The effect of piles and their loading on nearby retaining walls – an artificial neural network approach

Weiyang Zhang

A Thesis

in

The Department

of

Building, Civil and Environmental Engineering

Presented in Partial Fulfillment of the Requirements

for the Degree of

Master of Applied Science (Building, Civil and Environmental Engineering) at

Concordia University

Montreal, Quebec, Canada

August 2017

CONCORDIA UNIVERSITY

School of Graduate Studies

This is to certify that the thesis is prepared

By: Weiyang Zhang

Entitled: The effect of piles and their loading on nearby retaining walls – an artificial neural network approach

and submitted in partial fulfillment of the requirements of the degree of

Master of Applied Science (Building, Civil and Environmental Engineering)

complies with the regulations of the University and meets the accepted standards with respect to originality and quality.

Signed by the final Examining Committee:

Dr. A. M. Hanna Chair

Chair's name

Dr. A. Dolatabadi Examiner

Examiner's name

Dr. B. Li Examiner

Examiner's name

Dr. A. M. Zsaki Supervisor

Supervisor's name

Approved by ______________________________

Chair of Department or Graduate Program Director

__________2017 ______________________________

Dean of Faculty

ABSTRACT

The Effect of Piles and Their Loading on Nearby Retaining Walls – An Artificial Neural Network Approach

Weiyang Zhang

The assessment of stability of retaining walls that were constructed to prevent soil instability and collapse under the loads on nearby piles could be a sophisticated task. In urban areas, buildings or infrastructure are sometimes built relatively close to each other. Often pile foundations or groups of piles are used as the primary supporting systems and, inevitably, existing nearby retaining walls would be affected by these structures. The maximum wall deformation of these retaining walls was selected as a key factor to be determined to assess the retaining wall stability. In order to investigate the effect of loaded piles on the retaining wall, a set of parameters were selected such as the pile length, diameter and its location from the retaining wall. Considering all these parameters could lead to a large number of scenarios in order to establish the sensitivity of the system with respect to each variable. To reduce the required number of models needed to be analyzed, an Artificial Neural Network (ANN) was developed based on a representative dataset of base parameters. Similar to our brain, once the input (parameters) and output (maximum displacement and its location) baseline are given, the ANN is able to simulate and train by itself to provide a credible prediction of any corresponding scenario. Using the trained ANN model, for future designs engineers can predict a retaining wall maximum deformation and location under different geometrical scenarios, and as well to enhance or improve the serviceability of the entire pile-wall system.

Acknowledgements

I would like to express my deepest gratitude to my research supervisor Dr. Attila Michael Zsaki, who provided me the opportunity to carry out this research. His invaluable guidance and patience during the period of my graduate studies greatly assisted the success of my thesis research.

Furthermore, I extend my sincere appreciations and gratitude to my family who funded and supported my academic career with all their encouragement and love.

Authorization

I hereby declare that I am the sole author of the thesis.

I authorize The Concordia University of Civil Engineering Department to lend this thesis to other institutions or individuals for the purpose of scholarly research.

I also authorize The Concordia University of Civil Engineering Department to reproduce this thesis by photocopying or by other means, in total or in part, at the request of other institutions or individuals for the purpose of scholarly research.

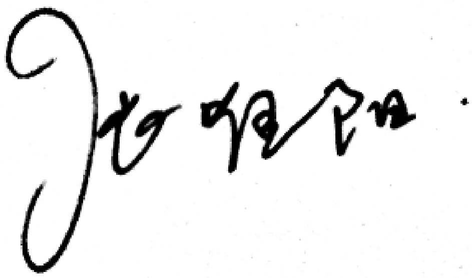

Weiyang Zhang

August 16

Table of Contents

List of Figures

List of Tables

Notation

The following symbols are used in this thesis

a; b	=	experimentally determined empirical coefficients;
A_j	=	a weighted sum activation function to trigger neurons in neural network;
A_p	=	pile cross section area;
b_0	=	bias at the single output neuron layer;
b_{HK}	=	bias at neuron *k* of the hidden layer ($k = 1, n$);
c'	=	effective cohesion of soil;
c_1'	=	cohesion of backfill soil;
c_2'; c	=	cohesion of clayey soil;
c_u	=	undrained shear strength;
D; B; d; D_2	=	pile diameter;
D_1	=	installation distance from pile to retaining wall;
D_{50}	=	mean particle size of the sand;
E	=	elastic modulus;
E_1	=	Young's modulus of backfill soil;
E_2	=	Young's modulus of clayey soil;
E_3	=	Young's modulus of retaining wall;
E_j	=	error function of each neuron in the neural network;
f	=	unit friction resistance at any depth;
f_{sig1}	=	sigmoid transfer function of each neuron in the hidden layer;
f_{sig2}	=	sigmoid transfer function of the neuron in the output layer.
H	=	distance between the pile base and the lower layer soil;
H_1	=	free height of retaining wall;
H_2	=	embedded depth of retaining wall;
H_3	=	retaining wall thickness;
H_{total}	=	total height of backfill;
I	=	moment of inertia;

K = earth coefficient;

K_a = Rankine active pressure coefficient;

K_h = soil displacement divided by the diameter of pile;

k_l = constant normal stiffness;

K_I = dimensionless stiffness number;

K_p = passive earth pressure coefficient;

K_{si} = initial shear stiffness;

L = length of the pile;

L' = a depth beyond which the unit frictional resistance stays as a constant value;

ΔL = incremental pile length;

M = bending moment at a certain depth;

N_q^*; N_c^* = Meyerhof's bearing capacity factors;

n = stiffness exponent;

O_j = a sigmoidal function representing the output in the neural network;

p = perimeter of the pile section;

p/pcs = the ratio of the initial confining pressure and the projection to the critical state line;

P_1 = area of the pressure diagram in sandy soil;

p_2 = active pressure at depth L;

p_a = atmospheric pressure;

P_i = input variable *I*;

q' = effective vertical stress at the level of the pile tip;

q_{ps} = ultimate unit point resistance of the stronger soil;

q_{pw} = ultimate unit point resistance of the weaker soil;

Q_p = tip resistance;

Q_s = shaft resistance;

Q_u = ultimate pile load;

$Q_{factored}$; Q_{ult} = factored ultimate load applied on top of the pile;

Rn = maximum normalized roughness;

R_t = maximum pile surface roughness measured as peak to peak over a skin length (L_m=0.8 to 2.5mm);

s/d = pile offset in percentage;

Δ_s = interface shear displacement;

Δu = soil displacement normal to the pile shaft in the interface;

$U(z)$ = final lateral displacement of the pile;

w_{ji} = input weights in the neural network;

W_{ik} = weight connection between input variable *i* (*i* = 1, m) and neuron *k* of the hidden layer;

W_k = weight of connection between neuron *k* of the hidden layer and the output layer;

x_i = inputs in the neural network;

z = depth under the surface of the ground;

$\bar{z}_1$ = center of pressure for the sandy soil;

σ'_0 = effective vertical stress at the depth under consideration;

σ_n = normal stress;

σ'_{nc} = normal effective stress at the soil-pile interaction;

$\Delta\sigma'_n$ = changes of normal effective stress during loading of the pile;

σ_r = radial stress;

σ_{r0} = initial radial stress;

σ_r/σ_{r0} = changes of radial stress;

σ_{v0} = initial vertical stress;

σ_v/σ_{v0} = changes of vertical stress;

δ = pile friction angle;

δ' = soil-pile friction angle;

δ_{wall} = angle of wall friction;

τ = interface shear stress;

τ_f = shear strength of interface;

τ_s = shear stress at the end of loading;

τ_{su} = mobilized ultimate shear stress;

τ_{ult} = asymptotic shear stress;

β = shear stress at the end of loading (τ_s) where s/d=30% and normalized with the initial vertical stress;

ϕ' = effective soil friction angle in the bearing stratum;

$\emptyset_1$; ϕ'_1; φ = sandy soil friction angle;

ϕ'_2 = friction angle of clayey soil;

ε_v = volumetric deformations for soils at different depths;

γ_1; γ = unit weight of sandy soil above the water table;

γ_2 = unit weight of clayey soil;

γ_w = unit weight of water;

Δ = outward displacement away from backfill at the top of the wall;

H = a constant value used for adjusting each weight in the neural network;

M = Poisson's ratio;

Chapter I. Introduction

1.1 Motivation

Geotechnical engineering, as a branch of civil engineering, could encounter a complex subject when analyzing the behavior of soil and its interaction with surrounding structures. When an in-place constructed (drilled, non-displacement) concrete pile that is axially loaded is placed close to a retaining wall, excessive deformation may occur and the stability of the wall could be affected. Foundations or pile support systems are commonly used in urban or offshore areas for various infrastructures, such as buildings or bridges. As shown in Figure 1.1.1, a group of pile foundations were constructed adjacent to a mechanically stabilized retaining wall. Depending on the geological and structural differences, the surrounding soils may be disturbed and reshaped into a denser or looser state when the pile is under the loading condition, which can potentially affect the stability of already existing nearby infrastructure. In this research, the main focus is on analyzing the behavior and deformation of an existing retaining wall under the condition that an adjacent existing pile is loaded by the maximum factored load.

Figure 1.1.1 Pile foundations for a bridge overpass structure located nearby a retaining wall (Weaver and Youn, 2008)

Current geotechnical approaches for the determination of the deformation of retaining walls have their limitations. A large number of models need to be established and the variety of combinations of key parameters including the soil properties, the free and embedded heights of the wall, the pile depth and pile-wall distance etc. are needed to be considered. However, by applying an artificial neural network (ANN), the number of models can be largely reduced by only providing typical samples and a well-trained ANN would be able to predict other scenarios.

1.2 Method of analysis

The mechanics of soil particles rearranging due to the disturbance caused by axially loaded piles is presented first in this thesis. In order to fully analyze a retaining wall system, the identification of key parameters would be the second objective which includes the retaining wall properties, soil properties and geometry of model, according to relevant references. After modeling and analyzing the adequate number of models using a finite element analysis method, an ANN was established. From which it was possible to predict the maximum wall deformation or inclination for other similar cases with the minimized prediction error procedure. In this thesis, all the values of key parameters were generated through a Monte Carlo sampling method. Two key software programs were used; RS2 (RocScience, 2017) for the finite element method (FEM) analysis and MATLAB (Mathworks, 2013) for developing the ANN.

In order to be able to analyze the model created in this thesis, the following assumptions shall be made:

- The pile was considered as an elastic concrete beam-column;
- The surrounding two layers of soils were considered as continuum medias;
- Absence of water table (drainage assumed behind and below the retaining wall);
- Homogeneous retaining walls were considered and the maximum free height and embedded depth were 11.7 and 14.4 meters respectively (from literature, as discuss later); and
- Distance between retaining wall and pile is kept within 5 meters (from literature, as discuss later).

1.3 Outcomes

Through using the developed ANN, it is possible to predict the maximum horizontal cantilever retaining wall deflection within an acceptable error range of 2.65 percent on average, with a maximum, and minimum error of 5.48, and 0.25 percent, respectively. By considering the inherent uncertainties regarding field soil properties, and geometric parameters, the ANNs performance would be acceptable in the geotechnical field. With given scenarios, instead of developing and using a FEM model, the ANNs analysis shall provide engineers with a more convenient and competent way of obtaining the corresponding results.

Chapter II. Literature Review

2.1 Soil deformation induced by axially loaded piles

In this thesis, the basic factors that control soil deformation will be presented and the corresponding retaining wall deformations due to the lateral stress changes or soil particle rearrangements will be considered as well.

Under the condition that a pile is axially loaded, within the maximum bearing capacity, the load would transfer to the surrounding soil and induce inevitable soil particle rearrangement and deformation of the soil mass. Since the shear stress along the pile shaft and the normal stress at the base are the prime triggering forces, the degree of soil deformation is determined by the magnitude of the loading and the roughness of pile-soil interaction. The ultimate bearing capacity of a single pile is calculated by the cumulative equilibrium forces that include the shaft resistance (Q_s) and tip resistance (Q_p). Because of the shaft resistance mobilization, the surrounding soil undergoes considerable straining and deforms in shear mode. Based on laboratory analysis, using physical model tests and shear tests, it was found that the degree of pile roughness and confining pressure controls the final mobilized shear stress of a given soil (D'Aguiar, 2007). Similarly, the pile-soil friction angle is dependent on the pile-soil interface roughness, soil grain gradation and the level of stress. By increasing the pile roughness, the value of pile-soil interaction friction angle could be the same as the soil's, and when soil failure occurs along the shaft, the maximum interface friction angle is equal to the mobilized soil friction angle. However, as for the tip resistance, it is mainly controlled by the soil behavior itself including the soil strength, initial state, shear stiffness, and volumetric compressibility (D'Aguiar, 2007).

To determine the soil behavior and failure pattern, a three-dimensional finite element analysis was done by D'Aguiar (2007) considering a non-displacement pile. Using the integrated critical state concept and a Mohr-Coulomb failure constitutive model, different models were compared with centrifuge test results. It was revealed that with the increased interface roughness of a pile, the shaft resistance was dramatically increased as well, however the tip resistance was not affected by the change of roughness. Also, the effects of increased roughness on soil behavior were shown on the bearing capacity of the pile. When the surrounding soil collapses, it only occurs within a thin layer adjacent to the pile shaft which indicated that the pile-soil interaction was strengthened. To determine the load transfer mechanism of the loaded pile, the evaluation of state paths, stress paths and stress transfer curves were presented by D'Aguiar (2007) with the maximum roughness (Rn >>). Figure 2.1.1 (a), where τ stands for the shear stress and σ_r for the radial stress, shows the stress and state paths of the soil (Toyoura sand, TS1) near an axially-loaded pile. From which, it is possible to observe that during loading, the escalation of the shear stress was followed by the increase of the lateral stress applied on the pile shaft. Also, the maximum shear stress increased with depth and which was independent from the radial stress. The author stated that during axial loading of a pile, the surrounding soil endured large straining and performed as in simple shear. As shown in the Figure 2.1.1(b), when soil undergoes shearing, it deforms either as contractively or dilatively depending on its relative density and initial state, which is illustrated by observing the variation of void ratio against the mean stress in the figure. In Figure 2.1.1(b), soil state paths at different depths began at the same initial void ratio with different confining pressures, and eventually all of them reached the critical state line (CSL) with different final void ratios.

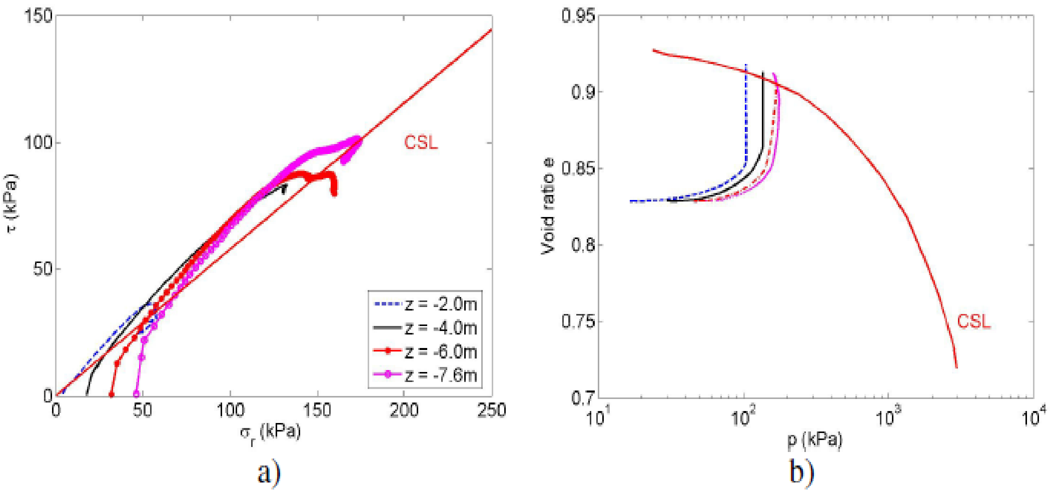

Figure 2.1.1 Stress and state paths at different depths along the pile shaft for TS1: a) Stress path in $\tau - \sigma_r$ plane; b) State path in $e - lnp$ plane (D'Aguiar, 2007)

Instead, the local stress transfer mechanism was illustrated in D'Aguiar (2007), through analyzing the shear stress changes at different depths against the pile tip settlement, as shown in Figure 2.1.2(a) where s/d stands for the pile offset in percentage, due to the increase in depth and confining pressure, the mobilized shear stress consequently increased. In addition, by comparing Figure 2.1.1(b) with Figure 2.1.2(b): during loading, the increase of normal stress was shown by the increase of the void ratio, and due to the dilation, the increasing friction transfer behavior illustrated in Figure 2.1.2(a) has been justified. Accordingly, because of the void ratio changes and the dilation, the constrained dilatancy resulted in the increase of normal and shear stress and thereafter contributed to the changes of pile resistance. In Figure 2.1.3, the changes of radial (σ_r/σ_{r0}) and vertical (σ_v/σ_{v0}) stress at different depths against the pile displacement are illustrated. Conclusions were made based on these two graphs that the stress distributions were dissipated ahead of the mesh boundary. From Figure 2.1.3(a), the effect of radial/lateral stress changes has been restrained and decreased under the dilatancy increases. Also, the vertical stress changes were less dependent on the change of depths (D'Aguiar, 2007).

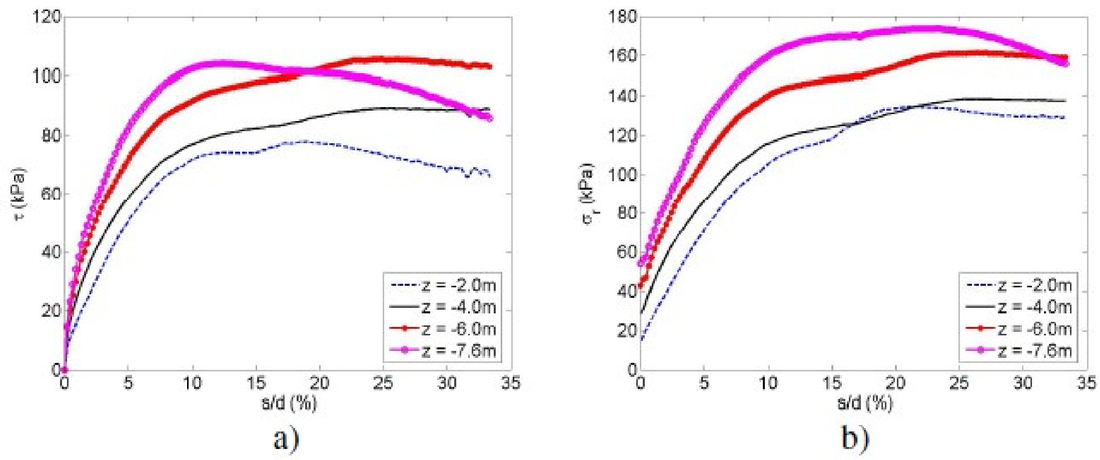

Figure 2.1.2 Local stress transfer curves along shaft for TS1, as a function of normalized head displacement: a) local shaft friction transfer; b) local radial stress transfer (D'Aguiar, 2007)

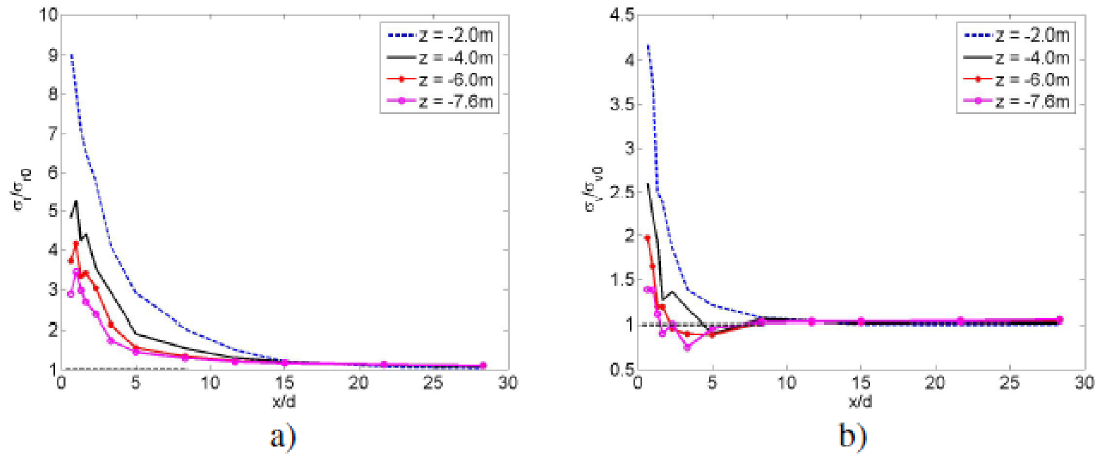

Figure 2.1.3 Variation of normalized stress with pile offset for different depths at s/d=30%: a) radial stress; b) vertical stress (D'Aguiar, 2007)

2.2 Pile shaft response

After a pile is installed into the ground, its resistance typically depends on the density of soil particles and the shaft friction. Normally, this resistance could change with different initial confining pressure and, even if having similar density, different soil types could also effect on the resistance change. As for the shaft friction, τ_s, in Fioravante (2002), the author stated that the following equation may be applied for its determination:

$$\tau_s = (\sigma'_{nc} + \Delta\sigma'_n)tan\delta \qquad (1)$$

where σ'_{nc} represents the normal effective stress at the soil-pile interaction, $\Delta\sigma'_n$ stands for the changes of normal effective stress during loading of the pile and δ is the pile friction angle (Fioravante, 2002).

Factors that control the mobilization and outcome of the shaft friction of pile in sandy soil are the interface zone, the “elastic spring”, and the constant normal stiffness model.

Specifically, the interface zone can be defined as a thin zone close to the pile shaft. The pile surface roughness would determine the magnitude of this zone, it generally varies between (2 to 5)*D_{50} to (10 to 15)*D_{50} for smooth pile and rough pile respectively, where D_{50} denotes for the mean particle size of the sand (Fioravante, 2002). After pile installation and loading, this interface zone was subjected to plastic straining. Similar to D’Aguiar (2007), the degree of the plastic straining was large enough to resemble as simple shear mode and dilative or contractive soil behavior could be expected. To examine in detail the influence of roughness, as shown in Figure 2.2.1, the normalized roughness was defined as $R_n = R_t/D_{50}$, where R_t represents the maximum pile surface roughness and measures as peak to peak over a skin length L_m=0.8 to 2.5mm (Fioravante, 2002). Furthermore, after defining the mobilized ultimate shear stress in the interface, τ_{su}, the author stated that when $R_n < 0.02$, the interface is smooth, no dilatancy occurred and the value of τ_{su} is low; when $R_n > 0.1$, which means the interface is totally rough and the value of τ_{su} is high yet not dependent on the roughness.

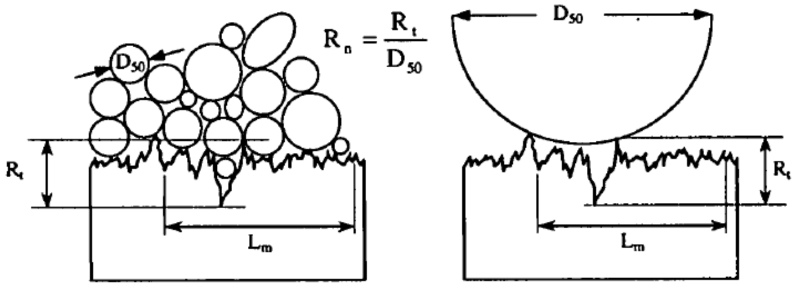

Figure 2.2.1 Definition of maximum roughness R_t and relative roughness R_n (Fioravante, 2002)

The "elastic spring", typically, is a phenomenon with the change of volume that interacts at the interface with the dilative or contractive behavior of soil, and the stress normal to the interface would be increased or decreased respectively. It has been stated that the increment of the effective stress $\Delta\sigma_n'$, for small diameter piles (laboratory model piles for instance), was inversely proportional to the pile radius and, for large scale piles with diameter $D \geq 500mm$, this effect can be ignored. For non-displacement piles, consequently, the influence of pile radius on the increment of shear stress should also be small enough to be neglected as well (Fioravante, 2002).

Furthermore, to test the mobilization of the skin friction along shaft, one of the simple shear test named "Interface Direct Shear Test" with constant normal stiffness (k_l) was conducted by some researchers (Fioravante, 2002; Lehane and White, 2005). Due to the relationships between stress changes and soil behavior, the following equation can be used to assure the constant normal stiffness will be applied during analysis:

$$k_l = \frac{\Delta\sigma_n'}{\Delta u} \tag{2}$$

where Δu is the soil displacement normal to the pile shaft in the interface (Fioravante, 2002).

From this relationship, if the surrounding soil along the pile undergoes dilation ($\Delta u > 0$), the applied normal stress would increase and, if contraction occurs ($\Delta u < 0$), the normal stress decreases accordingly. Following which, the centrifuge non-displacement pile tests were conducted to analyze the mobilization mechanism thoroughly provided by Fioravante (2002). Results had shown that the maximum unit shaft friction at the soil-pile interface is relying on the magnitude of the normalized roughness R_n. Specifically, for smooth surface piles with $R_n \cong 0.01$, the contraction of sand was generated and freely form the soil's initial state; for rough piles with $R_n \geq 0.13$, however, the dilation of sand at the interface was detected (Fioravante, 2002).

Accordingly, to define the mechanical behavior of a certain type of soil, the initial void ratio, or relative density, and the stress state are important to be known before analysis. The consequent influence of these parameters or soil state on the load settlement response can be interpreted by a stress state parameter and its distance to the critical state line (CSL). This stress state parameter was defined in D'Aguiar (2007) as "*the ratio of the initial confining pressure and the projection to the critical state line (p/pcs)*". To determine its importance on the shaft and base resistance, numerical models were established and analyzed with respect to different types of sandy soils, the TSi, ASi, and HSi, where index i stands for the different distances to the CSL.

Figure 2.2.2 illustrates the relationships between shaft resistance and pile offsets (Figure 2.2.2a) and the evolution of maximum shaft resistance mobilized with p/pcs values (Figure 2.2.2b). Specifically, in Figure 2.2.2(b), p represents the mean value of the initial confining pressure at approximately one third of the pile height from the bottom of the pile. The author (D'Aguiar, 2007) adopted that the lower the p/pcs values, or the further the distance of the initial states to the CSL, the higher the maximum shaft resistances were attained for all the soil samples. This was concluded by comparing the results with respect to the sand sample TS1 and TS2 that had 40% and 24% of relative density respectively. During loading, the loose sand (TS2) provided less shaft resistance as expected and for the dense sand (TS1), as shown in Figure 2.2.3(a), the greater the normal stress was mobilized. From Figure 2.2.4, moreover, for all the soil samples, they were first contracting and then dilating.

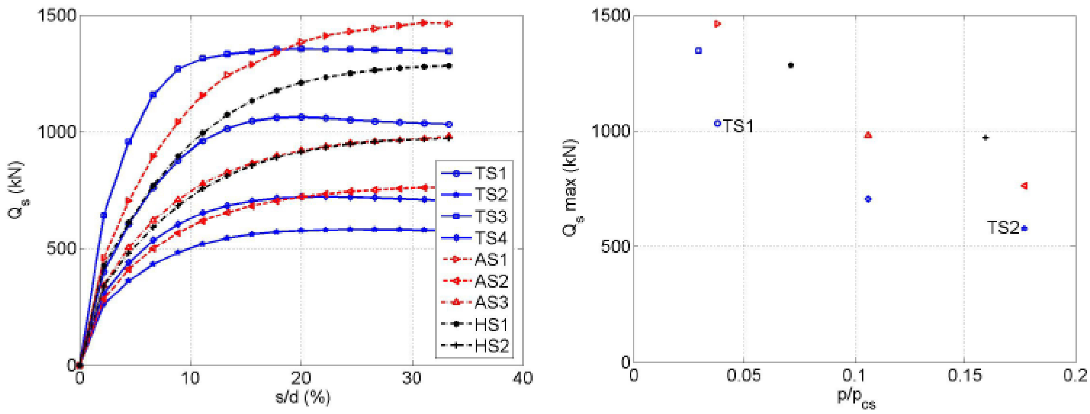

a) b)

Figure 2.2.2 Comparative results for different sand samples: a) load settlement curves for shaft; b) evolution of the maximum shaft resistance with the stress state parameter p/pcs (D'Aguiar, 2007)

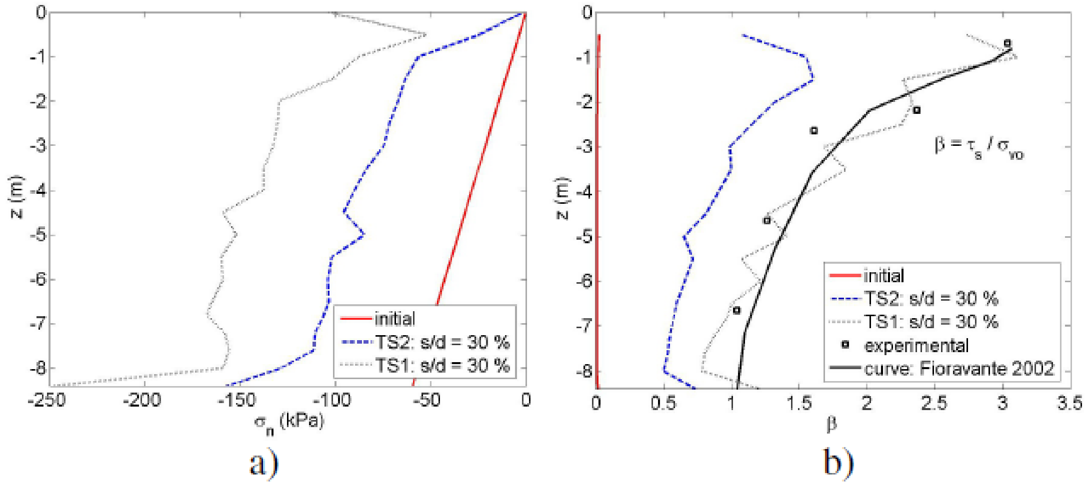

Figure 2.2.3 Comparative results for sands TS1 and TS2 at s/d=30%: a) normal stress distribution along shaft; b) normal shear stress distribution along shaft (D'Aguiar, 2007)

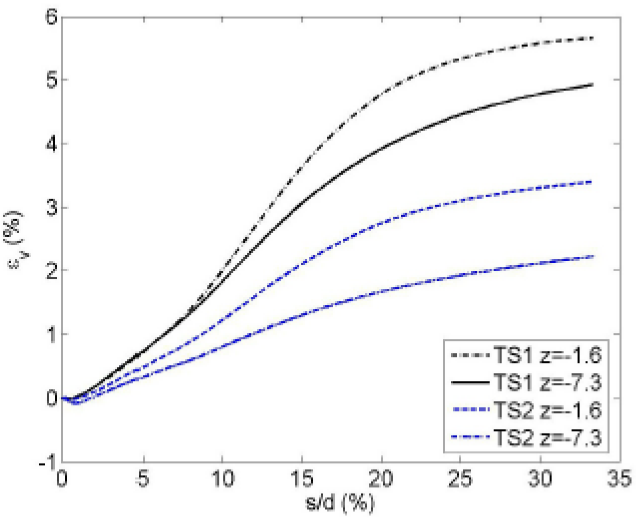

Figure 2.2.4 Comparative results for sands TS1 and TS2 at s/d=30%: evolution of volumetric deformations at different depths (D'Aguiar, 2007)

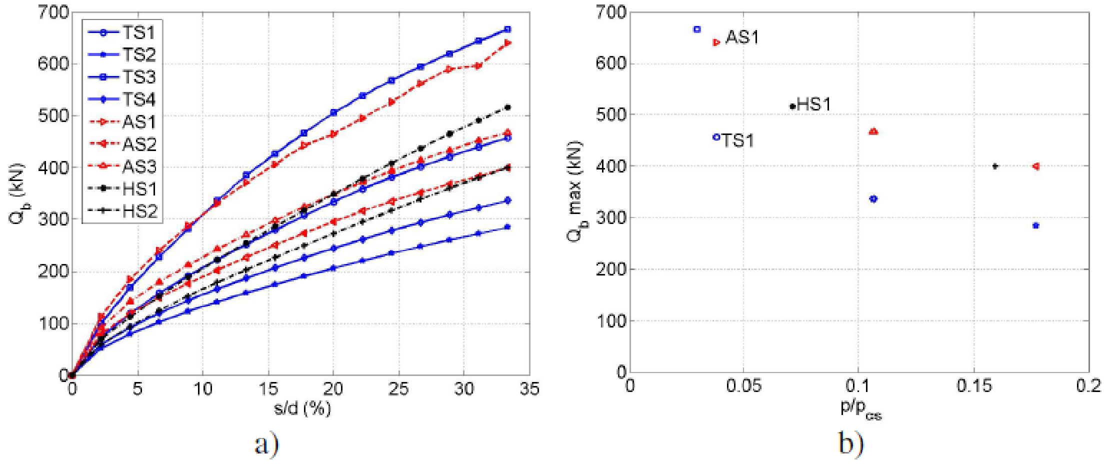

Figure 2.2.5 Comparative results for different sands: a) load settlement curves; b) evolution of the maximum base resistance with the stress state parameter p/pcs (D'Aguiar, 2007)

From above, we can establish that the changes of the volume of shear zone would determine the lateral stress behavior on the pile shaft, also, the lateral stress increases with the escalation of confinement pressure provided by the soil, and decreases with depth. In Figure 2.2.3(b), it was defined that the parameter β as the shear stress at the end of loading (τ_s) where s/d=30% and normalized with the initial vertical stress (σ_{v0}), therefore, $\beta = \tau_s/\sigma_{v0}$. From Figure 2.2.4, by comparing the volumetric deformations (ε_v) for soils at different depths (z=1.6m and 7.3m), the dilation was more noticeable under low stress environment. Therefore, with the increase of depth, the effect of restrained dilatancy in shear stress decreases so that the value of parameter β deformed progressively, which is corresponding with the result provided by Fioravante (2002).

2.3 Pile tip response

Similar to the pile shaft, the tip response, while the pile is being loaded, is mainly dependent on the soil initial state such as the density, shear stiffness and volumetric compressibility in compression and so on. For the same samples studied in Chapter 2.2, the analysis has been conducted by D'Aguiar (2007) as well. From which, in Figure 2.2.5(a), it is possible to notice that for all samples, the lower the density of the same type of soils was, the lower the provided tip resistance was. From Figure 2.2.5(b), the relationship between stress parameter p/pcs and the maximum tip resistance reveals that, with increasing the value of p/pcs, the consequent decreasing value of maximum tip resistance was generated.

By combining the shaft and tip resistance behavior, the author (D'Aguiar, 2007) stated that the key parameter, p/pcs, played a critical role in the determination of the prediction. During loading, with the changes of volume interaction between the interface and the constrained dilatancy, the behavior of the normal stress and shear stress can be determined.

2.4 Effect of loading on piles and a nearby retaining wall

During urban or offshore infrastructure construction, inevitably, an axially or laterally loaded pile would be installed adjacent to the retaining wall. The consequent lateral stress, shear stress changes, and the soil deformation induced by pile loading would trigger the deformation of retaining wall to a certain degree. If collapse happens, the outcome of which will pose a great threat to the stability of pile or pile foundation (Yu and Liang, 2010).

Unfortunately, the literature is quite limiting regarding this scenario (axially loading of piles near an existing retaining wall). However, related ones, on the subject of the laterally loaded pile effects on adjacent retaining walls were conducted by several authors, for example, Weaver and Youn (2008), and Chung (2005). In Yu and Liang (2010), Figure 2.4.1 shows a model of an axially loaded pile and a nearby retaining wall. Because the retaining structure serves a critical role in limiting the extra displacements of the retained soil, its stability is crucial in preventing the collapse of the soil and pile. If collapse of retaining wall occurs, tens of times increase of soil lateral movement can be expected and the greatest lateral soil displacement would be triggered around the ground surface, and decrease with depth (Yu and Liang, 2010).

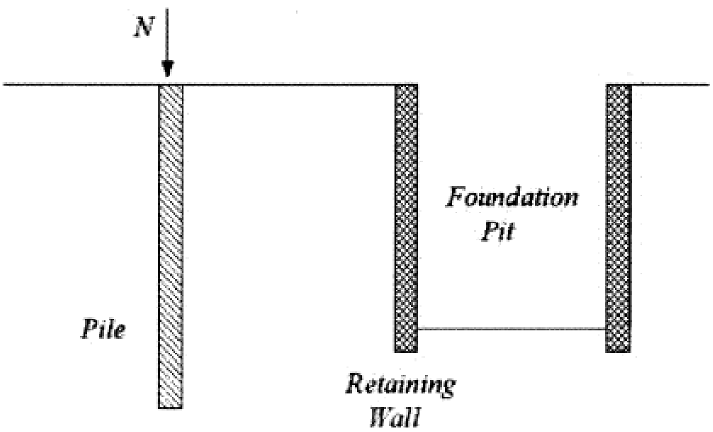

Figure 2.4.1 Layout of the axially loaded pile and retaining wall (Yu and Liang, 2010)

Given the relationships among the axial loading, bending moments of the pile, and displacement using the formula given in Yu and Liang (2010), it is possible to further investigate the pile and soil behavior before and after the retaining wall collapses:

$$K_U = \frac{U(z)}{d}, K_M = \frac{ML}{EI} \quad (3)$$

where $U(z)$ – the final lateral displacement of the pile; d – the diameter of the pile (m); M – the bending moment at a certain depth (kN*m); L – the length of the pile (m); E – elastic modulus (GPa); and I – moment of inertia (kg*m^2).

Figure 2.4.2 illustrates the comparative lateral soil displacement, from which, the resulting increase of soil movements induced by the collapse of the retaining wall can be perceived. Moreover, after the axial load ($K_N = 30\%$) was applied on the pile, comparative results are illustrated in Figure 2.4.3 and 2.4.4. Undoubtedly, from these two figures, the applied axial loading amplifies the horizontal displacements and bending moments of the pile; also, after the wall collapses, the two results, K_U and K_M, were significantly increased. In detail, in Figure 2.4.3, the resulting dimensionless pile head displacement behind a stable wall was increased from 0.0242 to 0.0294 (dimensionless) after the axial load was installed (increasing by 21.5%), and was augmented even more in the situation of the retaining wall collapses by 25.5% (Yu, 2010).

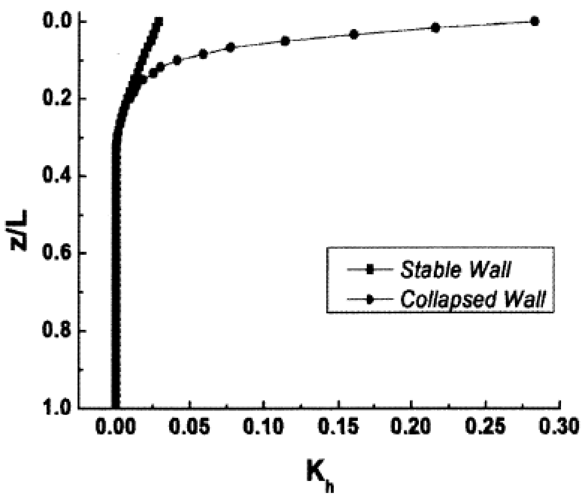

Figure 2.4.2 Comparison of lateral soil movement: z – depth under the surface of the ground (m); K_h - soil displacement divided by the diameter of pile (dimensionless) (Yu and Liang, 2010)

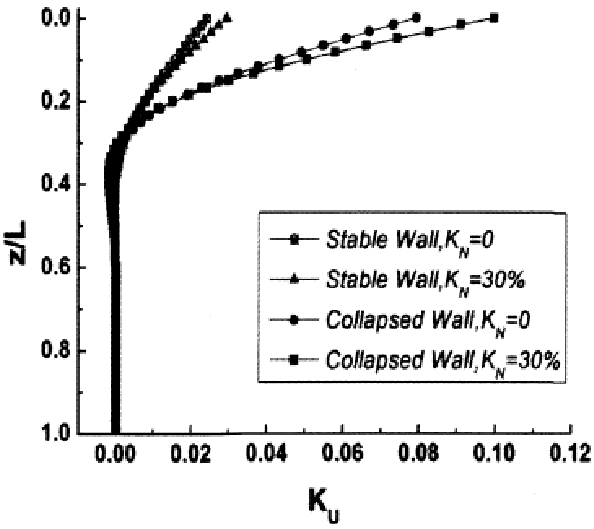

Figure 2.4.3 Comparison of dimensionless lateral displacements of pile (Yu and Liang, 2010)

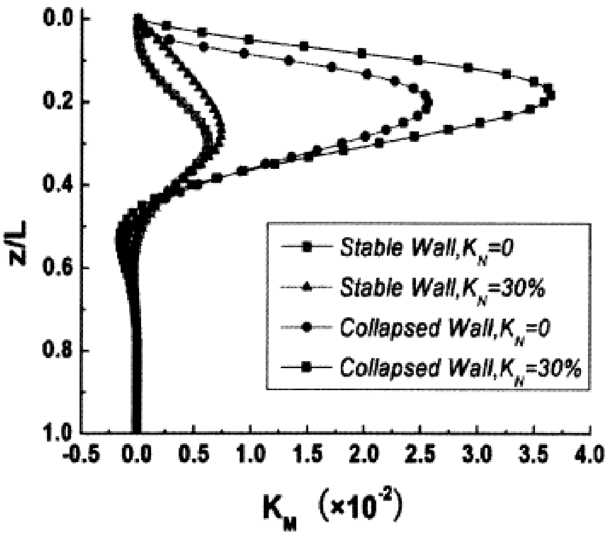

Figure 2.4.4 Comparison of dimensionless bending moment of pile (Yu and Liang, 2010)

Instead, from Figure 2.4.4, the changes of bending moments after the pile loading were increased from 0.0062 to 0.0074 (increasing by 19.4%) when the wall was stable; and raised from 0.0257 to 0.0364 (increasing by 41.6%) after the wall collapses, respectively.

Not only the case of axially-loaded piles, but some other literature have thoroughly examined the effects of laterally-loaded piles on a nearby retaining wall which can assist us in understanding the soil-pile and soil-retaining wall behaviors. Similarly, the effects of lateral loading on surrounding soils and retaining structures can be determined through numerical analysis. In bridge design, typically, it has been addressed in the 2004 American Association of Highway and State Transportation Officials (AASHTO) (Weaver and Youn, 2008), that the serviceability limit of pile head displacement shall not exceed 38mm. When the deformation of the pile occurs, the induced excessive horizontal stress may cause the collapse of the nearby retaining wall. Also, the interaction between pile and wall can change the lateral pile stiffness and, in the worst cases, this stiffness could be reduced dramatically (Weaver and Youn, 2008).

Using a non-linear three-dimensional finite element analysis, Chung (2005) investigated the interaction of a sheet pile wall and a nearby pile. As shown in Figure 2.4.5 and Figure 2.4.6, the increase of lateral stress acting on the retaining wall induced by the pile placed at 1.5 pile diameter from the wall can be noticed. When the pile was not sleeved with a lateral load of 5000kN, the lateral earth pressure acting on the wall varied from K_p to $3K_p$, where K_p stands for the passive earth pressure coefficient. Even though the pile sleeve could reduce a certain amount of the load transfer, the ultimate lateral earth pressure was greater than the at rest condition (Weaver and Youn, 2008). Following the distribution of stress changes, the horizontal displacement of wall can be expected and measured, see Figure 2.4.7. From which, for the sleeved pile resulted in smaller displacements due to the downward shear transfer mechanism as compared with the unsleeved ones (Chung, 2005), and it is possible to notice that the peak displacements were occurring at the top of the wall, which basically correspond to the result obtained in this thesis from numerical analysis of the axially loading conditions, as discussed in a subsequent chapter.

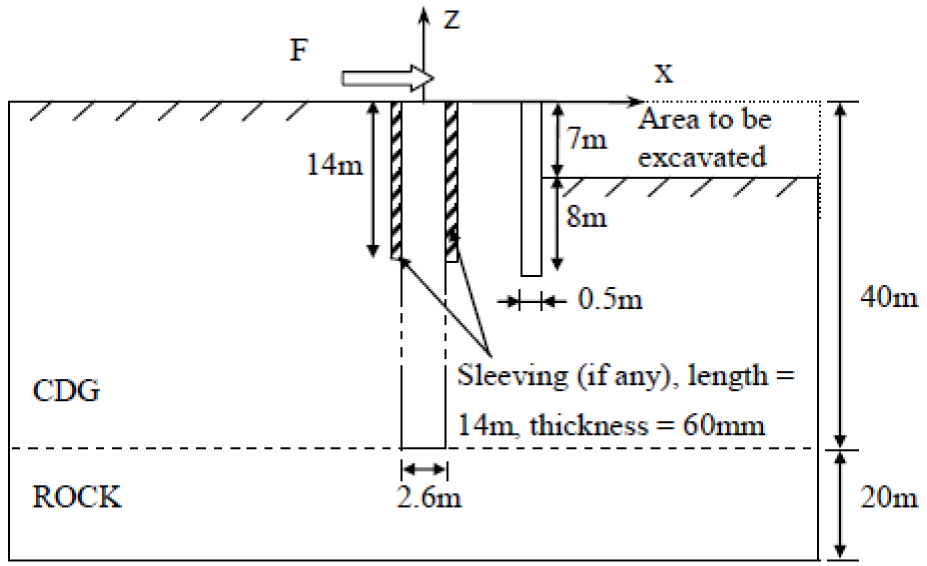

Figure 2.4.5 Pile and retaining wall system (Chung, 2005)

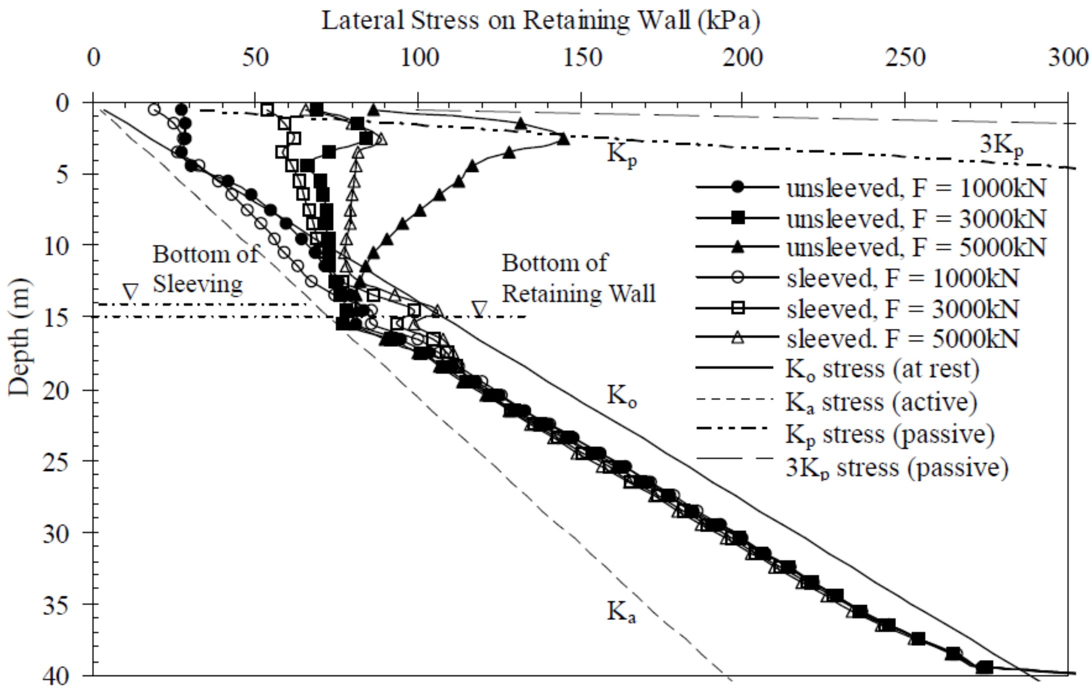

Figure 2.4.6 Lateral pressure acting on the retaining wall with a laterally loaded pile located 1.5 pile diameter from the wall (Chung, 2005)

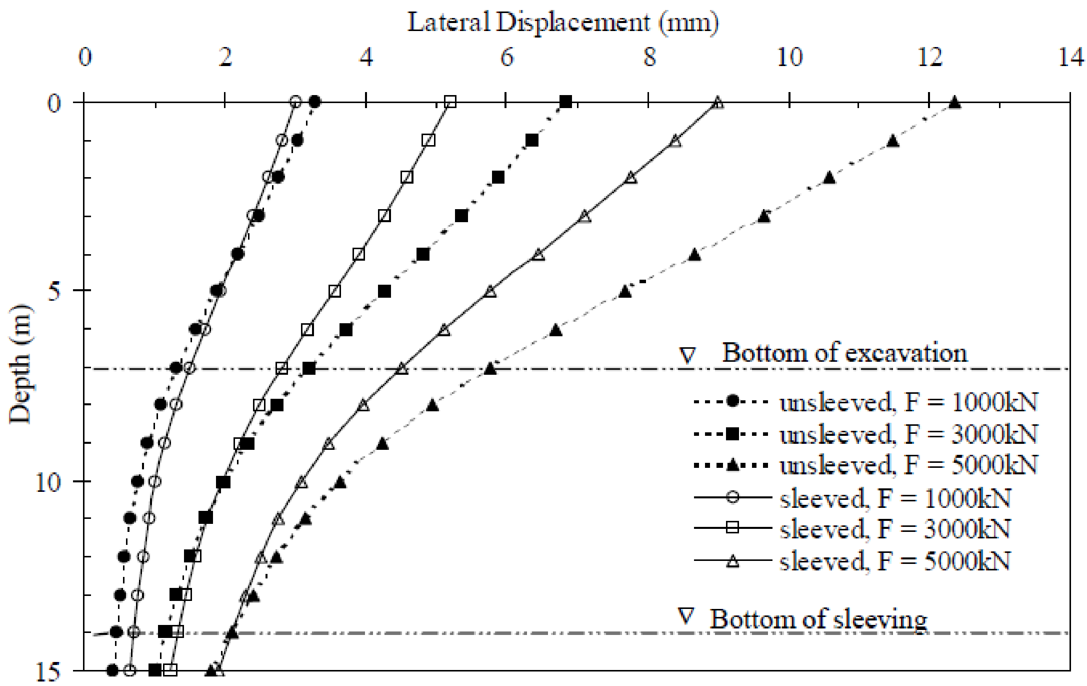

Figure 2.4.7 Lateral displacements of retaining wall along depth (Chung, 2005)

Since the axial or lateral loading on a pile could result in the lateral stress changes that contribute to the wall displacements, the effect of pile installation distance from the wall shall also be considered. Theoretically, the farther the pile is located from the wall, the smaller the effects would be transferred on the wall. In Weaver and Youn (2008), the authors have examined various situations including pile spacing of 2 to 8 pile diameters from the wall with a lateral loading, results of which are shown in Figure 2.4.8 and 2.4.9. In the analysis, the influence of wall bending stiffness has been considered that the sheet pile sections were given as PZ-22, PZ-27, PZ-35, and PZ-40. Also, the excavation depth was 4.6m and a 0.3m square pile was used. From Figure 2.4.8, the changes of horizontal earth pressure were limited within one passive and three times the passive earth pressure, and the peak value was obtained at about 5 pile diameters depth below the ground. From Figure 2.4.9, results are verifying that piles installed 8 or more pile diameters from the wall would have slight or negligible effects on the retaining wall (Weaver and Youn, 2008).

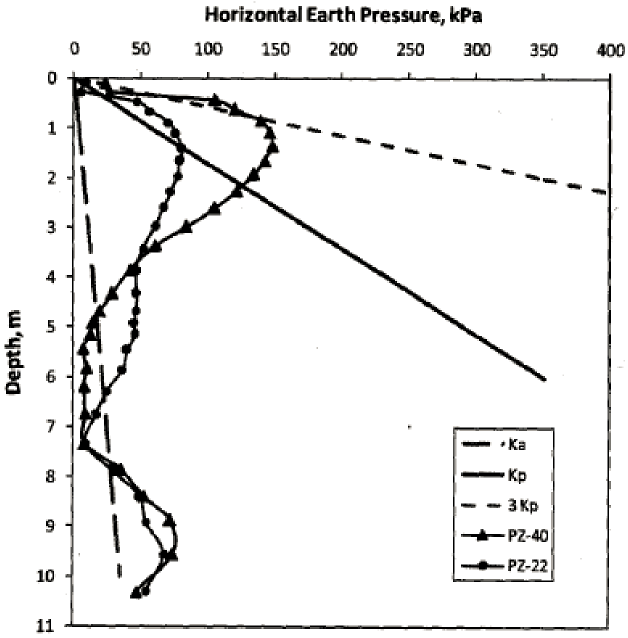

Figure 2.4.8 Horizontal earth pressure acting on the retaining wall for piles located two pile diameters from the wall (Weaver and Youn, 2008)

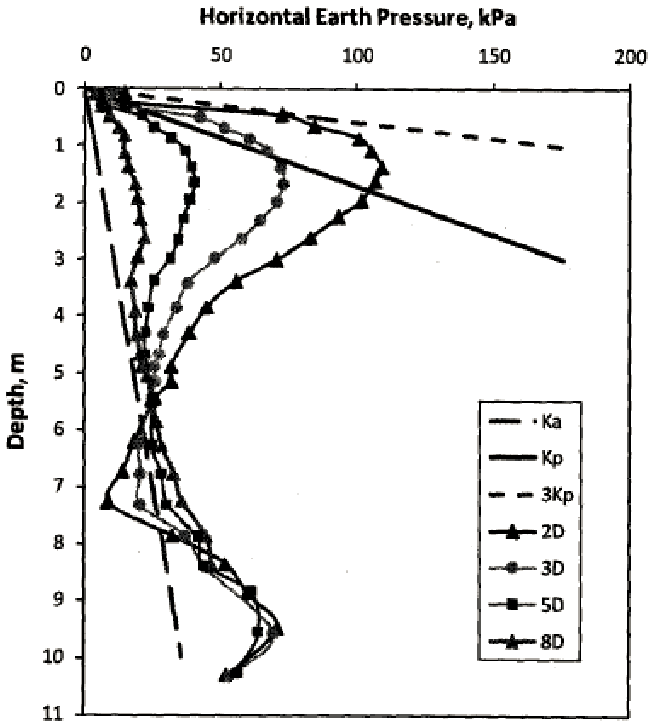

Figure 2.4.9 Horizontal earth pressure acting on the retaining wall for piles spaced 2 to 8 pile diameters from the wall (Weaver and Youn, 2008)

2.5 Pile bearing capacity

After the installation of closed-ended piles beside a retaining wall, the ultimate bearing capacity of these piles is dependent on the supporting soil condition which includes pile tip and shaft bearing capacities.

In total, as defined in Das (2007), the ultimate pile load can be expressed as:

$$Q_u = Q_p + Q_s \qquad (4)$$

where Q_p is the load carried at the pile tip and Q_s is the load carried by skin friction developed along the pile shaft.

If Q_s is too small, then $Q_u \approx Q_p$ and if there is no existing bedrock or rock-like material at the layer of pile tip, most of the resistance originates from the adhesion between pile and soil particles and, thus if Q_p is relatively small, then have $Q_u \approx Q_s$.

2.5.1 Bearing capacity in sand

Based on Meyerhof's method, in sandy soils where $c' = 0$, the cohesion of the soil supporting the pile tip is equal to zero, thus (Das, 2007):

$$Q_p = A_p q_p = A_p q' N_q^* \leq A_p q_l = A_p 50 N_q^* tan\phi' \quad (5)$$

where A_p is the pile cross section area, N_q^* is the bearing capacity factor which depends on the effective soil friction angle in the bearing stratum, ϕ', as shown in Figure 2.5.1.1, q_l is the limiting bearing resistance and q_p is the unit point resistance.

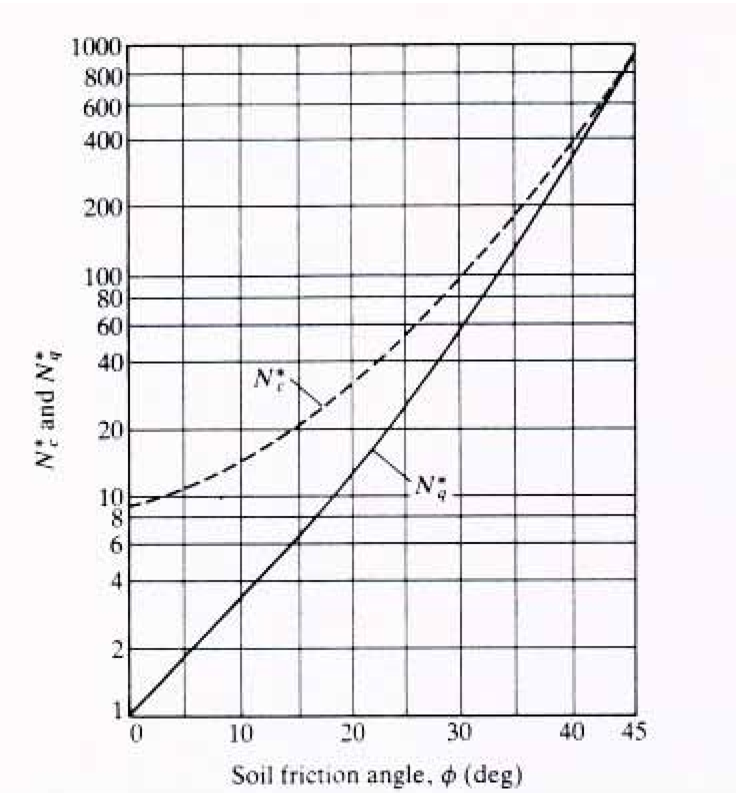

Figure 2.5.1.1 Meyerhof's bearing capacity factors, N_q^* and N_c^* (Meyerhof, 1976)

The total load carrying capacity of pile installed in clayey layer soil can be expressed as the following equation (Das, 2007):

$$Q_p = A_p q_p = A_p (q' N_q^* + c' N_c^*) \quad (6)$$

where q' is the effective vertical stress at the level of the pile tip and N_c^* is the Meyerhof's bearing capacity factor.

Since there is no available resource providing the precise values for determine the N_q^* and N_c^*, in the process of calculation, the following values (Table 2.5.1.1) of N_q^* and N_c^* were used correspondingly through estimation. From which, it is possible to conclude that the higher the value of friction angle is, a proportional increase of the value of N_q^* and N_c^* would be encountered.

Φ	1	2	3	4	5	6	7	8	9	10	11	12	13	14	15
N_c^*	9.5	9.7	10	10.5	11	11.5	12	13	14	15	16	17	18	19	21
N_q^*	1.1	1.2	1.4	1.7	1.9	2	2.1	3	3.3	3.5	3.8	4	5	6	7
Φ	16	17	18	19	20	21	22	23	24	25	26	27	28	29	30
N_c^*	23	27	28	30	33	35	38	40	45	55	60	65	75	90	95
N_q^*	7.5	8	9	10.5	13	14	16	17	20	28	30	35	40	50	59
Φ	31	32	33	34	35	36	37	38	39	40	41	42	43	44	45
N_c^*	105	120	150	170	190	200	250	300	350	400	420	520	610	800	1000
N_q^*	70	80	90	110	140	150	180	210	290	350	400	500	600	800	1000

Table 2.5.1.1 Values of N_q^* and N_c^* corresponding to the soil friction angle ϕ (Das, 2007)

For calculating the frictional resistance, Q_s, it can be addressed as (Das, 2007):

$$Q_s = \sum p \Delta L f \tag{7}$$

where, p is the perimeter of the pile section, ΔL is the incremental pile length over which p and f are taken as constant values, and f is the unit friction resistance at any depth z. In addition, Das (2007) illustrated that, for the unit frictional resistance f is given as:

$$f_{avg} = K\sigma_0' tan\delta' \tag{8}$$

where, K is the earth coefficient, σ_0' is the effective vertical stress at the depth under consideration and δ', which is the soil-pile friction angle, usually was taken as $0.5\phi' to\ 0.8\phi'$. In Seo et al. (2007), it suggested that the value of δ' varies between $0.8\phi'$ to ϕ', and in Józefiak et al.'s (2015) finite element analysis, it was assumed that the value of δ' is taken as equal to the value of ϕ'. To simplify the research, the value of δ' will be considered as:

$$\delta' = \phi' \tag{9}$$

The value of K, according to Das (2007) is:

$$K \approx 1 - sin\phi' to\ 1.4(1 - sin\phi') \tag{10}$$

Conservatively, when considering the effects of pile depth on shaft resistance in sand, the value of unit frictional resistance f stays as a constant value after $L' = 15D$, where D is the pile diameter. And from the ground to the depth $L' = 15D$, f is linearly increased by the increase of the installed depth, to calculate which, an average value $f_{av} = f/2$ was usually taken to represent the value of frictional resistance in. For non-displacement piles, the value of $K = 1.4(1 - sin\phi')$ for both clayey and sandy soils will be used.

In detail, when pile was in sandy soil, the following formulae were used for the calculation of pile shaft resistance:

$$Q_s = p * L * \frac{L * \gamma_1 K_{sand} * tan\emptyset_1}{2}; when\ L \leq H_1 + H_2\ and\ H_1 + H_2 \leq 15 * D; or\ L \leq 15 * D\ and\ 15 * D \leq\ H_1 + H_2 \quad (11)$$

$$Q_s = p * (L - 15D) * K_{sand} * 15D * \gamma_1 * tan\emptyset_1 + p * 15D * \frac{K_{sand} * 15D * \gamma_1 * tan\emptyset_1}{2}; when\ H_1 + H_2 > L > 15D \quad (12)$$

where γ_1 is the density of sandy soil, $\emptyset_1$ is the sandy soil friction angle, L is the pile length, p is the pile perimeter, H_1 is the free height of retaining wall, and H_2 is the embedded depth of retaining wall.

2.5.2 Bearing capacity in clayey soil

The major difference between clayey and sandy soils is the calculation of the frictional (shaft) resistance. In general, three methods are widely used: the α, λ, and β methods (Das, 2007), yet if overconsolidation ratio of the clay is not known, β method is not taken into consideration in the calculation. Since the water table is also not considered in the analysis, the undrained shear strength c_u is therefore inapplicable, hence, the method to calculate the bearing capacity where pile tip is located in clayey soils can be divided into the following scenarios;

When the pile tip is installed into the stronger (backfill) soil, but within a range of depth equal to $z_b = 0\ to\ 10B$, as illustrated in Figure 2.5.2.1, where B is the pile diameter (same as "D" denoted previously). This critical depth (10B) is different comparing with the case when the pile only penetrating through homogeneous sandy soil. The consequent end bearing capacity can be calculated by the following modified formula (Mitchell, 2005; Das, 2007):

$$q_b = q_{pw} + \frac{(q_{ps} - q_{pw})H}{10B} \quad (13)$$

where q_{pw} is the ultimate unit point resistance of the weaker soil, q_{ps} is the ultimate unit point resistance of the stronger soil and H is the distance between the pile base and the lower layer soil.

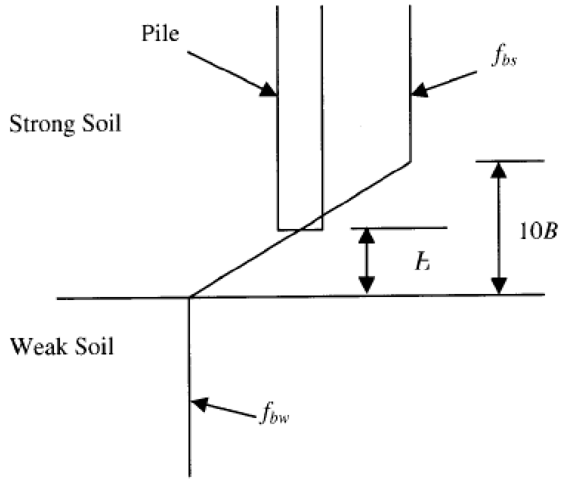

Figure 2.5.2.1 Relation between ultimate base resistance of pile and depth in strong layer overlying weak soil (Mitchell, 2005)

In Mitchell (2005), the value of ultimate unit point resistance of weaker soil was given by laboratory tests (pile jacking force), in this thesis, the value of q_{pw} was calculated by the formula when pile tip was in clayey soil. Combining with what is concluded above, the ultimate tip bearing capacity when the pile tip was penetrating into a certain distance (10B) above the clayey soils can be expressed as the following equation:

$$Q_p = A_p q' N^*_{qclay} + \frac{(\min(A_p 50 N^*_{qsand} tan\phi'_1, A_p q' N^*_{qsand}) - A_p q' N^*_{qclay})H}{10B}; \ when\ 0 < (H_1 + H_2 - L) < 10B; \quad (14)$$

where H_1 is the free height of wall, and H_2 is the embedded depth of wall.

Also, it is possible to deduce that when the pile tip was located beyond the critical depth of the stronger soil, the following holds:

$$Q_p = A_p(q' N^*_{qclay} + c' N^*_{c,clay}); when\ \ (L - H_1 - H_2) \geq 10B \quad (15)$$

where c' represents the corresponding cohesion of clayey soil.

According to Mitchell (2005) and Das (2007), similar as the method of calculation of the shaft resistance when pile was installed in sandy soil, it is also possible to calculate the consequent skin resistance when pile tip was in clayey soil. During calculation, the shaft resistance was cumulatively added together, like the sandy soil, to the considered thickness of 10D below the top of clayey soil as its critical depth for the calculation of skin resistance.

Through combining the shaft and pile tip resistances, the ultimate bearing capacity for a given pile installation scenario can be calculated. Also, taking a typical factor of safety (FS=3) into consideration, the factored ultimate load applied on top of the pile can be generated by the following formula (Das, 2007):

$$Q_{factored} = Q_u/FS \tag{16}$$

2.6 Numerical modeling of retaining walls

Retaining walls are one of the most widely used structures that can hold soil back and prevent its failure. No matter whether it is being used for supporting the backfill, existing slopes, or as excavation support, its stability is crucial for ensuring the safety and protection of property or construction activities.

Numerical analysis, such as the finite element method (FEM), is a useful tool for analyzing the earth pressure problems of soil-structure interaction. In the past decades, studies have been done concerning it; such as for analysis of the relationship between earth pressures and wall movements (Morgenstern and Eisenstein, 1970, Lambe, 1970).

To properly analyze the interactions between soil and wall, related assumptions for accurately obtaining the relationship shall be made. In Clough and Duncan (1971), they refer to that for most of the FEM, due to the difficulties of simulating the real situation occurring at the interface of soil and structure, the soil is modeled as perfectly rough particles that generate no slips on contacting surface. Furthermore, the authors also assumed that the interface is perfectly smooth, and there is no possibility of the shear stresses retarding the movement between wall and soil.

After the above assumptions, so as to represent the interface between wall and backfill, Clough and Duncan (1971) applied one-dimensional finite element analysis. It was mainly done based on the direct shear test of composite specimens and then incrementally changing properties of the interface and backfill, the relatively non-linear stress-displacement relationships were developed.

Initially, through a direct shear test, they found that the peak angle of wall friction (δ_{wall}) and soil specimen (sand) friction angle (φ) follow the relationship of δ_{wall}/φ= 0.8, and the stress-displacement curves can be expressed through an empirical equation (Clough and Duncan, 1971):

$$\tau = \frac{\Delta_s}{a + b\Delta_s} \tag{17}$$

where τ = interface shear stress, Δ_s = interface shear displacement, a and b are empirical coefficients which were determined experimentally.

After this, the authors managed to convert the hyperbolae curves into straight lines and by transposing equation (5), the following relationship was developed (Clough and Duncan, 1971):

$$\frac{\Delta_s}{\tau} = a + b\Delta_s \tag{18}$$

The purpose of this was to eliminate subjectivities and to be more standardized in the case of the stress-deformation relationship is not accurately hyperbolical.

Furthermore, they found that at where the stress-displacement curve reaches relatively large values of displacement, the relationship between asymptotic shear stress (τ_{ult}) and shear strength of interface (τ_f) can be expressed as:

$$\tau_f = \tau_{ult} R_f \tag{19}$$

Where the values of R_f were found to be in range from 0.82 to 0.95 (Clough and Duncan (1971)).

Being aware of that the initial shear stiffness, K_{si}, and the shear strength of the interface are dependent on the value of normal stress on the interface, the relationship between K_{si} and normal stress was expressed by:

$$K_{si} = K_I \gamma_w (\frac{\sigma_n}{p_a})^n \tag{20}$$

Also, the shear strength of the interface is proportional to normal stress, and it was expressed based on the angle of wall friction, δ_{wall} , therefore:

$$\tau_f = \sigma_n tan\delta_{wall} \tag{21}$$

Eventually, the relationship between the variation of shear stress and displacement can be developed as the following equation:

$$\tau = \frac{\Delta_s}{\frac{1}{K_I \gamma_w (\frac{\sigma_n}{p_a})^n} + \frac{R_f \Delta_s}{\sigma_n tan\delta_{wall}}} \tag{22}$$

where K_I is a dimensionless stiffness number; n = stiffness exponent; γ_w = unit weight of water in the same units of K_{si}; p_a = atmospheric pressure in the same units of normal stress σ_n; δ_{wall} = wall friction angle (Clough and Duncan, 1971).

From this equation, it is possible to calculate the non-linear, shear-dependent behavior of the interface and the shear stress under different displacements. It is mainly relying on four parameters: K_I, n, R_f,and δ_{wall} and their values can be determined through interface shear tests.

Based on what has been conducted of the interface behavior, proceeding analysis regarding the incremental change of properties of soil and interface has been analyzed. The author found that the maximum passive and the minimum active pressure generated from these changes were in good correspondence with the typical earth pressure theory.

For the rotating retaining wall supports, the medium dense sand backfill under the non-linear variation of pressure with depth, the active pressure condition will primarily be occurring at the top of wall, and when it is encountered through the entire height of the wall, the outward displacement away from backfill at the top of the wall, $\Delta,$ can be recorded to be $0.0023H_{total}$, where H_{total} is the total height of backfill.

In 1934, Terzaghi performed a series of tests on retaining walls, defining that the active condition on a rough wall encountered when $\frac{\Delta}{H_{total}} = 0.0014$ for dense sand and $\frac{\Delta}{H_{total}} = 0.0084$ for loose sand. The values obtained by Clough and Duncan for medium sand agreed with this theory.

In the same time, Clough and Duncan (1971) found that the dimension of active zone in the backfill would not be affected by the roughness of wall, and movements in backfill occur along a line that is inclined approximately at an angle of $45° + \emptyset/2$ from the horizontal base.

As for the translation of a retaining wall, results are nearly identical in comparison with the rotation of retaining walls: active condition for wall translation away from backfill was reached at where $\frac{\Delta}{H_{total}} = 0.0026$, in addition, the results of this amount of movement are identical for rough walls and smooth walls. Difference is if the walls are rough [δ_{wall}= (2/3) φ or δ_{wall}= φ], the minimum active pressure forces are almost 10% smaller than the smooth walls (δ_{wall} = 0) for displacement to occur. Meanwhile, the amount of inward movement where the maximum passive pressure condition encountered was detected to be almost one order of magnitude higher than of the outward movement.

Since the retaining wall deformation was normally triggered by the soil re-arrangement, based on the one-dimensional analysis, the two-dimensional FEM analysis would be necessary for further understanding the retaining wall behaviors. In GuhaRay (2015), the probabilistic analyses by using FEM have been used to analyze the cohesion-less and cohesive backfill soil retaining systems. As shown in Figure 2.6.1, and 2.6.2, the sheet pile wall retaining systems were modelled by PLAXIS 2D – V8 (GuhaRay, 2015), which used full fixity at the bottom and horizontal fixity at the sides. To conduct the FEM analysis, the initial condition of earth pressure has been simulated by geostatic stress condition, and the wall was modeled for plane strain condition so that any displacement or strain in z-direction would be zero. Moreover, GuhaRay (2015) modeled the soils as simple elastic-perfectly plastic Mohr-Coulomb model, and an elastoplastic model has been used to analyze the behavior of the interface in both cases. Notably, during the meshing stage, a cluster refinement around 1 m of the wall was used in each case.

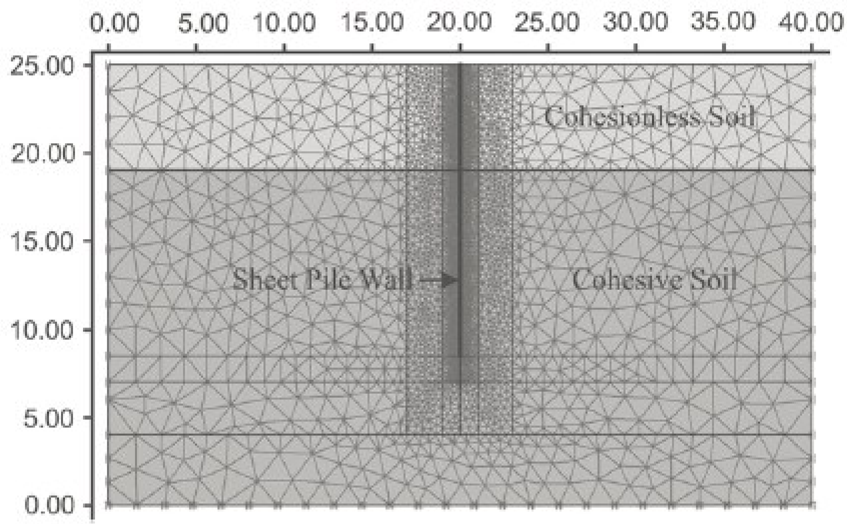

Figure 2.6.1 Meshing details of cohesion-less backfill retaining system (GuhaRay, 2015)

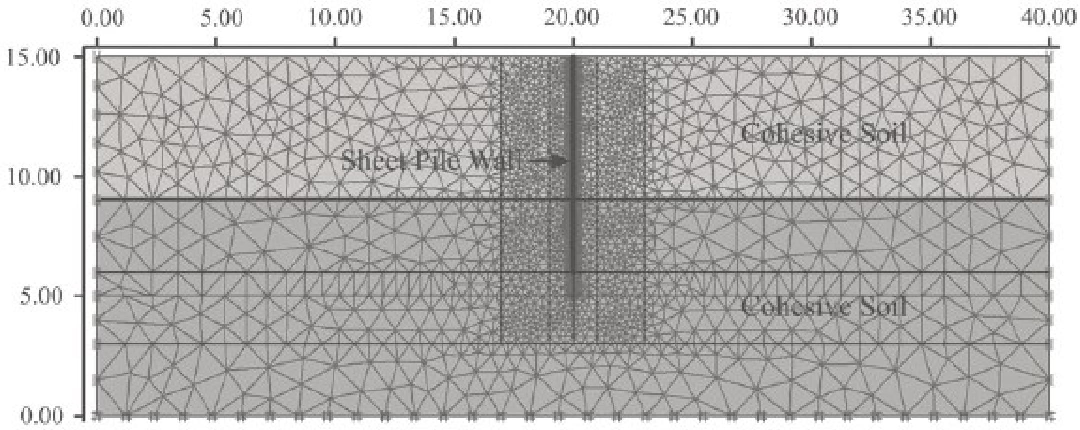

Figure 2.6.2 Meshing details of cohesive backfill retaining system (GuhaRay, 2015)

From the deformed results shown in Figure 2.6.3, and 2.6.4, GuhaRay stated that the factor of safety (FS) can be calculated through dividing the available shear strength by the shear strength at failure, which is called the *phi/c* reduction technique in *PLAXIS* (GuhaRay, 2015).

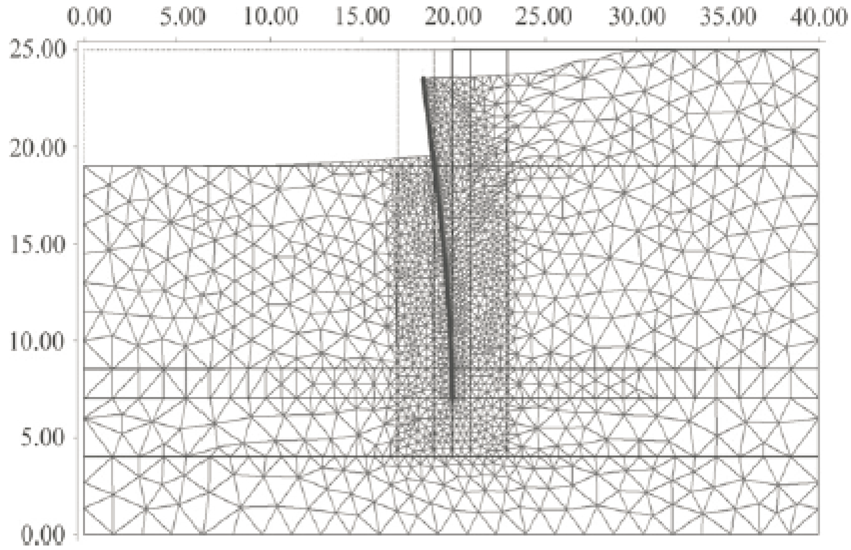

Figure 2.6.3 Deformed mesh of cohesion-less backfill retaining system (GuhaRay, 2015)

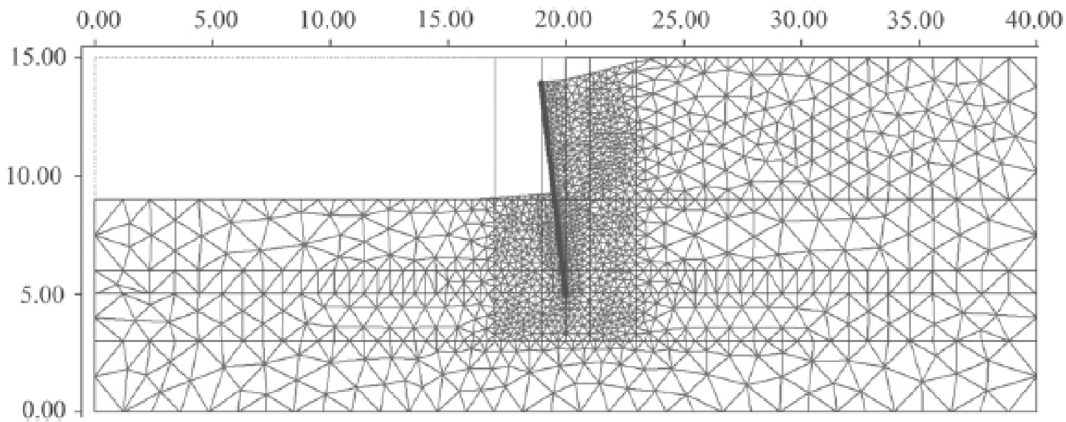

Figure 2.6.4 Deformed mesh of cohesive backfill retaining system (GuhaRay, 2015)

Tang (2011) stated that, the retaining wall deformation induced by excavation activities could be determined through FEM, however, the degree of uncertainties regarding the model or parameter cannot be reflected by the results. To solve it, the random finite element method (RFEM), which combines the random soil properties and Monte Carlo sampling method, has been used to estimate the wall deformation by taking the parameter uncertainty into consideration. Combining the non-linear FEM with random material properties generation techniques, the deficiency of conventional FEM regarding the geotechnical uncertainties can be solved. As been illustrated in Figure 2.6.5, to achieve the objective of analysis, the approach shall be consisted of two parts, which are the representative random variables in regarding the geotechnical uncertainties, and an adequate amount of FEM analyses to generate the relative frequency of maximum retaining wall deformation.

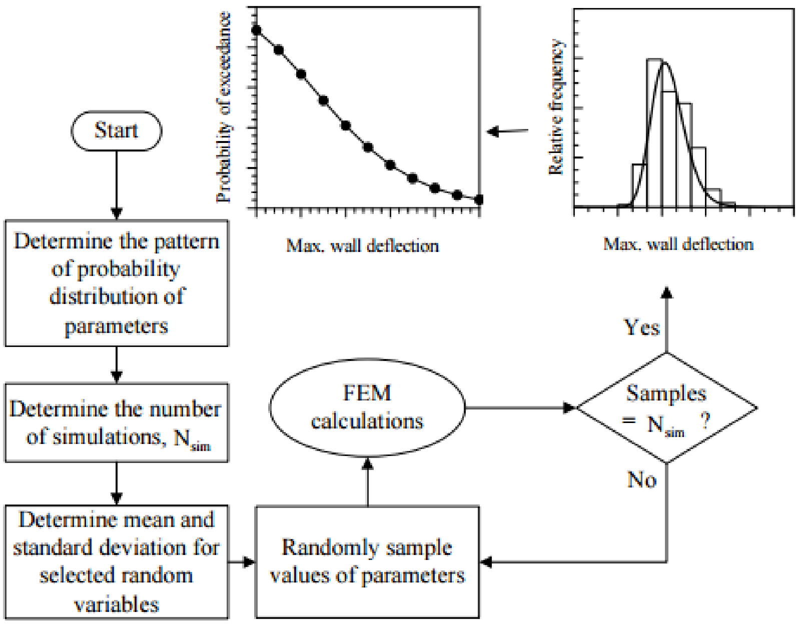

Figure 2.6.5 Random finite element method analysis procedure (Tang, 2011)

Herein, through combining the incremental one and, two-dimensional analyses, and the Monte Carlo sampling method, it is possible to analyze the interaction problem of soil-wall without neglecting the uncertainties of random field material properties. The minimum active and maximum passive pressure conditions have been conducted regarding wall displacement.

2.7 Artificial Neural Networks (ANNs)

2.7.1 General concepts

Artificial neural networks (ANNs) are a very useful tool that are being used in many areas of science and engineering and they have seen continual improvement for many years. Generally ANNs are methods that are fed inputs and they generate outputs through calculations; within all relevant elements are regarded as nodes and connected by reasonable connections between these nodes. By doing so, the basic networks can be easily developed. Nevertheless, the complexity of developing an advanced network such as a node, which can contain another network requires deeper and more detailed calculations among those nodes.

In ANNs, like our brain and inspired by the natural neurons, the nodes that obtain all the inputs and process them to generate the outputs are defined as "*artificial neurons*". Before the inputs are received and processed by activation functions, each of them will be multiplied by *weights (strength of the respective signals)*. The greater the *weight* of an individual neuron, the more influential or stronger will the inputs be. Also, weights can be negative which indicates the signal is inhibited by the negative weight. After which, inputs will be computed by a mathematical function that controls the *activation* of the neuron, and then the output can be generated, as shown in Figure 2.7.1.1. The types of ANNs and their functions can be different between each other through using different accepted values, algorithms, topology, etc. In this thesis, the backpropagation algorithm has been used, and which is one of the most common method used in layered feed-forward ANNs (Gershenson, 2003).

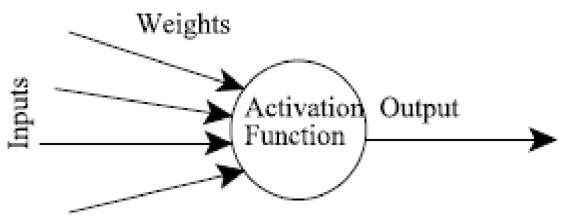

Figure 2.7.1.1 An artificial neuron network (Gershenson, 2003)

2.7.2 The backpropagation algorithm

For precise prediction, through the backpropagation algorithm, a three-layer, feed-forward ANN topology was developed in this thesis. In this system, as shown in Figure 2.7.2.1, the artificial neurons are organized into two or more layers and the signals will be send forward, and later the errors between the actual results and predicted outputs can propagate backwards. After the neurons in the *input layer* receive the input data, the output of a given database will be generated by the neurons in the *output layer*. Notably, the *hidden layer* enables the networks to compute complex associations among patterns, and the number of these layers could be one or more. The goal of this type of ANN model can be achieved by providing the algorithm with inputs and desired target results, through training and "self-learning", the errors can be calculated and minimized.

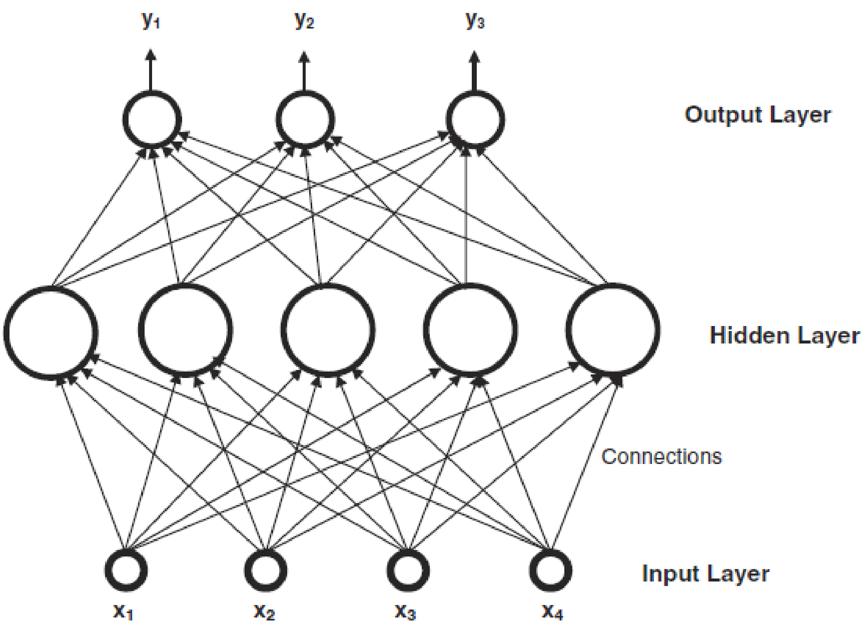

Figure 2.7.2.1 Typical artificial neuron network structure (Goh and Kulhawy, 2005)

The basic mathematical concepts regarding the backpropagation algorithm are common in the literature, for instance Gershenson (2003) is a good example.

To trigger the neurons and ANNs, and to perform the backpropagation algorithm, a weighted sum activation function (A_j) was used:

$$A_j(\bar{x}, \bar{w}) = \sum_{i=0}^{n} x_i w_{ji} \tag{23}$$

where x_i and w_{ji} represents the inputs and their weights respectively. From which it is possible to see that the activation function is dependent on the inputs and the weights only. To avoid the limitations from keeping the identity of output function be equal to the activation, yet allow the output to be dependent on inputs and their weights also, a sigmoidal function (O_j) representing the output has been widely used:

$$O_j(\bar{x}, \bar{w}) = \frac{1}{1 + e^{A_j(\bar{x}, \bar{w})}} \tag{24}$$

The outputs generated from the sigmoidal function were found to be very close to *zero* for large negative numbers, *0.5* if the numbers were zero, and very close to *zero* for large positive numbers. This would provide a smooth transition between high and low outputs of a neuron. After which, to reach the goal of the ANNs training, the desired output obtained from a given input shall be very close to the actual output. Which means that the difference between these two values should be minimized by adjusting the weights that control the magnitude of an error. The error function of each neuron can be defined as:

$$E_j(\bar{x}, \bar{w}, d) = (O_j(\bar{x}, \bar{w}) - d_j)^2 \tag{25}$$

The square of the difference between the desired and actual output can maintain the value of error to be positive. Based on this, for all the output layer neurons, the error of the system can be written as the following equation:

$$E(\bar{x}, \bar{w}, \bar{d}) = \sum_j (O_j(\bar{x}, \bar{w}) - d_j)^2 \tag{26}$$

Because the error is dependent on the inputs, outputs, and weights, through using the gradient descendent method as the equation shown below, it is possible to adjust each weight (Δw_{ji}) by multiplying the negative of a constant eta (η) with the derivative of E regarding to w_{ji}, which represents the dependence of the previous weight on the error of the system (Gershenson, 2003).

$$\Delta w_{ji} = -\eta \frac{\partial E}{\partial w_{ji}} \tag{27}$$

Since the Δw_{ji} is dependent on η and $\frac{\partial E}{\partial w_{ji}}$, to define the derivative of E in terms of w_{ji} would be the key to understanding the backpropagation algorithm. In short, the error is based on the output, which depends on the activation, or the weights. Therefore, through combining equations (25), (26), and (27), it is possible to write that:

$$\Delta w_{ji} = -\eta \frac{\partial E}{\partial O_j} \frac{\partial O_j}{\partial w_{ji}} = -\eta \frac{\partial E}{\partial O_j} \frac{\partial O_j}{\partial A_j} \frac{\partial A_j}{\partial w_{ji}} = -2\eta(O_j - d_j)O_j(1 - O_j)x_i \tag{28}$$

In this thesis, the ANNs were built by three layers: input layer, output layer, and hidden layer(s). Any additional layer would be unnecessary by taking the training time and practical purposes into consideration.

Chapter III. Key Parameters Representing Interaction Between Pile Loading and Retaining Wall Response

For the process of model generation of pile loading and retaining wall response, all related parameters affect the outcome of a model regarding the retaining wall behavior. Among these parameters, due to the difficulties of quantifying them all, some are critical and need to be identified before model building and simulation.

3.1 Soil properties

3.1.1 Soil properties of back-fill cohesionless (sandy) soils

Generally, piles or group piles are used as foundations or as supporting structures that carry and transfer loads to the surrounding soils. Engineers prefer to install piles into strong soil layers that provide higher tip and shaft resistance or bearing capacity. Most preferably, especially for the deep foundations, piles resting on a layer of rock is the best situation. In addition, in the absence of a rock layer, a layer of sand with gravel would also be suitable for supporting the piles. In this thesis, the retaining wall was used for preventing the failure of backfill soil particles, and which was primarily consisted by sands varying from dense to medium, and probably mixed with gravel (Structural Engineering Forum of India, 2017).

Different types of soils are representative of the variable conditions of back-fill soils (Swiss Standard, 1999; Koloski et al., 1989; Carter and Bentley, 1991; Obrzud and Truty, 2012), thus all relevant values of soil properties were within the corresponding range shown in Table 3.1.1. Therefore, in our RS2 FEM simulation, the soil properties listed as shown in Table 3.1.1 would be applied separately for obtaining different values of displacements.

Description	Soil friction angle (°)		Cohesion (kPa)	Unit weight (γdry) (kN/m^3)		Young's modulus (MPa)			Poisson's ratio (μ)
	min	max		min	max	loose	med.	dense	
Well graded gravel, sandy gravel, with little or no fines	33	40	0	20	22	30-80	80-160	160-320	-
Silty gravels, silty sandy gravels	30	40		20.5	22.5	-	-	-	-
Clayey gravels, clayey sandy gravels	28	35		18	21	-	-	-	-
Well graded sands, gravelly sands, with little or no fines	33	43		18.5	22.5	-	-	-	-
Sand	37	38		-	-	10-30	30-50	50-80	-
Loose sand	29	30		-	-	-	-	-	-
Medium sand	30	36		-	-	-	-	-	-
Dense sand	36	41		-	-	-	-	-	0.2-0.4
Silty sands	32	35		18	22.5	7-12	12-20	20-30	0.3-0.35
Clayey sands	30	40		19	20	-	-	-	0.2-0.3
Range	28-43		0	18-22.5		7 - 320			0.2-0.4

Table 3.1.1 Properties of different sandy soils (Swiss Standard, 1999; Koloski et al., 1989; Carter and Bentley, 1991; Obrzud and Truty, 2012)

3.1.2 Soil properties of cohesive foundation (clayey) soils

Since the water table is not considered between the boundary of backfill and foundation soils, the basic parameter values of clayey soils are shown in Table 3.1.2.

Clayey soil parameters				
Effective Cohesion, c' (kPa)	Friction angle, Φ' (°)	Unit Weight, γ (kN/m3)	Young's modulus, E (MPa)	Poisson's ratio (μ)
10	35	17.64	50	0.3
N/A	30	N/A	N/A	N/A
4.83	37.1	N/A	N/A	0.35
50	N/A	N/A	20	N/A
0	35	15.7	N/A	0.3
0 and 14.5	33	19.6 and 20	N/A	0.4 and 0.45
1 and 8.45	34	16 and 18.8	12.5	0.32
0	30	20	N/A	N/A
20	22	19.1 and 19.5	32 to 48.8	0.2
N/A	N/A	22 to 30	N/A	N/A
0.5	30	25.4	5.83	0.23
N/A	N/A	N/A	N/A	N/A
5	22	19	5	N/A
25	0	19.5	0.3	N/A
60	0	20	50	N/A
N/A	25 to 28	N/A	20	N/A
0-60	**0-37.1**	**15.7-25.4**	**0.3-50**	**0.2-0.45**

Table 3.1.2 Summary of clayey soil properties (Chung and Ng, 2005; Watson and Carder, 1991; Henke, 2010; Seed and Duncan, 1986; Athanasopoulos, 2011; Weaver and Youn, 2008; Poulos, 1994; Clough and Duncan, 1971; Hossain et al., 2012; Gunn and Clayton, 1992; Massarsch and Wersäll, 2013; Wang et al, 2012; Suzuki et al., 2010; Ford et al., 1991)

3.2 Geometric parameters

Before modeling, in addition to all the parameters mentioned above, geometric parameters that control the stability of entire system are important as well. In Table 3.2.1, the overall geometric properties are summarized. From where it is possible to select a credible modeling value range, for instance, the pile used in Chung and Ng (2005) was 2.6m diameter bored pile, which was not considered in this thesis due to its particular large diameter. Also, during modeling, the distance between the boundary and installed pile is required to be large enough to avoid neglecting any possible effects in the soil particles, and no potential influence of the boundary conditions occur during simulation (Grabe et al., 2014). Based on this, a choice of minimum 10 times of installed pile diameter was used.

Geometric parameters				
Retaining wall free end height (H_1) (m)	Retaining wall embedded depth (H_2) (m)	Pile diameter (D_2) (cm)	Installation depth (L)(m)	Installation distance from pile to retaining wall (D_1) (m)
7	8	2600	14	3.9
N/A	N/A	16, 30	5	0.5, 1, 2, 4, and 5
1.6 to 4.6	N/A	30	N/A	0.3 to 2.4
N/A	N/A	50	15	N/A
3 and 6	N/A	N/A	N/A	N/A
2m	N/A	N/A	N/A	N/A
6.486	0.914	N/A	N/A	N/A
11.71	8.29	N/A	N/A	N/A
8.4	8.6	N/A	N/A	N/A
N/A	N/A	30	26	N/A
N/A	N/A	24, 20,16	3.2	N/A
N/A	N/A	60	24	N/A
4	10	N/A	N/A	N/A
10.6	14.4	N/A	N/A	N/A
4	N/A	N/A	4.6	0.8 to 1.4
1.6-11.7	**0.914-14.4**	**16-60**	**3.2-26**	**0.3-5**

Table 3.2.1 Overall geometric parameters from literatures (Chung and Ng, 2005; Watson and Carder, 1991; Henke, 2010; Seed and Duncan, 1986; Athanasopoulos, 2011; Weaver and Youn, 2008; Poulos, 1994; Clough and Duncan, 1971; Hossain et al., 2012; Gunn and Clayton, 1992; Massarsch and Wersäll, 2013; Wang et al, 2012; Suzuki et al., 2010; Ford et al., 1991; Berg and Vulova, 2007)

3.2.1 Installation distance between retaining wall and pile

As has been previously addressed (Chapter 2.4), through combining the installed piles with an adjacent retaining wall in one system, the distance (D_1) of installation in between is one of the key parameters. Generally, the closer the installation, the more affected the wall would be, and larger deformations or displacements would be generated. Specifically, after experimental and numerical simulation, Weaver and Youn (2008) adopted that beyond a distance greater than 8 pile diameters, the laterally loaded pile would have negligible effects on the nearby retaining wall, and the excessive stresses acting on the retaining wall are barely significant. Thus, the modeling process in this thesis, the range of the pile-retaining wall distances were kept within 0.3m to 5m. This is also due to the selected pile sizes which varied from 0.16m to 0.6m (as shown in Table 3.2.1).

3.2.2 Pile diameters and installation depth

In Henke (2010), the piles used in the analysis were closed-ended, open-ended (pipe piles) and steel beams. In this thesis, in order to simulate the worst conditions where the greatest soil stresses changes would occur during installation, the author modeled the piles as closed-ended piles. Also, from other sources (Weaver and Youn 2008, Athanasopoulos et al. 2011, Massarsch and Wersäll, 2013), the range of the pile diameters was also included in Table 3.2.1.

For installed piles length, as mentioned in D'Aguiar (2007), the depth of the pile embedded in the ground was modeled as 20 meters, and the corresponding effects on surrounding soils were studied as illustrated in previous chapters (Chapter 2.1). Nevertheless, for model in this thesis, installed depth was increased to 26 meters based on other references (Chung and Ng, 2005; Poulos 1994; Wang et al, 2008; Massarsch and Wersäll, 2013). Within this range (see Table 2.3.1), the pile tip location controlled the final bearing capacity, and various situation derived from this range were considered thorough the numerical analysis.

3.2.3 Retaining wall properties

Retaining walls are one of the mainly used structure types for supporting and preventing possible failures against overturning and sliding of the retained soil mass. Thus, the height of the wall should be tall enough to carry different soil and external loading conditions. Different types of retaining walls may have their own advantages and limitations. For example, sheet pile walls were widely used as continuous waterfront structures, excavation, and temporary supports. GuhaRay (2015) stated that, for cantilever walls, the lateral support mainly contributed by the embedded portion and excessive stress might be induced owing to the large penetration depth. Therefore, a limit of free height of 5-6m shall be applied for the design of cantilever wall with steel sheet pilling. Instead, for other means of cantilever retaining wall, diaphragm concrete walls or bored pile walls were also commonly used with comparatively fewer limitations on their retained height above the ground. Often, these walls were used in areas with less site access or availability (Watson and Carder, 1991). In this thesis, for general analysis, retaining walls would not be limited to a certain type, while anchored or strutted systems were not considered in modeling for taking consideration of the worst scenarios.

3.2.3.1 Retaining wall height

In this thesis, as shown in Table 3.2.1, the range of values for the retaining wall free height and embedded or retained depth has been summarized. However, the value of embedded depth applied in the FEM modeling was not following the specific range, which instead, was used for correction and reference. This is because, based on a selected free height of the wall, the embedded depth can be designed according to the steps provided by Das (1999).

For cantilever retaining walls in the absence of water table, as shown in Figure 3.2.3.1.1, the relationships among all the linked parameters can be written as (Das, 1999):

$$p_2 = \gamma L K_a \tag{29}$$

$$P_1 = \frac{1}{2} L p_2 = \frac{1}{2} \gamma L^2 K_a \tag{30}$$

$$\bar{z}_1 = \frac{L}{3} \tag{31}$$

$$L_4 = \frac{D(4c - \gamma L) - \frac{1}{2}\gamma L^2 K_a}{4c} \tag{32}$$

where p_2 is the active pressure at depth L; γ is the unit weight of soil above the water table (same as γ_1 defined in this thesis); c is the cohesion of clayey soil (same as c_2' defined in this thesis); K_a is the Rankine active pressure coefficient = $tan^2(45 - \frac{\phi}{2})$; L is the free height of retaining wall (same as H_1 defined in this thesis); $\bar{z}_1$ is the center of pressure for the sandy soil and; P_1 is the area of the pressure diagram in sandy soil (Das, 1999).

From above, it is possible to calculate the theoretical depth of penetration, D (same as H2 defined in this thesis), from the following equation (Das, 1999):

$$D^2(4c - \gamma L) - 2DP_1 - \frac{P_1(P_1 + 12c\bar{z}_1)}{\gamma L + 2c} = 0 \tag{33}$$

therefore:

$$D = \frac{2P_1 \mp \sqrt{(-2P_1)^2 + 4(4c - \gamma L)(P_1\left(P_1 + 12c\frac{L}{3}\right)/(\gamma L + 2c)}}{2(4c - \gamma L)} \tag{34}$$

From equation (34), with a given value of retaining wall free height and relevant parameters, the embedded depth can be calculated. Notably, to keep the integrity of retaining wall free heights and embedded depths, in this thesis, all the calculated embedded depths used for FEM analysis were rounded to their nearest 0.25m.

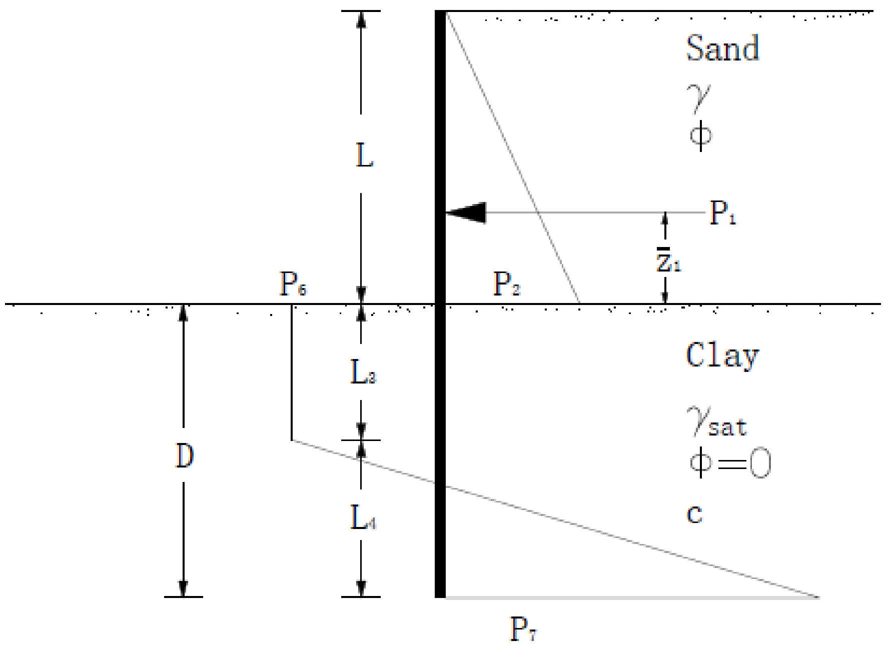

Figure 3.2.3.1.1 Cantilever wall penetrating clay (Das, 1999)

3.2.3.2 Retaining wall thickness

Retaining wall thickness is also another key factor that controls the stability of the wall. As seen from numerical stress analysis, the thicker the wall was, the less the deflection was generated under a certain load applied on top of the pile of which a further discussion will be presented in the chapter of FEM analysis. For modeling, the obtained range of values for the wall thicknesses were from 0.5 to 1.5m (Chung and Ng, 2005; Watson and Carder, 1991; and Kung et al., 2007).

3.2.3.3 Young's modulus of elasticity

In Kung et al. (2007), the authors summarized several case histories illustrating the properties of retaining walls, and like this thesis, they used them for ANN modeling. From which, the range of calculated Young's moduli for retaining walls (E3) was used for FEM analysis (Table 3.2.3.3.1).

Wall length (m)	Wall thickness (m)	Wall stiffness EI (kN*m^2/m)	Young's modulus E3 (MPa)
35	0.9	1505385	708
28	0.7	708295	885
31	0.8	915627	692
32.5	0.7	708295	762
21.5	0.6	446040	1153
22	0.6	446040	1126
28.5	0.7	708295	869
25	0.8	1057280	991
26	0.8	1057280	953
30	1.1	2748515	826
30	1.1	2748515	826
35	1.2	3568320	708
Range			692-1153

Table 3.2.3.3.1 Range of Young's of moduli for retaining walls (Kung et al., 2007)

3.3 Monte Carlo sampling method

After the summary of key parameters, the representative sampling of these ranges is necessary for the use in FEM analyses. By using a Monte Carlo sampling method (GuhaRay, 2015; Tang, 2011), it is possible to select a representative, yet random data for each parameter within its credible range. As shown in Table 3.3.1, an example of sampling for a model (Model 1) is illustrated. The same sampling procedure was used for all other models analyzed in this thesis and the corresponding parameter values for the other models were obtained similarly. By using this method, the randomness of all parameters used in building RS2 models was assured. Following which, by adding the corresponding maximum retaining wall displacements into the ANNs model, the database of the input and output for ANN models can therefore be determined.

Table 3.3.1 shows the generated random values of parameters for Model 1. Notably, for all models, the dimensions of the retaining wall free-height (H_1), wall thickness (H_3), and pile length (L) were kept in the nearest 0.25m; the values for the pile diameter (D_2), and the installation distance from the wall (D_1) were chosen in the nearest 0.05m. Also, for the soil friction angle, the relevant values were kept as integer numbers to correspond to Meyerhof's bearing capacity factors. For simplicity, all the other soil properties were kept in the same fashion.

By taking ϕ_1' as an example, the sampling procedure can be expressed as:

ϕ_1' range = [min - max] (35)

randomNumber=RAND() (36)

ϕ_1'_sampled=min+(max-min)*randomNumber (37)

And by taking H_1, and D_2 as examples, the round function was used to keep the random number values to their nearest 0.25m, and 0.05m respectively:

H_1_Round=Round(H_1_sampled*4,0)/4 (38)

D_2_Round=Round(D_2_sampled*20,0)/20 (39)

Model 1			
	Min	Max	Random Number
c_1'	0	0	0
Φ_1'	28	45	39
γ_1	18	22.5	20
E_1	7	320	55
c_2'	0	60	49
Φ_2'	0	37.1	25
γ_2	15.7	25.4	20
E_2	0.3	50	22
H_1	1.6	11.71	5.00
H_2	0.914	14.4	2.5
H_3	0.5	1.5	1
E3	692	1153	1125.1
D_1	0.3	5	3.95
D_2	0.16	0.6	0.5
L	3.2	26	10.75

Table 3.3.1 Model parameter sampling example

Chapter IV. Using the Finite Element Method to Model Pile Loading and Retaining Wall Response

4.1 Building FEM models for retaining wall analysis

With both theory explained and model parameters defined, the building and analysis of retaining wall models using FEM can be accomplished. Before starting the creation of models, some fundamental settings in the FEM modeling software should be initialized, as shown in Figure 4.1.1. Note that the field stress was defined as plane strain formulation, where the out of plane stress was the principal stress and normal to the plane of analysis. Since the water table was not considered in this thesis, the solid-fluid interaction was kept in default as uncoupled. Also, because the metric (MPa) units were needed, therefore, the units were set to Metric, stress as MPa.

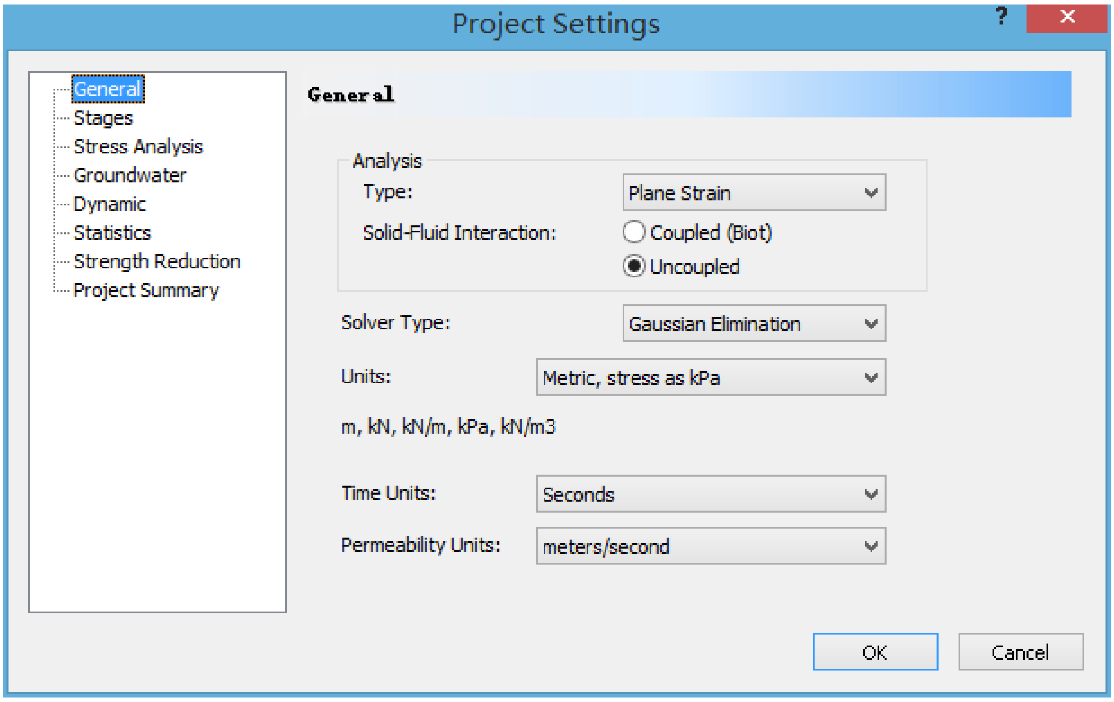

Figure 4.1.1 Fundamental project settings for all models in RS2

After which, the external boundaries should also be created. To eliminate the effect of the external boundaries on retaining wall behaviors, as mentioned in Chapter 3.2, a minimum of 10 times of the pile diameter distance was maintained between the pile and the external boundary. Also, in the process of modeling, the vertical boundaries were restrained in the horizontal (x) direction, and the bottom horizontal boundary was restrained in both x and y directions. This would allow the soil particles to deform properly under the influence of gravity and field stresses within the boundaries without excessive deformations.

Based on Monte Carlo sampling method, all relevant model parameters were used in each model accordingly. In this step, the initial element loading for sandy (backfill) soils was selected as body force only which allows the material to settle by its own weight; yet for clayey soils and the pile, it was chosen as body force with field stress (rocscience Inc., 2017). Also, for all the models, the pile properties were kept in consistent values, and for simplicity, all the Poisson's ratios were 0.2, which is a representative value for sandy soils. Typically, as seen in Figure 4.1.2, the retaining wall was initialized. The Poisson's ratio was set as 0.2 for all models, and the liner type, which represents the retaining wall, was selected as standard beam.

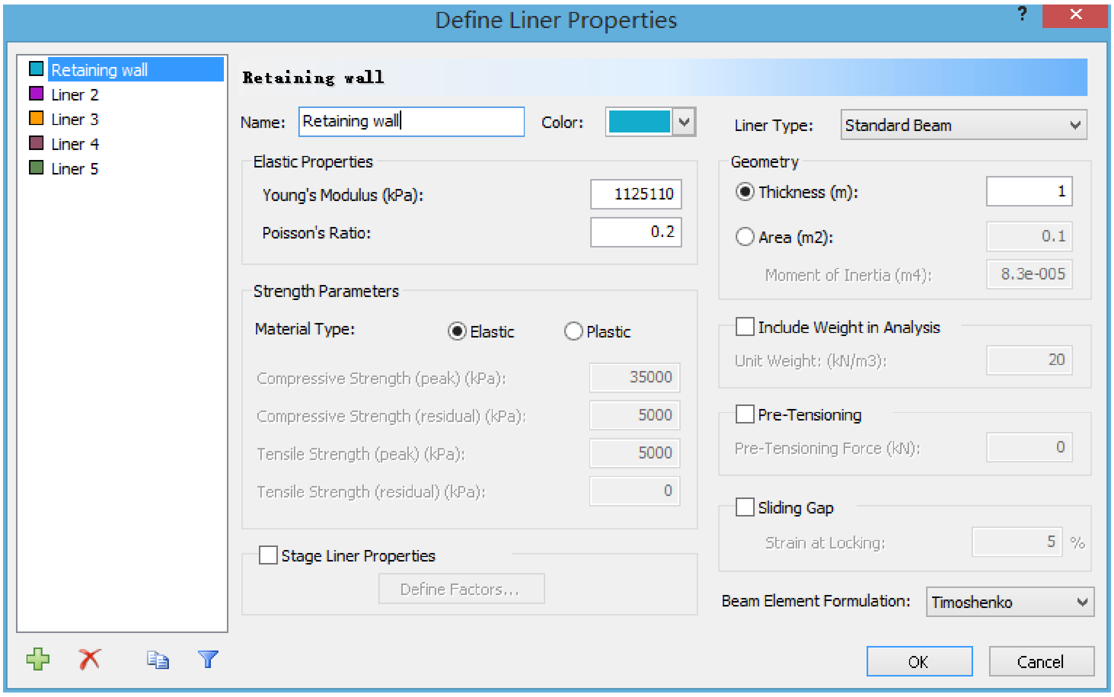

Figure 4.1.2 Material properties for retaining wall for a typical model

After making the assumptions that the pile was considered as an elastic concrete beam-column, two layers of soils surrounding the pile were kept as continuum media, and with drainage assumed behind the wall (no ground water), the phases of modeling can be illustrated in the following three steps.

The illustration for the three stages of modeling is given for a typical model (Model 1), and only stage 3 is demonstrated for the rest of 219 models (see Appendix). In stage 1, the initial soil-structure scenario was built, where a retaining wall separated the backfill (sandy soil) and clayey soils (Figure 4.1.3). In stage 2, an open-cut excavation was created on the left side (clayey soil) of retaining wall (Figure 4.1.4). In the final stage (stage 3), the pile was installed to a certain depth on the right side of retaining wall, and the designed ultimate service load was applied on top of the pile (Figure 4.1.5).

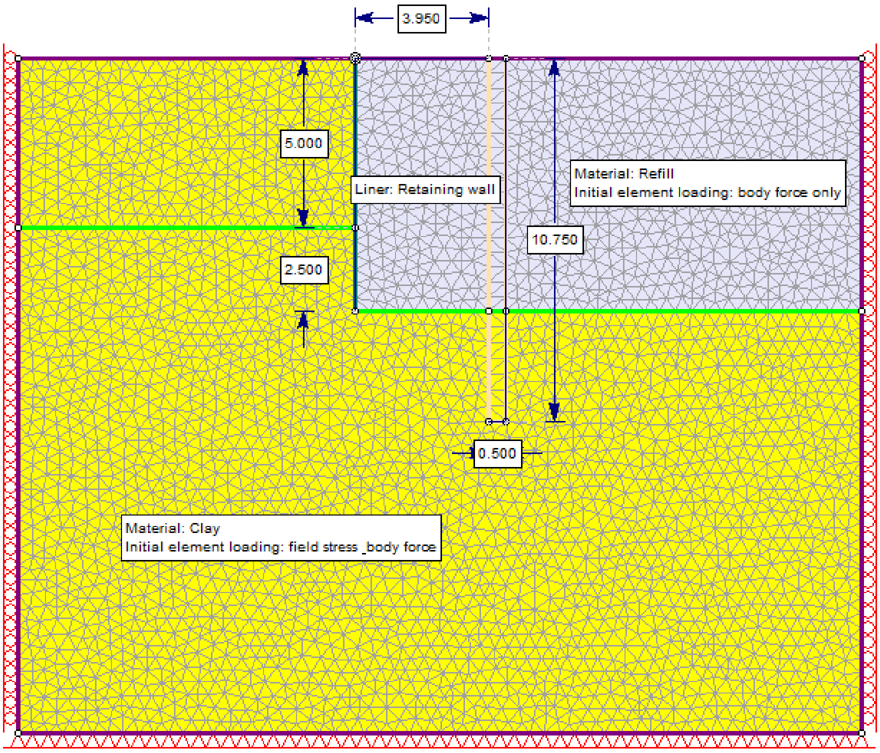

Figure 4.1.3 Stage 1: Initial state of modelling where retaining wall separates two layers of soil, without excavation in front of it

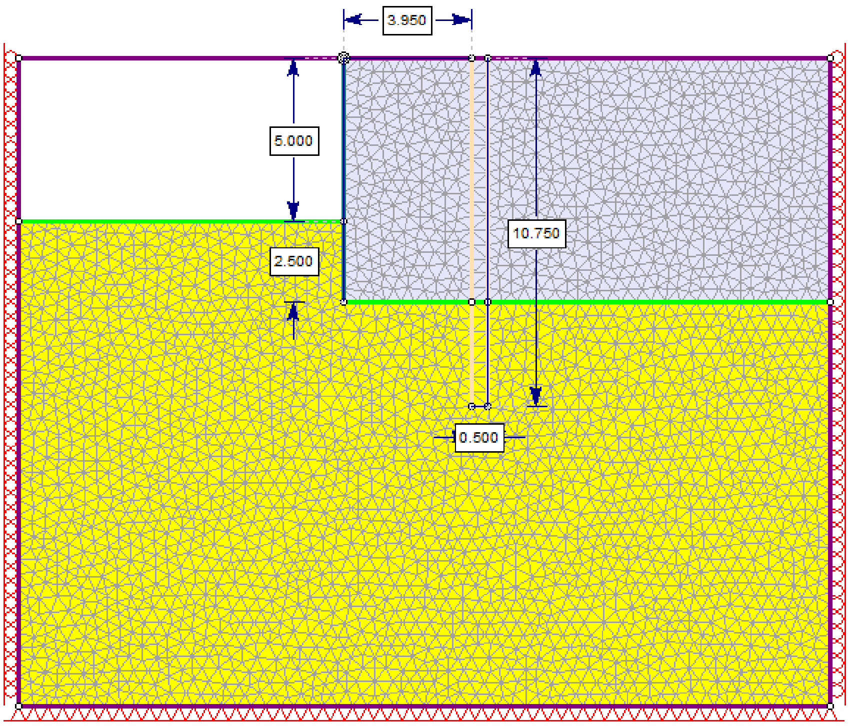

Figure 4.1.4 Stage 2: Open-cut excavation created on the left side of retaining wall

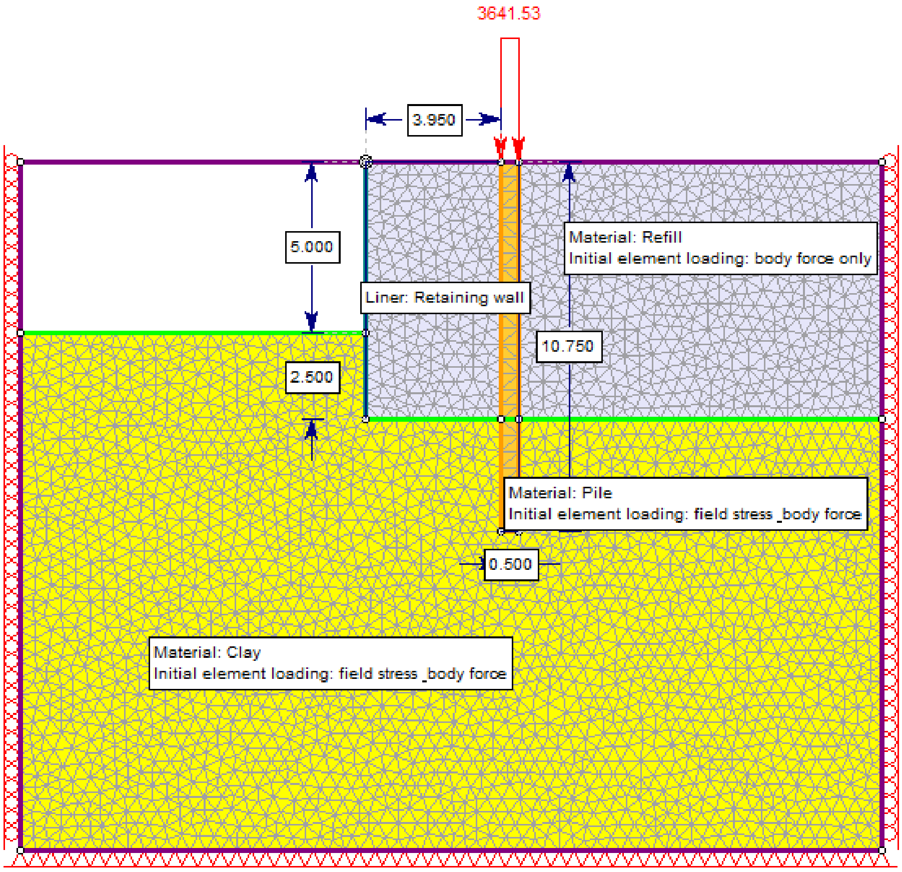

Figure 4.1.5 Stage 3: Pile installed on the right side of retaining wall and factored loading applied on the top of pile

Regarding the material constitutive models for all the models analyzed in this thesis, the yield criterion used was Mohr-Coulomb for the soils, while the pile and retaining wall were treated as linear elastic materials. In particular, the retaining interface was defined as joint-retaining wall-joint structure, and the properties of joint are shown in Figure 4.1.6. Only difference was the friction angle of the joint, which was defined as the same value as the maximum friction angle between sandy and clayey soils. Also, the same joint for each model was used along the boundary of the installed pile.

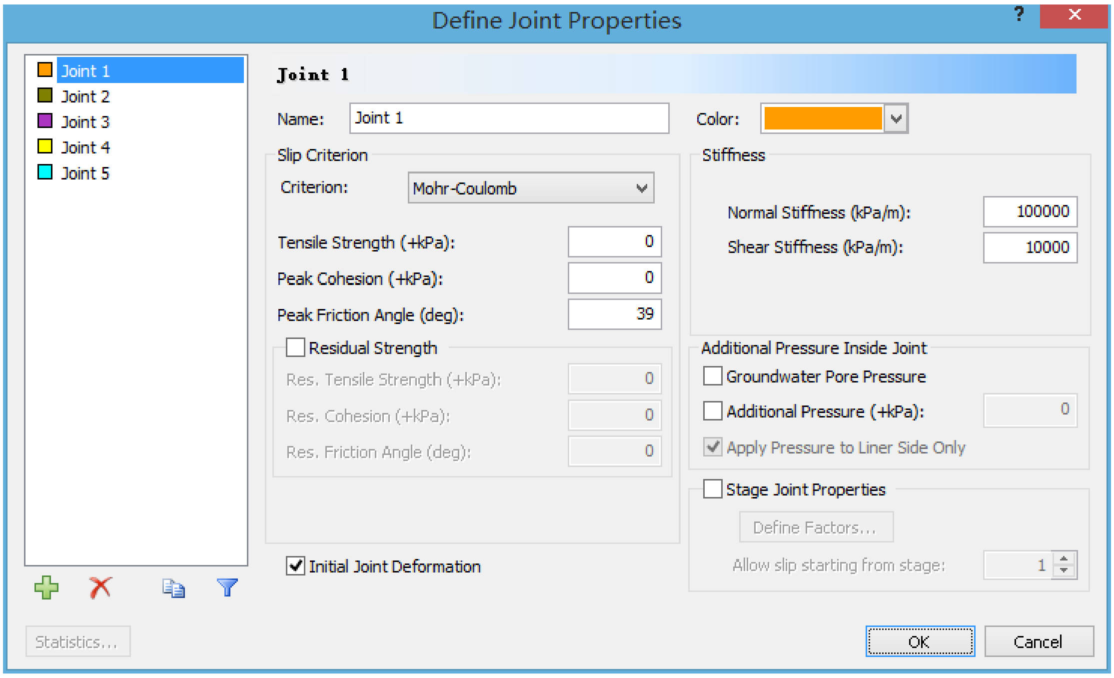

Figure 4.1.6 Joint properties for Model 1

A note on results of analysis and mesh convergence; it is well-understood from literature that the number of degrees of freedom, and implicitly the number of elements and nodes, can influence solution accuracy. The models presented in this thesis were subjected to a mesh convergence study to select the coarsest, yet most appropriate, level of mesh discretization. As shown on Figure 4.1.7, for example in the case of Model 1, four levels of discretization were considered (x0.75, x1.0, x1.5 and x2.0 number of nodes of the final accepted version). It appears that the coarsest mesh underestimates the maximum horizontal displacement of the retaining wall by about 30%, while the higher density meshes yield results that are only about 5% different than the accepted discretization. Thus, the x1.0 discretization level was accepted for the model. For the rest of the models in this thesis the same approach was taken to ensure the quality of results.

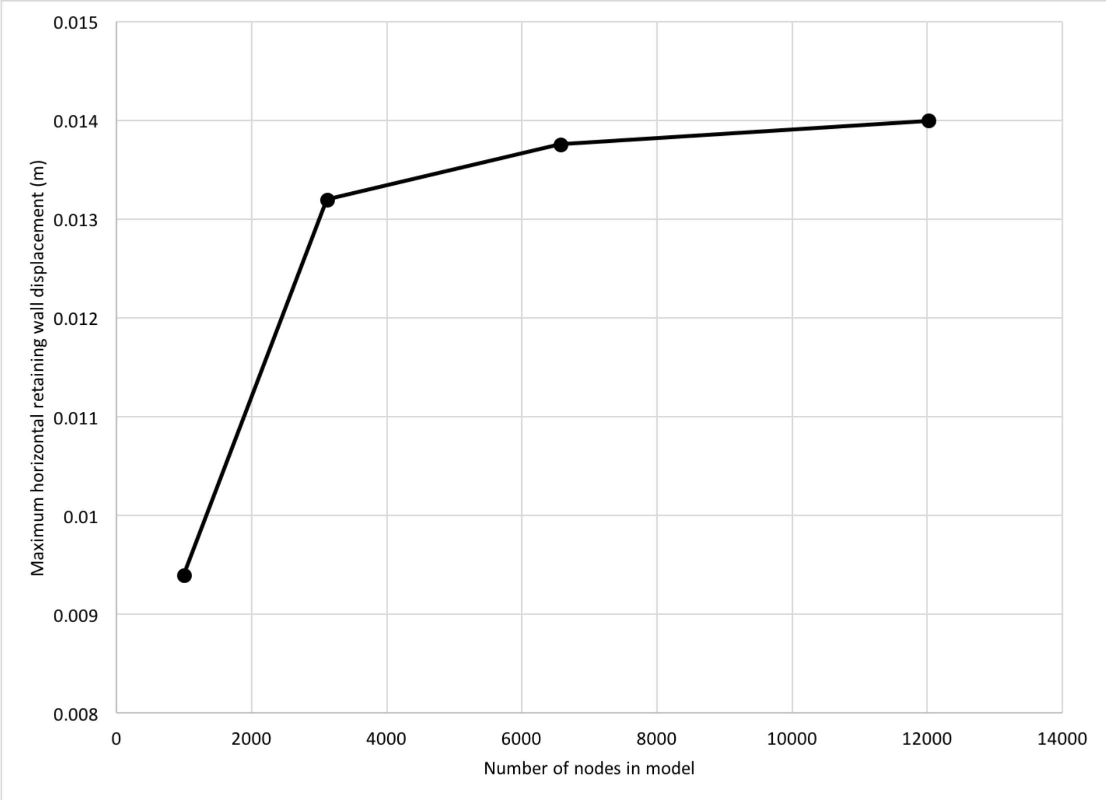

Figure 4.1.7 Mesh convergence results for Model 1

4.2 Discussion of FEM analysis results

After all the required model-building steps were properly established in RS2, the software could perform the calculations. Meanwhile, during the process of analyzing the models, some of them were not able to be converge which represented an unstable situation with excessive deformations, signifying failure. For obtaining the credible number of models and their results, the selection and filtering of results was necessarily. In total, in this thesis, 200 credible models for establishing the database of ANNs training were analyzed, and their corresponding results – maximum horizontal retaining wall displacements and their locations were given by the software. Figure 4.2.1 illustrates the deformed shape of retaining wall induced by an adjacent axially-loaded pile for a typical model (Model 1).

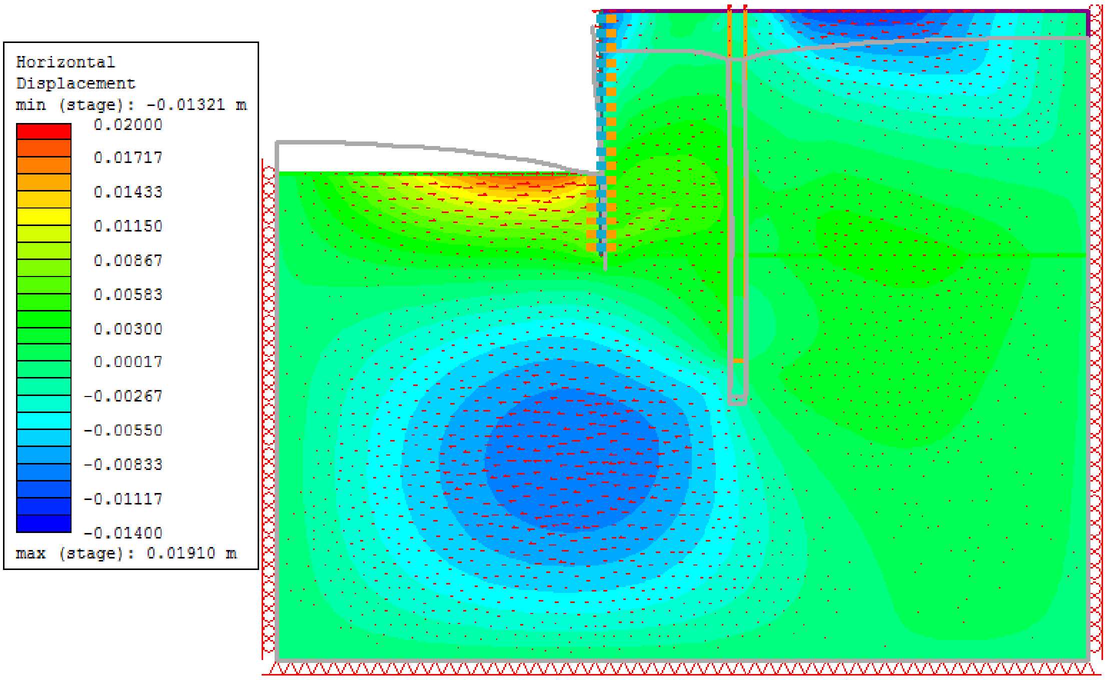

Figure 4.2.1 Deformed shape of Model 1

Based on the above, when the horizontal displacement of a retaining wall was negative, the direction of the wall deformation was away from the pile, and when the horizontal displacement of a retaining wall was positive, the direction of wall deformation was towards the pile.

Due to the limitation of the modeling software (RS2 from rocscience Inc.), the horizontal displacements of the liner (retaining wall) cannot be easily obtained. For most cases, the backfill soils along the wall deformed along with the wall; therefore, the horizontal displacements of backfill soils have been provided at the end of each summary for the illustration of retaining wall deformations. For some models, Model 50 for example, the actual retaining wall deformation was not coordinated with the soil deformation, therefore, a detailed view of cross-section of retaining wall and soil has provided a more precise result of wall displacement.

Figure 4.2.2 illustrates the frequency distribution of magnitude of maximum horizontal displacements for 200 models, which was divided into 10 bins by a width of 0.024531m. From which, it is possible to determine that 87 percent of displacements occurred in the range of -0.016393m to 0.008138m. It also revealed that for most cases, 149 out of 200 models, their values of maximum displacements were negative (e.g. away from the pile, into the excavated opening).

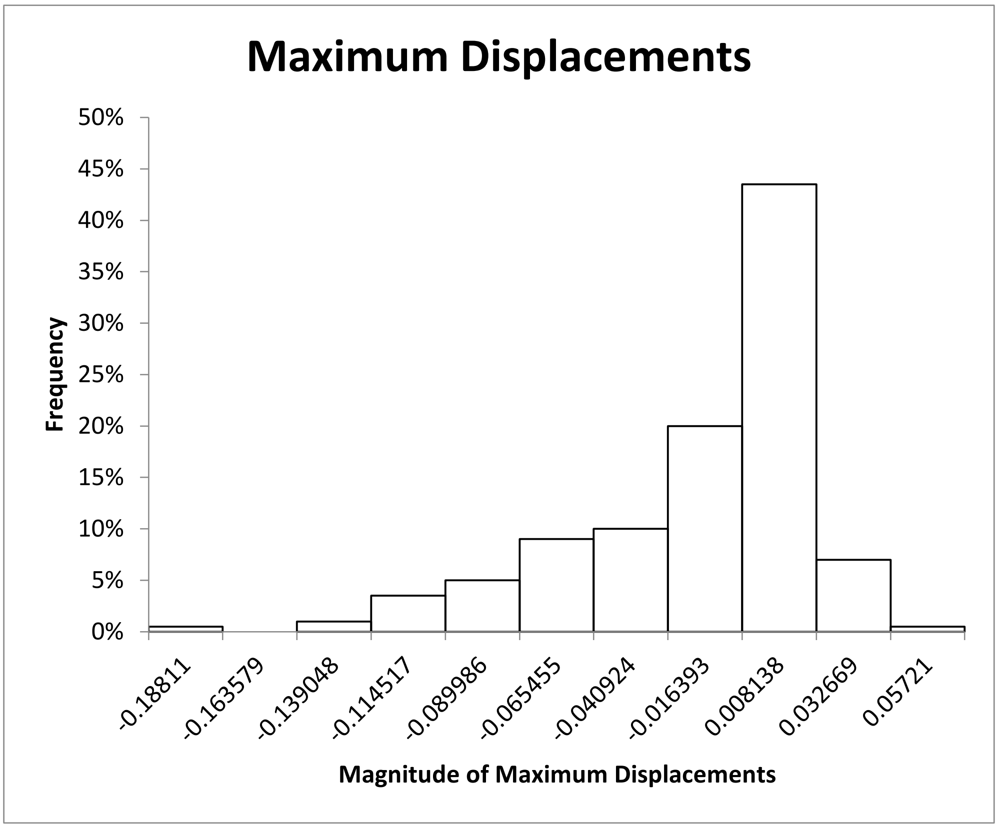

Figure 4.2.2 Distribution of maximum horizontal displacements for 200 models (in meter)

Figure 4.2.3 illustrates the frequency distribution of locations of maximum displacements for 200 models measured from the free tip of cantilever. Expectedly, as a cantilever structural system, its deformation behavior has shown that for most cases (160 out of 200 models), the locations of maximum displacements occurred at the start point of measurement, thus were equal to zero. Furthermore, the mean and standard deviations of the zero, non-zero and total locations of maximum displacements can be determined. The average location of maximum displacements for non-zero ones was equal to 5.23m with a standard deviation of 1.898m. Instead, a value of 1.045m represents the overall average location of maximum displacements along with a relatively higher standard deviation of 2.258m.

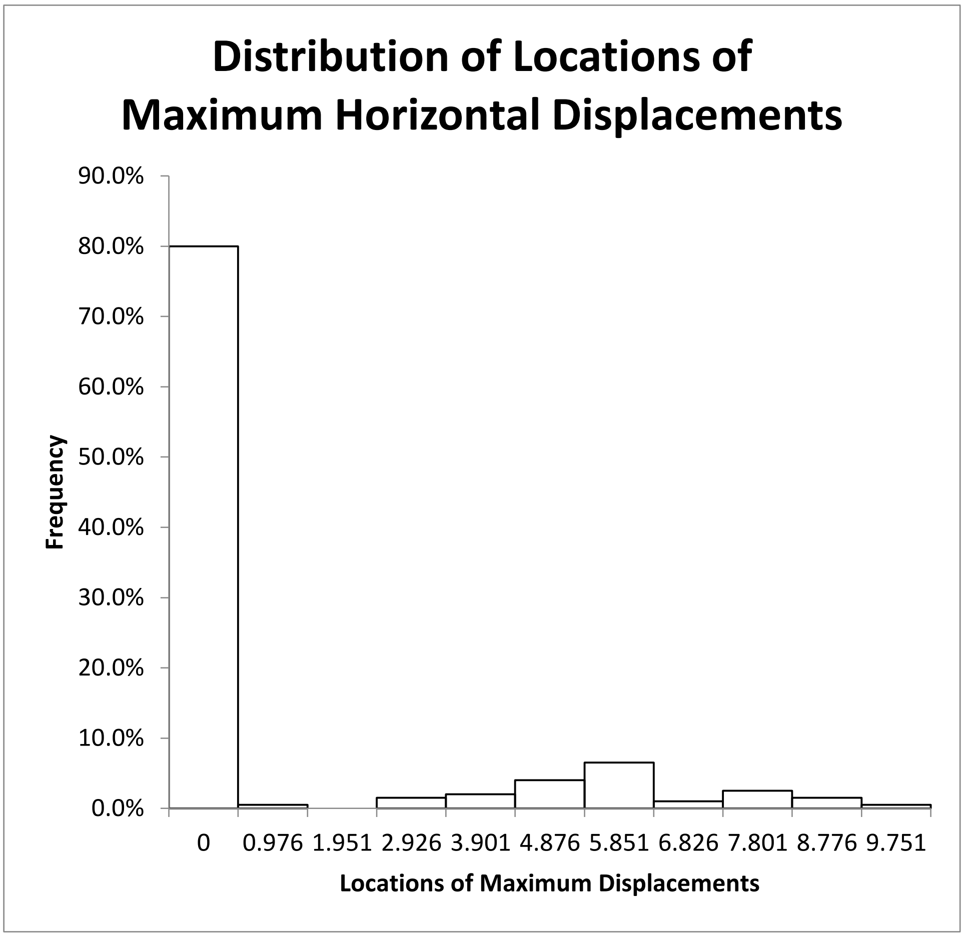

Figure 4.2.3 Distribution of locations of maximum displacements of 200 models (in meter)

Chapter V. The Development and Verification of Artificial Neural Networks (ANNs)

ANNs have been used in different domains to predict complex behavior, as discussed in Chapter II. Some of the researchers have analyzed the degree of retaining wall deflections under different external factors using ANN models. In those articles, FEM analyses were developed for generating all the relevant input data and which were thereafter applied in the ANN tools (Kung et al., 2007; Goh and Kulhawy, 2005). Kung et al. (2007) proposed that a simplified empirical chart method may not able to precisely predict the wall deflection induced by excavation in clayey soils, where only a limited number of variables have been used for making predictions. However, to establish the reliable ANN model as an alternative, a few of case histories can barely meet the minimum number needed, therefore, substantial hypothetical cases were indispensable for the development and training of ANNs. Based on Kung et al. (2007) and Goh and Kulhawy (2005), for a network with m input neurons, n hidden neurons, and a single output, the relationship among the input database and the output parameter, the maximum wall deflection δ_{hm}, can be written as:

$$\delta_{hm} = f_{sig2}\{b_0 + \sum_{k=1}^{n}[W_k f_{sig1}(b_{HK} + \sum_{i=1}^{m} W_{ik} P_i)]\} \quad (40)$$

where b_0 is the bias at the single output neuron layer; W_k is the weight of connection between neuron k of the hidden layer and the output layer; b_{HK} is the bias at neuron k of the hidden layer (k = 1, n); W_{ik} is the weight connection between input variable i (i = 1, m) and neuron k of the hidden layer; P_i is the input variable i; f_{sig1} is the sigmoid transfer function of each neuron in the hidden layer; and f_{sig2} is the sigmoid transfer function of the neuron in the output layer. These two transfer functions can be defined as:

$$f_N(\lambda) = \frac{1}{1+e^{-\lambda}} \text{ for } N = \text{sig1, sig2} \quad (41)$$

In this thesis, the number of input variables (m) is 16, which are the:

1. cohesion of backfill soil ($c_1' = 0$);
2. friction angle of backfill soil (ϕ_1');
3. unit weight of backfill soil (γ_1);
4. Young's modulus of backfill soil (E_1);
5. cohesion of clayey soil (c_2');
6. friction angle of clayey soil (ϕ_2');
7. unit weight of clayey soil (γ_2);
8. Young's modulus of clayey soil (E_2);
9. Young's of modulus of retaining wall (E_3);
10. retaining wall free height (H_1);
11. retaining wall embedded depth (H_2);
12. retaining wall thickness (H_3);
13. installation distance from pile to retaining wall (D_1);
14. pile diameter (D_2);
15. pile installation depth (L);
16. factored bearing capacity (Q_{ult}) of pile.

Notably, the input values of retaining wall embedded depth (H_2) and bearing capacity (Q_{ult}) were calculated dependent on their relevant parameters as discussed in previous chapters.

5.1 Introduction of establishing an ANNs using MATLAB

To establish an ANN model, a proper tool is essential for conducting the precise analyses and predictions. In this thesis, MATLAB (Mathworks, 2013) was chosen for establishing and training the ANN models. Within MATLAB, to create an ANN model, the Neural Network Toolbox was used, see Figure 5.1.1. Among all the four applications indicated in the toolbox, the application of input-output and curve fitting was chosen for the training.

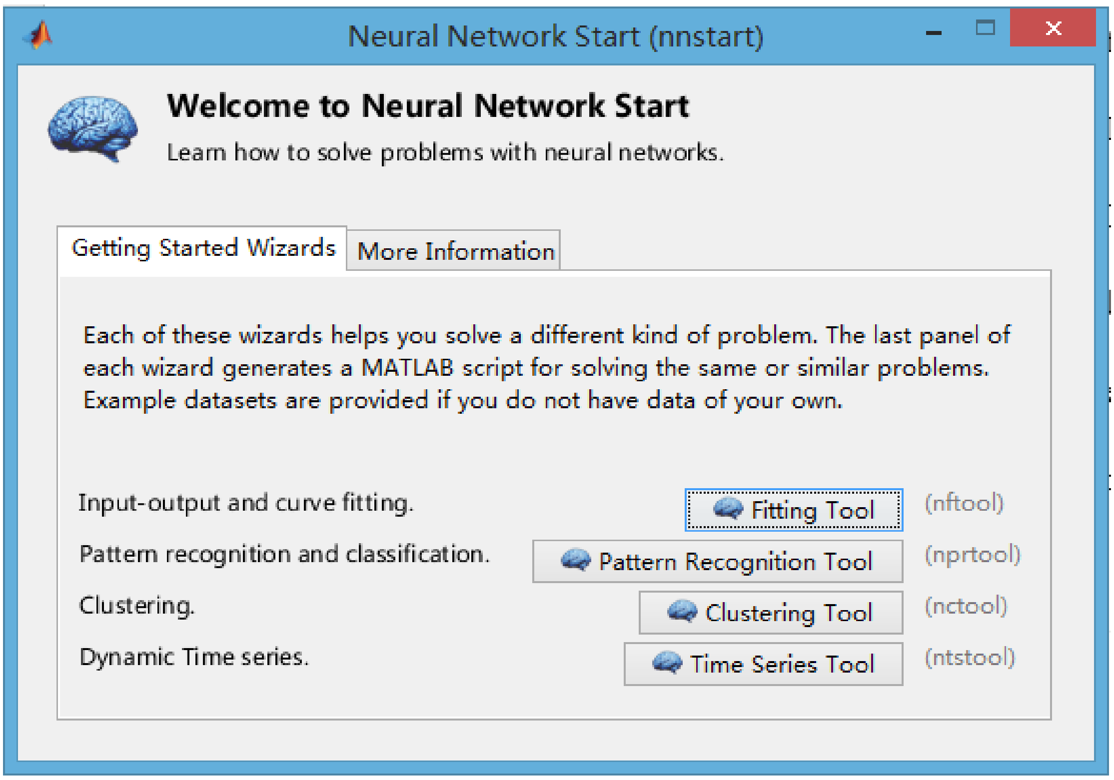

Figure 5.1.1 Neural Network Toolbox in MATLAB

In the fitting tool, the structure of the system was defined as a two-layer feed-forward network. Figure 5.1.2 briefly shows the relations among inputs, hidden layer output layer, and the output. To properly train the model, as discussed in Chapter 2.7, the backpropagation algorithm was used. However, MATLAB recommended three different algorithm functions which were Levenberg-Marquardt (*trainlm*), Bayesian regulation (*trainbr*), and the Scaled Conjugate Gradient (*trainscg*). In this thesis, the Levenberg-Marquardt algorithm was selected due to its highest processing speed and efficiency even though it requires more memory than the other two functions. Through optimizing the Newton's and Gradient Descent algorithms, the probability for being part of a local optimum can be avoided. In case of running out of memory during the training, the *trainscg* function should be used. Fortunately, the database obtained from FEM analyses did not exceed the limit and the performance was acceptable, as will be discussed later.

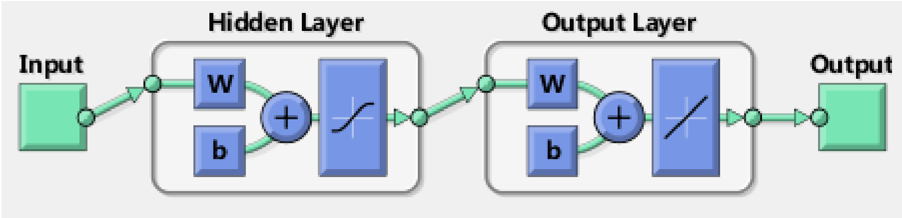

Figure 5.1.2 Neural network in MATLAB

By default, a MATLAB neural network randomly selects 70% of the inputs for training, 15% for validation and 15% for testing, as shown in Figure 5.1.3. By adjusting the percentage for validation and testing, it is possible to obtain different regression results (R), yet in this thesis, the original defaults were used.

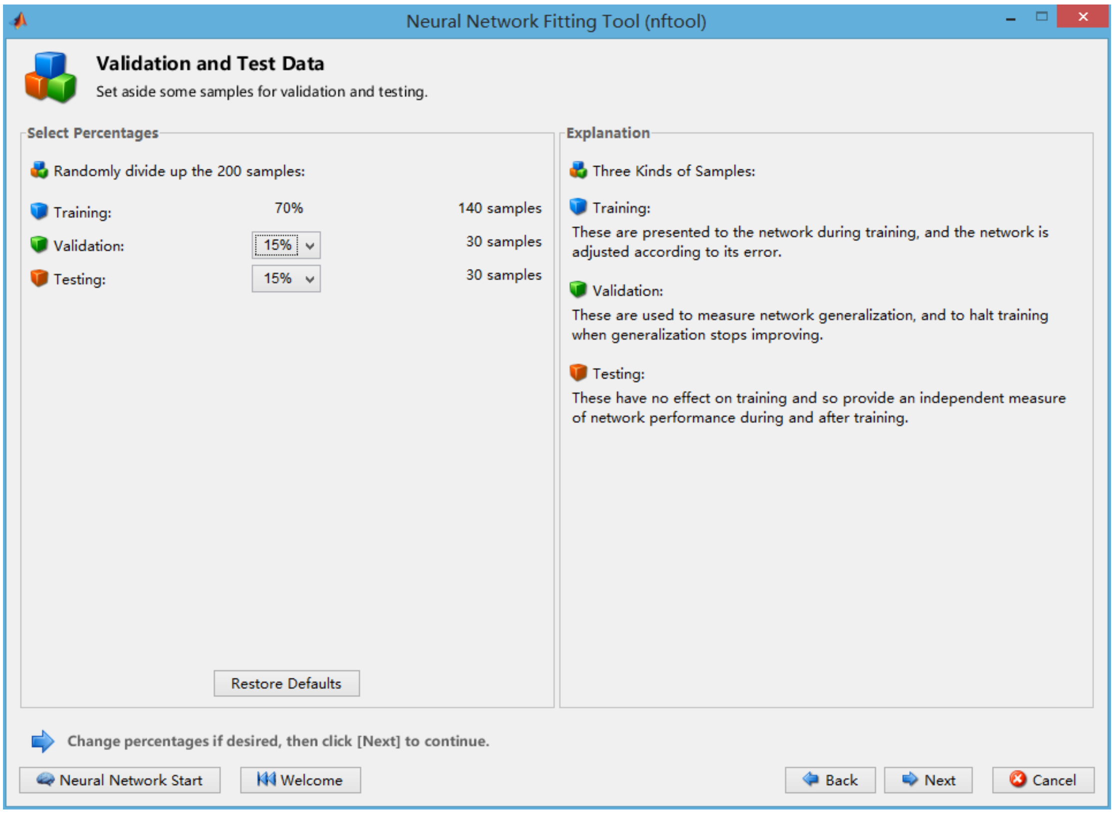

Figure 5.1.3 Percentage of training, validation, and testing in neural network

5.2 Sample filtering

Since the objective of the ANN's training is to minimize the value of error between target output and expected output, it is important to assure the input database was credible (e.g. all models resulted in converged, physically feasible outcomes).

Among all the models created by FEM analyses, some were not able to converge, in which the number of iterations during analysis exceeded the maximum tolerance (500), meaning that the deformations obtained by the FEM were violating the small-strain assumption of the FEM formulation. Figure 5.2.1 shows the consequence of these outcomes; thus, it was necessary to avoid using them and replace them with converged models. The reasons led to this can be different such as the excessive axial loading on pile, extreme weak clayey soil supporting strong backfill soil, not enough space between pile and external boundary, retaining wall was too thin, etc. Especially if the free height of retaining wall was designed beyond 10m, based on Equation (35) and combing with all relevant parameters, a credible embedded depth requires the friction angle of backfill soil to be extremely large which often led to an unstable situation. Accordingly, the highest retaining wall free height in all the models was 9.25m, and the correspond backfill soil friction angle was 42 degrees (Model 34), which led to a 14m embedded depth. However, the largest maximum horizontal retaining wall displacement among all the models was -0.41636m for Model 192 (Figure 5.2.2). Comparing with Model 177 (Figure 5.2.3), which has similar retaining wall heights yet with different pile installation location, the induced maximum retaining wall displacement was only -0.02355m. The reason for the excessive displacement can be attributed to the relatively thinner thickness of retaining wall, and closer installation distance between pile and wall.

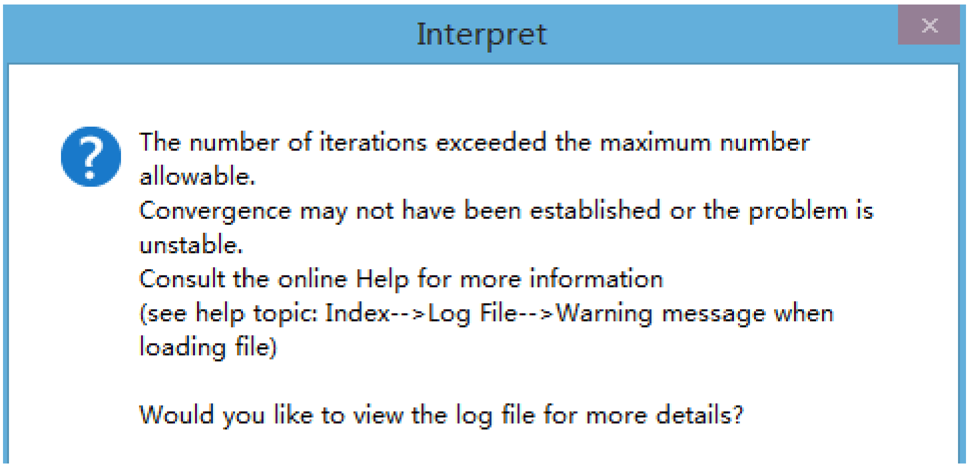

Figure 5.2.1 Unstable situation during FEM analysis

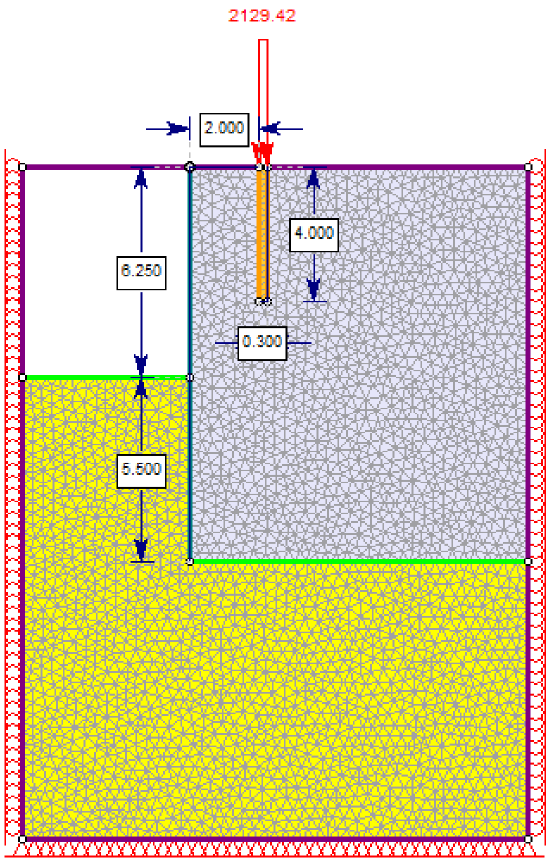

Figure 5.2.2 Original unmodified Model 192

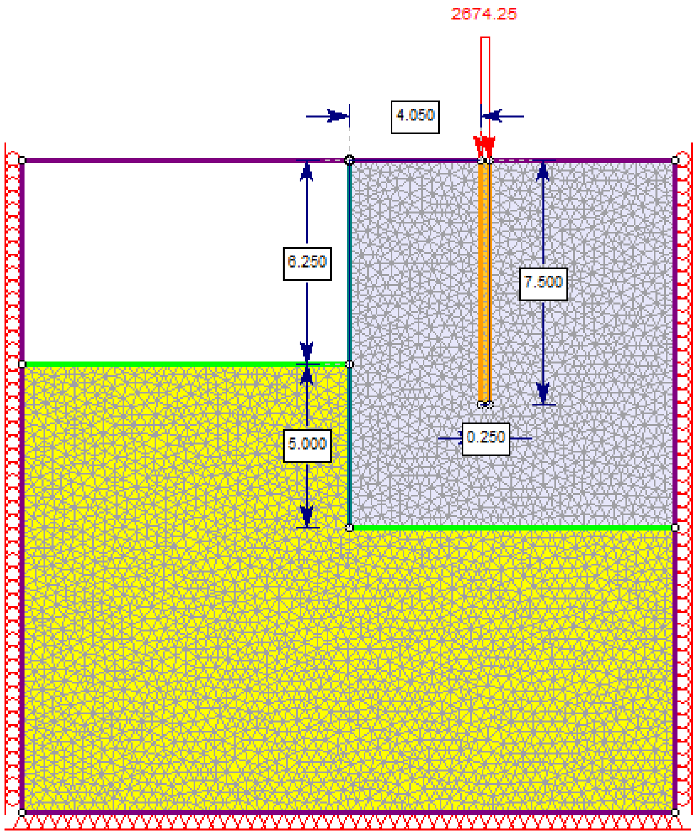

Figure 5.2.3 Model 177

From above, the database of ANNs training was modified by re-modeling all the non-convergent models into ones that converged. Fortunately, only 10 models resulted in the maximum horizontal displacements greater than 0.1m in absolute value. Also, only three out of these ten results were greater than 0.2m, which were Model 76, 169, and 192. These three outlier samples were replaced by new models in the process of training, owing to their unrepresentativeness. Changes were made only regarding to the thickness of retaining wall for keeping the randomness of other parameters. After adjusting these models, the improvement of training performance (error difference between expected and actual output) was observed, as illustrated by Figures 5.2.4 and 5.2.5.

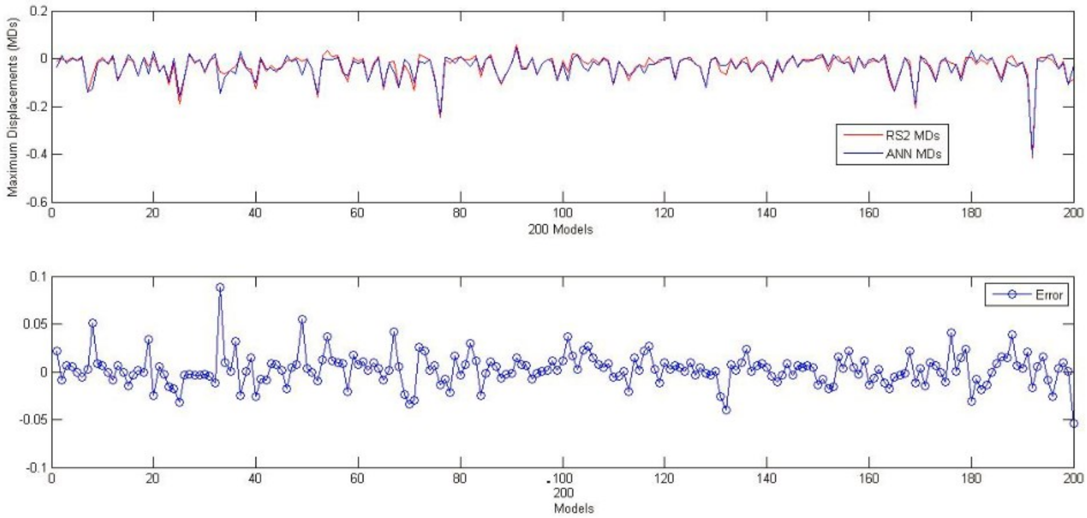

Figure 5.2.4 ANNs training and error (in meters) before replacing outlier samples regarding to the Maximum Horizontal Displacements

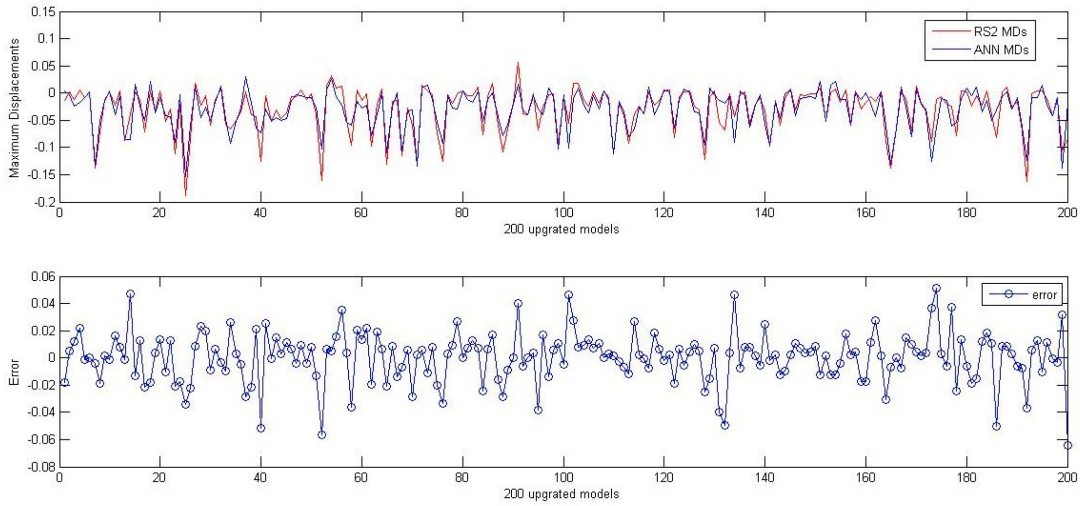

Figure 5.2.5 ANNs training and error (in meters) after replacing outlier models regarding to the Maximum Horizontal Displacements

The top diagram in Figure 5.2.4 and 5.2.5 shows the value of maximum displacements (MDs) of retaining wall obtained from 200 RS2 models (blue) and output values (red) generated from the neural network. Comparing these two diagrams, the maximum absolute values of MDs were significantly reduced from 0.4m to 0.19m, which contributed to the decrease of error range from [-0.06m, 0.09m] to [-0.06m, 0.05m] as shown in the lower diagram of each figure. Comparatively, the distribution of the locations of MDs will be discussed in the following chapter due to its particularity.

5.3 MATLAB ANNs training scripts

As discussed in Chapter 5.1, through using the Neural Network Toolbox, it is possible to conduct the training by MATLAB itself. However, the Mean Squared Error (MSE), which represents the average squared difference between outputs and targets, and the Regression (R) values, which can measure the correlation between targets and outputs, derived from the toolbox were not acceptable as shown in Figure 5.3.1. No matter how the number of neurons in hidden layer was changed, the consequent results were still not satisfactory since the R values were significantly smaller than 0.9 of the validation and testing results. To lower the value of MSE as closer to zero, and increase the value of R as closer to 1 as possible, a script written in MATLAB for the ANNs training was necessary.

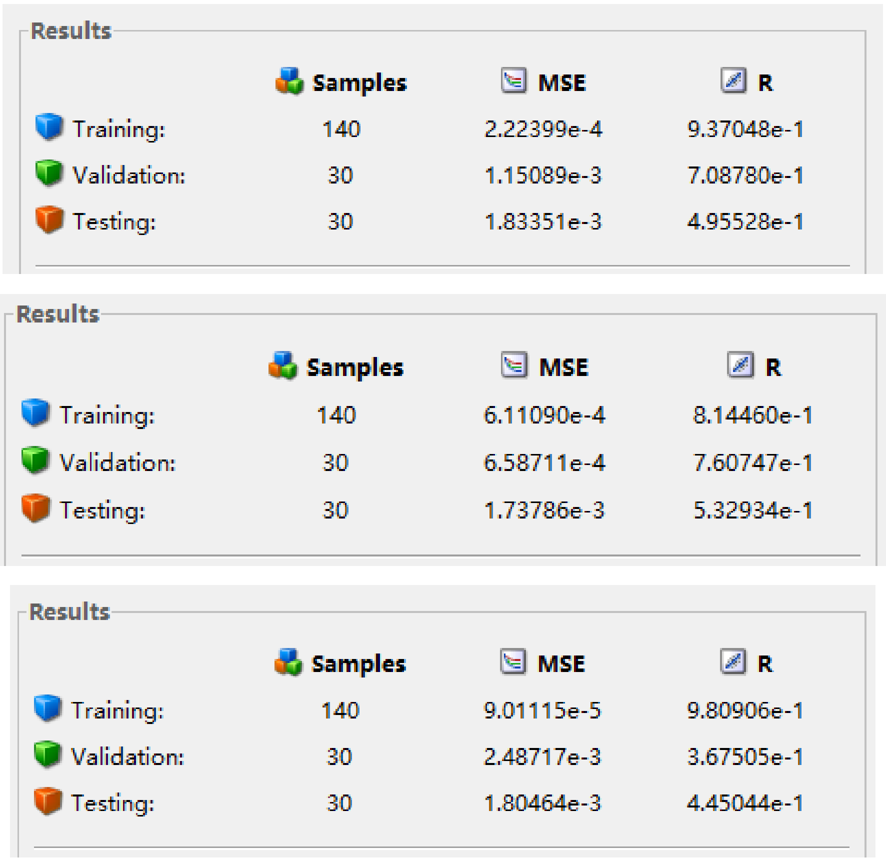

Results

	Samples	MSE	R
Training:	140	2.22399e-4	9.37048e-1
Validation:	30	1.15089e-3	7.08780e-1
Testing:	30	1.83351e-3	4.95528e-1

Results

	Samples	MSE	R
Training:	140	6.11090e-4	8.14460e-1
Validation:	30	6.58711e-4	7.60747e-1
Testing:	30	1.73786e-3	5.32934e-1

Results

	Samples	MSE	R
Training:	140	9.01115e-5	9.80906e-1
Validation:	30	2.48717e-3	3.67505e-1
Testing:	30	1.80464e-3	4.45044e-1

Figure 5.3.1 MSE and R values derived from Neural Network Toolbox training when number of neurons in hidden layer was 25, 30, and 35, respectively

Accordingly, the script in MATLAB for ANNs training was developed as shown in Appendix along with the interpretation of each code. Input values of 1 – 15 were obtained by using Monte Carlo sampling method through Excel as mentioned in Chapter 3.2, and input values for the 16th parameter, which represents the axial-loading, were derived using the formulae mentioned in Chapter 2.5.

- […data…] see Appendix

```
inputdata=[input_1; input_2; input_3;input_4; input_5; input_6;input_7; input_8;
input_9;input_10; input_11; input_12;input_13; input_14;
input_15;input_16;];%building input 16*200 matrix
outputdata=target_1;%building output 1*200 matrix
figure(1);
subplot(2,1,1)
plot(outputdata,'r');%plot the RS2 MDs on the top diagram in red 'r=red'
hold on;
net=newff(inputdata,outputdata,[35,35],{'tansig','purelin'},'trainlm');%ANN
building
net.trainparam.epochs=50;
net.trainparam.goal=1e-10;
net=train(net,inputdata,outputdata);%R=0.74348, not good enough
net=train(net,inputdata,outputdata);%R=0.86834, not good enough
net=train(net,inputdata,outputdata);%R=0.86831, not good enough
net=train(net,inputdata,outputdata);%R=0.88589, not good enough
net=train(net,inputdata,outputdata);%R=0.91261, not good enough
net=train(net,inputdata,outputdata);%R=0.94716, not good enough
net=train(net,inputdata,outputdata);%R=0.95338, good enough, training stop
outputdata_net=sim(net,inputdata);%ANN calculates the maximum displacements of
retaining wall
error=outputdata-outputdata_net;%errors between the RS2 MDs and ANN MDs for 200
models

plot(outputdata_net,'b');%plot the ANN MDs in top diagram in blue 'b=blue'
subplot(2,1,2)
```

```
plot(error,'o-');plot the errors in the bottom diagram

x = [0 29 20 287 48 16 19 6 3.25 1.5 0.75 1045397 2.6 0.3 4.5 939.77]';%test model
1, convert a 1*16 matrix (16 sample of 1 element) to a 16*1(1 sample of 16 elements)
matrix
y=sim(net, x);%ANN simulation results regarding to dataset x
```

To assure the script was functioning as intended, initially, the uniformity for matrix sizes of inputs and output should be guaranteed. As shown above, for inputs 1 – 16, since each row represents one element in the network, by combining all input datum, each input column represented 16 elements of each sample, respectively. To check whether the *newff* network was well functioning was by observing the differences between *outputdata* and *outputdata_net* as shown in Figure 5.2.5. For clarification, the *outputdata* which obtained from FEM analyses has been defined in red color, and *outputdata_net* generated from the ANN was drawn in blue. Notably, the script from above described only the *outputdata* representing the maximum horizontal displacements of retaining wall, it's corresponding location has been written in a separate script.

From the above, the fundamental function of the neural network was written in a FeedForwardent network term as:

```
net=newff(inputdata,outputdata,[35,35],{'tansig','purelin'},'trainlm');
```

where the [35,35] represents the number of neurons in two hidden layers; *tansig* is a Hyperbolic tangent sigmoid transfer function for the input layer (Figure 5.3.1); *purelin* is a linear transfer function for output layer (Figure 5.3.2); and *trainlm* is the backpropagation algorithm as defined in Chapter 5.1.

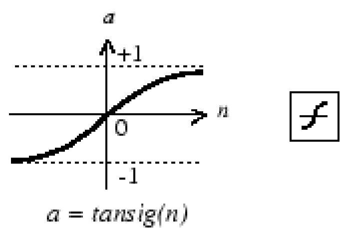

Figure 5.3.1 Tan-Sigmoid transfer function (Mathworks, 2013)

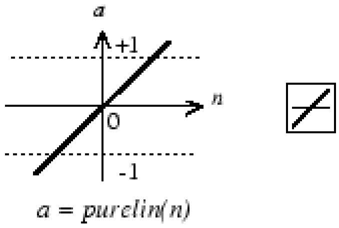

Figure 5.3.2 Linear transfer function (Mathworks, 2013)

Similarly, to predict the locations of maximum horizontal displacements, all relevant inputs and operational functions were kept as the same, only except the number of training cycles, the colors used in graphing, and target values in accordance with the FEM analyses were changed to:

-
```
target_2=[…data…] see Appendix;
plot(outputdata,'b');% plot the RS2 MDs locations on the top diagram in blue

net=train(net,inputdata,outputdata);%R=0.60837, not good enough
net=train(net,inputdata,outputdata);%R=0.71751, not good enough
net=train(net,inputdata,outputdata);%R=0.83166, the best result, training stop
plot(outputdata_net,'r'); plot the ANN MDs locations on the top diagram in red
```

From the script above, it can be noticed that 160 out of 200 (80%) values were equal to zero. This is due to the nature of cantilever retaining wall behavior that, under a certain lateral stress decreasingly distributed along the wall, the location of maximum horizontal displacement should be generated at its top, at the tip of the cantilever. In terms of which, the derived result from ANNs was not uniformly distributed, and the differences between *outputdata* and *outputdata_net* is shown in Figure 5.3.3.

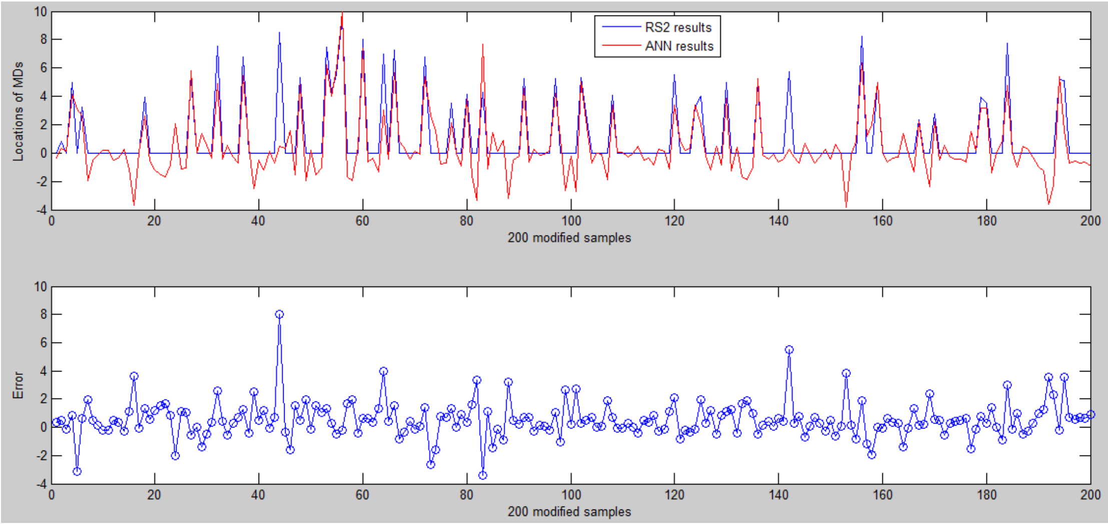

Figure 5.3.3 Neural network training and error (in meters) differences between *outputdata* and *outputdata_net* regarding the locations of MDs

5.4 ANNs training results and testing

Once the framework of ANNs was established, the results after running shall be as satisfactory (high R-value) as possible to predict similar scenarios. Figure 5.4.1 illustrates the structure of the ANNs. In this thesis, since the output layers have been defined separately for the maximum horizontal displacements and their locations, their corresponding results should be concluded respectively.

5.4.1 Maximum horizontal displacements

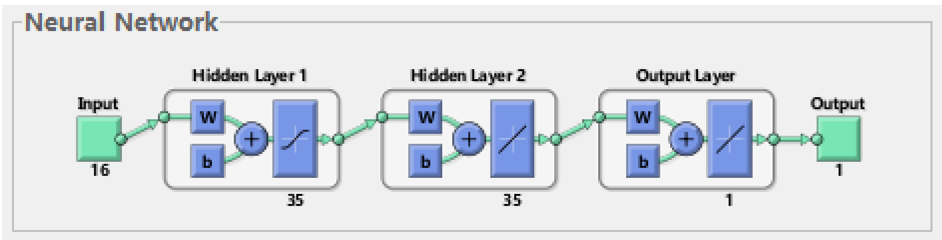

Figure 5.4.1.1 ANNs analysis structure

To improve the performance of neural networks, and for obtaining the optimized results, an adequate number of samples should be assured in the first place. In this thesis, 200 samples were used and which gave us the expected result. From the result shown in Figure 5.4.2 regarding to the maximum horizontal displacements, all samples were uniformly distributed in a systematic form, and the global Regression (R) value was desirable. Initially, the R-value was not acceptable at all (R=0.74348), in terms of which, revisions including retraining or increasing the number of training cycles in the network, and adjusting the number of neurons in each layer led to the R-value that was closer to 1 as possible. In the process of ANNs analysis, the percentages of sample distributions in terms of training, validation, and testing were divided into 70%, 15%, and 15% respectively, as discussed earlier. Accordingly, training samples were critical to the network adjustments based on its error, and to generalized the network, validation samples can stop the training whenever there is no improvement. As for the testing samples, they were separated from the previous two types and randomly chosen by the network to measure the overall performance.

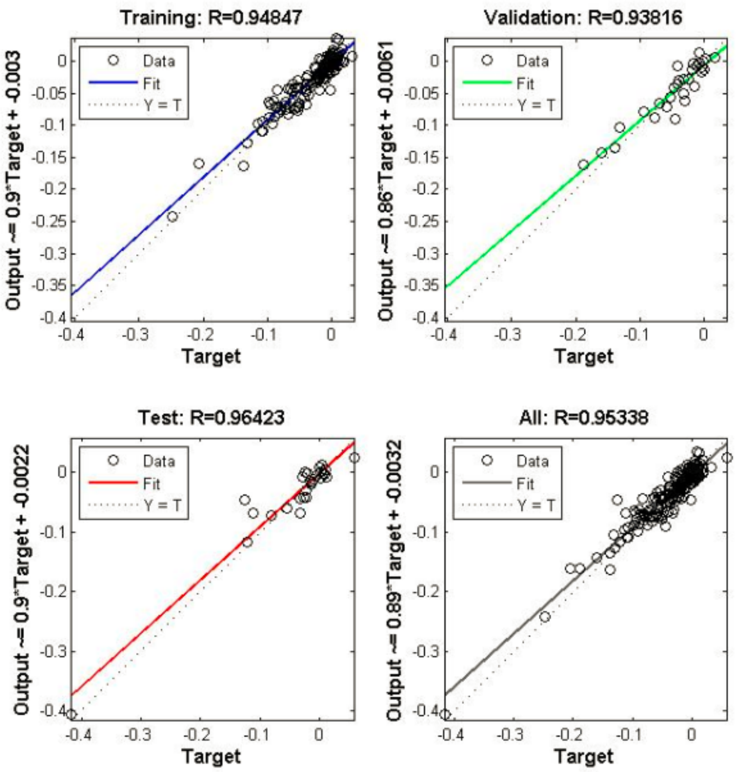

Figure 5.4.1.2 ANNs regression result regarding to the maximum horizontal displacements

5.4.2 Locations of maximum horizontal displacements

By sorting 200 model results as shown in Figure 5.4.2.1 with respect to the locations of maximum displacements (MDs), it can be observed that for quite a few (80%) cases the ANNs prediction should be zero. As stated earlier, this is due to the maximum displacement occuring at the free tip of the cantilever (location of origin of measurements, at zero), which is the expected behavior of the structural system. However, since there is no clear and unique functional relationship regarding this situation, the prediction of locations was not as accurate as the magnitude of the displacements (R was only =0.83166), as shown in Figure 5.4.2.2, and no matter how the changes were made in the script, the R-value could not be greater than 0.9.

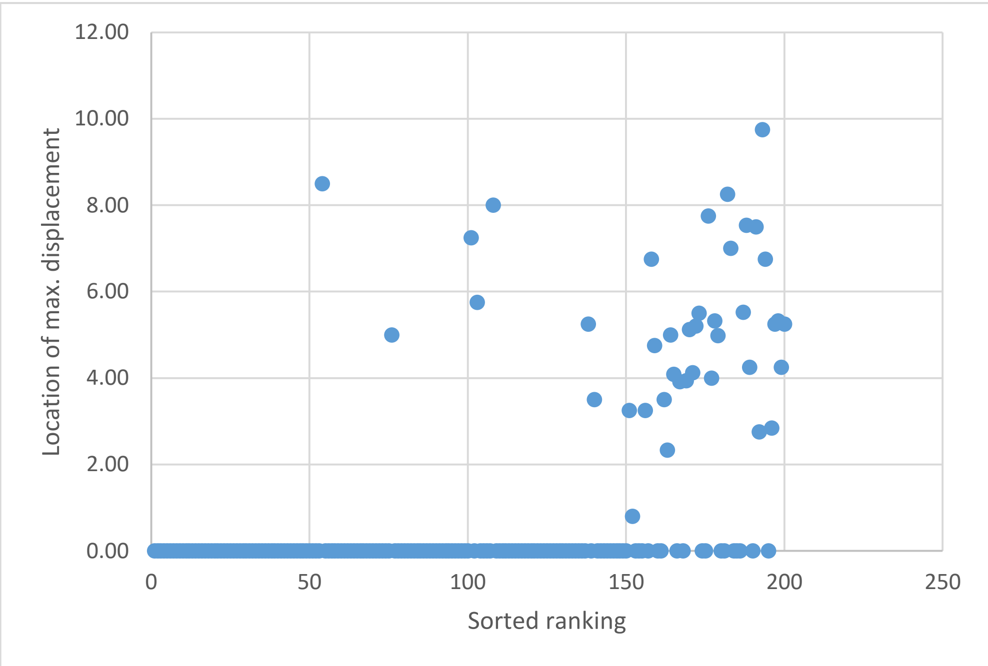

Figure 5.4.2.1 Distribution of locations of MDs measured from the top of retaining wall

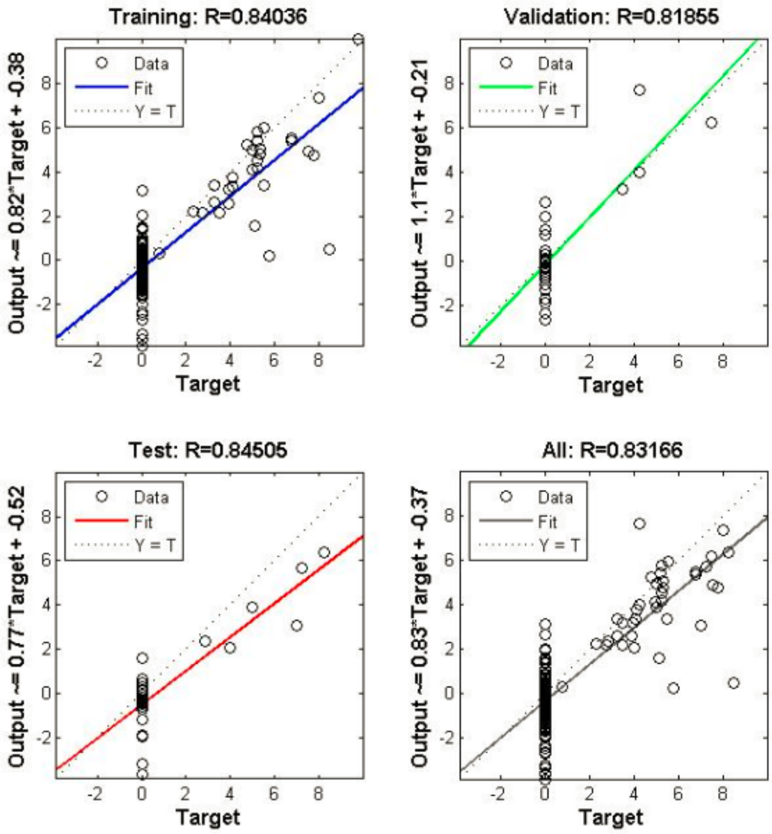

Figure 5.4.2.2 ANNs regression result regarding to the locations of MDs

In addition, the magnitude of maximum displacement vs. the location of maximum magnitude (Figure 5.4.2.3) and the location of max. displacement vs. its sorted ranking (Figure 5.4.2.4), as illustrated below, support the fact that the maximum horizontal displacement usually, and most frequently will be encountered at the top of retaining wall.

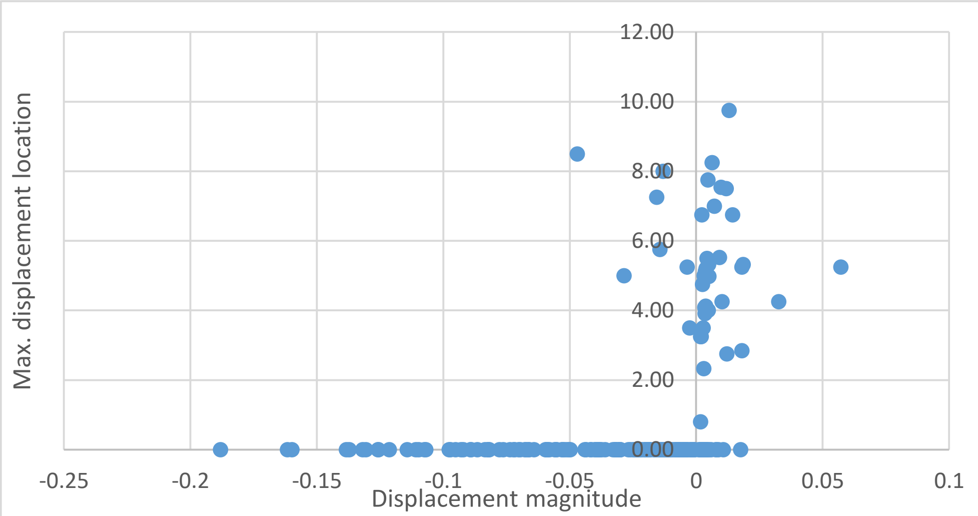

Figure 5.4.2.3 Displacement magnitude vs. maximum displacement location

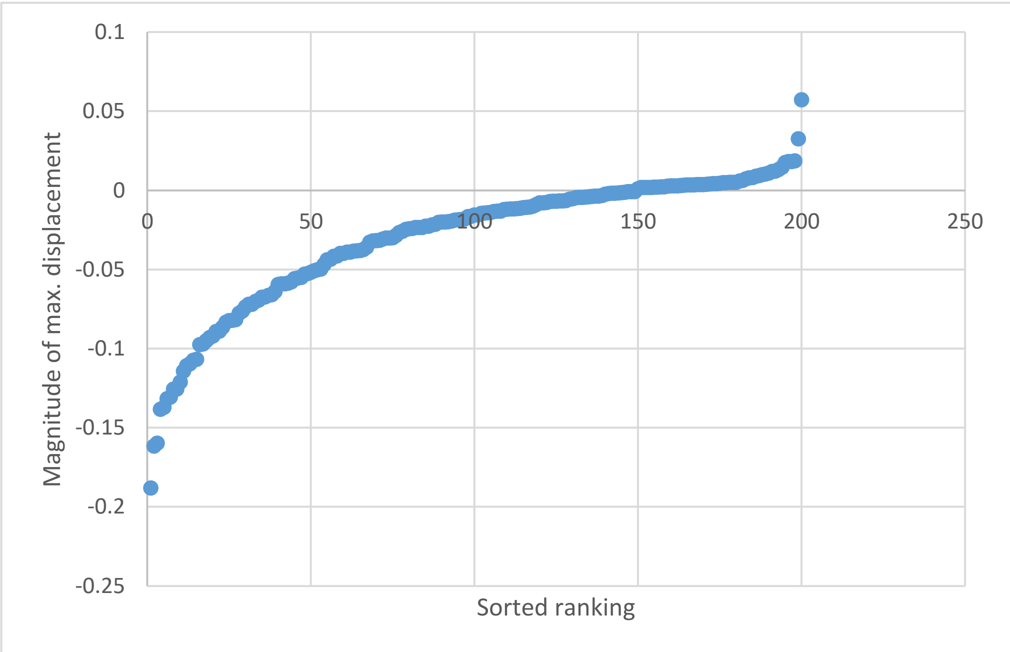

Figure 5.4.2.4 Magnitude of maximum displacement vs. its sorted ranking

5.5 ANN's prediction

Since the maximum horizontal displacements normally occurred at the top of retaining wall as discussed in the previous chapter, the objective of the ANNs prediction will be focused on the magnitude of maximum displacements (MDs) only. To qualitatively evaluate the accuracy of prediction, the percentage of error between expected (RS2_MDs) and actual (ANNs_MDs) outputs for 20 extra test samples, established and analyzed by FEM analyses, should be estimated by the following equation:

$$Error(\%) = \frac{\left||RS2\_MD| - |ANNs\_MD|\right|}{|RS2\_MD|} * 100\% \quad (42)$$

By applying the equation, as shown in Table 5.5.1 and 5.5.2, the overall average error was 2.652 percent, while the maximum and minimum errors were 5.478 percent, and 0.253 percent respectively. Which, for example, represents that for Test 19, the ANNs predicted the maximum horizontal displacement of retaining wall as 0.06208m, which is 0.0034m smaller than the actual result from RS2 analysis (0.06548m); and for Test 4, the prediction difference is only 0.00001m, which is negligible. Notably, during the process of ANN prediction, all the testing sample parameters were different than the ones used in ANN training.

	Backfill soil properties				Clayey soil properties				Geometric properties		
	c_1'	ϕ_1'	γ_1	E_1	c_2'	ϕ_2'	γ_2	E_2	H_1	H_2	H_3
Test 1	0	29	20	287	48	16	19	6	3.25	1.5	0.75
Test 2	0	37	18	65	39	31	23	37	7	10.5	1.25
Test 3	0	42	20	142	51	13	24	46	6.25	3.5	1.25
Test 4	0	35	19	89	23	15	18	47	3.5	3.75	1.25
Test 5	0	41	20	40	53	26	25	34	6	3	0.75
Test 6	0	33	21	136	49	18	22	30	3.25	1.25	0.75
Test 7	0	29	18	253	40	20	23	27	6	6.5	1.25
Test 8	0	42	21	96	24	7	18	45	3.5	3.75	0.5
Test 9	0	37	22	53	31	32	23	43	4	3.5	1.25
Test 10	0	31	19	132	22	9	21	3	3.75	5.75	0.5
Test 11	0	29	21	161	56	17	23	46	4.25	2	1
Test 12	0	29	20	290	22	21	22	12	3.25	4.25	0.75
Test 13	0	37	21	189	33	35	17	4	4	2.75	1
Test 14	0	43	22	178	47	18	17	12	5.25	2.75	0.75
Test 15	0	35	18	20	41	22	24	37	5.25	3.5	0.5
Test 16	0	36	21	285	51	7	19	36	5.75	3.75	1.25
Test 17	0	40	21	268	36	2	16	23	6	11.75	0.5
Test 18	0	39	22	80	25	19	18	46	3.5	4	0.5
Test 19	0	40	19	228	41	3	16	2	7.5	13	1.5
Test 20	0	37	18	103	54	8	20	39	9.25	10.75	1.25

Table 5.5.1 20 test sample parameters

	Geometric properties				Loading	ANN MDs	RS2 MDs	Error
	E3	D_1	D_2	L	Q(ult)			
Test 1	1045397	2.6	0.3	4.5	939.77	-0.02870	-0.02754	0.04212
Test 2	775995	3.95	0.5	14.5	7396.27	-0.03440	-0.035684	0.03598
Test 3	1102658	2.8	0.35	12.75	2080.22	-0.00961	-0.01003663	0.04258
Test 4	978106	2.85	0.35	11	1491.03	0.00406	0.00405	0.00253
Test 5	1010299	0.75	0.5	15	6127.46	-0.06045	-0.06096	0.00834
Test 6	805595	1.8	0.6	9.5	1451.38	-0.01126	-0.01146984	0.01827
Test 7	692511	3.6	0.4	24.5	5330.89	-0.03274	-0.03181	0.02916
Test 8	1047976	2.45	0.6	21.5	1301.10	-0.00720	-0.00706	0.01983
Test 9	737967	1.65	0.3	11.5	9552.95	-0.02167	-0.021420133	0.01161
Test 10	1024512	2	0.4	18	1844.12	-0.02879	-0.02962	0.02812
Test 11	991211	0.75	0.2	6	1579.36	-0.03254	-0.0311	0.04640
Test 12	969323	4.5	0.5	20.5	3982.29	0.00746	0.00785	0.04927
Test 13	914332	1.25	0.2	4	2692.34	-0.06322	-0.0618	0.02300
Test 14	934799	3.5	0.3	20.75	3367.14	-0.01339	-0.01382	0.03109
Test 15	753416	2.4	0.5	12.25	2962.62	-0.11493	-0.11891	0.03347
Test 16	844429	1.2	0.5	17	1627.80	-0.01448	-0.01467	0.01272
Test 17	797878	1	0.25	9.5	6254.88	-0.13909	-0.13716	0.01408
Test 18	713630	3.05	0.5	11.25	1770.49	-0.01649	-0.01683	0.01998
Test 19	729321	1.6	0.2	13.75	6853.91	-0.06548	-0.06208	0.05478
Test 20	1043888	1	0.4	20.25	3234.32	-0.13115	-0.13209	0.00708
							Average	0.02652

Table 5.5.2 20 test sample parameters and errors between RS2 results and ANNs prediction

Based on the results, the established ANNs in this thesis can predict the magnitude of horizontal maximum displacements within an acceptable error range. Where the acceptable error range is in the context of knowing soil properties, which are seldom known better than approximately 10-20 percent within their true mean values. For other similar cases, instead of using FEM analysis software, the object of prediction can be achieved simply through the neural network with provided corresponding input parameters. Expectedly, the locations of MDs for these 20 test samples were behaving according to the nature of cantilever retaining wall, as shown in Table 5.5.3, through FEM analyses, only 2 out of 20 (10%) samples acted differently and the rest test samples were indicating that the maximum horizontal deflection occurred on the top of retaining wall.

	Backfill soil properties				Clayey soil properties				Geometric properties							Loading	Location of MD
	c_1'	ϕ_1'	γ_1	E_1	c_2'	ϕ_2'	γ_2	E_2	H_1	H_2	H_3	E_3	D_1	D_2	L	Q(ult)	ANN Results
Test 1	0	29	20	287	48	16	19	6	3.25	1.5	0.75	1045397	2.6	0.3	4.5	939.77	0.0
Test 2	0	37	18	65	39	31	23	37	7	10.5	1.25	775995	3.95	0.5	14.5	7396.27	0.0
Test 3	0	42	20	142	51	13	24	46	6.25	3.5	1.25	1102658	2.8	0.35	12.75	2080.22	0.0
Test 4	0	35	19	89	23	15	18	47	3.5	3.75	1.25	978106	2.85	0.35	11	1491.03	4.33
Test 5	0	41	20	40	53	26	25	34	6	3	0.75	1010299	0.75	0.5	15	6127.46	0.0
Test 6	0	33	21	136	49	18	22	30	3.25	1.25	0.75	805595	1.8	0.6	9.5	1451.38	0.0
Test 7	0	29	18	253	40	20	23	27	6	6.5	1.25	692511	3.6	0.4	24.5	5330.89	0.0
Test 8	0	42	21	96	24	7	18	45	3.5	3.75	0.5	1047976	2.45	0.6	21.5	1301.10	0.0
Test 9	0	37	22	53	31	32	23	43	4	3.5	1.25	737967	1.65	0.3	11.5	9552.95	0.0
Test 10	0	31	19	132	22	9	21	3	3.75	5.75	0.5	1024512	2	0.4	18	1844.12	0.0
Test 11	0	29	21	161	56	17	23	46	4.25	2	1	991211	0.75	0.2	6	1579.36	0.0
Test 12	0	29	20	290	22	21	22	12	3.25	4.25	0.75	969323	4.5	0.5	20.5	3982.29	4.19
Test 13	0	37	21	189	33	35	17	4	4	2.75	1	914332	1.25	0.2	4	2692.34	0.0
Test 14	0	43	22	178	47	18	17	12	5.25	2.75	0.75	934799	3.5	0.3	20.75	3367.14	0.0
Test 15	0	35	18	20	41	22	24	37	5.25	3.5	0.5	753416	2.4	0.5	12.25	2962.62	0.0
Test 16	0	36	21	285	51	7	19	36	5.75	3.75	1.25	844429	1.2	0.5	17	1627.80	0.0
Test 17	0	40	21	268	36	2	16	23	6	11.75	0.5	797878	1	0.25	9.5	6254.88	0.0
Test 18	0	39	22	80	25	19	18	46	3.5	4	0.5	713630	3.05	0.5	11.25	1770.49	0.0
Test 19	0	40	19	228	41	3	16	2	7.5	13	1.5	729321	1.6	0.2	13.75	6853.91	0.0
Test 20	0	37	18	103	54	8	20	39	9.25	10.75	1.25	1043888	1	0.4	20.25	3234.32	0.0

Table 5.5.3 FEM results of the locations of MDs for 20 test samples.

Chapter VI Conclusion and Summary

6.1 Remarks

The objective of this thesis was to determine the influence of axially-loaded piles adjacent to existing retaining walls on the stability of retaining walls. Since the system is comprised of multiple interacting elements, such as a pile, the retaining wall, backfill and foundation soils, the Finite Element Method was used due to its ability to model deformations and induced stresses in both the soil and retaining wall. It was concluded that the behavior of the retaining wall can be characterized by determining the magnitude and location of the maximum horizontal displacement induced by a nearby axially-loaded pile. However, due a large number of possible combination of model parameters, a ANN was developed predict the retaining wall deflection thus reducing the need to generate FEM models for each and every possible scenario.

As input parameters for each FEM model (in addition to soil properties, pile length, retaining wall height, etc.) the ultimate pile load was computed based on the fundamental principles of soil mechanics and Meyerhof's bearing capacity theory. Similarly, the depth of embedment for a retaining wall was calculated using these principles as well. Thus, using all these parameters, models were built in a FEM analysis software (RS2) and analyzed. Adapting the Mohr-Coulomb failure criterion, the backfill and the relatively weaker clayey soils were initialized within their credible parameter ranges. Various model parameters were sampled using a Monte Carlo sampling method. The water table was not considered due to the assumption of full drainage behind the retaining wall. Thus, the retaining wall deflection behavior was analyzed and quantified for the following ANNs modeling.

Based on over 200 credible models, the ANN was built and trained according to the model input values and their outputs (the magnitude of maximum horizontal retaining wall deflection, and its location). Predictions were made by using the trained ANN, which used the backpropagation and Levenberg-Marquardt neural network algorithms within MATLAB. These algorithms can assure the time efficiency of systems even though they require more memory. The training process was terminated at the point where it could not be improved further using the default settings. However, after the quality and quantity of dataset were assured to be credible, to further enhance the performance of the ANN, improvements were made regarding the training cycles, and the number of neurons in neural networks until the regression value (R) was as close to unity as possible.

As a final check, the developed ANN was used to predict the results of a fully independent (not used in training, testing or validation of the ANN) set of 20 sample models that were analyzed resulting in acceptable values in terms of the magnitude of predicted deflection. The average error was 2.652%, thus the efficiency and preciseness of the neural network assured that it could be used to estimate the magnitude of maximum horizontal deflection within the context of knowing parameters in geotechnical engineering. However, due to the nature of cantilever retaining wall (maximum deflection at the free tip) and the limitation of prediction, the location of maximum deflection was found to be at the top of the wall for most cases (over 80%), making it difficult for the ANN to find a precise correlation between the input values and the computed outputs.

Combining the FEM analyses and ANNs results, in terms of future researches or practical designs, the resulting maximum retaining wall horizontal displacements induced by nearby axially-loaded piles can be predicted through simply using the neural networks developed in this thesis with given corresponding parameter values. With these results, engineers can evaluate the stability of pile-wall system, therefore to decide if further enhancement shall be applied to increase the serviceability of the retaining wall and to prevent failure.

6.2 Limitations

6.2.1 Limitation of model parameters

As addressed in Chapter 1, although representing a credible situation, a limitation of the retaining wall – pile model is the soil condition that consists of backfill soil overlying a relatively weaker layer of clayey soil, and due to the absence of ground water with assumed drainage along the retaining wall, the effect of water table was not considered in this thesis.

Secondly, the effect of excavation induced retaining wall deformation on its own was not analyzed. This is because comparing with the load induced deformation, the excavation induced displacement was comparatively much smaller, which can be found in FEM analysis software. Also, since the object of this thesis was to determine the effects of axially loaded pile on nearby retaining wall, the excavation induced effects were neglected.

In addition, all models were created based on numerical approach, no experimental work has been conducted.

6.2.2 Limitation of ANNs

Since the ANN was developed based on the results of FEM analysis, all the relevant parameter sizes were kept as the same. Thus, the networks scripts in this thesis were limited by the scale of input parameters and their conditions such as no groundwater and assumed continuous retaining wall (in the third dimension). Once any new parameter needs to be considered, the ANNs in this thesis may not be applicable, which requires the network to be re-coded, re-trained and re-verified. Although the prediction of ANNs was accurate regarding the maximum displacements of retaining wall, however, the existence of ground water can seldom be avoided in practical engineering.

Another shortcoming of the applicability of ANNs is its high dependency on the input and target values. If any un-realistic (non-physical) FEM model behavior was not filtered out, the accuracy of prediction will be drastically reduced. Also, any change made in FEM analysis, such as adding the ground water table, could result in the need to the recreate and re-analyze all models used for training. In conclusion, before training the ANNs, the accuracy and credibility of inputs and target database need to be assured.

References

1. Lu, A. D.D., and Yeung, A. T. (2011) Risk Analysis of Pile Pressing-In on an Adjacent Earth-Retaining Wall. *Geo-Risk 2011*, pp. 948-954.
2. Athanasopoulos, G., Vlachakis, V., and Pelekis, P. (2011). Installation and Performance of a Steel Sheet Pile Wall for Supporting an Excavation in Urban Environment. *Geo-Frontiers 2011*, pp. 3370-3380.
3. Berg, R., and Vulova, C. (2007) Effects of Pile Driving Through a Full-Height Precast Concrete Panel Faced, Geogrid-Reinforced, Mechanically Stabilized Earth (MSE) Wall. *Case Studies In Earth Retaining Structures*, pp. 1-10.
4. Carter, M., and Bentley, S. P. (1991). *Correlations of Soil Properties*. Pentech Press Publishers.
5. Chung, I., and Ng, C. (2005). Three Dimensional Numerical Investigations of the Influence of Sleeved Piles on the Stability of Retailing Wall. *Advances in Deep Foundations*, pp. 1-9.
6. Clough, G.W., and Duncan, J.M. (1971) Finite Element Analyses of Retaining Wall. *ASCE Journal of the Soil Mechanics and Foundation Division*, 97 (SM12), pp. 1657-1673.
7. D'Aguiar, S. C., Lopez-Caballero, F., Modaressi, A., and Santos, J. (2007). Implication of Soil Behavior in Load Transfer Mechanisms of Axially Loaded Single Piles. *Advances in Measurement and Modeling of Soil Behavior*, pp. 1-10.
8. Das, B.M. (1999), *Principles of Foundation Engineering*, 4th Edition, PWS Publishing, Pacific Grove, CA.
9. Das, B.M. (2007) *Fundamentals of Geotechnical Engineering. 3rd Edition, CL-engineering.*
10. Dijkstra, J., Broere, W., and Van Tol, A.F. (2008). Modeling Displacement Pile Installation in a Finite Element Method. *Proceedings of the 2Nd BGA International Conference on Foundations, ICOF2008.*
11. Dijkstra, J., Broere, W., and Van Tol, A.F. (2009). Eulerian simulation Of The Installation Process of a Displacement Pile. *Geotechnical Special Publication*, 186, pp. 135-142.
12. Fioravante, V. (2002). On The Shaft Friction Modelling of Non-displacement Piles in Sand. *Soils and Foundations*, 42(2), 23-33.
13. Ford, C. J., Candler, C. J., and Chartes, F. R. D. (1991). The monitoring and Back Analysis of a Large Retaining Wall in Lias Clay. *Proc., 10th Eur. Conf. Soil Mech. Found. Engrg., Vol. 2*, Balkema,

Rotterdam, The Netherlands, 707–710.

14. Gao, C., and Ling, J (2008) Numerical Simulation of Static Piling Process in Layered Soils. *Zhongguo Tiedao Kexue/China Railway Science*, 29, (2), pp 23-27.
15. Gershenson, C. (2003). *Artificial Neural Networks for Beginners*. arXiv preprint cs/0308031.
16. Goh, A. T. C., and Kulhawy, F. H. (2005). Reliability Assessment of Serviceability Performance of Braced Retaining Walls Using a Neural Network Approach. *International Journal for Numerical and Analytical Methods in Geomechanics*, 29(6), pp. 627-642.
17. Goh, A. T., Wong, K. S., and Broms, B. B. (1995). Estimation of Lateral Wall Movements in Braced Excavations Using Neural Networks. *Canadian Geotechnical Journal*, 32(6), pp. 1059-1064.
18. Grabe, J., Pucker, T. and Hamann, T. (2014). Numerical Simulation of Pile Installation Processes in Dry and Saturated Granular Soils. *Numerical Methods in Geotechnical Engineering - Proceedings of the 8th European Conference on Numerical Methods in Geotechnical Engineering, NUMGE 2014*, v 1, pp. 663-668.
19. GuhaRay, A., and Baidya, D. K. (2015). Reliability-Based Analysis of Cantilever Sheet Pile Walls Backfilled With Different Soil Types Using the Finite-Element Approach. *International Journal of Geomechanics*, 15(6), 06015001.
20. Gunn, M.J., and Clayton, C.R.I. (1992). Installing Effects and Their Importance in the Design of Earth-Retaining Structures. *Geotechnique*, 42(1), pp. 137-141.
21. Henke, S. (2010) Influence of Pile Installation on Adjacent Structures. *International Journal for Numerical and Analytical Methods in Geomechanics*, 34(11), pp. 1191-1210.
22. Hossain, M., Kibria, G., Khan, M., Hossain, J., and Taufiq, T. (2012). Effects of Backfill Soil on Excessive Movement of MSE Wall. J. *Perform. Constr. Facil.*, 26(6), pp. 793–802.
23. Józefiak, K., Zbiciak, A., Maślakowski, M., and Piotrowski, T. (2015). Numerical Modeling and Bearing Capacity Analysis of Pile Foundation. *Procedia Engineering*, 111, pp. 356-363.
24. Koloski, J. W., Schwarz, S. D., and Tubbs, D. W. (1989). Geotechnical Properties of Geologic Materials. *Engineering geology in Washington*, 1, pp. 19-24.
25. Kung, G. T., Hsiao, E. C., Schuster, M., and Juang, C. H. (2007). A Neural Network Approach to Estimating Deflection of Diaphragm Walls Caused by Excavation in Clays. *Computers and Geotechnics*, 34(5), pp. 385-396.

26. Lambe, T. W. (1970) Braced Excavations. Preprint Proceedings. *Specialty Conference on Lateral Stresses in the Ground Design of Earth-Retaining Structures*, Cornell University, pp. 149-218.
27. Lehane, B. M., and White, D. J. (2005). Lateral Stress Changes and Shaft Friction for Model Displacement Piles in Sand. *Canadian Geotechnical Journal*, 42(4), pp. 1039-1052.
28. Li, Y.N., and Li, J.P. (2014). Discrete Element Modeling of Jacked Piles in Granular Soil. *Electronic Journal of Geotechnical Engineering*, 19, pp. 1109-1122.
29. Massarsch, K. and Wersäll, C. (2013) Cumulative Lateral Soil Displacement Due to Pile Driving in Soft Clay. *Sound Geotechnical Research to Practice*: pp. 462-479.
30. Mathworks, Inc.: 2013, Matlab version R2013a, https://www.mathworks.com/products/new_products/release2013a.html
31. Meyerhof, G.G. (1976), Bearing Capacity and Settlement of Pile Foundations. *ASCE Journal of Geotechnical Engineering Division*, Vol. 102, No. GT3, Proc. Paper 11962, pp. 195-228.
32. Mitchell, P. W. (2005), Bearing Capacity of Jacked Piles in a Layered Soil Profile. *Australian Geomechanics Journal*, 40(2), pp. 89-98.
33. Morgenstern, N. R., and Eisenstein, Z. (1970) Methods of Estimating Lateral Loads and Deformations. Preprint Proceedings. *Specialty Conference on Lateral Stresses in the Ground Design of Earth-Retaining Structures*, Cornell University, June 1970, pp. 51-105.
34. Obrzud, R., and Truty, A. (2012). The Hardening Soil Model – A Practical Guidebook. *Zace Services*.
35. Pham, H.D., Engin, H.K., Brinkgreve, R.B.J., and Van Tol, A.F. (2010). Modeling of Installation of Driven Piles Using Hypoplasticity. *Numerical Methods in Geotechnical Engineering - Proceedings of the 7th European Conference on Numerical Methods in Geotechnical Engineering*, pp. 261-266.
36. Poulos, H.G. (1994) Effect of Pile Driving on Adjacent Piles in Clay. *Canadian Geotechnical Journal*, 31(6), pp. 856-867.
37. Rauf, A. (2012). Estimation of Pile Capacity by Optimizing Dynamic Pile Driving Formulae. *UWSpace*. *http://hdl.handle.net/10012/6651*.
38. RocScience, Inc. (2017) Phase2, Finite Element Analysis for Excavations and Slopes version 9.0. Documentation, https://www.rocscience.com/rocscience/products/rs2
39. Rosti, F., and Abu-Farsakh, M. (2015). Numerical Simulation of Pile Installation and Setup for Bayou Lacassine Site. *Geotechnical Special Publication*, v GSP 256, pp. 1152-1161.

40. Said, I., De Gennaro, V., and Frank, R. (2009) Axisymmetric Finite Element Analysis of Pile Loading Tests. *Computers and Geotechnics*, 36(1-2), pp. 6-19.

41. Seed, R., and Duncan, J. (1986). FE Analyses: Compaction - Induced Stresses and Deformations, *J. Geotech. Engrg*., 112(1), pp. 23–43.

42. Seo, H., Yildirim, I., and Prezzi, M. (2009). Assessment of the Axial Load Response of an H Pile Driven in Multilayered Soil. *ASCE* J. Geotech. Geoenviron. Eng., 10.1061/(ASCE)GT.1943-5606.0000156, pp. 1789-1804.

43. Sharma, S. (2011) Teaching Retaining Wall Design with Case Histories. *Geo-Frontiers* 2011: pp. 2877-2886.doi: 10.1061/41165(397)295.

44. Structural Engineering Forum of India. (2017) Properties of Soils, http://www.sefindia.org/forum/files/appc_soil_properties_718.pdf (accessed May 08, 2017)

45. Suzuki, M., Shahin, H.M., and Nakai, T. (2010). Numerical Analysis on Ground Behavior for Construction of Displacement Pile. *Geotechnical Special Publication*, 205 GSP, pp. 300-307.

46. Swiss Standard, S. N. (1999). 670 010b. *Characteristic Coefficients of Soils*. Association of Swiss Road and Traffic Engineers, Zurich.

47. Tang, Y. G. (2011). Probabilistic Analysis of Retaining Wall in Deep Excavation. Geotechnical Risk Assessment and Management, GSP 224, pp. 217-224.

48. Wang, F.T., Tao, X. X., and Sun, J. (2008) Influence of Backfill Cohesion on Seismic Displacement of Gravity Retaining Wall. *The 14th World Conference on Earthquake Engineering*, October 12-17, 2008, Beijing, China.

49. Wang, Z., Miao, L., and Wang, F. (2012). Theoretical and Numerical Analysis of Jacked Pile in Sand. *GeoCongress*: pp. 245-254.

50. Watson, G.V.R., and Carder, D.R. (1994) Comparison of the Measured and Computed Performance of a Propped Bored Pile Retaining Wall at Walthamstow. *Proceedings of the Institution of Civil Engineers Geotechnical Engineering*, 107(3), pp. 127-133.

51. Weaver, T., and Youn, H. (2008) Pile Foundation Interaction With a Nearby Retaining Wall. *41st Symposium on Engineering Geology and Geotechnical Engineering 2008*, pp. 67-76.

52. Yang, Z., Jardine, R., Zhu, B., and Rimoy, S. (2014). Stresses Developed Around Displacement Piles Penetration in Sand. *ASCE J. Geotech. Geoenviron. Eng.*, 140(3), 04013027.

53. Yu, C., and Du, G. (2010). Numerical Simulation on a Tube-installed Displacement Pile in Sand Using Stress-Controlled Method. *Geotechnical Special Publication*, n 205 GSP, pp 308-314.

54. Yu, F., Chu, F., and Liang, F. Y. (2010). A Preliminary Study on the Behavior of Axially Loaded Single Pile Subjected to Lateral Soil Movement behind a Retaining Wall. *Deep and Underground Excavations,* pp. 76-83.

Appendix

ANN input values

```
input_1=[0  0   0   0   0   0   0   0   0   0   0   0   0   0   0   0   0   0   0   0   0   0   0
0   0   0   0   0   0   0   0   0   0   0   0   0   0   0   0   0   0   0   0   0   0   0   0   0
0   0   0   0   0   0   0   0   0   0   0   0   0   0   0   0   0   0   0   0   0   0   0   0   0
0   0   0   0   0   0   0   0   0   0   0   0   0   0   0   0   0   0   0   0   0   0   0   0   0
0   0   0   0   0   0   0   0   0   0   0   0   0   0   0   0   0   0   0   0   0   0   0   0   0
0   0   0   0   0   0   0   0   0   0   0   0   0   0   0   0   0   0   0   0   0   0   0   0   0
0   0   0   0   0   0   0   0   0   0   0   0   0   0   0   0   0   0   0   0   0   0   0   0   0
0   0   0   0   0   0   0   0   0   0   0   0   0   0   0   0   0   0   0   0   0   0   0   0   0
0   0]; %values of backfill soil cohesion of 200 models
input_2=[39 36  29  30  39  39  28  35  30  45  36  39  42  39  32  30  28  35  30  41  29  32
31  30  37  28  45  37  41  42  37  30  29  42  41  33  38  44  41  42  33  39  29  36  38  42
31  37  36  28  37  33  34  31  31  31  37  29  29  45  39  41  29  35  37  31  30  40  43  34
41  36  38  33  39  35  36  36  39  39  29  40  45  38  44  30  31  34  42  37  45  38  37  32
40  37  38  28  41  30  41  39  38  35  43  39  36  32  32  43  40  38  38  36  33  43  32  36
33  40  30  35  36  38  40  38  34  38  38  38  31  42  37  36  32  43  35  31  45  32  37  42
31  34  40  42  30  32  37  29  38  28  35  31  38  43  42  33  42  28  39  33  33  44  37  31
34  36  37  34  36  31  37  38  28  30  36  42  38  40  40  43  38  33  33  37  43  35  32  29
30  36  30  41  31  39  41  40  30  32]; %values of backfill soil friction angle of 200 models
input_3=[20 21  22  22  21  21  22  21  19  22  19  21  20  22  21  22  21  19  20  21  20  18
19  19  21  21  19  20  21  19  20  22  22  19  19  19  22  19  20  20  21  20  18  18  20  21
20  21  21  22  22  20  22  20  19  18  21  21  20  21  21  20  21  20  19  21  21  21  22  20
19  20  18  20  18  18  19  21  21  22  18  19  18  21  18  20  20  22  22  21  21  21  21  21
21  19  22  22  19  21  19  19  22  20  20  20  22  19  22  20  21  21  19  18  21  21  21  20
22  19  18  19  19  21  21  21  21  18  19  21  18  21  20  22  19  22  22  22  21  20  21  20
22  21  18  21  18  19  22  18  22  22  20  22  20  19  20  19  20  21  21  18  21  20  19  21
22  18  22  18  19  19  18  18  19  19  18  18  22  22  22  20  22  21  18  18  22  20  18  20
```

```
20  21  18  22  19  20  22  22  20  20];%values of backfill soil unit weights of 200 models
input_4=[55 220 147 258 241 148 77  64  256 280 267 191 17  105 73  295 193 89  216 124 237
166 264 48  90  106 40  281 299 49  109 76  100 257 37  54  285 83  40  99  136 143 253 110
138 96  158 140 291 228 53  21  22  158 132 68  252 161 290 122 309 111 226 130 132 189 198
112 178 70  248 20  109 171 116 20  232 285 202 80  302 39  279 174 290 14  172 26  184 257
10  107 248 36  107 227 175 238 123 253 123 9   202 57  201 152 41  296 189 244 62  195 34
260 213 32  233 96  297 121 135 19  184 117 47  107 279 115 155 150 41  136 284 49  300 221
117 32  263 272 70  208 225 223 154 162 310 252 28  314 46  256 311 142 254 228 205 195 250
271 74  229 216 191 15  264 82  156 26  223 156 295 89  136 314 188 302 262 131 151 283 145
114 108 28  123 77  15  244 35  249 37  202 215 254 81  49  100 276 234];%values of backfill
soil Young's of modulus of 200 models
input_5=[49 22  55  34  32  15  53  36  22  43  18  10  55  44  56  45  37  23  47  52  45  56
51  23  42  36  21  50  21  42  19  15  40  52  56  41  16  20  53  56  49  48  40  41  38  24
38  25  42  52  31  40  29  41  22  18  42  56  22  45  59  52  37  17  34  33  59  38  47  35
38  14  31  26  35  41  43  51  54  25  45  51  37  59  50  24  47  52  45  39  50  51  57  55
51  29  25  52  58  18  58  25  31  48  53  37  54  21  56  50  41  37  46  42  43  34  41  42
59  46  11  36  47  29  53  58  38  58  33  26  35  33  51  58  35  34  46  57  48  48  34  33
44  31  15  51  28  49  18  20  12  46  14  16  49  25  52  12  50  34  35  49  25  51  52  51
14  50  46  21  39  51  51  12  30  52  43  46  20  21  48  23  44  54  59  60  19  21  53  51
56  48  32  10  9   60  36  57  59  45];%values of clayey soil cohesion of 200 models
input_6=[25 17  28  21  6   11  31  30  26  28  28  7   31  31  12  14  2   15  28  15  23  15
29  4   37  31  32  10  20  10  27  5   11  15  30  24  0   2   26  20  18  29  20  25  30  7
1   15  2   19  10  21  11  28  9   13  8   17  21  25  18  17  25  12  37  35  16  28  18  14
17  7   26  5   15  33  6   7   15  19  0   15  32  26  2   28  27  15  26  7   31  15  30  9
20  19  23  2   28  15  27  15  20  15  30  5   5   7   16  34  19  15  17  30  31  2   25  25
13  6   27  17  0   34  21  24  13  36  16  21  22  30  7   25  23  11  14  24  0   20  24  30
2   26  26  30  16  13  22  14  15  29  19  27  27  11  30  1   24  2   24  28  25  24  31  24
11  18  16  15  15  29  20  32  11  18  14  29  13  23  4   8   14  2   13  3   30  26  10  3
17  20  6   28  12  13  15  13  24  7];%values of clayey soil friction angle of 200 models
```

```
input_7=[20 23  20  20  23  22  25  18  23  18  18  18  23  16  18  21  18  18  21  20  24  18
17  22  23  21  21  19  20  20  23  25  23  22  20  16  17  17  25  18  22  22  23  18  17  18
20  17  16  24  23  24  21  22  21  20  25  23  22  16  22  23  20  24  16  17  17  18  17  18
21  18  25  17  21  24  20  19  20  18  22  17  20  25  23  25  20  23  25  18  24  19  18  17
19  17  22  18  24  23  24  24  18  18  20  16  24  23  22  16  20  21  19  23  25  17  17  17
20  25  23  22  21  22  23  19  24  17  24  20  25  18  17  20  23  22  24  16  19  22  25  16
22  20  19  17  22  23  16  21  19  17  21  23  20  23  18  16  18  21  19  24  22  22  20  25
19  18  25  16  20  16  18  16  21  20  17  25  18  23  24  24  20  24  24  21  17  20  23  19
16  16  19  22  18  20  16  18  18  18];%values of clayey soil unit weights of 200 models
input_8=[22.4   44.1    20.7    23.1    14.9    27.9    38.1    44.7    38.5    21.5    10.1
10.0    32.9    43.4    13.5    46.7    6.7 47.2    43.2    21.4    48.2    19.8    35.2    6.0
39.2    31.8    31.9    20.4    48.5    29.8    41.4    21.7    27.5    17.6    27.0    28.3
42.7    25.7    33.9    41.6    29.5    39.2    26.7    4.0 36.3    45.0    14.5    26.4
47.0    8.8 42.6    21.0    7.4 6.4 3.2 0.3 32.9    46.0    12.4    5.2 23.7    17.0    44.0
2.0 5.3 4.1 47.4    24.7    11.6    49.0    6.1 20.2    35.0    14.2    14.0    37.0    29.3
36.0    43.5    45.9    30.3    48.6    41.9    27.4    25.3    44.1    43.0    47.3    11.4
25.3    23.7    38.1    13.2    8.2 38.1    38.1    5.0 20.7    41.2    19.3    41.2    31.7
16.2    8.2 46.8    25.0    24.4    15.7    29.1    46.2    21.4    6.5 0.7 37.3    20.8
31.5    35.5    28.8    23.6    20.5    35.6    17.9    25.1    6.6 22.9    36.9    8.6 9.6
24.9    40.6    5.6 28.7    17.8    26.8    13.9    47.7    28.1    44.4    13.1    27.0
42.5    33.0    22.6    30.4    8.2 38.2    30.1    13.6    44.3    6.3 7.4 43.7    39.4
38.8    12.4    19.5    40.6    6.9 3.1 3.7 42.9    38.7    14.8    45.5    29.7    44.3
12.4    17.5    47.8    42.9    7.2 44.2    20.7    33.3    23.8    29.0    21.3    22.4
19.0    10.9    42.9    41.4    37.3    30.1    27.0    45.4    22.1    45.7    43.3    2.9
42.8    26.9    38.6    42.3    22.8    35.6    30.3    29.9    24.5    24.4];%value of clayey
soil Young's of modulus of 200 models
input_9=[5.0    2.00    4.00    4.50    5.00    2.00    6   6.00    3.75    2.25    3.50
1.50    4   6.25    2.75    3.75    6.00    3.5 6.25    3.50    6.50    3   5.25    3.75    3
5.25    3.75    7.00    3.75    7.00    3.00    2.50    6.00    9.25    4.75    3.75    2.50
```

```
4.00    6   3.75    3.25    6.75    6   5.25    6.50    3.5 3.75    4.00    4.75    3.00    4
6.00    3.75    3   3.75    3.25    7.00    4.25    3.25    5.25    4.25    8.50    3   2.75
5.25    4   4   6.50    5.25    5.25    6.75    2.50    2.50    3.25    6.50    5.25    3.50
5.75    3   3.5 4.25    3.25    3.25    8.5 4.25    2.75    7.00    5   7.00    5.75    4.00
5.50    6.50    4.50    5.50    5.50    3.00    2.50    4.00    2.75    4.00    4.25    3.25
5.25    5.00    2.75    4.75    3.00    2.75    6.00    5.75    5.50    6.50    6.75    5.75
4.75    2.75    4.00    4.75    4.00    1.75    6.25    4.25    2.25    3.00    6.25    5.75
5.75    4.00    3.00    3.75    4.00    3.50    6.00    3.75    3.25    5.75    3.75    5.50
6.50    5.25    3.75    6.75    4.25    2.50    5.00    2.75    4.00    2.50    2.50    1.75
6.50    1.75    2.25    5.00    4.25    6.25    1.75    3.75    5.00    3.25    5.75    2.25
5.00    3.25    6.75    2.00    4.25    6.00    2.75    4.00    7.00    7.50    2.25    4.25
6.00    6.25    6.00    3.00    2.25    6.50    3.75    6.00    4.00    6.25    8.5 2.5 3.25
7   5.25    7.50    6.25    2.25    1.75    1.75    5.5 4.75    4.00    7.50    4.50];%values
of retaining wall free height of 200 models
input_10=[2.5   1.00    2.00    5.75    6.50    1.75    5.75    14.00   7.25    0.5 8.75
1.50    1.25    7.25    1   2   13.00   3.75    6.25    1.25    8.25    1   3.00    5.50    1
7.50    5.00    6.50    11.25   6.75    4.00    8.00    13.25   14.00   1.75    1.75    4.25
12.50   3   1.25    1.25    5.75    6.5 3.25    11.25   3.75    2.25    7.50    3.25    1.25
3.5 7.75    3.75    1.25    5.75    6.50    13.25   2   4.25    2.75    1.50    9.50    1.75
4.25    5.50    3.25    1.75    11.25   2.75    5.75    9.00    8.50    1.00    2.75    9.25
3.5 1.50    3.75    1   4   2.25    1   1   8.5 1.25    2   9.25    3   11.00   6.75    1.25
3.25    4.00    2.25    3.00    13.25   2.25    1.00    1.25    4.75    1.25    5.00    2.00
3.25    2.00    1.00    2.25    3.25    1.00    3.25    5.00    6.75    5.25    6.75    5.75
4.00    1.25    2.00    2.25    1.50    2.25    10.25   2.00    1.00    1.00    3.50    7.25
2.50    2.50    2.00    2.25    2.50    1.25    3.75    2.25    1.50    5.25    1.50    2.75
6.00    7.75    2.00    13.00   4.25    2.50    2.25    1.50    1.75    2.75    2.00    2.50
11.25   1.25    3.00    2.50    4.00    3.50    1.75    1.25    7.75    1.50    3.50    1.25
2.00    1.00    7.00    3.00    1.75    5.75    2.00    2.00    6.50    6.25    3.50    4.75
4.25    5.00    3.25    4.25    1.25    6.25    4.25    6.25    1.75    3.50    6.25    2
```

4.00 5.25 3.5 8.00 5.5 1 5.75 5.25 2.5 4.25 1.50 6.75 2.75];%values of retaining wall embedded depth of 200 models

input_11=[1 0.5 1 1.5 1.25 0.75 1.25 0.75 0.75 1 0.75 1 1 1 1.25
1 1.25 1.25 1.5 1.25 1 0.5 1.25 0.75 1 1 0.5 1 1.25 1 0.75 1
1.25 1.5 1 0.5 0.75 1.25 0.75 1 1.25 1 1.25 1.5 0.5 0.5 0.75 1.5 1 1
1.25 1 1.25 0.75 0.75 1.25 1.25 1 1.25 0.75 1 1 0.75 0.5
0.75 1 1.5 0.75 0.75 0.75 0.75 0.5 1.5 0.75 0.75 0.75 0.75 1.25
1.25 1.25 0.75 1 0.75 0.75 0.75 1 1.25 0.5 1 1.25 1 0.75 1.5
1.25 0.75 1 0.5 1 0.5 1.5 0.5 0.75 1 1 1 1.25 0.75 1.25 1.5 1 1 1
1.25 1.25 1.25 0.5 1.25 0.75 1.25 0.75 1.25 1.5 0.75 1.5 0.5 1.25
0.75 0.75 0.75 0.75 1.25 1.25 1 1.25 0.75 1.5 0.75 0.75 1 1
1 0.75 1.5 0.75 1.5 1 0.75 1 1 1.5 0.75 1.25 0.5 1.25 1.25 1 1.25
0.5 0.75 1.5 0.75 1.5 1 1 0.75 1.25 0.5 0.75 0.75 0.75 1.25 1.5 1.25
1.25 1.25 1.25 1.25 1 0.5 1.25 1.25 0.75 1.5 1.25 1 1.25 1.25
1.5 1.5 1.5 1.5 1.25 1.25 0.75 0.5 1.25 0.5 1 1.5 1];%values of retaining wall thickness of 200 models

input_12=[1125106 1050759 726230 749602 1090178 837517 1005536 987126
1103341 709078 1135916 969742 895565 1070677 1046517 967035 703394
978106 703078 765782 975416 897387 1149355 738893 1108965 743782 1150628
1022344 942513 1085462 881766 1096506 949846 1105146 896118 779715
1081705 754741 1010299 799362 805595 1003680 692511 732027 1106731
1047976 906244 948275 1121572 1030254 737967 737797 1007597 1068473
824512 692552 894792 991211 969323 904192 943736 1148533 862776 968168 896126
914332 721011 978517 934799 759730 1017867 1131896 924199 802922 962361
753416 707047 744429 1035688 713630 1103809 845731 1074505 1101455
1034884 1137481 822417 926898 1049763 776202 964895 1034083 972029
735283 1034083 761964 711252 771263 1052548 812624 1052548 753682 994453
991164 752053 832622 991893 1073769 1020754 924573 1043321 716636 917299
1107295 1090142 1135082 1065744 753136 726080 1141747 762877 720007

```
925735  782914  823087  771626  1034534    1037255    1006702    942301  1083762
887754  1058765    1107325    1003695    865357  1053188    860002  966153  1091735
699417  960039  730351  1026710    893472  757076  856251  945657  1032435    851665
848901  917274  923173  1000793    753665  1035158    871250  701003  1042987    1106052
699916  698011  693943  975094  827263  958596  897833  1107442    1080558    797415
745816  1132329    700966  1105974    731874  974438  824030  859412  976564  928973
1096175    842356  925617  1111265    899082  965515  998263  949483  785758  882212
1116838    991567  920209  1129907    1004124    705803  1041786    943939  1101381
972109 ];%values of retaining wall Young's of modulus of 200 models
input_13=[3.95  3.15   3.95   4.80   3.75   1.95   1.3 2.80   1.65   4.85   1.50
1.00   1.55   0.95   2.8 1.95   0.70   2.85   2.9 4.95   0.70   0.75   1.00   1.55
0.9 1.60   2.10   2.45   2.45   1.65   2.40   4.55   1.05   3.00   1.40   0.35
1.05   3.90   0.75   0.85   1.8 3.55   3.6 4.55   3.15   2.45   2.55   3.80   2.00
2.85   1.65   1.90   2.75   2.8 5   2.55   3.25   2.75   4.5 0.55   4.70   4.20   1.8
2.95   0.45   1.25   3.75   1.75   3.5 4.85   1.05   2.05   3.20   2.65   1.55   2.4
3.20   1.2 2.8 4.05   0.7 1.85   2.75   2.35   2.3 3.1 1.15   0.6 2.05   3.95   4.55
3.45   4.55   2.20   3.45   3.35   1.00   0.85   0.90   0.50   0.90   4.10   1.95
2.20   4.50   4.00   1.25   4.05   0.75   2.45   2.60   2.10   3.00   2.95   4.45
2.75   4.65   4.50   0.90   2.05   4.90   2.90   2.85   2.35   3.05   0.60   1.4
4.80   2.40   0.45   2.00   1.90   1.50   2.40   3.85   1.80   1.85   2.15   3.80
2.30   4.70   4.50   2.15   5.00   2.75   2.80   2.35   2.85   0.85   1.70   1.20
3.45   3.35   4.90   2.10   1.30   3.35   4.00   4.75   2.30   1.20   0.70   2.90
2.05   0.50   1.75   0.95   1.15   1.00   4.10   1.55   4.05   0.80   1.00   3.45
0.45   4.05   3.80   0.80   1.45   4.65   4.90   0.90   4.80   4.35   3.55   2.75
3.70   3.7 2.95   0.35   2   1.45   2.55   0.45   0.5 2.00   2.85   0.30
2.20];%velues of installation distance from pile to wall of 200 models
input_14=[0.5  0.45   0.35   0.40   0.30   0.20   0.4 0.30   0.45   0.35   0.50
0.45   0.4 0.30   0.35   0.25   0.35   0.35   0.45   0.45   0.60   0.55   0.55
0.55   0.4 0.40   0.55   0.40   0.30   0.40   0.35   0.50   0.35   0.25   0.45
```

```
0.35    0.55    0.15    0.5 0.3 0.6 0.55    0.4 0.45    0.40    0.6 0.45    0.25    0.30    0.60
0.2 0.20    0.35    0.4 0.4 0.30    0.20    0.2 0.5 0.50    0.35    0.45    0.6 0.25    0.35
0.2 0.45    0.55    0.3 0.25    0.15    0.30    0.20    0.55    0.35    0.5 0.55    0.5 0.45
0.5 0.55    0.55    0.5 0.3 0.45    0.35    0.20    0.4 0.30    0.30    0.50    0.50    0.45
0.30    0.50    0.35    0.55    0.25    0.35    0.50    0.35    0.35    0.20    0.30    0.25
0.25    0.55    0.45    0.45    0.30    0.50    0.55    0.30    0.50    0.30    0.30    0.30
0.55    0.25    0.20    0.45    0.55    0.50    0.35    0.25    0.35    0.3 0.45    0.30
0.35    0.45    0.45    0.35    0.25    0.30    0.60    0.50    0.25    0.30    0.40    0.60
0.35    0.15    0.25    0.25    0.40    0.20    0.20    0.20    0.40    0.35    0.45    0.30
0.20    0.25    0.40    0.45    0.40    0.50    0.40    0.40    0.20    0.30    0.55    0.20
0.50    0.50    0.50    0.30    0.40    0.20    0.50    0.20    0.15    0.50    0.25    0.25
0.45    0.50    0.15    0.30    0.30    0.55    0.40    0.15    0.6 0.5 0.55    0.55    0.55
0.50    0.3 0.5 0.50    0.30    0.2 0.25    0.40    0.45    0.40];%values of pile diameter of
200 models
input_15=[10.75 20.50   23.00   24.00   14.75   10.75   11.5    15.00   22.00   15.5    8.75
20.00   8   21.00   15.25   6.25    21.50   11  16.75   18.25   16.25   4.25    9.50    15.75
6   10.25   21.25   23.75   12.75   25.25   4.75    10.75   8.75    14.50   13.75   10.75
25.00   7.50    15  7.5 9.5 19.75   24.5    6.25    21.75   21.5    14.50   15.00   11.75
17.75   11.5    3.25    10.50   20.25   18  7.25    20.75   15  20.5    21.75   7.00    22.75
9.25    24.25   6.00    4   7.5 15.25   20.75   21.75   6.75    13.75   21.25   9.25    21.75
12.25   9.00    17  5.25    11.25   12.25   13  20.75   23  11.25   24.5    14.00   13.25
12.25   17.75   17.25   10.00   12.75   22.25   7.00    25.25   18.25   21.50   6.50    7.50
6.50    8.50    15.75   10.75   6.50    9.25    13.00   17.25   21.00   6.25    18.50   10.00
6.50    6.00    25.75   24.25   16.25   4.00    9.25    18.25   3.50    5.50    23.50   22.00
14.25   17.50   25.75   5.00    15.75   23.75   5.50    19.00   18.50   9.75    9.00    20.25
25.50   25.00   15.25   13.00   20.25   22.50   20.50   13.50   11.00   11.00   4.00    7.50
6.75    3.75    18.00   23.50   5.50    13.50   10.00   19.50   13.00   10.75   18.00   12.00
13.50   24.75   6.50    17.50   3.50    12.00   16.00   10.75   11.75   7.75    5.25    25.25
13.00   3.25    22.00   22.25   7.50    6.25    17.75   22.75   12.00   7.25    23.75   19.00
```

11.25 16.75 11.75 8.50 25.5 7 8.50 4 3.25 20.25 12.00 19.75 25.75 15.50 4.75 11.25];%values of pile installation depth of 200 models

input_16=[3641.53 2993.89 9759.04 5070.49 2048.96 1164.41 9546.62 3877.89 7605.78 5894.22 3089.42 941.97 6669.37 12142.14 1475.51 1235.24 2970.81 1491.03 7644.64 2374.46 4520.89 724.57 4858.76 1149.09 11964.56 4214.01 14776.06 3004.55 6576.71 2982.60 2643.10 1413.65 1549.97 9532.13 8062.39 2498.96 508.07 13860.00 6127.46 1739.48 1451.38 10707.33 5330.89 2454.61 10938.64 1301.10 695.40 2659.57 1271.57 3259.14 1735.92 1269.25 1405.13 8682.51 1844.12 1408.87 3965.07 2954.11 3982.29 5680.91 1579.91 4504.78 2814.33 2930.78 2804.28 1120.22 1214.98 7040.28 3367.14 3116.51 6669.16 1763.32 8348.34 588.29 3618.19 11687.66 582.85 1627.80 847.24 1770.49 377.00 1433.55 14119.99 9968.54 652.37 11343.59 2763.54 2263.43 9367.19 2345.65 12804.35 1712.60 7497.53 2028.39 2943.20 4631.32 4030.77 794.30 3983.30 1180.71 3529.21 2307.95 3057.19 1887.34 6174.32 656.50 1059.35 1236.99 3062.49 9997.14 3331.18 2665.67 3421.77 2181.35 19847.05 1580.53 4642.32 1942.65 1648.30 1638.98 1360.52 1922.44 417.80 21252.16 3454.35 4857.59 4026.59 5321.95 2564.83 4424.75 1518.23 9189.88 1168.99 4266.10 2384.21 1787.20 3859.25 5696.61 1039.55 3314.23 5967.10 9919.54 3645.37 4790.67 3277.61 6259.94 834.46 1304.46 1539.57 511.76 2064.74 10917.35 809.70 5536.43 4441.10 2125.93 7367.29 292.70 4119.93 1735.61 3199.20 12132.50 2195.52 4662.70 3512.97 3626.04 1246.05 1588.04 2852.72 784.82 1634.14 10448.32 3648.41 3056.10 2181.26 4007.57 2674.25 7162.74 1793.25 5664.25 3300.17 3385.05 3337.41 1007.21 2158.05 1920.72 5211.82 2633.54 2808.96 790.70 1352.29 2129.42 266.28 8215.11 1274.72 2829.08 3479.09 1768.80 839.47 1090.13]; %values of factored ultimate axial-loading of 200 models

target_1=[-0.01321 0.00171 -0.01225 0.004951457 -0.00899 0.00169622 -0.13716

-0.07203 -0.01163 0.00213 -0.02265 0.00338 -0.08656 -0.0383 0.00201 -0.01175 -0.07201 0.00343 -0.03193 0.00427 -0.05274 -0.02997 -0.11083 -0.01992 -0.18811 -0.08183 0.0181 -0.0215 -0.00537 -0.05906 -0.01139 0.00984 -0.058 -0.066 -0.04983 -0.03203 0.002219 -0.03992 -0.04355 -0.1257 -0.00476 -0.05196 -0.03025 -0.04709 -0.03604 -0.00651 -0.00677 0.00489 -0.01205 -0.00085 -0.0392 -0.15984 0.0119 0.032559 0.009236 0.01299 -0.05024 -0.0952 0.00587 -0.01314 -0.00126 -0.09764 -0.02001 0.00718 -0.13067 -0.015667 -0.01394 -0.1143 -0.02681 -0.05924 -0.13184 0.01443 0.00346 -0.00398 -0.07365 -0.12577 -0.0026 -0.01949 -0.002 0.00373 -0.00461 -0.00413 0.01019 -0.07624 -0.00583 0.01751 -0.05871 -0.10744 -0.06647 -0.01869 0.0572 -0.03744 -0.03912 -0.002 -0.06771 -0.02412 -0.00364 -0.00176 -0.09307 -0.00779 -0.05513 0.01853 0.0181 -0.01344 -0.02345 0.00184 -0.01889 0.00336 -0.00806 -0.10973 -0.01816 -0.04176 -0.09214 -0.03858 -0.02357 -0.03812 0.0027 -0.02192 -0.01417 0.00423 0.00505 -0.08241 -0.00687 0.00201 0.004698 -0.02483 -0.03157 -0.12133 -0.0069 0.00307 -0.05316 -0.0674 -0.00083 -0.04406 -0.00364 0.00253 -0.05547 -0.02022 -0.00804 -0.03281 -0.09715 -0.01438 -0.05958 -0.01078 0.00776 -0.03075 -0.00336 -0.00443 -0.00204 -0.0008 0.00886 -0.05091 0.00099 0.008 -0.01671 0.00624 -0.05593 0.00426 -0.028577 -0.01637 -0.0072 -0.01568 0.00275 -0.0892 -0.1384 -0.06408 0.00293 -0.01056 -0.07018 0.01213 -0.01842 -0.03023 -0.08904 -0.01109 -0.00685 -0.02011 -0.02355 -0.0778 0.00361 0.00277 -0.0244 -0.00427 -0.02271 0.00469 -0.03996 -0.08216 0.001818 0.010759 -0.02601 -0.0146 -0.06954 -0.16166 -0.00153 0.00388 0.00362 -0.00997 -0.04156 -0.01182 -0.10695 -0.0835];%values of maximum horizontal displacement of retaining wall obtained from RS2 of 200 models

target_2=[0.00 0.80 0.00 4.979 0.00 3.25 0.00 0.00 0.00 0.00 0.00 0.00 0.00 0.00 0.00 0.00 0.00 3.916666667 0.00 0.00 0.00 0.00 0.00 0.00 0.00 0.00 5.25 0.00 0.00 0.00 0.00 7.537 0.00 0.00 0.00 0.00 6.75 0.00 0.00 0.00 0.00 0.00 0.00 8.50 0.00 0.00 0.00 5.3235 0.00 0.00 0.00 0.00 7.50 4.25 5.519 9.75 0.00 0.00

```
0.00    8.00    0.00    0.00    0.00    7.00    0.00    7.25    0.00    0.00    0.00    0.00

0.00    6.750   0.00    0.00    0.00    0.00    3.50    0.00    0.00    4.124   0.00    0.00

4.25    0.00    0.00    0.00    0.00    0.00    0.00    0.00    5.25    0.00    0.00    0.00

0.00    0.00    5.25    0.00    0.00    0.00    0.00    5.32    2.844   0.00    0.00    0.00

0.00    4.083   0.00    0.00    0.00    0.00    0.00    0.00    0.00    0.00    0.00    0.00

0.00    5.50    0.00    0.00    0.00    3.25    4.00    0.00    0.00    0.00    0.00    5.00

0.00    0.00    0.00    0.00    0.00    4.75    0.00    0.00    0.00    0.00    0.00    5.75

0.00    0.00    0.00    0.00    0.00    0.00    0.00    0.00    0.00    0.00    0.00    0.00

0.00    8.25    0.00    0.00    5.00    0.00    0.00    0.00    0.00    0.00    0.00    0.00

2.33    0.00    0.00    2.75    0.00    0.00    0.00    0.00    0.00    0.00    0.00    0.00

3.94    3.5 0.00    0.00    0.00    7.75    0.00    0.00    0.00    0.00    0.00    0.00

0.00    0.00    0.00    5.2 5.125   0.00    0.00    0.00    0.00    0.00];%values of the
location of maximum horizontal displacement measured from the top of the retaining wall for
200 models
```

The summary of modelling

Model 1:

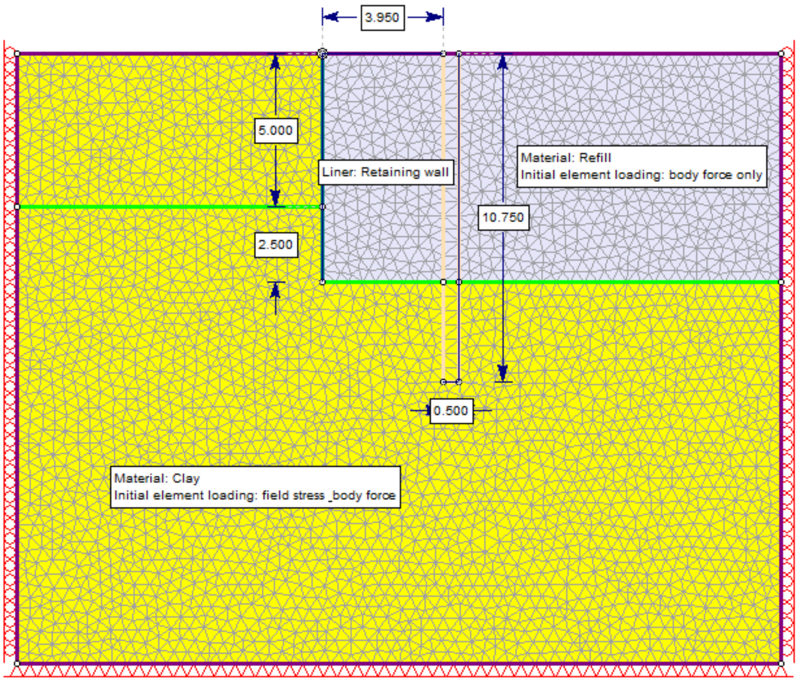

M (Model) 1.1: Stage 1: Initial state of modelling where retaining wall separates two layers of soil

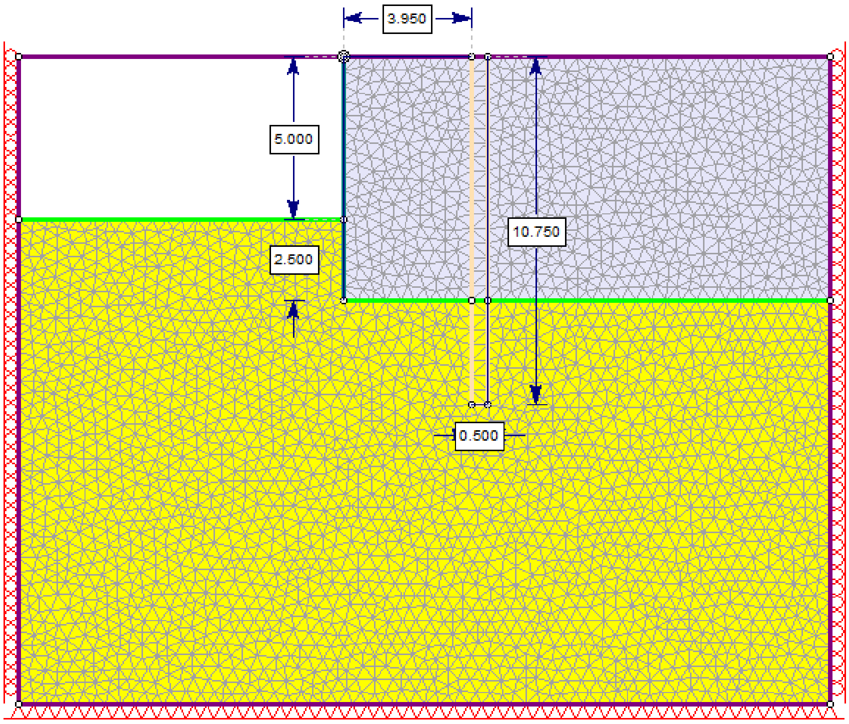

M (Model) 1.2: Stage 2: Open-cut excavation applied on the left side of retaining wall

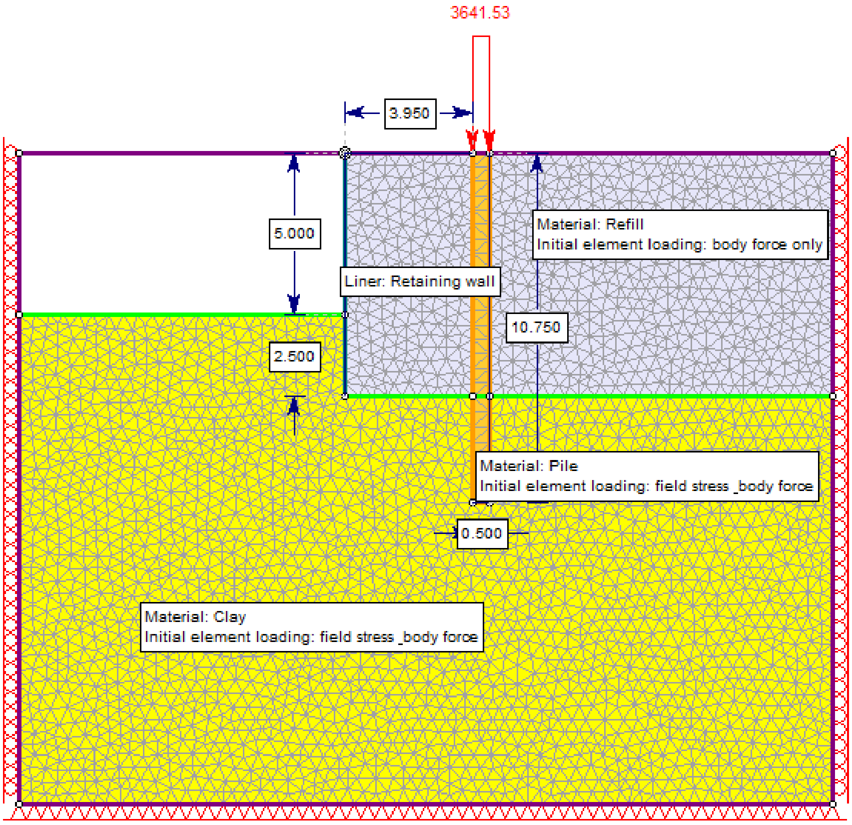

M (Model) 1.3: Stage 3: Pile installed on the right side of retaining wall and factored loading applied on the top of pile

C_1'	ϕ_1'	γ_1	E_1	C_2'	ϕ_2'	γ_2	E_2	H_1	H_2	H_3	E_3	D_1	D_2	L	Qult
0	39	20	55	49	25	20	22	5.0	2.5	1	1125106	3.95	0.5	10.75	3641.53

M (Model) 1.4: Parameter values

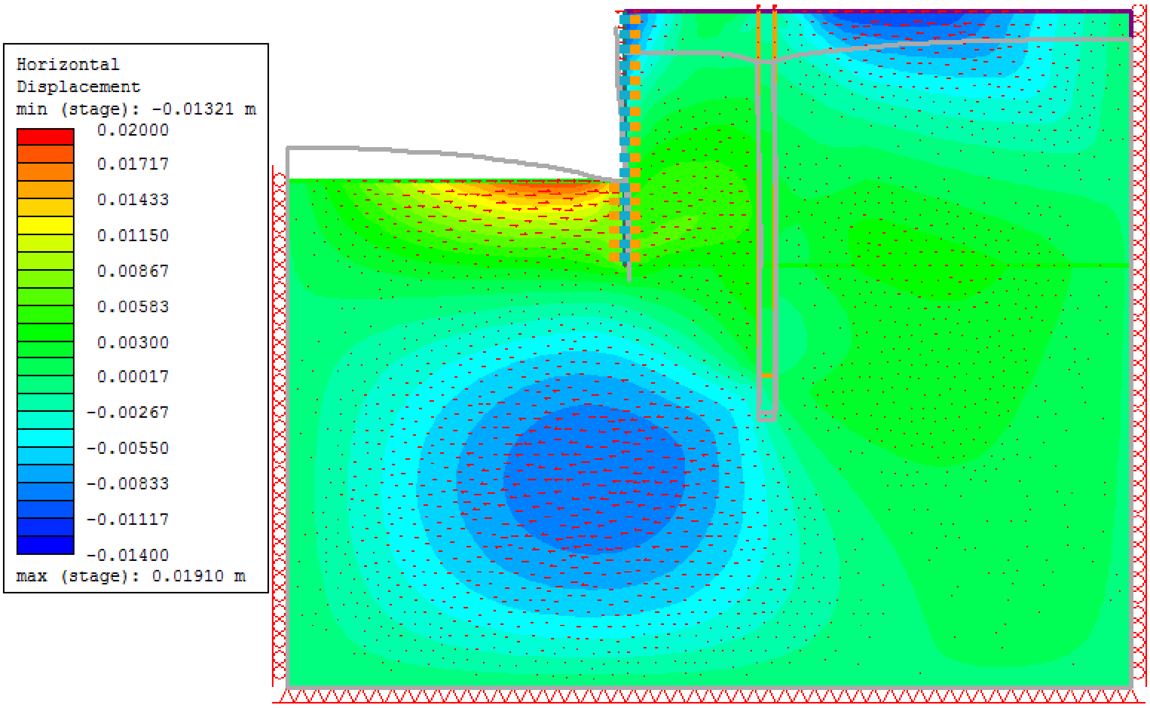

M (Model) 1.5: Deformed model (stage 3)

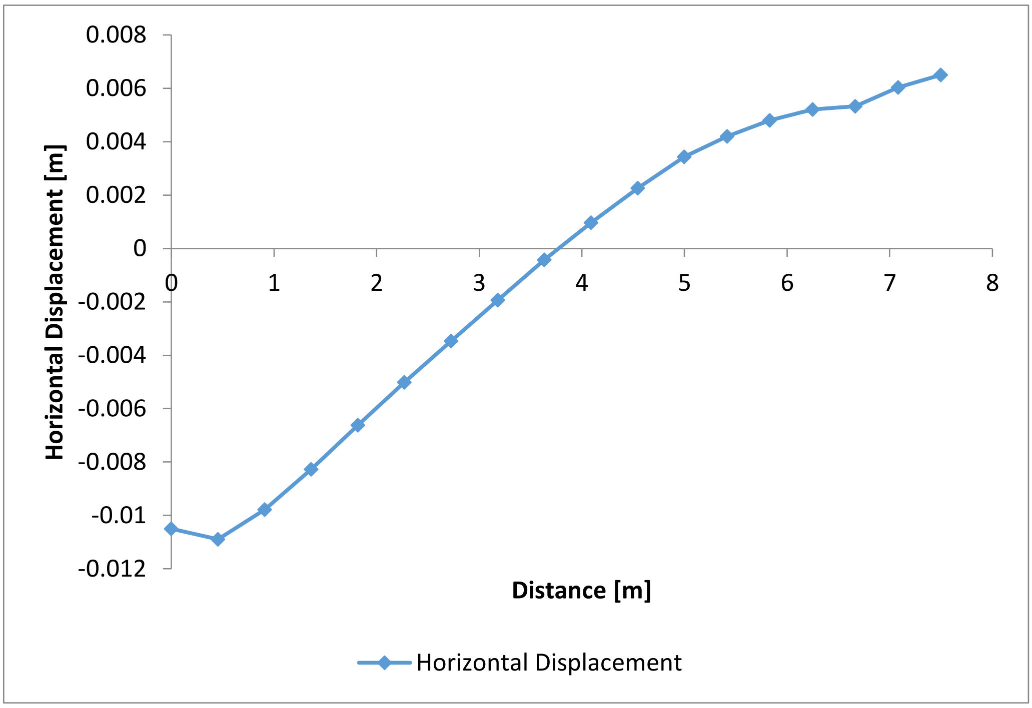

M (Model) 1.6: Horizontal displacement of soil along retaining wall

Retaining wall maximum horizontal displacement: -0.01321m

Distance from point of maximum displacement in retaining wall to the top of backfill soil: 0.0m

Model 2:

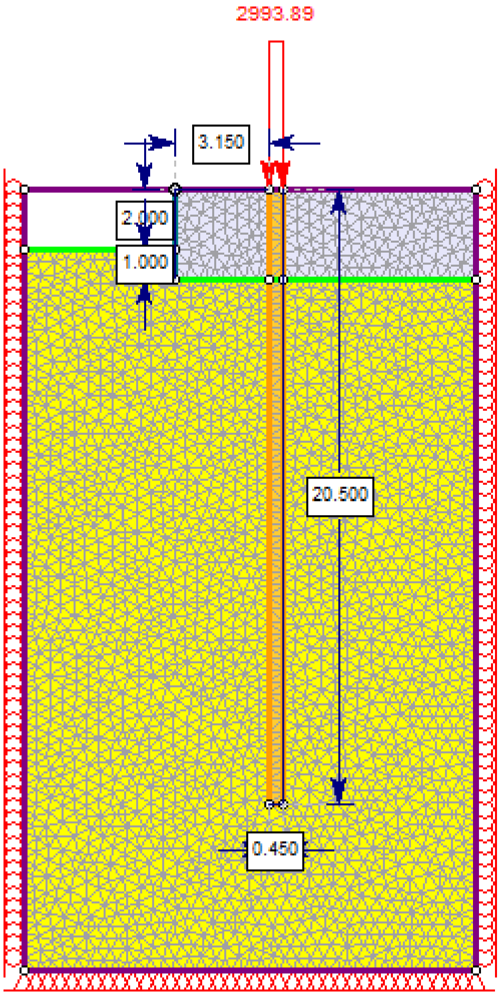

M 2.1: Original model (stage 3)

C'_1	ϕ'_1	γ_1	E_1	C'_2	ϕ'_2	γ_2	E_2	H_1	H_2	H_3	E_3	D_1	D_2	L	Qult
0	36	21	220	22	17	23	44.1	2.00	1	0.5	1050759	3.15	0.45	20.5	2993.89

M 2.2: Parameter values

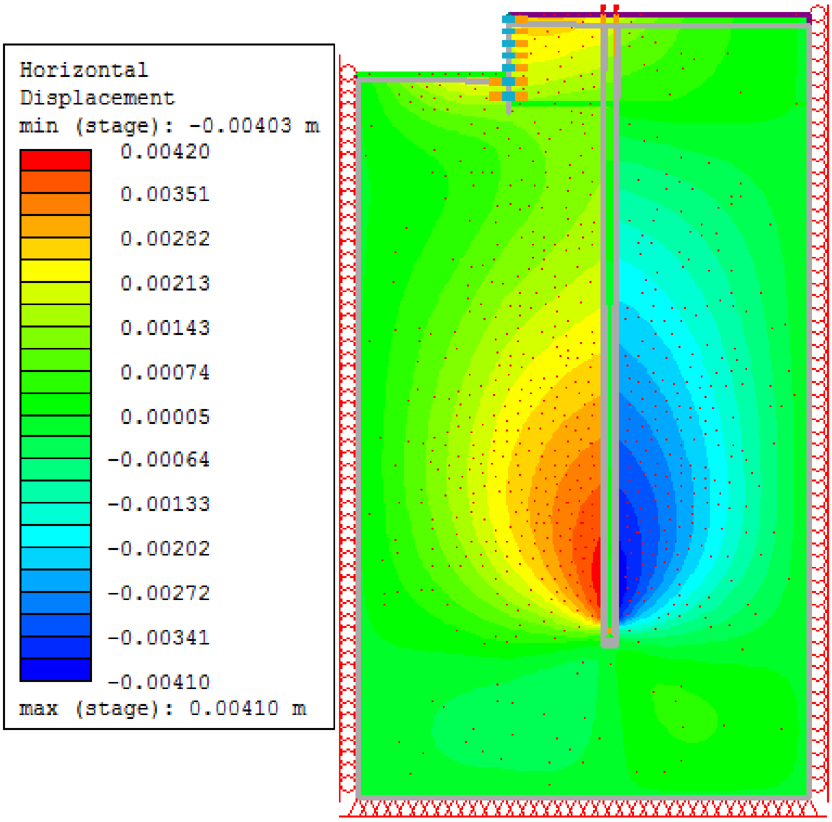

M 2.3: Deformed model (stage 3)

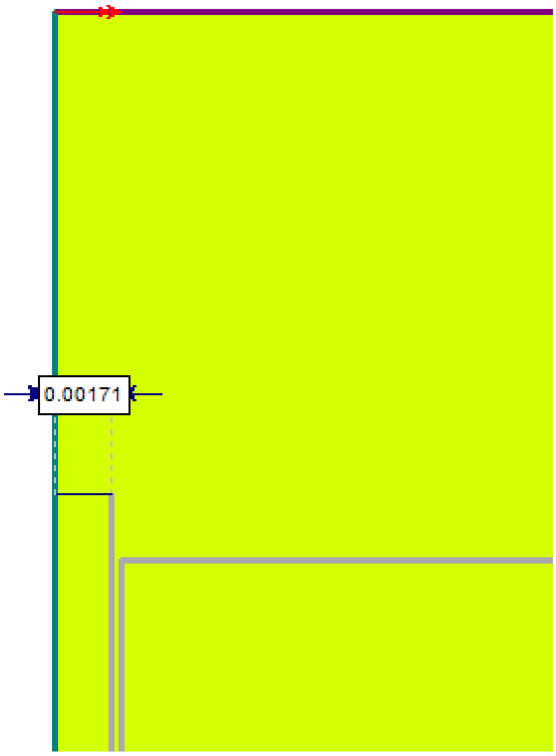

M 2.4: Detailed view of cross-section of retaining wall and soil (stage 3)

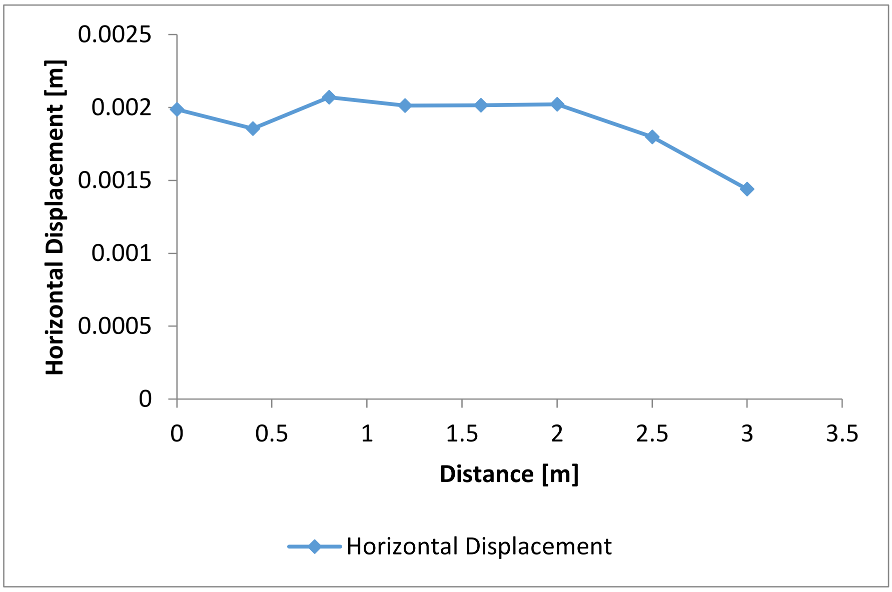

M 2.5: Horizontal displacement of soil along retaining wall

Retaining wall maximum horizontal displacement: 0.00171m

Distance from point of maximum displacement in retaining wall to the top of backfill soil: 0.0m

Model 3:

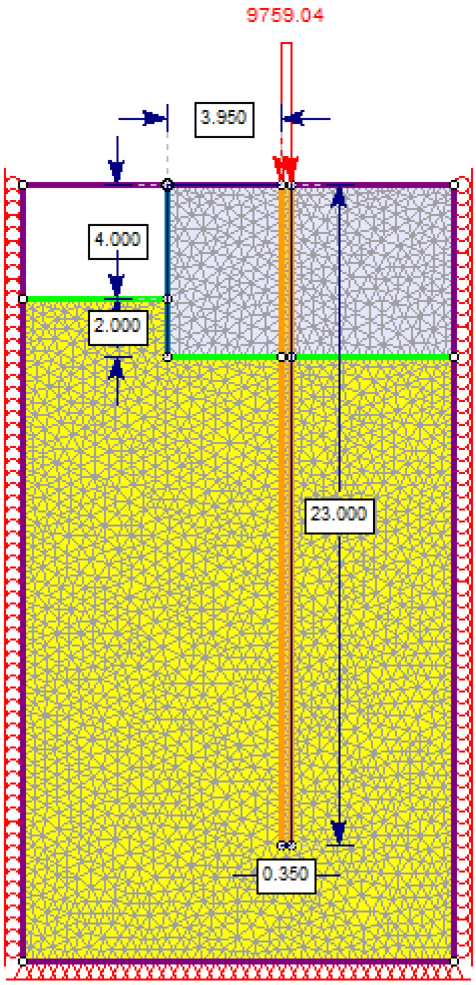

M 3.1: Original model (stage 3)

C_1'	ϕ_1'	γ_1	E_1	C_2'	ϕ_2'	γ_2	E_2	H_1	H_2	H_3	E_3	D_1	D_2	L	Qult
0	29	22	147	55	28	20	20.7	4.00	2	1	726230	3.95	0.35	23	9759.04

M 3.1: Parameter values

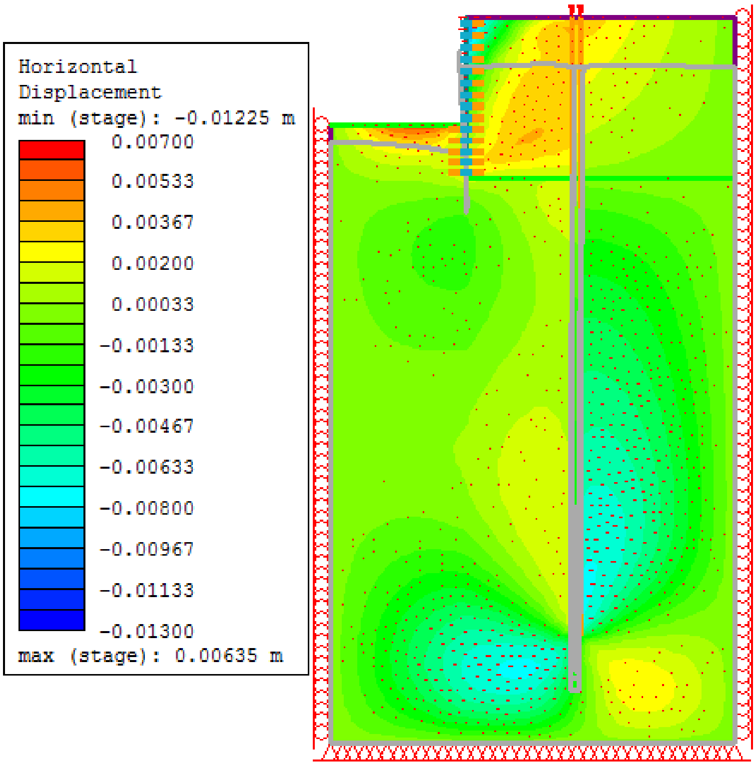

M 3.3: Deformed model (stage 3)

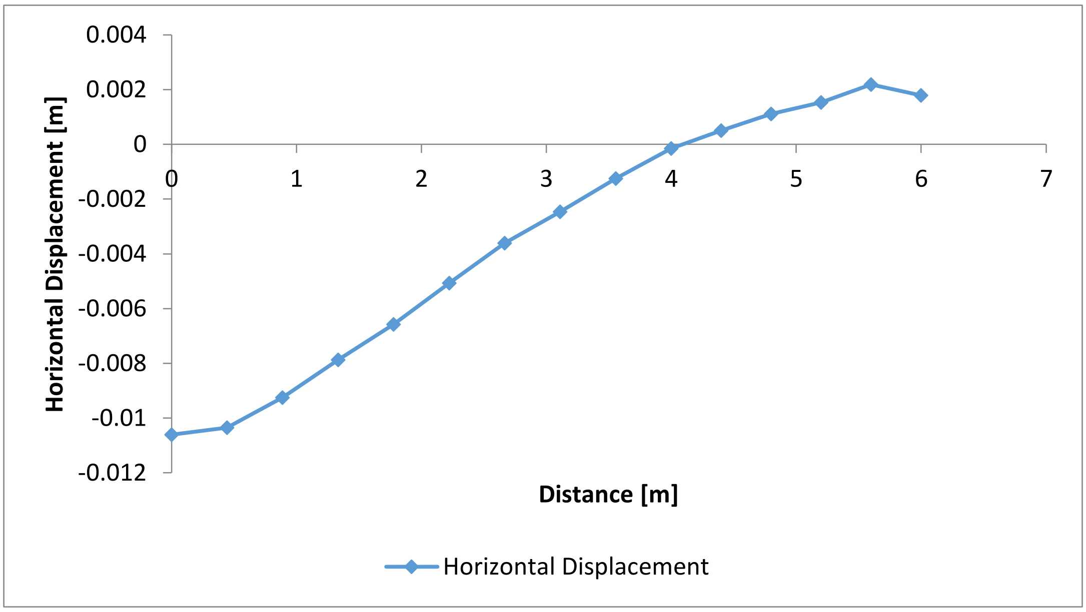

M 3.4: Horizontal displacement of soil along retaining wall

Retaining wall maximum horizontal displacement: -0.01225m

Distance from point of maximum displacement in retaining wall to the top of backfill soil: 0.0m

Model 4:

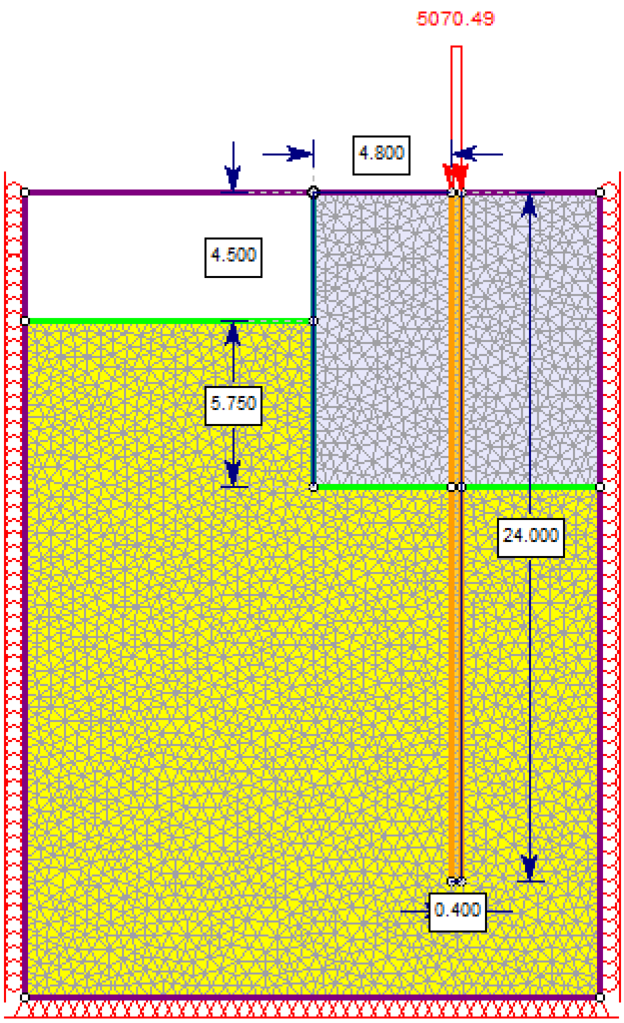

M 4.1: Original model (stage 3)

C_1'	ϕ_1'	γ_1	E_1	C_2'	ϕ_2'	γ_2	E_2	H_1	H_2	H_3	E_3	D_1	D_2	L	Qult
0	30	22	258	34	21	20	23.1	4.50	5.75	1.5	749602	4.8	0.4	24	5070.49

M 4.2: Parameter values

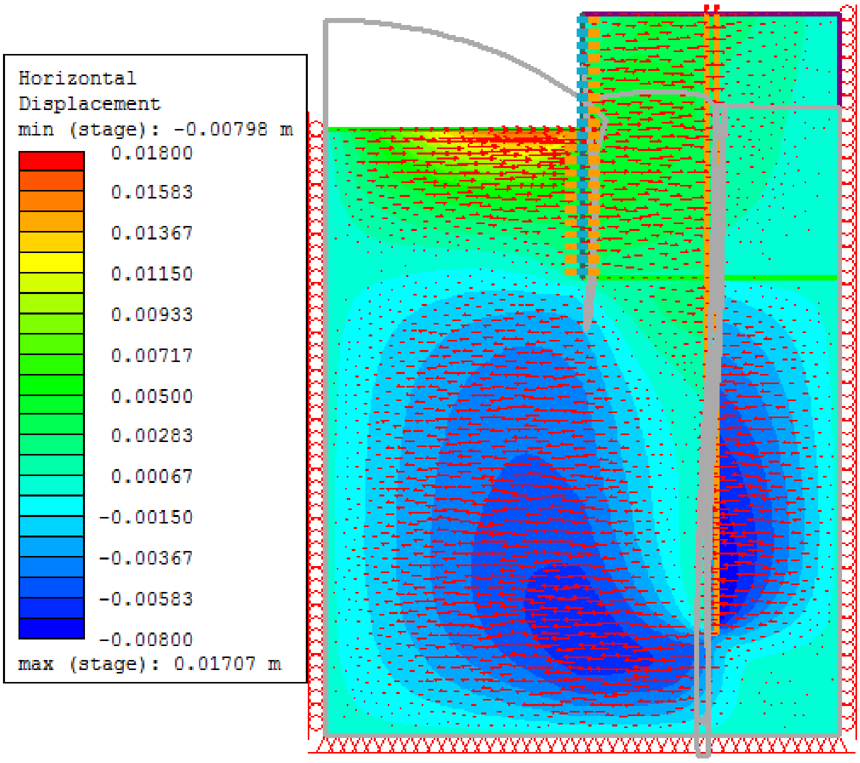

M 4.3: Deformed model (stage 3)

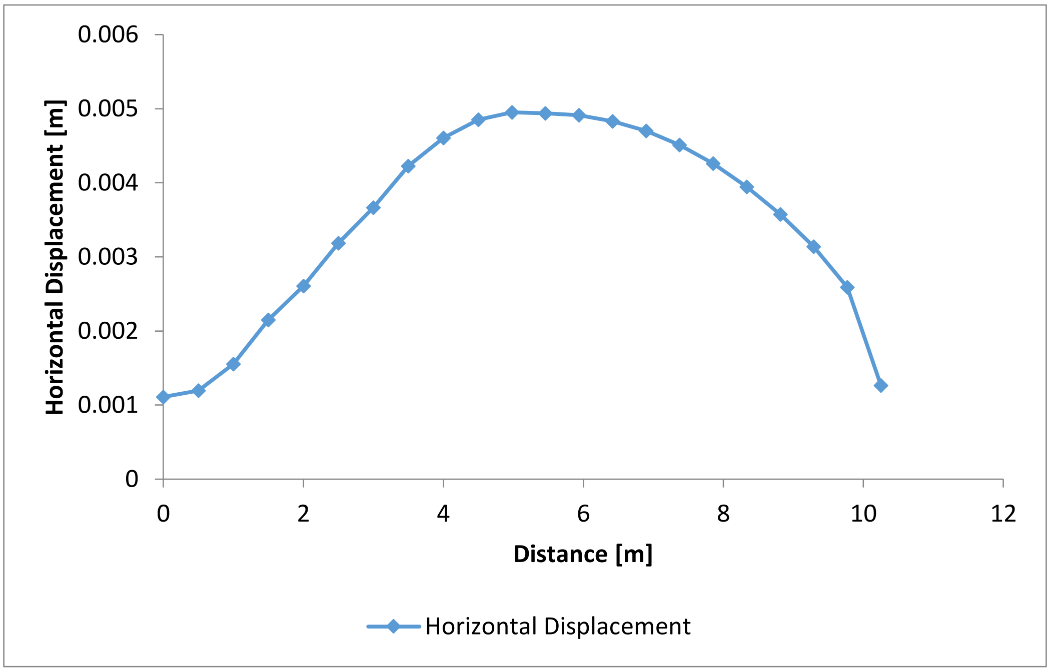

M 4.4: Horizontal displacement of soil along retaining wall

Retaining wall maximum horizontal displacement: 0.004951457m

Distance from point of maximum displacement in retaining wall to the top of backfill soil: 4.979m

Model 5:

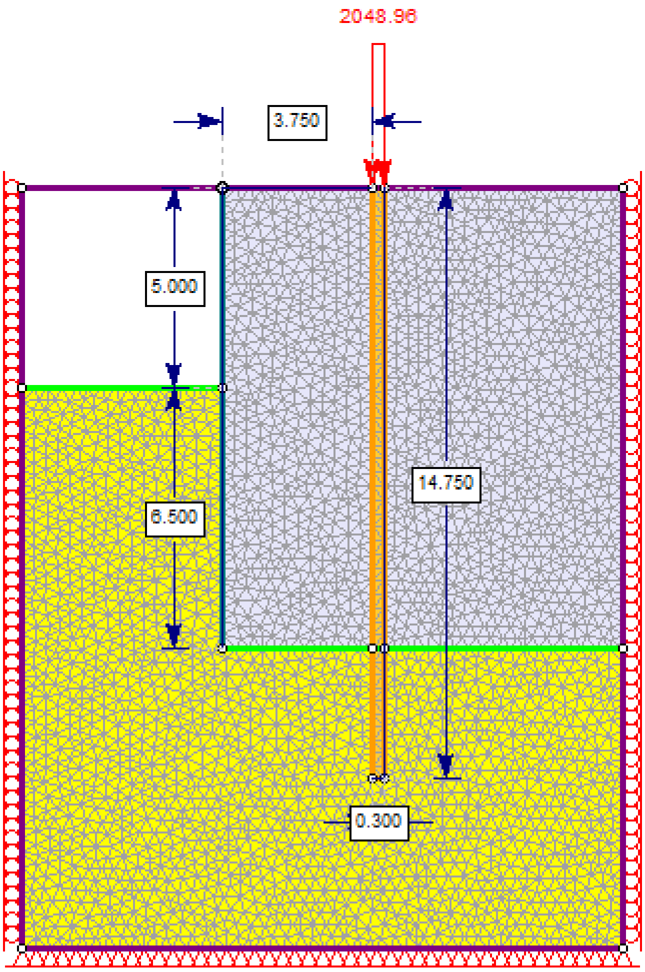

M 5.1: Original model (stage 3)

C_1'	ϕ_1'	γ_1	E_1	C_2'	ϕ_2'	γ_2	E_2	H_1	H_2	H_3	E_3	D_1	D_2	L	Qult
0	39	21	241	32	6	23	14.9	5.00	6.5	1.25	1090178	3.75	0.3	14.75	2048.96

M 5.2: Parameter values

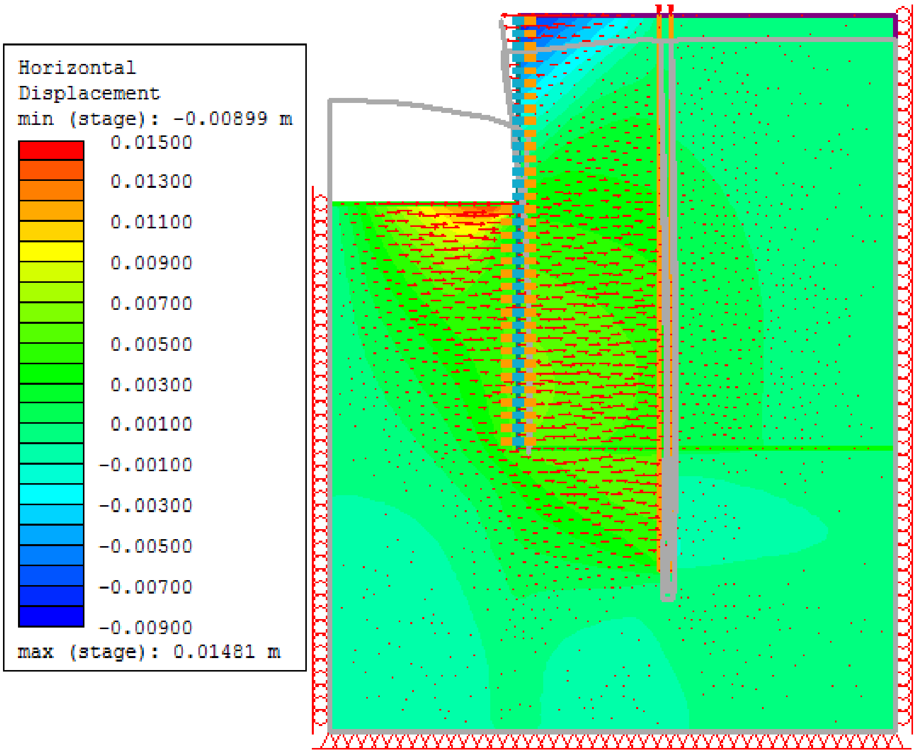

M 5.3: Deformed model (stage 3)

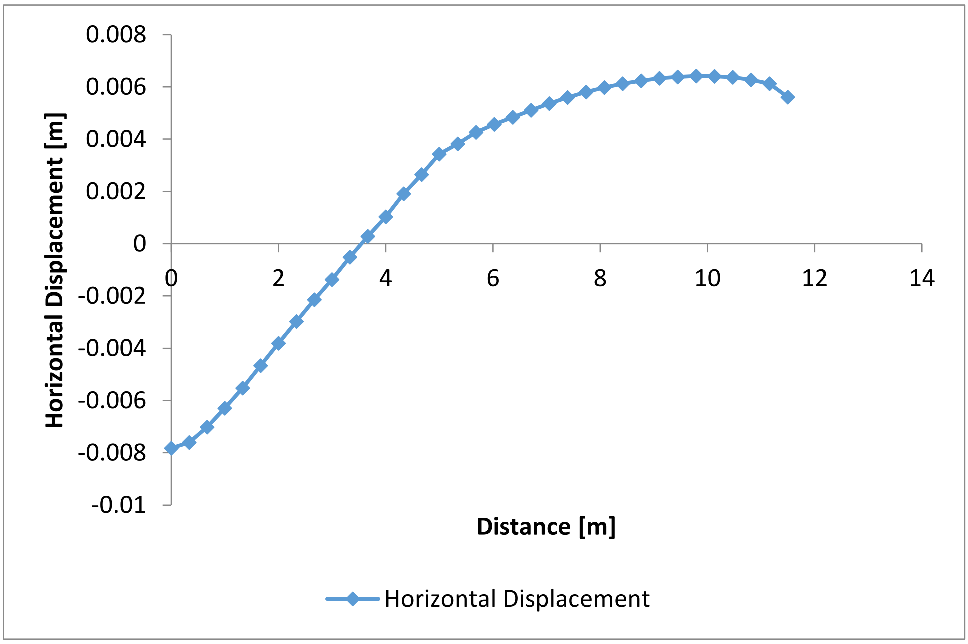

M 5.4: Horizontal displacement of soil along retaining wall

Retaining wall maximum horizontal displacement: -0.00899m

Distance from point of maximum displacement in retaining wall to the top of backfill soil: 0.0 m

Model 6:

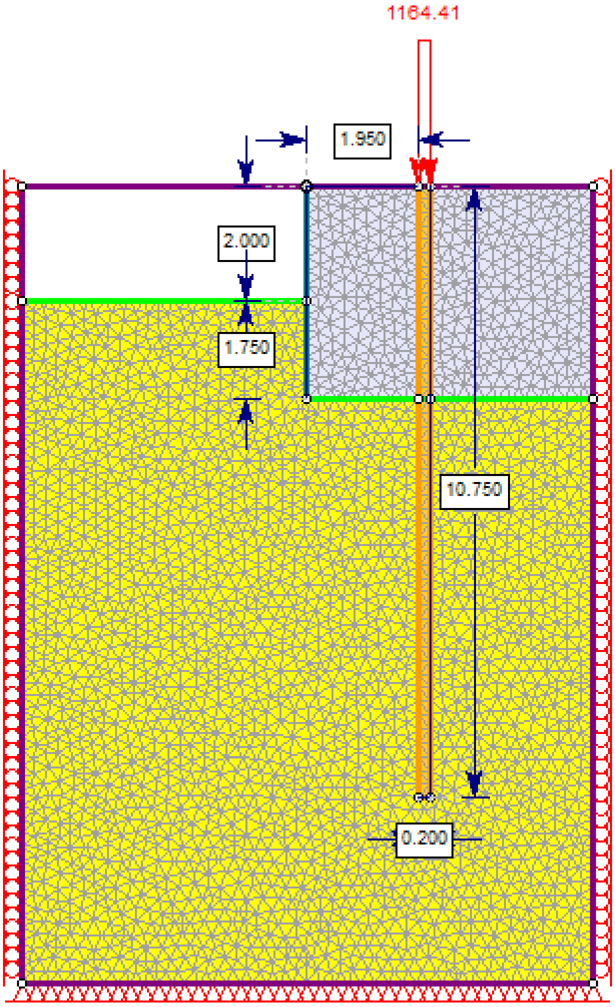

M 6.1: Original model (stage 3)

C'_1	ϕ'_1	γ_1	E_1	C'_2	ϕ'_2	γ_2	E_2	H_1	H_2	H_3	E_3	D_1	D_2	L	Qult
0	39	21	148	15	11	22	27.9	2.00	1.75	0.75	837517	1.95	0.2	10.75	1164.41

M 6.2: Parameter values

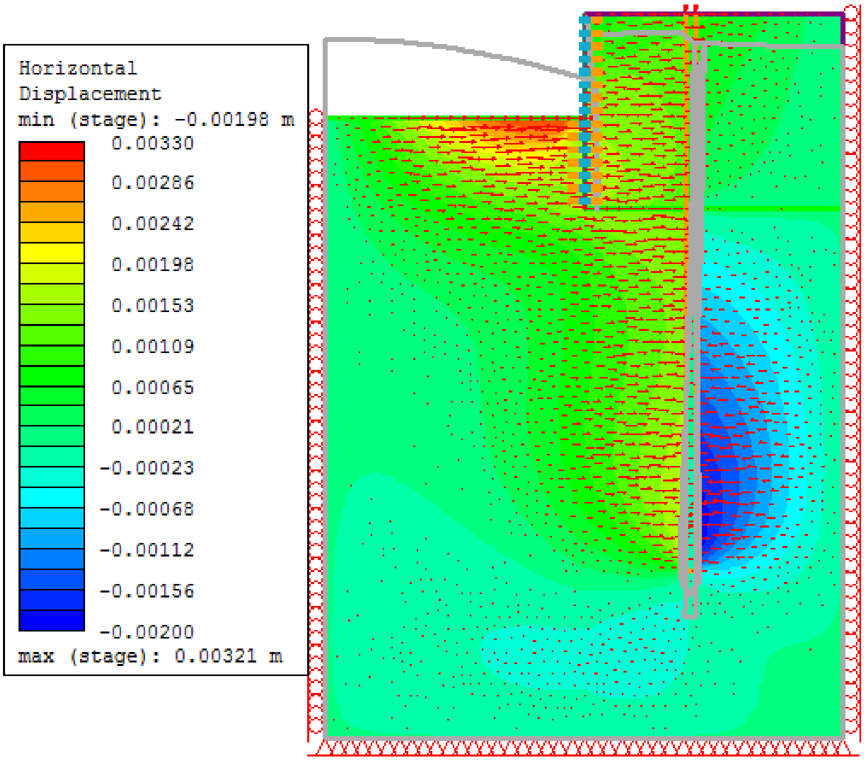

M 6.3: Deformed model (stage 3)

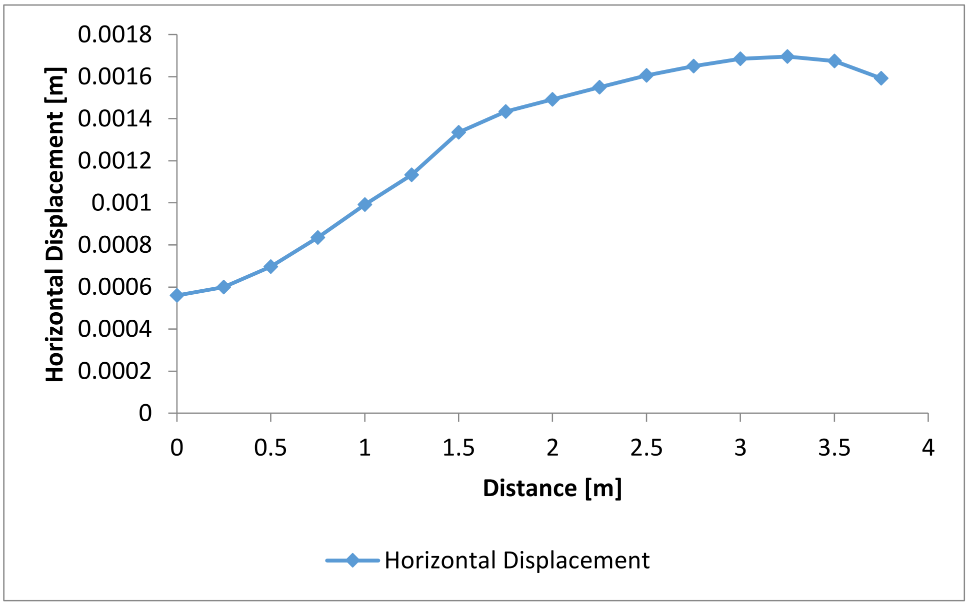

M 6.4: Horizontal displacement of soil along retaining wall

Retaining wall maximum horizontal displacement: 0.00169622m

Distance from point of maximum displacement in retaining wall to the top of backfill soil: 3.25m

Model 7:

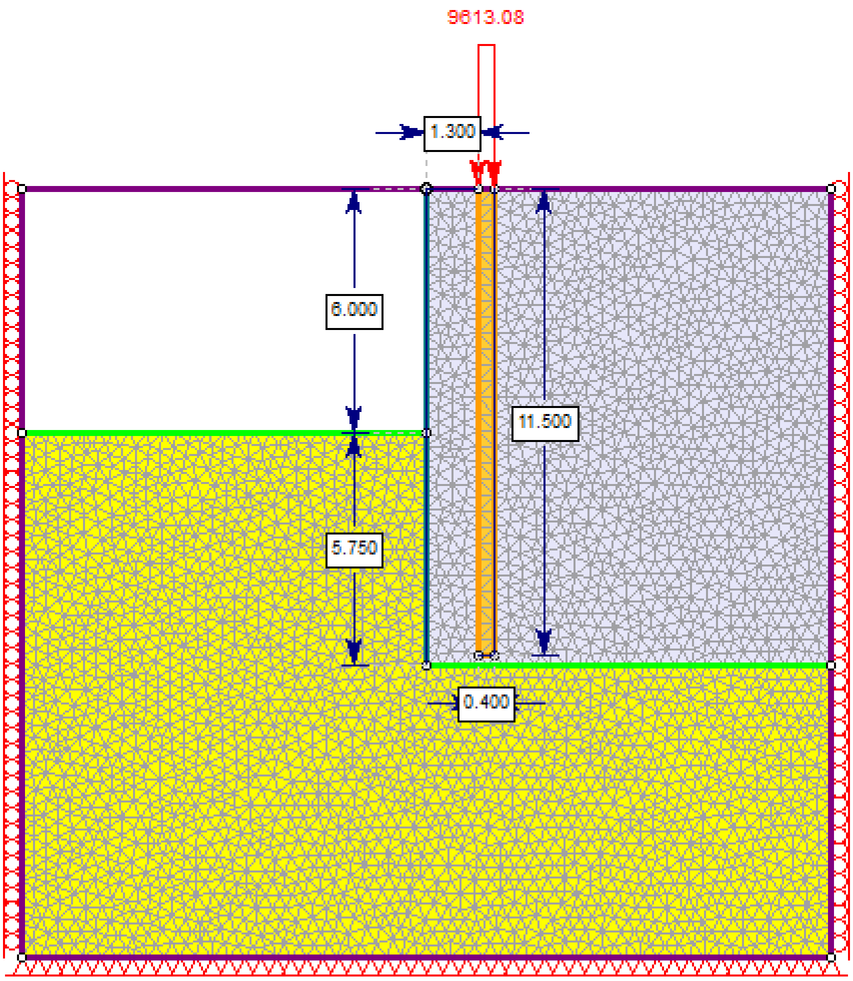

M 7.1: Original model (stage 3)

C'_1	ϕ'_1	γ_1	E_1	C'_2	ϕ'_2	γ_2	E_2	H_1	H_2	H_3	E_3	D_1	D_2	L	Qult
0	28	22	77	53	31	25	38	6.00	5.75	1.25	1005536	1.3	0.4	11.5	9546.62

M 7.2: Parameter values

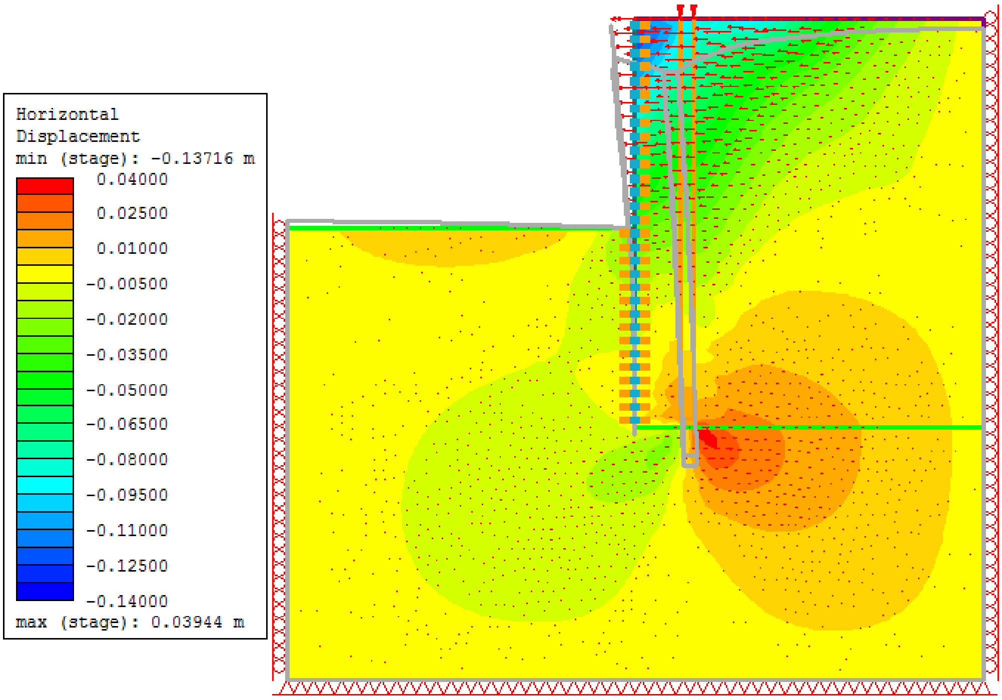

M 7.3: Deformed model (stage 3)

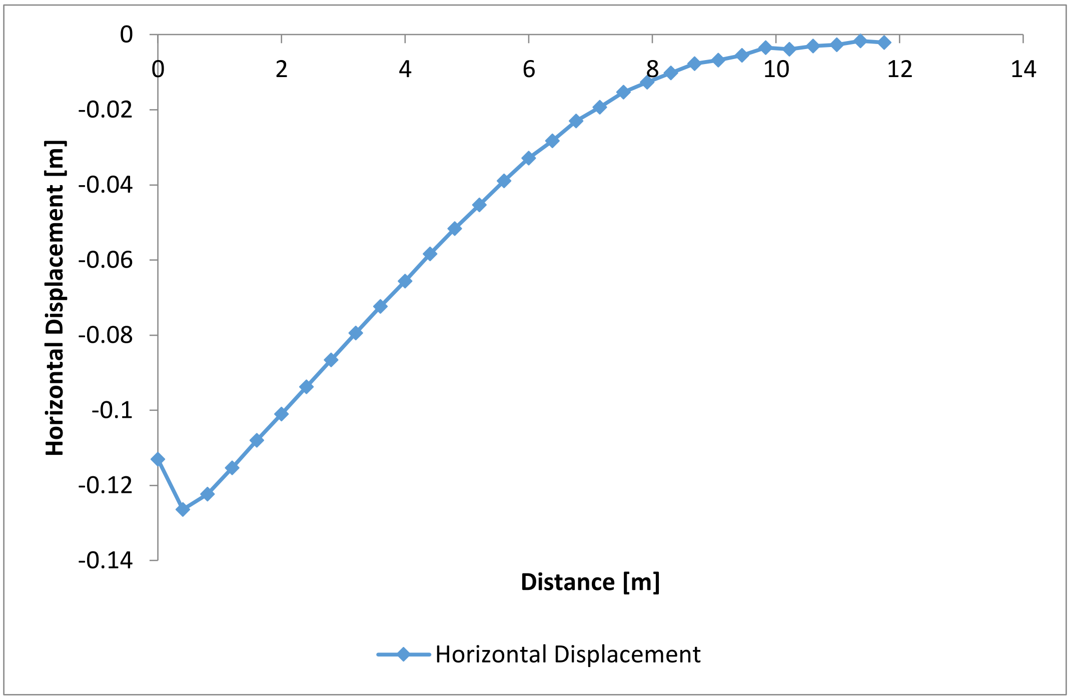

M 7.4: Horizontal displacement of soil along retaining wall

Retaining wall maximum horizontal displacement: -0.13716m

Distance from point of maximum displacement in retaining wall to the top of backfill soil: 0.0m

Model 8:

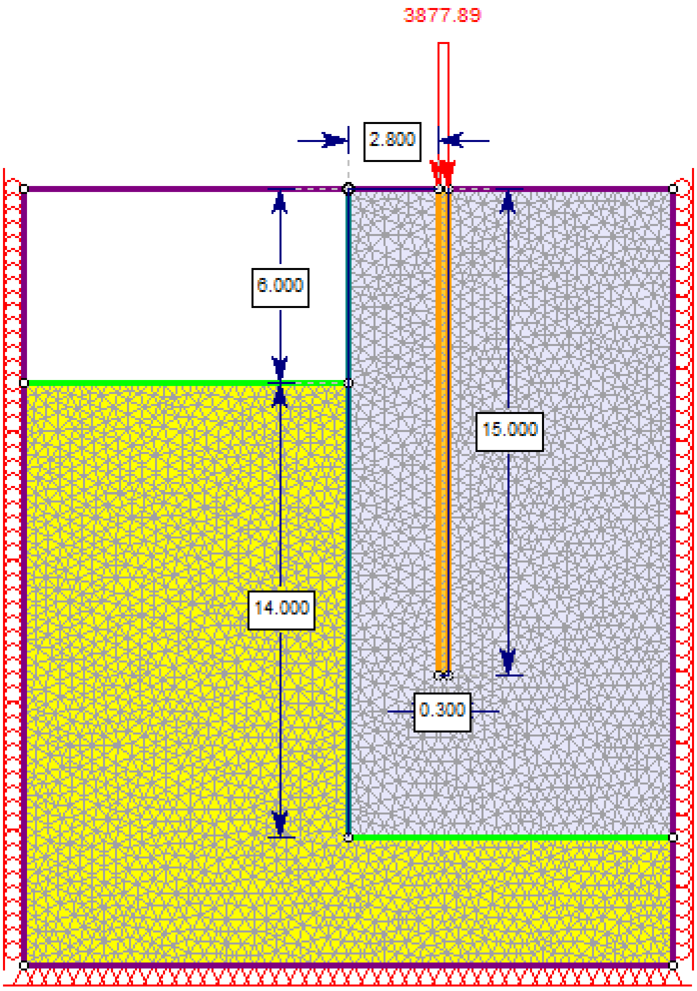

M 8.1: Original model (stage 3)

C_1'	ϕ_1'	γ_1	E_1	C_2'	ϕ_2'	γ_2	E_2	H_1	H_2	H_3	E_3	D_1	D_2	L	Qult
0	35	21	64	36	30	18	44.7	6.00	14	0.75	987126	2.8	0.3	15	3877.89

M 8.2: Parameter values

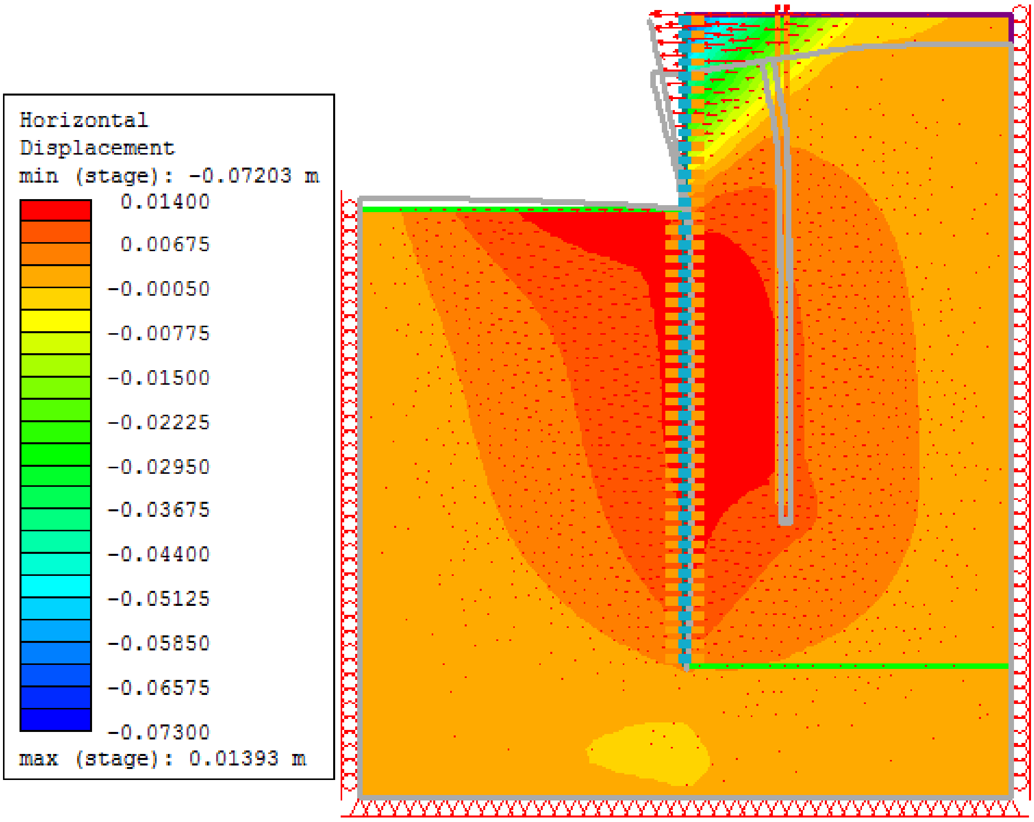

M 8.3: Deformed model (stage 3)

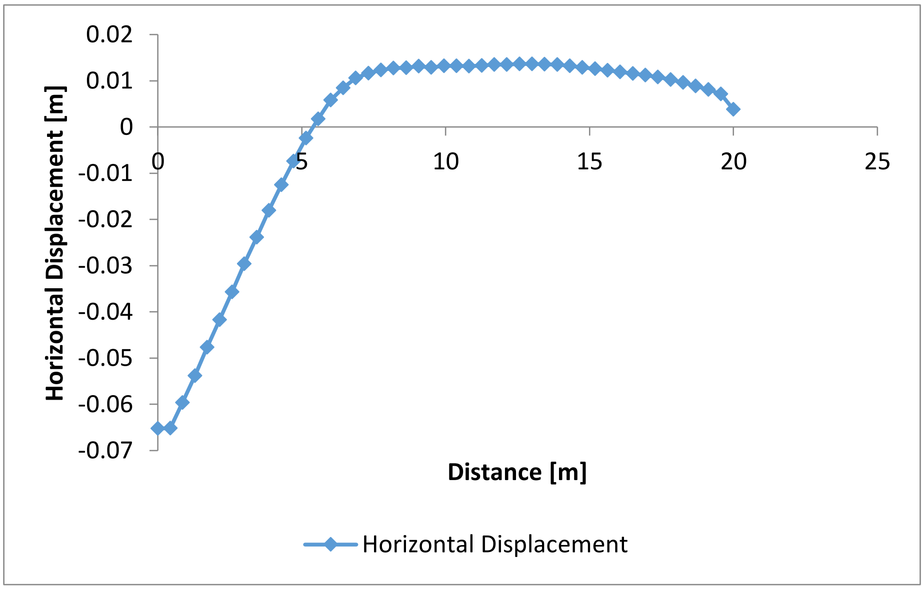

M 8.4: Horizontal displacement of soil along retaining wall

Retaining wall maximum horizontal displacement: -0.07203m

Distance from point of maximum displacement in retaining wall to the top of backfill soil: 0.0m

Model 9:

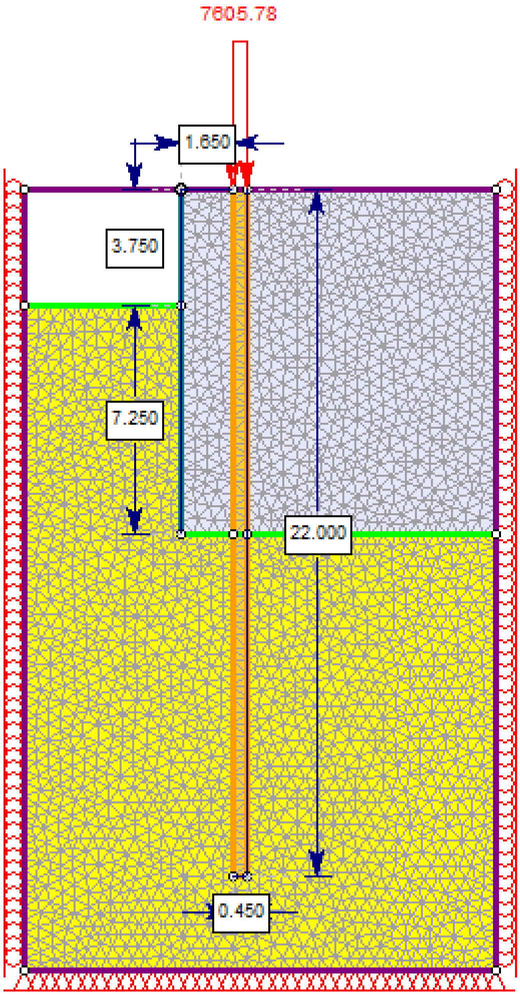

M 9.1: Original model (stage 3)

C_1'	ϕ_1'	γ_1	E_1	C_2'	ϕ_2'	γ_2	E_2	H_1	H_2	H_3	E_3	D_1	D_2	L	Qult
0	30	19	256	22	26	23	38.5	3.75	7.25	0.75	1103341	1.65	0.45	22	7605.78

M 9.2: Parameter values

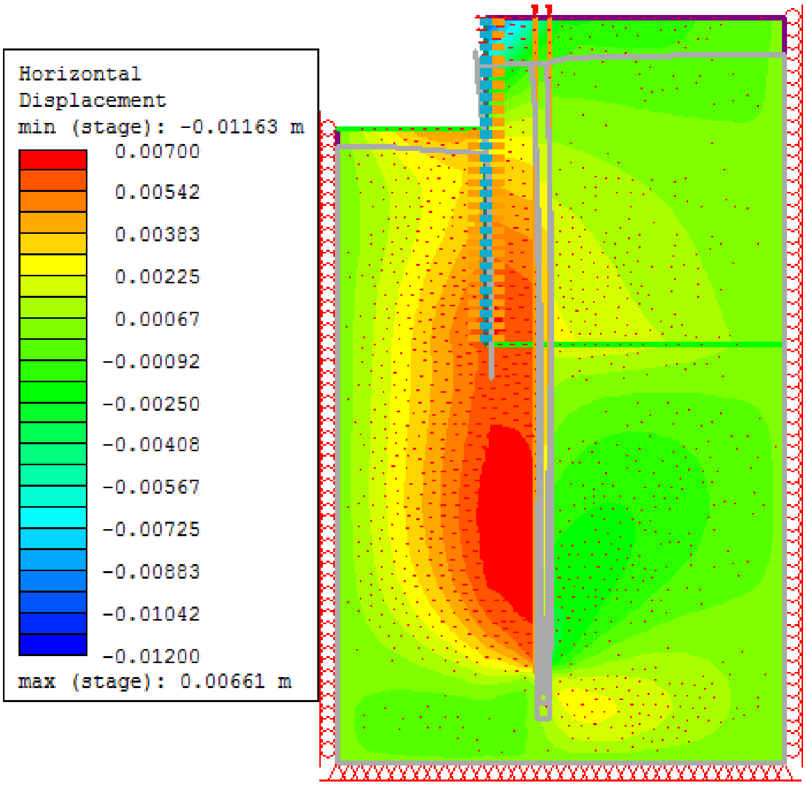

M 9.3: Deformed model (stage 3)

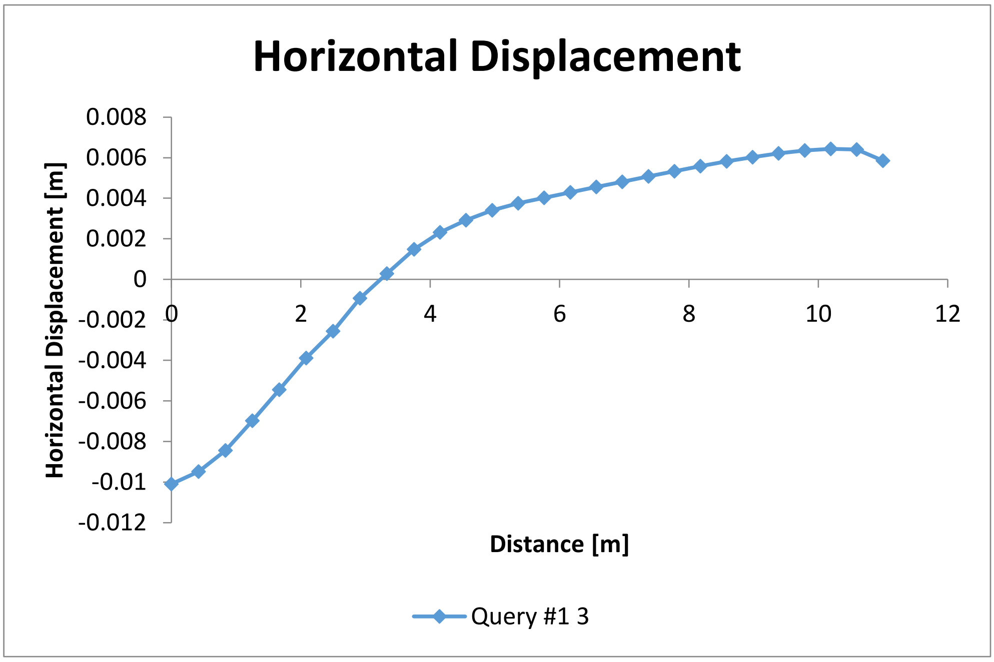

M 9.4: Horizontal displacement of soil along retaining wall

Retaining wall maximum horizontal displacement: -0.01163m

Distance from point of maximum displacement in retaining wall to the top of backfill soil: 0.0m

Model 10:

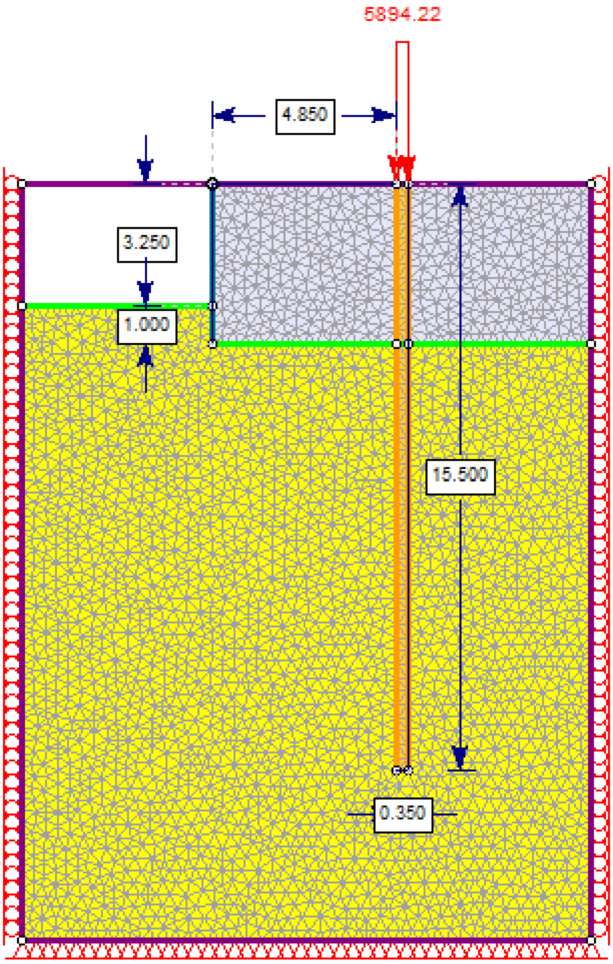

M 10.1: Original model (stage 3)

C_1'	ϕ_1'	γ_1	E_1	C_2'	ϕ_2'	γ_2	E_2	H_1	H_2	H_3	E_3	D_1	D_2	L	Qult
0	45	22	280	43	28	18	22	2.25	0.5	1	709078	4.85	0.35	22.5	5894.22

M 10.2: Parameter values

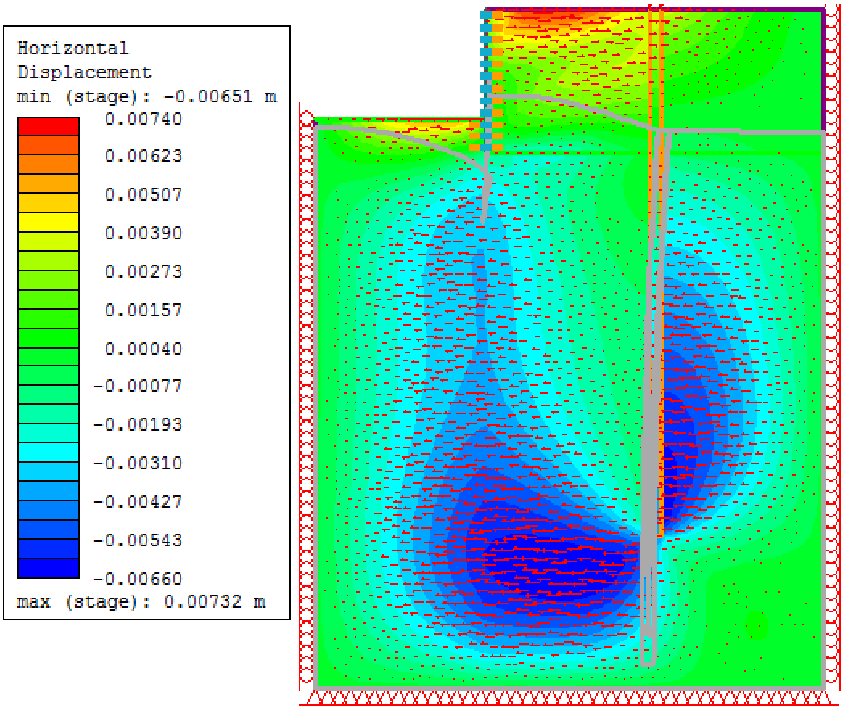

M 10.3: Deformed model (stage 3)

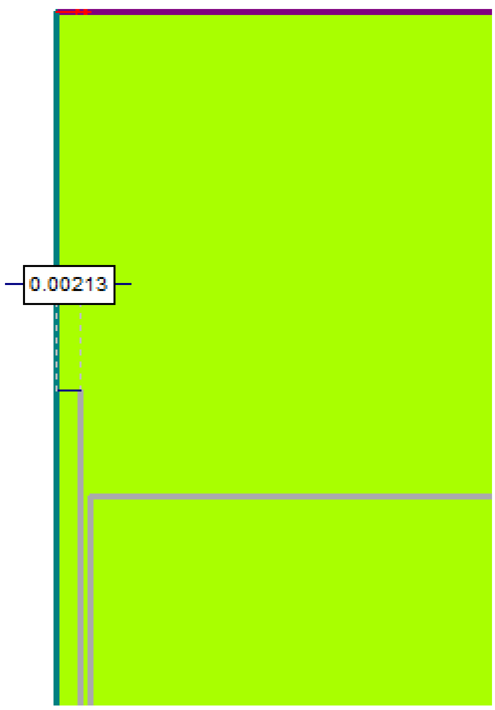

M 10.4: Detailed view of cross-section of retaining wall and soil (stage 3)

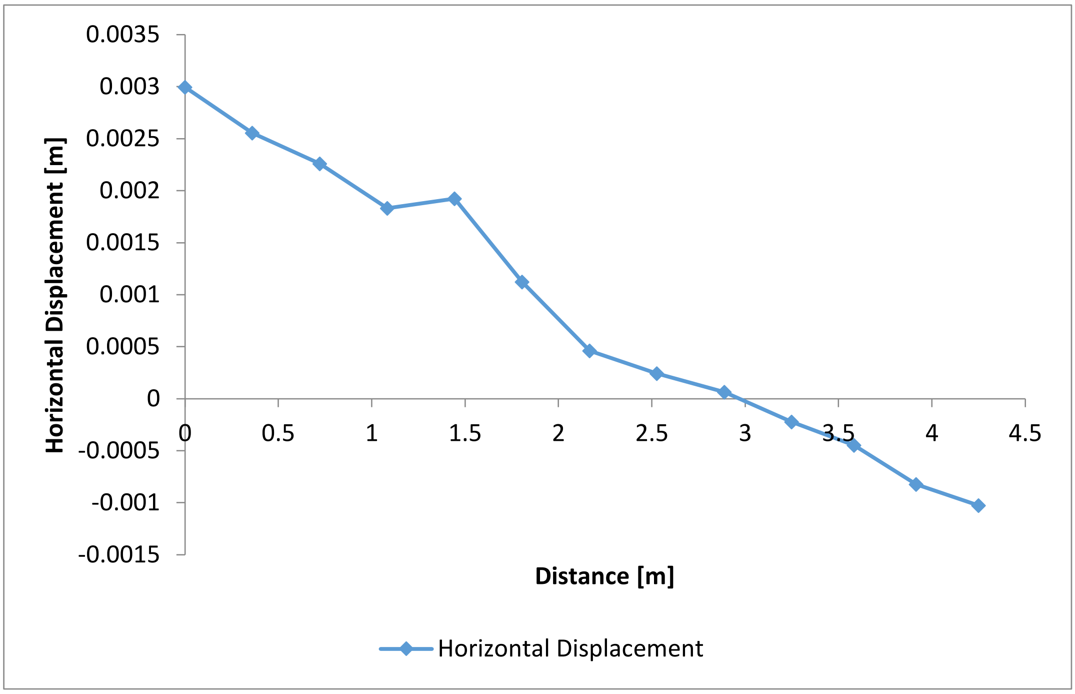

M 10.5: Horizontal displacement of soil along retaining wall

Retaining wall maximum horizontal displacement: 0.00213m

Distance from point of maximum displacement in retaining wall to the top of backfill soil: 0.0m

Model 11:

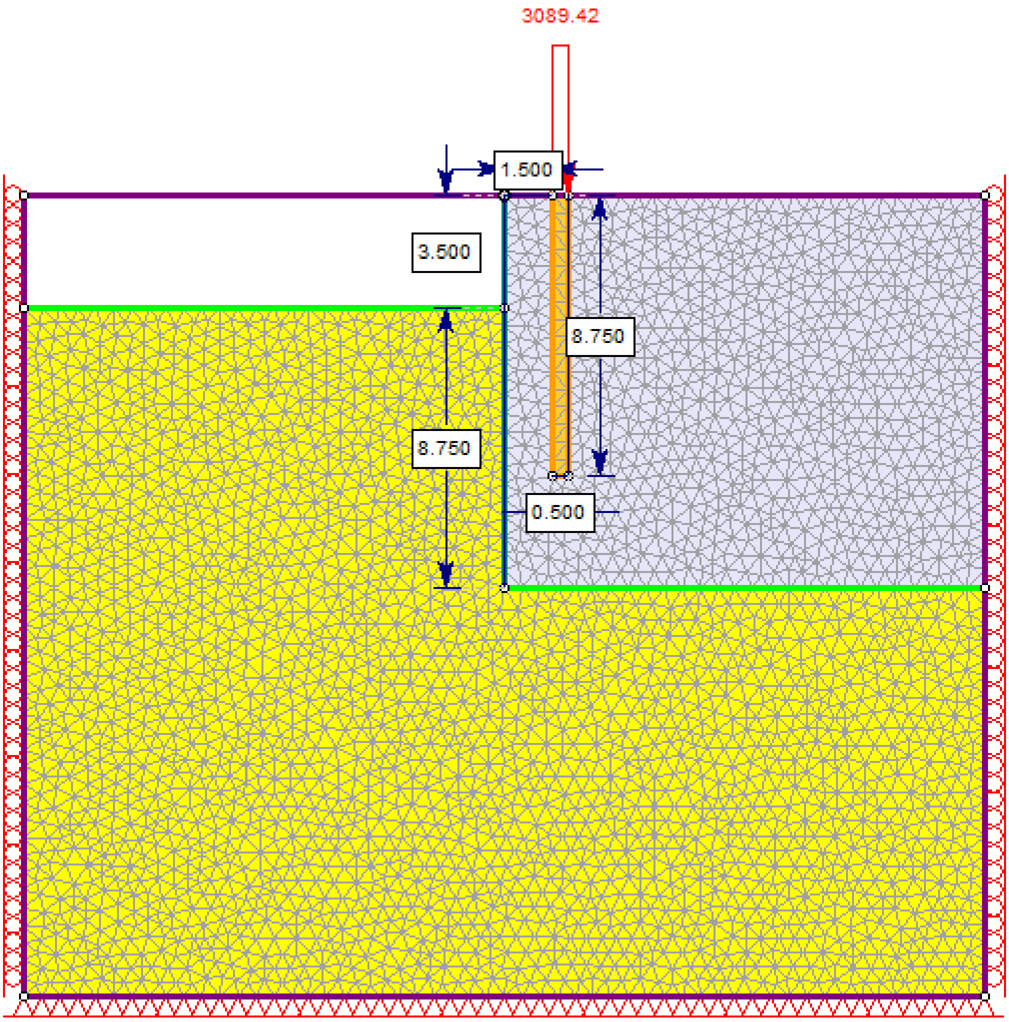

M 11.1: Original model (stage 3)

C'_1	ϕ'_1	γ_1	E_1	C'_2	ϕ'_2	γ_2	E_2	H_1	H_2	H_3	E_3	D_1	D_2	L	Qult
0	36	19	267	18	28	18	10.1	3.50	8.75	0.75	1135916	1.5	0.5	8.75	3089.42

M 11.2: Parameter values

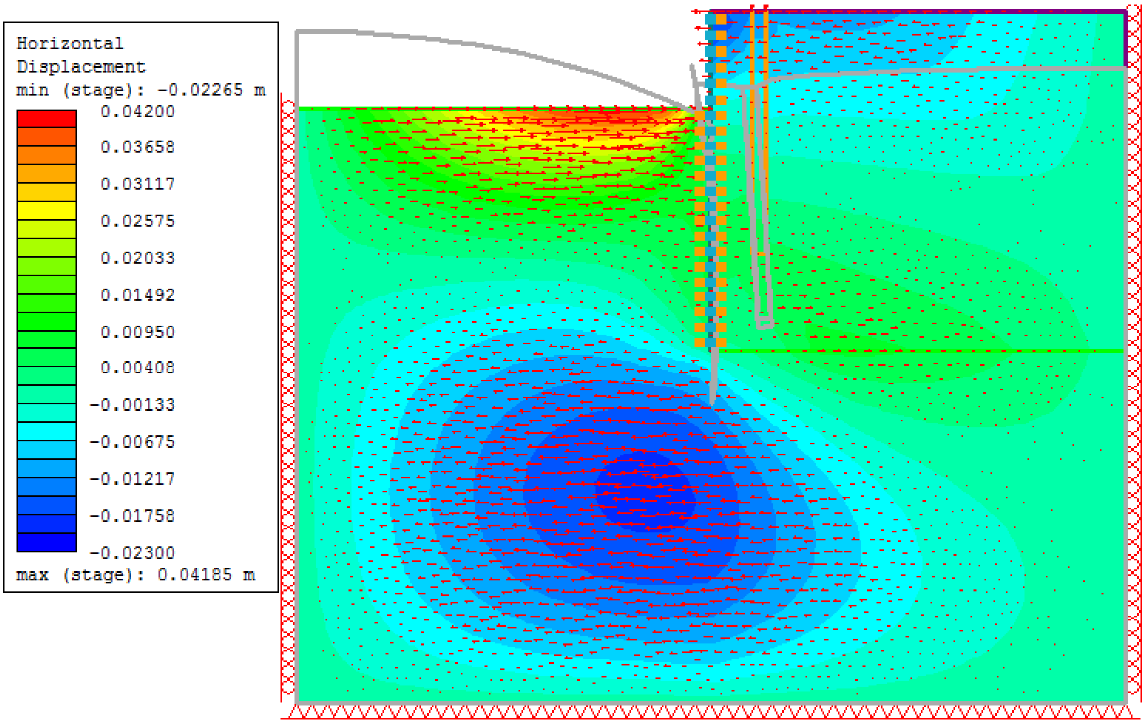

M 11.3: Deformed model (stage 3)

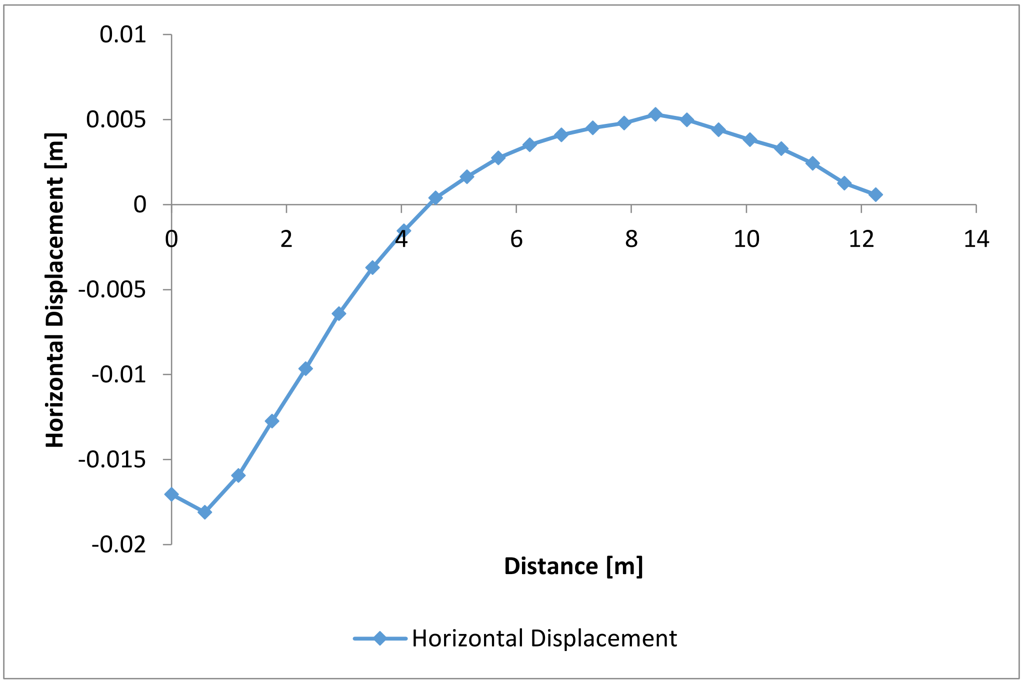

M 11.4: Horizontal displacement of soil along retaining wall

Retaining wall maximum horizontal displacement: -0.02265m

Distance from point of maximum displacement in retaining wall to the top of backfill soil: 0.0m

Model 12:

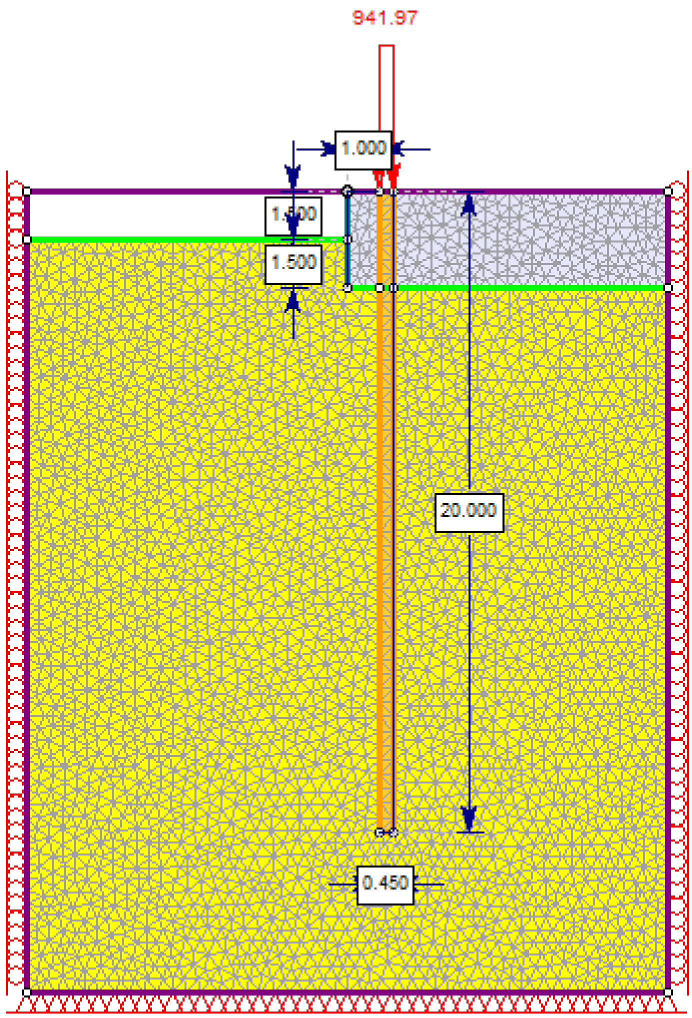

M 12.1: Original model (stage 3)

C_1'	ϕ_1'	γ_1	E_1	C_2'	ϕ_2'	γ_2	E_2	H_1	H_2	H_3	E_3	D_1	D_2	L	Qult
0	39	21	191	10	7	18	10.0	1.50	1.5	1	969742	1	0.45	20	941.97

M 12.2: Parameter values

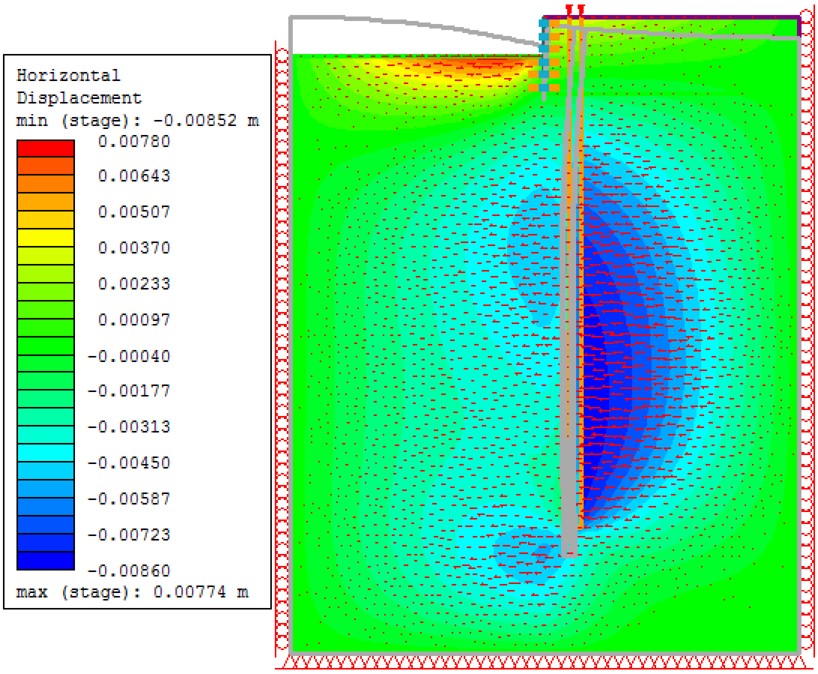

M 12.3: Deformed model (stage 3)

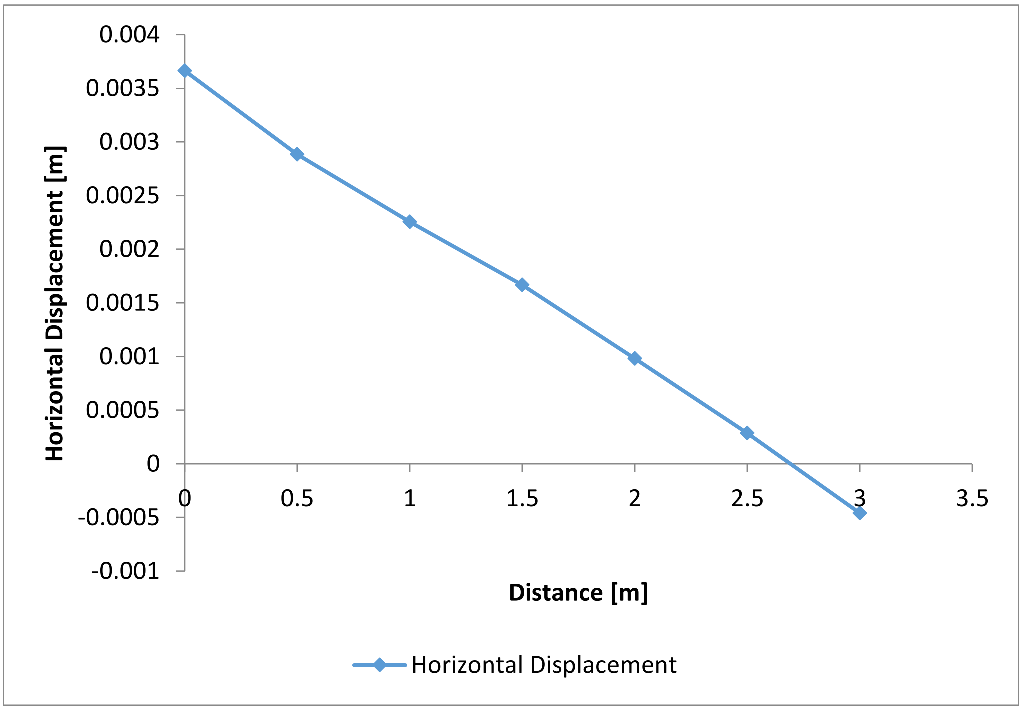

M 12.4: Horizontal displacement of soil along retaining wall

Retaining wall maximum horizontal displacement: 0.00338m

Distance from point of maximum displacement in retaining wall to the top of backfill soil: 0.0m

Model 13:

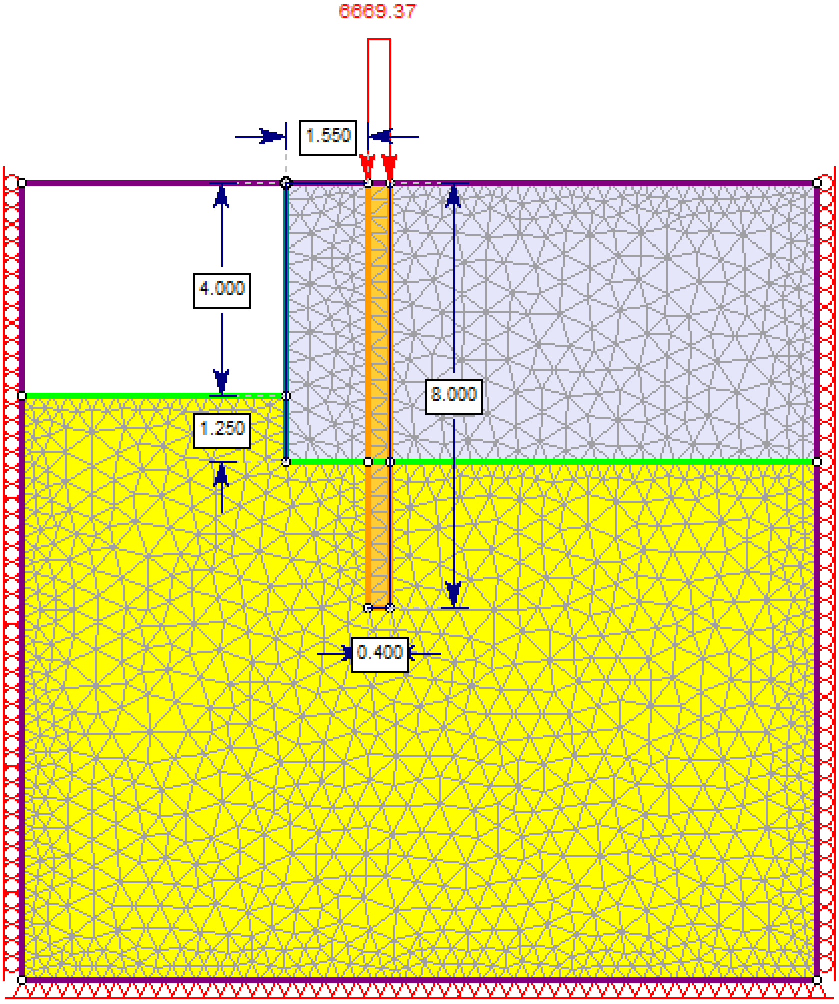

M 13.1: Original model (stage 3)

C'_1	ϕ'_1	γ_1	E_1	C'_2	ϕ'_2	γ_2	E_2	H_1	H_2	H_3	E_3	D_1	D_2	L	Qult
0	42	20	17	55	31	23	33	4.00	1.25	1	895565	1.55	0.4	8	6669.37

M 13.2: Parameter values

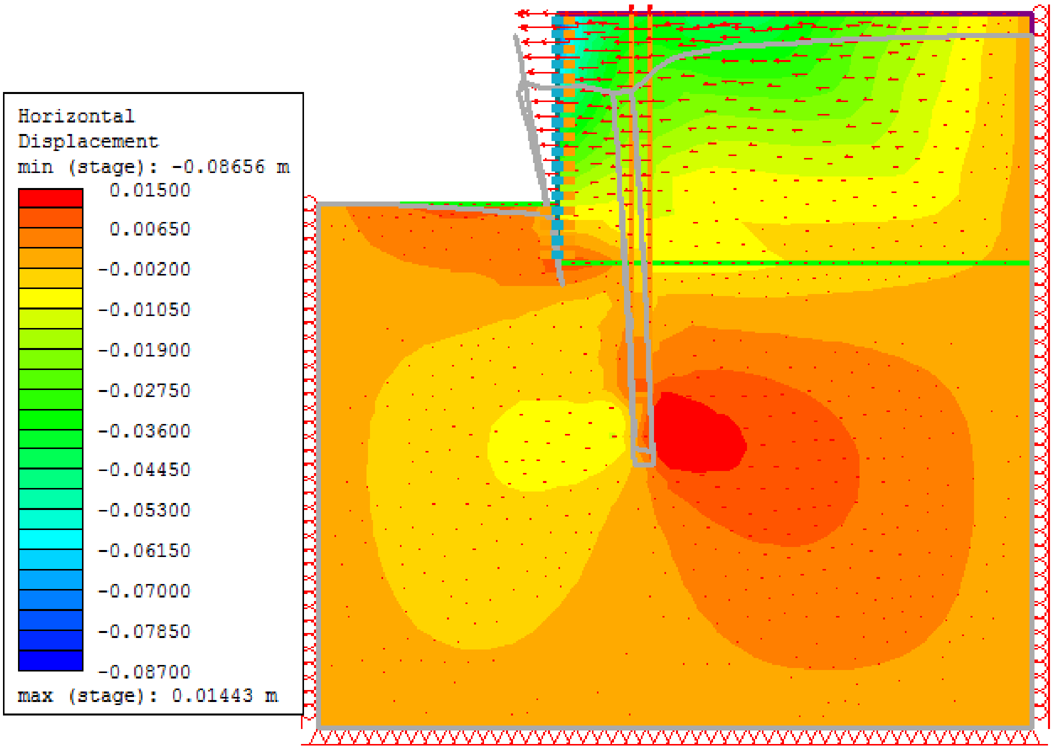

M 13.3: Deformed model (stage 3)

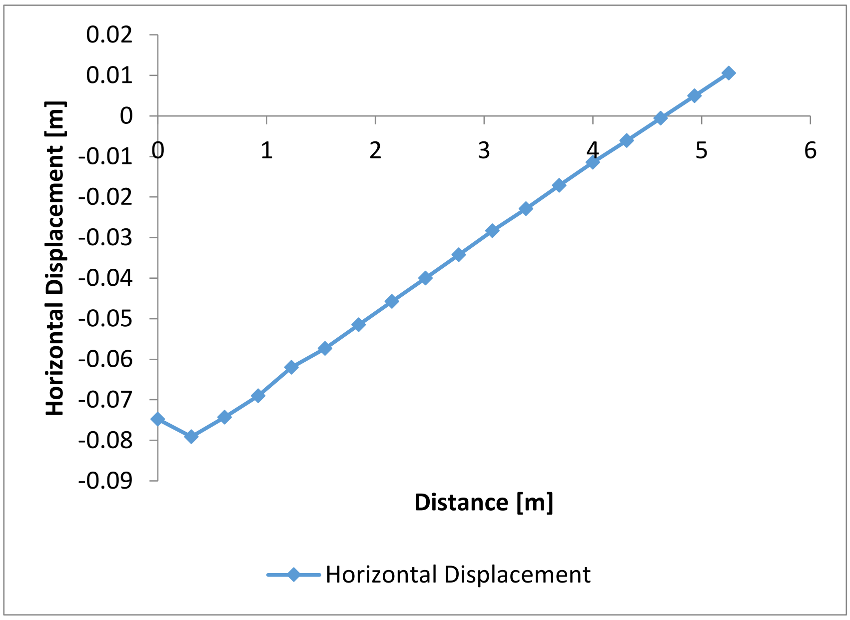

M 13.4: Horizontal displacement of soil along retaining wall

Retaining wall maximum horizontal displacement: -0.08656m

Distance from point of maximum displacement in retaining wall to the top of backfill soil: 0.0m

Model 14:

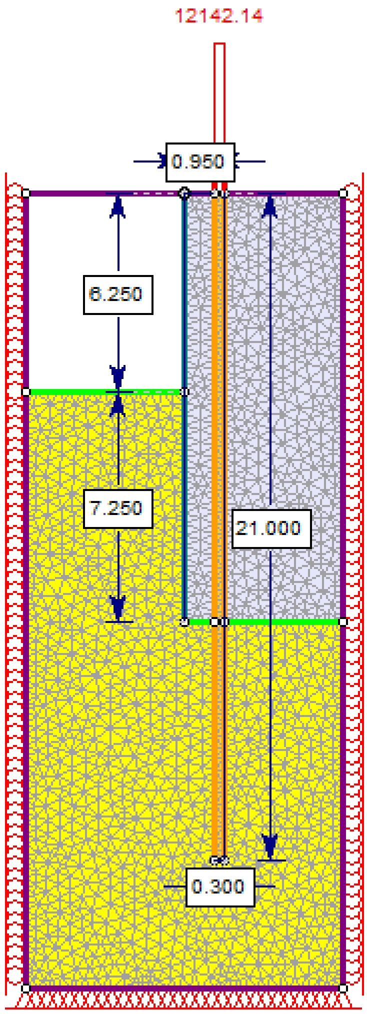

M 14.1: Original model (stage 3)

C_1'	ϕ_1'	γ_1	E_1	C_2'	ϕ_2'	γ_2	E_2	H_1	H_2	H_3	E_3	D_1	D_2	L	Qult
0	39	22	105	44	31	16	43.4	6.25	7.25	1	1070677	0.95	0.3	21	6737.45

M 14.2: Parameter values

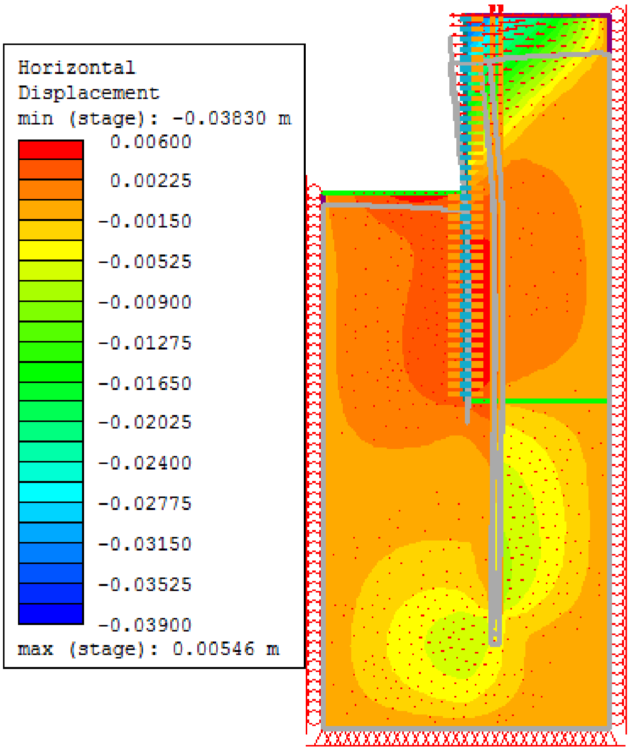

M 14.3: Deformed model (stage 3)

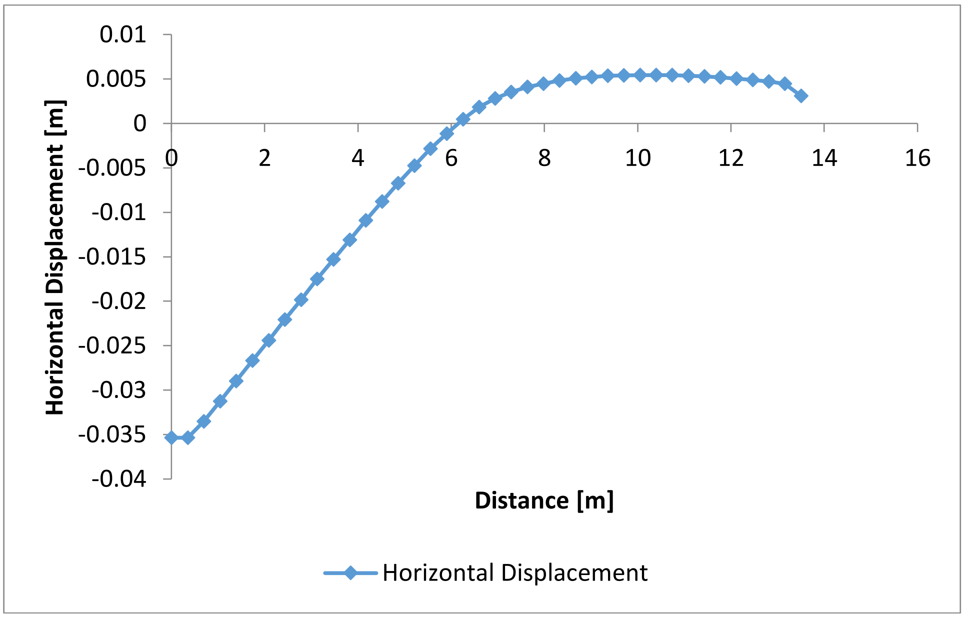

M 14.4: Horizontal displacement of soil along retaining wall

Retaining wall maximum horizontal displacement: -0.0383m

Distance from point of maximum displacement in retaining wall to the top of backfill soil: 0.0m

Model 15:

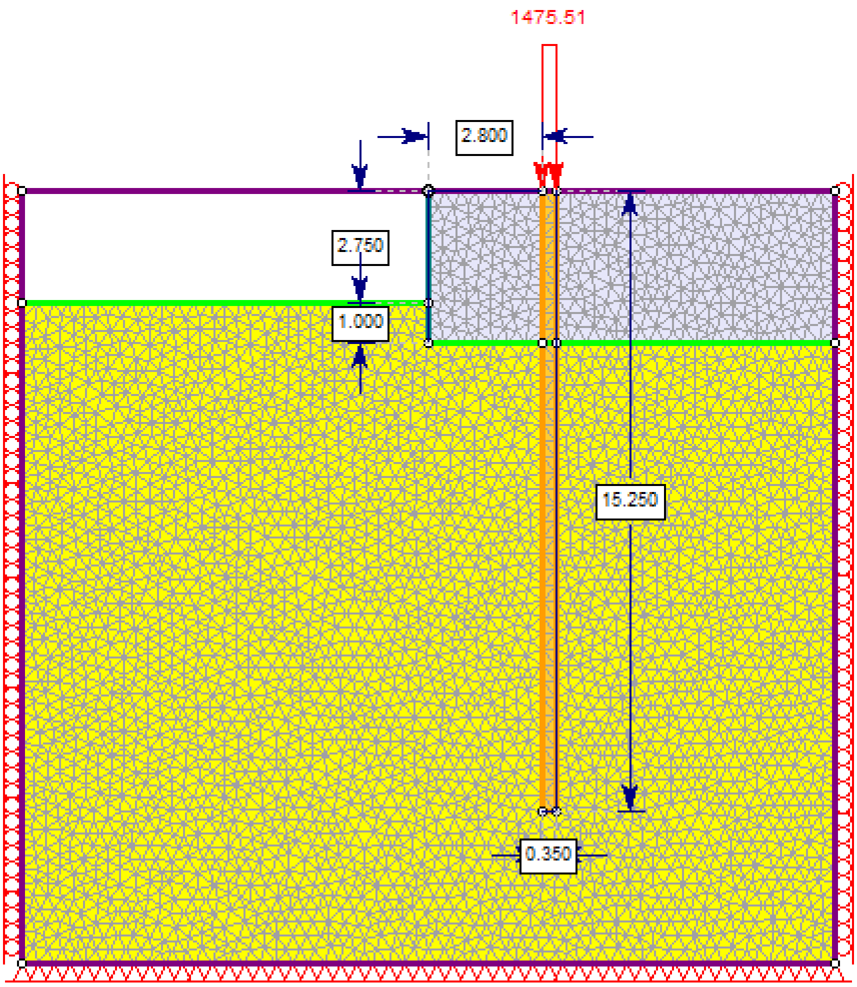

M 15.1: Original model (stage 3)

C_1'	ϕ_1'	γ_1	E_1	C_2'	ϕ_2'	γ_2	E_2	H_1	H_2	H_3	E_3	D_1	D_2	L	Qult
0	32	21	73	56	12	18	13.5	2.75	1	1.25	1046517	2.8	0.35	15.25	1068.77

M 15.2: Parameter values

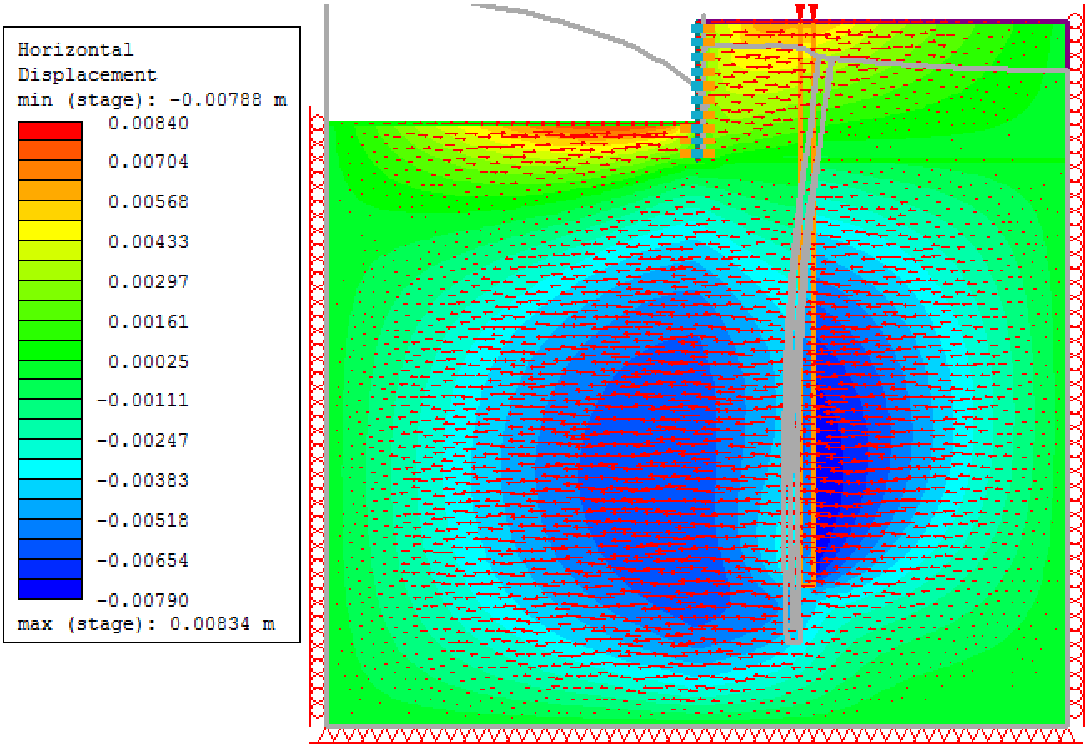

M 15.3: Deformed model (stage 3)

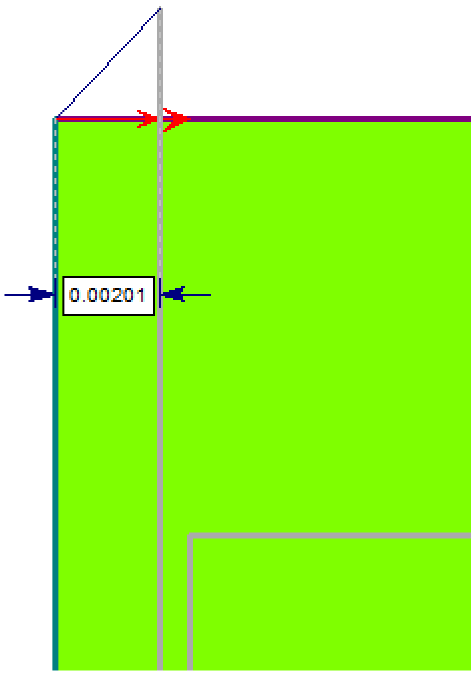

M 15.4: Detailed view of cross-section of retaining wall and soil (stage 3)

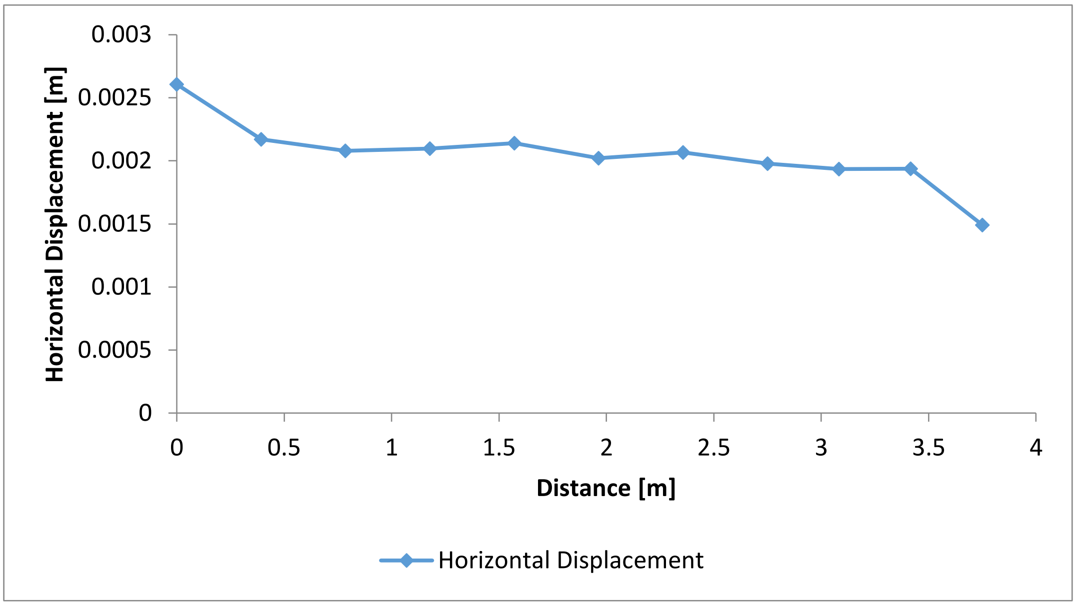

M 15.4: Horizontal displacement of soil along retaining wall

Retaining wall maximum horizontal displacement: 0.00201m

Distance from point of maximum displacement in retaining wall to the top of backfill soil: 0.0m

Model 16:

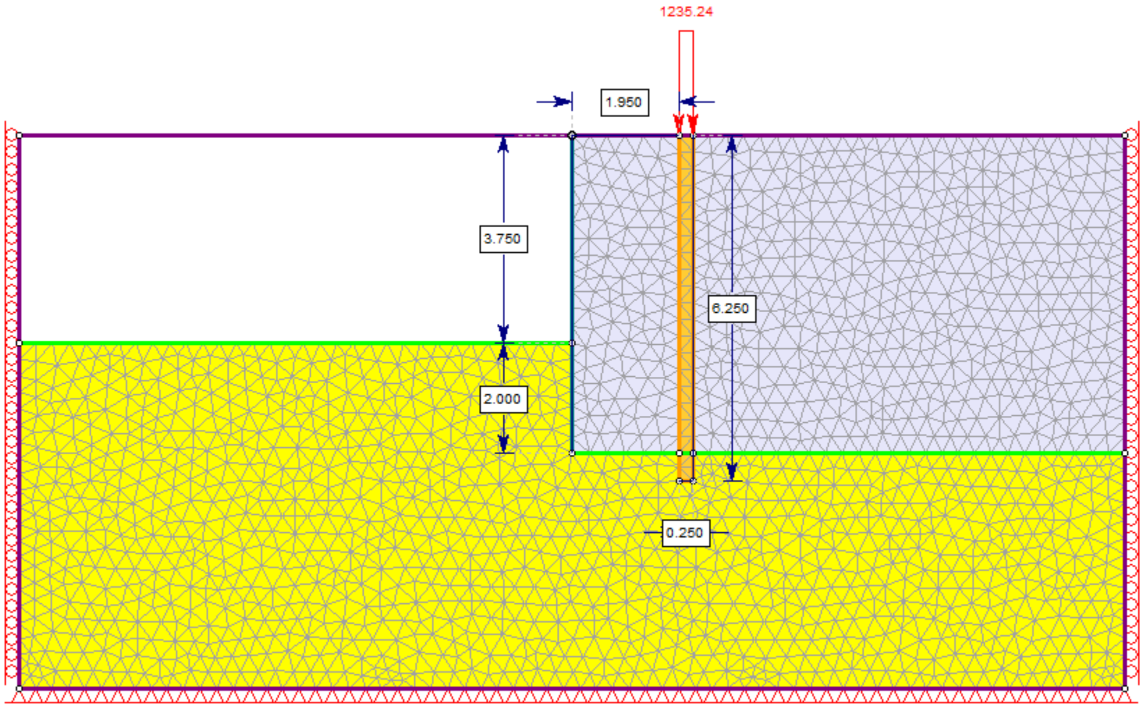

M 16.1: Original model (stage 3)

C'_1	ϕ'_1	γ_1	E_1	C'_2	ϕ'_2	γ_2	E_2	H_1	H_2	H_3	E_3	D_1	D_2	L	Qult
0	30	22	295	45	14	21	46	3.75	2	1	967035	1.95	0.25	14.5	1235.24

M 16.2: Parameter values

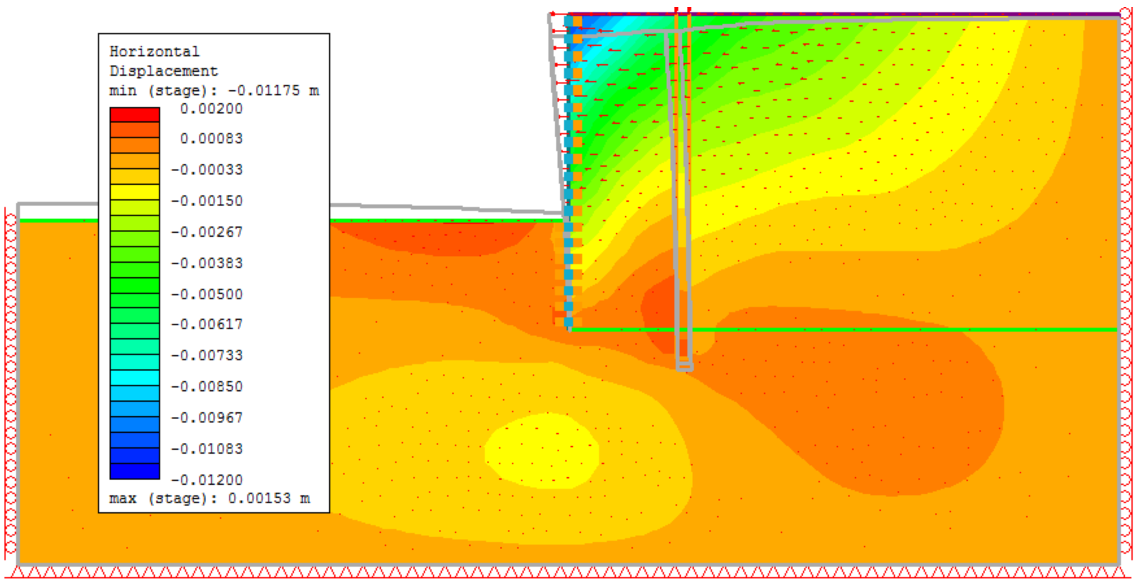

M 16.3: Deformed model (stage 3)

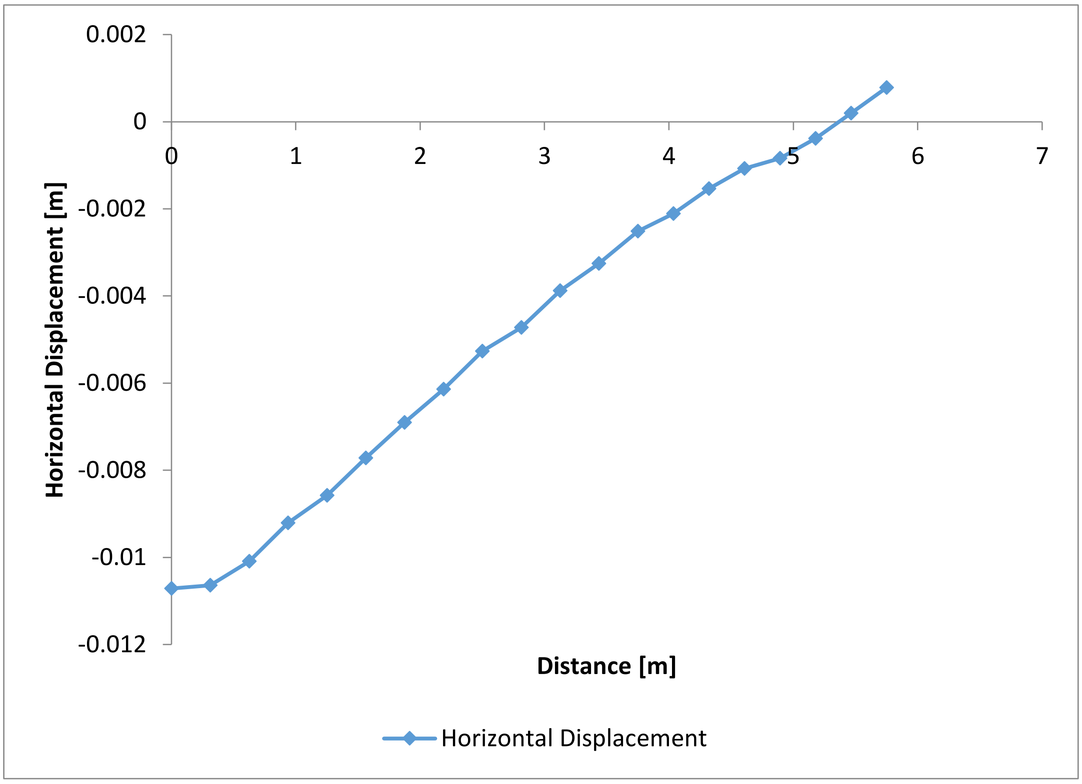

M 16.4: Horizontal displacement of soil along retaining wall

Retaining wall maximum horizontal displacement: -0.01175m

Distance from point of maximum displacement in retaining wall to the top of backfill soil: 0.0m

Model 17:

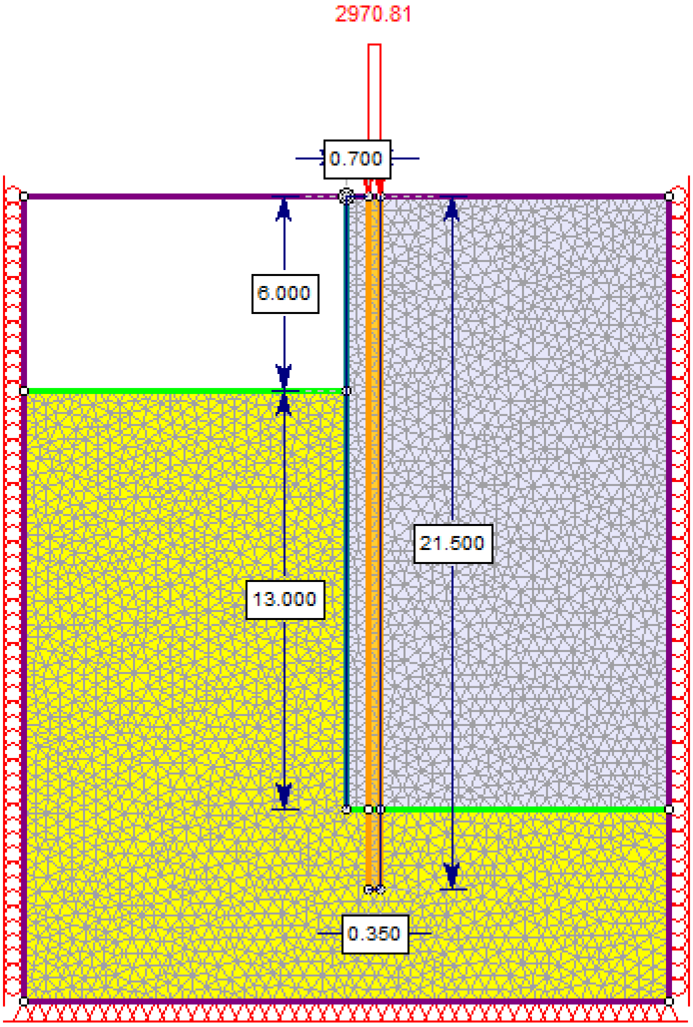

M 17.1: Original model (stage 3)

C_1'	ϕ_1'	γ_1	E_1	C_2'	ϕ_2'	γ_2	E_2	H_1	H_2	H_3	E_3	D_1	D_2	L	Qult
0	28	21	193	37	2	18	6.7	6.00	13	1.25	703394	0.7	0.35	21.5	2970.81

M 17.2: Parameter values

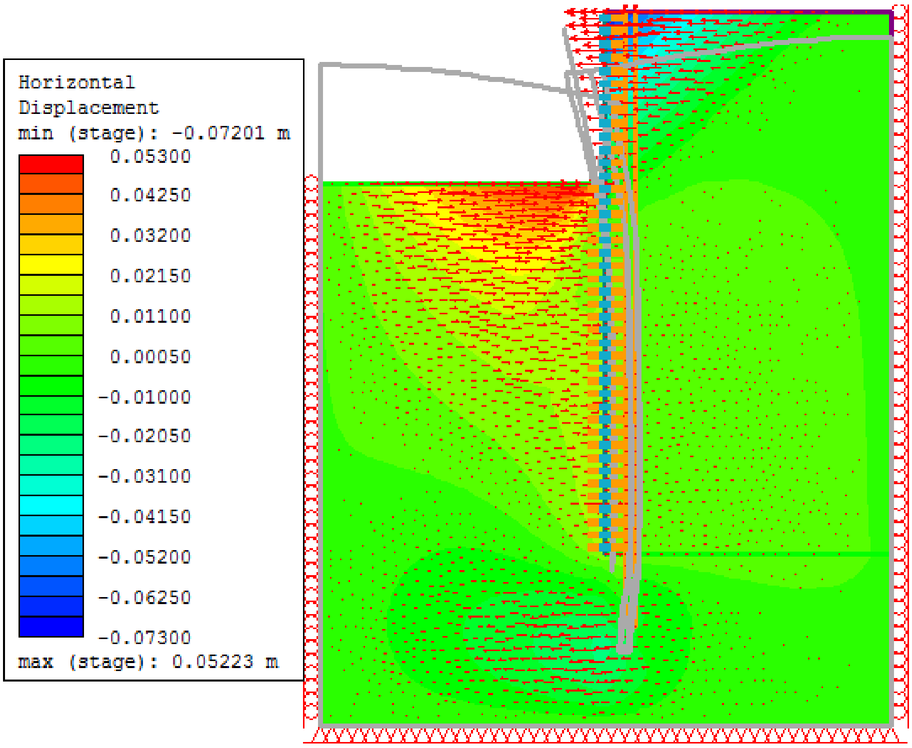

M 17.3: Deformed model (stage 3)

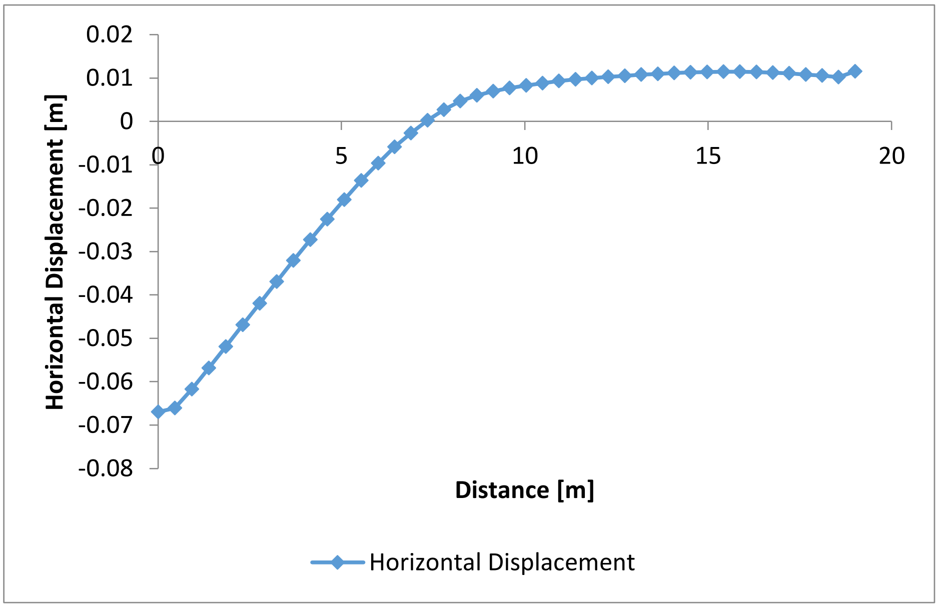

M 17.4: Horizontal displacement of soil along retaining wall

Retaining wall maximum horizontal displacement: -0.07201m

Distance from point of maximum displacement in retaining wall to the top of backfill soil: 0.0m

Model 18:

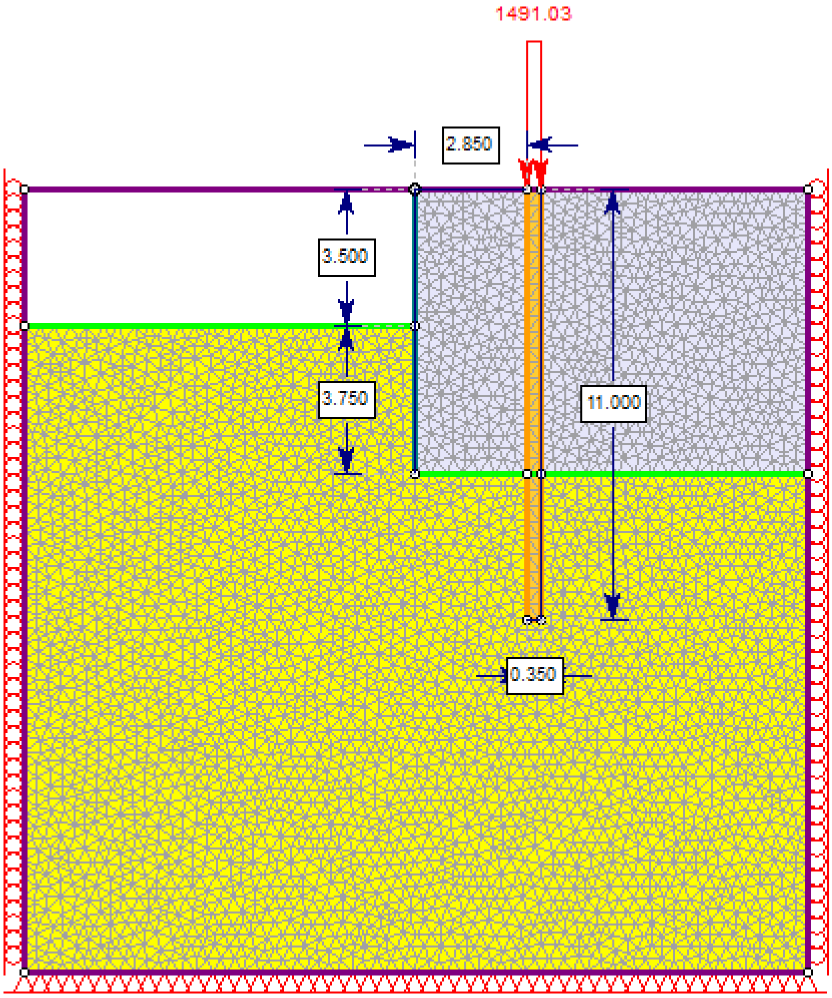

M 18.1: Original model (stage 3)

C'_1	ϕ'_1	γ_1	E_1	C'_2	ϕ'_2	γ_2	E_2	H_1	H_2	H_3	E_3	D_1	D_2	L	Qult
0	35	19	89	23	15	18	47.2	3.50	3.75	1.25	978106	2.85	0.35	11	1491.03

M 18.2: Parameter values

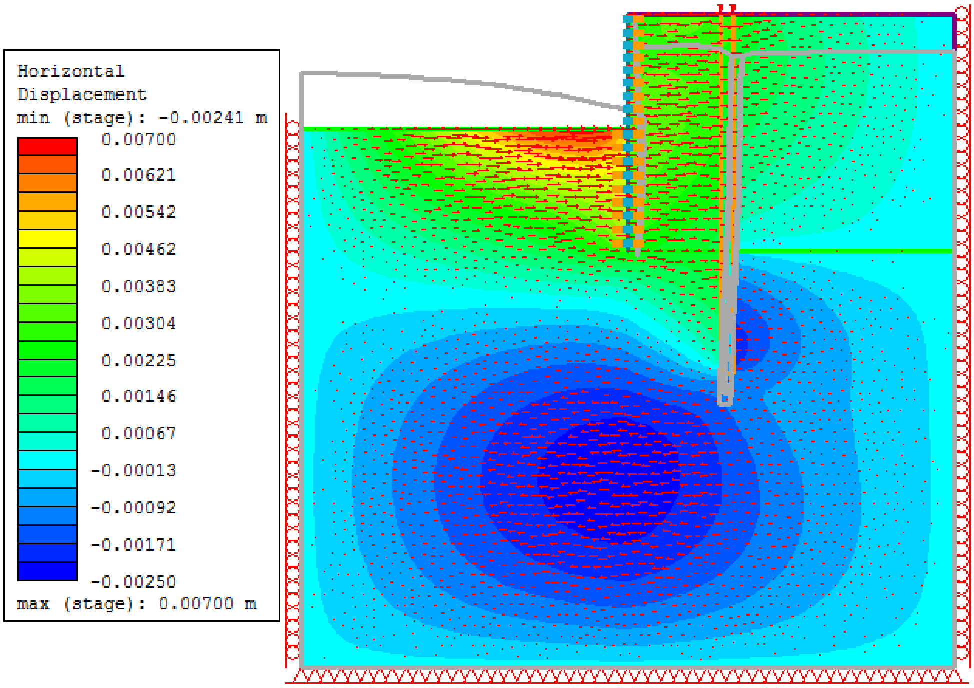

M 18.3: Deformed model (stage 3)

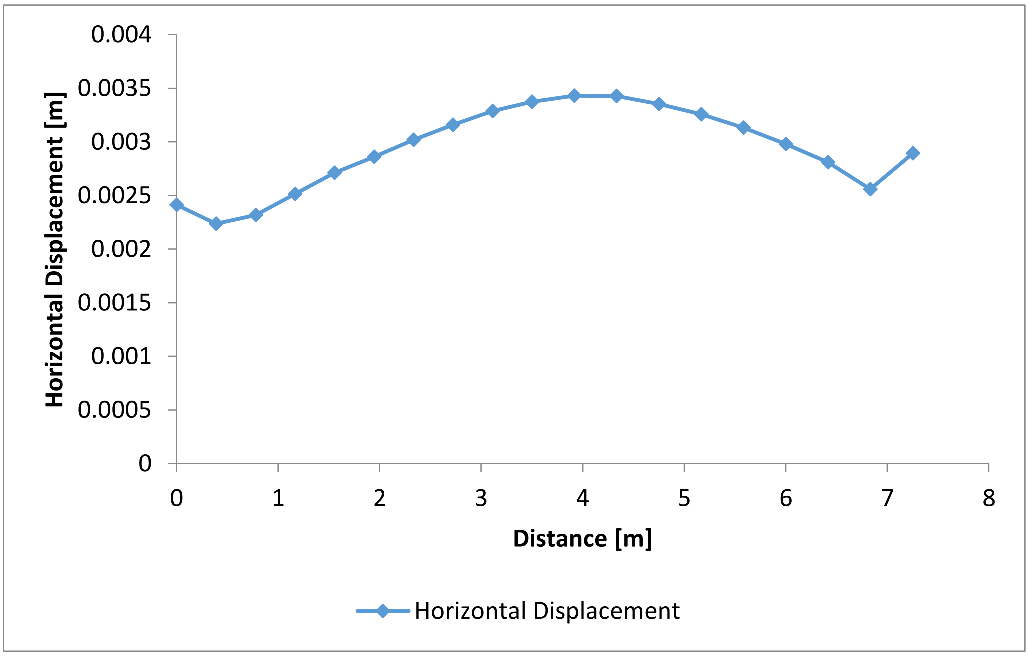

M 18.4: Horizontal displacement of soil along retaining wall

Retaining wall maximum horizontal displacement: 0.00343m

Distance from point of maximum displacement in retaining wall to the top of backfill soil: 3.916666667m

Model 19:

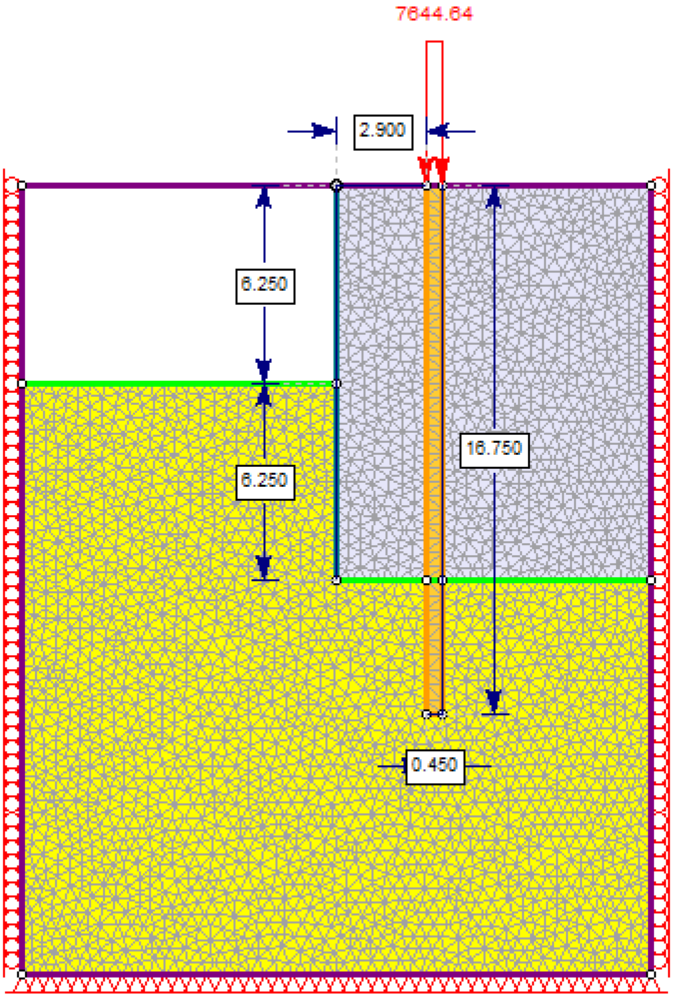

M 19.1: Original model (stage 3)

C_1'	ϕ_1'	γ_1	E_1	C_2'	ϕ_2'	γ_2	E_2	H_1	H_2	H_3	E_3	D_1	D_2	L	Qult
0	30	20	216	47	28	21	43.2	6.25	6.25	1.5	703078	2.9	0.45	16.75	3453.57

M 19.2: Parameter values

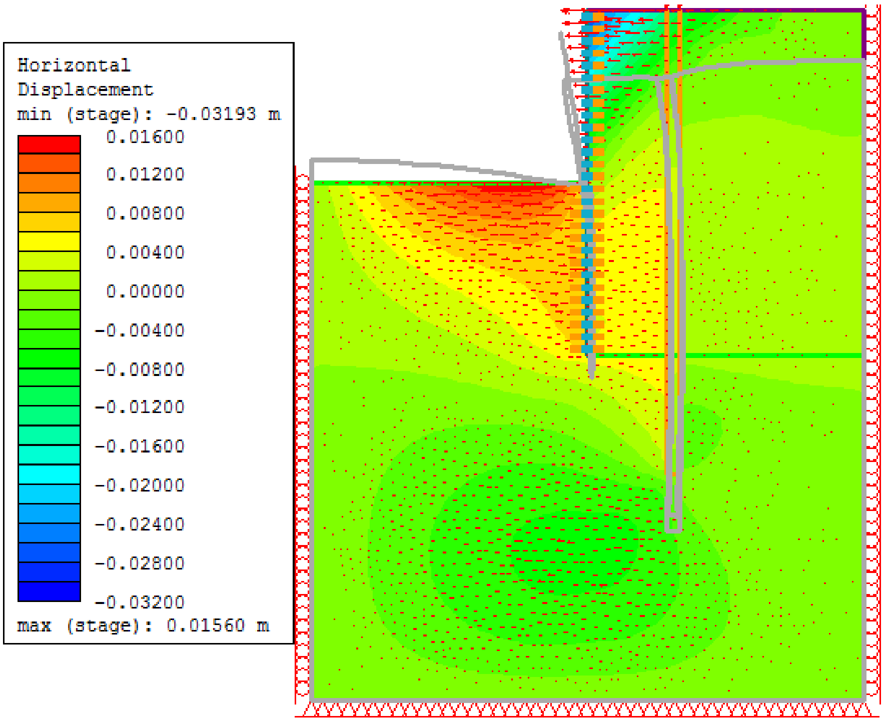

M 19.3: Deformed model (stage 3)

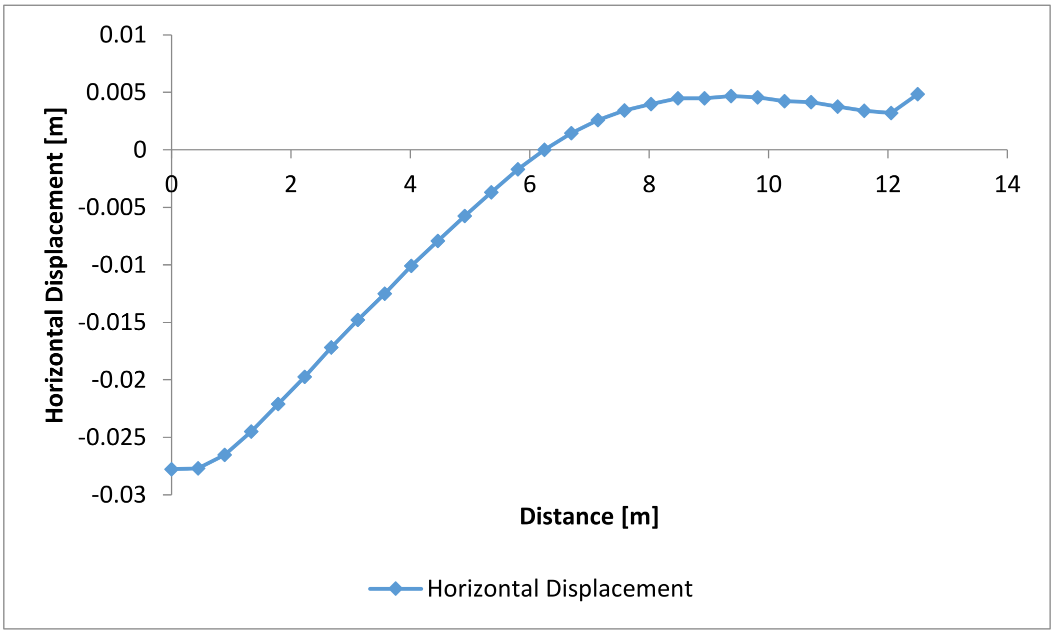

M 19.4: Horizontal displacement of soil along retaining wall

Retaining wall maximum horizontal displacement: -0.03193m

Distance from point of maximum displacement in retaining wall to the top of backfill soil: 0.0m

Model 20:

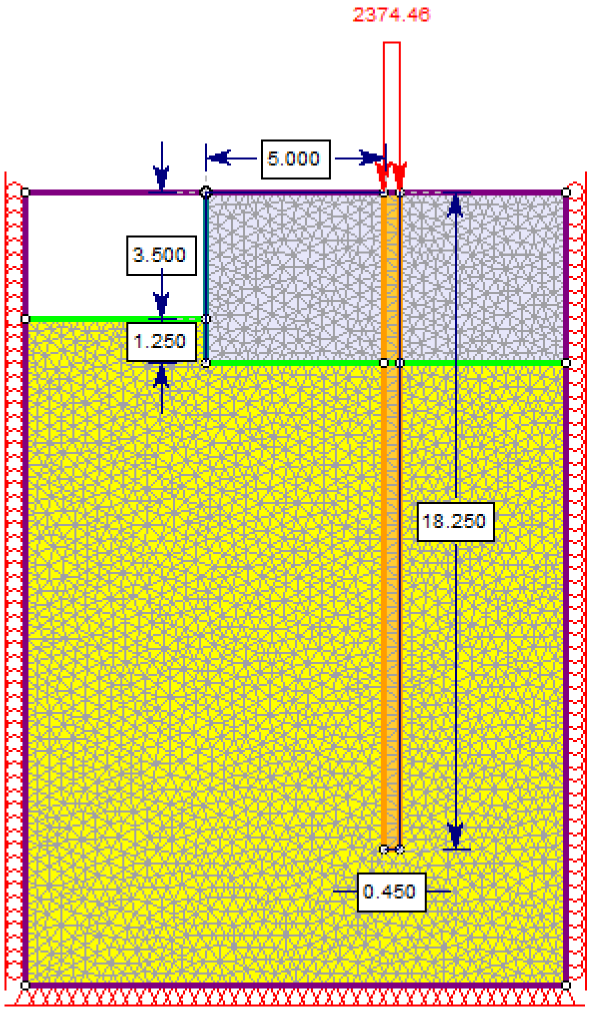

M 20.1: Original model (stage 3)

C_1'	ϕ_1'	γ_1	E_1	C_2'	ϕ_2'	γ_2	E_2	H_1	H_2	H_3	E_3	D_1	D_2	L	Qult
0	41	21	124	52	15	20	21.4	3.50	1.25	1.25	765782	4.95	0.45	18.25	2374.46

M 20.2: Parameter values

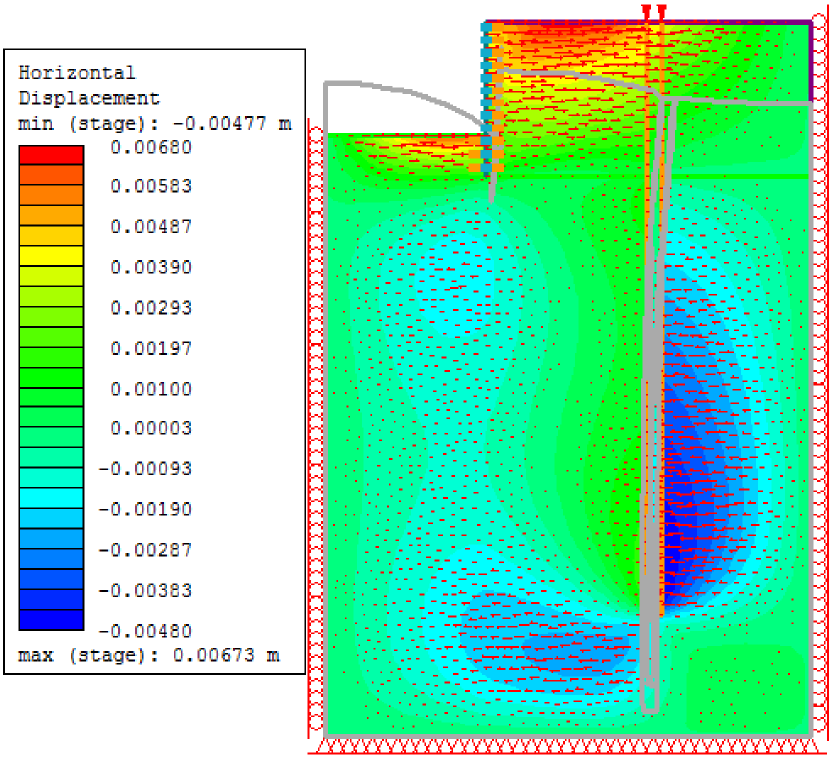

M 20.3: Deformed model (stage 3)

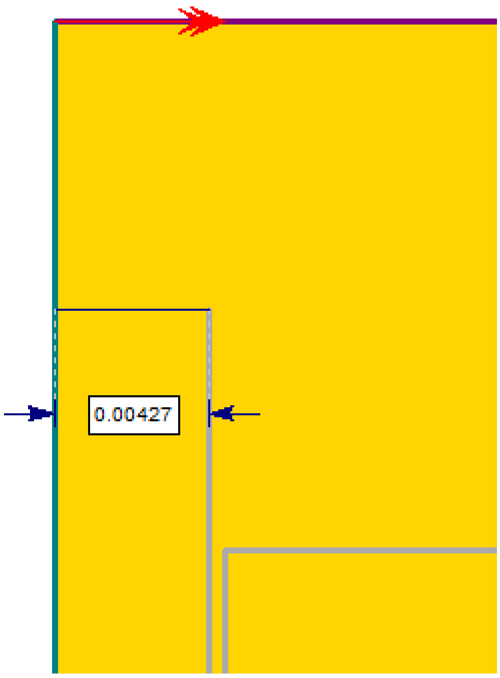

M 20.4: Detailed view of cross-section of retaining wall and soil (stage 3)

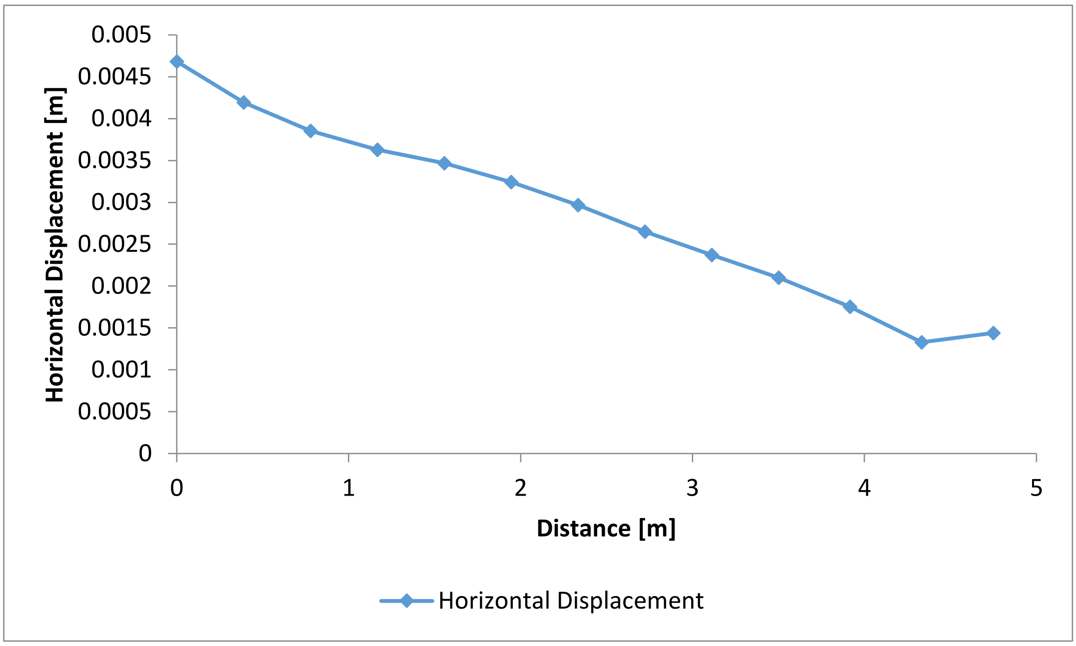

M 20.5: Horizontal displacement of soil along retaining wall

Retaining wall maximum horizontal displacement: 0.00427m

Distance from point of maximum displacement in retaining wall to the top of backfill soil: 0.0m

Model 21:

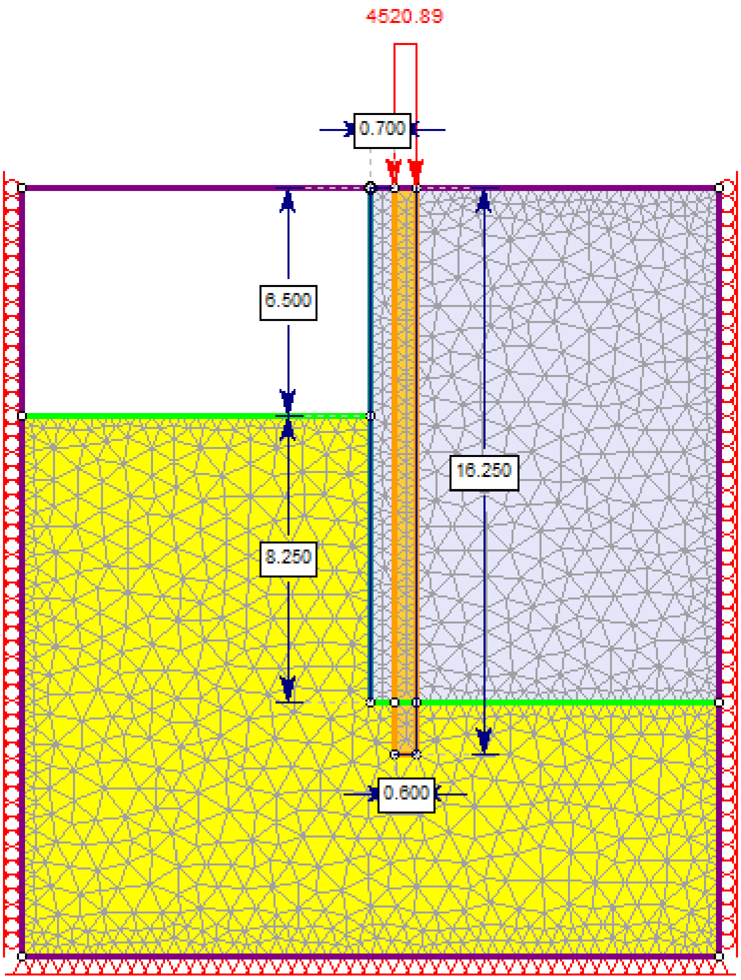

M 21.1: Original model (stage 3)

C_1'	ϕ_1'	γ_1	E_1	C_2'	ϕ_2'	γ_2	E_2	H_1	H_2	H_3	E_3	D_1	D_2	L	Qult
0	29	20	237	45	23	24	48.2	6.50	8.25	1	975416	0.7	0.6	16.25	4520.89

M 21.2: Parameter values

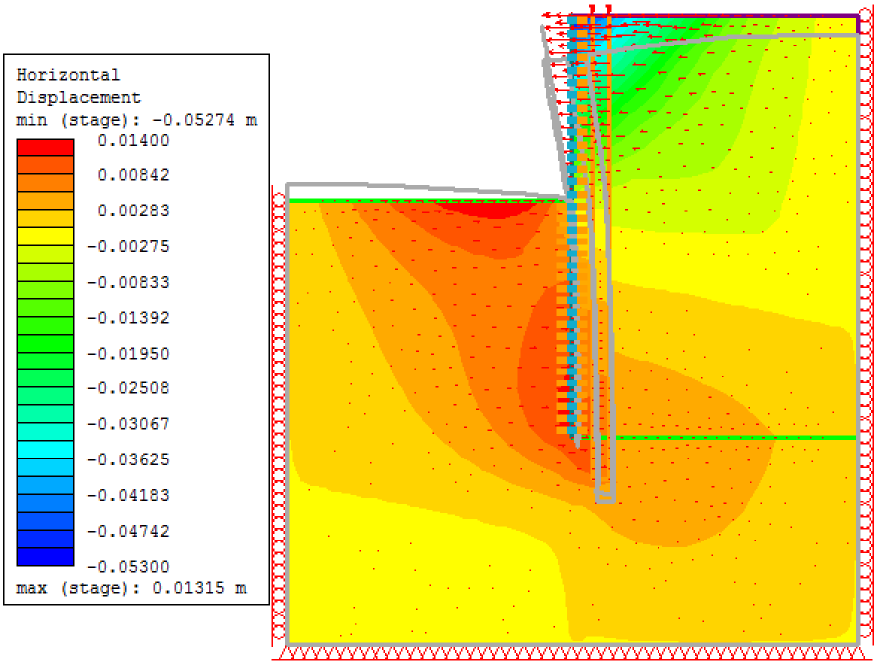

M 21.3: Deformed model (stage 3)

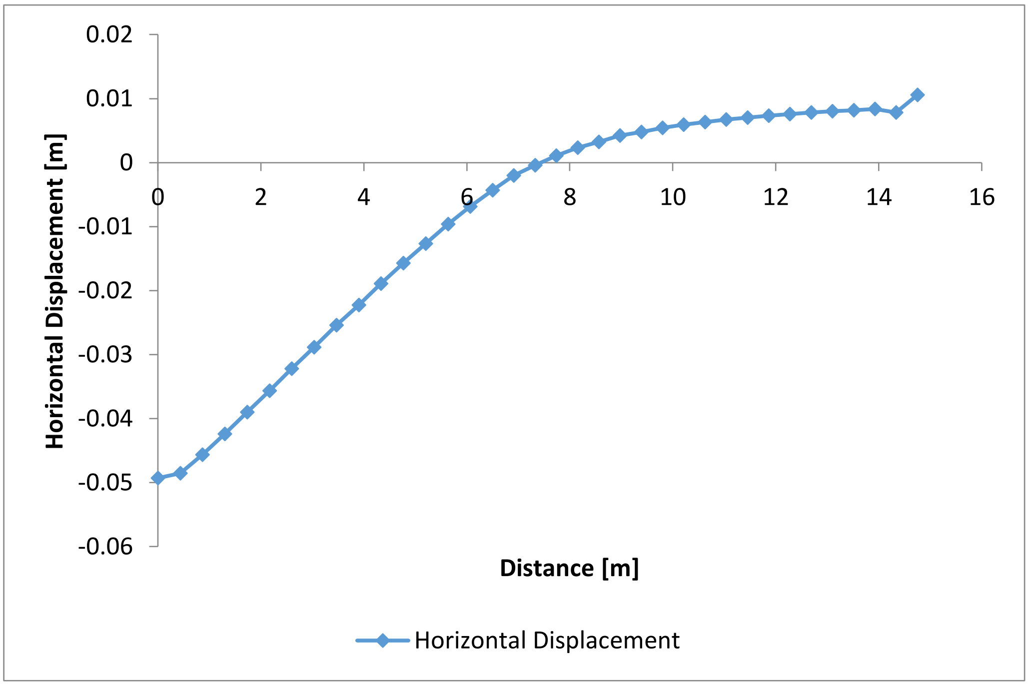

M 21.4: Horizontal displacement of soil along retaining wall

Retaining wall maximum horizontal displacement: -0.05274m

Distance from point of maximum displacement in retaining wall to the top of backfill soil: 0.0m

Model 22:

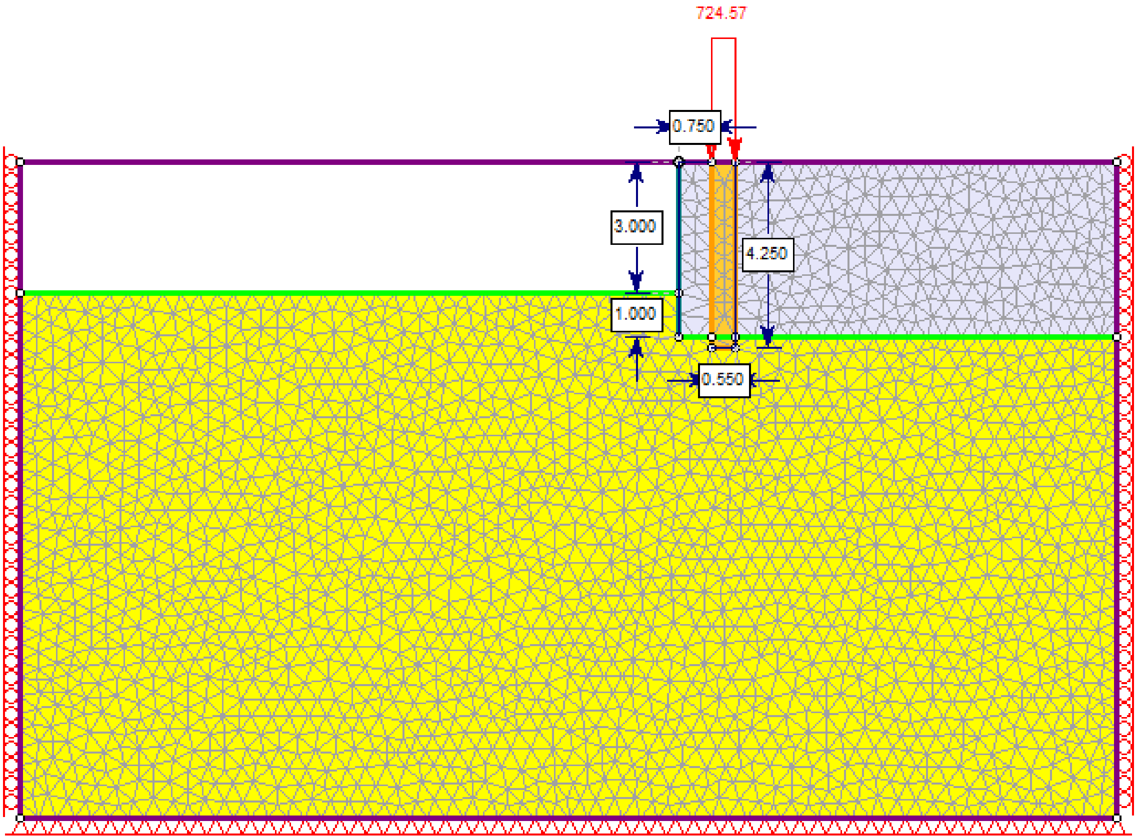

M 22.1: Original model (stage 3)

C_1'	ϕ_1'	γ_1	E_1	C_2'	ϕ_2'	γ_2	E_2	H_1	H_2	H_3	E_3	D_1	D_2	L	Qult
0	32	18	166	56	15	18	19.8	3.00	1	0.5	897387	0.75	0.55	4.25	724.57

M 22.2: Parameter values

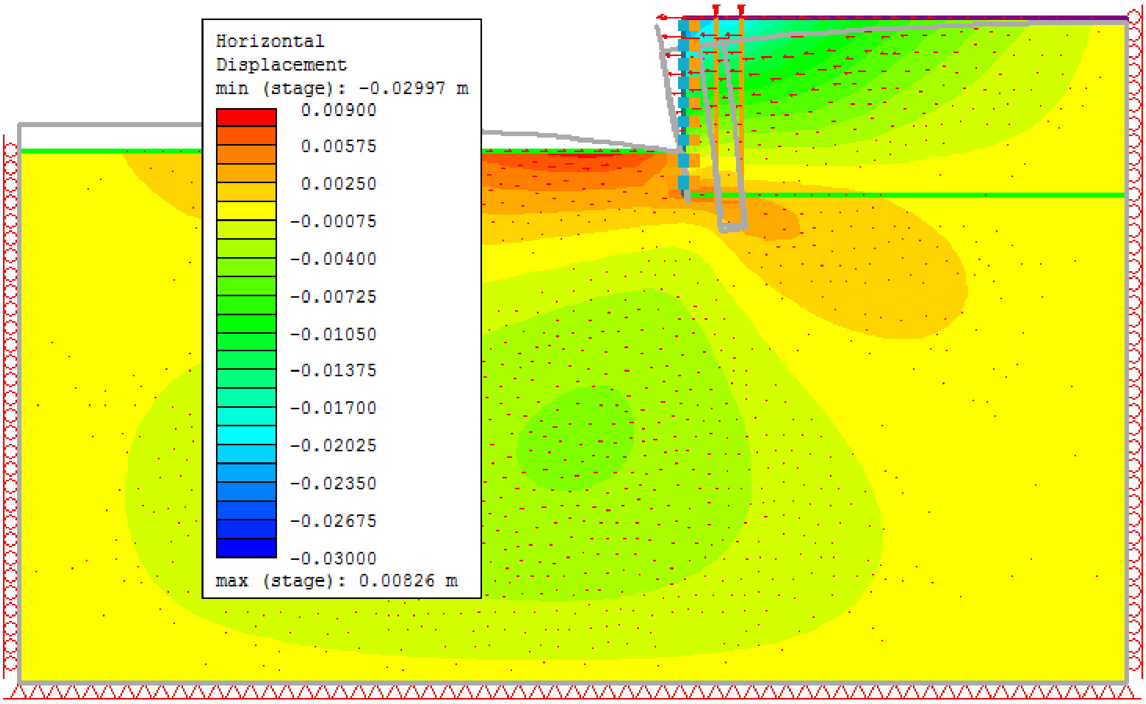

M 22.3: Deformed model (stage 3)

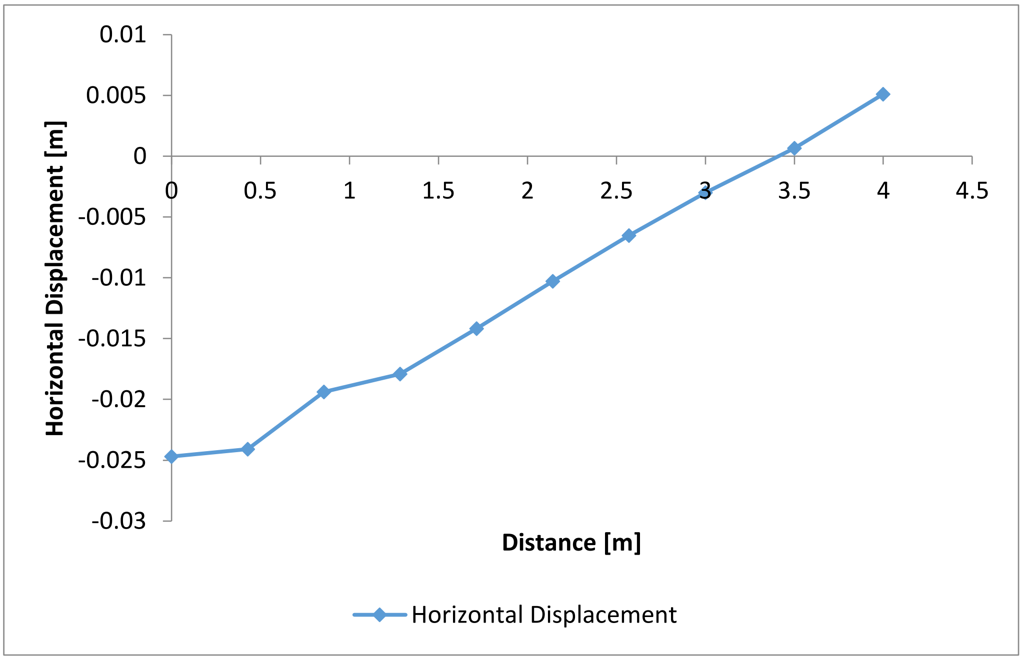

M 22.4: Horizontal displacement of soil along retaining wall

Retaining wall maximum horizontal displacement: -0.02997m

Distance from point of maximum displacement in retaining wall to the top of backfill soil: 0.0m

Model 23:

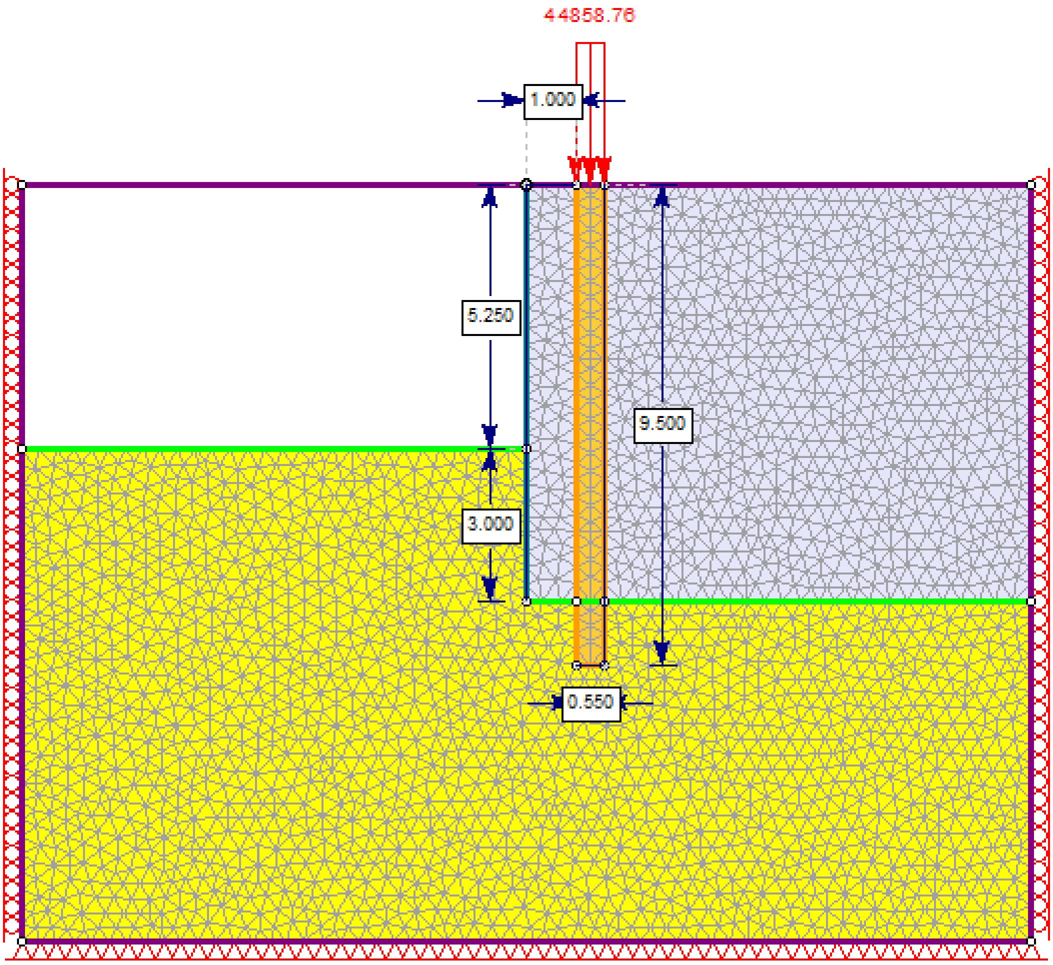

M 23.1: Original model (stage 3)

C'_1	ϕ'_1	γ_1	E_1	C'_2	ϕ'_2	γ_2	E_2	H_1	H_2	H_3	E_3	D_1	D_2	L	Qult
0	31	19	264	51	29	17	35.2	5.25	3	1.25	1149355	1	0.55	9.5	4858.76

M 23.2: Parameter values

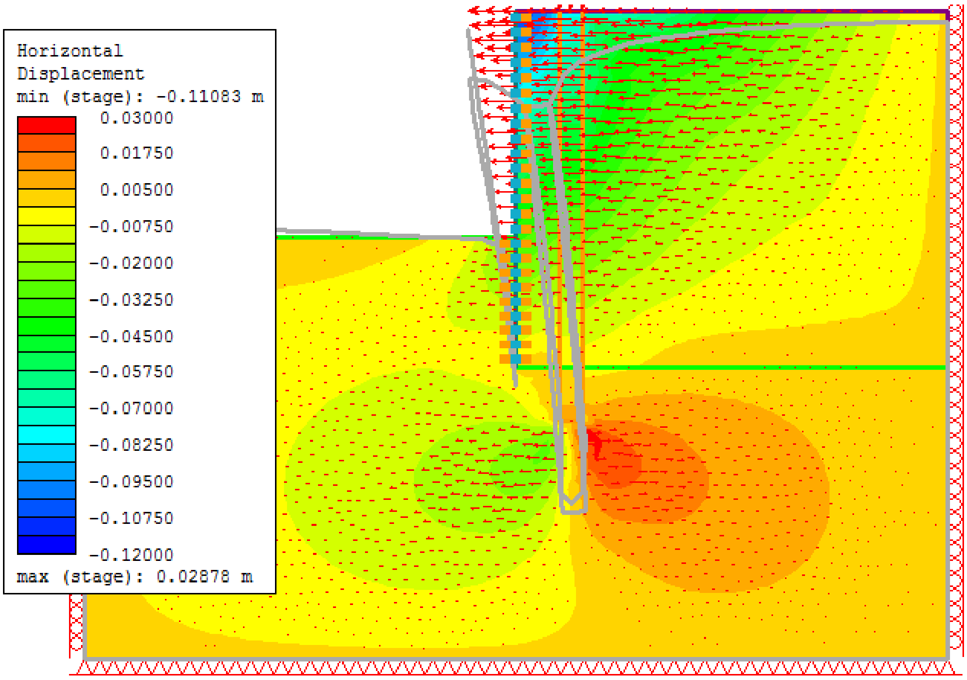

M 23.3: Deformed model (stage 3)

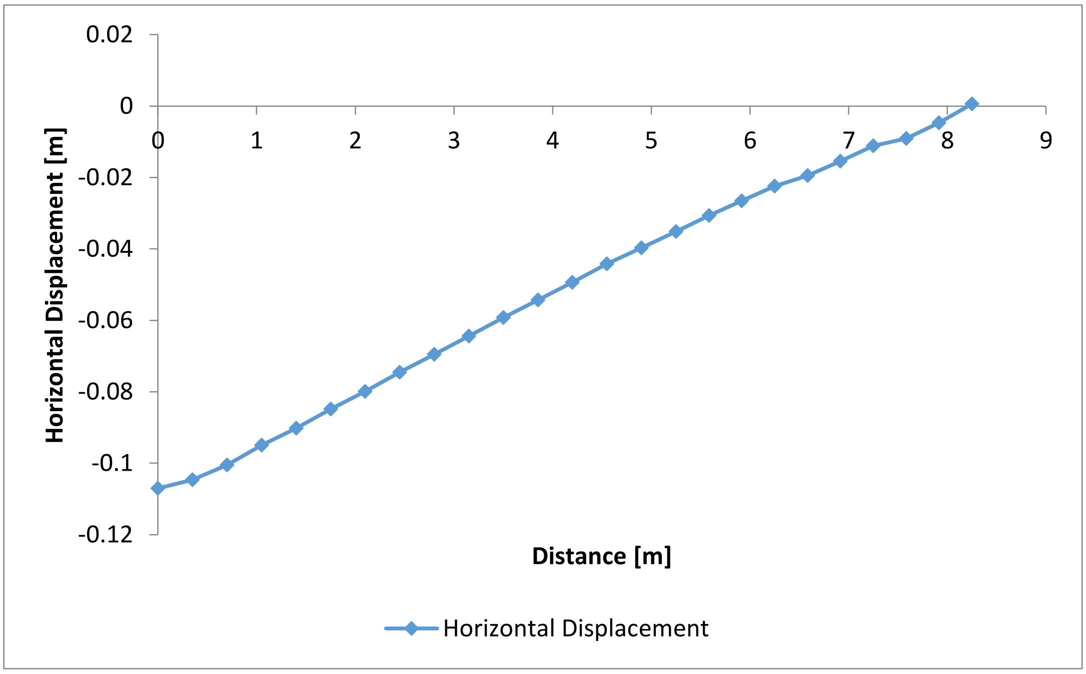

M 23.4: Horizontal displacement of soil along retaining wall

Retaining wall maximum horizontal displacement: -0.11083m

Distance from point of maximum displacement in retaining wall to the top of backfill soil: 0.0m

Model 24:

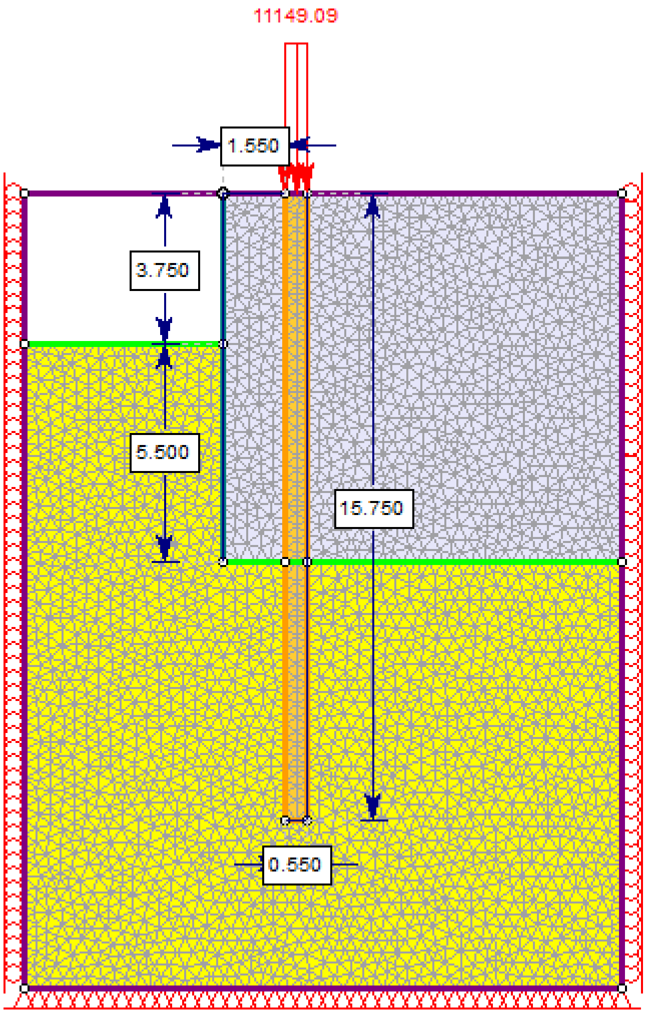

M 24.1: Original model (stage 3)

C_1'	ϕ_1'	γ_1	E_1	C_2'	ϕ_2'	γ_2	E_2	H_1	H_2	H_3	E_3	D_1	D_2	L	Qult
0	30	19	48	23	4	22	6.0	3.75	5.5	0.75	738893	1.55	0.55	15.75	1149.09

M 24.2: Parameter values

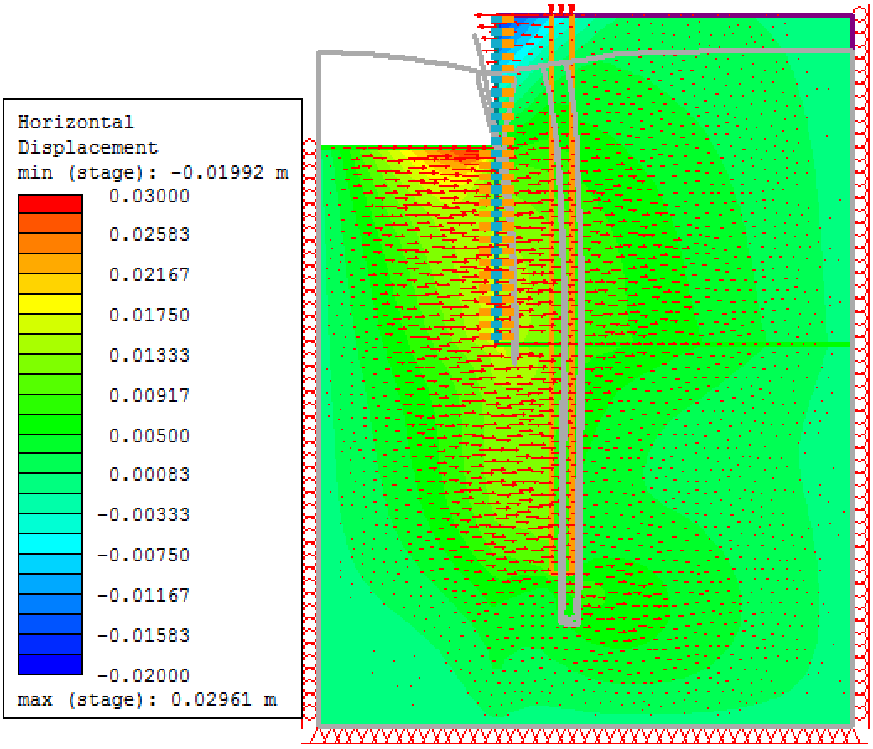

M 24.3: Deformed model (stage 3)

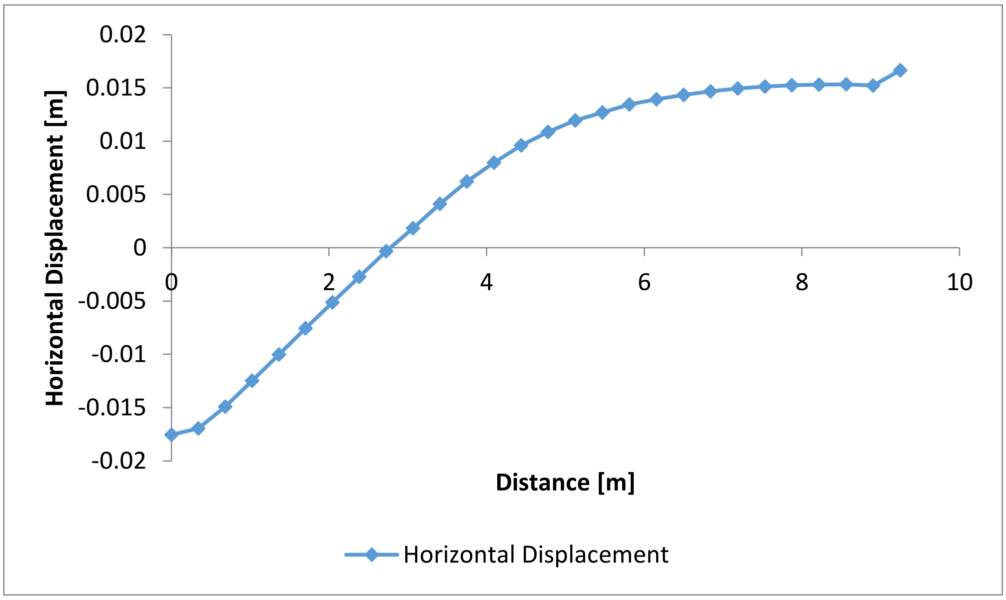

M 24.4: Horizontal displacement of soil along retaining wall

Retaining wall maximum horizontal displacement: -0.01992m

Distance from point of maximum displacement in retaining wall to the top of backfill soil: 0.0m

Model 25:

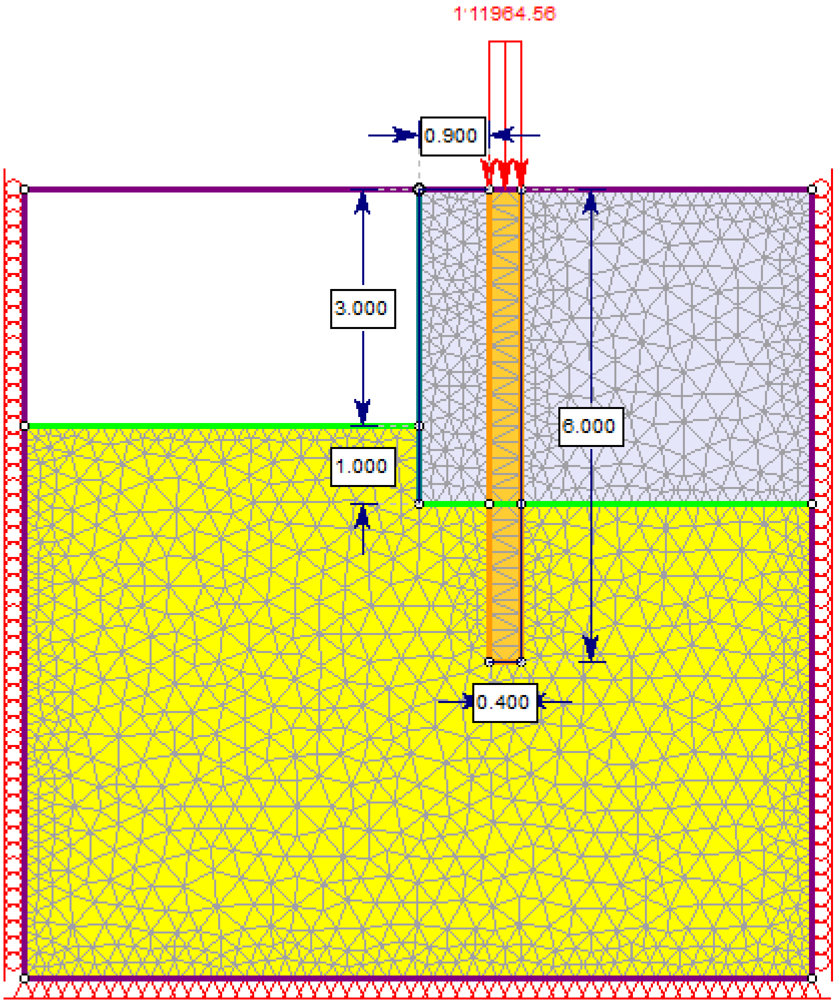

M 25.1: Original model (stage 3)

C_1'	ϕ_1'	γ_1	E_1	C_2'	ϕ_2'	γ_2	E_2	H_1	H_2	H_3	E_3	D_1	D_2	L	Qult
0	37	21	90	42	37	23	39.2	3.00	1	1	1108965	0.9	0.4	6	11964.56

M 25.2: Parameter values

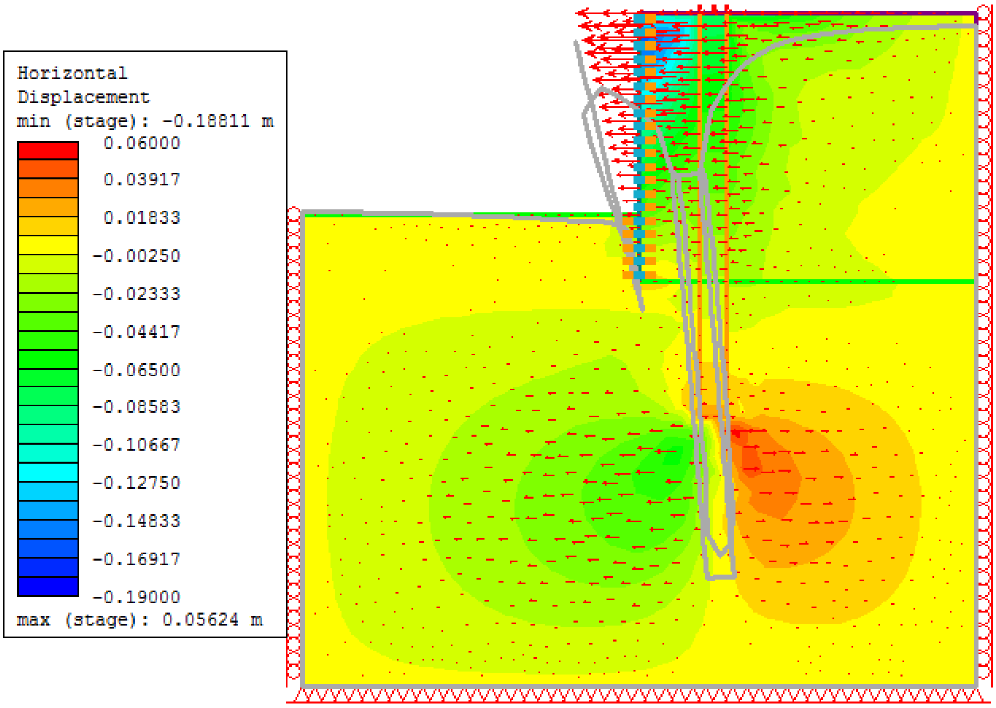

M 25.3: Deformed model (stage 3)

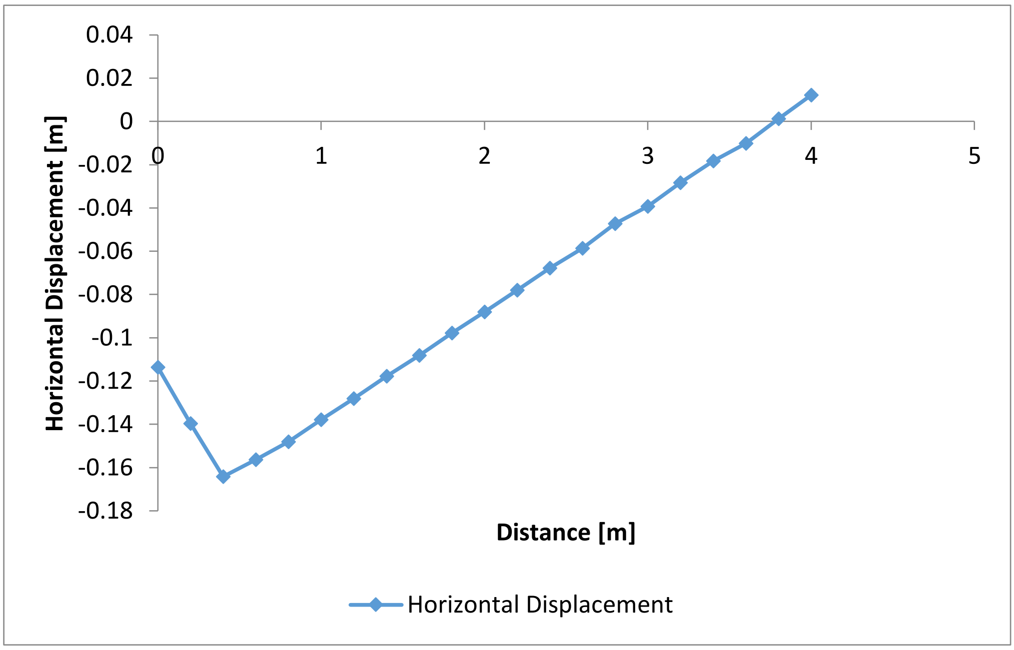

M 25.4: Horizontal displacement of soil along retaining wall

Retaining wall maximum horizontal displacement: -0.18811m

Distance from point of maximum displacement in retaining wall to the top of backfill soil: 0.0m

Model 26:

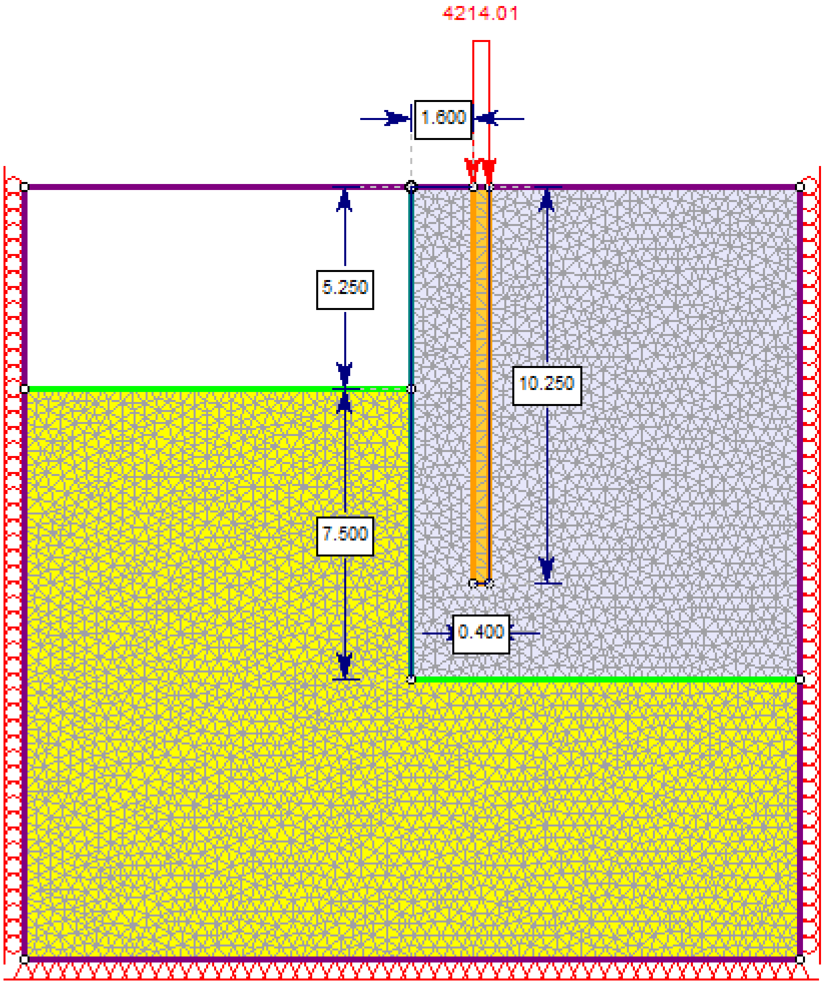

M 26.1: Original model (stage 3)

C'_1	ϕ'_1	γ_1	E_1	C'_2	ϕ'_2	γ_2	E_2	H_1	H_2	H_3	E_3	D_1	D_2	L	Qult
0	28	21	106	36	31	21	31.8	5.25	7.5	1	743782	1.6	0.4	10.25	4214.01

M 26.2: Parameter values

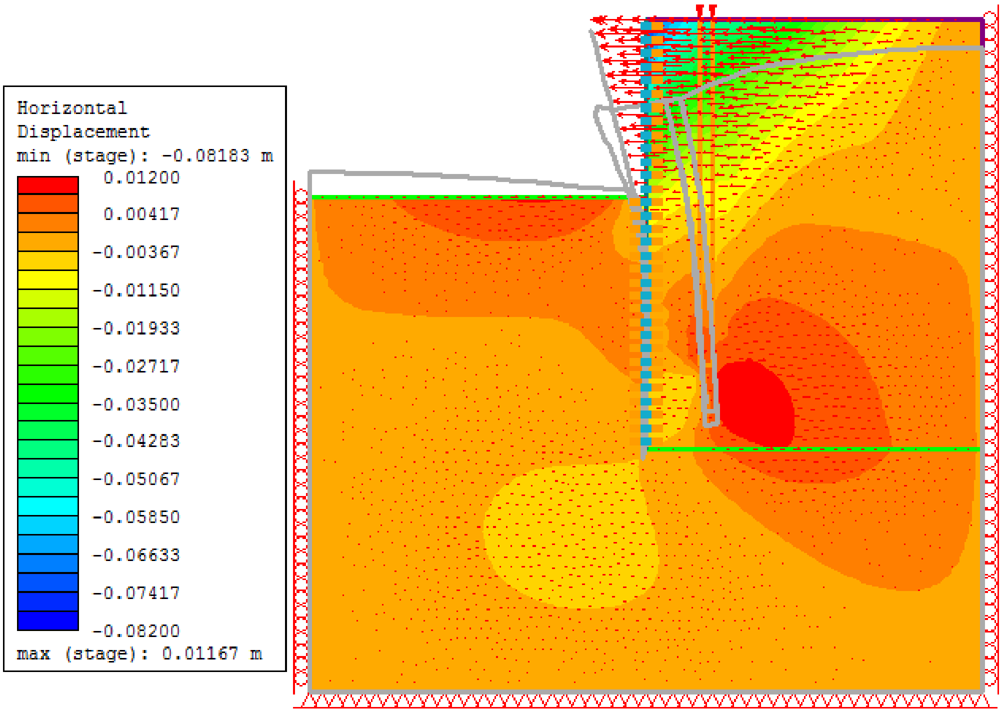

M 26.3: Deformed model (stage 3)

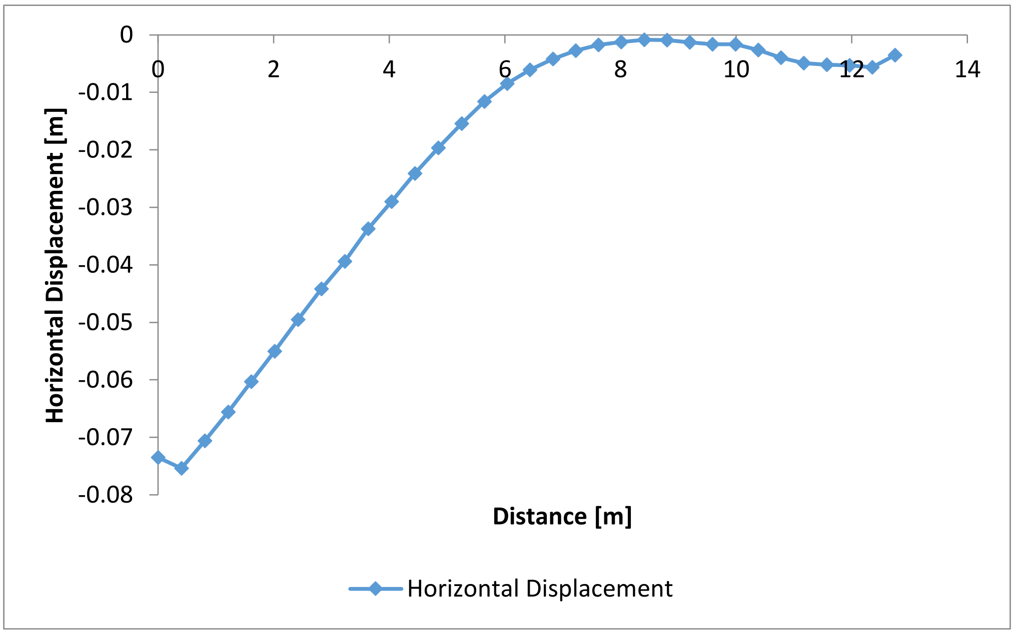

M 26.4: Horizontal displacement of soil along retaining wall

Retaining wall maximum horizontal displacement: -0.08183m

Distance from point of maximum displacement in retaining wall to the top of backfill soil: 0.0m

Model 27:

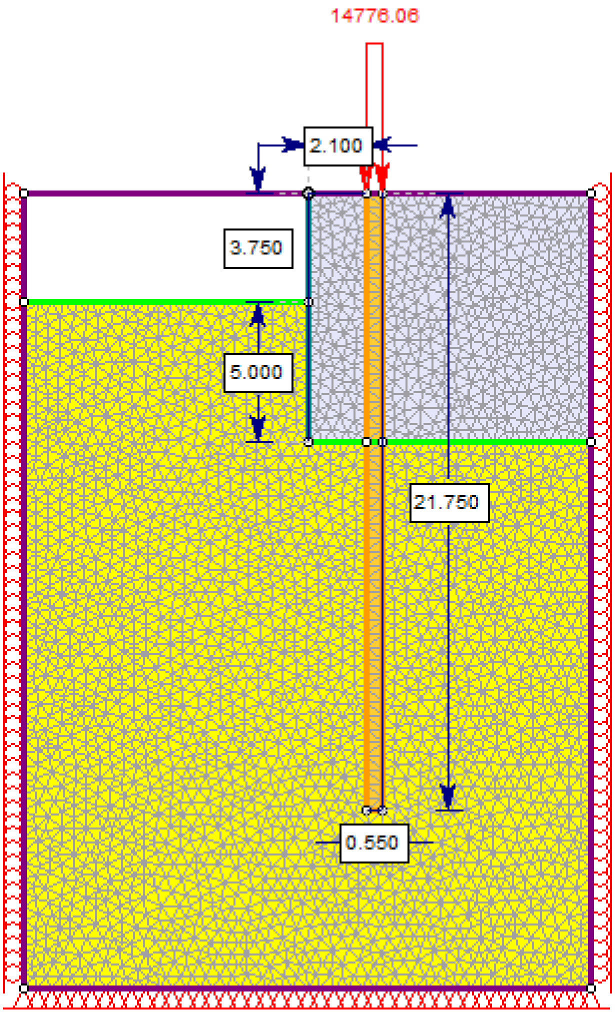

M 27.1: Original model (stage 3)

C_1'	ϕ_1'	γ_1	E_1	C_2'	ϕ_2'	γ_2	E_2	H_1	H_2	H_3	E_3	D_1	D_2	L	Qult
0	45	19	40	21	32	21	31.9	3.75	5	0.5	1150628	2.1	0.55	21.25	14776.06

M 27.2: Parameter values

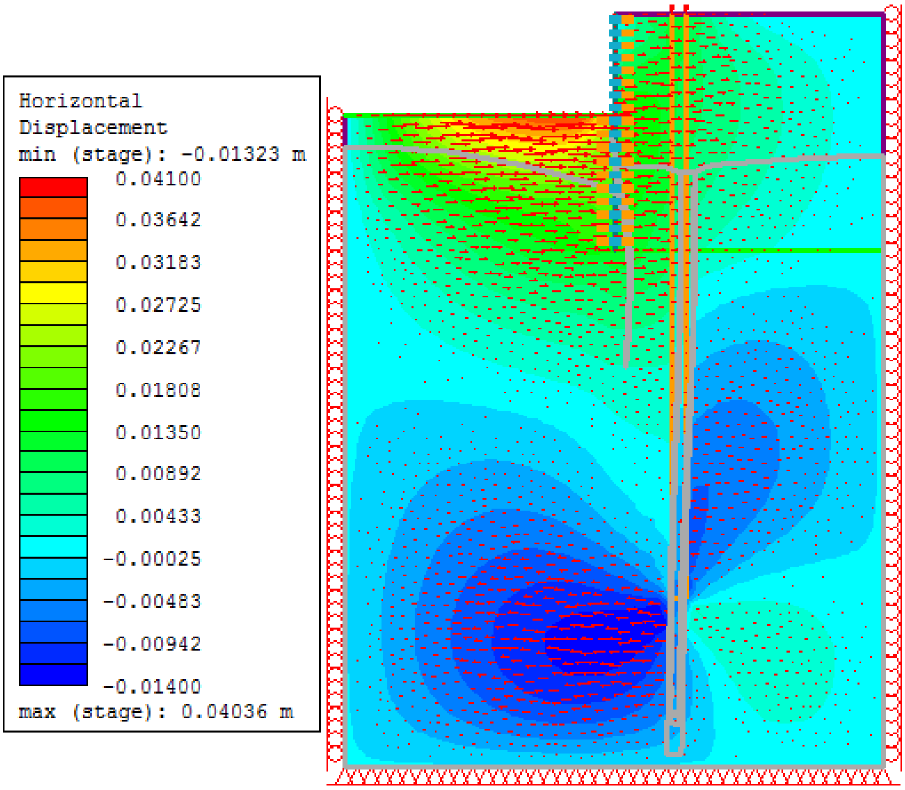

M 27.3: Deformed model (stage 3)

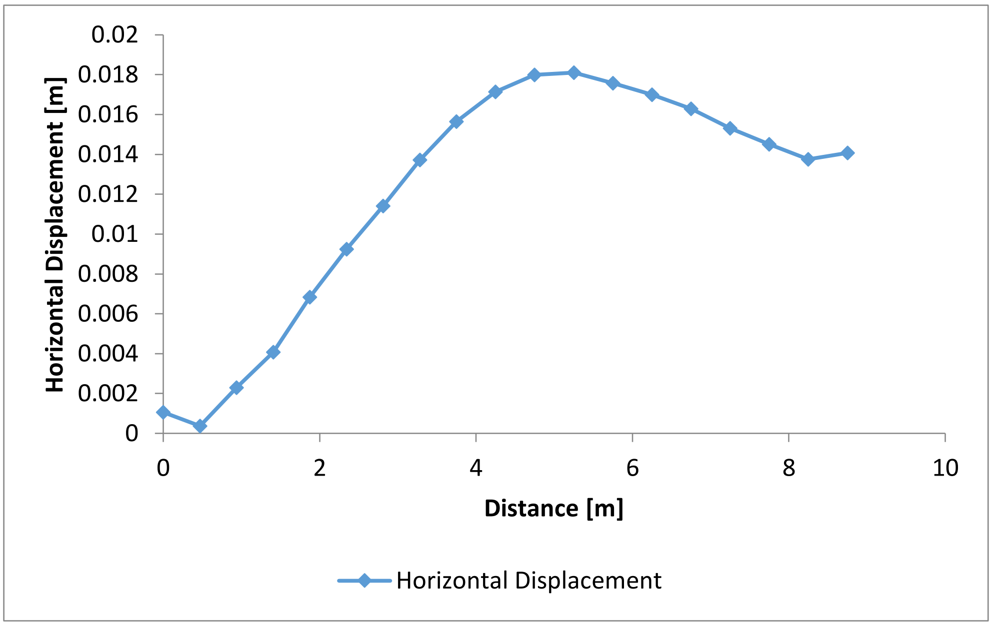

M 27.4: Horizontal displacement of soil along retaining wall

Retaining wall maximum horizontal displacement: 0.0181m

Distance from point of maximum displacement in retaining wall to the top of backfill soil: 5.25m

Model 28:

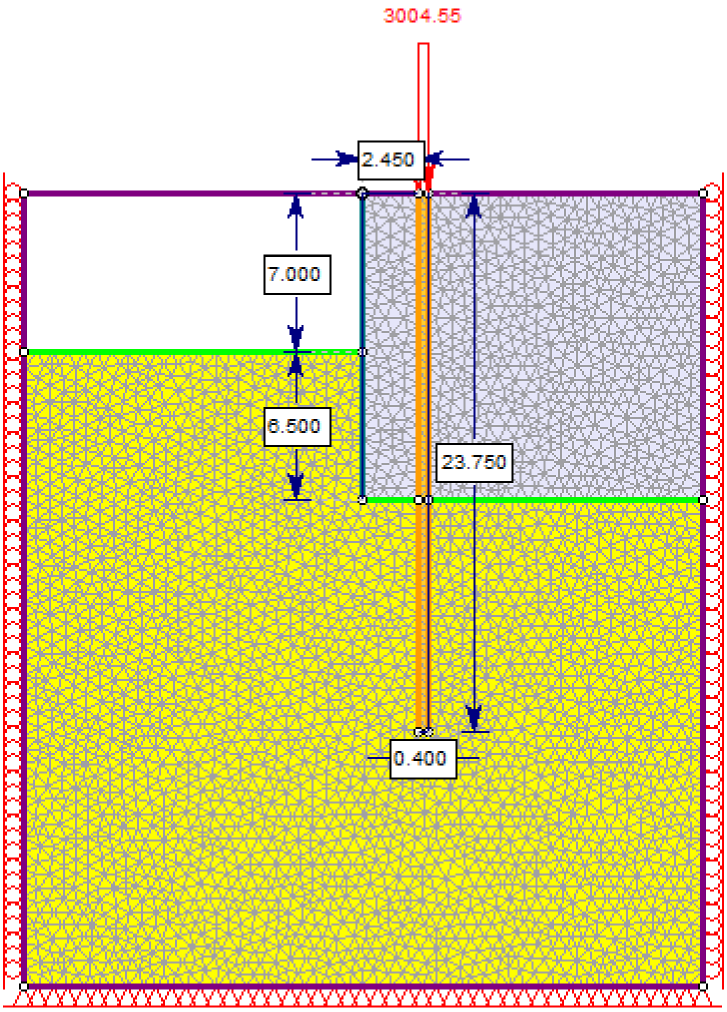

M 28.1: Original model (stage 3)

C_1'	ϕ_1'	γ_1	E_1	C_2'	ϕ_2'	γ_2	E_2	H_1	H_2	H_3	E_3	D_1	D_2	L	Qult
0	37	20	281	50	10	19	20.4	7.00	6.5	1	1022344	2.45	0.4	23.75	3004.55

M 28.2: Parameter values

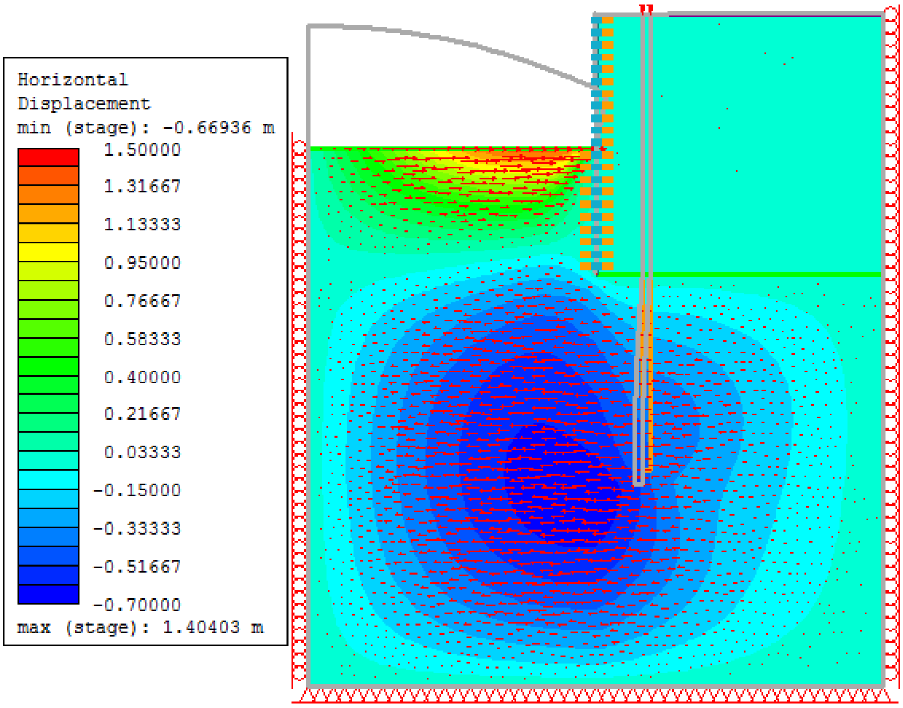

M 28.3: Deformed model (stage 3)

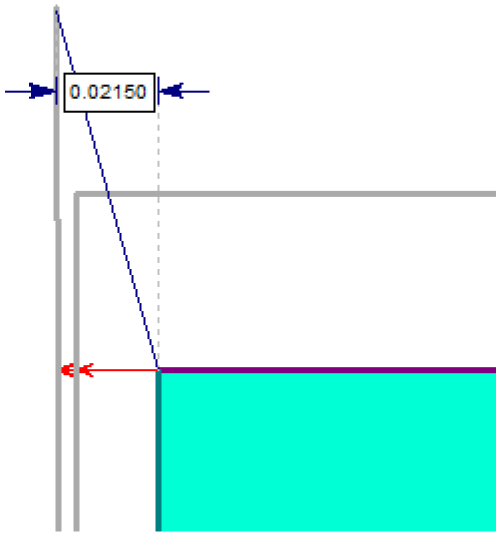

M 28.4: Detailed view of cross-section of retaining wall and soil (stage 3)

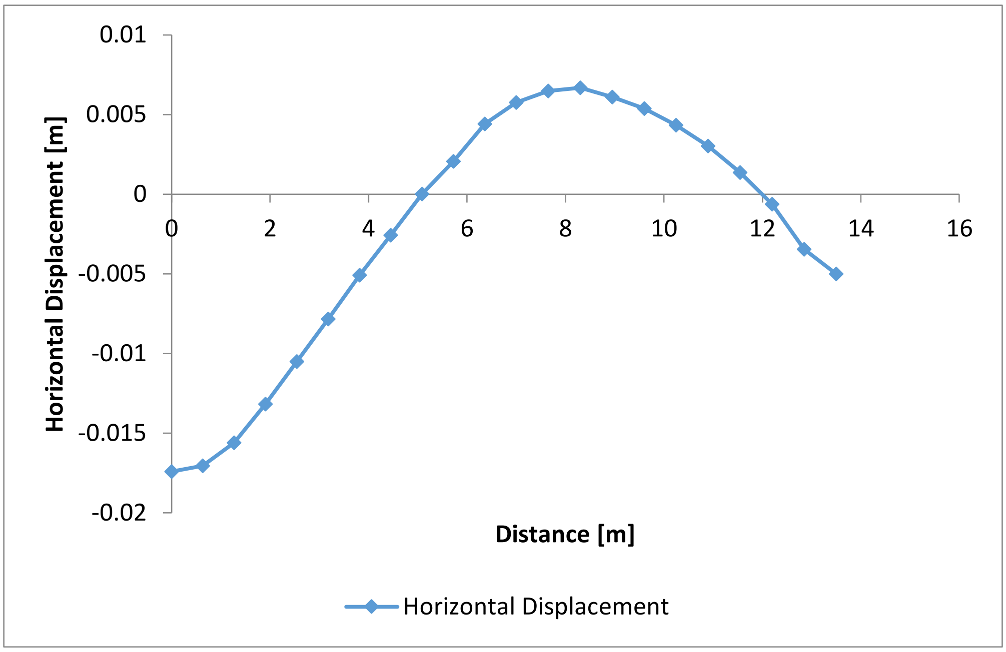

M 28.5: Horizontal displacement of soil along retaining wall

Retaining wall maximum horizontal displacement: -0.0215m

Distance from point of maximum displacement in retaining wall to the top of backfill soil: 0.0m

Model 29:

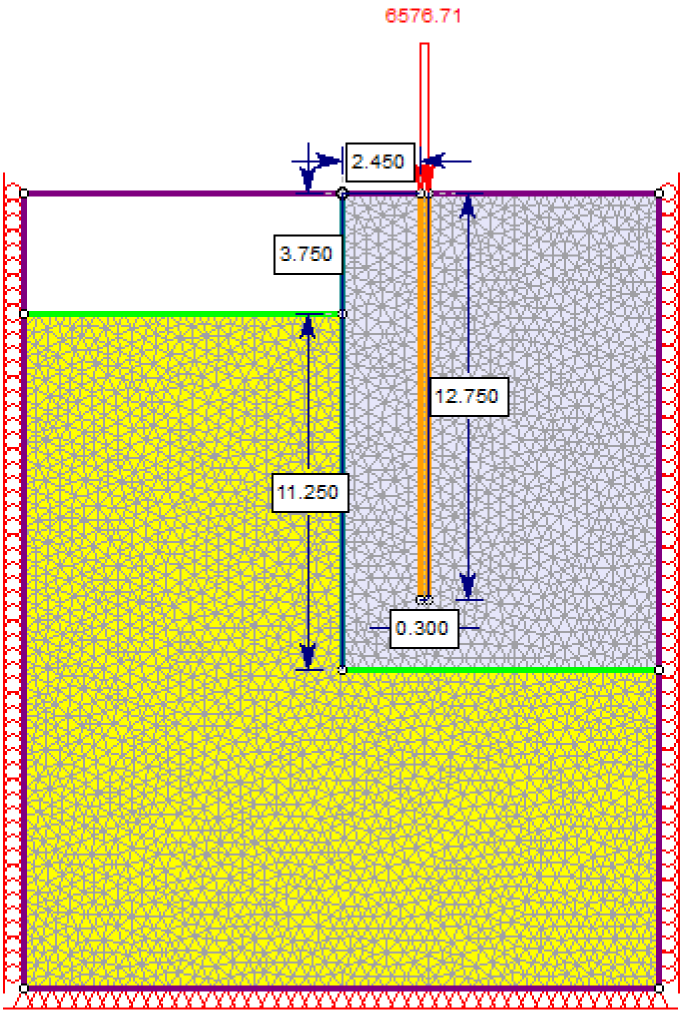

M 29.1: Original model (stage 3)

C_1'	ϕ_1'	γ_1	E_1	C_2'	ϕ_2'	γ_2	E_2	H_1	H_2	H_3	E_3	D_1	D_2	L	Qult
0	41	21	299	21	20	20	48.5	3.75	11.25	1.5	942513	2.45	0.3	12.75	6576.71

M 29.2: Parameter values

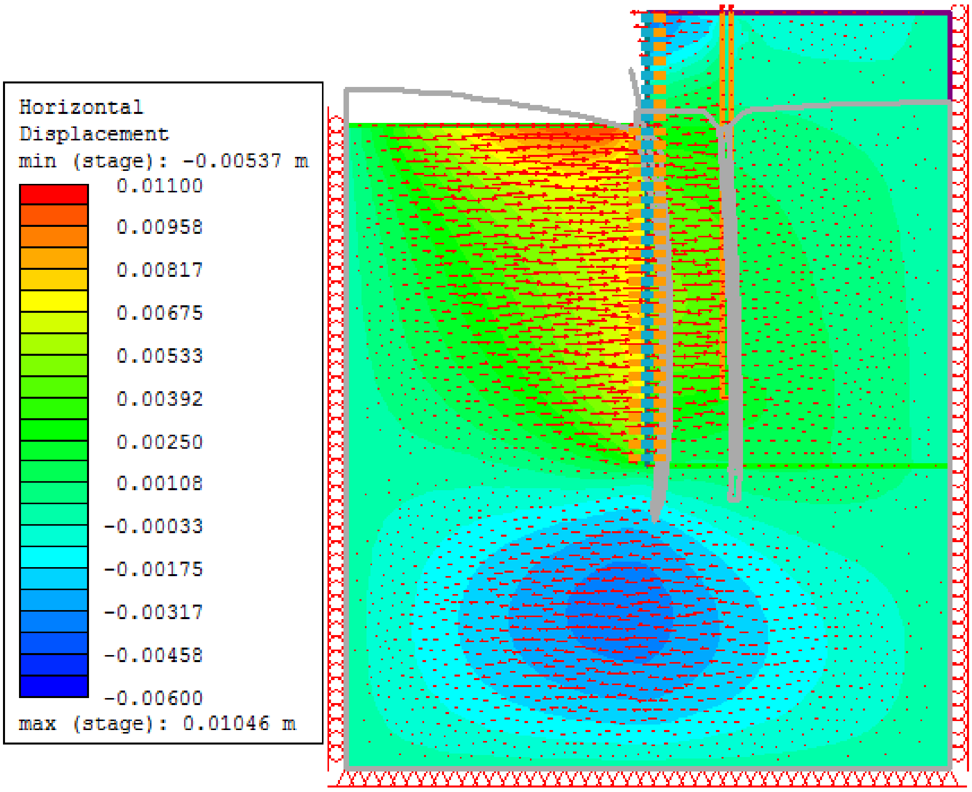

M 29.3: Deformed model (stage 3)

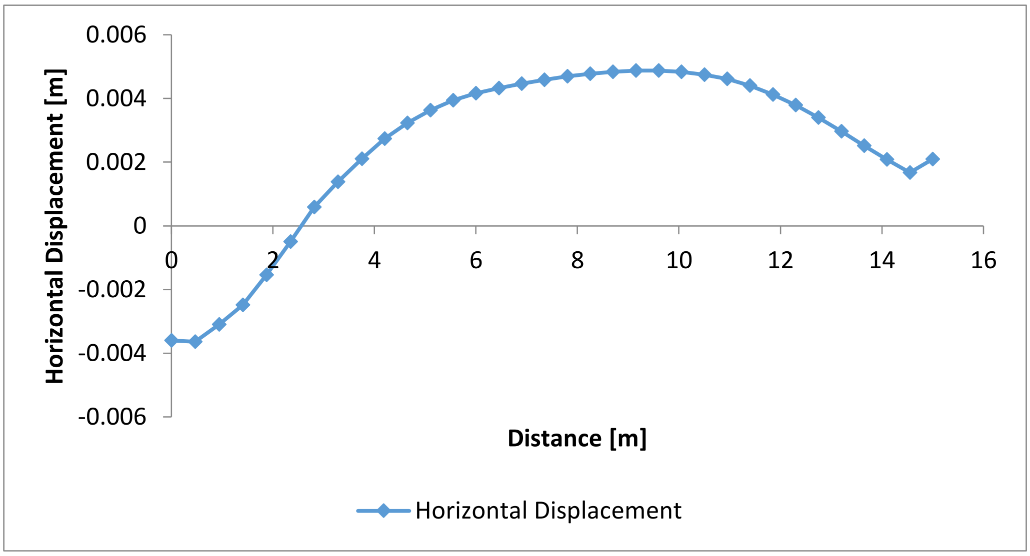

M 29.4: Horizontal displacement of soil along retaining wall

Retaining wall maximum horizontal displacement: -0.00537m

Distance from point of maximum displacement in retaining wall to the top of backfill soil: 0.0m

Model 30:

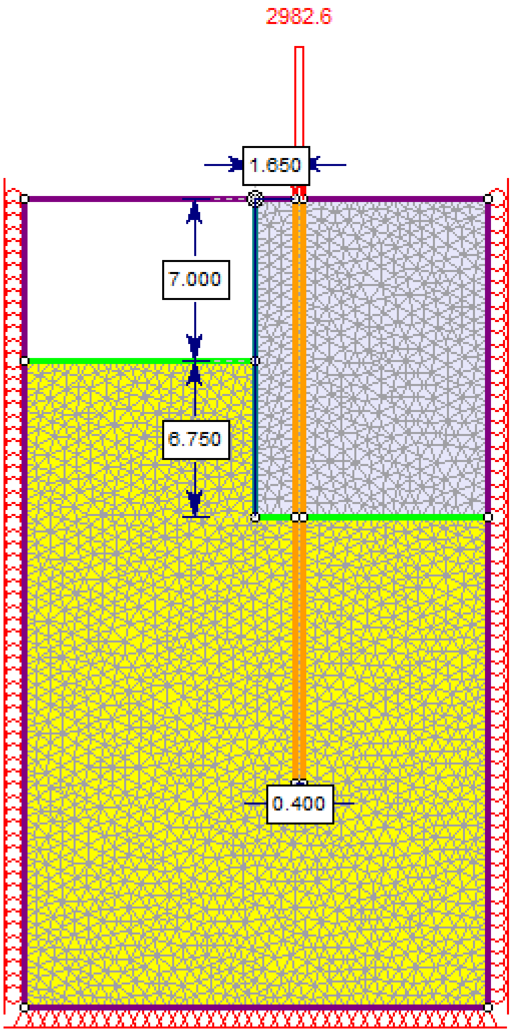

M 30.1: Original model (stage 3)

C_1'	ϕ_1'	γ_1	E_1	C_2'	ϕ_2'	γ_2	E_2	H_1	H_2	H_3	E_3	D_1	D_2	L	Qult
0	42	19	49	42	10	20	29.8	7.00	6.75	1	1085462	1.65	0.4	25.25	2982.6

M 30.2: Parameter values

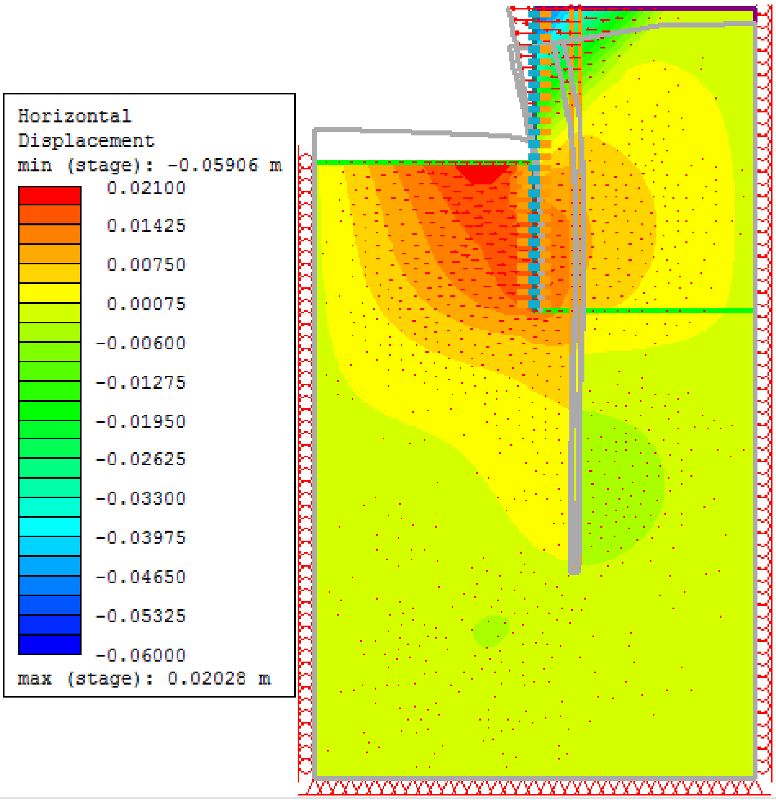

M 30.3: Deformed model (stage 3)

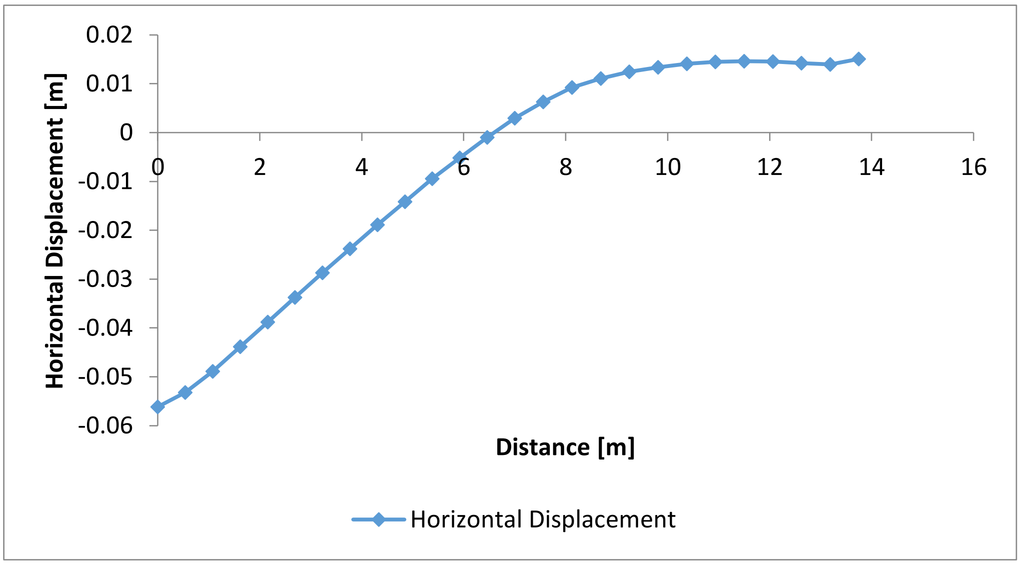

M 30.4: Horizontal displacement of soil along retaining wall

Retaining wall maximum horizontal displacement: -0.05906m

Distance from point of maximum displacement in retaining wall to the top of backfill soil: 0.0m

Model 31:

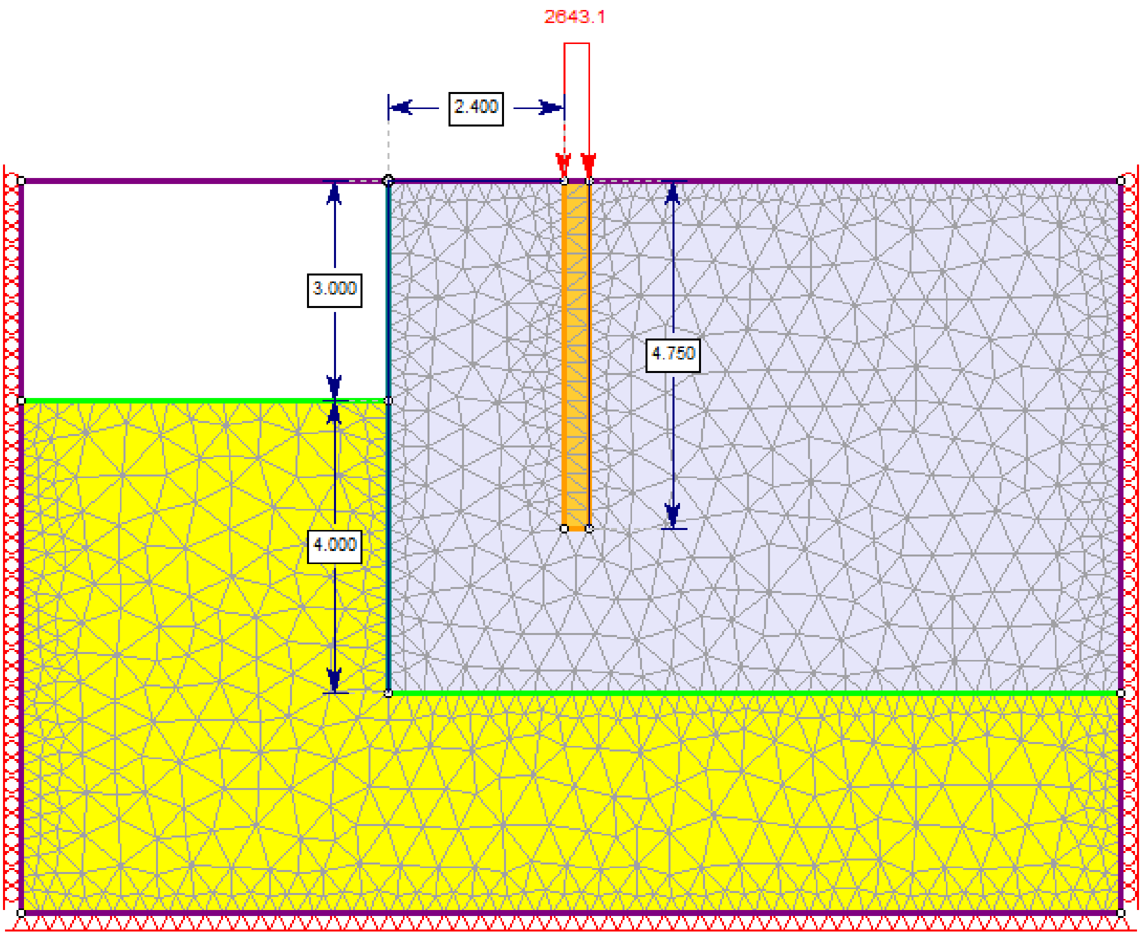

M 31.1: Original model (stage 3)

C_1'	ϕ_1'	γ_1	E_1	C_2'	ϕ_2'	γ_2	E_2	H_1	H_2	H_3	E_3	D_1	D_2	L	Qult
0	37	20	109	19	27	23	41.4	3.00	4	0.75	881766	2.4	0.35	4.75	2643.1

M 31.2: Parameter values

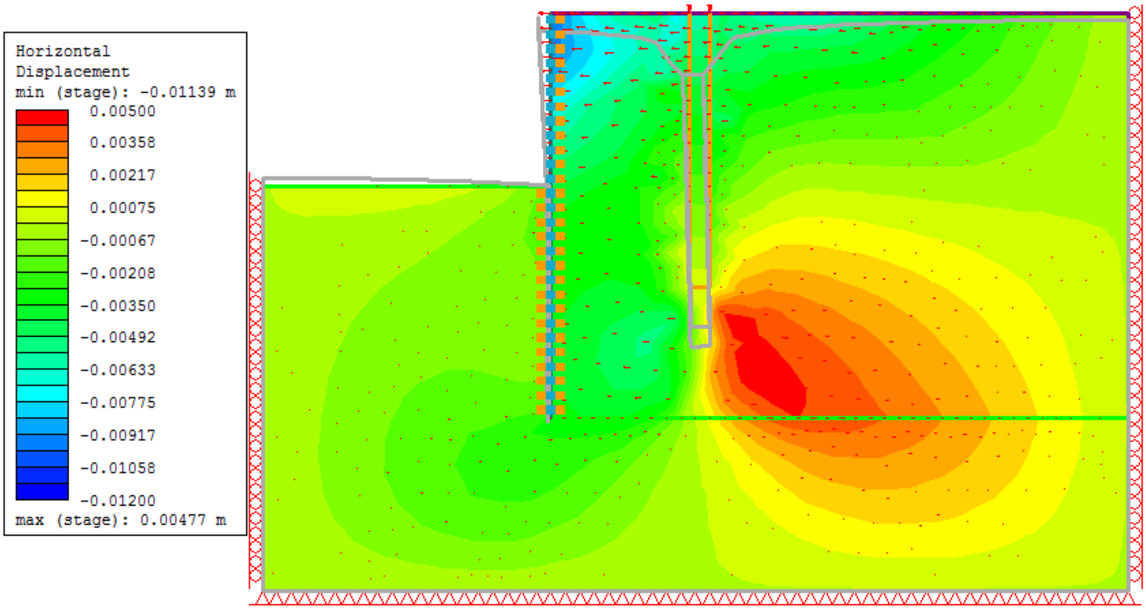

M 31.3: Deformed model (stage 3)

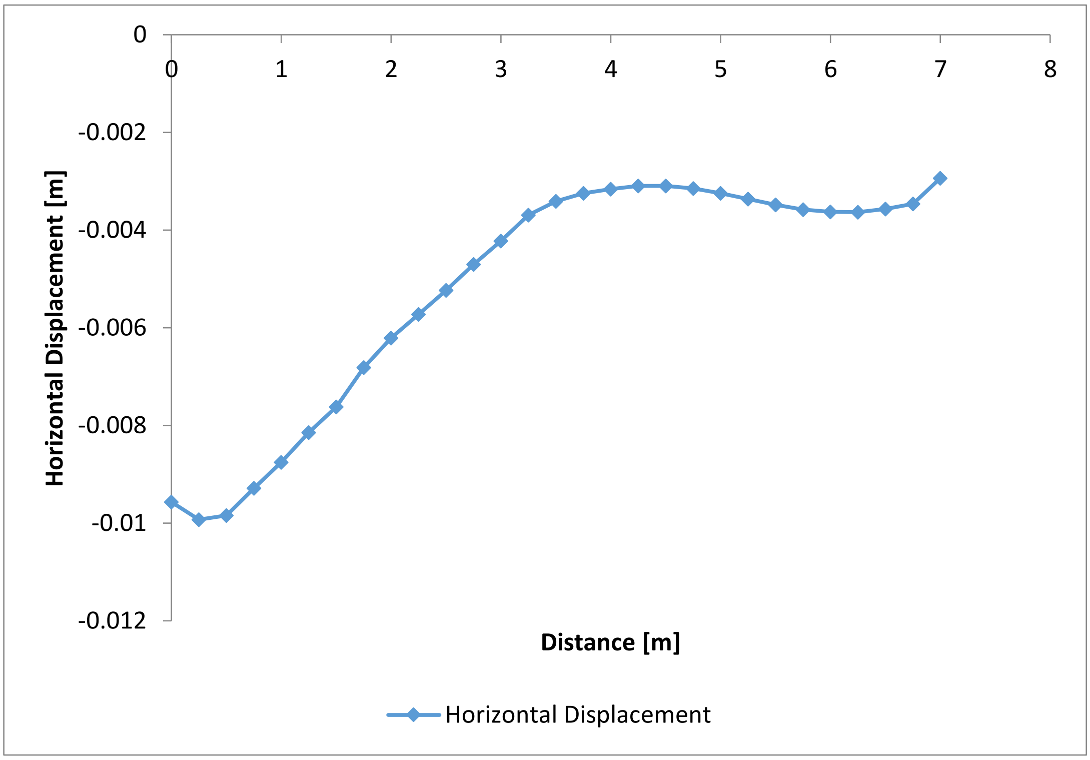

M 31.4: Horizontal displacement of soil along retaining wall

Retaining wall maximum horizontal displacement: -0.01139m

Distance from point of maximum displacement in retaining wall to the top of backfill soil: 0.0m

Model 32:

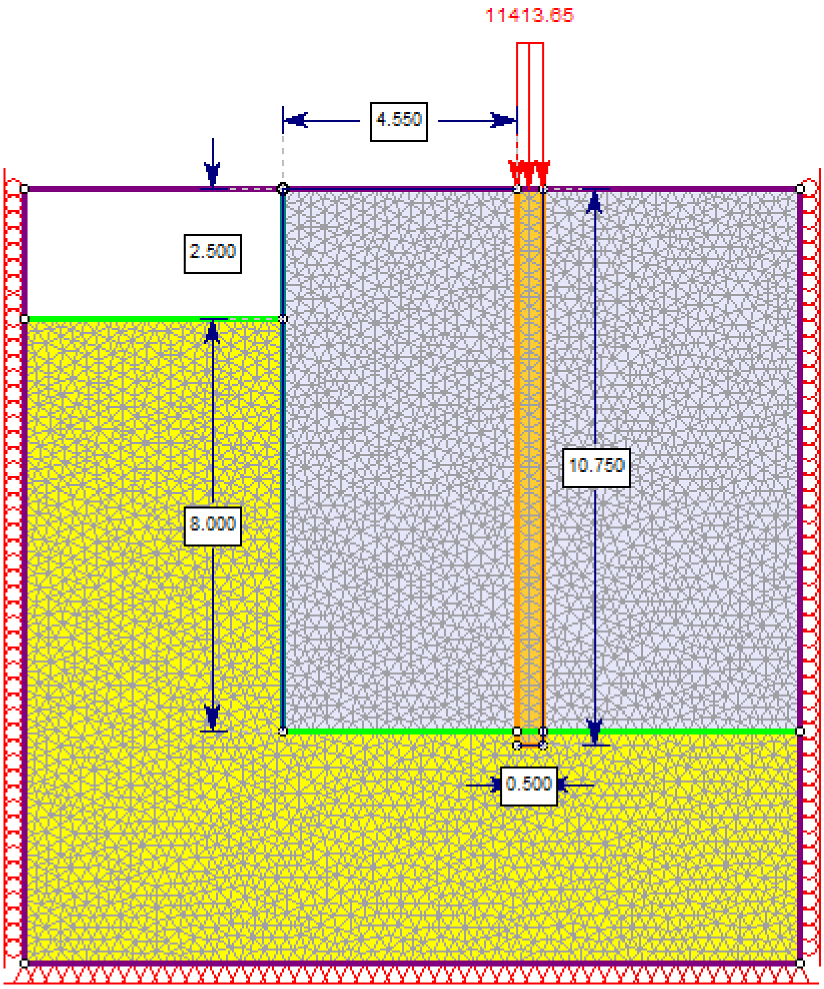

M 32.1: Original model (stage 3)

C_1'	ϕ_1'	γ_1	E_1	C_2'	ϕ_2'	γ_2	E_2	H_1	H_2	H_3	E_3	D_1	D_2	L	Qult
0	30	22	76	15	5	25	21.7	2.50	8	1	1096506	4.55	0.5	10.75	1413.65

M 32.2: Parameter values

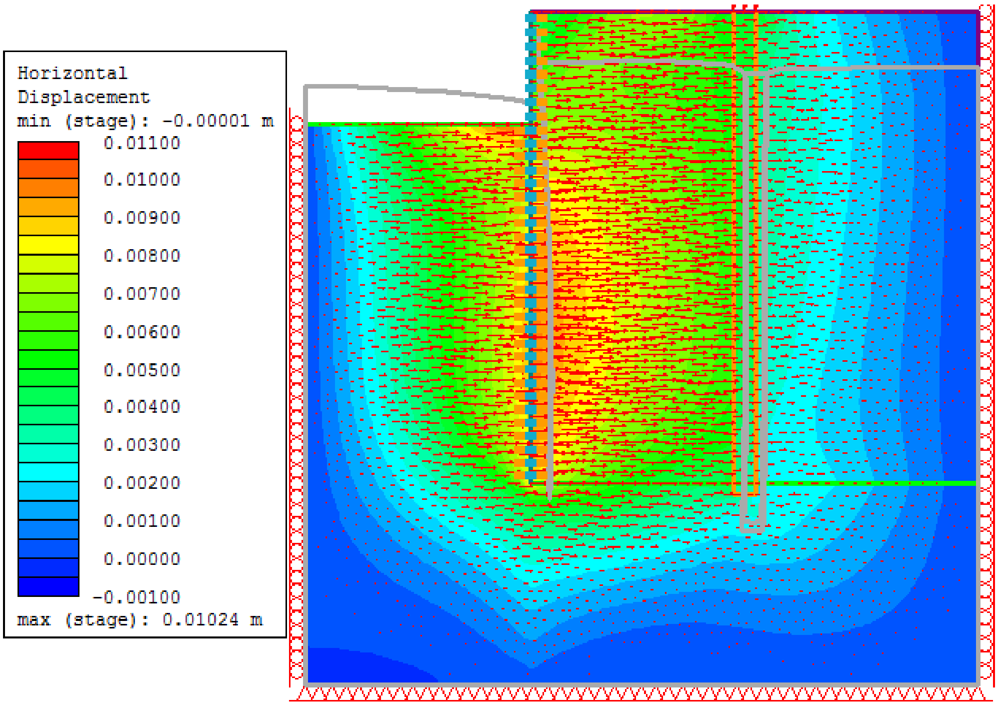

M 32.3: Deformed model (stage 3)

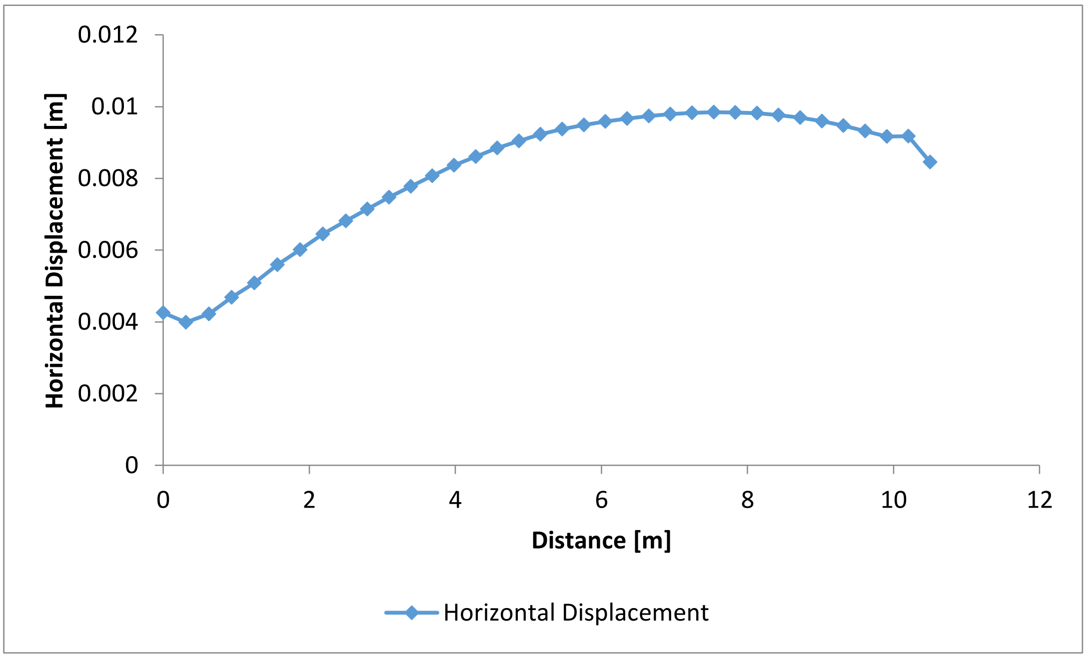

M 32.4: Horizontal displacement of soil along retaining wall

Retaining wall maximum horizontal displacement: 0.00984m

Distance from point of maximum displacement in retaining wall to the top of backfill soil: 7.537m

Model 33:

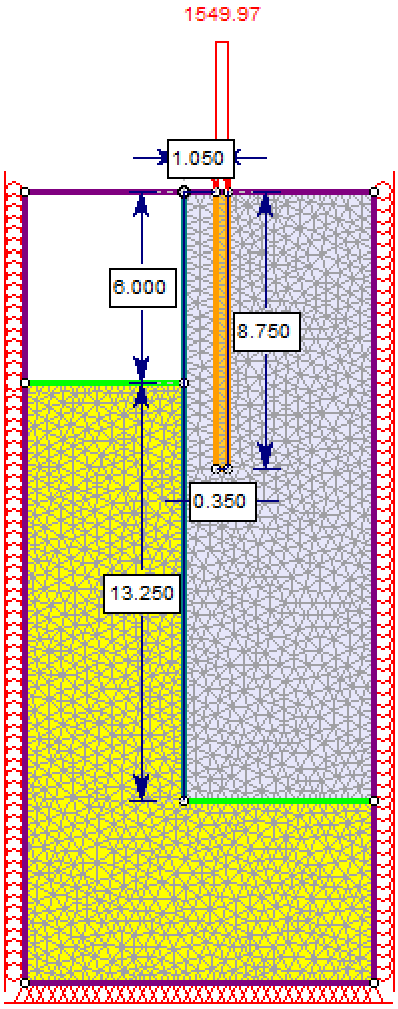

M 33.1: Original model (stage 3)

C_1'	ϕ_1'	γ_1	E_1	C_2'	ϕ_2'	γ_2	E_2	H_1	H_2	H_3	E_3	D_1	D_2	L	Qult
0	29	22	100	40	11	23	27.5	6.00	13.25	1.25	949846	1.05	0.35	8.75	1549.97

M 33.2: Parameter values

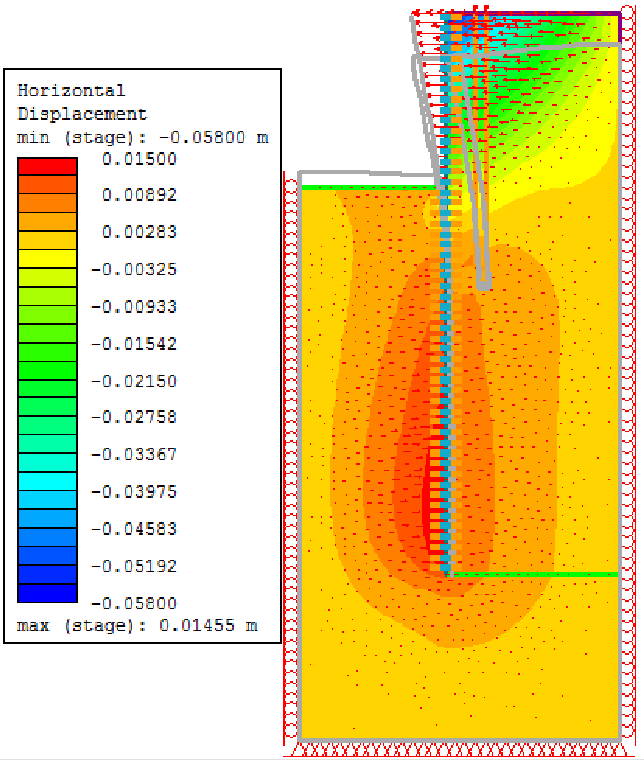

M 33.3: Deformed model (stage 3)

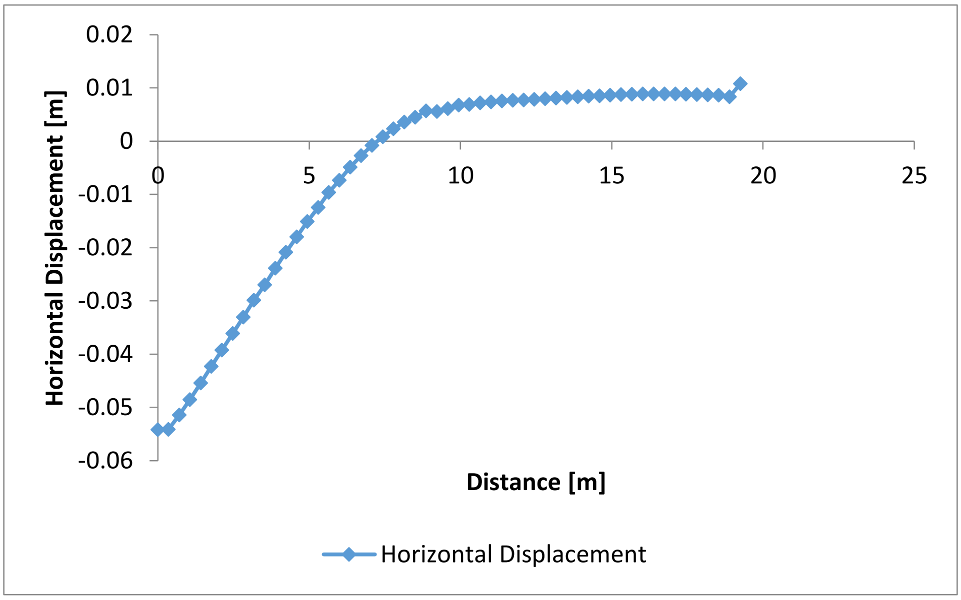

M 33.4: Horizontal displacement of soil along retaining wall

Retaining wall maximum horizontal displacement: -0.058m

Distance from point of maximum displacement in retaining wall to the top of backfill soil: 0.0m

Model 34:

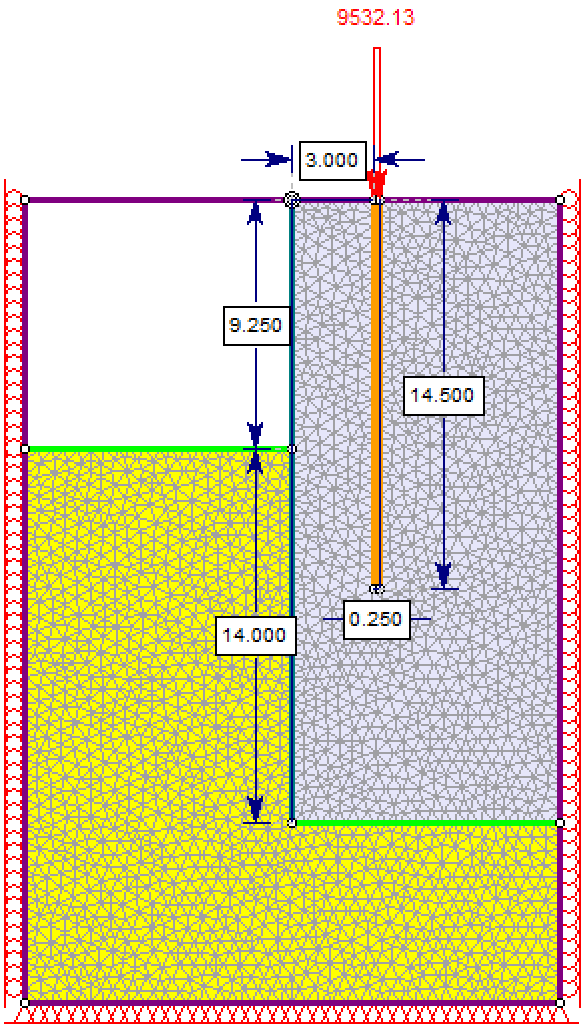

M 34.1: Original model (stage 3)

C'_1	ϕ'_1	γ_1	E_1	C'_2	ϕ'_2	γ_2	E_2	H_1	H_2	H_3	E_3	D_1	D_2	L	Qult
0	42	19	257	52	15	22	17.6	9.25	14	1.5	1105146	3	0.25	14.5	9532.13

M 34.2: Parameter values

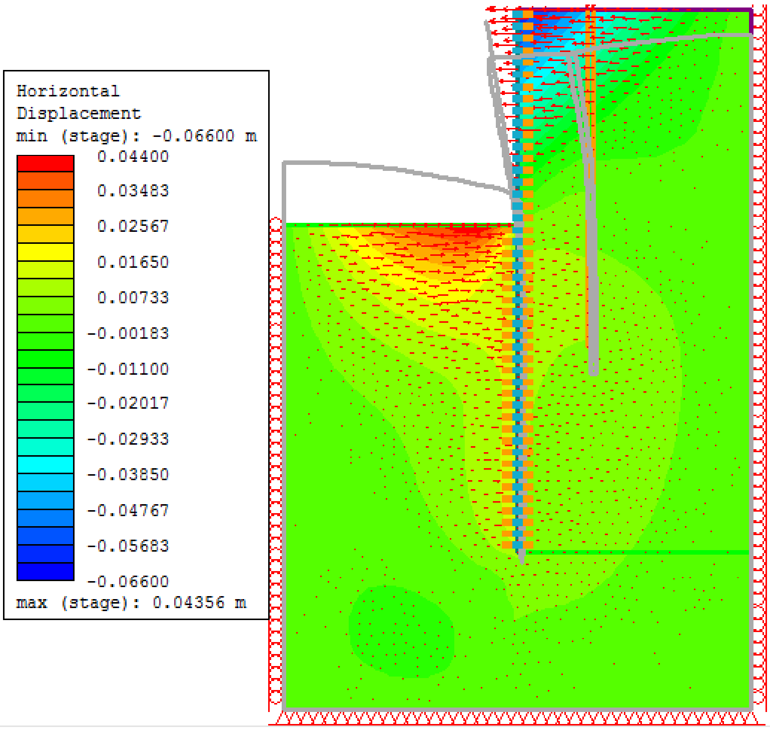

M 34.3: Deformed model (stage 3)

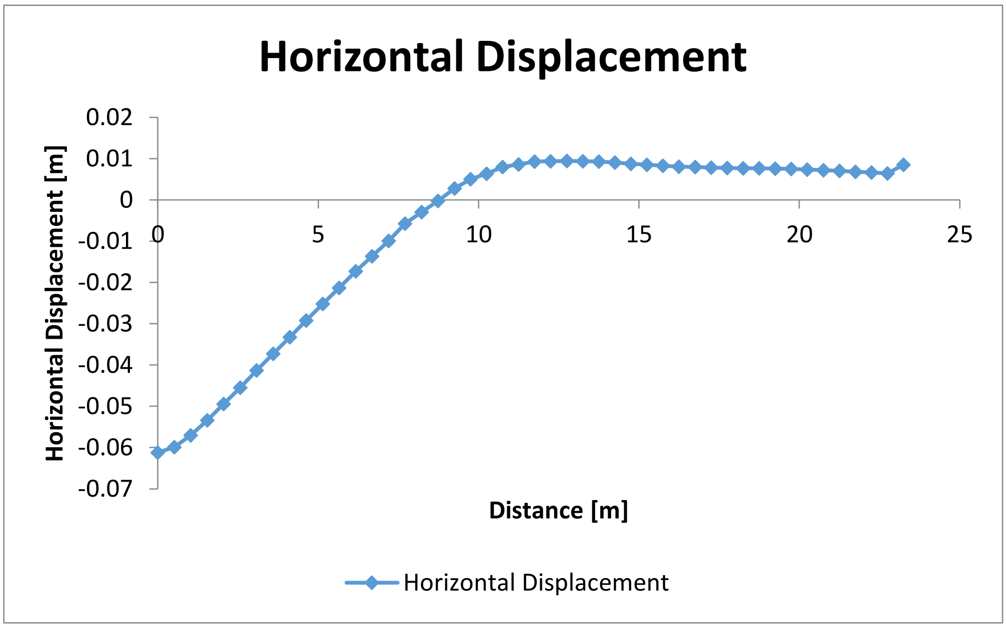

M 34.4: Horizontal displacement of soil along retaining wall

Retaining wall maximum horizontal displacement: -0.066m

Distance from point of maximum displacement in retaining wall to the top of backfill soil: 0.0m

Model 35:

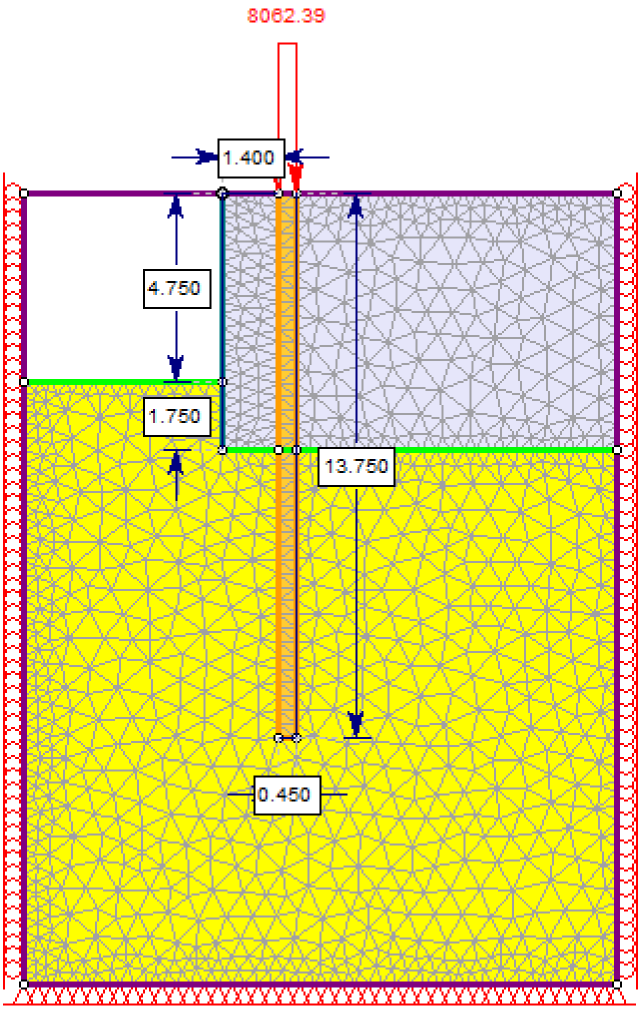

M 35.1: Original model (stage 3)

C'_1	ϕ'_1	γ_1	E_1	C'_2	ϕ'_2	γ_2	E_2	H_1	H_2	H_3	E_3	D_1	D_2	L	Qult
0	41	19	37	56	30	20	27.0	4.75	1.75	1	896118	1.4	0.45	13.75	8062.39

M 35.2: Parameter values

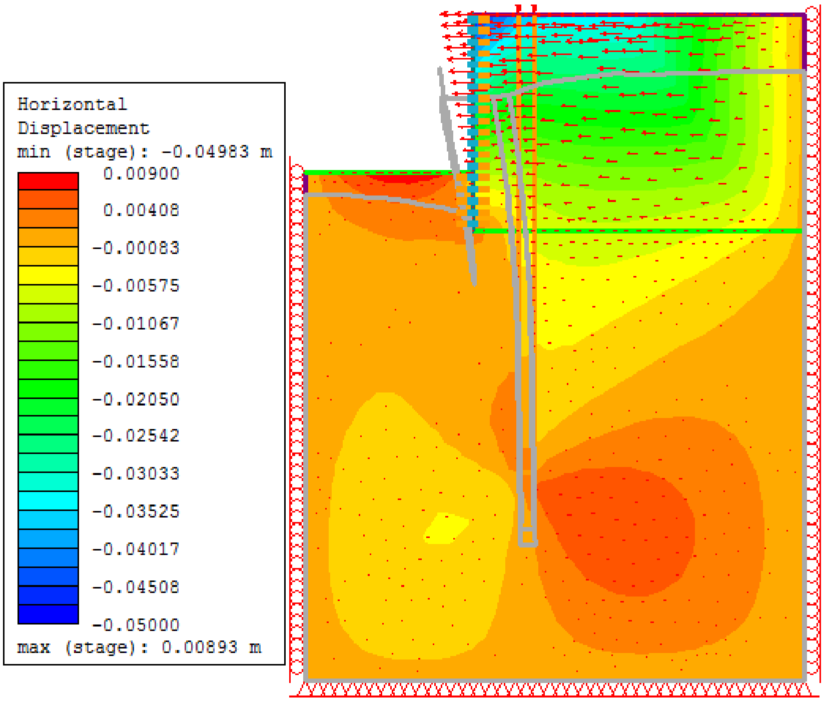

M 35.3: Deformed model (stage 3)

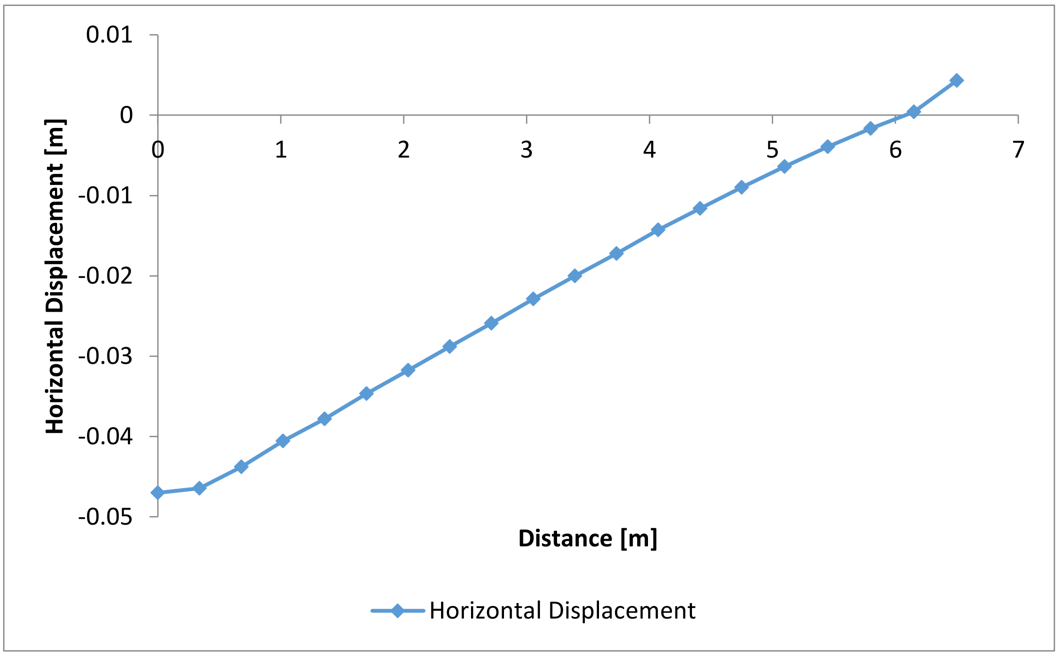

M 35.4: Horizontal displacement of soil along retaining wall

Retaining wall maximum horizontal displacement: -0.04983m

Distance from point of maximum displacement in retaining wall to the top of backfill soil: 0.0m

Model 36:

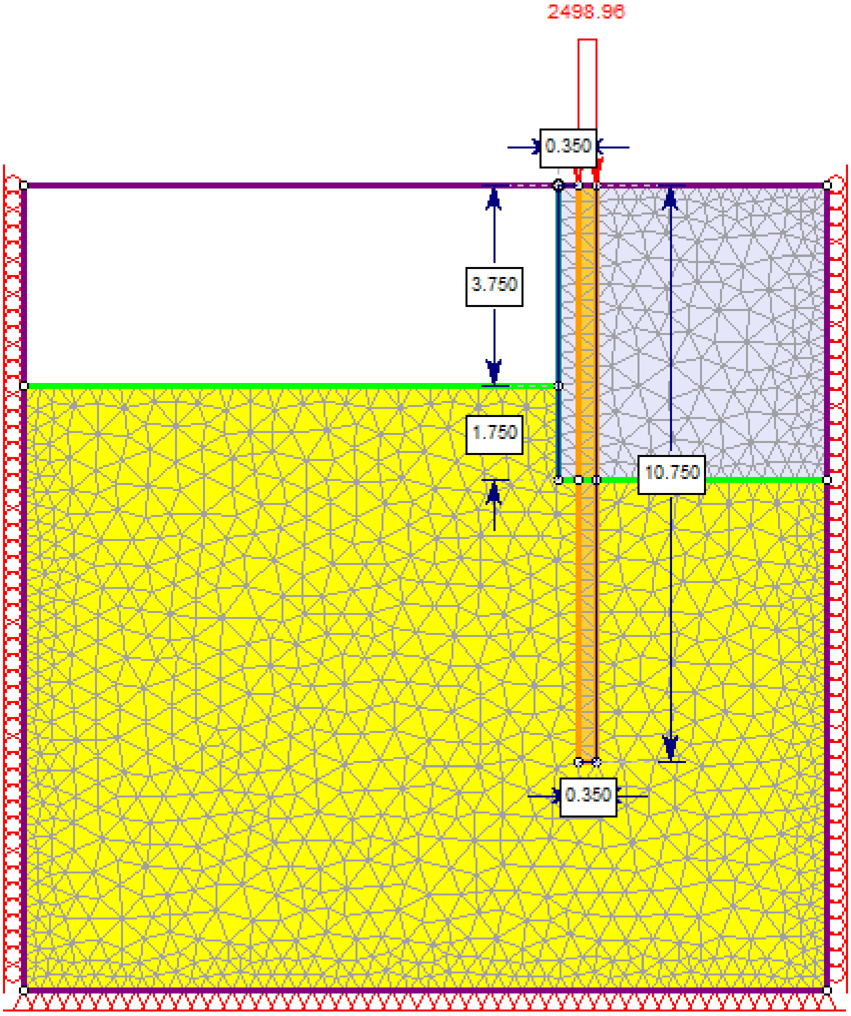

M 36.1: Original model (stage 3)

C_1'	ϕ_1'	γ_1	E_1	C_2'	ϕ_2'	γ_2	E_2	H_1	H_2	H_3	E_3	D_1	D_2	L	Qult
0	33	19	54	41	24	16	28.3	3.75	1.75	0.5	779715	0.35	0.35	10.75	2498.96

M 36.2: Parameter values

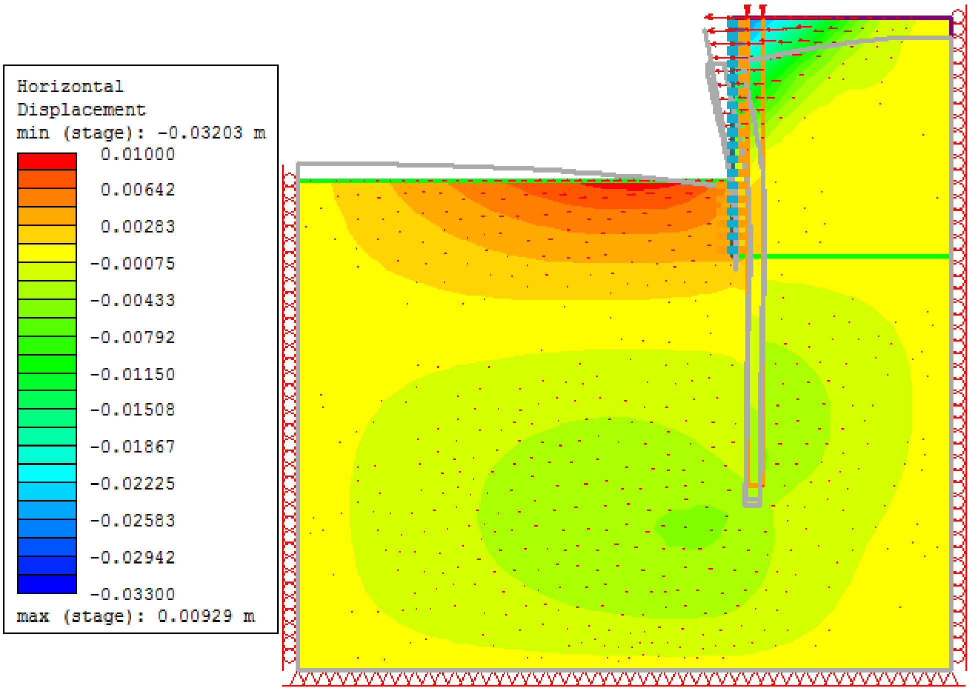

M 36.3: Deformed model (stage 3)

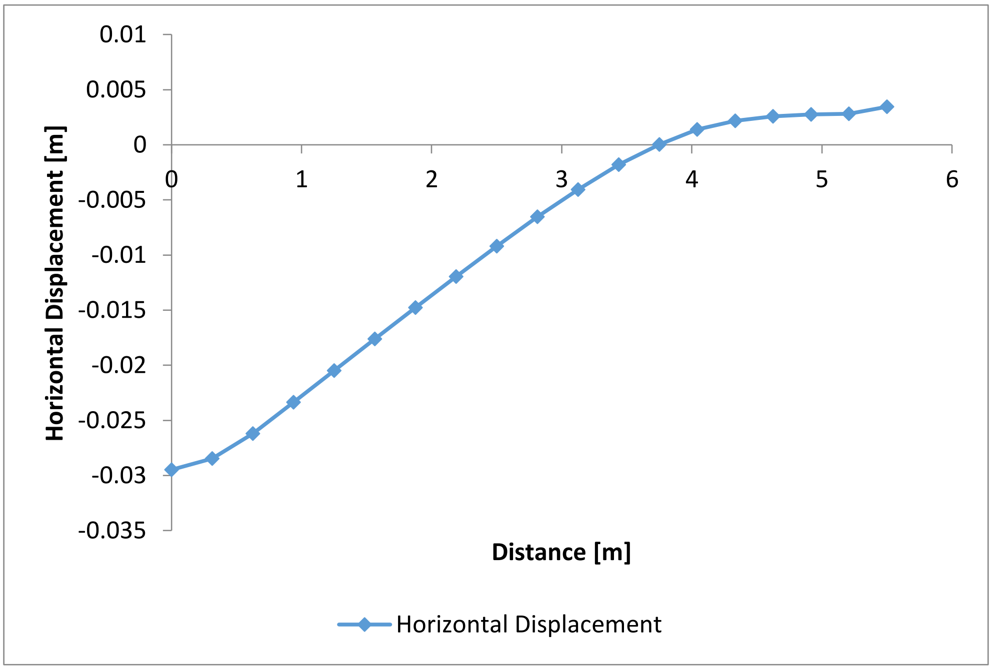

M 36.4: Horizontal displacement of soil along retaining wall

Retaining wall maximum horizontal displacement: -0.03203m

Distance from point of maximum displacement in retaining wall to the top of backfill soil: 0.0m

Model 37:

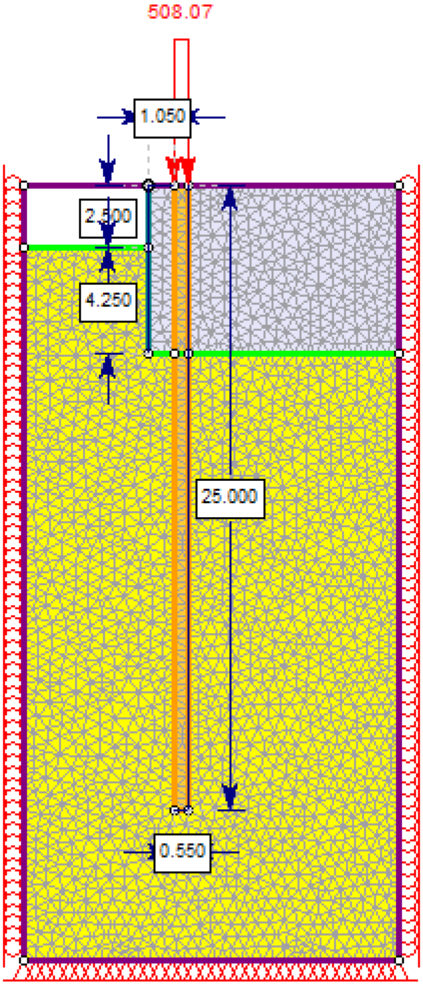

M 37 1: Original model (stage 3)

C'_1	ϕ'_1	γ_1	E_1	C'_2	ϕ'_2	γ_2	E_2	H_1	H_2	H_3	E_3	D_1	D_2	L	Qult
0	38	22	285	16	0	17	42.7	2.50	4.25	0.75	1081705	1.05	0.55	25	508.07

M 37.2: Parameter values

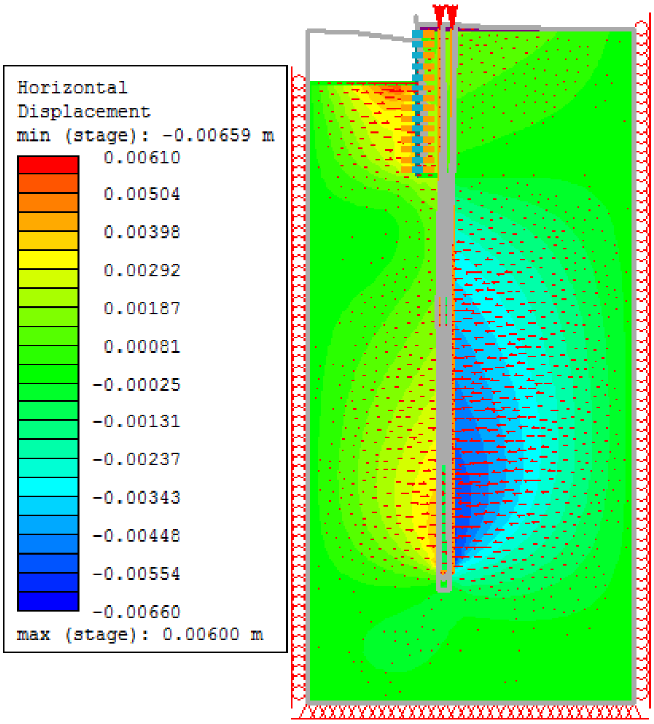

M 37.3: Deformed model (stage 3)

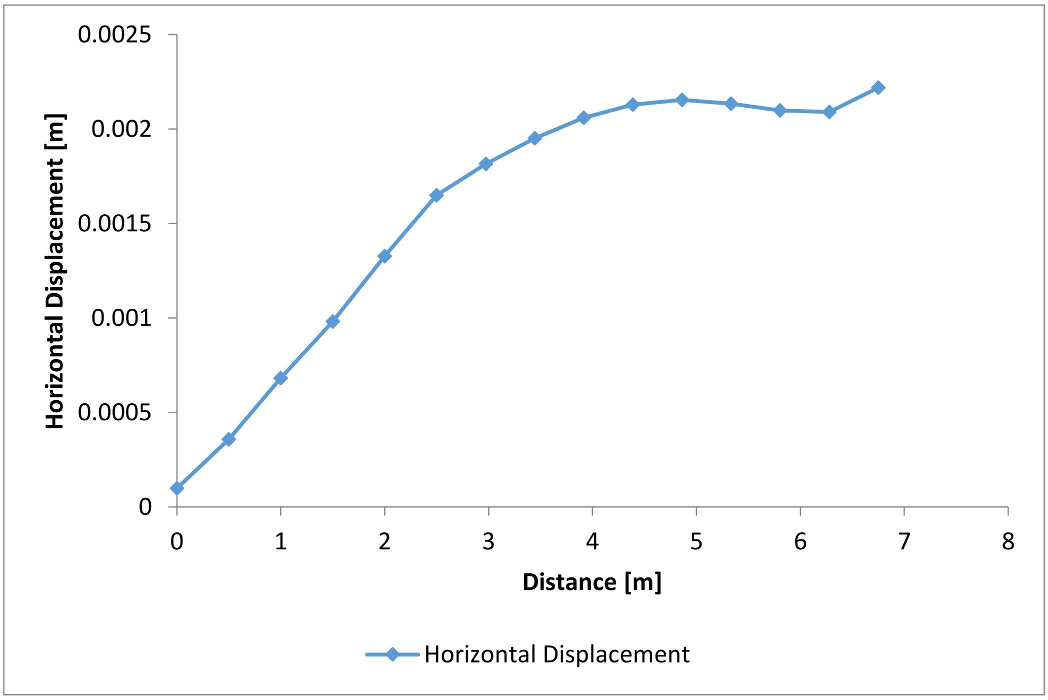

M 37.4: Horizontal displacement of soil along retaining wall

Retaining wall maximum horizontal displacement: 0.002219m

Distance from point of maximum displacement in retaining wall to the top of backfill soil: 6.75m

Model 38:

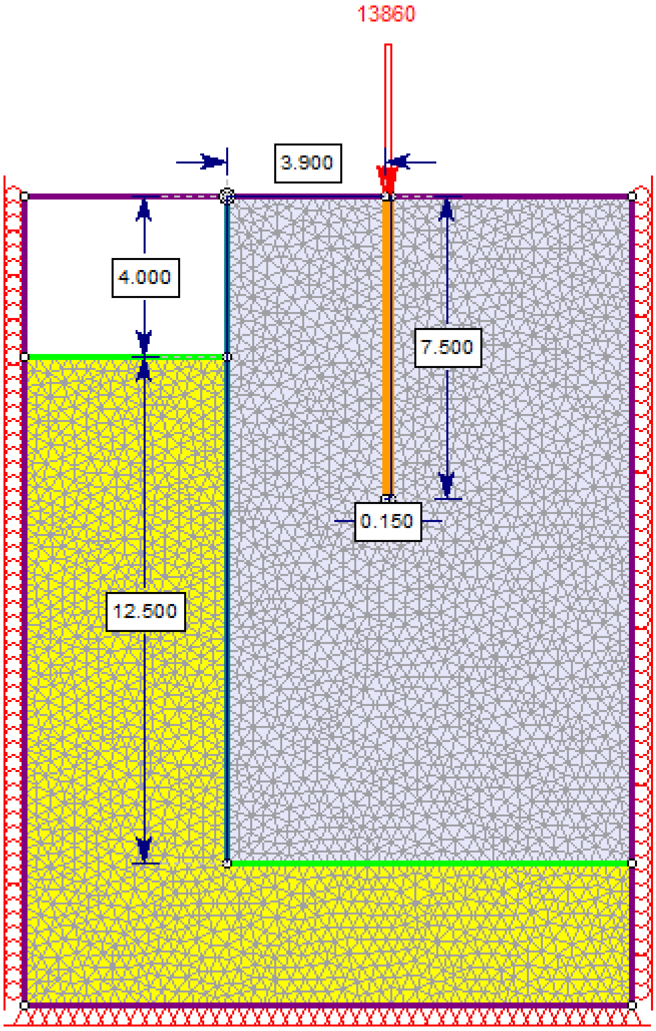

M 38.1: Original model (stage 3)

C'_1	ϕ'_1	γ_1	E_1	C'_2	ϕ'_2	γ_2	E_2	H_1	H_2	H_3	E_3	D_1	D_2	L	Qult
0	44	19	83	20	2	17	25.7	4.00	12.5	1.25	754741	3.9	0.15	7.5	13860.0

M 38.2: Parameter values

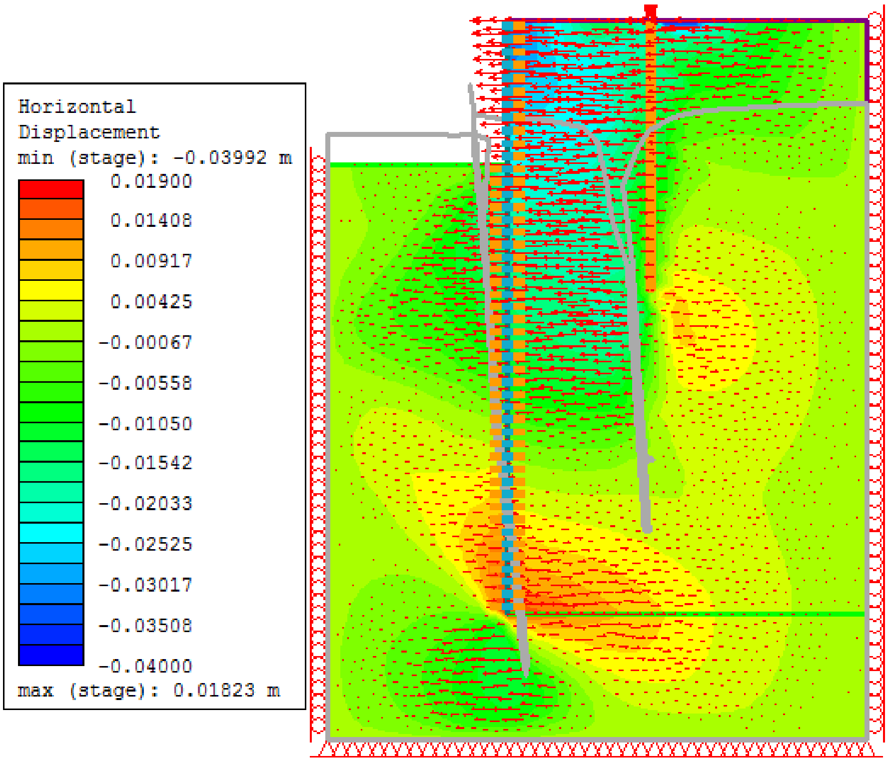

M 38.3: Deformed model (stage 3)

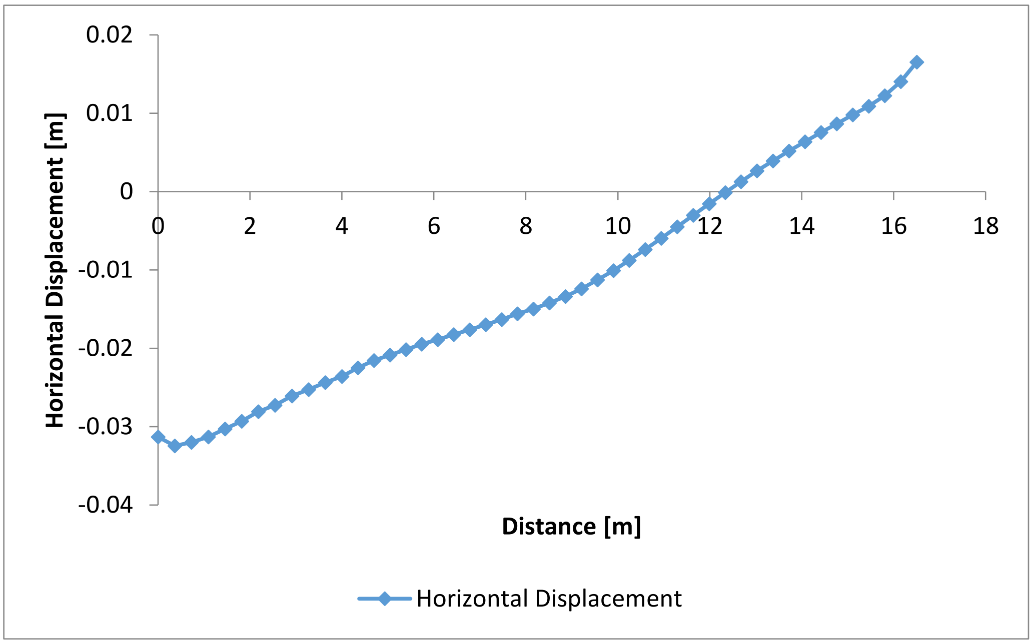

M 38.4: Horizontal displacement of soil along retaining wall

Retaining wall maximum horizontal displacement: -0.03992m

Distance from point of maximum displacement in retaining wall to the top of backfill soil: 0.0m

Model 39:

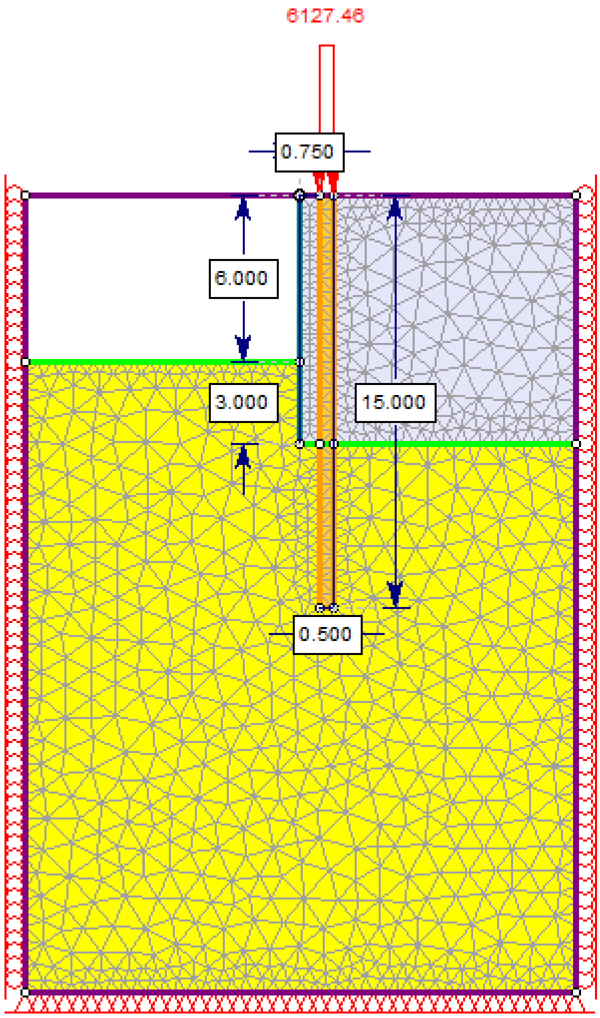

M 39.1: Original model (stage 3)

C'_1	ϕ'_1	γ_1	E_1	C'_2	ϕ'_2	γ_2	E_2	H_1	H_2	H_3	E_3	D_1	D_2	L	Qult
0	41	20	40	53	26	25	33.9	6.00	3	0.75	1010299	0.75	0.5	15	6127.46

M 39.2: Parameter values

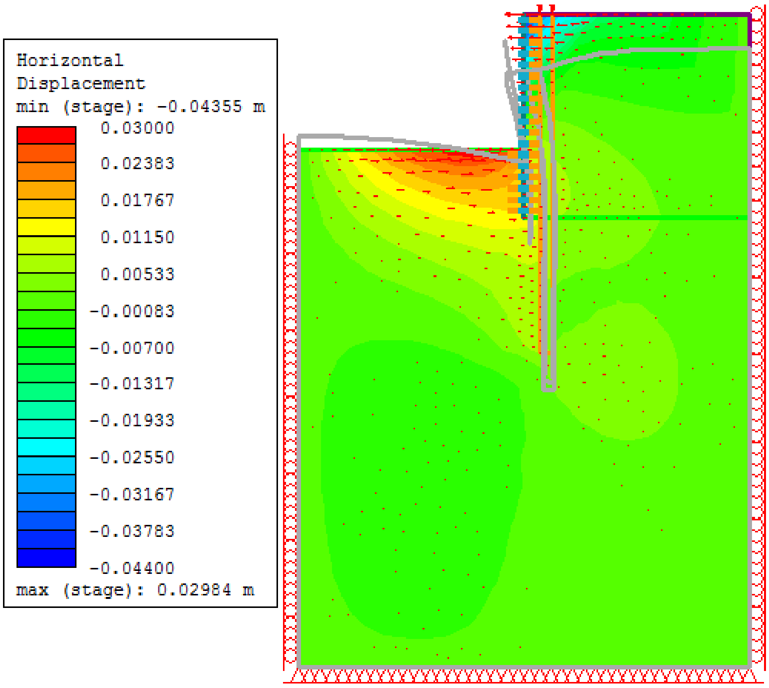

M 39.3: Deformed model (stage 3)

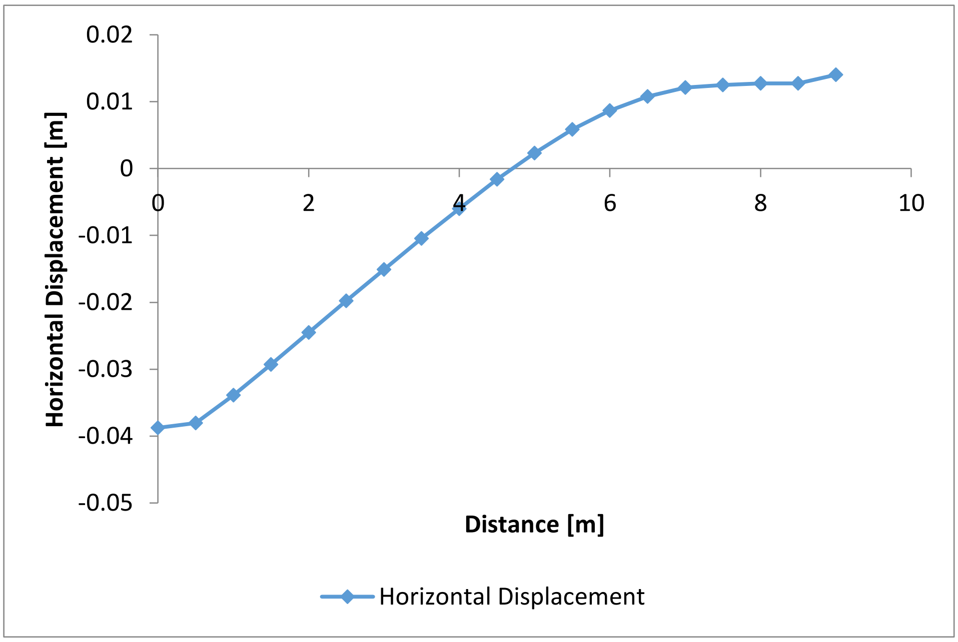

M 39.4: Horizontal displacement of soil along retaining wall

Retaining wall maximum horizontal displacement: -0.04355m

Distance from point of maximum displacement in retaining wall to the top of backfill soil: 0.0m

Model 40:

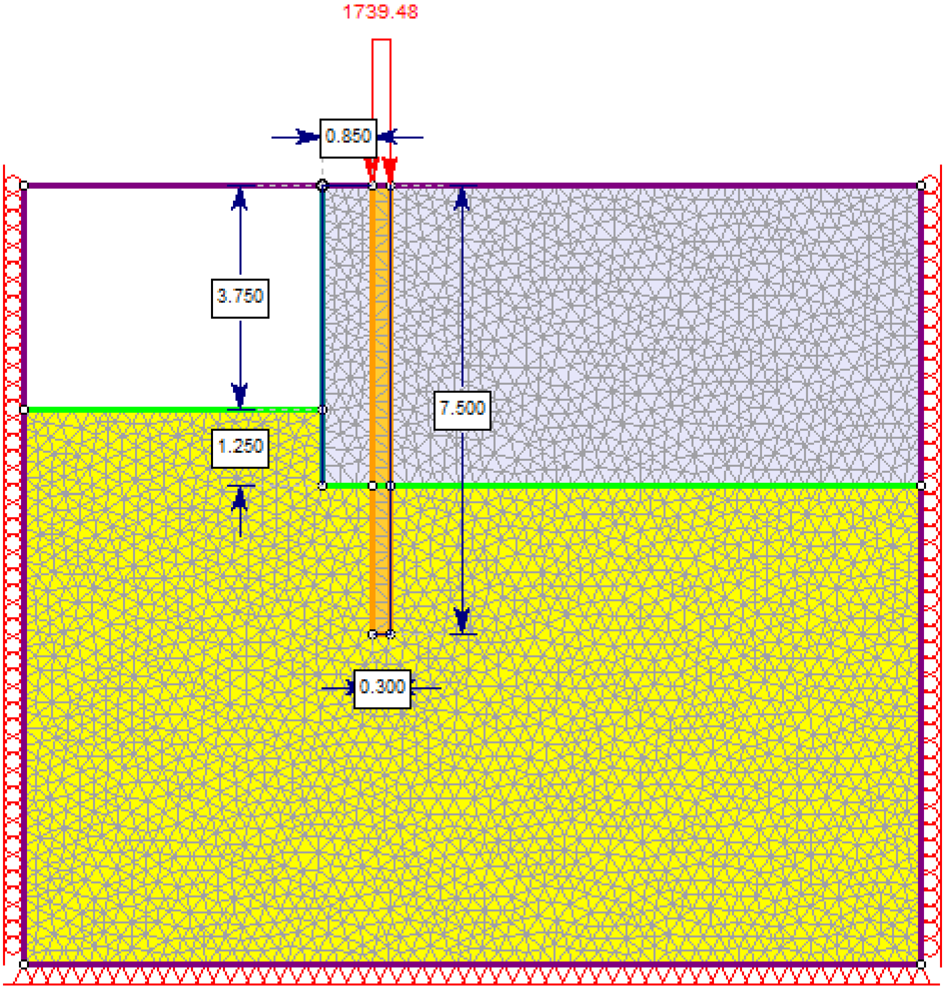

M 40.1: Original model (stage 3)

C'_1	ϕ'_1	γ_1	E_1	C'_2	ϕ'_2	γ_2	E_2	H_1	H_2	H_3	E_3	D_1	D_2	L	Qult
0	42	20	99	56	20	18	41.6	3.75	1.25	1	799362	0.85	0.3	7.5	1739.48

M 40.2: Parameter values

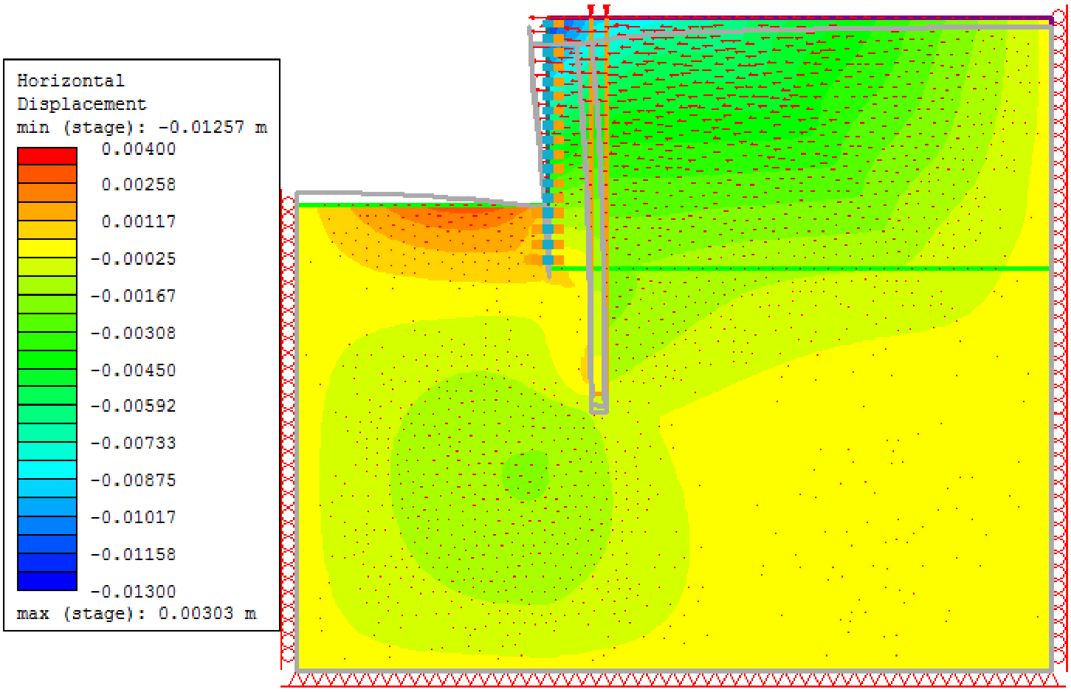

M 40.3: Deformed model (stage 3)

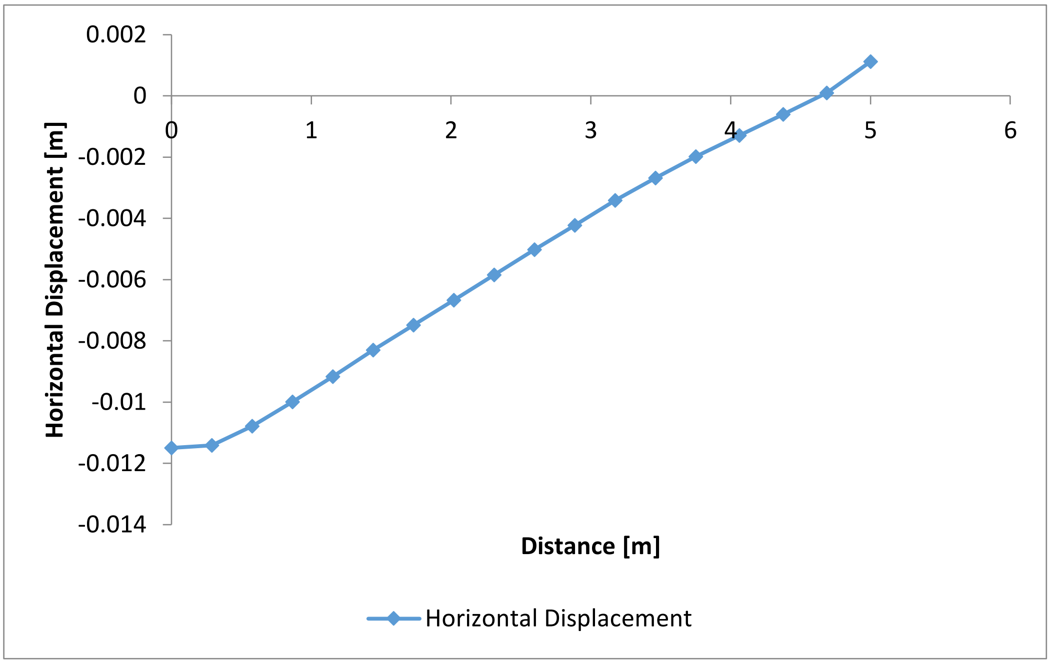

M 40.4: Horizontal displacement of soil along retaining wall

Retaining wall maximum horizontal displacement: -0.1257m

Distance from point of maximum displacement in retaining wall to the top of backfill soil: 0.0m

Model 41:

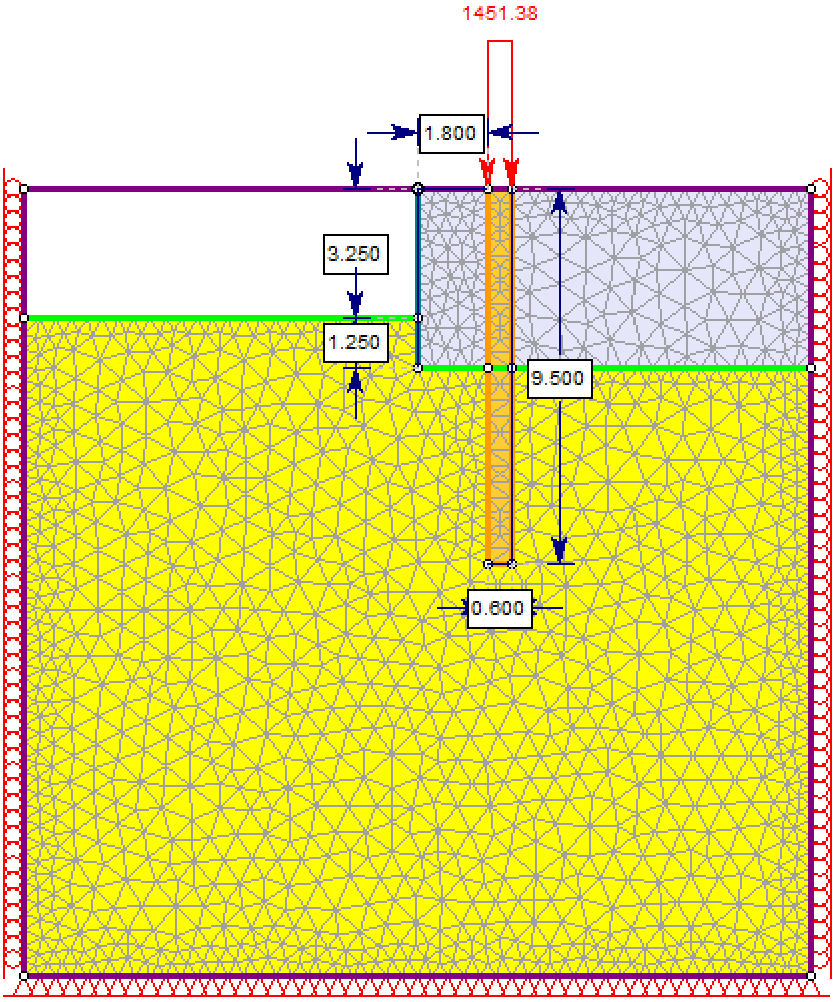

M 41.1: Original model (stage 3)

C'_1	ϕ'_1	γ_1	E_1	C'_2	ϕ'_2	γ_2	E_2	H_1	H_2	H_3	E_3	D_1	D_2	L	Qult
0	33	21	136	49	18	22	29.5	3.25	1.25	1.25	805595	1.8	0.6	9.5	1451.38

M 41.2: Parameter values

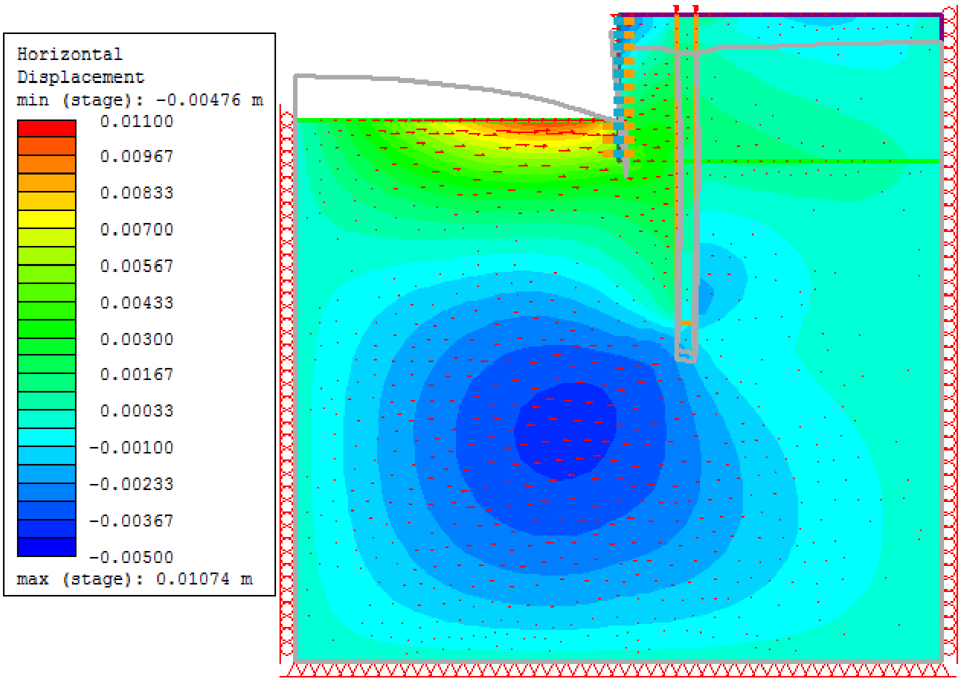

M 41.3: Deformed model (stage 3)

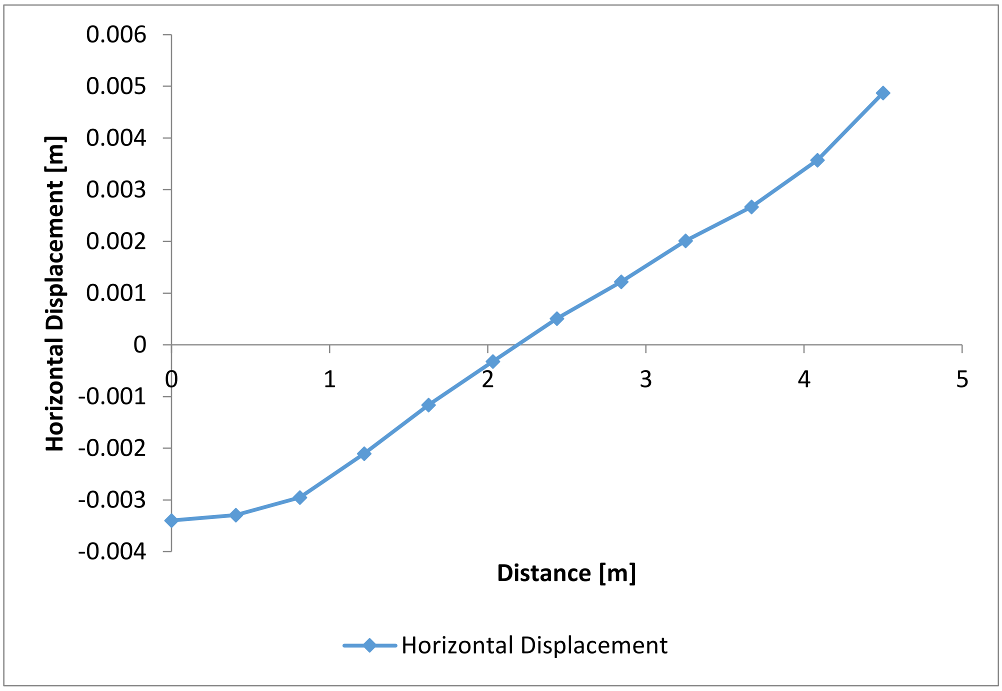

M 41.4: Horizontal displacement of soil along retaining wall

Retaining wall maximum horizontal displacement: -0.00476m

Distance from point of maximum displacement in retaining wall to the top of backfill soil: 0.0m

Model 42:

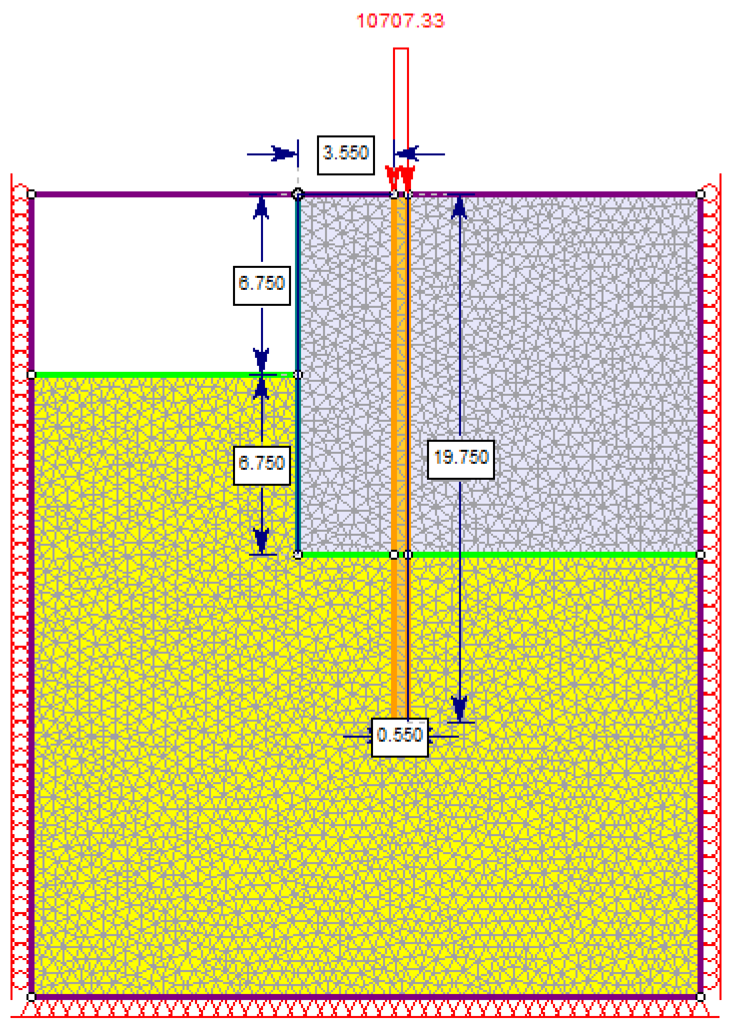

M 42.1: Original model (stage 3)

C_1'	ϕ_1'	γ_1	E_1	C_2'	ϕ_2'	γ_2	E_2	H_1	H_2	H_3	E_3	D_1	D_2	L	Qult
0	39	20	143	48	29	22	39.2	6.75	5.75	1	1003680	3.55	0.55	19.75	10707.33

M 42.2: Parameter values

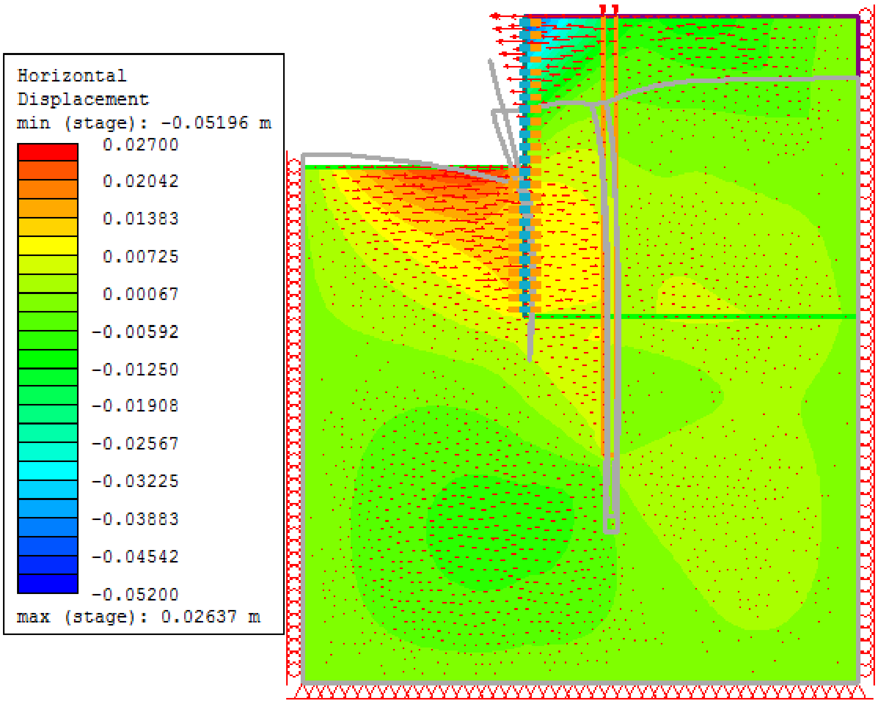

M 42.3: Deformed model (stage 3)

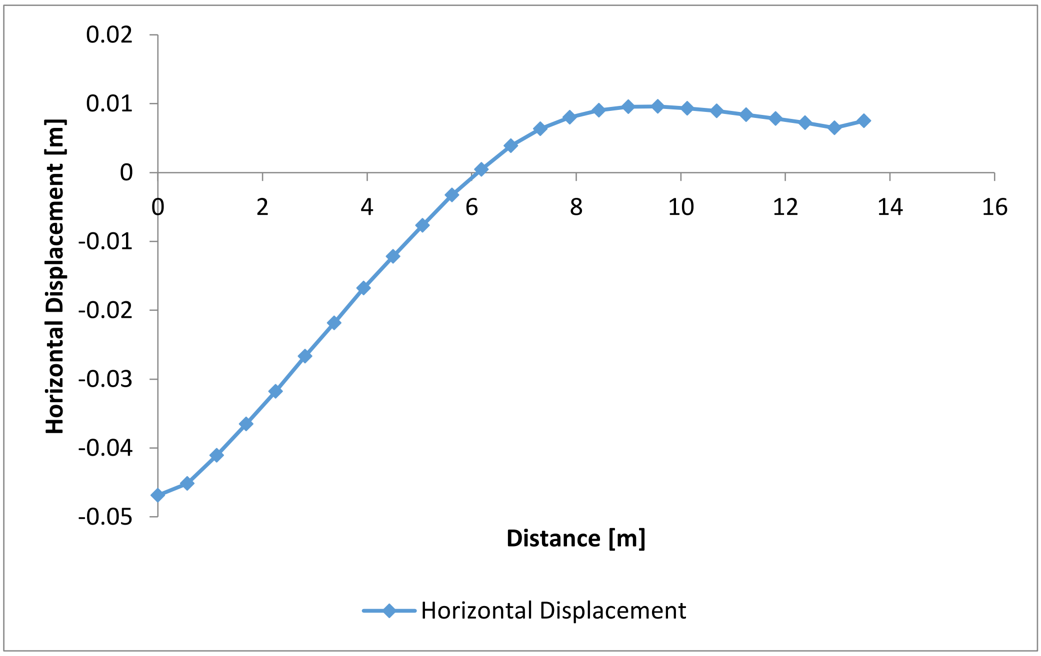

M 42.4: Horizontal displacement of soil along retaining wall

Retaining wall maximum horizontal displacement: -0.05196m

Distance from point of maximum displacement in retaining wall to the top of backfill soil: 0.0m

Model 43:

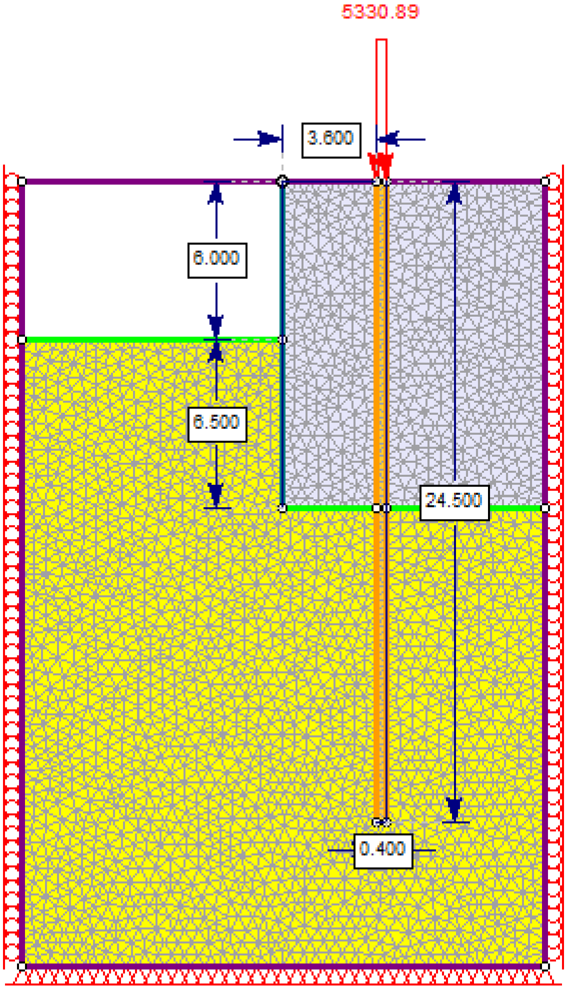

M 43.1: Original model (stage 3)

C_1'	ϕ_1'	γ_1	E_1	C_2'	ϕ_2'	γ_2	E_2	H_1	H_2	H_3	E_3	D_1	D_2	L	Qult
0	29	18	253	40	20	23	26.7	6.00	6.5	1.25	692511	3.6	0.4	24.5	5330.89

M 43.2: Parameter values

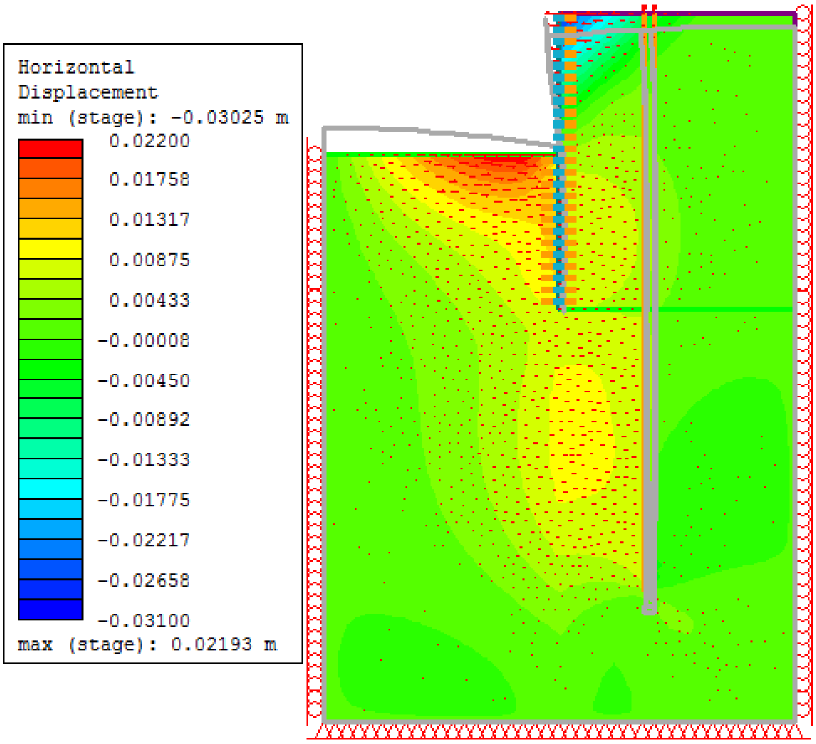

M 43.3: Deformed model (stage 3)

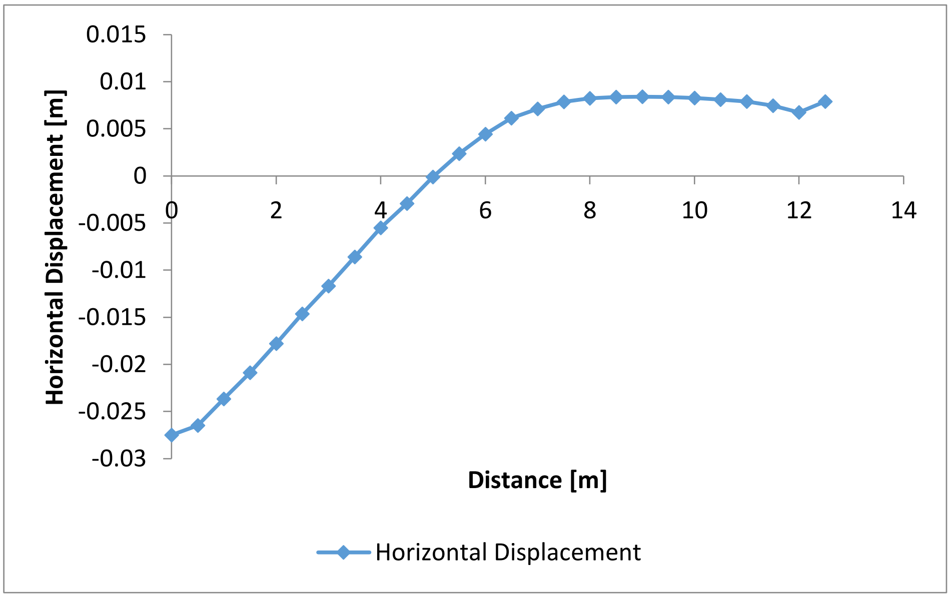

M 43.4: Horizontal displacement of soil along retaining wall

Retaining wall maximum horizontal displacement: -0.03025m

Distance from point of maximum displacement in retaining wall to the top of backfill soil: 0.0m

Model 44:

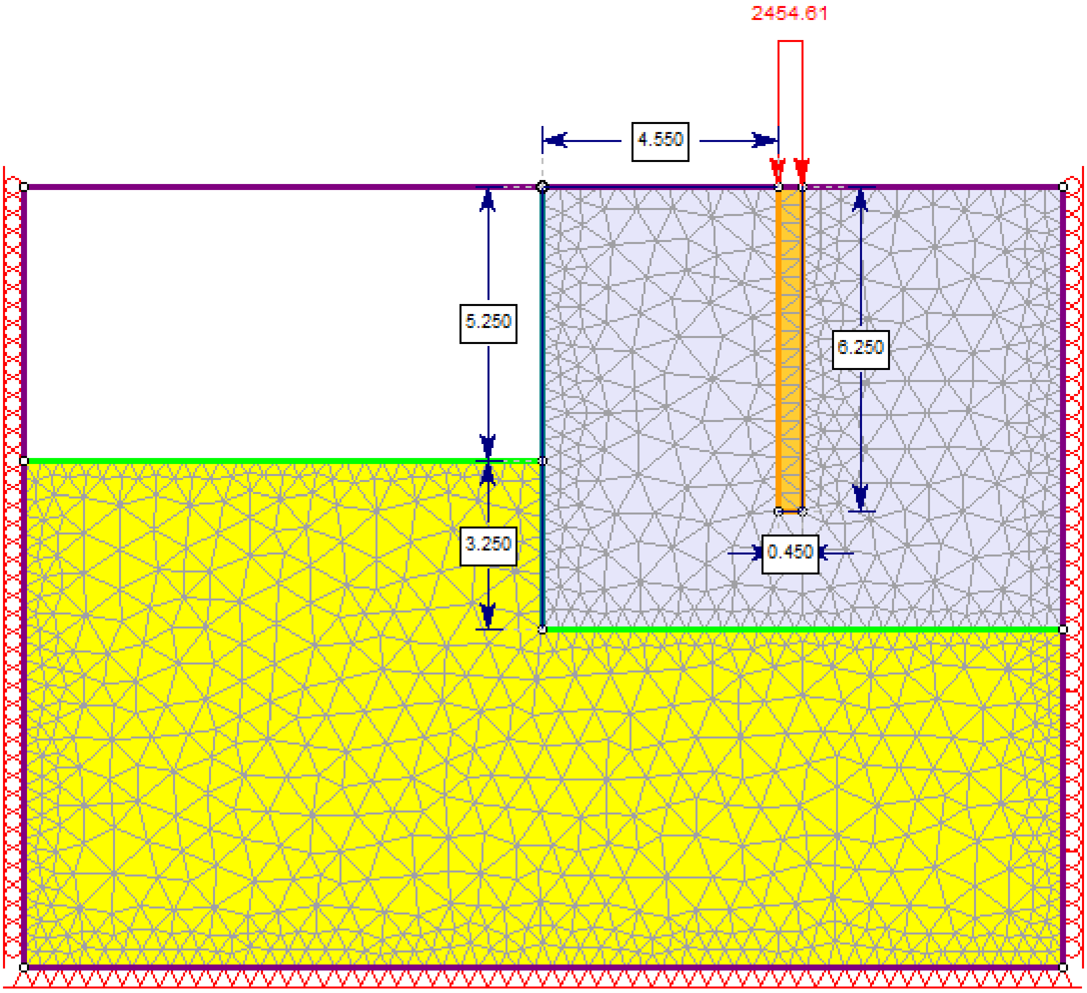

M 44.1: Original model (stage 3)

C_1'	ϕ_1'	γ_1	E_1	C_2'	ϕ_2'	γ_2	E_2	H_1	H_2	H_3	E_3	D_1	D_2	L	Qult
0	36	18	110	41	25	18	4.0	5.25	3.25	1.5	732027	4.55	0.45	6.25	2454.61

M 44.2: Parameter values

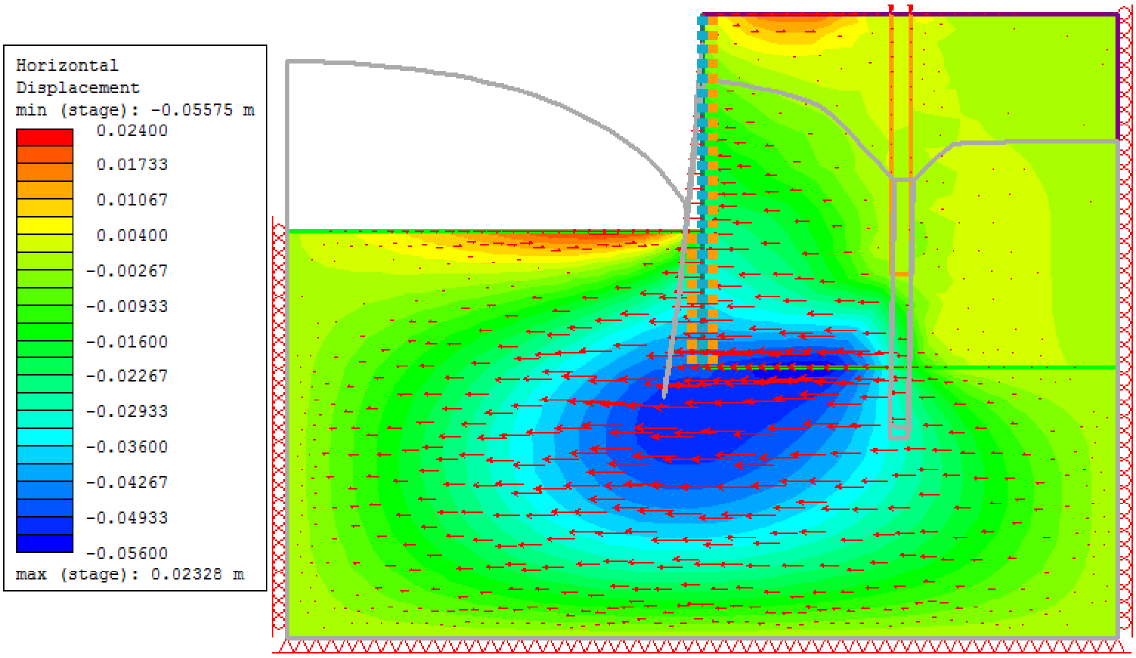

M 44.3: Deformed model (stage 3)

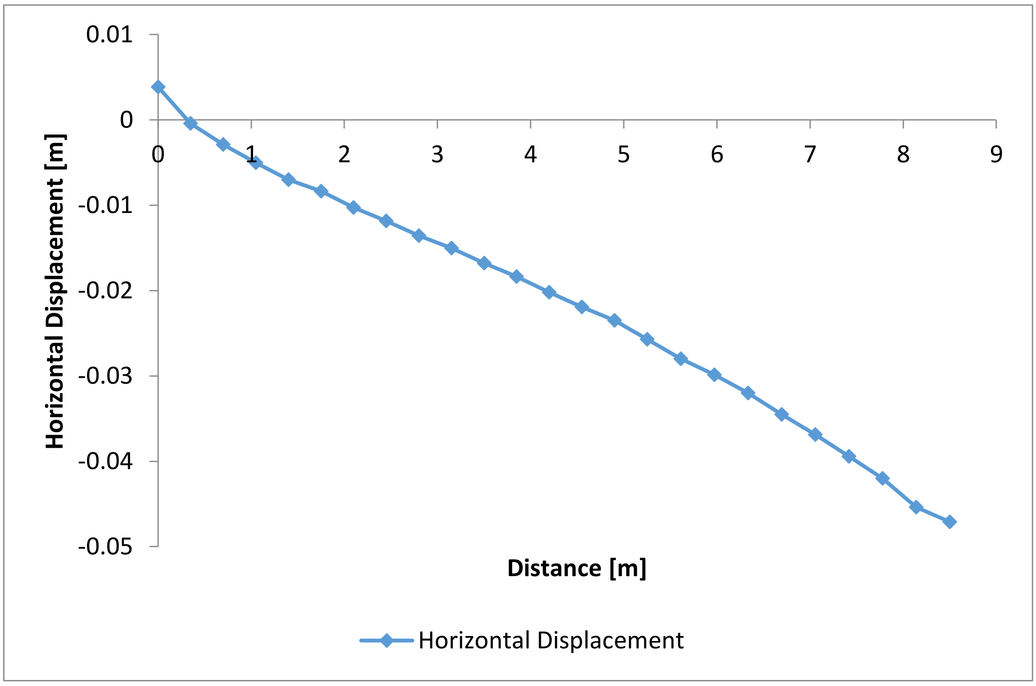

M 44.4: Horizontal displacement of soil along retaining wall

Retaining wall maximum horizontal displacement: -0.04709m

Distance from point of maximum displacement in retaining wall to the top of backfill soil: 8.5m

Model 45:

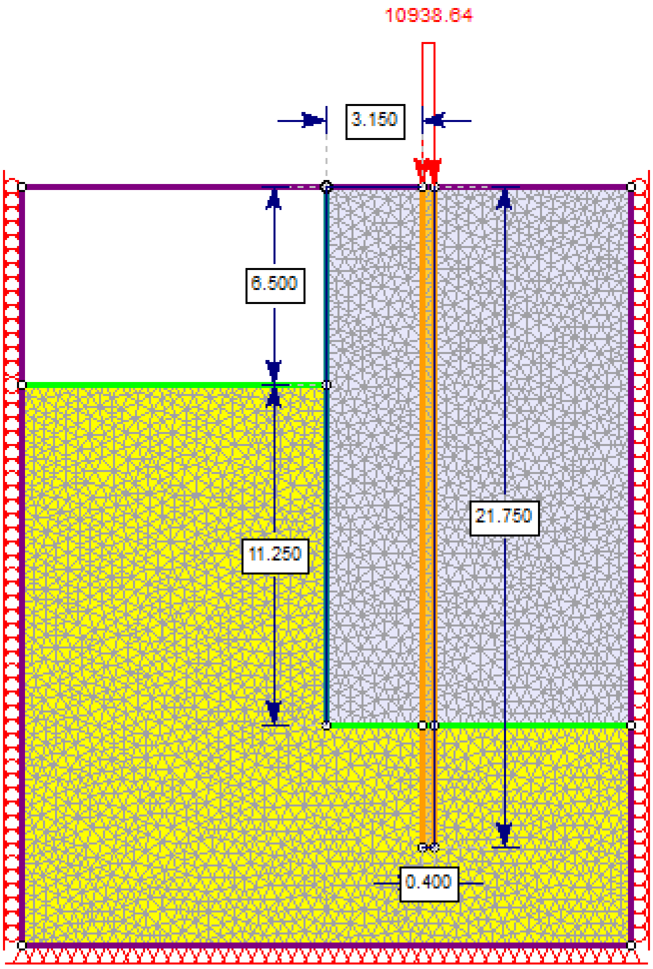

M 45.1: Original model (stage 3)

C_1'	ϕ_1'	γ_1	E_1	C_2'	ϕ_2'	γ_2	E_2	H_1	H_2	H_3	E_3	D_1	D_2	L	Qult
0	38	20	138	38	30	17	36.3	6.50	11.25	0.5	1106731	3.15	0.4	21.75	10938.64

M 45.2: Parameter values

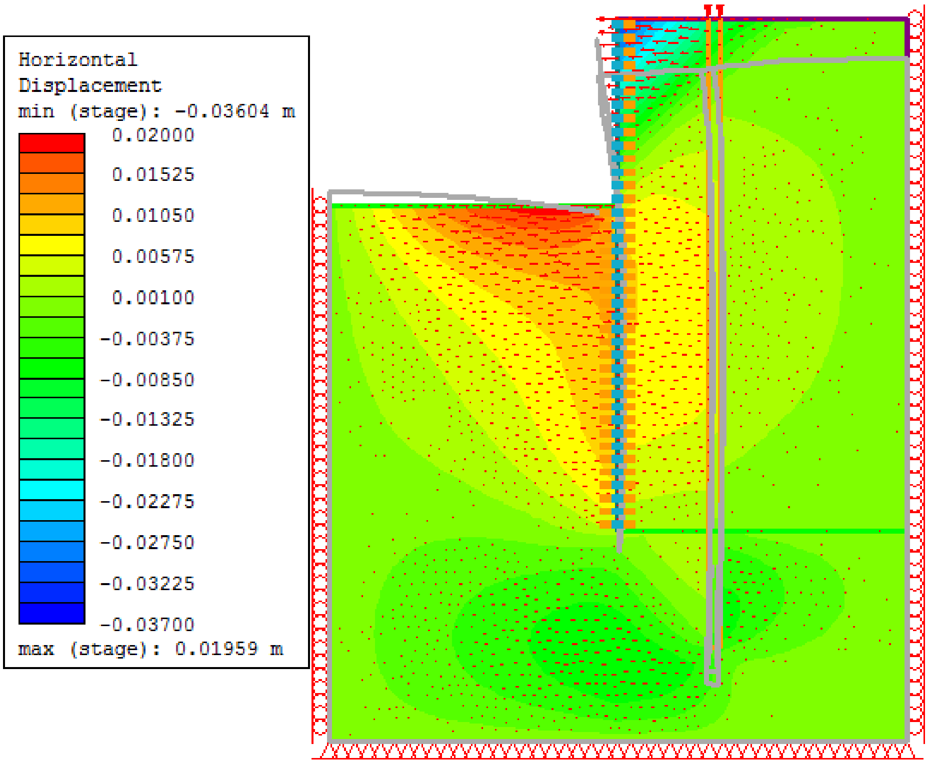

M 45.3: Deformed model (stage 3)

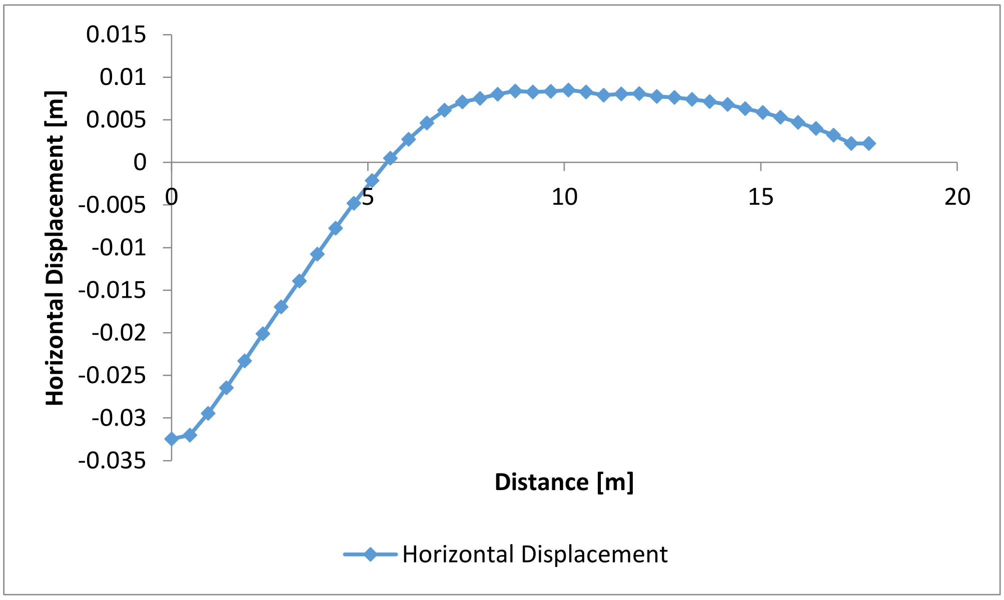

M 45.4: Horizontal displacement of soil along retaining wall

Retaining wall maximum horizontal displacement: -0.03604m

Distance from point of maximum displacement in retaining wall to the top of backfill soil: 0.0m

Model 46:

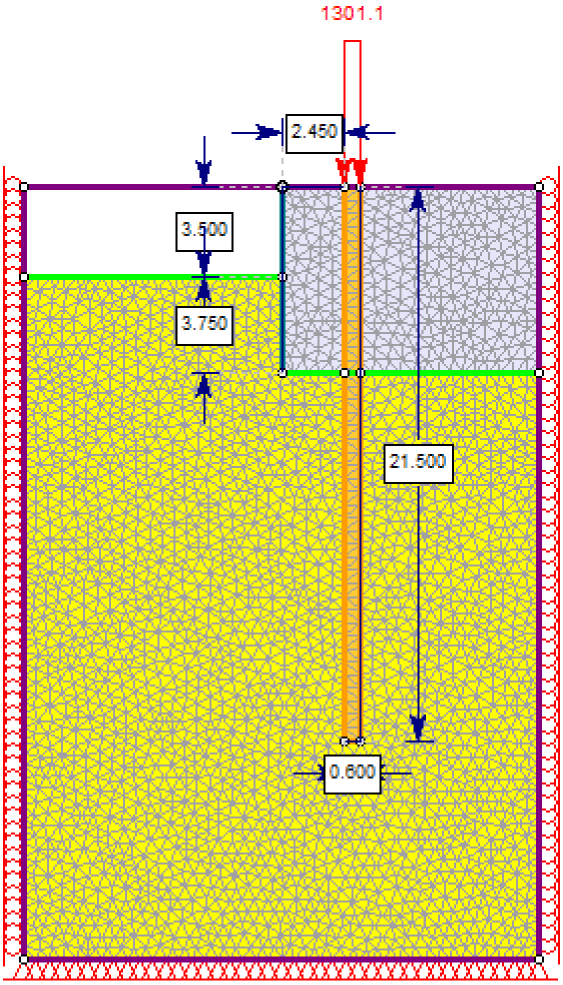

M 46.1: Original model (stage 3)

C_1'	ϕ_1'	γ_1	E_1	C_2'	ϕ_2'	γ_2	E_2	H_1	H_2	H_3	E_3	D_1	D_2	L	Qult
0	42	21	96	24	7	18	45.0	3.50	3.75	0.5	1047976	2.45	0.6	21.5	1301.1

M 46.2: Parameter values

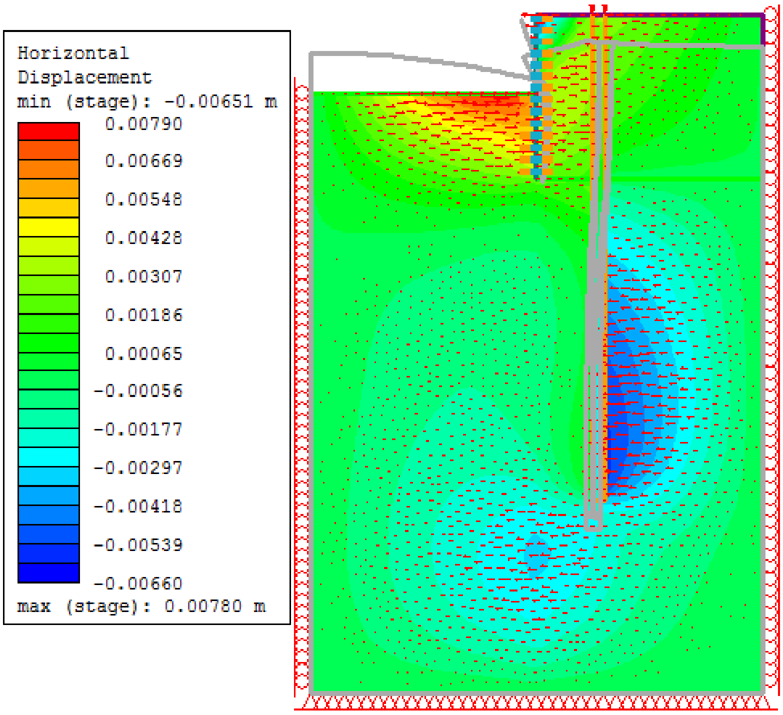

M 46.3: Deformed model (stage 3)

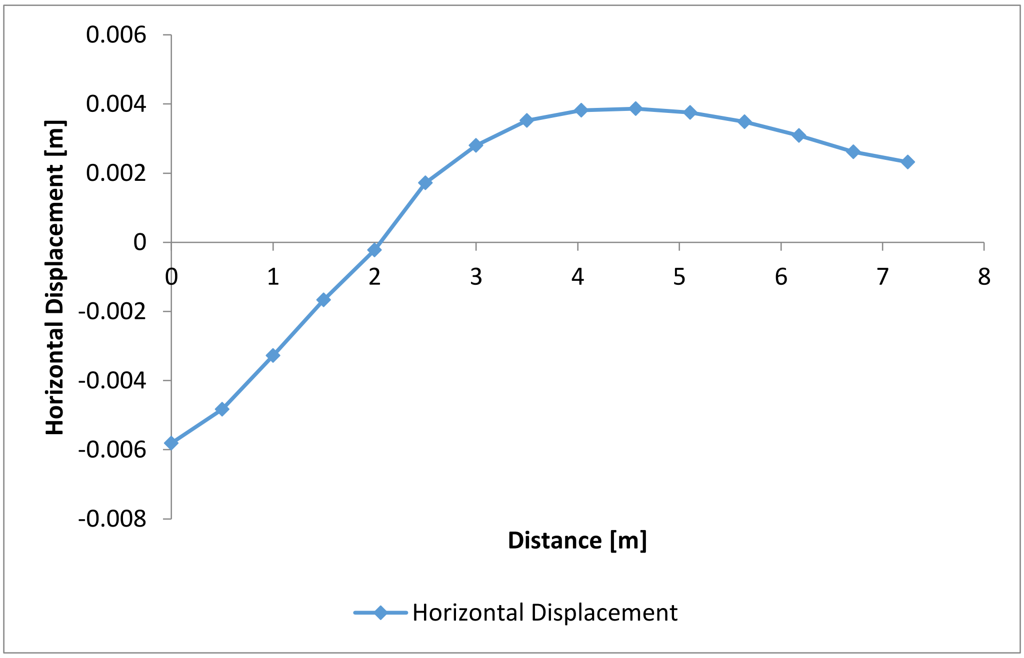

M 46.4: Horizontal displacement of soil along retaining wall

Retaining wall maximum horizontal displacement: -0.00651m

Distance from point of maximum displacement in retaining wall to the top of backfill soil: 0.0m

Model 47:

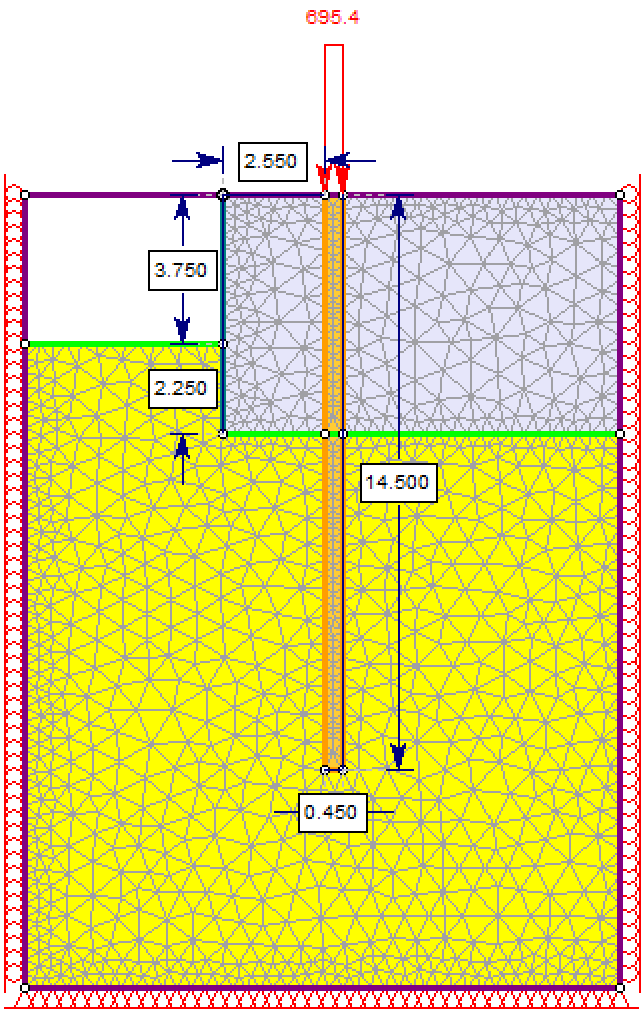

M 47.1: Original model (stage 3)

C_1'	ϕ_1'	γ_1	E_1	C_2'	ϕ_2'	γ_2	E_2	H_1	H_2	H_3	E_3	D_1	D_2	L	Qult
0	31	20	158	38	1	20	14.5	3.75	2.25	0.75	906244	2.55	0.45	14.5	695.4

M 47.2: Parameter values

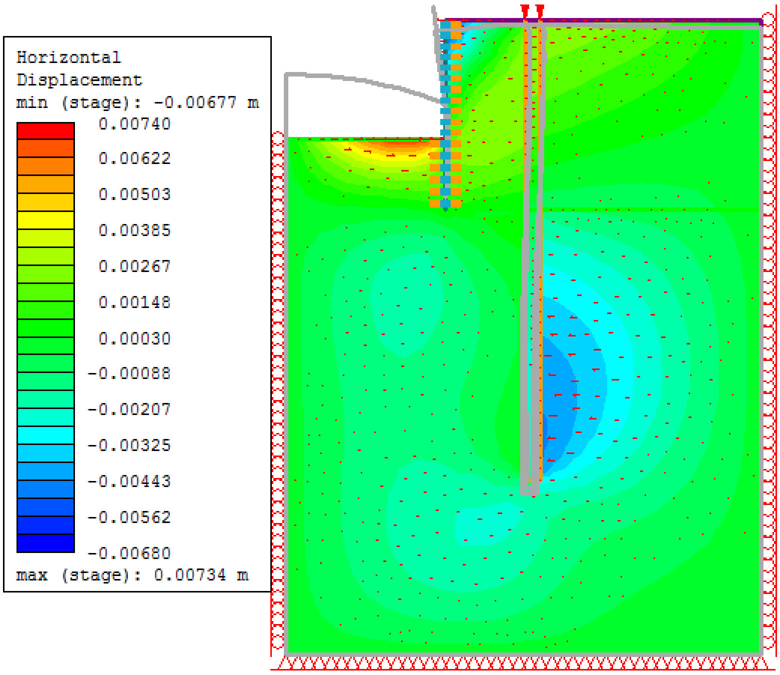

M 47.3: Deformed model (stage 3)

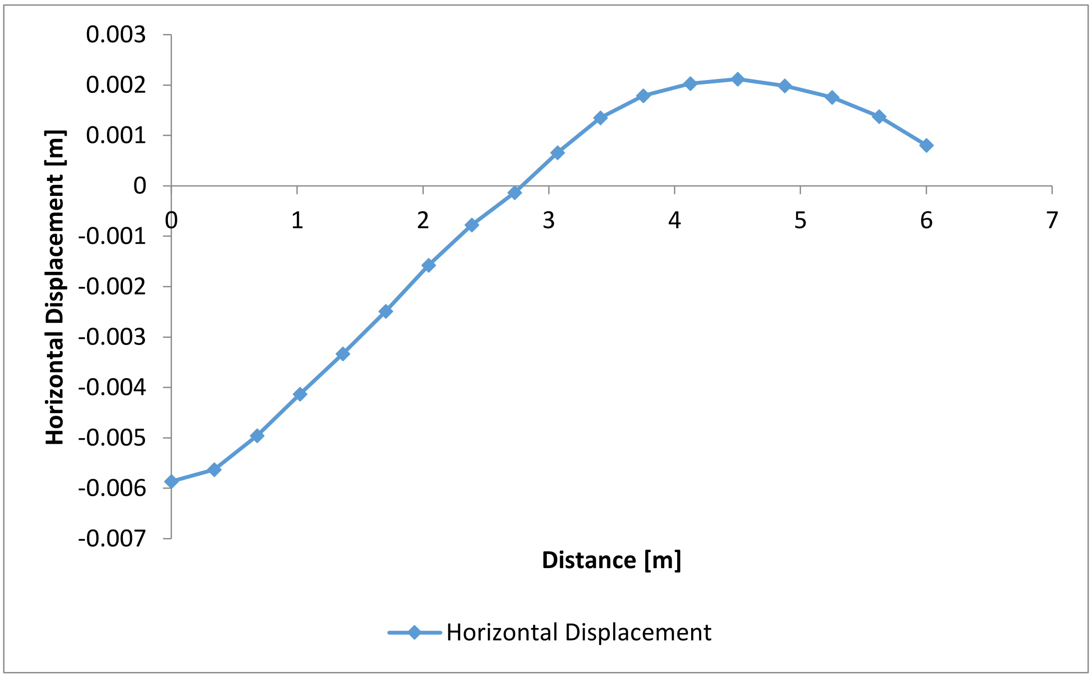

M 47.4: Horizontal displacement of soil along retaining wall

Retaining wall maximum horizontal displacement: -0.00677m

Distance from point of maximum displacement in retaining wall to the top of backfill soil: 0.0m

Model 48:

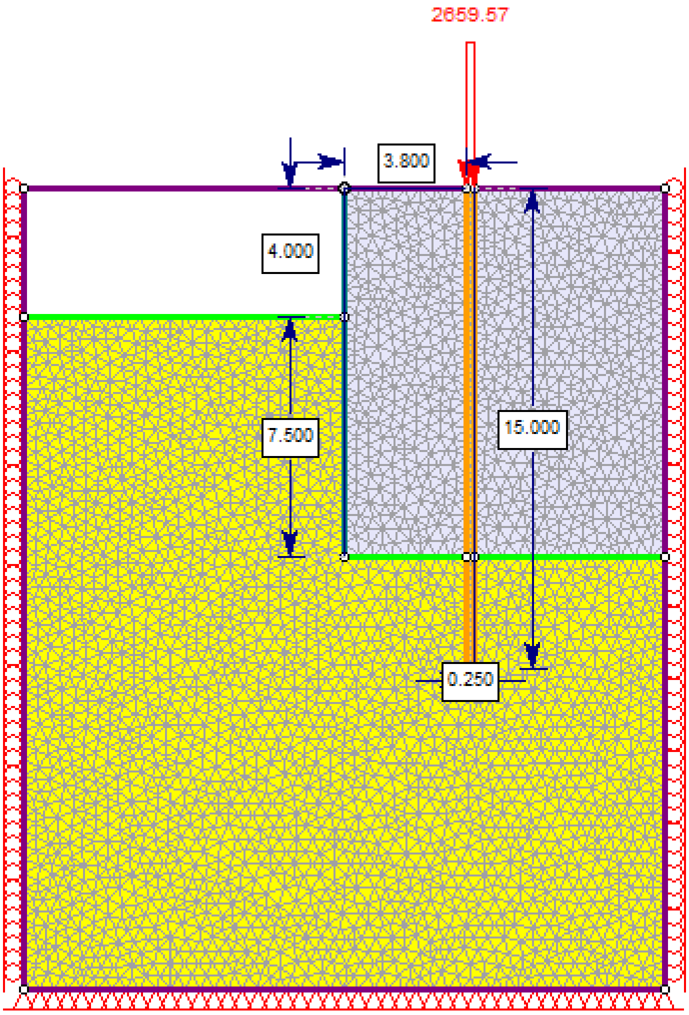

M 48.1: Original model (stage 3)

C'_1	ϕ'_1	γ_1	E_1	C'_2	ϕ'_2	γ_2	E_2	H_1	H_2	H_3	E_3	D_1	D_2	L	Qult
0	37	21	140	25	15	17	26.4	4.00	7.5	1.5	948275	3.8	0.25	15	2659.57

M 48.2: Parameter values

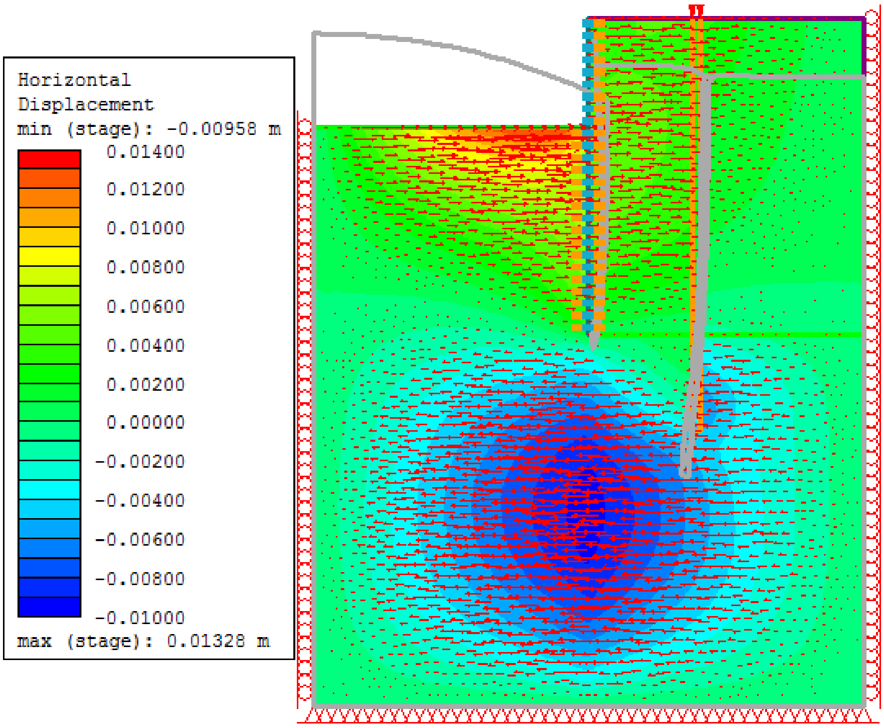

M 48.3: Deformed model (stage 3)

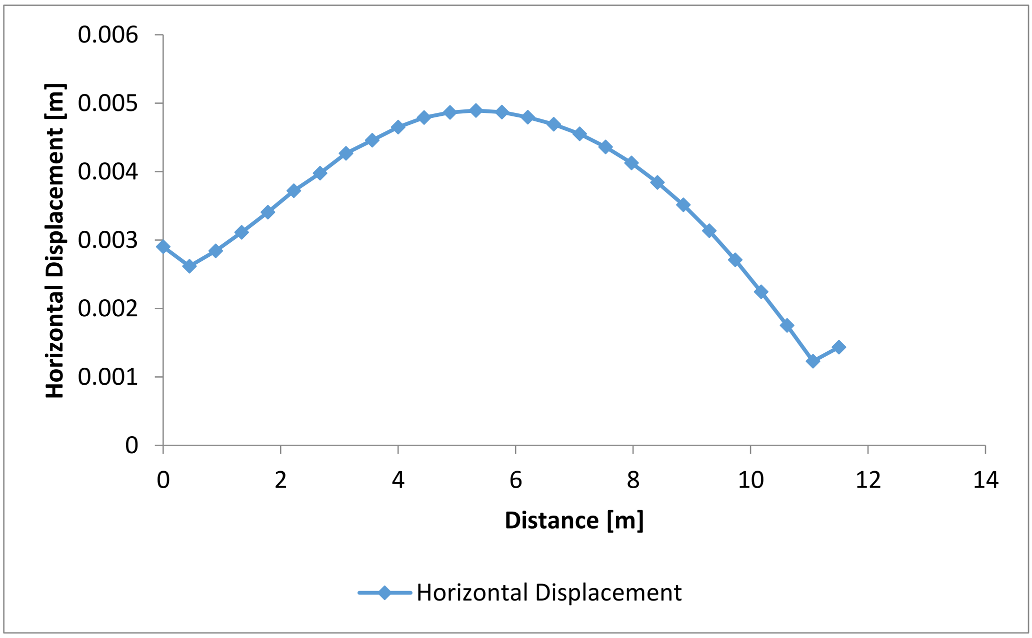

M 48.4: Horizontal displacement of soil along retaining wall

Retaining wall maximum horizontal displacement: 0.00489m

Distance from point of maximum displacement in retaining wall to the top of backfill soil: 5.3235m

Model 49:

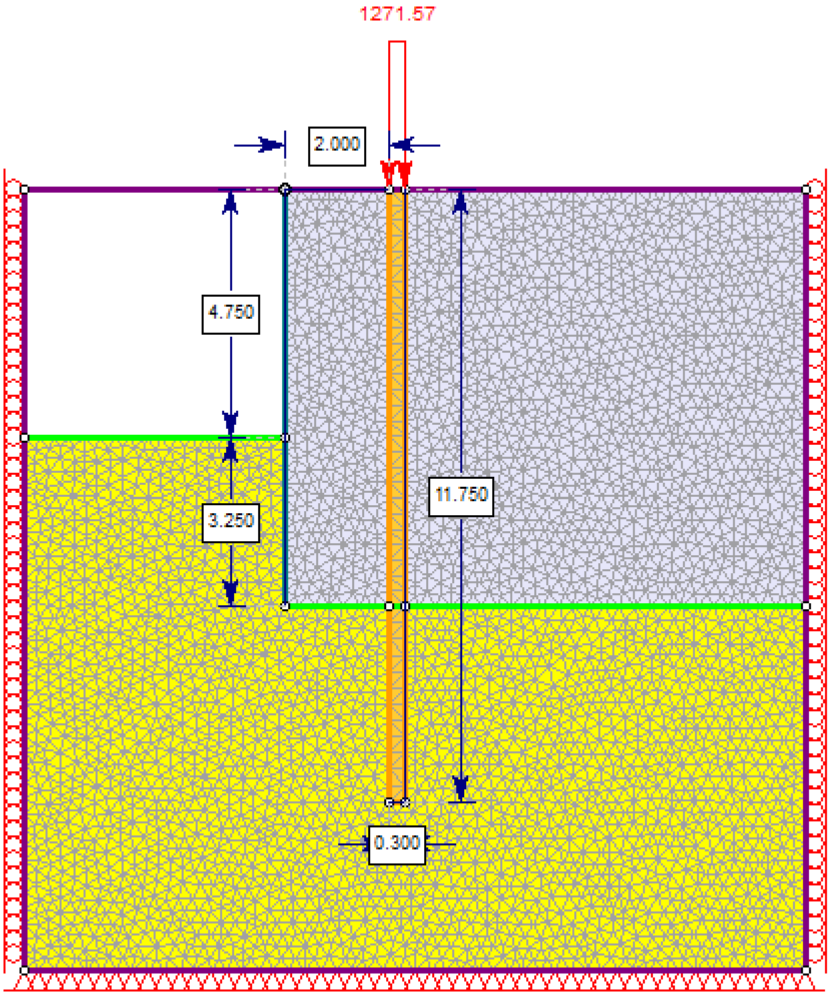

M 49.1: Original model (stage 3)

C'_1	ϕ'_1	γ_1	E_1	C'_2	ϕ'_2	γ_2	E_2	H_1	H_2	H_3	E_3	D_1	D_2	L	Qult
0	36	21	291	42	2	16	47.0	4.75	3.25	1	1121572	2	0.3	11.75	1271.57

M 49.2: Parameter values

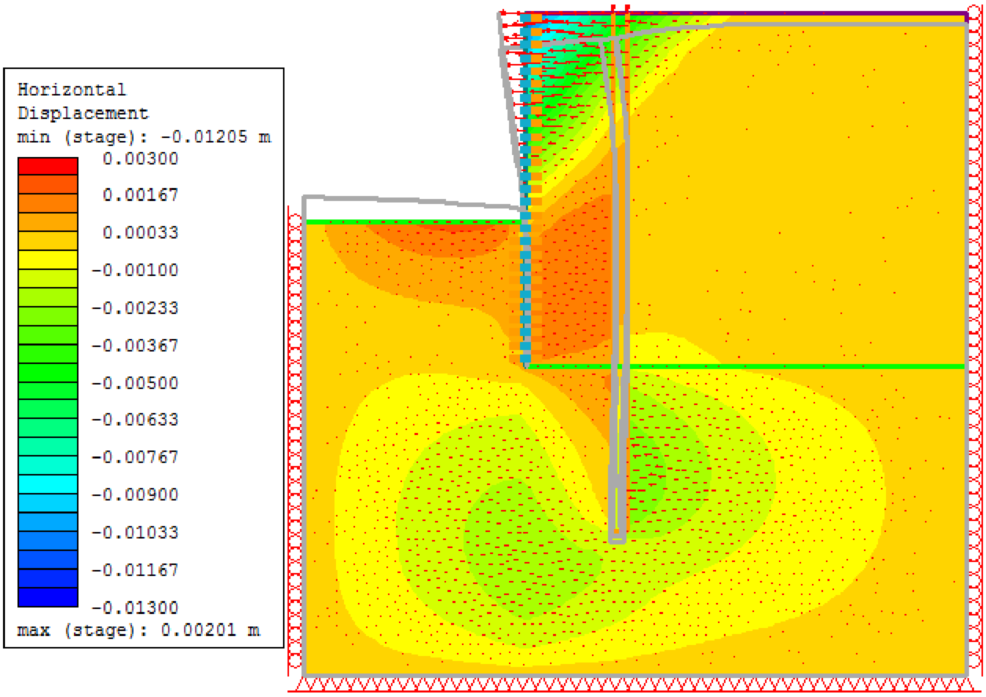

M 49.3: Deformed model (stage 3)

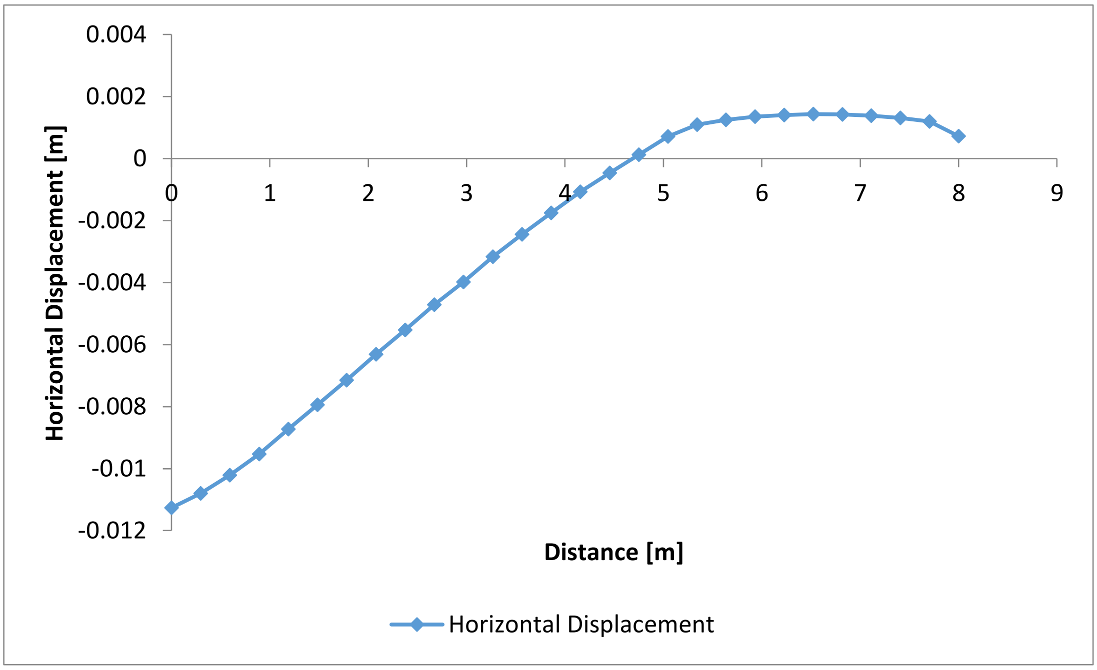

M 49.4: Horizontal displacement of soil along retaining wall

Retaining wall maximum horizontal displacement: -0.01205m

Distance from point of maximum displacement in retaining wall to the top of backfill soil: 0.0m

Model 50:

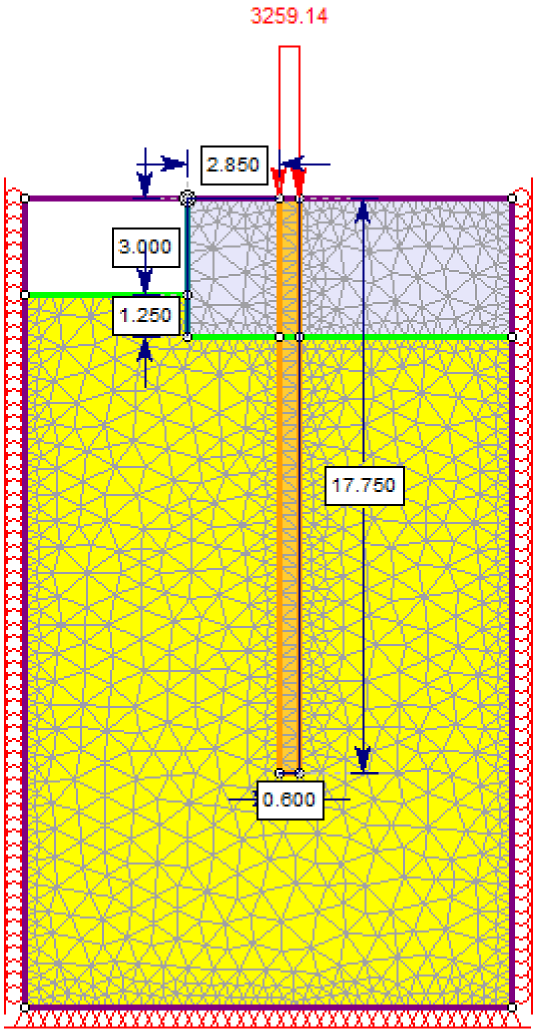

M 50.1: Original model (stage 3)

C_1'	ϕ_1'	γ_1	E_1	C_2'	ϕ_2'	γ_2	E_2	H_1	H_2	H_3	E_3	D_1	D_2	L	Qult
0	28	22	228	52	19	24	8.8	3.00	1.25	1	1030254	2.85	0.6	17.75	3259.14

M 50.2: Parameter values

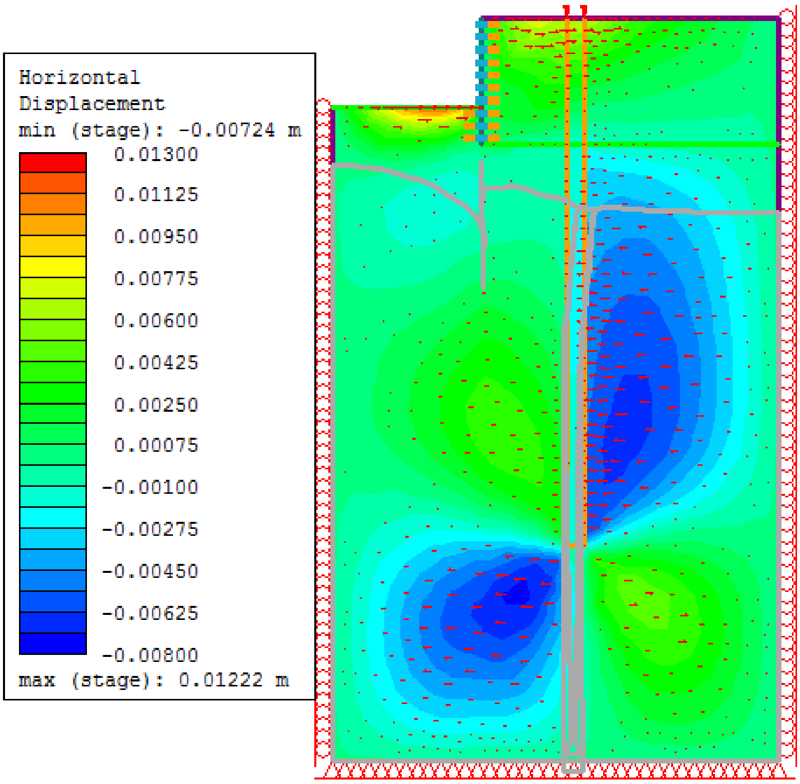

M 50.3: Deformed model (stage 3)

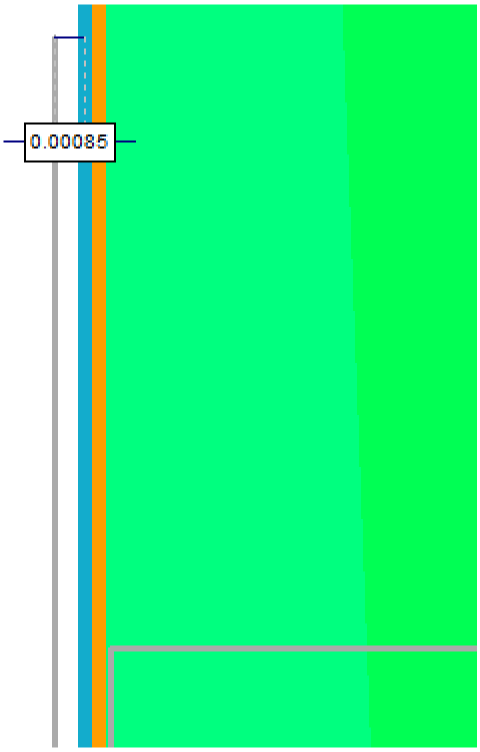

M 50.4: Detailed view of cross-section of retaining wall and soil (stage 3)

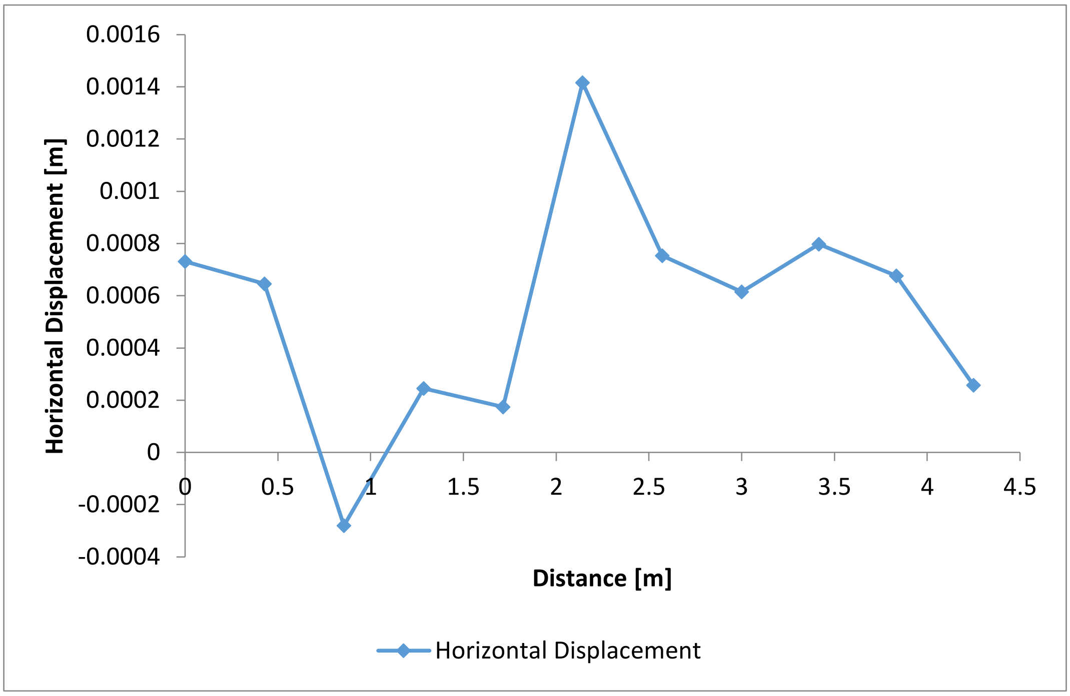

M 50.5: Horizontal displacement of soil along retaining wall

Retaining wall maximum horizontal displacement: -0.00085m

Distance from point of maximum displacement in retaining wall to the top of backfill soil: 0.0m

Model 51:

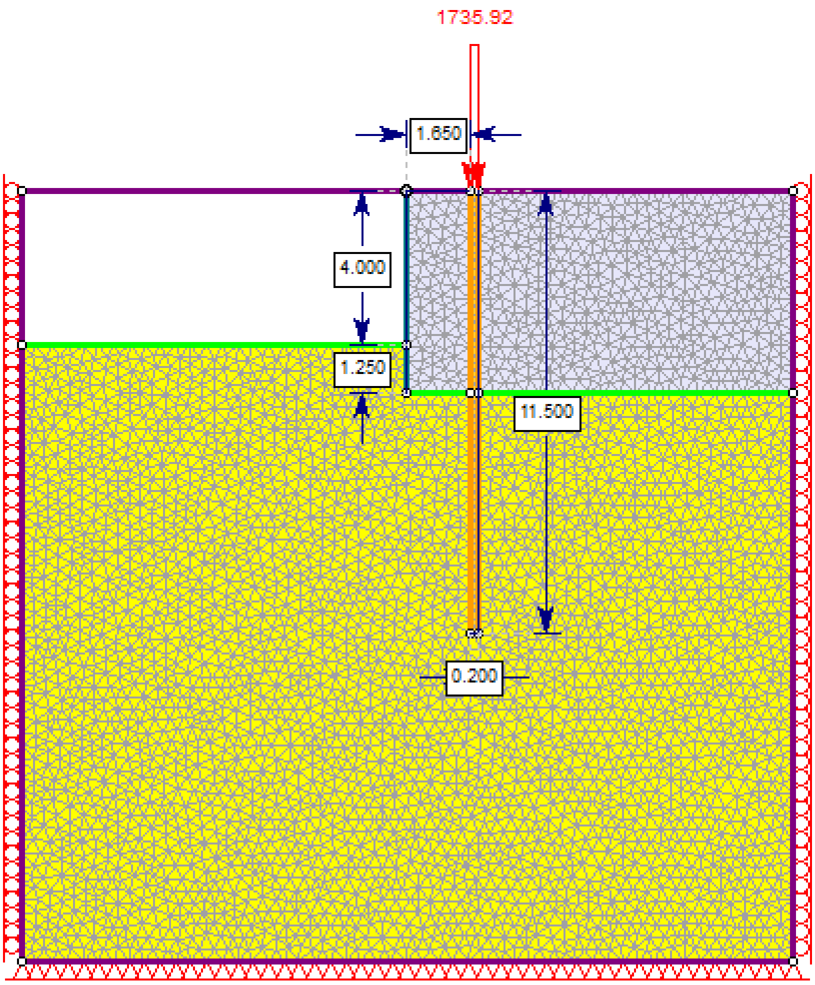

M 51.1: Original model (stage 3)

C'_1	ϕ'_1	γ_1	E_1	C'_2	ϕ'_2	γ_2	E_2	H_1	H_2	H_3	E_3	D_1	D_2	L	Qult
0	37	22	53	31	10	23	42.6	4.00	3.5	1.25	737967	1.65	0.2	11.5	1735.92

M 51.2: Parameter values

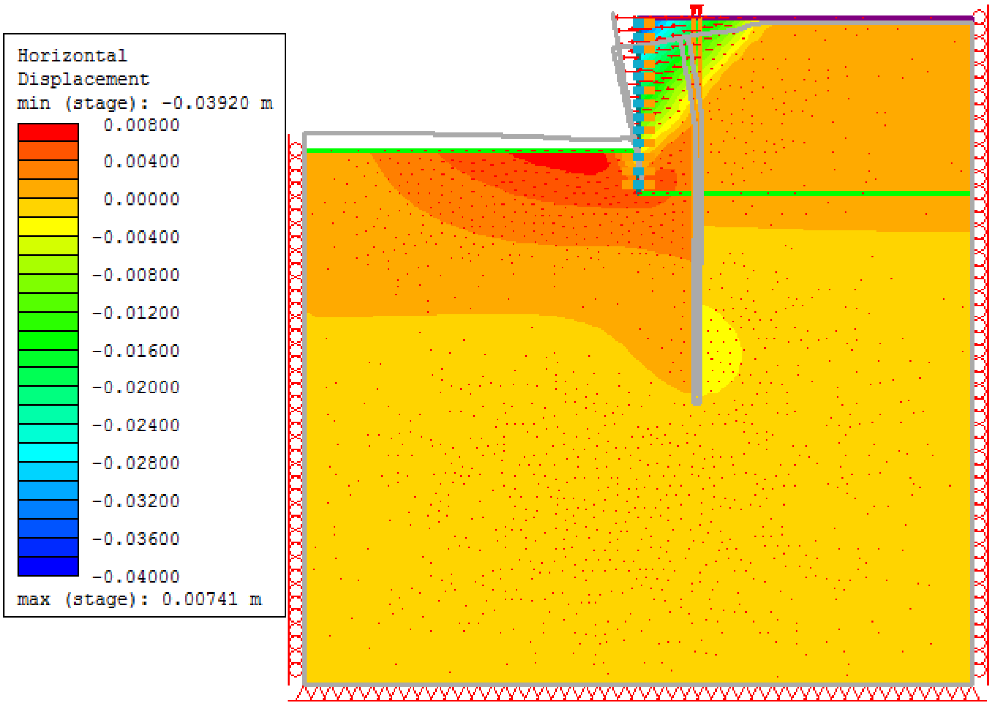

M 51.3: Deformed model (stage 3)

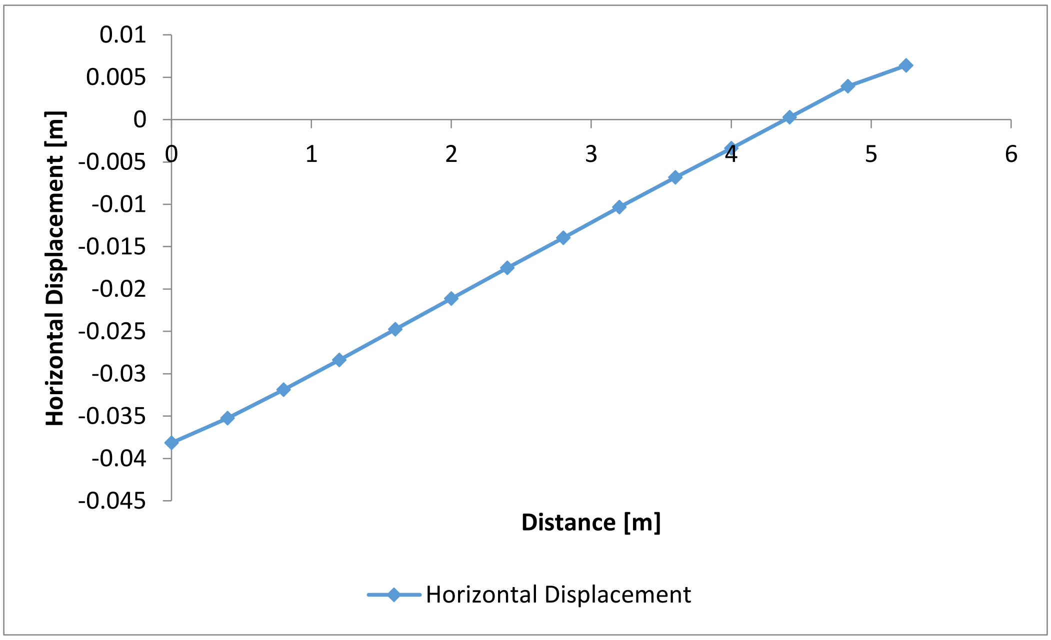

M 51.4: Horizontal displacement of soil along retaining wall

Retaining wall maximum horizontal displacement: -0.0392m

Distance from point of maximum displacement in retaining wall to the top of backfill soil: 0.0m

Model 52:

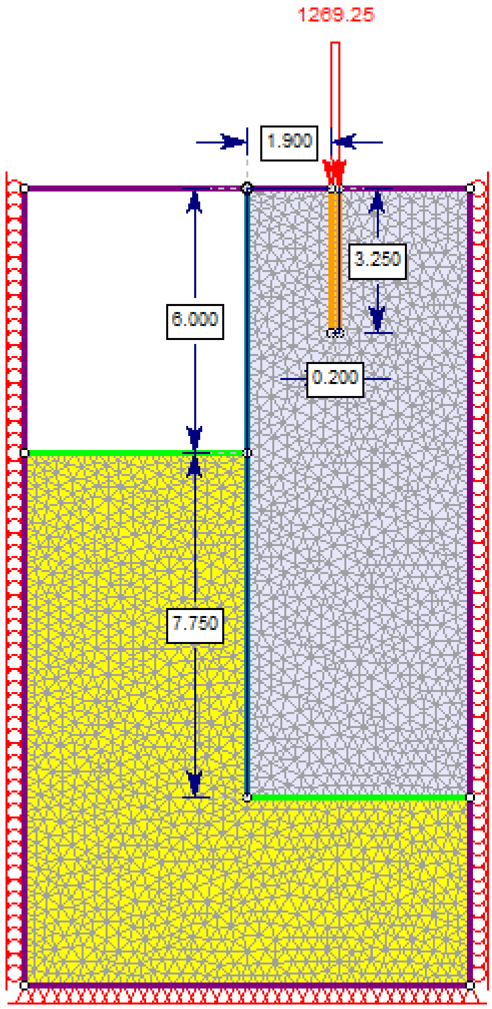

M 52.1: Original model (stage 3)

C_1'	ϕ_1'	γ_1	E_1	C_2'	ϕ_2'	γ_2	E_2	H_1	H_2	H_3	E_3	D_1	D_2	L	Qult
0	33	20	21	40	21	24	21.0	6.00	7.75	1	737797	1.9	0.2	3.25	1269.25

M 52.2: Parameter values

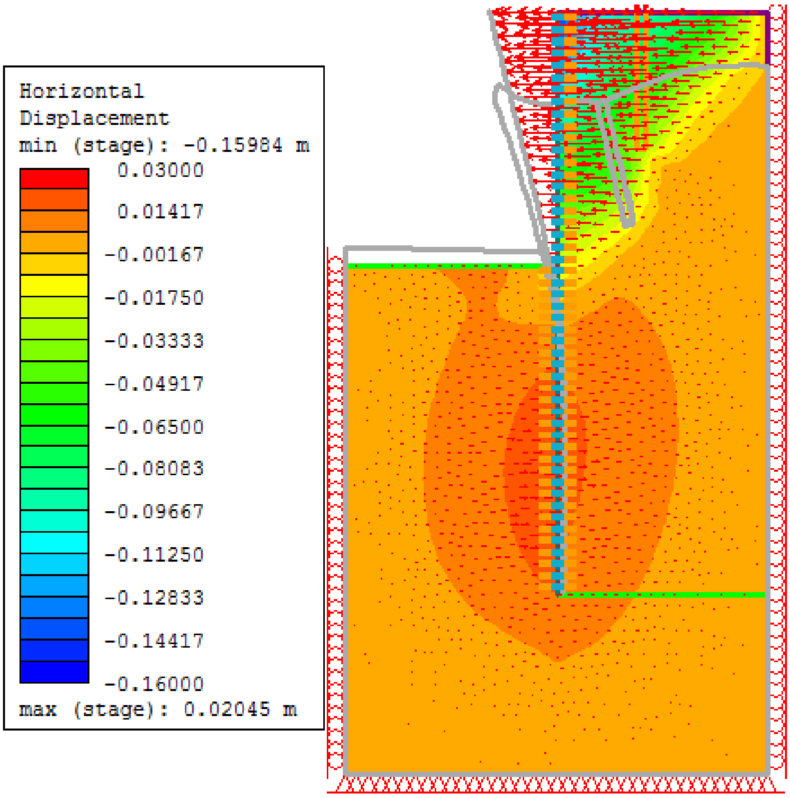

M 52.3: Deformed model (stage 3)

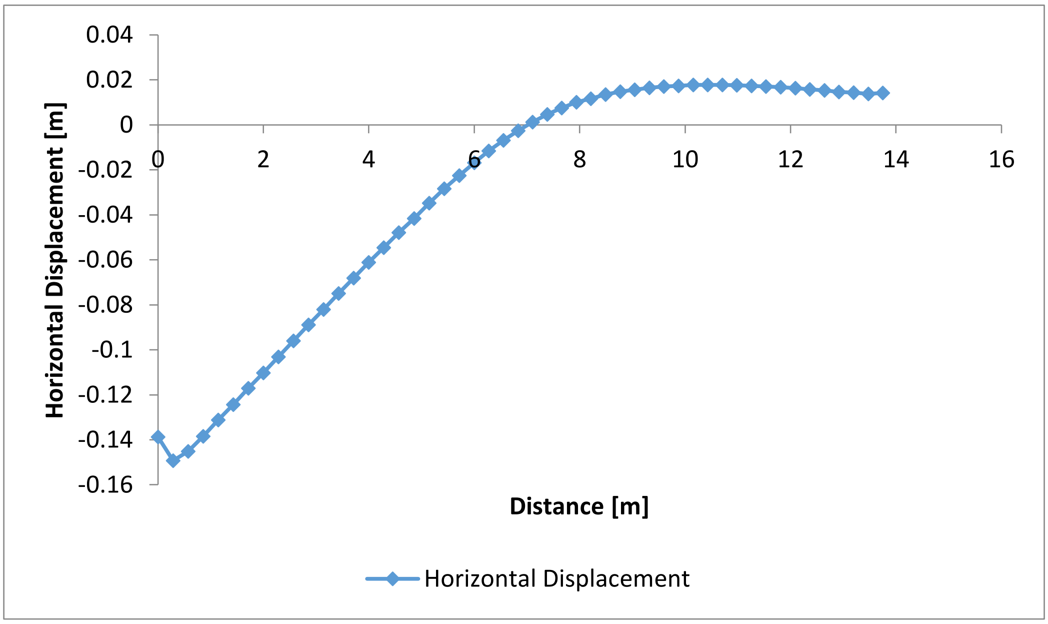

M 52.4: Horizontal displacement of soil along retaining wall

Retaining wall maximum horizontal displacement: -0.15984m

Distance from point of maximum displacement in retaining wall to the top of backfill soil: 0.0m

Model 53:

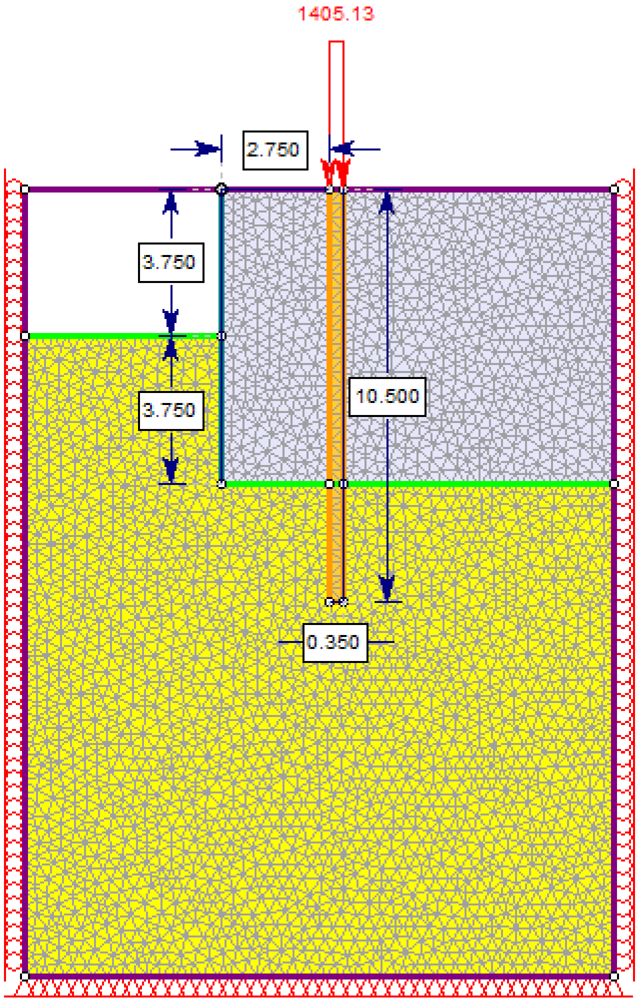

M 53.1: Original model (stage 3)

C_1'	ϕ_1'	γ_1	E_1	C_2'	ϕ_2'	γ_2	E_2	H_1	H_2	H_3	E_3	D_1	D_2	L	Qult
0	34	22	22	29	11	21	7.4	3.75	3.75	1.25	1007597	2.75	0.35	10.5	1405.13

M 53.2: Parameter values

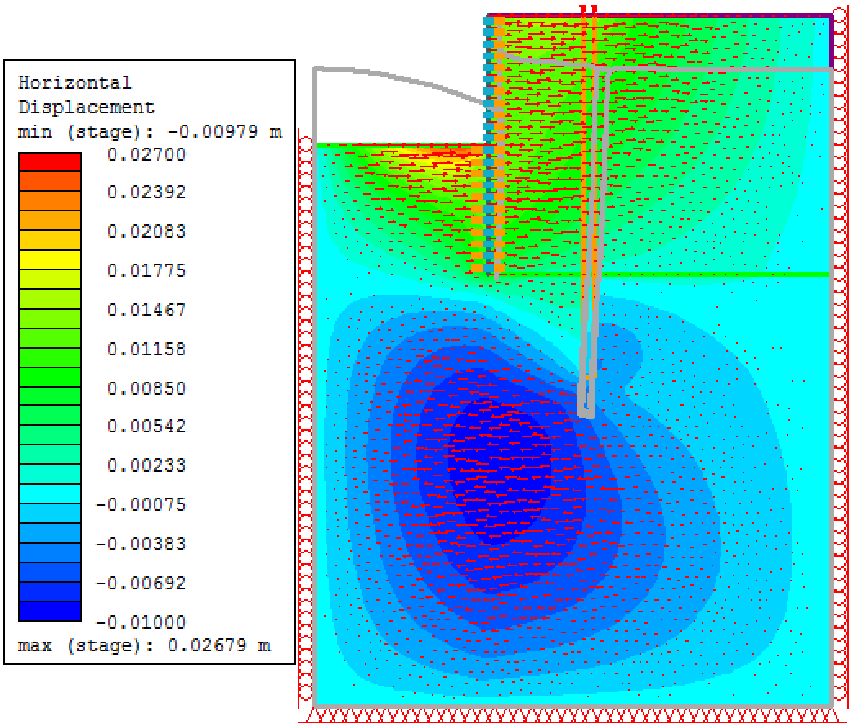

M 53.3: Deformed model (stage 3)

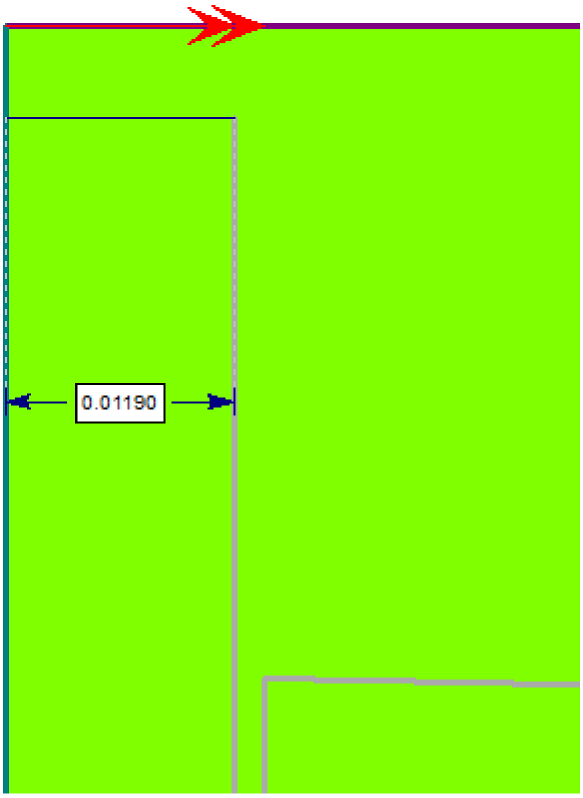

M 53.4: Detailed view of cross-section of retaining wall and soil (stage 3)

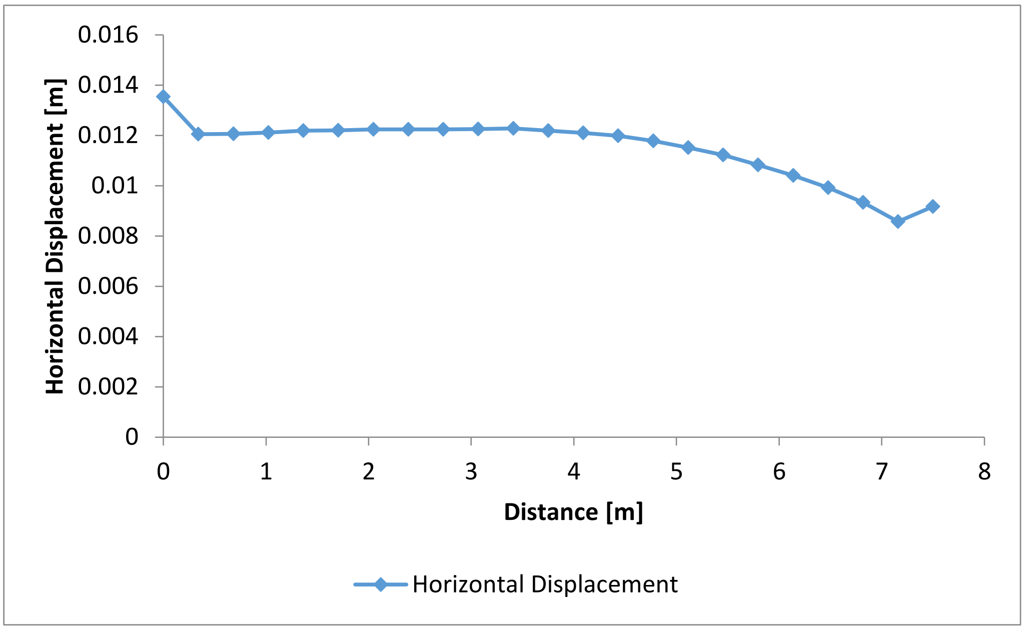

M 53.5: Horizontal displacement of soil along retaining wall

Retaining wall maximum horizontal displacement: 0.0119m

Distance from point of maximum displacement in retaining wall to the top of backfill soil: 0.0 m

Model 54:

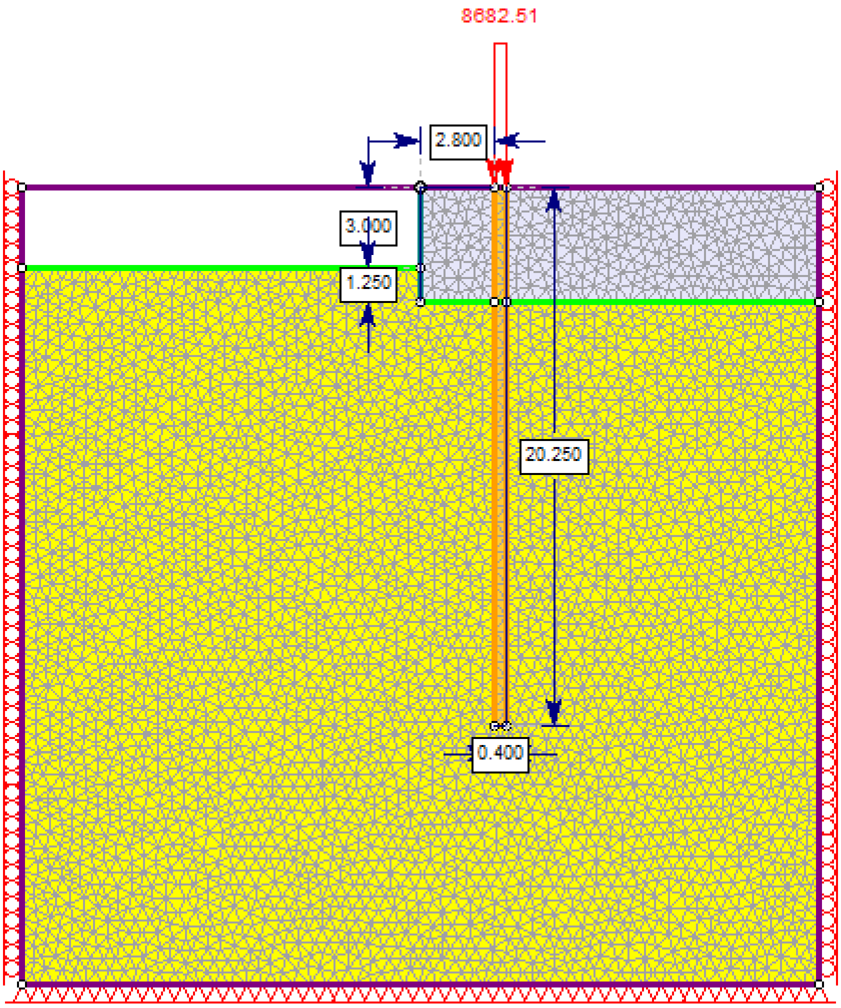

M 54.1: Original model (stage 3)

C_1'	ϕ_1'	γ_1	E_1	C_2'	ϕ_2'	γ_2	E_2	H_1	H_2	H_3	E_3	D_1	D_2	L	Qult
0	31	20	158	41	28	22	6.4	3.00	1.25	0.75	1068473	2.8	0.4	20.25	8682.51

M 54.2: Parameter values

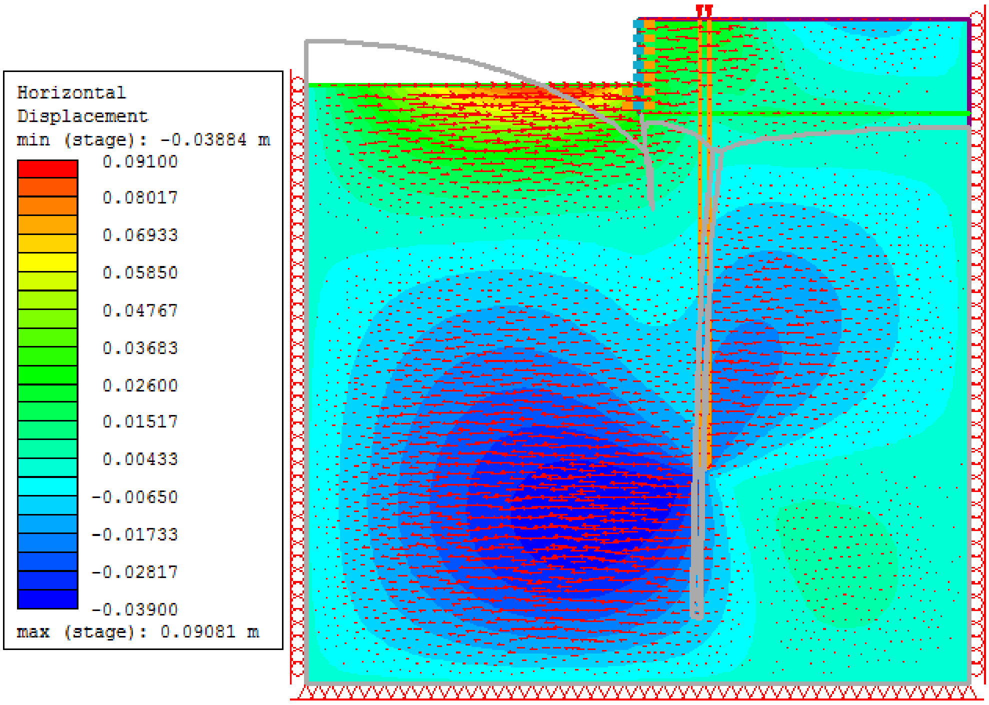

M 54.3: Deformed model (stage 3)

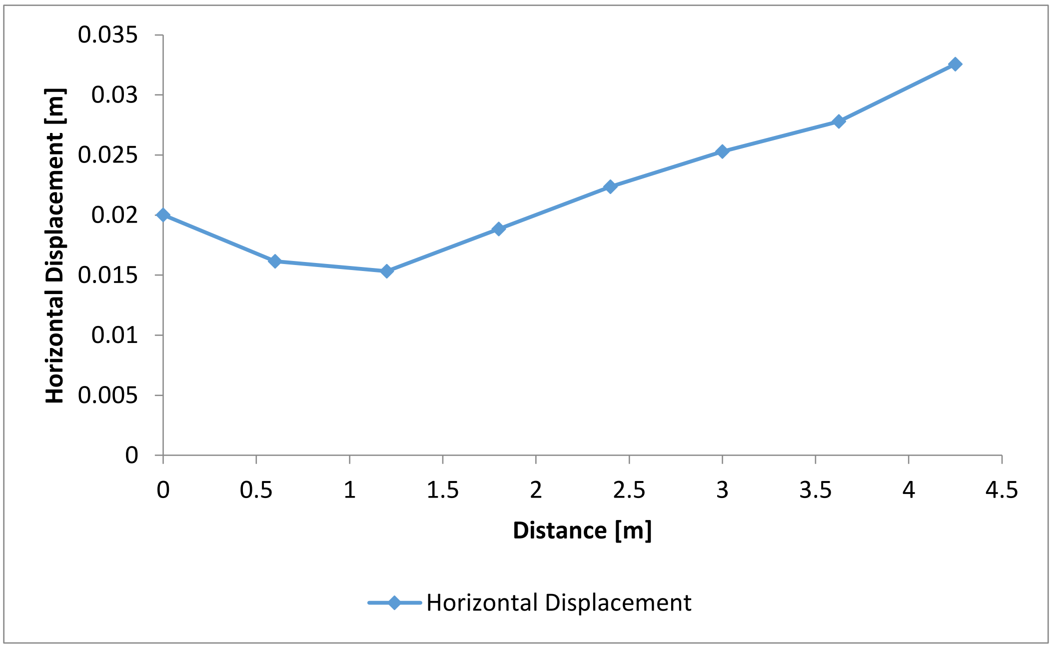

M 54.4: Horizontal displacement of soil along retaining wall

Retaining wall maximum horizontal displacement: 0.032559m

Distance from point of maximum displacement in retaining wall to the top of backfill soil: 4.25m

Model 55:

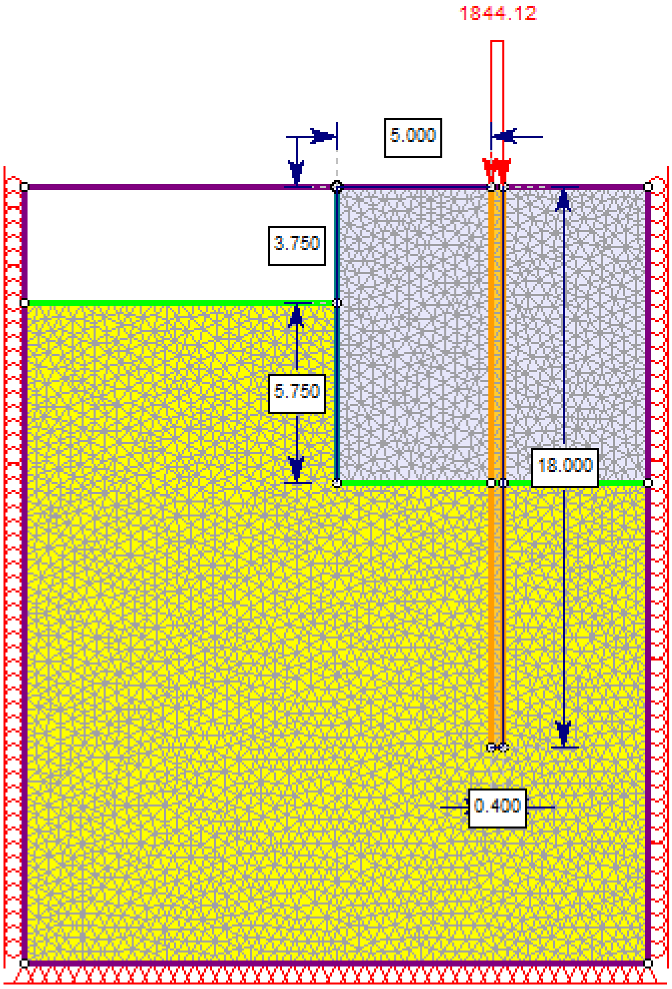

M 55.1: Original model (stage 3)

C_1'	ϕ_1'	γ_1	E_1	C_2'	ϕ_2'	γ_2	E_2	H_1	H_2	H_3	E_3	D_1	D_2	L	Qult
0	31	19	132	22	9	21	3.2	3.75	5.75	0.75	824512	5	0.4	18	1844.12

M 55.2: Parameter values

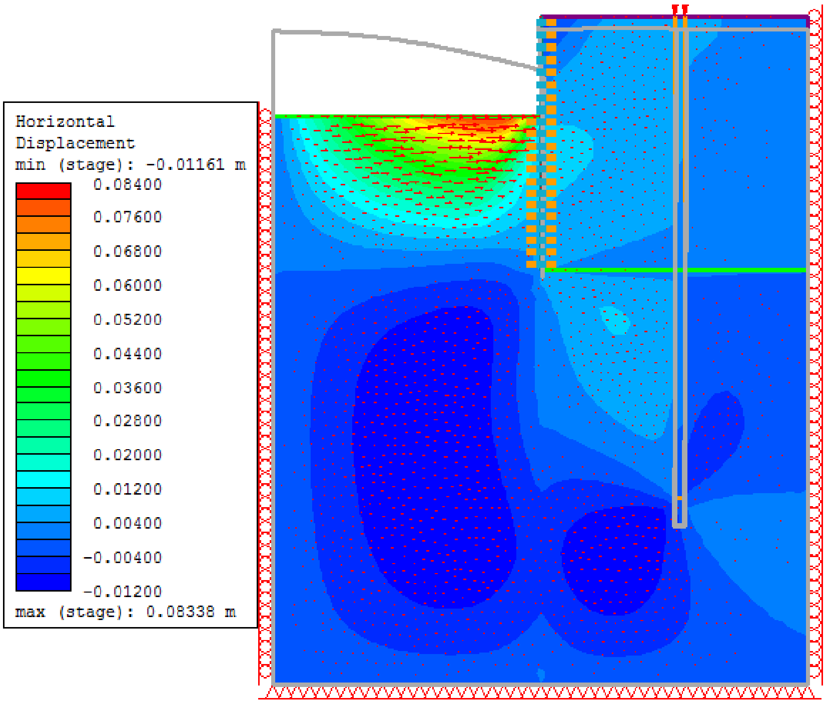

M 55.3: Deformed model (stage 3)

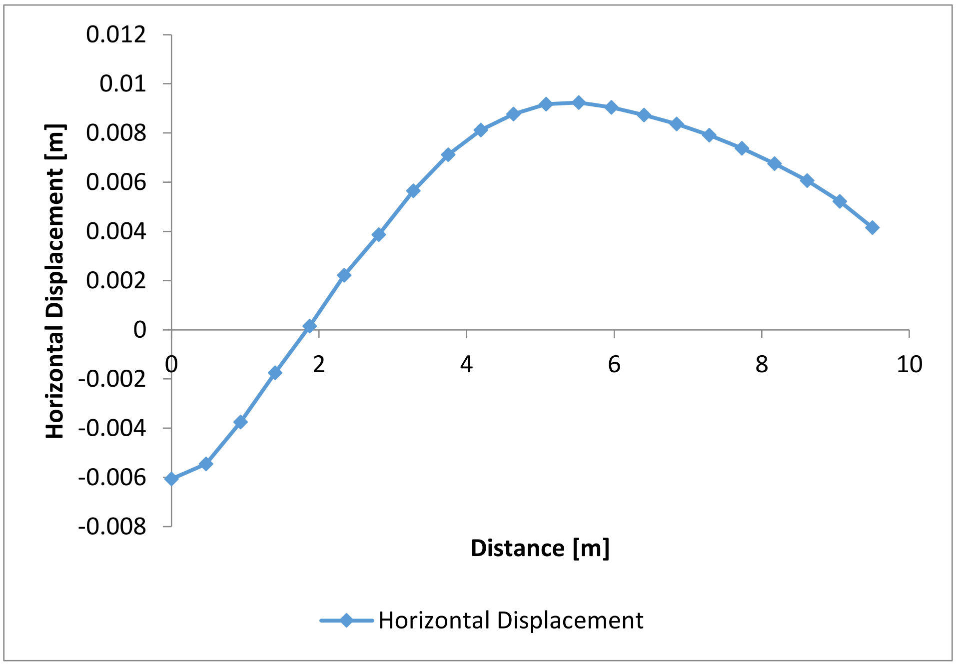

M 55.4: Horizontal displacement of soil along retaining wall

Retaining wall maximum horizontal displacement: 0.009236m

Distance from point of maximum displacement in retaining wall to the top of backfill soil: 5.519m

Model 56:

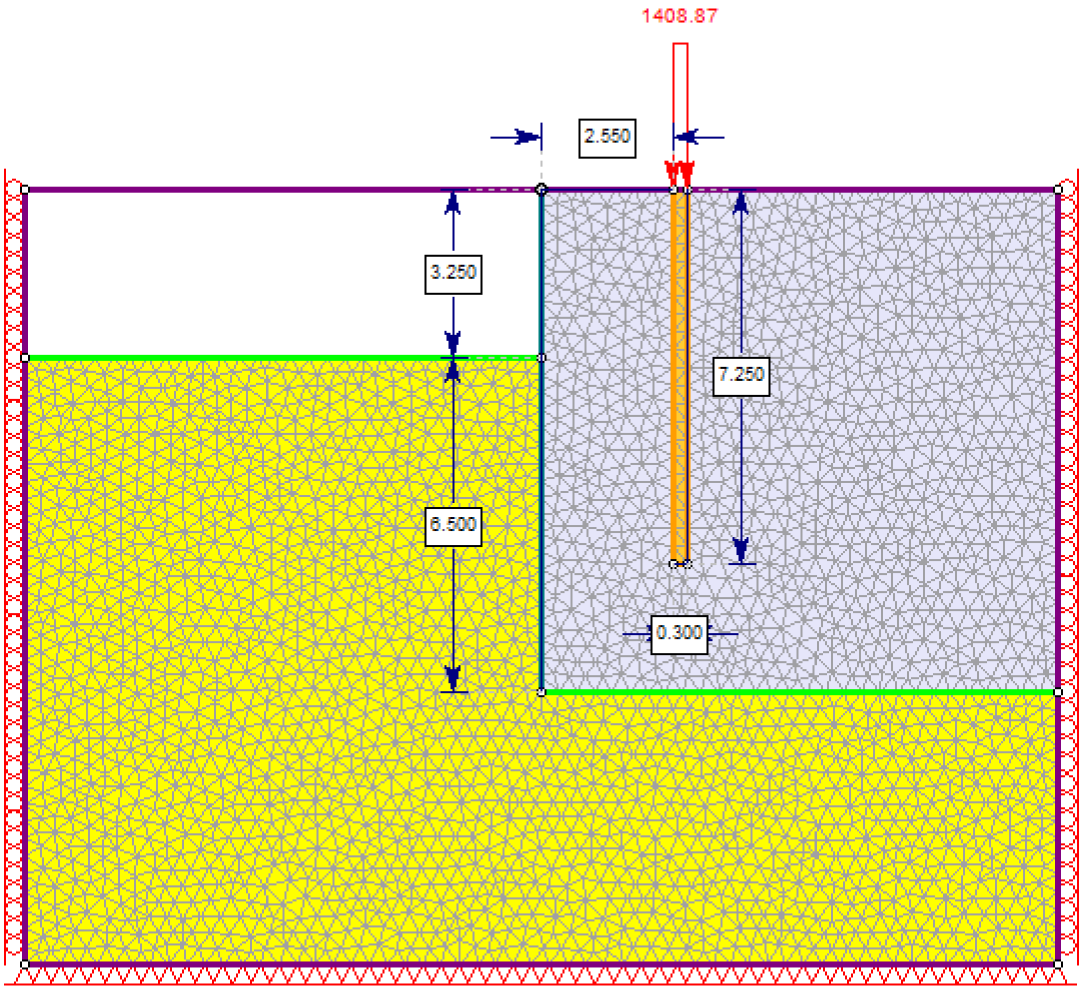

M 56.1: Original model (stage 3)

C'_1	ϕ'_1	γ_1	E_1	C'_2	ϕ'_2	γ_2	E_2	H_1	H_2	H_3	E_3	D_1	D_2	L	Qult
0	31	18	68	18	13	20	0.3	3.25	6.5	1.25	692552	2.55	0.3	7.25	1408.87

M 56.2: Parameter values

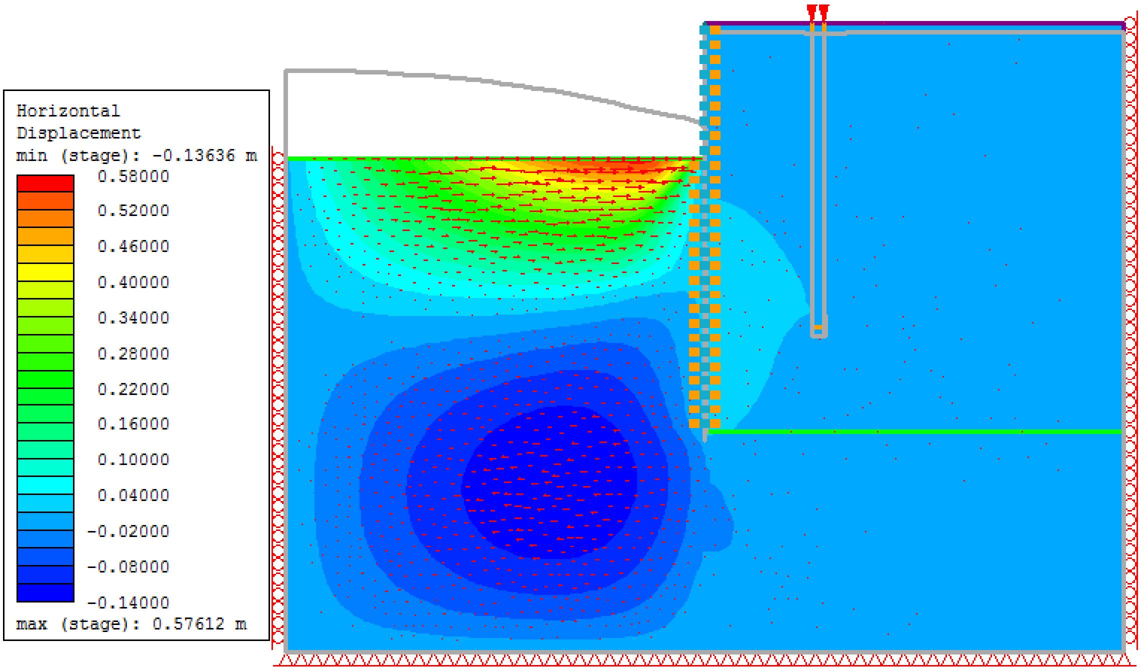

M 56.3: Deformed model (stage 3)

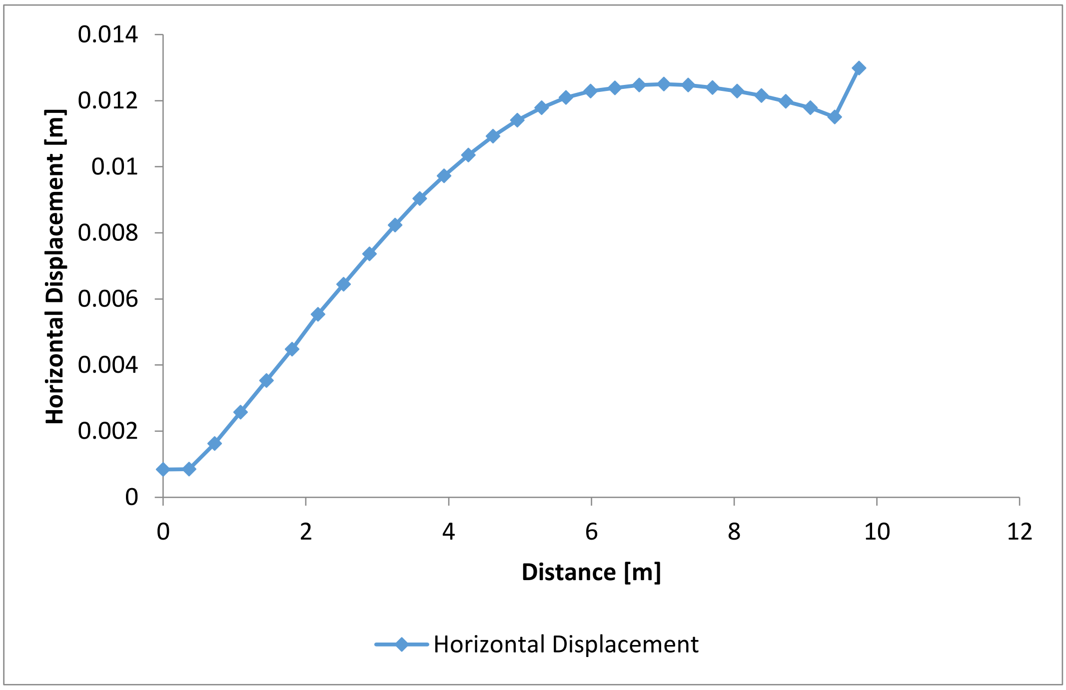

M 56.4: Horizontal displacement of soil along retaining wall

Retaining wall maximum horizontal displacement: 0.01299m

Distance from point of maximum displacement in retaining wall to the top of backfill soil: 9.75m

Model 57:

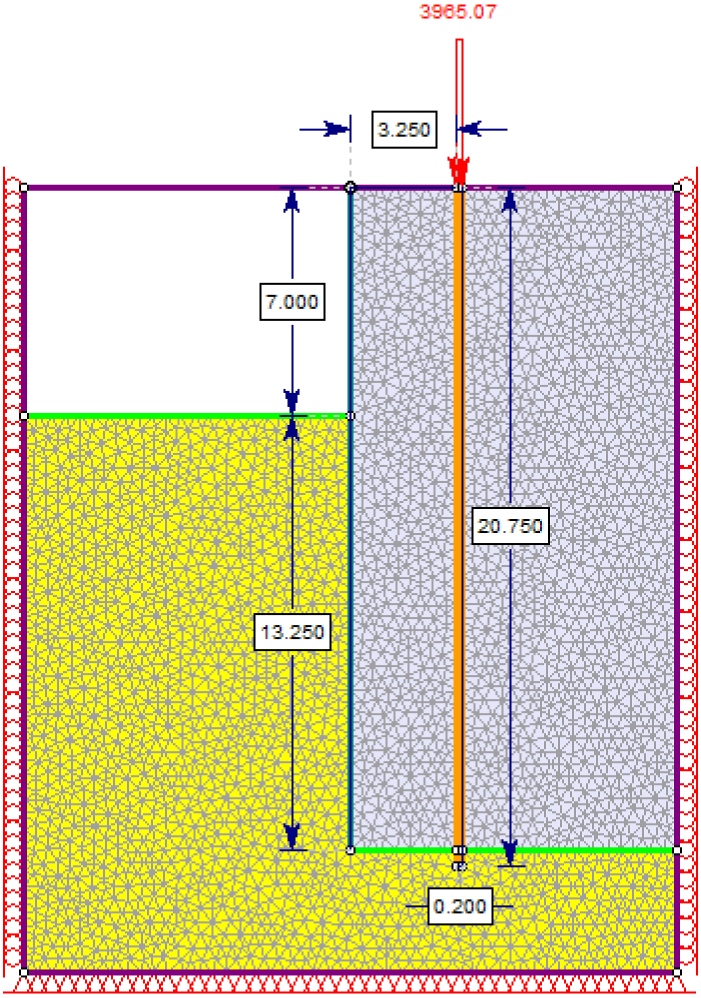

M 57.1: Original model (stage 3)

C_1'	ϕ_1'	γ_1	E_1	C_2'	ϕ_2'	γ_2	E_2	H_1	H_2	H_3	E_3	D_1	D_2	L	Qult
0	37	21	252	42	8	25	32.9	7.00	13.25	1.25	894792	3.25	0.2	20.75	3965.07

M 57.2: Parameter values

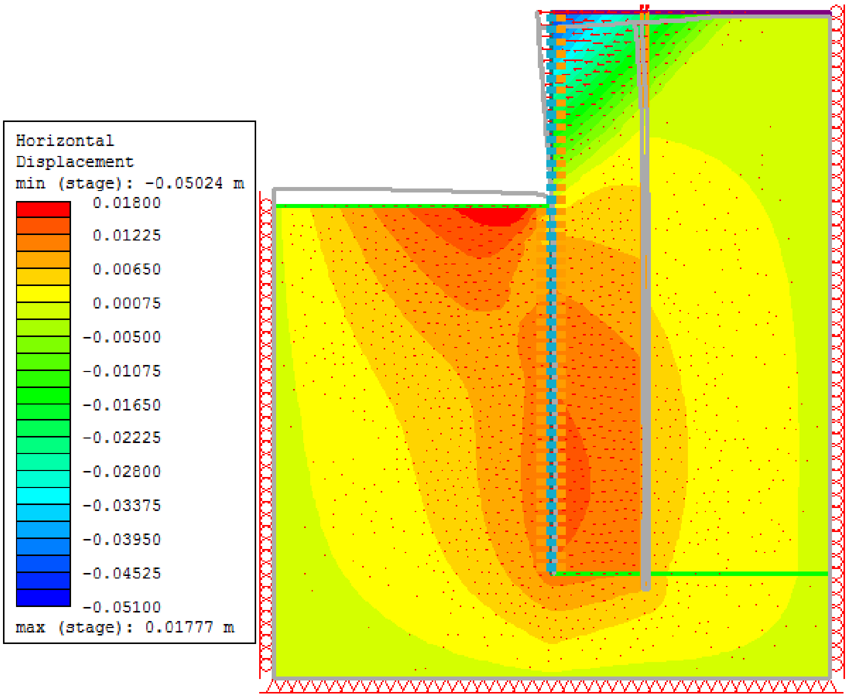

M 57.3: Deformed model (stage 3)

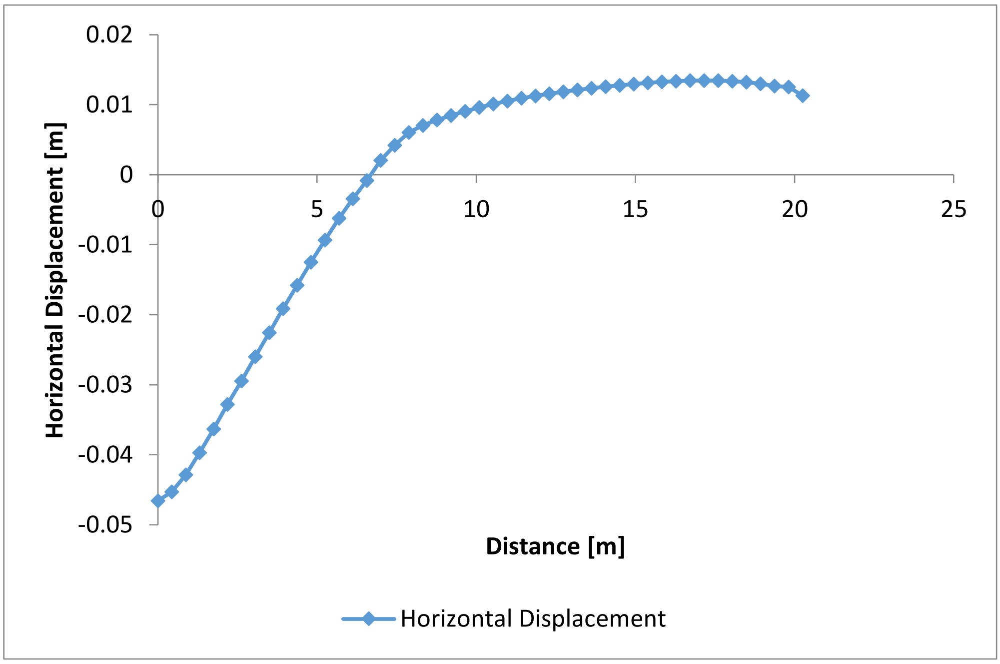

M 57.4: Horizontal displacement of soil along retaining wall

Retaining wall maximum horizontal displacement: -0.05024m

Distance from point of maximum displacement in retaining wall to the top of backfill soil: 0.0m

Model 58:

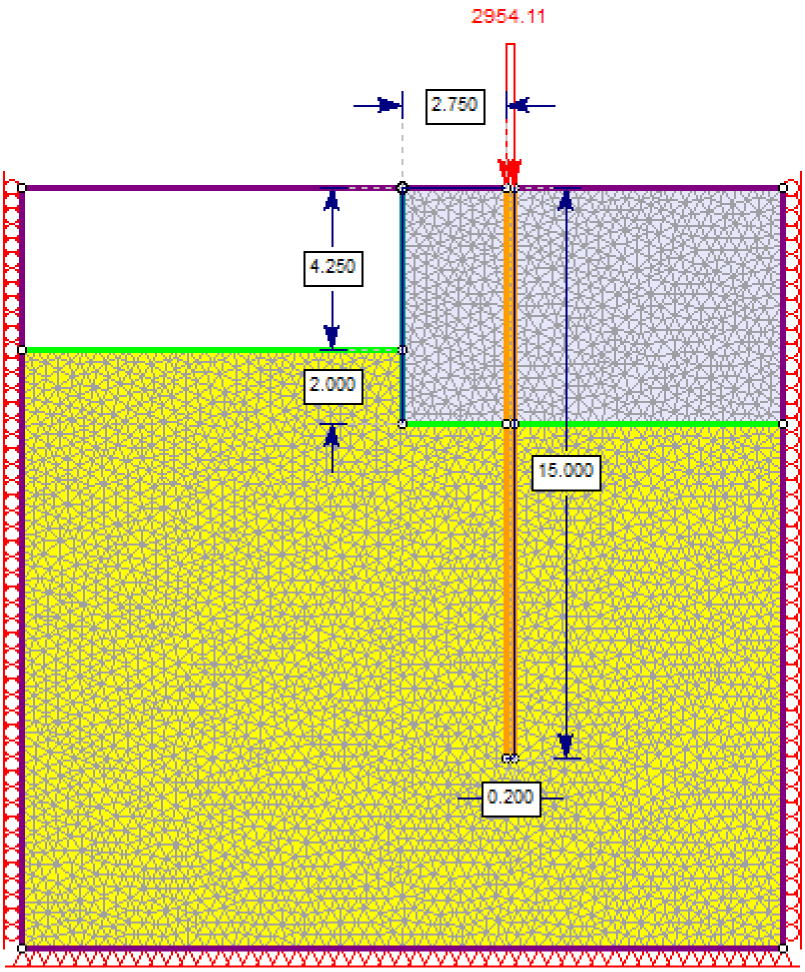

M 58.1: Original model (stage 3)

C_1'	ϕ_1'	γ_1	E_1	C_2'	ϕ_2'	γ_2	E_2	H_1	H_2	H_3	E_3	D_1	D_2	L	Qult
0	29	21	161	56	17	23	46.0	4.25	2	1	991211	2.75	0.2	15	2954.11

M 58.2: Parameter values

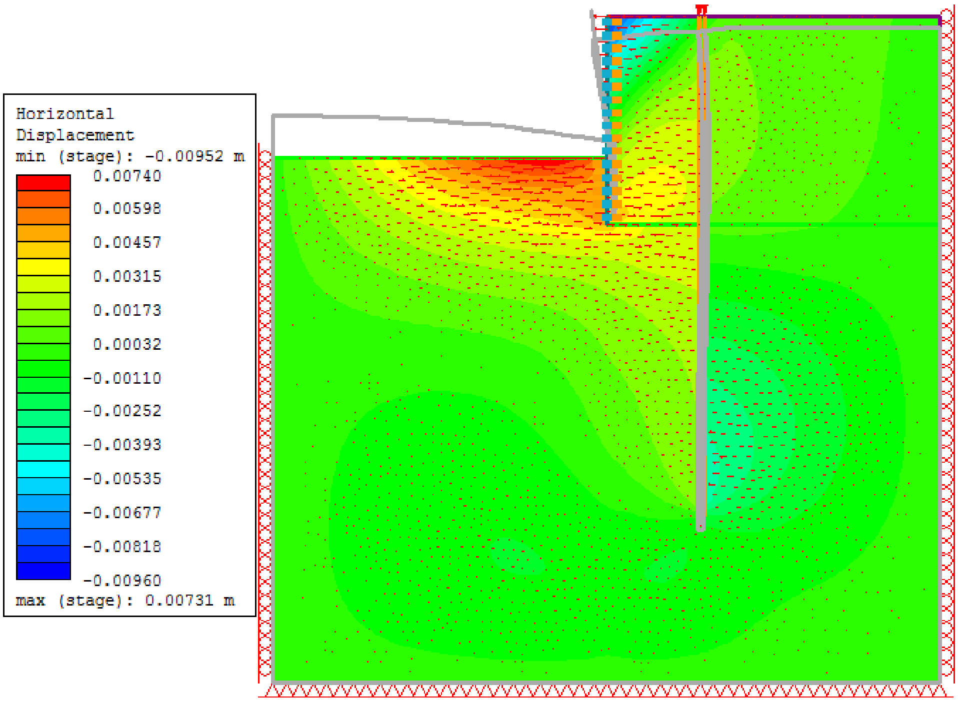

M 58.3: Deformed model (stage 3)

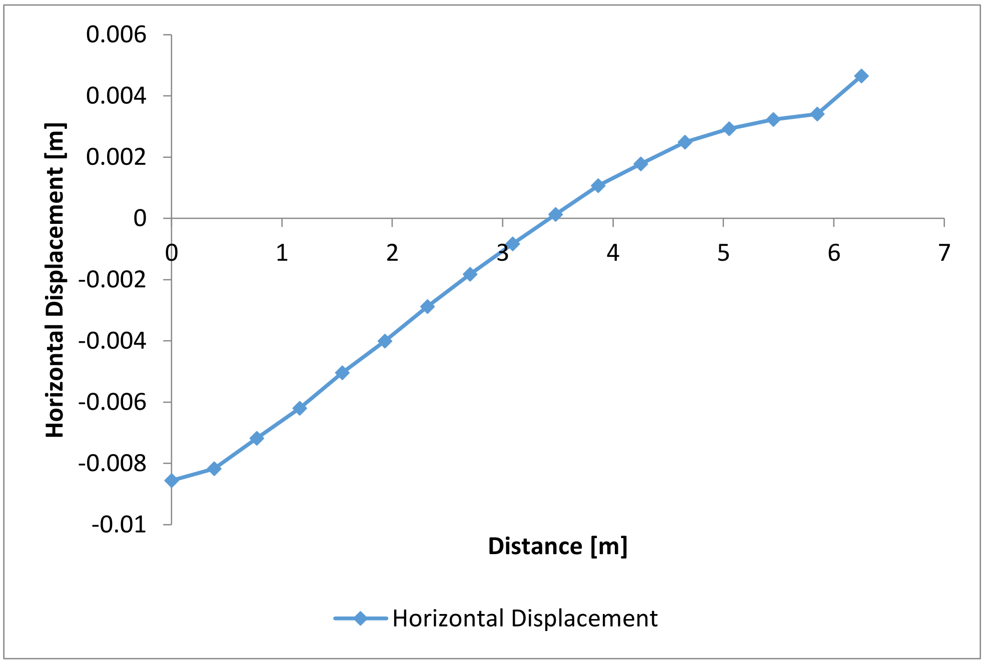

M 58.4: Horizontal displacement of soil along retaining wall

Retaining wall maximum horizontal displacement: -0.0952m

Distance from point of maximum displacement in retaining wall to the top of backfill soil: 0.0m

Model 59:

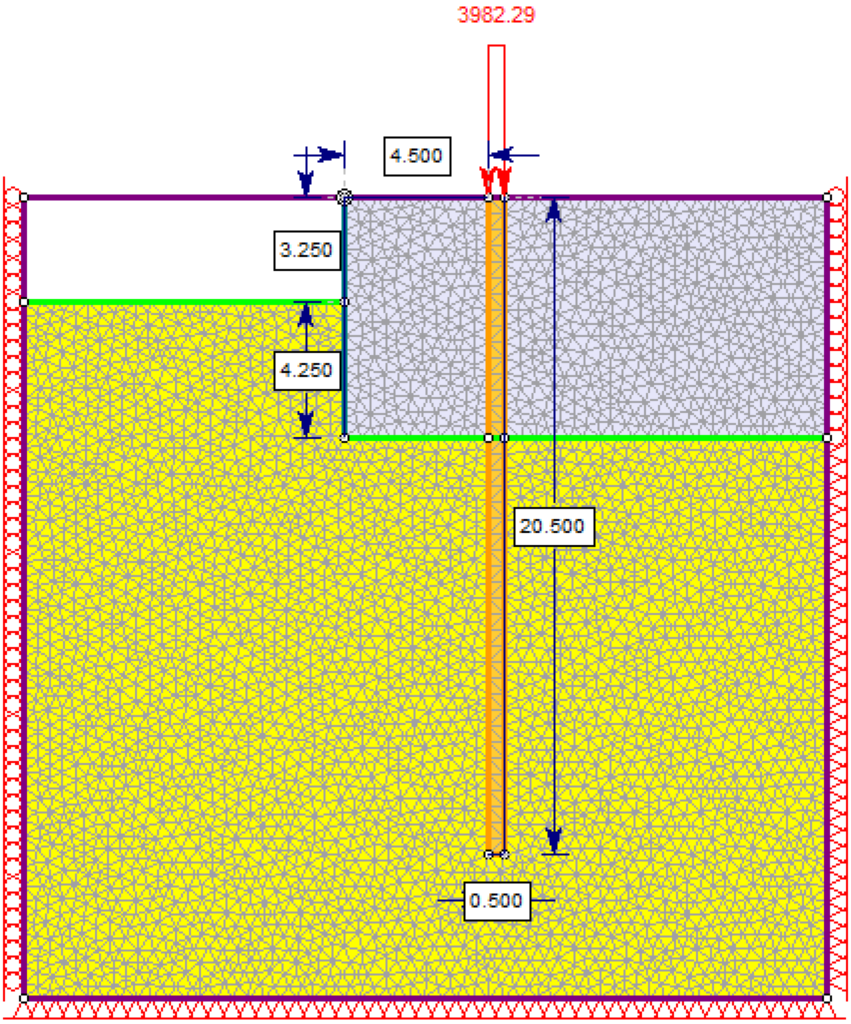

M 59.1: Original model (stage 3)

C'_1	ϕ'_1	γ_1	E_1	C'_2	ϕ'_2	γ_2	E_2	H_1	H_2	H_3	E_3	D_1	D_2	L	Qult
0	29	20	290	22	21	22	12.4	3.25	4.25	1.25	969323	4.5	0.5	20.5	3982.29

M 59.2: Parameter values

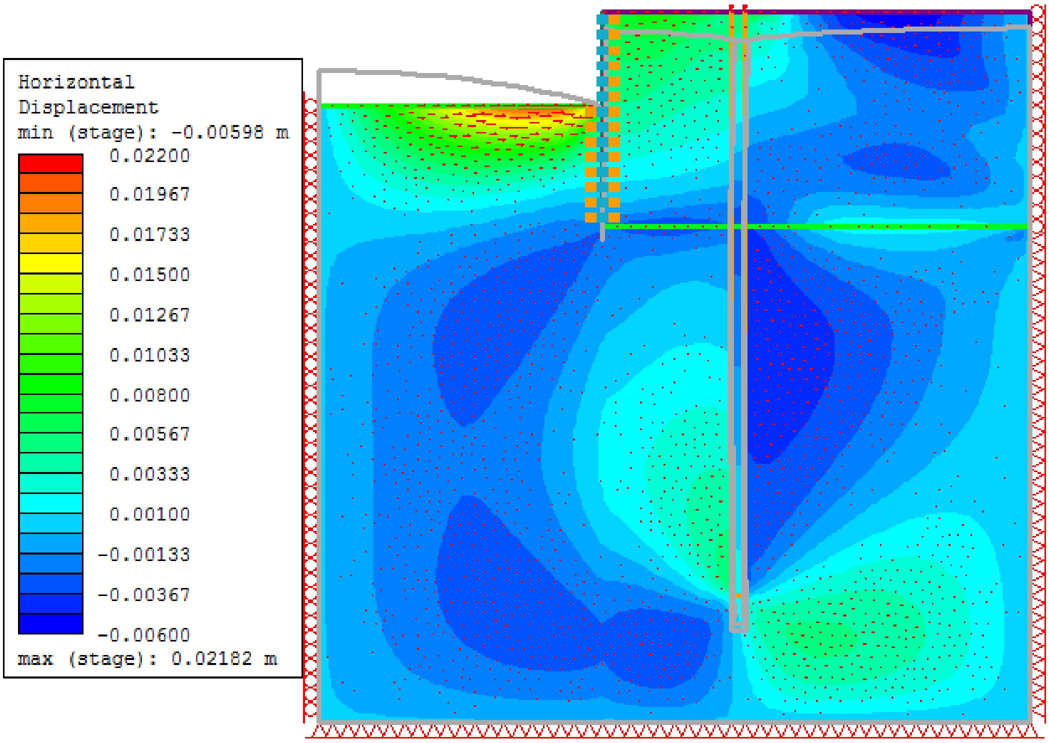

M 59.3: Deformed model (stage 3)

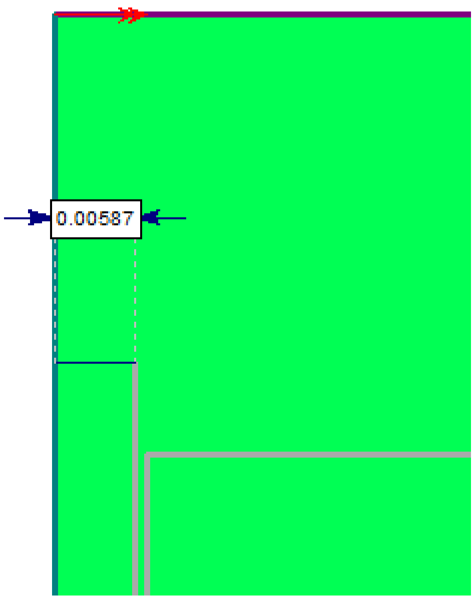

M 59.4: Detailed view of cross-section of retaining wall and soil (stage 3)

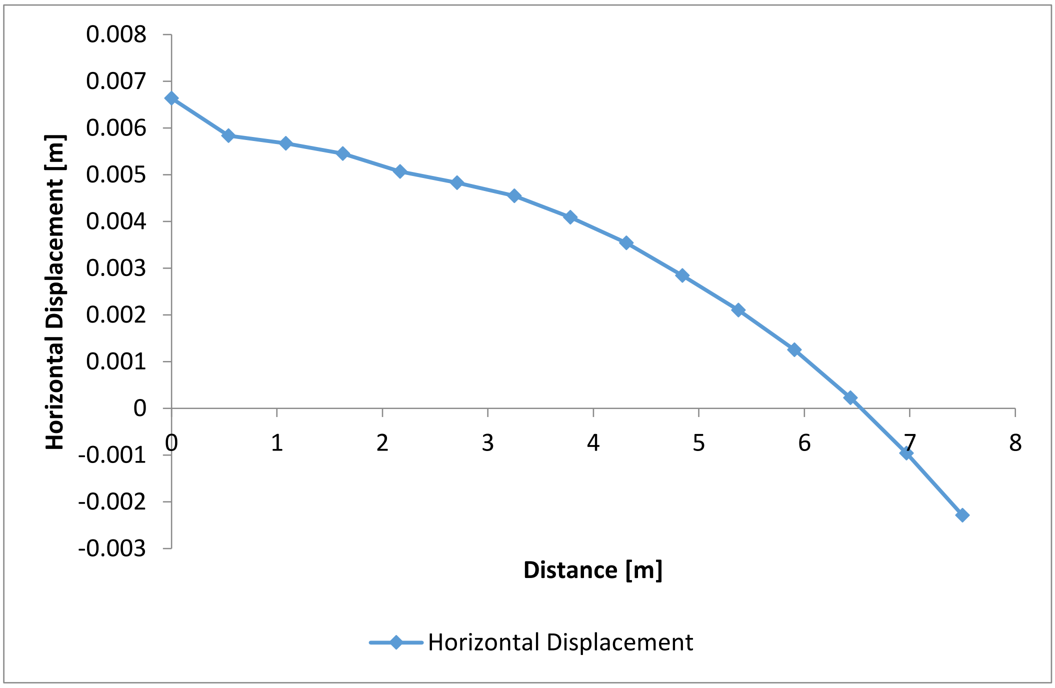

M 59.5: Horizontal displacement of soil along retaining wall

Retaining wall maximum horizontal displacement: 0.00587m

Distance from point of maximum displacement in retaining wall to the top of backfill soil: 0.0m

Model 60:

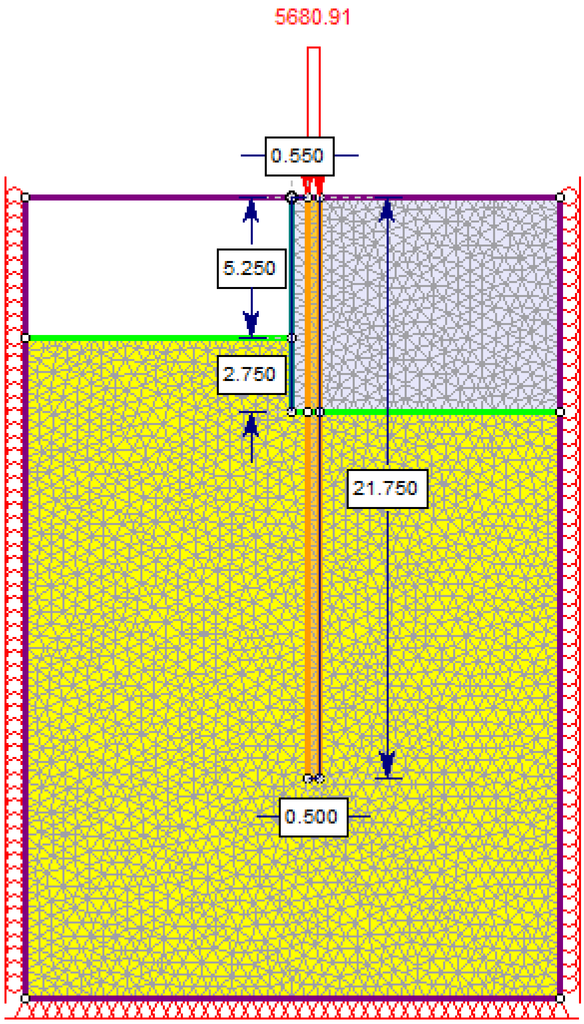

M 60.1: Original model (stage 3)

C_1'	ϕ_1'	γ_1	E_1	C_2'	ϕ_2'	γ_2	E_2	H_1	H_2	H_3	E_3	D_1	D_2	L	Qult
0	45	21	122	45	25	16	5.2	5.25	2.75	0.75	904192	0.55	0.5	21.75	5680.91

M 60.2: Parameter values

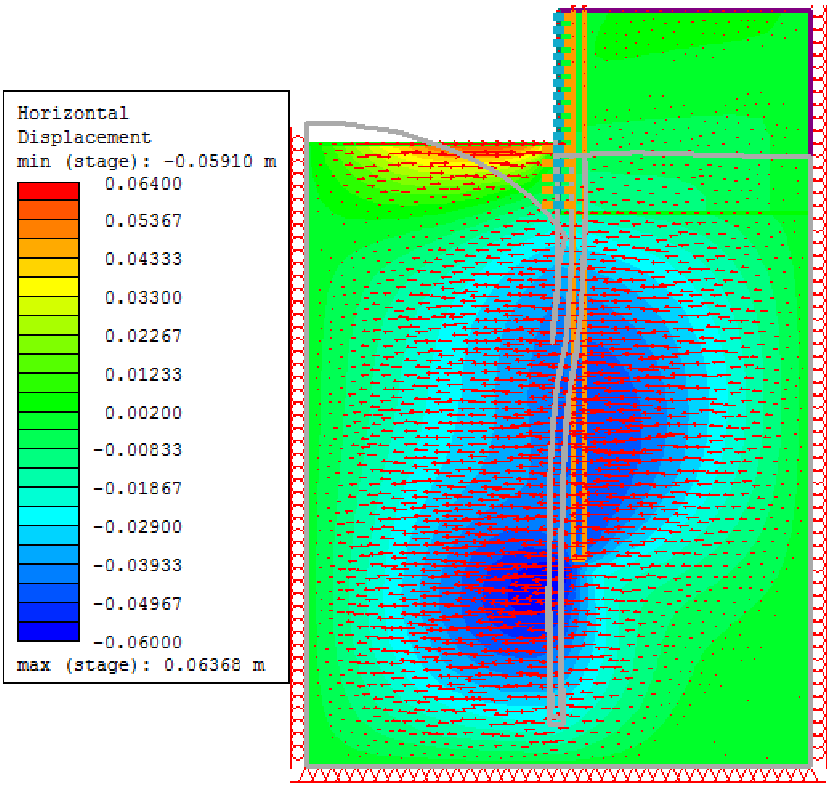

M 60.3: Deformed model (stage 3)

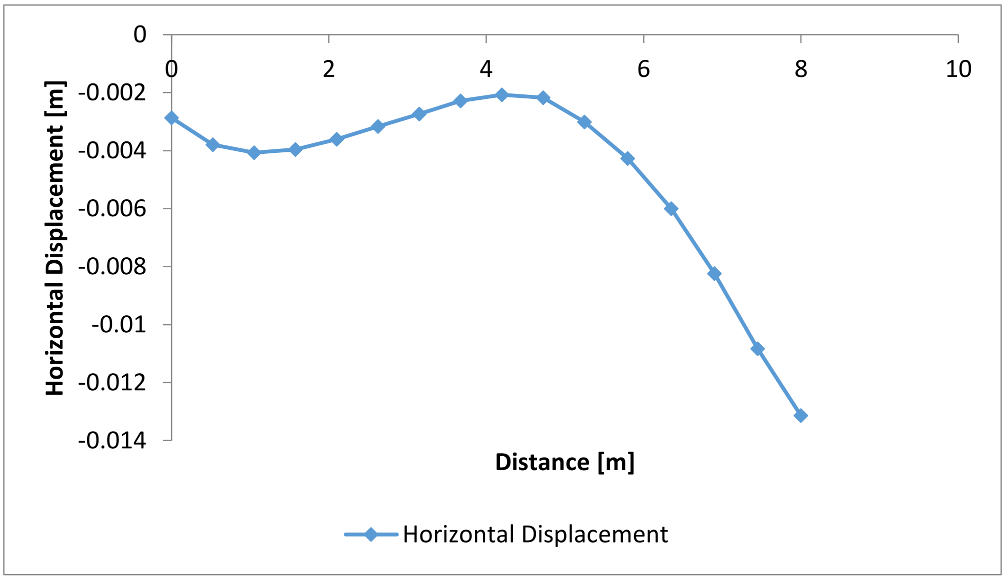

M 60.4: Horizontal displacement of soil along retaining wall

Retaining wall maximum horizontal displacement: -0.01314m

Distance from point of maximum displacement in retaining wall to the top of backfill soil: 8.0m

Model 61:

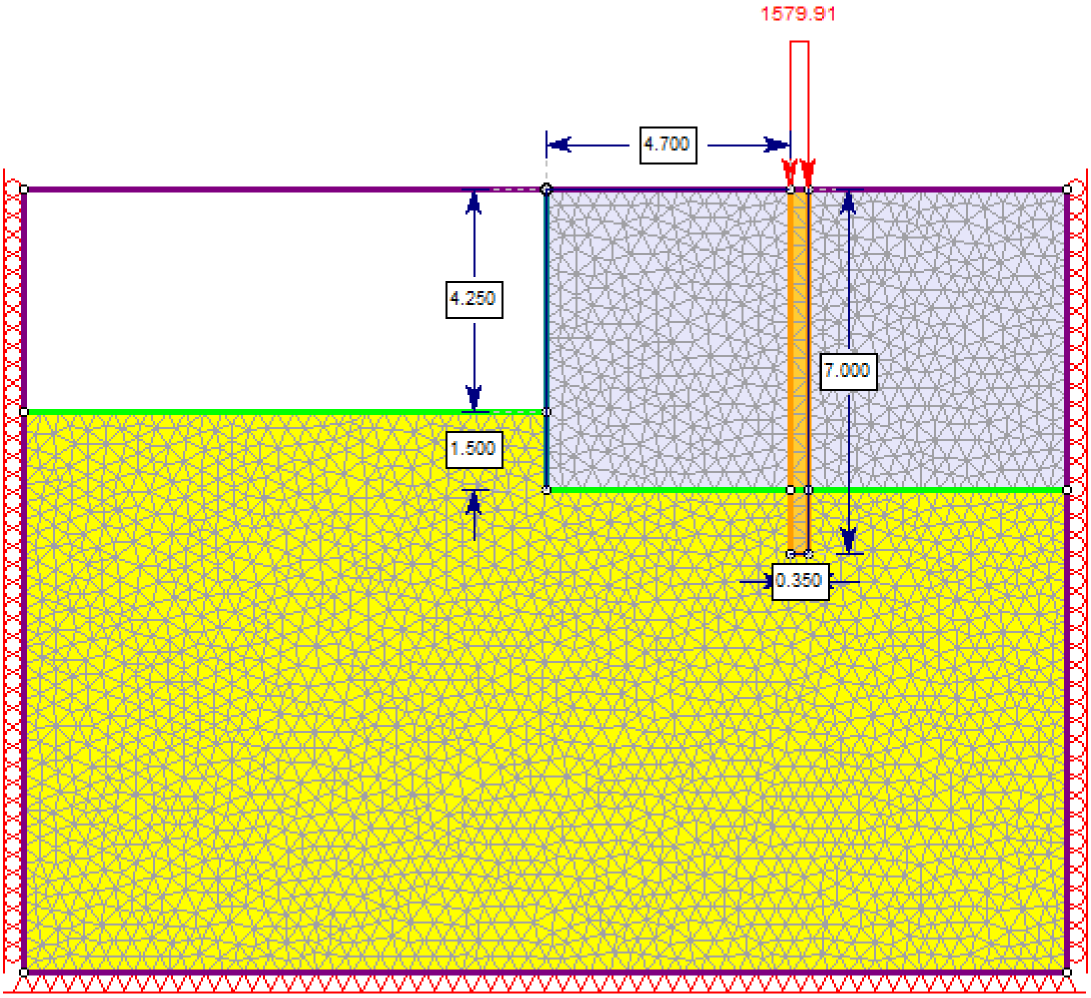

M 61.1: Original model (stage 3)

C_1'	ϕ_1'	γ_1	E_1	C_2'	ϕ_2'	γ_2	E_2	H_1	H_2	H_3	E_3	D_1	D_2	L	Qult
0	39	21	309	59	18	22	23.7	4.25	1.5	1	943736	4.7	0.35	7	1579.91

M 61.2: Parameter values

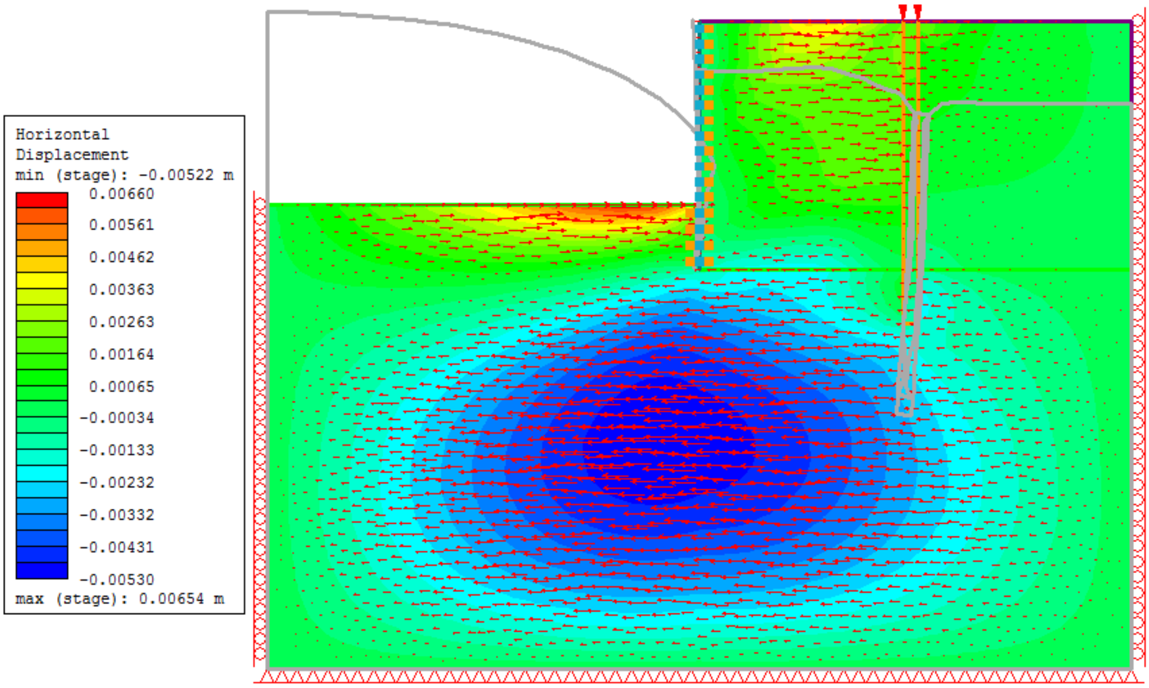

M 61.3: Deformed model (stage 3)

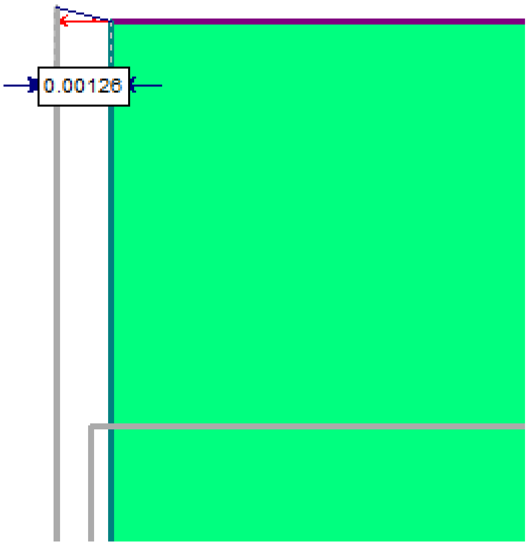

M 61.4: Detailed view of cross-section of retaining wall and soil (stage 3)

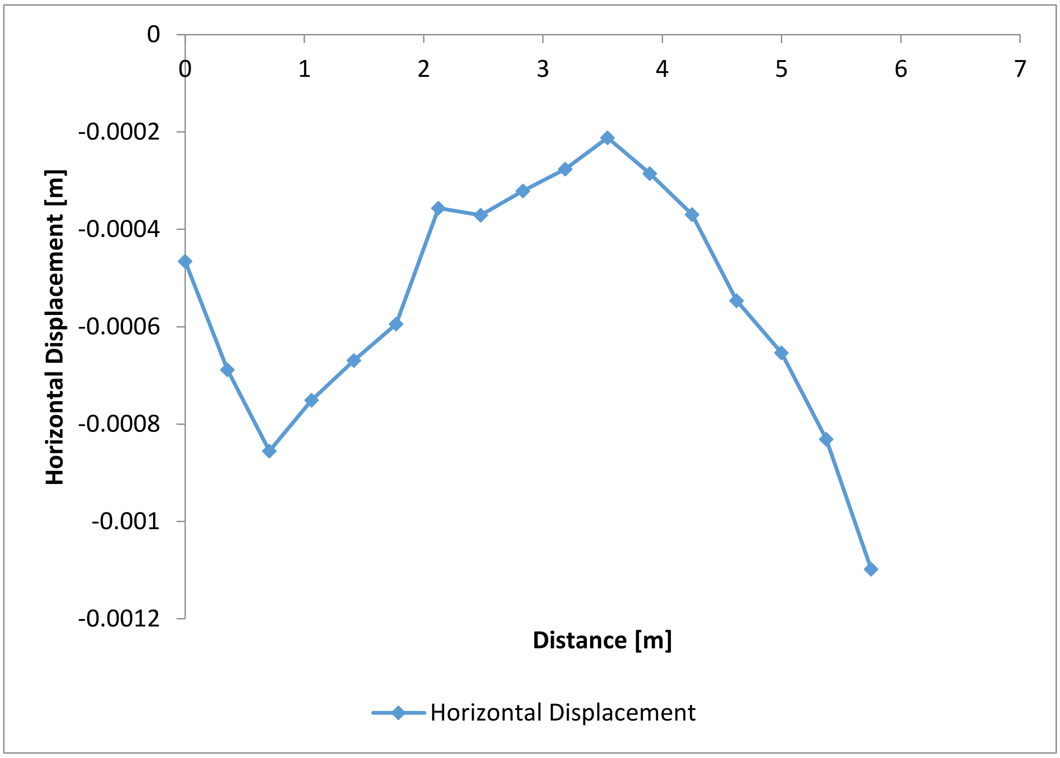

M 61.5: Horizontal displacement of soil along retaining wall

Retaining wall maximum horizontal displacement: -0.00126m

Distance from point of maximum displacement in retaining wall to the top of backfill soil: 0.0m

Model 62:

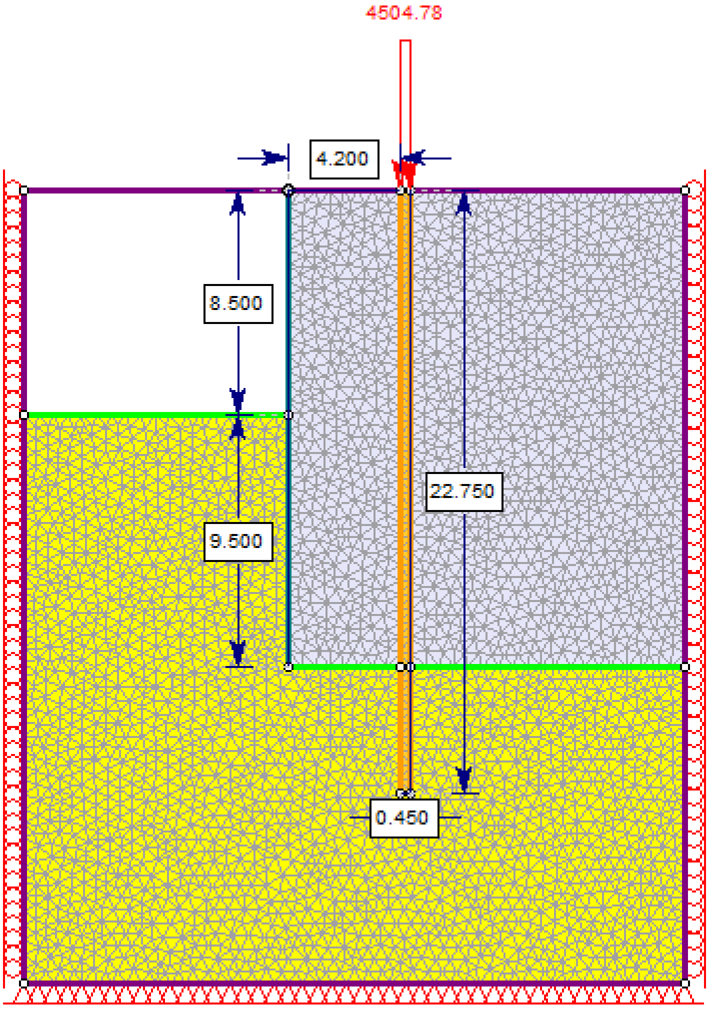

M 62.1: Original model (stage 3)

C'_1	ϕ'_1	γ_1	E_1	C'_2	ϕ'_2	γ_2	E_2	H_1	H_2	H_3	E_3	D_1	D_2	L	Qult
0	41	20	111	52	17	23	17.0	8.50	9.5	1	1148533	4.2	0.45	22.75	4504.78

M 62.2: Parameter values

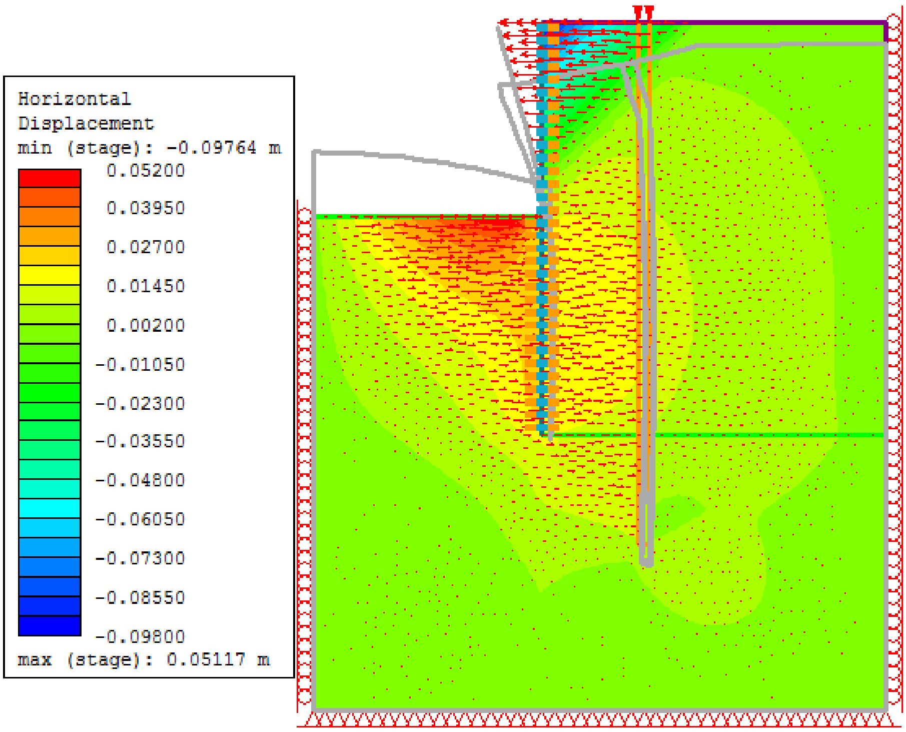

M 62.3: Deformed model (stage 3)

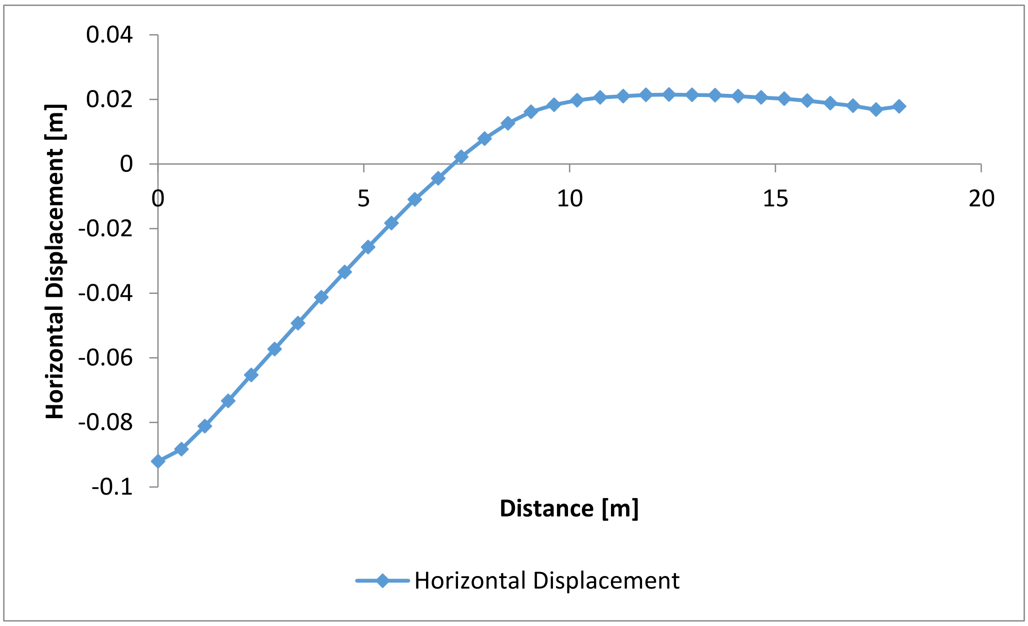

M 62.4: Horizontal displacement of soil along retaining wall

Retaining wall maximum horizontal displacement: -0.09764m

Distance from point of maximum displacement in retaining wall to the top of backfill soil: 0.0m

Model 63:

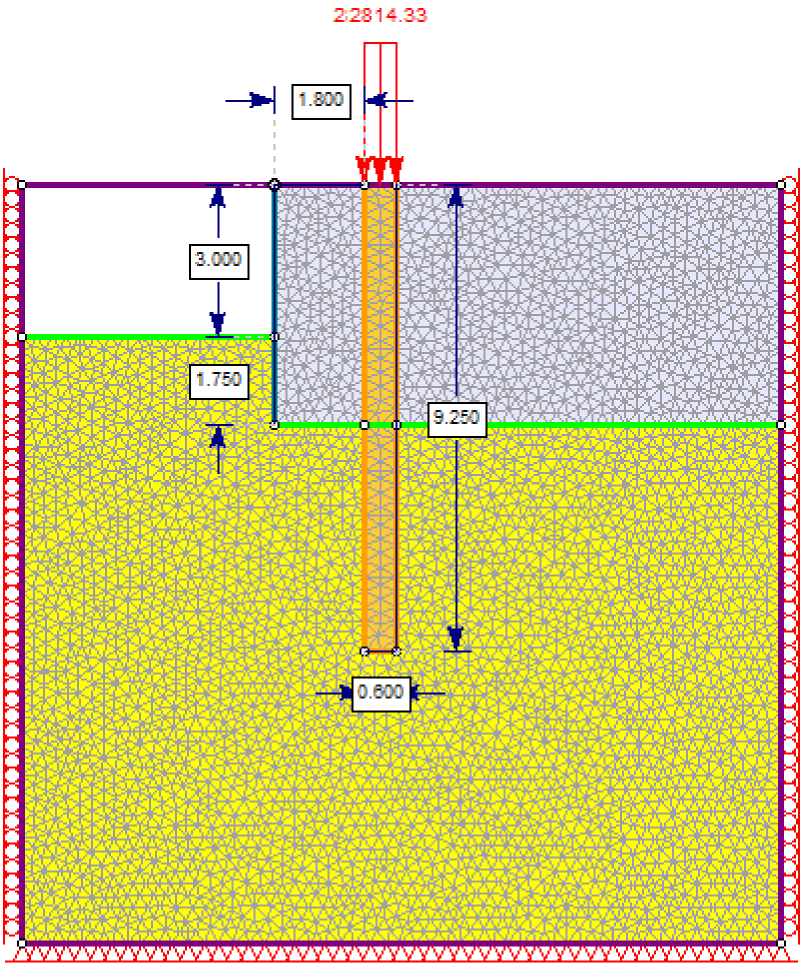

M 63.1: Original model (stage 3)

C_1'	ϕ_1'	γ_1	E_1	C_2'	ϕ_2'	γ_2	E_2	H_1	H_2	H_3	E_3	D_1	D_2	L	Qult
0	29	21	226	37	25	20	44.0	3.00	1.75	0.75	862776	1.8	0.6	9.25	2814.33

M 63.2: Parameter values

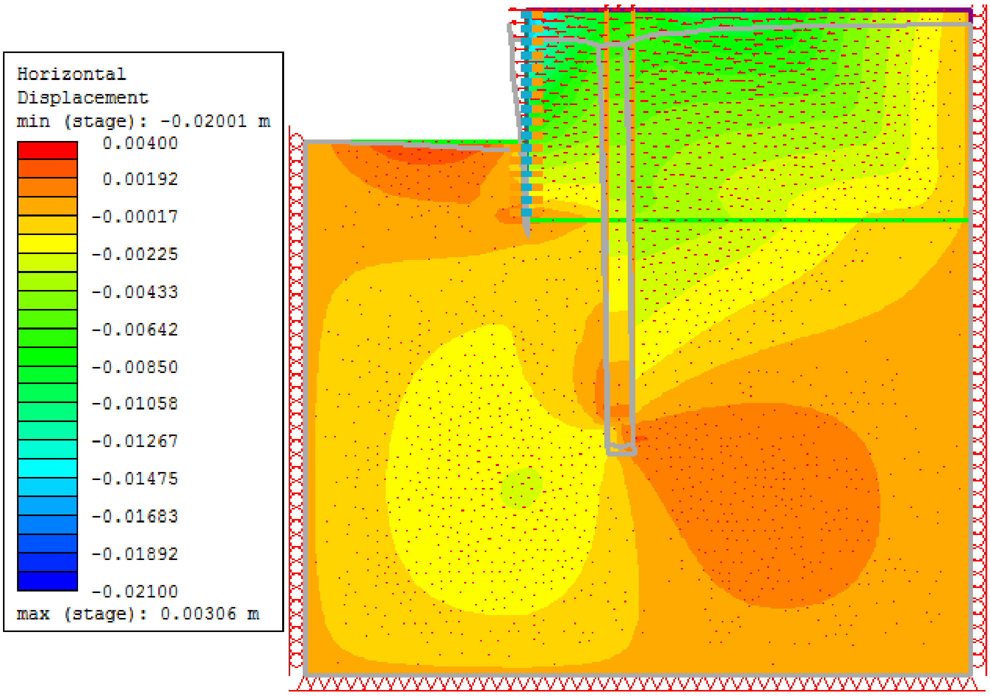

M 63.3: Deformed model (stage 3)

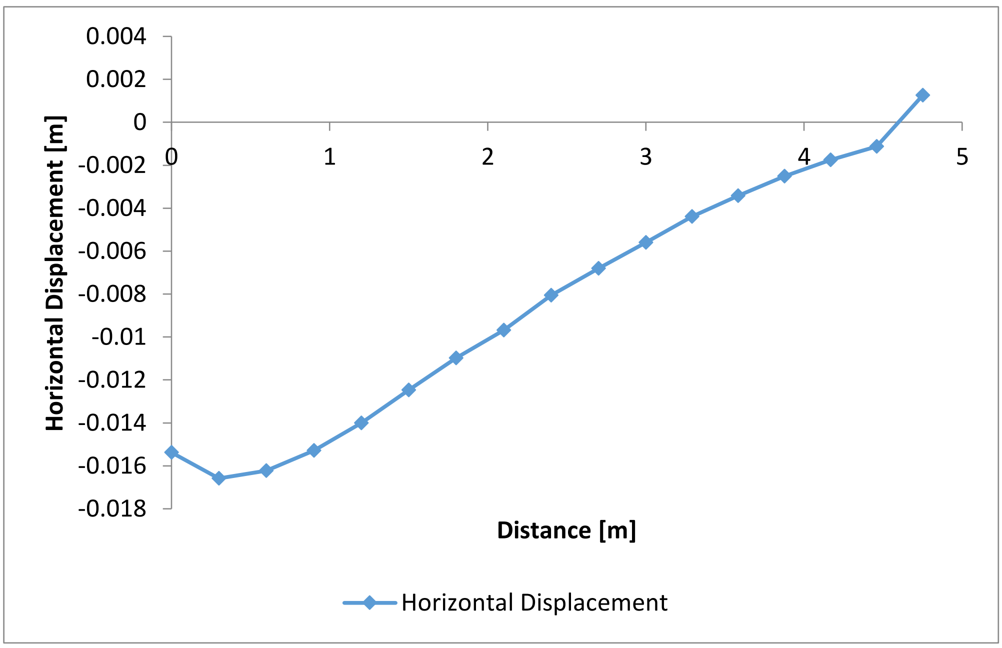

M 63.4: Horizontal displacement of soil along retaining wall

Retaining wall maximum horizontal displacement: -0.02001m

Distance from point of maximum displacement in retaining wall to the top of backfill soil: 0.0m

Model 64:

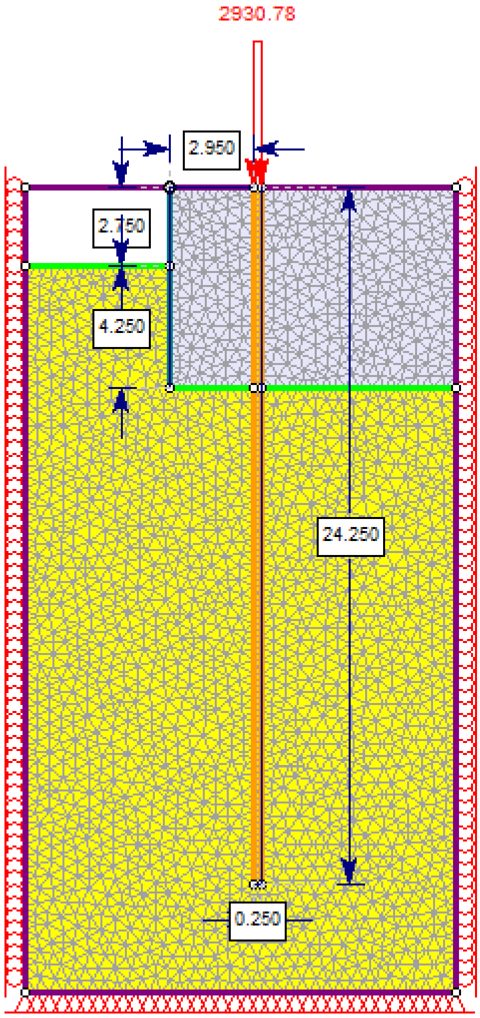

M 64.1: Original model (stage 3)

C'_1	ϕ'_1	γ_1	E_1	C'_2	ϕ'_2	γ_2	E_2	H_1	H_2	H_3	E_3	D_1	D_2	L	Qult
0	35	20	130	17	12	24	2.0	2.75	4.25	0.5	968168	2.95	0.25	24.25	2930.78

M 64.2: Parameter values

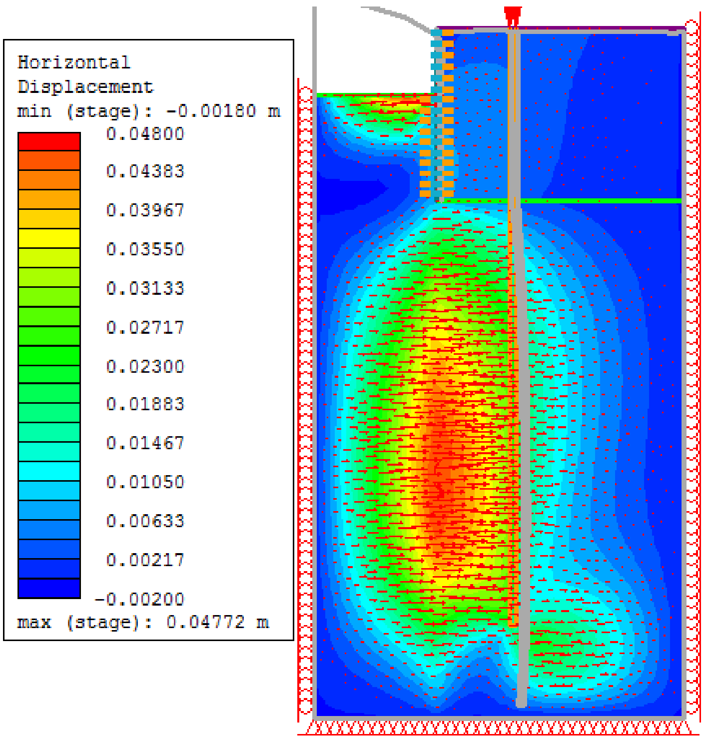

M 64.3: Deformed model (stage 3)

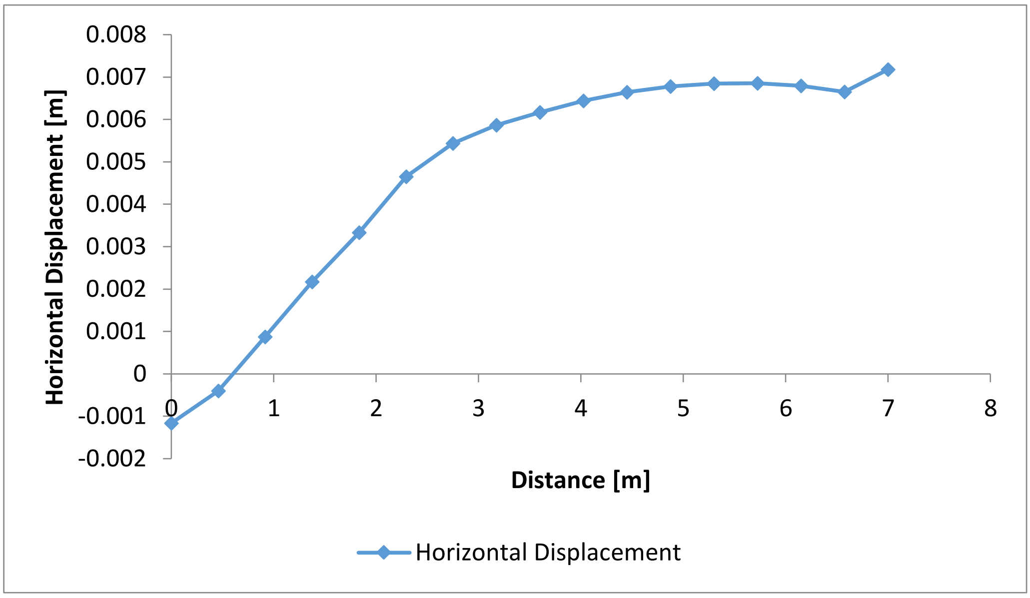

M 64.4: Horizontal displacement of soil along retaining wall

Retaining wall maximum horizontal displacement: 0.00718m

Distance from point of maximum displacement in retaining wall to the top of backfill soil: 7.0m

Model 65:

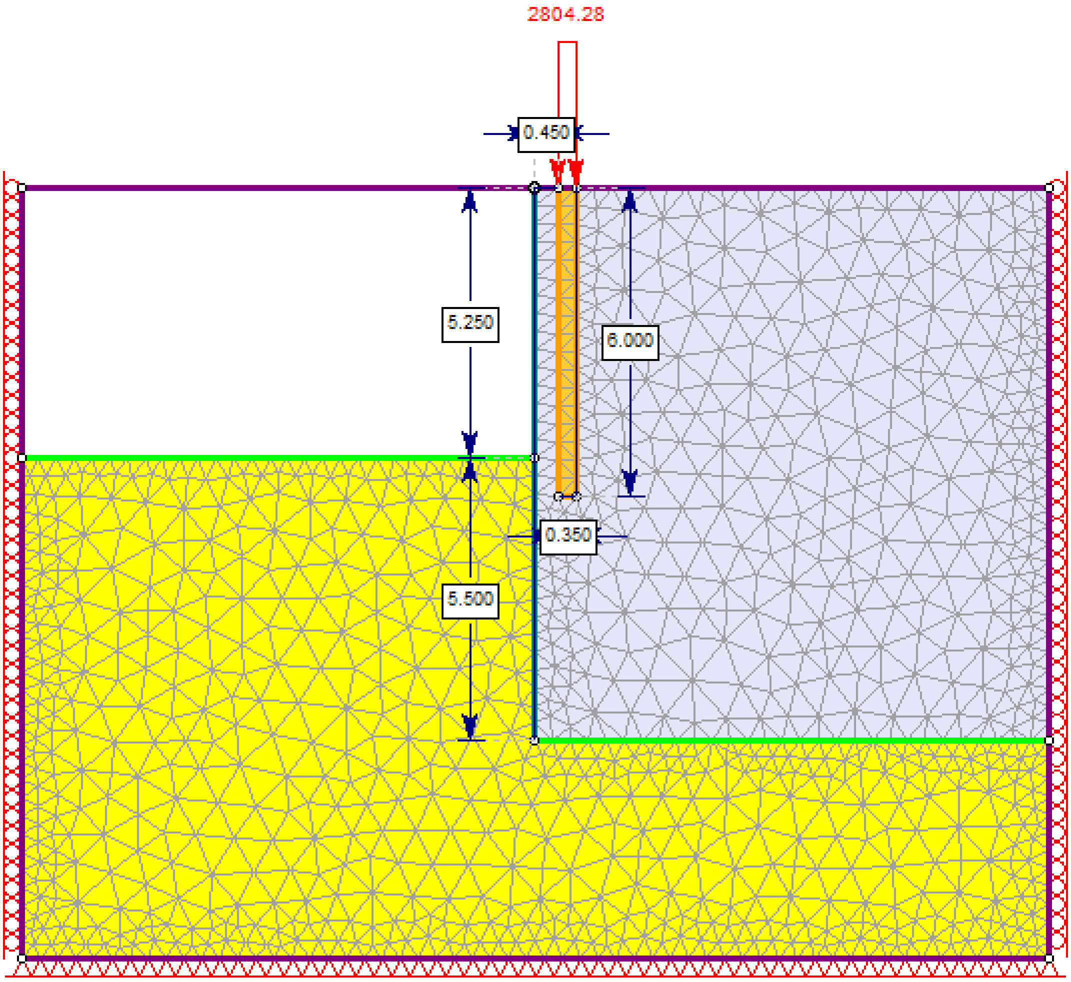

M 65.1: Original model (stage 3)

C_1'	ϕ_1'	γ_1	E_1	C_2'	ϕ_2'	γ_2	E_2	H_1	H_2	H_3	E_3	D_1	D_2	L	Qult
0	37	19	132	34	37	16	5.3	5.25	5.5	0.75	896126	0.45	0.35	6	2804.28

M 65.2: Parameter values

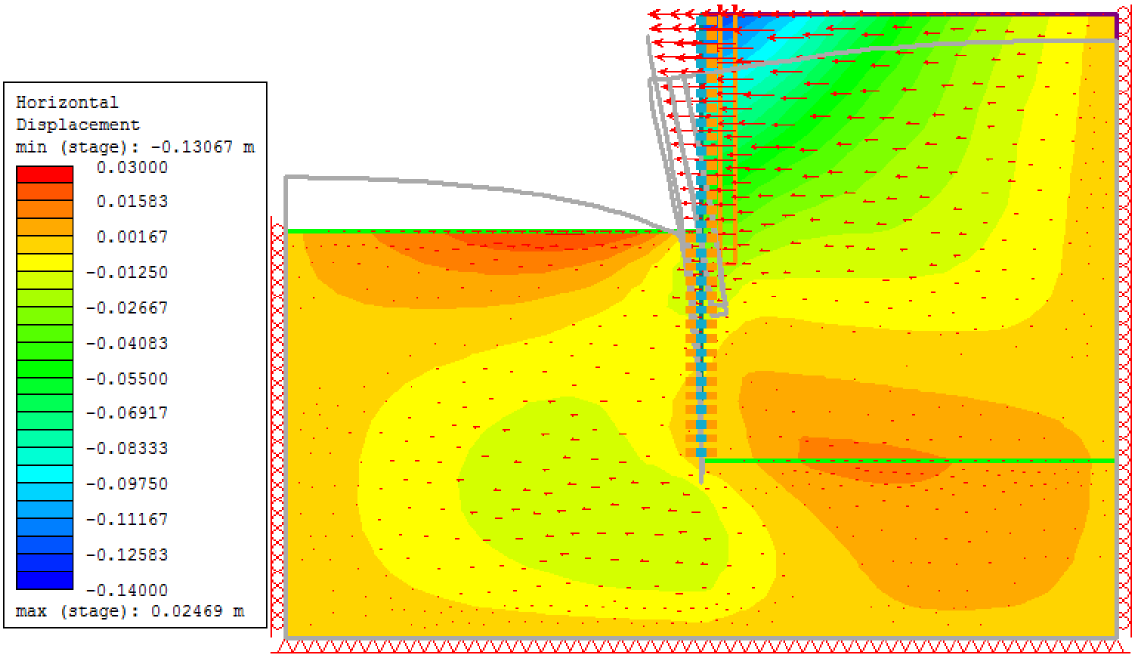

M 65.3: Deformed model (stage 3)

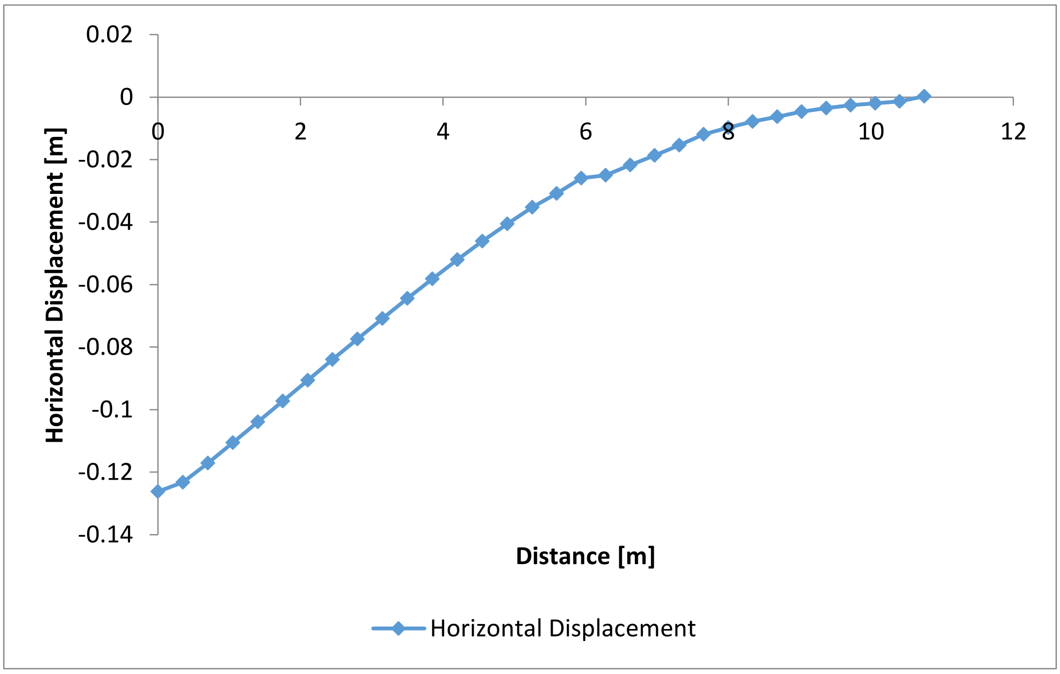

M 65.4: Horizontal displacement of soil along retaining wall

Retaining wall maximum horizontal displacement: -0.13067m

Distance from point of maximum displacement in retaining wall to the top of backfill soil: 0.0m

Model 66:

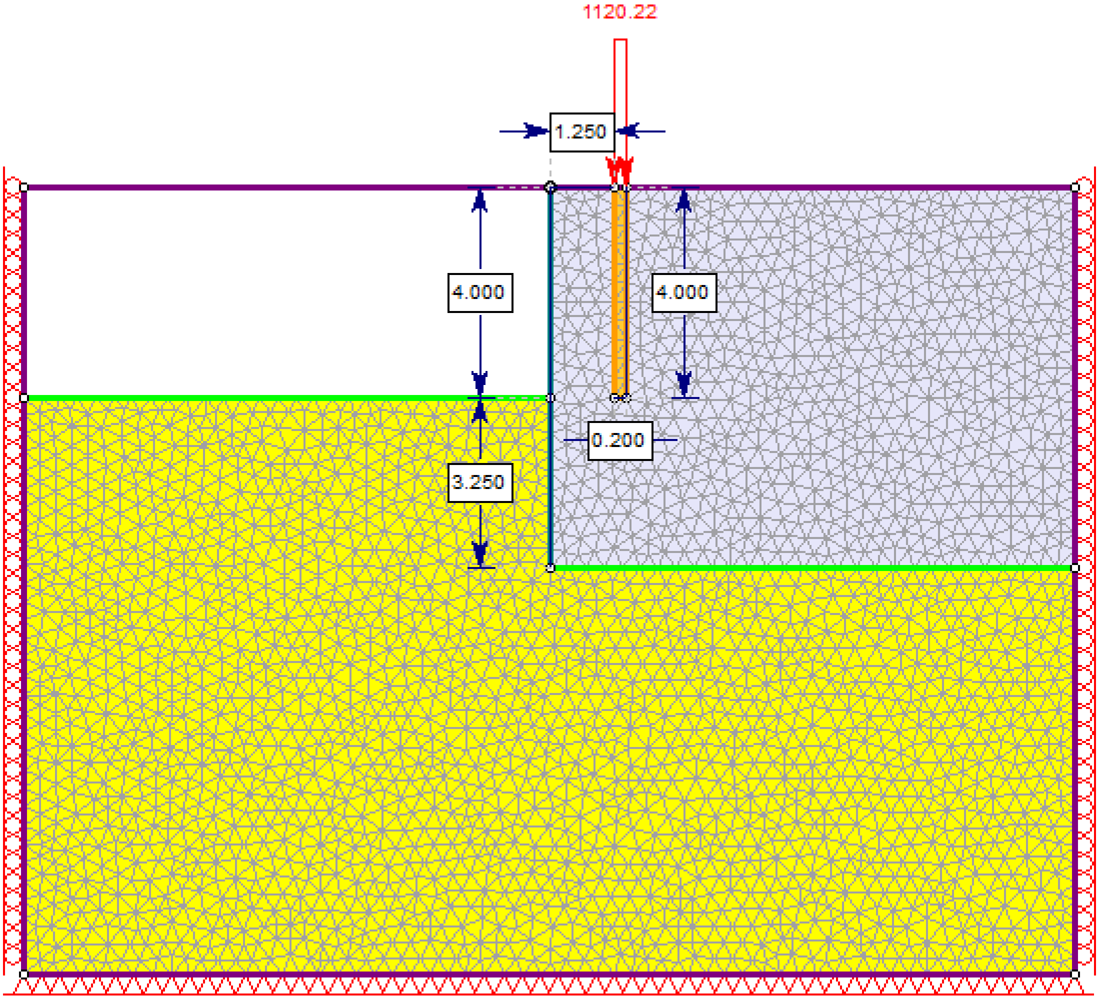

M 66.1: Original model (stage 3)

C'_1	ϕ'_1	γ_1	E_1	C'_2	ϕ'_2	γ_2	E_2	H_1	H_2	H_3	E_3	D_1	D_2	L	Qult
0	31	21	189	33	35	17	4.1	4.00	3.25	1	914332	1.25	0.2	4	1120.22

M 66.2: Parameter values

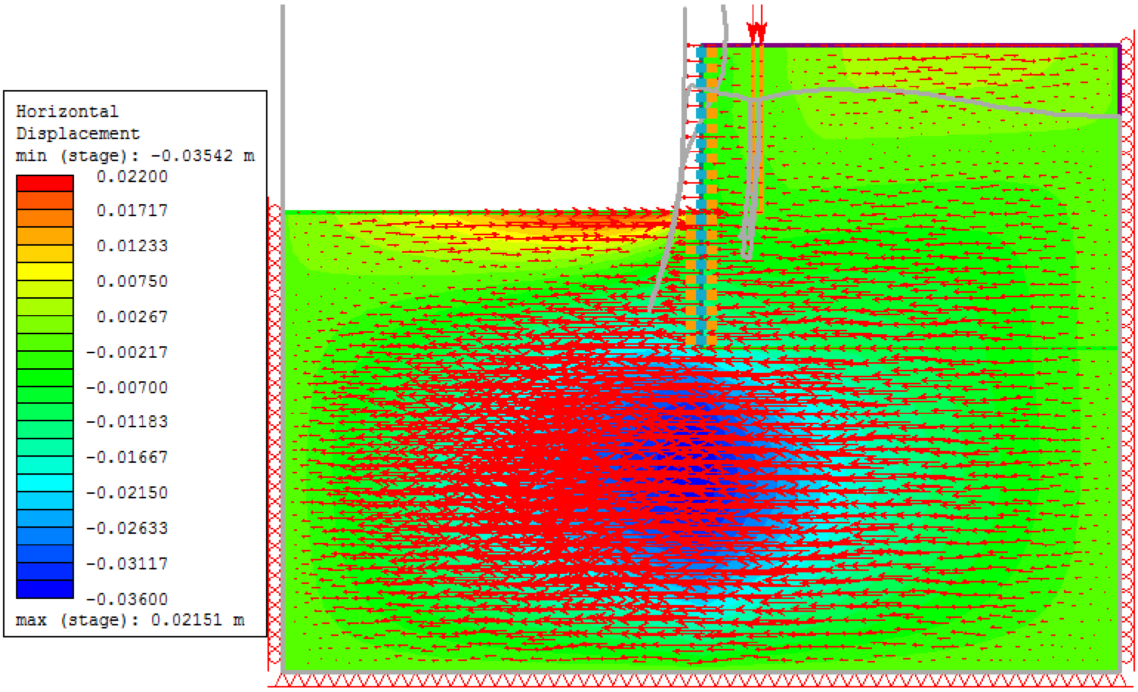

M 66.3: Deformed model (stage 3)

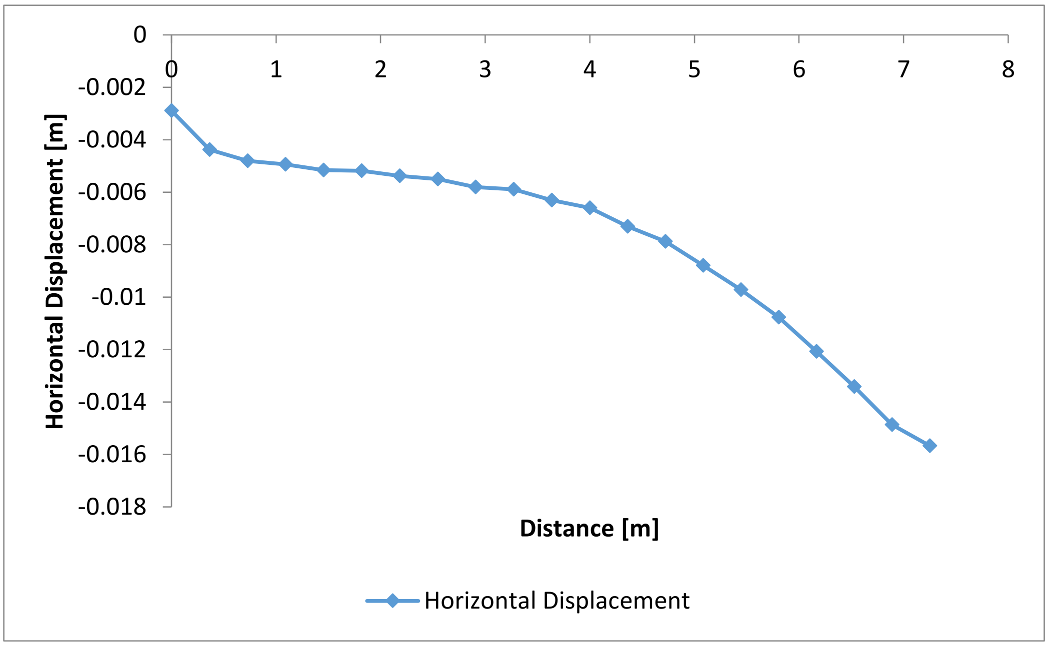

M 66.4: Horizontal displacement of soil along retaining wall

Retaining wall maximum horizontal displacement: -0.015667m

Distance from point of maximum displacement in retaining wall to the top of backfill soil: 7.25m

Model 67:

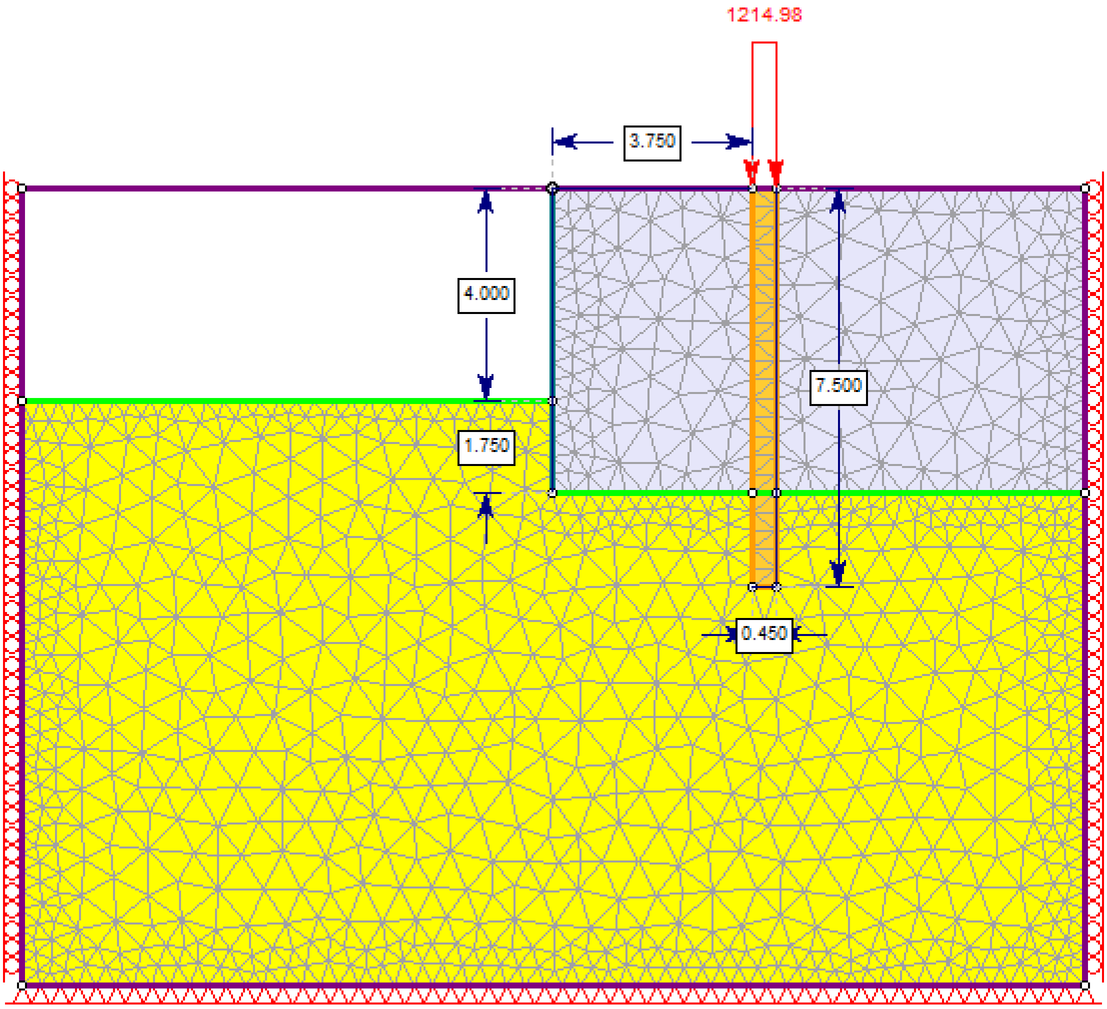

M 67.1: Original model (stage 3)

C_1'	ϕ_1'	γ_1	E_1	C_2'	ϕ_2'	γ_2	E_2	H_1	H_2	H_3	E_3	D_1	D_2	L	Qult
0	30	21	198	59	16	17	47.4	4.00	1.75	1.5	721011	3.75	0.45	7.5	1214.98

M 67.2: Parameter values

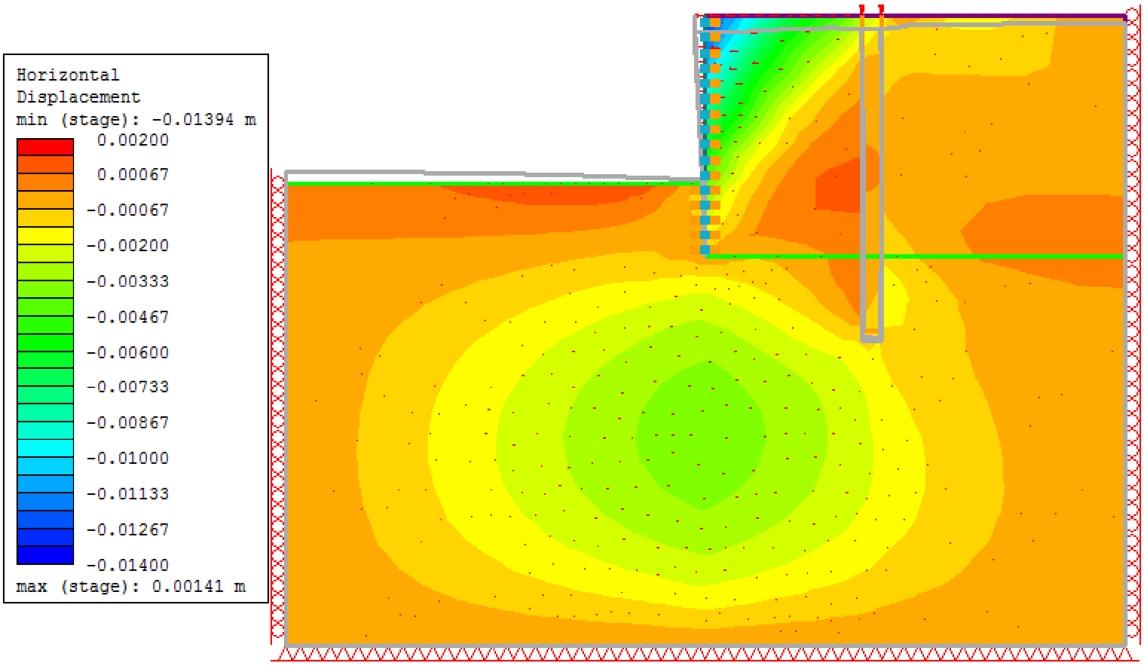

M 67.3: Deformed model (stage 3)

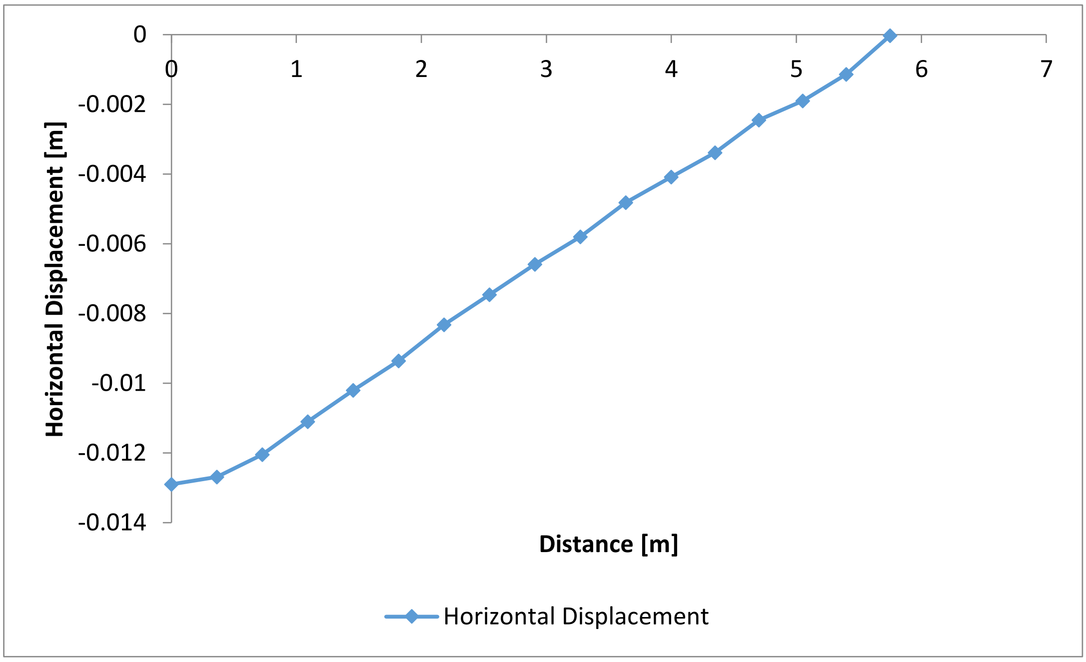

M 67.4: Horizontal displacement of soil along retaining wall

Retaining wall maximum horizontal displacement: -0.01394m

Distance from point of maximum displacement in retaining wall to the top of backfill soil: 0.0m

Model 68:

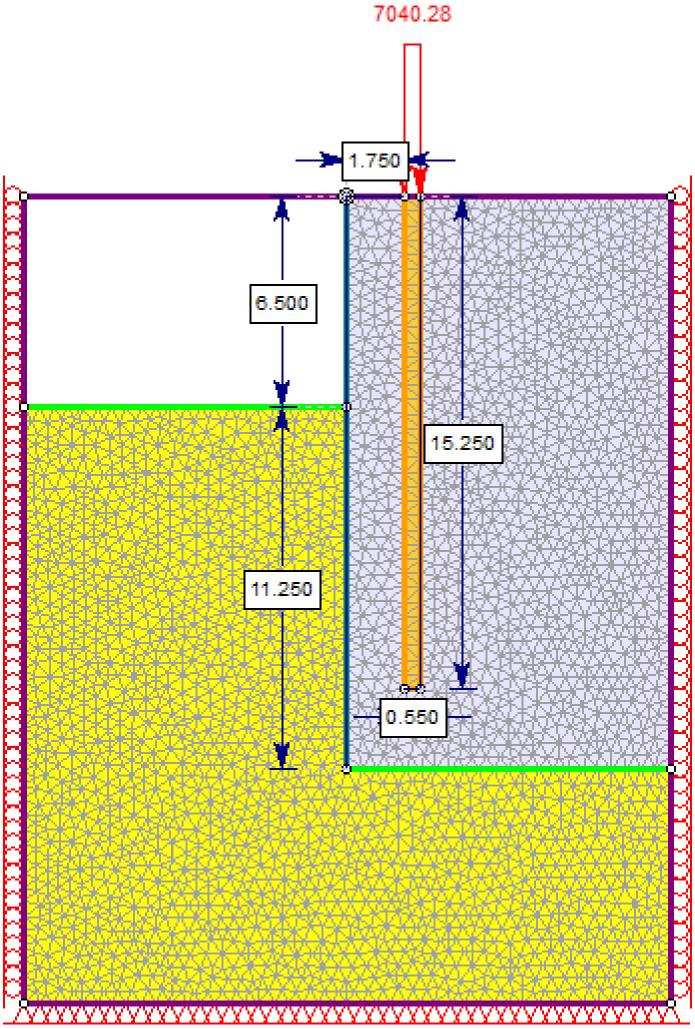

M 68.1: Original model (stage 3)

C_1'	ϕ_1'	γ_1	E_1	C_2'	ϕ_2'	γ_2	E_2	H_1	H_2	H_3	E_3	D_1	D_2	L	Qult
0	40	21	112	38	28	18	24.7	6.50	11.25	0.75	978517	1.75	0.55	15.25	7040.28

M 68.2: Parameter values

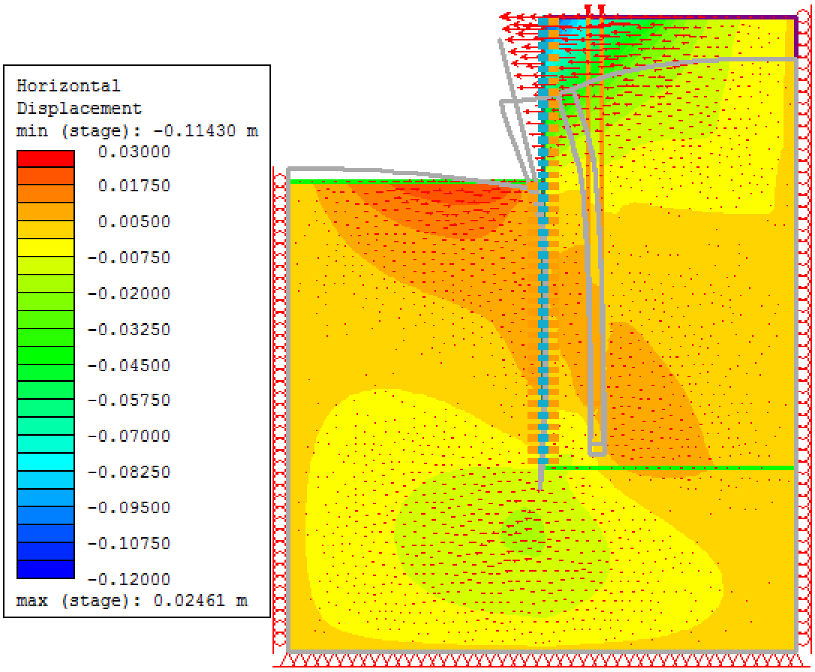

M 68.3: Deformed model (stage 3)

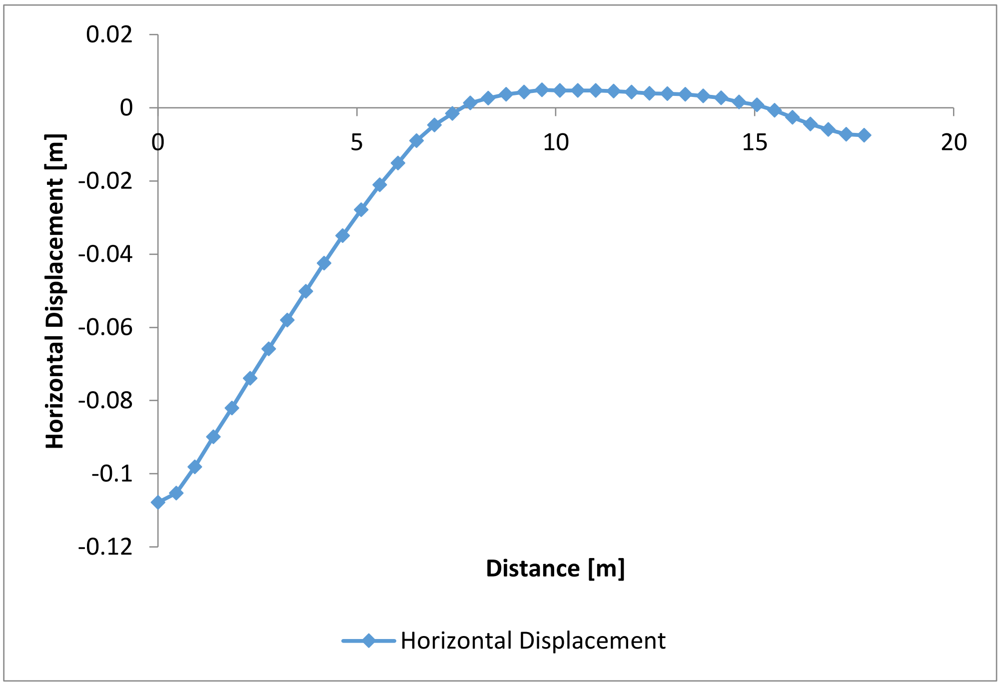

M 68.4: Horizontal displacement of soil along retaining wall

Retaining wall maximum horizontal displacement: -0.1143m

Distance from point of maximum displacement in retaining wall to the top of backfill soil: 0.0m

Model 69:

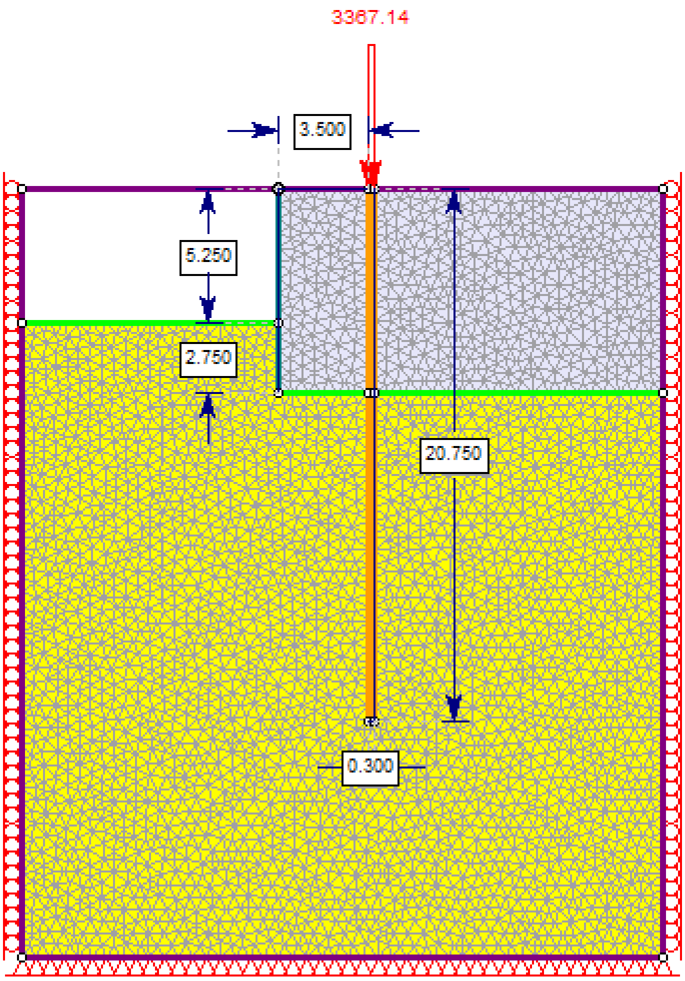

M 69.1: Original model (stage 3)

C_1'	ϕ_1'	γ_1	E_1	C_2'	ϕ_2'	γ_2	E_2	H_1	H_2	H_3	E_3	D_1	D_2	L	Qult
0	43	22	178	47	18	17	11.6	5.25	2.75	0.75	934799	3.5	0.3	20.75	3367.14

M 69.2: Parameter values

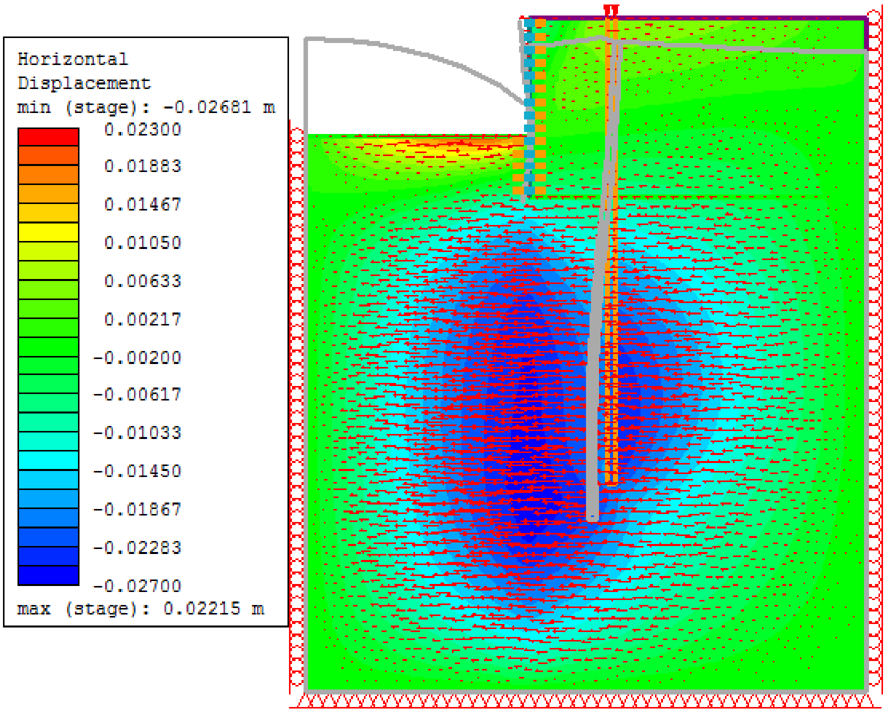

M 69.3: Deformed model (stage 3)

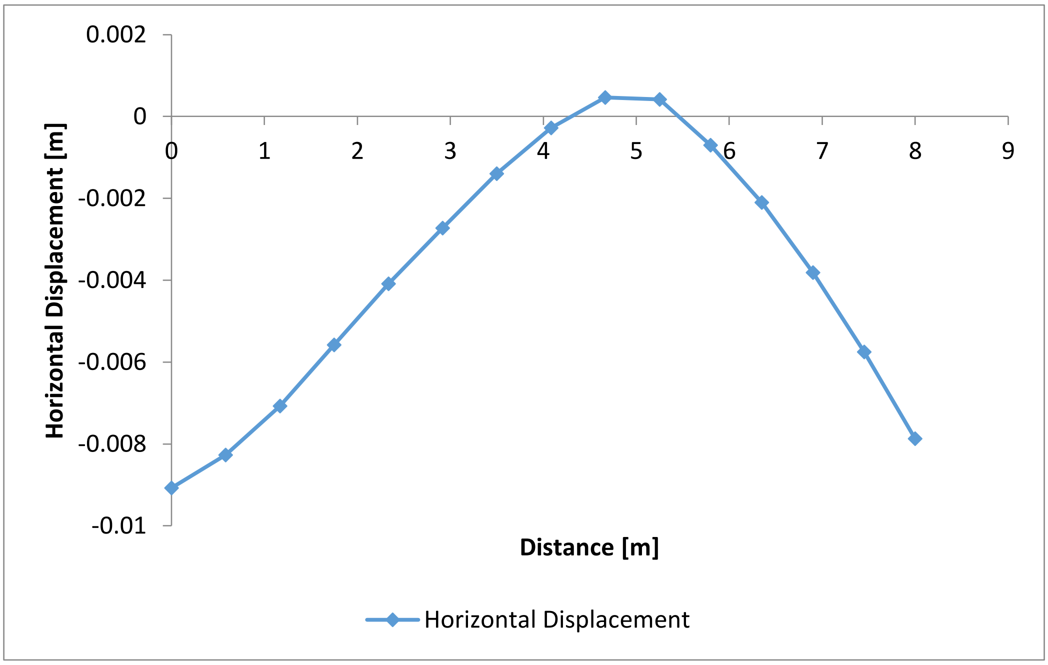

M 69.5: Horizontal displacement of soil along retaining wall

Retaining wall maximum horizontal displacement: -0.02681m

Distance from point of maximum displacement in retaining wall to the top of backfill soil: 0.0m

Model 70:

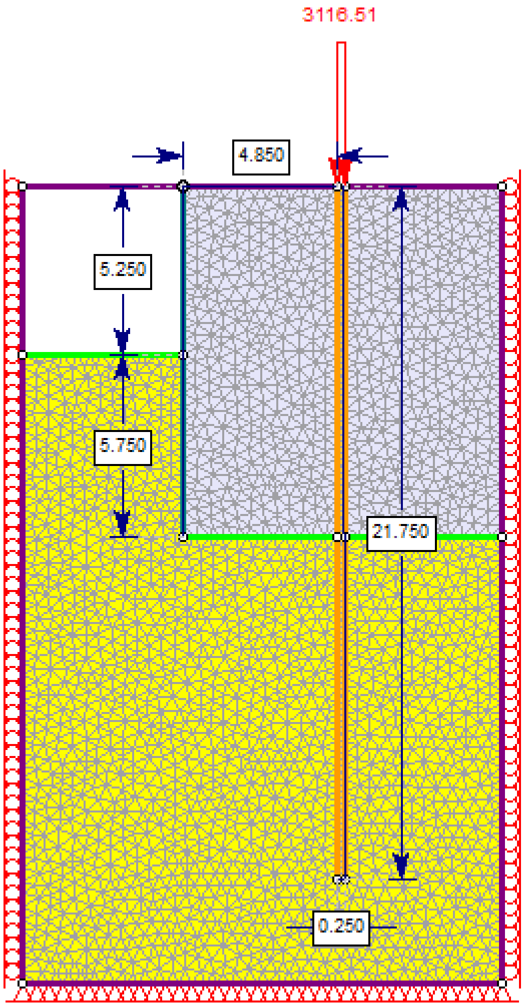

M 70.1: Original model (stage 3)

C_1'	ϕ_1'	γ_1	E_1	C_2'	ϕ_2'	γ_2	E_2	H_1	H_2	H_3	E_3	D_1	D_2	L	Qult
0	34	20	70	35	14	18	49.0	5.25	5.75	0.75	759730	4.85	0.25	21.75	3116.51

M 70.2: Parameter values

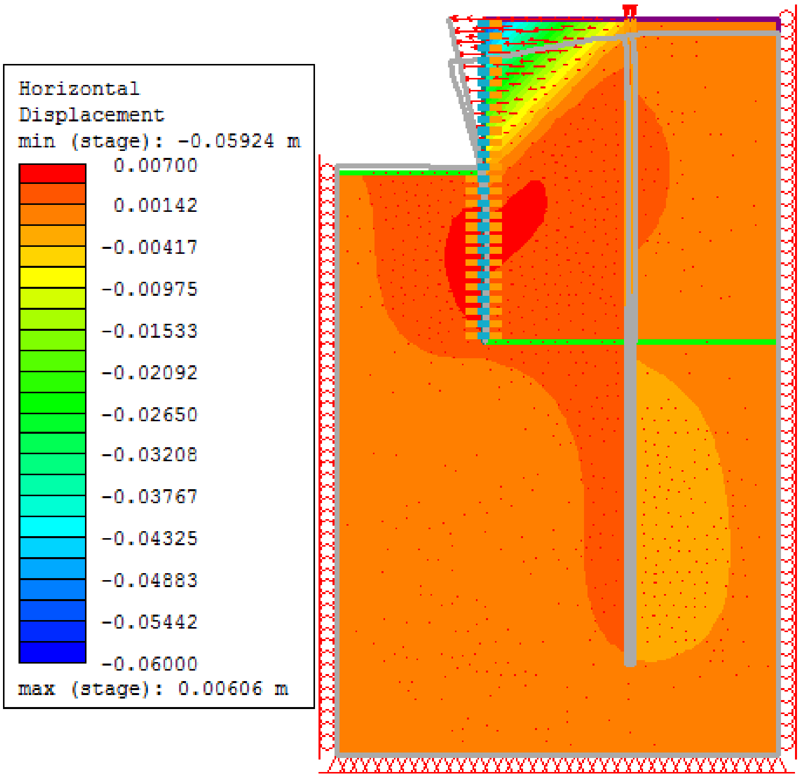

M 70.3: Deformed model (stage 3)

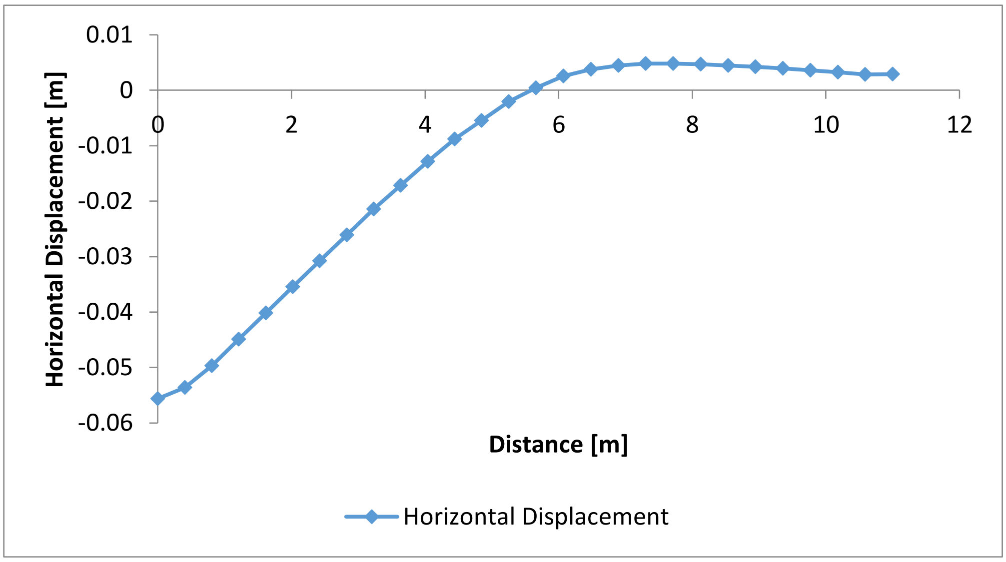

M 70.4: Horizontal displacement of soil along retaining wall

Retaining wall maximum horizontal displacement: -0.05924m

Distance from point of maximum displacement in retaining wall to the top of backfill soil: 0.0m

Model 71:

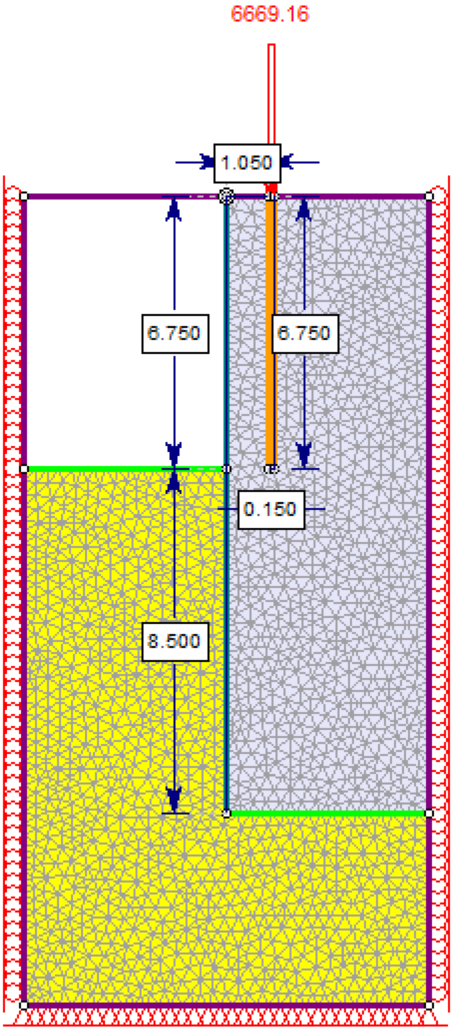

M 71.1: Original model (stage 3)

C_1'	ϕ_1'	γ_1	E_1	C_2'	ϕ_2'	γ_2	E_2	H_1	H_2	H_3	E_3	D_1	D_2	L	Qult
0	41	19	248	38	17	21	6.1	6.75	9	0.75	1017867	1.05	0.15	6.75	6669.16

M 71.2: Parameter values

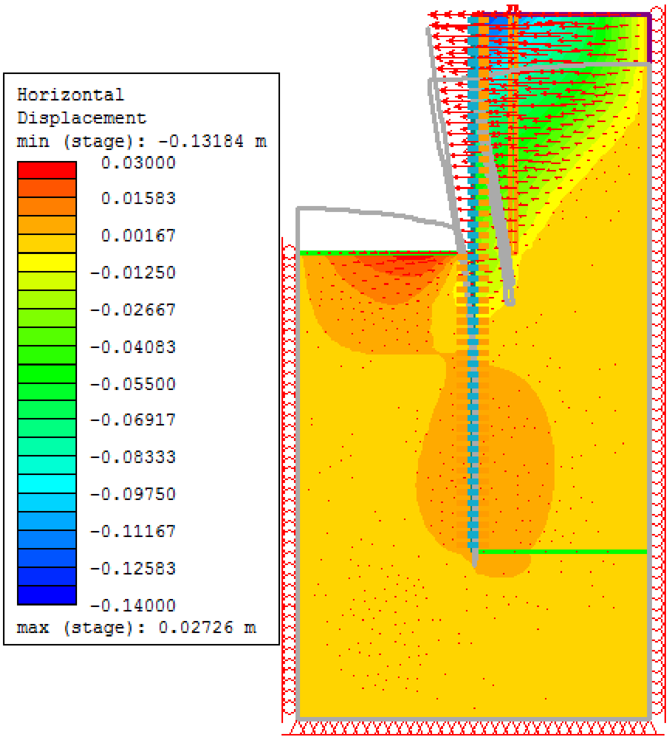

M 71.3: Deformed model (stage 3)

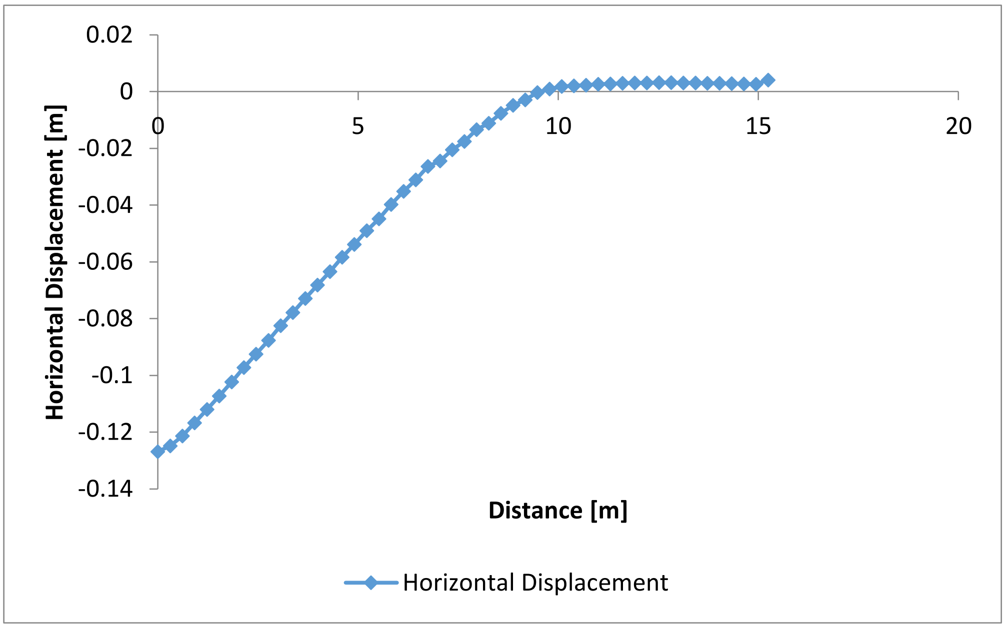

M 71.4: Horizontal displacement of soil along retaining wall

Retaining wall maximum horizontal displacement: -0.13184m

Distance from point of maximum displacement in retaining wall to the top of backfill soil: 0.0m

Model 72:

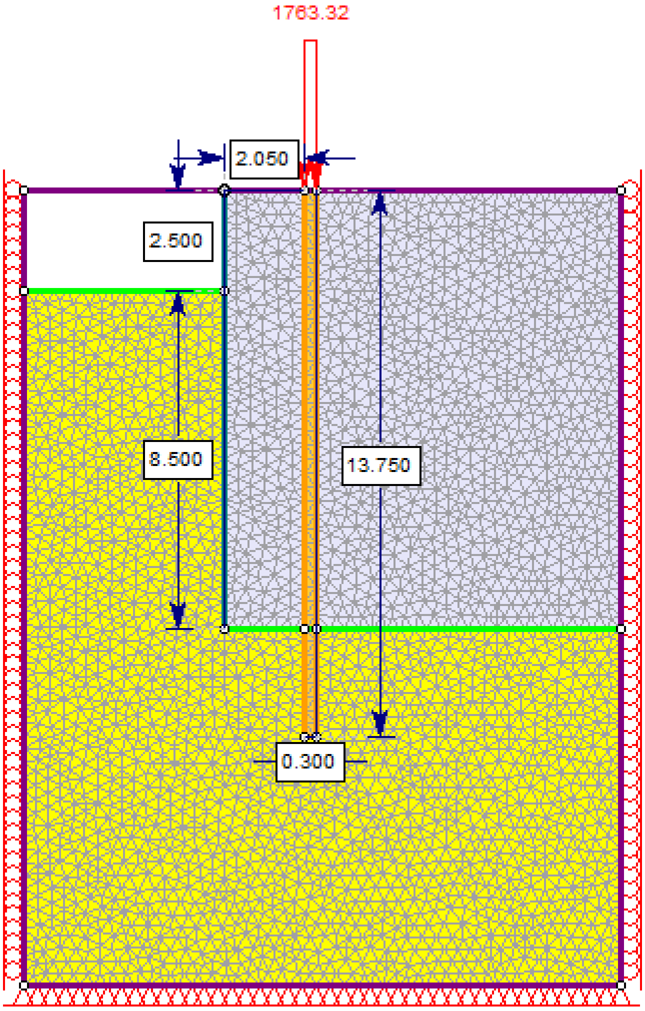

M 72.1: Original model (stage 3)

C'_1	ϕ'_1	γ_1	E_1	C'_2	ϕ'_2	γ_2	E_2	H_1	H_2	H_3	E_3	D_1	D_2	L	Qult
0	36	20	20	14	7	18	20.2	2.50	8.5	0.5	1131896	2.05	0.3	13.75	4142.59

M 72.2: Parameter values

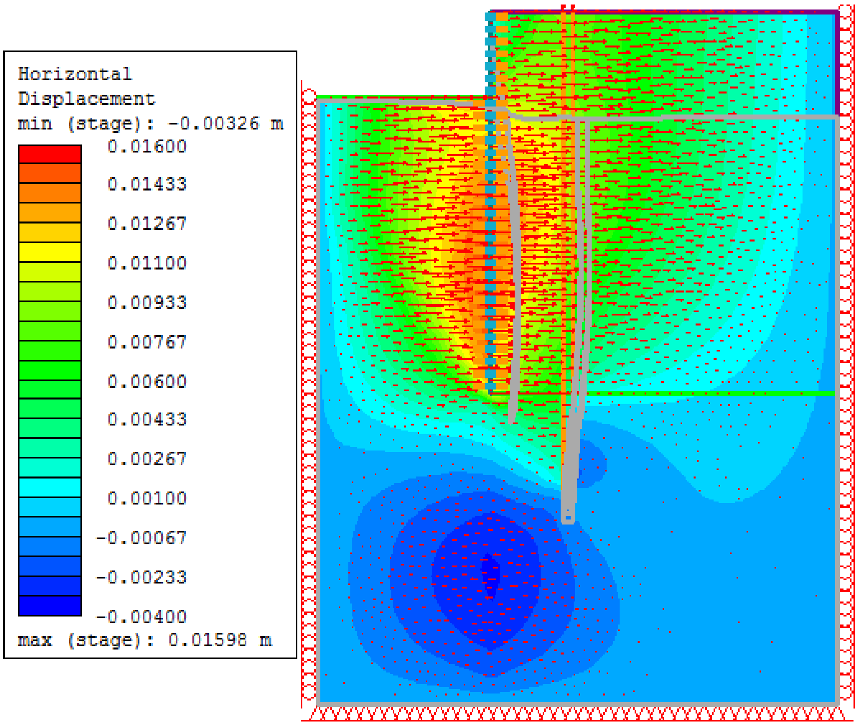

M 72.3: Deformed model (stage 3)

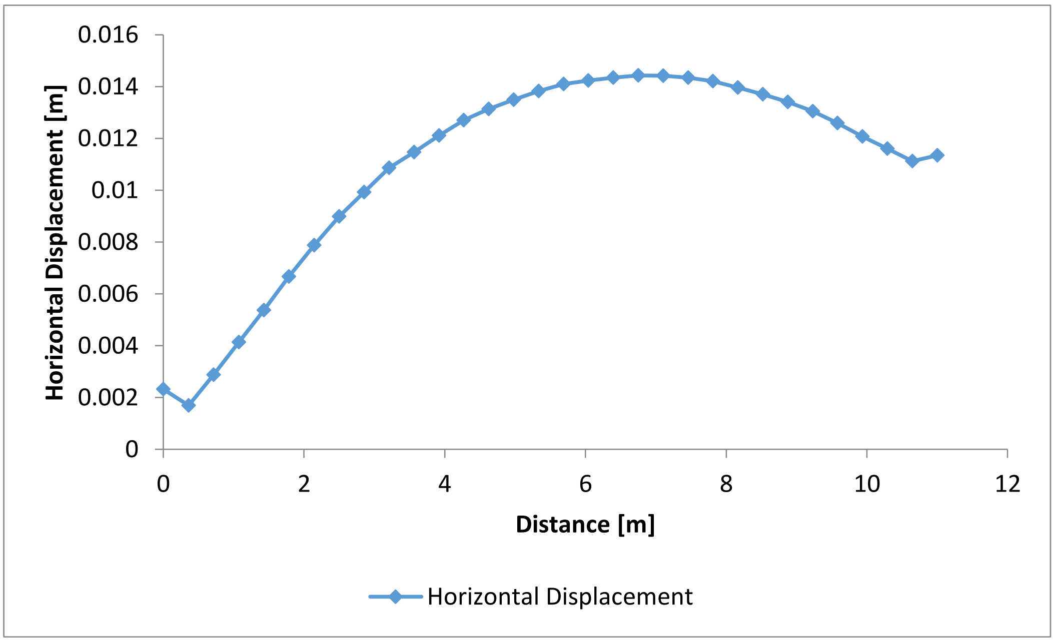

M 72.4: Horizontal displacement of soil along retaining wall

Retaining wall maximum horizontal displacement: 0.01443m

Distance from point of maximum displacement in retaining wall to the top of backfill soil: 6.75m

Model 73:

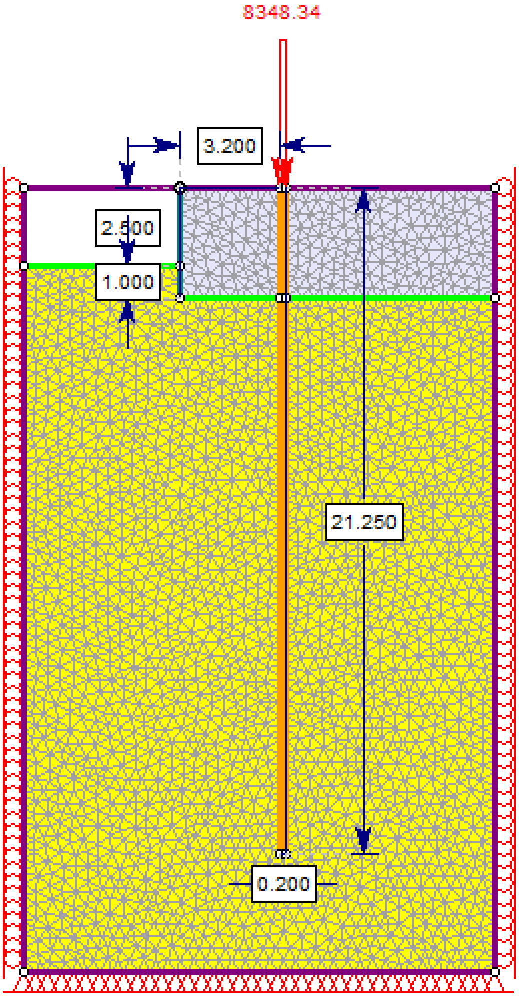

M 73.1: Original model (stage 3)

C_1'	ϕ_1'	γ_1	E_1	C_2'	ϕ_2'	γ_2	E_2	H_1	H_2	H_3	E_3	D_1	D_2	L	Qult
0	38	18	109	31	26	25	35.0	2.50	1	1.5	924199	3.2	0.2	21.25	8348.34

M 73.2: Parameter values

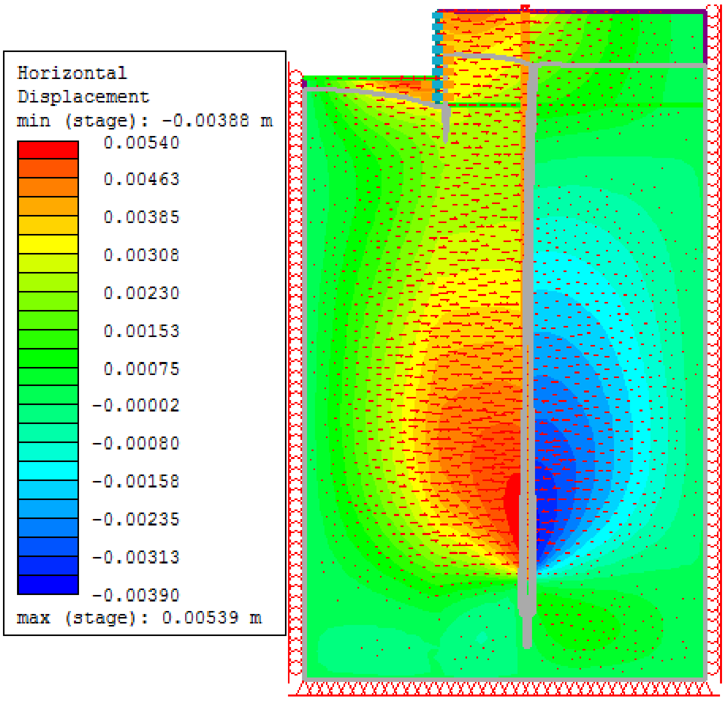

M 73.3: Deformed model (stage 3)

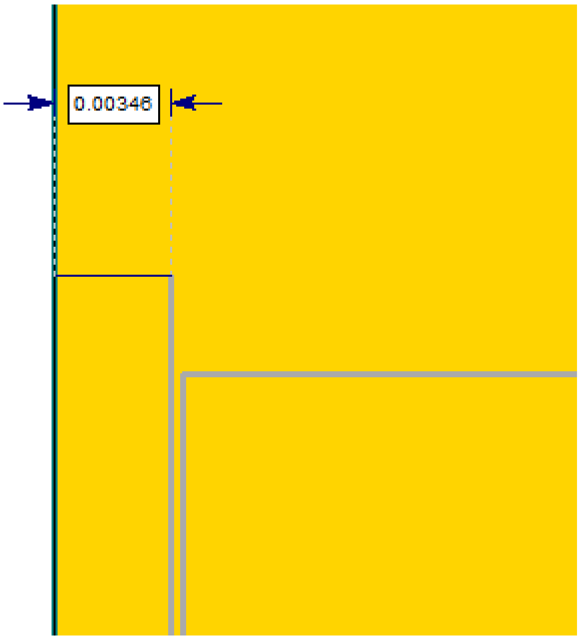

M 73.4: Detailed view of cross-section of retaining wall and soil (stage 3)

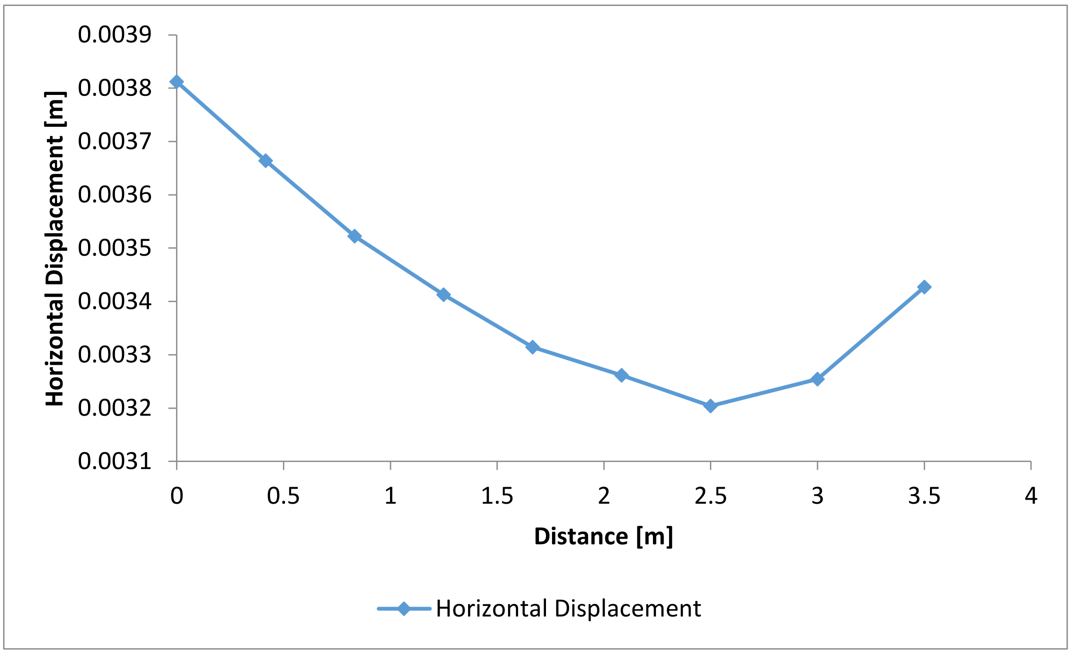

M 73.5: Horizontal displacement of soil along retaining wall

Retaining wall maximum horizontal displacement: 0.00346m

Distance from point of maximum displacement in retaining wall to the top of backfill soil: 0.0m

Model 74:

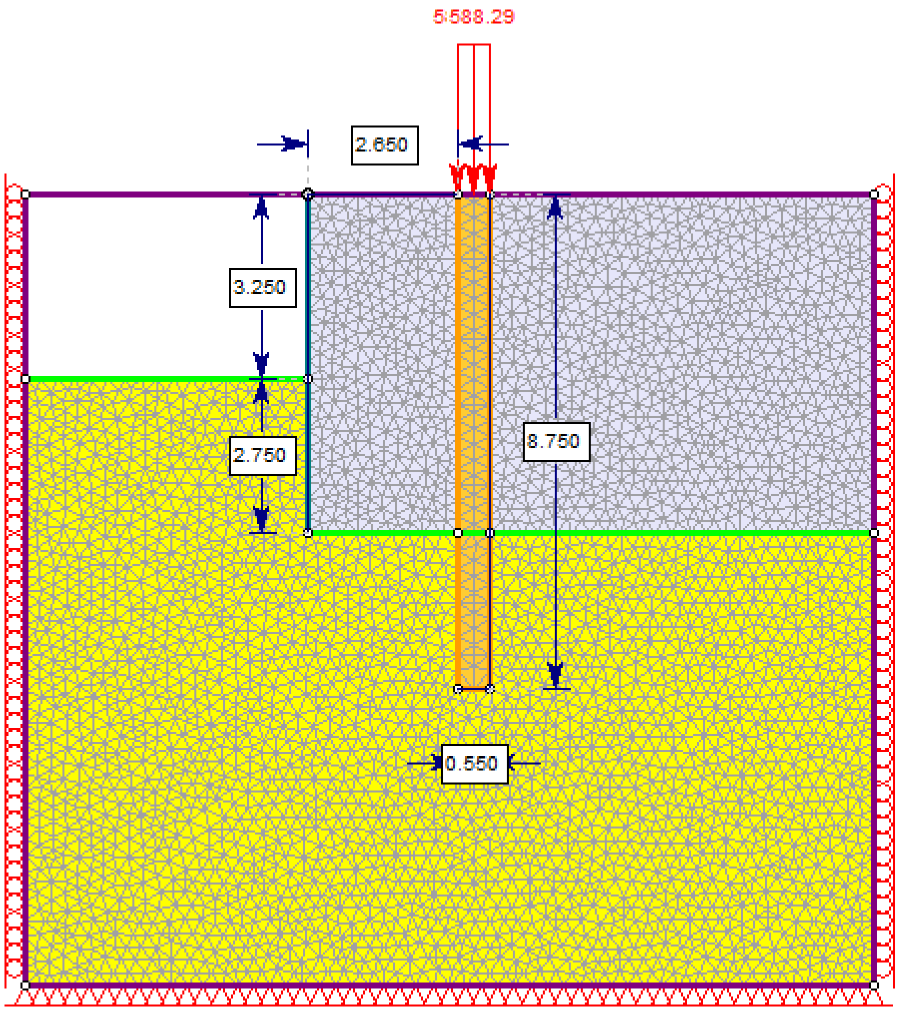

M 74.1: Original model (stage 3)

C_1'	ϕ_1'	γ_1	E_1	C_2'	ϕ_2'	γ_2	E_2	H_1	H_2	H_3	E_3	D_1	D_2	L	Qult
0	33	20	171	26	5	17	14.2	3.25	2.75	0.75	802922	2.65	0.55	9.25	588.29

M 74.2: Parameter values

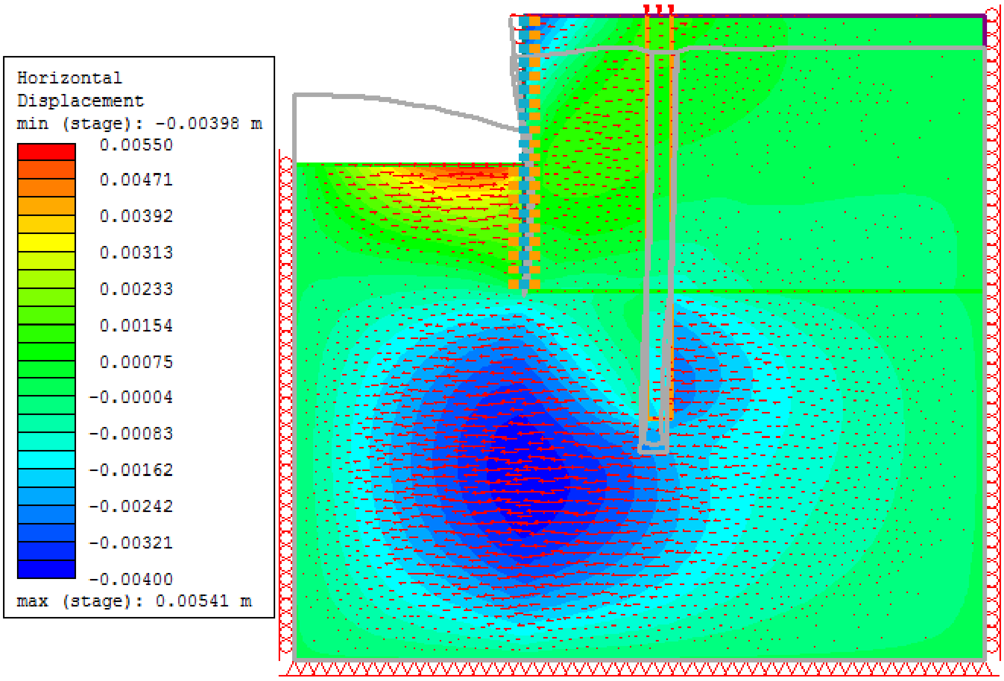

M 74.3: Deformed model (stage 3)

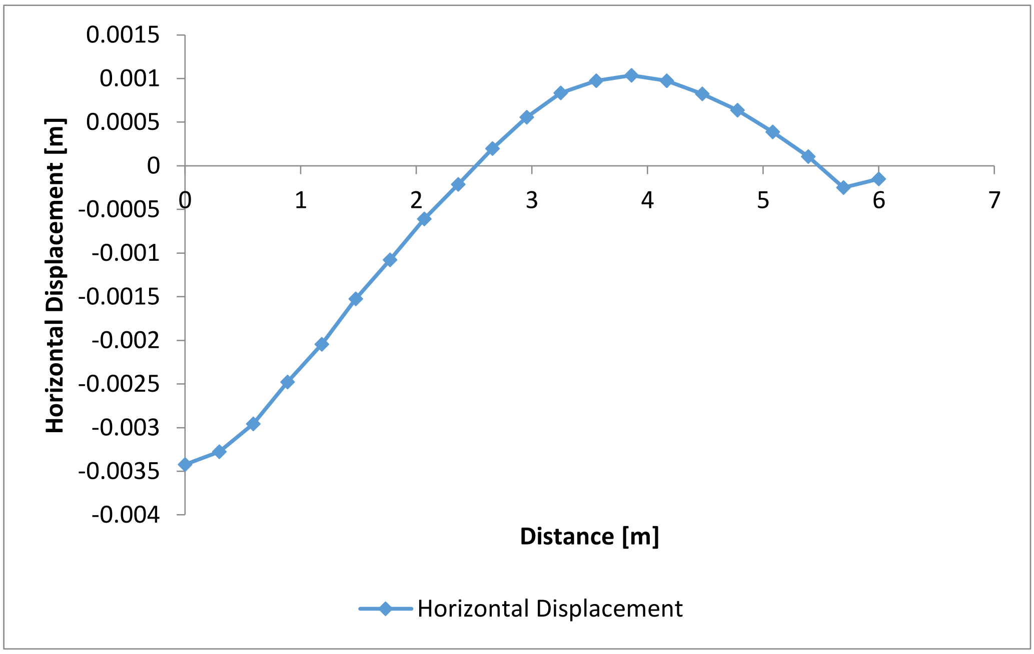

M 74.4: Horizontal displacement of soil along retaining wall

Retaining wall maximum horizontal displacement: -0.00398m

Distance from point of maximum displacement in retaining wall to the top of backfill soil: 0.0m

Model 75:

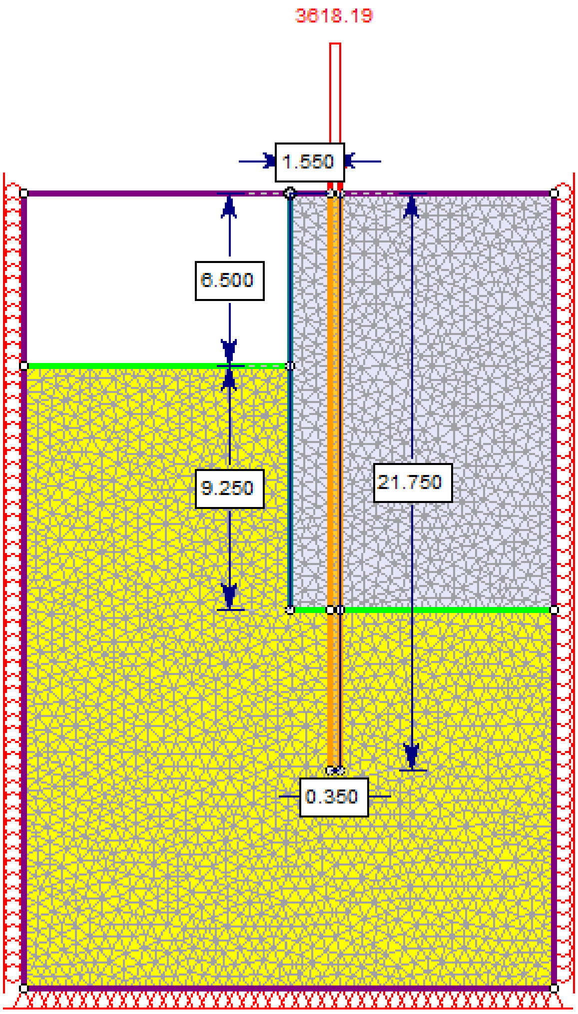

M 75.1: Original model (stage 3)

C_1'	ϕ_1'	γ_1	E_1	C_2'	ϕ_2'	γ_2	E_2	H_1	H_2	H_3	E_3	D_1	D_2	L	Qult
0	39	18	116	35	15	21	14.0	6.50	9.25	0.75	962361	1.55	0.35	21.75	3618.19

M 75.2: Parameter values

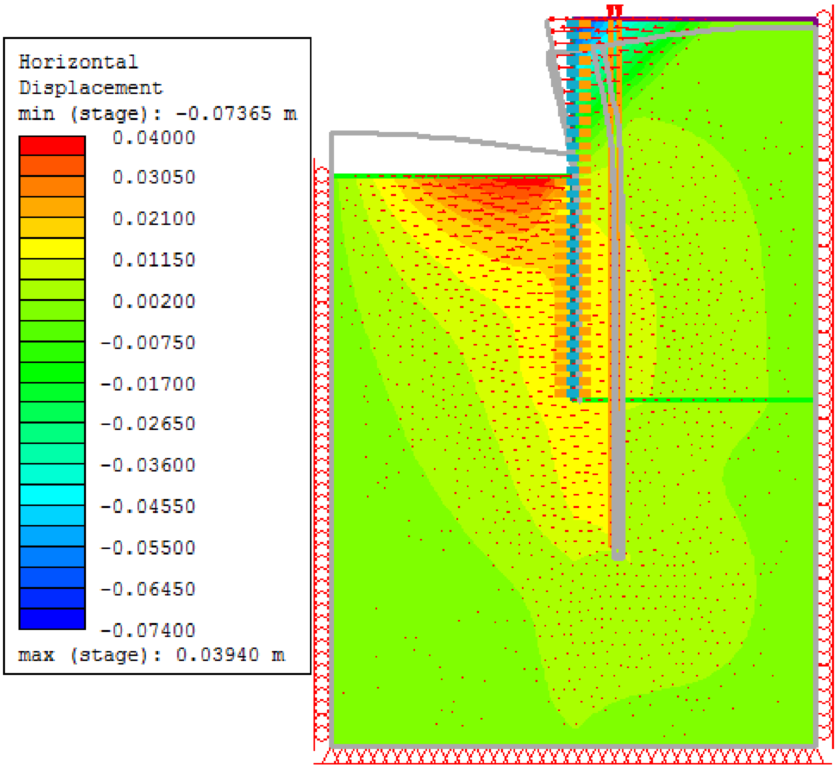

M 75.3: Deformed model (stage 3)

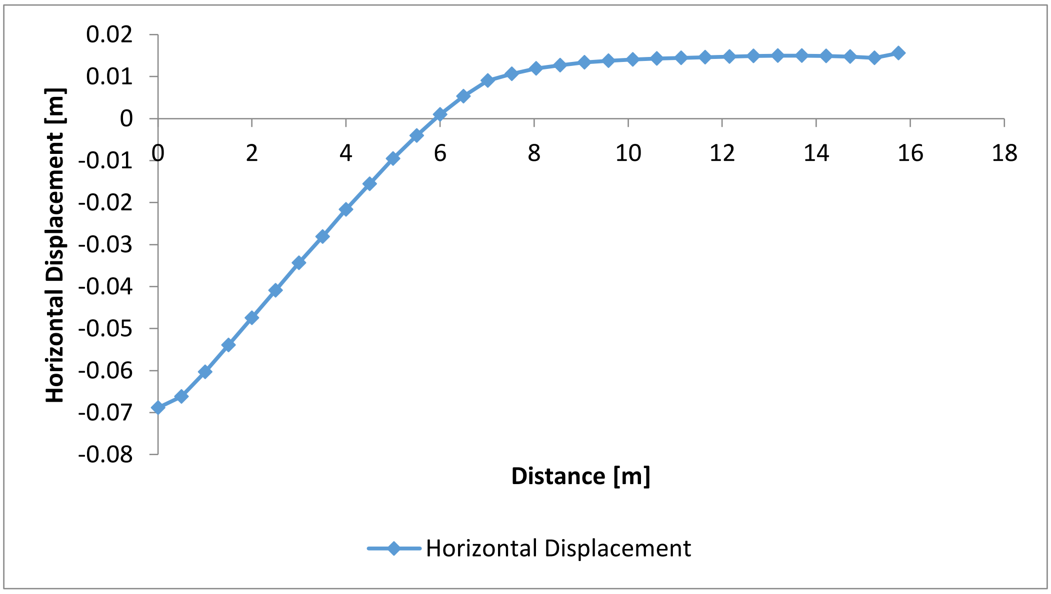

M 75.4: Horizontal displacement of soil along retaining wall

Retaining wall maximum horizontal displacement: -0.07365m

Distance from point of maximum displacement in retaining wall to the top of backfill soil: 0.0m

Model 76:

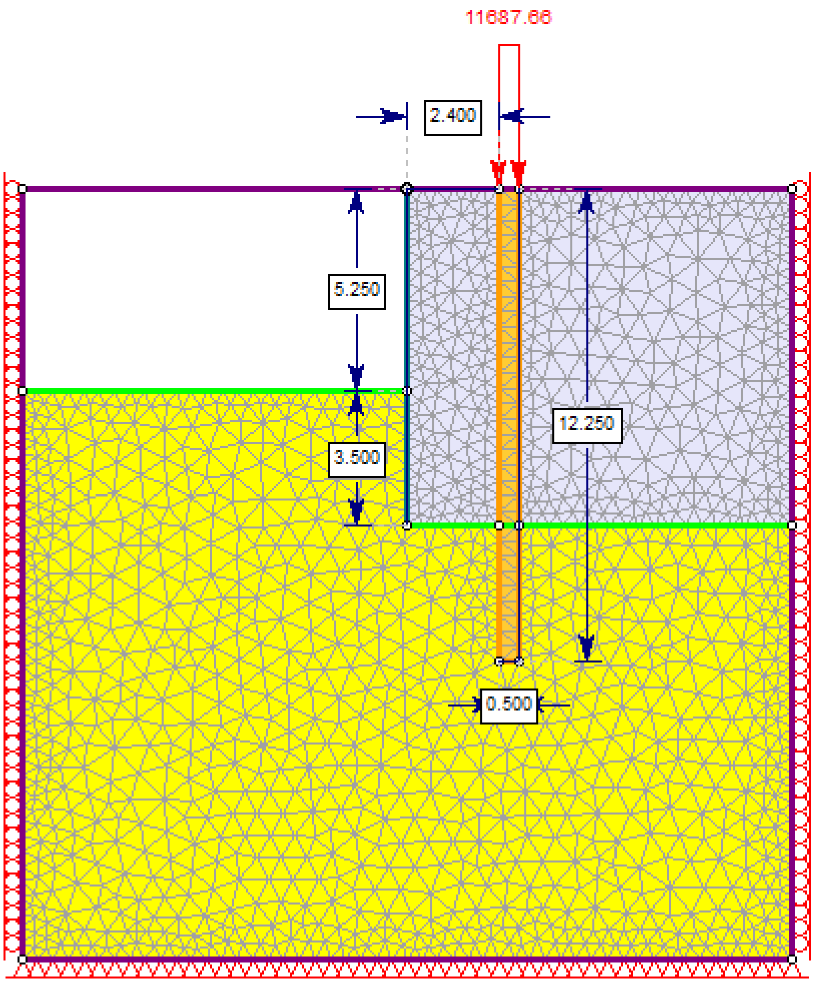

M 76.1: Original model (stage 3)

C_1'	ϕ_1'	γ_1	E_1	C_2'	ϕ_2'	γ_2	E_2	H_1	H_2	H_3	E_3	D_1	D_2	L	Qult
0	35	18	20	41	33	24	37.0	5.25	3.5	0.75	753416	2.4	0.5	12.25	11687.66

M 76.2: Parameter values

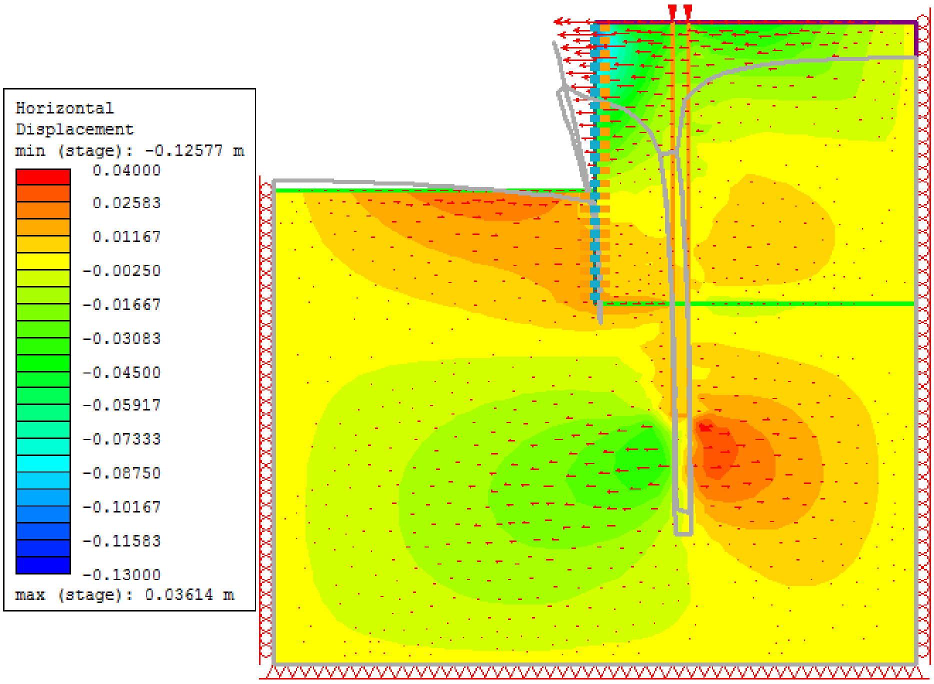

M 76.3: Deformed model (stage 3)

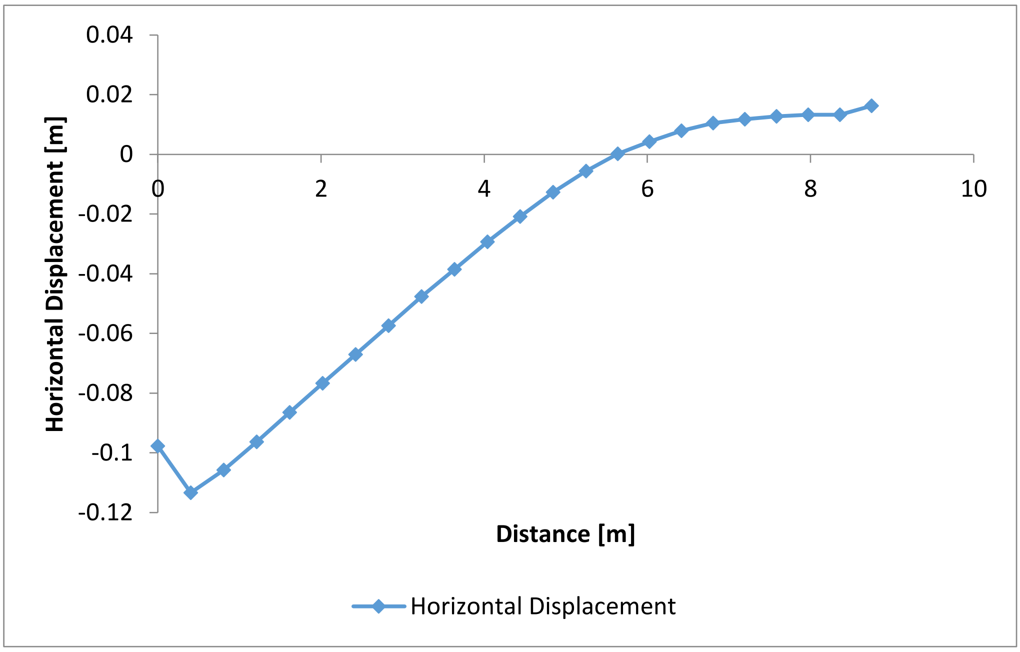

M 76.4: Horizontal displacement of soil along retaining wall

Retaining wall maximum horizontal displacement: -0.12577m

Distance from point of maximum displacement in retaining wall to the top of backfill soil: 0.0m

Model 77:

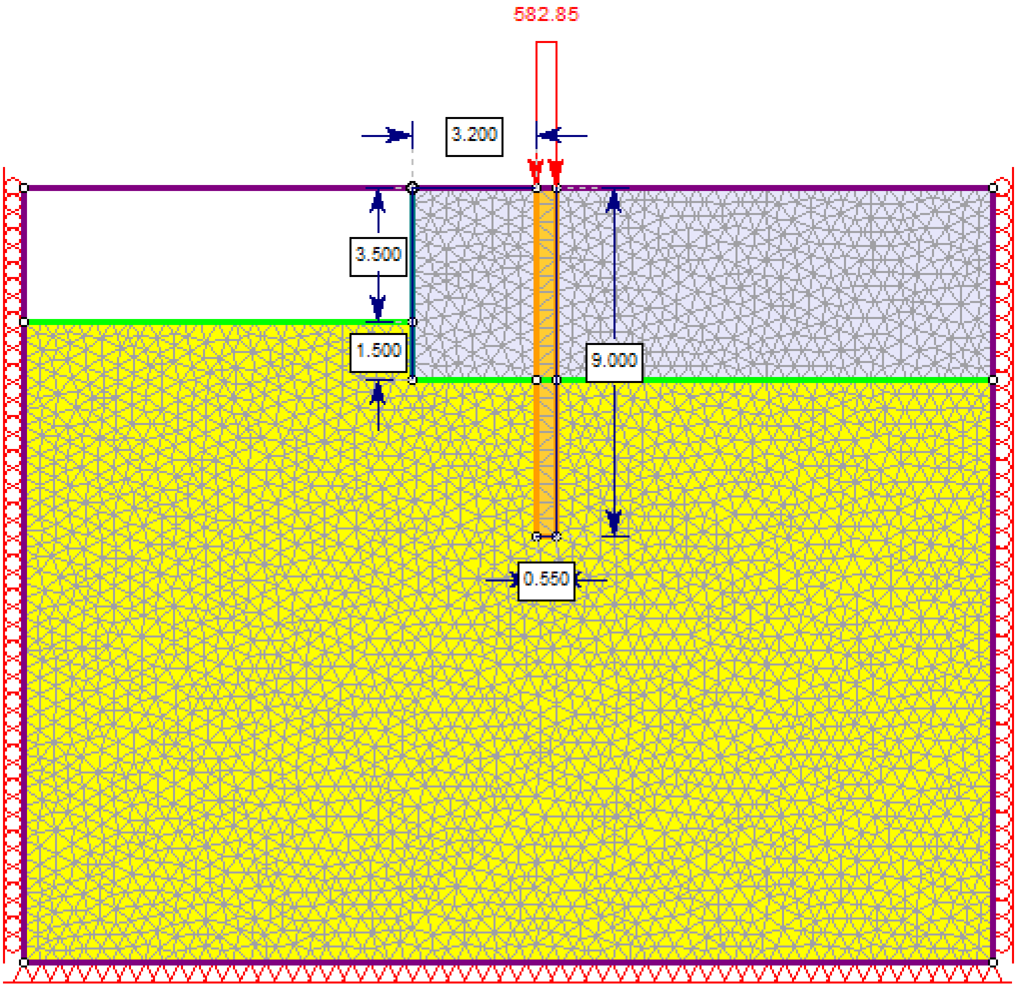

M 77.1: Original model (stage 3)

C'_1	ϕ'_1	γ_1	E_1	C'_2	ϕ'_2	γ_2	E_2	H_1	H_2	H_3	E_3	D_1	D_2	L	Qult
0	36	19	232	43	6	20	29.3	3.50	1.5	0.75	707047	3.2	0.55	9	582.85

M 77.2: Parameter values

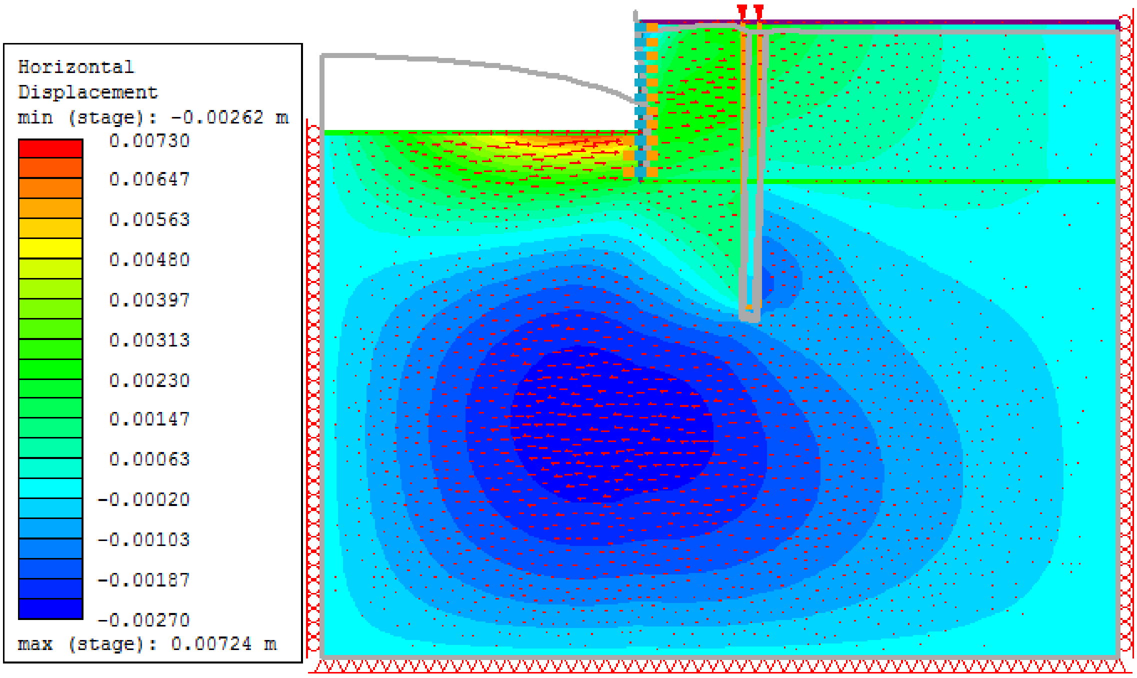

M 77.3: Deformed model (stage 3)

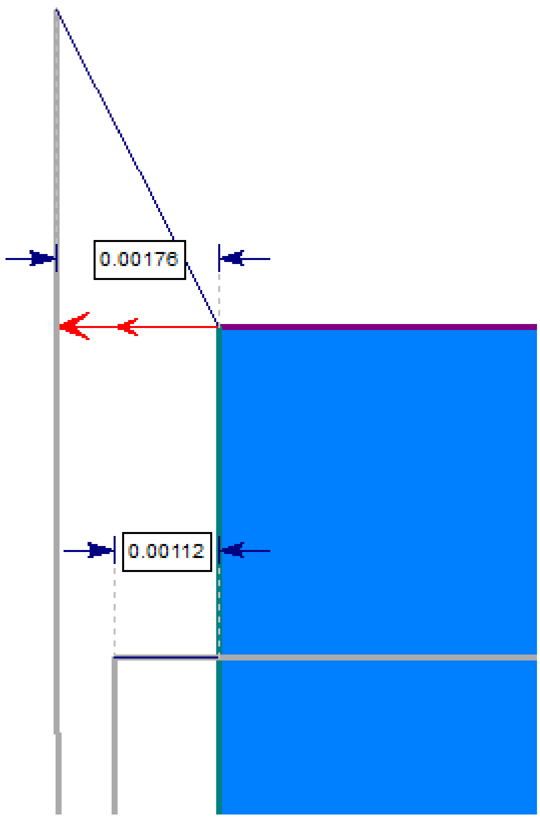

M 77.4: Detailed view of cross-section of retaining wall and soil (stage 3)

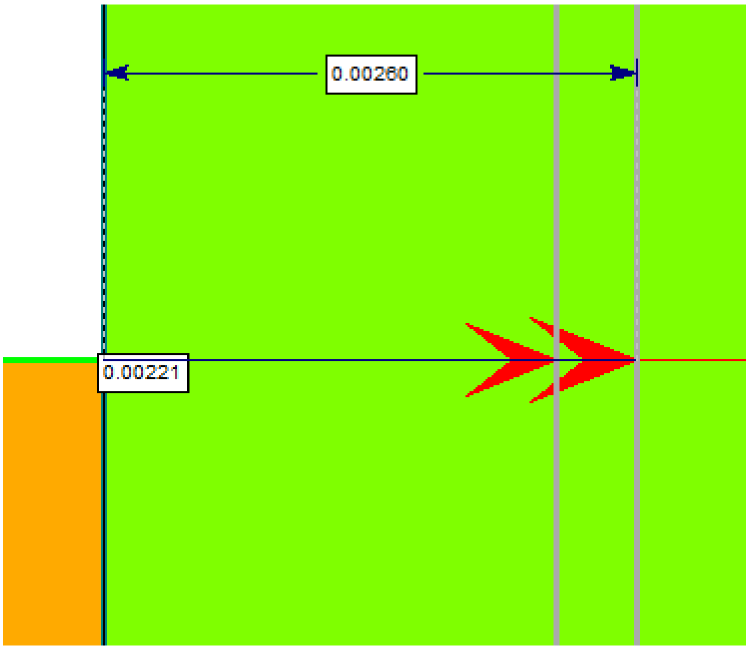

M 77.5: Detailed view of cross-section of retaining wall and soil (stage 3)

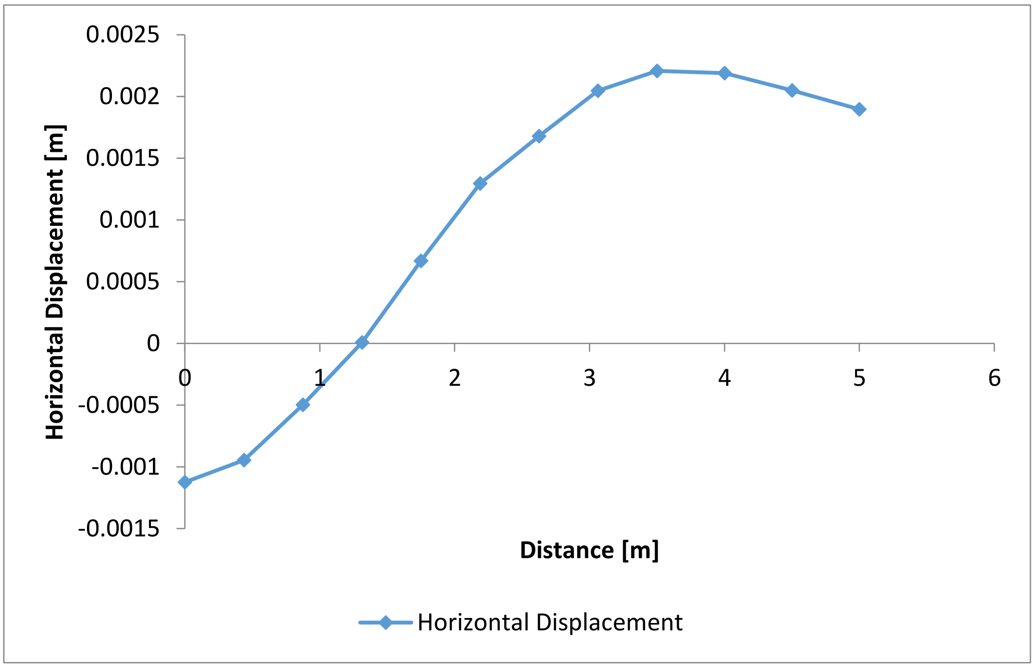

M 77.6: Horizontal displacement of soil along retaining wall

Retaining wall maximum horizontal displacement: -0.0026m

Distance from point of maximum displacement in retaining wall to the top of backfill soil: 3.5m

Model 78:

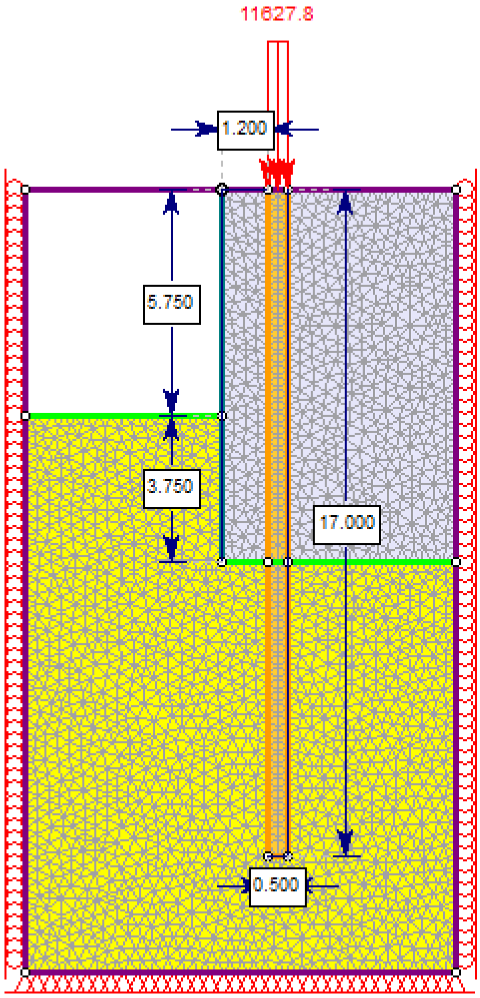

M 78.1: Original model (stage 3)

C_1'	ϕ_1'	γ_1	E_1	C_2'	ϕ_2'	γ_2	E_2	H_1	H_2	H_3	E_3	D_1	D_2	L	Qult
0	36	21	285	51	7	19	36.0	5.75	3.75	1.25	744429	1.2	0.5	17	1627.8

M 78.2: Parameter values

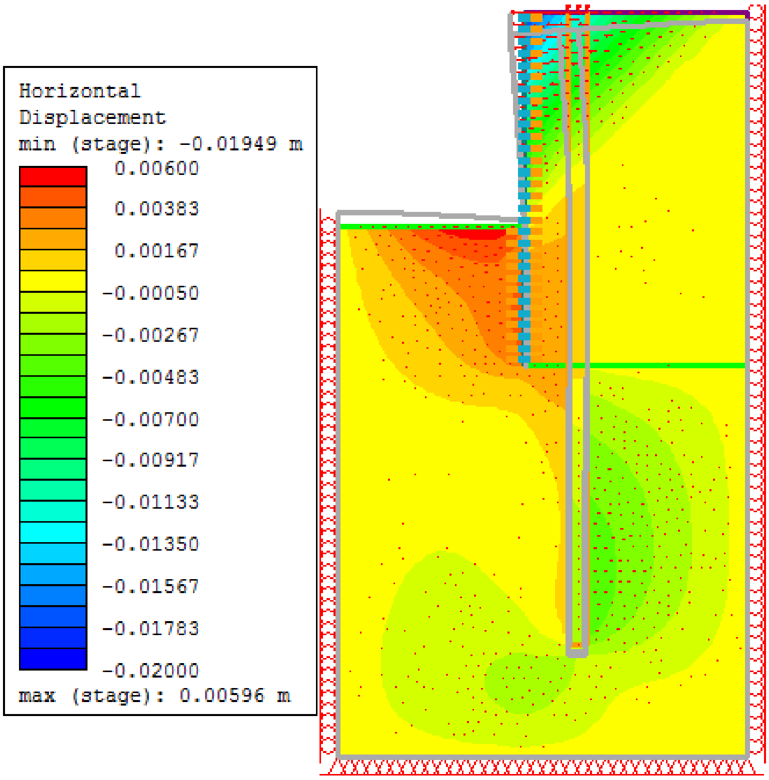

M 78.3: Deformed model (stage 3)

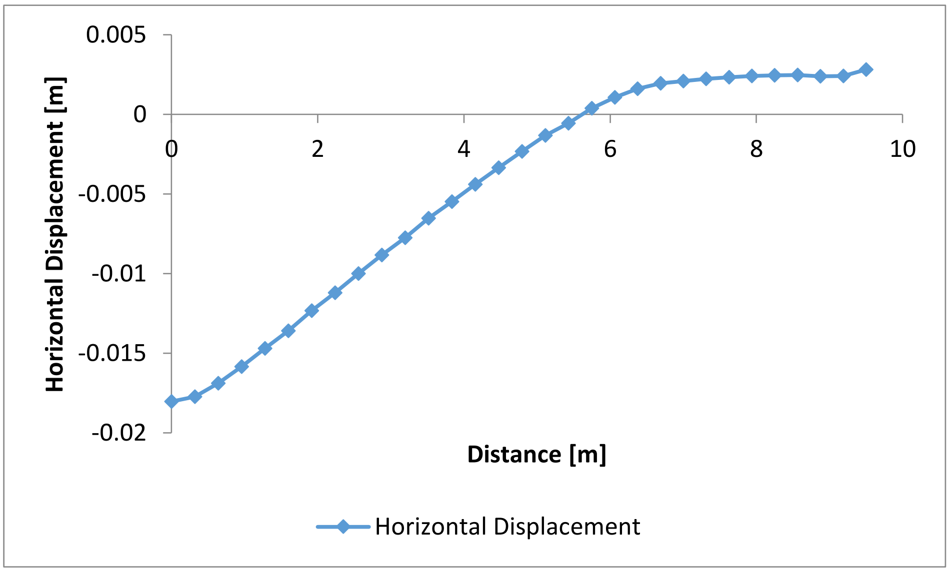

M 78.4: Horizontal displacement of soil along retaining wall

Retaining wall maximum horizontal displacement: -0.01949m

Distance from point of maximum displacement in retaining wall to the top of backfill soil: 0.0m

Model 79:

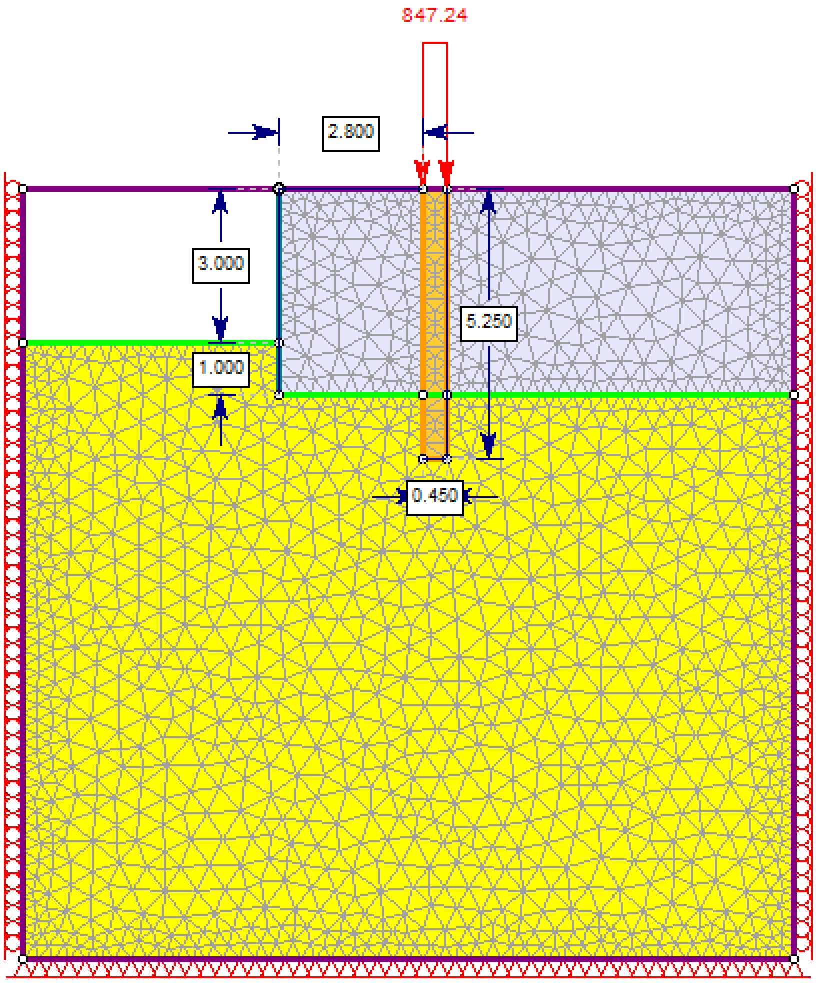

M 79.1: Original model (stage 3)

C_1'	ϕ_1'	γ_1	E_1	C_2'	ϕ_2'	γ_2	E_2	H_1	H_2	H_3	E_3	D_1	D_2	L	Qult
0	39	21	202	54	15	20	43.5	3.00	1	1.25	1035688	2.8	0.45	5.25	847.24

M 79.2: Parameter values

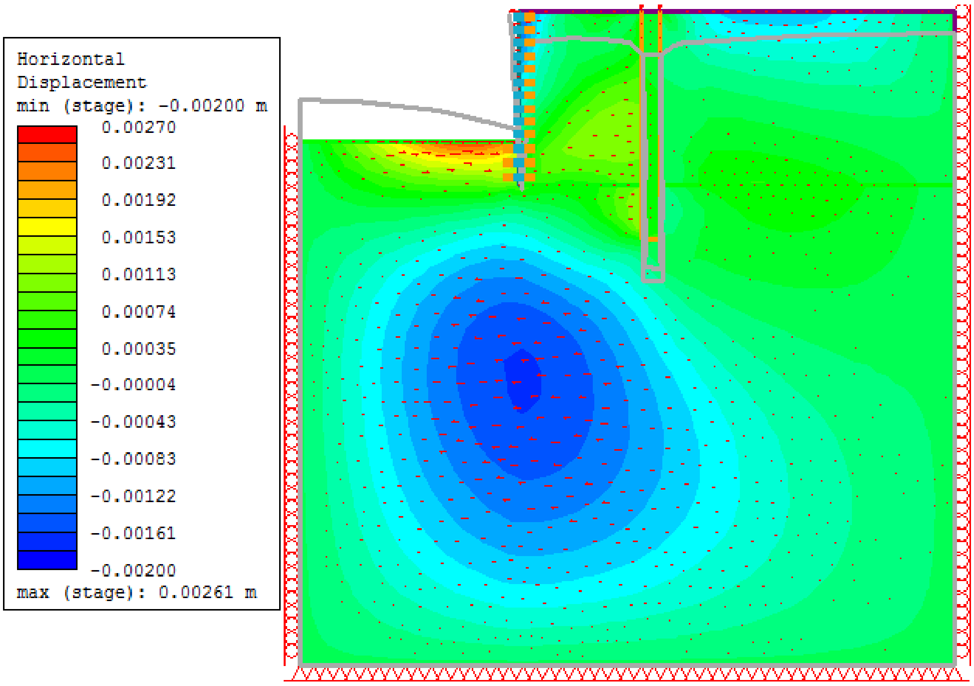

M 79.3: Deformed model (stage 3)

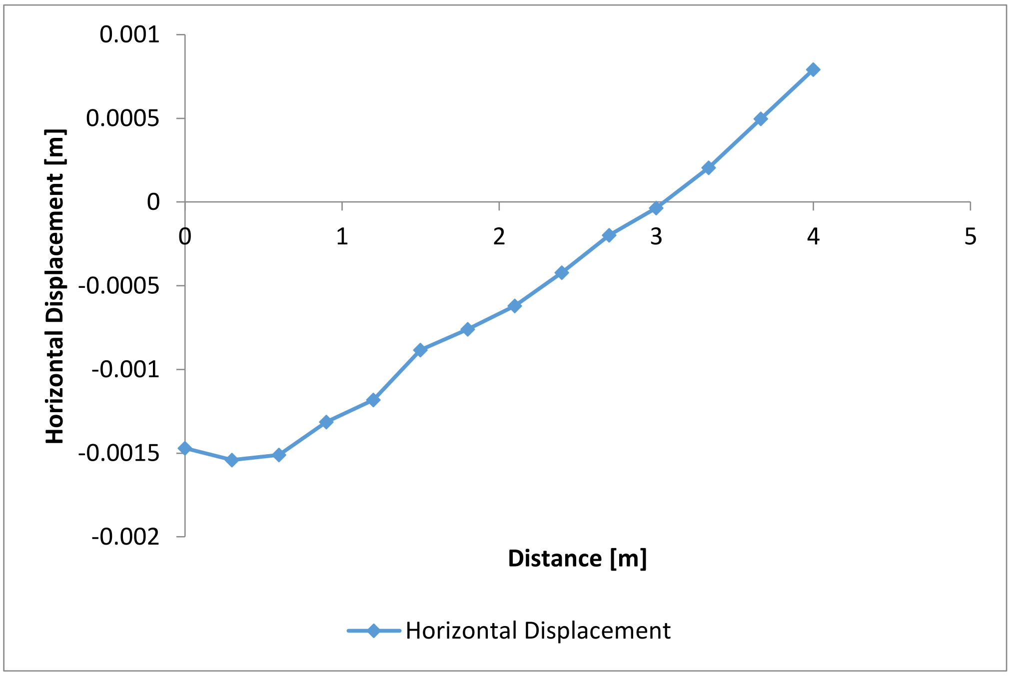

M 79.5: Horizontal displacement of soil along retaining wall

Retaining wall maximum horizontal displacement: -0.002m

Distance from point of maximum displacement in retaining wall to the top of backfill soil: 0.0m

Model 80:

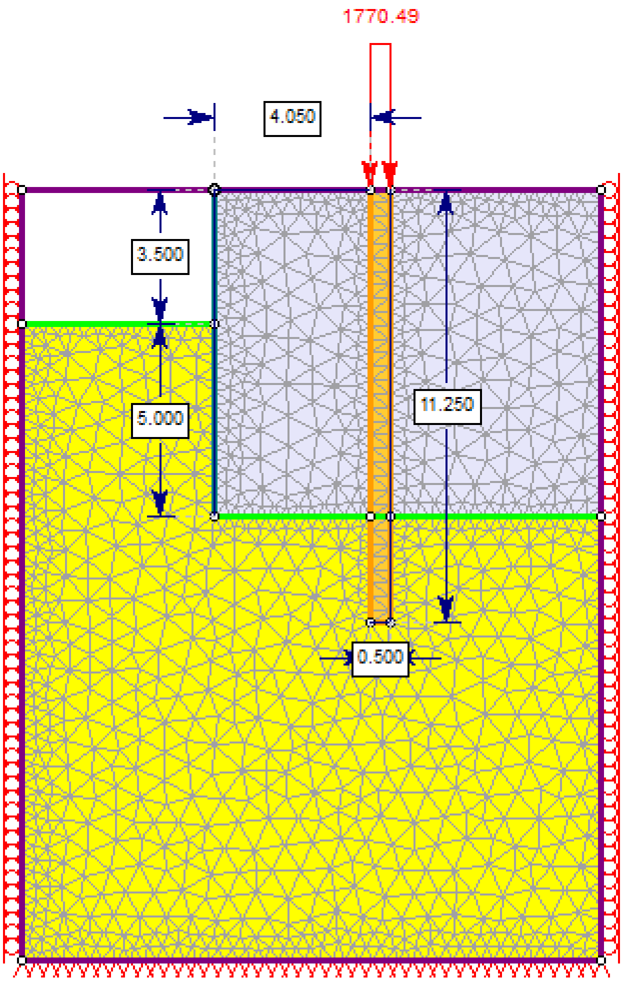

M 80.1: Original model (stage 3)

C'_1	ϕ'_1	γ_1	E_1	C'_2	ϕ'_2	γ_2	E_2	H_1	H_2	H_3	E_3	D_1	D_2	L	Qult
0	39	22	80	25	19	18	45.9	3.50	4	1.25	713630	4.05	0.5	11.25	1770.49

M 80.2: Parameter values

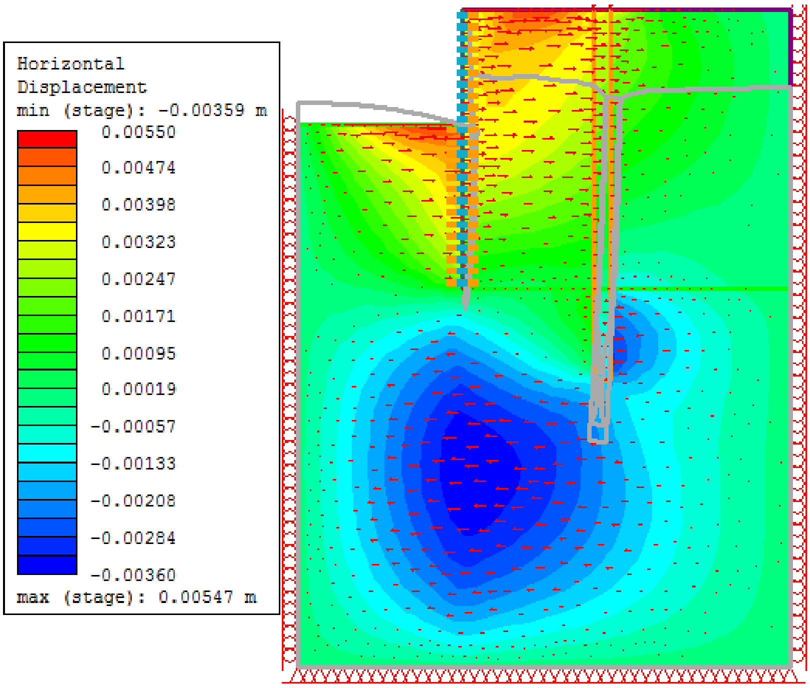

M 80.3: Deformed model (stage 3)

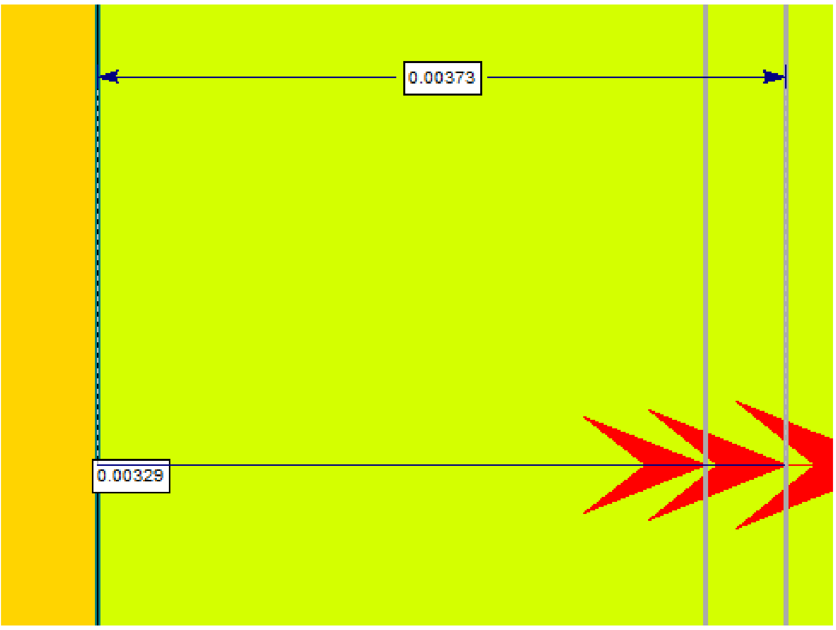

M 80.4: Detailed view of cross-section of retaining wall and soil (stage 3)

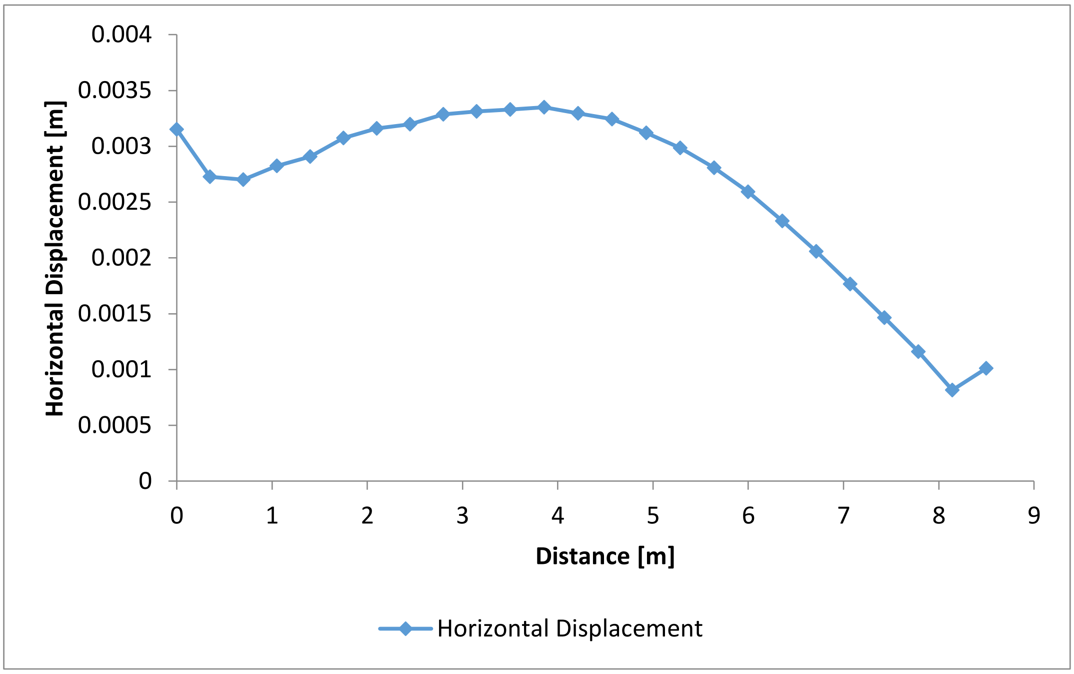

M 80.5: Horizontal displacement of soil along retaining wall

Retaining wall maximum horizontal displacement: 0.00373m

Distance from point of maximum displacement in retaining wall to the top of backfill soil: 4.124m

Model 81:

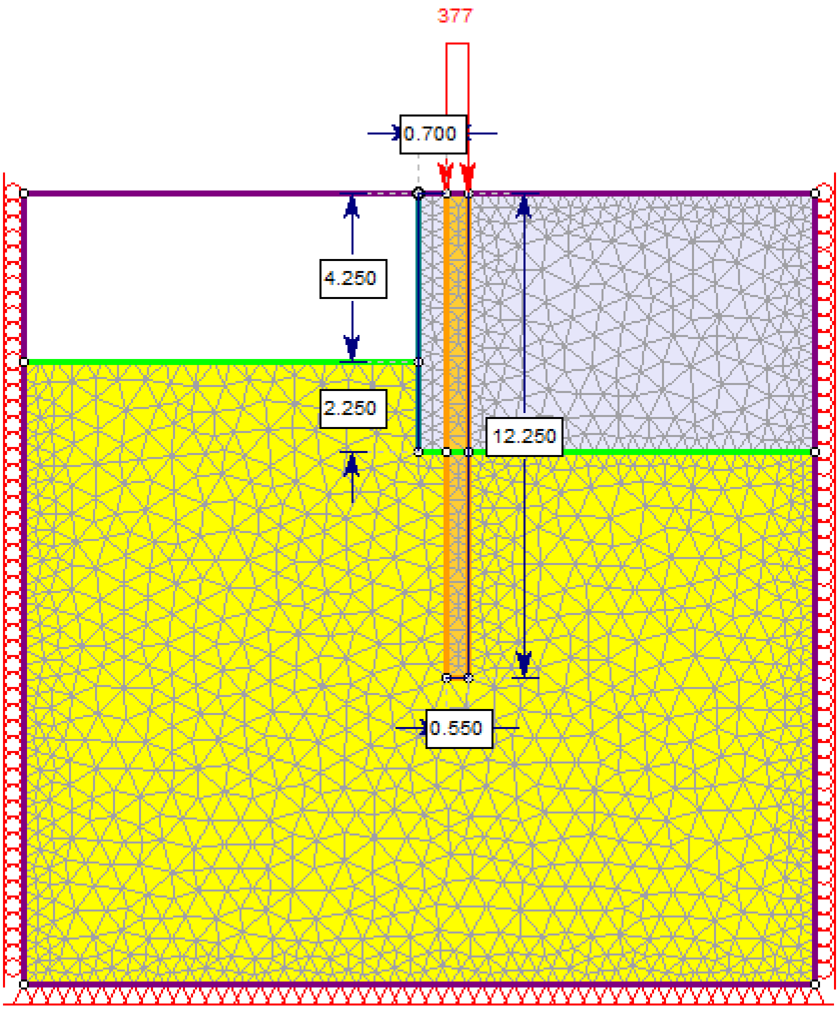

M 81.1: Original model (stage 3)

C'_1	ϕ'_1	γ_1	E_1	C'_2	ϕ'_2	γ_2	E_2	H_1	H_2	H_3	E_3	D_1	D_2	L	Qult
0	29	18	302	45	0	22	30.3	4.25	2.25	0.75	1103809	0.7	0.55	12.25	377

M 81.2: Parameter values

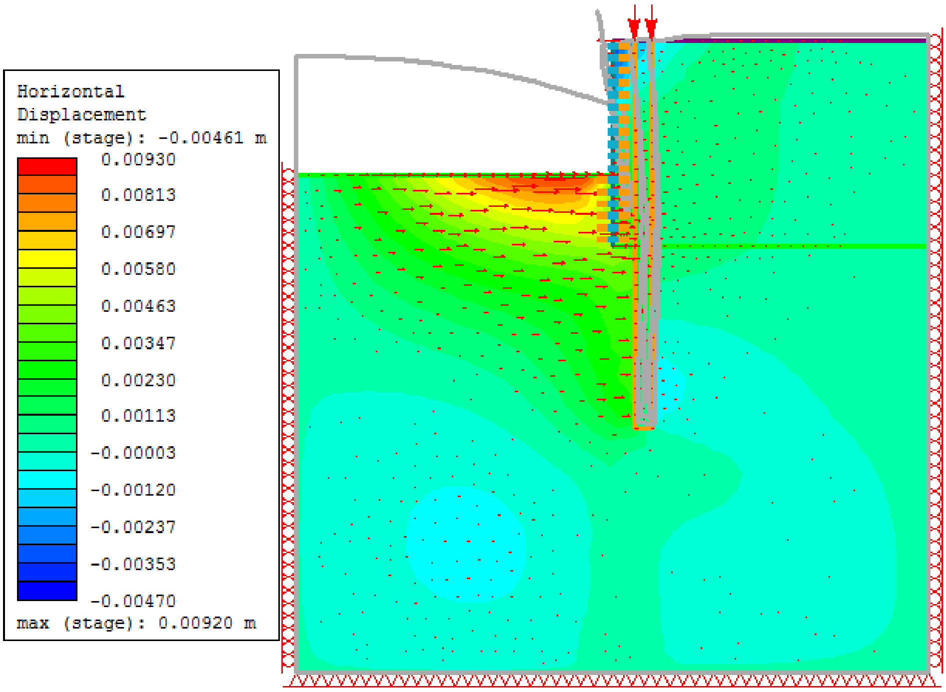

M 81.3: Deformed model (stage 3)

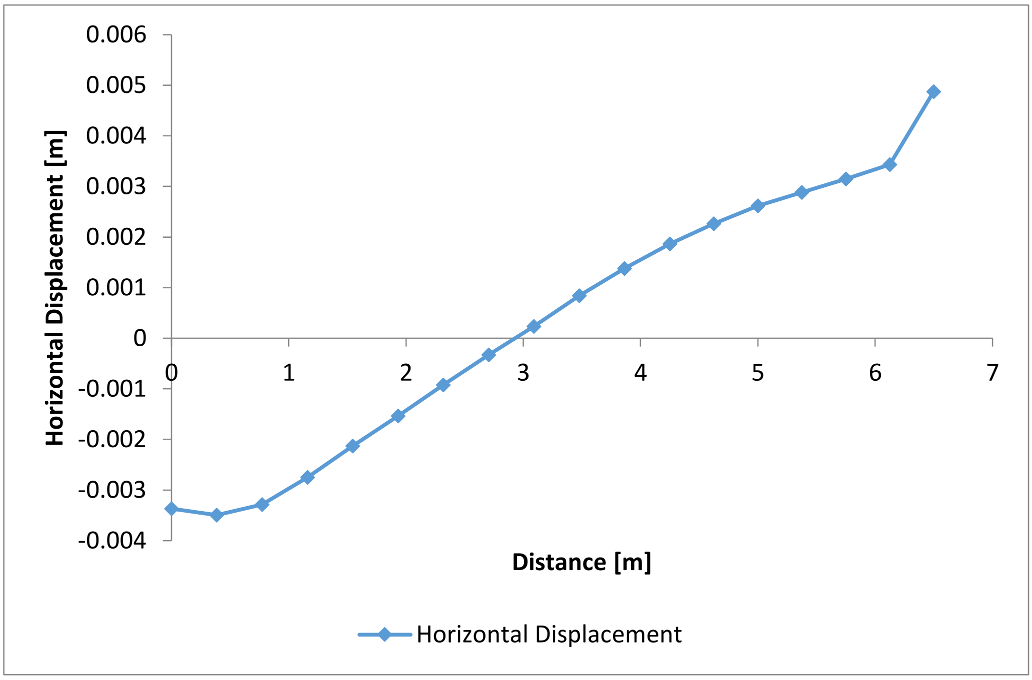

M 81.4: Horizontal displacement of soil along retaining wall

Retaining wall maximum horizontal displacement: -0.00461m

Distance from point of maximum displacement in retaining wall to the top of backfill soil: 0.0m

Model 82:

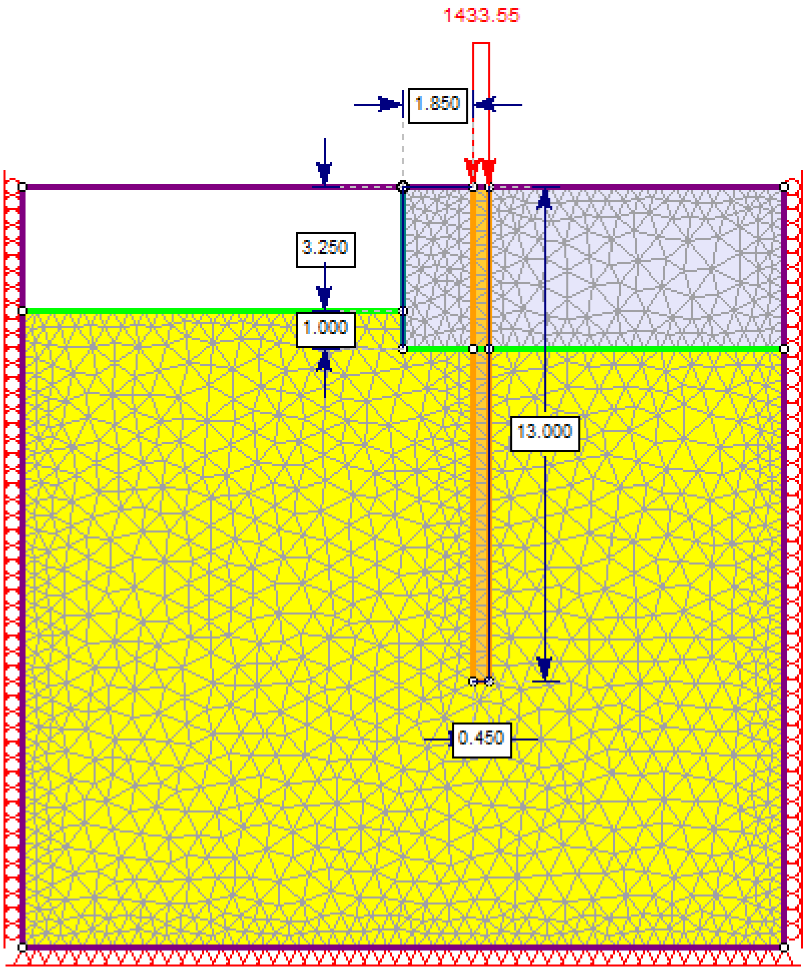

M 82.1: Original model (stage 3)

C_1'	ϕ_1'	γ_1	E_1	C_2'	ϕ_2'	γ_2	E_2	H_1	H_2	H_3	E_3	D_1	D_2	L	Qult
0	40	19	39	51	15	17	48.6	3.25	1	1	845731	1.85	0.55	13	1433.55

M 82.2: Parameter values

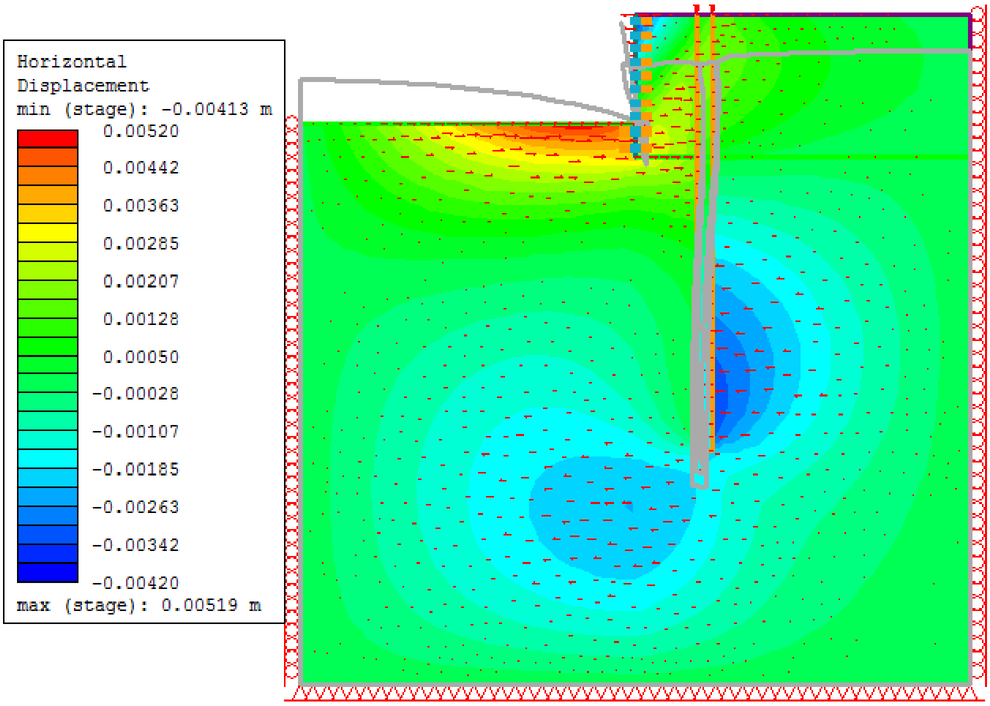

M 82.3: Deformed model (stage 3)

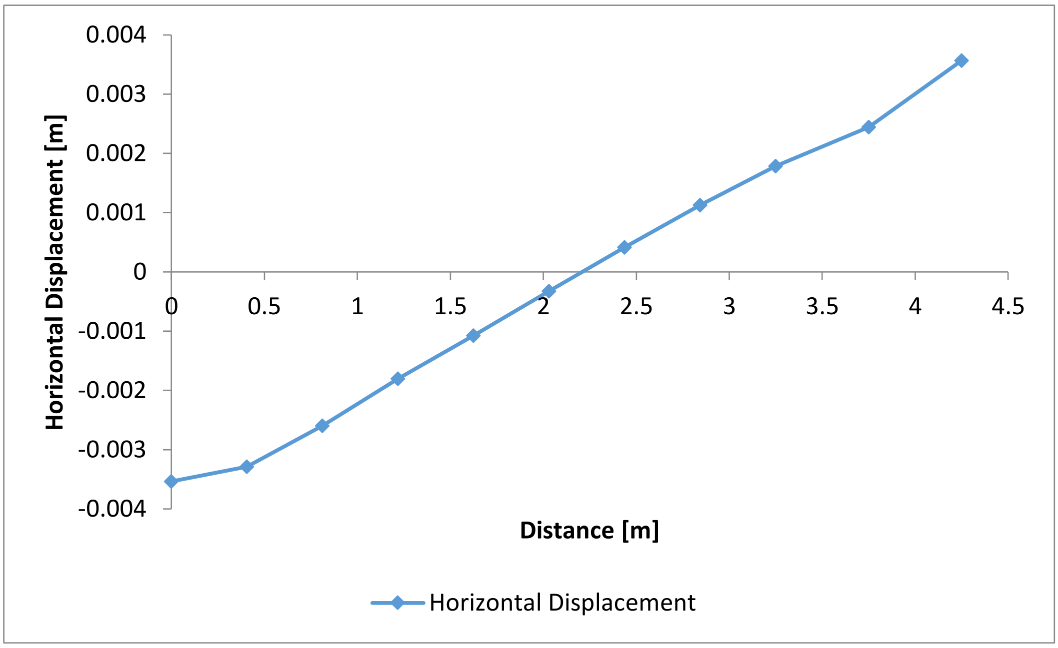

M 82.4: Horizontal displacement of soil along retaining wall

Retaining wall maximum horizontal displacement: -0.00413m

Distance from point of maximum displacement in retaining wall to the top of backfill soil: 0.0m

Model 83:

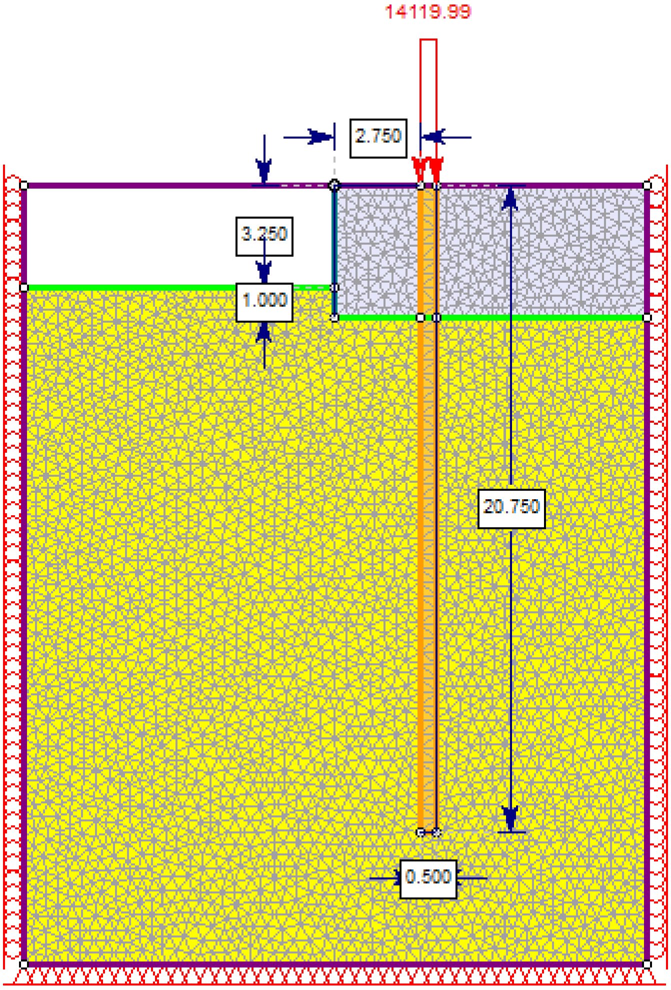

M 83.1: Original model (stage 3)

C_1'	ϕ_1'	γ_1	E_1	C_2'	ϕ_2'	γ_2	E_2	H_1	H_2	H_3	E_3	D_1	D_2	L	Qult
0	45	18	279	37	32	20	41.9	3.25	1	0.75	1074505	2.75	0.5	20.75	14119.99

M 83.2: Parameter values

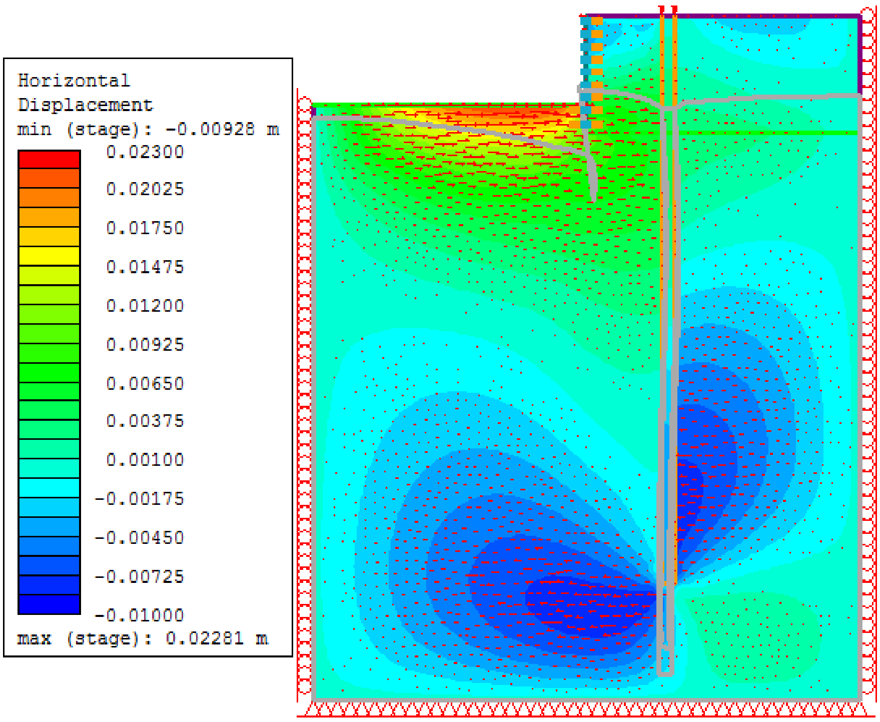

M 83.3: Deformed model (stage 3)

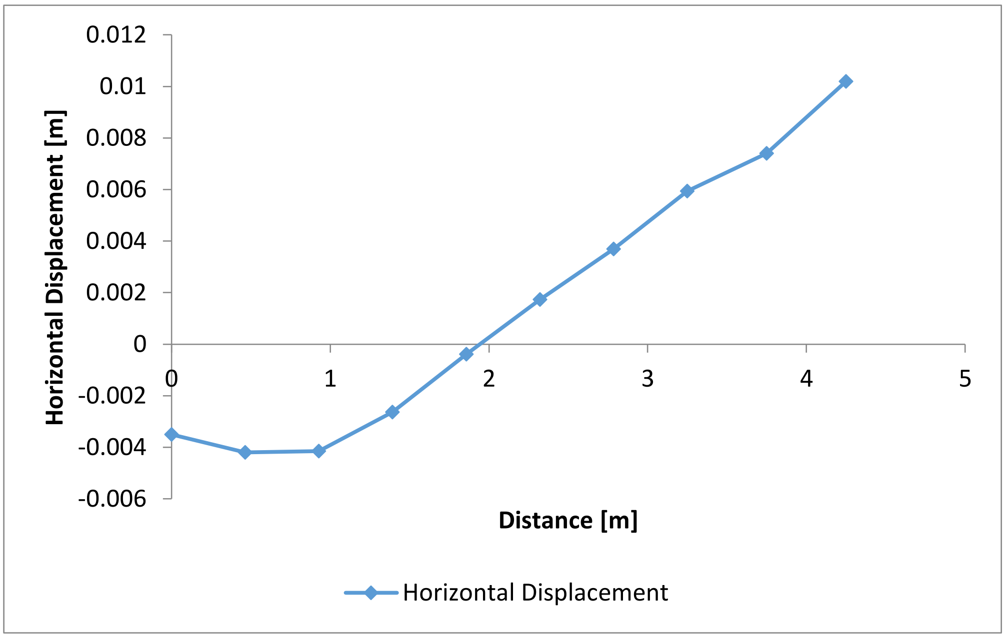

M 83.4: Horizontal displacement of soil along retaining wall

Retaining wall maximum horizontal displacement: 0.01019m

Distance from point of maximum displacement in retaining wall to the top of backfill soil: 4.25m

Model 84:

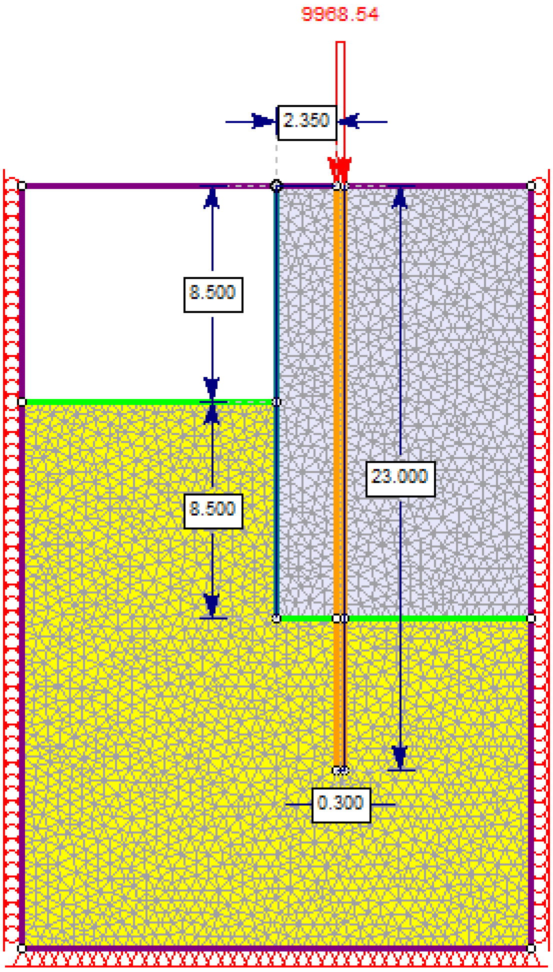

M 84.1: Original model (stage 3)

C'_1	ϕ'_1	γ_1	E_1	C'_2	ϕ'_2	γ_2	E_2	H_1	H_2	H_3	E_3	D_1	D_2	L	Qult
0	38	21	174	59	26	25	27.4	8.50	8.50	1.25	1101455	2.35	0.3	23	9968.54

M 84.2: Parameter values

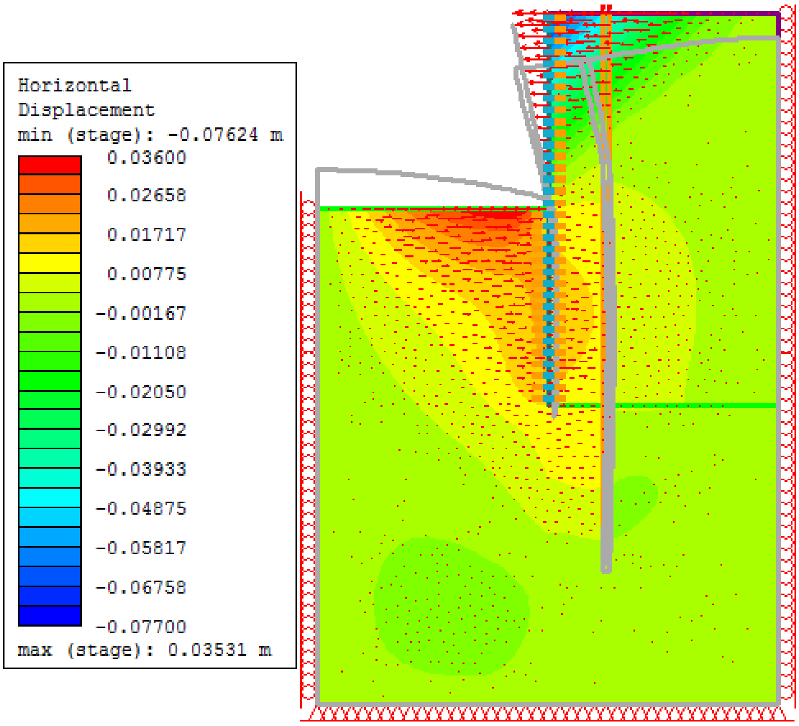

M 84.3: Deformed model (stage 3)

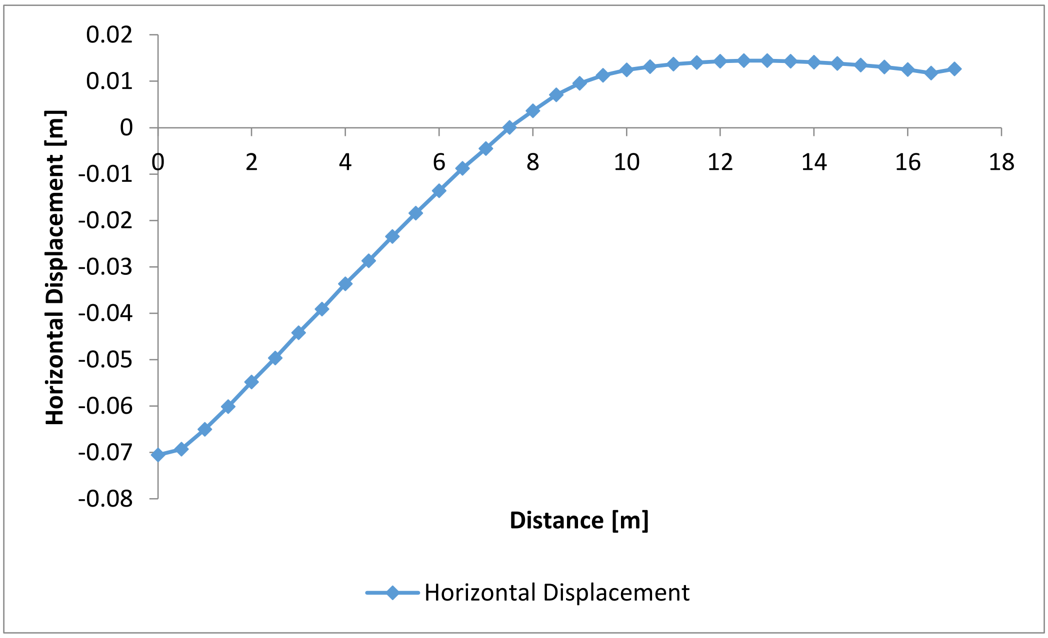

M 84.4: Horizontal displacement of soil along retaining wall

Retaining wall maximum horizontal displacement: -0.07624m

Distance from point of maximum displacement in retaining wall to the top of backfill soil: 0.0m

Model 85:

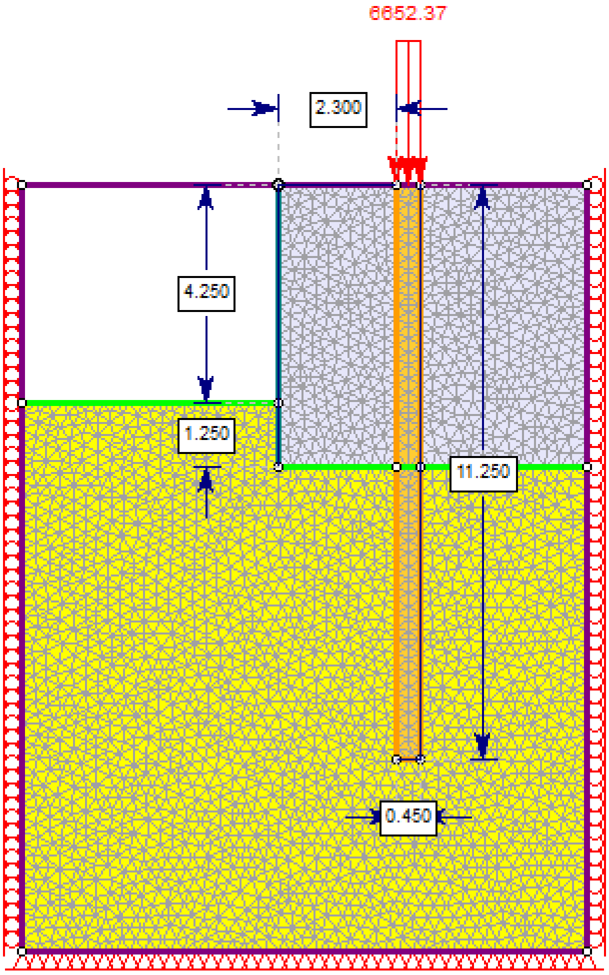

M 85.1: Original model (stage 3)

C_1'	ϕ_1'	γ_1	E_1	C_2'	ϕ_2'	γ_2	E_2	H_1	H_2	H_3	E_3	D_1	D_2	L	Qult
0	44	18	290	50	2	23	25.3	4.25	1.25	0.75	1034884	2.3	0.45	11.25	6652.37

M 85.2: Parameter values

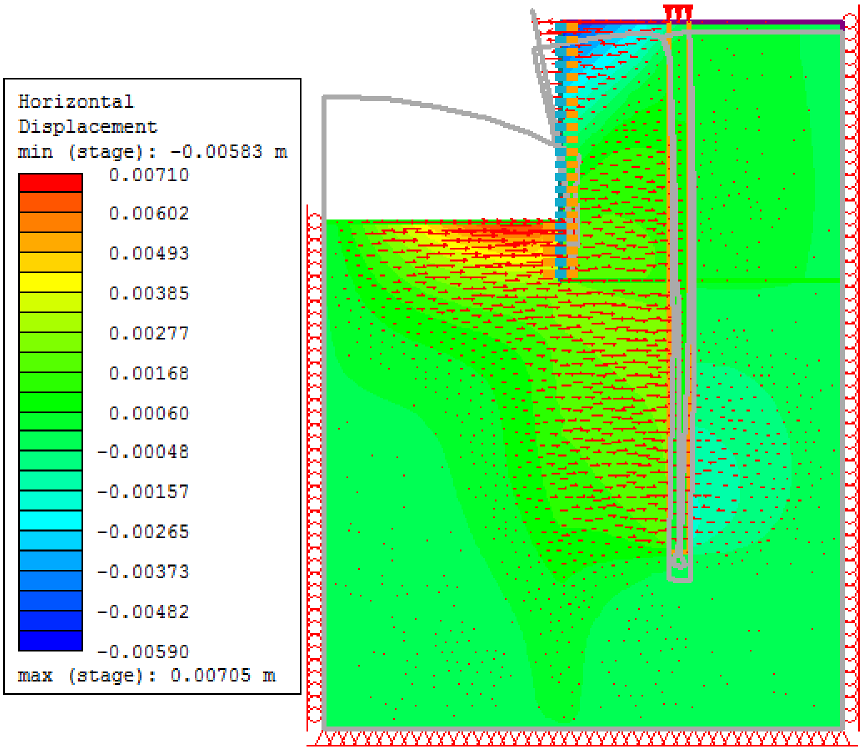

M 85.3: Deformed model (stage 3)

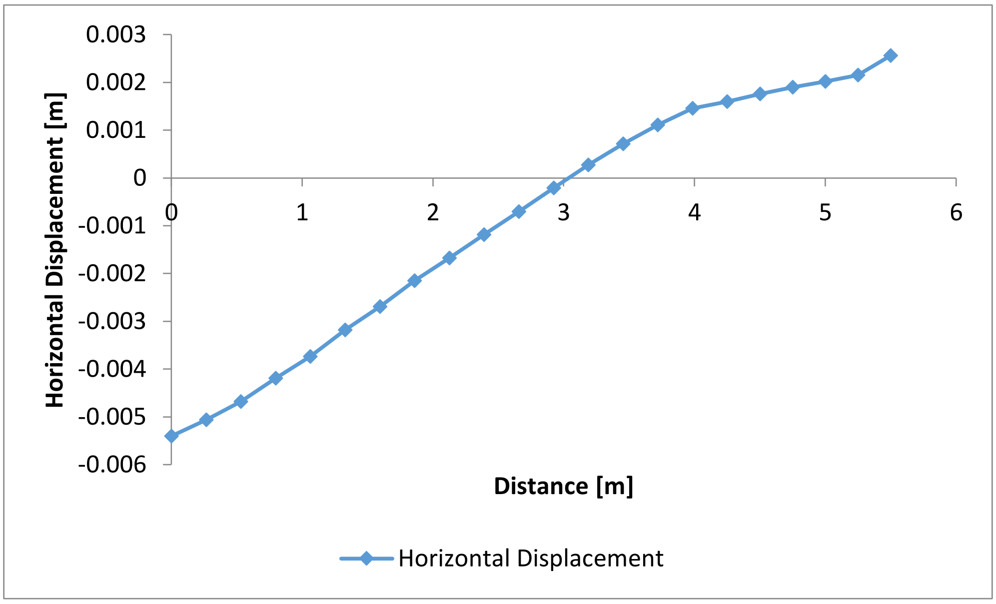

M85.4: Horizontal displacement of soil along retaining wall

Retaining wall maximum horizontal displacement: -0.00583m

Distance from point of maximum displacement in retaining wall to the top of backfill soil: 0.0m

Model 86:

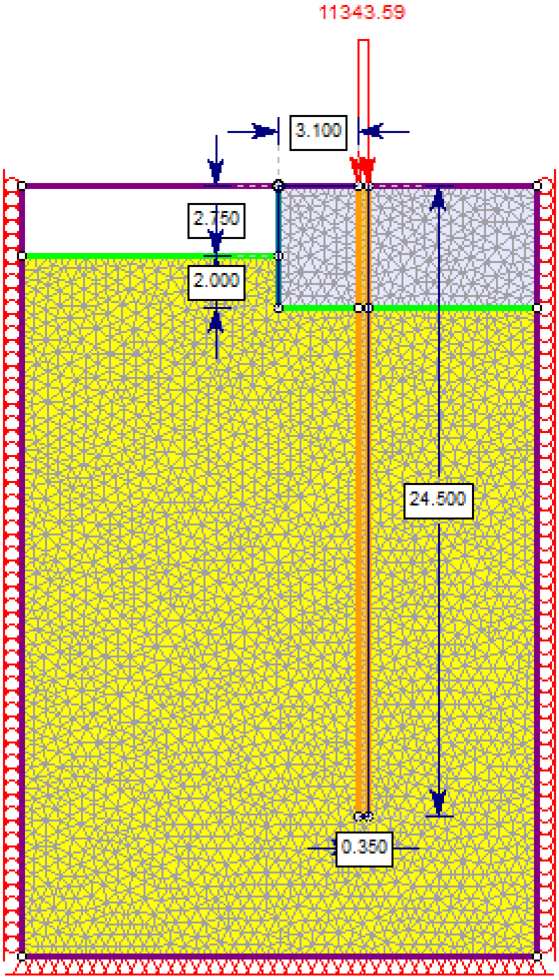

M 86.1: Original model (stage 3)

C'_1	ϕ'_1	γ_1	E_1	C'_2	ϕ'_2	γ_2	E_2	H_1	H_2	H_3	E_3	D_1	D_2	L	Qult
0	30	20	14	24	28	25	44.1	2.75	2	1	1137481	3.1	0.35	24.5	11343.59

M 86.2: Parameter values

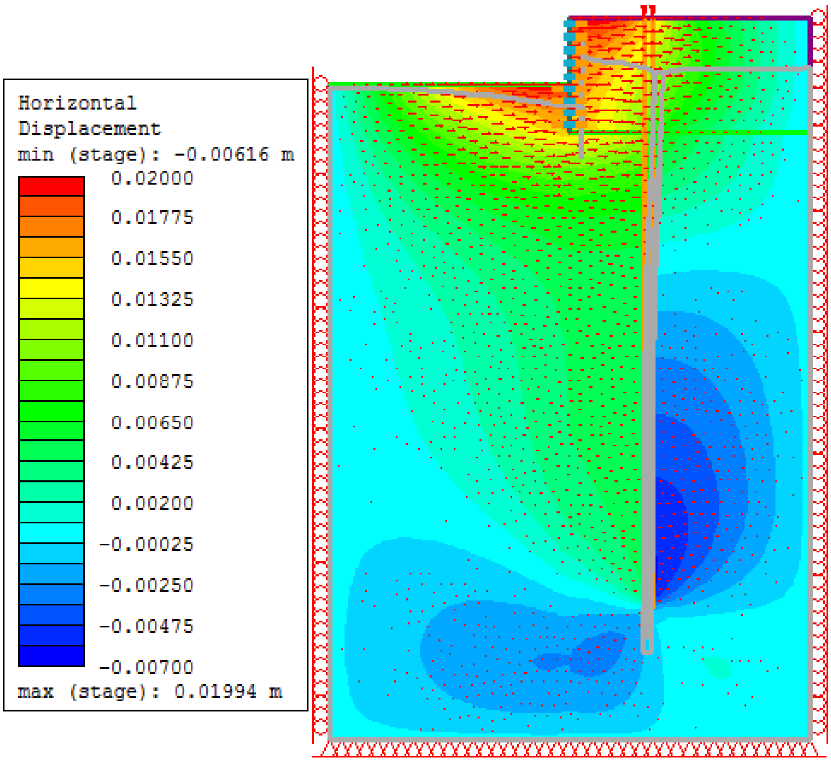

M 86.3: Deformed model (stage 3)

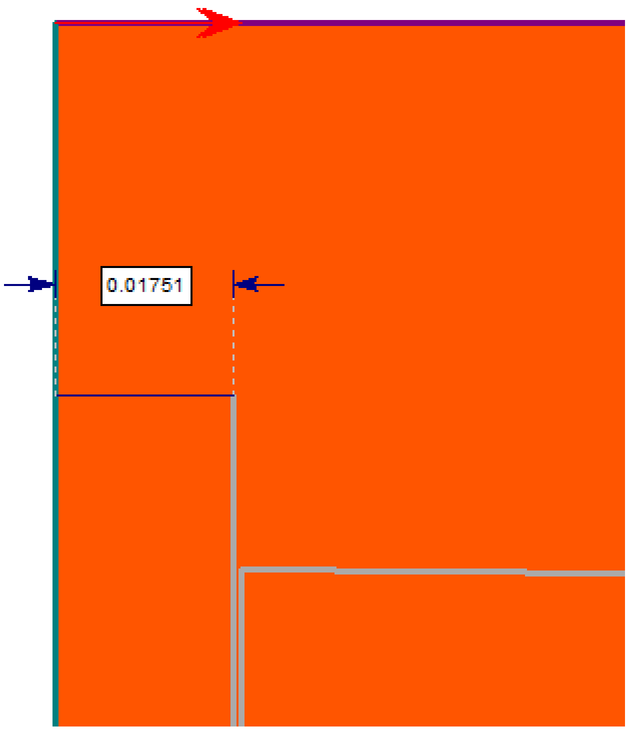

M 86.4: Detailed view of cross-section of retaining wall and soil (stage 3)

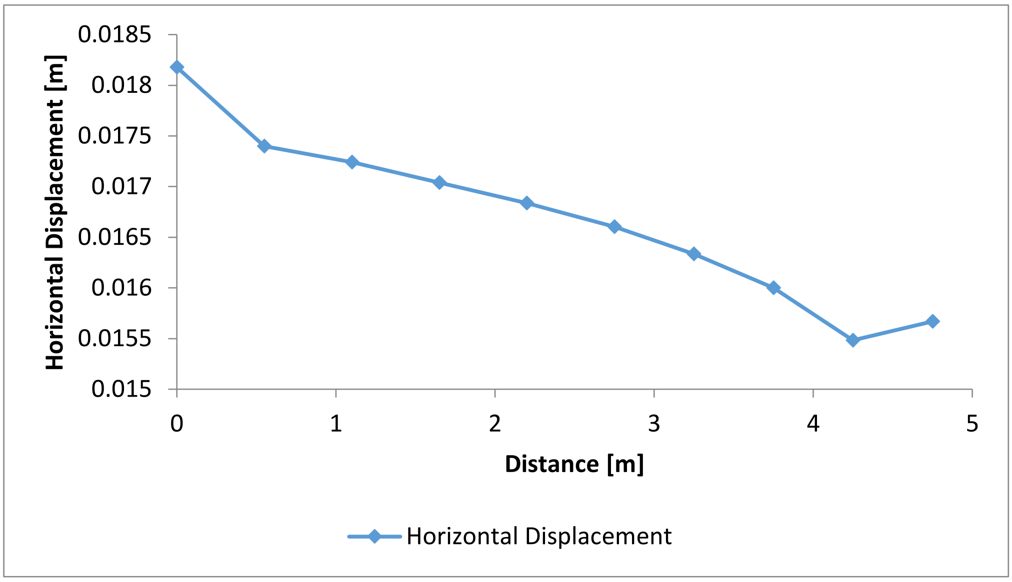

M 86.5: Horizontal displacement of soil along retaining wall

Retaining wall maximum horizontal displacement: 0.01751m

Distance from point of maximum displacement in retaining wall to the top of backfill soil: 0.0m

Model 87:

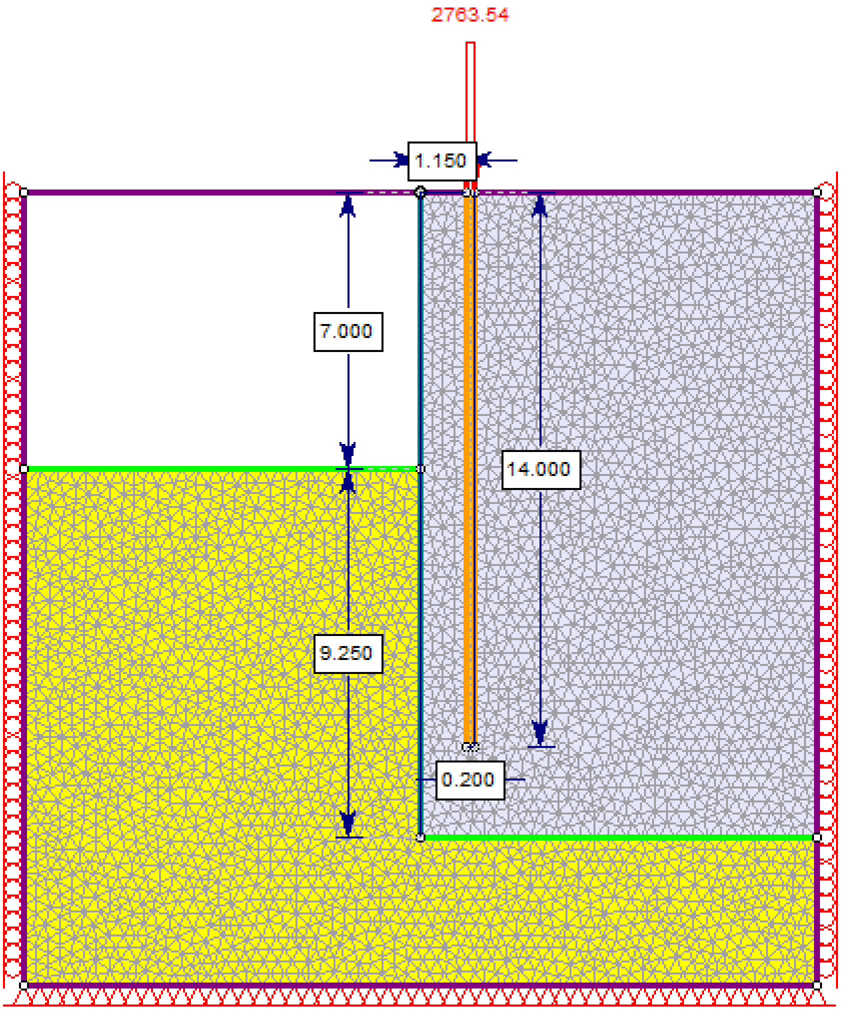

M 87.1: Original model (stage 3)

C'_1	ϕ'_1	γ_1	E_1	C'_2	ϕ'_2	γ_2	E_2	H_1	H_2	H_3	E_3	D_1	D_2	L	Qult
0	31	20	172	47	27	20	43.0	7.00	9.25	1.25	822417	1.15	0.2	14	2763.54

M 87.2: Parameter values

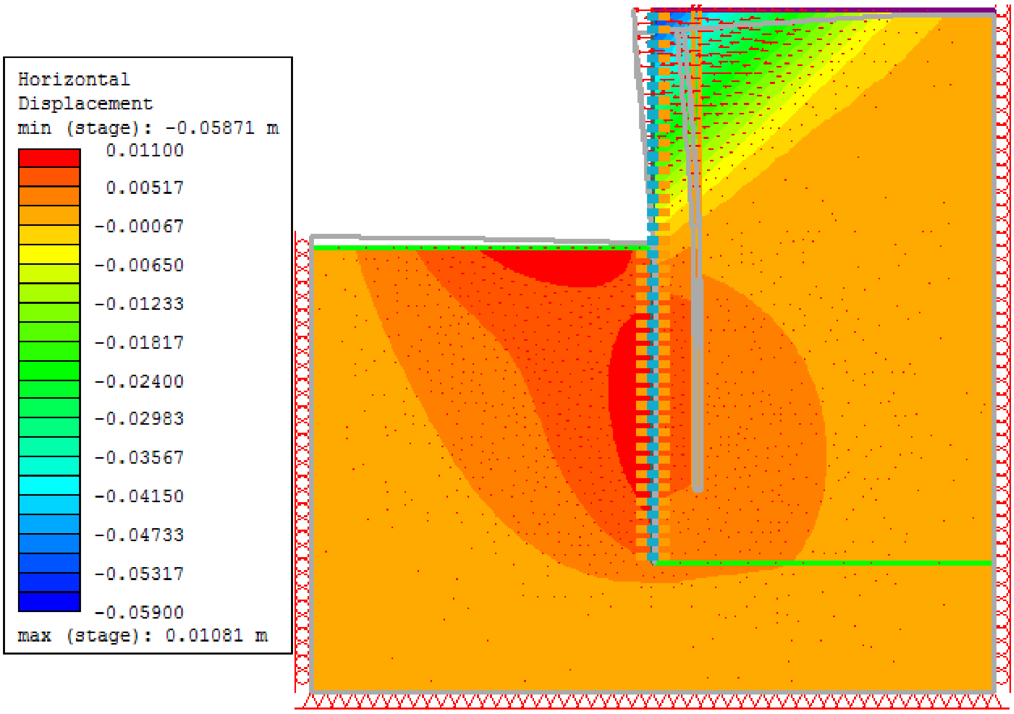

M 87.3: Deformed model (stage 3)

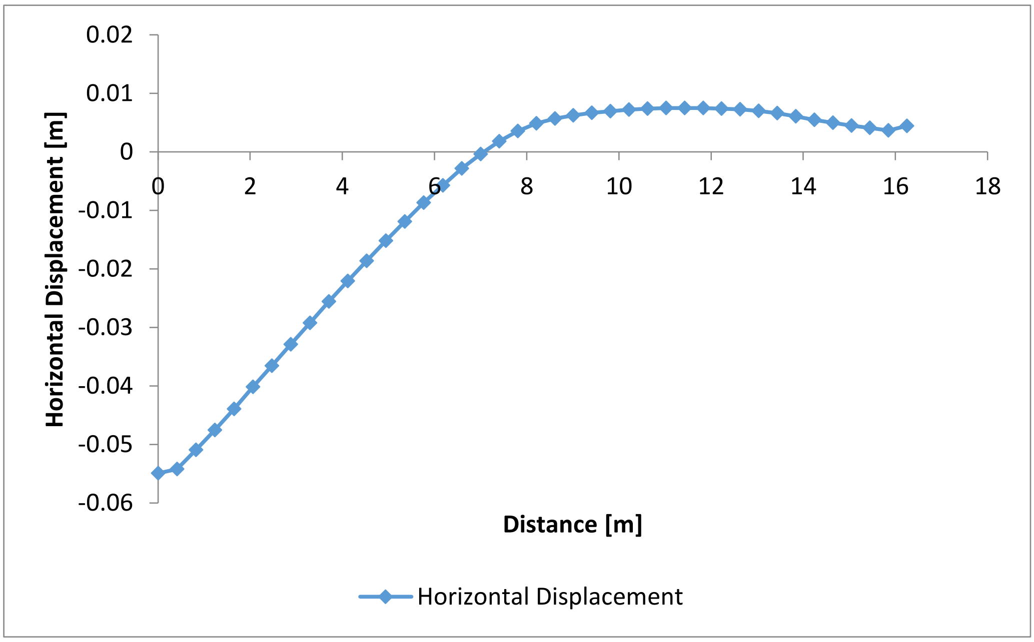

M 87.4: Horizontal displacement of soil along retaining wall

Retaining wall maximum horizontal displacement: -0.05871m

Distance from point of maximum displacement in retaining wall to the top of backfill soil: 0.0m

Model 88:

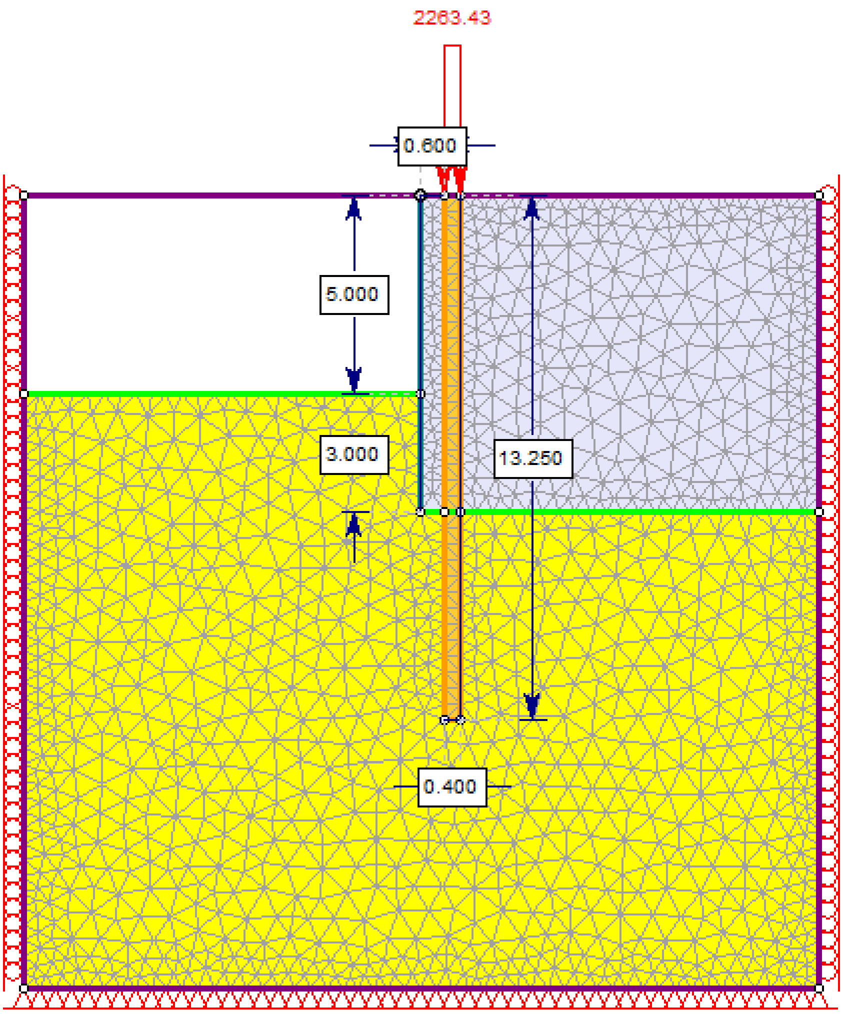

M 88.1: Original model (stage 3)

C_1'	ϕ_1'	γ_1	E_1	C_2'	ϕ_2'	γ_2	E_2	H_1	H_2	H_3	E_3	D_1	D_2	L	Qult
0	35	20	45	59	21	18	21.4	6.50	4	1	714763	0.75	0.55	4	2263.43

M 88.2: Parameter values

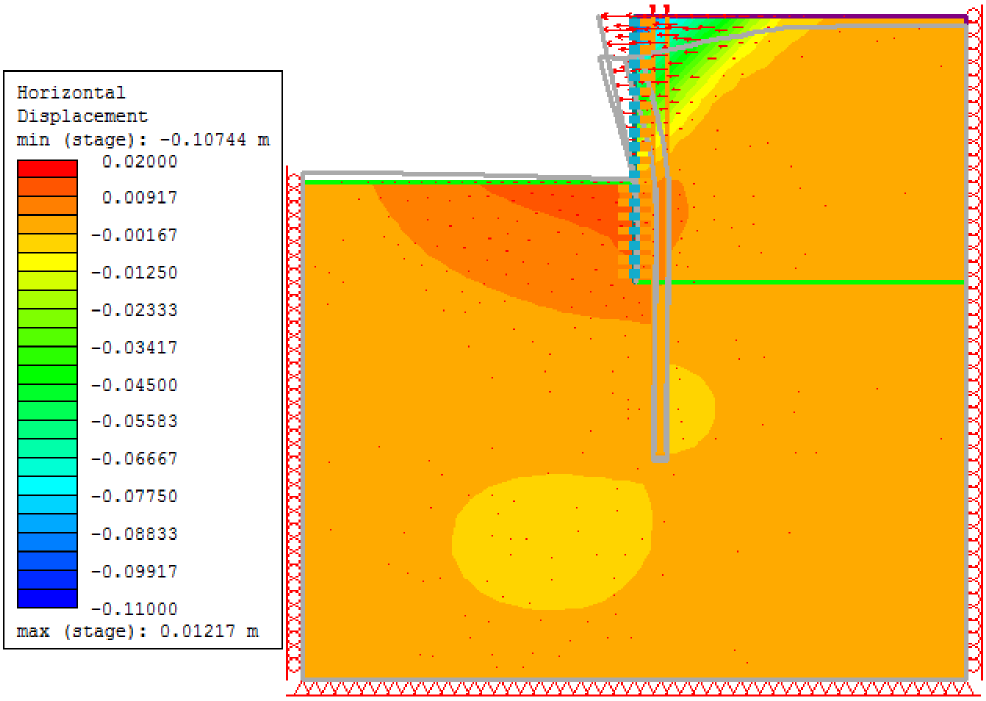

M 88.3: Deformed model (stage 3)

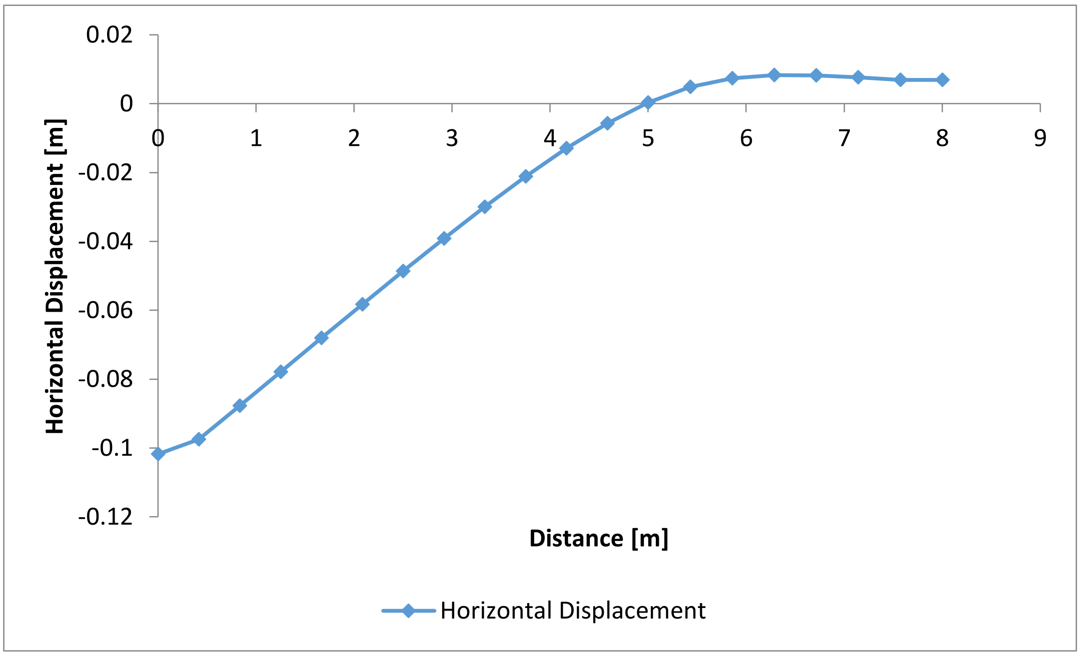

M 88.4: Horizontal displacement of soil along retaining wall

Retaining wall maximum horizontal displacement: -0.10744m

Distance from point of maximum displacement in retaining wall to the top of backfill soil: 0.0m

Model 89:

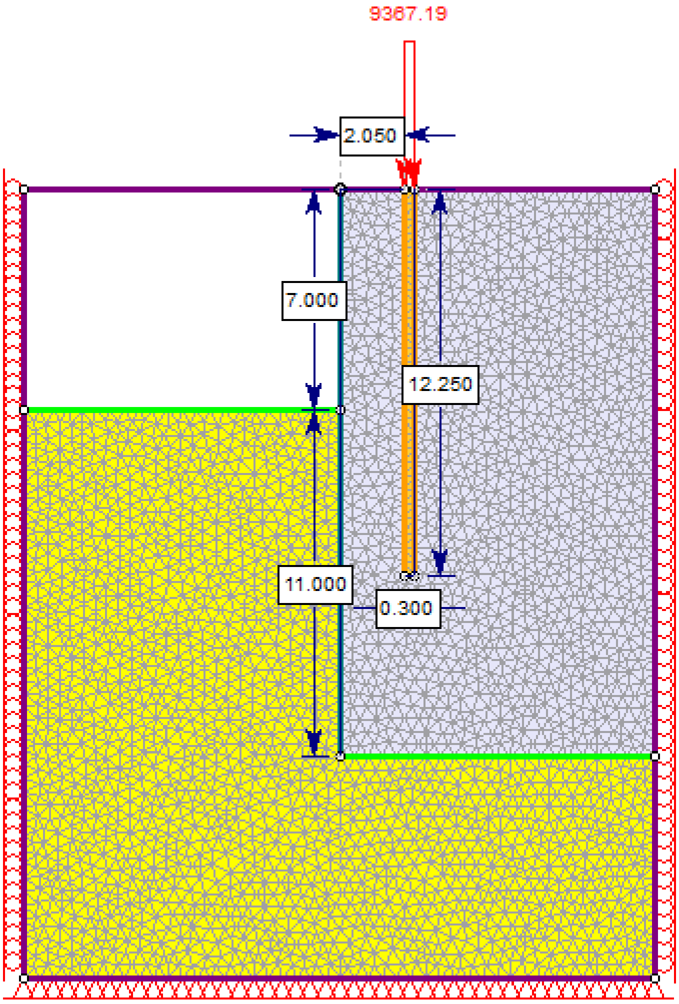

M 89.1: Original model (stage 3)

C'_1	ϕ'_1	γ_1	E_1	C'_2	ϕ'_2	γ_2	E_2	H_1	H_2	H_3	E_3	D_1	D_2	L	Qult
0	42	22	184	45	26	25	11.4	7.00	11	1	1049763	2.05	0.3	12.25	9367.19

M 89.2: Parameter values

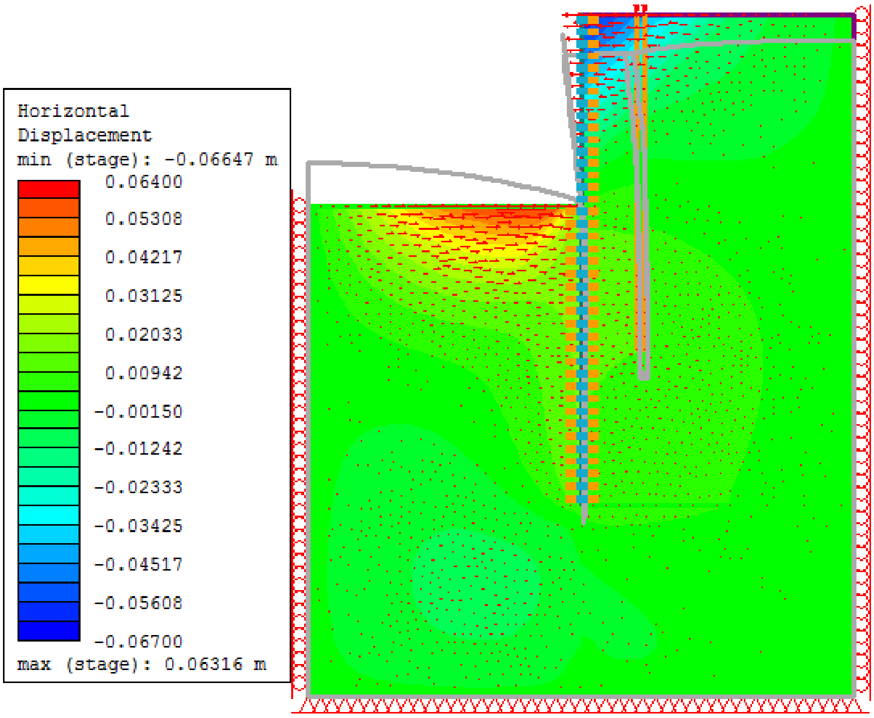

M 89.3: Deformed model (stage 3)

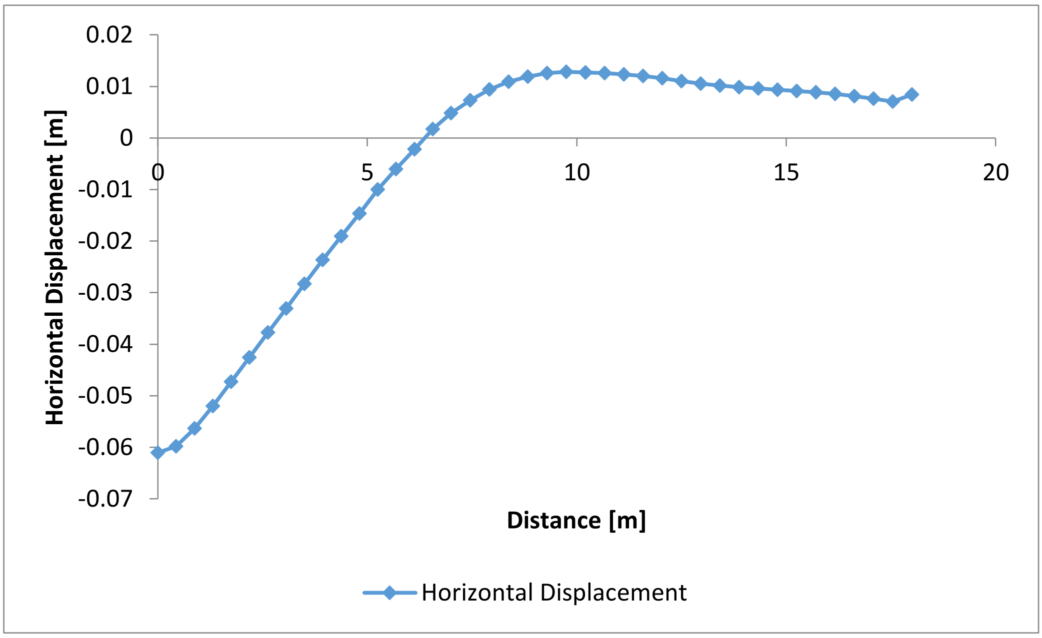

M 89.4: Horizontal displacement of soil along retaining wall

Retaining wall maximum horizontal displacement: -0.06647m

Distance from point of maximum displacement in retaining wall to the top of backfill soil: 0.0m

Model 90:

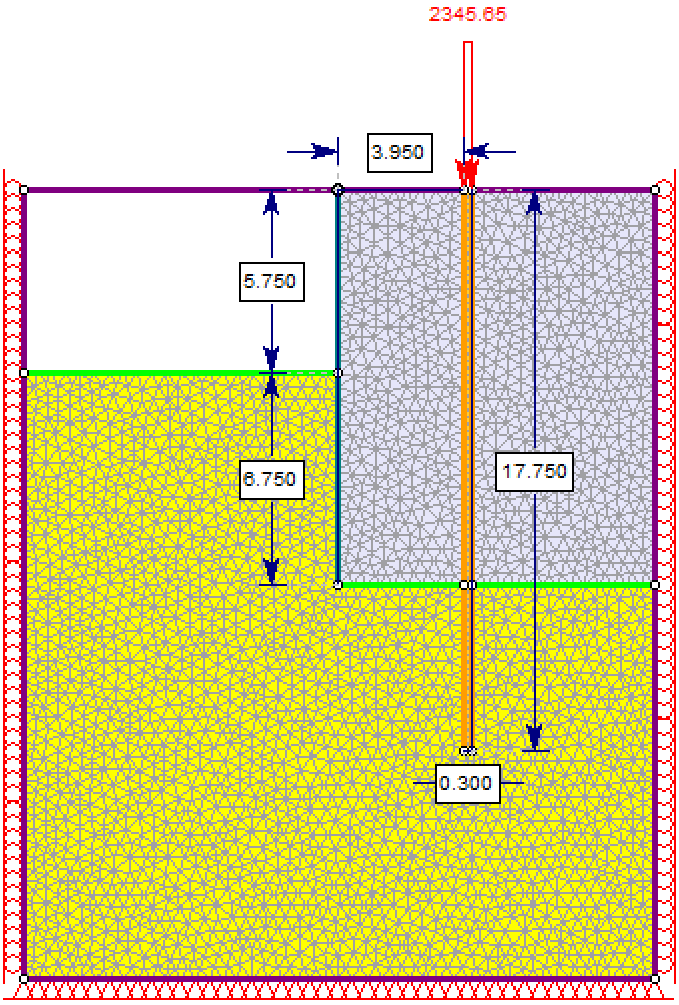

M 90.1: Original model (stage 3)

C_1'	ϕ_1'	γ_1	E_1	C_2'	ϕ_2'	γ_2	E_2	H_1	H_2	H_3	E_3	D_1	D_2	L	Qult
0	37	21	257	39	7	18	25.3	5.75	6.75	1.25	776202	3.95	0.3	17.75	2345.65

M 90.2: Parameter values

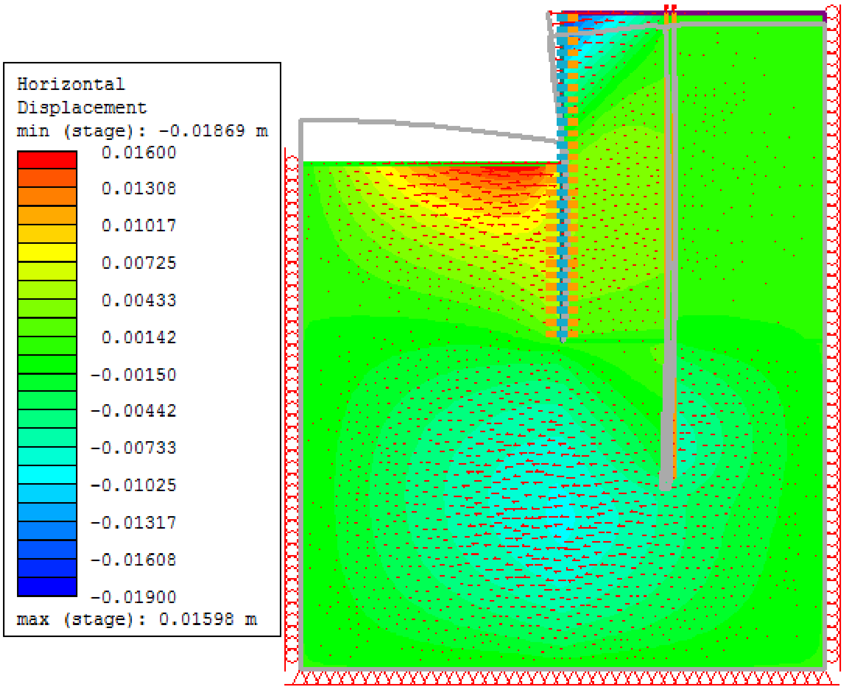

M 90.3: Deformed model (stage 3)

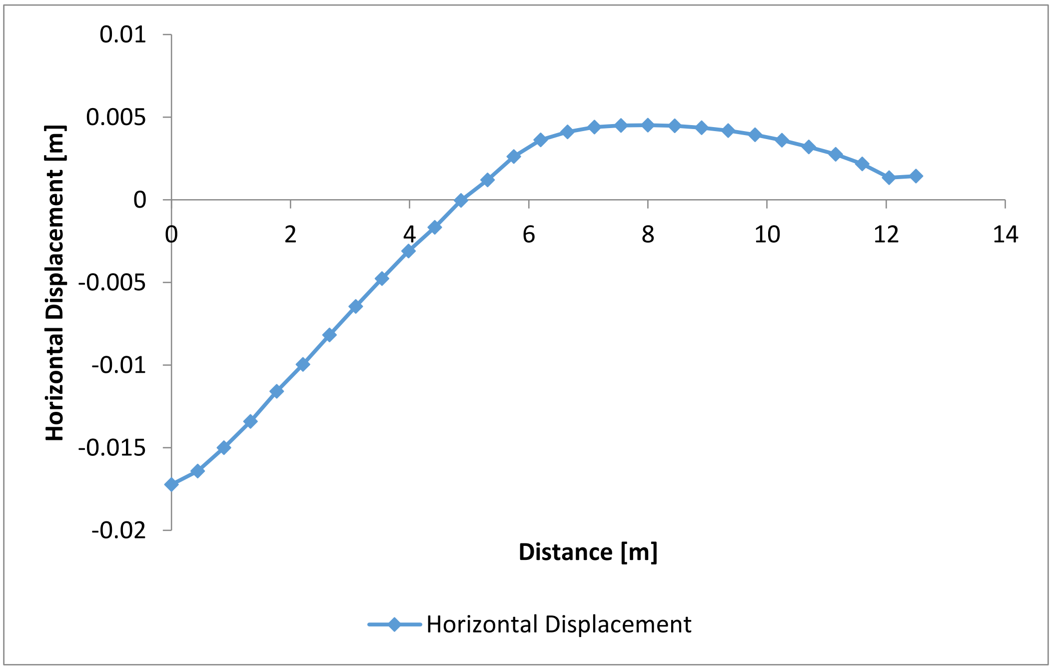

M 90.4: Horizontal displacement of soil along retaining wall

Retaining wall maximum horizontal displacement: -0.01869m

Distance from point of maximum displacement in retaining wall to the top of backfill soil: 0.0m

Model 91:

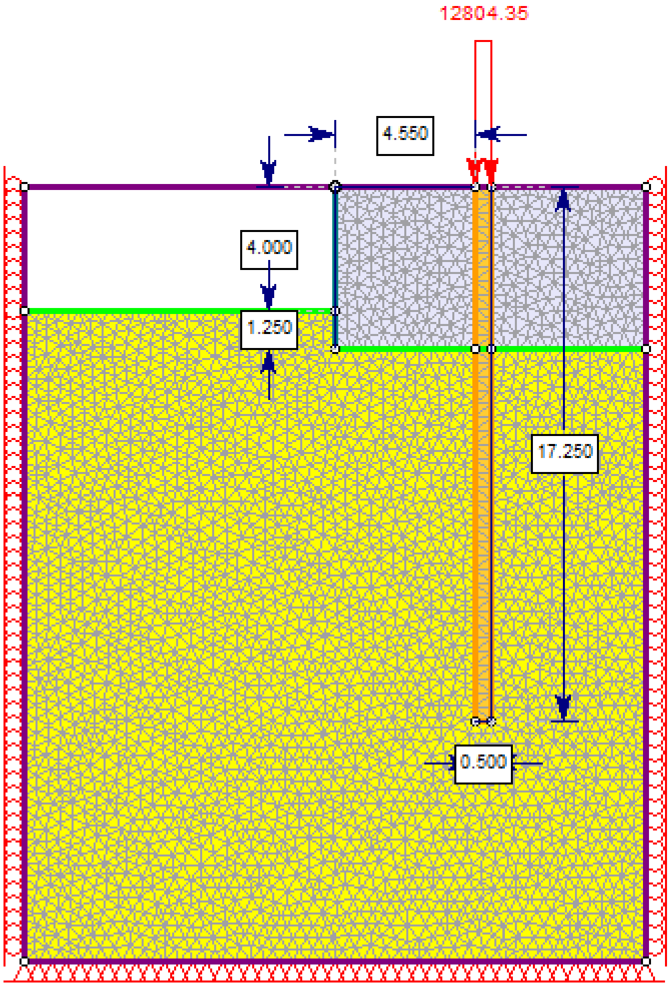

M 91.1: Original model (stage 3)

C_1'	ϕ_1'	γ_1	E_1	C_2'	ϕ_2'	γ_2	E_2	H_1	H_2	H_3	E_3	D_1	D_2	L	Qult
0	45	21	10	50	31	24	23.7	4.00	1.25	1	964895	4.55	0.5	17.25	12804.35

M 91.2: Parameter values

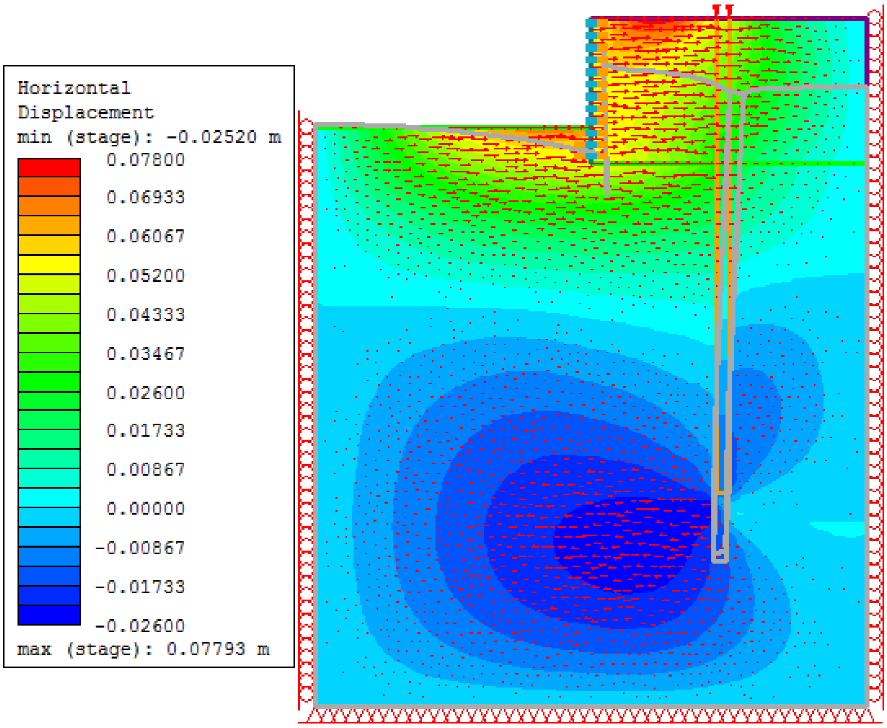

M 91.3: Deformed model (stage 3)

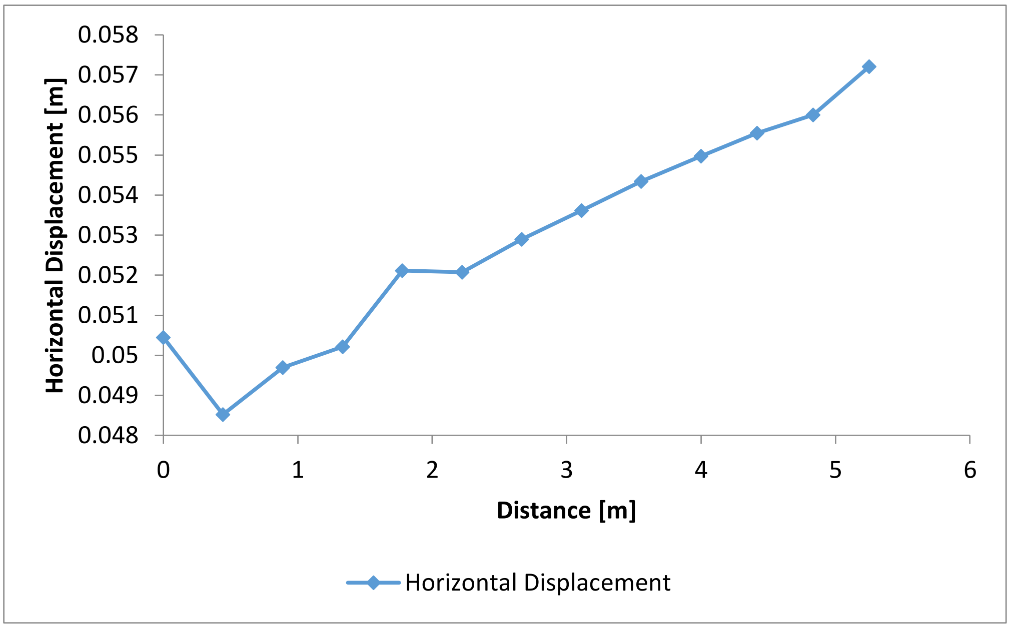

M 91.4: Horizontal displacement of soil along retaining wall

Retaining wall maximum horizontal displacement: 0.0572m

Distance from point of maximum displacement in retaining wall to the top of backfill soil: 5.25m

Model 92:

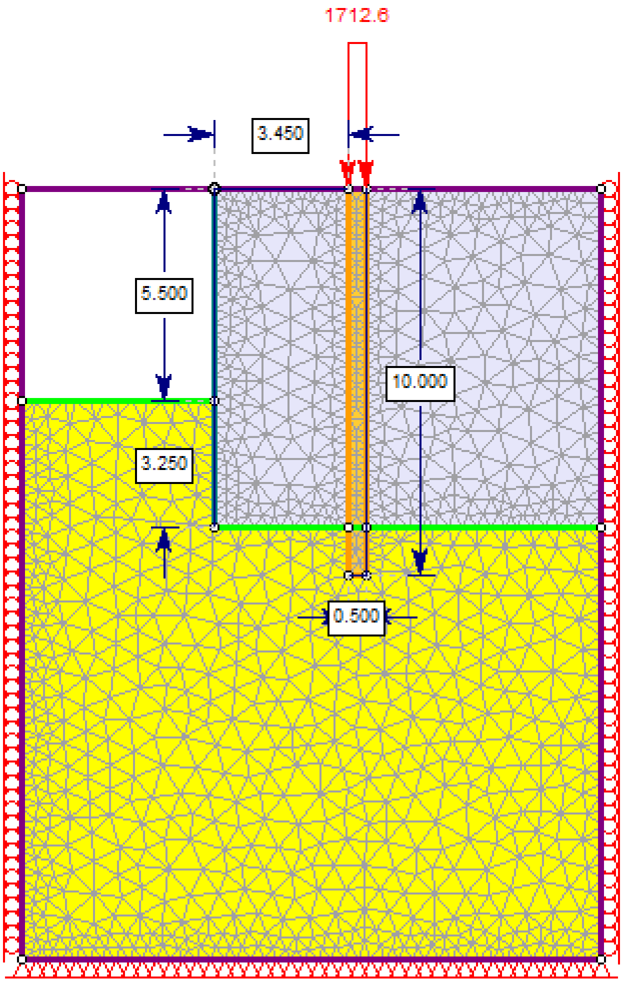

M 92.1: Original model (stage 3)

C_1'	ϕ_1'	γ_1	E_1	C_2'	ϕ_2'	γ_2	E_2	H_1	H_2	H_3	E_3	D_1	D_2	L	Qult
0	38	21	107	51	15	19	38.1	5.50	3.25	0.75	1034083	3.45	0.5	10	1712.6

M 92.2: Parameter values

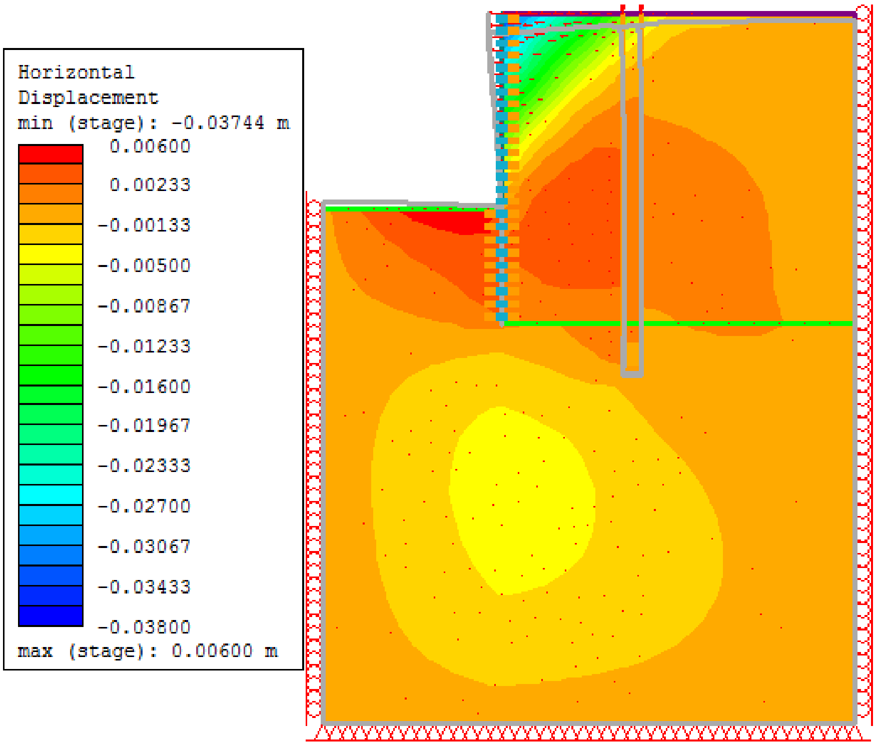

M 92.3: Deformed model (stage 3)

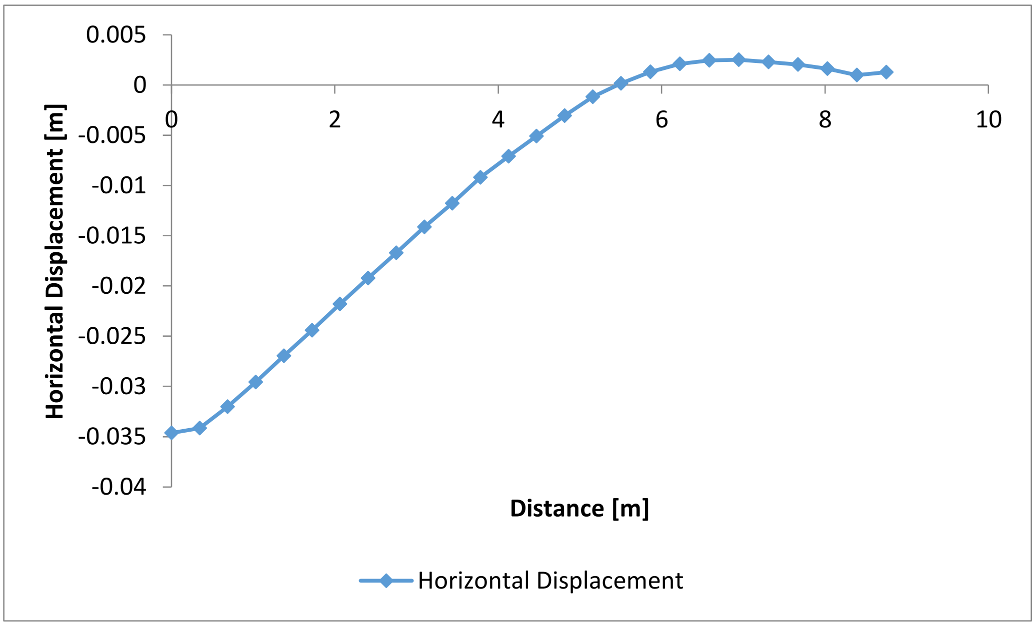

M 92.4: Horizontal displacement of soil along retaining wall

Retaining wall maximum horizontal displacement: -0.03744m

Distance from point of maximum displacement in retaining wall to the top of backfill soil: 0.0m

Model 93:

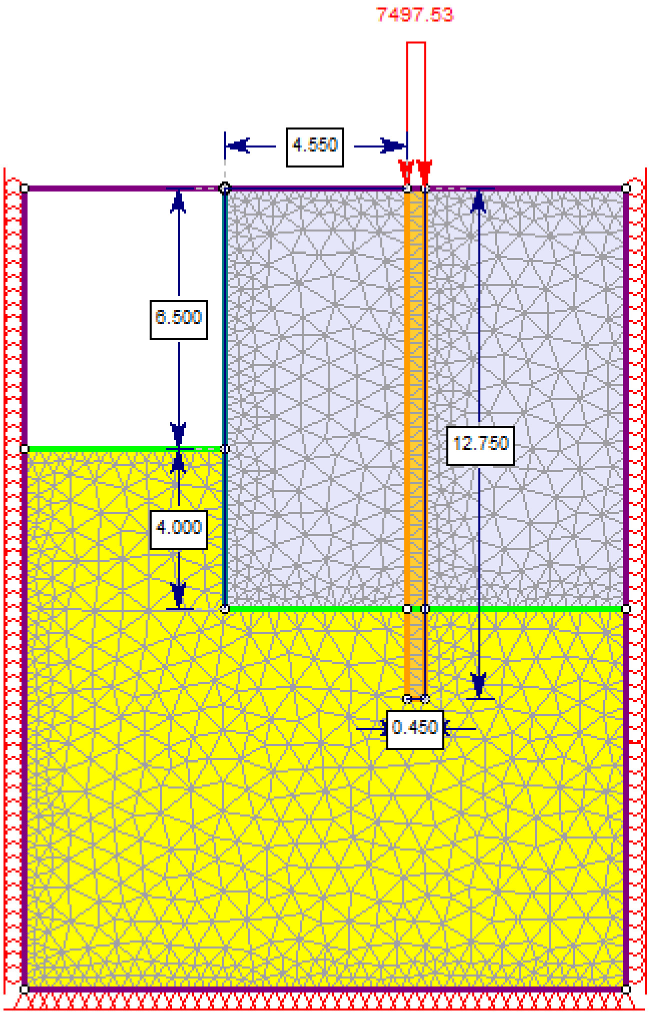

M 93.1: Original model (stage 3)

C_1'	ϕ_1'	γ_1	E_1	C_2'	ϕ_2'	γ_2	E_2	H_1	H_2	H_3	E_3	D_1	D_2	L	Qult
0	37	21	248	57	30	18	13.2	6.50	4	1.5	972029	4.55	0.45	12.75	7497.53

M 93.2: Parameter values

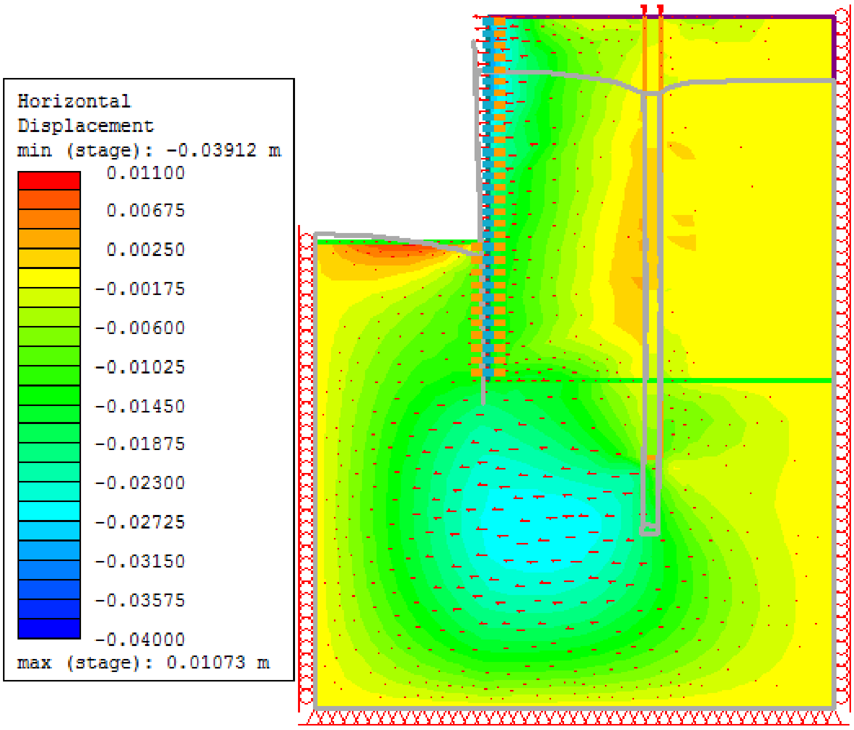

M 93.3: Deformed model (stage 3)

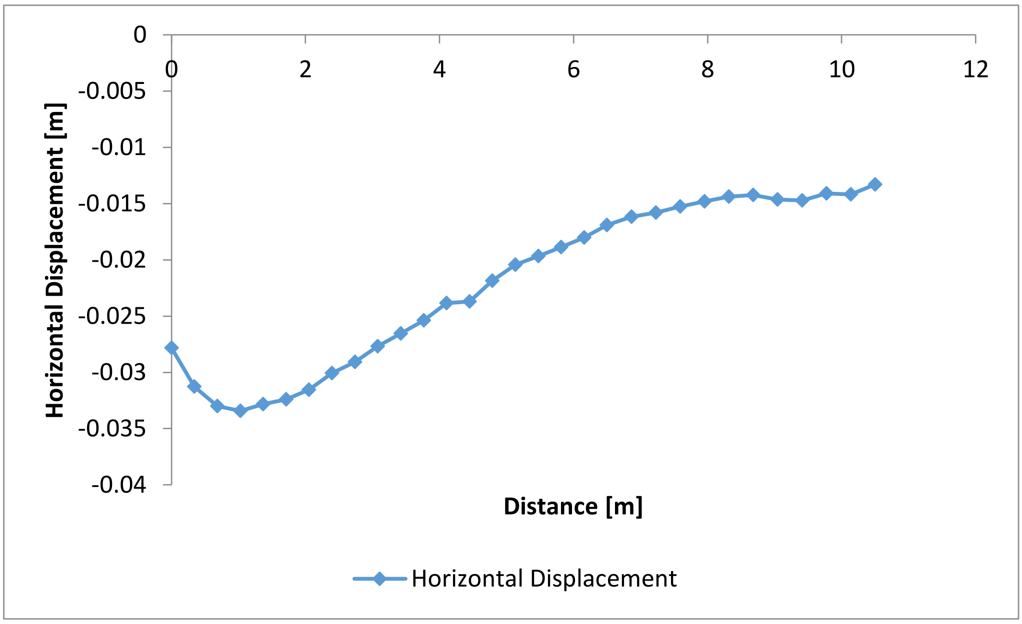

M 93.4: Horizontal displacement of soil along retaining wall

Retaining wall maximum horizontal displacement: -0.03912m

Distance from point of maximum displacement in retaining wall to the top of backfill soil: 0.0m

Model 94:

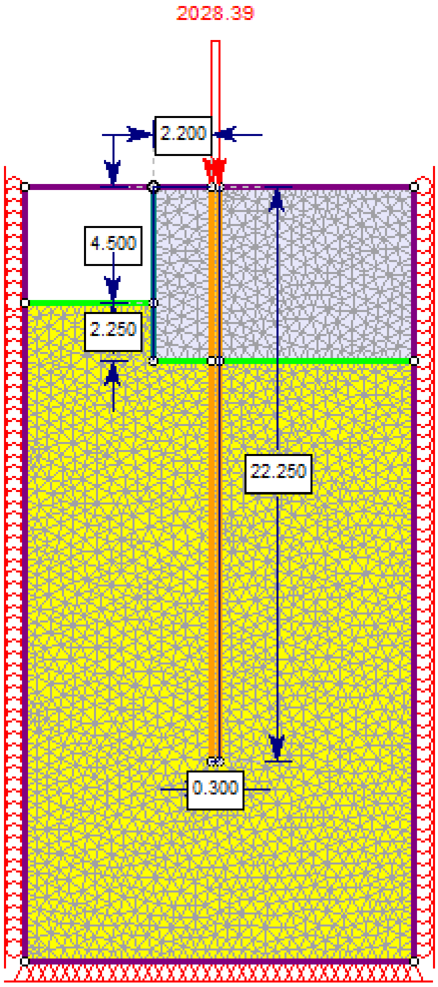

M 94.1: Original model (stage 3)

C_1'	ϕ_1'	γ_1	E_1	C_2'	ϕ_2'	γ_2	E_2	H_1	H_2	H_3	E_3	D_1	D_2	L	Qult
0	32	21	36	55	9	17	8.2	4.50	2.25	1.25	735283	2.2	0.3	22.25	2028.39

M 94.2: Parameter values

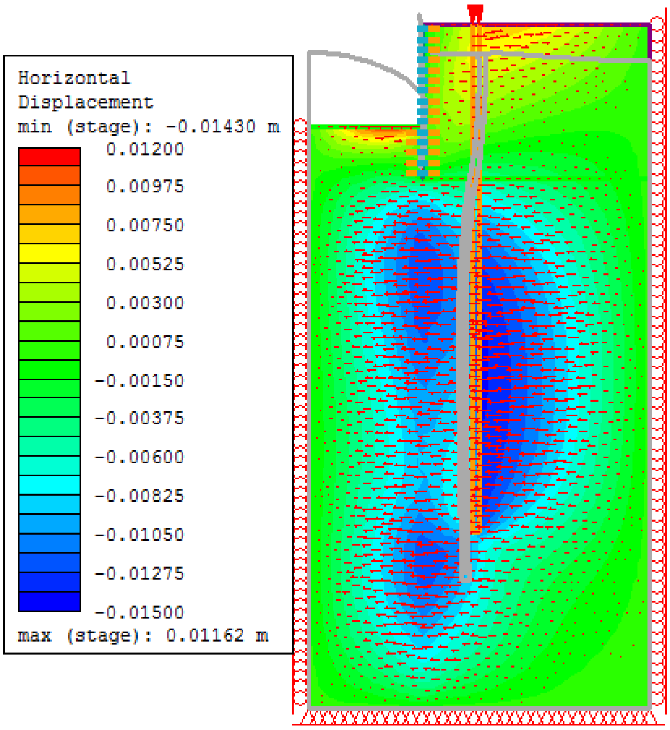

M 94.3: Deformed model (stage 3)

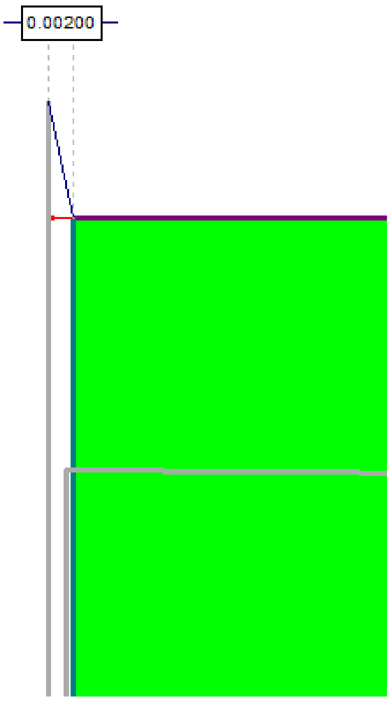

M 94.4: Detailed view of cross-section of retaining wall and soil (stage 3)

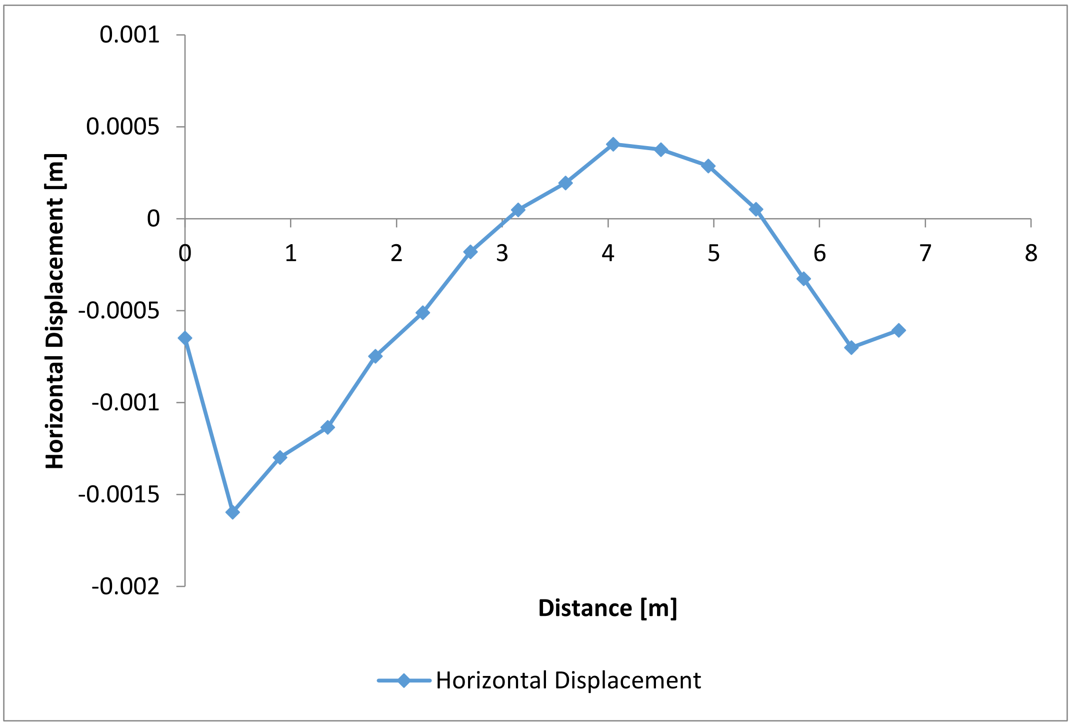

M 94.5: Horizontal displacement of soil along retaining wall

Retaining wall maximum horizontal displacement: -0.002m

Distance from point of maximum displacement in retaining wall to the top of backfill soil: 0.0m

Model 95:

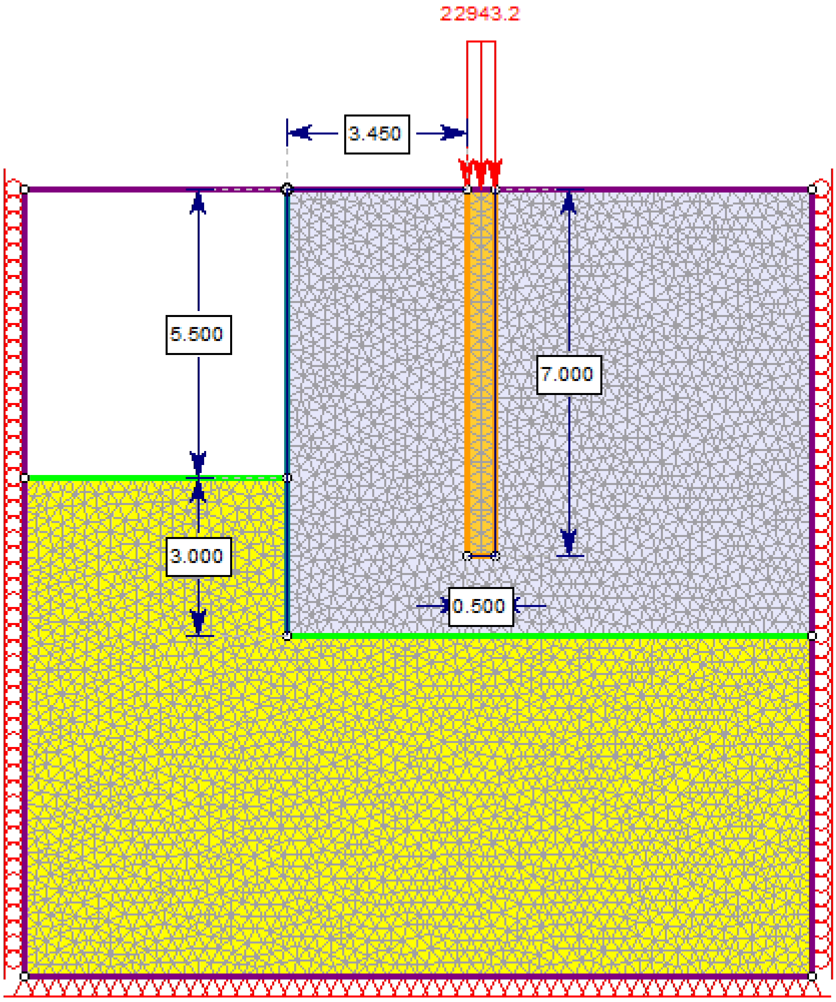

M 95.1: Original model (stage 3)

C'_1	ϕ'_1	γ_1	E_1	C'_2	ϕ'_2	γ_2	E_2	H_1	H_2	H_3	E_3	D_1	D_2	L	Qult
0	40	21	107	51	20	19	38.1	5.50	3	0.75	1034083	3.45	0.5	7	2943.2

M 95.2: Parameter values

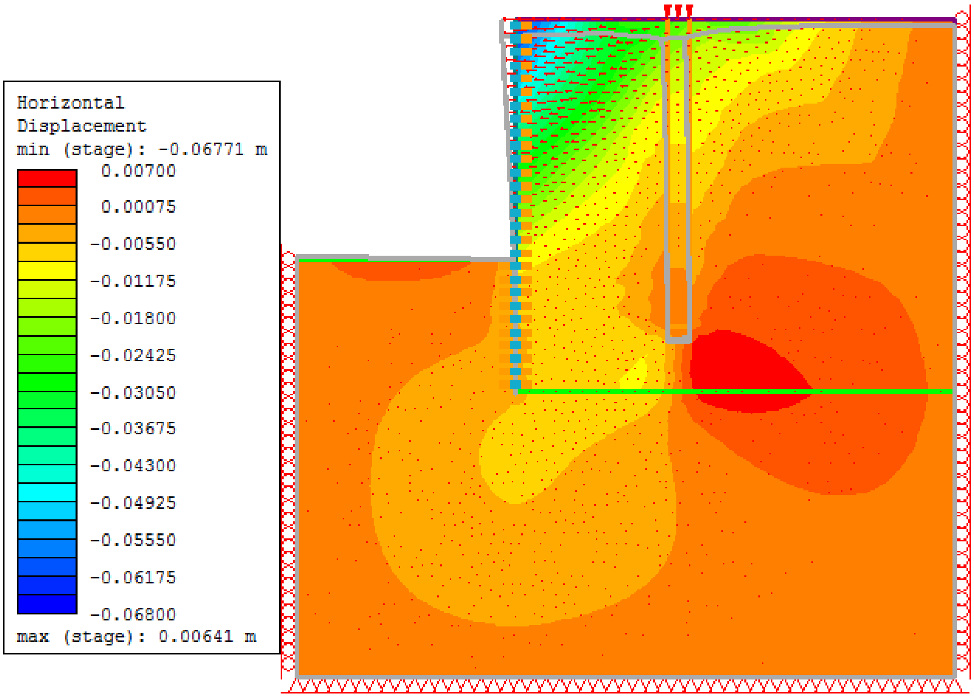

M 95.3: Deformed model (stage 3)

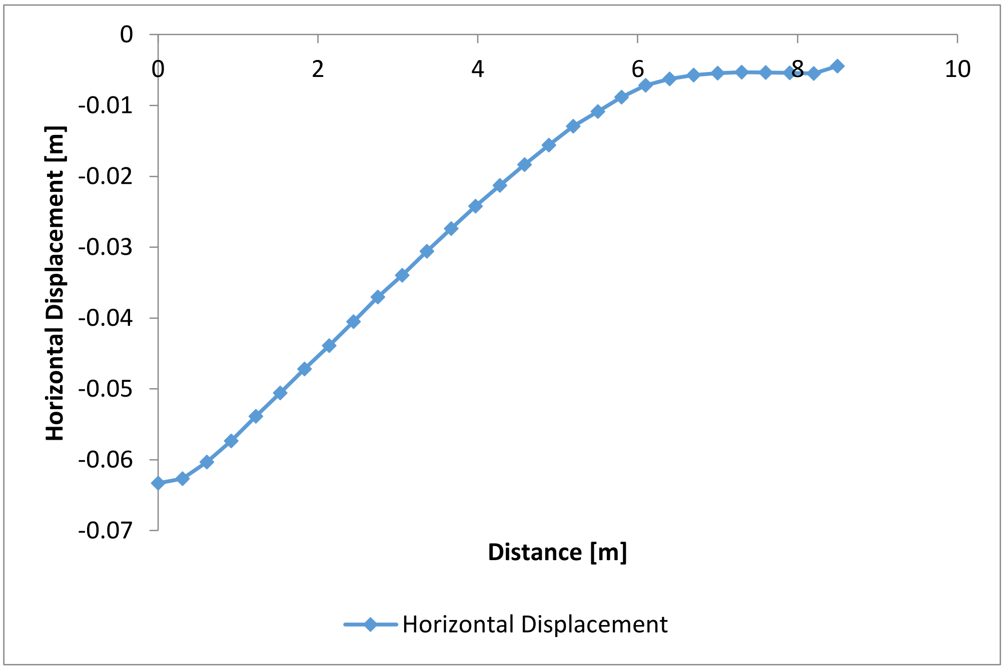

M 95.4: Horizontal displacement of soil along retaining wall

Retaining wall maximum horizontal displacement: -0.06771m

Distance from point of maximum displacement in retaining wall to the top of backfill soil: 0.0m

Model 96:

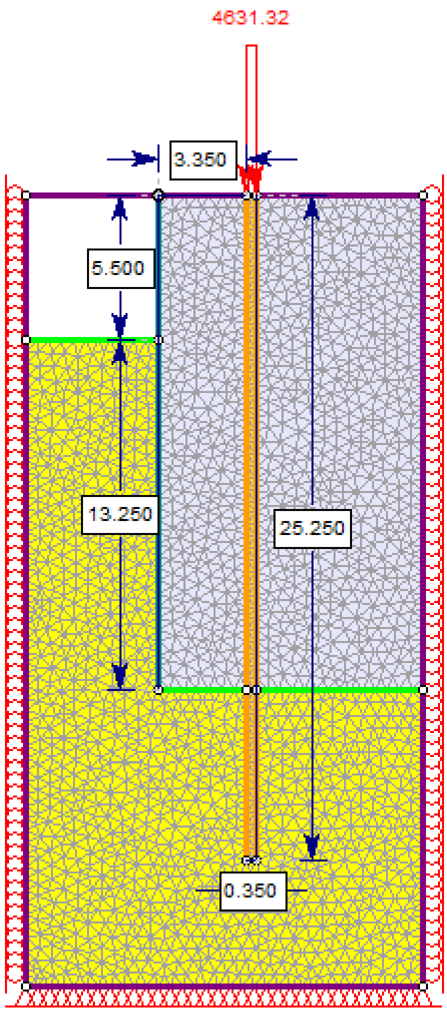

M 96.1: Original model (stage 3)

C_1'	ϕ_1'	γ_1	E_1	C_2'	ϕ_2'	γ_2	E_2	H_1	H_2	H_3	E_3	D_1	D_2	L	Qult
0	37	19	227	29	19	17	38.1	5.50	13.25	1	761964	3.35	0.35	25.25	4631.32

M 96.2: Parameter values

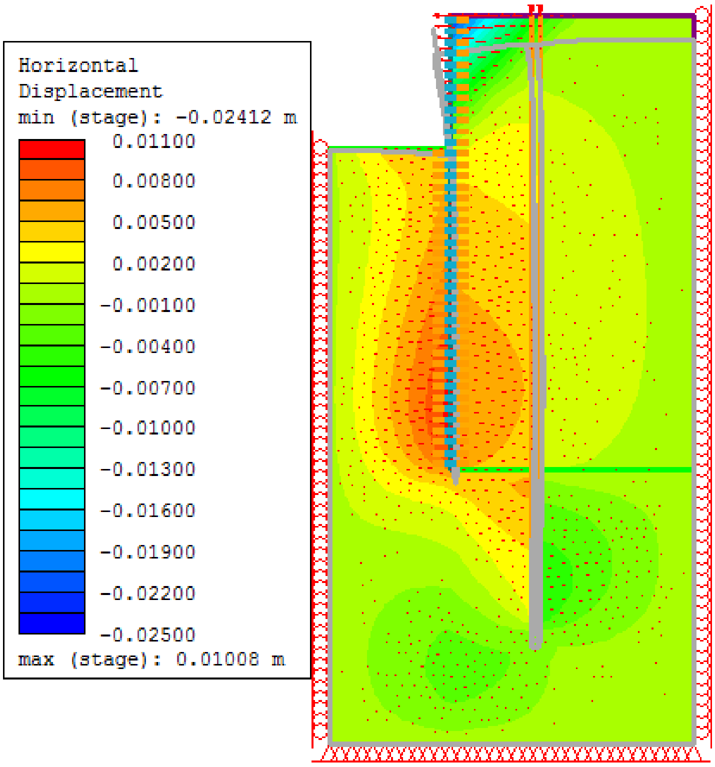

M 96.3: Deformed model (stage 3)

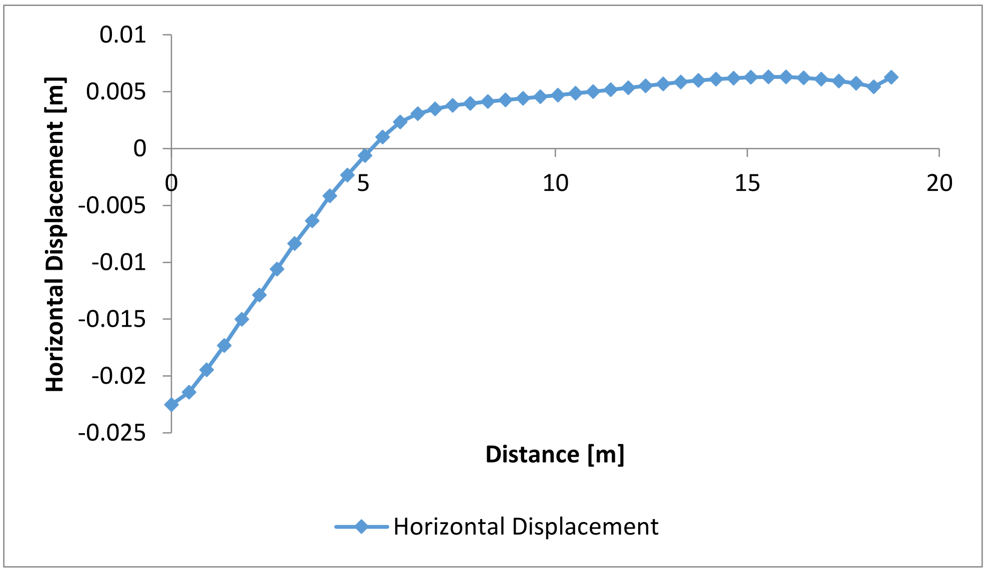

M 96.4: Horizontal displacement of soil along retaining wall

Retaining wall maximum horizontal displacement: -0.02412m

Distance from point of maximum displacement in retaining wall to the top of backfill soil: 0.0m

Model 97:

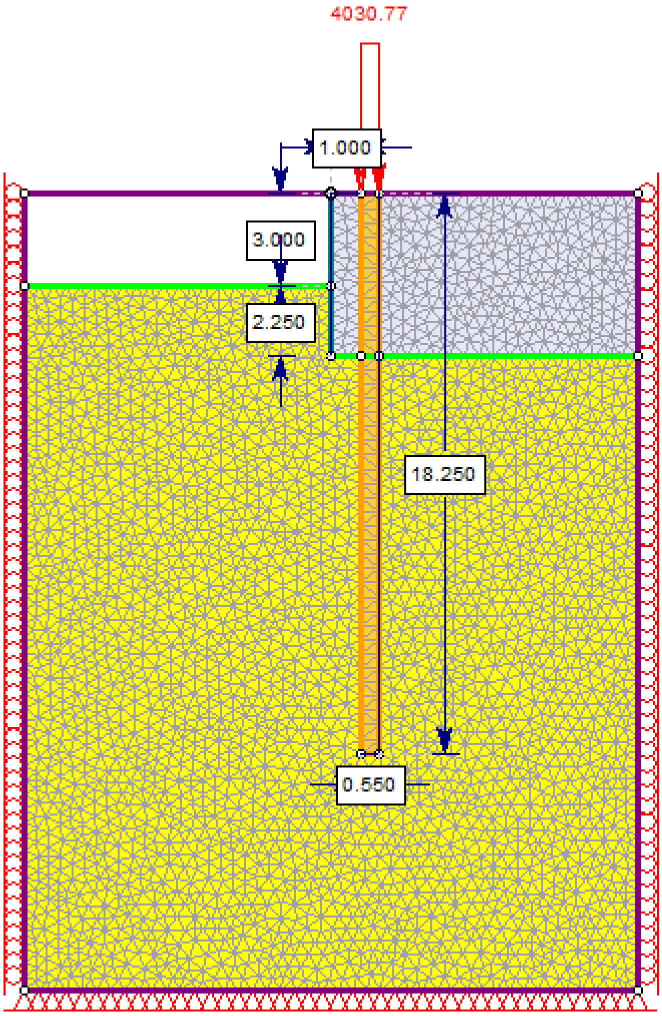

M 97.1: Original model (stage 3)

C_1'	ϕ_1'	γ_1	E_1	C_2'	ϕ_2'	γ_2	E_2	H_1	H_2	H_3	E_3	D_1	D_2	L	Qult
0	38	22	175	25	23	22	5.0	3.00	2.25	0.5	711252	1	0.55	18.25	4030.77

M 97.2: Parameter values

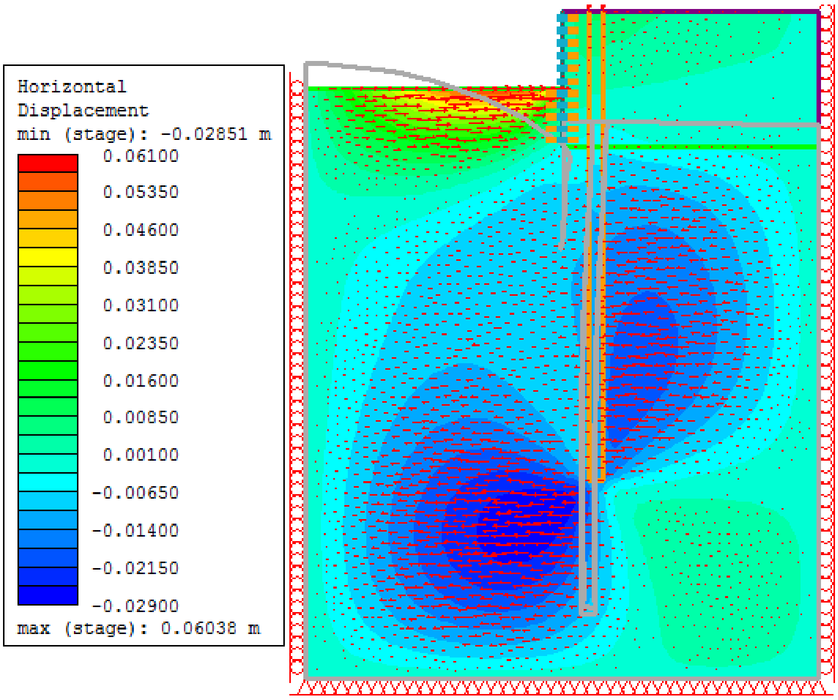

M 97.3: Deformed model (stage 3)

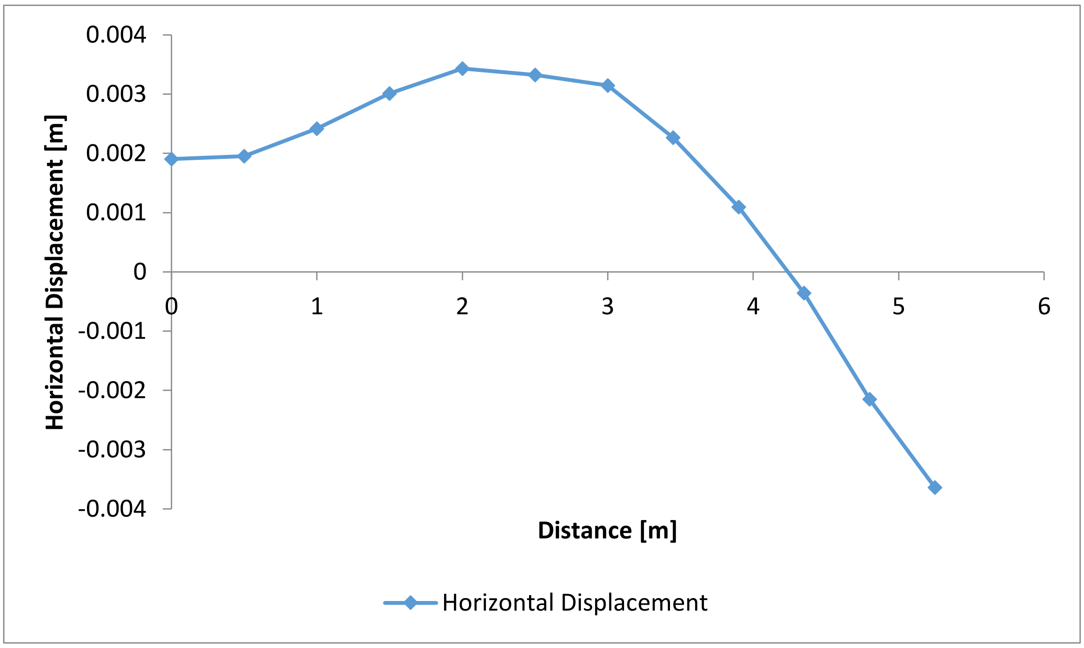

M 97.4: Horizontal displacement of soil along retaining wall

Retaining wall maximum horizontal displacement: -0.00364m

Distance from point of maximum displacement in retaining wall to the top of backfill soil: 5.25m

Model 98:

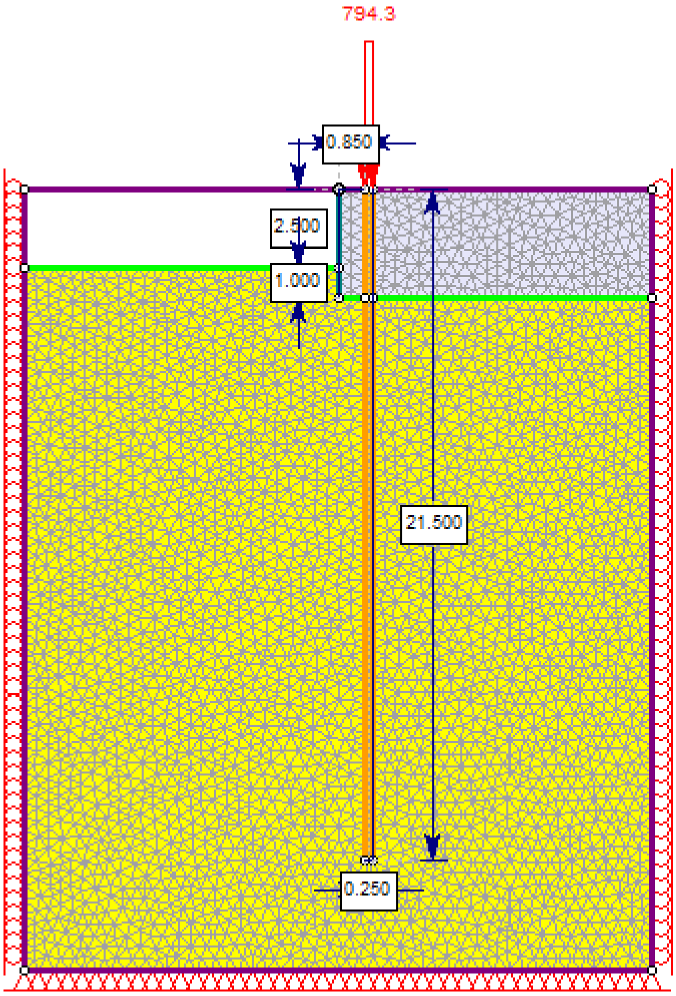

M 98.1: Original model (stage 3)

C_1'	ϕ_1'	γ_1	E_1	C_2'	ϕ_2'	γ_2	E_2	H_1	H_2	H_3	E_3	D_1	D_2	L	Qult
0	28	22	238	52	2	18	20.7	2.50	1	1	771263	0.85	0.25	21.5	794.3

M 98.2: Parameter values

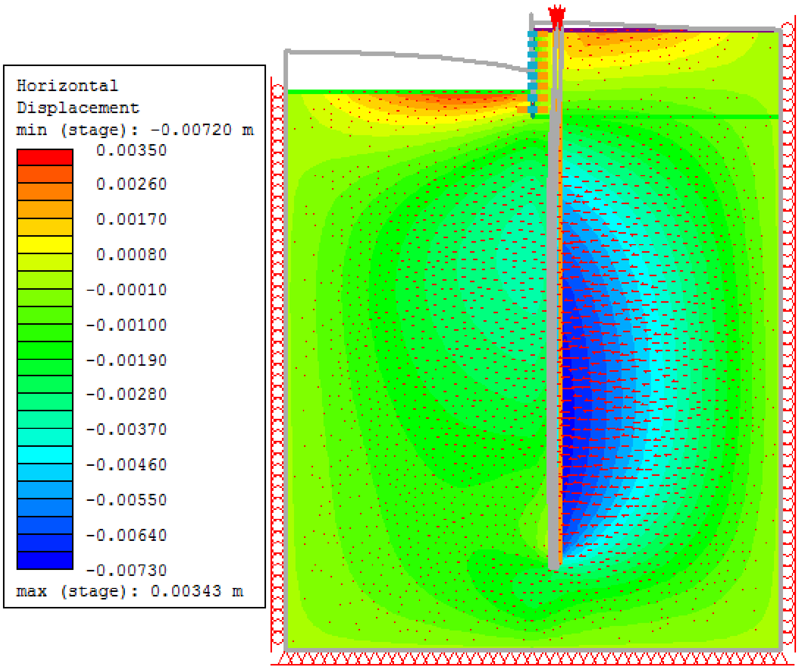

M 98.3: Deformed model (stage 3)

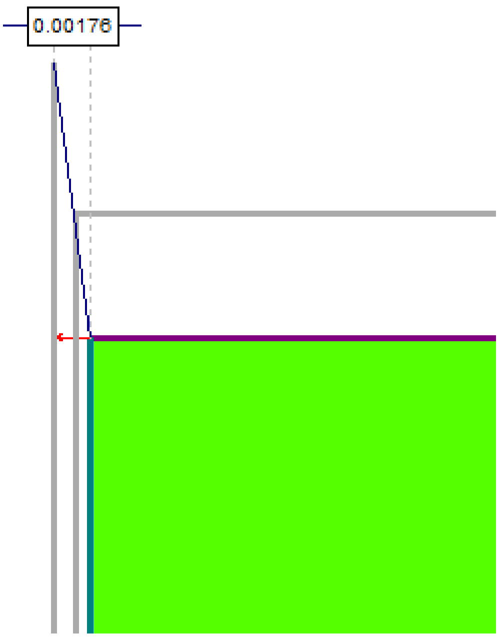

M 98.4: Detailed view of cross-section of retaining wall and soil (stage 3)

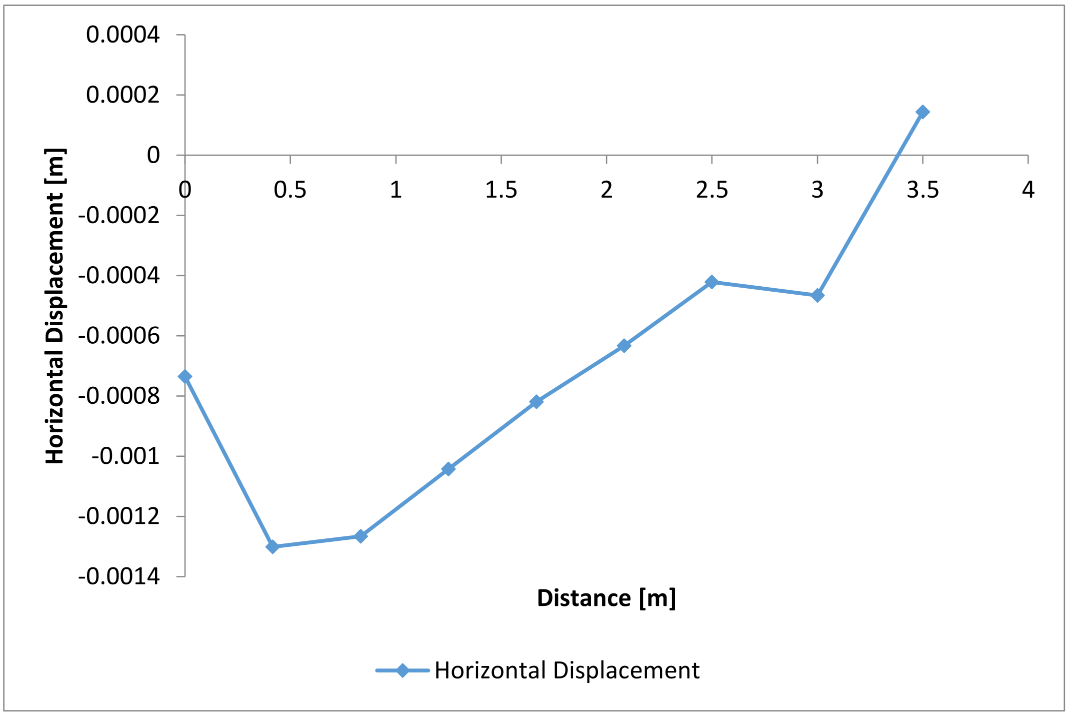

M 98.5: Horizontal displacement of soil along retaining wall

Retaining wall maximum horizontal displacement: -0.00176m

Distance from point of maximum displacement in retaining wall to the top of backfill soil: 0.0m

Model 99:

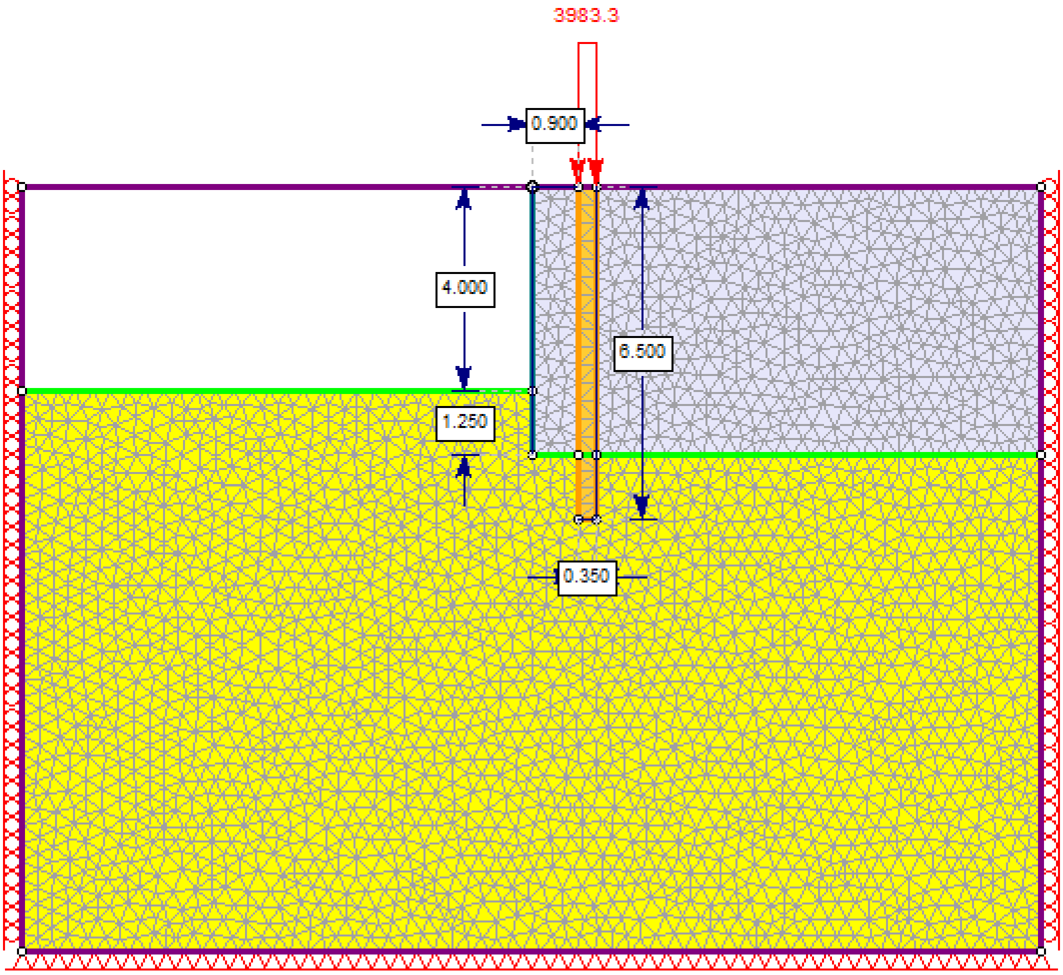

M 99.1: Original model (stage 3)

C_1'	ϕ_1'	γ_1	E_1	C_2'	ϕ_2'	γ_2	E_2	H_1	H_2	H_3	E_3	D_1	D_2	L	Qult
0	41	19	123	58	28	24	41.2	4.00	1.25	0.5	1052548	0.9	0.35	6.5	3983.3

M 99.2: Parameter values

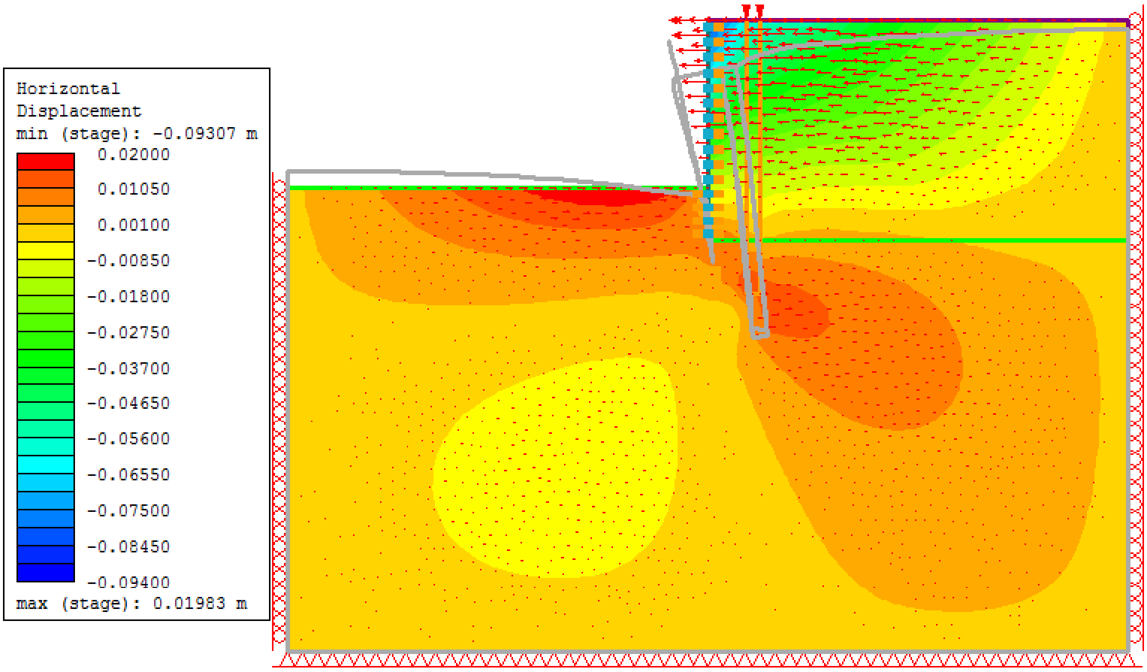

M 99.3: Deformed model (stage 3)

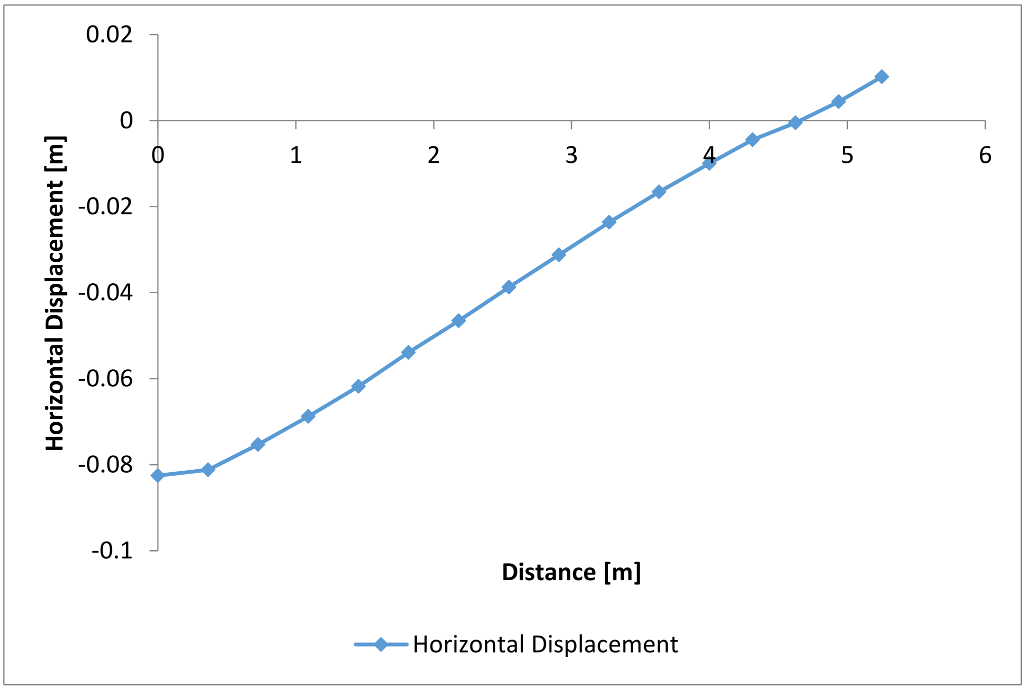

M 99.4: Horizontal displacement of soil along retaining wall

Retaining wall maximum horizontal displacement: -0.09307m

Distance from point of maximum displacement in retaining wall to the top of backfill soil: 0.0m

Model 100:

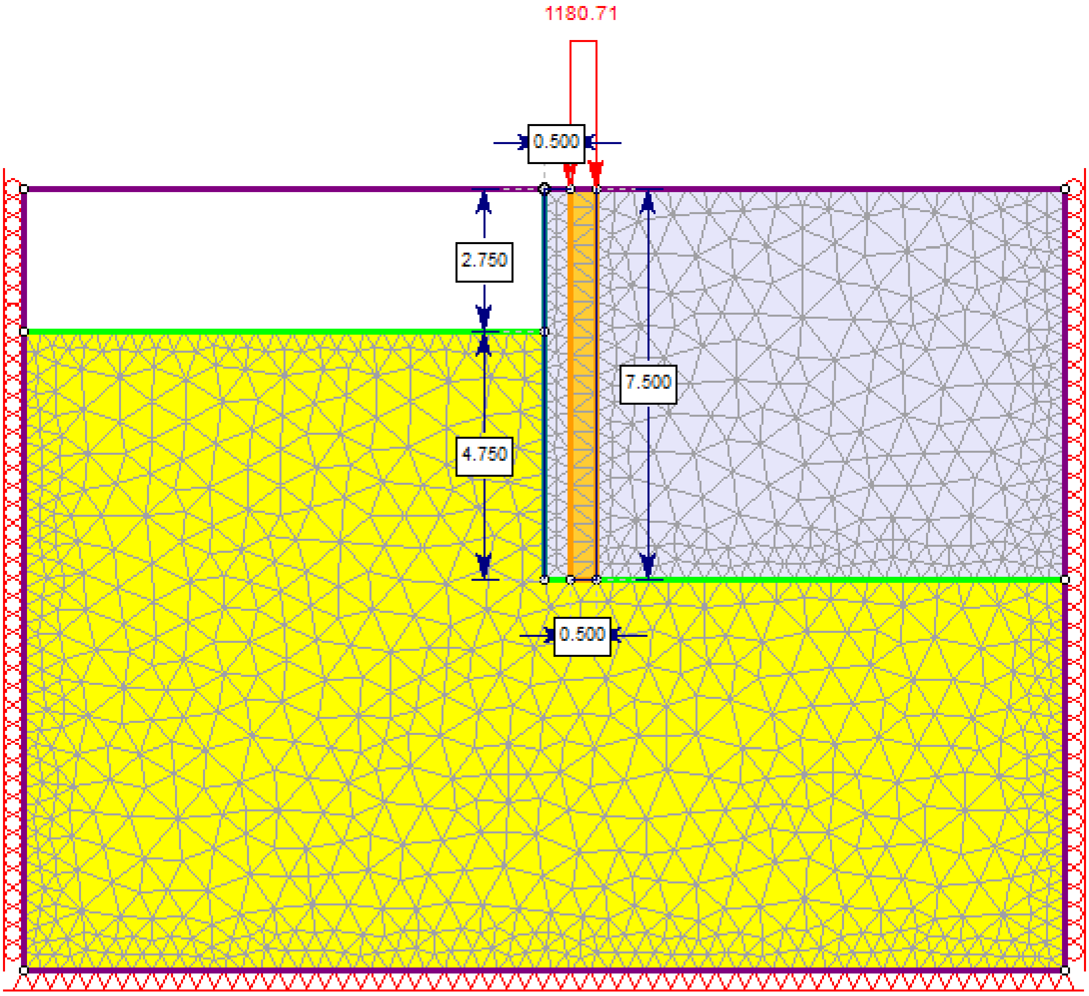

M 100.1: Original model (stage 3)

C_1'	ϕ_1'	γ_1	E_1	C_2'	ϕ_2'	γ_2	E_2	H_1	H_2	H_3	E_3	D_1	D_2	L	Qult
0	30	21	253	15	29	23	19.3	2.75	4.75	1.5	812624	0.5	0.5	7.5	1180.71

M 100.2: Parameter values

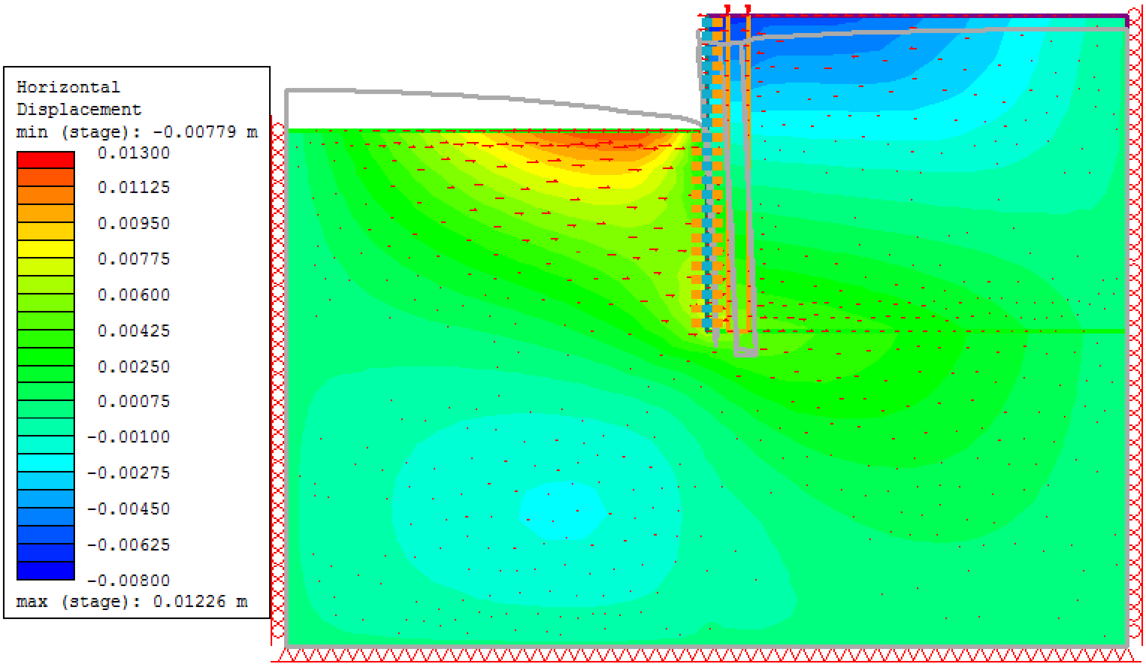

M 100.3: Deformed model (stage 3)

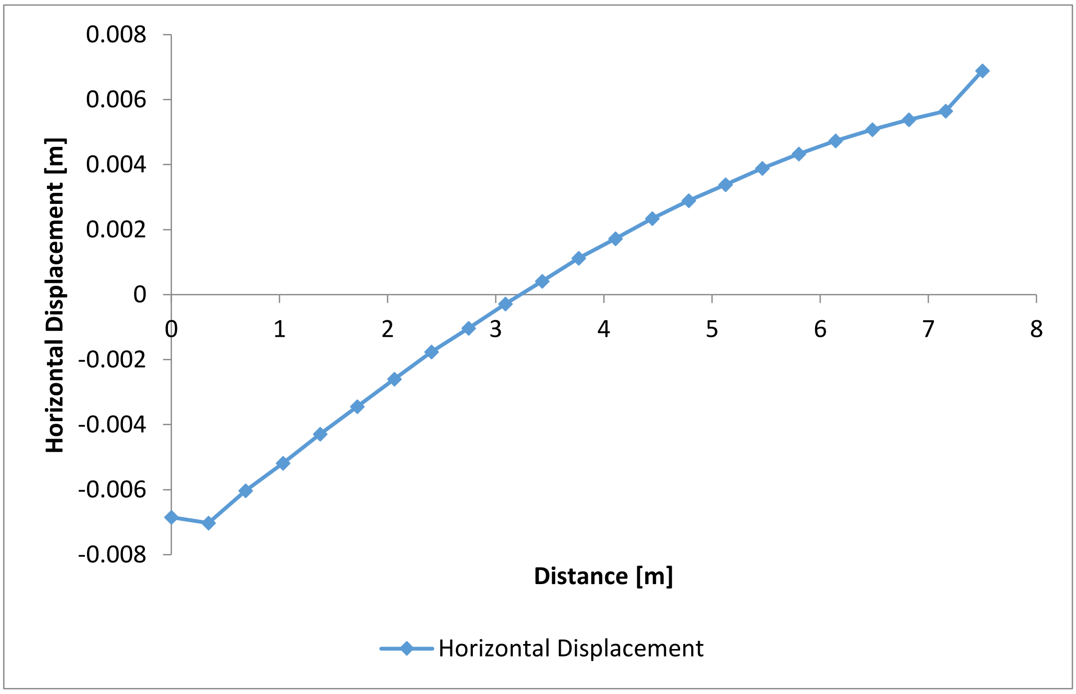

M 100.4: Horizontal displacement of soil along retaining wall

Retaining wall maximum horizontal displacement: -0.00779m

Distance from point of maximum displacement in retaining wall to the top of backfill soil: 0.0m

Model 101:

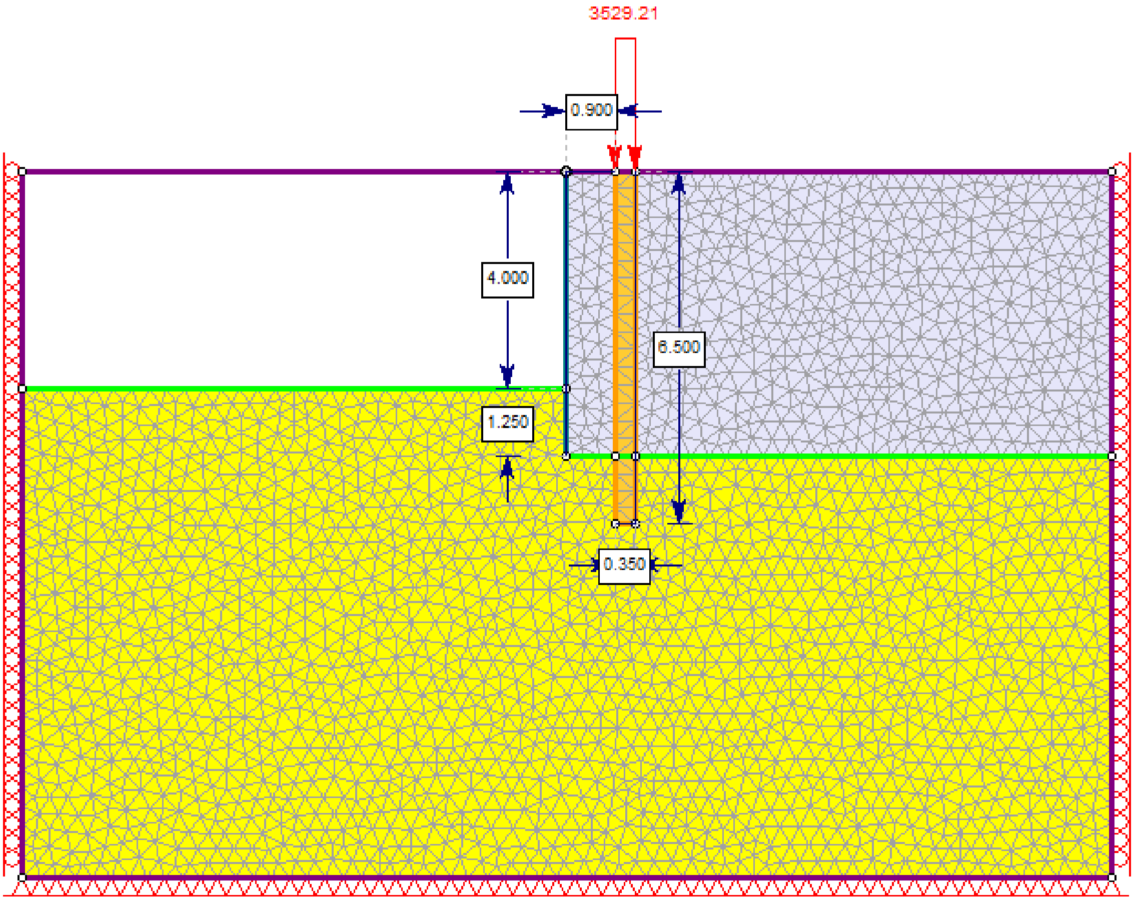

M 101.1: Original model (stage 3)

C_1'	ϕ_1'	γ_1	E_1	C_2'	ϕ_2'	γ_2	E_2	H_1	H_2	H_3	E_3	D_1	D_2	L	Qult
0	41	19	123	58	27	24	41.2	4.00	1.25	0.5	1052548	0.9	0.35	6.5	3529.21

M 101.2: Parameter values

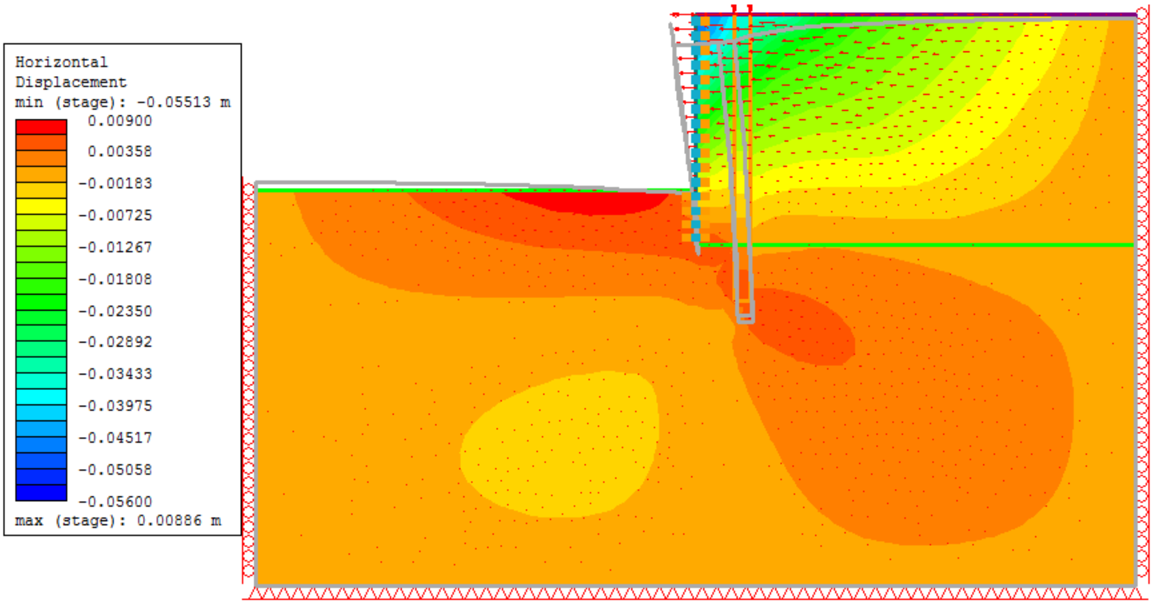

M 101.3: Deformed model (stage 3)

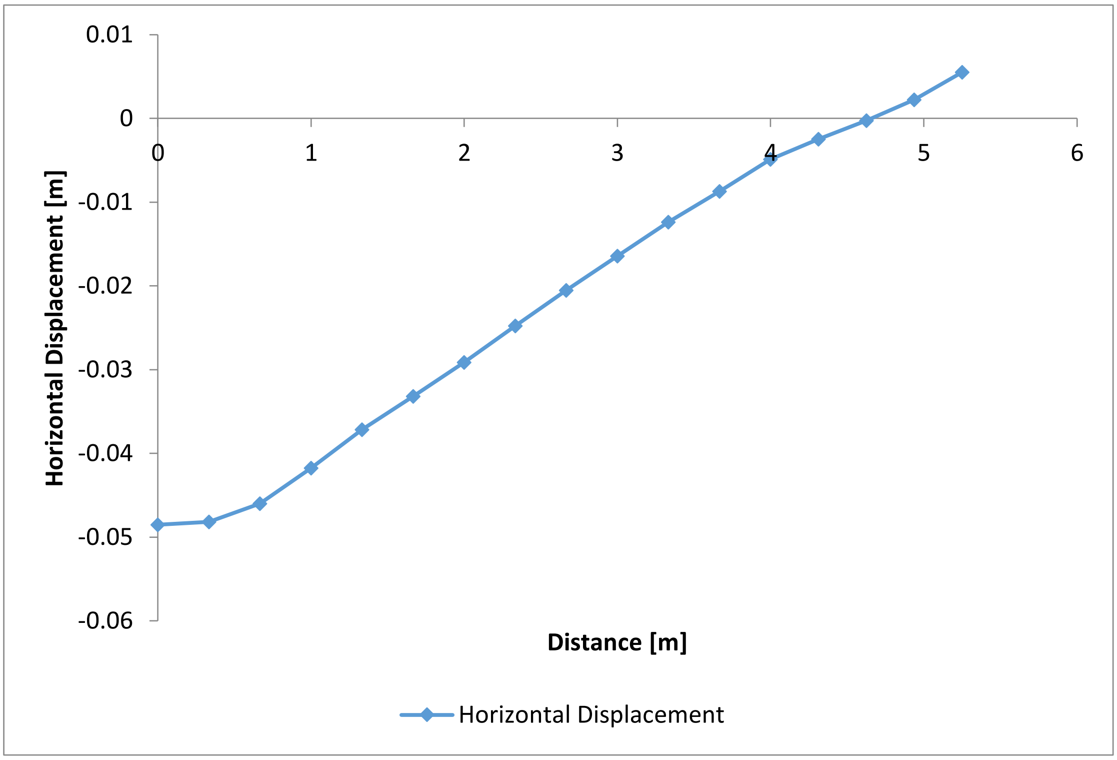

M 101.4: Horizontal displacement of soil along retaining wall

Retaining wall maximum horizontal displacement: -0.05513m

Distance from point of maximum displacement in retaining wall to the top of backfill soil: 0.0m

Model 102:

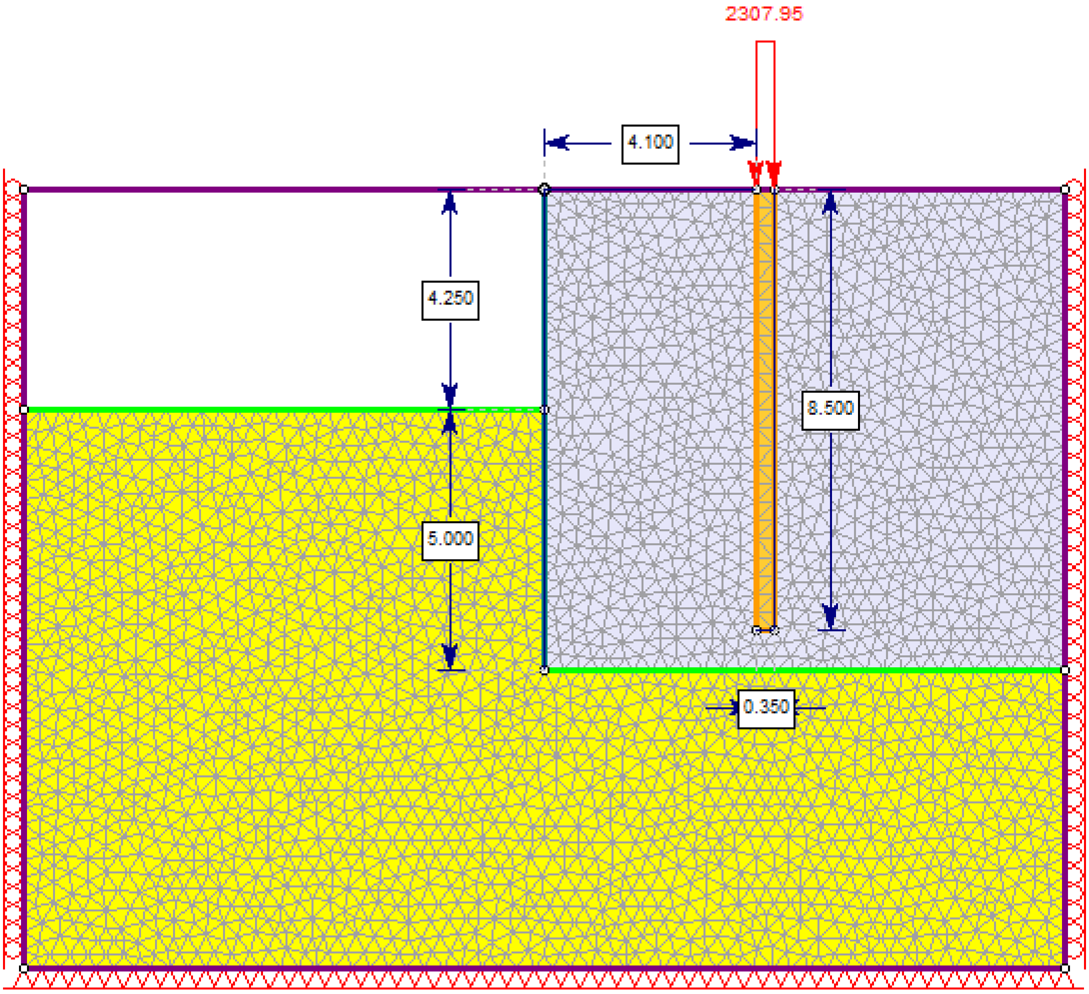

M 102.1: Original model (stage 3)

C'_1	ϕ'_1	γ_1	E_1	C'_2	ϕ'_2	γ_2	E_2	H_1	H_2	H_3	E_3	D_1	D_2	L	Qult
0	39	19	9	25	15	24	31.7	4.25	5	0.75	753682	4.1	0.35	8.5	2307.95

M 102.2: Parameter values

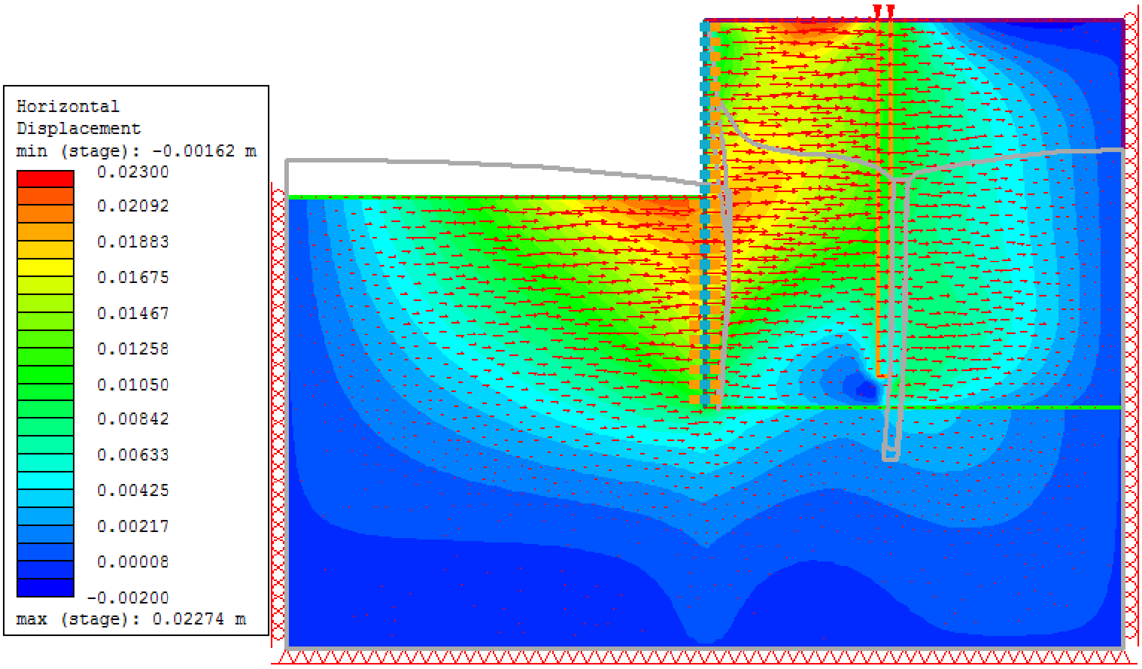

M 102.3: Deformed model (stage 3)

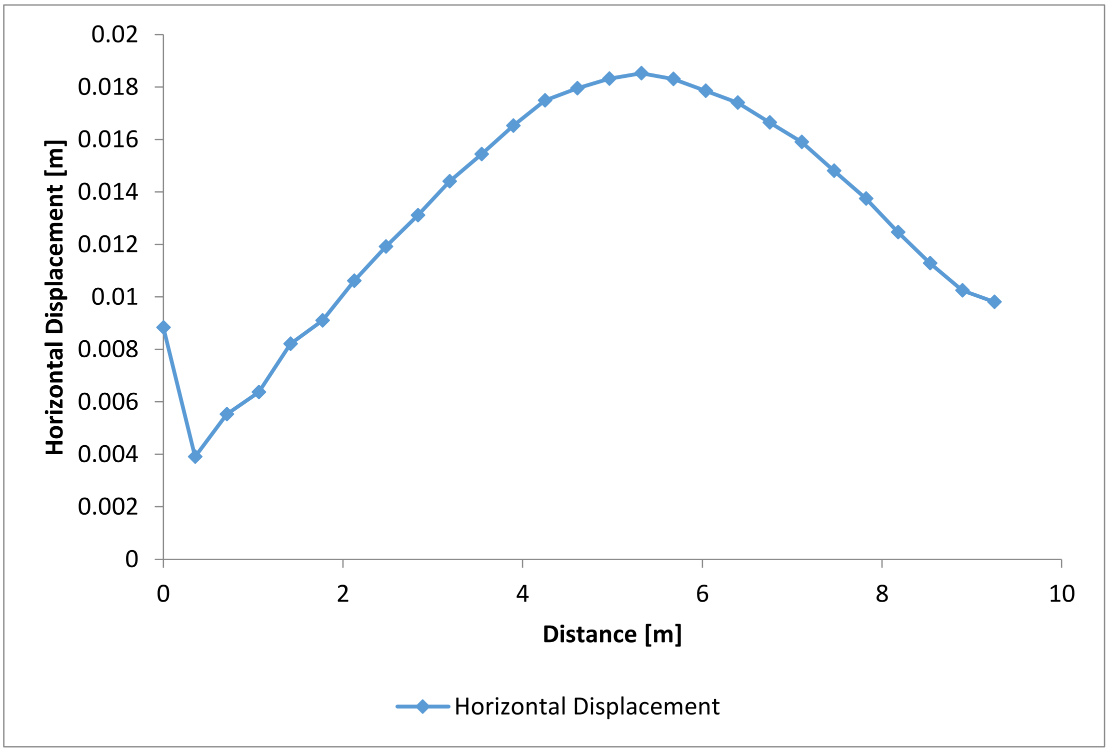

M 102.5: Horizontal displacement of soil along retaining wall

Retaining wall maximum horizontal displacement: 0.01853m

Distance from point of maximum displacement in retaining wall to the top of backfill soil: 5.32m

Model 103:

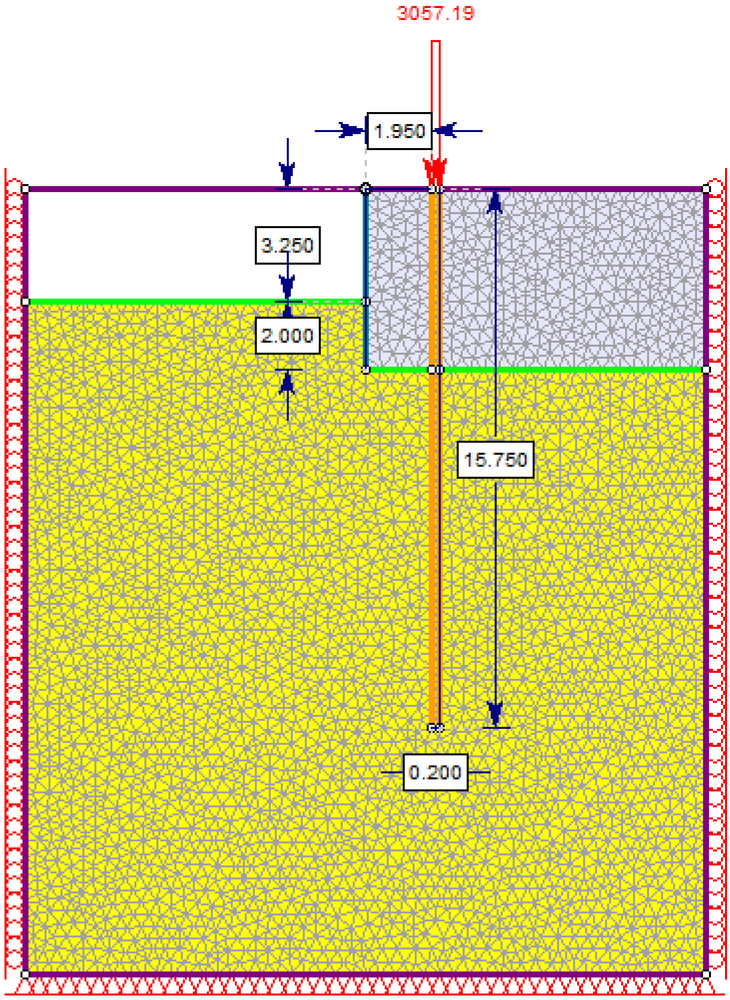

M 103.1: Original model (stage 3)

C'_1	ϕ'_1	γ_1	E_1	C'_2	ϕ'_2	γ_2	E_2	H_1	H_2	H_3	E_3	D_1	D_2	L	Qult
0	38	22	202	31	20	18	16.2	3.25	2	1	994453	1.95	0.2	15.75	3057.19

M 103.2: Parameter values

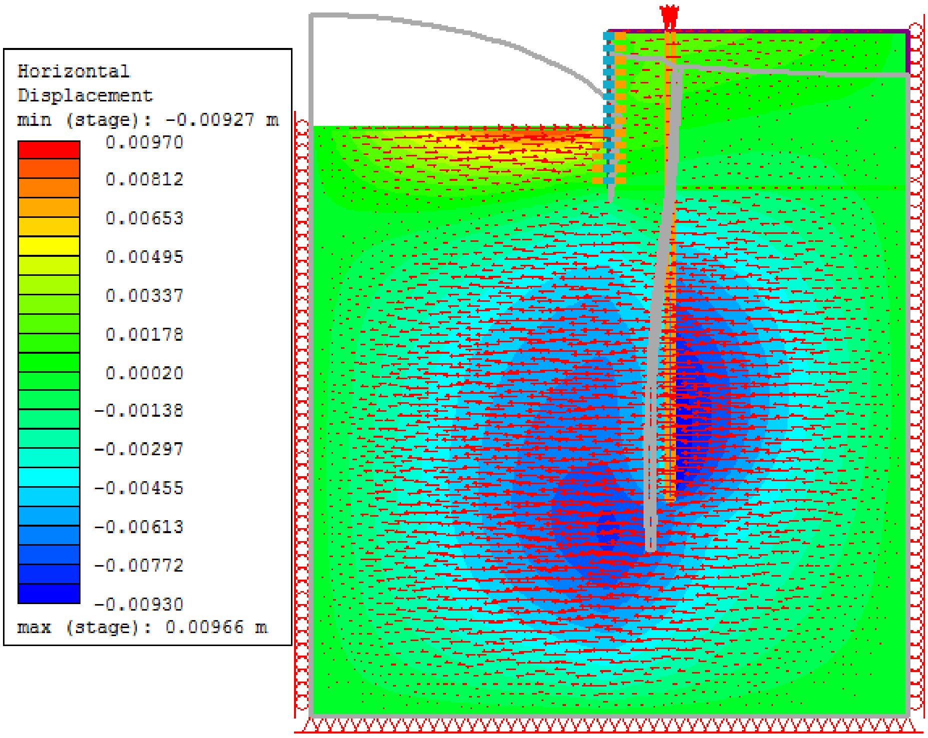

M 103.3: Deformed model (stage 3)

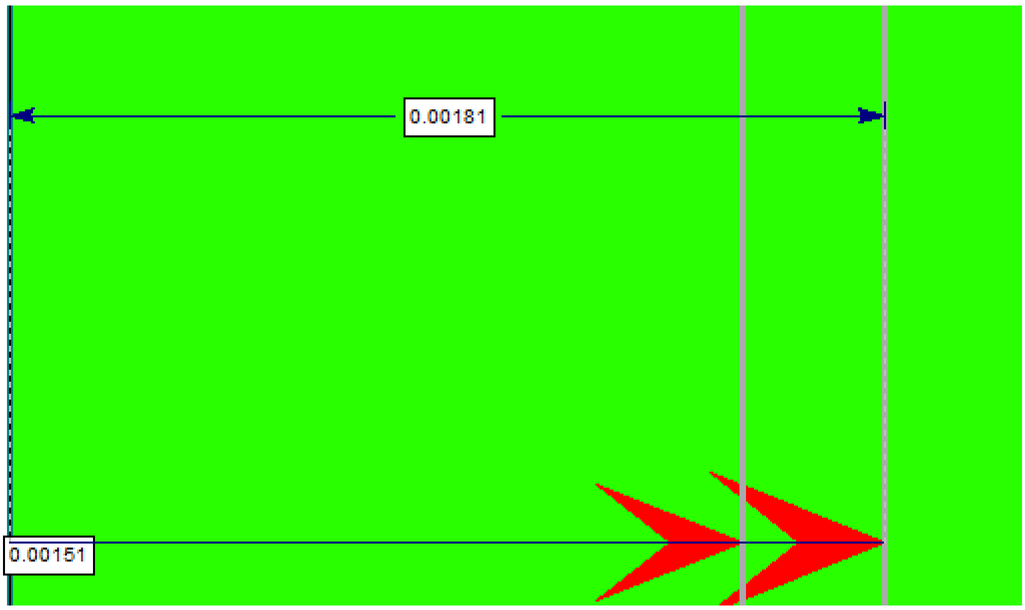

M 103.4: Detailed view of cross-section of retaining wall and soil (stage 3)

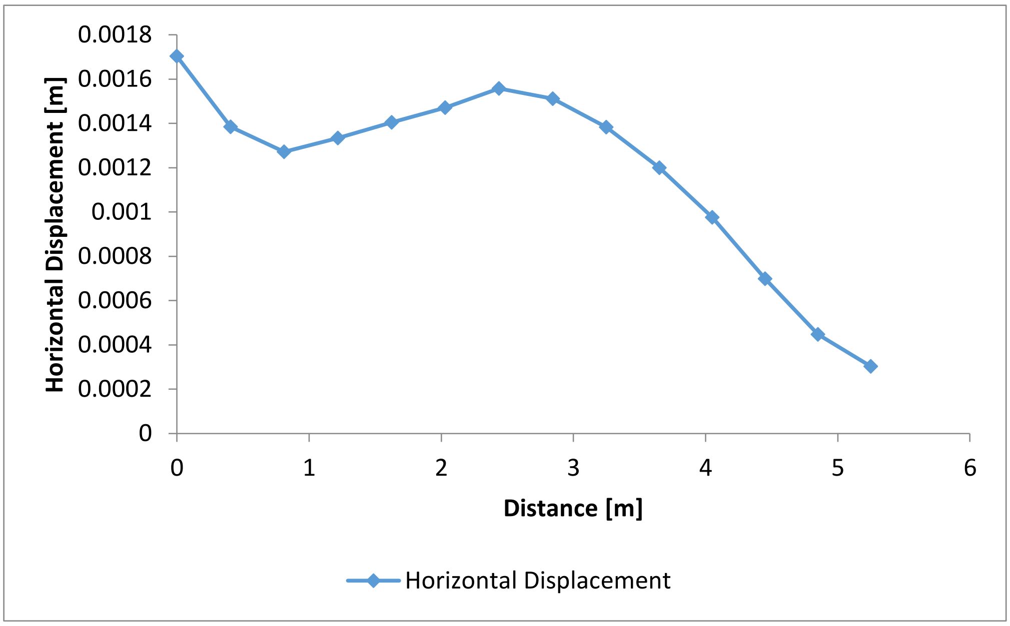

M 103.5: Horizontal displacement of soil along retaining wall

Retaining wall maximum horizontal displacement: 0.0181m

Distance from point of maximum displacement in retaining wall to the top of backfill soil: 2.844m

Model 104:

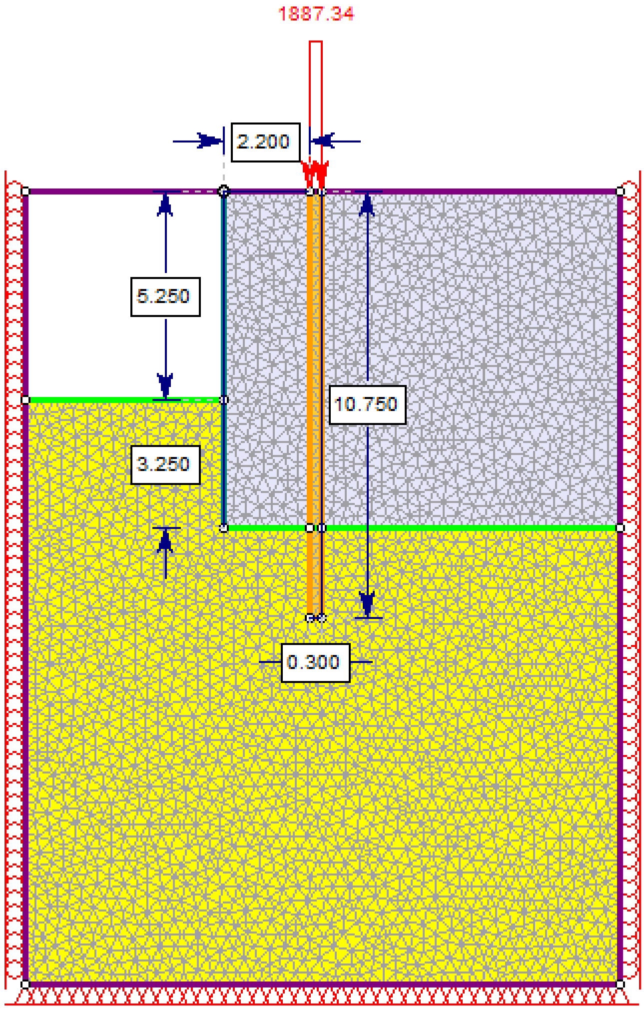

M 104.1: Original model (stage 3)

C_1'	ϕ_1'	γ_1	E_1	C_2'	ϕ_2'	γ_2	E_2	H_1	H_2	H_3	E_3	D_1	D_2	L	Qult
0	35	20	57	48	15	18	8.2	5.25	3.25	1	991164	2.2	0.3	10.75	1887.34

M 104.2: Parameter values

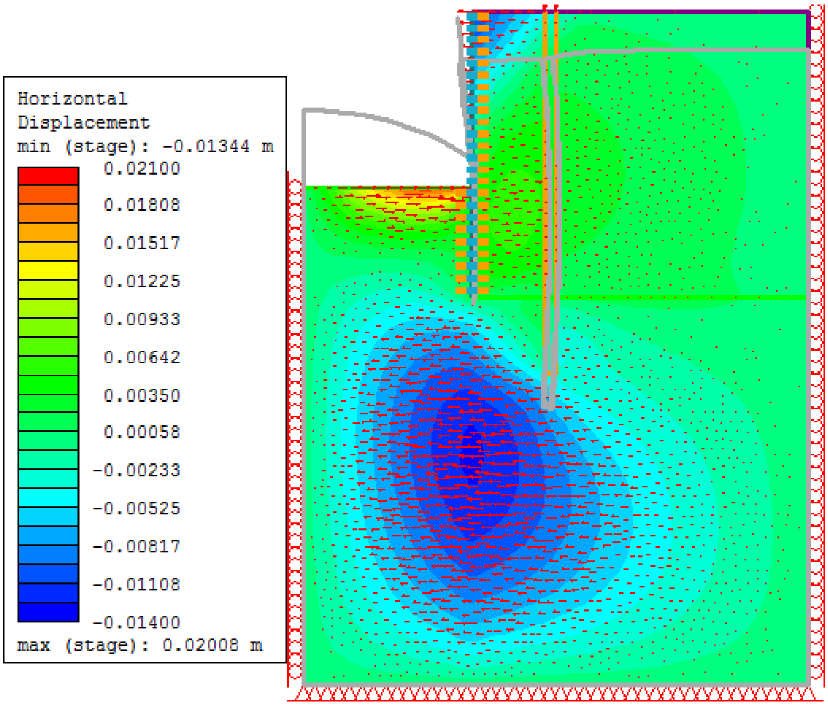

M 104.3: Deformed model (stage 3)

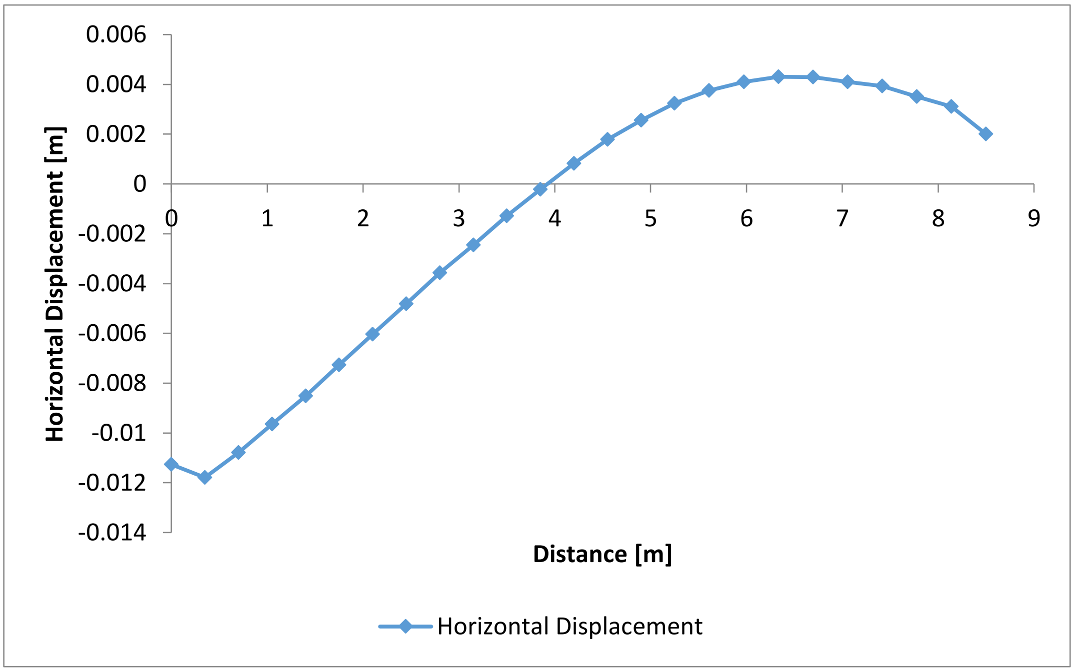

M 104.4: Horizontal displacement of soil along retaining wall

Retaining wall maximum horizontal displacement: -0.01344m

Distance from point of maximum displacement in retaining wall to the top of backfill soil: 0.0m

Model 105:

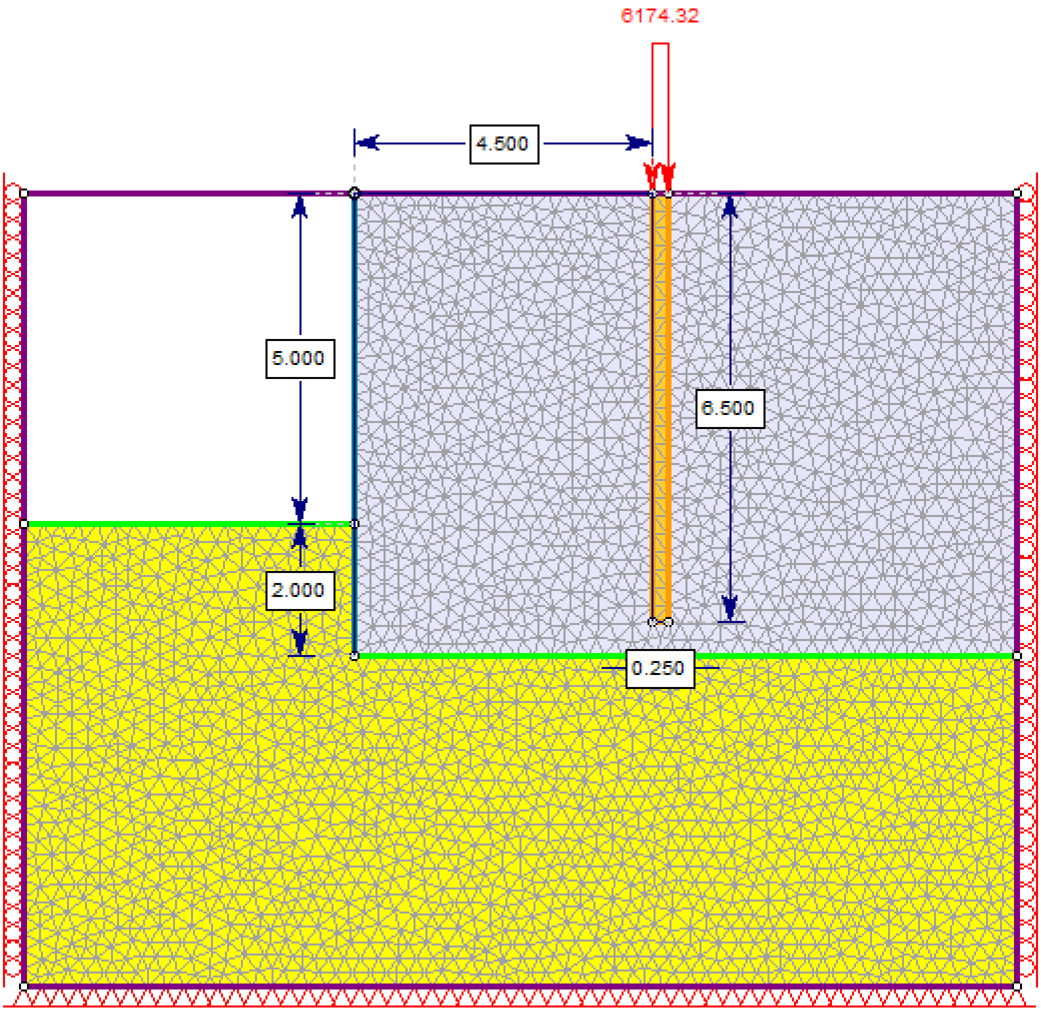

M 105.1: Original model (stage 3)

C'_1	ϕ'_1	γ_1	E_1	C'_2	ϕ'_2	γ_2	E_2	H_1	H_2	H_3	E_3	D_1	D_2	L	Qult
0	43	20	201	53	30	20	46.8	5.00	2	1	752053	4.5	0.25	6.5	6174.32

M 105.2: Parameter values

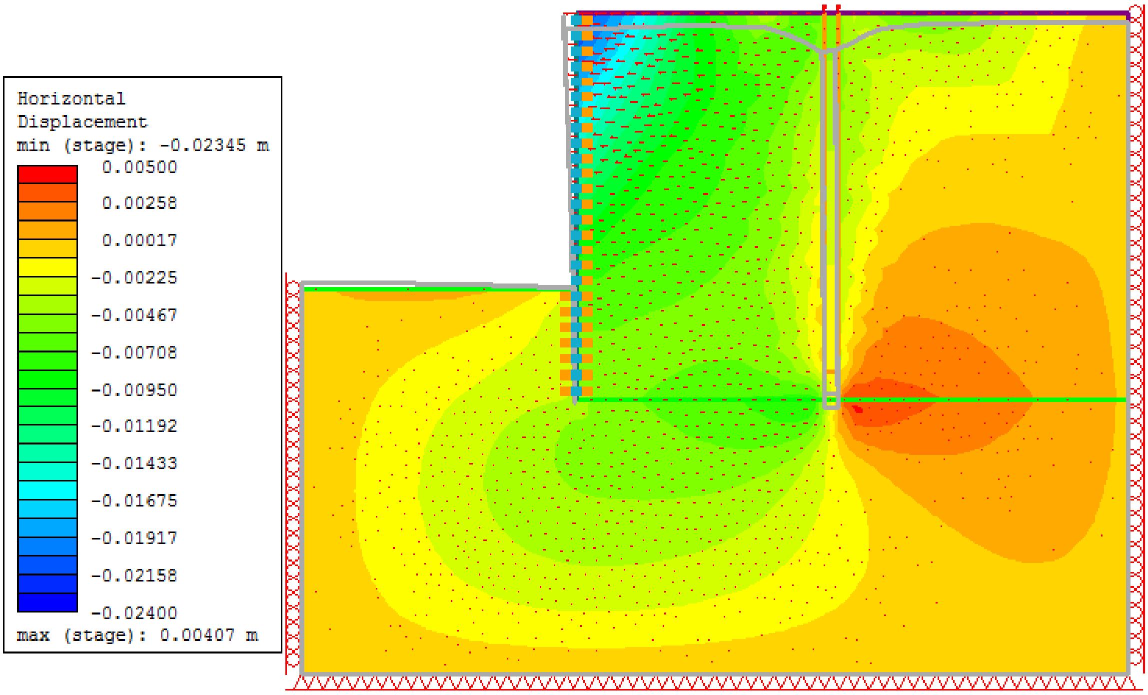

M 105.3: Deformed model (stage 3)

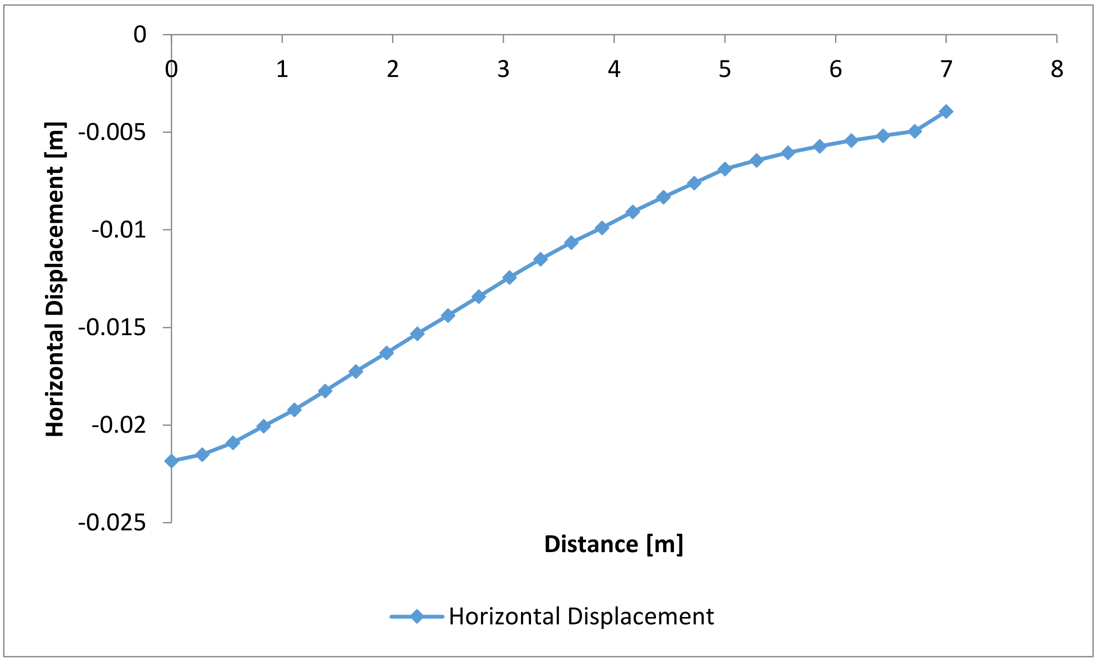

M 105.4: Horizontal displacement of soil along retaining wall

Retaining wall maximum horizontal displacement: -0.02345m

Distance from point of maximum displacement in retaining wall to the top of backfill soil: 0.0m

Model 106:

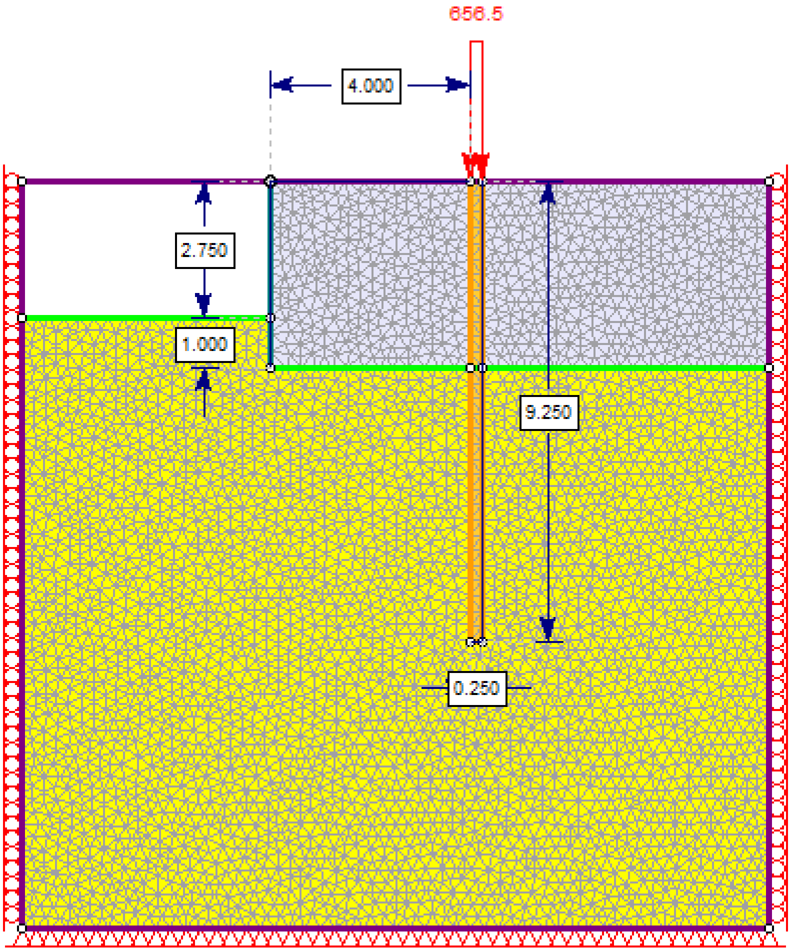

M 106.1: Original model (stage 3)

C'_1	ϕ'_1	γ_1	E_1	C'_2	ϕ'_2	γ_2	E_2	H_1	H_2	H_3	E_3	D_1	D_2	L	Qult
0	39	20	152	37	5	16	25.0	2.75	1	1.25	832622	4	0.25	9.25	656.5

M 106.2: Parameter values

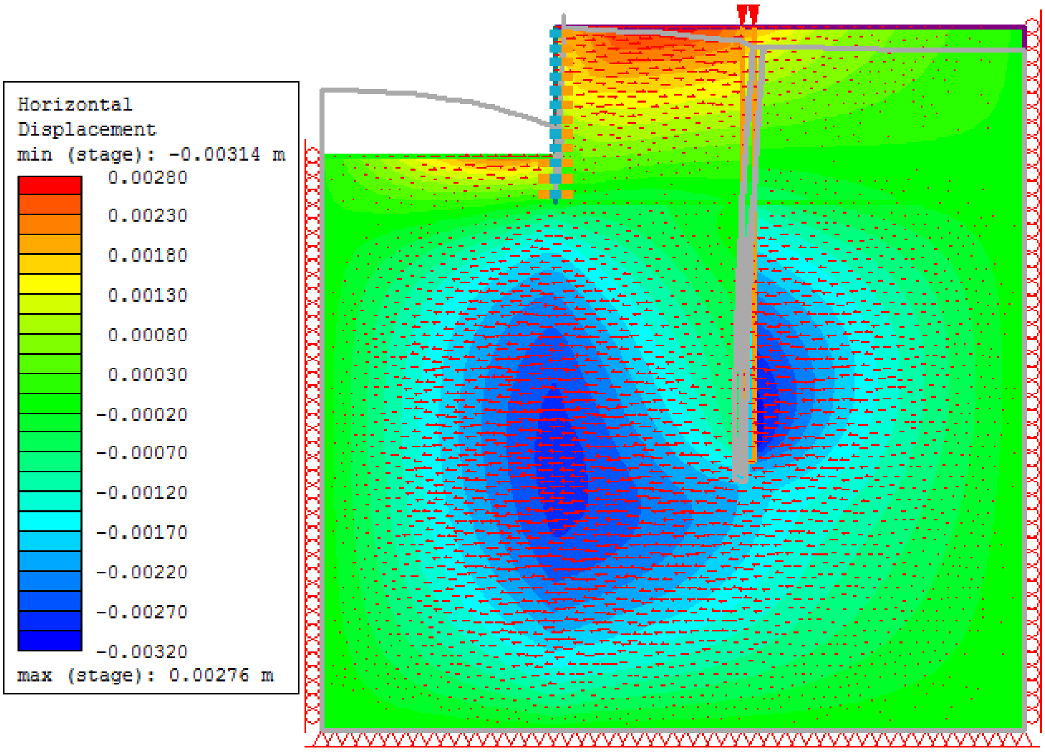

M 106.3: Deformed model (stage 3)

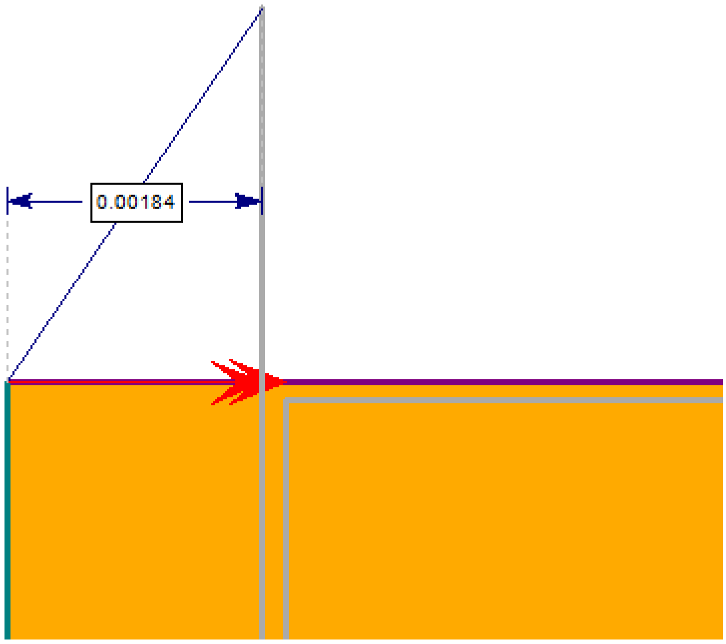

M 106.4: Detailed view of cross-section of retaining wall and soil (stage 3)

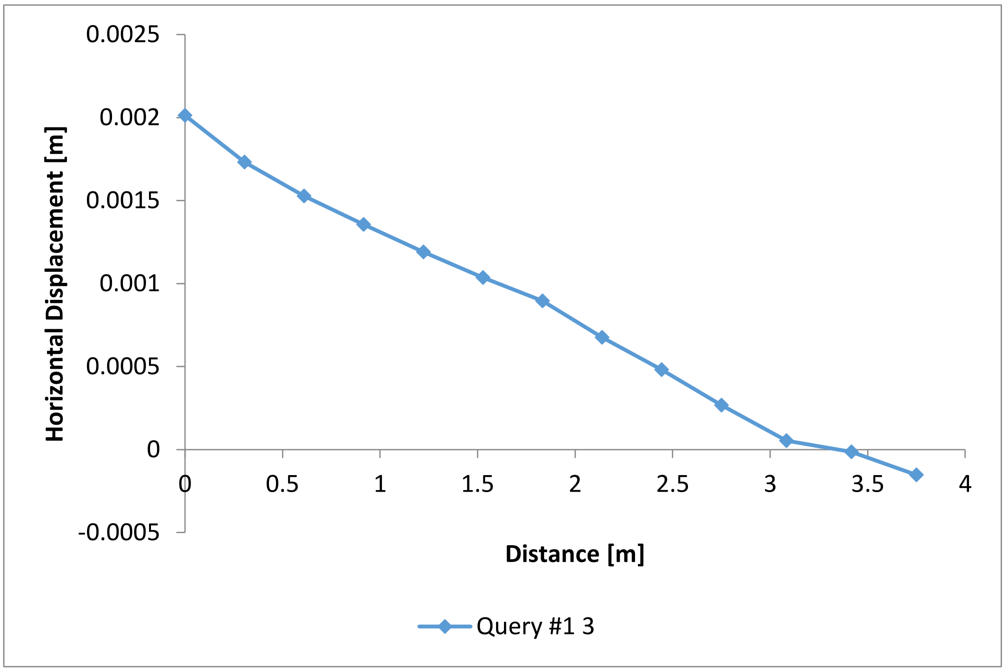

M 106.5: Horizontal displacement of soil along retaining wall

Retaining wall maximum horizontal displacement: 0.00184m

Distance from point of maximum displacement in retaining wall to the top of backfill soil: 0.0m

Model 107:

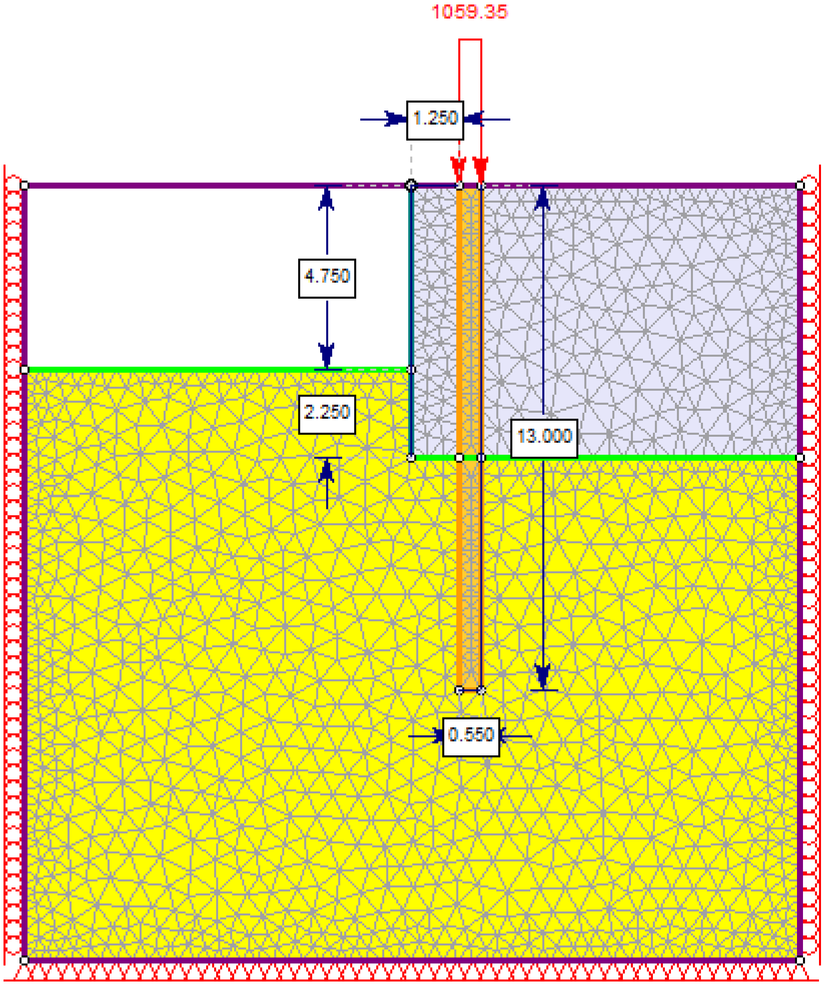

M 107.1: Original model (stage 3)

C_1'	ϕ_1'	γ_1	E_1	C_2'	ϕ_2'	γ_2	E_2	H_1	H_2	H_3	E_3	D_1	D_2	L	Qult
0	36	22	41	54	5	24	24.4	4.75	2.25	0.75	991893	1.25	0.55	13	1059.35

M 107.2: Parameter values

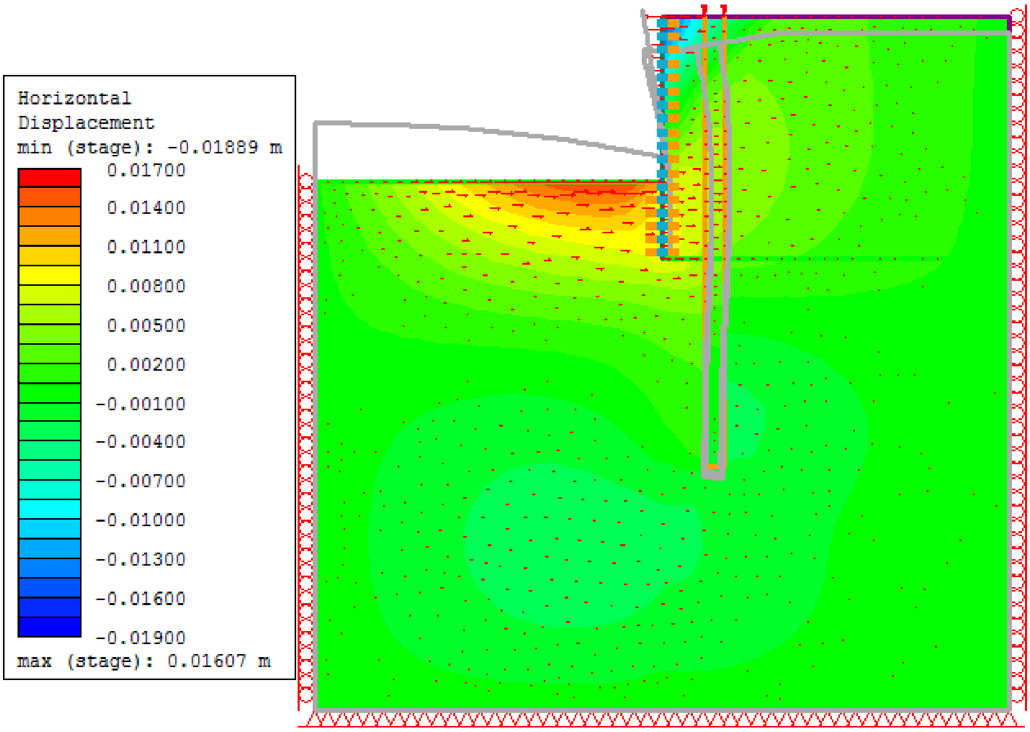

M 107.3: Deformed model (stage 3)

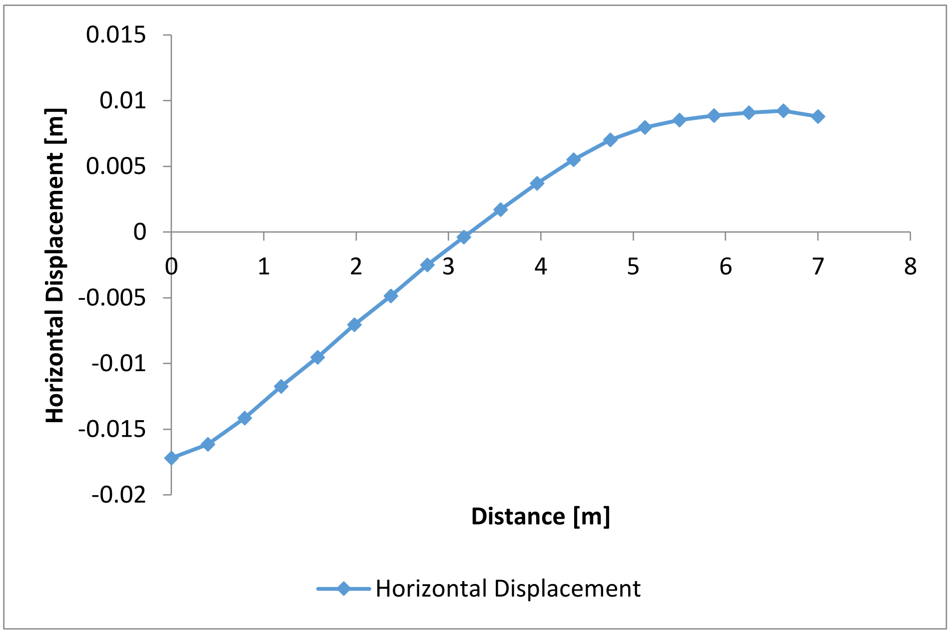

M 107.4: Horizontal displacement of soil along retaining wall

Retaining wall maximum horizontal displacement: -0.01889m

Distance from point of maximum displacement in retaining wall to the top of backfill soil: 0.0m

Model 108:

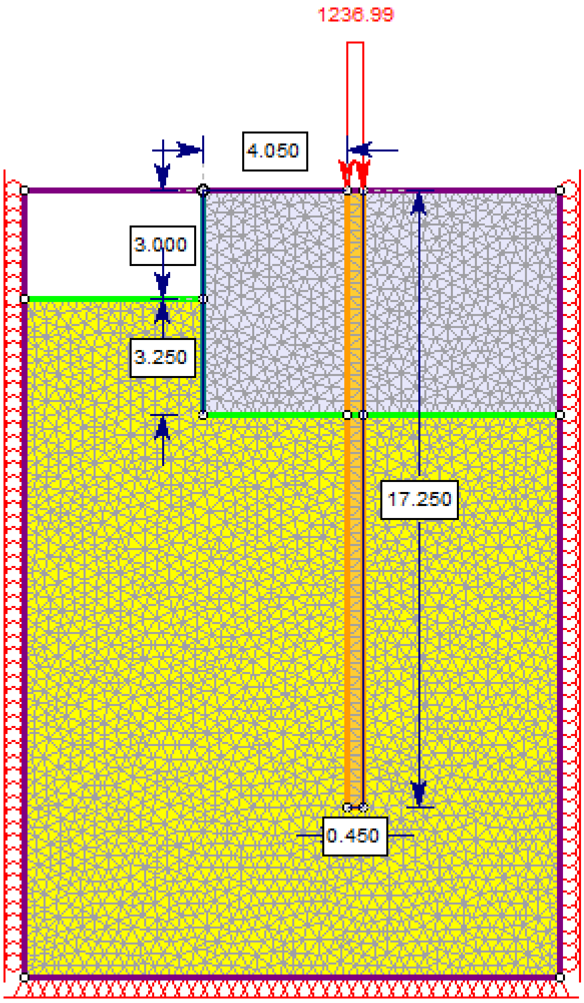

M 108.1: Original model (stage 3)

C'_1	ϕ'_1	γ_1	E_1	C'_2	ϕ'_2	γ_2	E_2	H_1	H_2	H_3	E_3	D_1	D_2	L	Qult
0	32	19	296	21	7	23	15.7	3.00	3.25	1.25	1073769	4.05	0.45	17.25	1236.99

M 108.2: Parameter values

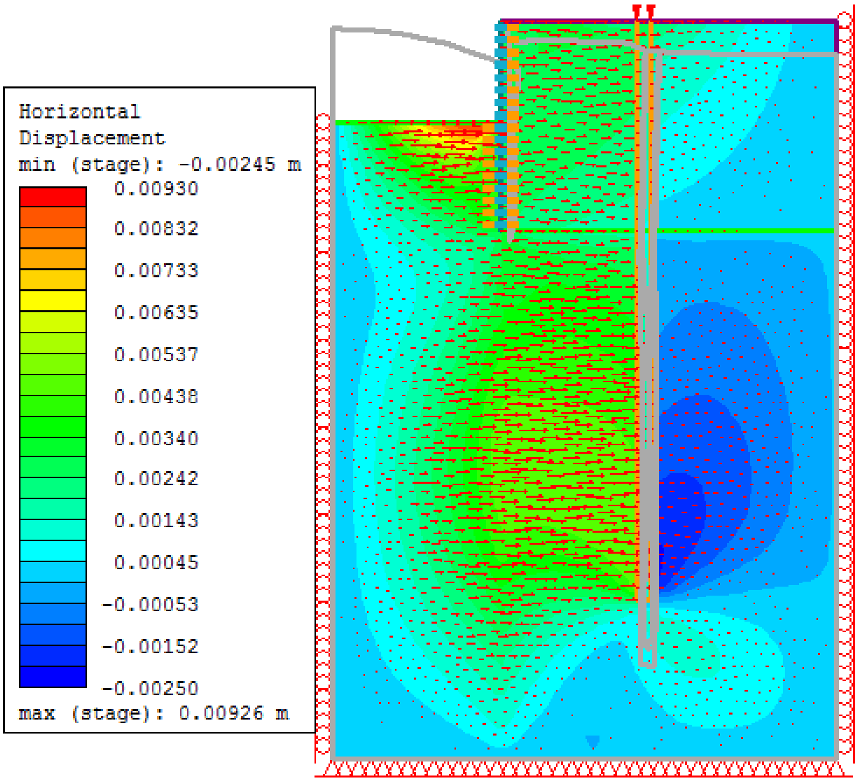

M 108.3: Deformed model (stage 3)

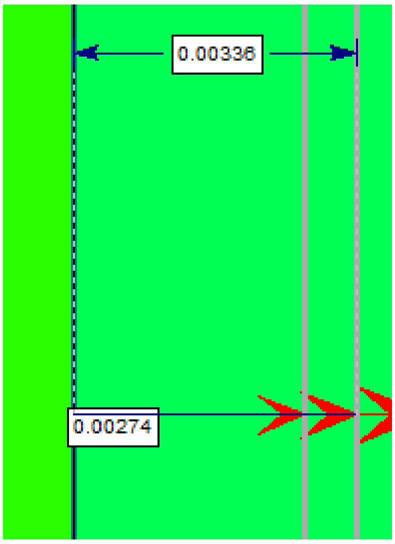

M 108.4: Detailed view of cross-section of retaining wall and soil (stage 3)

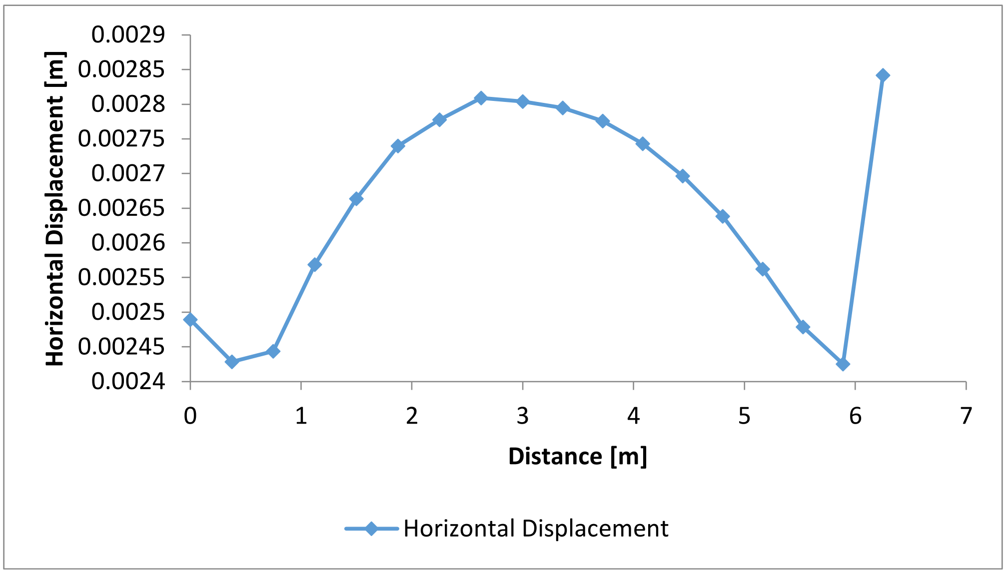

M 108.5: Horizontal displacement of soil along retaining wall

Retaining wall maximum horizontal displacement: 0.00336m

Distance from point of maximum displacement in retaining wall to the top of backfill soil: 4.083m

Model 109:

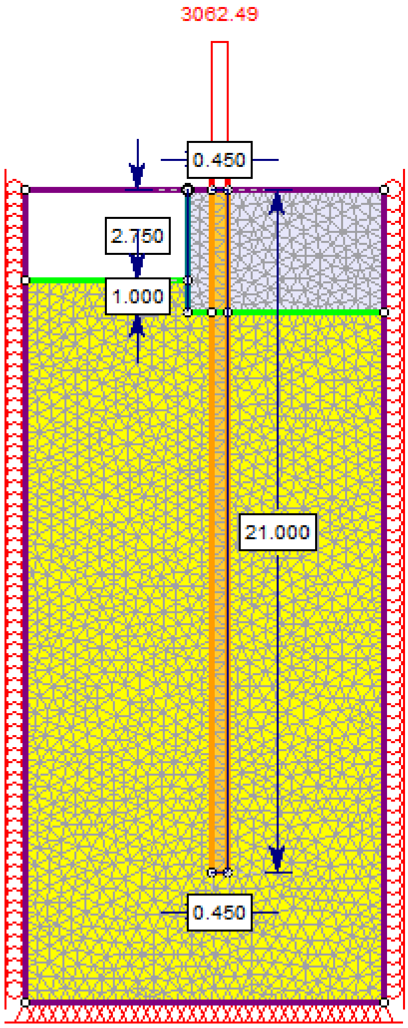

M 109.1: Original model (stage 3)

C_1'	ϕ_1'	γ_1	E_1	C_2'	ϕ_2'	γ_2	E_2	H_1	H_2	H_3	E_3	D_1	D_2	L	Qult
0	32	22	189	56	16	22	29.1	2.75	1	1.5	1020754	0.75	0.45	21	3062.49

M 109.2: Parameter values

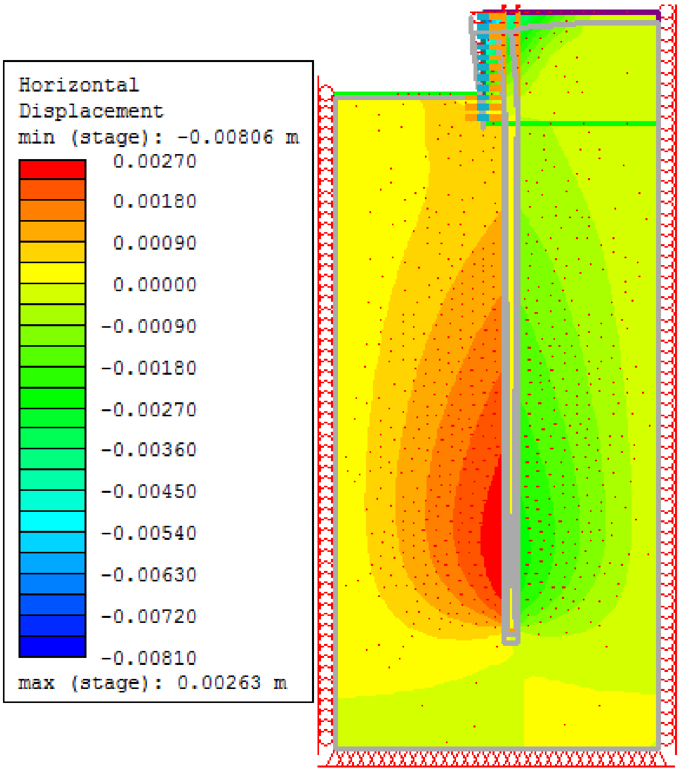

M 109.3: Deformed model (stage 3)

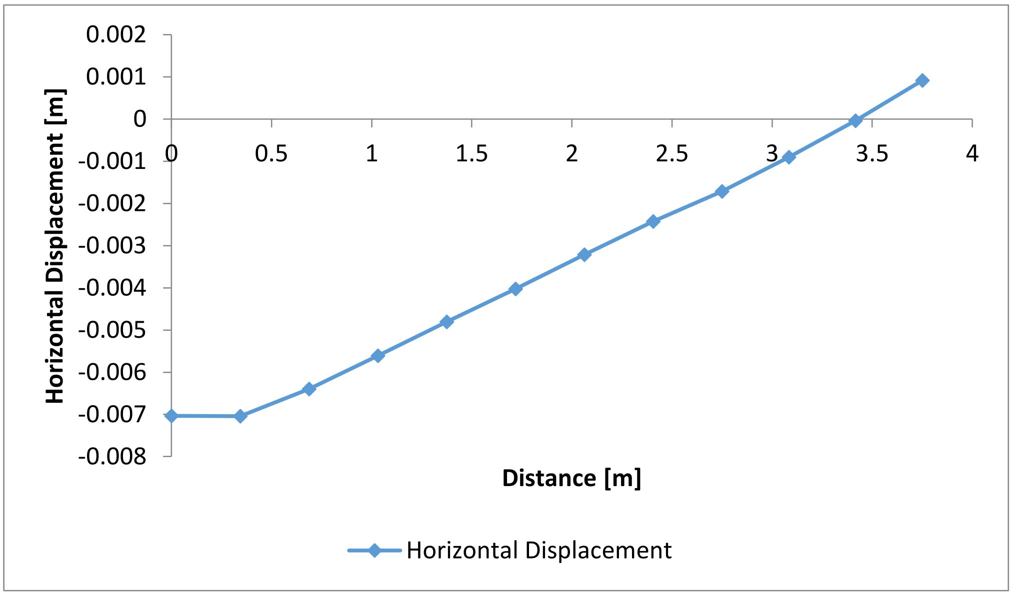

M 109.4: Horizontal displacement of soil along retaining wall

Retaining wall maximum horizontal displacement: -0.00806m

Distance from point of maximum displacement in retaining wall to the top of backfill soil: 0.0m

Model 110:

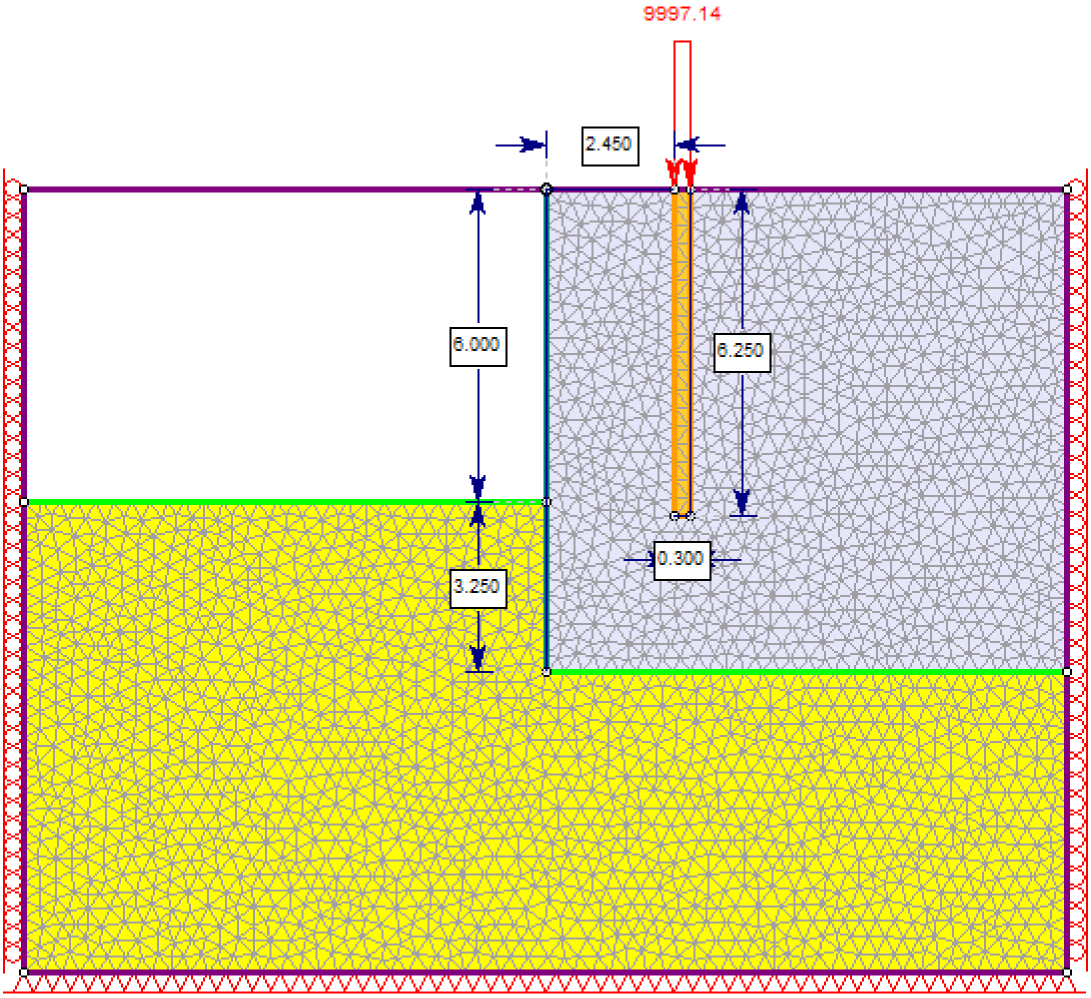

M 110.1: Original model (stage 3)

C'_1	ϕ'_1	γ_1	E_1	C'_2	ϕ'_2	γ_2	E_2	H_1	H_2	H_3	E_3	D_1	D_2	L	Qult
0	43	20	244	50	34	16	46.2	6.00	3.25	1	924573	2.45	0.3	6.25	9997.14

M 110.2: Parameter values

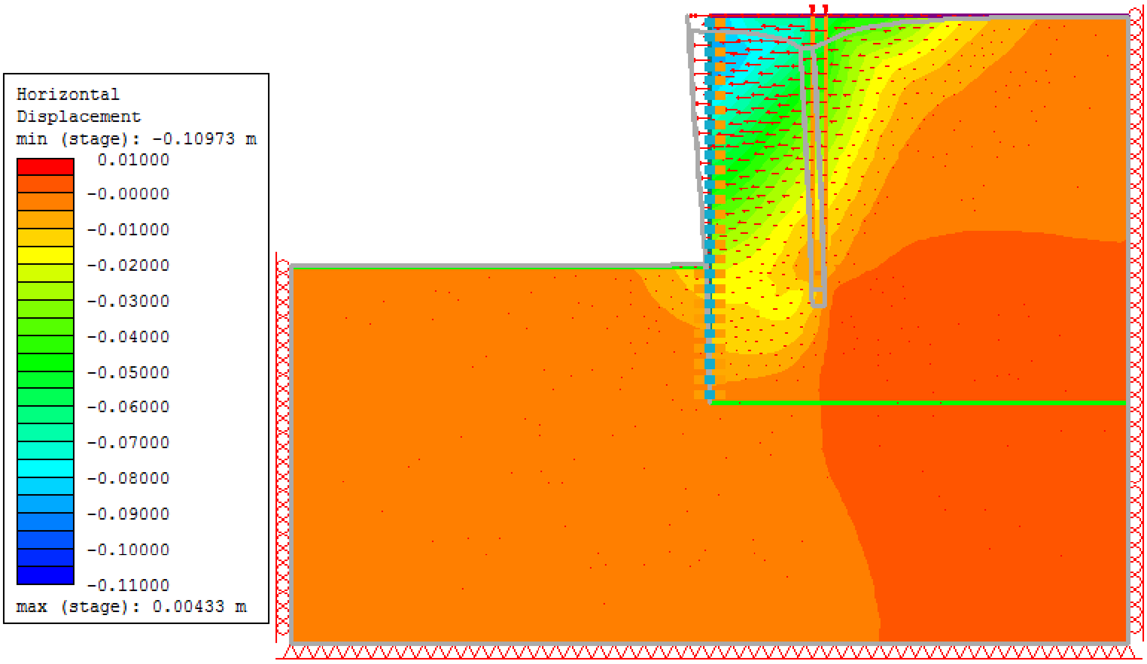

M 110.3: Deformed model (stage 3)

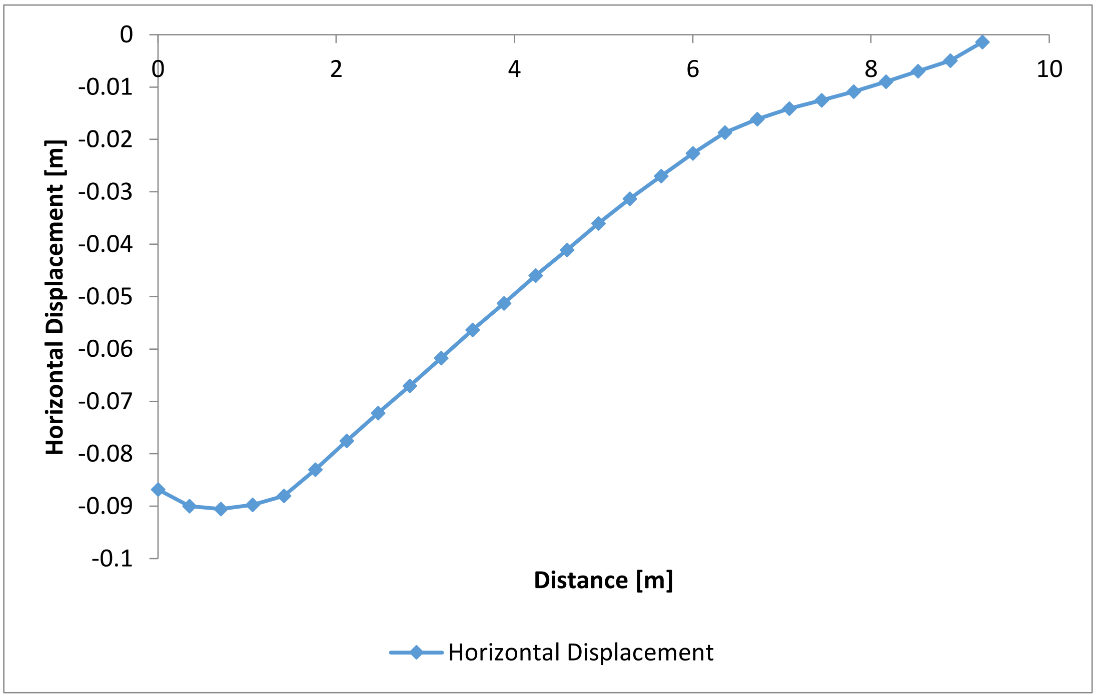

M 110.4: Horizontal displacement of soil along retaining wall

Retaining wall maximum horizontal displacement: -0.10973m

Distance from point of maximum displacement in retaining wall to the top of backfill soil: 0.0m

Model 111:

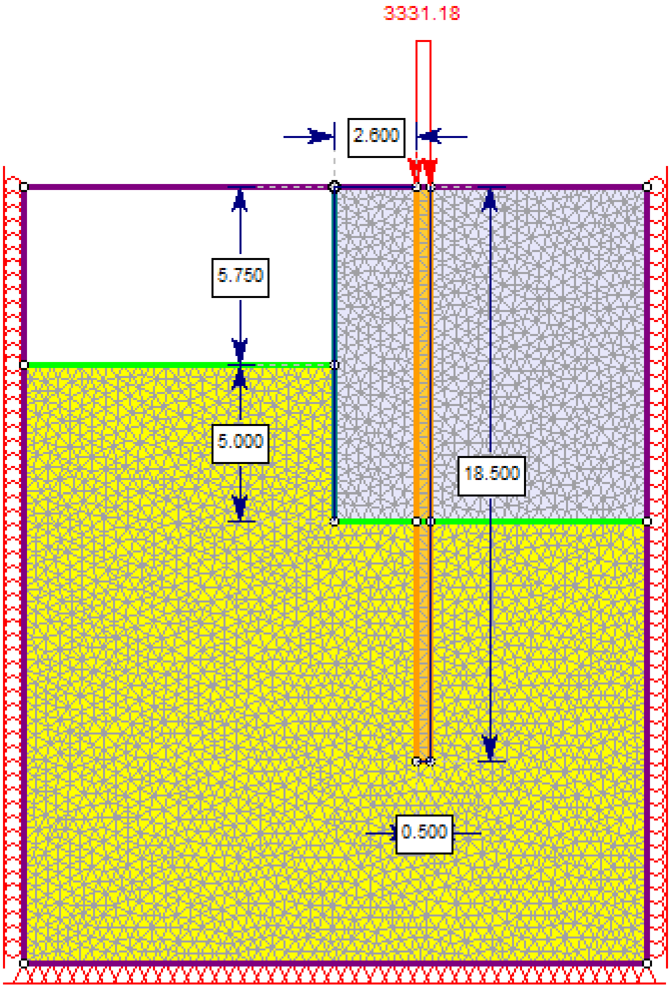

M 111.1: Original model (stage 3)

C_1'	ϕ_1'	γ_1	E_1	C_2'	ϕ_2'	γ_2	E_2	H_1	H_2	H_3	E_3	D_1	D_2	L	Qult
0	40	21	62	41	19	20	21.4	5.75	5	1	1043321	2.6	0.5	18.5	3331.18

M 111.2: Parameter values

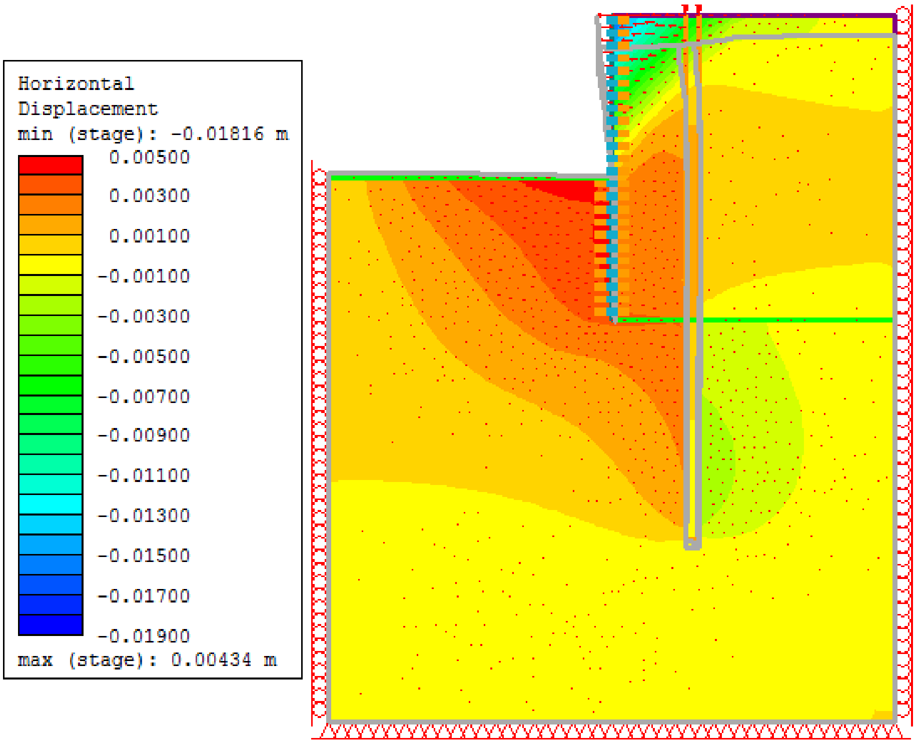

M 111.3: Deformed model (stage 3)

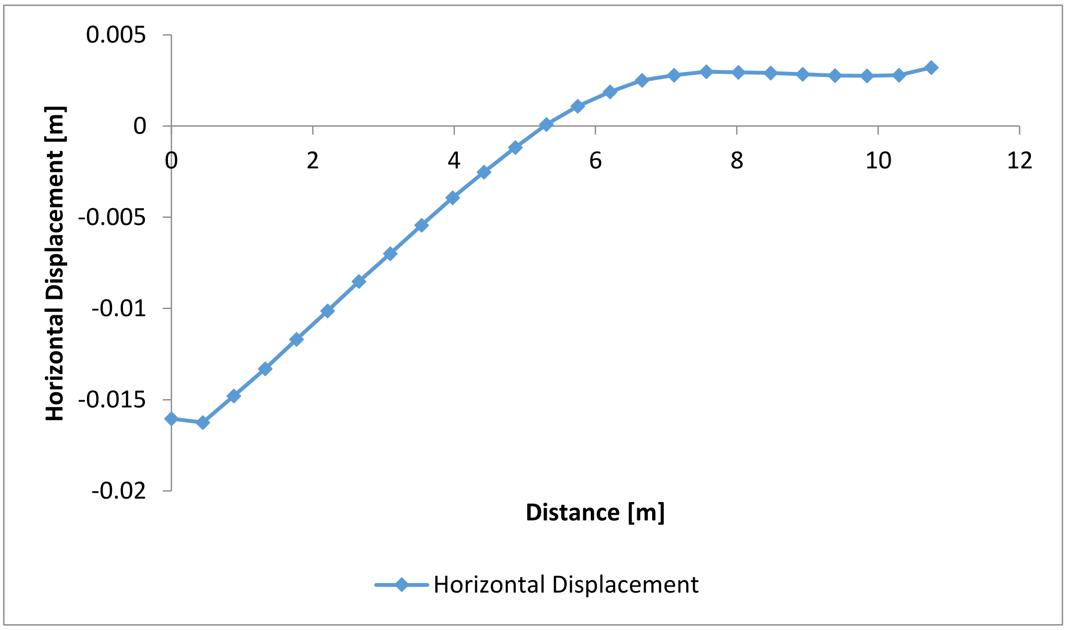

M 111.4: Horizontal displacement of soil along retaining wall

Retaining wall maximum horizontal displacement: -0.01816m

Distance from point of maximum displacement in retaining wall to the top of backfill soil: 0.0m

Model 112:

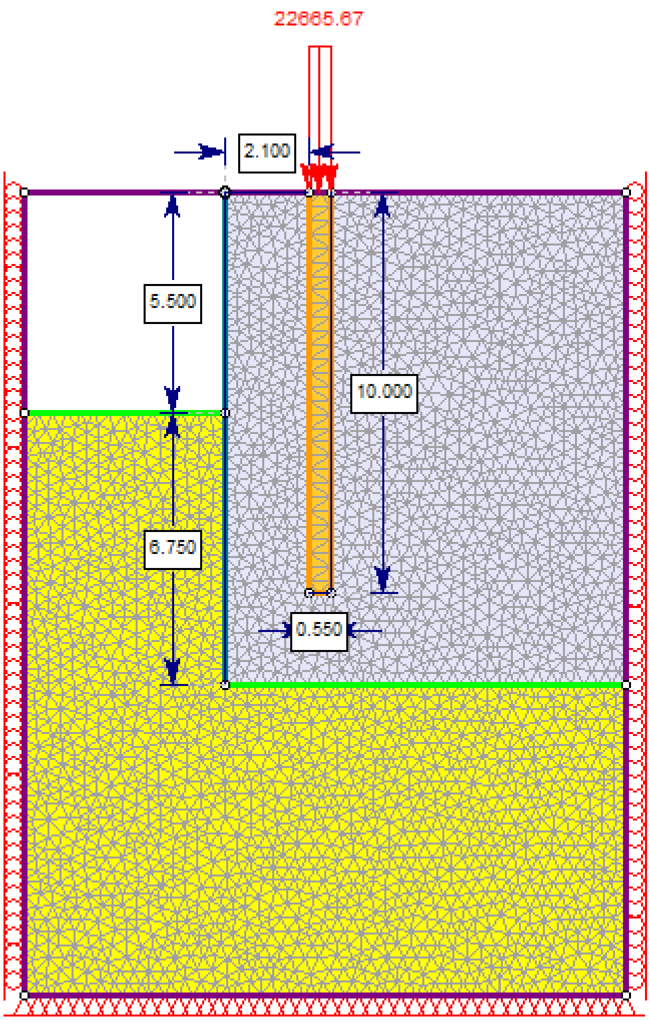

M 112.1: Original model (stage 3)

C'_1	ϕ'_1	γ_1	E_1	C'_2	ϕ'_2	γ_2	E_2	H_1	H_2	H_3	E_3	D_1	D_2	L	Qult
0	38	21	195	37	15	21	6.5	5.50	6.75	1	716636	2.1	0.55	10	2665.67

M 112.2: Parameter values

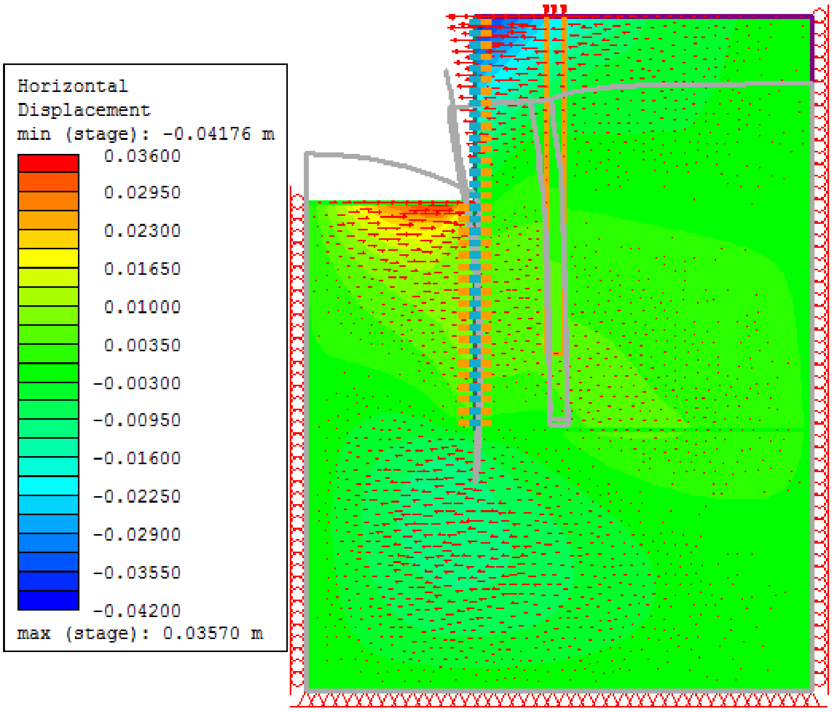

M 112.3: Deformed model (stage 3)

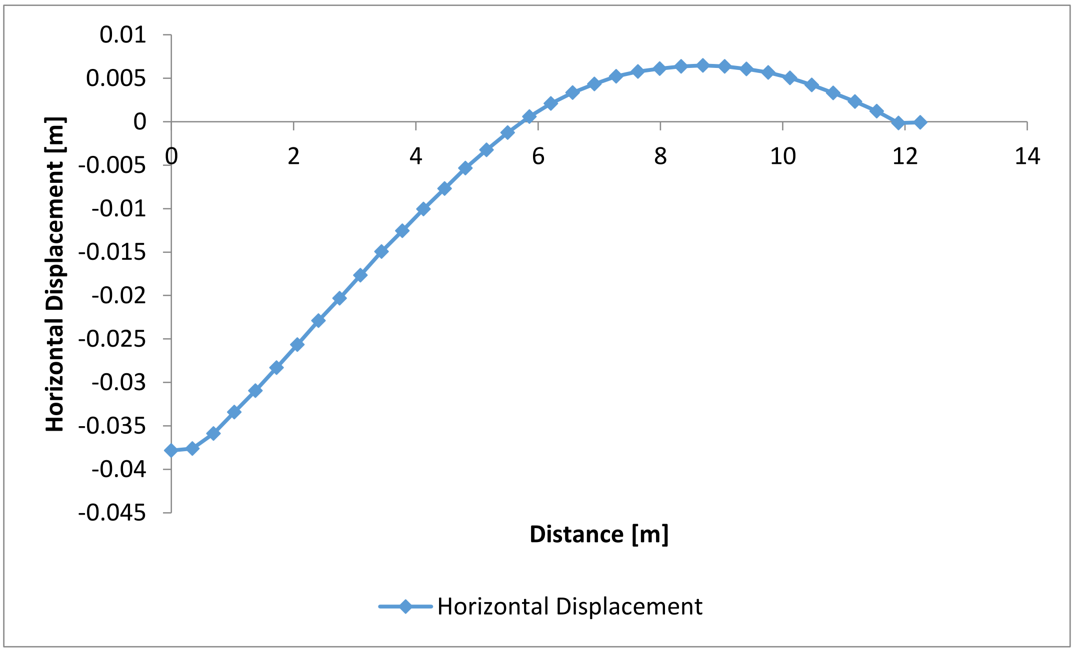

M 112.4: Horizontal displacement of soil along retaining wall

Retaining wall maximum horizontal displacement: -0.04176m

Distance from point of maximum displacement in retaining wall to the top of backfill soil: 0.0m

Model 113:

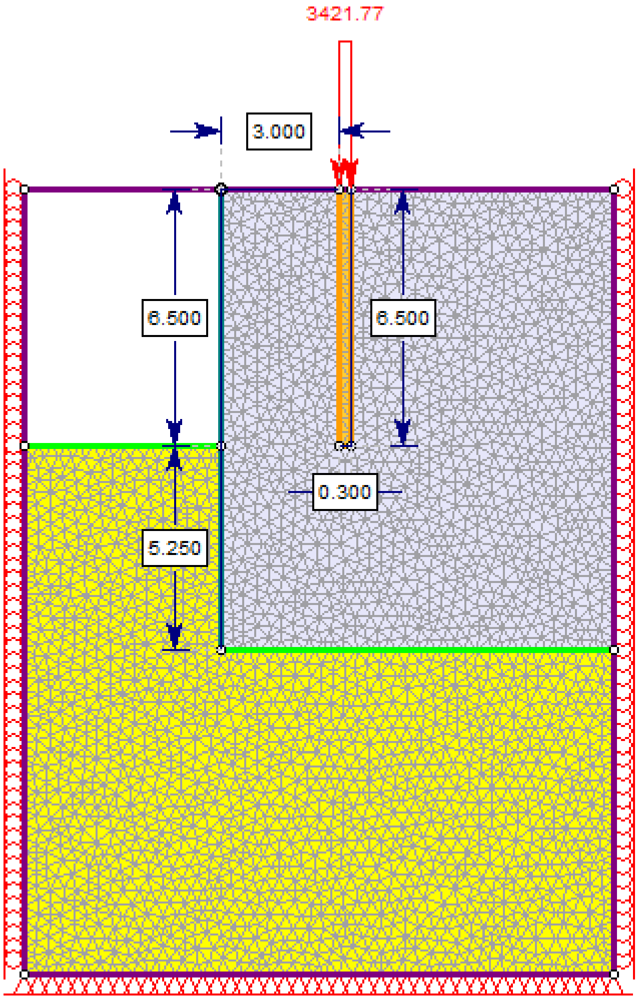

M 113.1: Original model (stage 3)

C'_1	ϕ'_1	γ_1	E_1	C'_2	ϕ'_2	γ_2	E_2	H_1	H_2	H_3	E_3	D_1	D_2	L	Qult
0	38	19	34	46	17	19	0.7	6.50	5.25	1.25	917299	3	0.3	6.5	3421.77

M 113.2: Parameter values

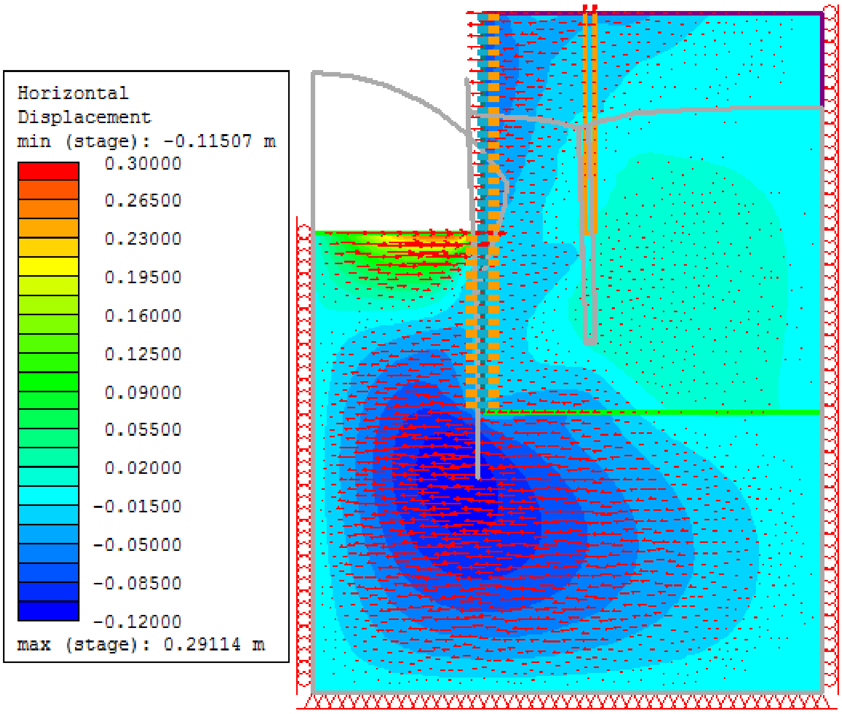

M 113.3: Deformed model (stage 3)

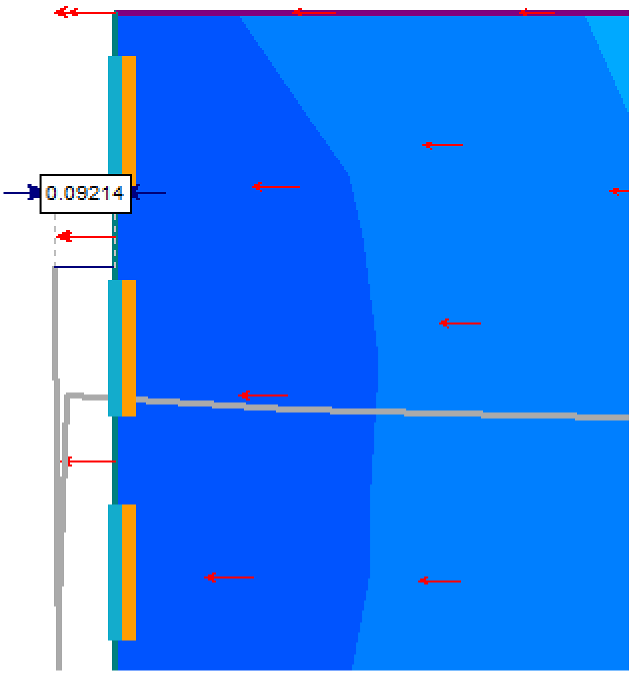

M 113.4: Detailed view of cross-section of retaining wall and soil (stage 3)

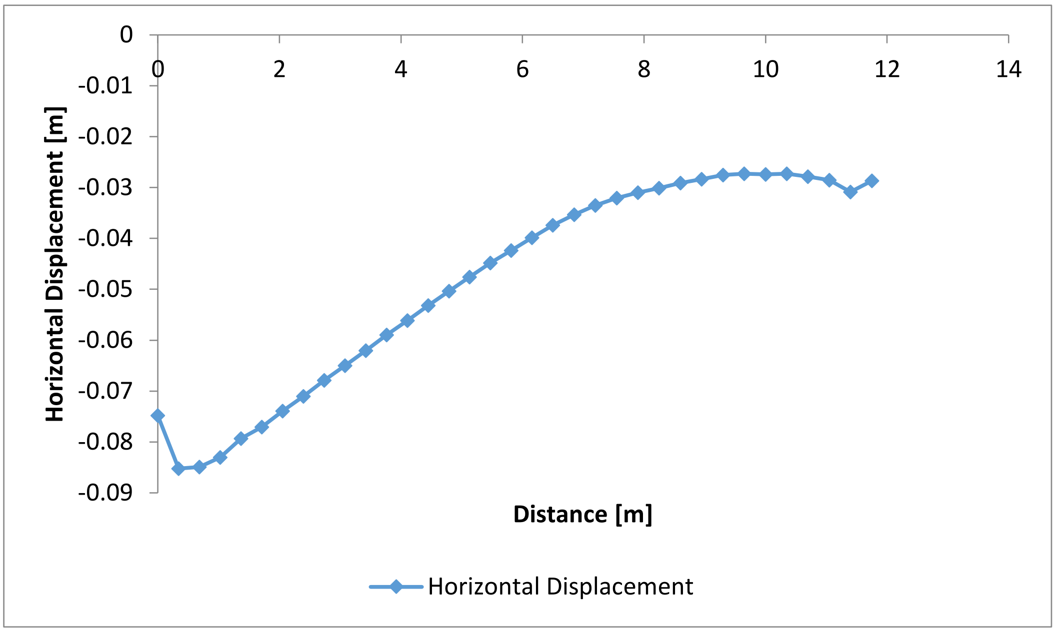

M 113.5: Horizontal displacement of soil along retaining wall

Retaining wall maximum horizontal displacement: -0.09214m

Distance from point of maximum displacement in retaining wall to the top of backfill soil: 0.0m

Model 114:

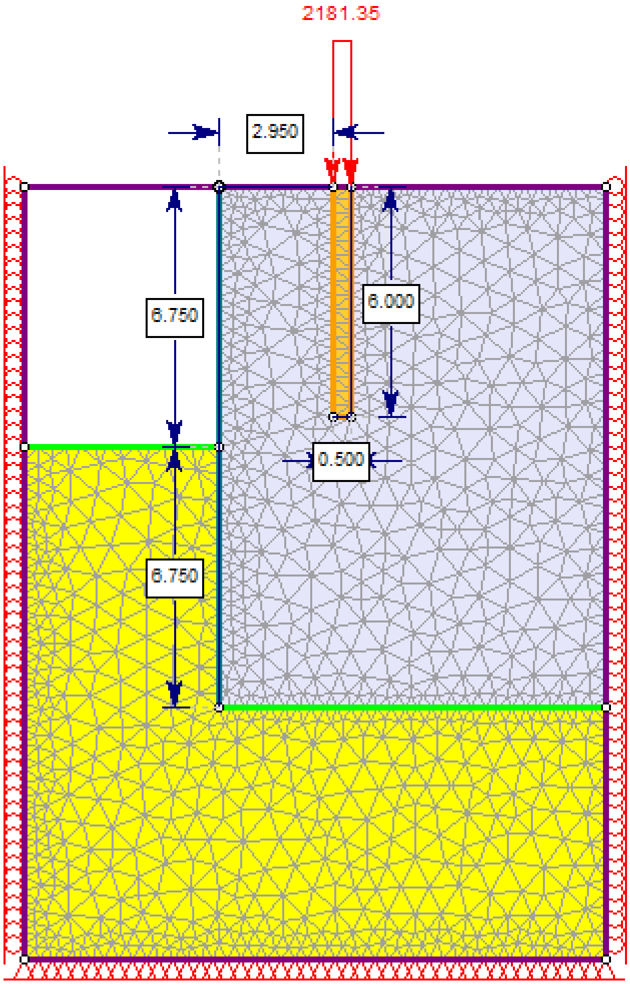

M 114.1: Original model (stage 3)

C_1'	ϕ_1'	γ_1	E_1	C_2'	ϕ_2'	γ_2	E_2	H_1	H_2	H_3	E_3	D_1	D_2	L	Qult
0	36	18	260	42	30	23	37.3	6.75	6.75	1.25	1107295	2.95	0.5	6	2181.35

M 114.2: Parameter values

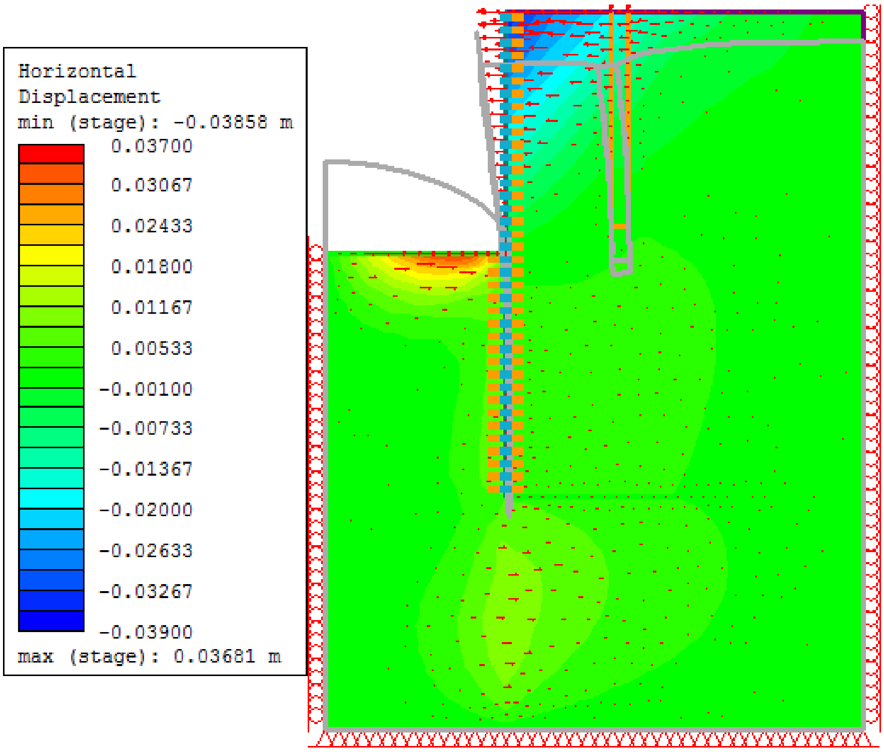

M 114.3: Deformed model (stage 3)

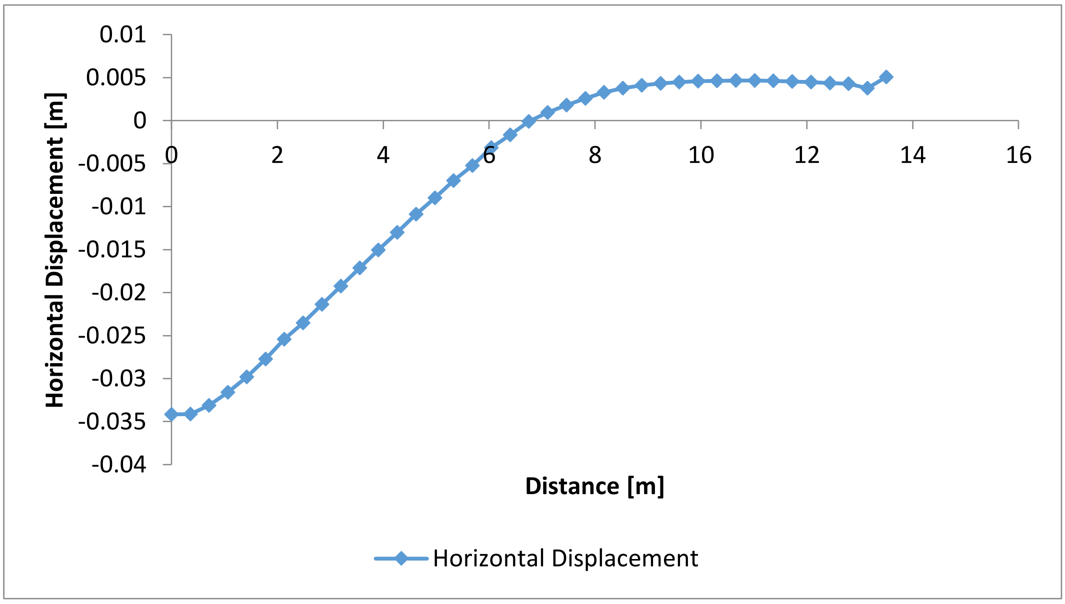

M 114.4: Horizontal displacement of soil along retaining wall

Retaining wall maximum horizontal displacement: -0.03858m

Distance from point of maximum displacement in retaining wall to the top of backfill soil: 0.0m

Model 115:

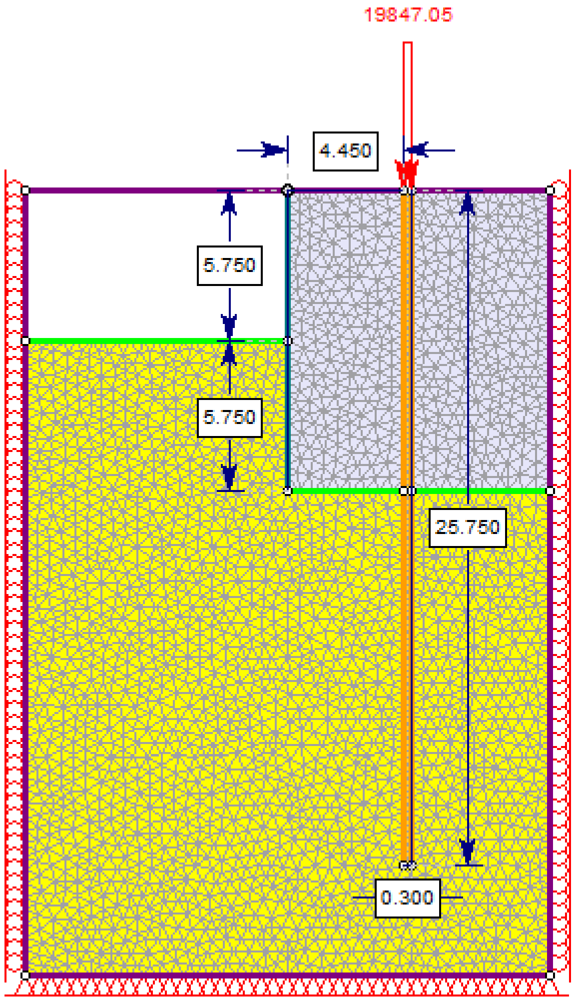

M 115.1: Original model (stage 3)

C'_1	ϕ'_1	γ_1	E_1	C'_2	ϕ'_2	γ_2	E_2	H_1	H_2	H_3	E_3	D_1	D_2	L	Qult
0	33	21	213	43	31	25	20.8	5.75	5.75	1.25	1090142	4.45	0.3	25.75	19847.05

M 115.2: Parameter values

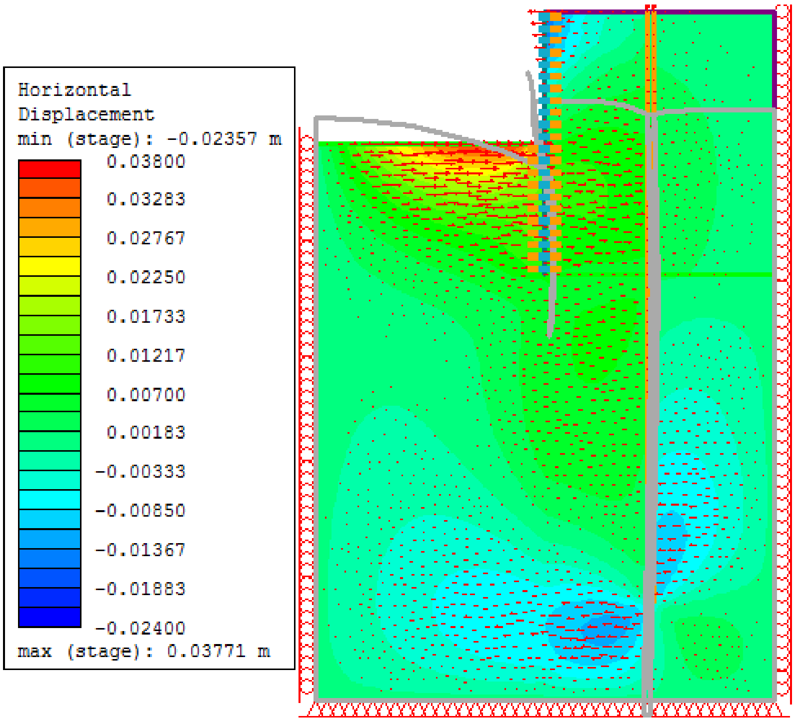

M 115.3: Deformed model (stage 3)

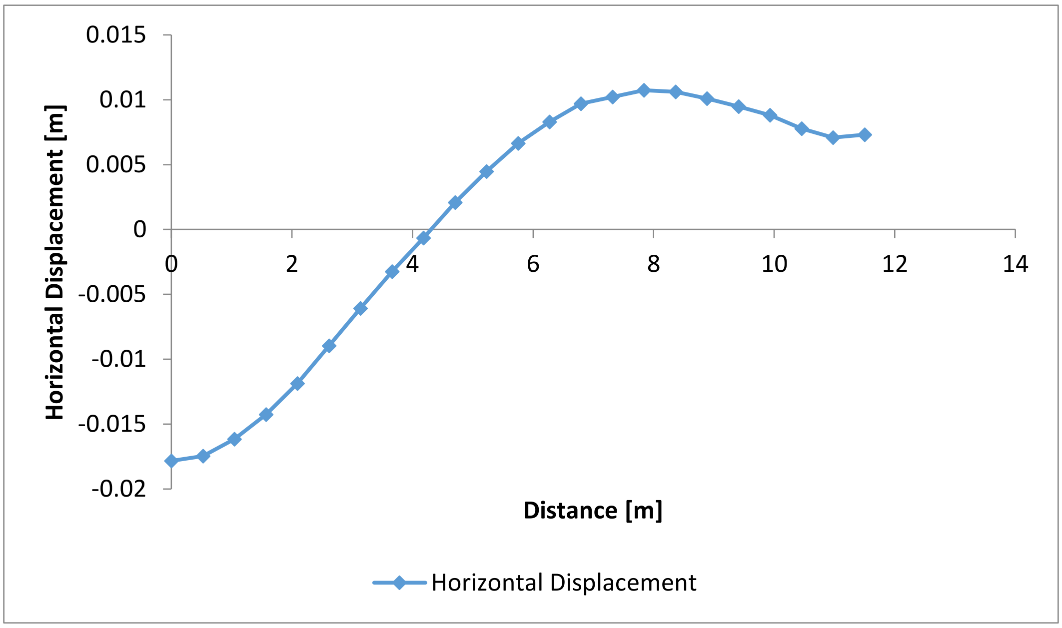

M 115.4: Horizontal displacement of soil along retaining wall

Retaining wall maximum horizontal displacement: -0.02357m

Distance from point of maximum displacement in retaining wall to the top of backfill soil: 0.0m

Model 116:

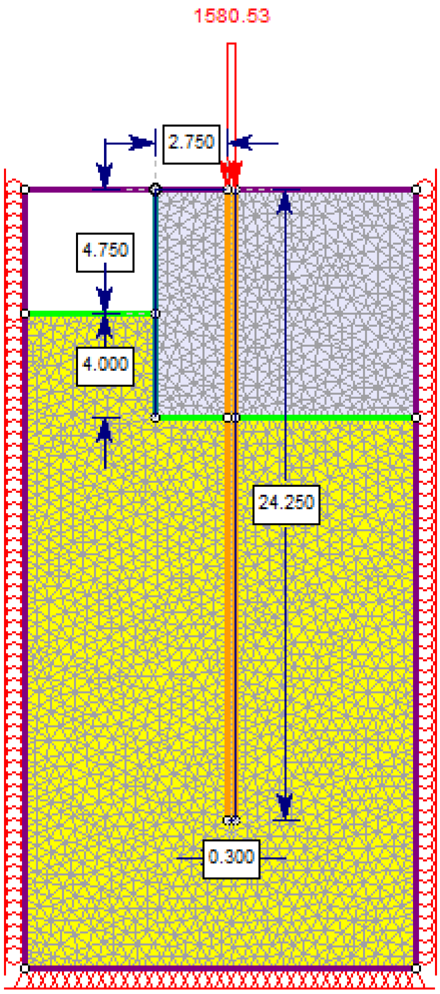

M 116.1: Original model (stage 3)

C_1'	ϕ_1'	γ_1	E_1	C_2'	ϕ_2'	γ_2	E_2	H_1	H_2	H_3	E_3	D_1	D_2	L	Qult
0	43	21	32	34	2	17	31.5	4.75	4	0.5	1135082	2.75	0.3	24.25	1580.53

M 116.2: Parameter values

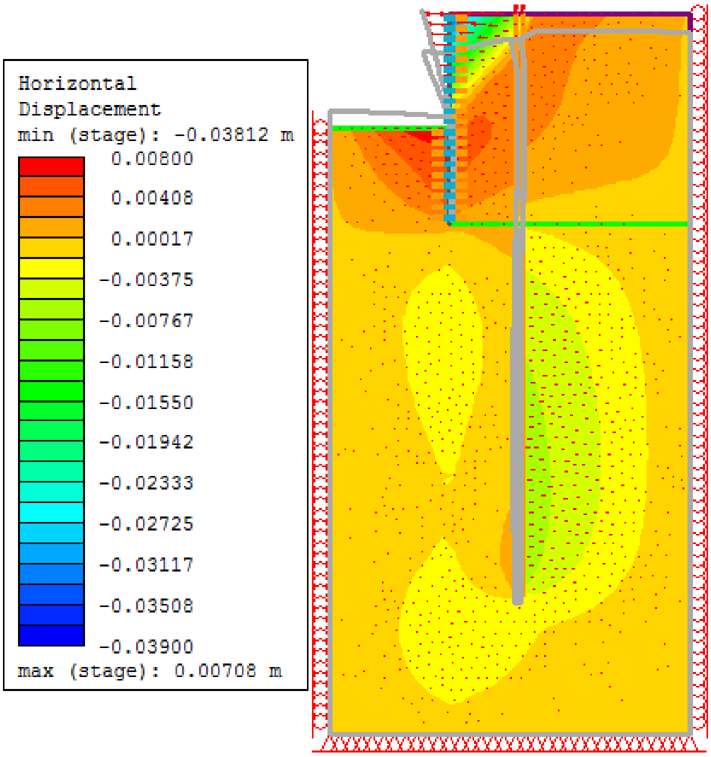

M 116.3: Deformed model (stage 3)

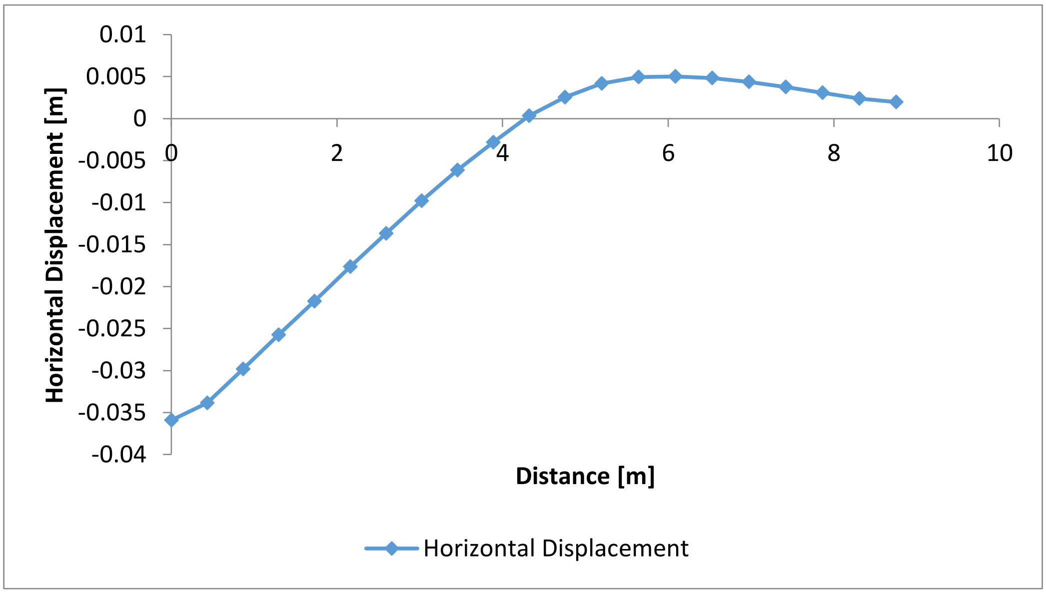

M 116.4: Horizontal displacement of soil along retaining wall

Retaining wall maximum horizontal displacement: -0.03812m

Distance from point of maximum displacement in retaining wall to the top of backfill soil: 0.0m

Model 117:

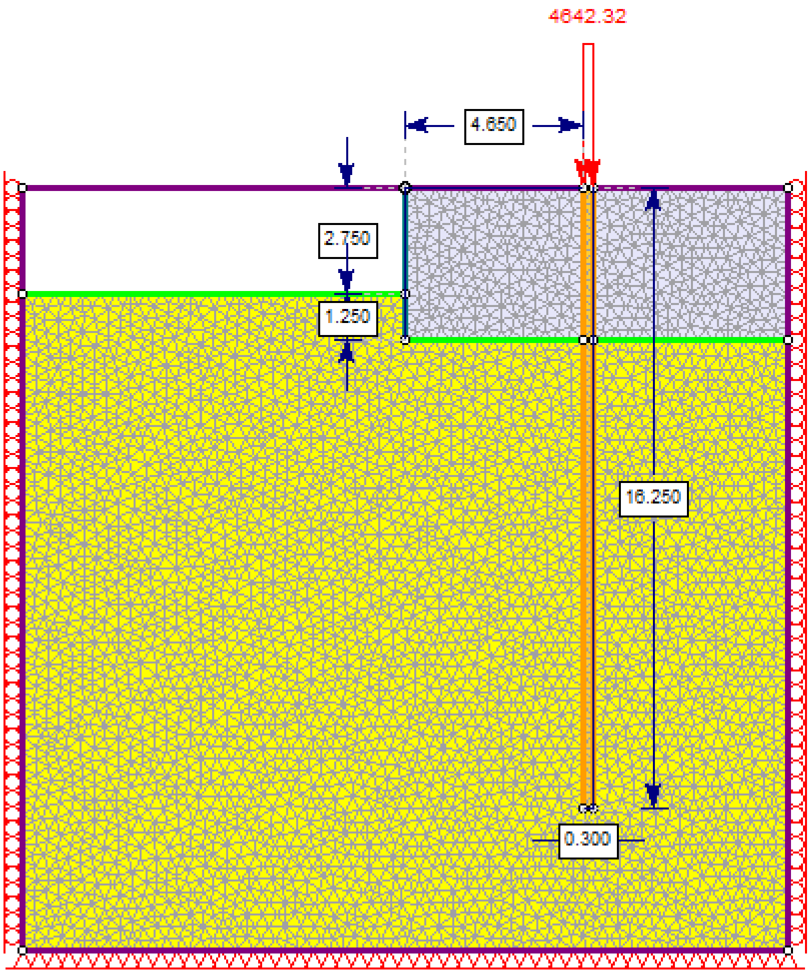

M 117.1: Original model (stage 3)

C_1'	ϕ_1'	γ_1	E_1	C_2'	ϕ_2'	γ_2	E_2	H_1	H_2	H_3	E_3	D_1	D_2	L	Qult
0	32	21	233	41	25	17	35.5	2.75	1.25	1.25	1065744	4.65	0.3	16.25	4642.32

M 117.2: Parameter values

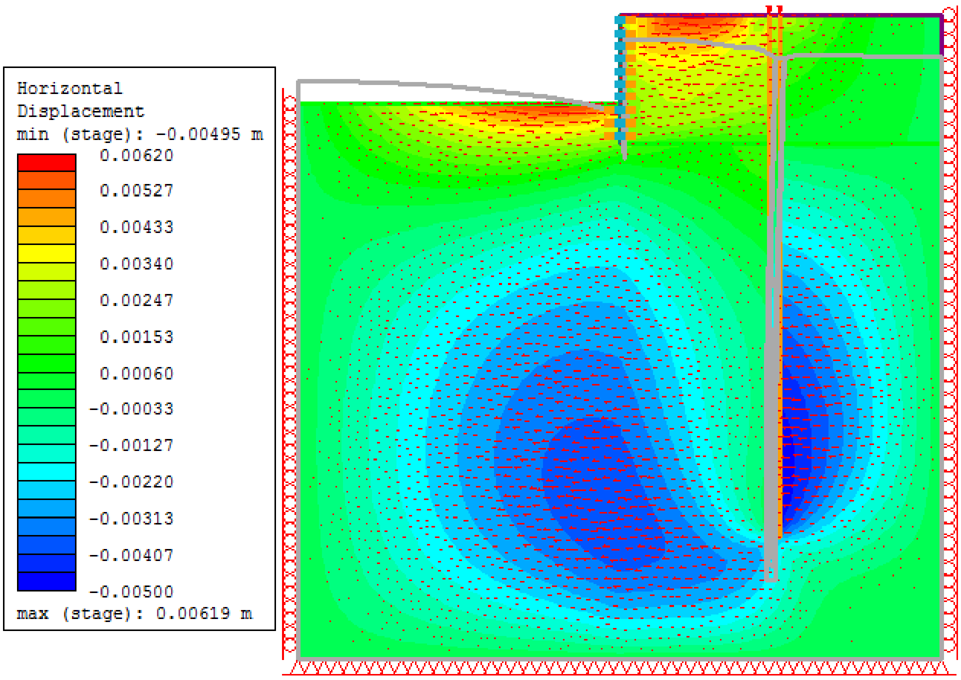

M 117.3: Deformed model (stage 3)

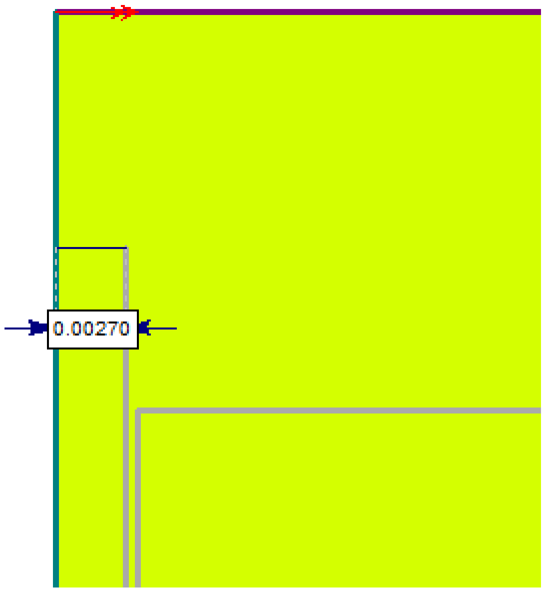

M 117.4: Detailed view of cross-section of retaining wall and soil (stage 3)

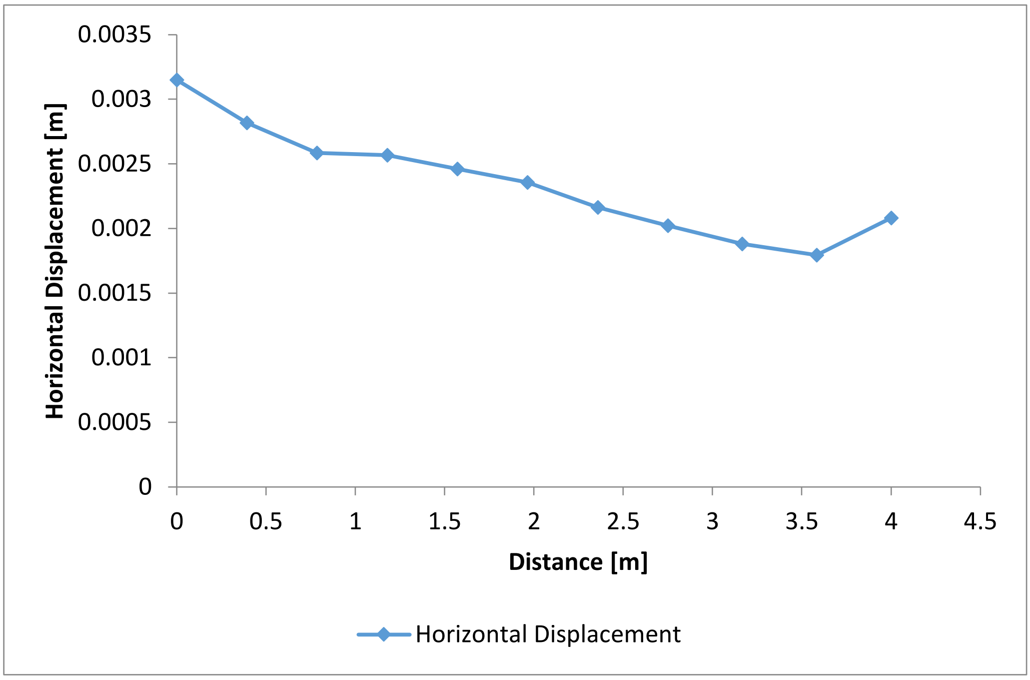

M 117.5: Horizontal displacement of soil along retaining wall

Retaining wall maximum horizontal displacement: 0.0027m

Distance from point of maximum displacement in retaining wall to the top of backfill soil: 0.0m

Model 118:

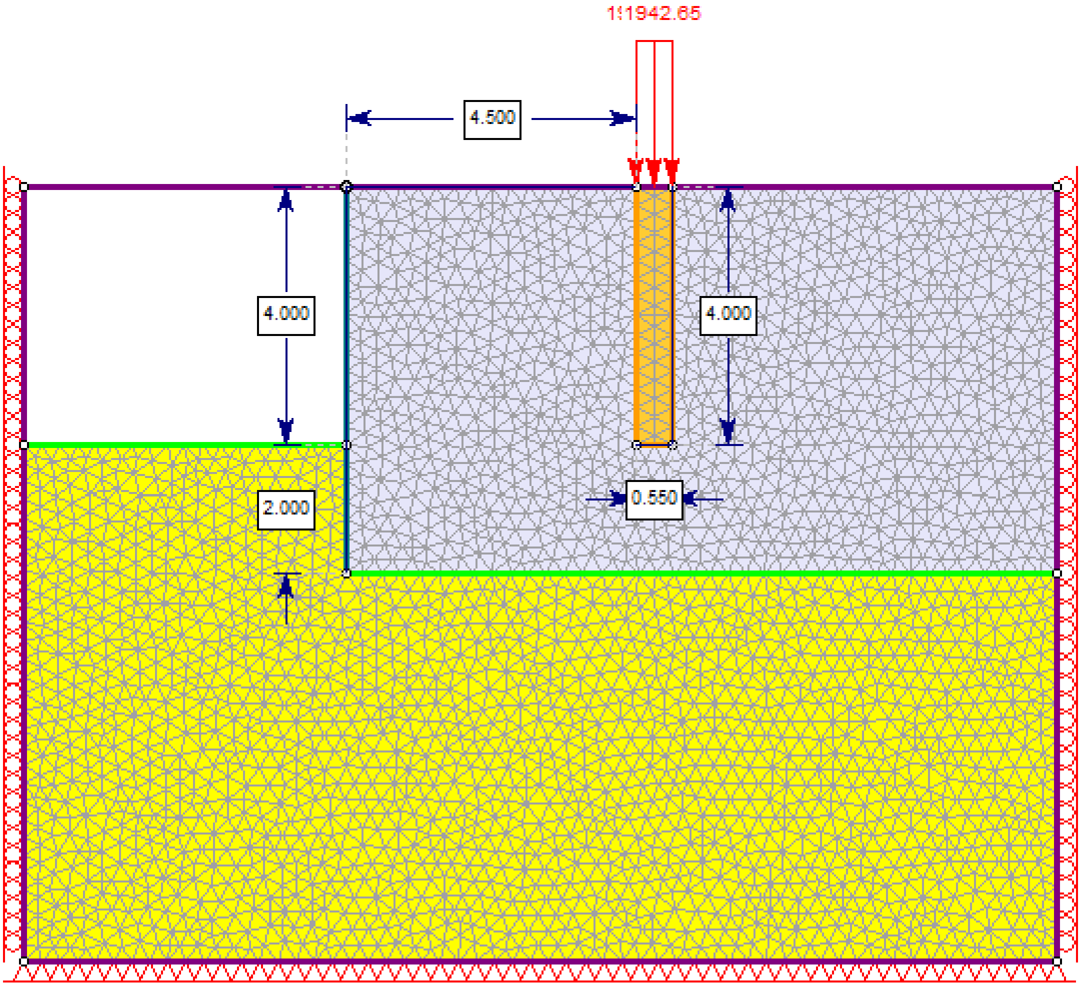

M 118.1: Original model (stage 3)

C_1'	ϕ_1'	γ_1	E_1	C_2'	ϕ_2'	γ_2	E_2	H_1	H_2	H_3	E_3	D_1	D_2	L	Qult
0	36	20	96	42	25	17	28.8	4.00	2	0.75	753136	4.5	0.55	4	1942.16

M 118.2: Parameter values

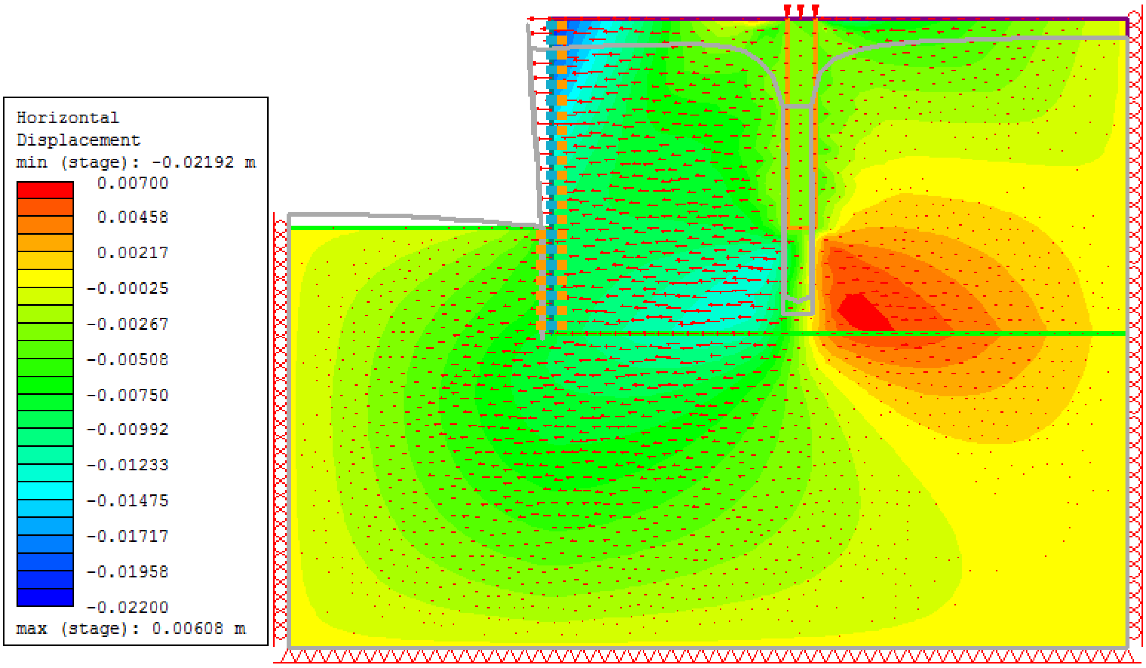

M 118.3: Deformed model (stage 3)

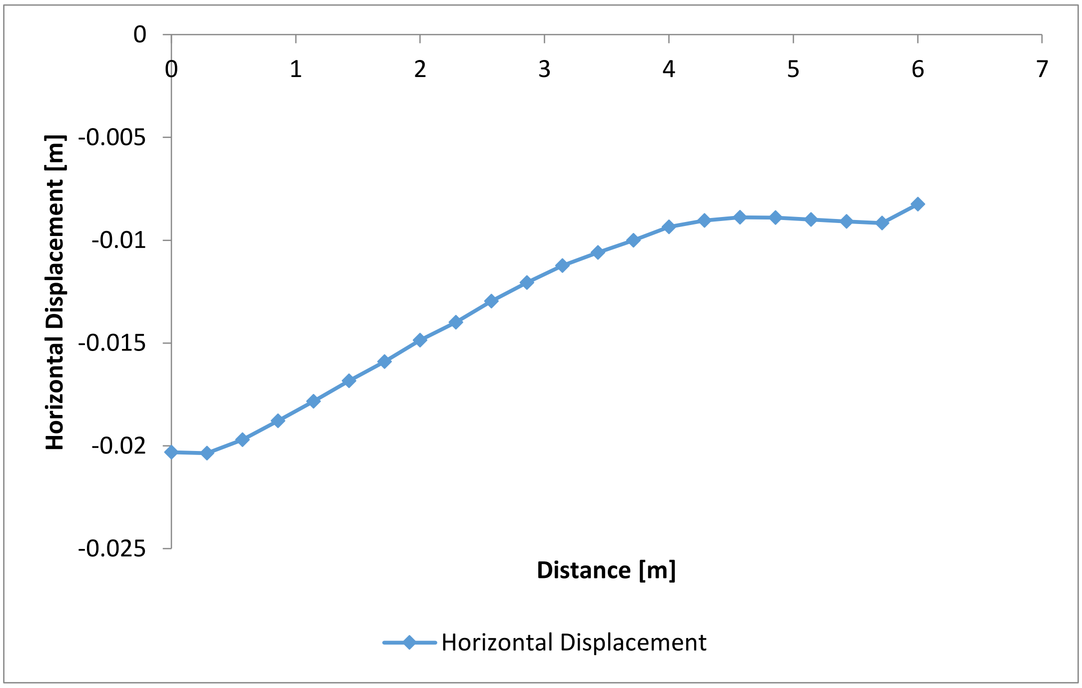

M 118.4: Horizontal displacement of soil along retaining wall

Maximum horizontal displacement of retaining wall: -0.02192m

Distance from point of maximum displacement in retaining wall to the top of backfill soil: 0.0m

Model 119:

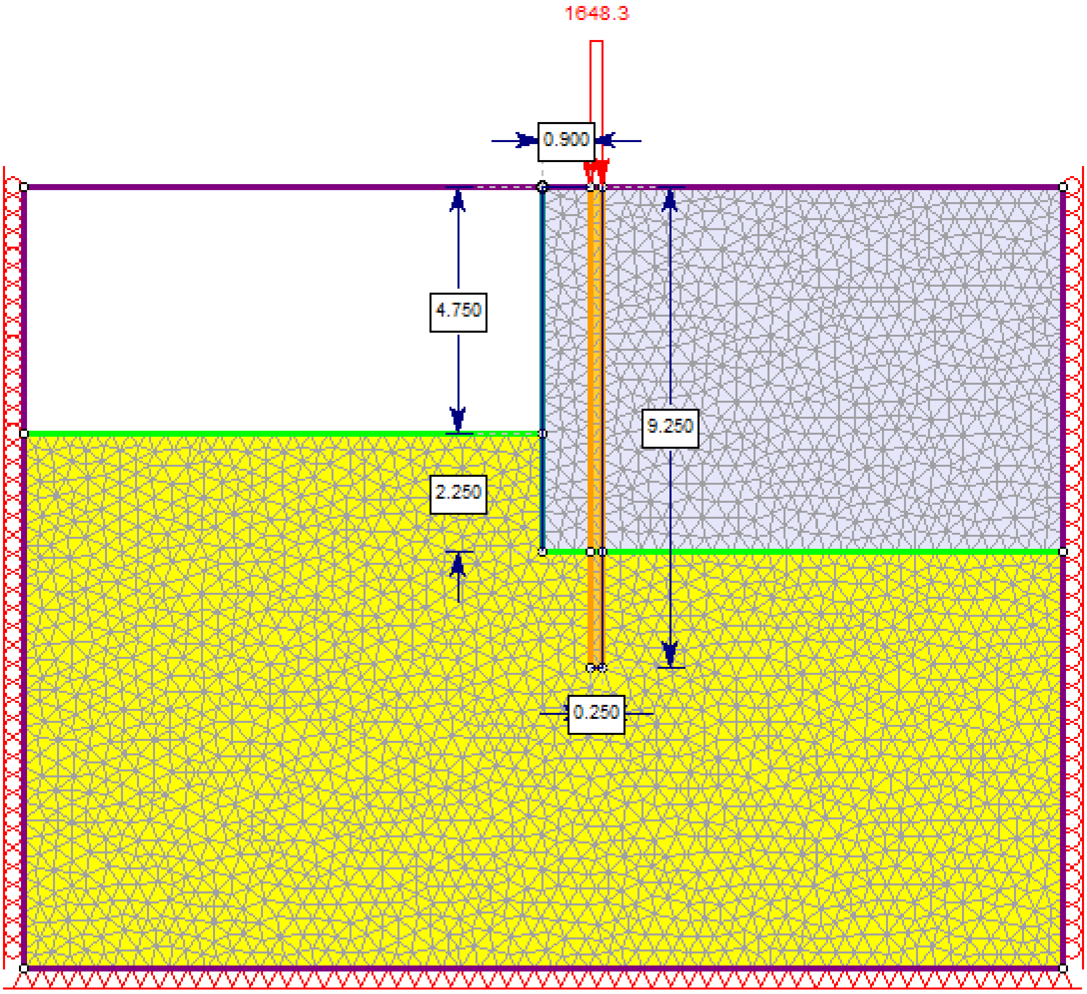

M 119.1: Original model (stage 3)

C'_1	ϕ'_1	γ_1	E_1	C'_2	ϕ'_2	γ_2	E_2	H_1	H_2	H_3	E_3	D_1	D_2	L	Qult
0	33	22	297	59	13	20	23.6	4.75	2.25	1.25	726080	0.9	0.25	9.25	1648.3

M 119.2: Parameter values

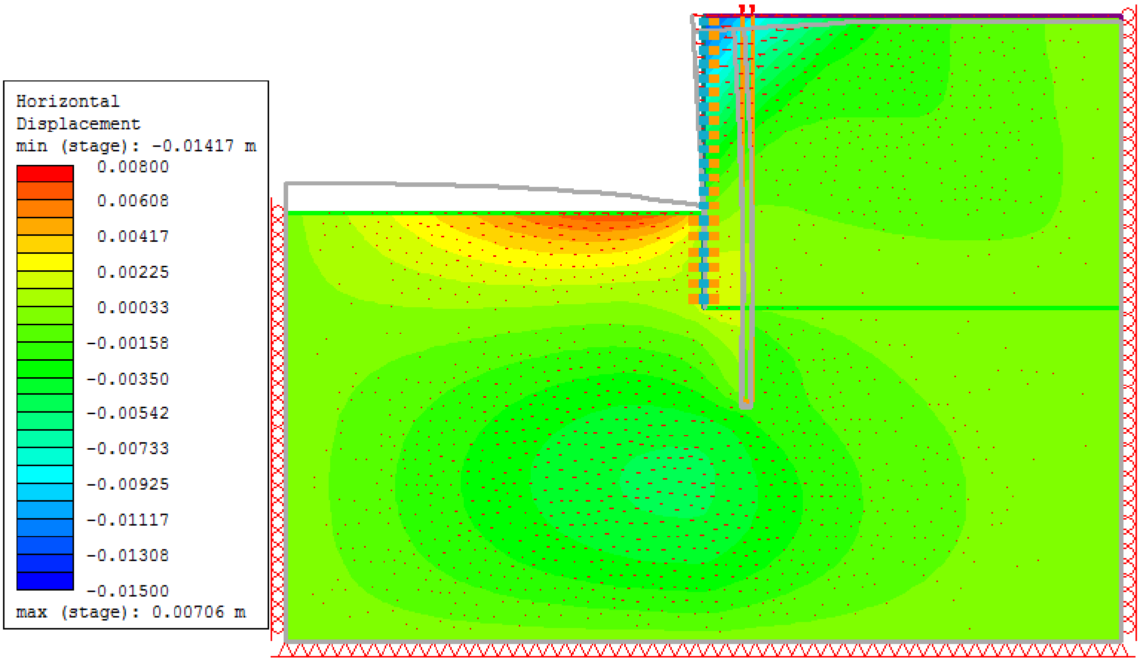

M 119.3: Deformed model (stage 3)

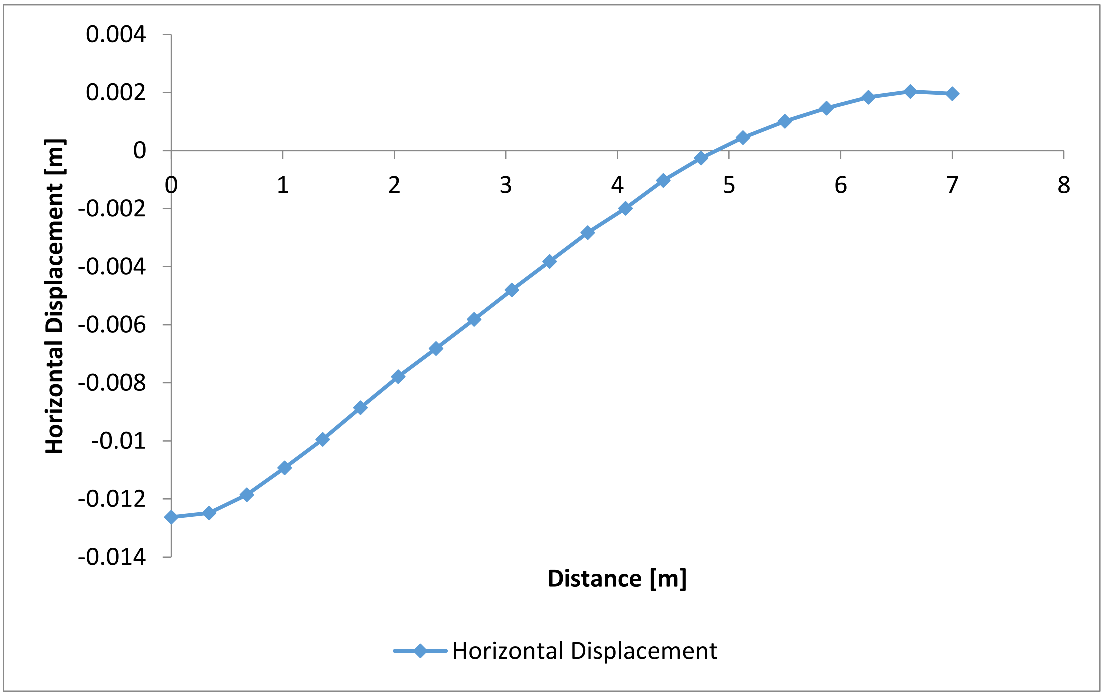

M 119.4: Horizontal displacement of soil along retaining wall

Retaining wall maximum horizontal displacement: -0.01417m

Distance from point of maximum displacement in retaining wall to the top of backfill soil: 0.0m

Model 120:

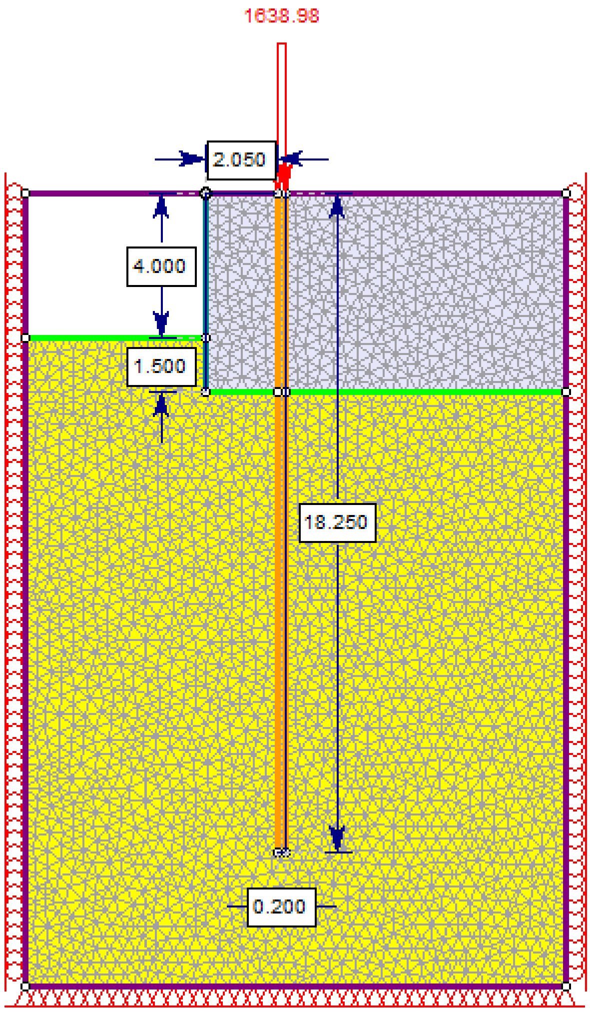

M 120.1: Original model (stage 3)

C'_1	ϕ'_1	γ_1	E_1	C'_2	ϕ'_2	γ_2	E_2	H_1	H_2	H_3	E_3	D_1	D_2	L	Qult
0	40	19	121	46	6	25	20.5	4.00	1.5	0.75	1141747	2.05	0.2	18.25	1638.98

M 120.2: Parameter values

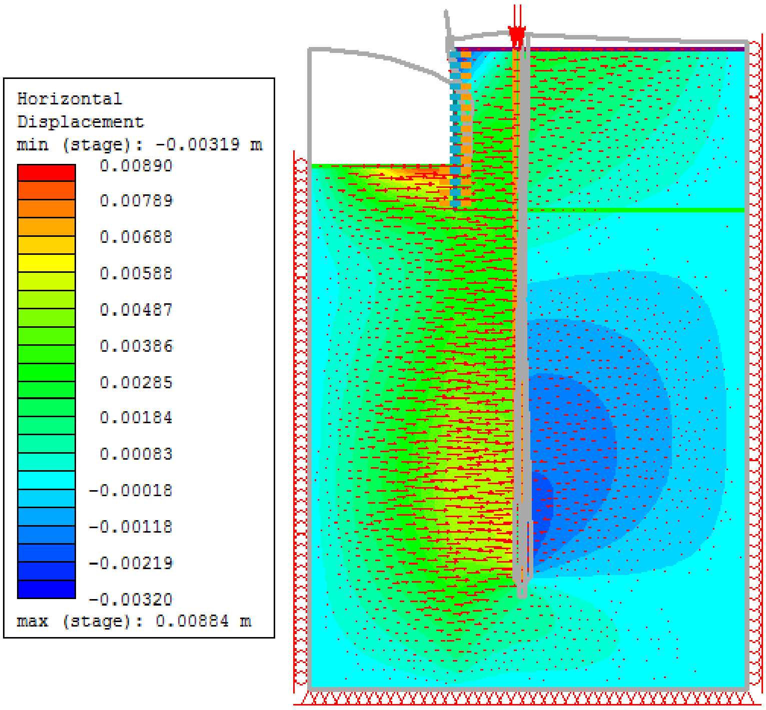

M 120.3: Deformed model (stage 3)

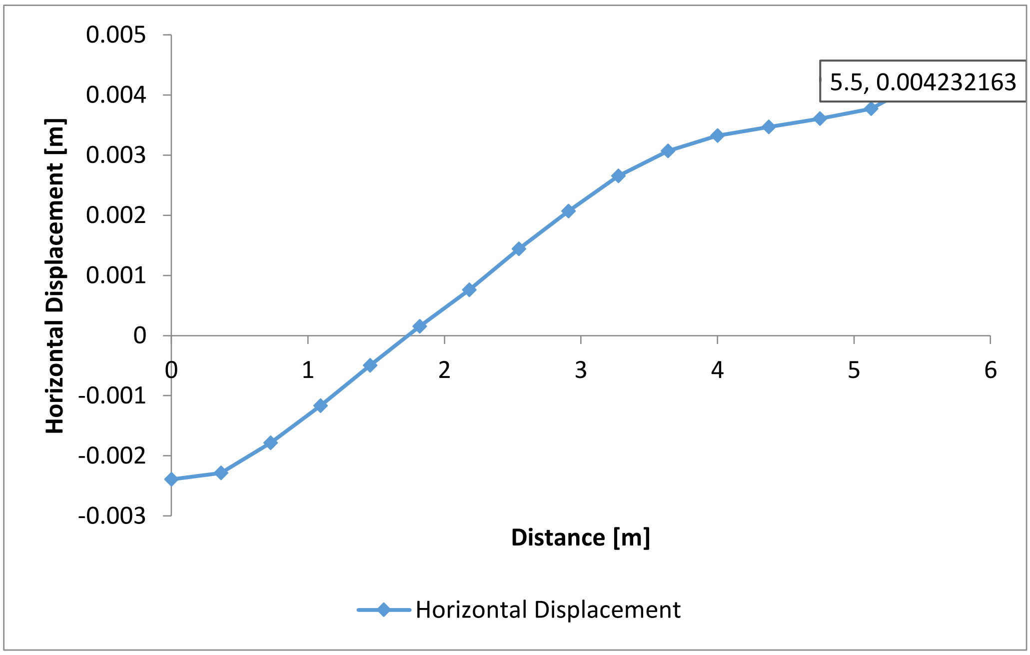

M 120.4: Horizontal displacement of soil along retaining wall

Retaining wall maximum horizontal displacement: 0.00423m

Distance from point of maximum displacement in retaining wall to the top of backfill soil: 5.5m

Model 121:

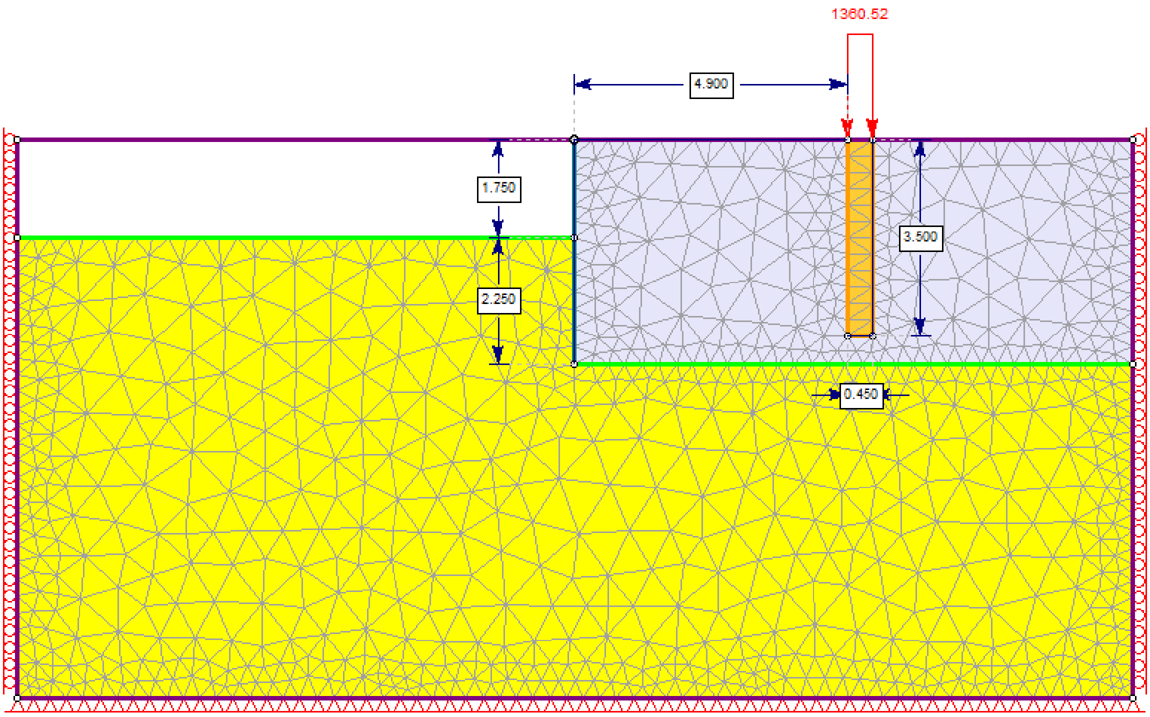

M 121.1: Original model (stage 3)

C_1'	ϕ_1'	γ_1	E_1	C_2'	ϕ_2'	γ_2	E_2	H_1	H_2	H_3	E_3	D_1	D_2	L	Qult
0	30	18	135	11	27	23	35.6	1.75	2.25	1.25	762877	4.9	0.45	3.5	1360.52

M 121.2: Parameter values

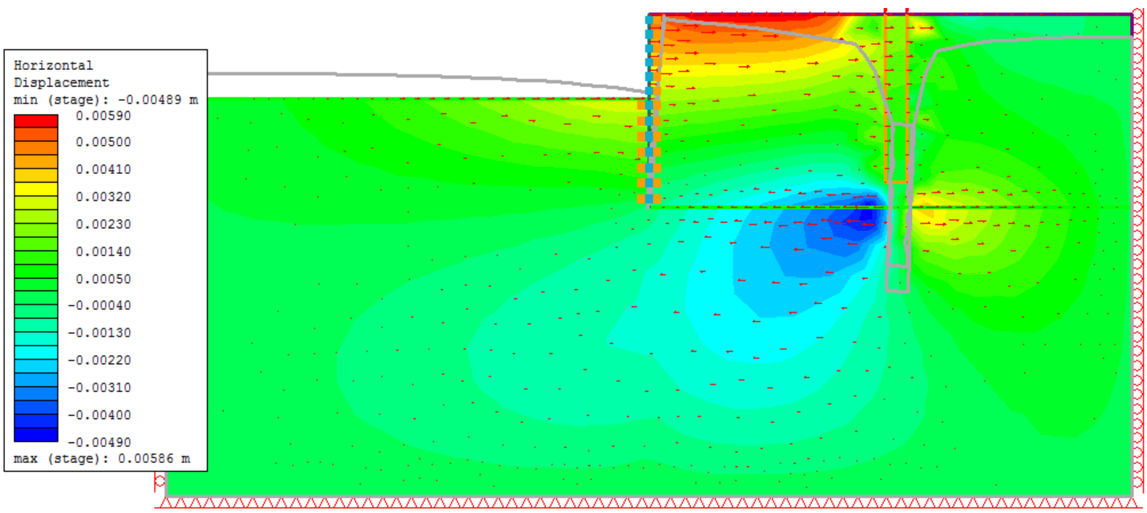

M 121.3: Deformed model (stage 3)

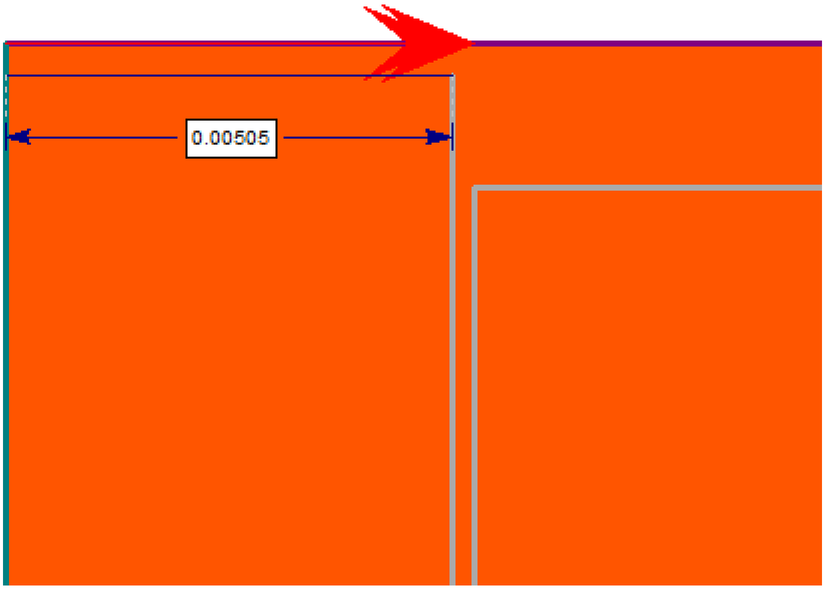

M 121.4: Detailed view of cross-section of retaining wall and soil (stage 3)

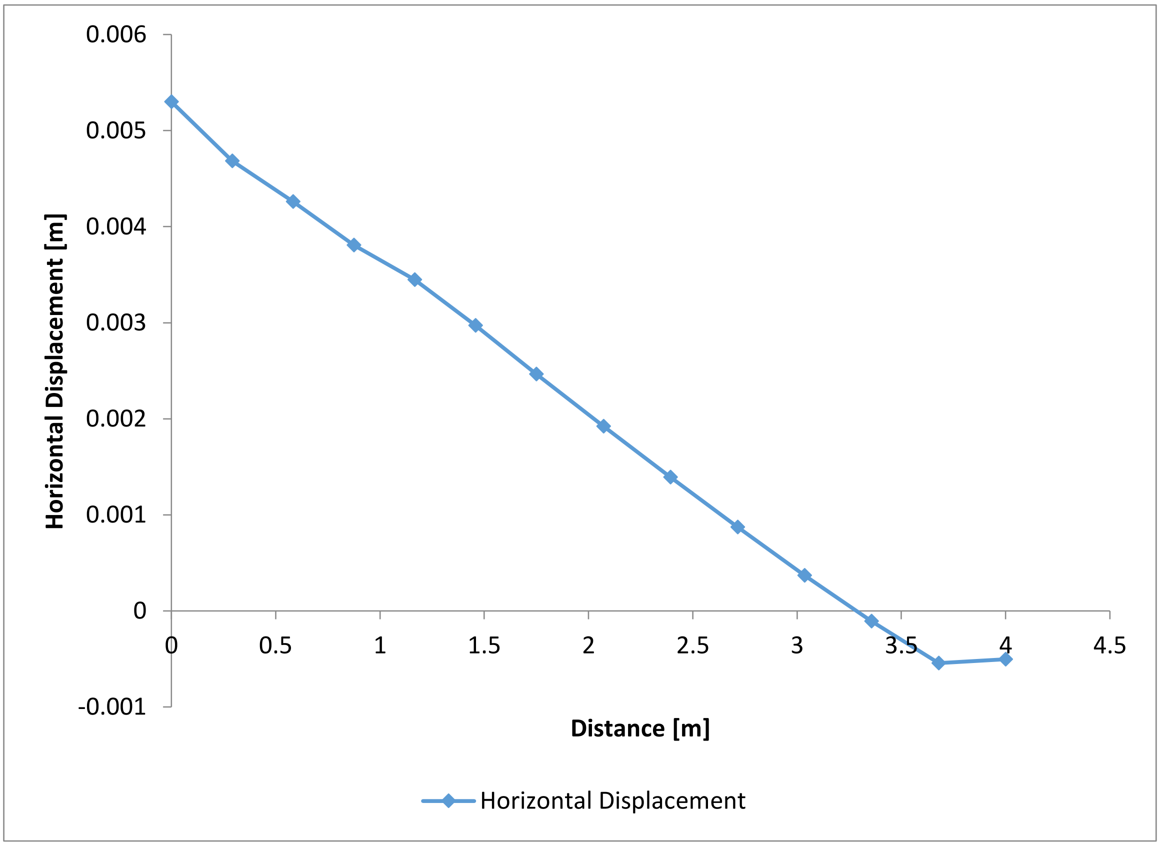

M 121.5: Horizontal displacement of soil along retaining wall

Retaining wall maximum horizontal displacement: 0.00505m

Distance from point of maximum displacement in retaining wall to the top of backfill soil: 0.0m

Model 122:

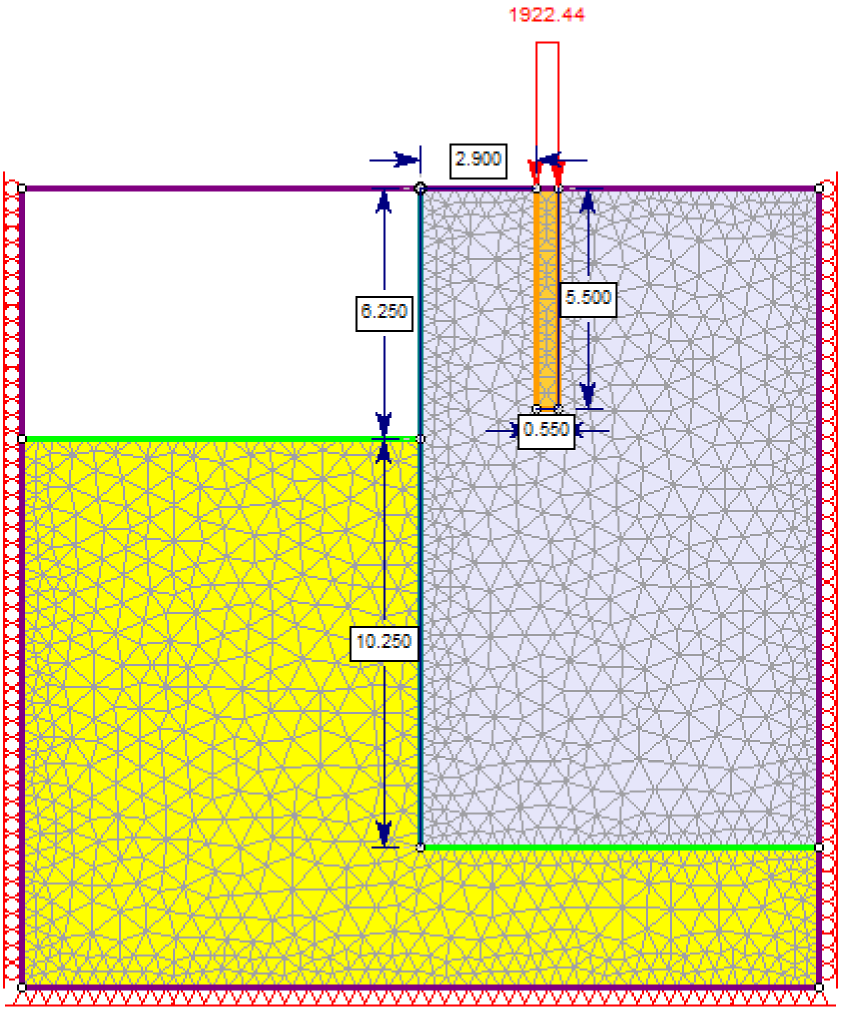

M 122.1: Original model (stage 3)

C'_1	ϕ'_1	γ_1	E_1	C'_2	ϕ'_2	γ_2	E_2	H_1	H_2	H_3	E_3	D_1	D_2	L	Qult
0	35	19	19	36	17	22	17.9	6.25	10.25	1.5	720007	2.9	0.55	5.5	1922.44

M 122.2: Parameter values

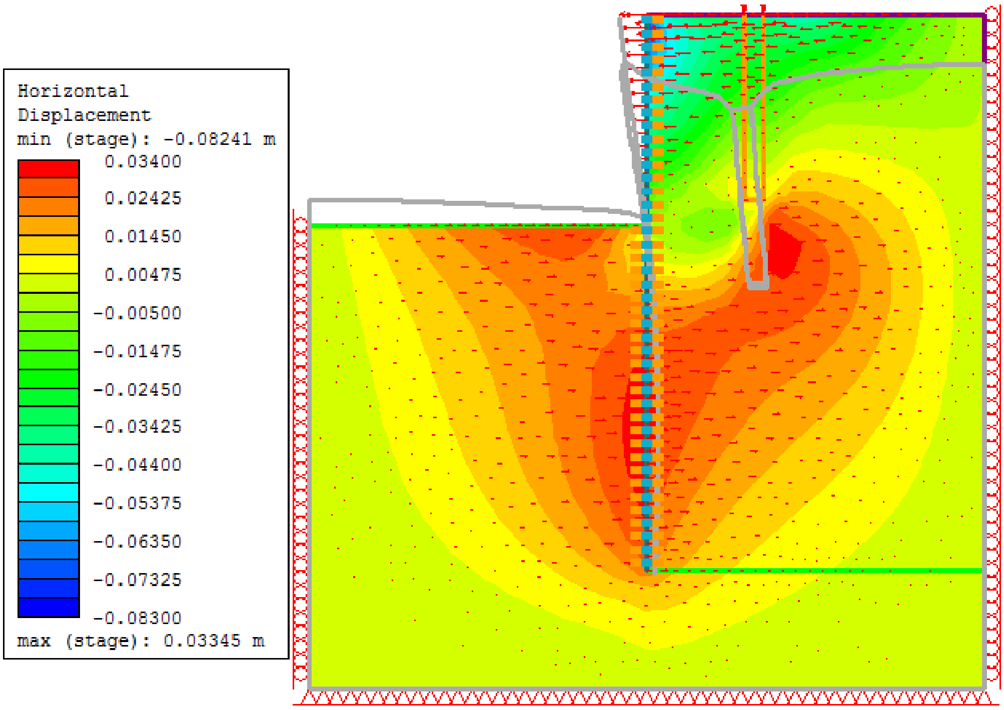

M 122.3: Deformed model (stage 3)

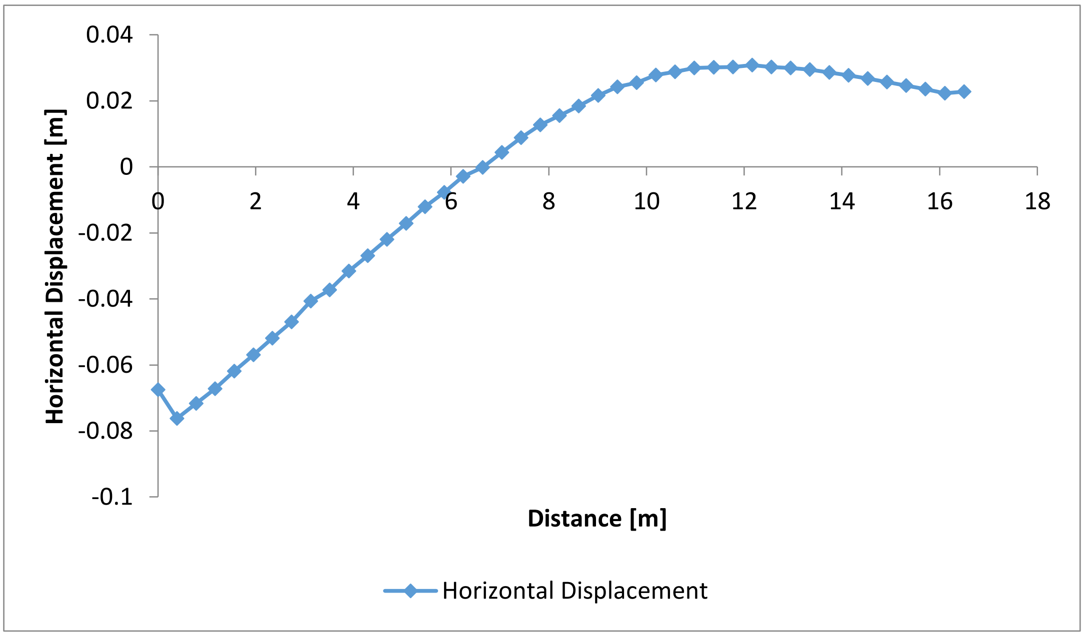

M 122.4: Horizontal displacement of soil along retaining wall

Retaining wall maximum horizontal displacement: -0.08241m

Distance from point of maximum displacement in retaining wall to the top of backfill soil: 0.0m

Model 123:

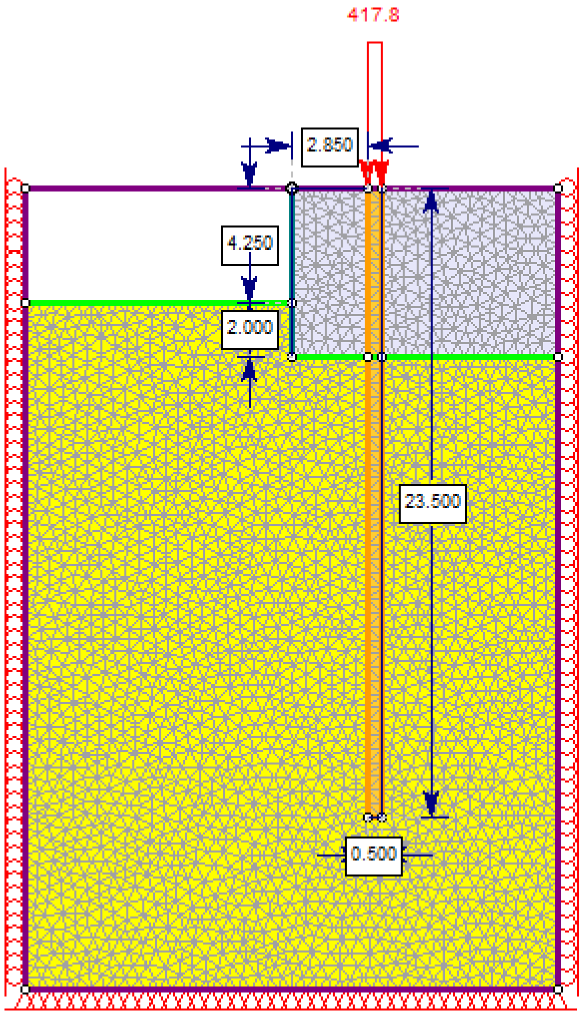

M 123.1: Original model (stage 3)

C'_1	ϕ'_1	γ_1	E_1	C'_2	ϕ'_2	γ_2	E_2	H_1	H_2	H_3	E_3	D_1	D_2	L	Qult
0	36	19	184	47	0	21	25.1	4.25	2	0.75	925735	2.85	0.5	23.5	417.8

M 123.2: Parameter values

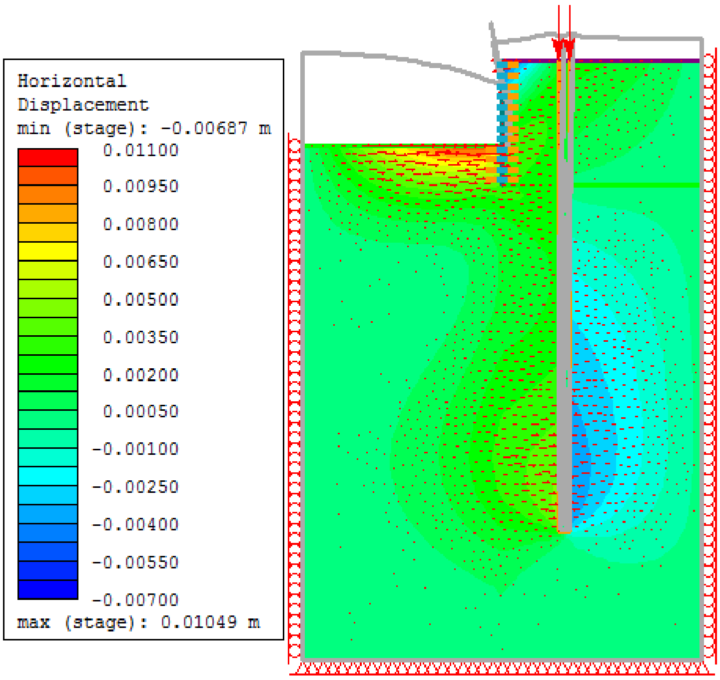

M 123.3: Deformed model (stage 3)

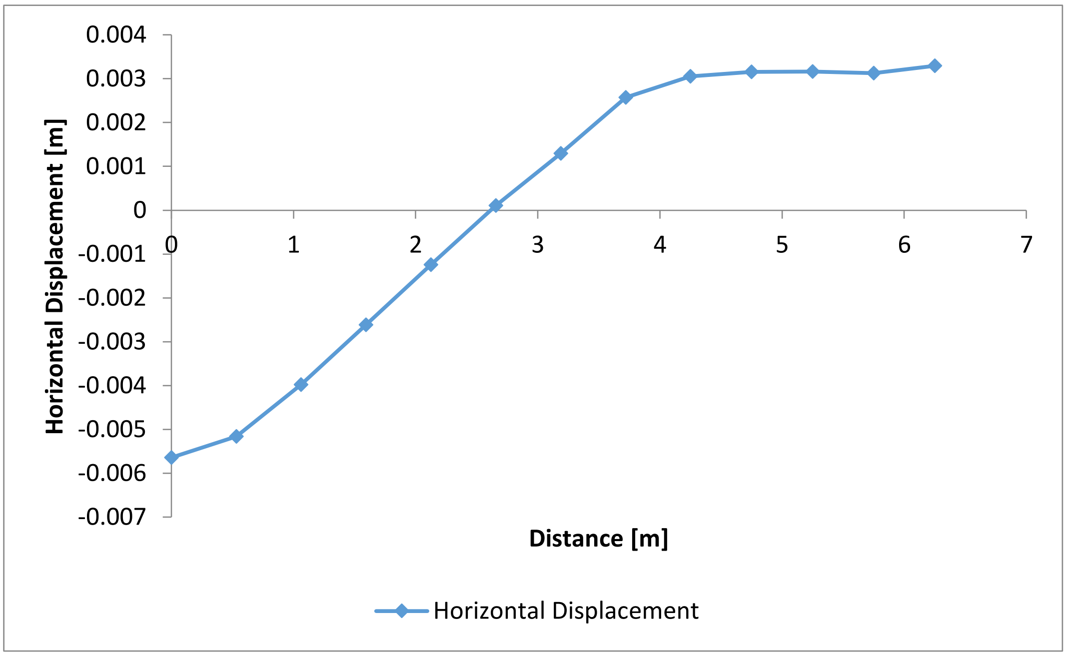

M 123.4: Horizontal displacement of soil along retaining wall

Retaining wall maximum horizontal displacement: -0.00687m

Distance from point of maximum displacement in retaining wall to the top of backfill soil: 0.0m

Model 124:

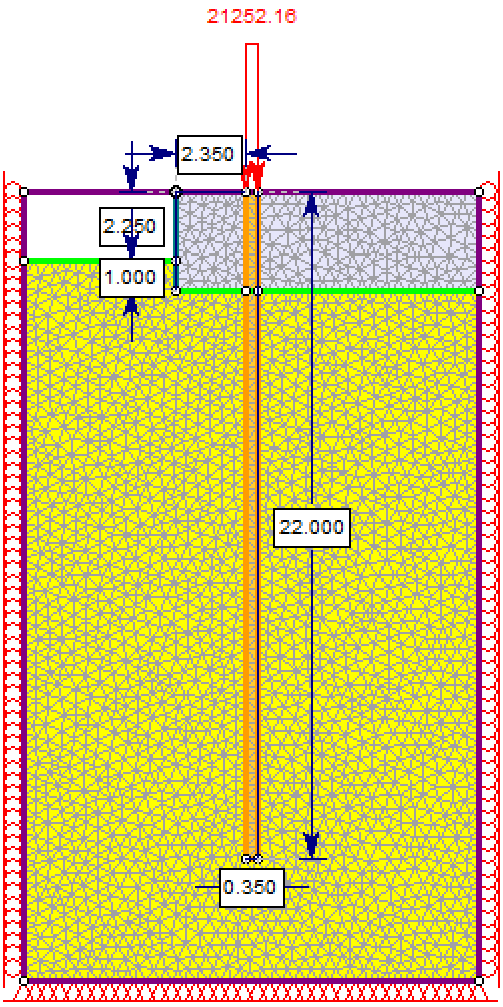

M 124.1: Deformed model (stage 3)

C_1'	ϕ_1'	γ_1	E_1	C_2'	ϕ_2'	γ_2	E_2	H_1	H_2	H_3	E_3	D_1	D_2	L	Qult
0	38	21	117	29	34	22	6.6	2.25	1	1.5	782914	2.35	0.35	22	21252.16

M 124.2: Parameter values

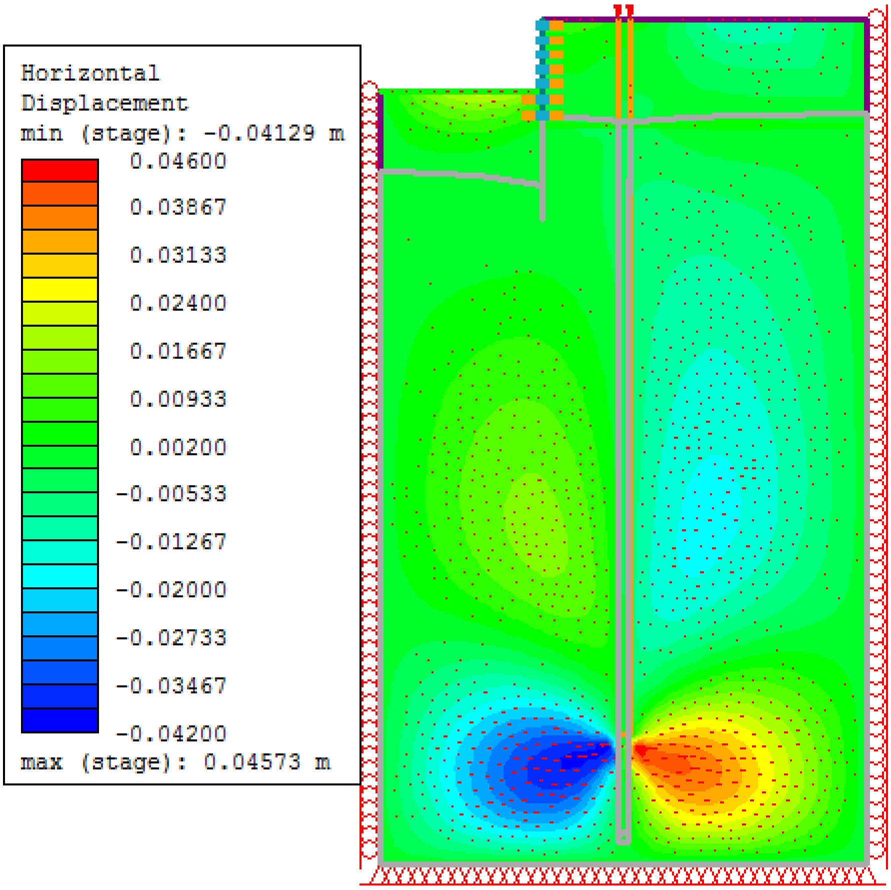

M 124.3: Deformed model (stage 3)

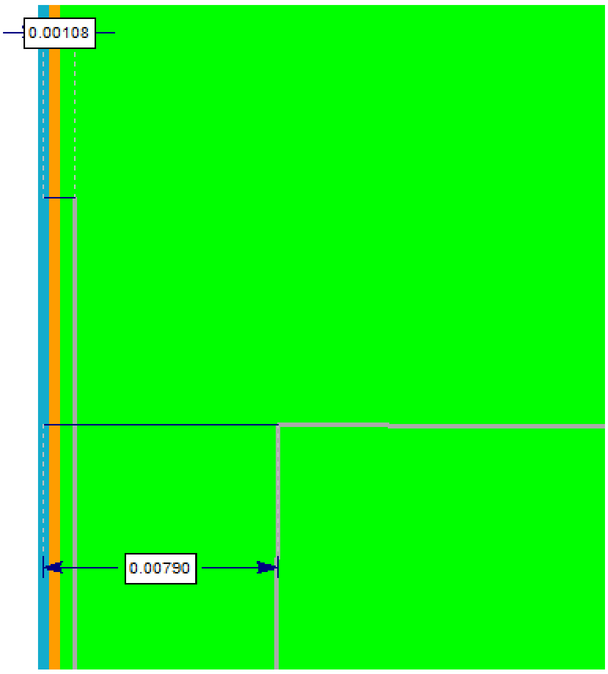

M 124.4: Detailed view of cross-section of retaining wall and soil (stage 3)

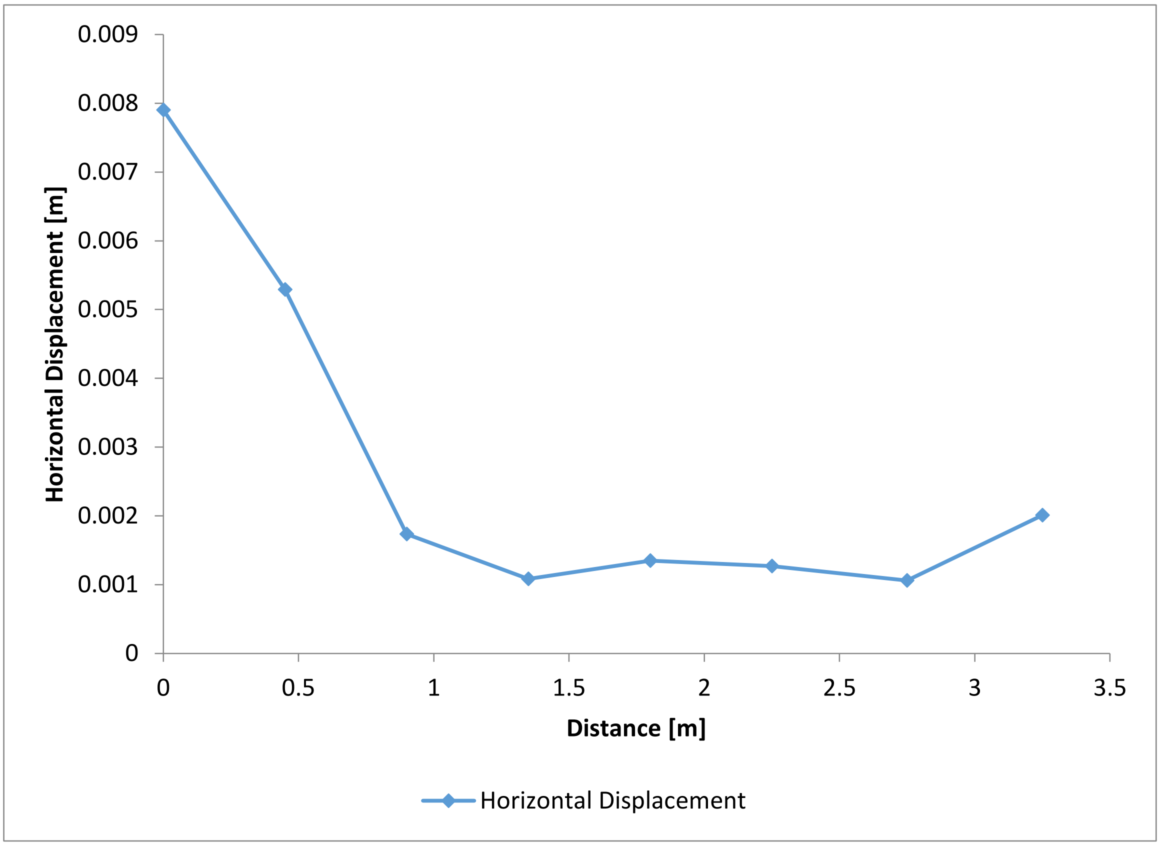

M 124.5: Horizontal displacement of soil along retaining wall

Retaining wall maximum horizontal displacement: 0.00201m

Distance from point of maximum displacement in retaining wall to the top of backfill soil: 3.25m

Model 125:

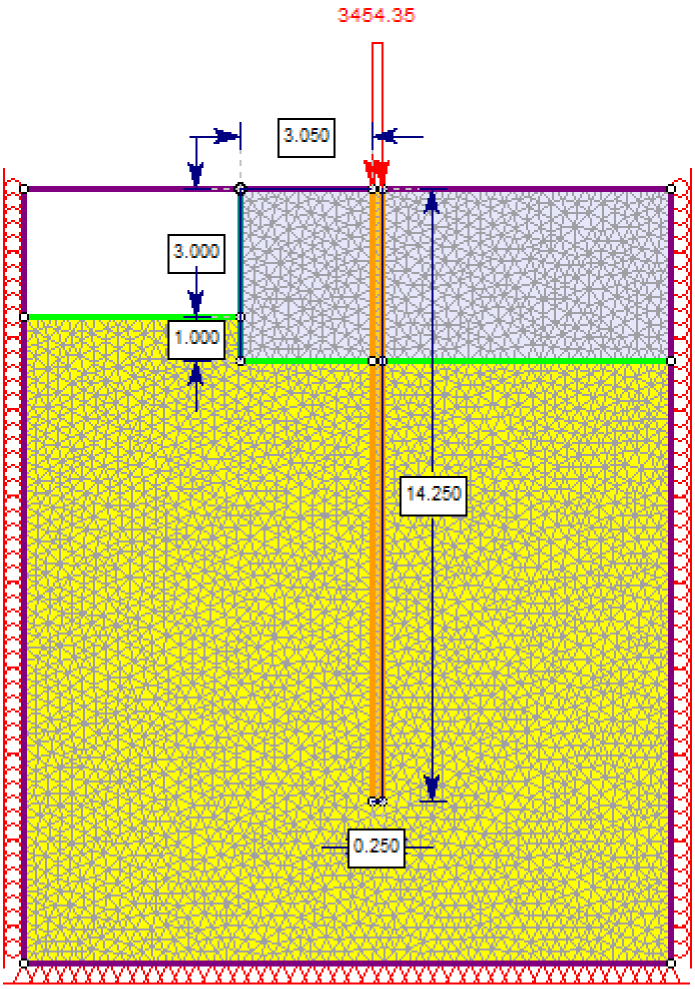

M 125.1: Original model (stage 3)

C_1'	ϕ_1'	γ_1	E_1	C_2'	ϕ_2'	γ_2	E_2	H_1	H_2	H_3	E_3	D_1	D_2	L	Qult
0	40	21	47	53	21	23	22.9	3.00	1	0.5	823087	3.05	0.25	14.25	3454.35

M 125.2: Parameter values

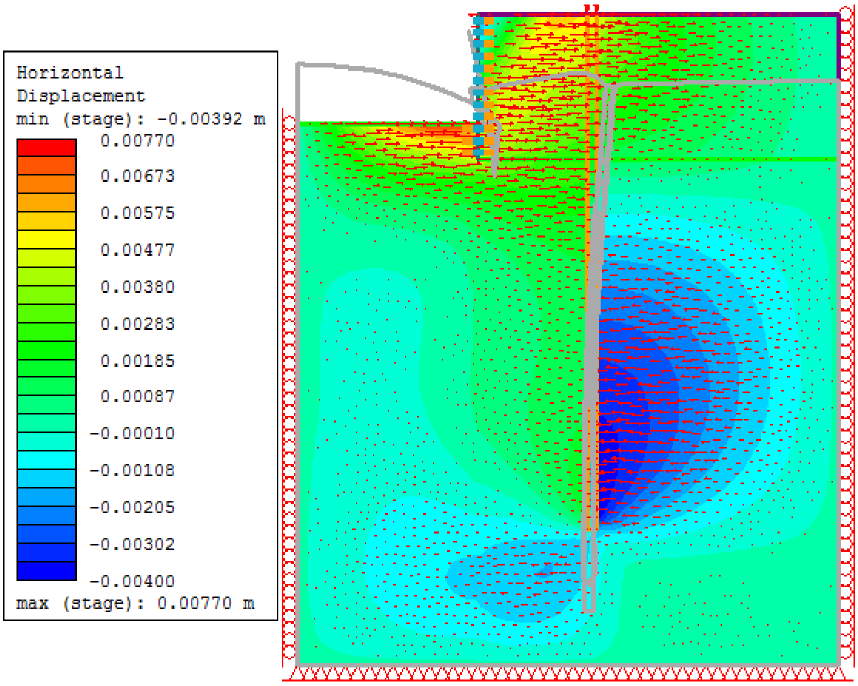

M 125.3: Deformed model (stage 3)

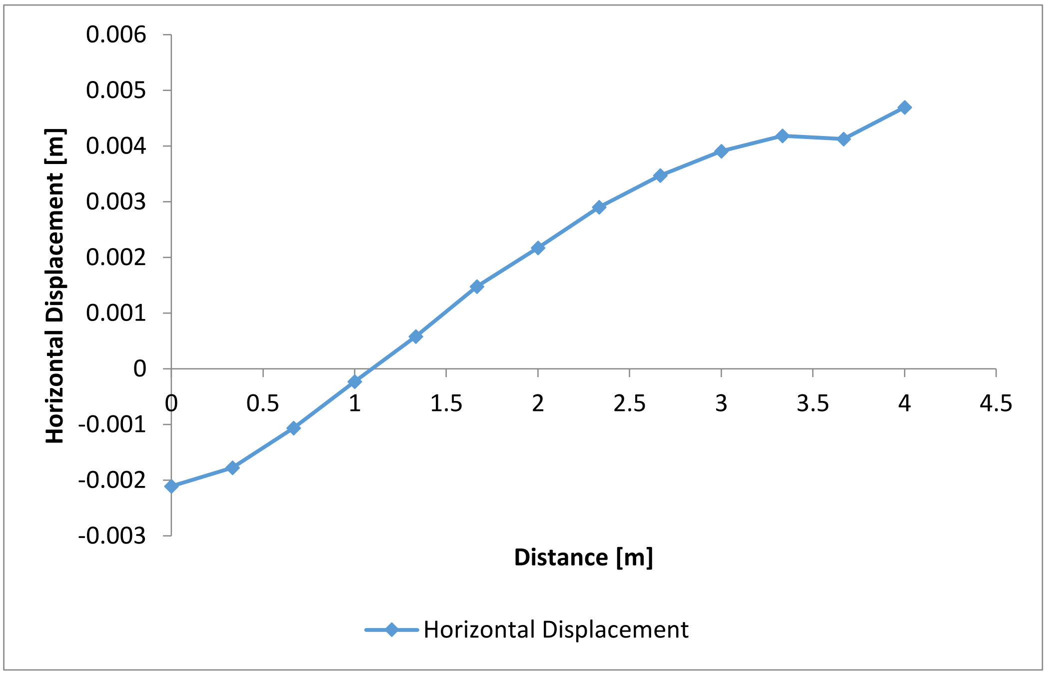

M 125.4: Horizontal displacement of soil along retaining wall

Retaining wall maximum horizontal displacement: 0.004698m

Distance from point of maximum displacement in retaining wall to the top of backfill soil: 4.0m

Model 126:

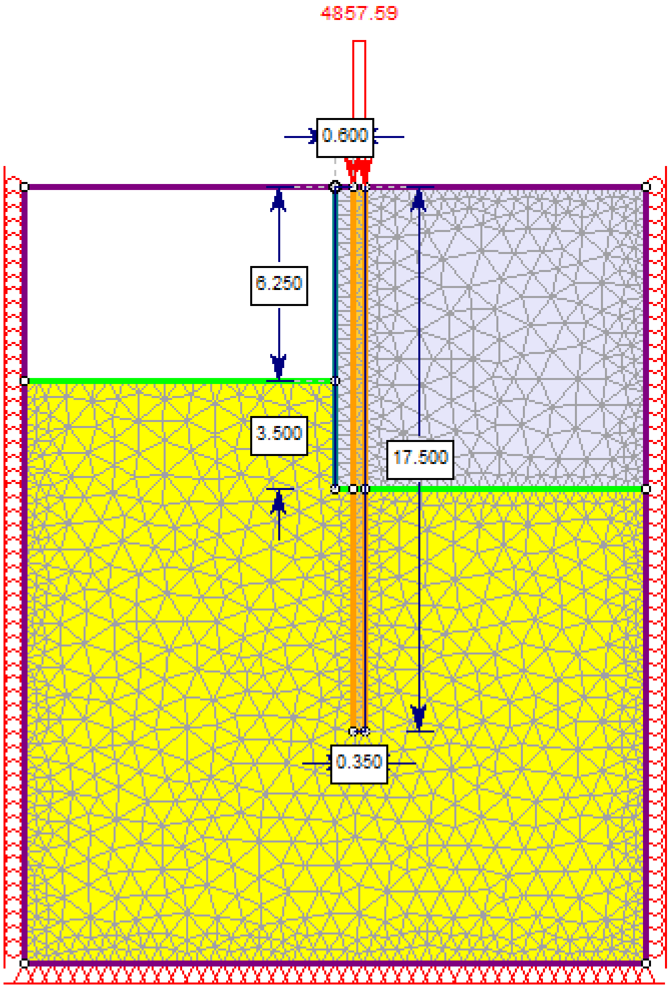

M 126.1: Original model (stage 3)

C_1'	ϕ_1'	γ_1	E_1	C_2'	ϕ_2'	γ_2	E_2	H_1	H_2	H_3	E_3	D_1	D_2	L	Qult
0	38	21	107	58	24	19	36.9	6.25	3.5	1.25	771626	0.6	0.35	17.5	4857.59

M 126.2: Parameter values

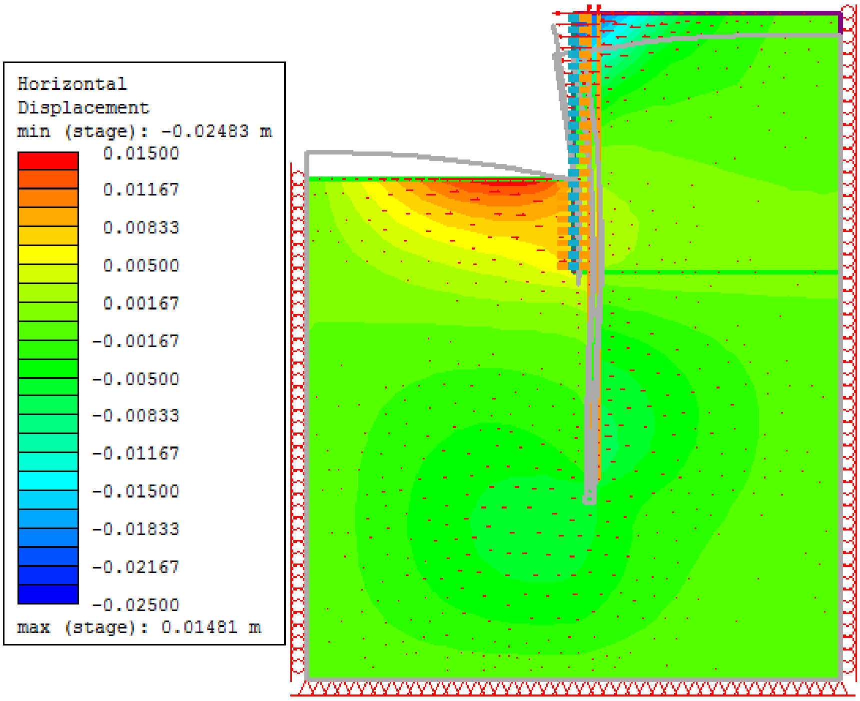

M 126.3: Deformed model (stage 3)

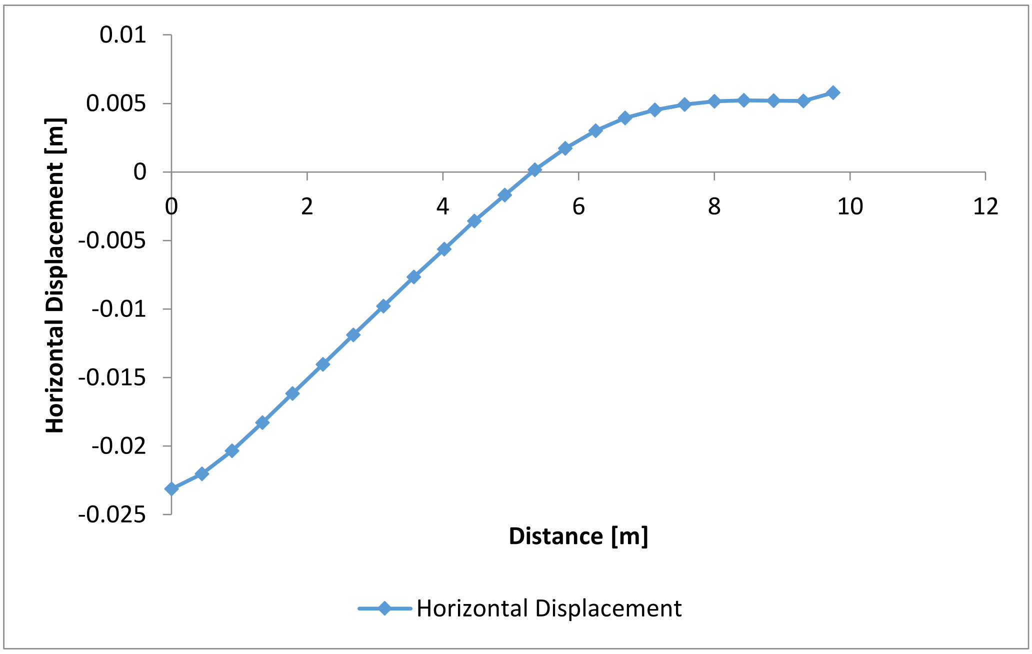

M 126.4: Horizontal displacement of soil along retaining wall

Retaining wall maximum horizontal displacement: -0.02483m

Distance from point of maximum displacement in retaining wall to the top of backfill soil: 0.0m

Model 127:

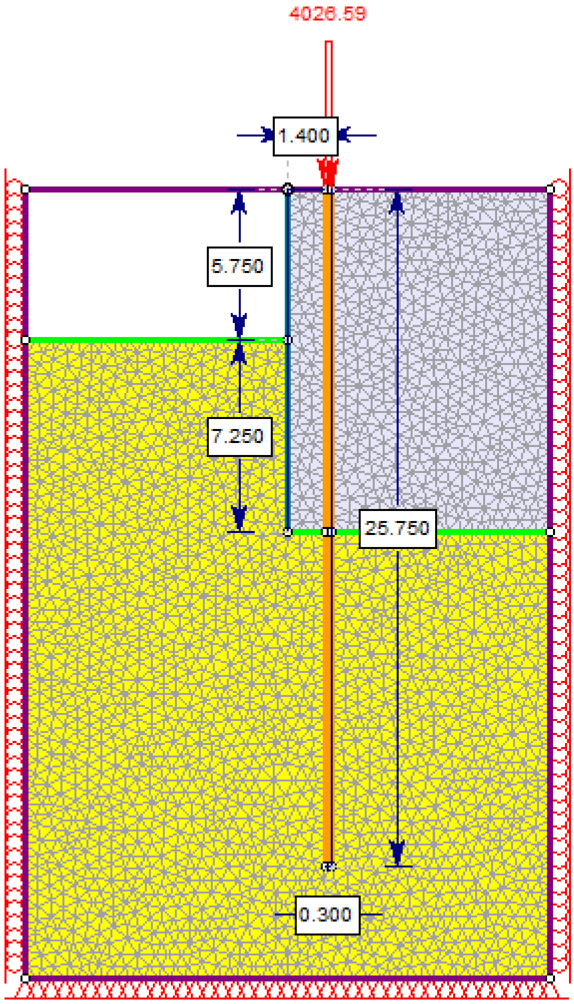

M 127.1: Original model (stage 3)

C'_1	ϕ'_1	γ_1	E_1	C'_2	ϕ'_2	γ_2	E_2	H_1	H_2	H_3	E_3	D_1	D_2	L	Qult
0	39	22	48	42	36	16	22.5	6.00	6.5	0.5	1101651	1.85	0.5	17.5	4026.59

M 127.2: Parameter values

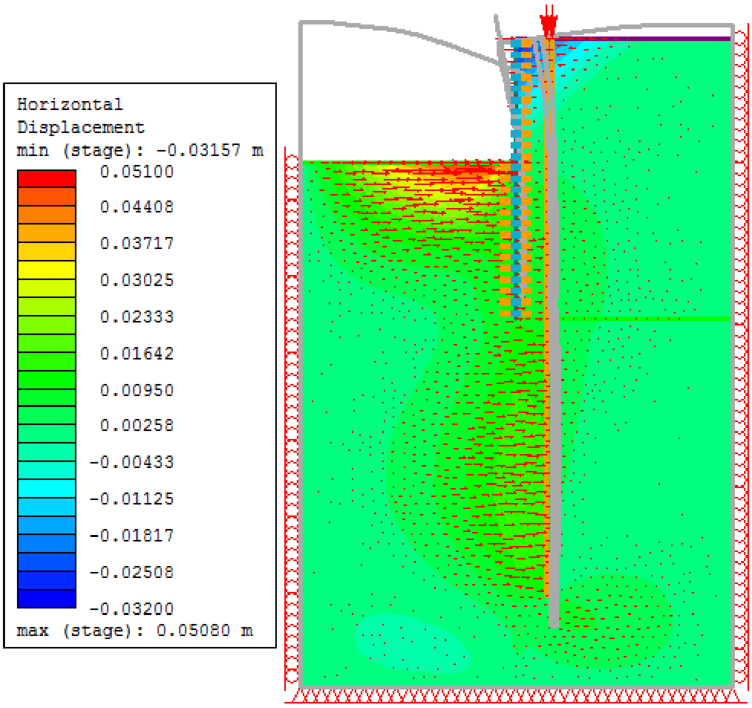

M 127.3: Deformed model (stage 3)

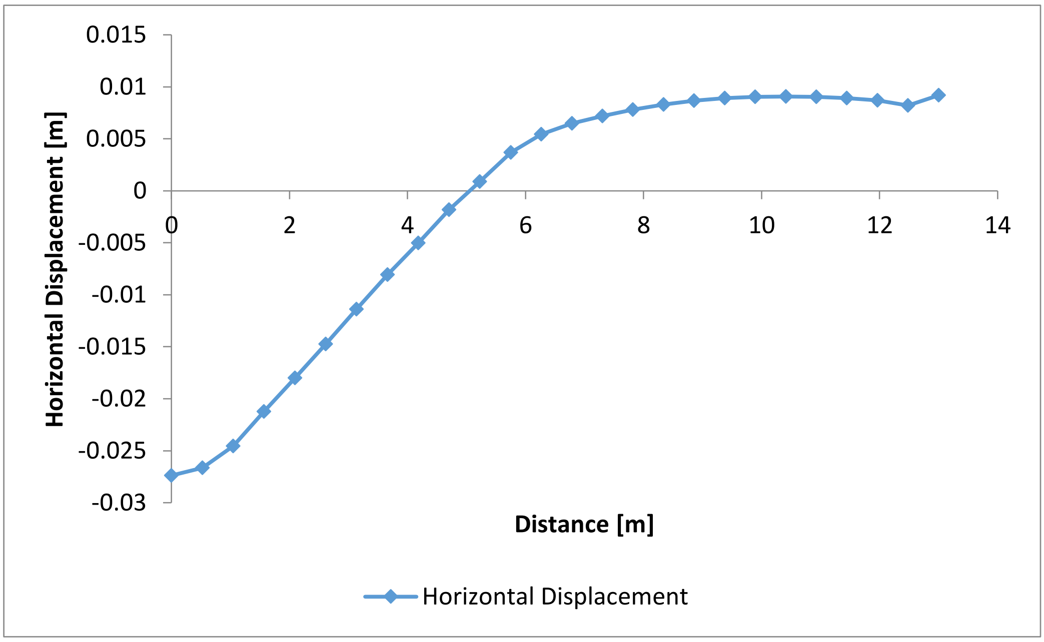

M 127.4: Horizontal displacement of soil along retaining wall

Retaining wall maximum horizontal displacement: -0.03157m

Distance from point of maximum displacement in retaining wall to the top of backfill soil: 0.0m

Model 128:

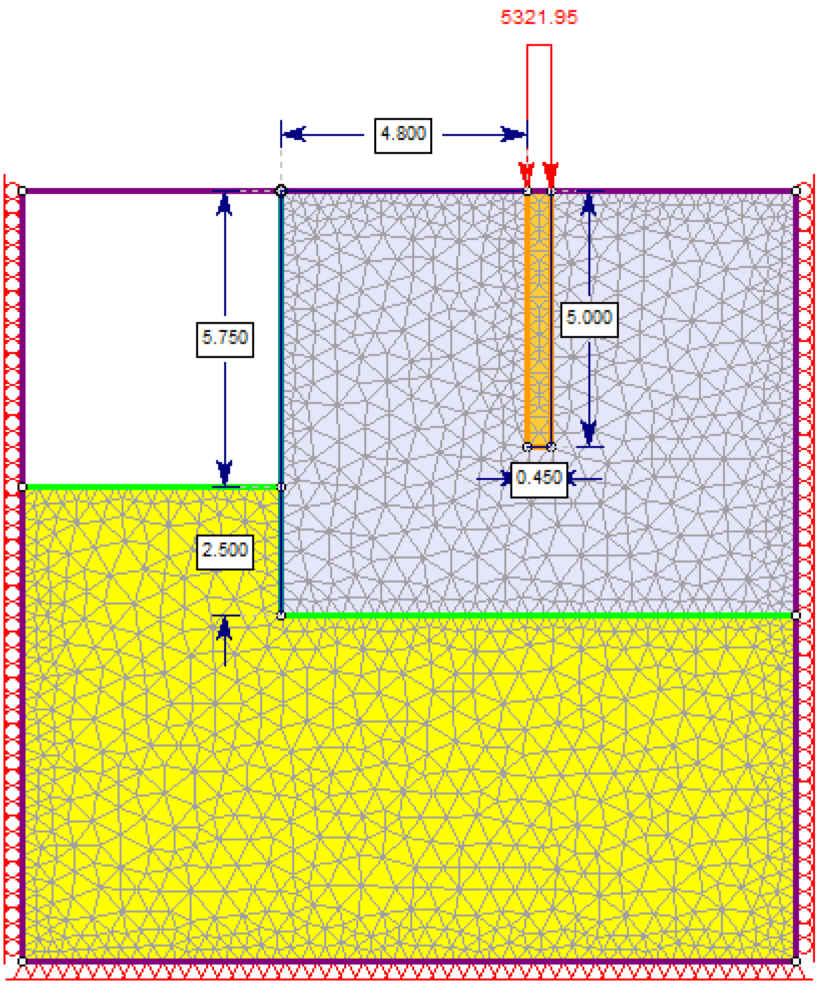

M 128.1: Original model (stage 3)

C_1'	ϕ_1'	γ_1	E_1	C_2'	ϕ_2'	γ_2	E_2	H_1	H_2	H_3	E_3	D_1	D_2	L	Qult
0	40	18	115	58	36	17	9.6	5.75	2.5	0.75	1037255	4.8	0.45	5	5321.95

M 128.2: Parameter values

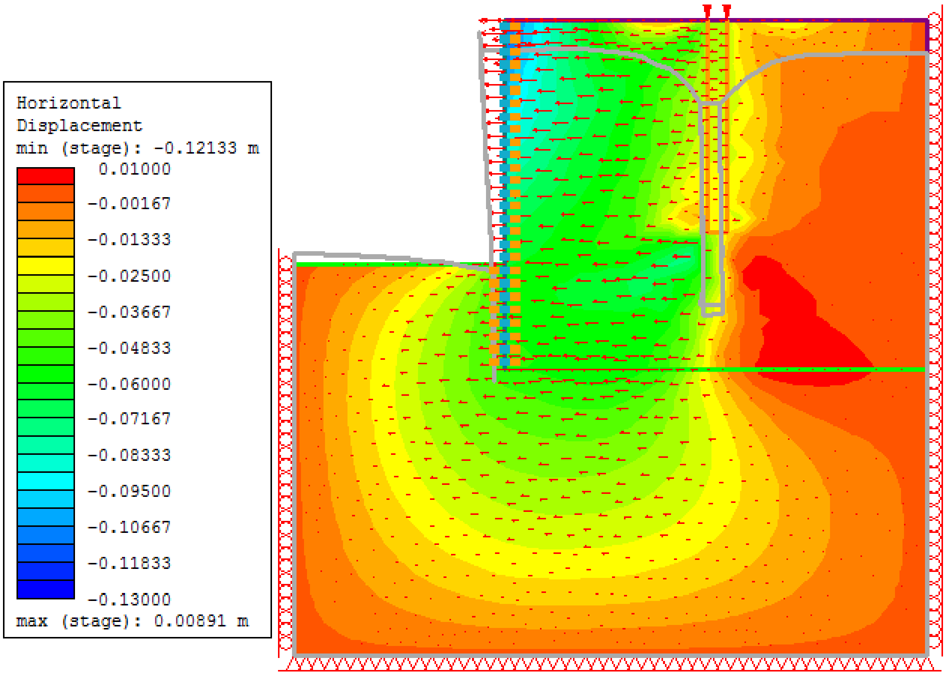

M 128.3: Deformed model (stage 3)

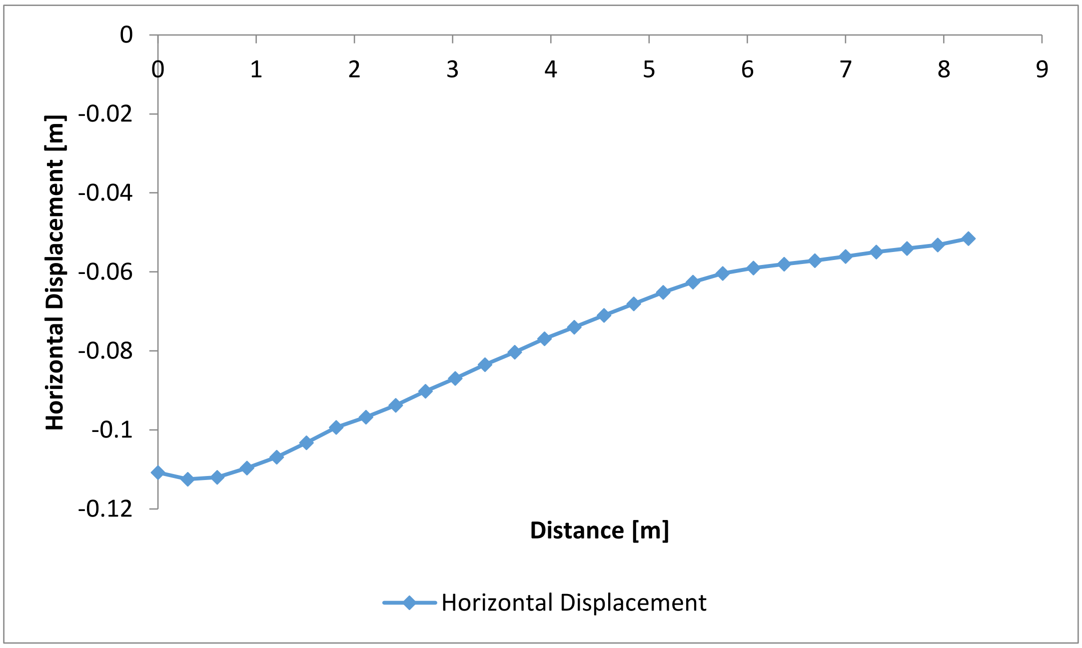

M 128.4: Horizontal displacement of soil along retaining wall

Retaining wall maximum horizontal displacement: -0.12133m

Distance from point of maximum displacement in retaining wall to the top of backfill soil: 0.0m

Model 129:

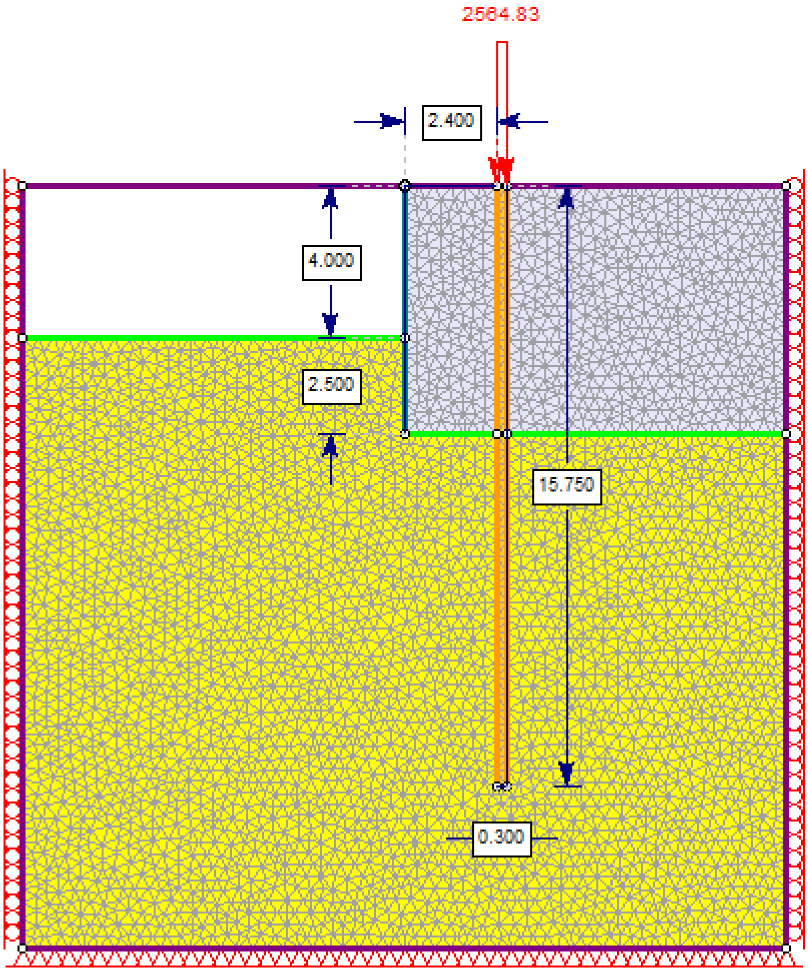

M 129.1: Original model (stage 3)

C_1'	ϕ_1'	γ_1	E_1	C_2'	ϕ_2'	γ_2	E_2	H_1	H_2	H_3	E_3	D_1	D_2	L	Qult
0	38	19	155	33	16	24	24.9	4.00	2.5	0.75	1006702	2.4	0.3	15.75	2564.83

M 129.2: Parameter values

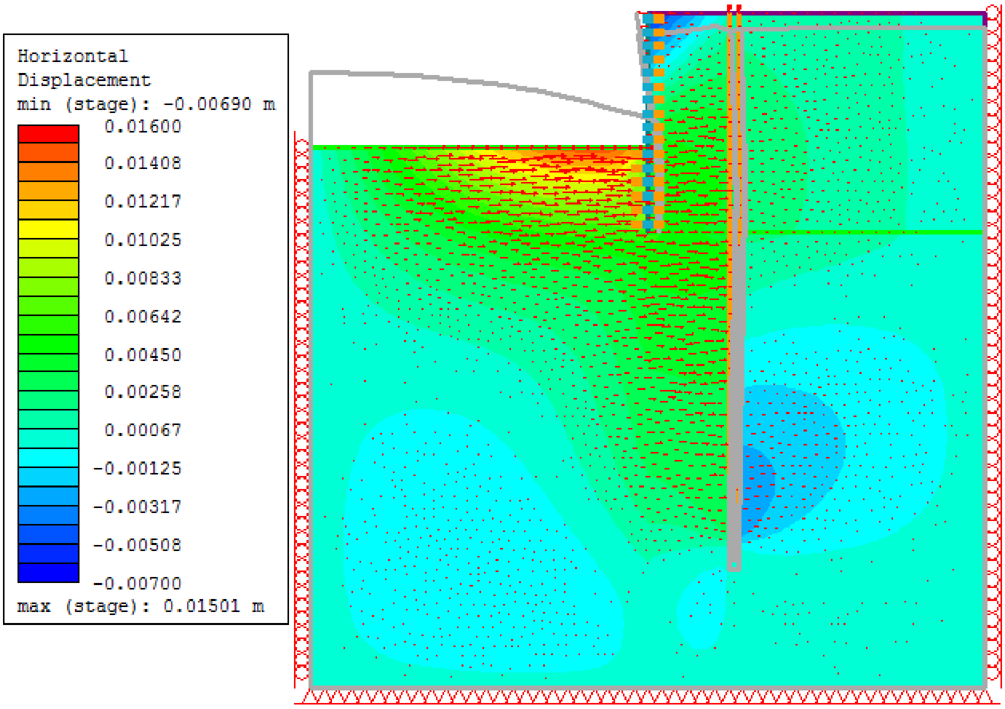

M 129.3: Deformed model (stage 3)

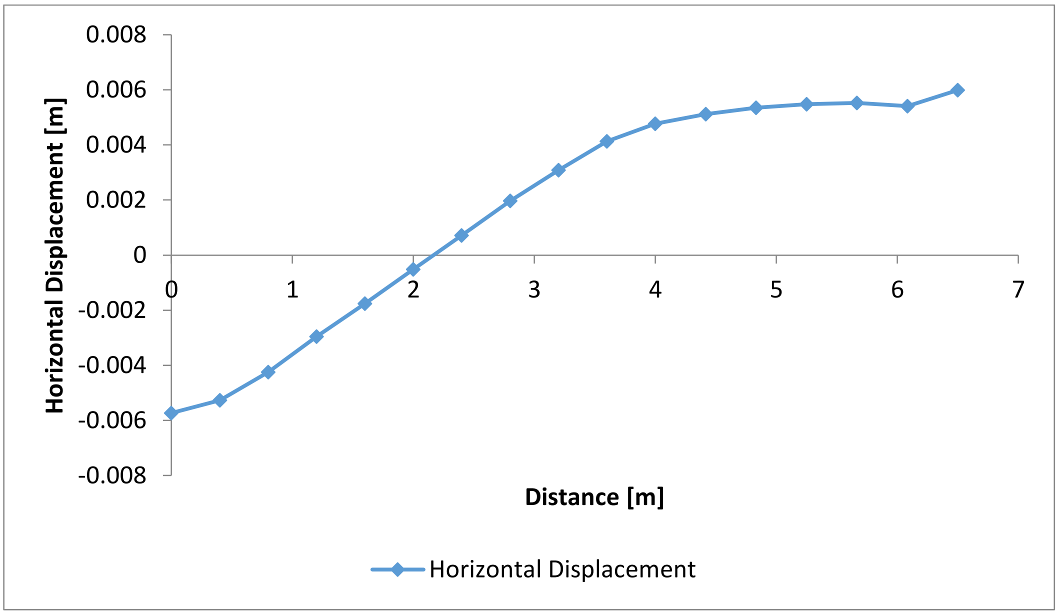

M 129.4: Horizontal displacement of soil along retaining wall

Retaining wall maximum horizontal displacement: -0.0069m

Distance from point of maximum displacement in retaining wall to the top of backfill soil: 0.0m

Model 130:

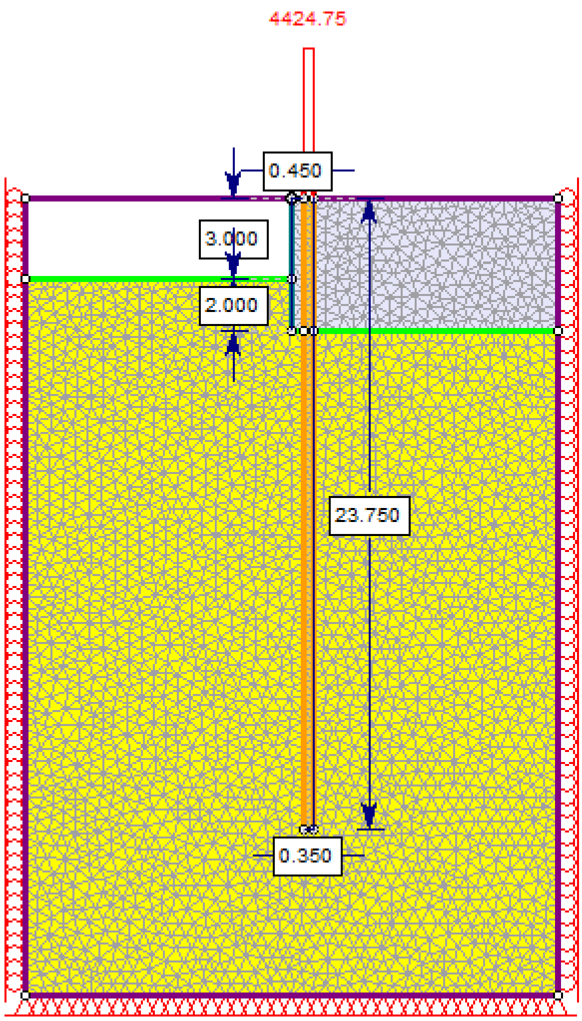

M 130.1: Original model (stage 3)

C_1'	ϕ_1'	γ_1	E_1	C_2'	ϕ_2'	γ_2	E_2	H_1	H_2	H_3	E_3	D_1	D_2	L	Qult
0	38	21	150	26	21	20	40.6	3.00	2	0.75	942301	0.45	0.35	23.75	4424.75

M 130.2: Parameter values

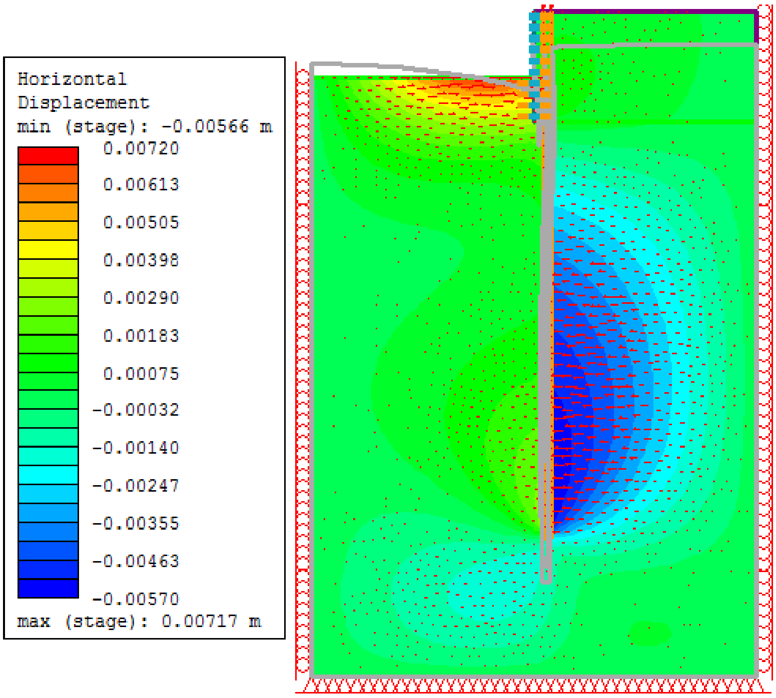

M 130.3: Deformed model (stage 3)

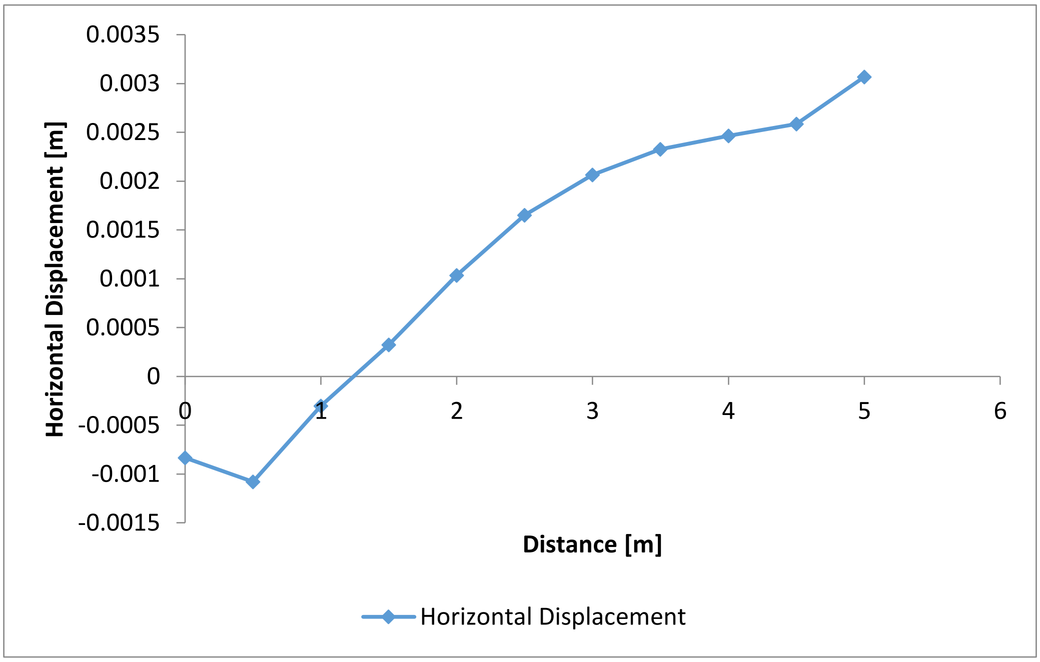

M 130.4: Horizontal displacement of soil along retaining wall

Retaining wall maximum horizontal displacement: 0.00307m

Distance from point of maximum displacement in retaining wall to the top of backfill soil: 5.0m

Model 131:

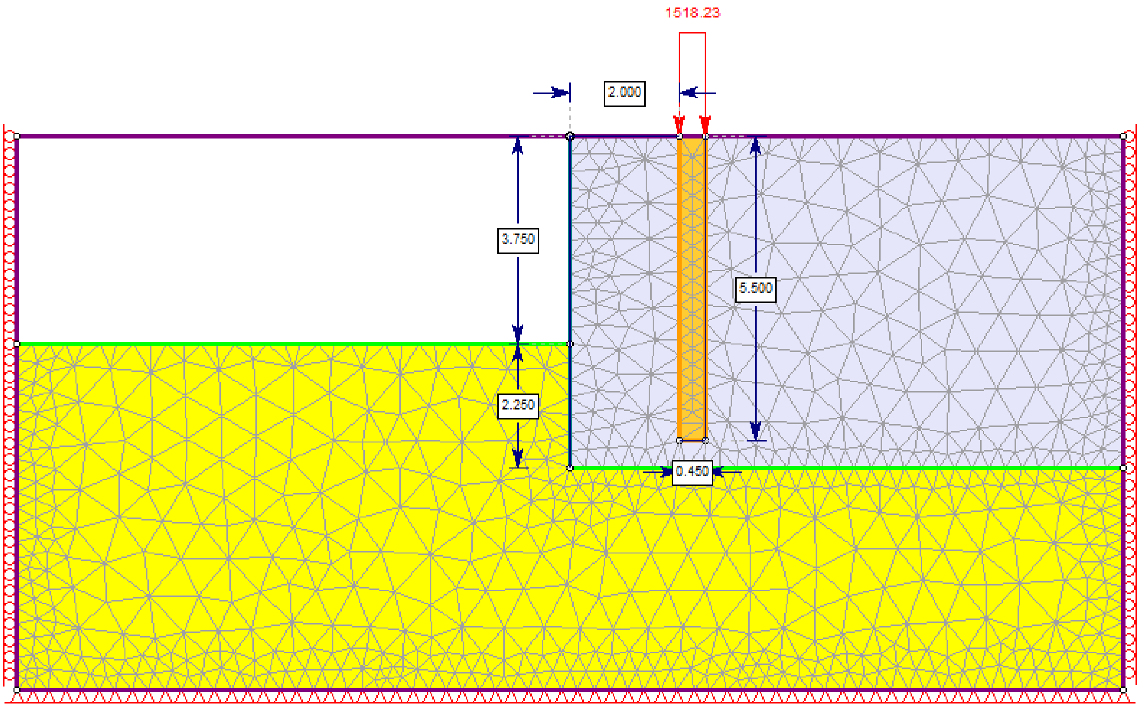

M 131.1: Original model (stage 3)

C'_1	ϕ'_1	γ_1	E_1	C'_2	ϕ'_2	γ_2	E_2	H_1	H_2	H_3	E_3	D_1	D_2	L	Qult
0	31	18	41	35	31	25	5.6	3.75	2.25	1.25	1083762	2	0.45	5.5	1518.23

M 131.2: Parameter values

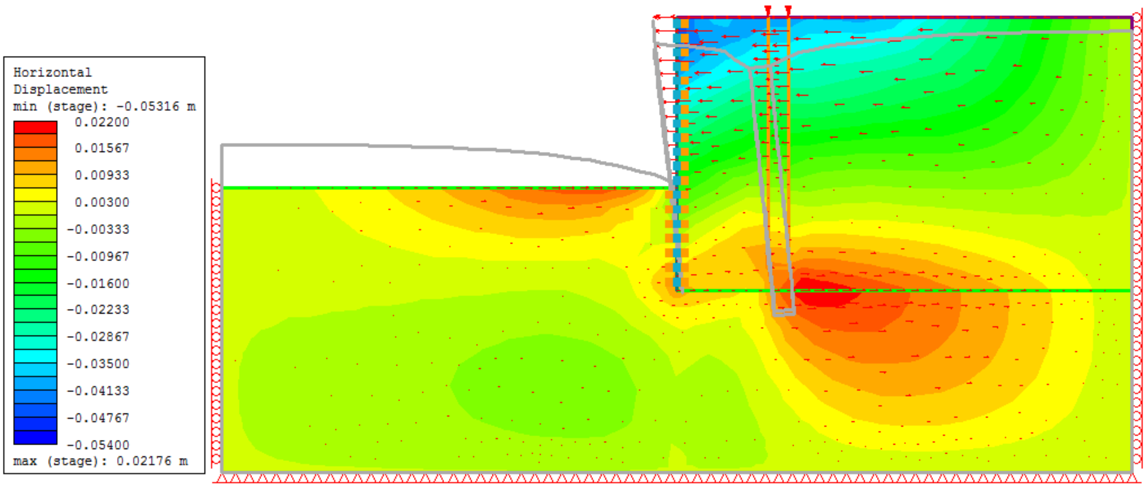

M 131.3: Deformed model (stage 3)

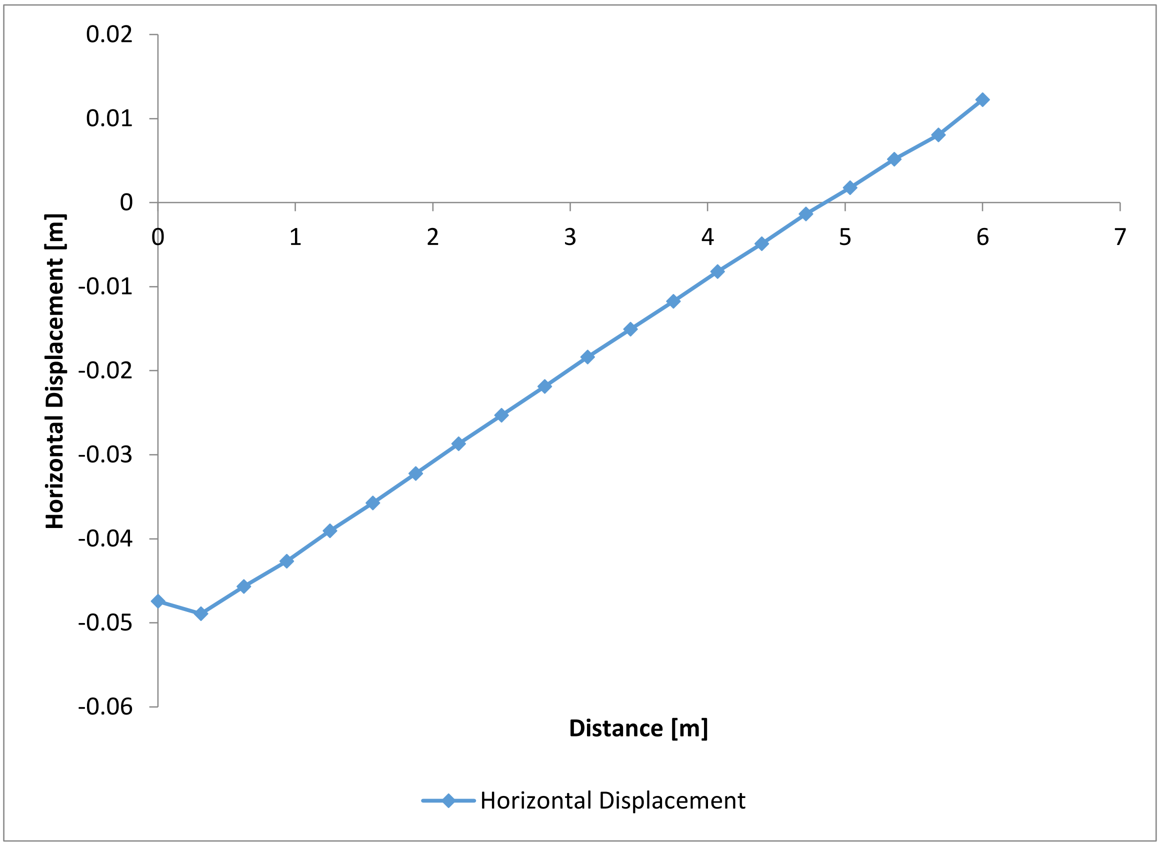

M 131.4: Horizontal displacement of soil along retaining wall

Retaining wall maximum horizontal displacement: -0.05316m

Distance from point of maximum displacement in retaining wall to the top of backfill soil: 0.0m

Model 132:

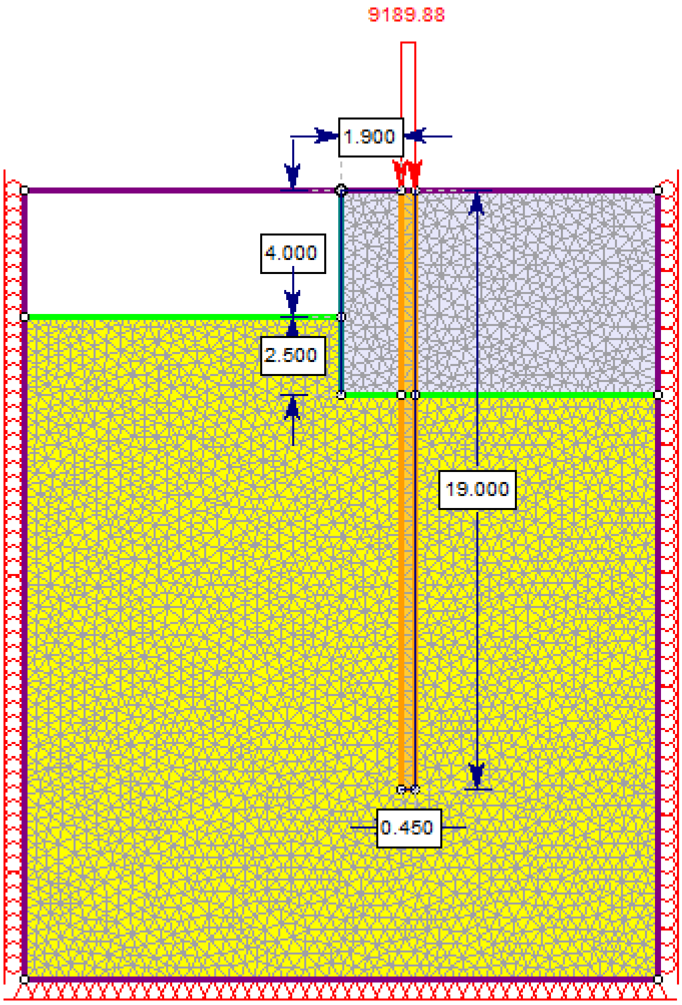

M 132.1: Original model (stage 3)

C'_1	ϕ'_1	γ_1	E_1	C'_2	ϕ'_2	γ_2	E_2	H_1	H_2	H_3	E_3	D_1	D_2	L	Qult
0	42	21	136	33	30	18	28.7	4.00	2.5	1.25	887754	1.9	0.45	19	9189.88

M 132.2: Parameter values

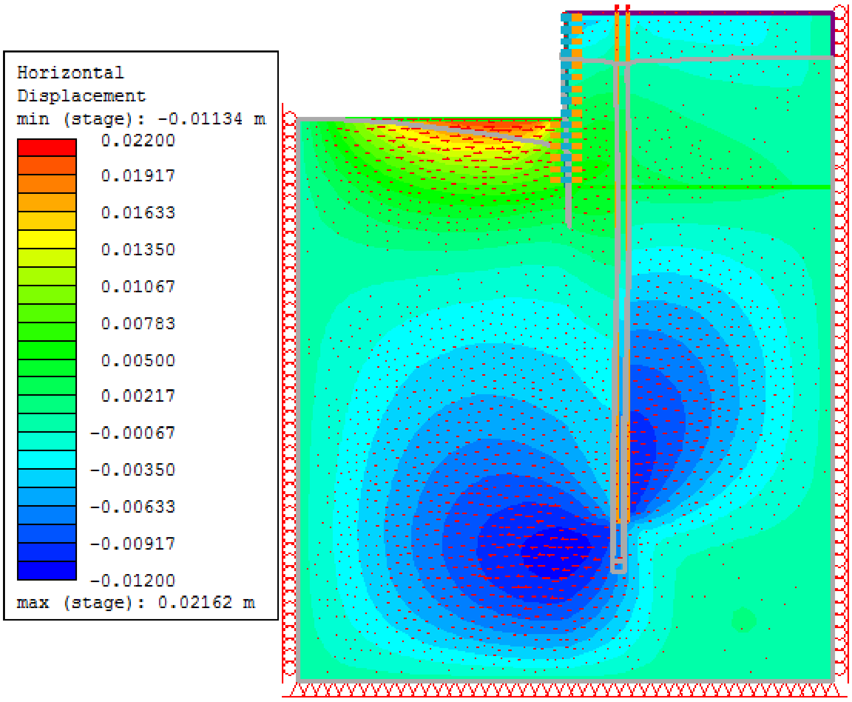

M 132.3: Deformed model (stage 3)

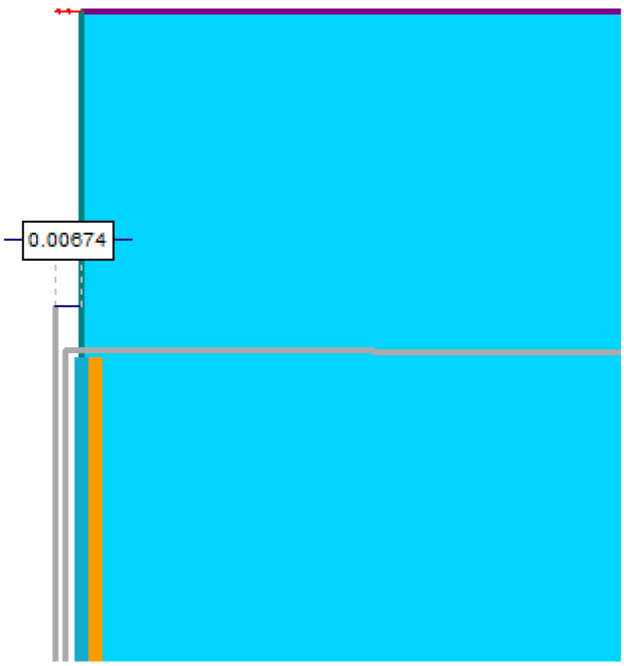

M 132.4: Detailed view of cross-section of retaining wall and soil (stage 3)

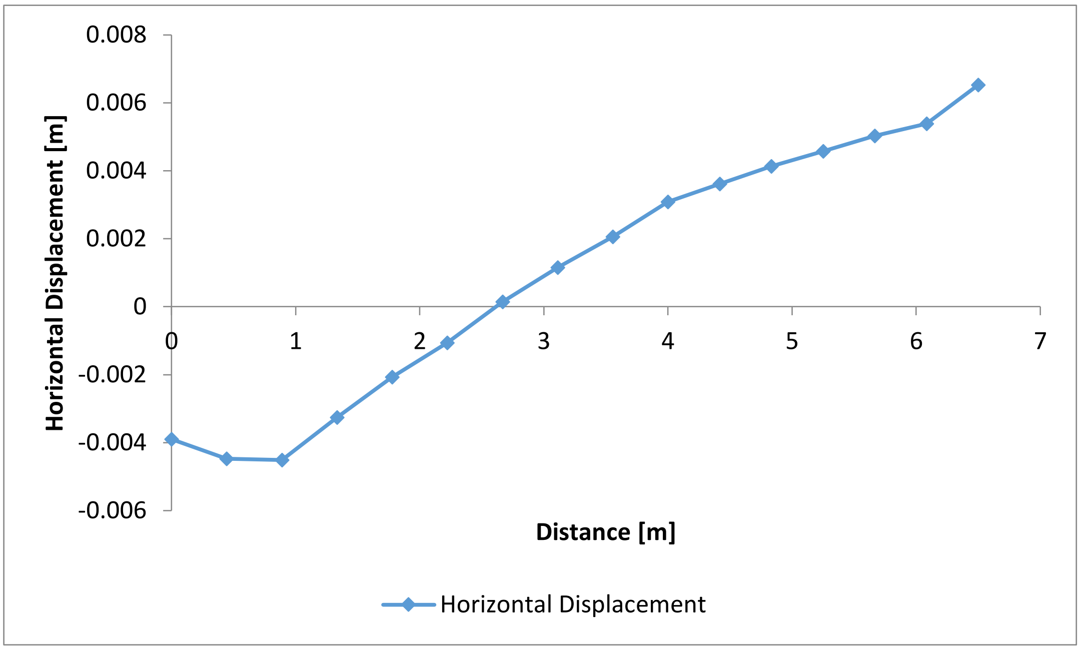

M 132.5: Horizontal displacement of soil along retaining wall

Retaining wall maximum horizontal displacement: -0.0674m

Distance from point of maximum displacement in retaining wall to the top of backfill soil: 0.0m

Model 133:

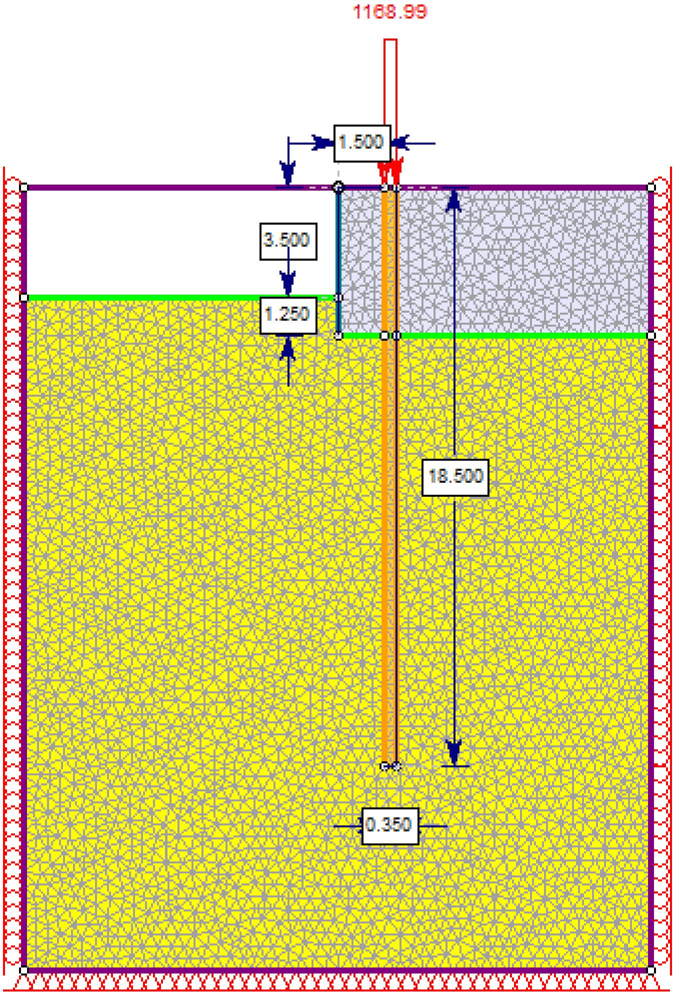

M 133.1: Original model (stage 3)

C_1'	ϕ_1'	γ_1	E_1	C_2'	ϕ_2'	γ_2	E_2	H_1	H_2	H_3	E_3	D_1	D_2	L	Qult
0	37	20	284	51	7	17	17.8	3.50	1.25	1	1058765	1.5	0.35	18.5	1168.99

M 133.2: Parameter values

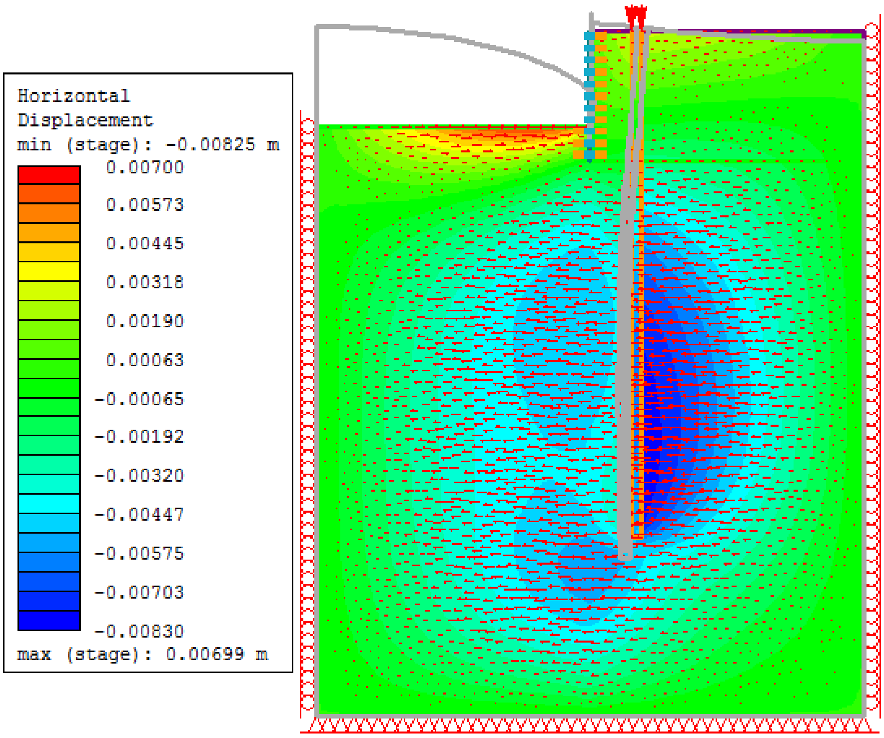

M 133.3: Deformed model (stage 3)

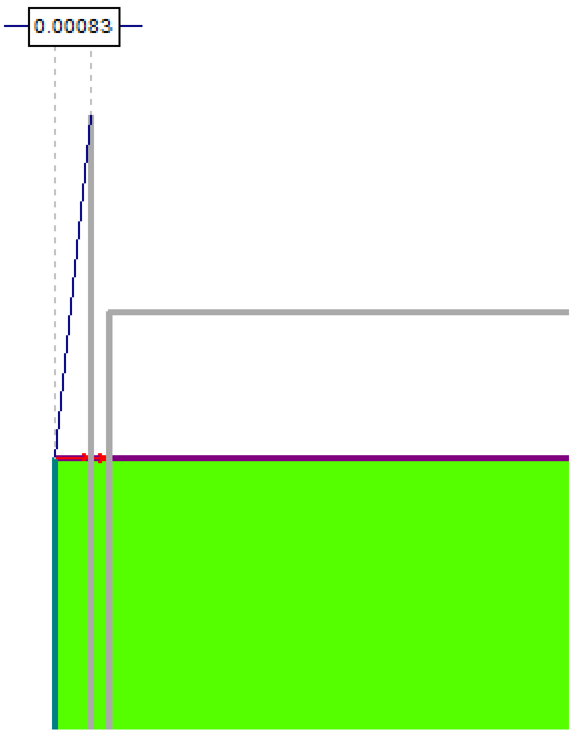

M 133.4: Detailed view of cross-section of retaining wall and soil (stage 3)

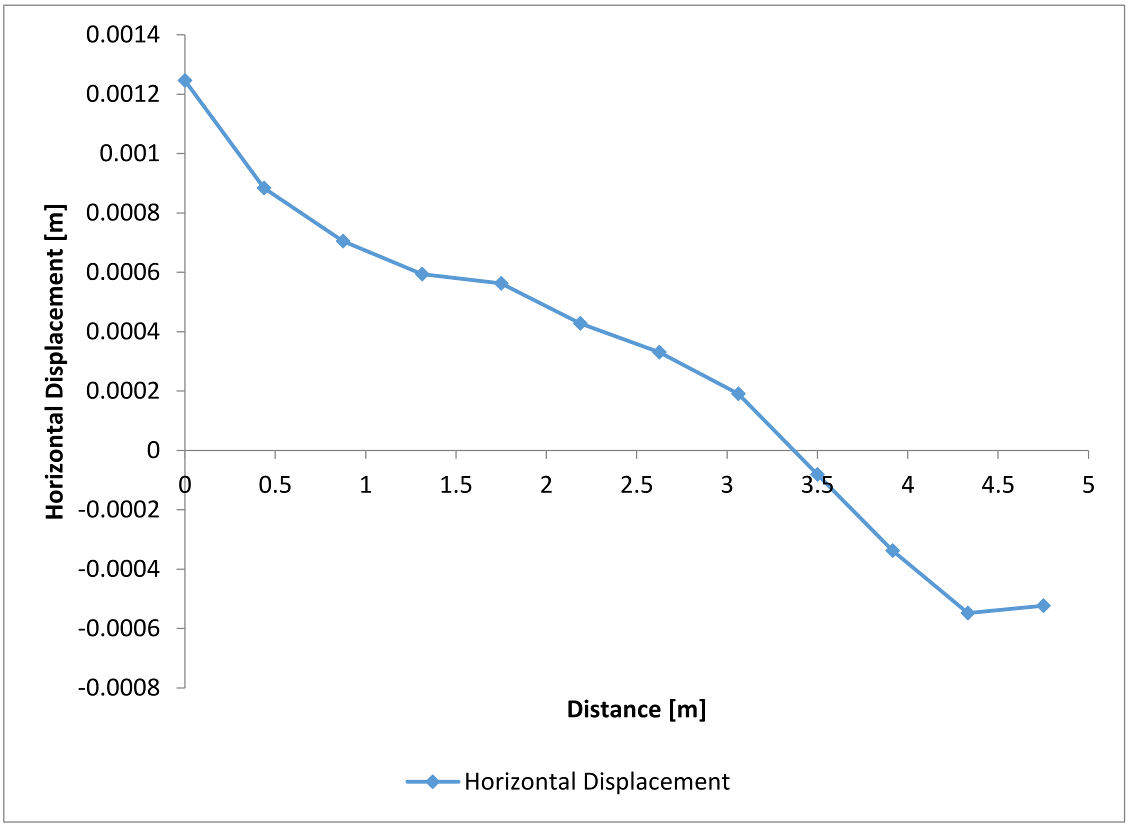

M 133.5: Horizontal displacement of soil along retaining wall

Retaining wall maximum horizontal displacement: -0.00083m

Distance from point of maximum displacement in retaining wall to the top of backfill soil: 0.0m

Model 134:

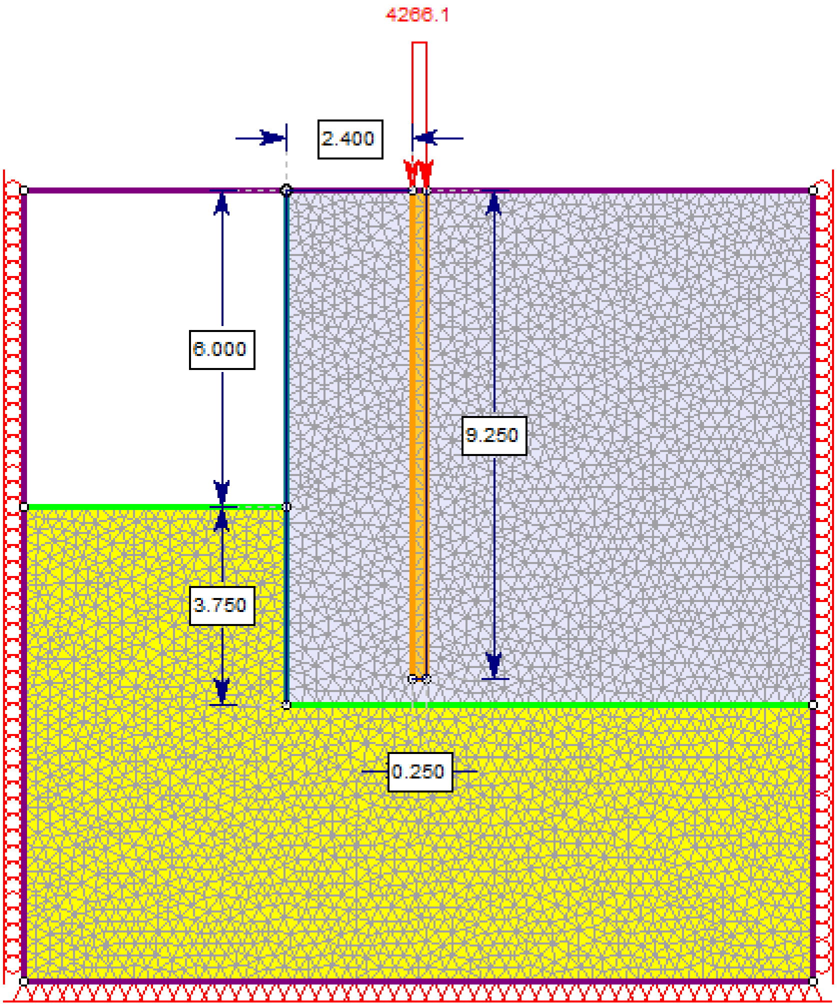

M 134.1: Original model (stage 3)

C_1'	ϕ_1'	γ_1	E_1	C_2'	ϕ_2'	γ_2	E_2	H_1	H_2	H_3	E_3	D_1	D_2	L	Qult
0	36	22	49	58	32	20	26.8	6.00	3.75	0.75	1107325	2.4	0.25	9.75	4266.1

M 134.2: Parameter values

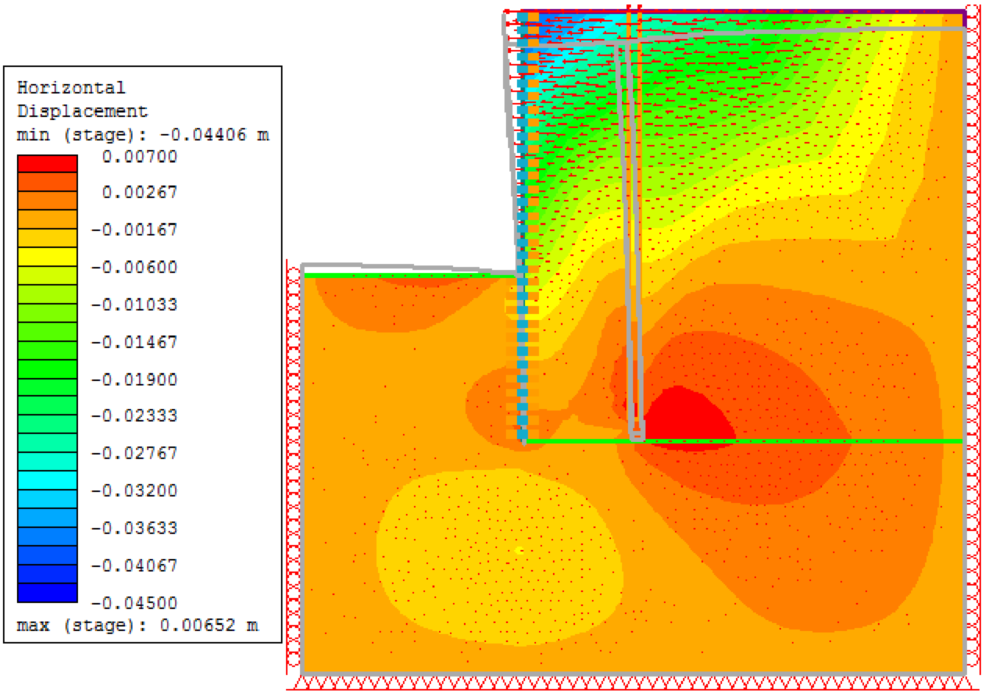

M 134.3: Deformed model (stage 3)

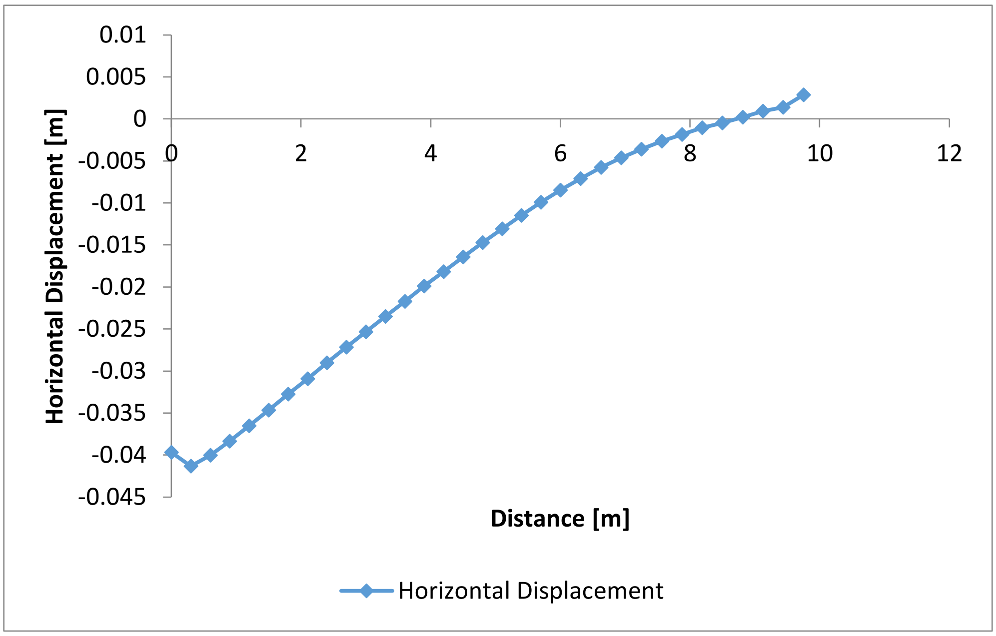

M 134.4: Horizontal displacement of soil along retaining wall

Retaining wall maximum horizontal displacement: -0.04406m

Distance from point of maximum displacement in retaining wall to the top of backfill soil: 0.0m

Model 135:

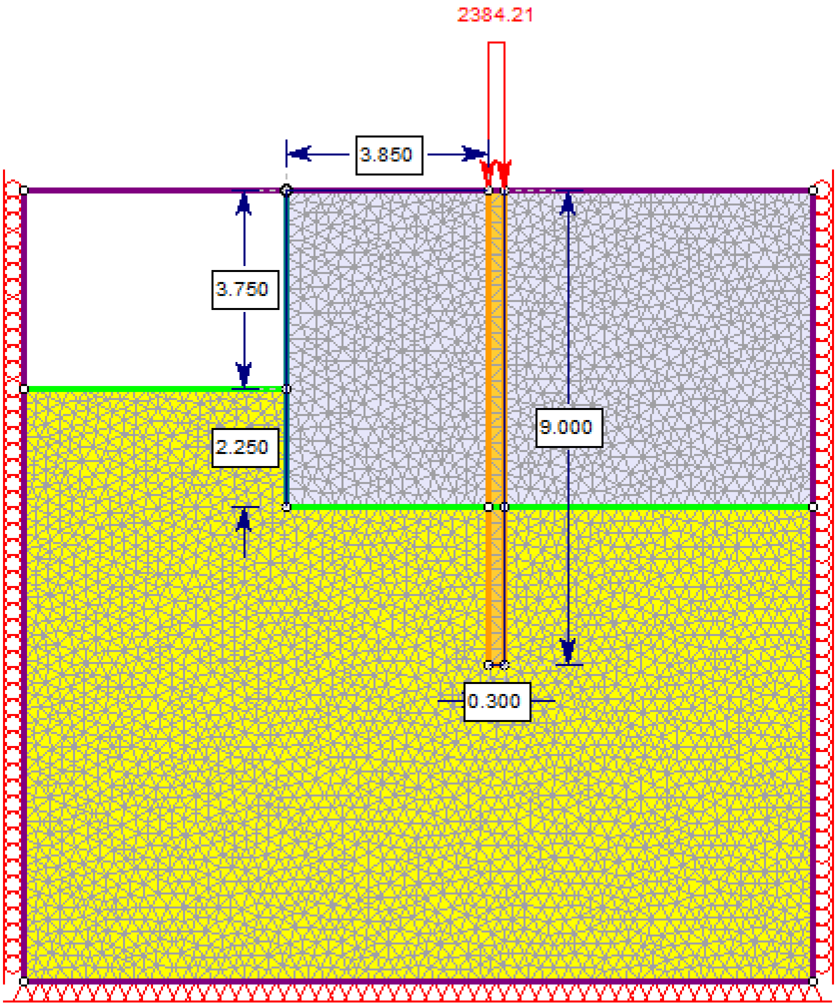

M 135.1: Original model (stage 3)

C'_1	ϕ'_1	γ_1	E_1	C'_2	ϕ'_2	γ_2	E_2	H_1	H_2	H_3	E_3	D_1	D_2	L	Qult
0	32	19	300	35	23	23	13.9	3.75	2.25	0.75	1003695	3.85	0.3	9	2384.21

M 135.2: Parameter values

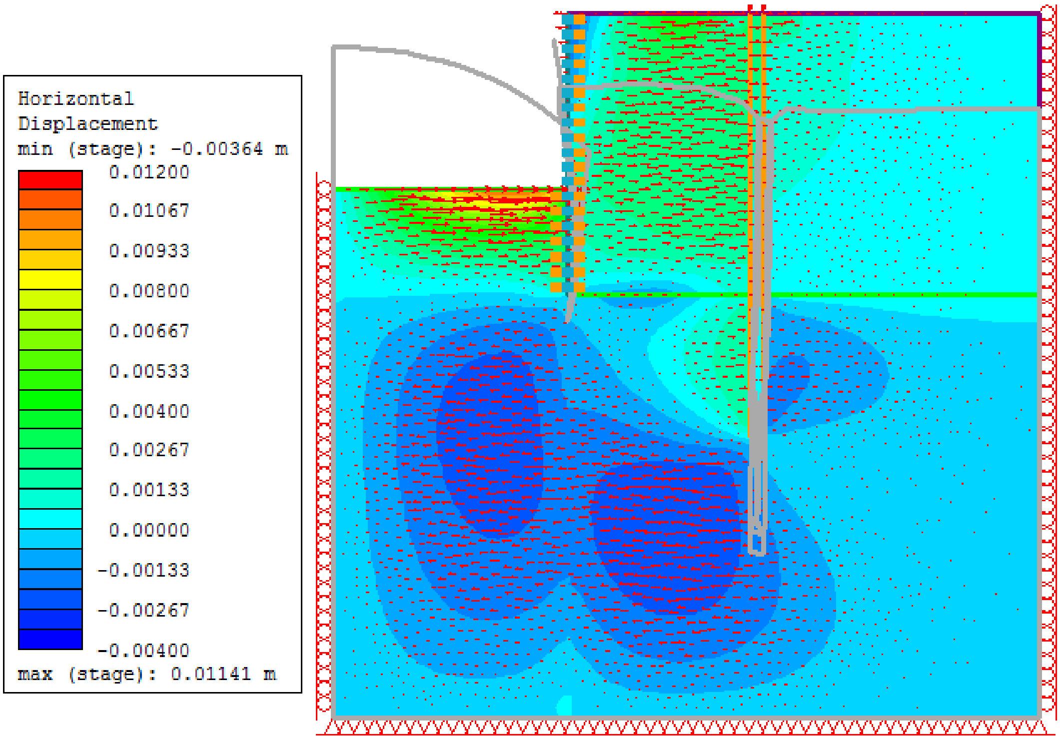

M 135.3: Deformed model (stage 3)

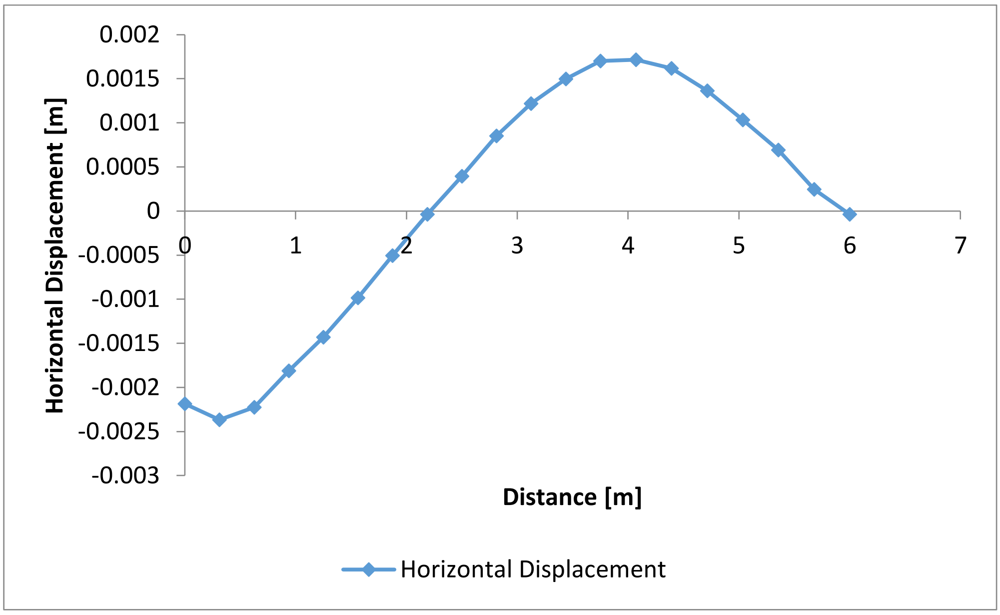

M 135.4: Horizontal displacement of soil along retaining wall

Retaining wall maximum horizontal displacement: -0.00364m

Distance from point of maximum displacement in retaining wall to the top of backfill soil: 0.0m

Model 136:

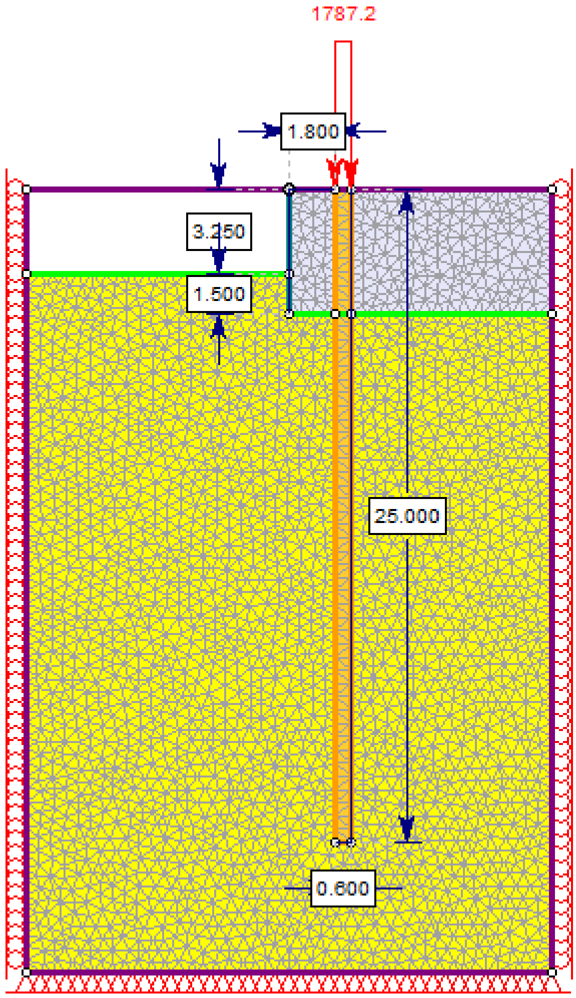

M 136.1: Original model (stage 3)

C'_1	ϕ'_1	γ_1	E_1	C'_2	ϕ'_2	γ_2	E_2	H_1	H_2	H_3	E_3	D_1	D_2	L	Qult
0	43	22	221	34	11	22	47.7	3.25	1.5	1.5	865357	1.8	0.6	20.25	1787.2

M 136.2: Parameter values

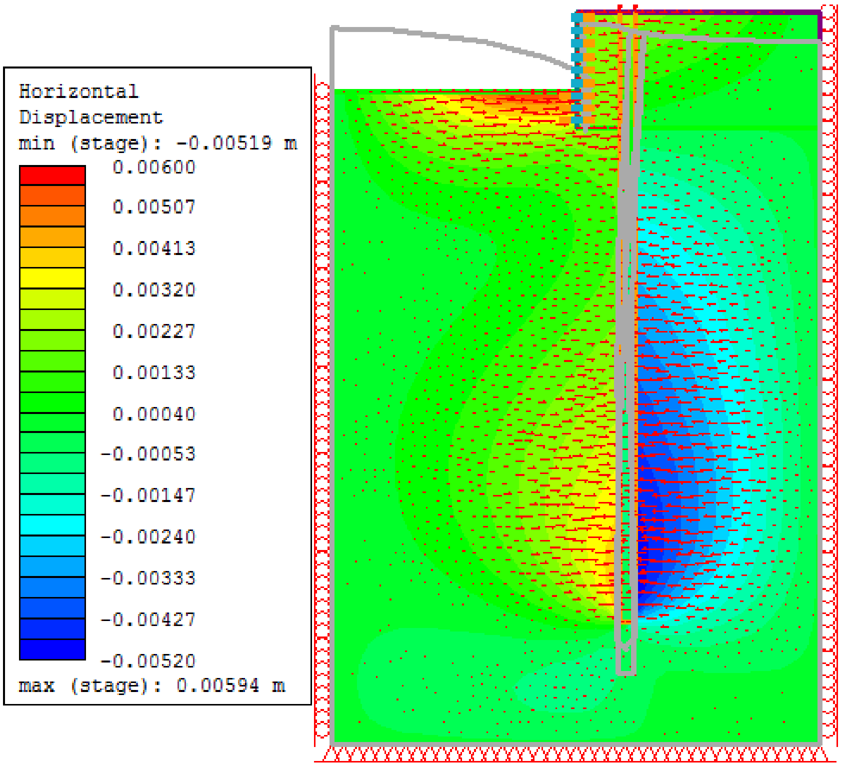

M 136.3: Deformed model (stage 3)

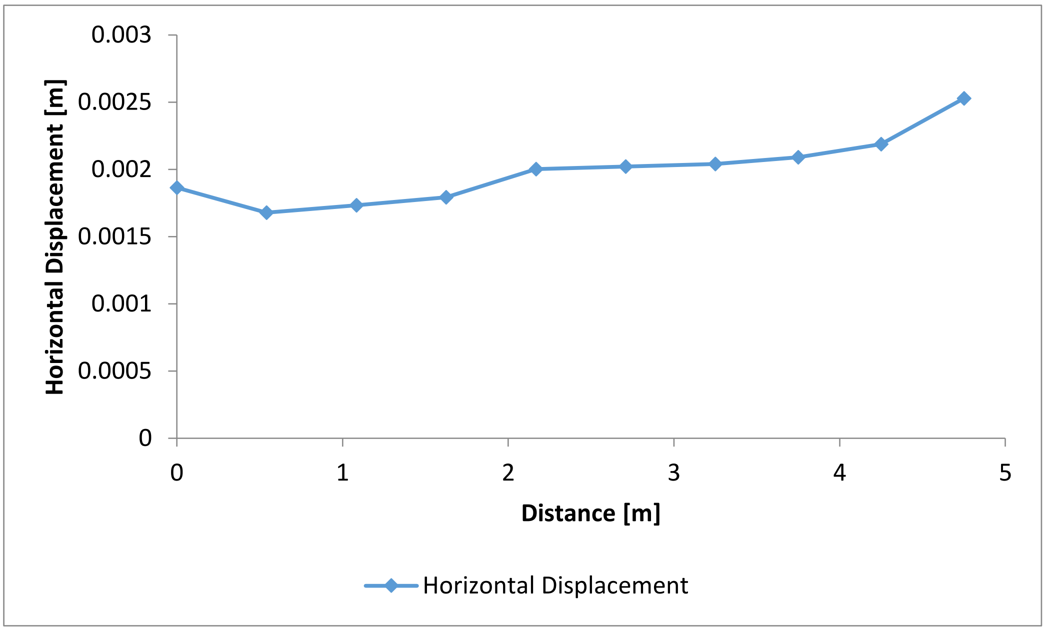

M 136.4: Horizontal displacement of soil along retaining wall

Retaining wall maximum horizontal displacement: 0.00253m

Distance from point of maximum displacement in retaining wall to the top of backfill soil: 4.75m

Model 137:

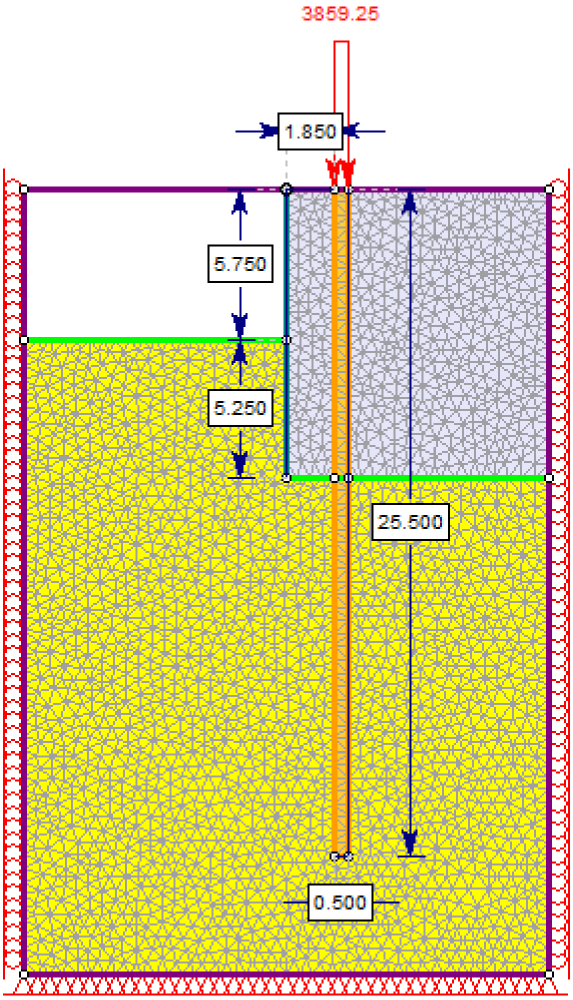

M 137.1: Original model (stage 3)

C'_1	ϕ'_1	γ_1	E_1	C'_2	ϕ'_2	γ_2	E_2	H_1	H_2	H_3	E_3	D_1	D_2	L	Qult
0	35	22	117	46	14	24	28.1	5.75	5.25	0.75	1053188	1.85	0.5	25.5	3859.25

M 137.2: Parameter values

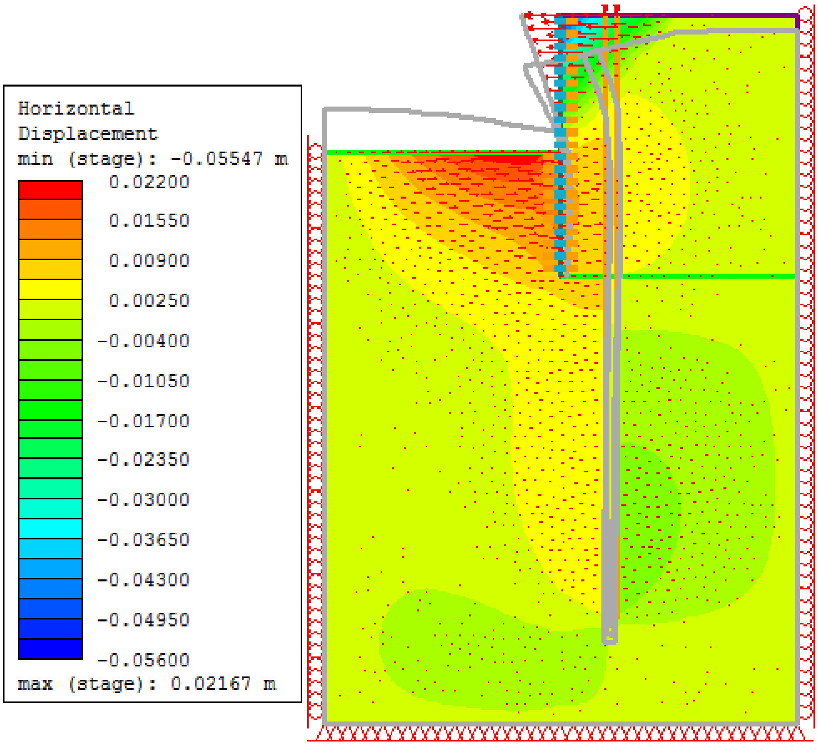

M 137.3: Deformed model (stage 3)

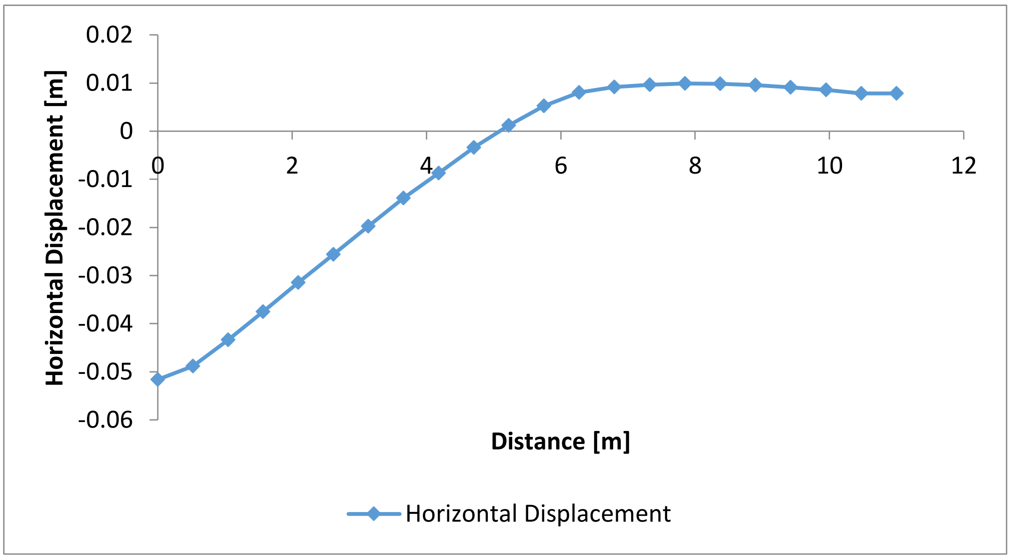

M 137.4: Horizontal displacement of soil along retaining wall

Retaining wall maximum horizontal displacement: -0.05547m

Distance from point of maximum displacement in retaining wall to the top of backfill soil: 0.0m

Model 138:

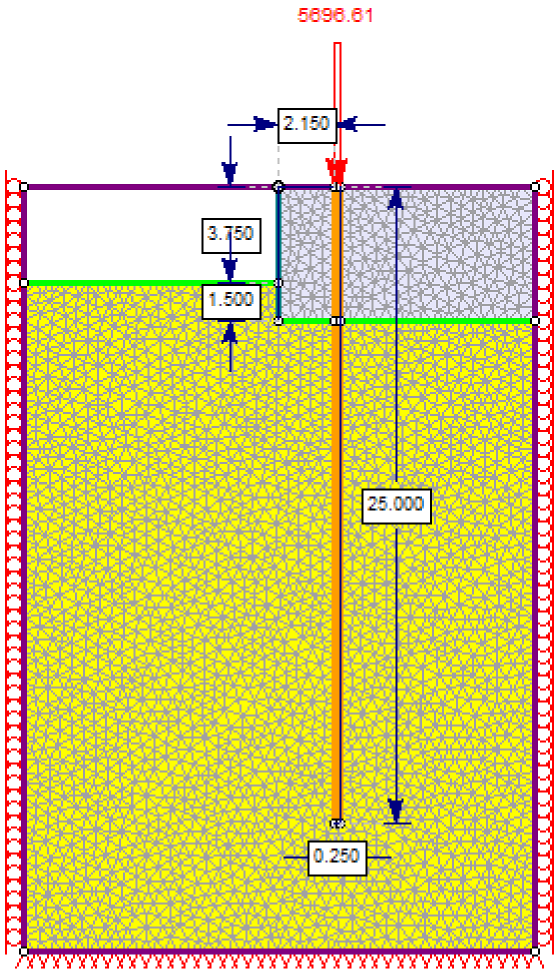

M 138.1: Original model (stage 3)

C'_1	ϕ'_1	γ_1	E_1	C'_2	ϕ'_2	γ_2	E_2	H_1	H_2	H_3	E_3	D_1	D_2	L	Qult
0	31	22	32	57	24	16	44.4	3.75	1.5	0.75	860002	2.15	0.25	25	5696.61

M 138.2: Parameter values

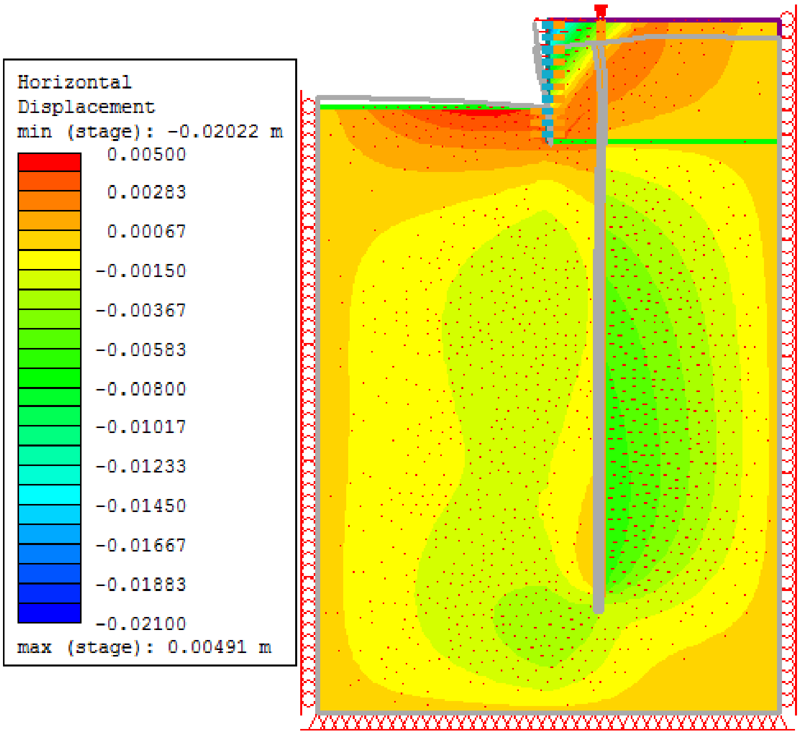

M 138.3: Deformed model (stage 3)

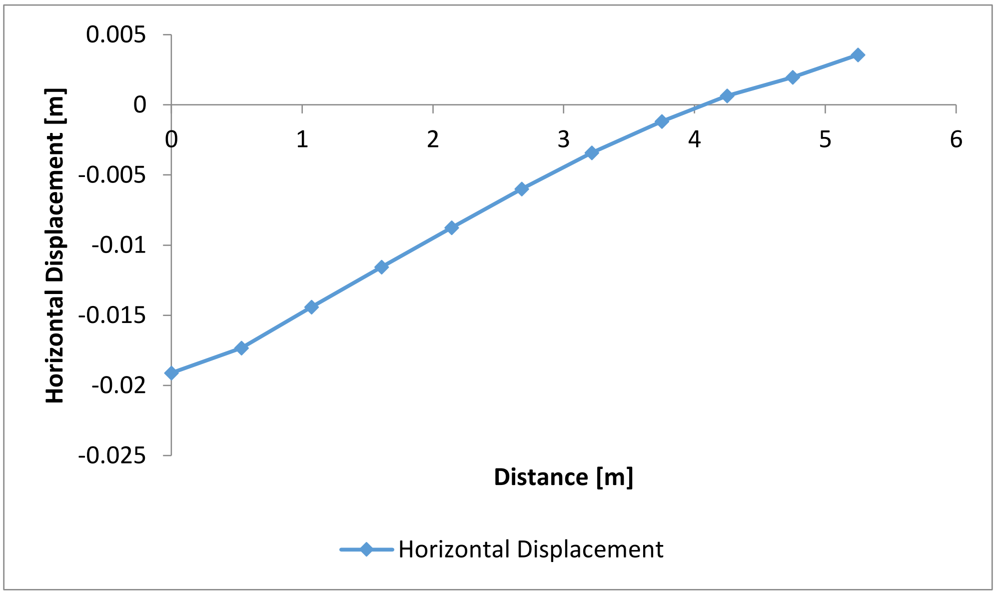

M 138.4: Horizontal displacement of soil along retaining wall

Retaining wall maximum horizontal displacement: -0.02022m

Distance from point of maximum displacement in retaining wall to the top of backfill soil: 0.0m

Model 139:

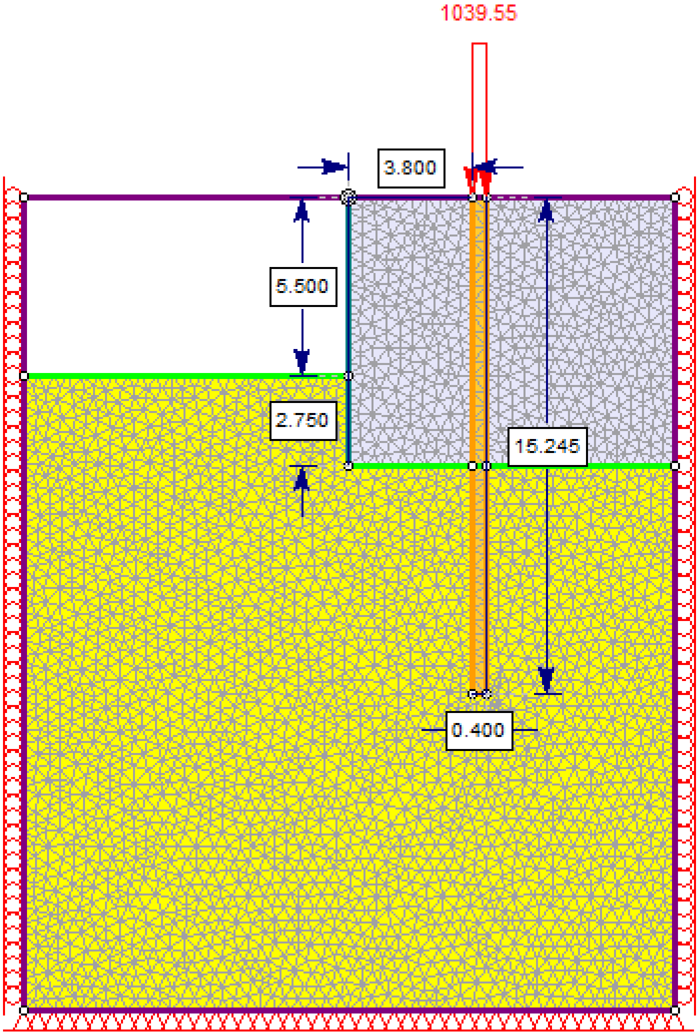

M 139.1: Original model (stage 3)

C'_1	ϕ'_1	γ_1	E_1	C'_2	ϕ'_2	γ_2	E_2	H_1	H_2	H_3	E_3	D_1	D_2	L	Qult
0	45	21	263	48	0	19	13.1	5.50	2.75	1	966153	3.8	0.3	15.25	1039.55

M 139.2: Parameter values

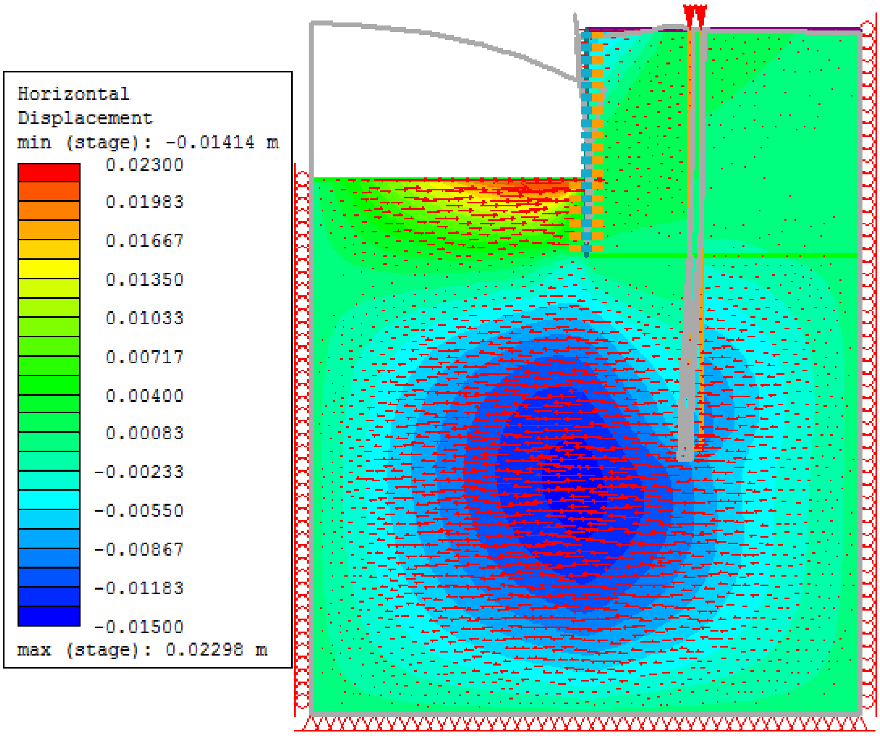

M 139.3: Deformed model (stage 3)

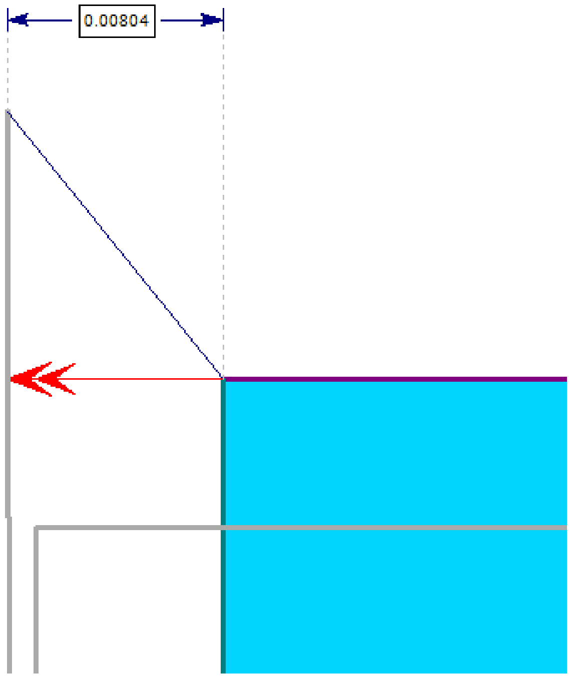

M 139.4: Detailed view of cross-section of retaining wall and soil (stage 3)

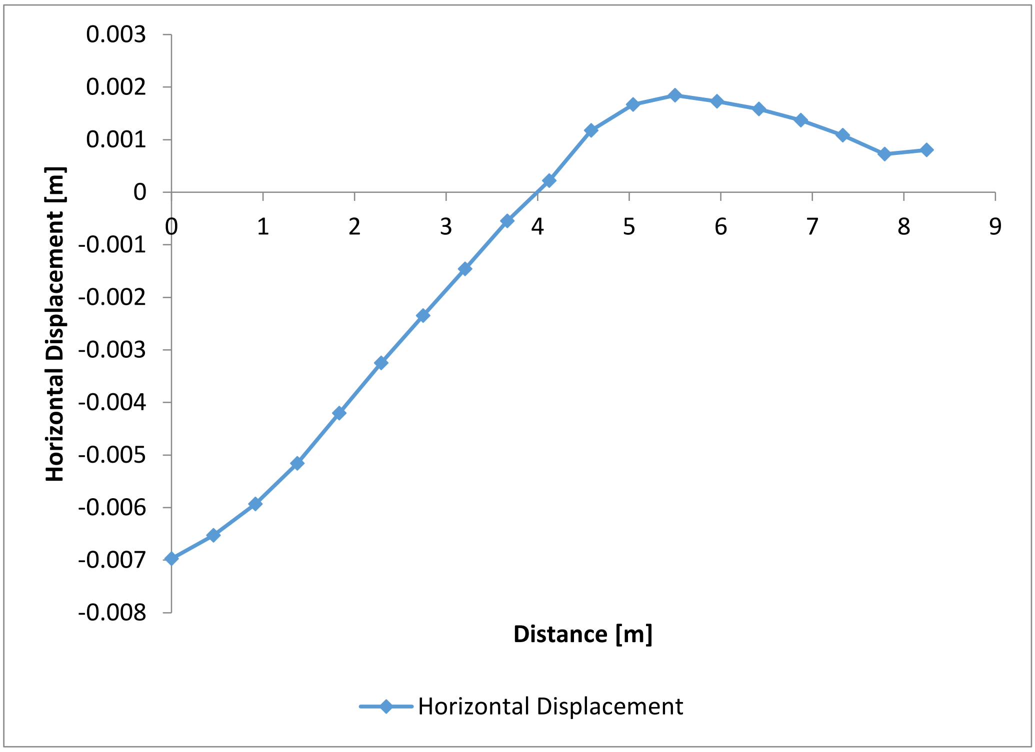

M 139.5: Horizontal displacement of soil along retaining wall

Retaining wall maximum horizontal displacement: -0.00804m

Distance from point of maximum displacement in retaining wall to the top of backfill soil: 0.0m

Model 140:

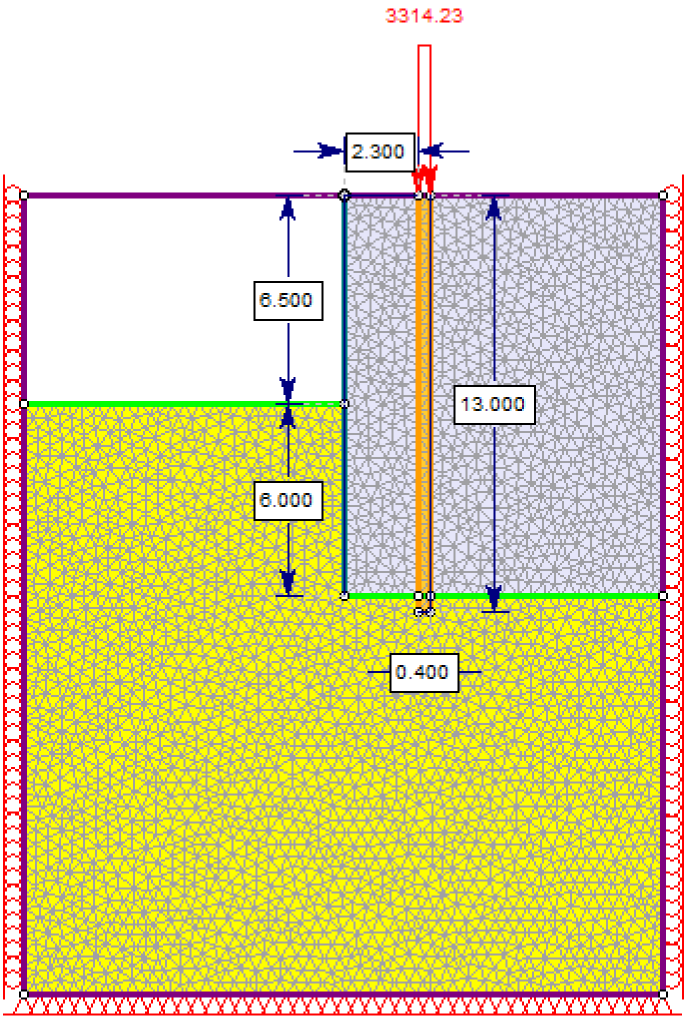

M 140.1: Original model (stage 3)

C_1'	ϕ_1'	γ_1	E_1	C_2'	ϕ_2'	γ_2	E_2	H_1	H_2	H_3	E_3	D_1	D_2	L	Qult
0	32	20	272	48	20	22	27.0	6.50	6	1	1091735	2.3	0.4	13	3314.23

M 140.2: Parameter values

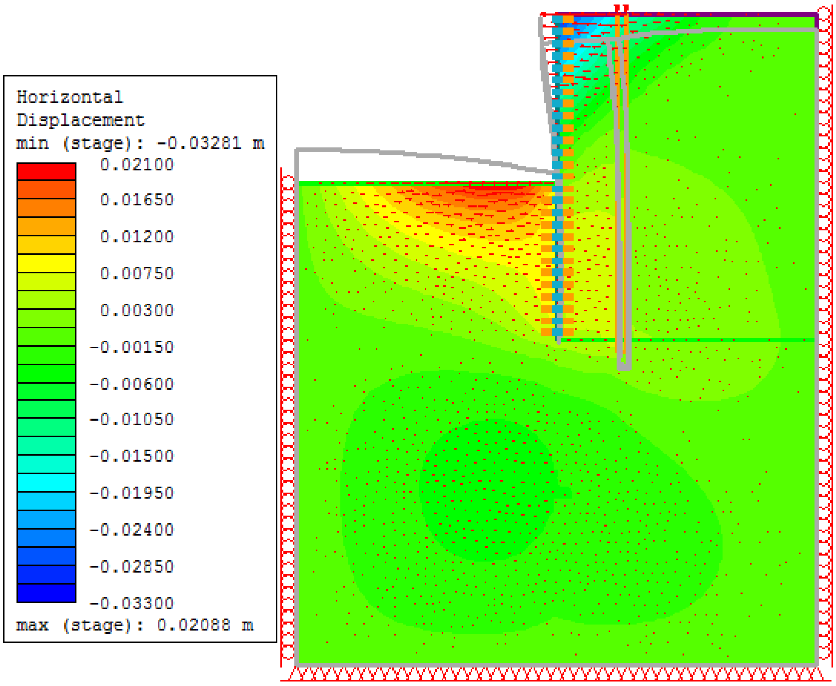

M 140.3: Deformed model (stage 3)

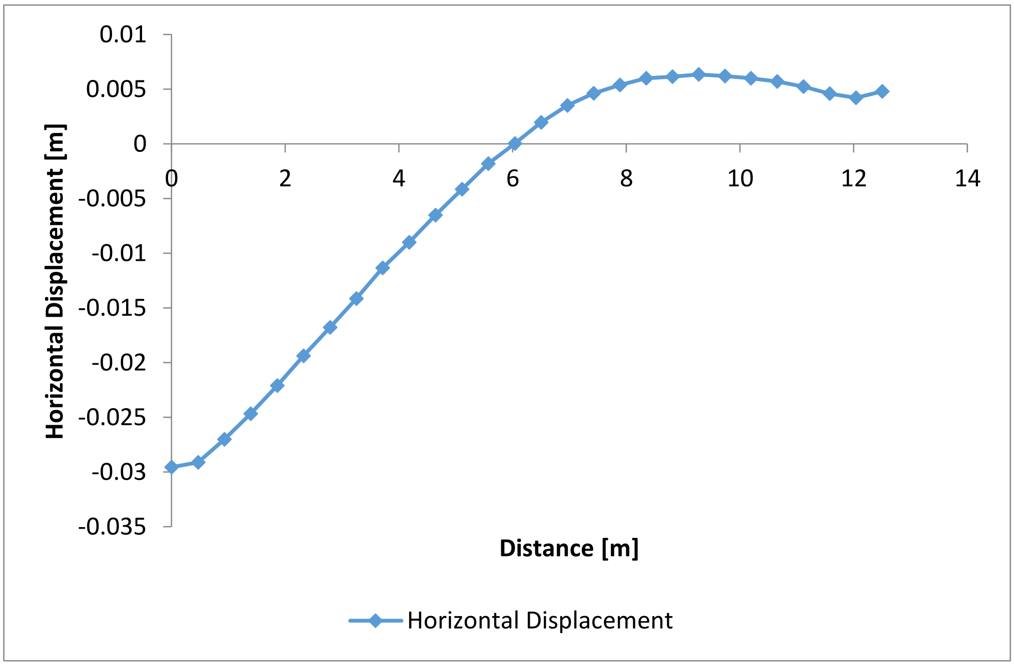

M 140.4: Horizontal displacement of soil along retaining wall

Retaining wall maximum horizontal displacement: -0.03281m

Distance from point of maximum displacement in retaining wall to the top of backfill soil: 0.0m

Model 141:

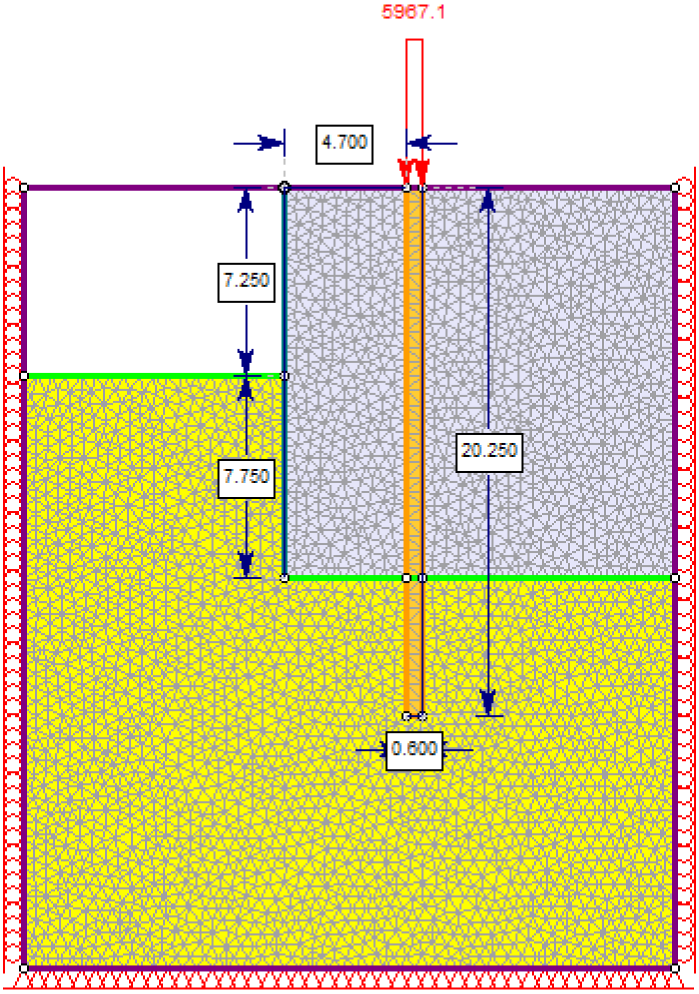

M 141.1: Original model (stage 3)

C_1'	ϕ_1'	γ_1	E_1	C_2'	ϕ_2'	γ_2	E_2	H_1	H_2	H_3	E_3	D_1	D_2	L	Qult
0	37	21	70	34	24	25	42.5	5.25	7.75	1	699417	4.7	0.6	20.25	5967.1

M 141.2: Parameter values

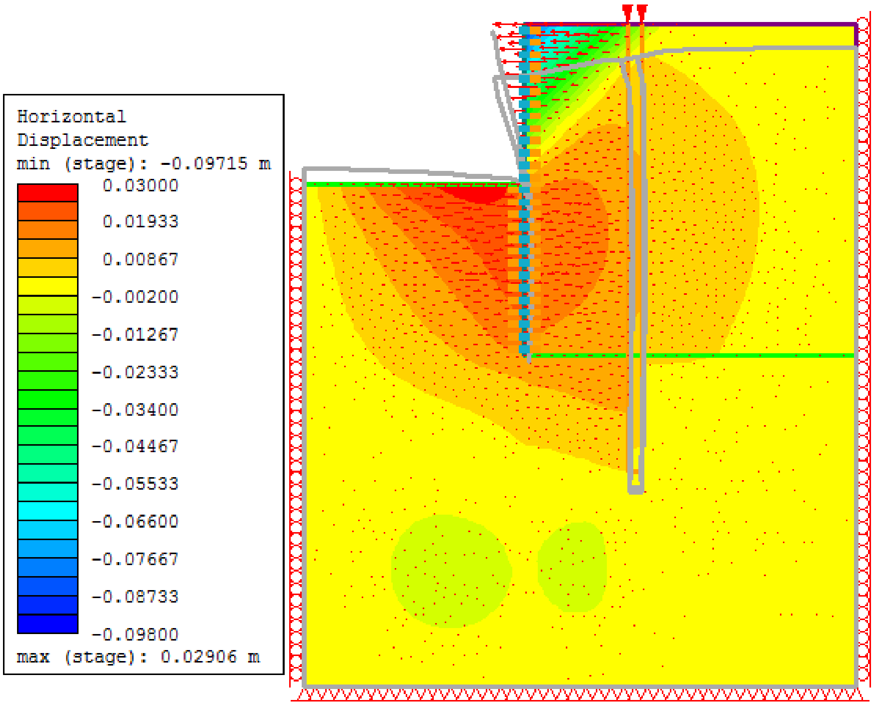

M 141.3: Deformed model (stage 3)

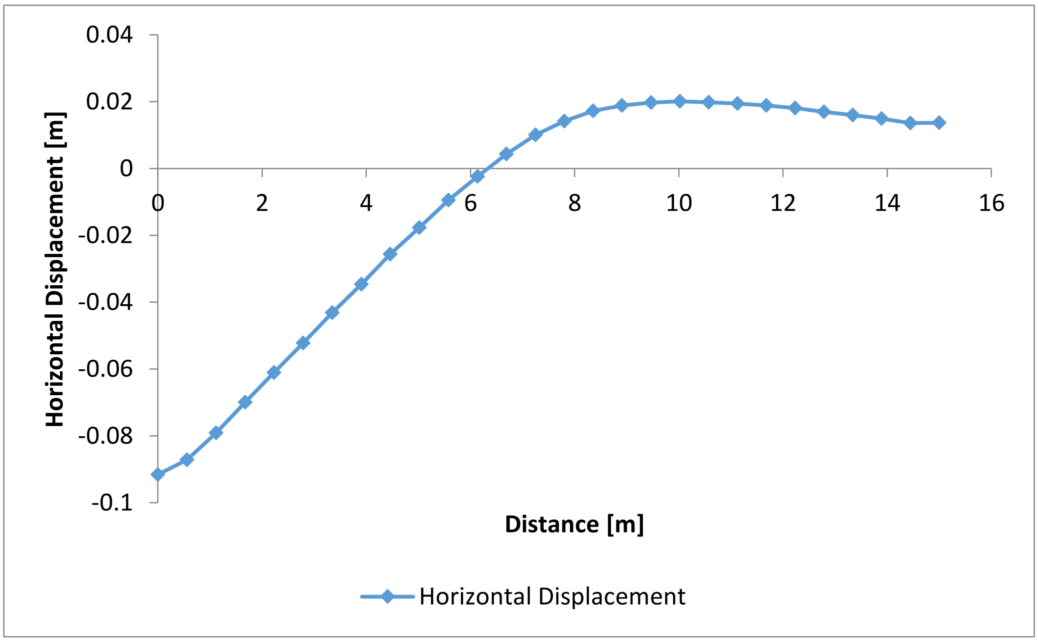

M 141.4: Horizontal displacement of soil along retaining wall

Retaining wall maximum horizontal displacement: -0.09715m

Distance from point of maximum displacement in retaining wall to the top of backfill soil: 0.0m

Model 142:

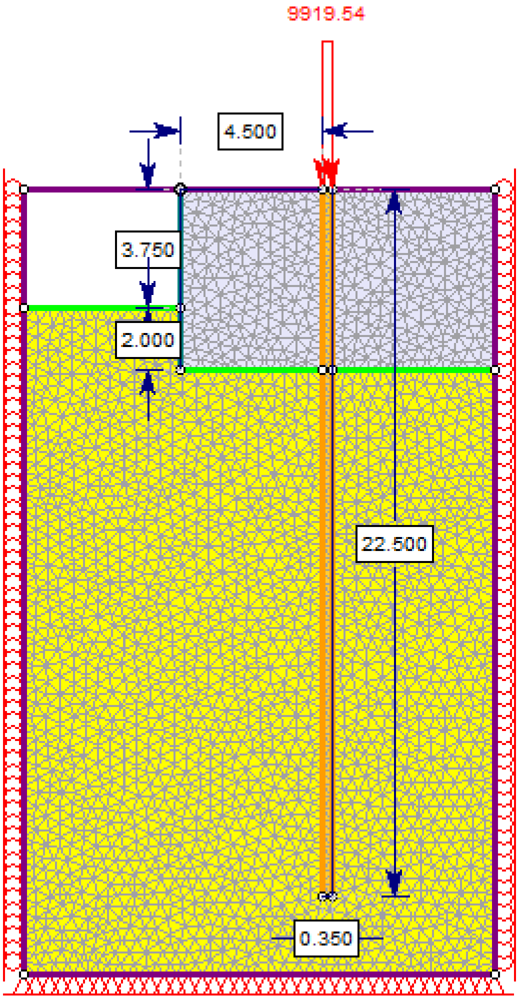

M 142.1: Original model (stage 3)

C_1'	ϕ_1'	γ_1	E_1	C_2'	ϕ_2'	γ_2	E_2	H_1	H_2	H_3	E_3	D_1	D_2	L	Qult
0	42	20	208	33	30	16	33.0	3.75	2	0.75	960039	4.5	0.35	22.5	9919.54

M 142.2: Parameter values

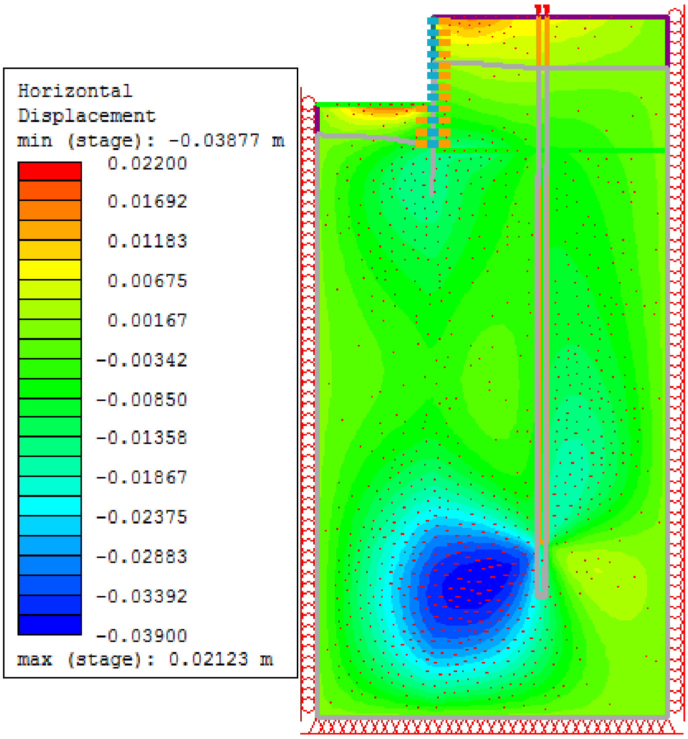

M 142.3: Deformed model (stage 3)

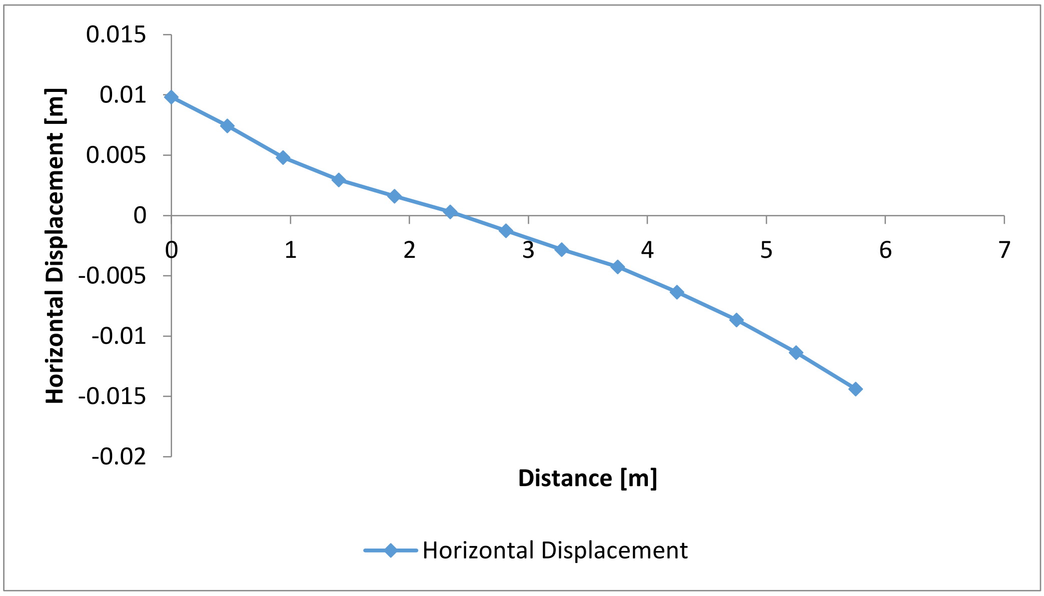

M 142.4: Horizontal displacement of soil along retaining wall

Retaining wall maximum horizontal displacement: -0.01438m

Distance from point of maximum displacement in retaining wall to the top of backfill soil: 5.75m

Model 143:

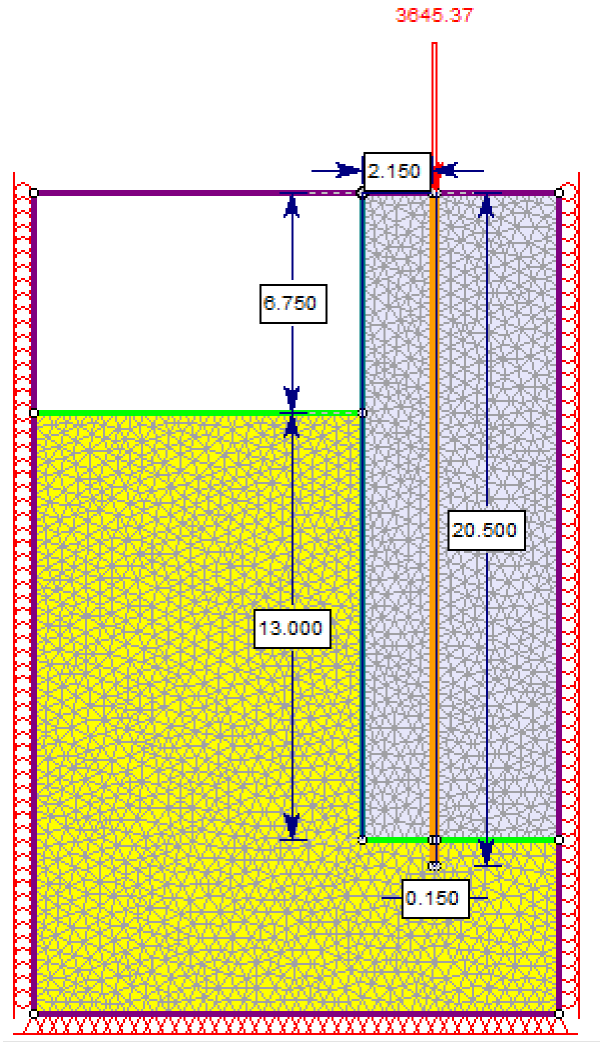

M 143.1: Original model (stage 3)

C_1'	ϕ_1'	γ_1	E_1	C_2'	ϕ_2'	γ_2	E_2	H_1	H_2	H_3	E_3	D_1	D_2	L	Qult
0	31	22	225	44	2	22	22.6	6.75	13	1.5	730351	2.15	0.15	20.5	3654.37

M 143.2: Parameter values

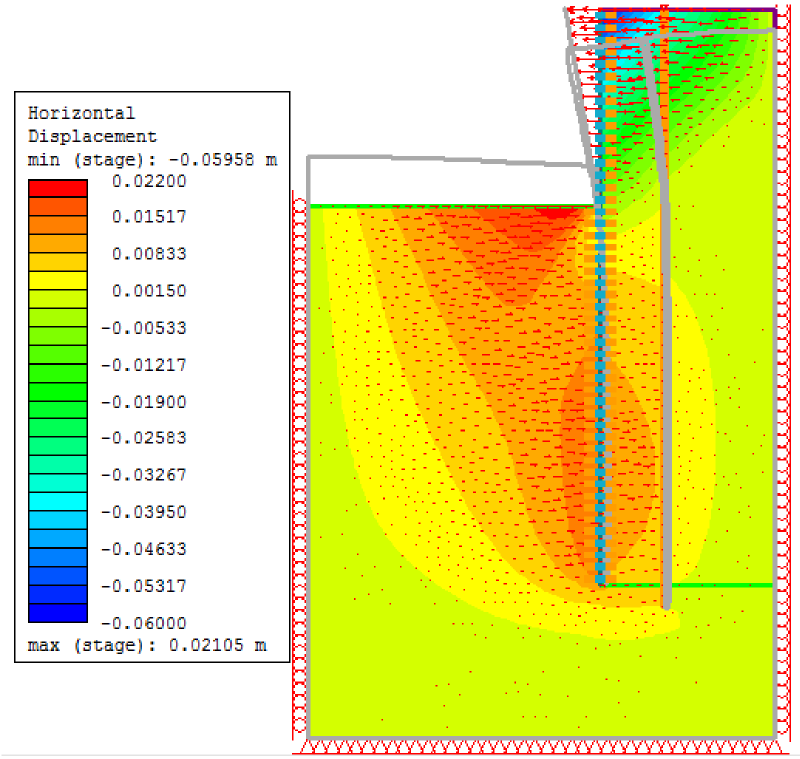

M 143.3: Deformed model (stage 3)

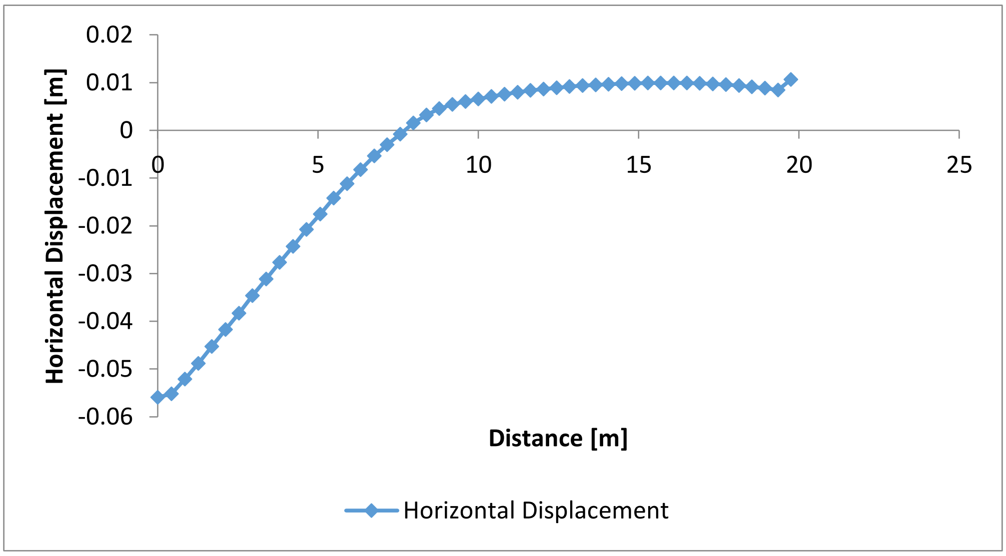

M 143.4: Horizontal displacement of soil along retaining wall

Retaining wall maximum horizontal displacement: -0.05958m

Distance from point of maximum displacement in retaining wall to the top of backfill soil: 0.0m

Model 144:

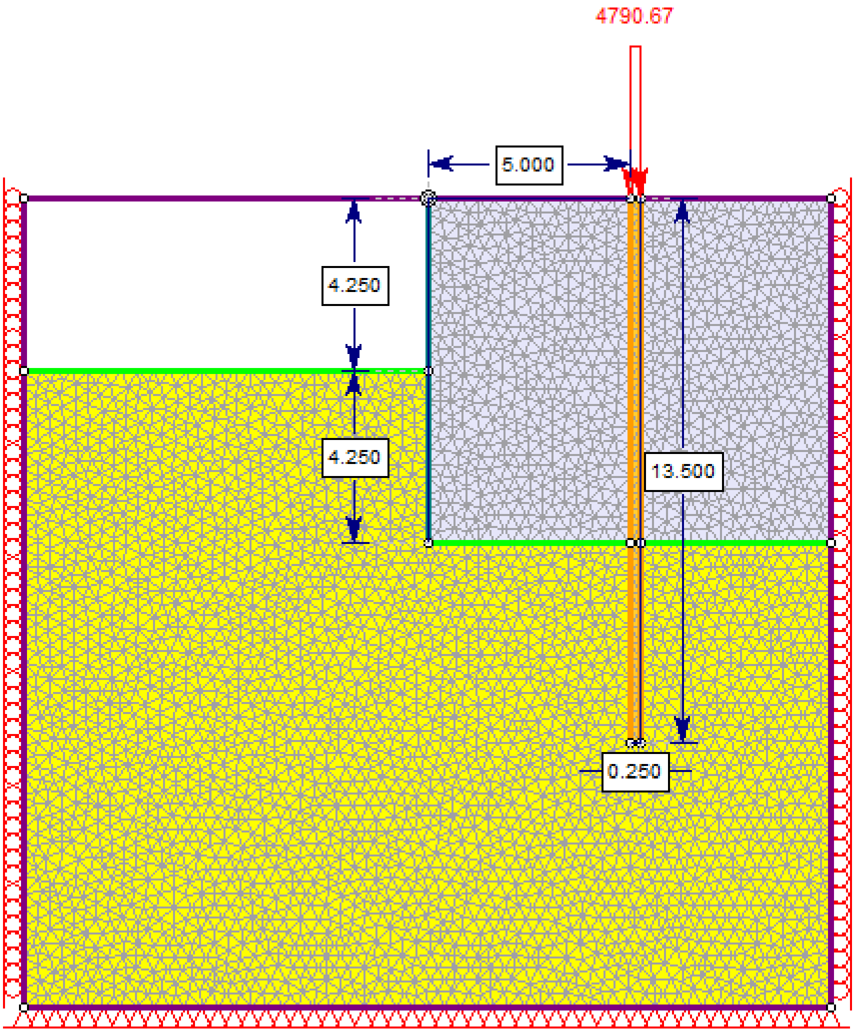

M 144.1: Original model (stage 3)

C_1'	ϕ_1'	γ_1	E_1	C_2'	ϕ_2'	γ_2	E_2	H_1	H_2	H_3	E_3	D_1	D_2	L	Qult
0	34	21	223	31	26	20	30.4	4.25	4.25	0.75	1026710	5	0.25	13.5	4790.67

M 144.2: Parameter values

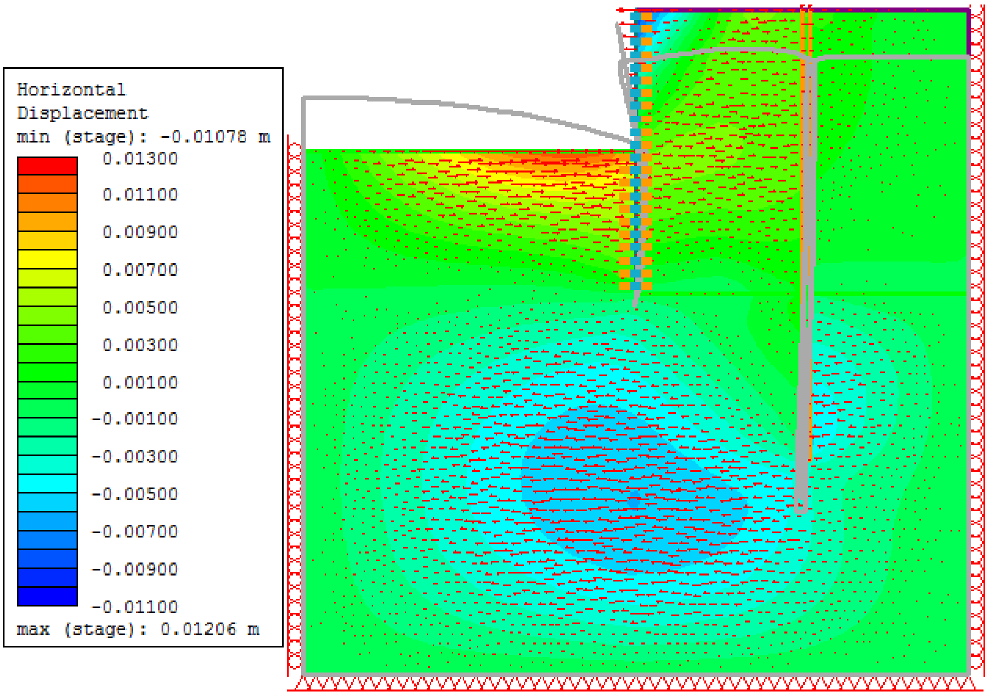

M 144.3: Deformed model (stage 3)

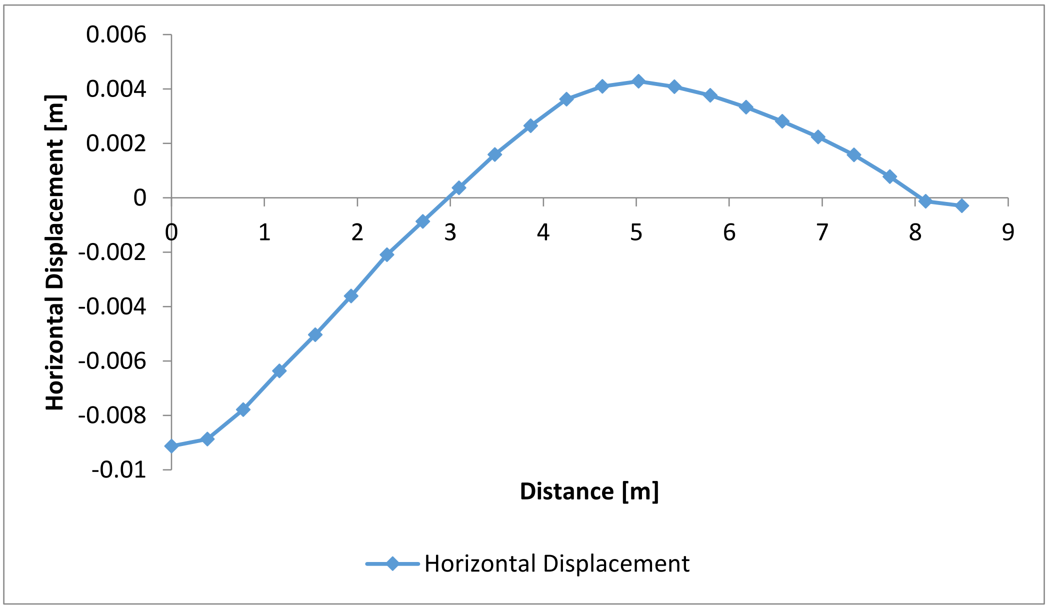

M 144.4: Horizontal displacement of soil along retaining wall

Retaining wall maximum horizontal displacement: -0.01078m

Distance from point of maximum displacement in retaining wall to the top of backfill soil: 0.0m

Model 145:

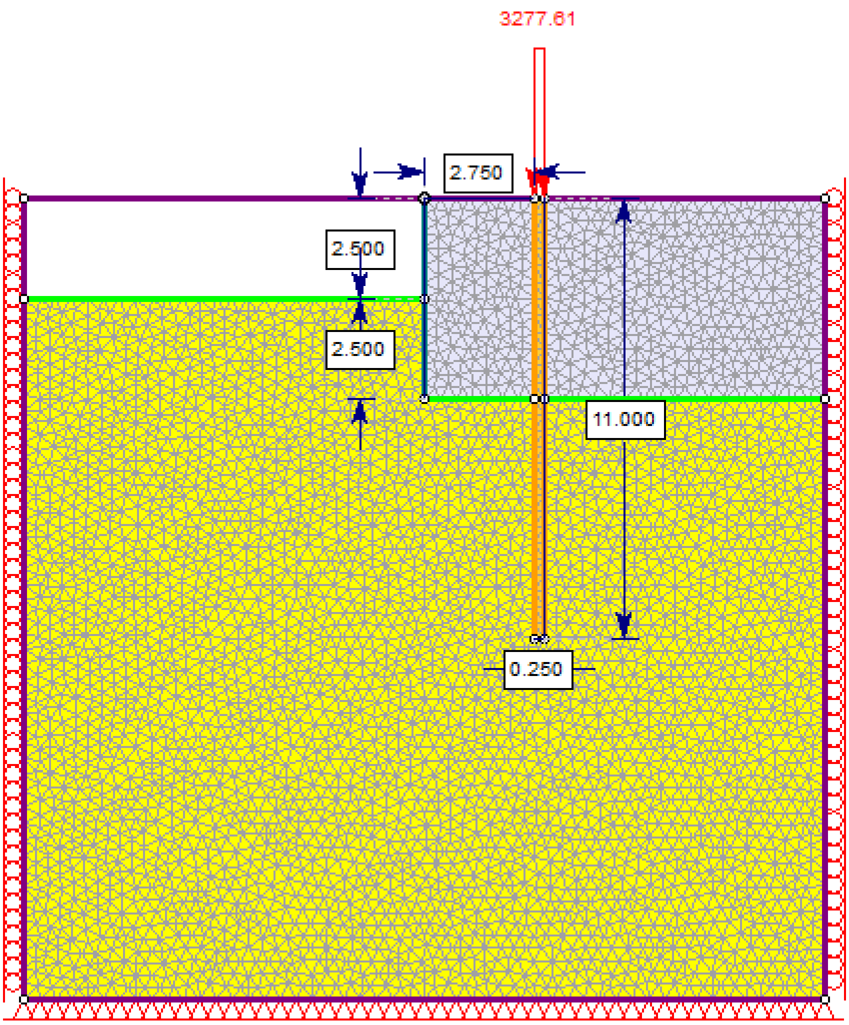

M 145.1: Original model (stage 3)

C_1'	ϕ_1'	γ_1	E_1	C_2'	ϕ_2'	γ_2	E_2	H_1	H_2	H_3	E_3	D_1	D_2	L	Qult
0	40	18	154	15	26	19	8.2	2.50	2.5	1.5	893472	2.75	0.25	11	3277.61

M 145.2: Parameter values

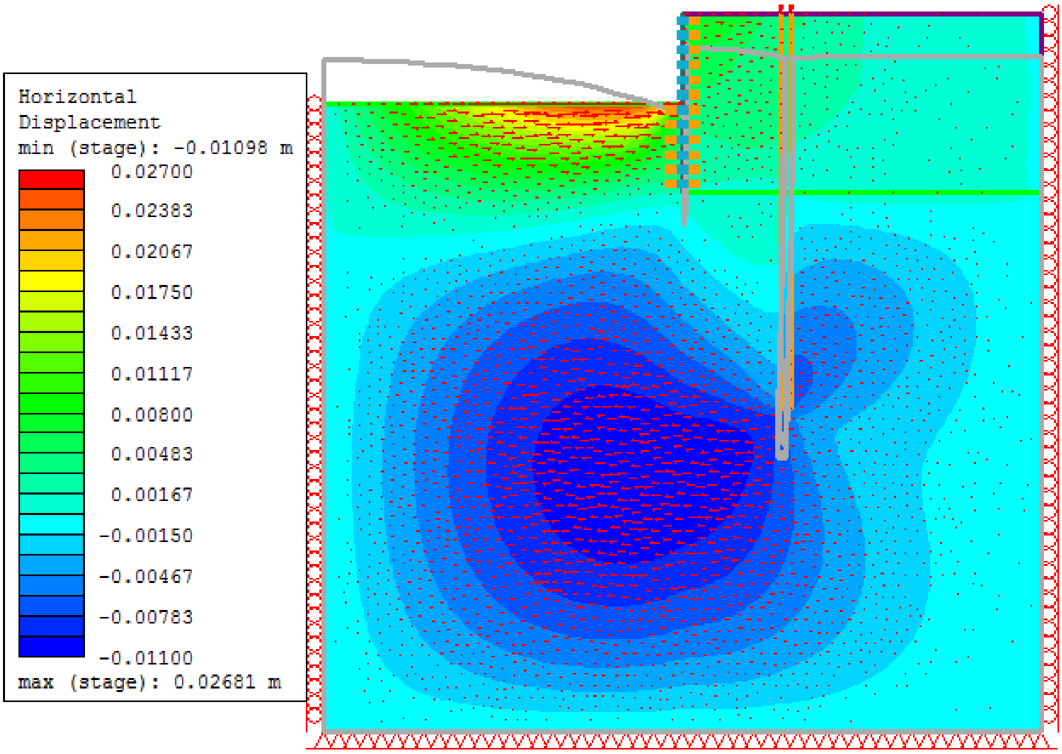

M 145.3: Deformed model (stage 3)

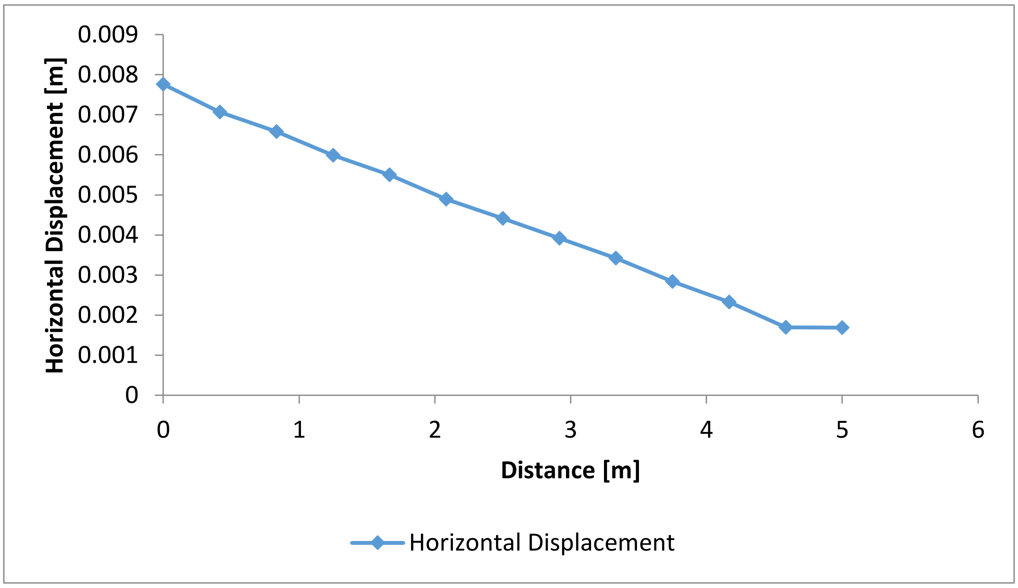

M 145.4: Horizontal displacement of soil along retaining wall

Retaining wall maximum horizontal displacement: 0.00776m

Distance from point of maximum displacement in retaining wall to the top of backfill soil: 0.0m

Model 146:

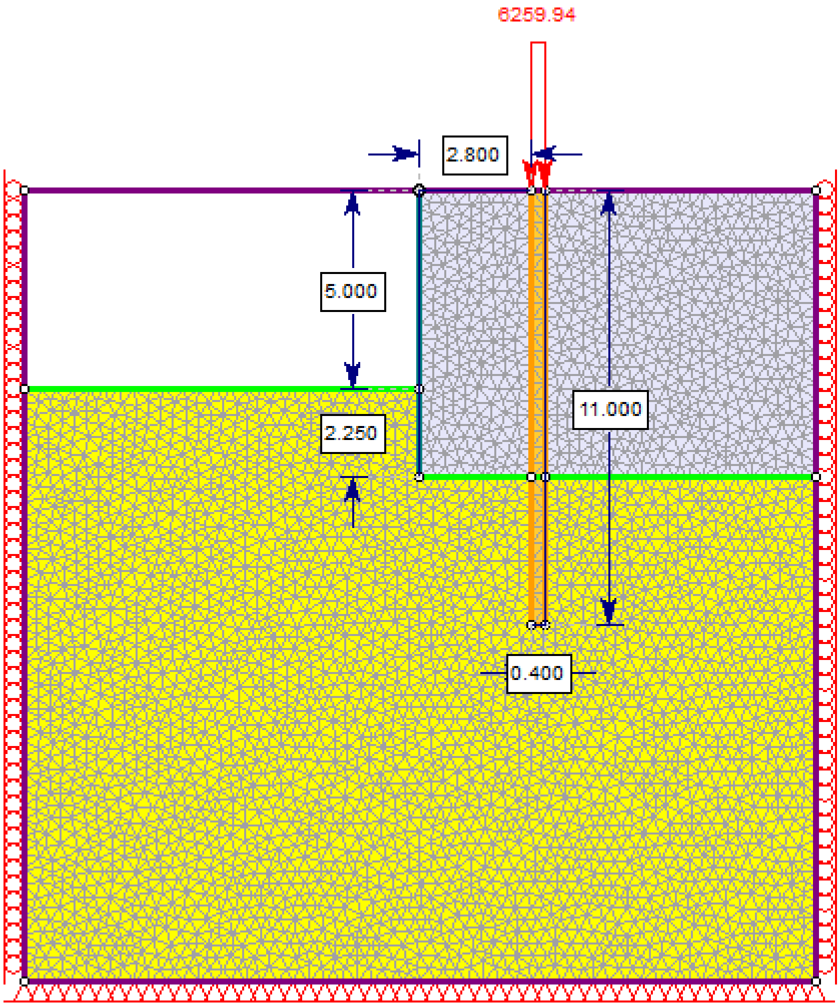

M 146.1: Original model (stage 3)

C_1'	ϕ_1'	γ_1	E_1	C_2'	ϕ_2'	γ_2	E_2	H_1	H_2	H_3	E_3	D_1	D_2	L	Qult
0	42	21	162	51	30	17	38.2	5.00	2.25	1	757076	2.8	0.4	11	6259.94

M 146.2: Parameter values

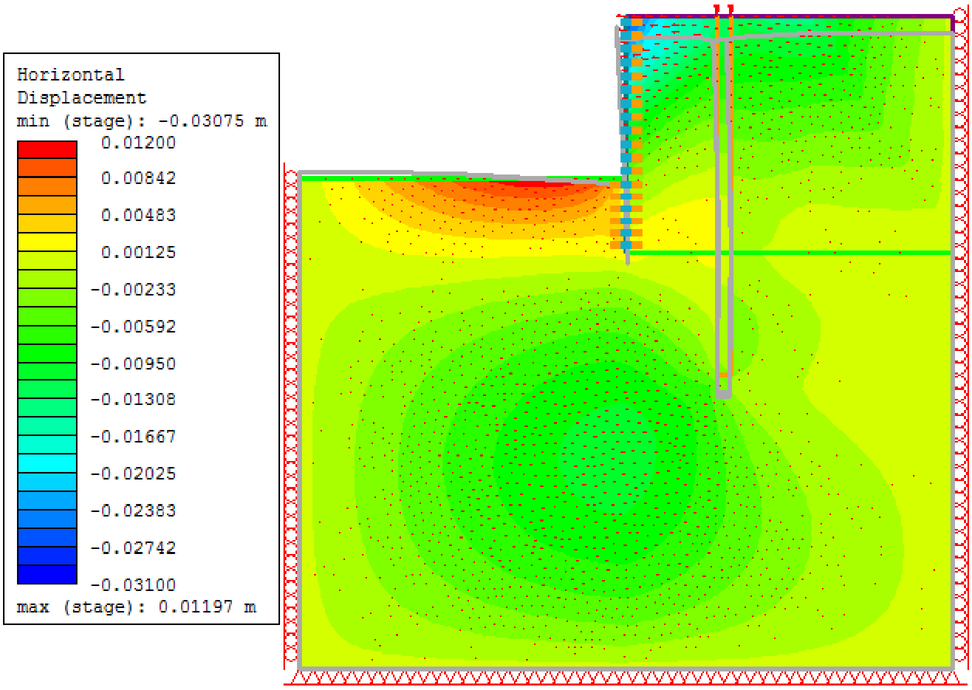

M 146.3: Deformed model (stage 3)

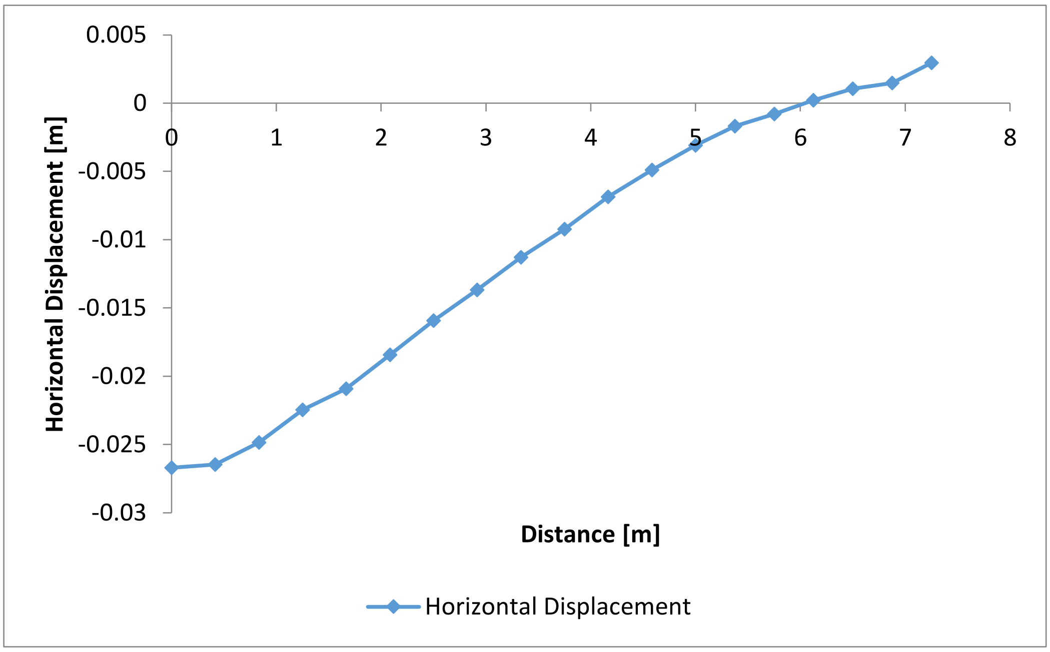

M 146.4: Horizontal displacement of soil along retaining wall

Retaining wall maximum horizontal displacement: -0.03075m

Distance from point of maximum displacement in retaining wall to the top of backfill soil: 0.0m

Model 147:

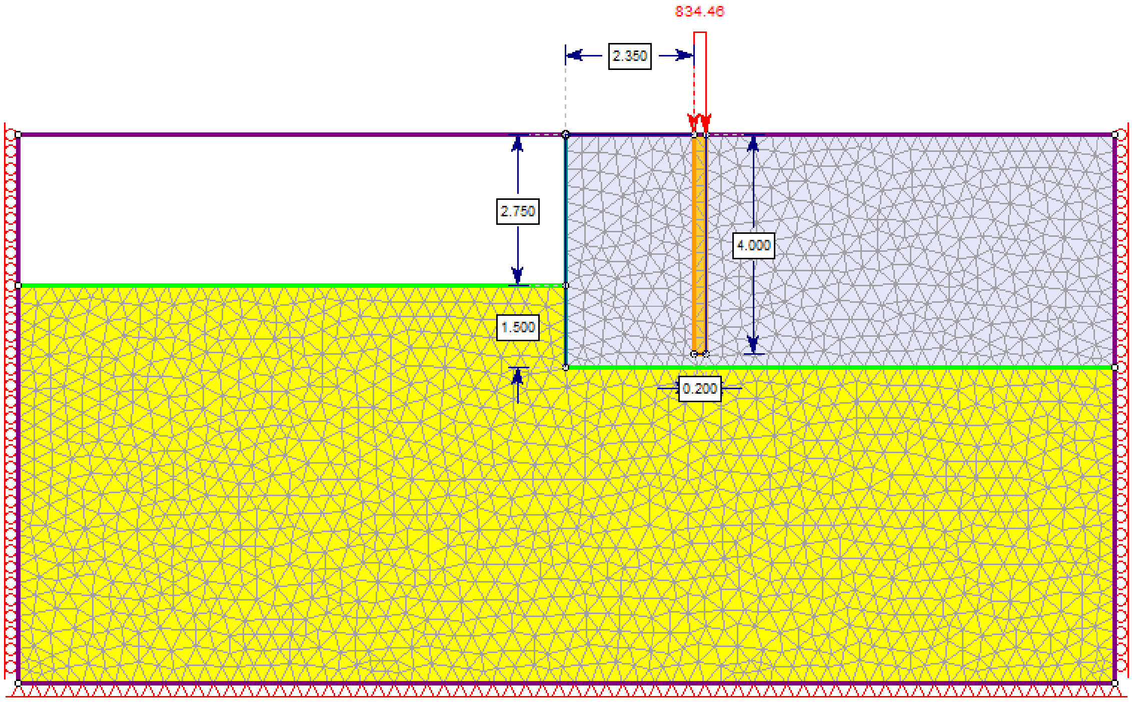

M 147.1: Original model (stage 3)

C'_1	ϕ'_1	γ_1	E_1	C'_2	ϕ'_2	γ_2	E_2	H_1	H_2	H_3	E_3	D_1	D_2	L	Qult
0	30	18	310	28	16	22	30.1	2.75	1.5	0.75	856251	2.35	0.2	4	834.46

M 147.2: Parameter values

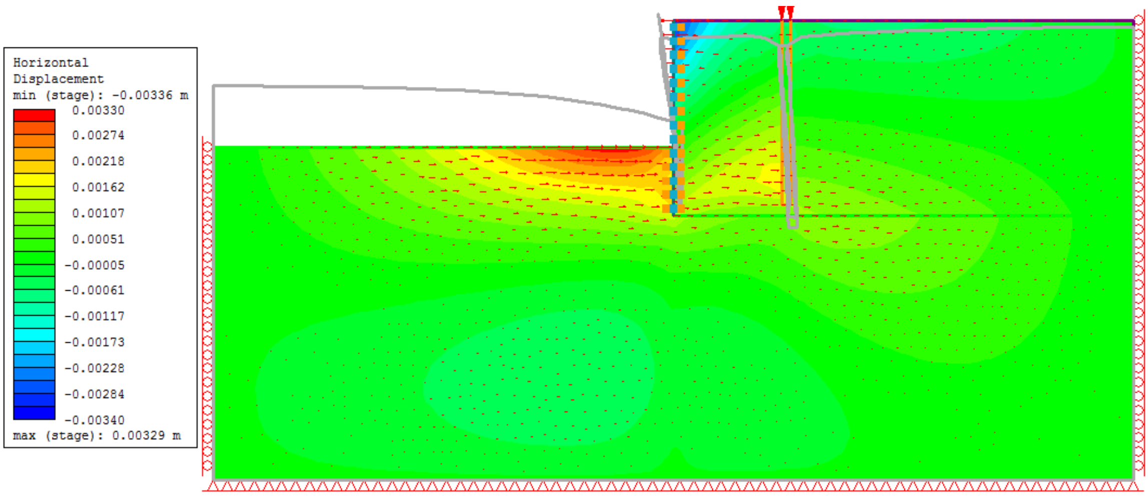

M 147.3: Deformed model (stage 3)

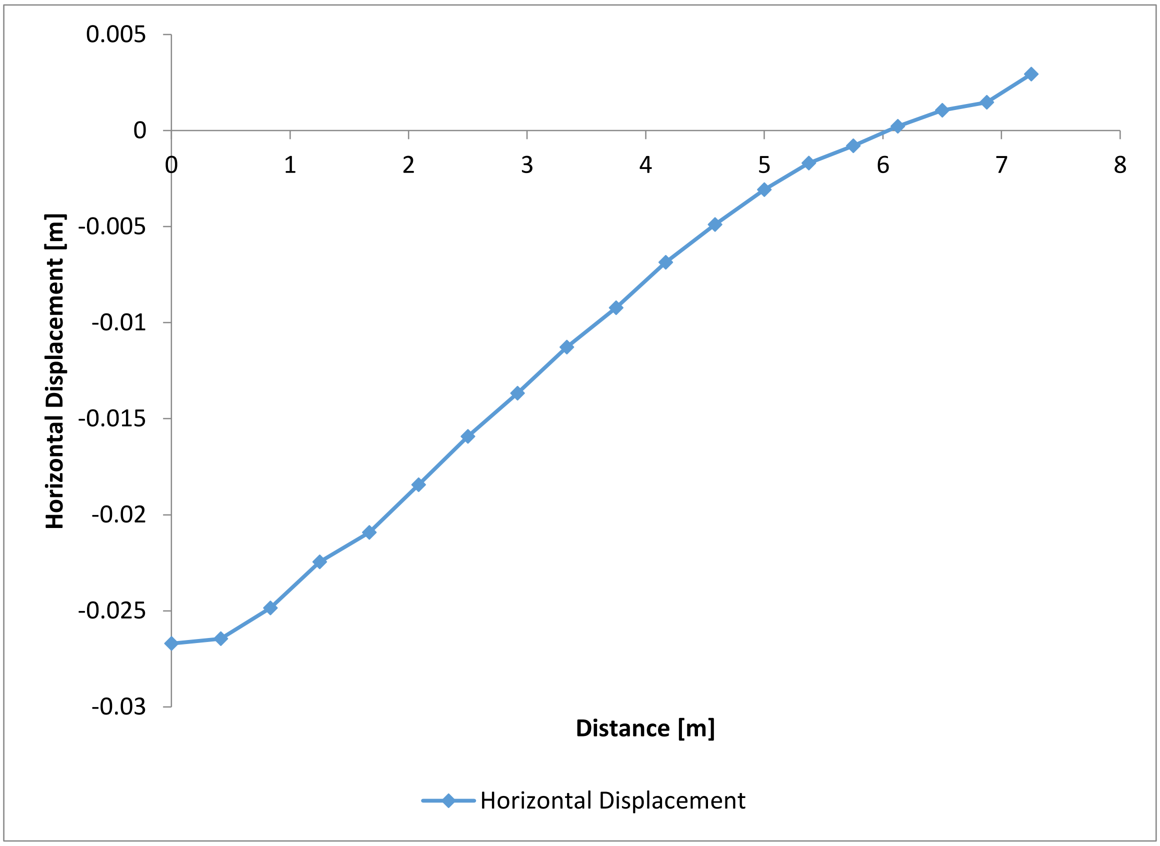

M 147.4: Horizontal displacement of soil along retaining wall

Retaining wall maximum horizontal displacement: -0.00336m

Distance from point of maximum displacement in retaining wall to the top of backfill soil: 0.0m

Model 148:

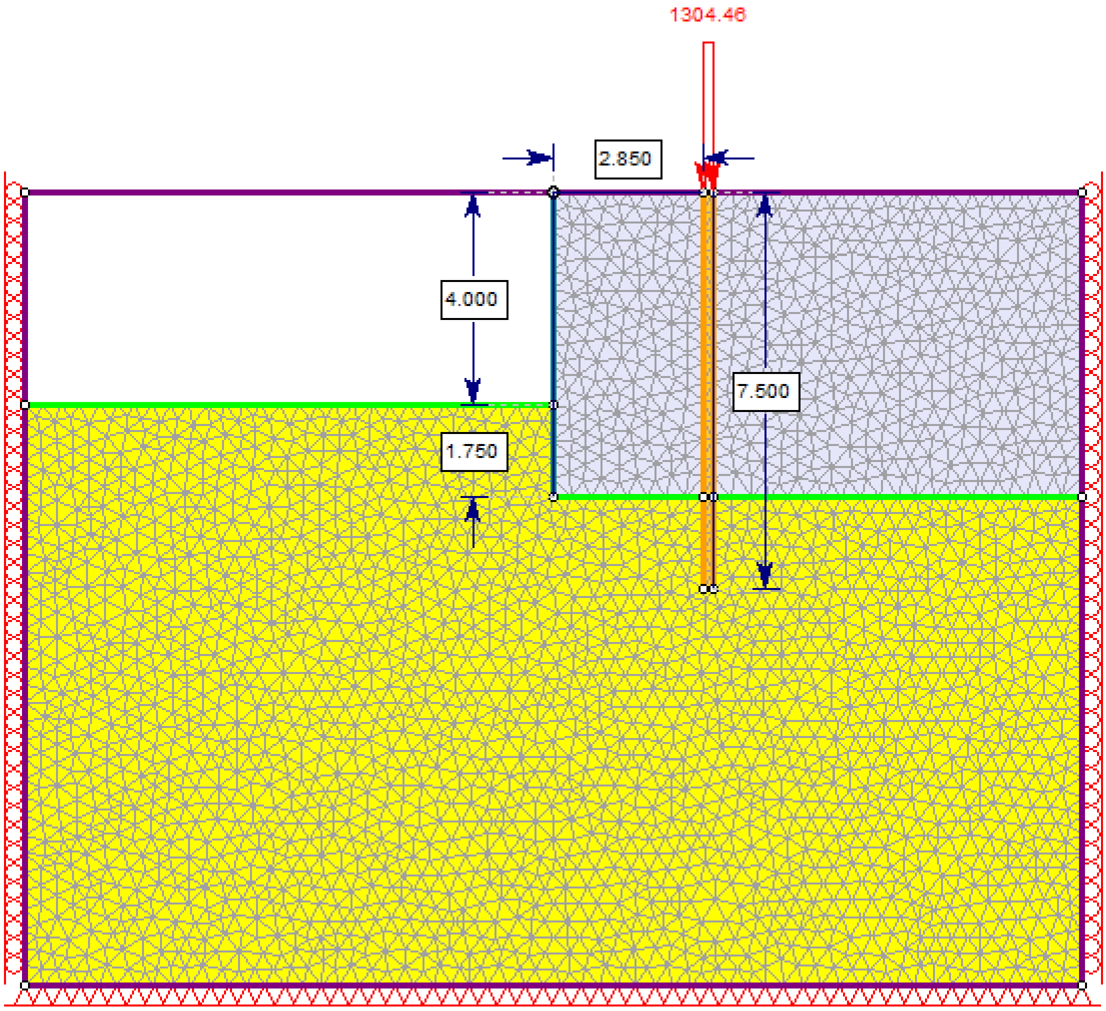

M 148.1: Original model (stage 3)

C_1'	ϕ_1'	γ_1	E_1	C_2'	ϕ_2'	γ_2	E_2	H_1	H_2	H_3	E_3	D_1	D_2	L	Qult
0	32	19	252	49	13	23	13.6	4.00	1.75	1	945657	2.85	0.2	7.5	1304.46

M 148.2: Parameter values

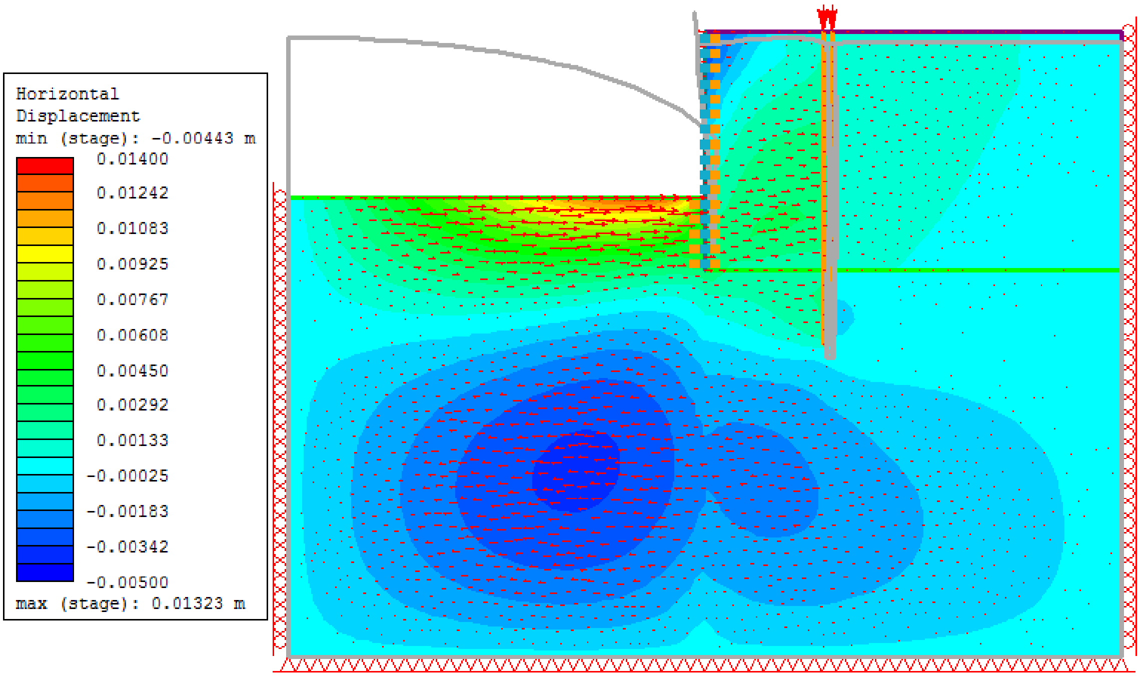

M 148.3: Deformed model (stage 3)

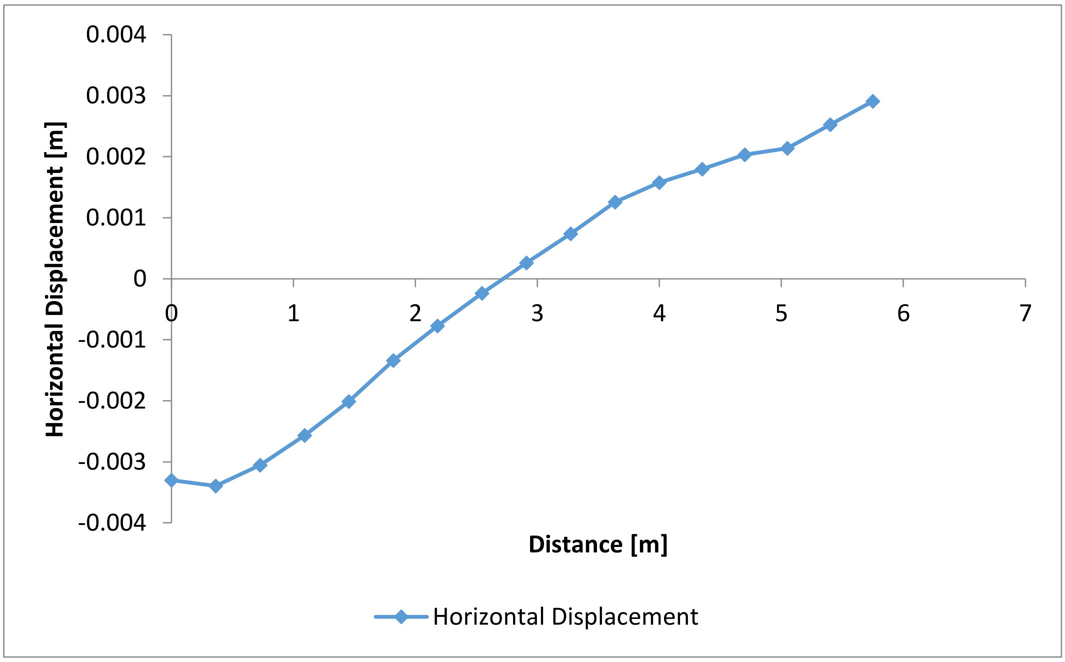

M 148.4: Horizontal displacement of soil along retaining wall

Retaining wall maximum horizontal displacement: -0.00443m

Distance from point of maximum displacement in retaining wall to the top of backfill soil: 0.0m

Model 149:

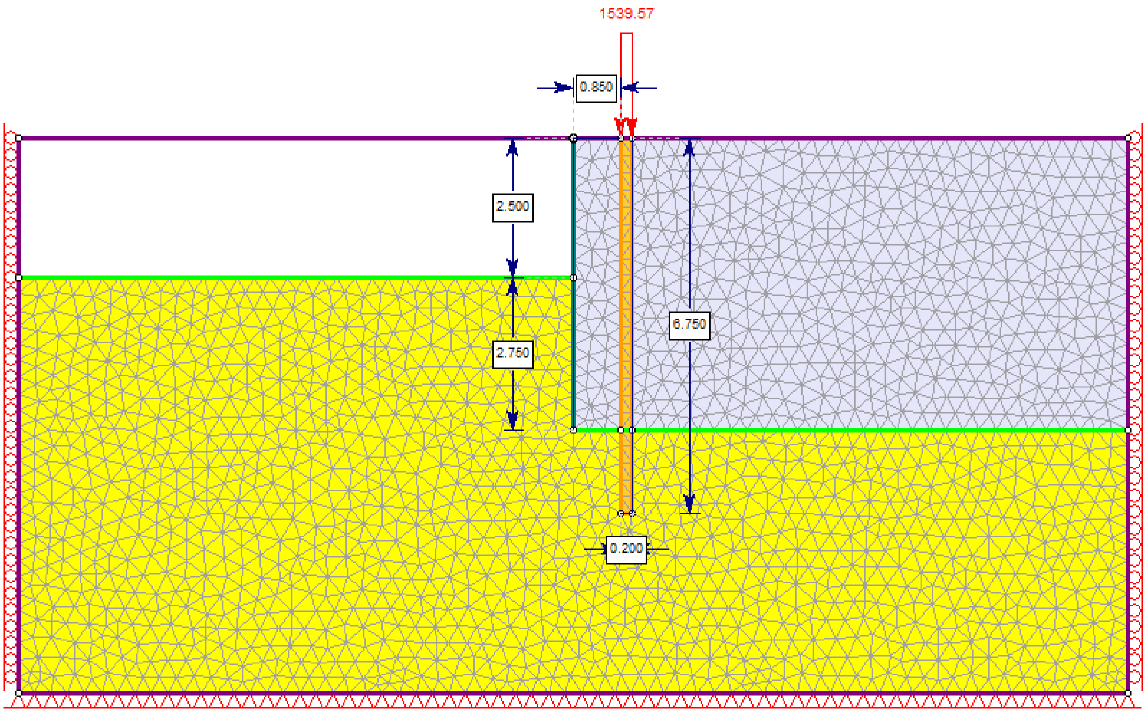

M 149.1: Original model (stage 3)

[illegible]	ϕ'_1	γ_1	E_1	C'_2	ϕ'_2	γ_2	E_2	H_1	H_2	H_3	E_3	D_1	D_2	L	Qult
[illegible]	37	22	28	18	22	16	44.3	2.50	2.75	1	1032435	0.85	0.2	6.75	1539.57

M 149.2: Parameter values

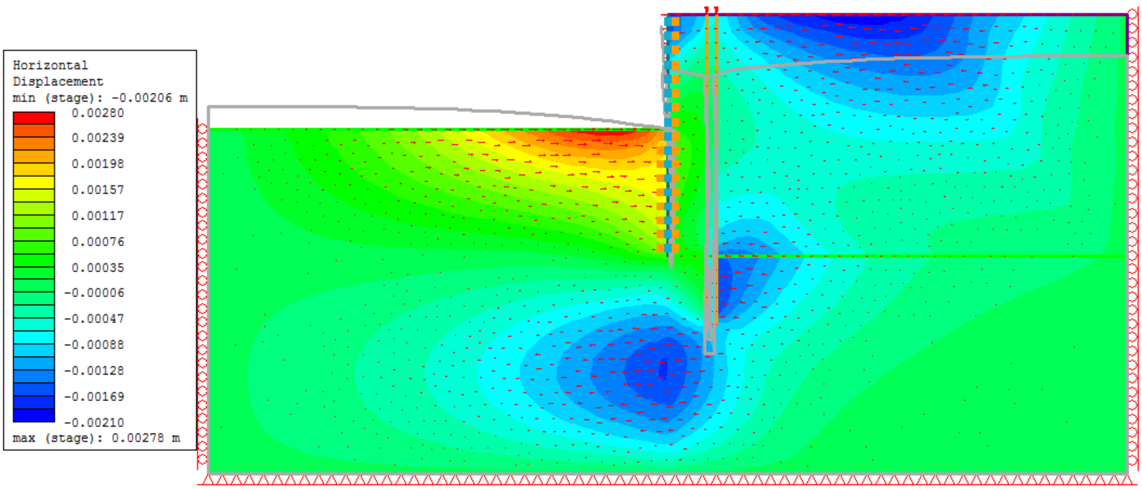

M 149.3: Deformed model (stage 3)

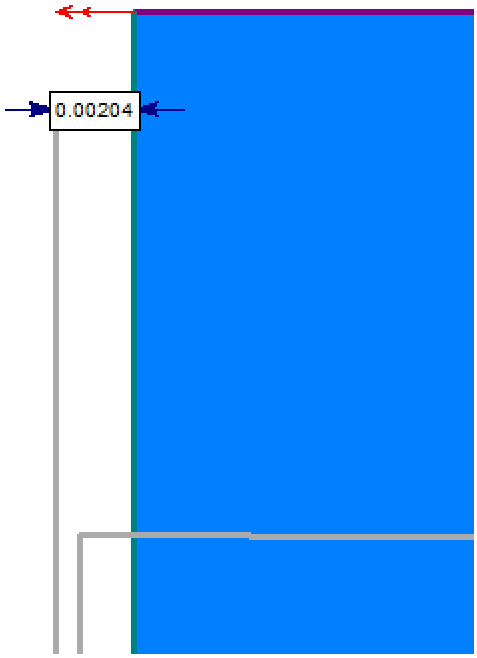

M 149.4: Detailed view of cross-section of retaining wall and soil (stage 3)

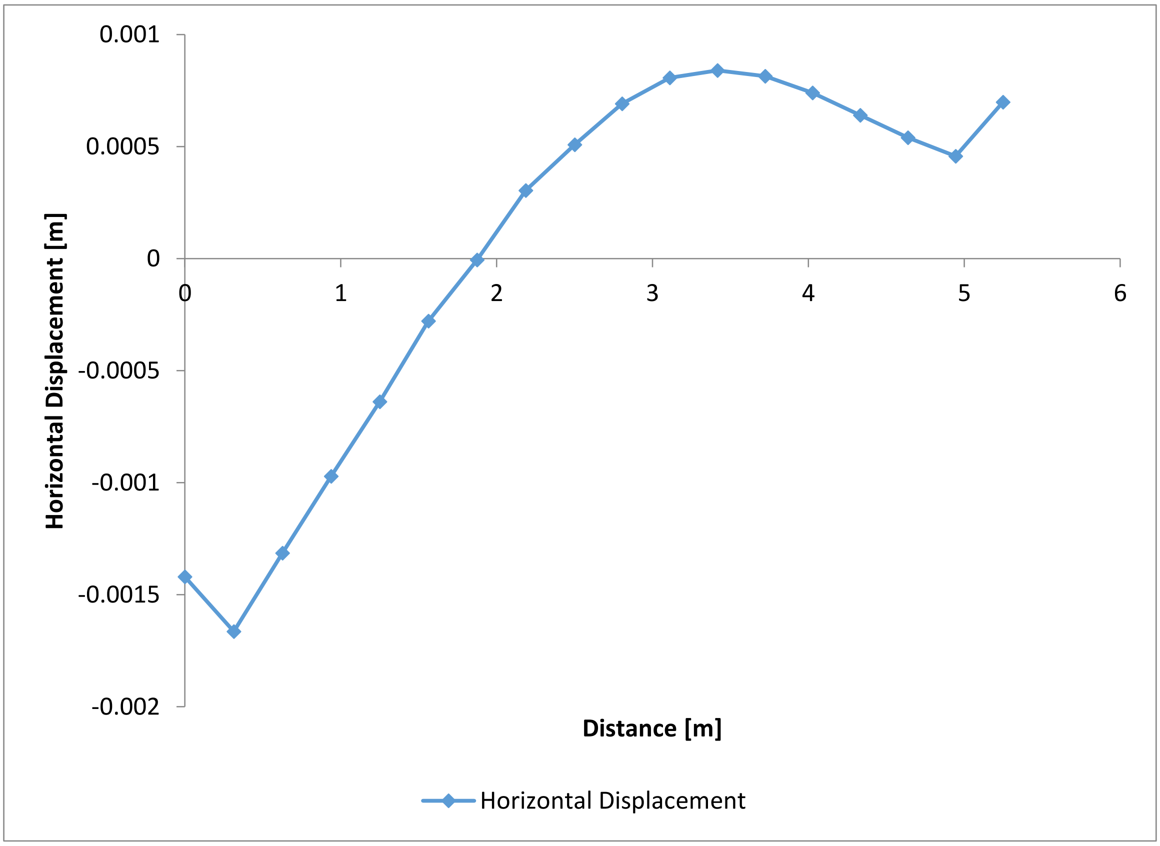

M 149.5: Horizontal displacement of soil along retaining wall

Retaining wall maximum horizontal displacement: -0.00204m

Distance from point of maximum displacement in retaining wall to the top of backfill soil: 0.0m

Model 150:

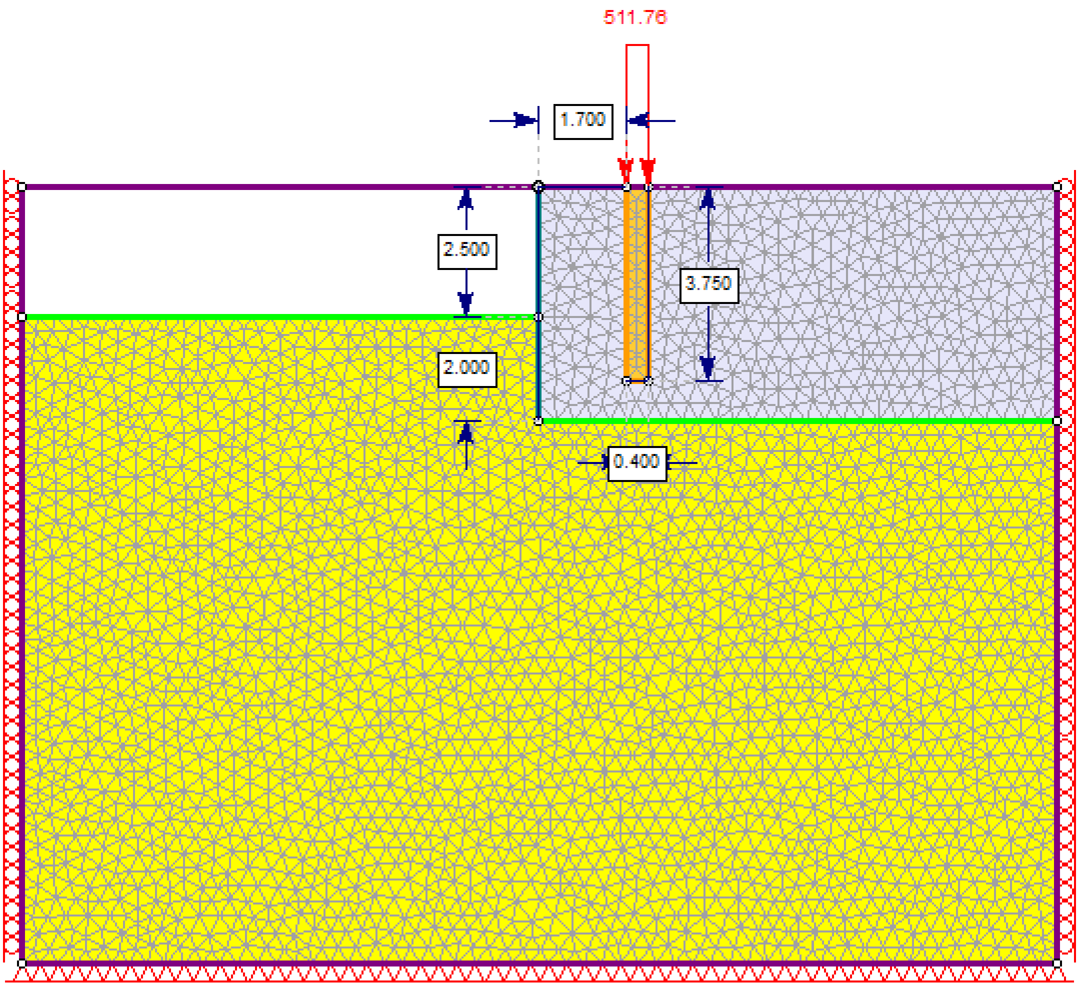

M 150.1: Original model (stage 3)

C'_1	ϕ'_1	γ_1	E_1	C'_2	ϕ'_2	γ_2	E_2	H_1	H_2	H_3	E_3	D_1	D_2	L	Qult
0	29	18	314	20	14	21	6.3	2.50	2	1.5	851665	1.7	0.4	3.75	511.76

M 150.2: Parameter values

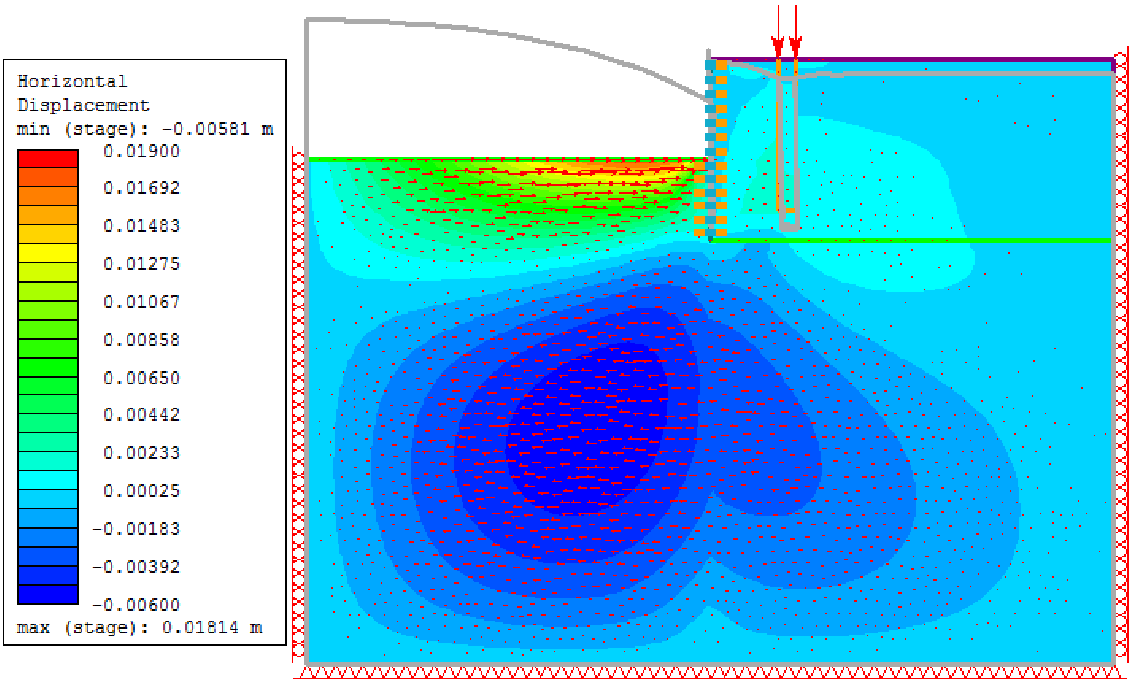

M 150.3: Deformed model (stage 3)

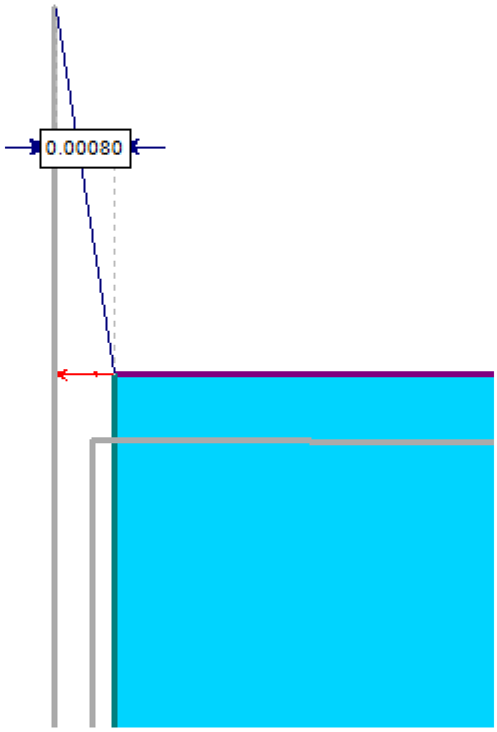

M 150.4: Detailed view of cross-section of retaining wall and soil (stage 3)

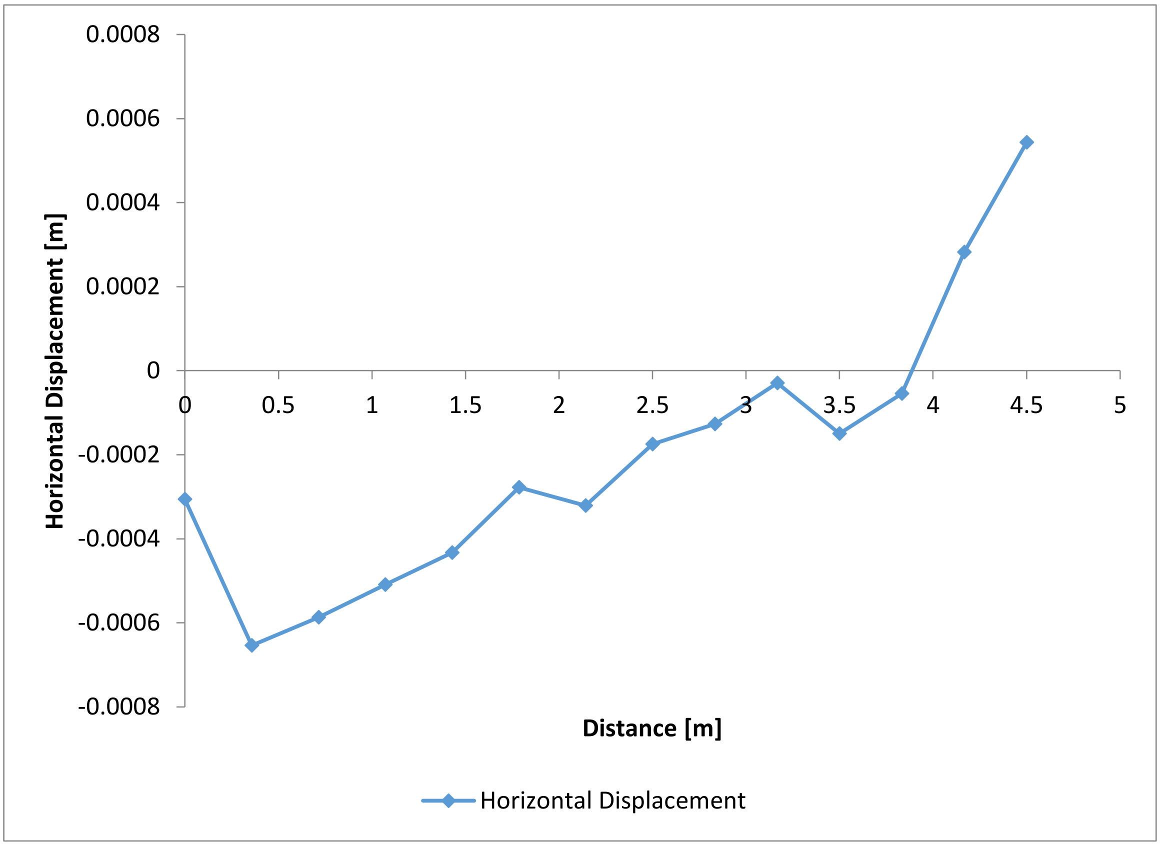

M 150.5: Horizontal displacement of soil along retaining wall

Retaining wall maximum horizontal displacement: -0.0008m

Distance from point of maximum displacement in retaining wall to the top of backfill soil: 0.0m

Model 151:

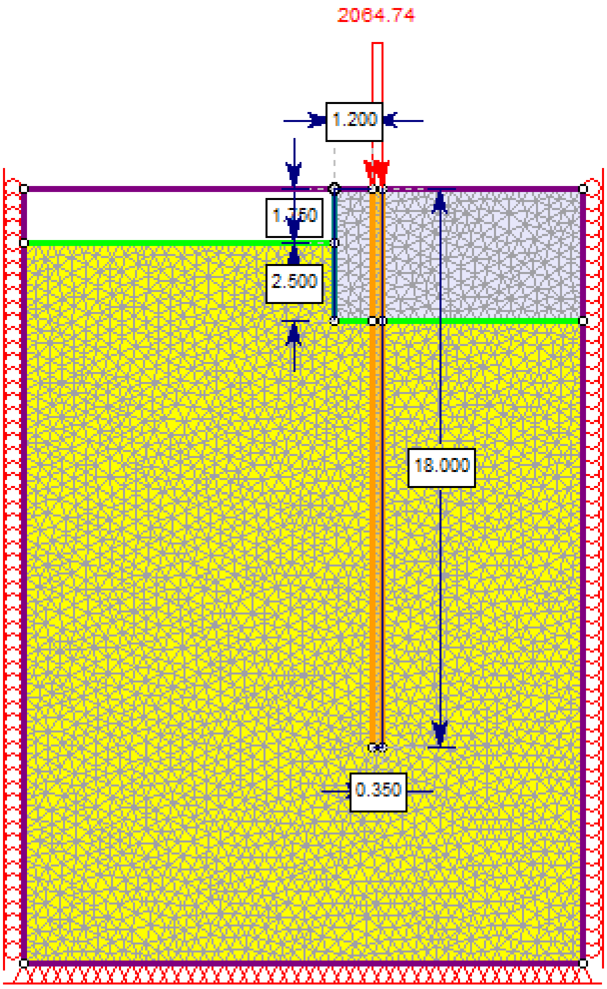

M 151.1: Original model (stage 3)

C_1'	ϕ_1'	γ_1	E_1	C_2'	ϕ_2'	γ_2	E_2	H_1	H_2	H_3	E_3	D_1	D_2	L	Qult
0	38	22	46	12	15	19	7.4	1.75	2.5	0.75	848901	1.2	0.35	18	2064.74

M 151.2: Parameter values

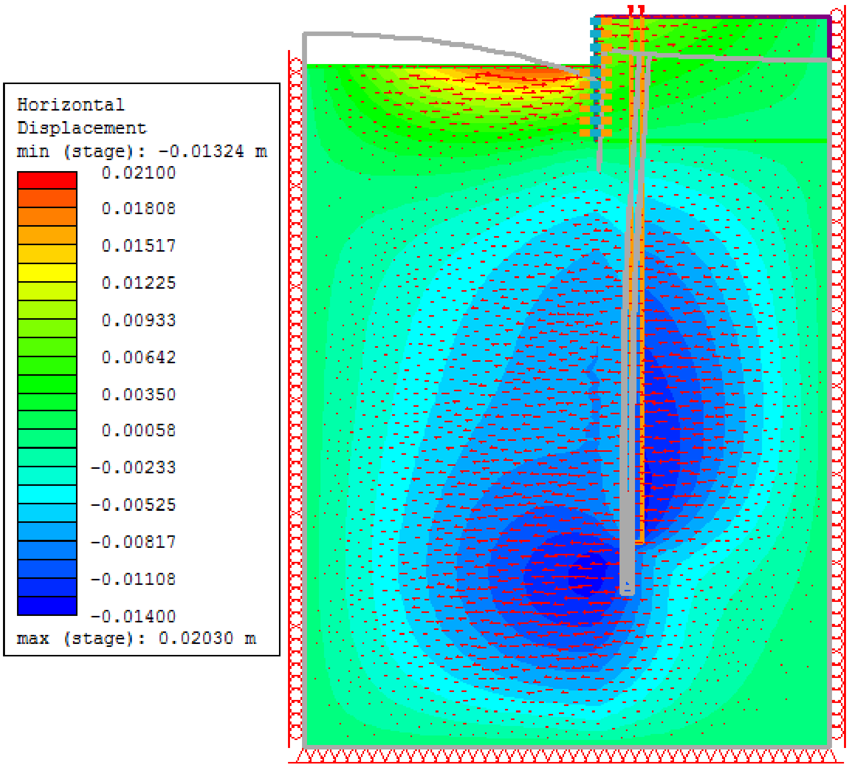

M 151.3: Deformed model (stage 3)

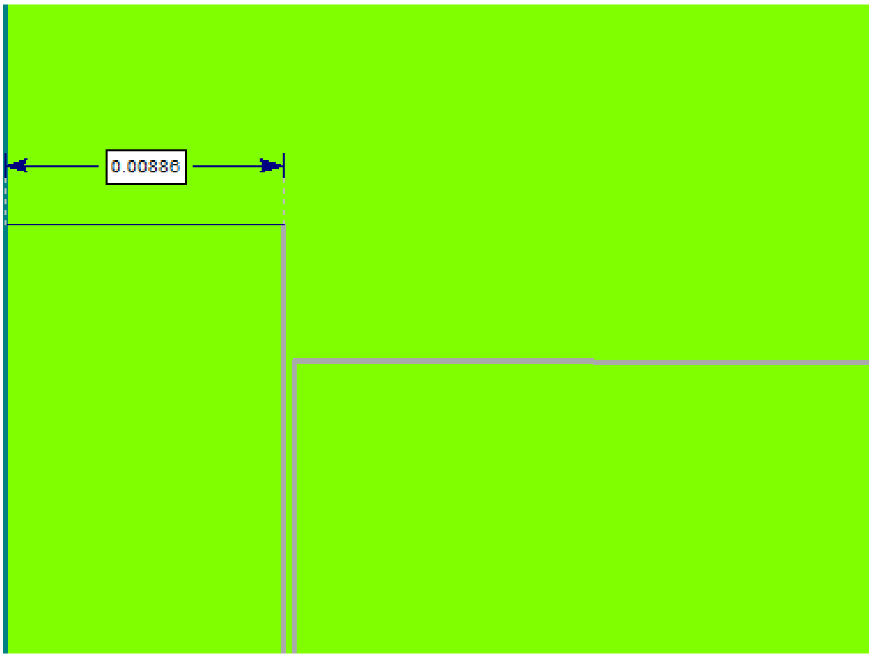

M 151.4: Detailed view of cross-section of retaining wall and soil (stage 3)

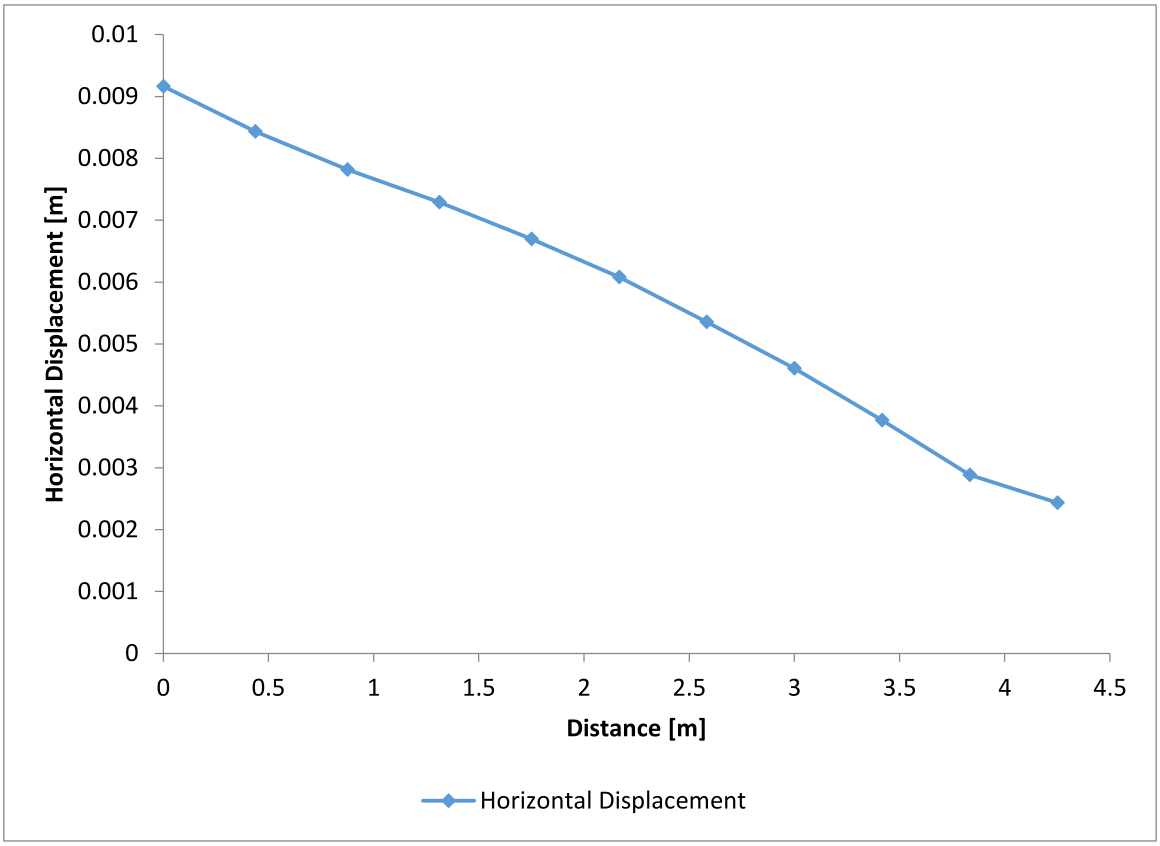

M 151.4: Horizontal displacement of soil along retaining wall

Retaining wall maximum horizontal displacement: 0.00886m

Distance from point of maximum displacement in retaining wall to the top of backfill soil: 0.0m

Model 152:

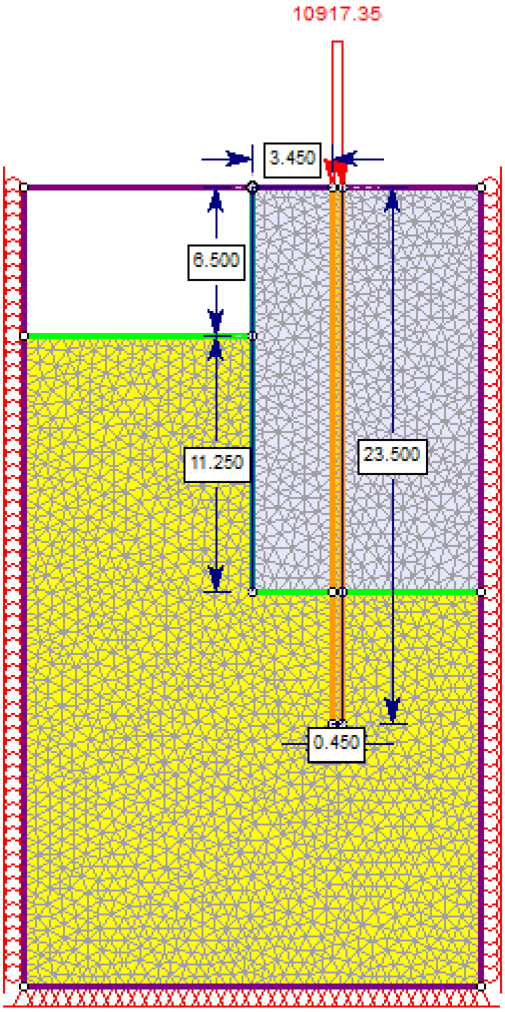

M 152.1: Original model (stage 3)

C'_1	ϕ'_1	γ_1	E_1	C'_2	ϕ'_2	γ_2	E_2	H_1	H_2	H_3	E_3	D_1	D_2	L	Qult
0	28	22	256	46	29	17	43.7	6.50	11.25	1.25	917274	3.45	0.45	23.5	10917.35

M 152.2: Parameter values

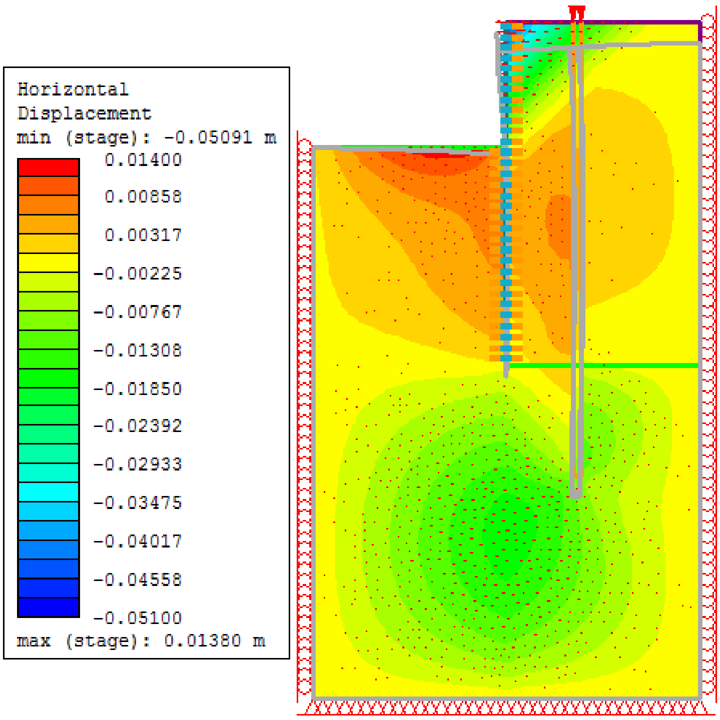

M 152.3: Deformed model (stage 3)

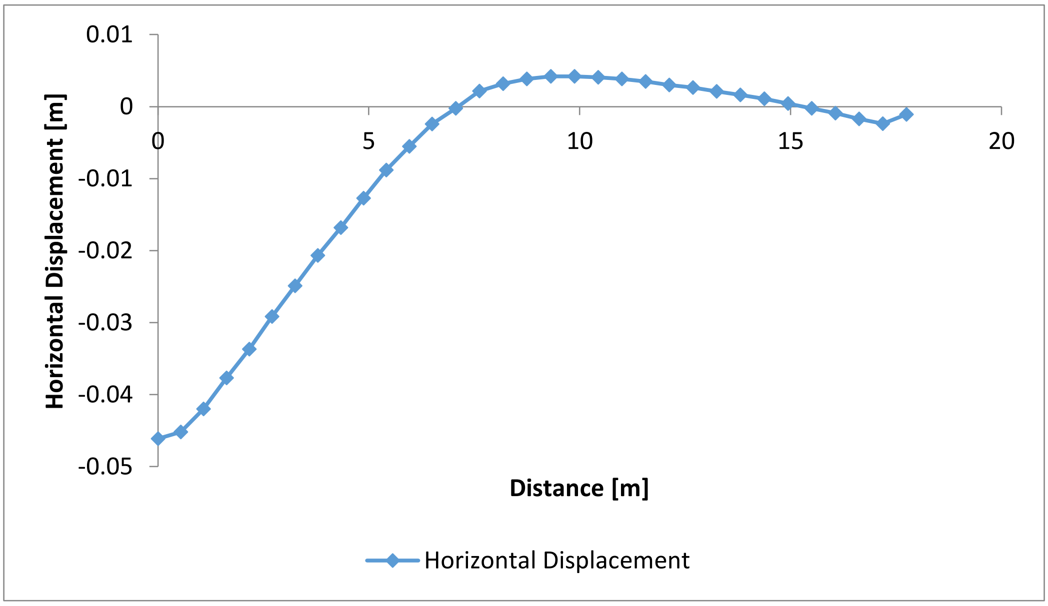

M 152.4: Horizontal displacement of soil along retaining wall

Retaining wall maximum horizontal displacement: -0.05091m

Distance from point of maximum displacement in retaining wall to the top of backfill soil: 0.0m

Model 153:

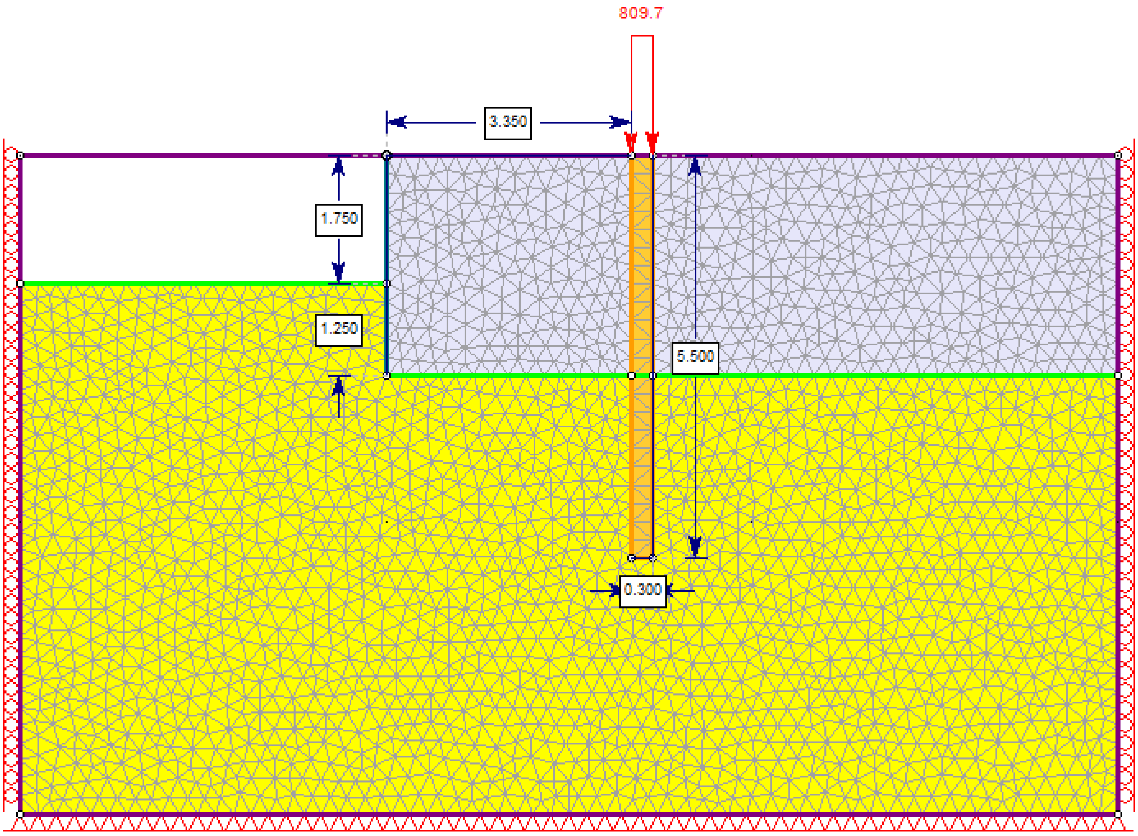

M 153.1: Original model (stage 3)

C_1'	ϕ_1'	γ_1	E_1	C_2'	ϕ_2'	γ_2	E_2	H_1	H_2	H_3	E_3	D_1	D_2	L	Qult
0	35	20	311	14	19	21	39.4	1.75	1.25	0.5	923173	3.35	0.3	5.5	809.7

M 153.2: Parameter values

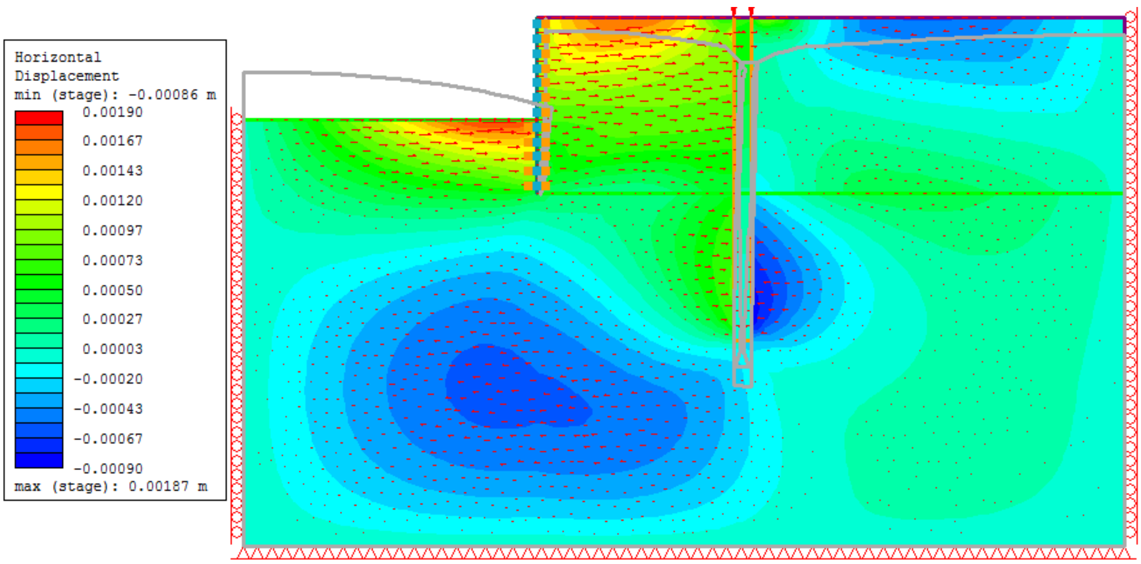

M 153.3: Deformed model (stage 3)

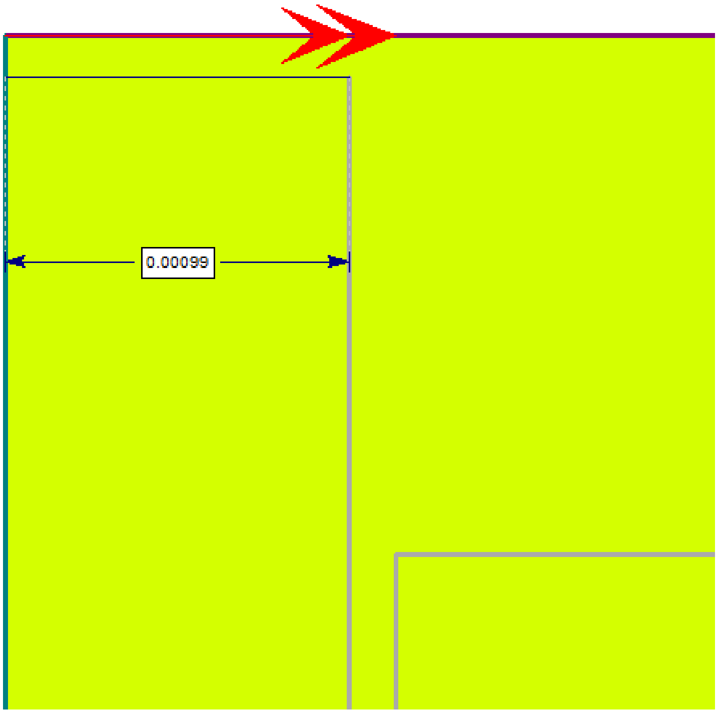

M 153.4: Detailed view of cross-section of retaining wall and soil (stage 3)

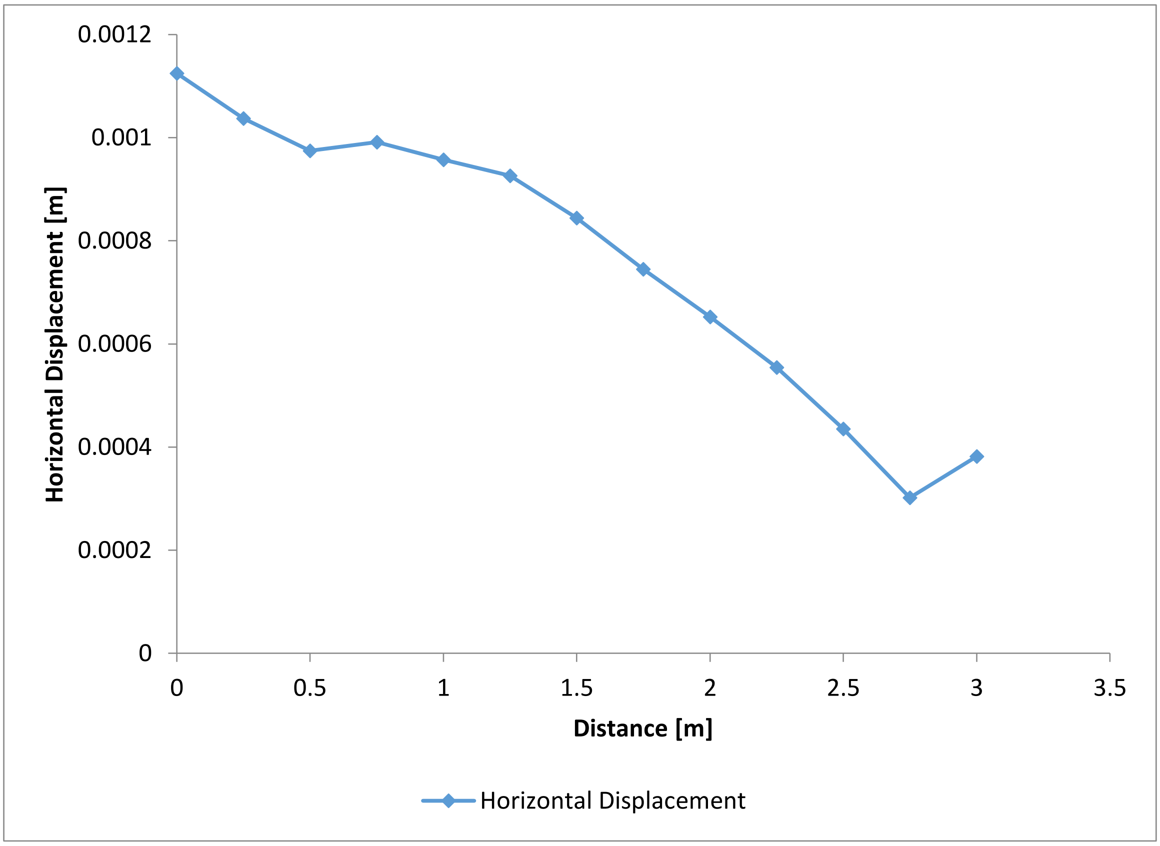

M 153.5: Horizontal displacement of soil along retaining wall

Retaining wall maximum horizontal displacement: 0.00099m

Distance from point of maximum displacement in retaining wall to the top of backfill soil: 0.0m

Model 154:

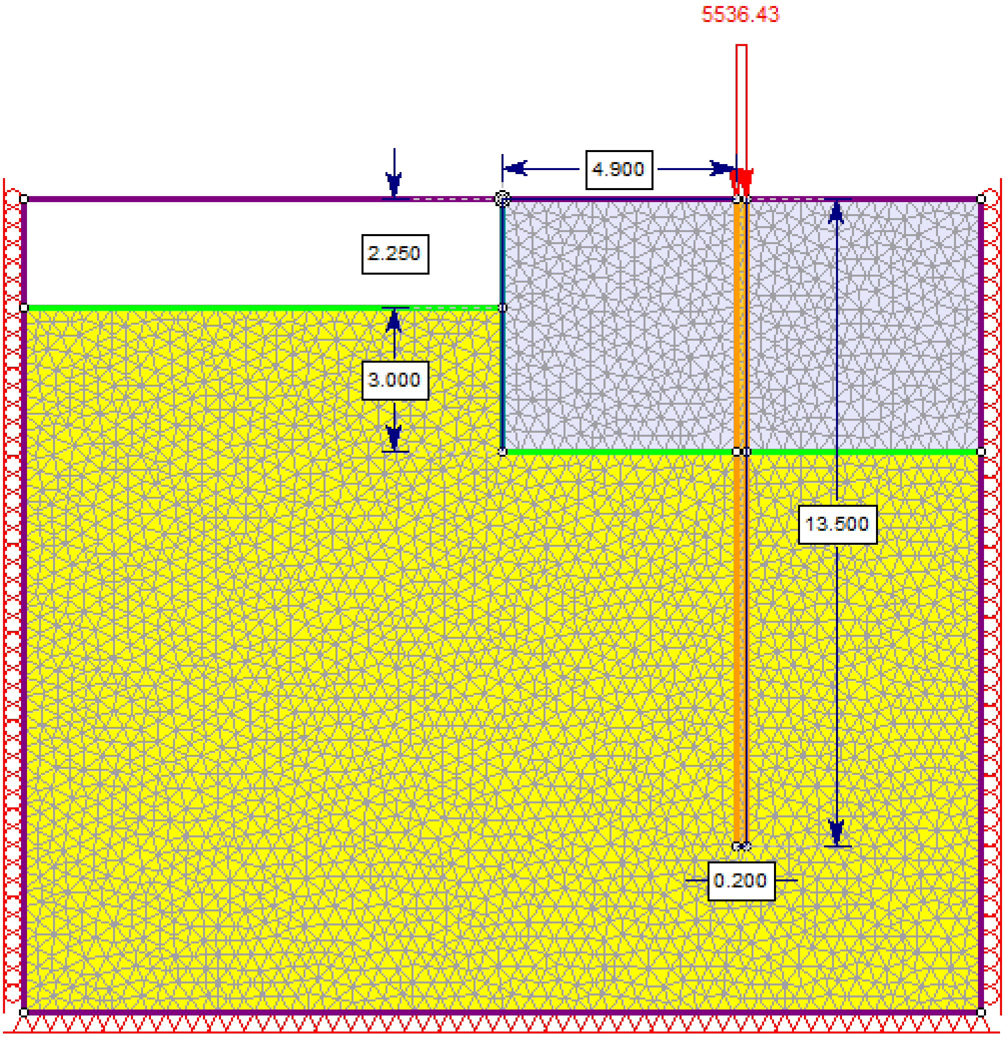

M 154.1: Original model (stage 3)

C_1'	ϕ_1'	γ_1	E_1	C_2'	ϕ_2'	γ_2	E_2	H_1	H_2	H_3	E_3	D_1	D_2	L	Qult
0	31	22	142	16	27	23	38.8	2.25	3	1.25	1000793	4.9	0.2	13.5	5536.43

M 154.2: Parameter values

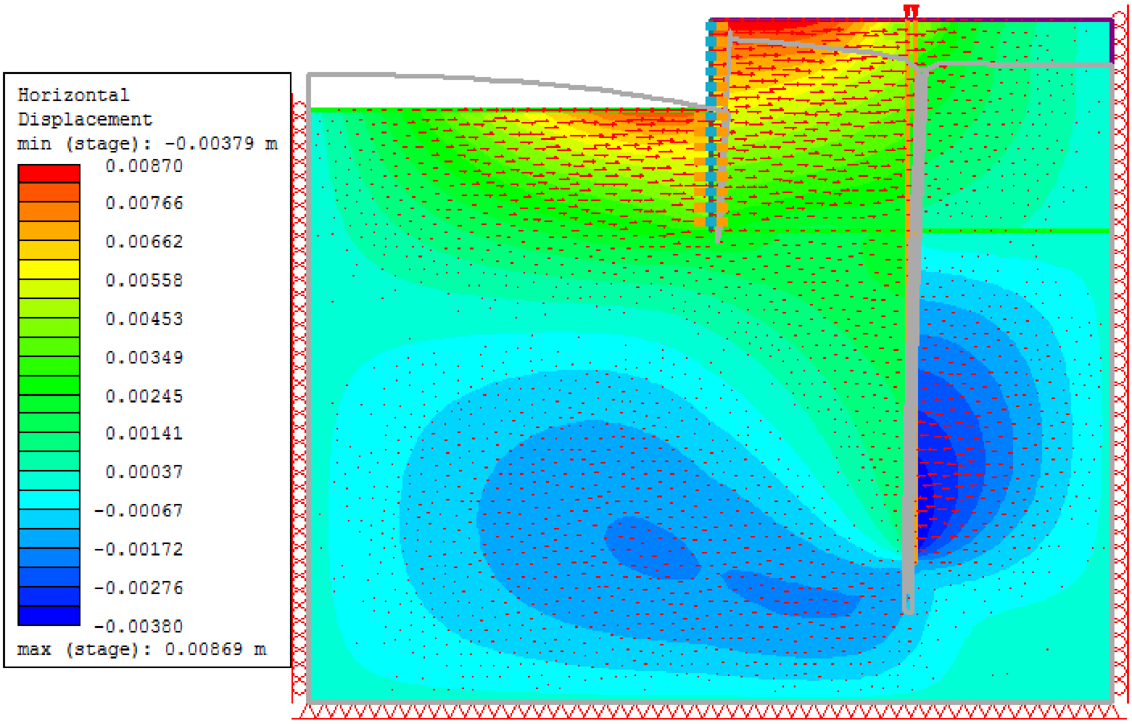

M 154.3: Deformed model (stage 3)

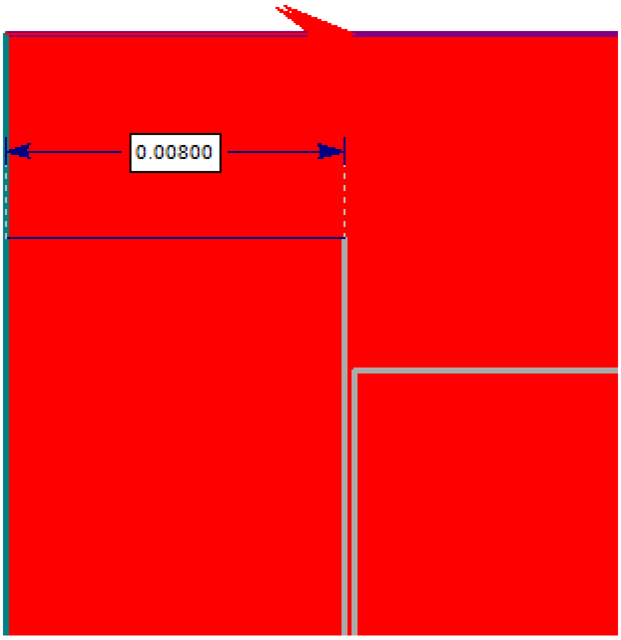

M 154.4: Detailed view of cross-section of retaining wall and soil (stage 3)

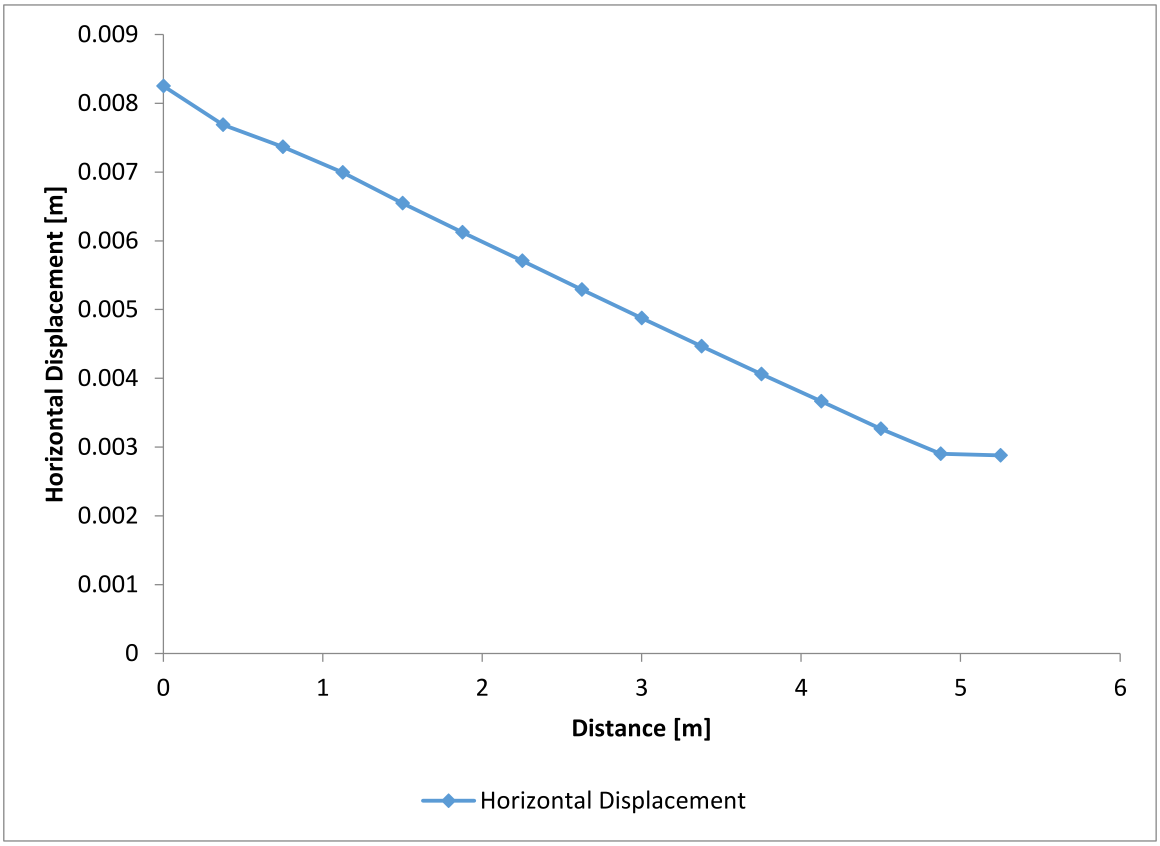

M 154.5: Horizontal displacement of soil along retaining wall

Retaining wall maximum horizontal displacement: 0.008m

Distance from point of maximum displacement in retaining wall to the top of backfill soil: 0.0m

Model 155:

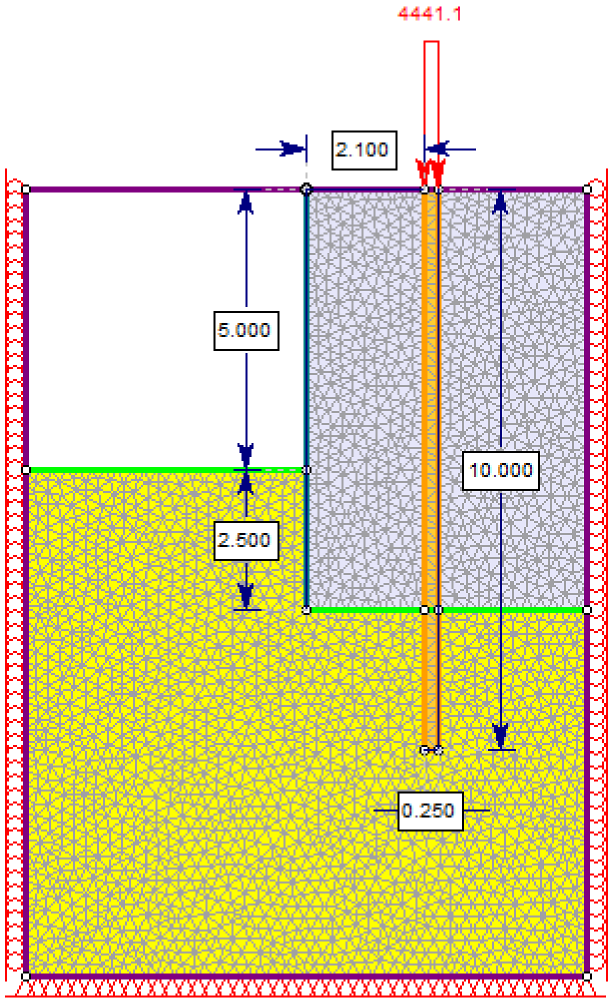

M 155.1: Original model (stage 3)

C_1'	ϕ_1'	γ_1	E_1	C_2'	ϕ_2'	γ_2	E_2	H_1	H_2	H_3	E_3	D_1	D_2	L	Qult
0	38	20	254	49	27	20	12.4	5.00	2.5	1.25	753665	2.1	0.25	10	4441.1

M 155.2: Parameter values

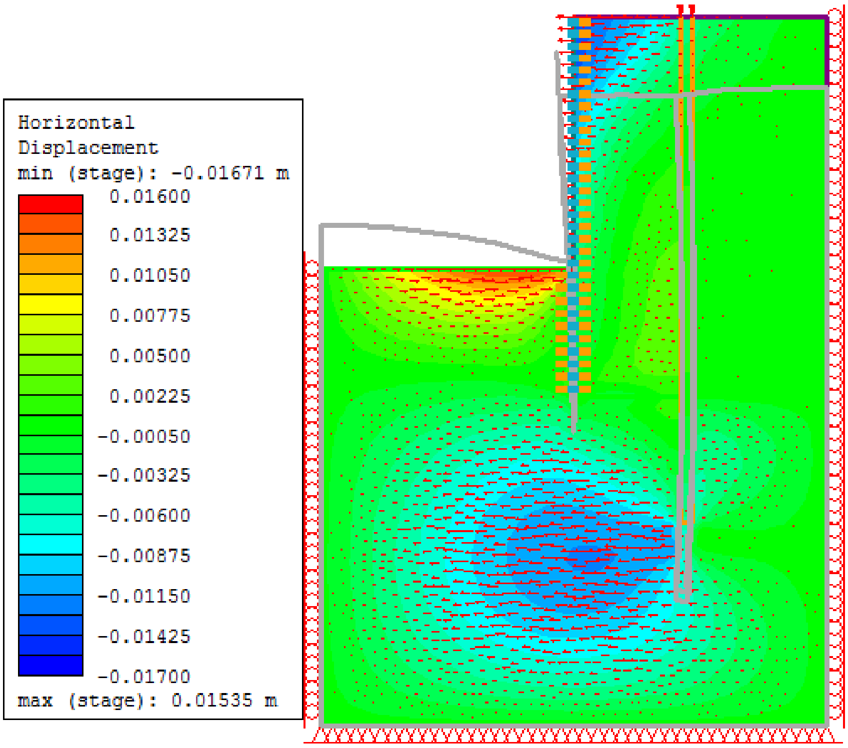

M 155.3: Deformed model (stage 3)

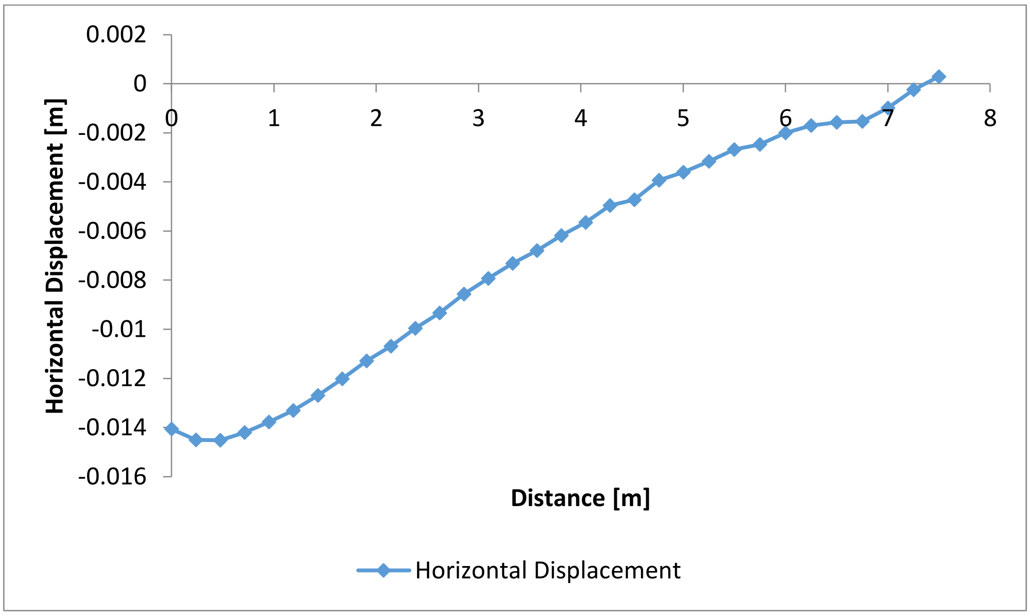

M 155.4: Horizontal displacement of soil along retaining wall

Retaining wall maximum horizontal displacement: -0.01671m

Distance from point of maximum displacement in retaining wall to the top of backfill soil: 0.0m

Model 156:

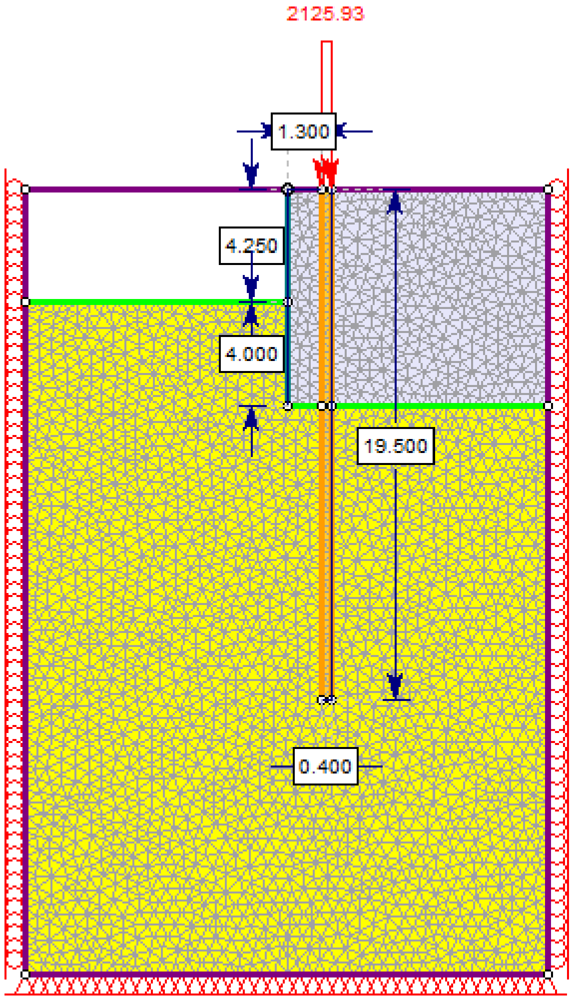

M 156.1: Original model (stage 3)

C'_1	ϕ'_1	γ_1	E_1	C'_2	ϕ'_2	γ_2	E_2	H_1	H_2	H_3	E_3	D_1	D_2	L	Qult
0	43	19	228	25	11	23	19.5	4.25	4	1	1035158	1.3	0.4	19.5	2125.93

M 156.2: Parameter values

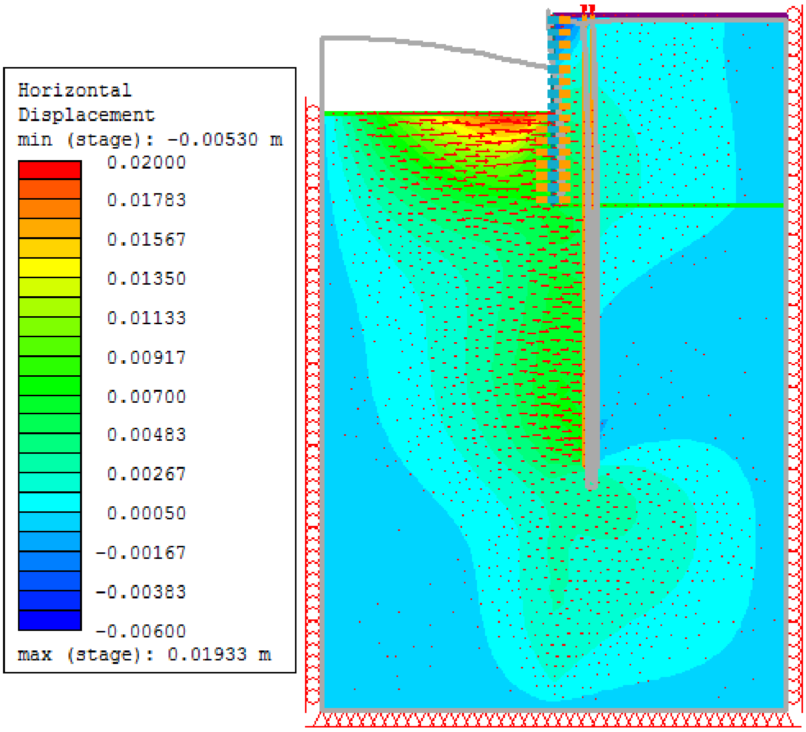

M 156.3: Deformed model (stage 3)

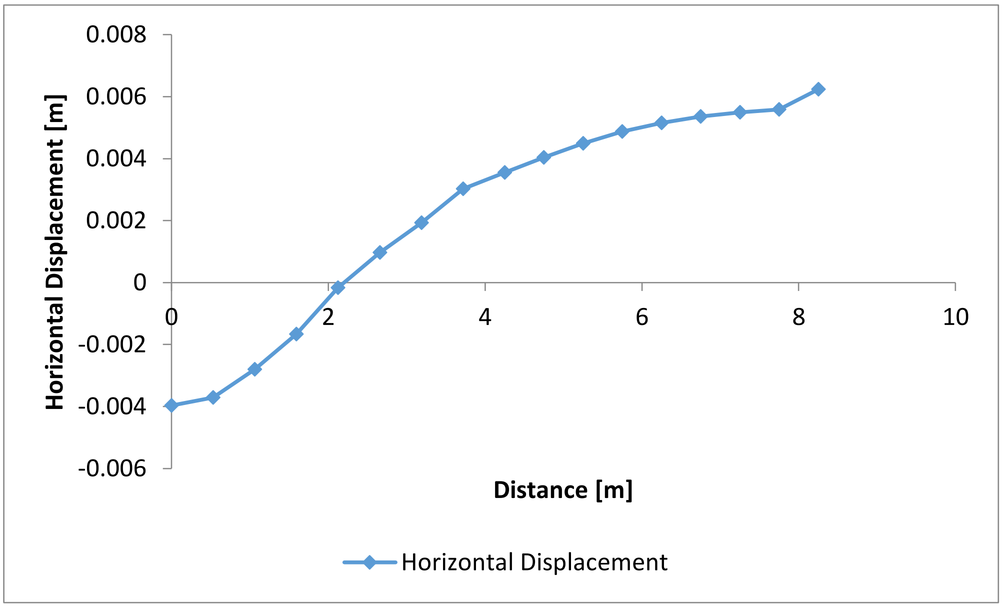

M 156.4: Horizontal displacement of soil along retaining wall

Retaining wall maximum horizontal displacement: 0.00624m

Distance from point of maximum displacement in retaining wall to the top of backfill soil: 8.25m

Model 157:

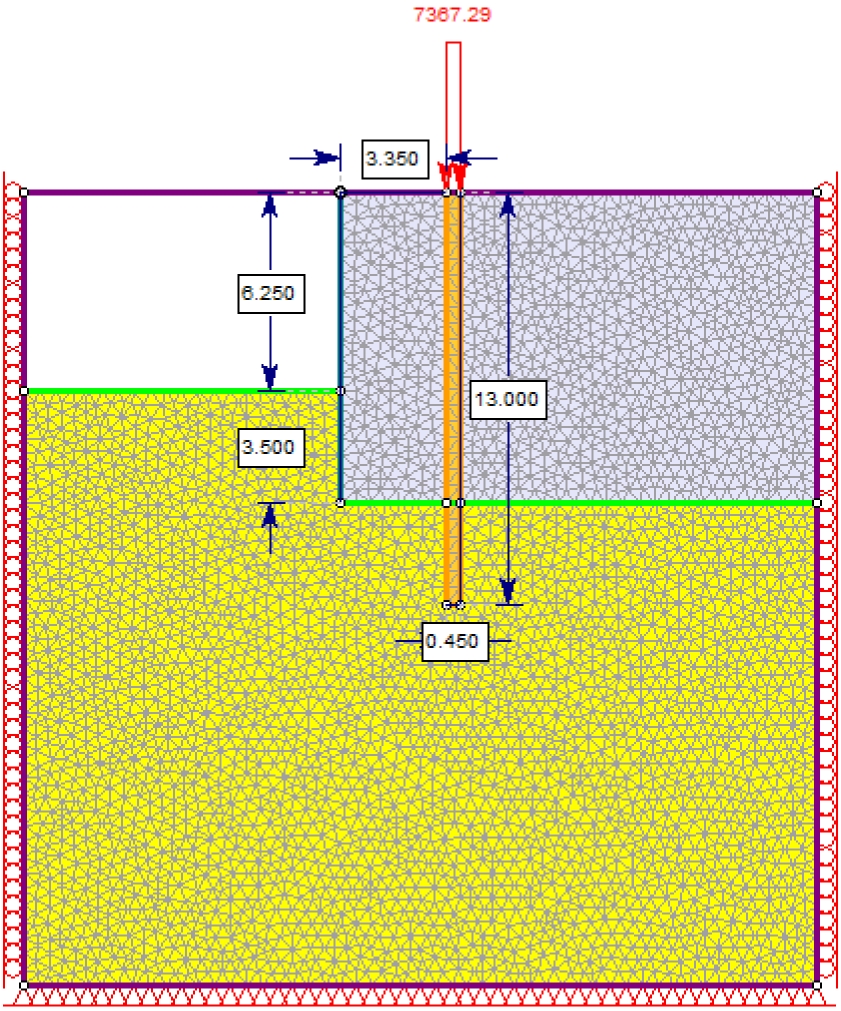

M 157.1: Original model (stage 3)

C_1'	ϕ_1'	γ_1	E_1	C_2'	ϕ_2'	γ_2	E_2	H_1	H_2	H_3	E_3	D_1	D_2	L	Qult
0	42	20	205	52	30	18	40.6	6.25	3.5	1.25	871250	3.35	0.45	13	7367.29

M 157.2: Parameter values

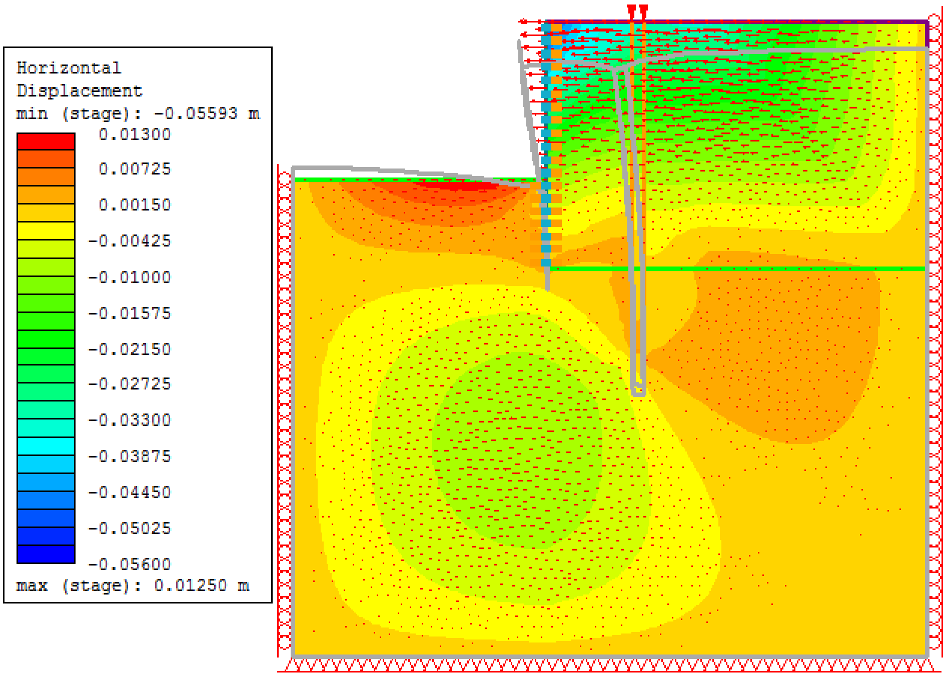

M 157.3: Deformed model (stage 3)

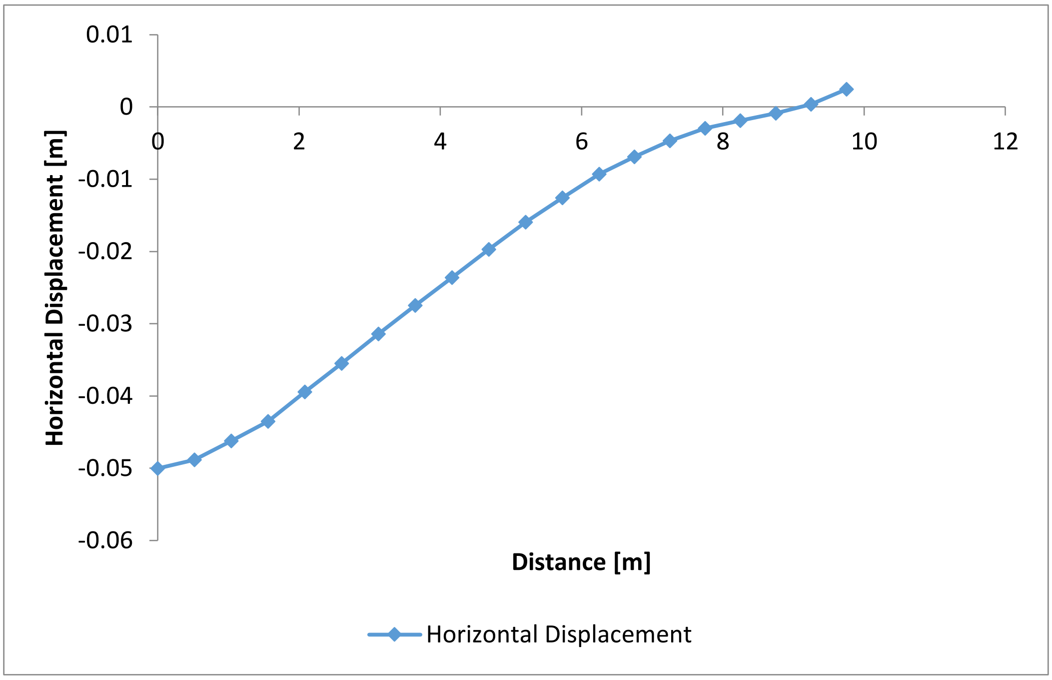

M 157.4: Horizontal displacement of soil along retaining wall

Retaining wall maximum horizontal displacement: -0.05593m

Distance from point of maximum displacement in retaining wall to the top of backfill soil: 0.0m

Model 158:

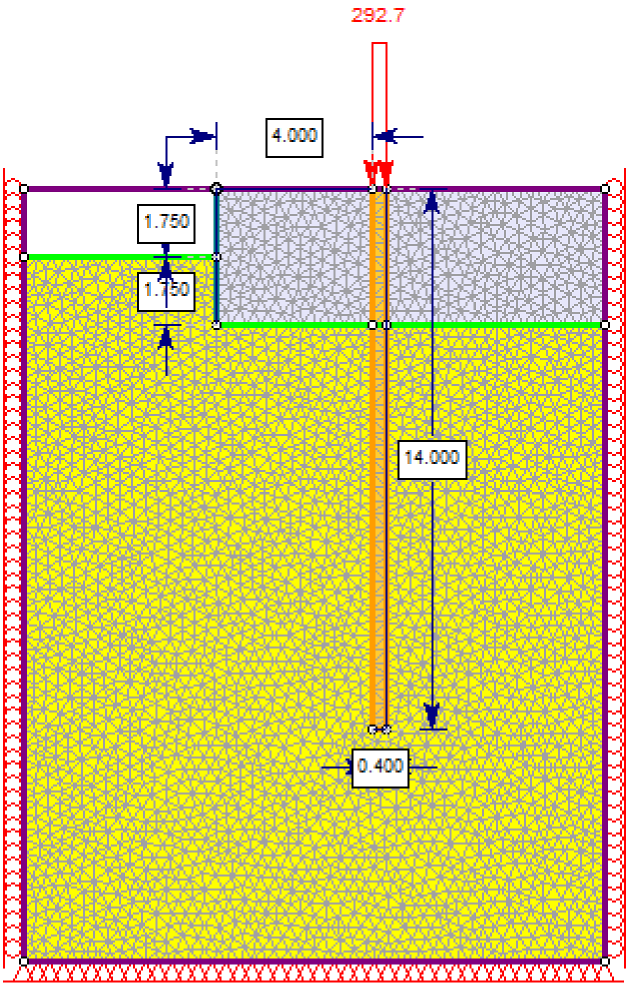

M 158.1: Original model (stage 3)

C'_1	ϕ'_1	γ_1	E_1	C'_2	ϕ'_2	γ_2	E_2	H_1	H_2	H_3	E_3	D_1	D_2	L	Qult
0	33	19	195	12	1	16	6.9	1.75	1.75	0.5	701003	4	0.4	10.75	292.7

M 158.2: Parameter values

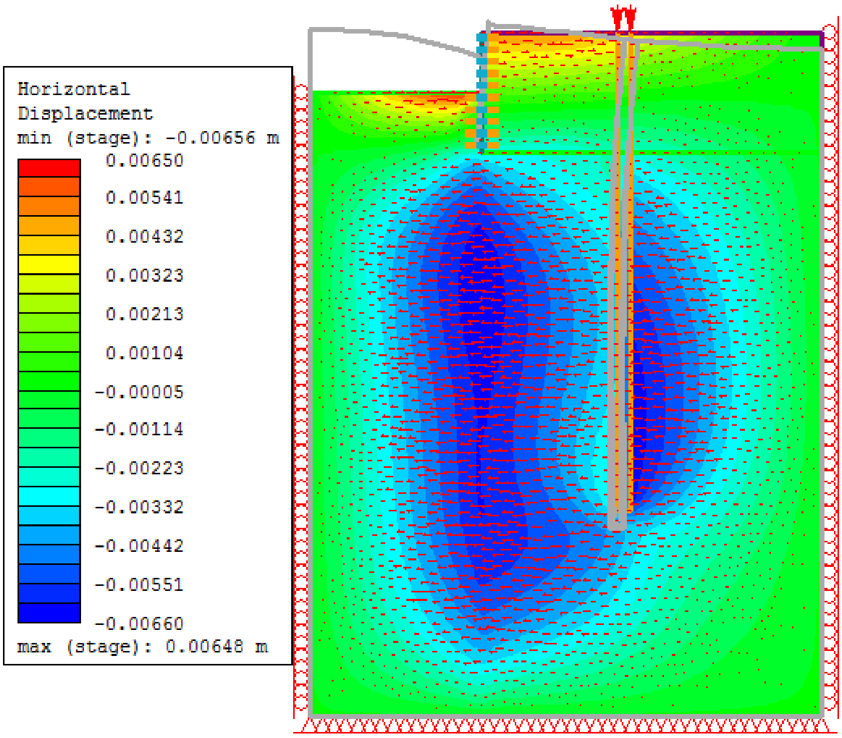

M 158.3: Deformed model (stage 3)

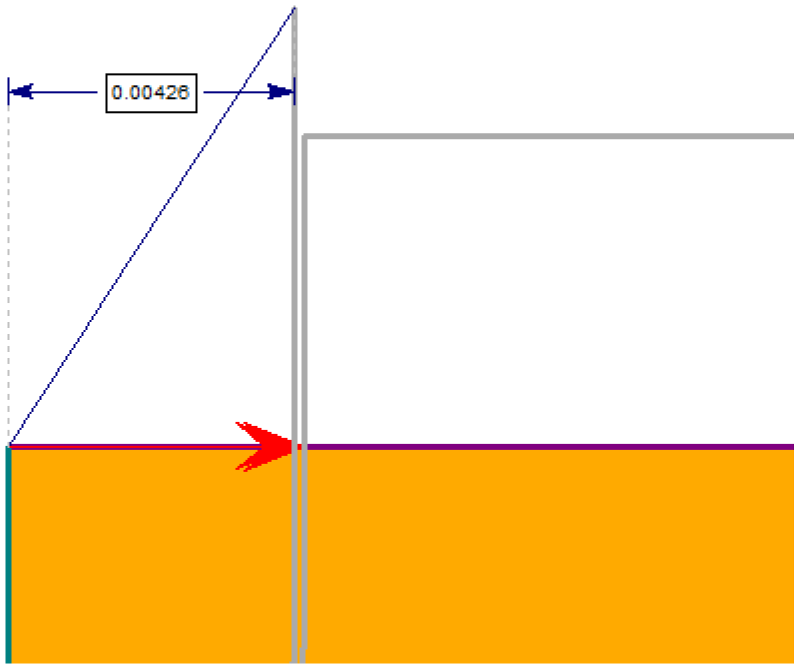

M 158.4: Detailed view of cross-section of retaining wall and soil (stage 3)

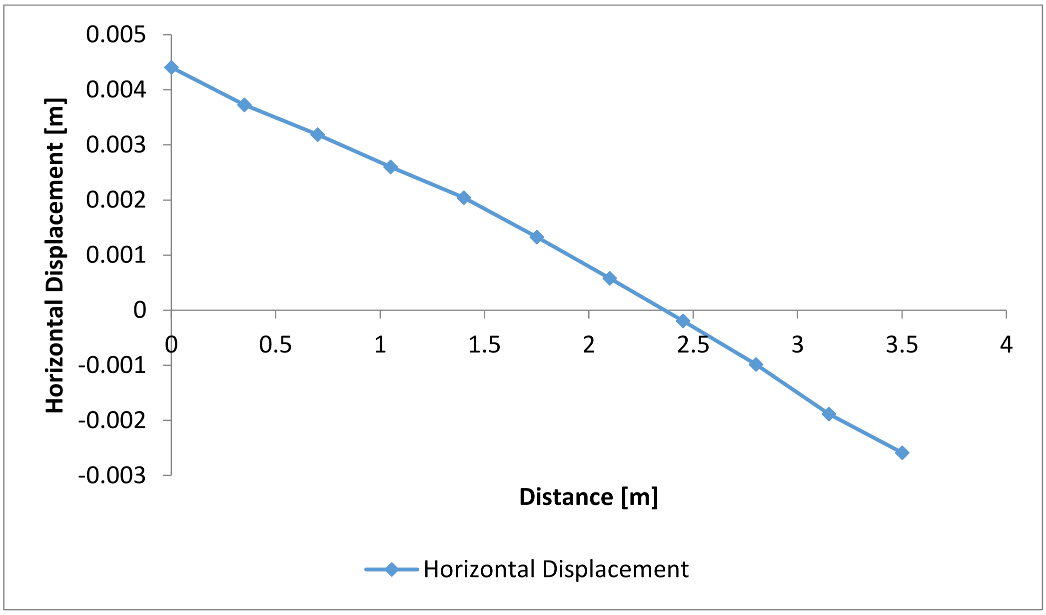

M 158.5: Horizontal displacement of soil along retaining wall

Retaining wall maximum horizontal displacement: 0.00426m

Distance from point of maximum displacement in retaining wall to the top of backfill soil: 0.0m

Model 159:

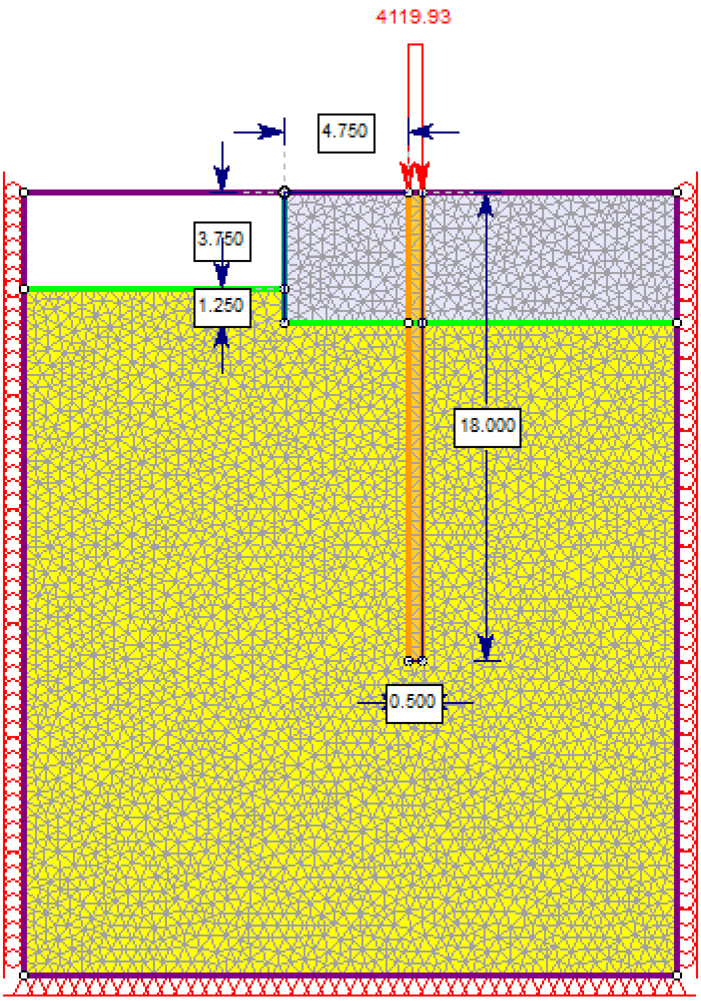

M 159.1: Original model (stage 3)

C'_1	ϕ'_1	γ_1	E_1	C'_2	ϕ'_2	γ_2	E_2	H_1	H_2	H_3	E_3	D_1	D_2	L	Qult
0	42	20	250	50	24	18	3.1	3.75	1.25	0.75	1042987	4.75	0.5	18	4119.93

M 159.2: Parameter values

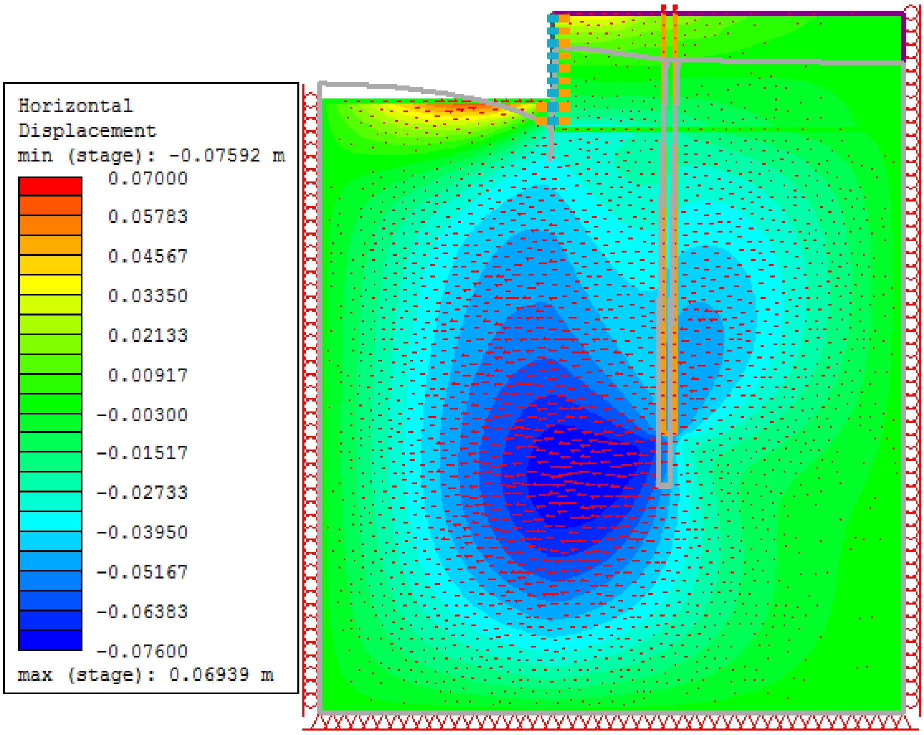

M 159.3: Deformed model (stage 3)

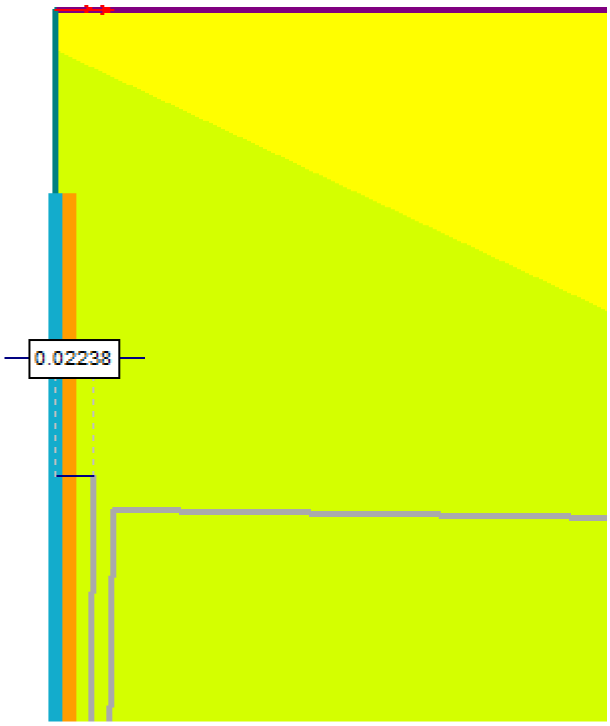

M 159.4: Detailed view of cross-section of retaining wall and soil (stage 3)

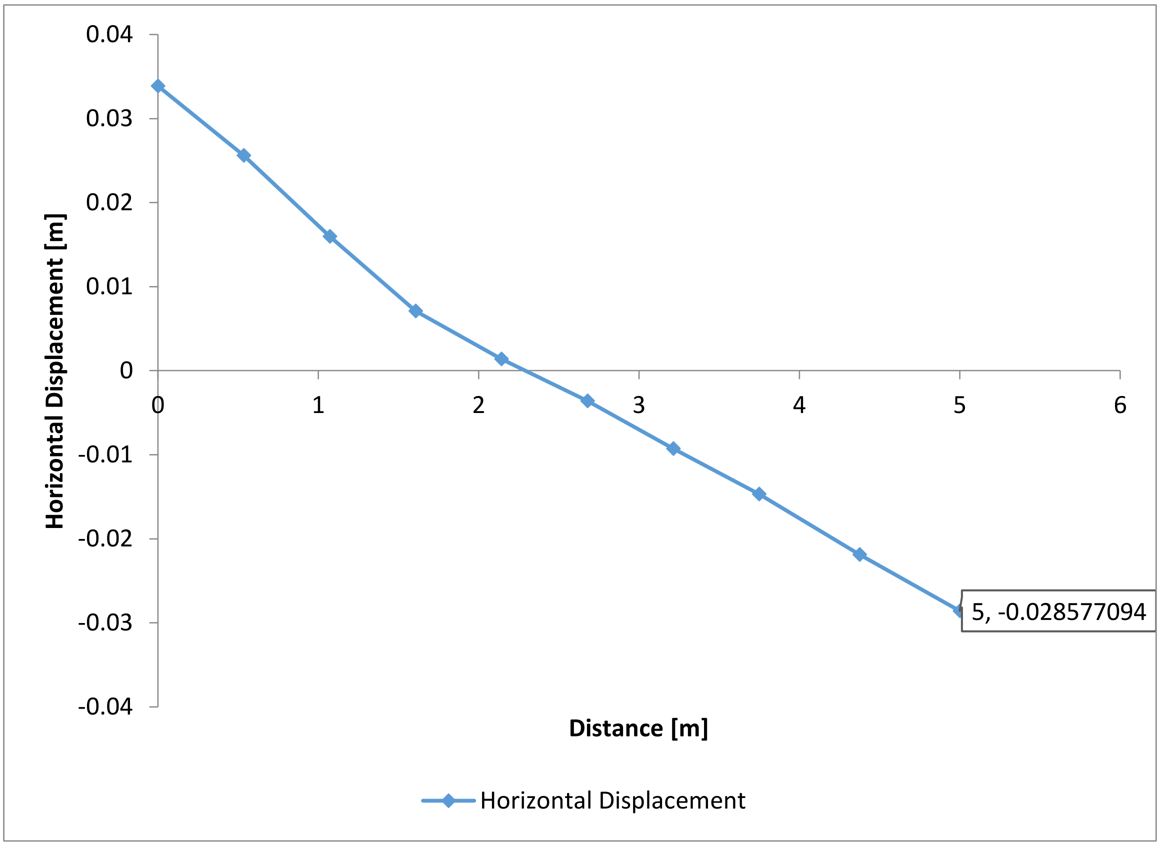

M 159.5: Horizontal displacement of soil along retaining wall

Retaining wall maximum horizontal displacement: -0.028577m

Distance from point of maximum displacement in retaining wall to the top of backfill soil: 5.0m

Model 160:

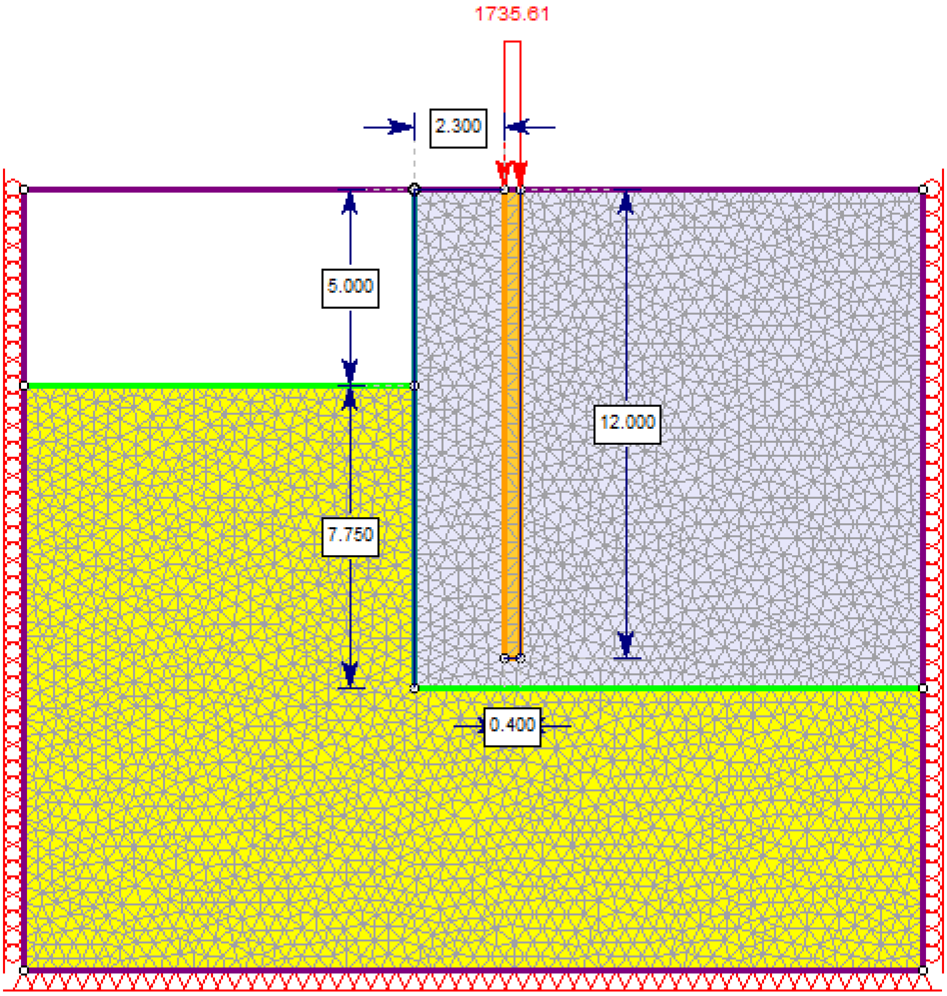

M 160.1: Original model (stage 3)

C'_1	ϕ'_1	γ_1	E_1	C'_2	ϕ'_2	γ_2	E_2	H_1	H_2	H_3	E_3	D_1	D_2	L	Qult
0	28	21	271	34	2	21	3.7	5.00	7.75	1.5	1106052	2.3	0.4	12	1735.61

M 160.2: Parameter values

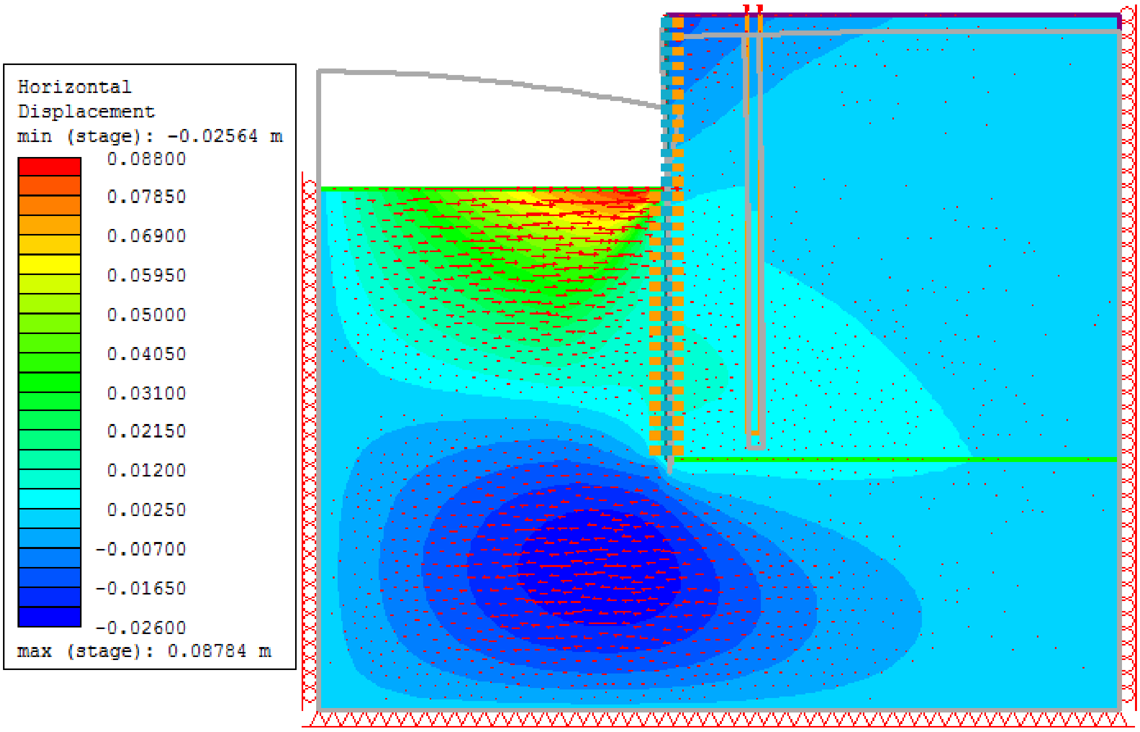

M 160.3: Deformed model (stage 3)

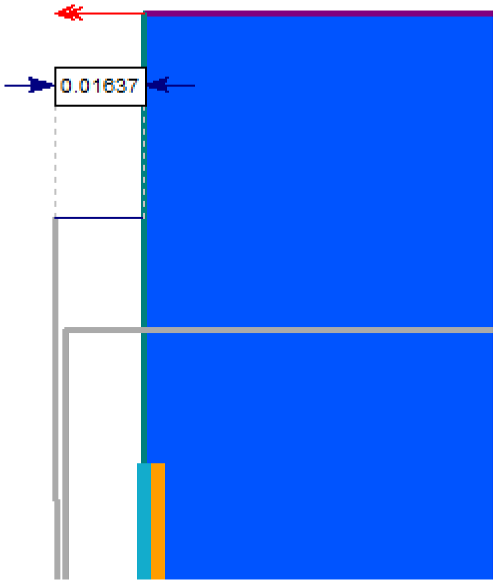

M 160.4: Detailed view of cross-section of retaining wall and soil (stage 3)

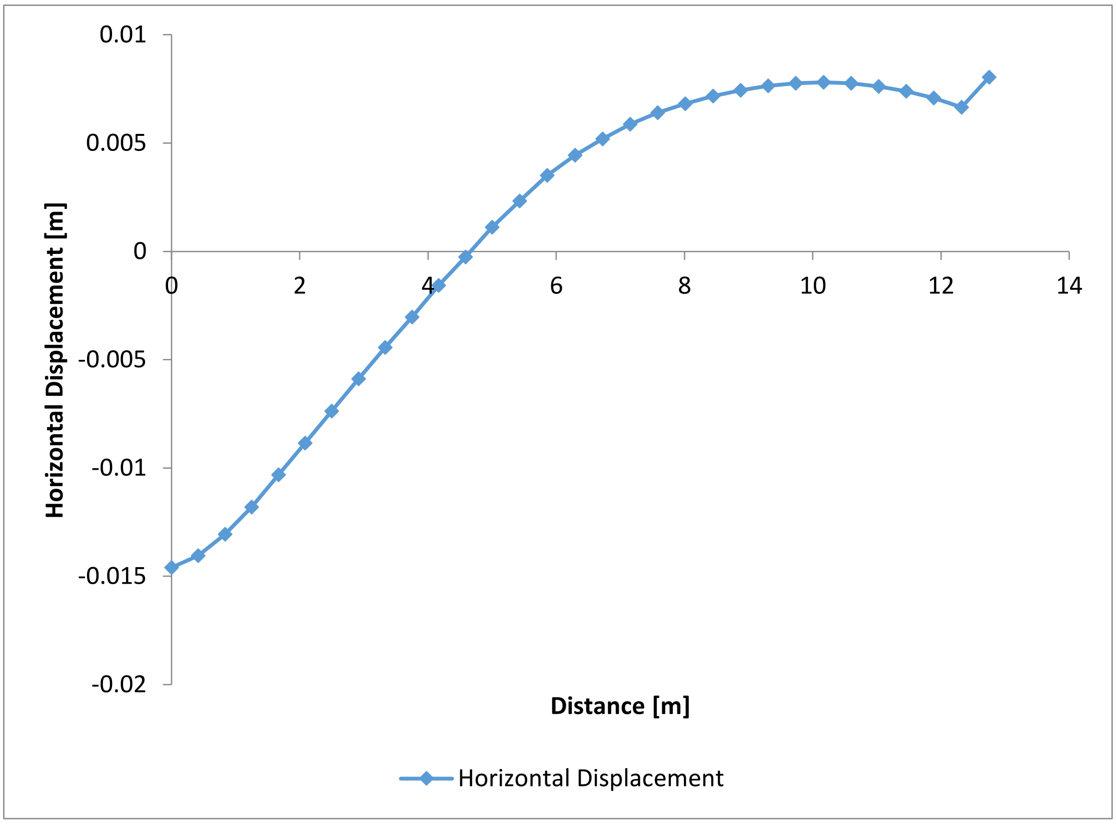

M 160.5: Horizontal displacement of soil along retaining wall

Retaining wall maximum horizontal displacement: -0.01637m

Distance from point of maximum displacement in retaining wall to the top of backfill soil: 0.0m

Model 161:

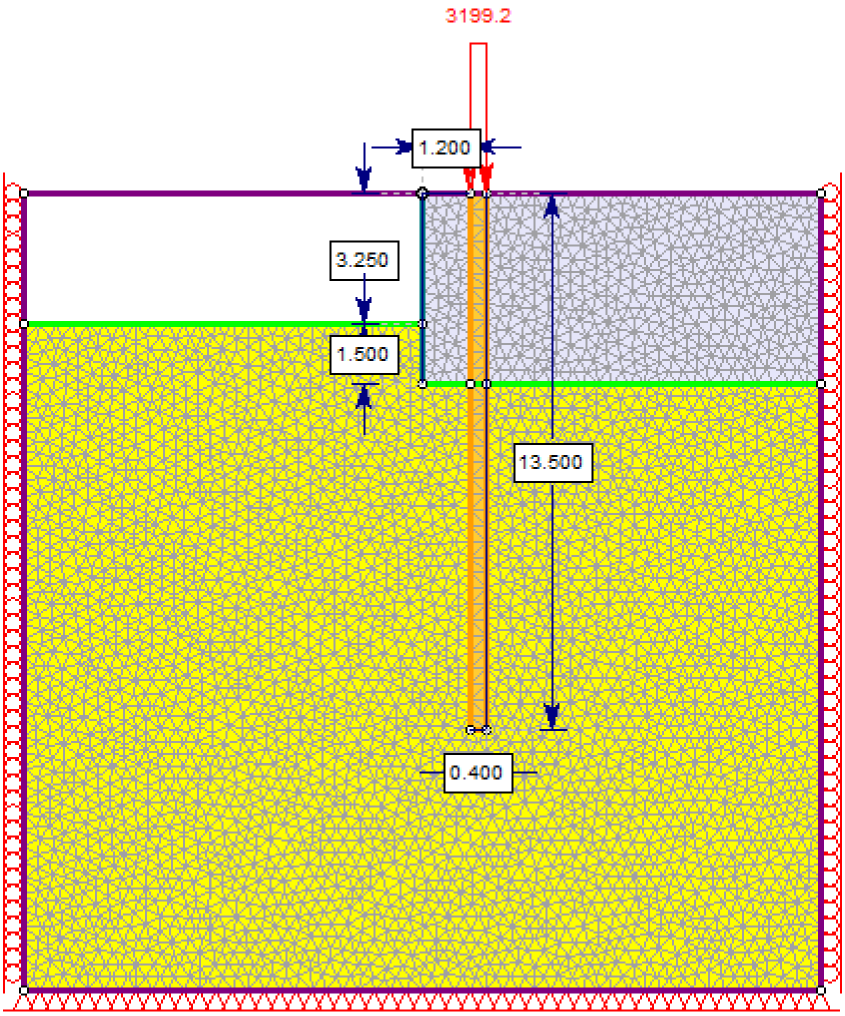

M 161.1: Original model (stage 3)

C_1'	ϕ_1'	γ_1	E_1	C_2'	ϕ_2'	γ_2	E_2	H_1	H_2	H_3	E_3	D_1	D_2	L	Qult
0	39	21	74	35	24	19	42.9	3.25	1.5	0.75	699916	1.2	0.4	13.5	3199.2

M 161.2: Parameter values

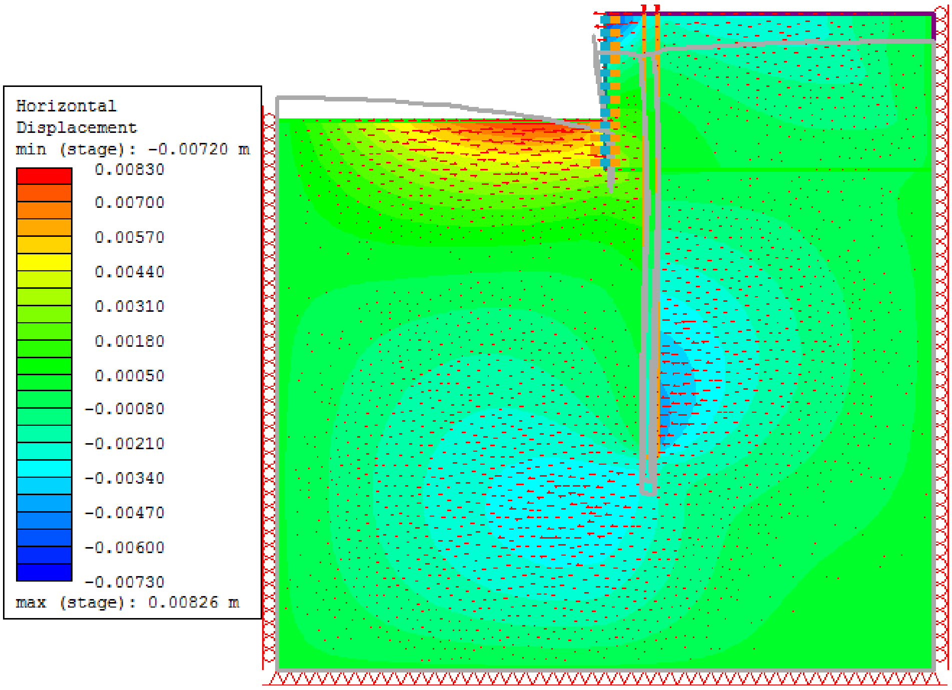

M 161.3: Deformed model (stage 3)

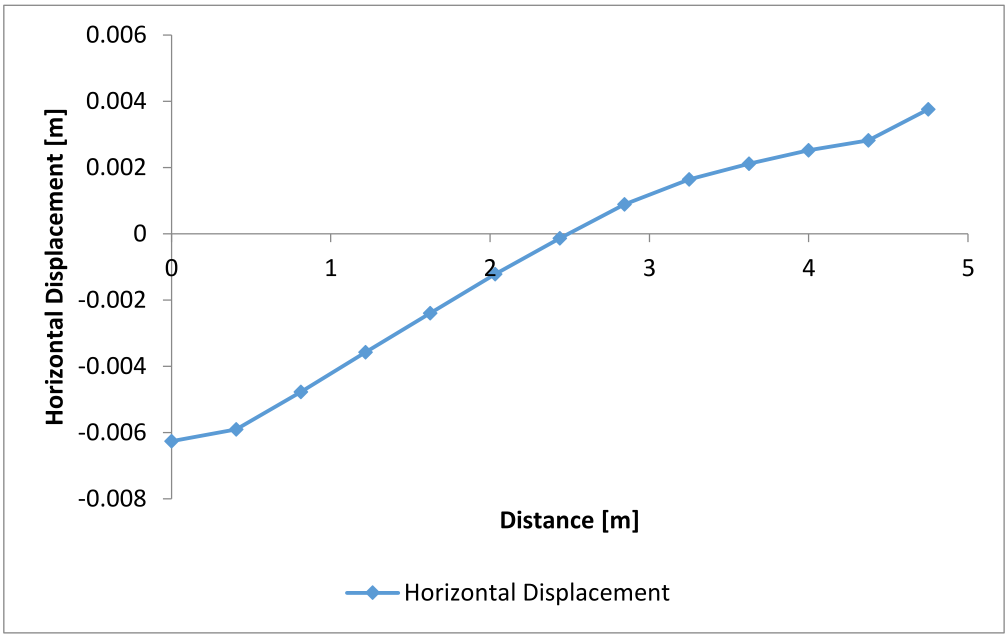

M 161.4: Horizontal displacement of soil along retaining wall

Retaining wall maximum horizontal displacement: -0.0072m

Distance from point of maximum displacement in retaining wall to the top of backfill soil: 0.0m

Model 162:

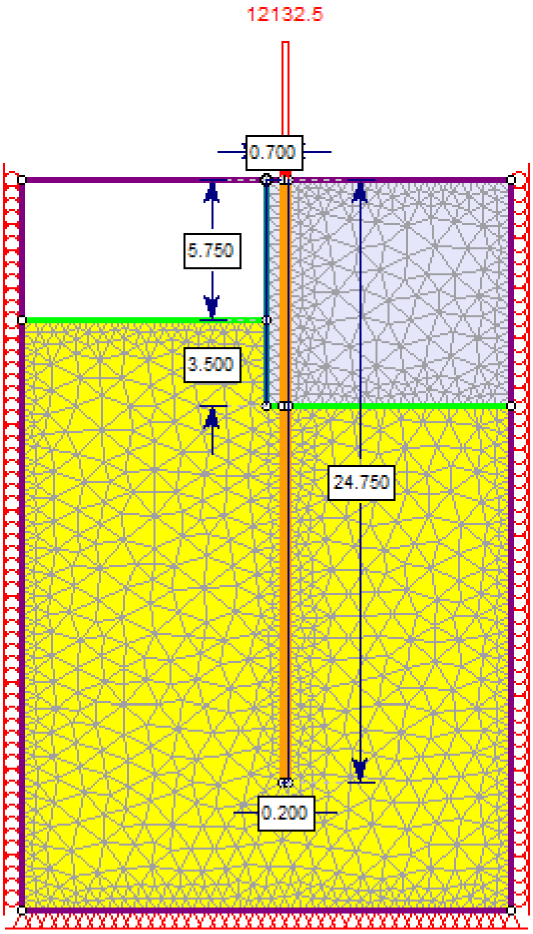

M 162.1: Original model (stage 3)

C_1'	ϕ_1'	γ_1	E_1	C_2'	ϕ_2'	γ_2	E_2	H_1	H_2	H_3	E_3	D_1	D_2	L	Qult
0	33	18	229	49	28	24	38.7	5.75	3.5	1.5	698011	0.7	0.2	24.75	12132.5

M 162.2: Parameter values

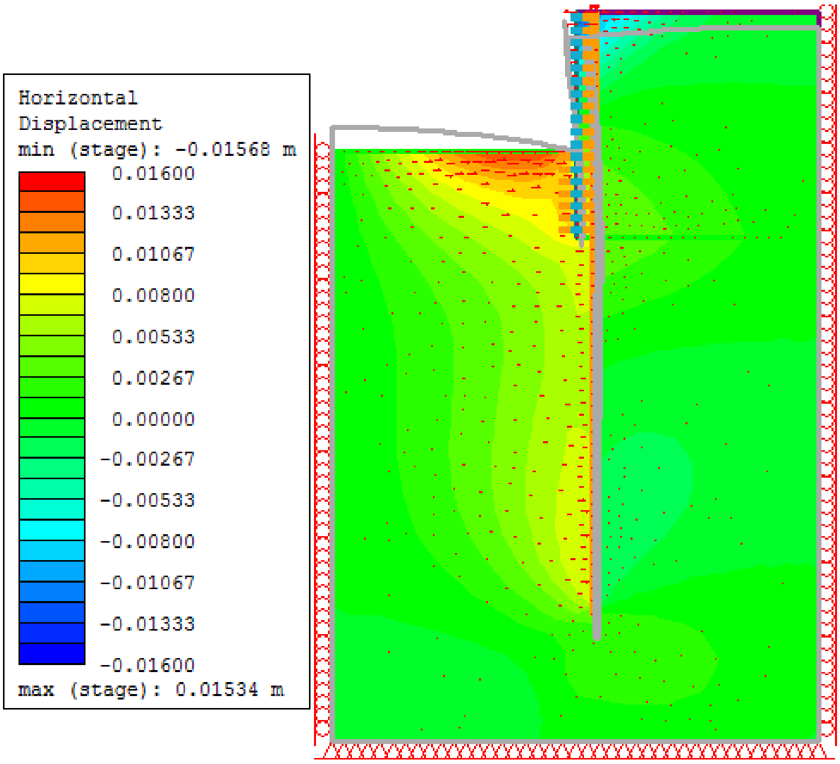

M 162.3: Deformed model (stage 3)

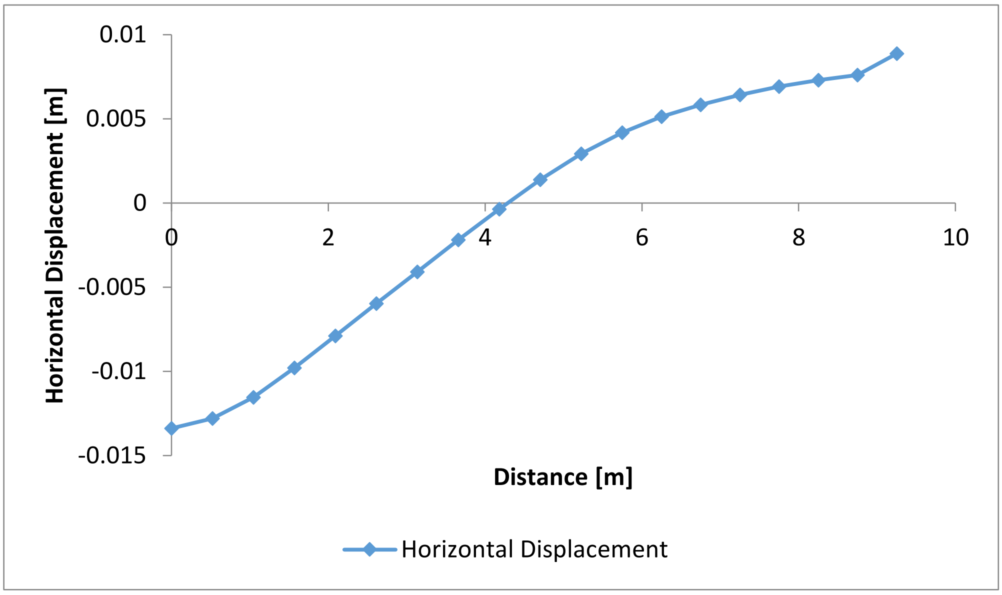

M 162.4: Horizontal displacement of soil along retaining wall

Retaining wall maximum horizontal displacement: -0.01568m

Distance from point of maximum displacement in retaining wall to the top of backfill soil: 0.0m

Model 163:

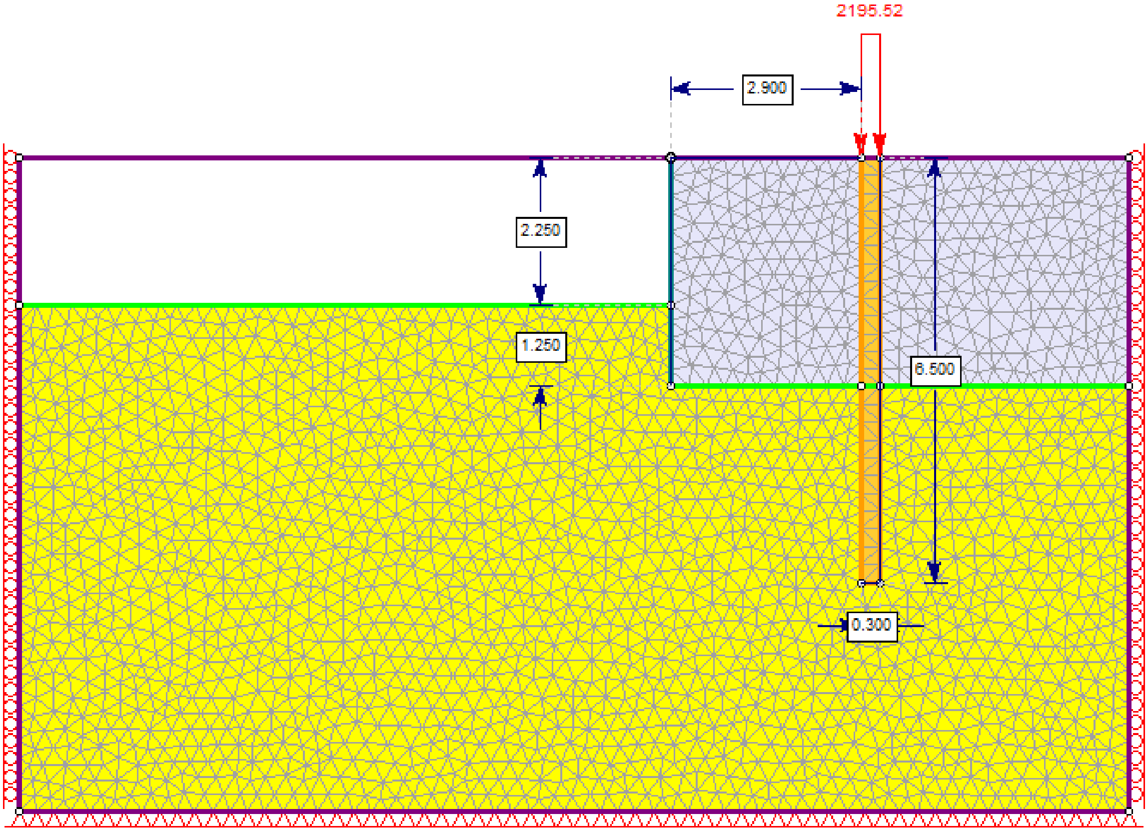

M 163.1: Original model (stage 3)

C_1'	ϕ_1'	γ_1	E_1	C_2'	ϕ_2'	γ_2	E_2	H_1	H_2	H_3	E_3	D_1	D_2	L	Qult
0	33	21	216	25	25	22	14.8	2.25	1.25	1	693943	2.9	0.3	6.5	2195.52

M 163.2: Parameter values

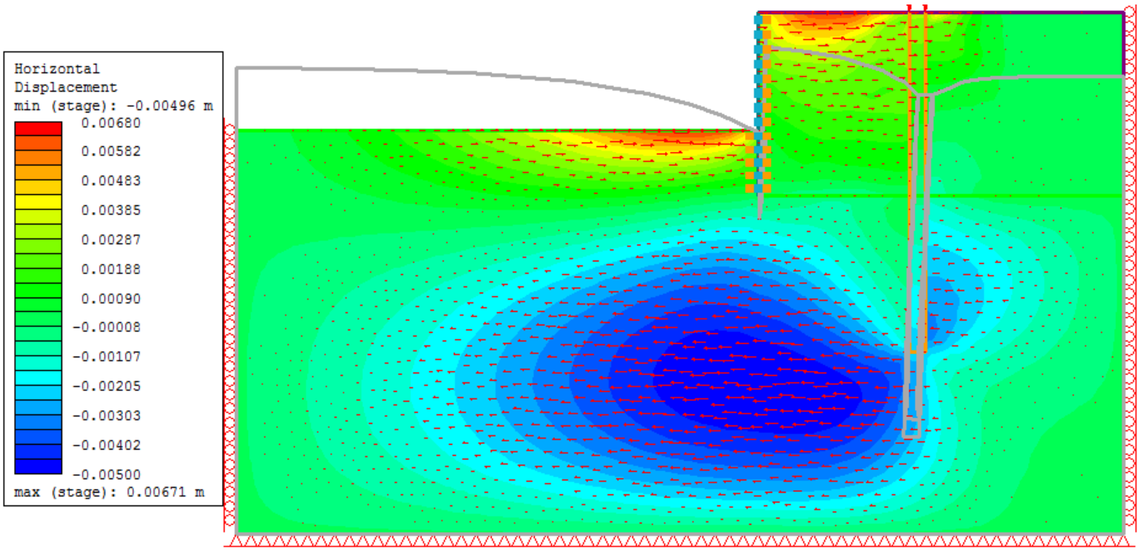

M 163.3: Deformed model (stage 3)

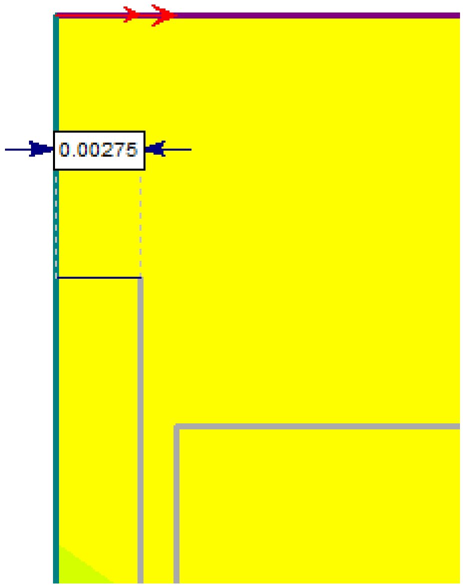

M 163.4: Detailed view of cross-section of retaining wall and soil (stage 3)

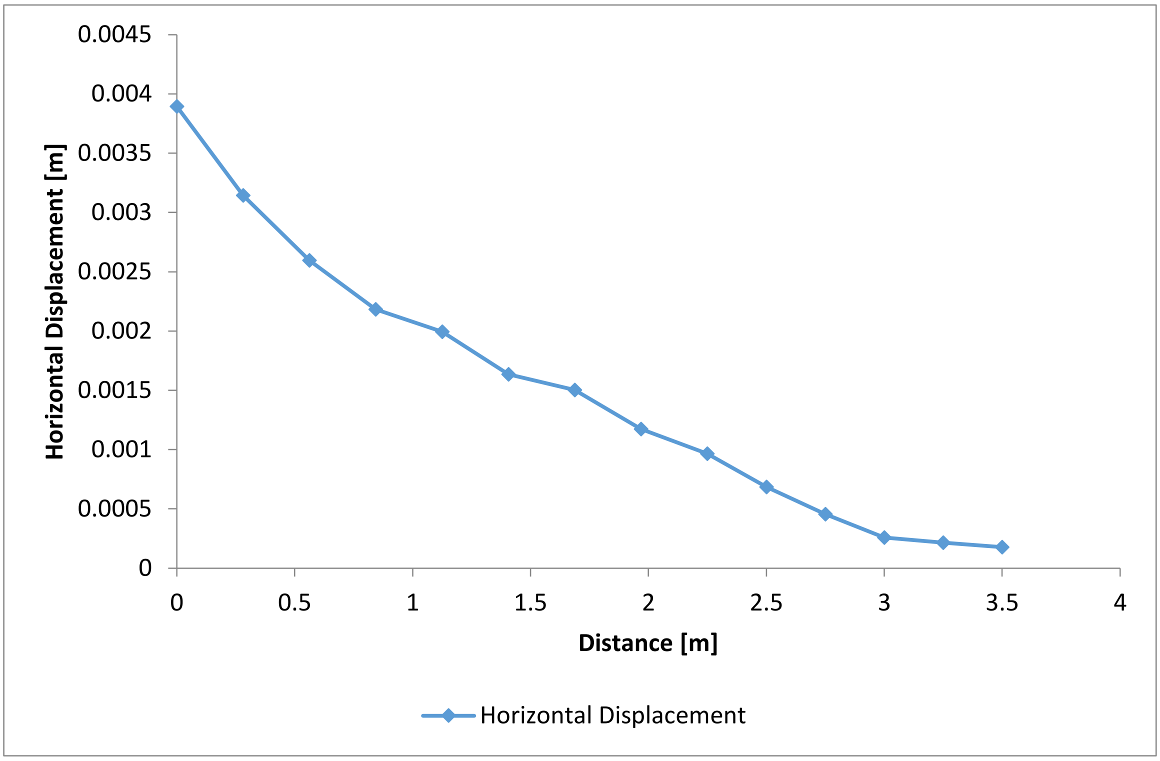

M 163.5: Horizontal displacement of soil along retaining wall

Retaining wall maximum horizontal displacement: 0.00275m

Distance from point of maximum displacement in retaining wall to the top of backfill soil: 0.0m

Model 164:

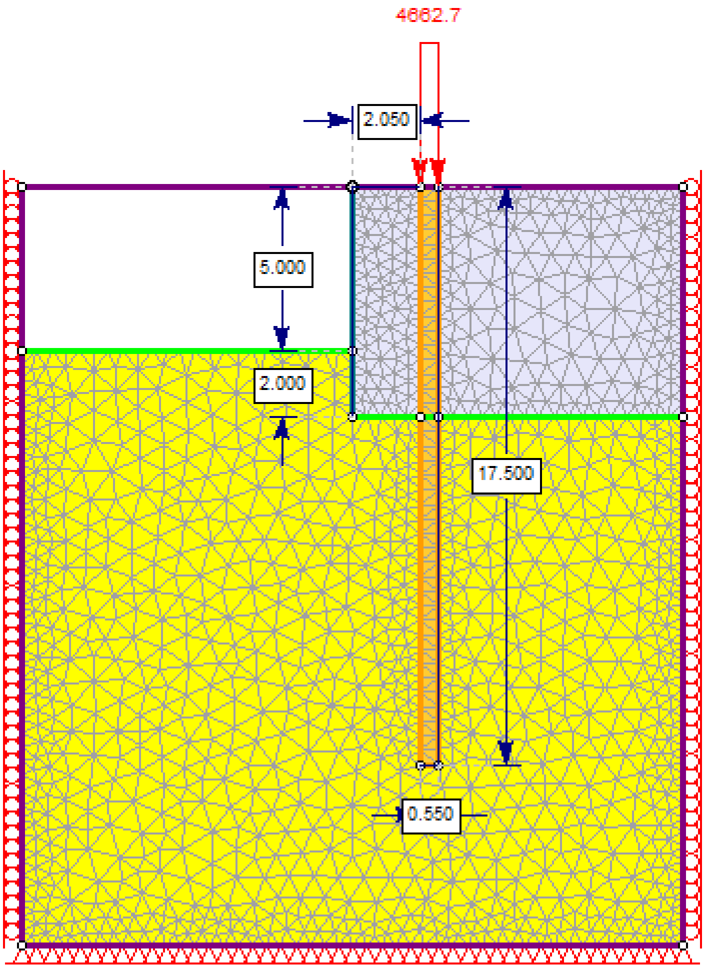

M 164.1: Original model (stage 3)

C_1'	ϕ_1'	γ_1	E_1	C_2'	ϕ_2'	γ_2	E_2	H_1	H_2	H_3	E_3	D_1	D_2	L	Qult
0	44	20	191	51	24	22	45.5	5.00	2	1	975094	2.05	0.55	17.5	4662.7

M 164.2: Parameter values

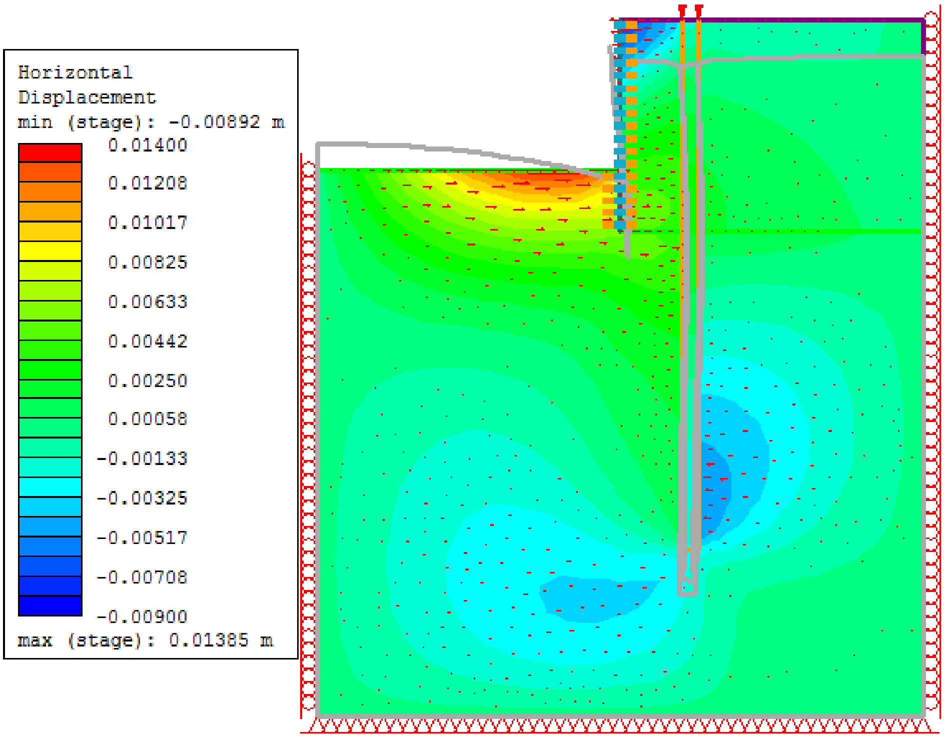

M 164.3: Detailed view of cross-section of retaining wall and soil (stage 3)

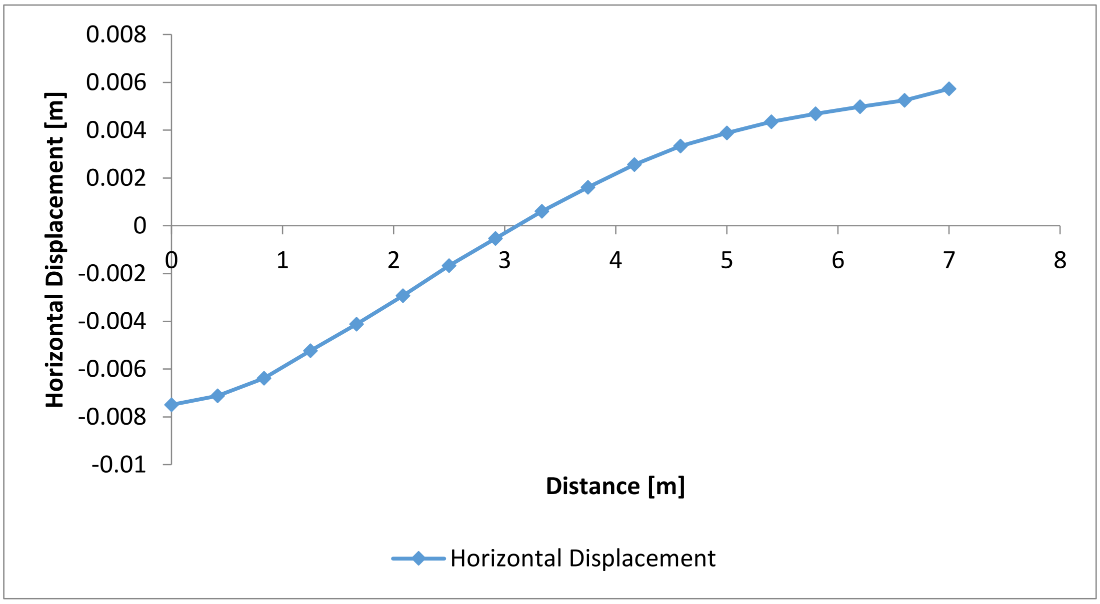

M 164.4: Horizontal displacement of soil along retaining wall

Retaining wall maximum horizontal displacement: -0.0892m

Distance from point of maximum displacement in retaining wall to the top of backfill soil: 0.0m

Model 165:

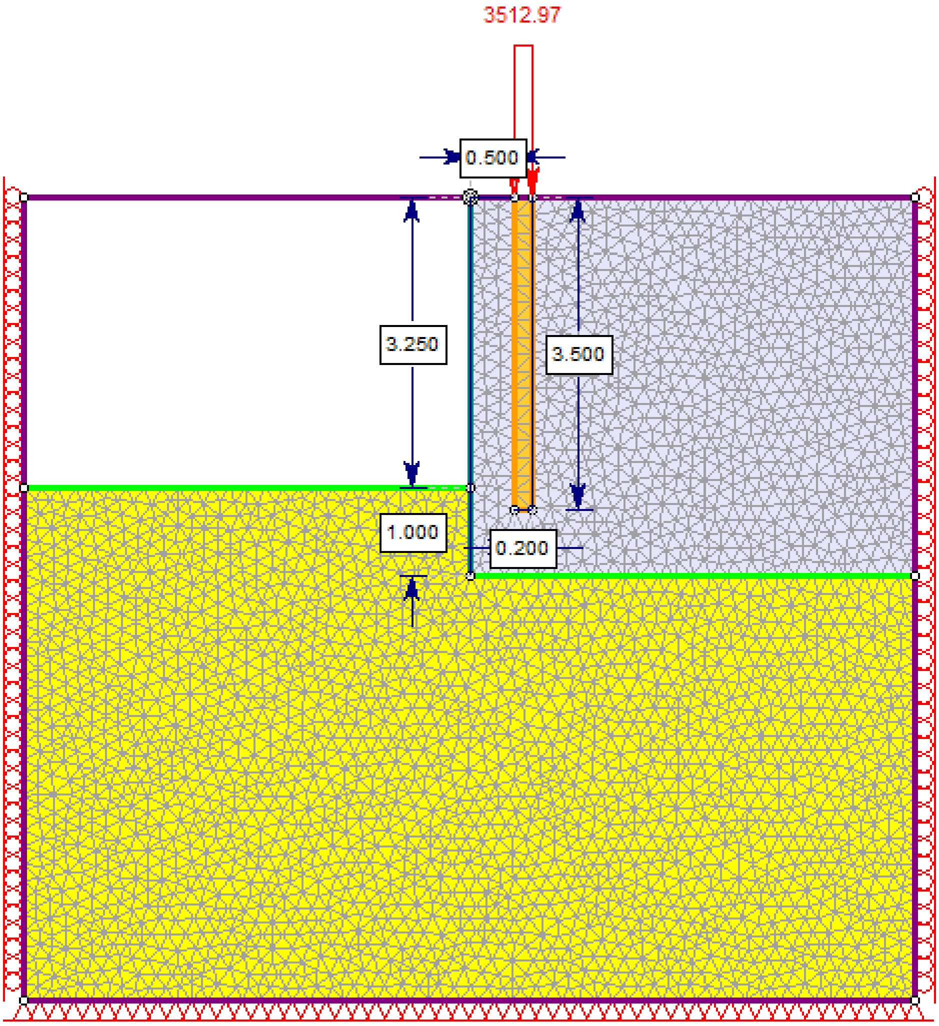

M 165.1: Original model (stage 3)

C_1'	ϕ_1'	γ_1	E_1	C_2'	ϕ_2'	γ_2	E_2	H_1	H_2	H_3	E_3	D_1	D_2	L	Qult
0	37	19	15	52	31	20	29.7	3.25	1	0.75	827263	0.5	0.2	3.5	3512.97

M 165.2: Parameter values

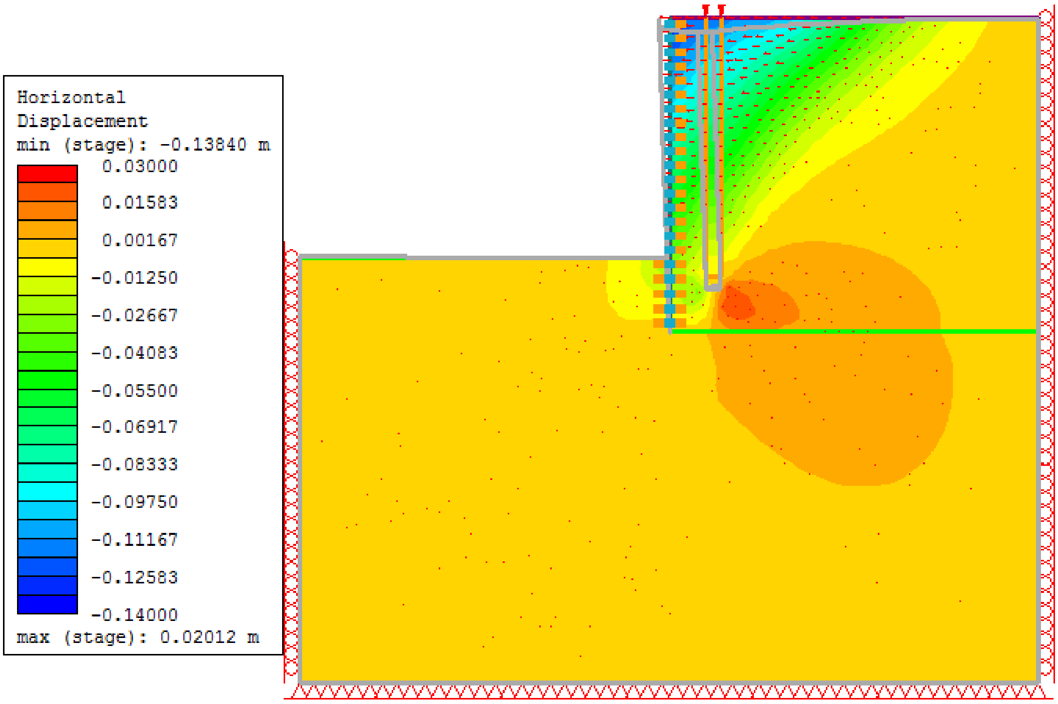

M 165.3: Deformed model (stage 3)

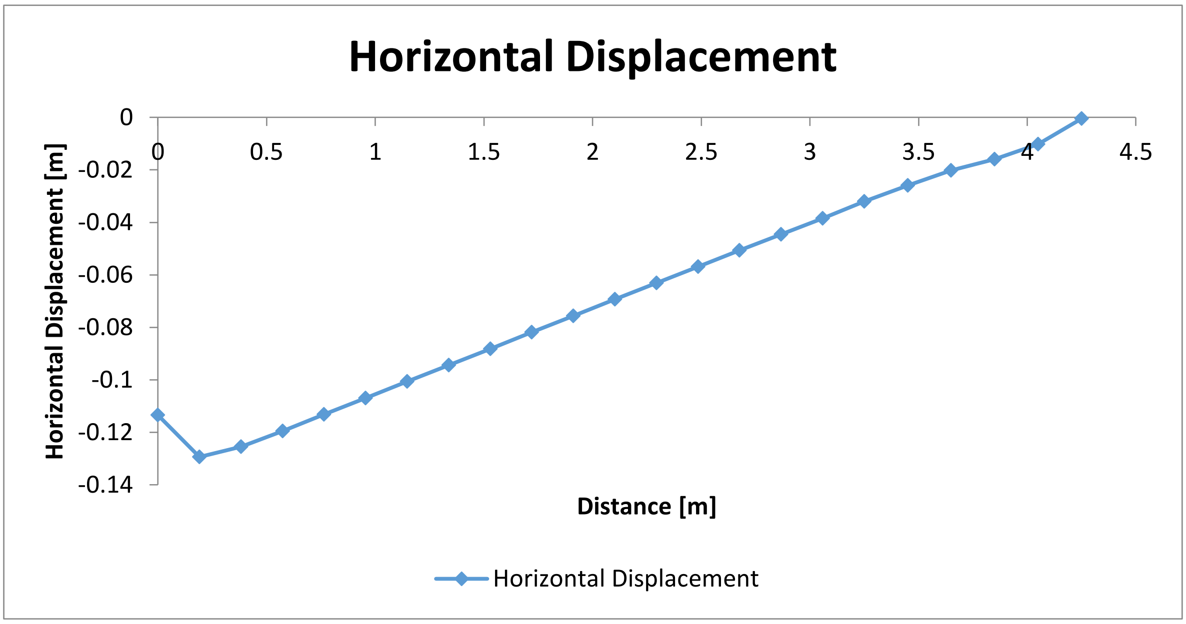

M 165.4: Horizontal displacement of soil along retaining wall

Retaining wall maximum horizontal displacement: -0.1384m

Distance from point of maximum displacement in retaining wall to the top of backfill soil: 0.0m

Model 166:

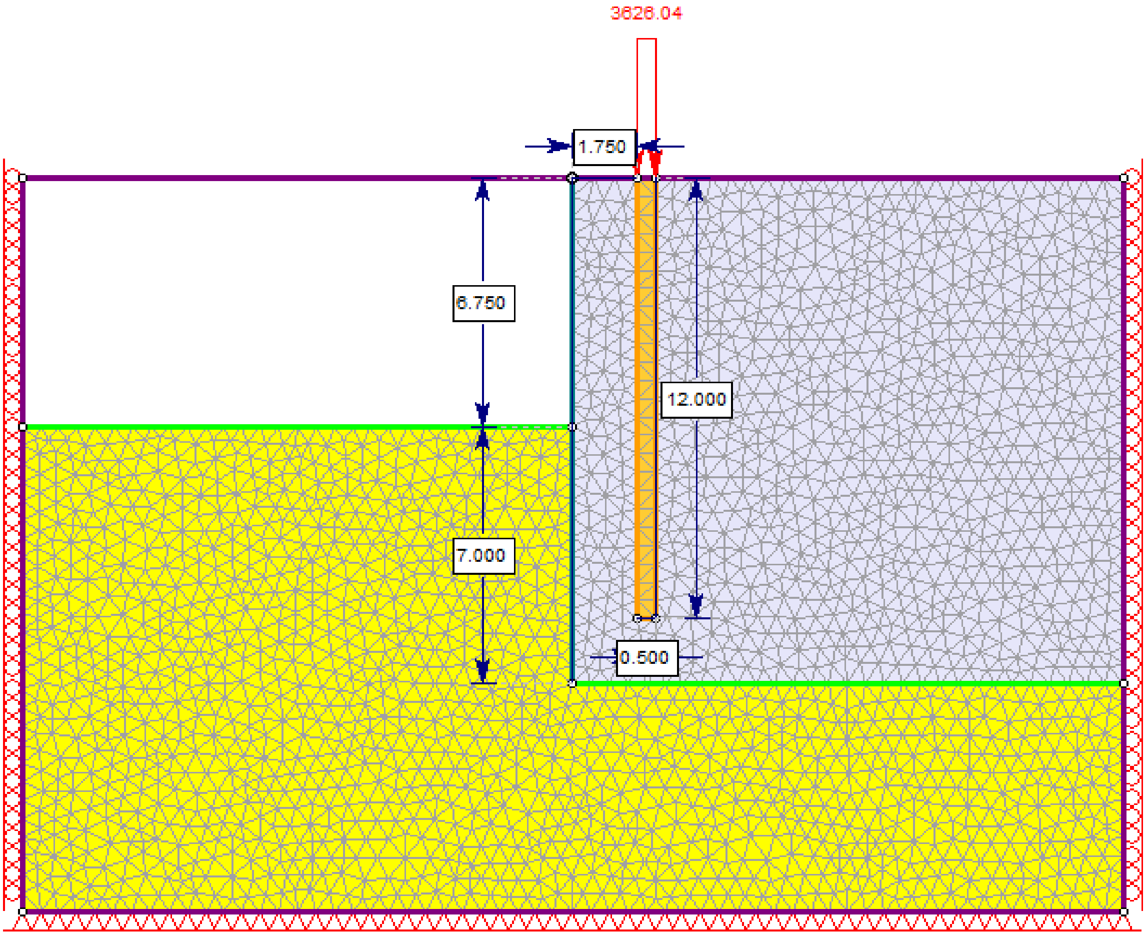

M 166.1: Original model (stage 3)

C_1'	ϕ_1'	γ_1	E_1	C_2'	ϕ_2'	γ_2	E_2	H_1	H_2	H_3	E_3	D_1	D_2	L	Qult
0	31	21	264	51	24	25	44.3	6.75	7	1.25	958596	1.75	0.5	12	3626.04

M 166.2: Parameter values

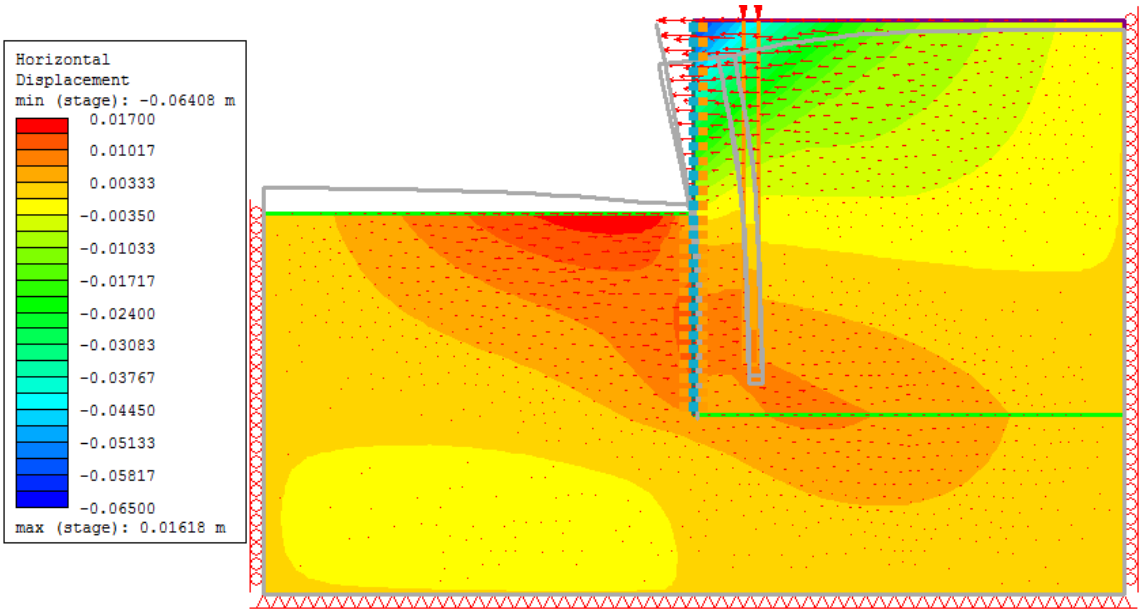

M 166.3: Deformed model (stage 3)

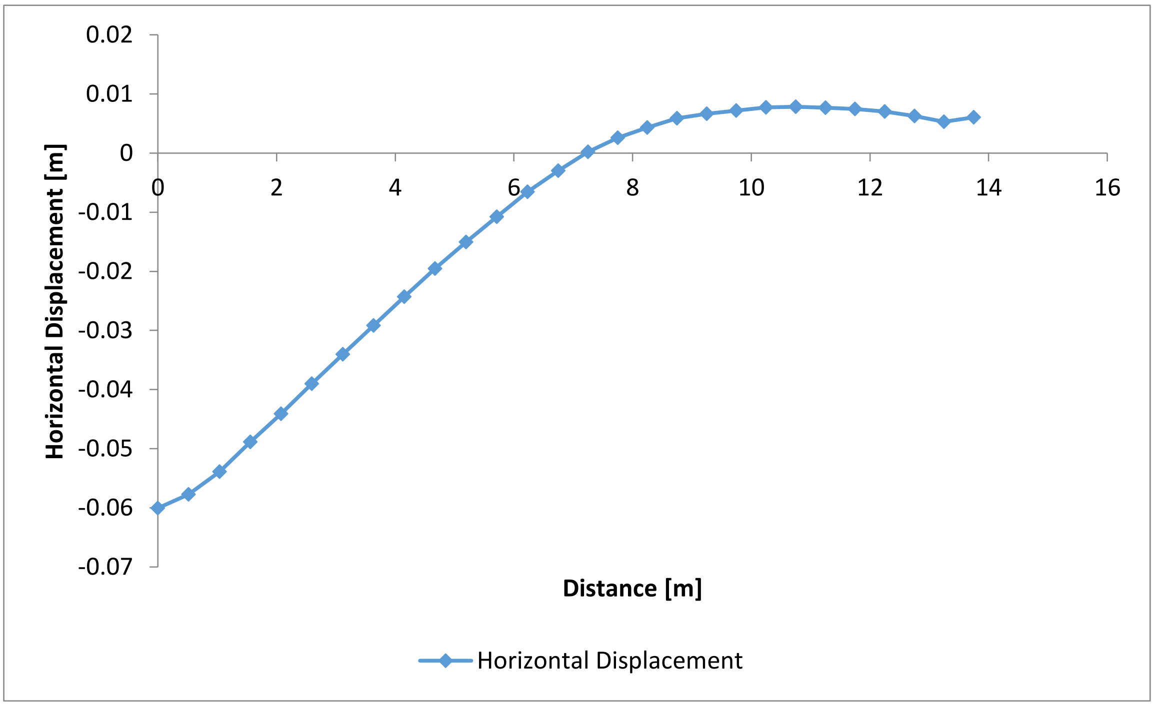

M 166.4: Horizontal displacement of soil along retaining wall

Retaining wall maximum horizontal displacement: -0.06408m

Distance from point of maximum displacement in retaining wall to the top of backfill soil: 0.0m

Model 167:

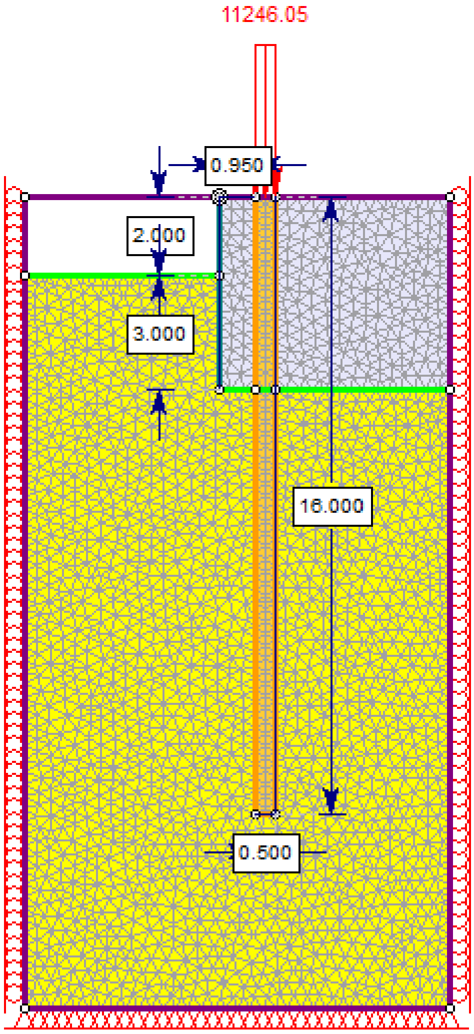

M 167.1: Original model (stage 3)

C_1'	ϕ_1'	γ_1	E_1	C_2'	ϕ_2'	γ_2	E_2	H_1	H_2	H_3	E_3	D_1	D_2	L	Qult
0	34	22	82	14	11	19	12.4	2.00	3	0.5	897833	0.95	0.5	16	1246.05

M 167.2: Parameter values

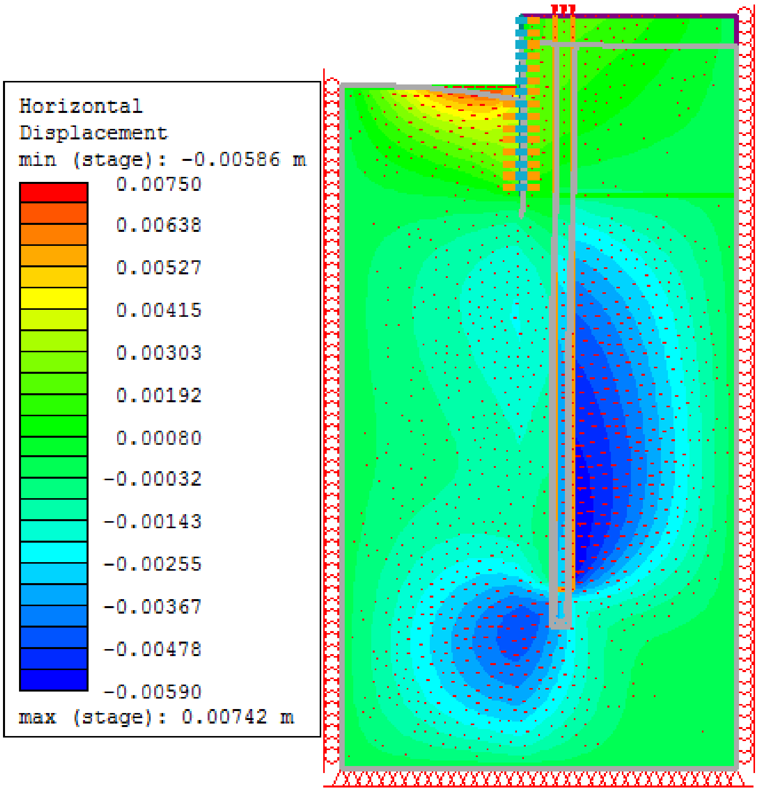

M 167.3: Deformed model (stage 3)

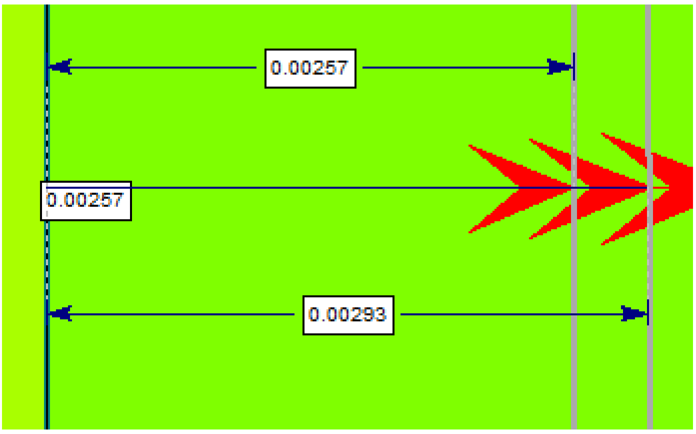

M 167.4: Detailed view of cross-section of retaining wall and soil (stage 3)

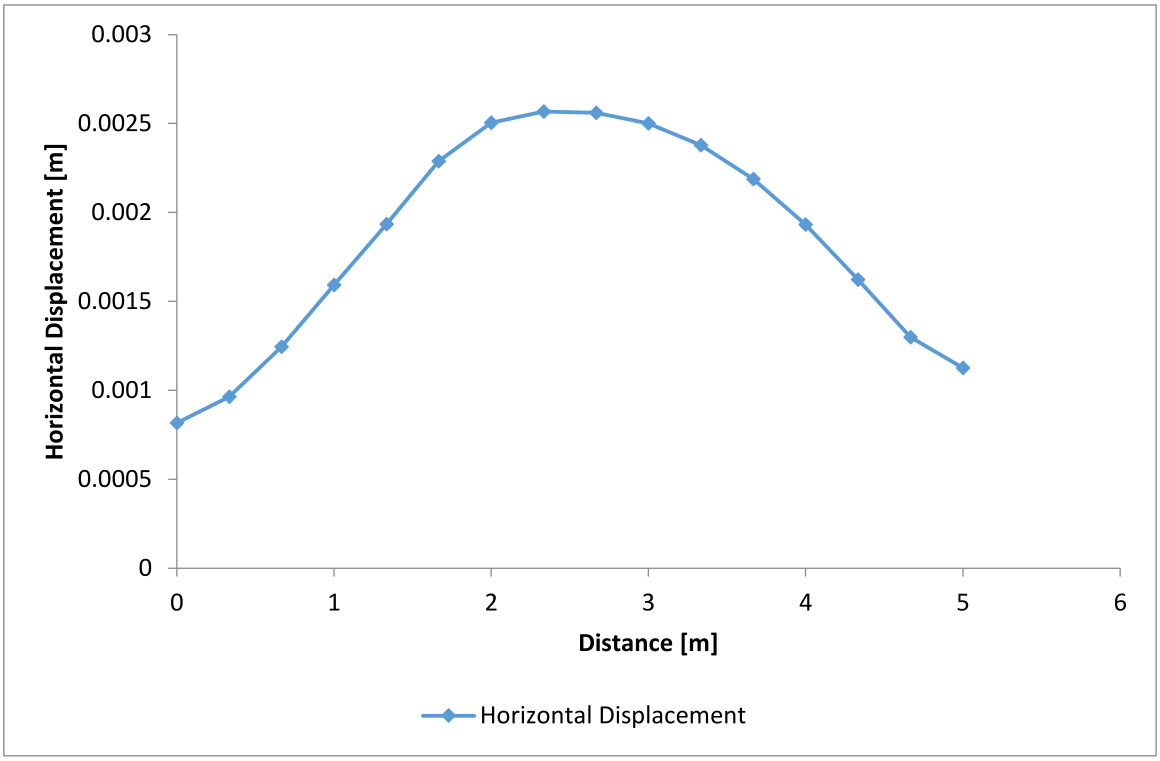

M 167.5: Horizontal displacement of soil along retaining wall

Retaining wall maximum horizontal displacement: 0.00293m

Distance from point of maximum displacement in retaining wall to the top of backfill soil: 2.33m

Model 168:

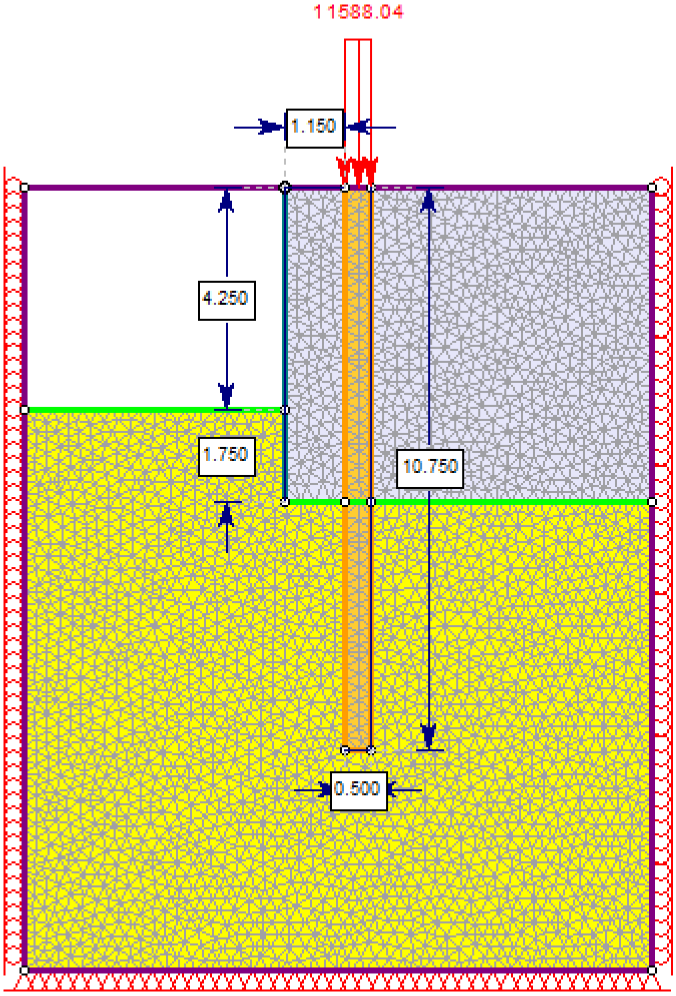

M 168.1: Original model (stage 3)

C'_1	ϕ'_1	γ_1	E_1	C'_2	ϕ'_2	γ_2	E_2	H_1	H_2	H_3	E_3	D_1	D_2	L	Qult
0	36	18	156	50	18	18	17.5	4.25	1.75	0.75	1107442	1.15	0.5	10.75	1588.04

M 168.2: Parameter values

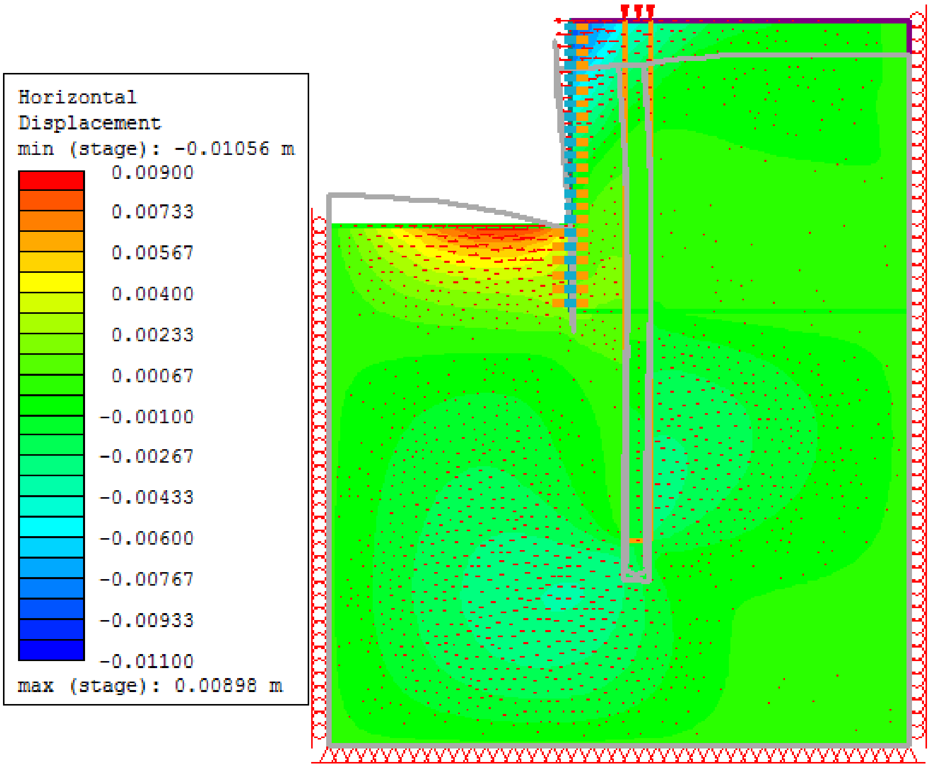

M 168.3: Deformed model (stage 3)

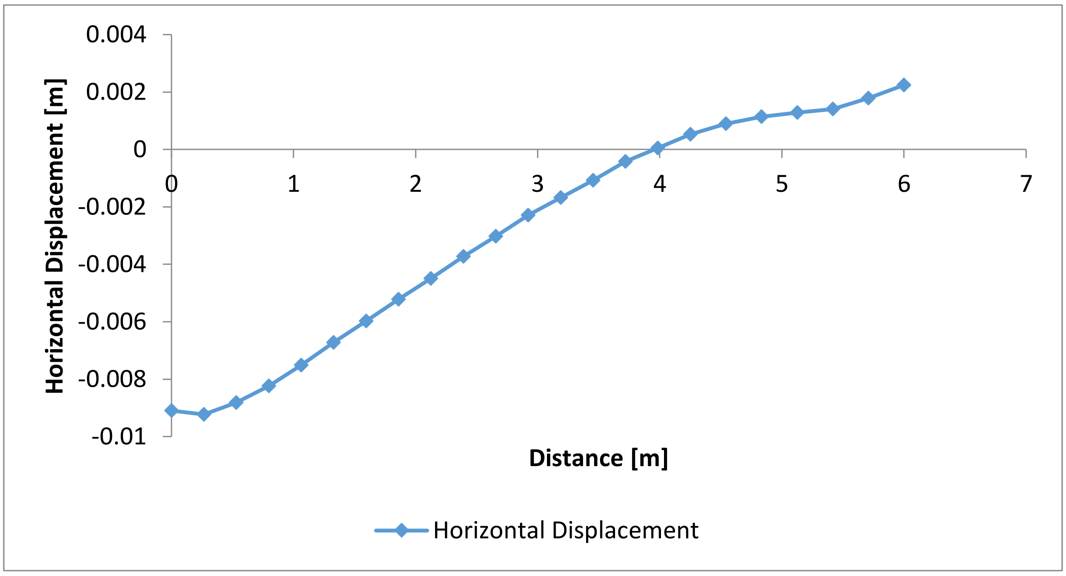

M 168.4: Horizontal displacement of soil along retaining wall

Retaining wall maximum horizontal displacement: -0.01056m

Distance from point of maximum displacement in retaining wall to the top of backfill soil: 0.0m

Model 169:

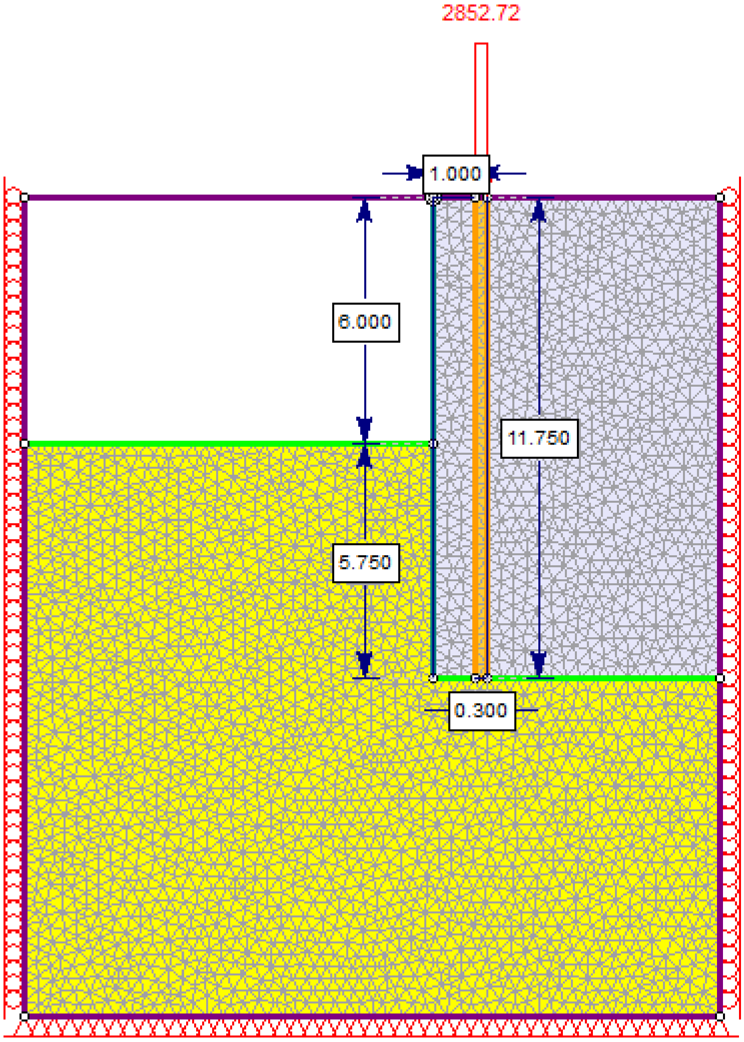

M 169.1: Original model (stage 3)

C_1'	ϕ_1'	γ_1	E_1	C_2'	ϕ_2'	γ_2	E_2	H_1	H_2	H_3	E_3	D_1	D_2	L	Qult
0	37	22	26	46	16	25	47.8	6.00	5.75	0.75	1080558	1	0.3	11.75	2852.72

M 169.2: Parameter values

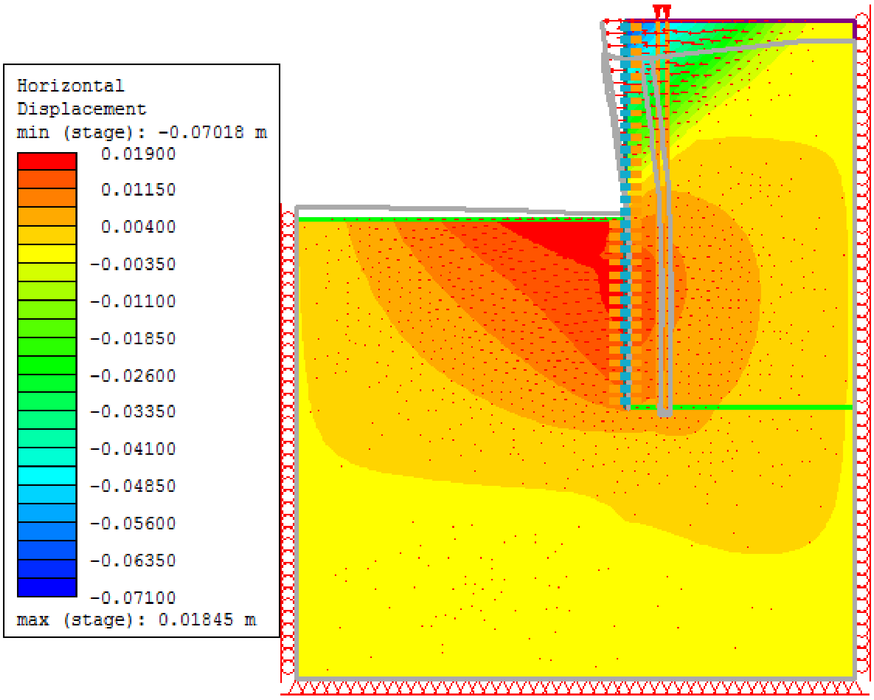

M 169.3: Deformed model (stage 3)

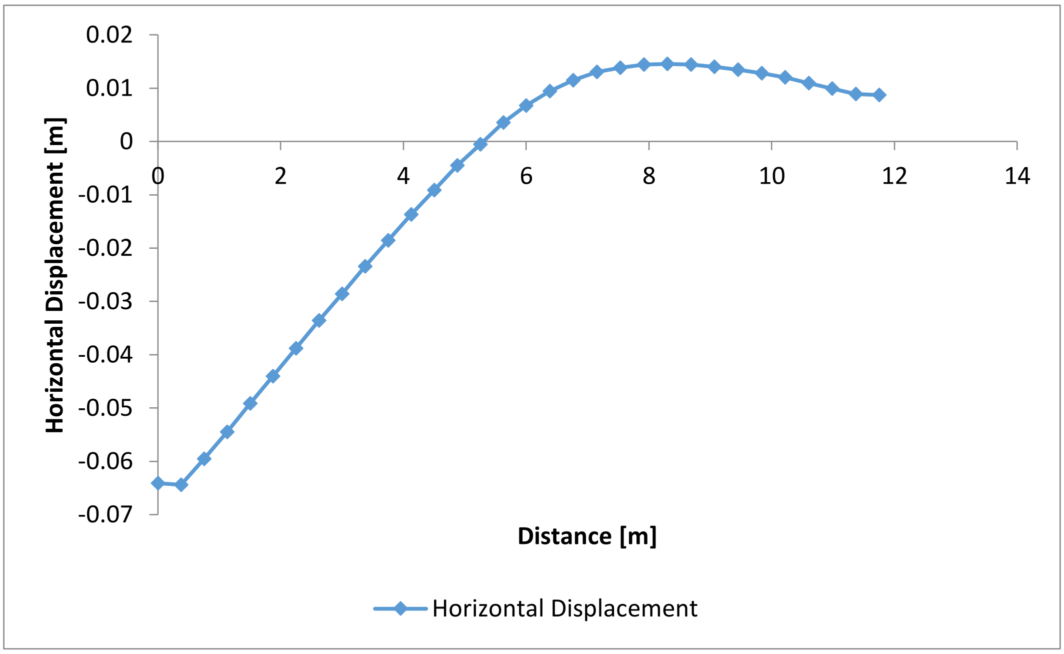

M 169.4: Horizontal displacement of soil along retaining wall

Retaining wall maximum horizontal displacement: -0.07018m

Distance from point of maximum displacement in retaining wall to the top of backfill soil: 0.0m

Model 170:

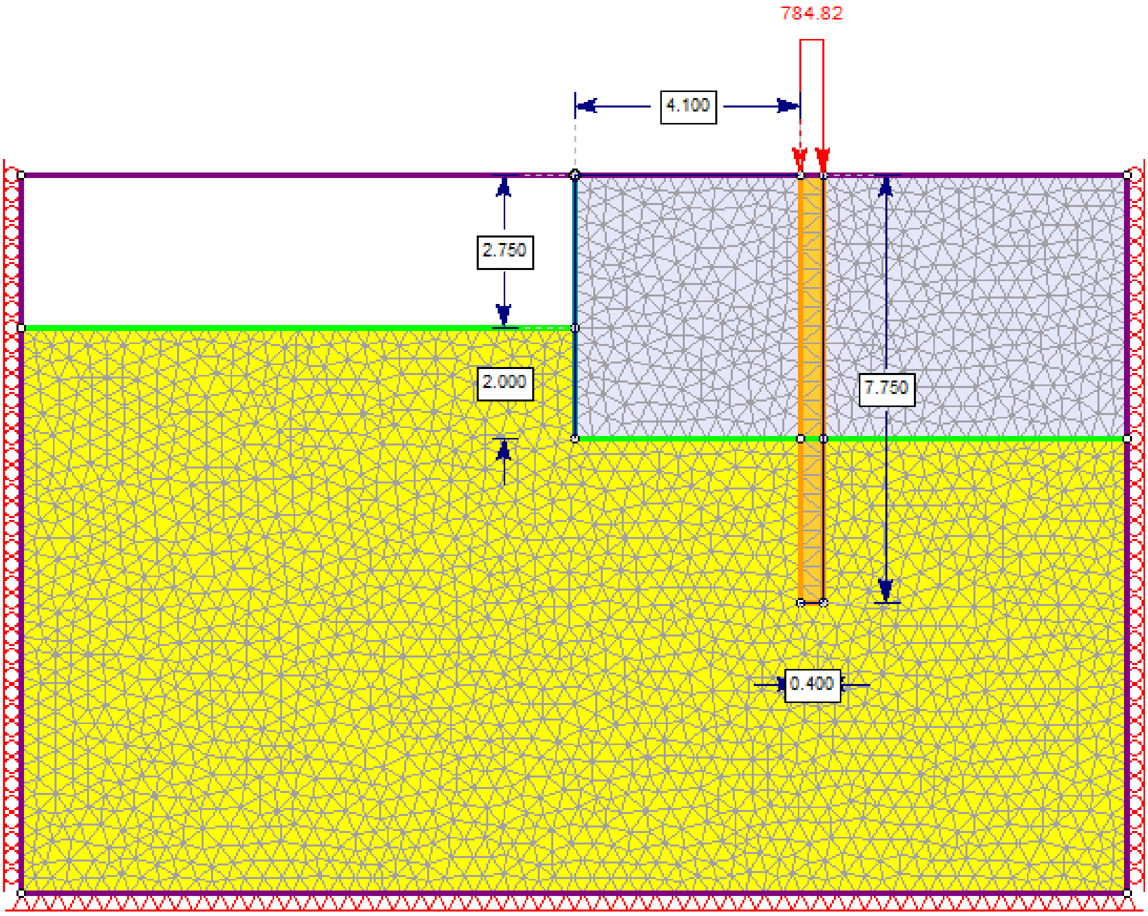

M 170.1: Original model (stage 3)

C_1'	ϕ_1'	γ_1	E_1	C_2'	ϕ_2'	γ_2	E_2	H_1	H_2	H_3	E_3	D_1	D_2	L	Qult
0	34	18	223	21	15	16	42.9	2.75	2	0.75	797415	4.1	0.4	7.75	784.82

M 170.2: Parameter values

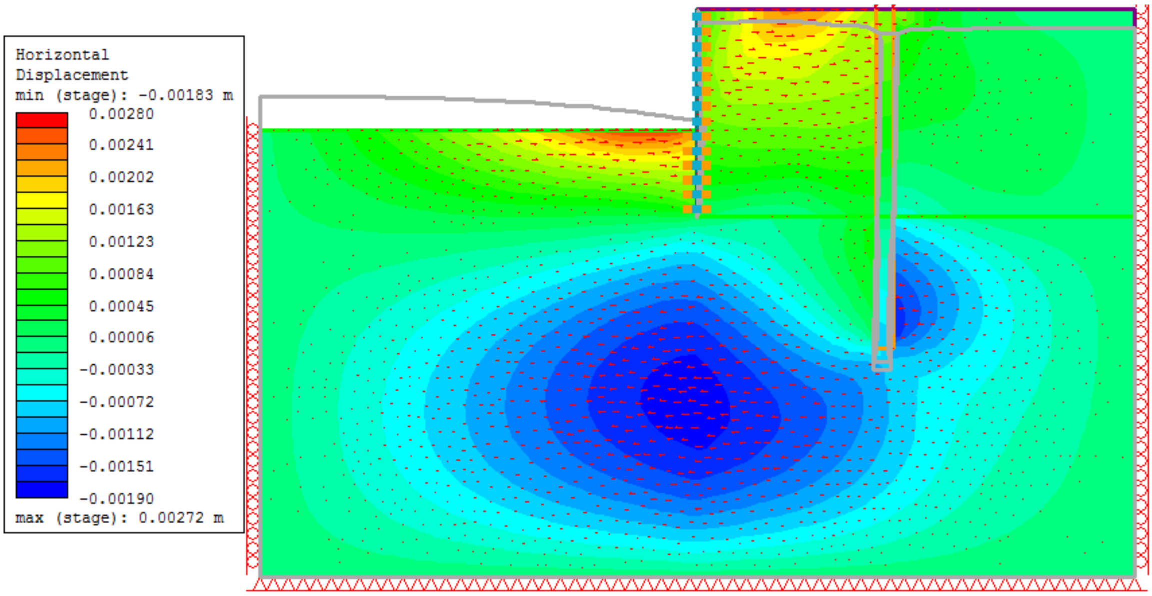

M 170.3: Deformed model (stage 3)

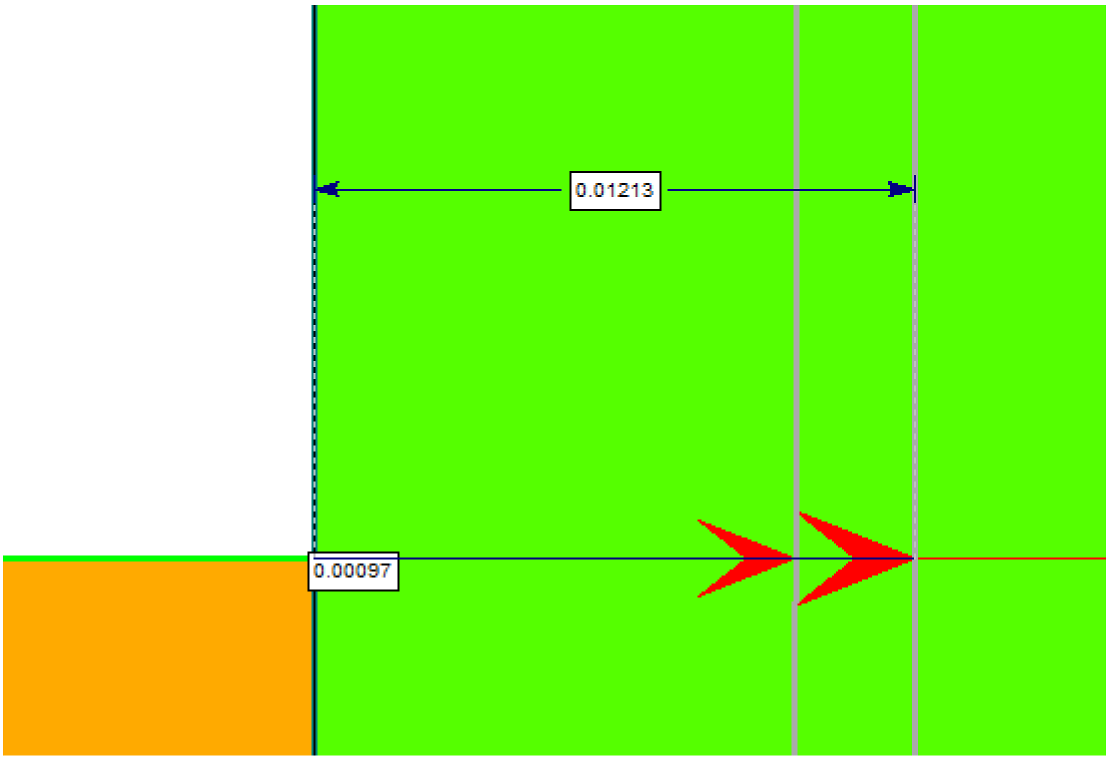

M 170.4: Detailed view of cross-section of retaining wall and soil (stage 3)

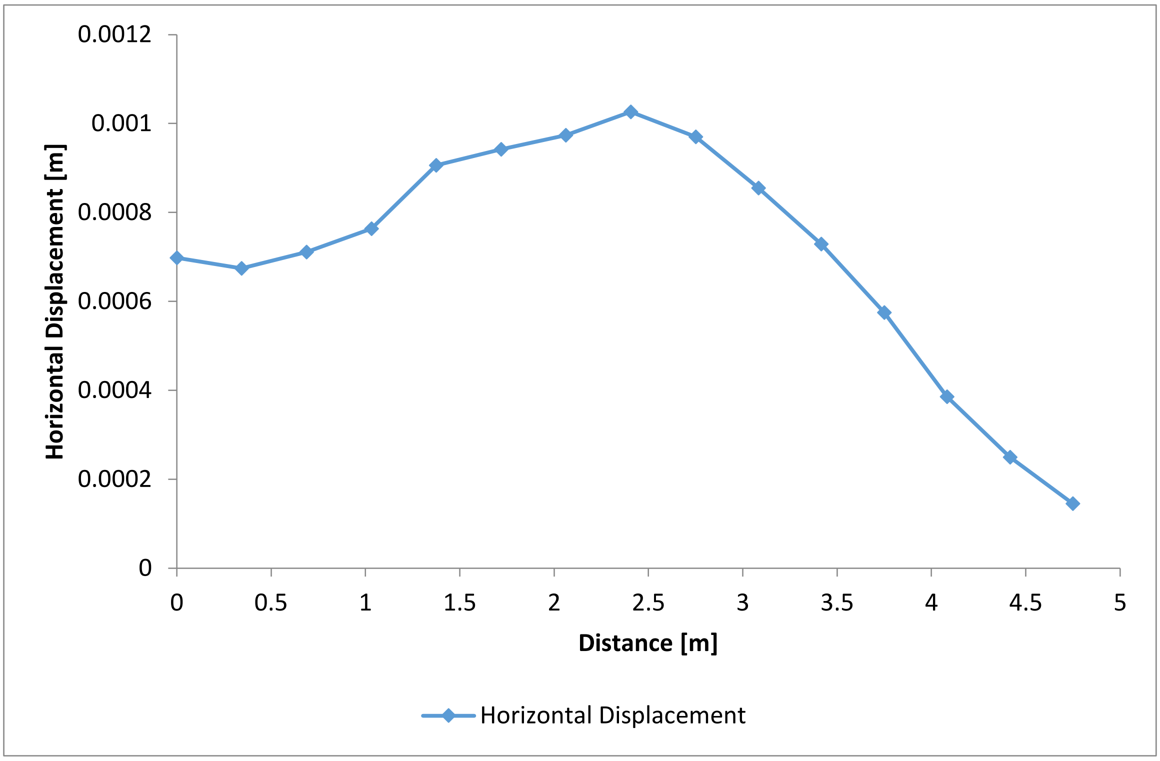

M 170.5: Horizontal displacement of soil along retaining wall

Retaining wall maximum horizontal displacement: 0.01213m

Distance from point of maximum displacement in retaining wall to the top of backfill soil: 2.75m

Model 171:

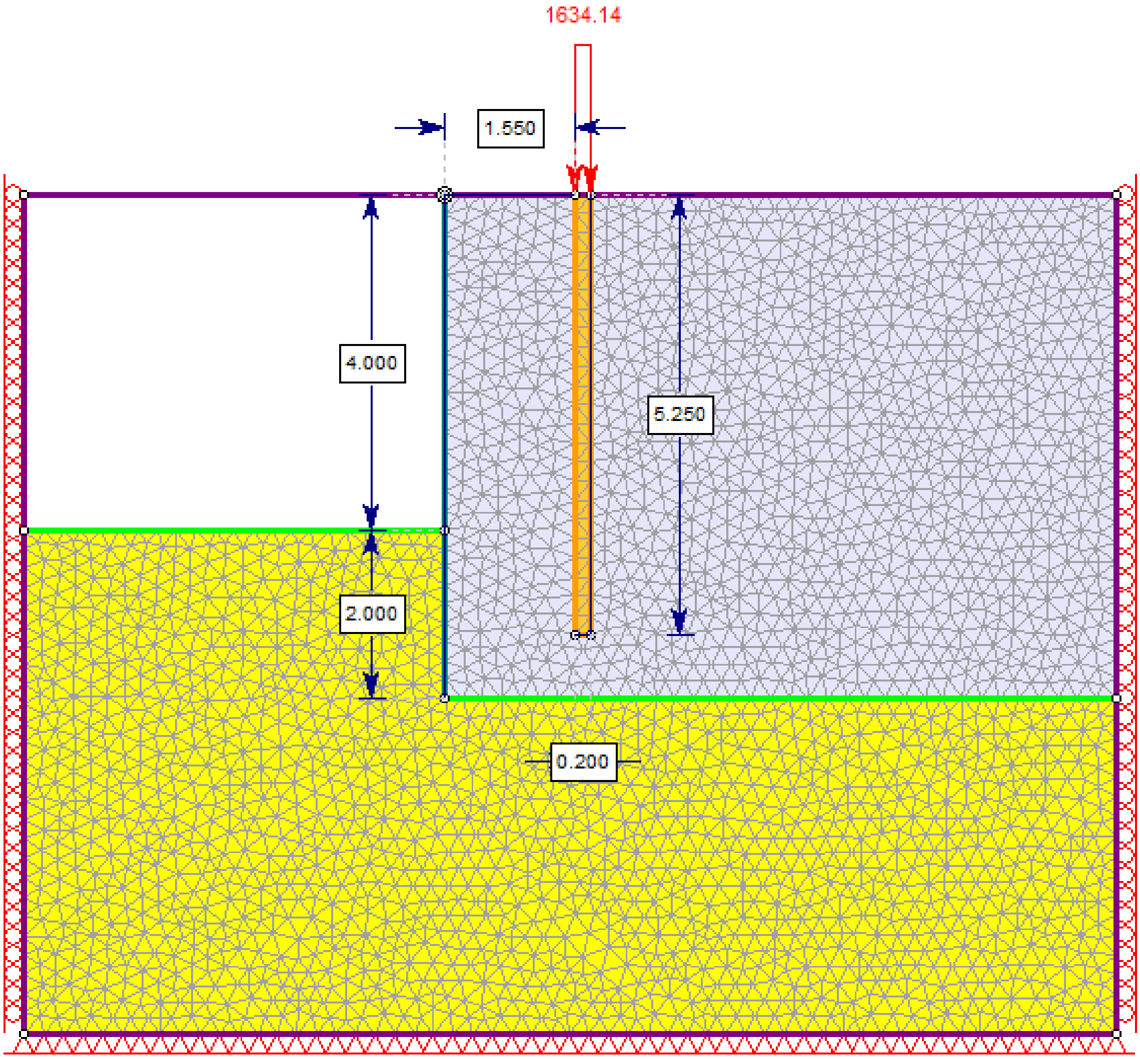

M 171.1: Original model (stage 3)

C_1'	ϕ_1'	γ_1	E_1	C_2'	ϕ_2'	γ_2	E_2	H_1	H_2	H_3	E_3	D_1	D_2	L	Qult
0	36	19	156	39	15	20	7.2	4.00	2	1.25	745816	1.55	0.2	5.25	1634.14

M 171.2: Parameter values

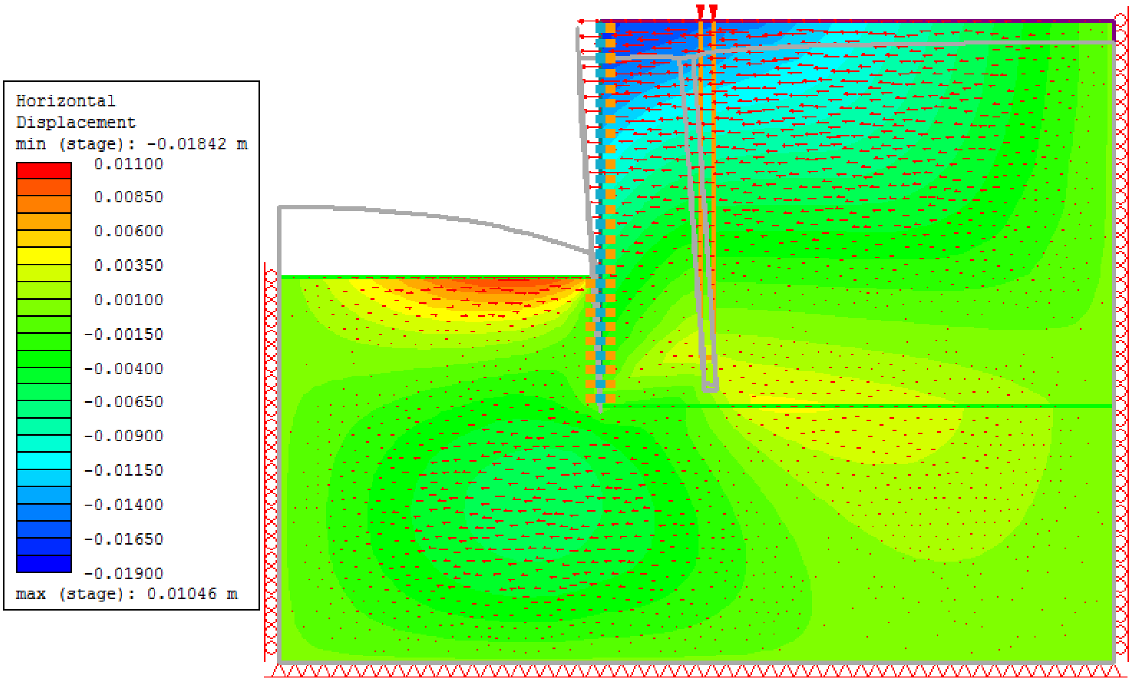

M 171.3: Deformed model (stage 3)

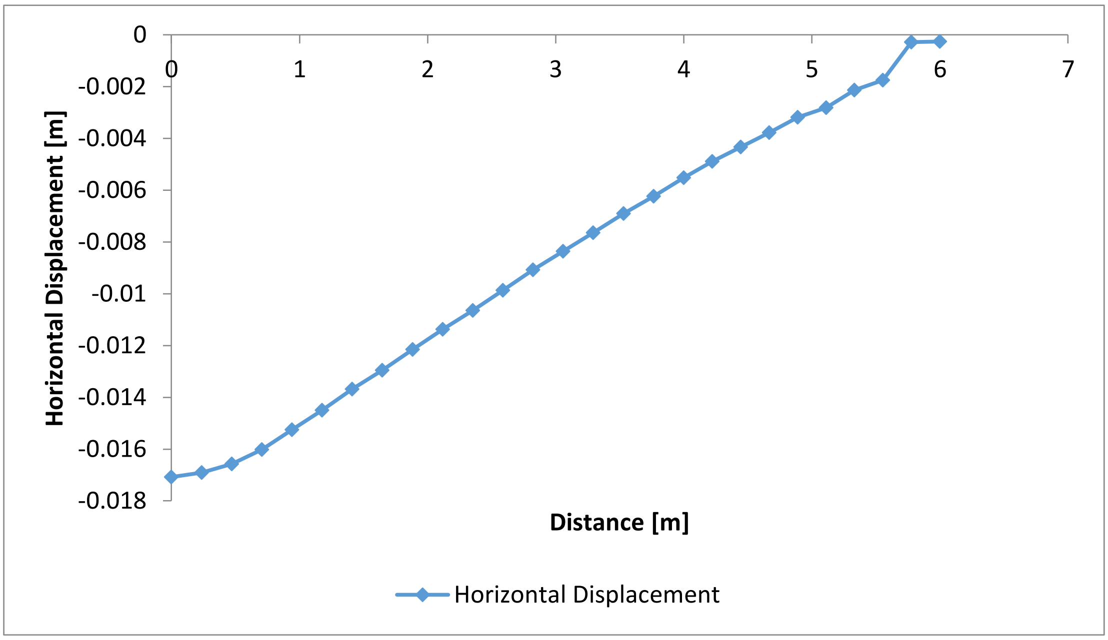

M 171.4: Horizontal displacement of soil along retaining wall

Retaining wall maximum horizontal displacement: -0.01842m

Distance from point of maximum displacement in retaining wall to the top of backfill soil: 0.0m

Model 172:

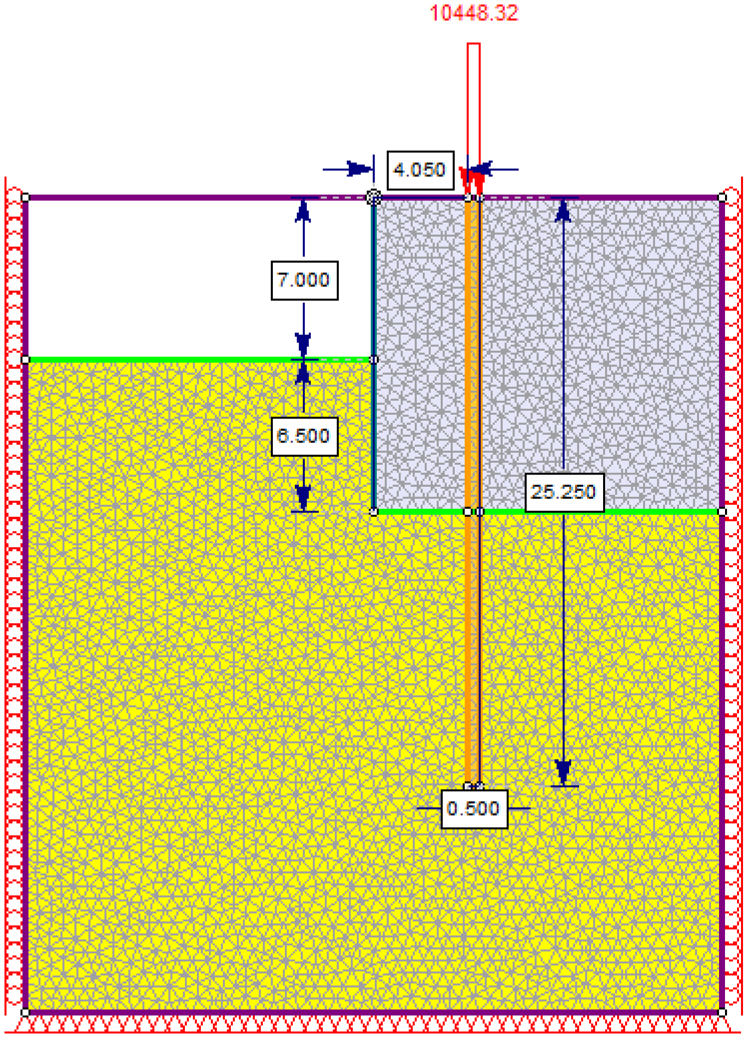

M 172.1: Original model (stage 3)

C_1'	ϕ_1'	γ_1	E_1	C_2'	ϕ_2'	γ_2	E_2	H_1	H_2	H_3	E_3	D_1	D_2	L	Qult
0	31	19	295	51	29	16	44.2	7.00	6.5	1.5	1132329	4.05	0.5	25.25	10448.32

M 172.2: Parameter values

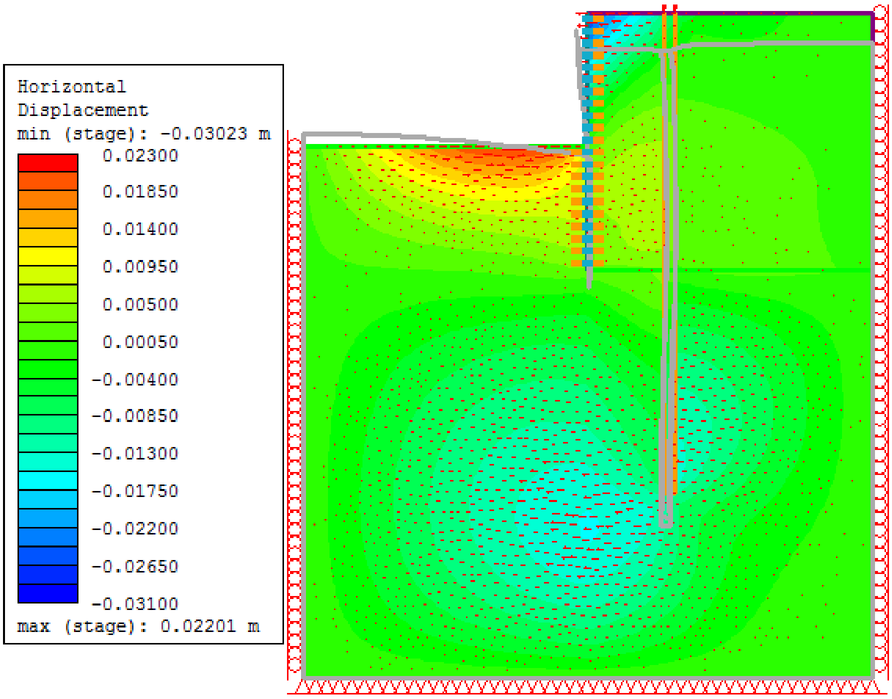

M 172.3: Deformed model (stage 3)

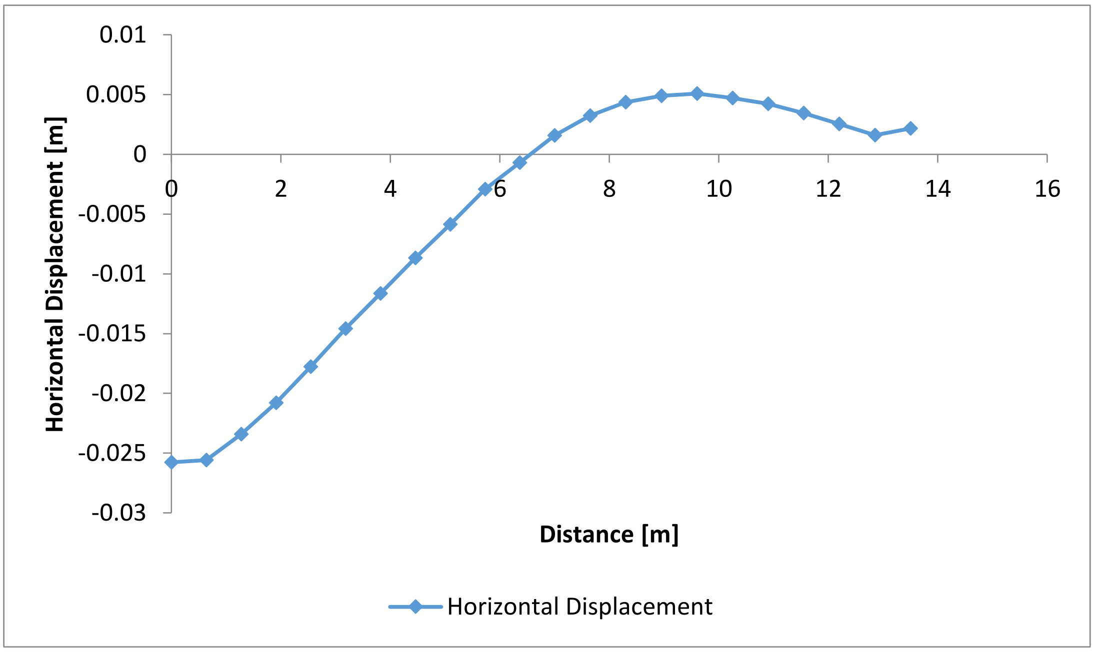

M 172.4: Horizontal displacement of soil along retaining wall

Retaining wall maximum horizontal displacement: -0.03023m

Distance from point of maximum displacement in retaining wall to the top of backfill soil: 0.0m

Model 173:

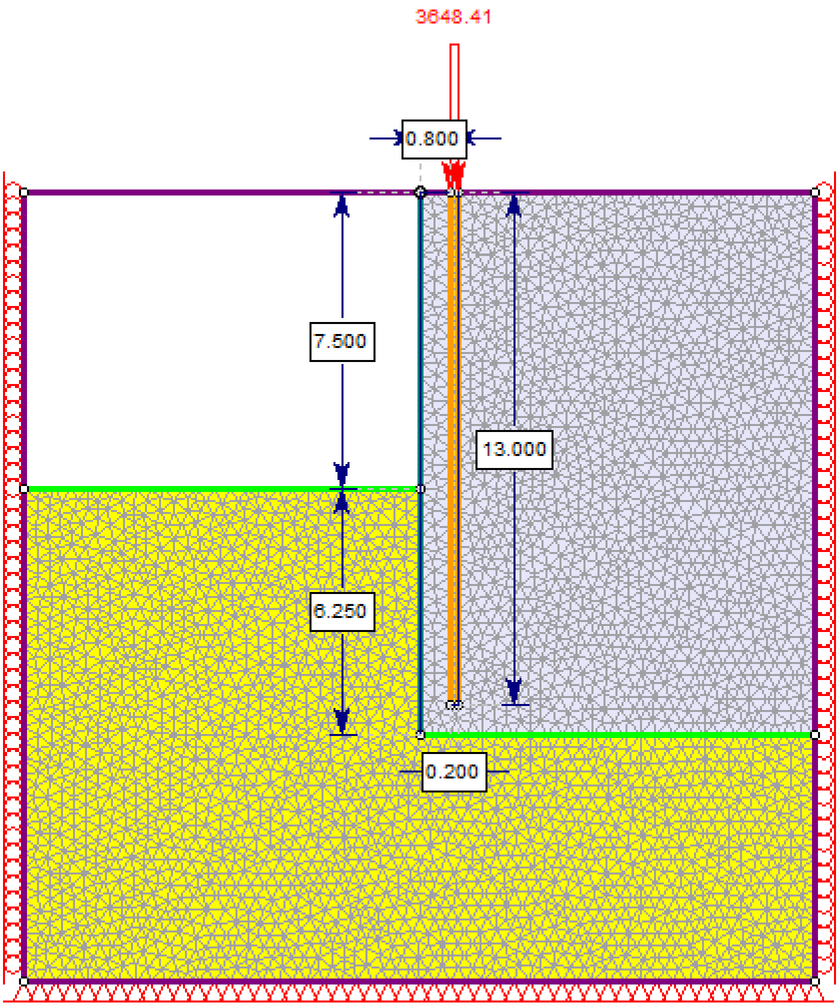

M 173.1: Original model (stage 3)

C_1'	ϕ_1'	γ_1	E_1	C_2'	ϕ_2'	γ_2	E_2	H_1	H_2	H_3	E_3	D_1	D_2	L	Qult
0	37	18	89	51	20	18	20.7	7.50	6.25	1.25	700966	0.8	0.2	13	3648.41

M 173.2: Parameter values

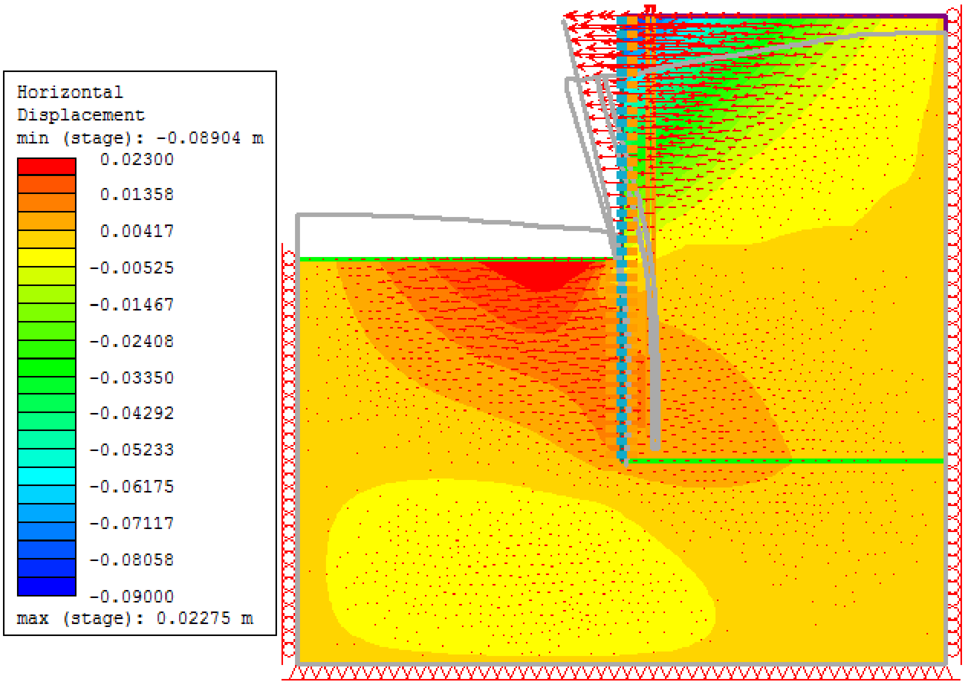

M 173.3: Deformed model (stage 3)

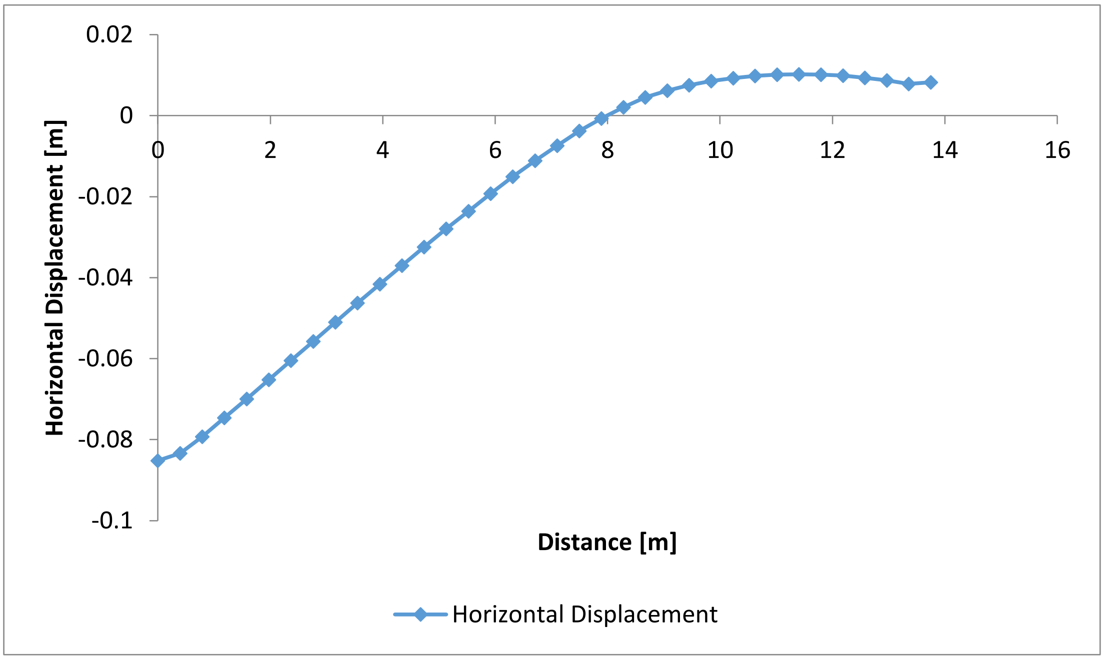

M 173.4: Horizontal displacement of soil along retaining wall

Retaining wall maximum horizontal displacement: -0.08904m

Distance from point of maximum displacement in retaining wall to the top of backfill soil: 0.0m

Model 174:

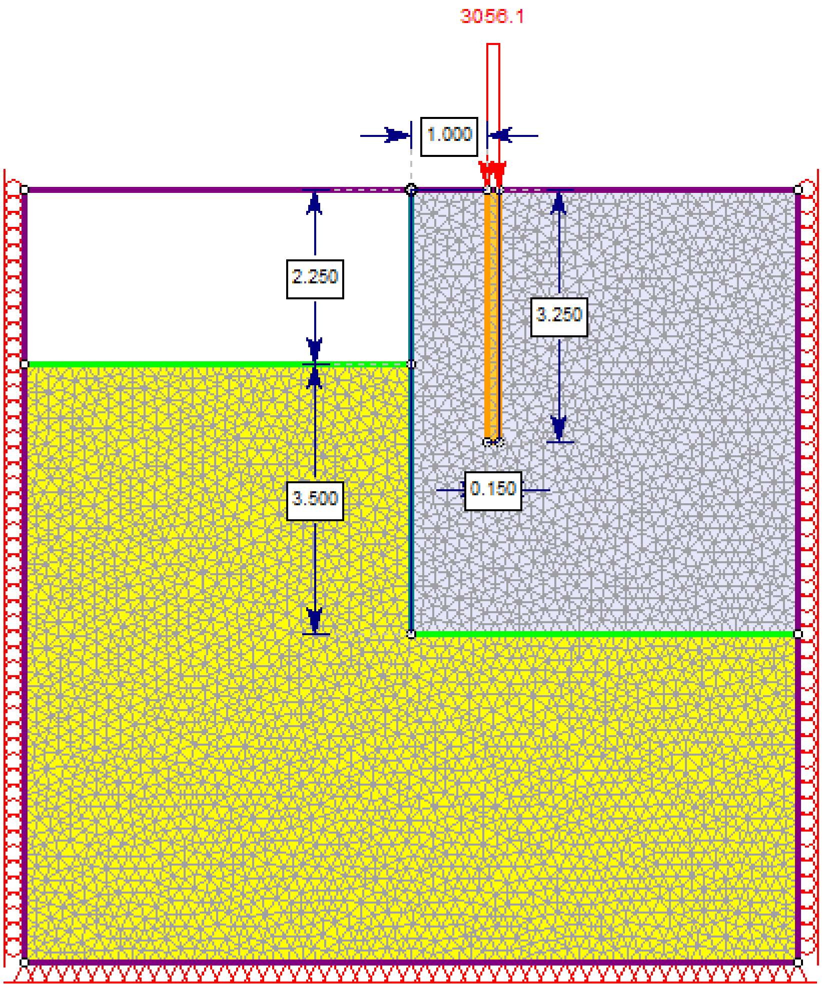

M 174.1: Original model (stage 3)

C'_1	ϕ'_1	γ_1	E_1	C'_2	ϕ'_2	γ_2	E_2	H_1	H_2	H_3	E_3	D_1	D_2	L	Qult
0	38	18	136	12	32	16	33.3	2.25	3.5	1.25	1105974	1	0.15	3.25	3056.1

M 174.2: Parameter values

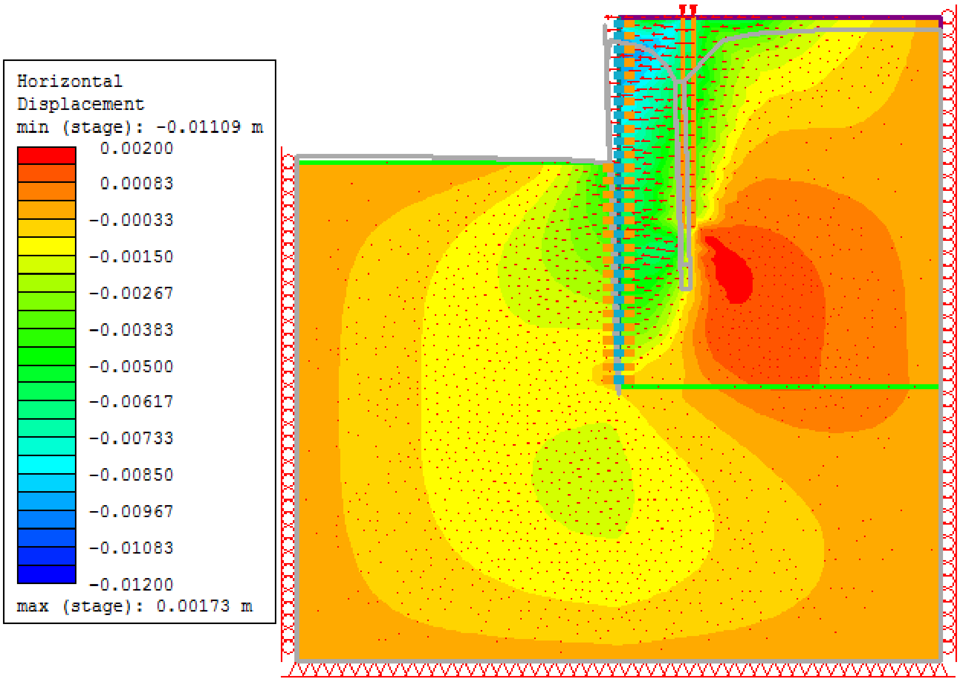

M 174.3: Deformed model (stage 3)

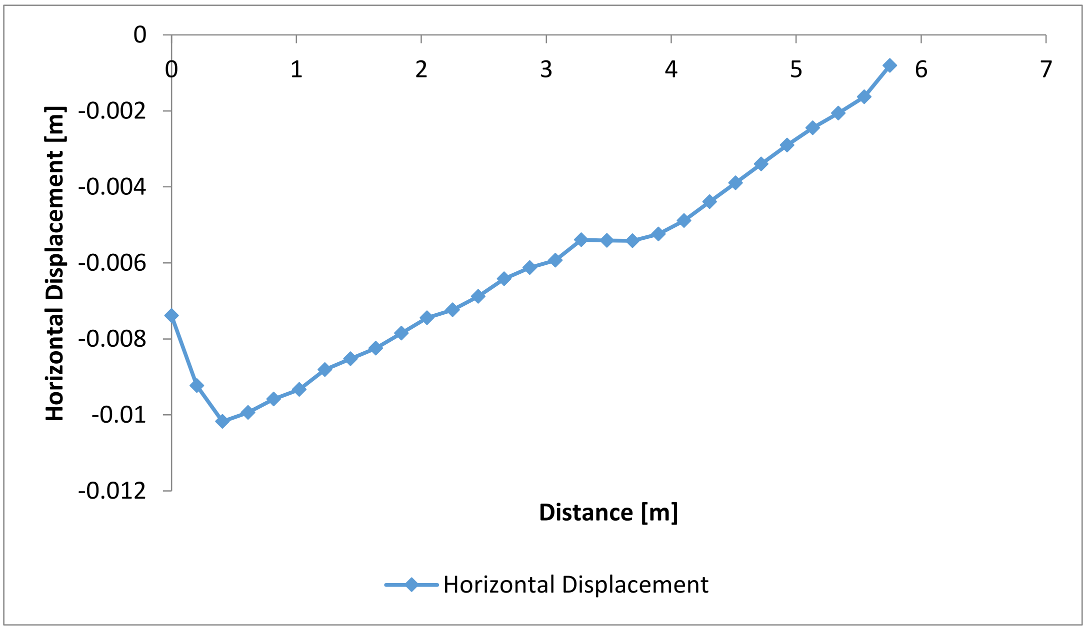

M 174.4: Horizontal displacement of soil along retaining wall

Retaining wall maximum horizontal displacement: -0.01109m

Distance from point of maximum displacement in retaining wall to the top of backfill soil: 0.0m

Model 175:

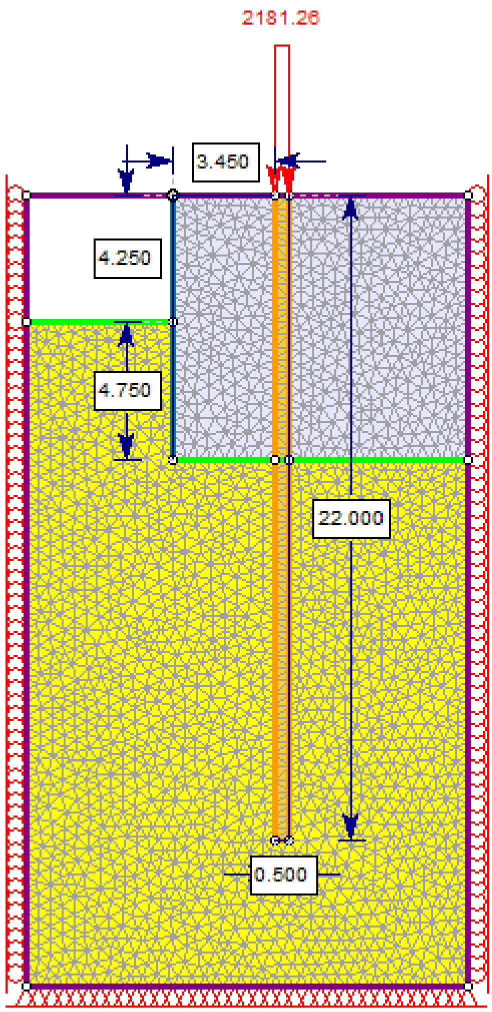

M 175.1: Original model (stage 3)

C'_1	ϕ'_1	γ_1	E_1	C'_2	ϕ'_2	γ_2	E_2	H_1	H_2	H_3	E_3	D_1	D_2	L	Qult
0	28	19	314	30	11	21	23.8	4.25	4.75	1.25	731874	3.45	0.5	22	2181.26

M 175.2: Parameter values

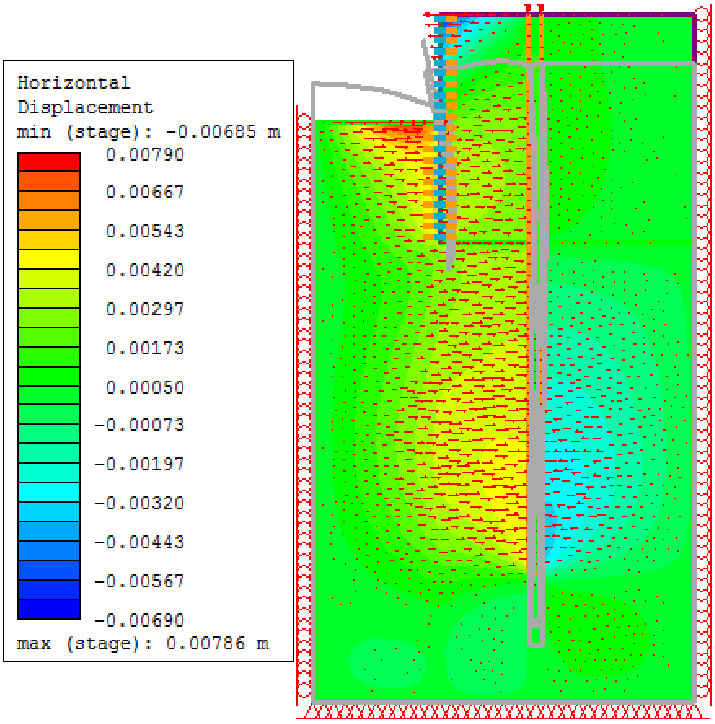

M 175.3: Deformed model (stage 3)

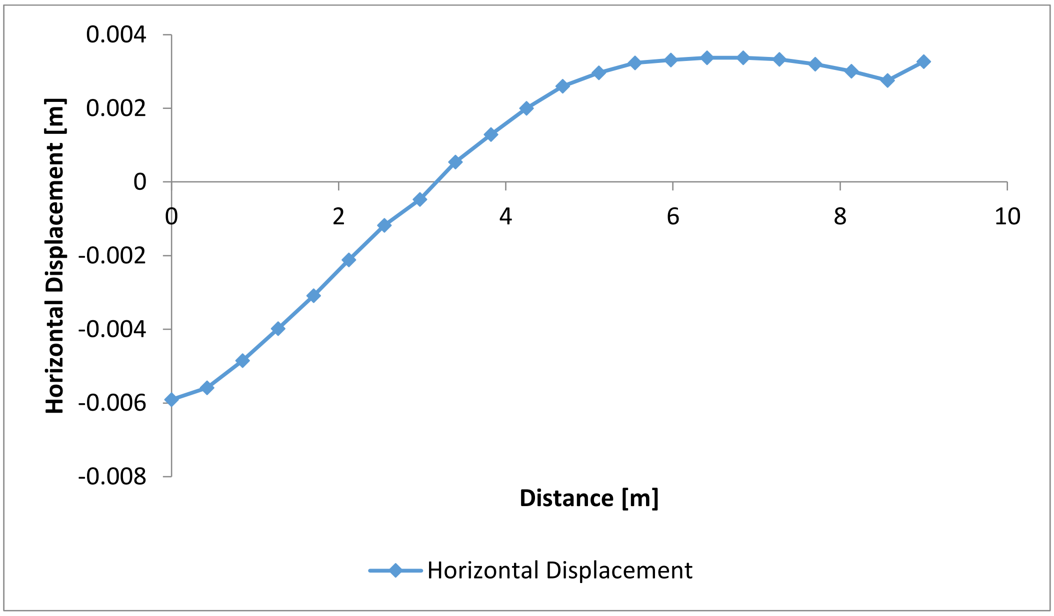

M 175.4: Horizontal displacement of soil along retaining wall

Retaining wall maximum horizontal displacement: -0.00685m

Distance from point of maximum displacement in retaining wall to the top of backfill soil: 0.0m

Model 176:

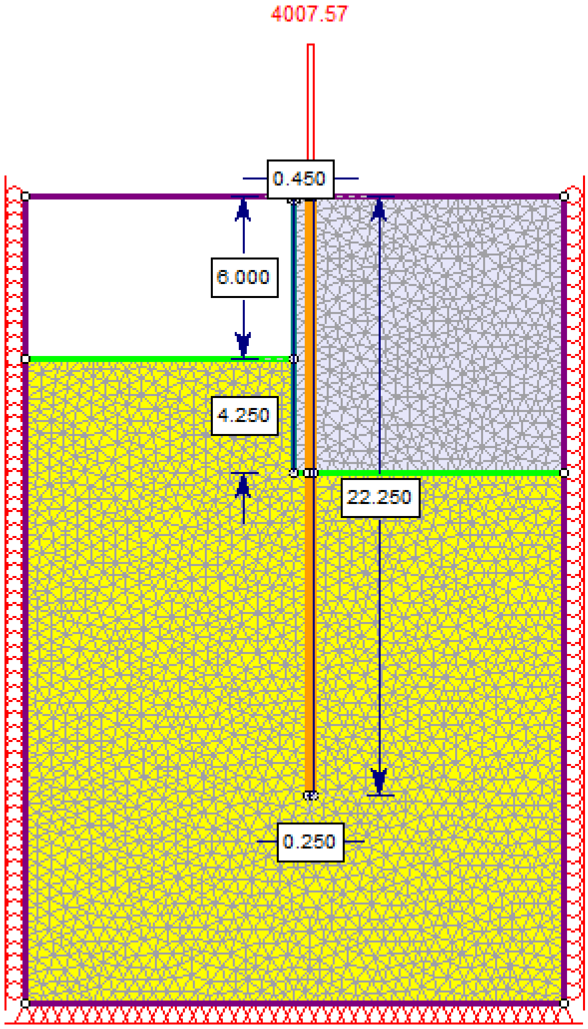

M 176.1: Original model (stage 3)

C'_1	ϕ'_1	γ_1	E_1	C'_2	ϕ'_2	γ_2	E_2	H_1	H_2	H_3	E_3	D_1	D_2	L	Qult
0	30	19	188	52	18	20	29.0	6.00	4.25	1.25	974438	0.45	0.25	22.25	4007.57

M 176.2: Parameter values

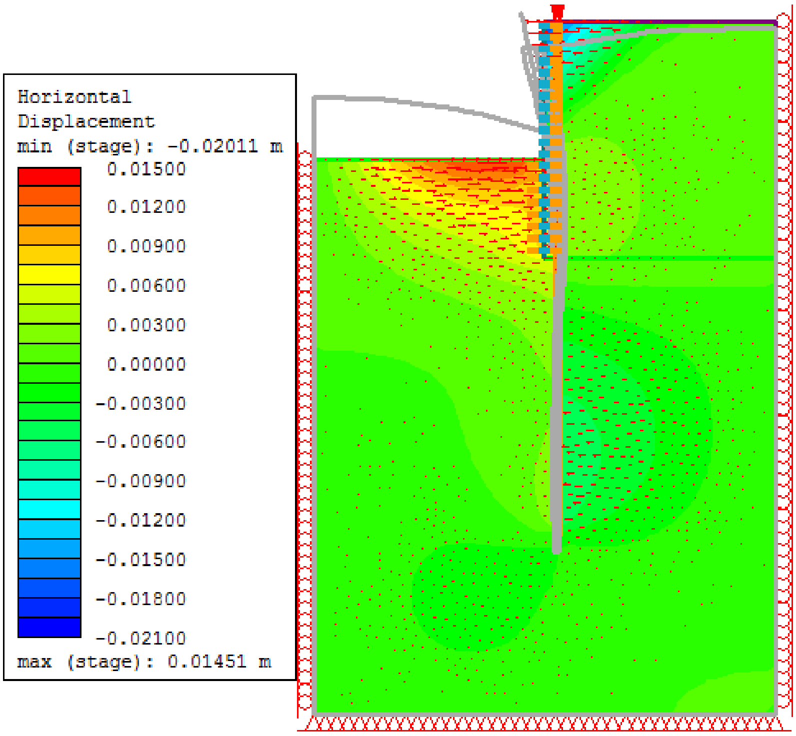

M 176.3: Deformed model (stage 3)

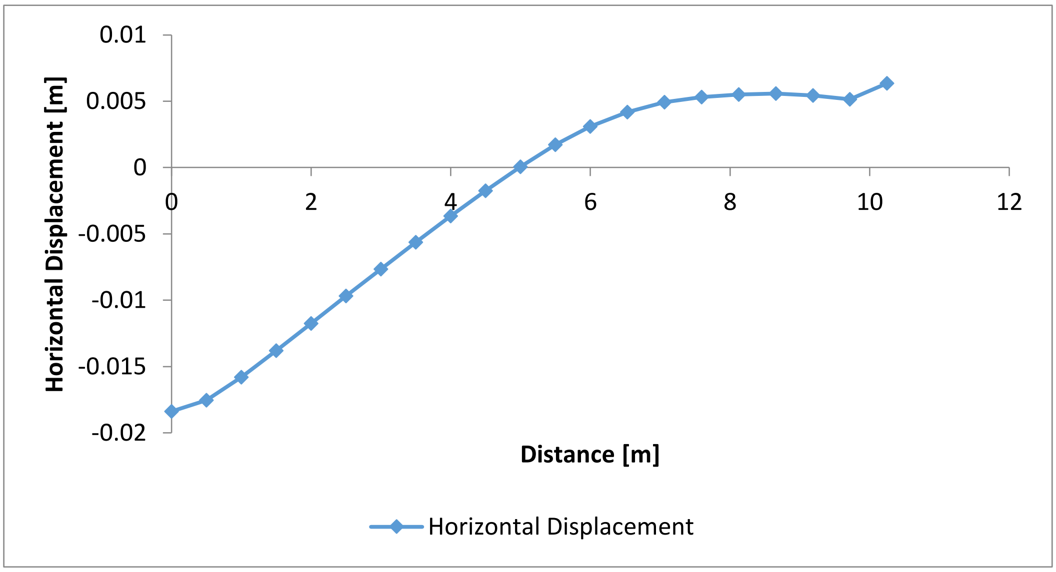

M 176.4: Horizontal displacement of soil along retaining wall

Retaining wall maximum horizontal displacement: -0.02011m

Distance from point of maximum displacement in retaining wall to the top of backfill soil: 0.0m

Model 177:

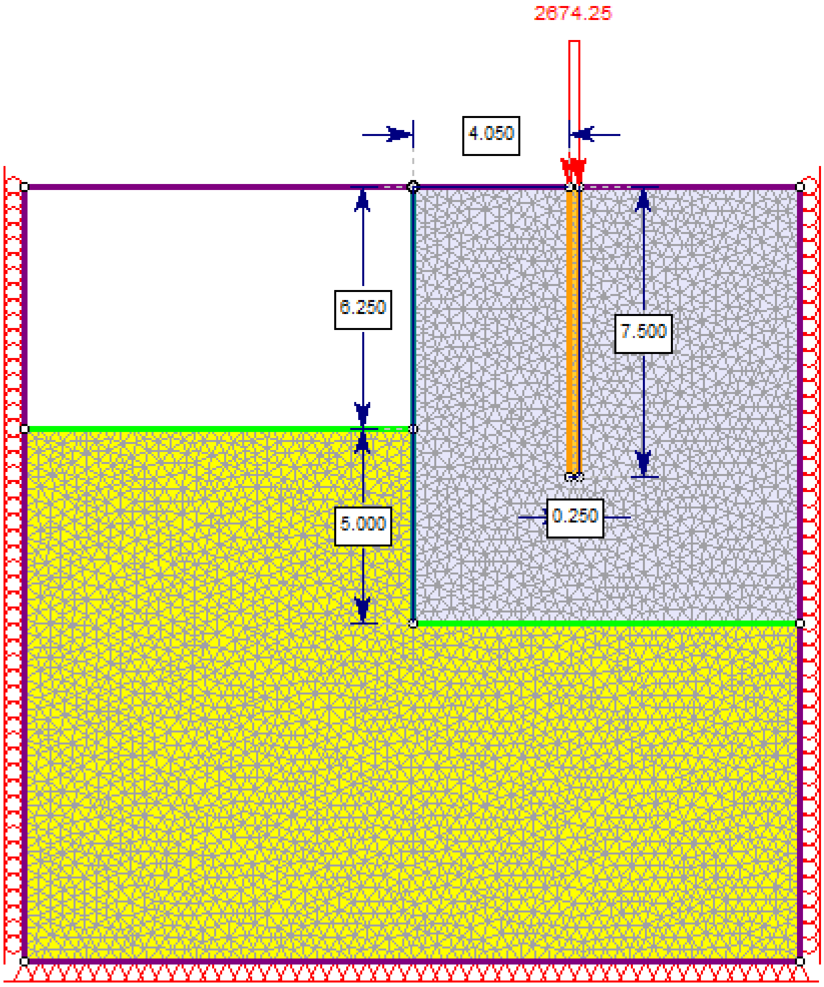

M 177.1: Original model (stage 3)

C_1'	ϕ_1'	γ_1	E_1	C_2'	ϕ_2'	γ_2	E_2	H_1	H_2	H_3	E_3	D_1	D_2	L	Qult
0	36	18	302	43	14	17	21.3	6.25	5	1.25	824030	4.05	0.25	7.5	2674.25

M 177.2: Parameter values

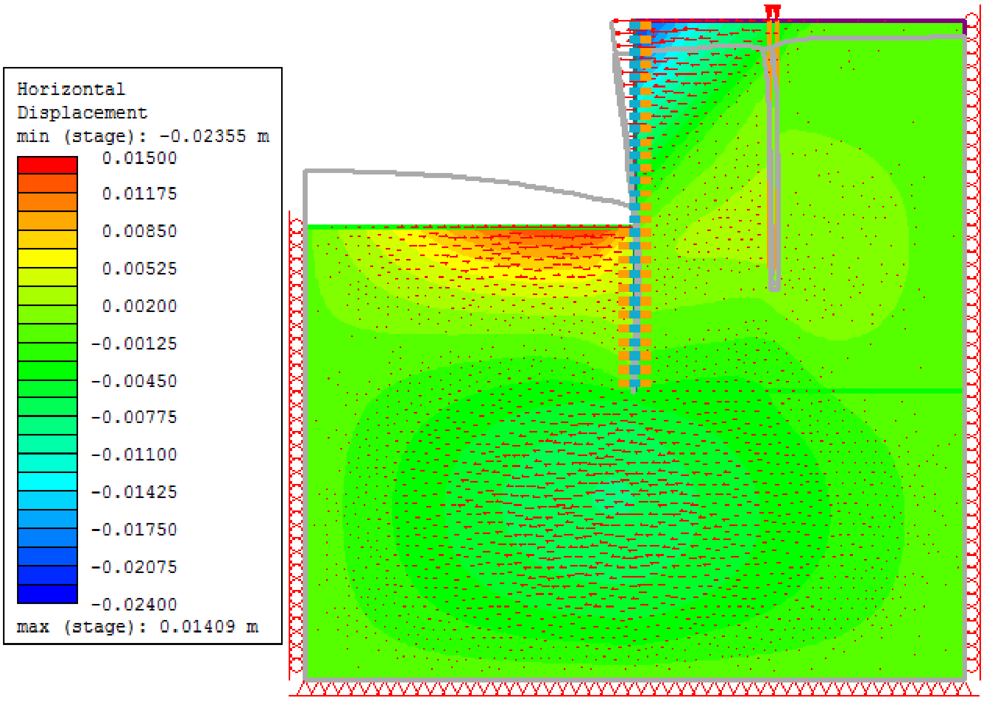

M 177.3: Deformed model (stage 3)

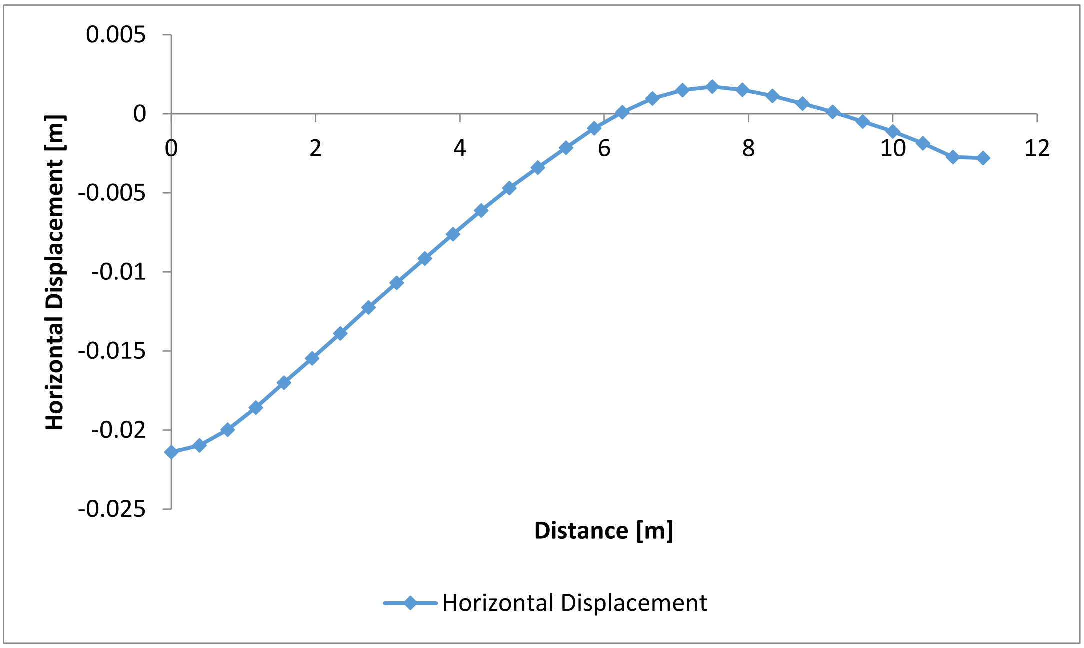

M 177.4: Horizontal displacement of soil along retaining wall

Retaining wall maximum horizontal displacement: -0.02355m

Distance from point of maximum displacement in retaining wall to the top of backfill soil: 0.0m

Model 178:

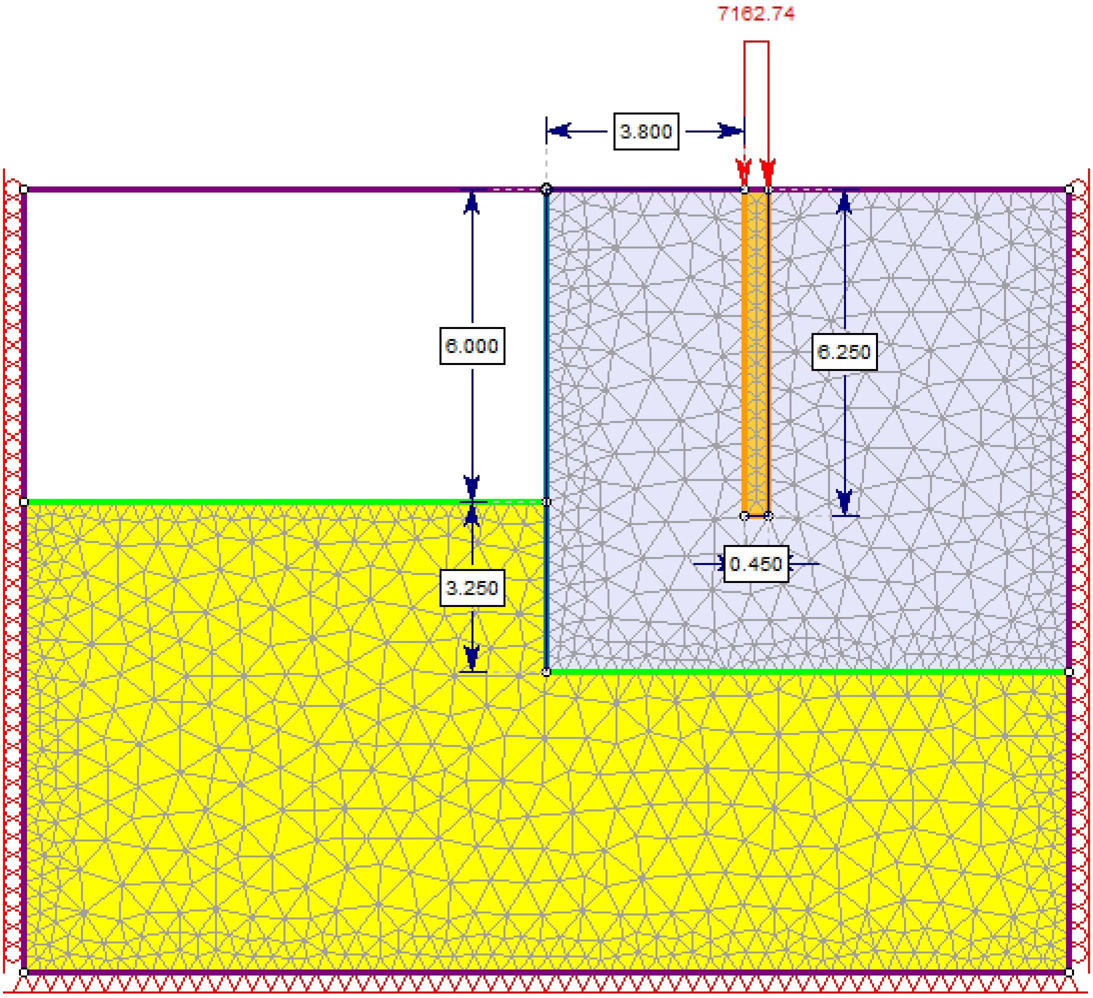

M 178.1: Original model (stage 3)

C_1'	ϕ_1'	γ_1	E_1	C_2'	ϕ_2'	γ_2	E_2	H_1	H_2	H_3	E_3	D_1	D_2	L	Qult
0	42	18	262	46	29	25	22.4	6.00	3.25	1	859412	3.8	0.45	6.25	7162.74

M 178.2: Parameter values

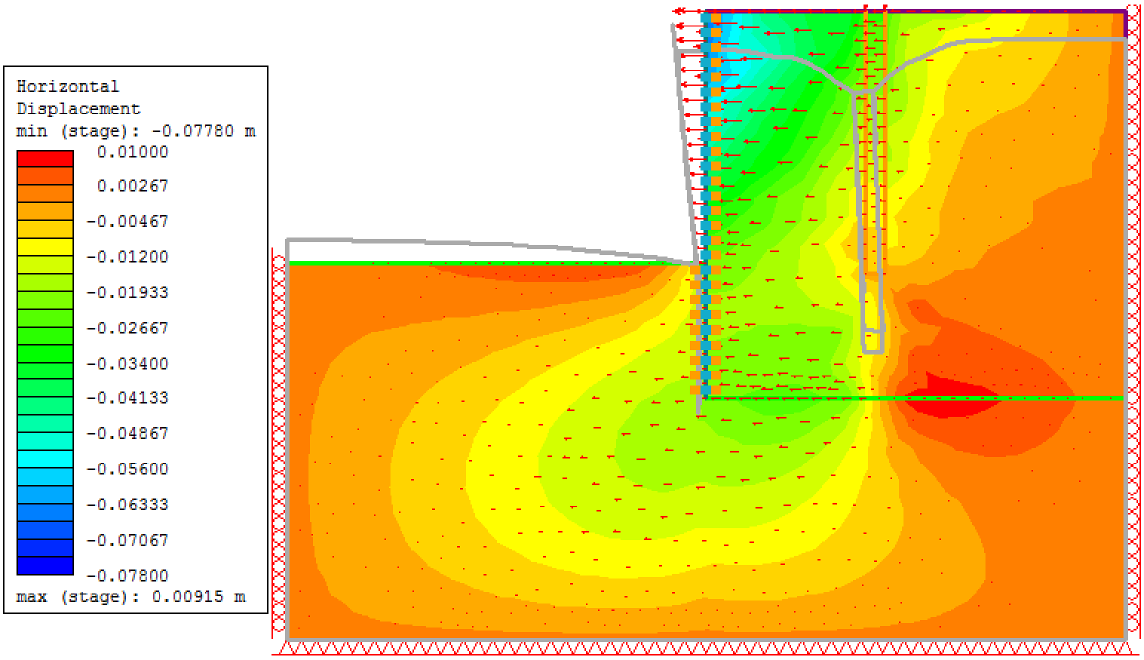

M 178.3: Deformed model (stage 3)

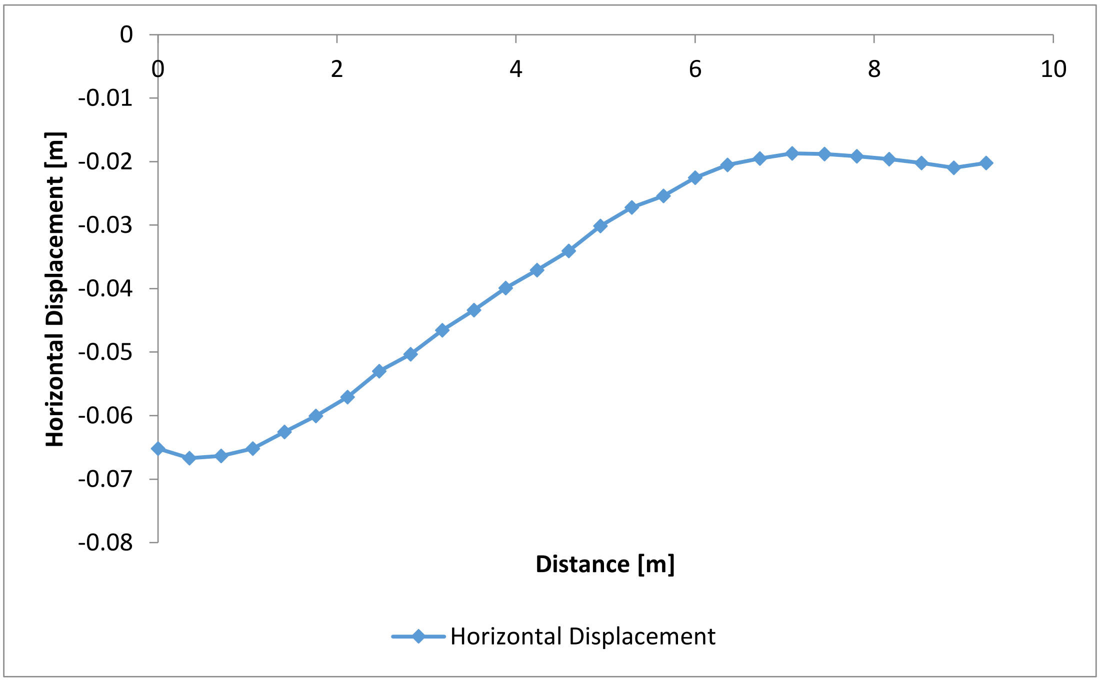

M 178.4: Horizontal displacement of soil along retaining wall

Retaining wall maximum horizontal displacement: -0.0778m

Distance from point of maximum displacement in retaining wall to the top of backfill soil: 0.0m

Model 179:

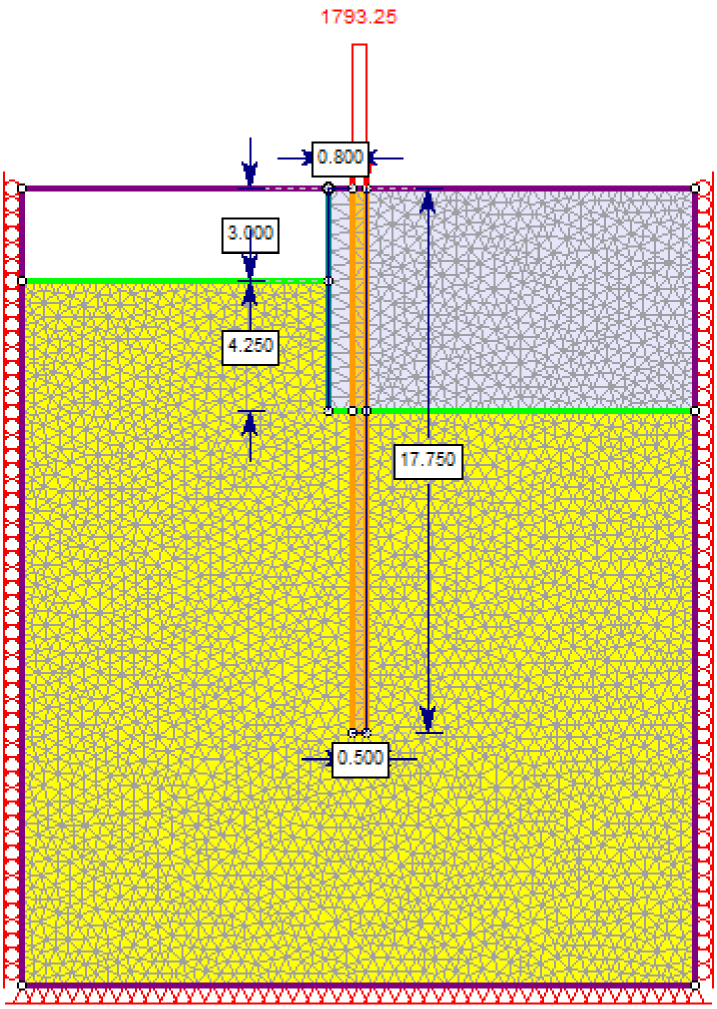

M 179.1: Original model (stage 3)

C_1'	ϕ_1'	γ_1	E_1	C_2'	ϕ_2'	γ_2	E_2	H_1	H_2	H_3	E_3	D_1	D_2	L	Qult
0	38	22	131	20	13	18	19.0	3.00	4.25	0.5	976564	0.8	0.5	17.75	1793.25

M 179.2: Parameter values

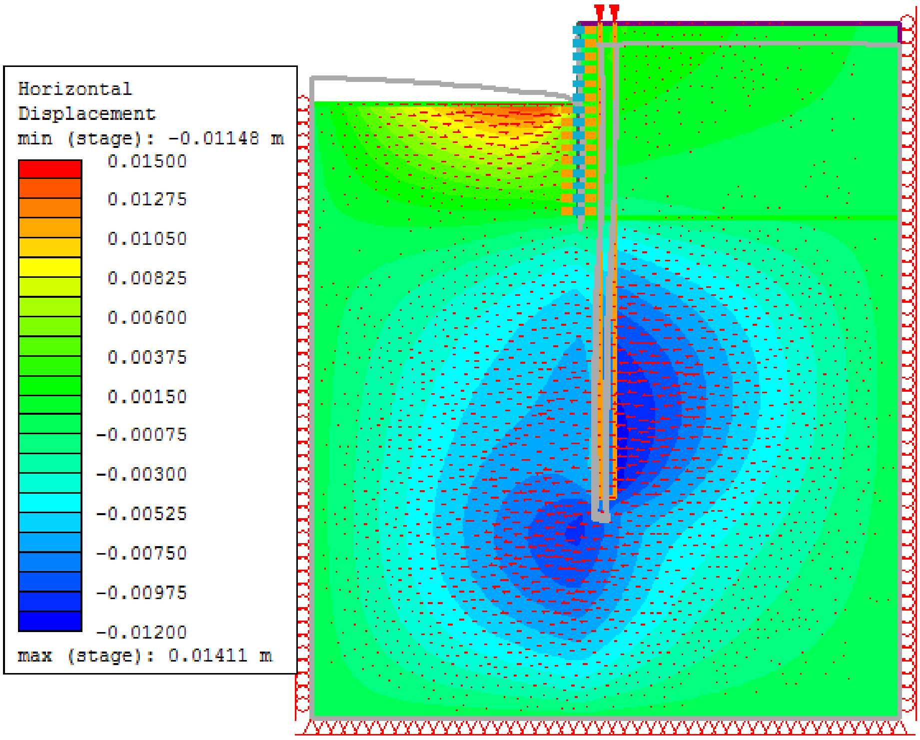

M 179.3: Deformed model (stage 3)

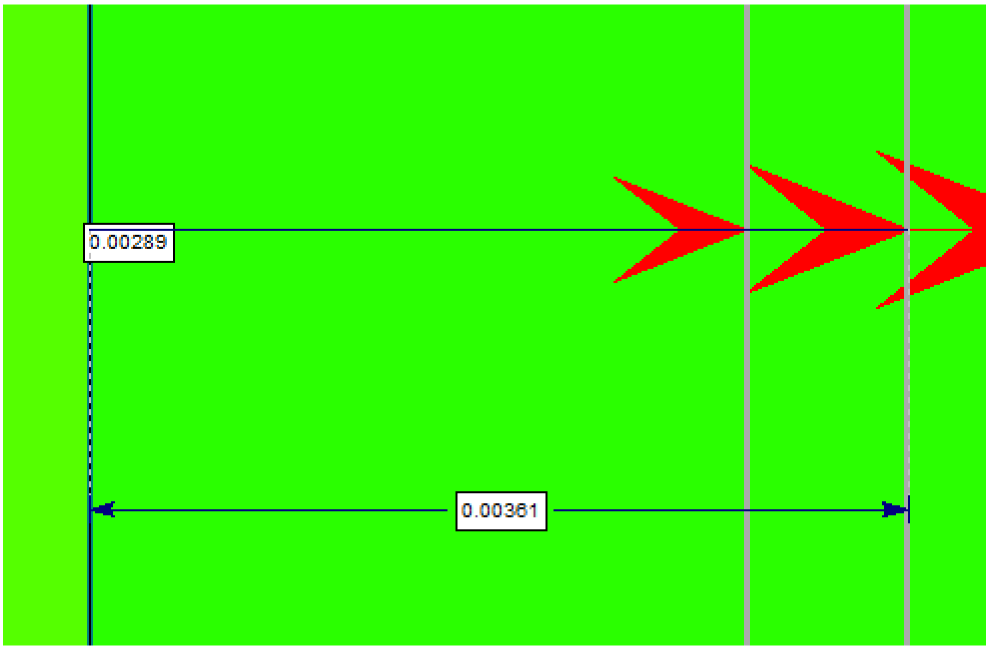

M 179.4: Detailed view of cross-section of retaining wall and soil (stage 3)

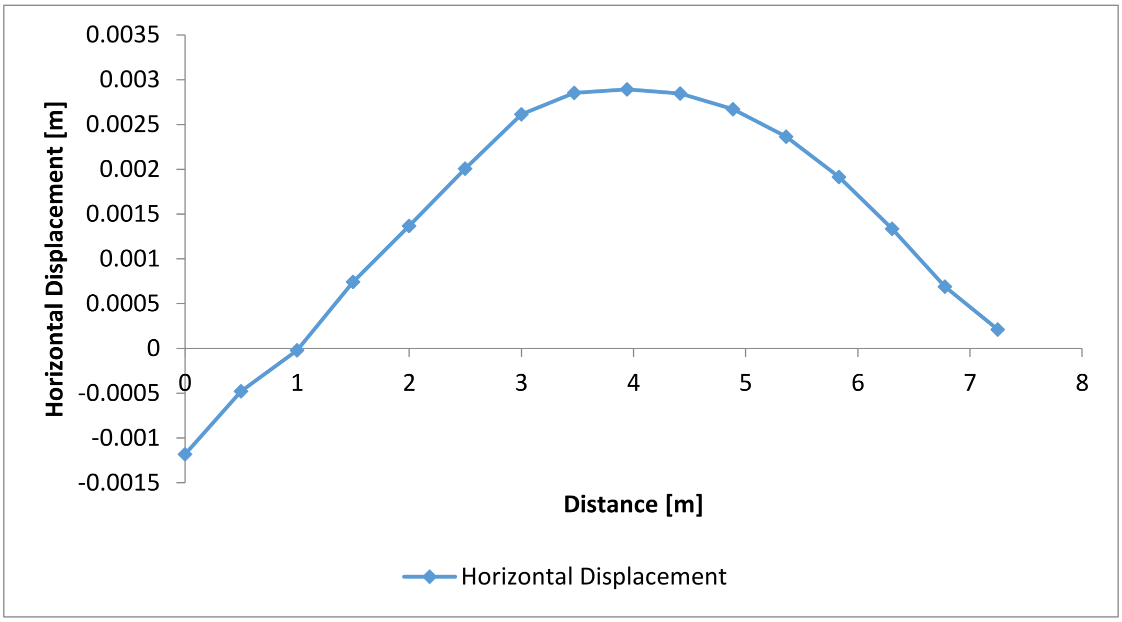

M 179.5: Horizontal displacement of soil along retaining wall

Retaining wall maximum horizontal displacement: 0.00361m

Distance from point of maximum displacement in retaining wall to the top of backfill soil: 3.94m

Model 180:

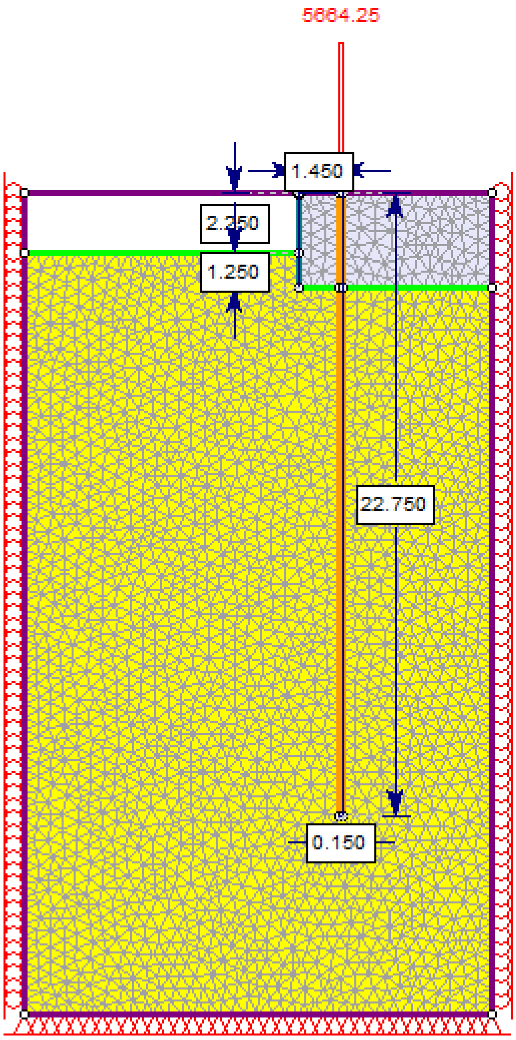

M 180.1: Original model (stage 3)

C_1'	ϕ_1'	γ_1	E_1	C_2'	ϕ_2'	γ_2	E_2	H_1	H_2	H_3	E_3	D_1	D_2	L	Qult
0	40	22	151	21	23	23	10.9	2.25	1.25	1.25	928973	1.45	0.15	22.75	5664.25

M 180.2: Parameter values

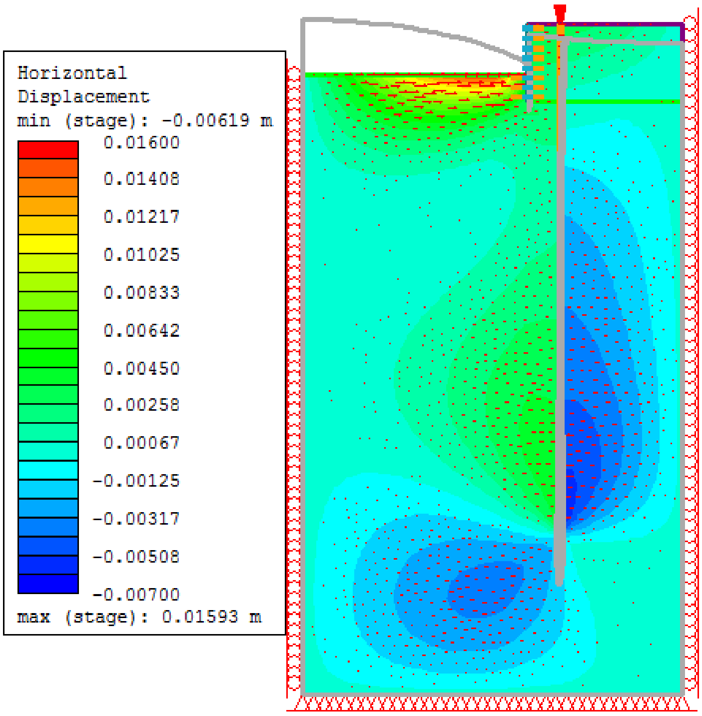

M 180.3: Deformed model (stage 3)

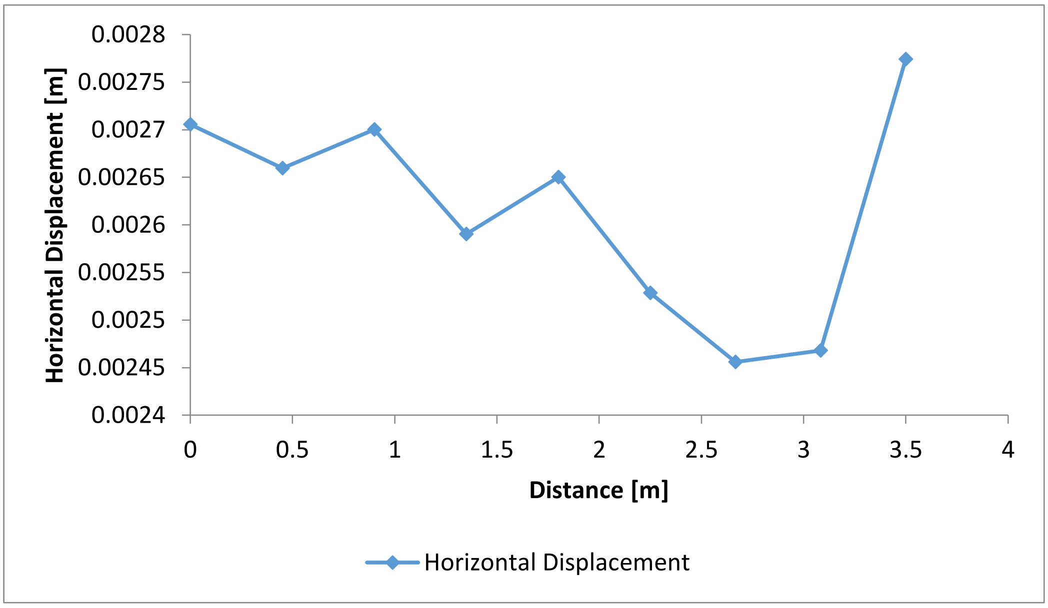

M 180.4: Horizontal displacement of soil along retaining wall

Retaining wall maximum horizontal displacement: 0.00277m

Distance from point of maximum displacement in retaining wall to the top of backfill soil: 3.5m

Model 181:

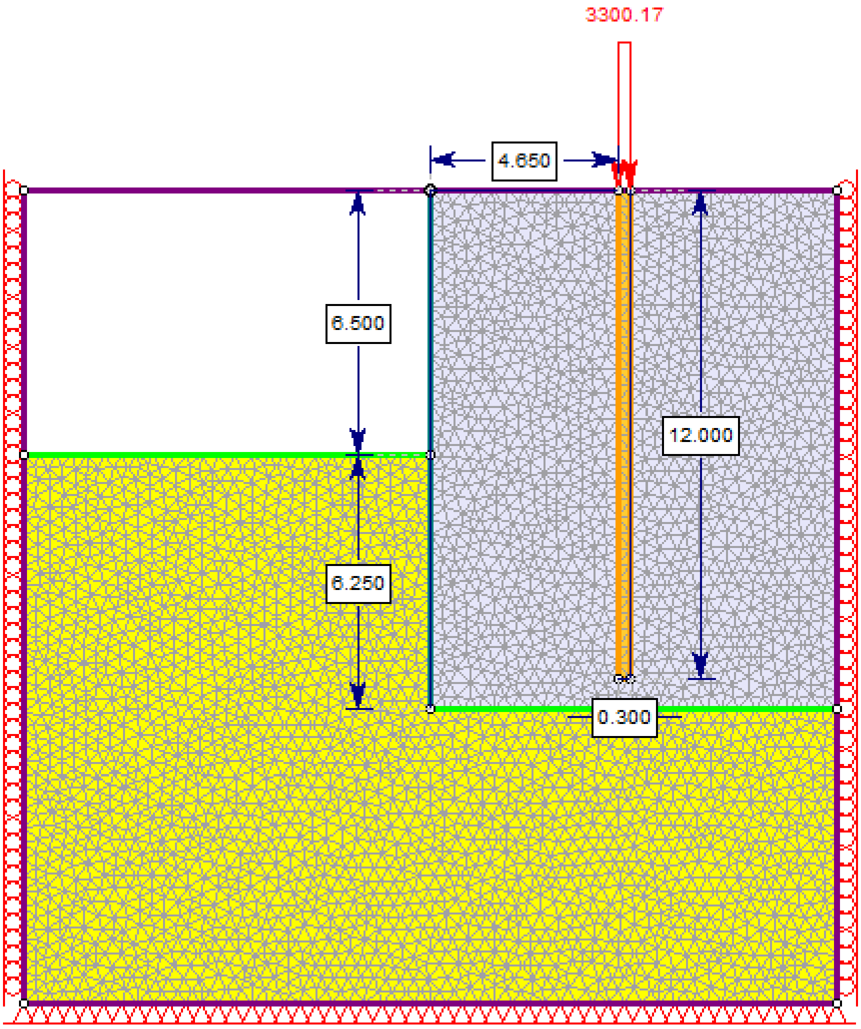

M 181.1: Original model (stage 3)

C_1'	ϕ_1'	γ_1	E_1	C_2'	ϕ_2'	γ_2	E_2	H_1	H_2	H_3	E_3	D_1	D_2	L	Qult
0	40	22	283	48	4	24	42.9	6.50	6.25	1.25	1096175	4.65	0.3	12	3300.17

M 181.2: Parameter values

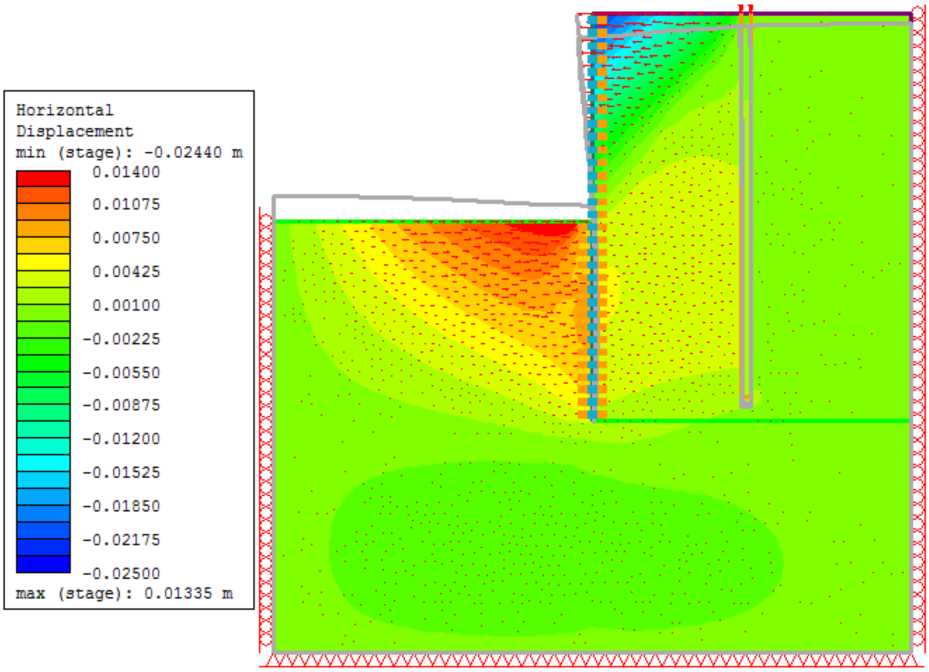

M 181.3: Deformed model (stage 3)

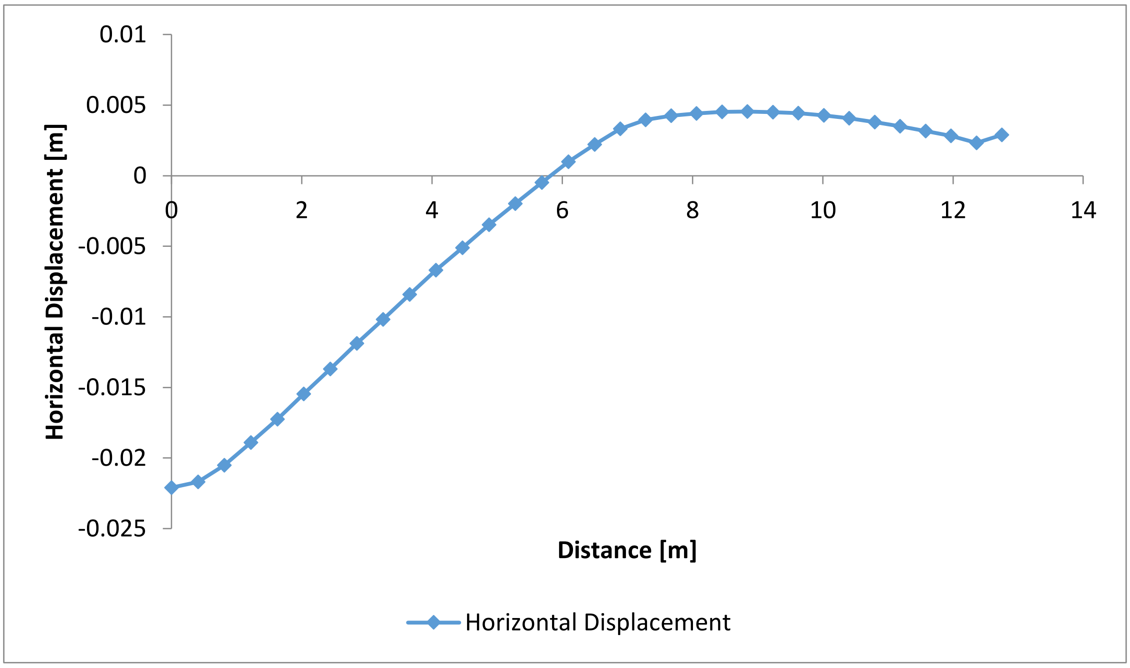

M 181.4: Horizontal displacement of soil along retaining wall

Retaining wall maximum horizontal displacement: -0.0244m

Distance from point of maximum displacement in retaining wall to the top of backfill soil: 0.0m

Model 182:

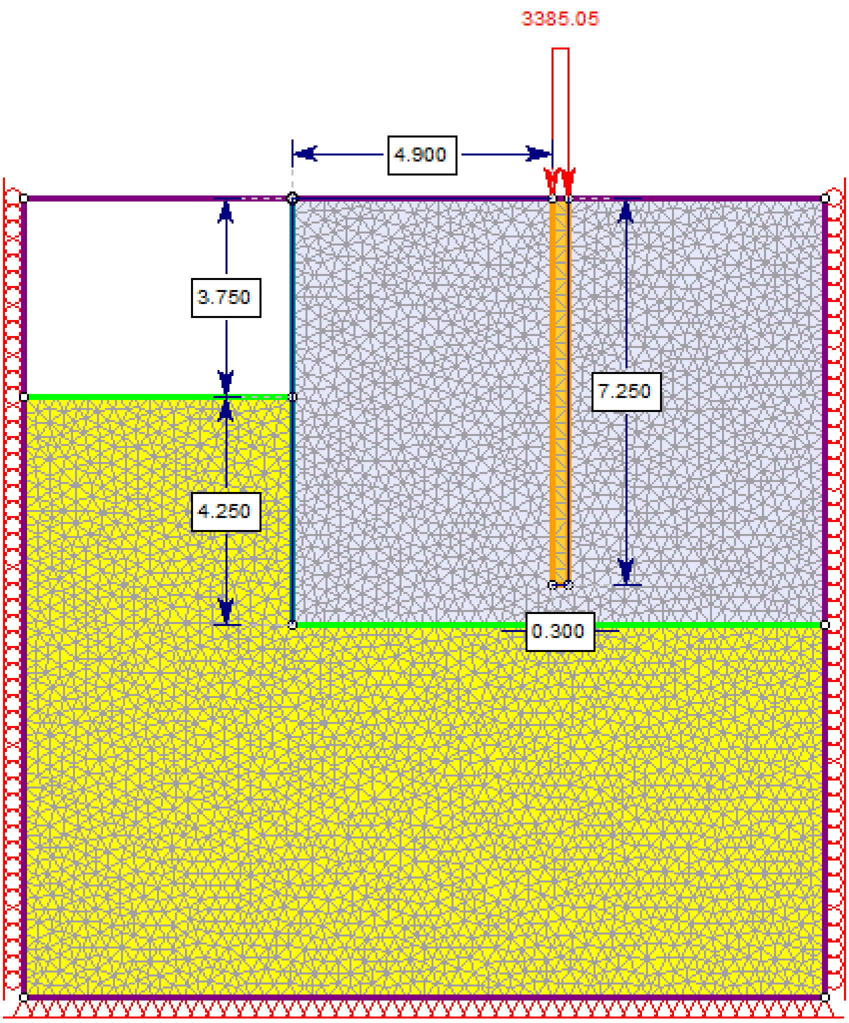

M 182.1: Original model (stage 3)

C_1'	ϕ_1'	γ_1	E_1	C_2'	ϕ_2'	γ_2	E_2	H_1	H_2	H_3	E_3	D_1	D_2	L	Qult
0	43	20	145	23	8	24	41.4	3.75	4.25	0.75	842356	4.9	0.3	7.25	3385.05

M 182.2: Parameter values

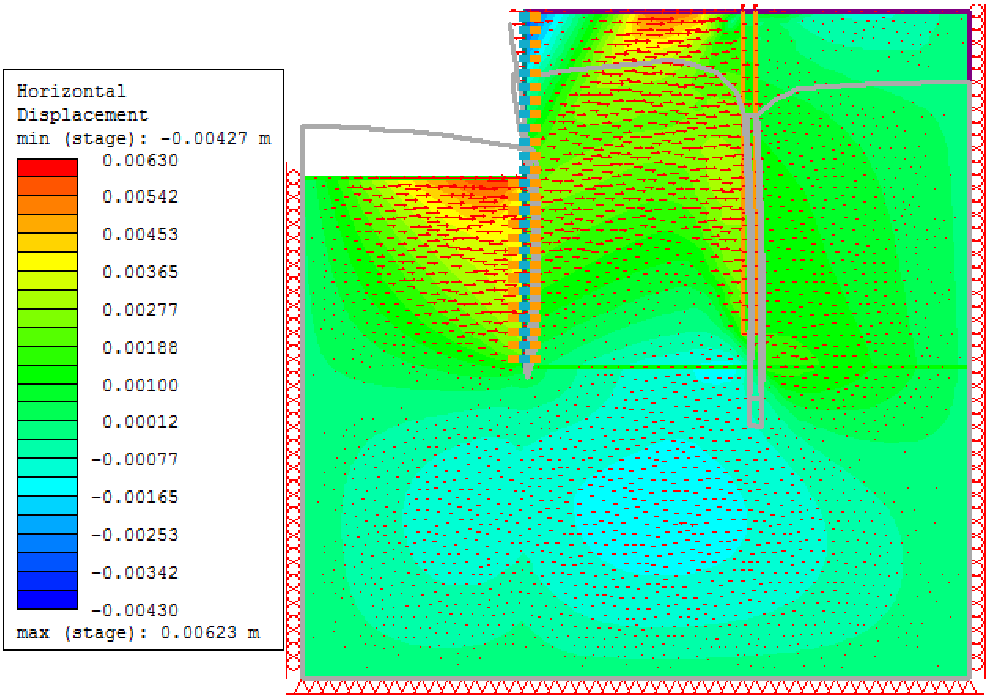

M 182.3: Deformed model (stage 3)

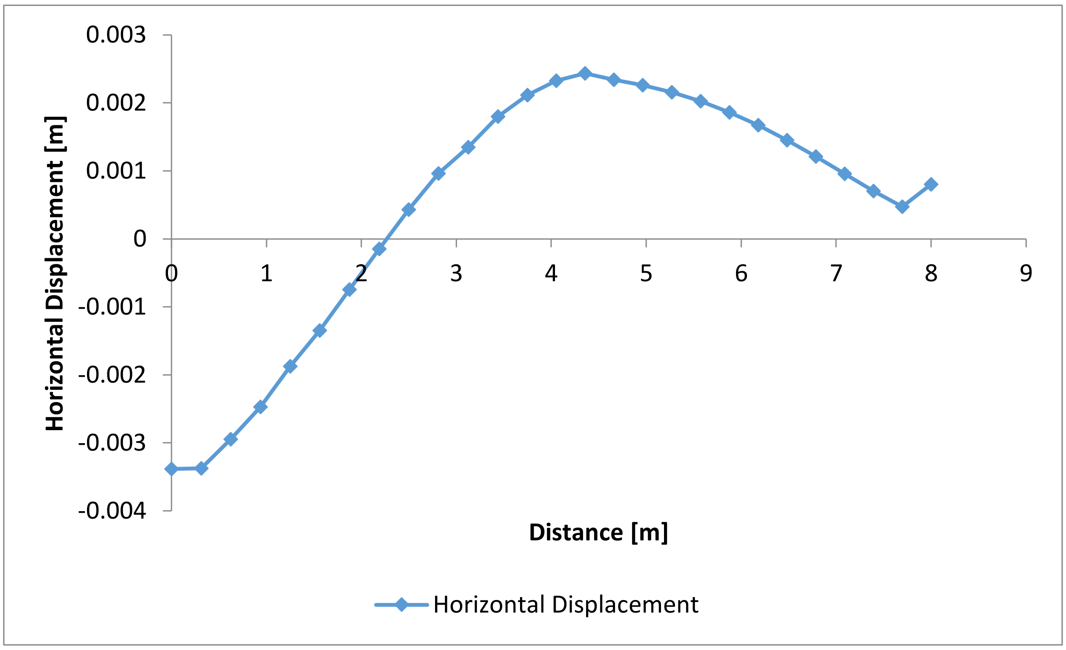

M 182.4: Horizontal displacement of soil along retaining wall

Retaining wall maximum horizontal displacement: -0.00427m

Distance from point of maximum displacement in retaining wall to the top of backfill soil: 0.0m

Model 183:

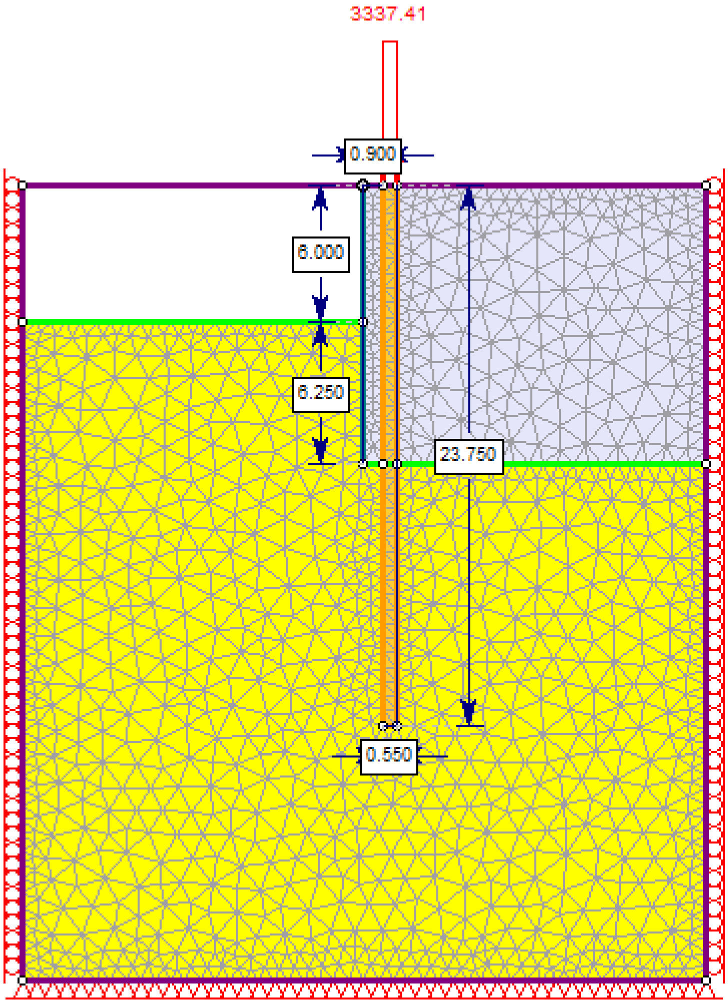

M 183.1: Original model (stage 3)

C_1'	ϕ_1'	γ_1	E_1	C_2'	ϕ_2'	γ_2	E_2	H_1	H_2	H_3	E_3	D_1	D_2	L	Qult
0	38	22	114	44	14	20	37.3	6.00	6.25	1.5	925617	0.9	0.55	23.75	3337.41

M 183.2: Parameter values

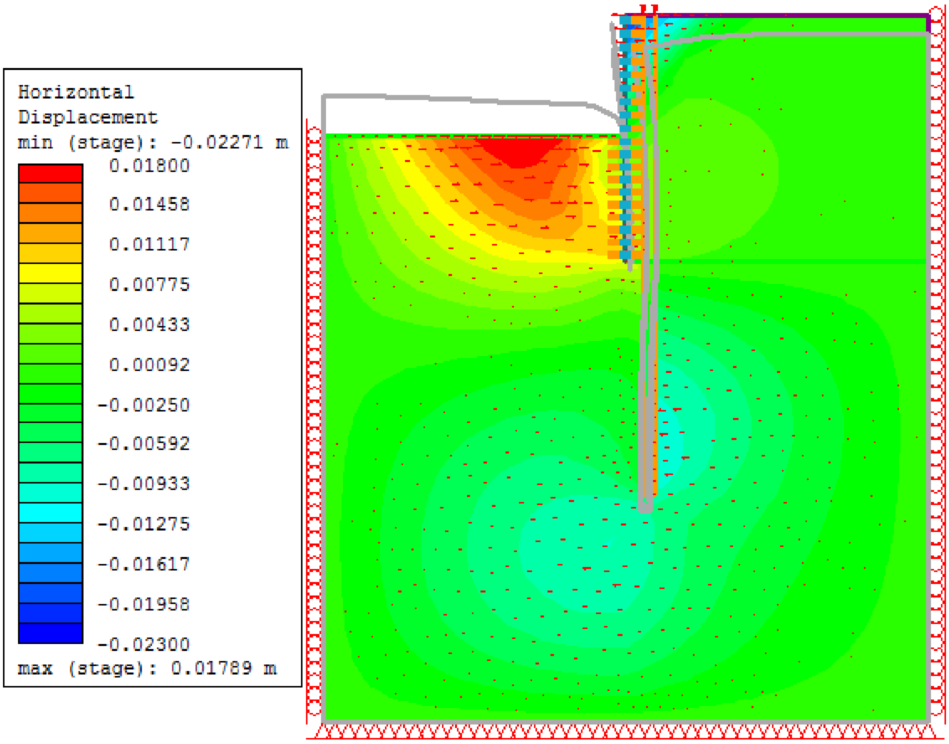

M 183.3: Deformed model (stage 3)

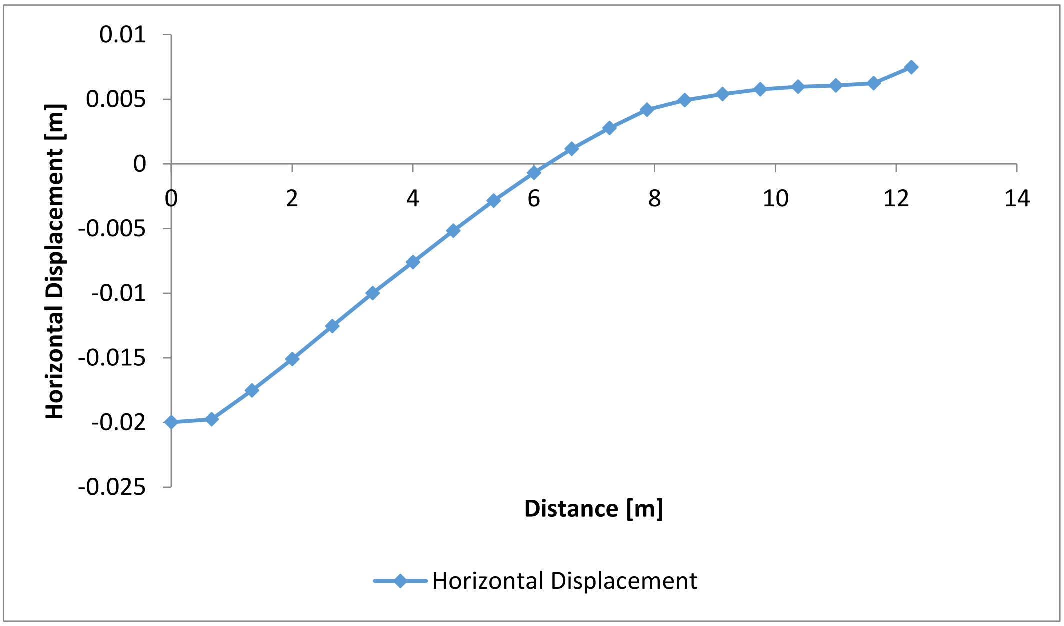

M 183.4: Horizontal displacement of soil along retaining wall

Retaining wall maximum horizontal displacement: -0.02271m

Distance from point of maximum displacement in retaining wall to the top of backfill soil: 0.0m

Model 184:

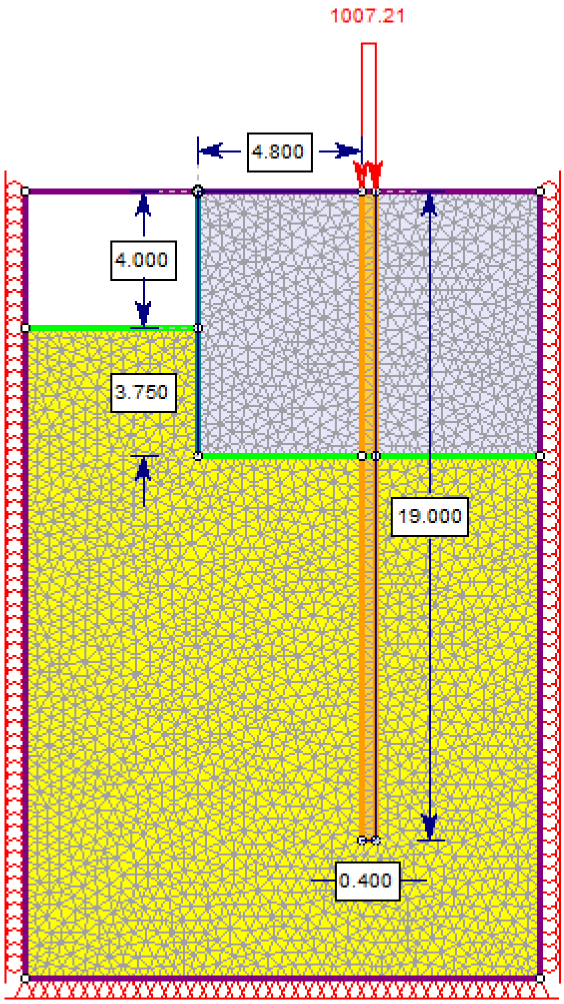

M 184.1: Original model (stage 3)

C'_1	ϕ'_1	γ_1	E_1	C'_2	ϕ'_2	γ_2	E_2	H_1	H_2	H_3	E_3	D_1	D_2	L	Qult
0	33	21	108	54	2	24	30.1	4.00	1.75	1.25	1111265	4.8	0.4	19	1007.21

M 184.2: Parameter values

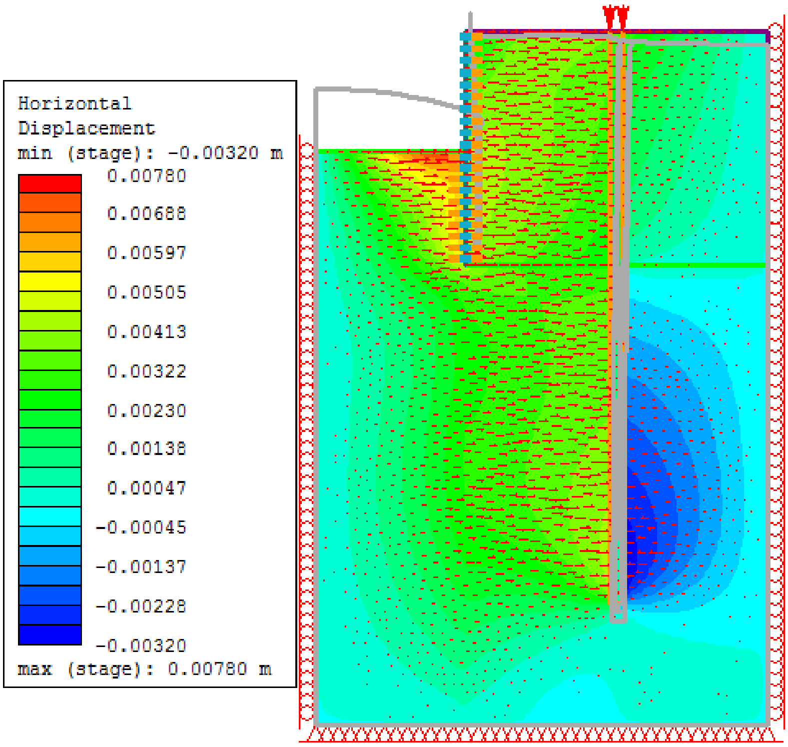

M 184.3: Deformed model (stage 3)

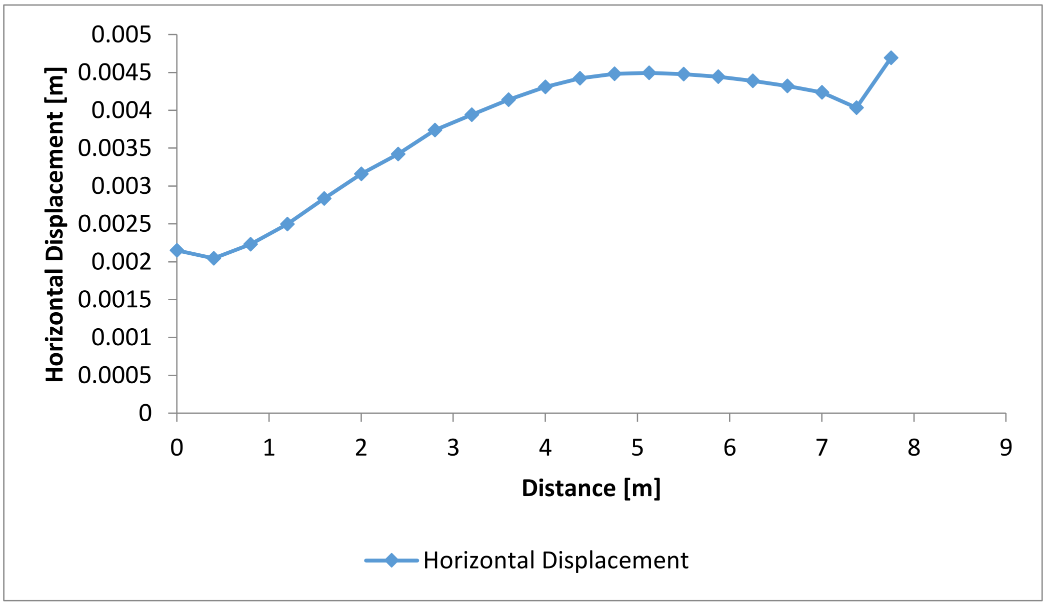

M 184.5: Horizontal displacement of soil along retaining wall

Retaining wall maximum horizontal displacement: 0.00469m

Distance from point of maximum displacement in retaining wall to the top of backfill soil: 7.75m

Model 185:

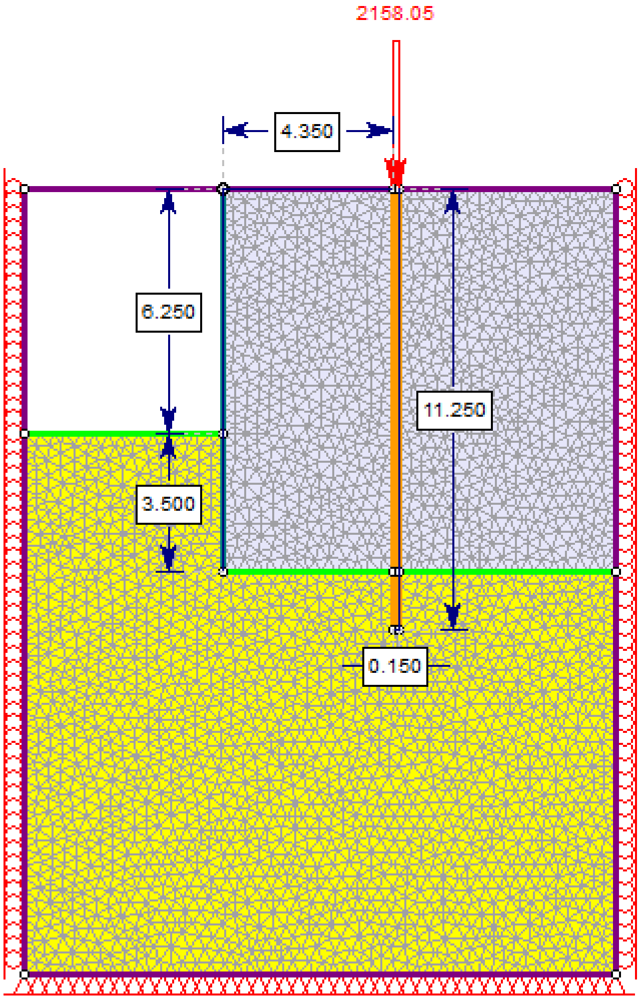

M 185.1: Original model (stage 3)

C_1'	ϕ_1'	γ_1	E_1	C_2'	ϕ_2'	γ_2	E_2	H_1	H_2	H_3	E_3	D_1	D_2	L	Qult
0	33	18	28	59	13	24	27.0	6.25	3.5	1	899082	4.35	0.15	11.25	2158.05

M 185.2: Parameter values

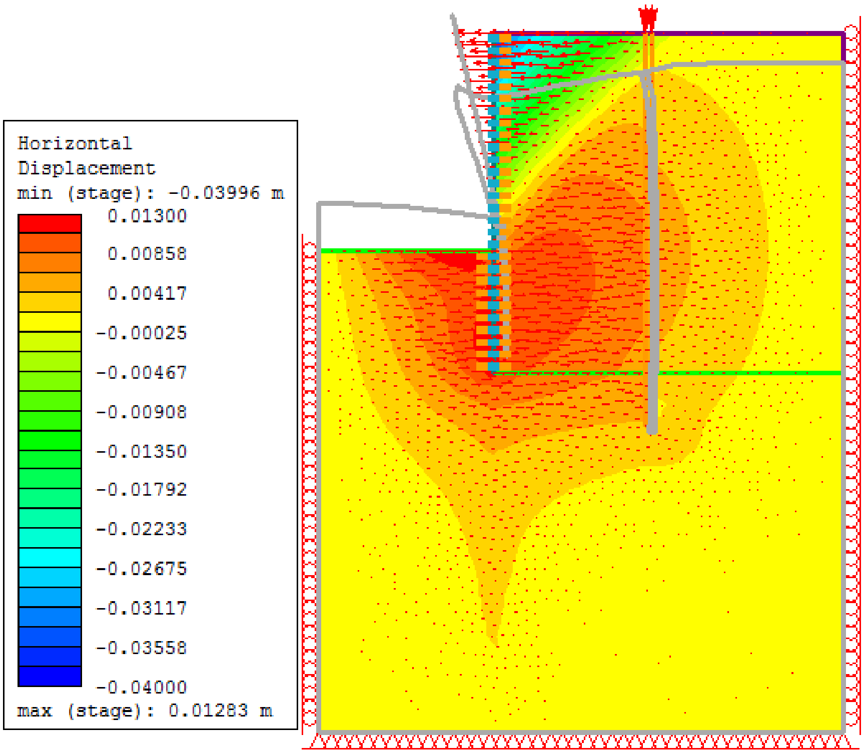

M 185.3: Deformed model (stage 3)

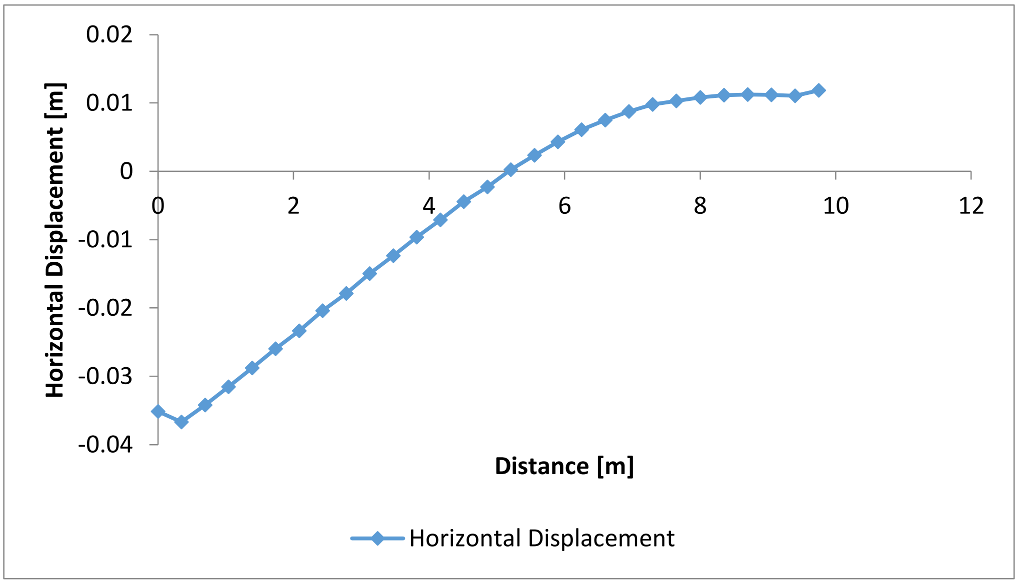

M 185.4: Horizontal displacement of soil along retaining wall

Retaining wall maximum horizontal displacement: -0.03996m

Distance from point of maximum displacement in retaining wall to the top of backfill soil: 0.0m

Model 186:

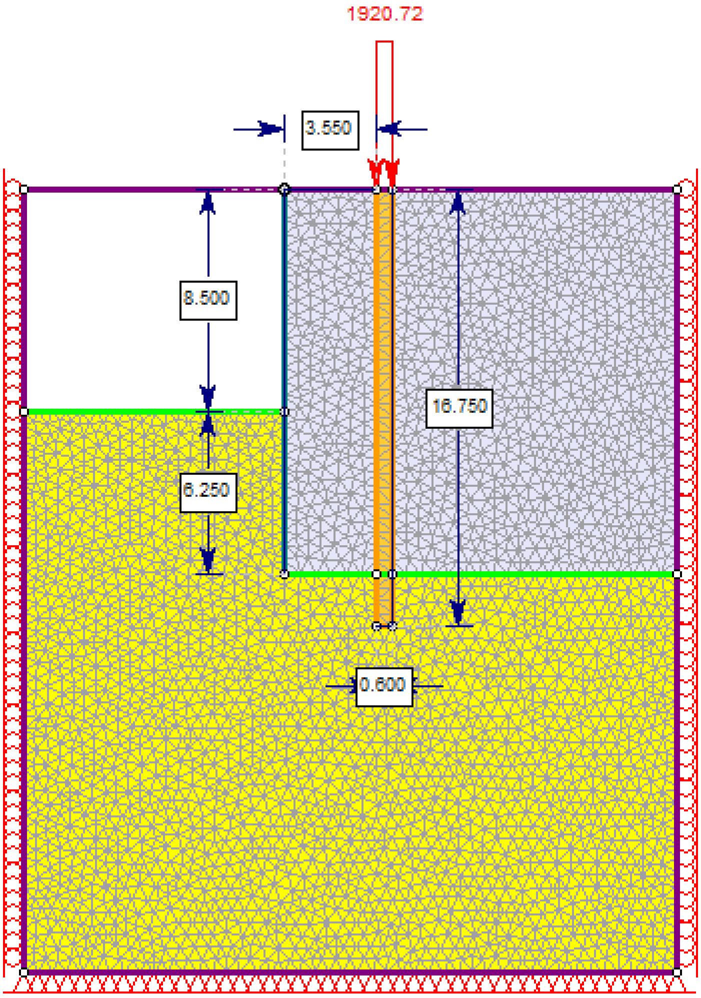

M 186.1: Original model (stage 3)

C_1'	ϕ_1'	γ_1	E_1	C_2'	ϕ_2'	γ_2	E_2	H_1	H_2	H_3	E_3	D_1	D_2	L	Qult
0	37	18	123	60	3	21	45.4	8.50	6.25	1.25	965515	3.55	0.6	16.75	1920.72

M 186.2: Parameter values

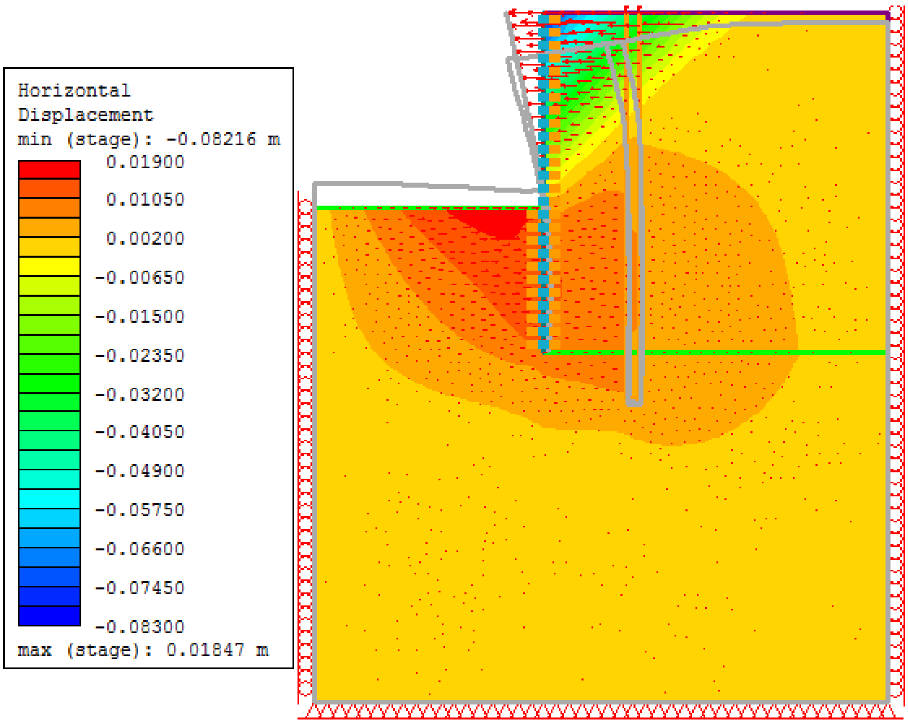

M 186.3: Deformed model (stage 3)

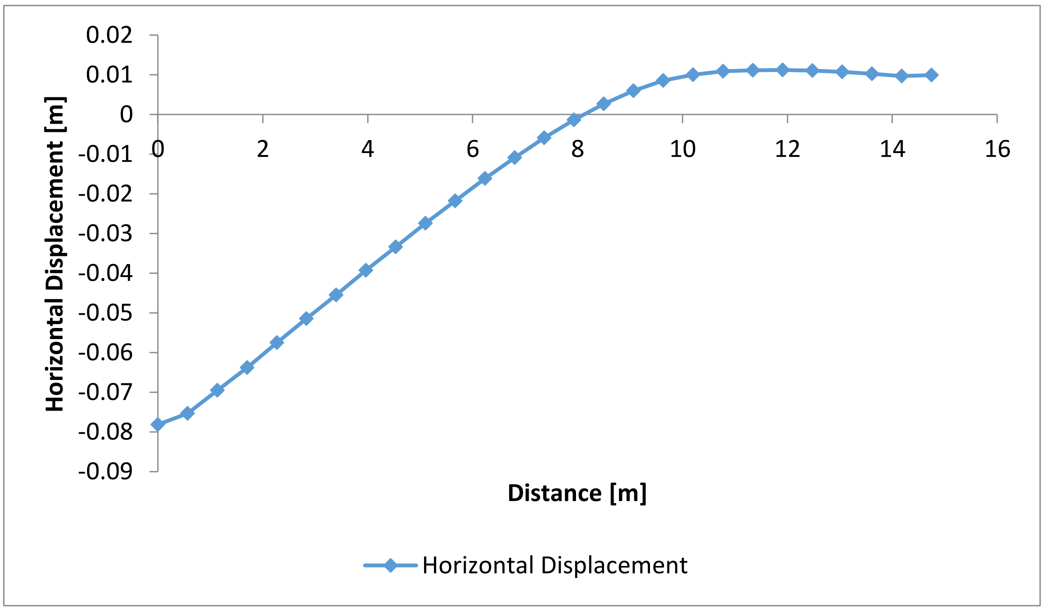

M 186.4: Horizontal displacement of soil along retaining wall

Retaining wall maximum horizontal displacement: -0.08216m

Distance from point of maximum displacement in retaining wall to the top of backfill soil: 0.0m

Model 187:

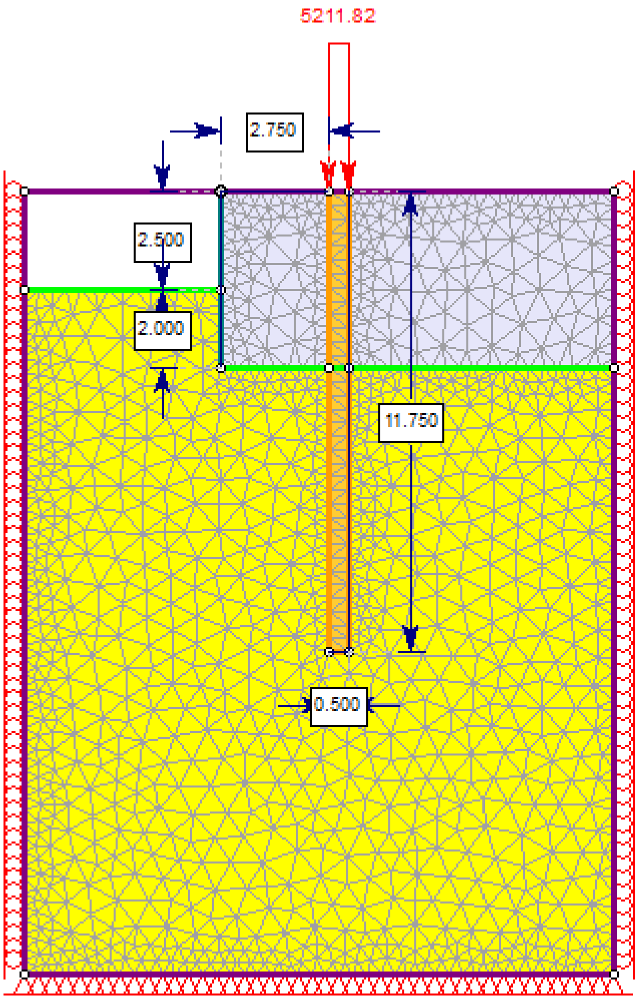

M 187.1: Original model (stage 3)

C_1'	ϕ_1'	γ_1	E_1	C_2'	ϕ_2'	γ_2	E_2	H_1	H_2	H_3	E_3	D_1	D_2	L	Qult
0	43	22	77	19	30	17	22.1	2.50	2	1.25	998263	2.75	0.5	11.75	5211.82

M 187.2: Parameter values

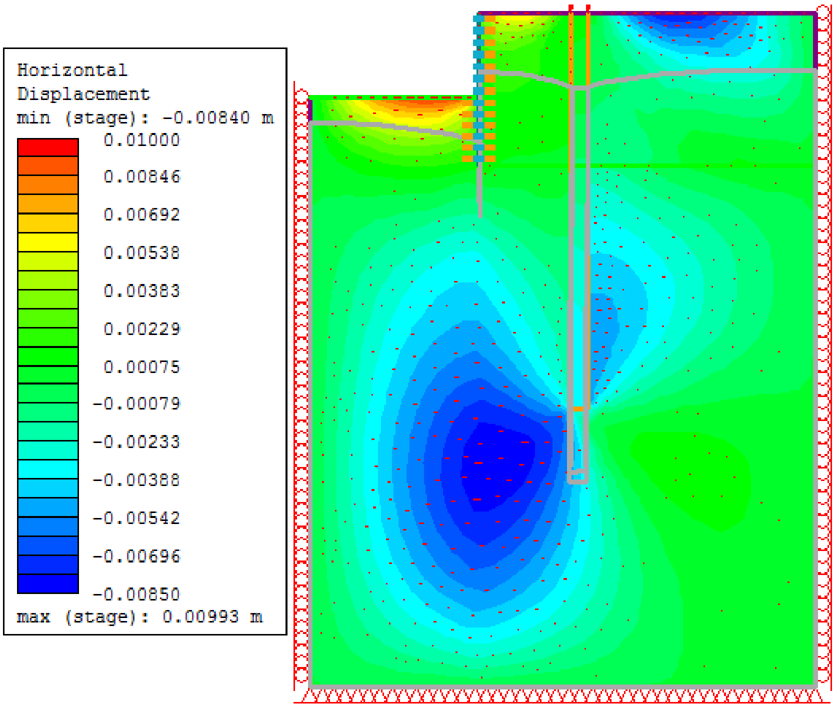

M 187.3: Deformed model (stage 3)

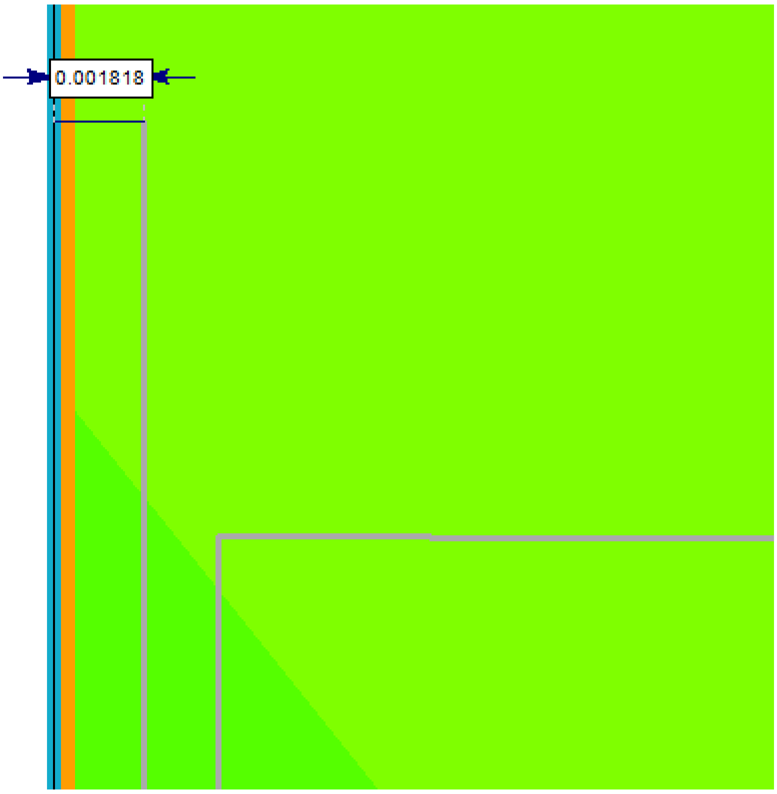

M 187.4: Detailed view of cross-section of retaining wall and soil (stage 3)

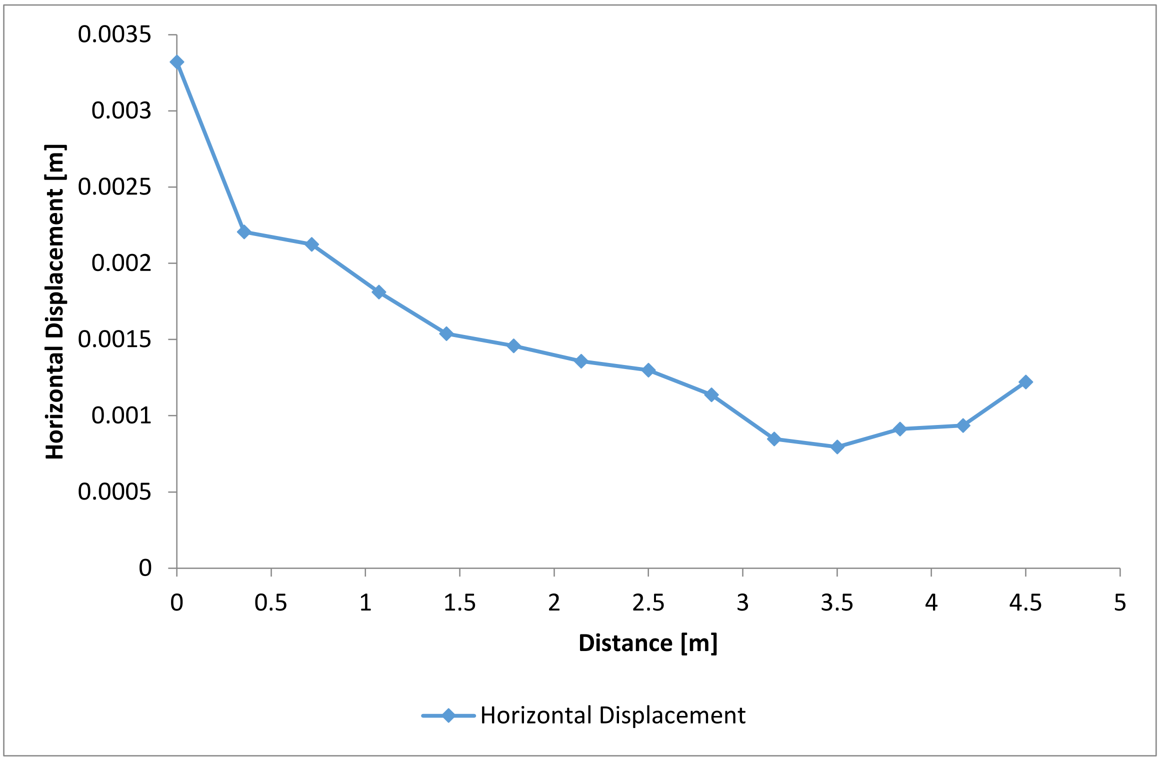

M 187.5: Horizontal displacement of soil along retaining wall

Retaining wall maximum horizontal displacement: 0.001818m

Distance from point of maximum displacement in retaining wall to the top of backfill soil: 0.0m

Model 188:

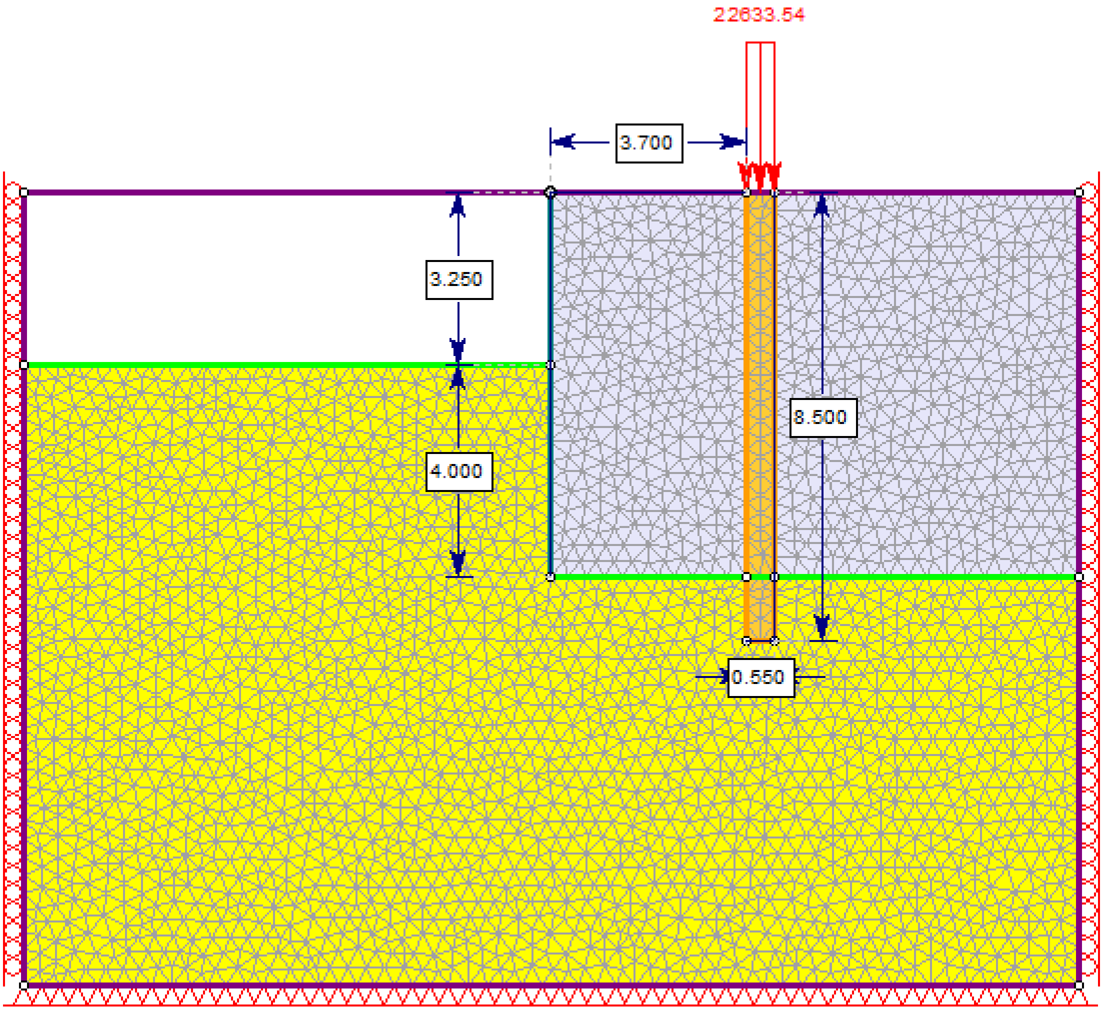

M 188.1: Original model (stage 3)

C'_1	ϕ'_1	γ_1	E_1	C'_2	ϕ'_2	γ_2	E_2	H_1	H_2	H_3	E_3	D_1	D_2	L	Qult
0	35	20	15	21	26	20	45.7	3.25	4	1.5	949483	3.7	0.55	8.5	2633.54

M 188.2: Parameter values

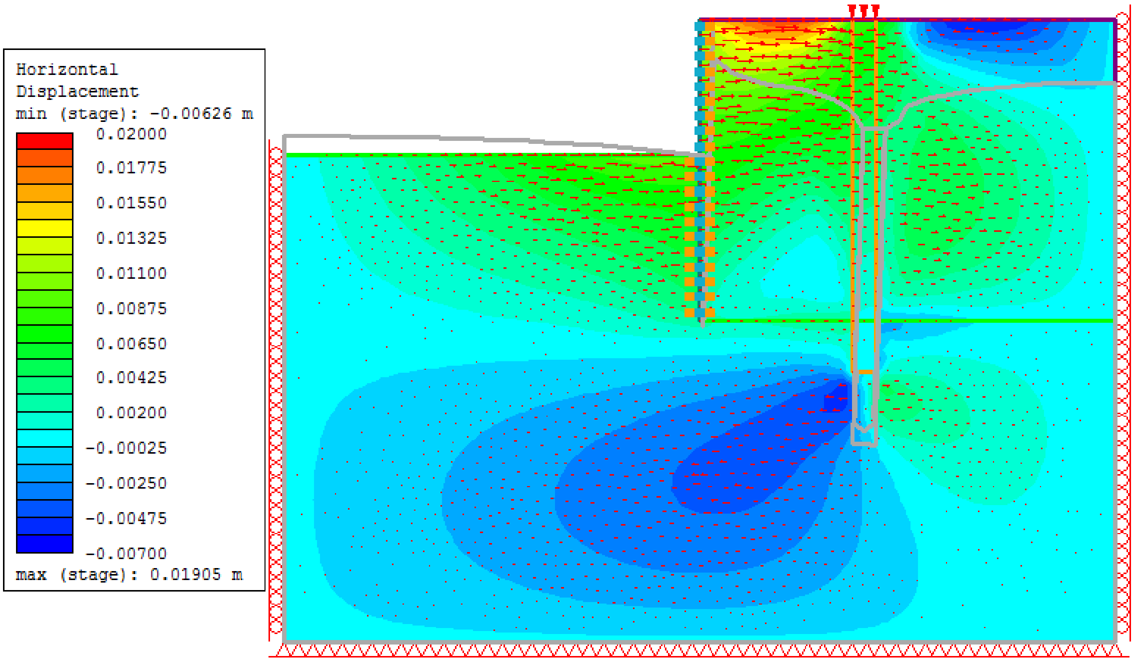

M 188.3: Deformed model (stage 3)

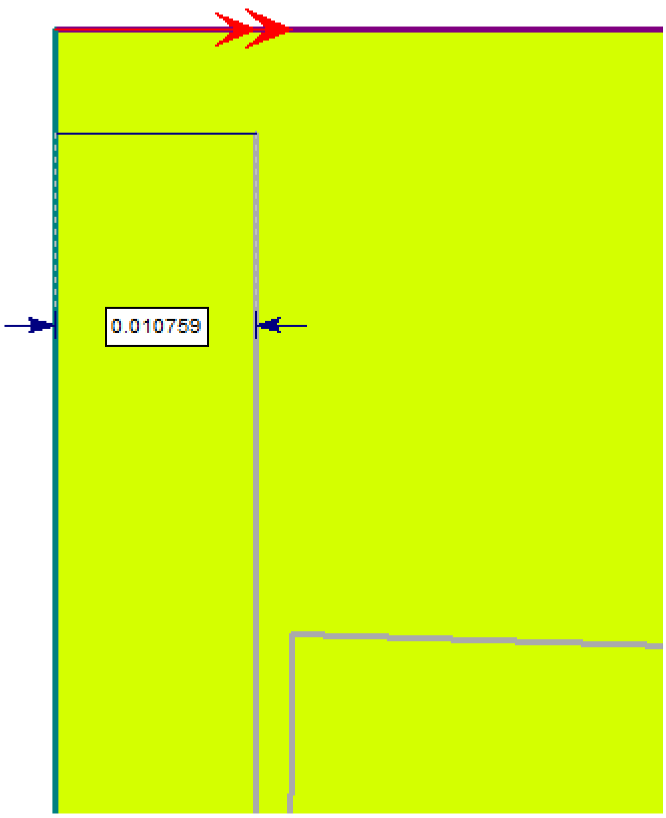

M 188.4: Detailed view of cross-section of retaining wall and soil (stage 3)

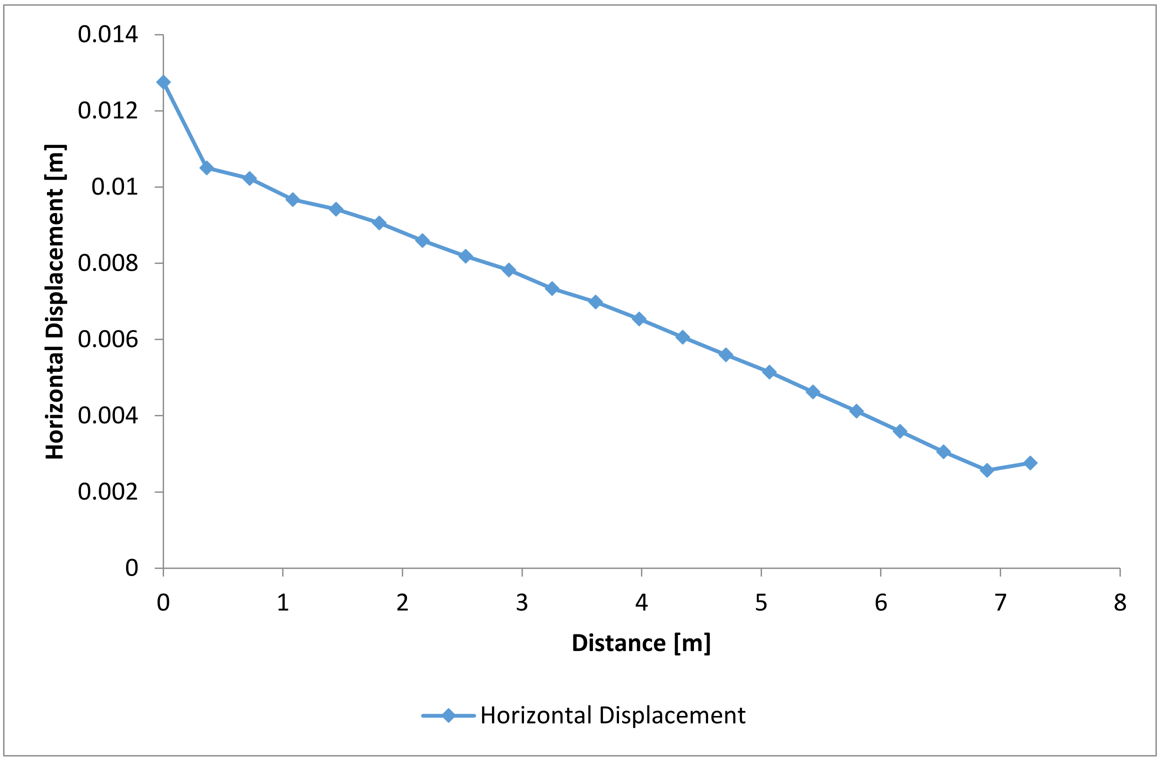

M 188.5: Horizontal displacement of soil along retaining wall

Retaining wall maximum horizontal displacement: 0.010759m

Distance from point of maximum displacement in retaining wall to the top of backfill soil: 0.0m

Model 189:

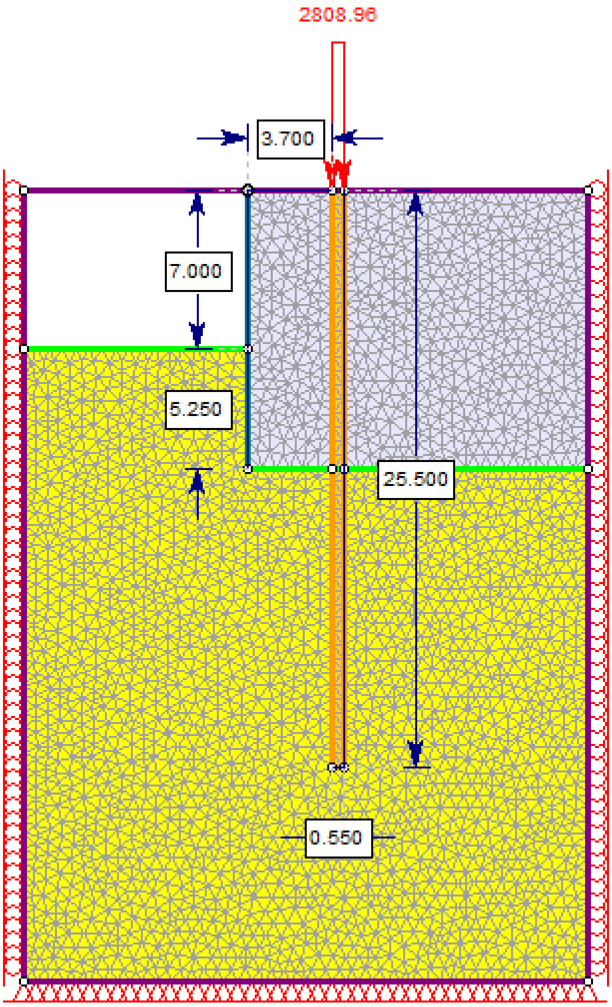

M 189.1: Original model (stage 3)

C_1'	ϕ_1'	γ_1	E_1	C_2'	ϕ_2'	γ_2	E_2	H_1	H_2	H_3	E_3	D_1	D_2	L	Qult
0	32	18	244	53	10	23	43.3	7.00	5.25	1.5	785758	3.7	0.55	25.5	2808.96

M 189.2: Parameter values

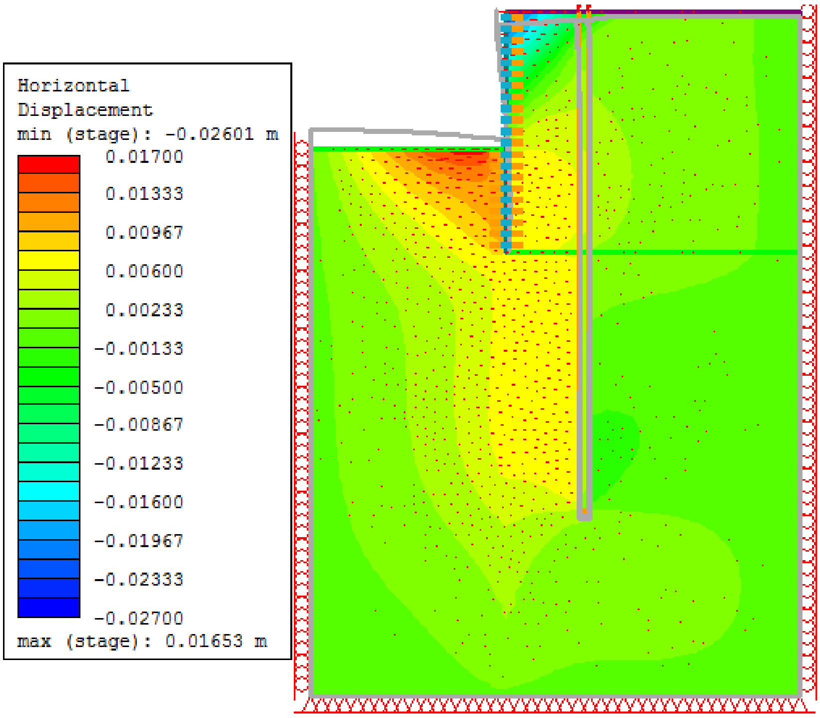

M 189.3: Deformed model (stage 3)

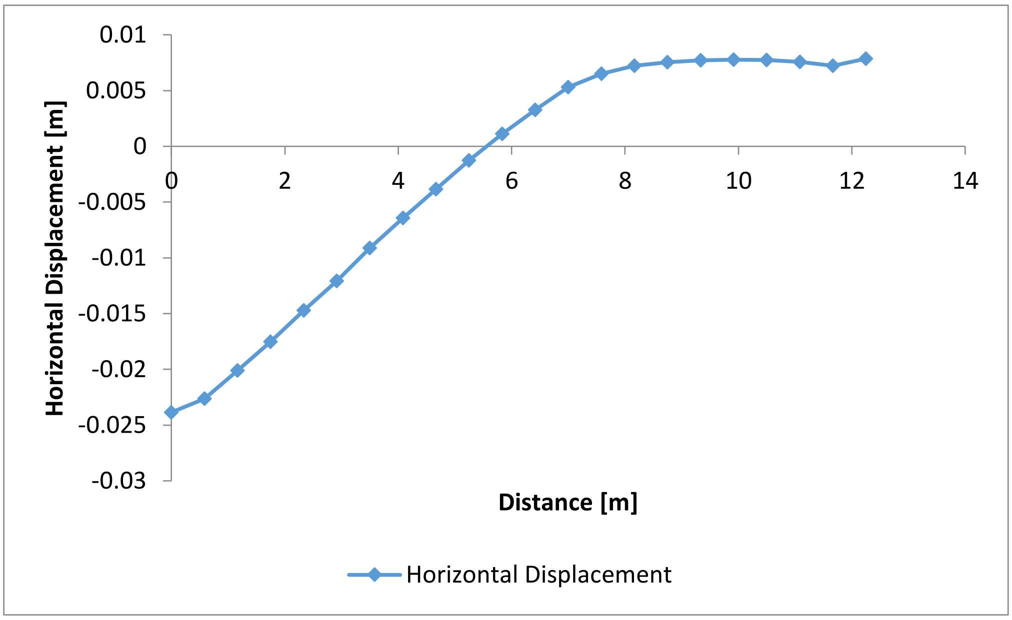

M 189.4: Horizontal displacement of soil along retaining wall

Retaining wall maximum horizontal displacement: -0.02601m

Distance from point of maximum displacement in retaining wall to the top of backfill soil: 0.0m

Model 190:

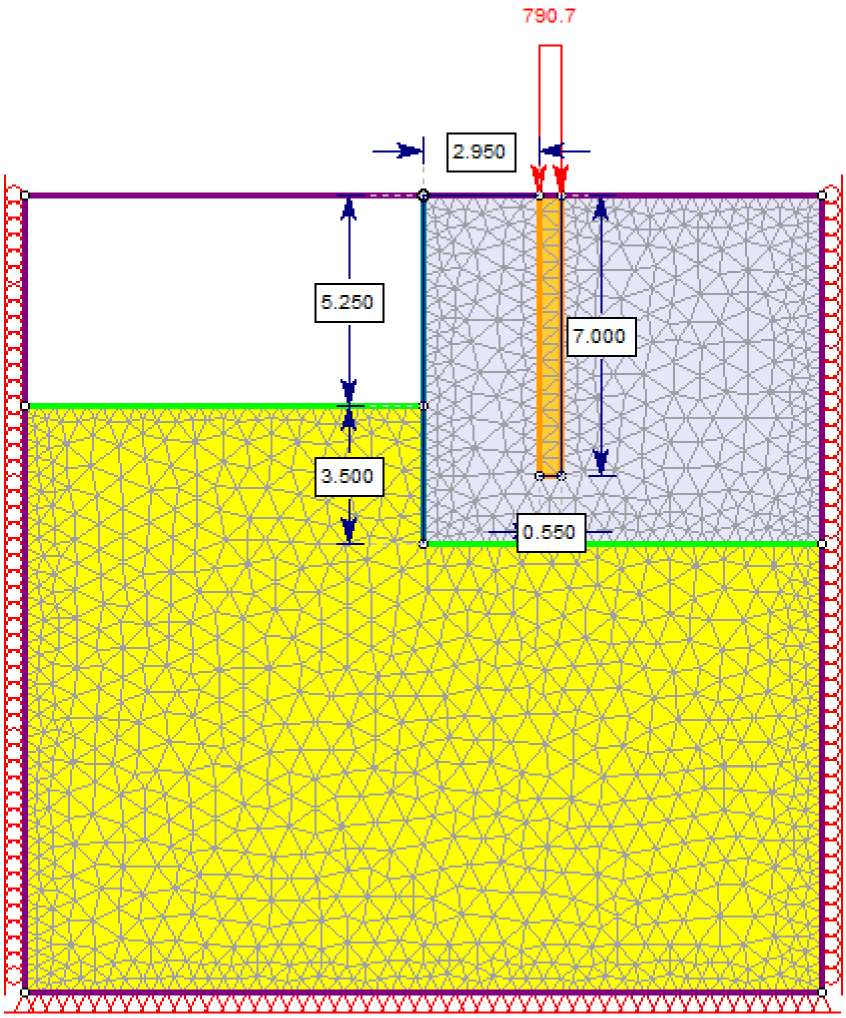

M 190.1: Original model (stage 3)

C'_1	ϕ'_1	γ_1	E_1	C'_2	ϕ'_2	γ_2	E_2	H_1	H_2	H_3	E_3	D_1	D_2	L	Qult
0	29	20	35	51	3	19	2.9	5.25	3.5	1.5	882212	2.95	0.55	7	790.7

M 190.2: Parameter values

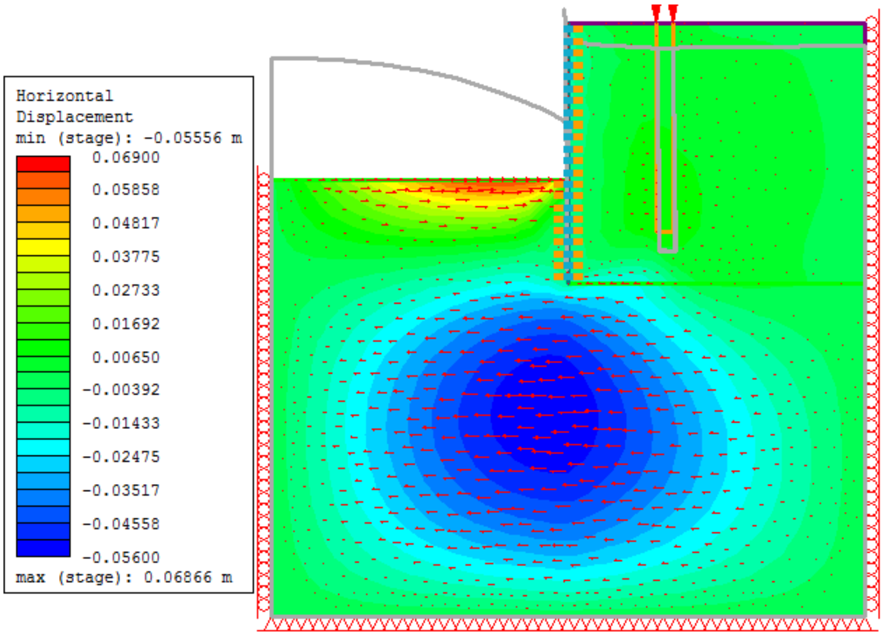

M 190.3: Deformed model (stage 3)

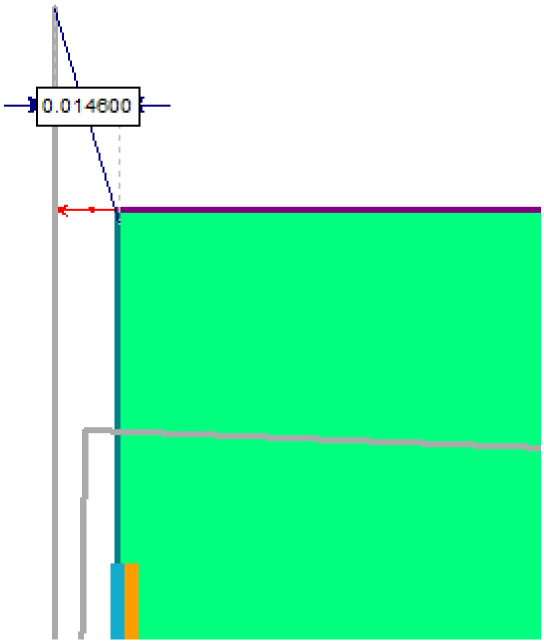

M 190.4: Detailed view of cross-section of retaining wall and soil (stage 3)

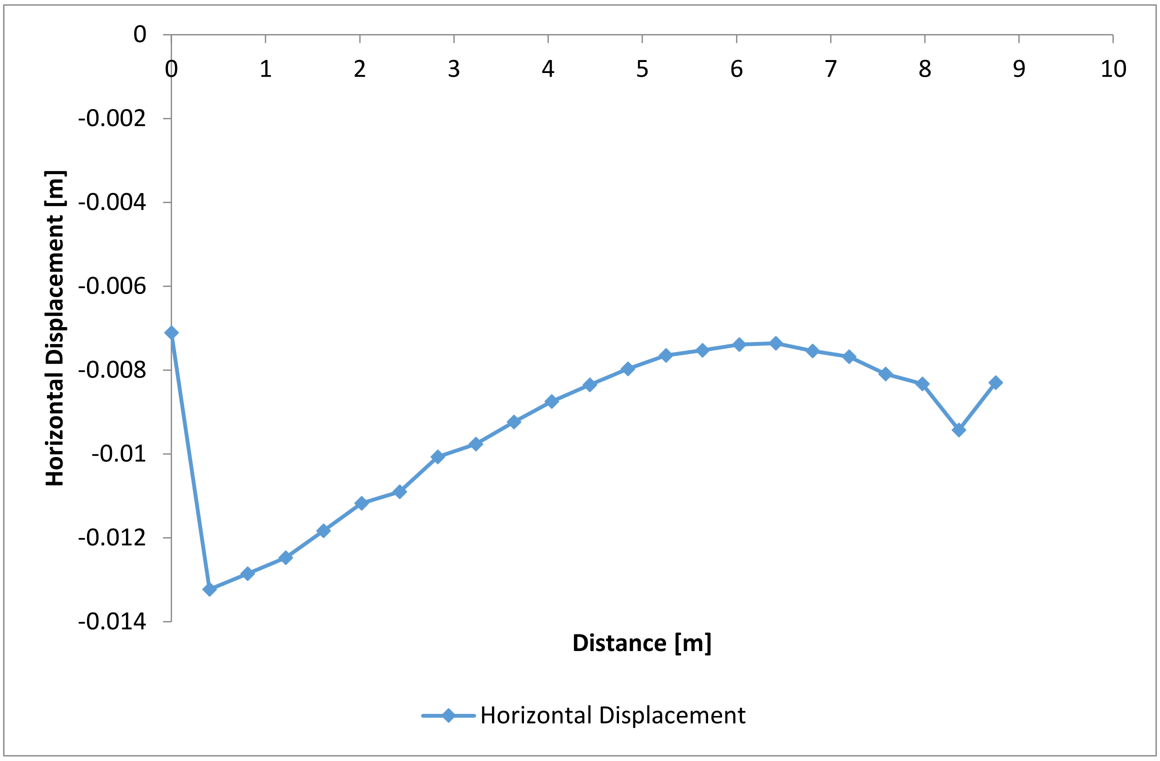

M 190.5: Horizontal displacement of soil along retaining wall

Retaining wall maximum horizontal displacement: -0.0146m

Distance from point of maximum displacement in retaining wall to the top of backfill soil: 0.0m

Model 191:

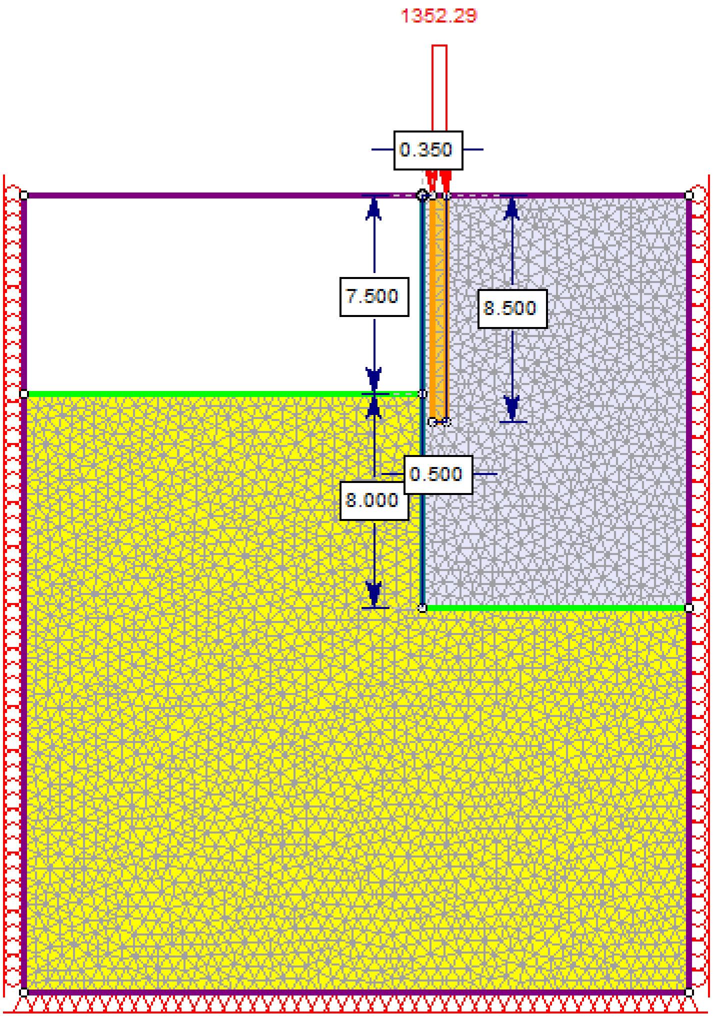

M 191.1: Original model (stage 3)

C_1'	ϕ_1'	γ_1	E_1	C_2'	ϕ_2'	γ_2	E_2	H_1	H_2	H_3	E_3	D_1	D_2	L	Qult
0	30	20	249	56	17	16	42.8	7.50	8	1.5	1116838	0.35	0.5	8.5	1352.29

M 191.2: Parameter values

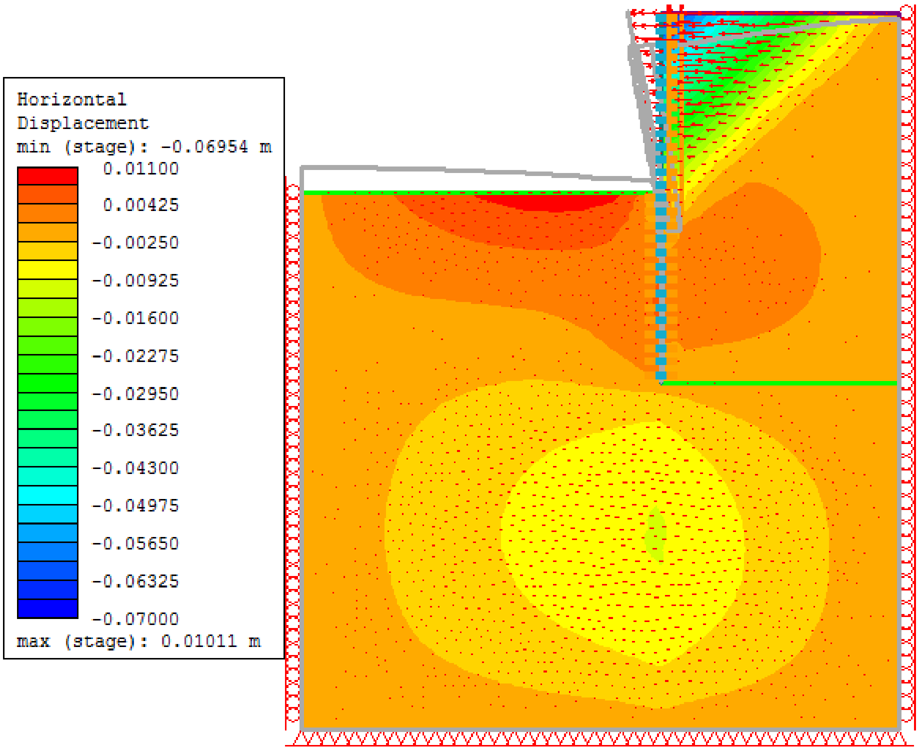

M 191.3: Deformed model (stage 3)

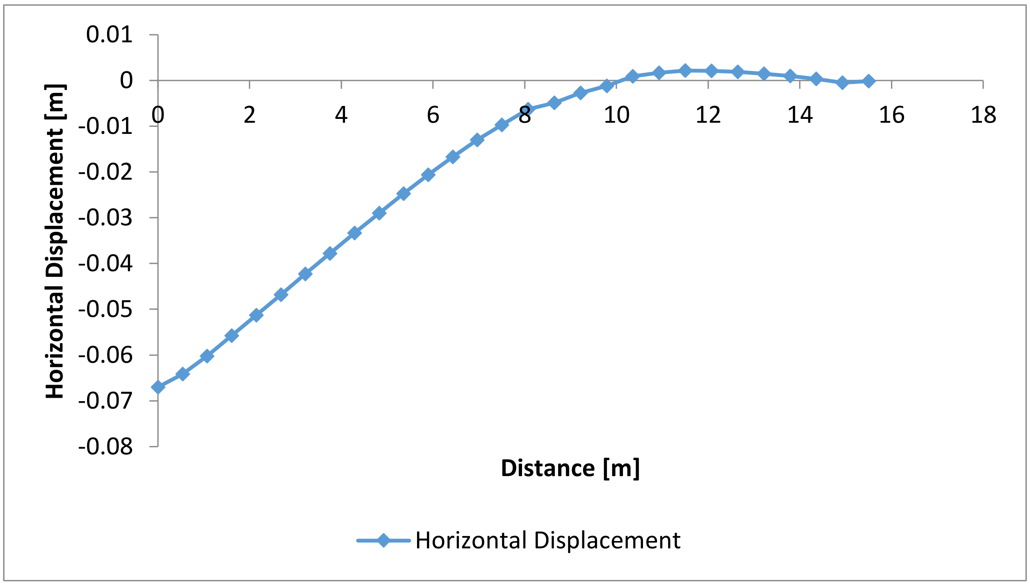

M 191.4: Horizontal displacement of soil along retaining wall

Retaining wall maximum horizontal displacement: -0.06954m

Distance from point of maximum displacement in retaining wall to the top of backfill soil: 0.0m

Model 192:

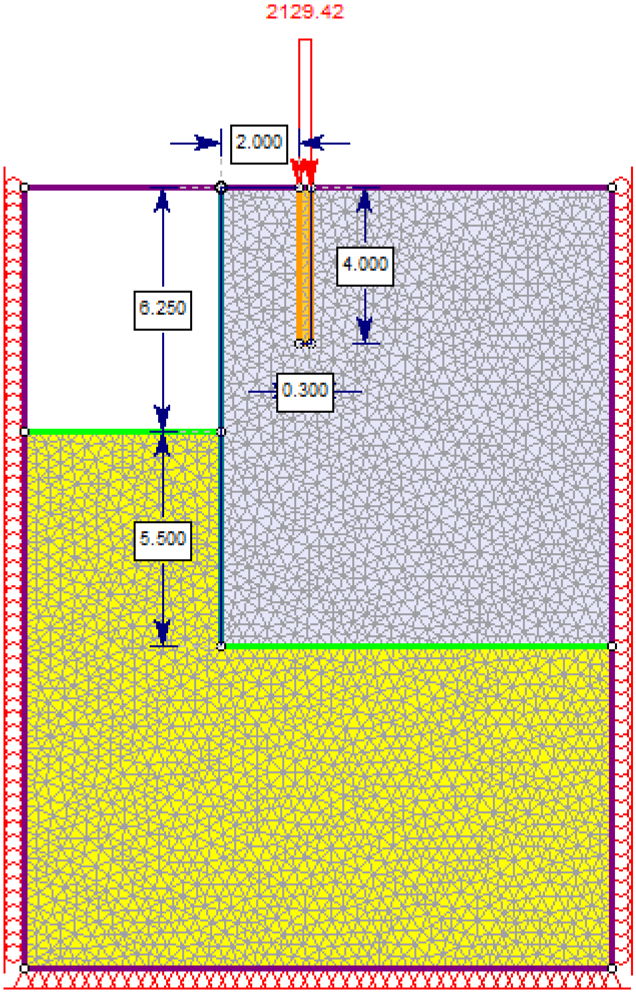

M 192.1: Original model (stage 3)

C_1'	ϕ_1'	γ_1	E_1	C_2'	ϕ_2'	γ_2	E_2	H_1	H_2	H_3	E_3	D_1	D_2	L	Qult
0	36	21	37	48	20	16	26.9	6.25	5.5	0.75	991567	2	0.3	4	2129.42

M 192.2: Parameter values

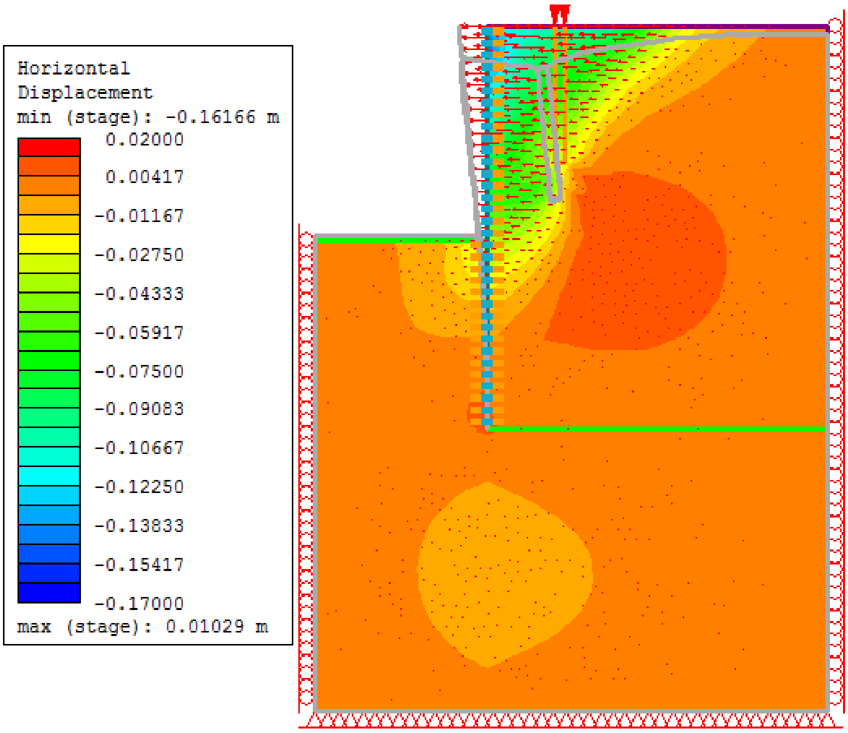

M 192.3: Deformed model (stage 3)

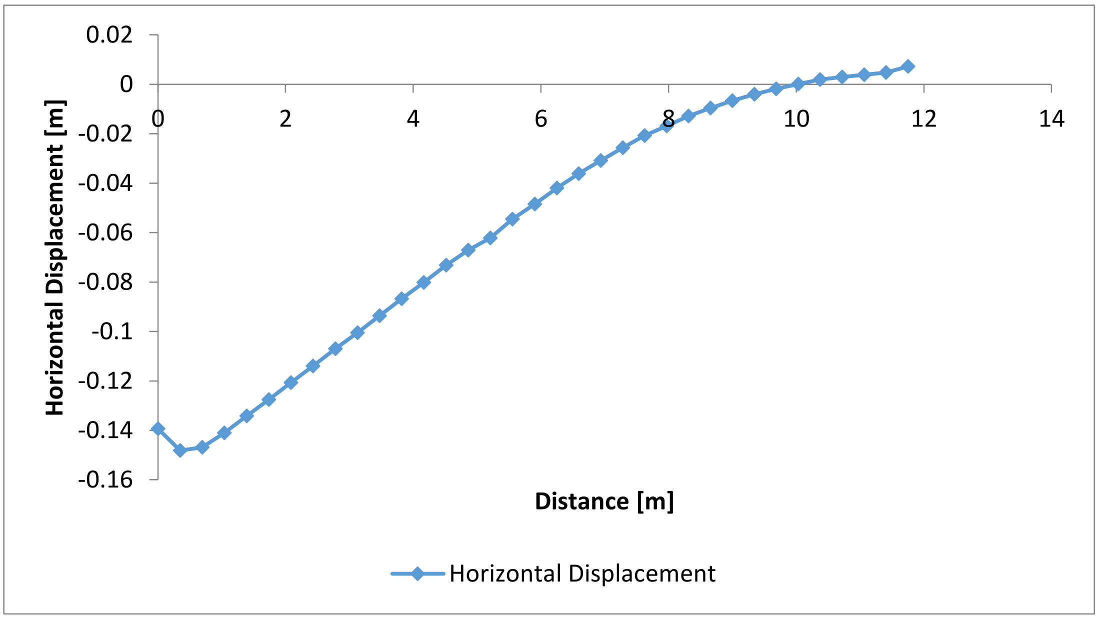

M 192.4: Horizontal displacement of soil along retaining wall

Retaining wall maximum horizontal displacement: -0.16166m

Distance from point of maximum displacement in retaining wall to the top of backfill soil: 0.0m

Model 193:

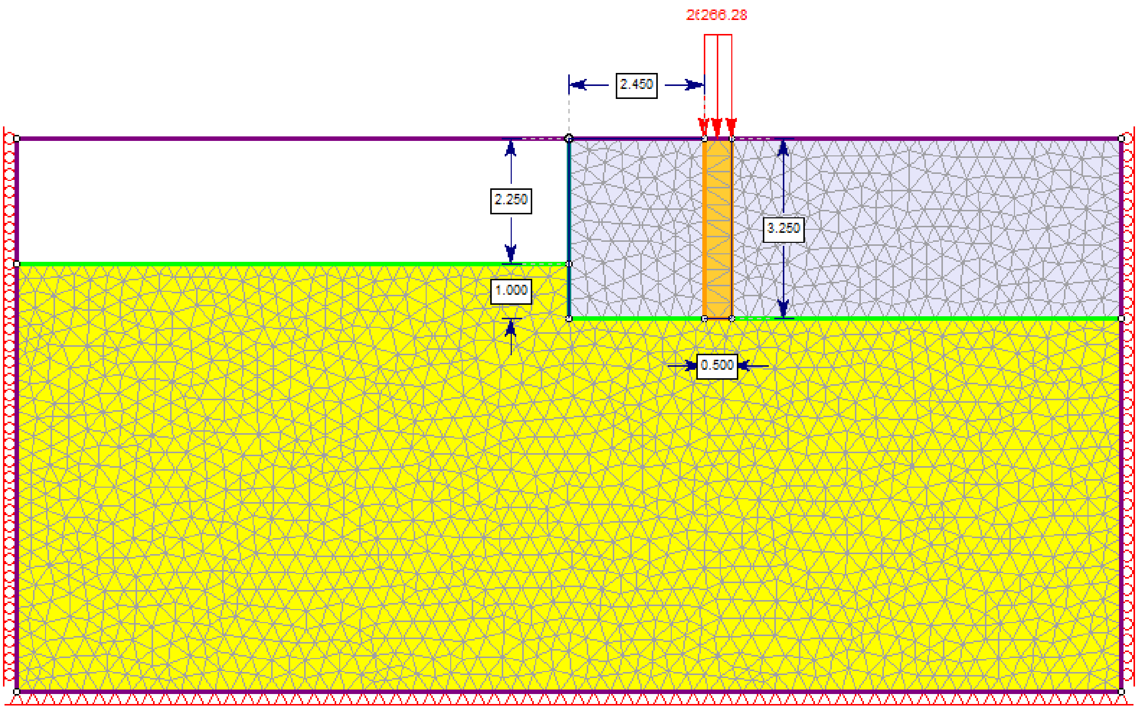

M 193.1: Original model (stage 3)

C_1'	ϕ_1'	γ_1	E_1	C_2'	ϕ_2'	γ_2	E_2	H_1	H_2	H_3	E_3	D_1	D_2	L	Qult
0	30	18	202	32	6	19	38.6	2.25	1	1.25	920209	1.45	0.5	3.25	266.28

M 193.2: Parameter values

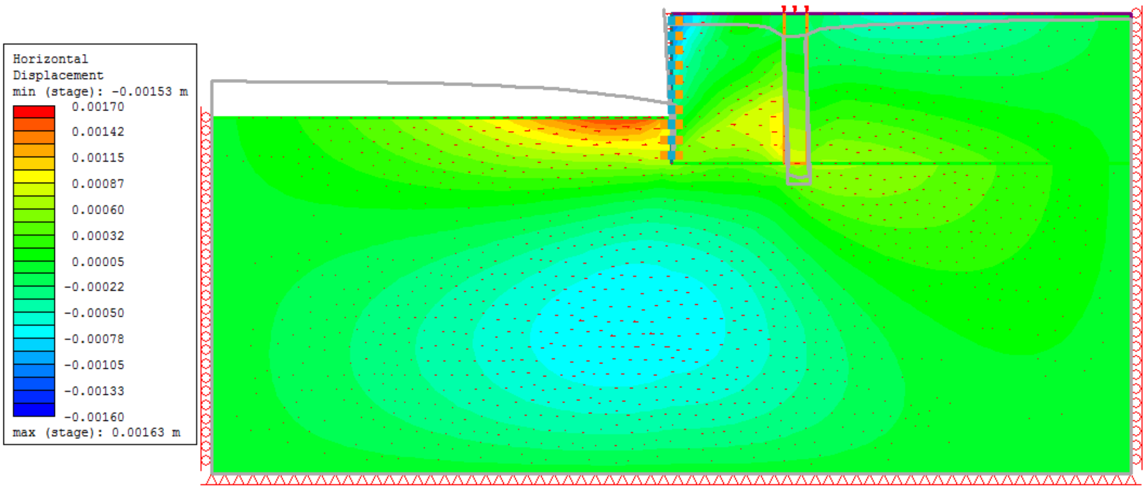

M 193.3: Deformed model (stage 3)

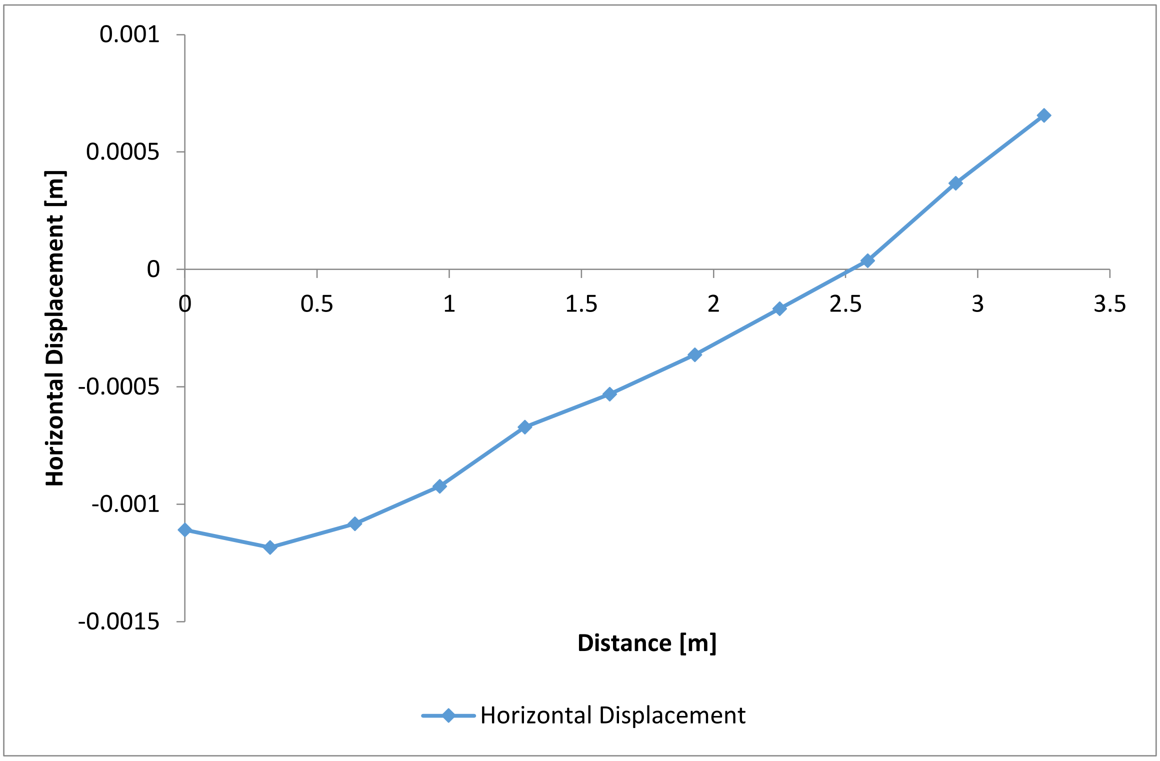

M 193.4: Horizontal displacement of soil along retaining wall

Retaining wall maximum horizontal displacement: -0.00153m

Distance from point of maximum displacement in retaining wall to the top of backfill soil: 0.0m

Model 194:

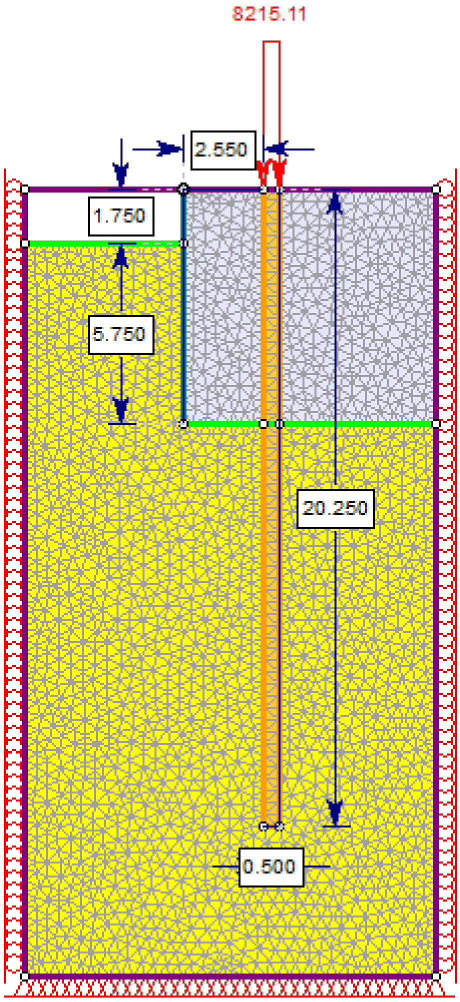

M 194.1: Original model (stage 3)

C'_1	ϕ'_1	γ_1	E_1	C'_2	ϕ'_2	γ_2	E_2	H_1	H_2	H_3	E_3	D_1	D_2	L	Qult
0	41	22	215	10	28	22	42.3	1.75	5.75	0.75	1129907	2.55	0.5	20.25	8215.11

M 194.2: Parameter values

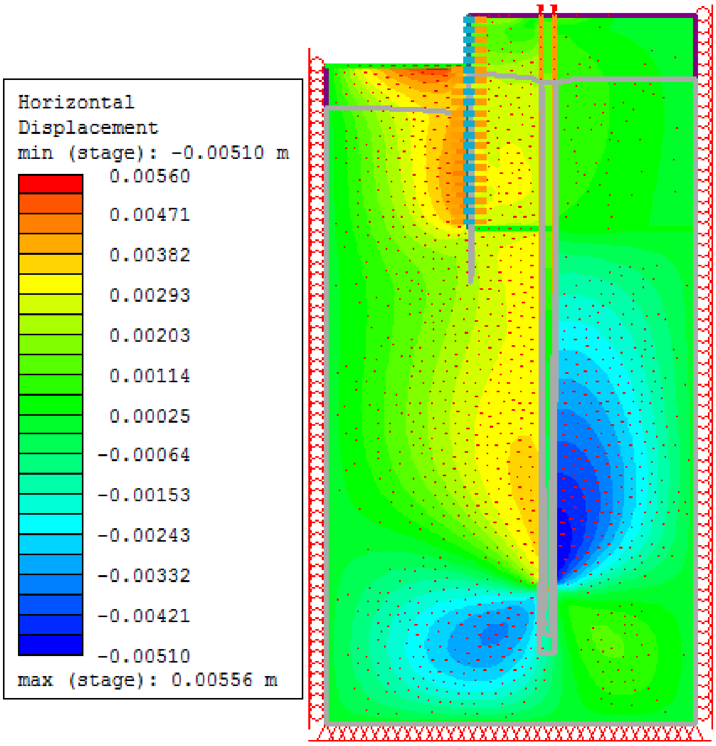

M 194.3: Deformed model (stage 3)

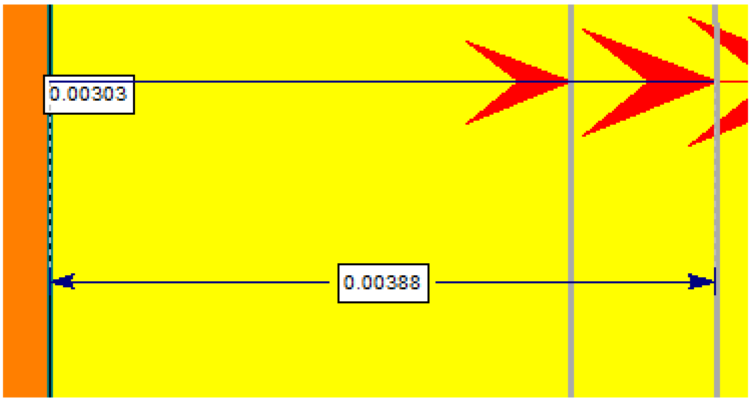

M 194.4: Detailed view of cross-section of retaining wall and soil (stage 3)

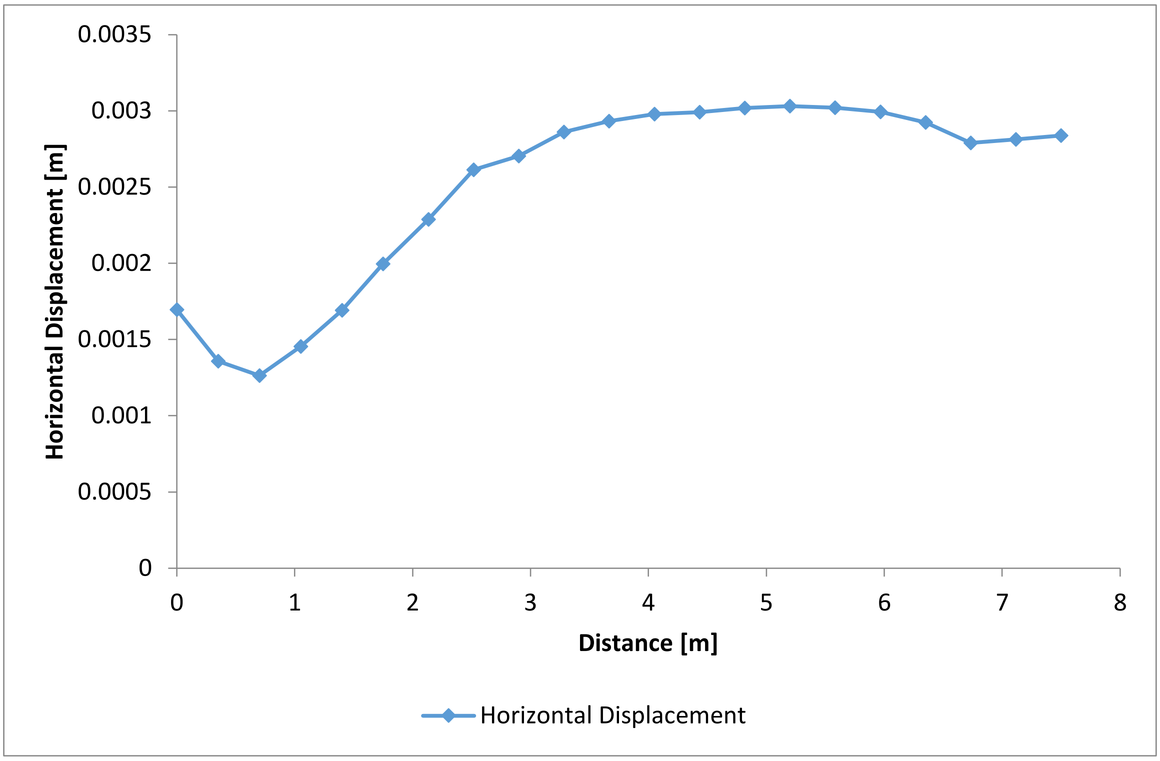

M 194.5: Horizontal displacement of soil along retaining wall

Retaining wall maximum horizontal displacement: 0.00388m

Distance from point of maximum displacement in retaining wall to the top of backfill soil: 5.2m

Model 195:

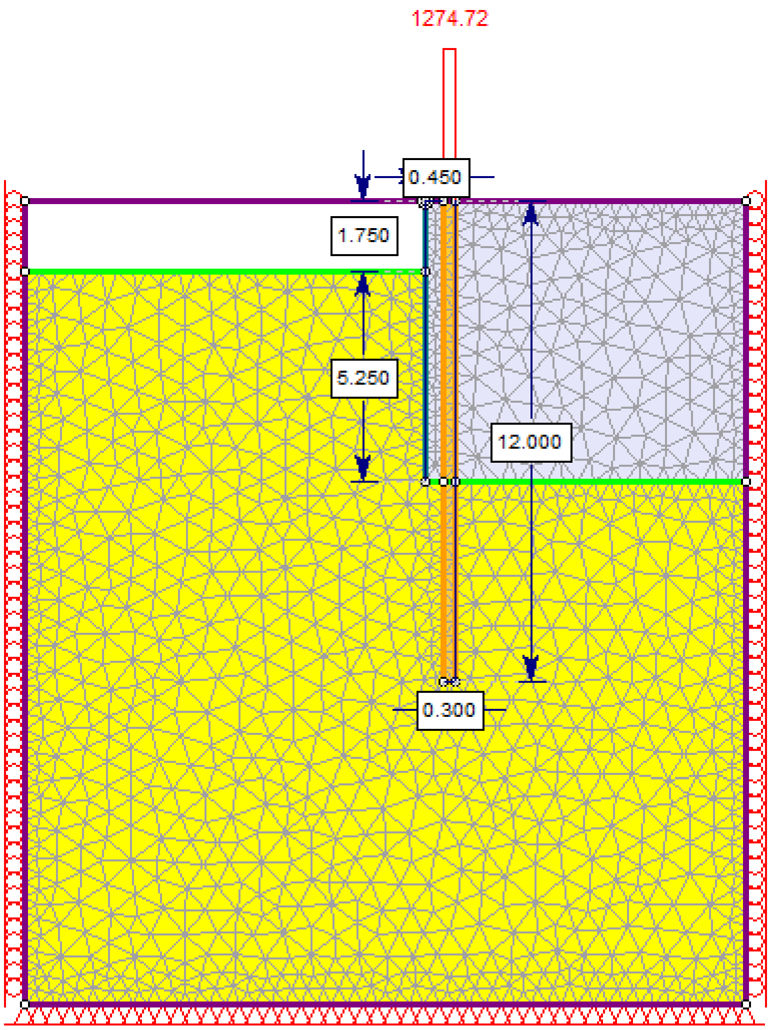

M 195.1: Original model (stage 3)

C_1'	ϕ_1'	γ_1	E_1	C_2'	ϕ_2'	γ_2	E_2	H_1	H_2	H_3	E_3	D_1	D_2	L	Qult
0	31	19	254	9	12	18	22.8	1.75	5.25	0.5	1004124	0.45	0.3	12	1274.72

M 195.2: Parameter values

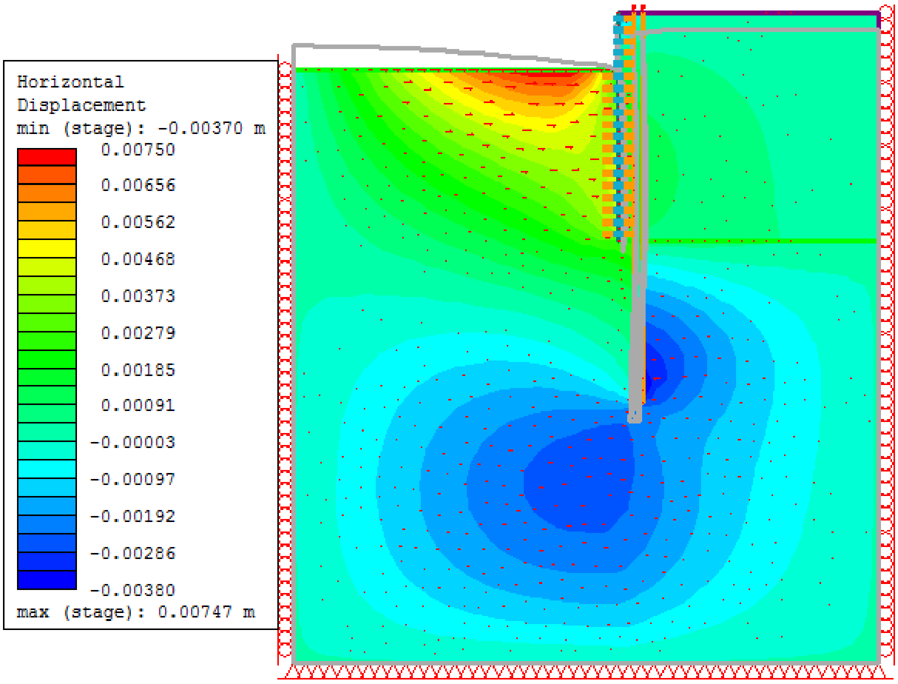

M 195.3: Deformed model (stage 3)

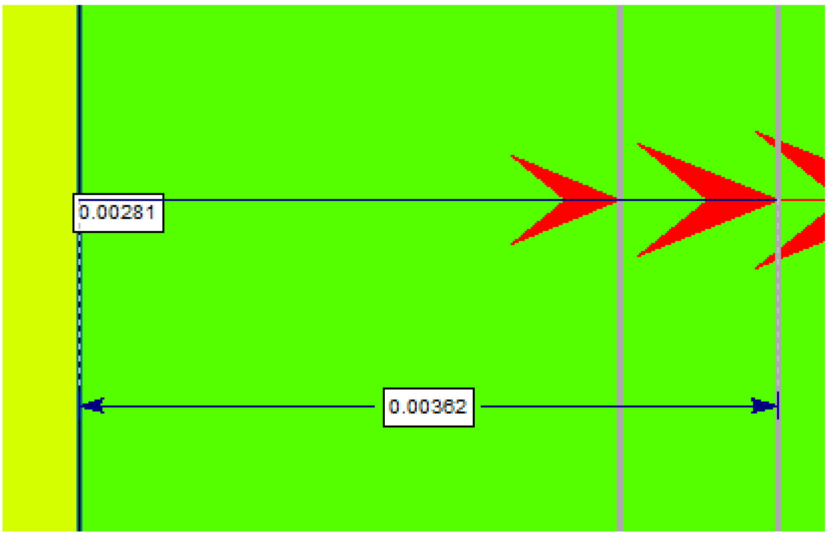

M 195.4: Detailed view of cross-section of retaining wall and soil (stage 3)

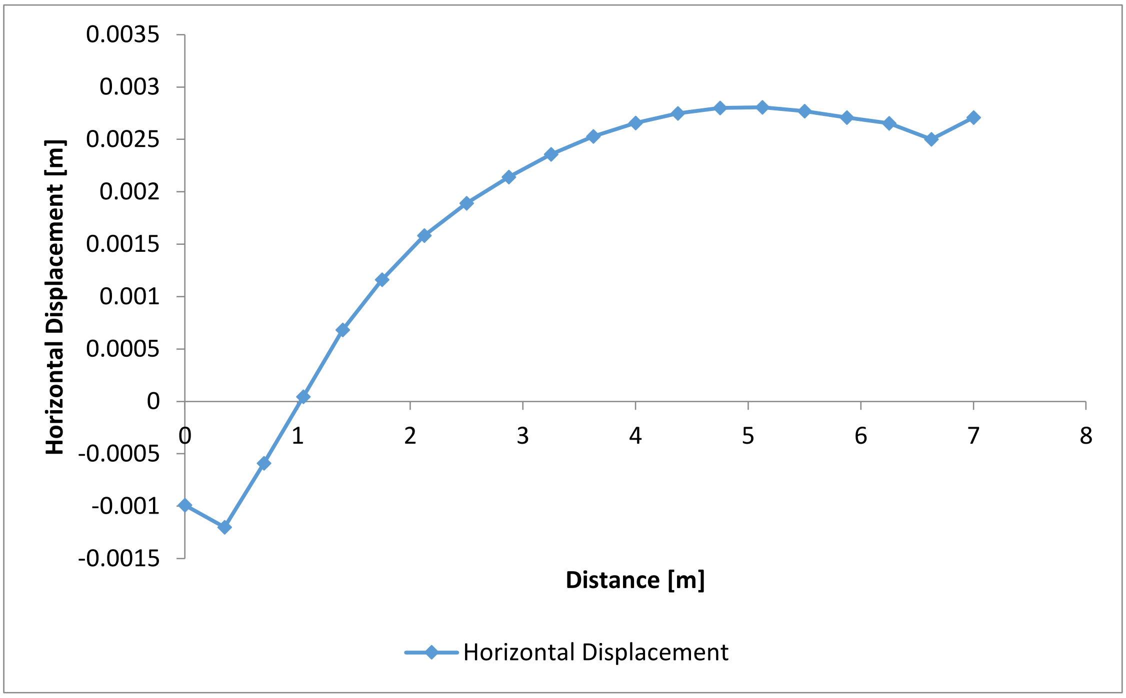

M 195.5: Horizontal displacement of soil along retaining wall

Retaining wall maximum horizontal displacement: 0.00362m

Distance from point of maximum displacement in retaining wall to the top of backfill soil: 5.125m

Model 196:

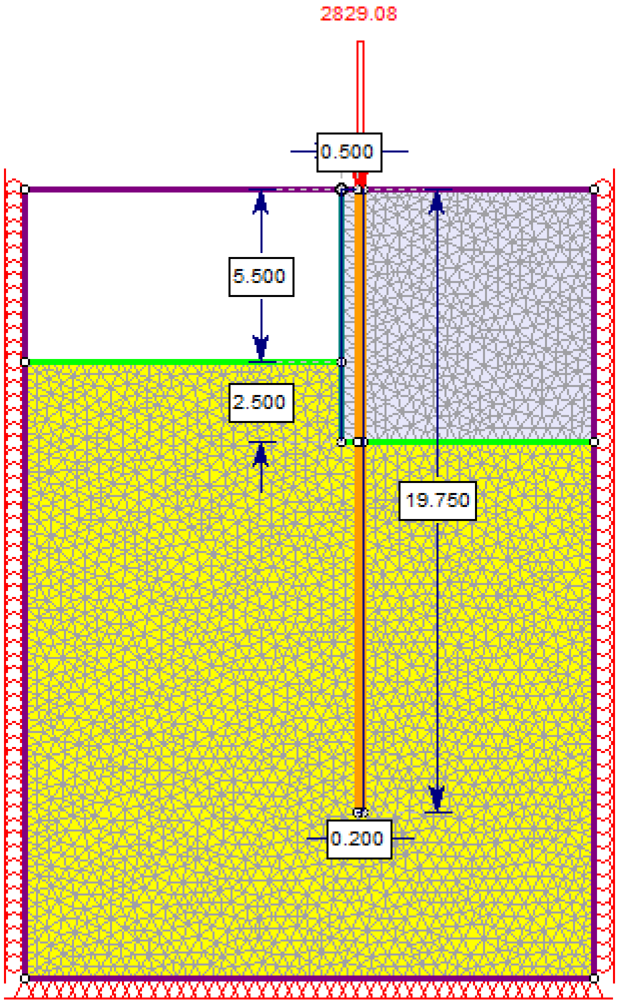

M 196.1: Original model (stage 3)

C'_1	ϕ'_1	γ_1	E_1	C'_2	ϕ'_2	γ_2	E_2	H_1	H_2	H_3	E_3	D_1	D_2	L	Qult
0	39	20	81	60	13	20	35.6	5.50	2.5	1.25	705803	0.5	0.2	19.75	2829.08

M 196.2: Parameter values

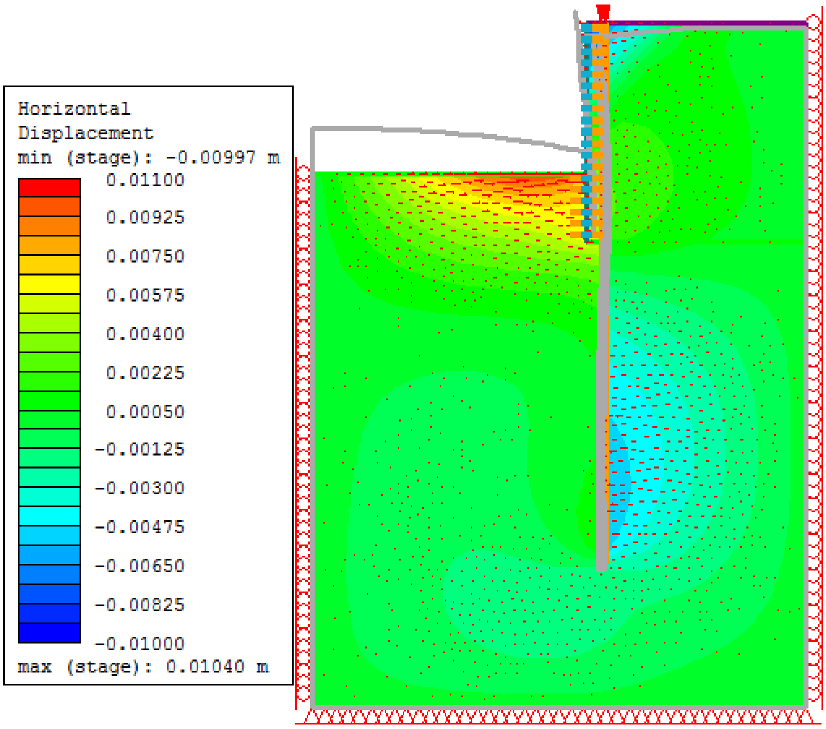

M 196.3: Deformed model (stage 3)

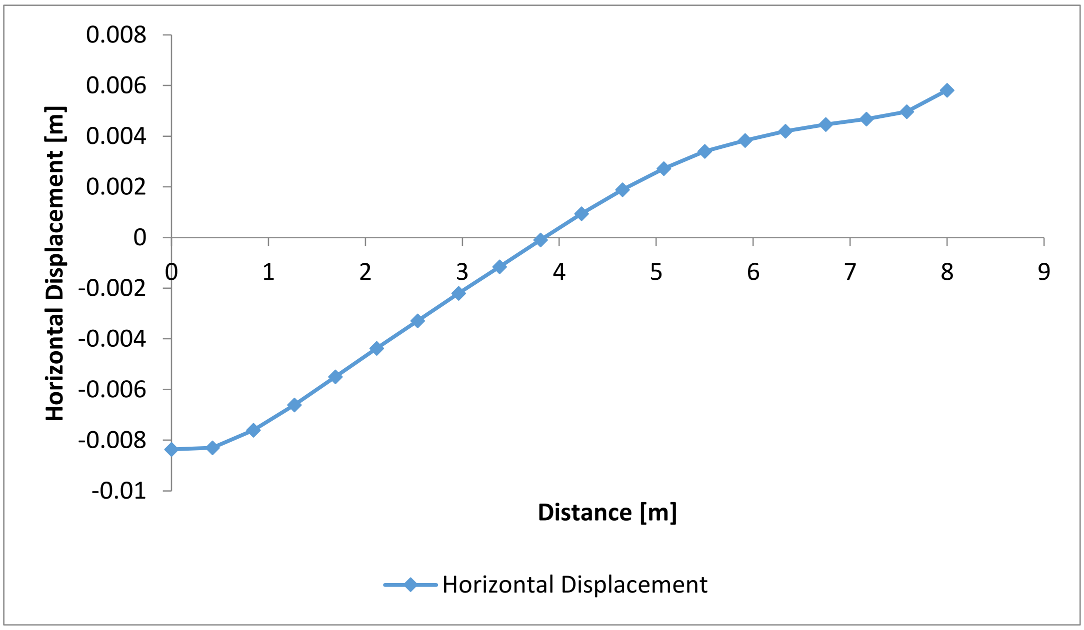

M 196.4: Horizontal displacement of soil along retaining wall

Retaining wall maximum horizontal displacement: -0.00997m

Distance from point of maximum displacement in retaining wall to the top of backfill soil: 0.0m

Model 197:

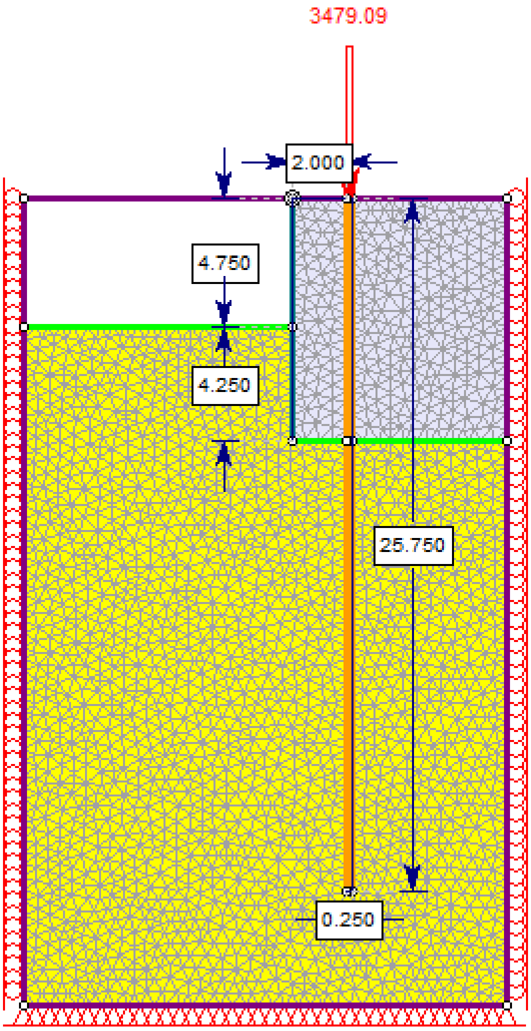

M 197.1: Original model (stage 3)

C'_1	ϕ'_1	γ_1	E_1	C'_2	ϕ'_2	γ_2	E_2	H_1	H_2	H_3	E_3	D_1	D_2	L	Qult
0	41	22	49	36	15	16	30.3	4.75	4.25	0.5	1041786	2	0.25	25.75	3479.09

M 197.2: Parameter values

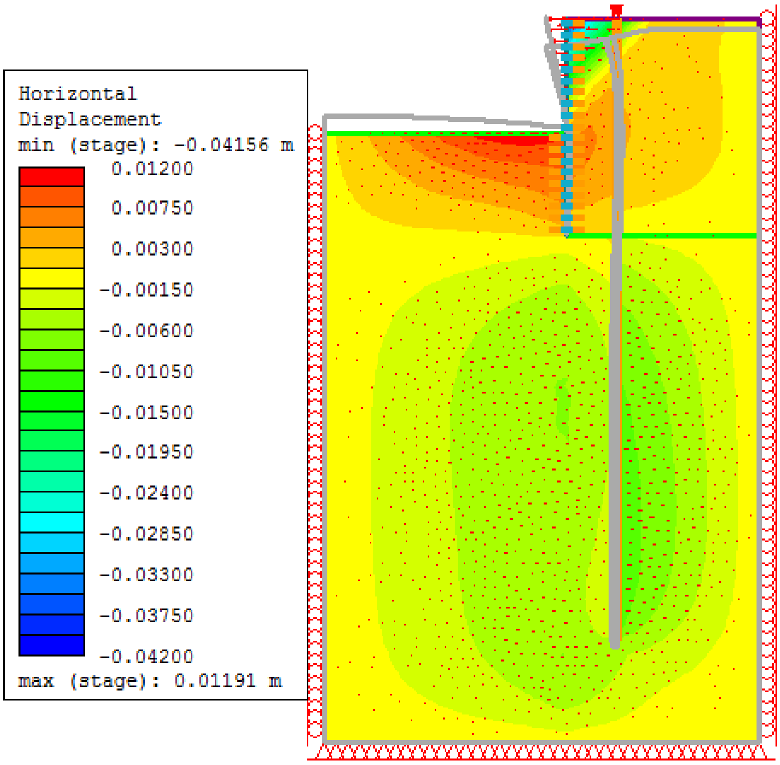

M 197.3: Deformed model (stage 3)

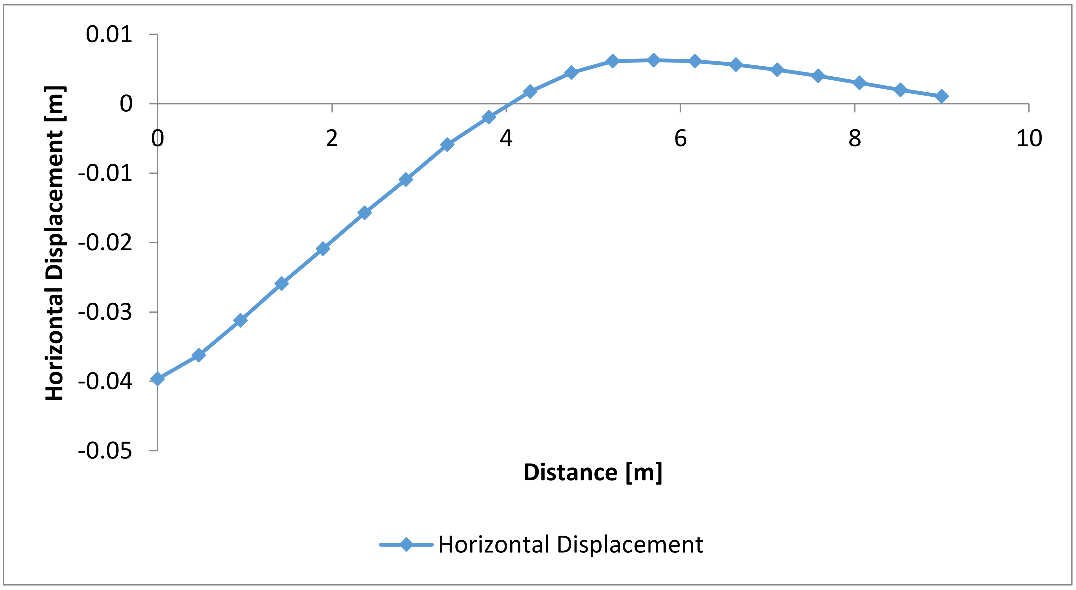

M 197.4: Horizontal displacement of soil along retaining wall

Retaining wall maximum horizontal displacement: -0.04156m

Distance from point of maximum displacement in retaining wall to the top of backfill soil: 0.0m

Model 198:

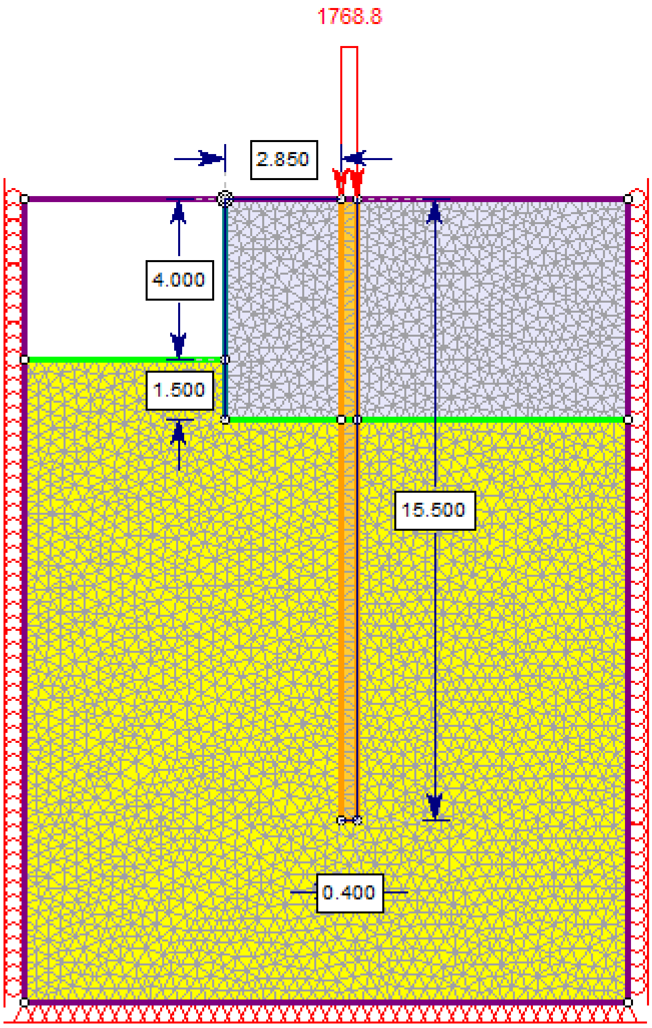

M 198.1: Original model (stage 3)

C'_1	ϕ'_1	γ_1	E_1	C'_2	ϕ'_2	γ_2	E_2	H_1	H_2	H_3	E_3	D_1	D_2	L	Qult
0	40	22	100	57	13	18	29.9	4.00	1.5	1	943939	2.85	0.4	15.5	1768.8

M 198.2: Parameter values

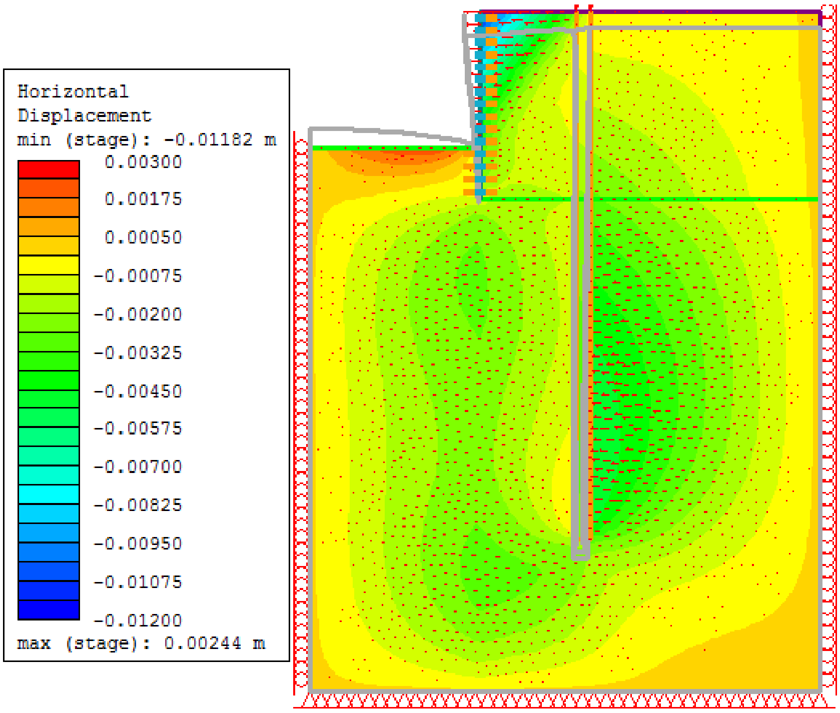

M 198.3: Deformed model (stage 3)

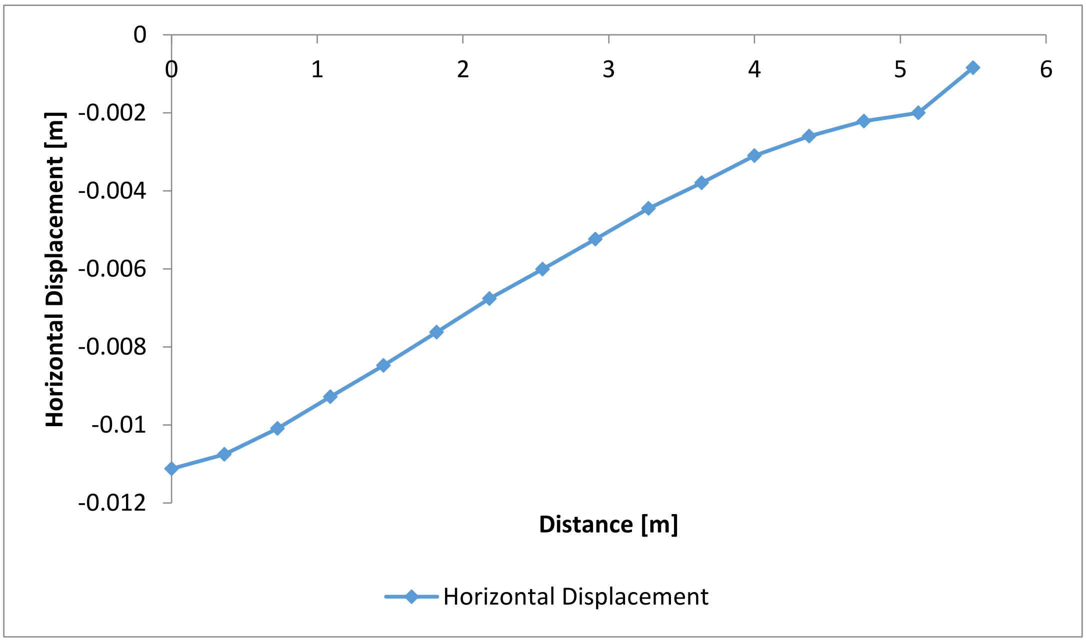

M 198.4: Horizontal displacement of soil along retaining wall

Retaining wall maximum horizontal displacement: -0.01182m

Distance from point of maximum displacement in retaining wall to the top of backfill soil: 0.0m

Model 199:

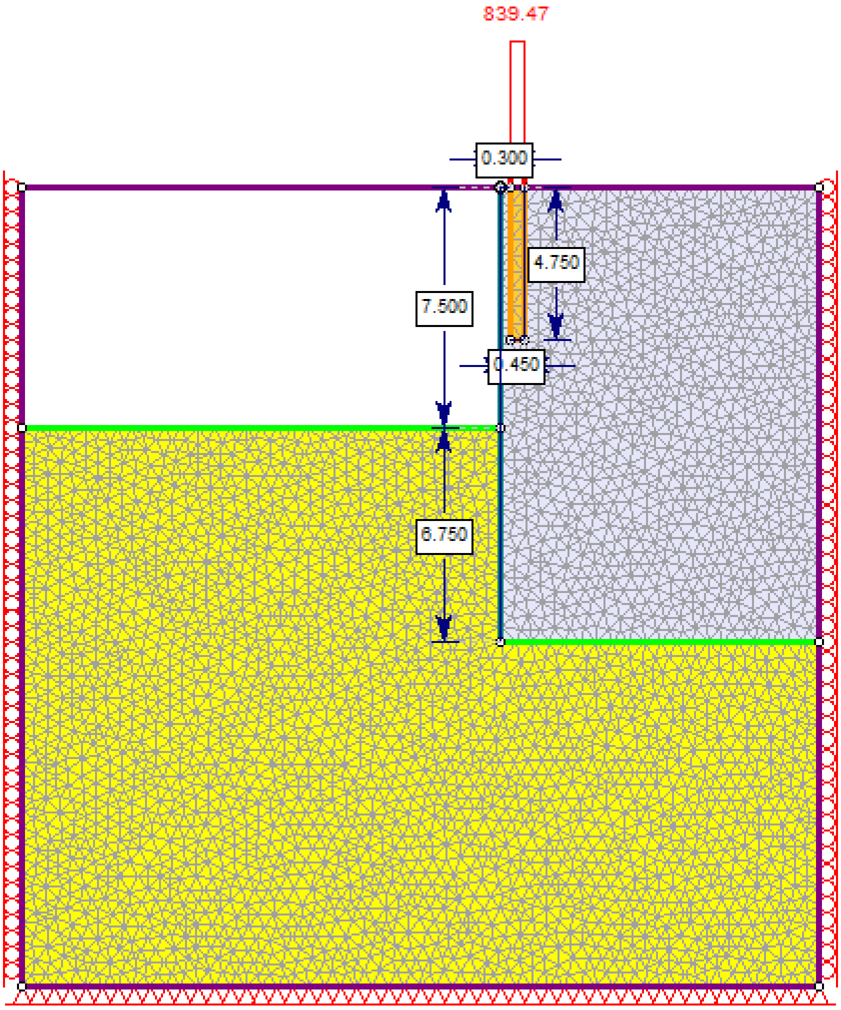

M 199.1: Original model (stage 3)

C_1'	ϕ_1'	γ_1	E_1	C_2'	ϕ_2'	γ_2	E_2	H_1	H_2	H_3	E_3	D_1	D_2	L	Qult
0	30	20	276	59	24	18	24.5	7.50	6.75	1.5	1101381	0.3	0.45	4.75	839.47

M 199.2: Parameter values

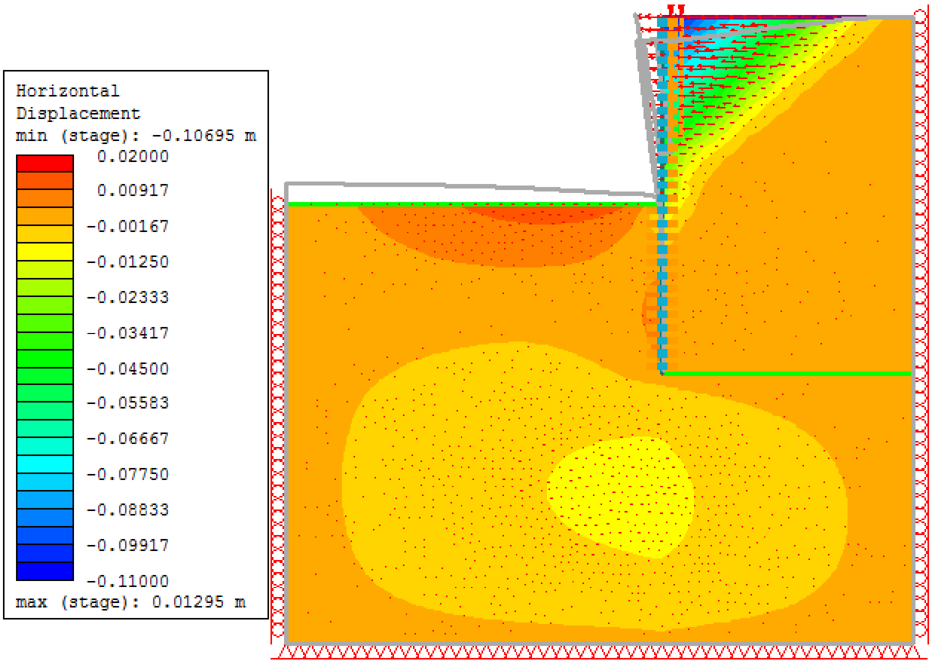

M 199.3: Deformed model (stage 3)

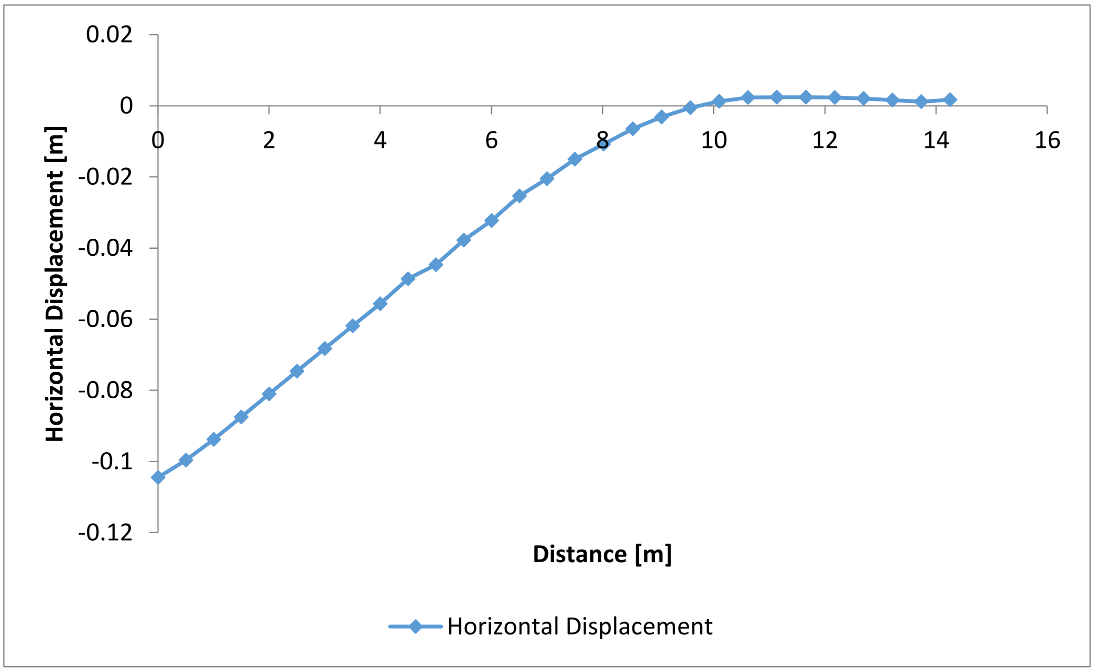

M 199.4: Horizontal displacement of soil along retaining wall

Retaining wall maximum horizontal displacement: -0.10695m

Distance from point of maximum displacement in retaining wall to the top of backfill soil: 0.0m

Model 200:

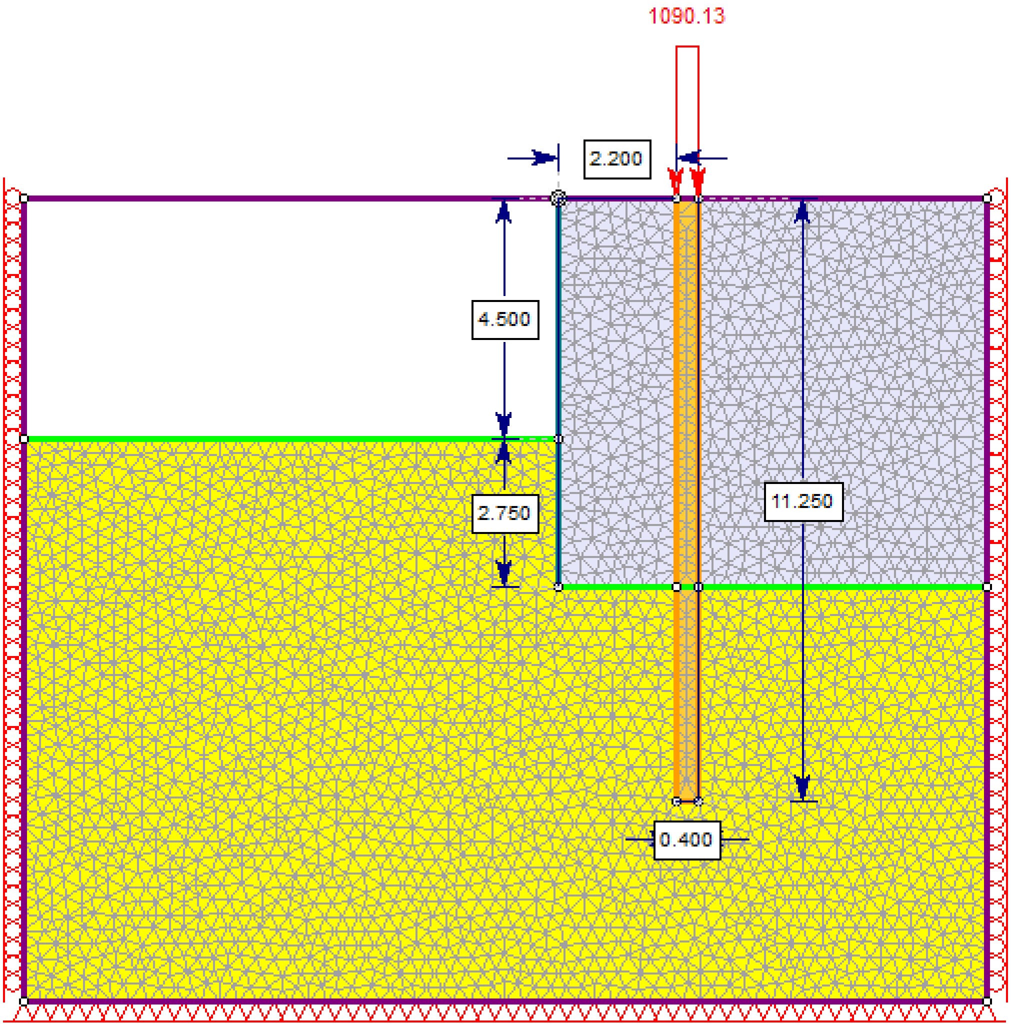

M 200.1: Original model (stage 3)

C'_1	ϕ'_1	γ_1	E_1	C'_2	ϕ'_2	γ_2	E_2	H_1	H_2	H_3	E_3	D_1	D_2	L	Qult
0	32	20	234	45	7	18	24.4	4.50	2.75	1	972109	2.2	0.4	11.25	1090.13

M 200.2: Parameter values

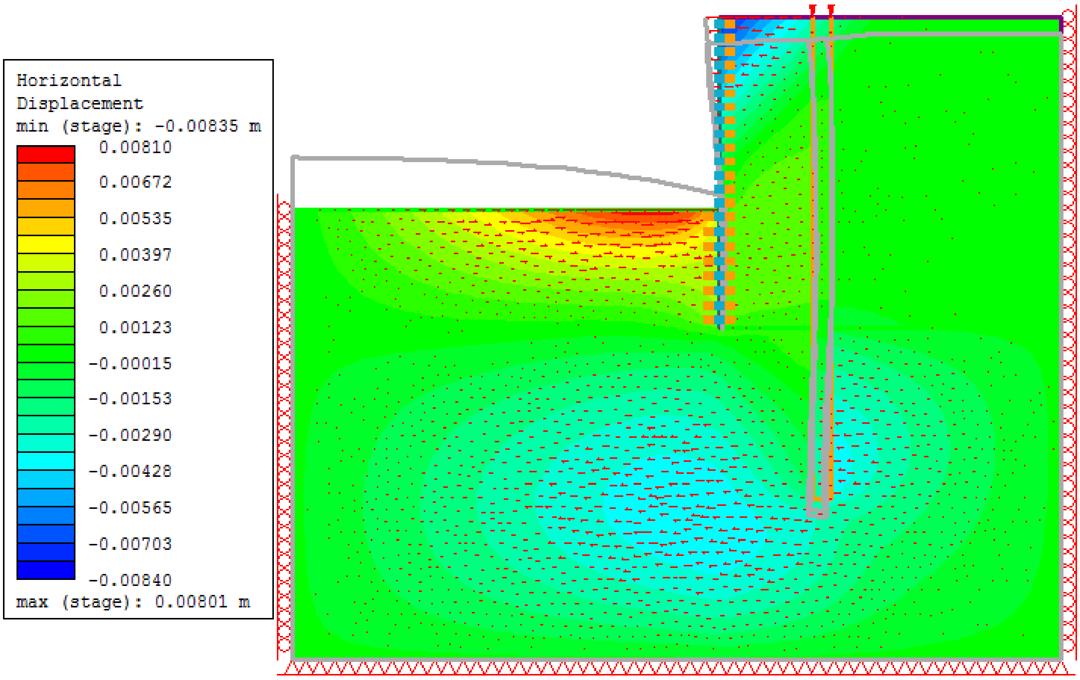

M 200.3: Deformed model (stage 3)

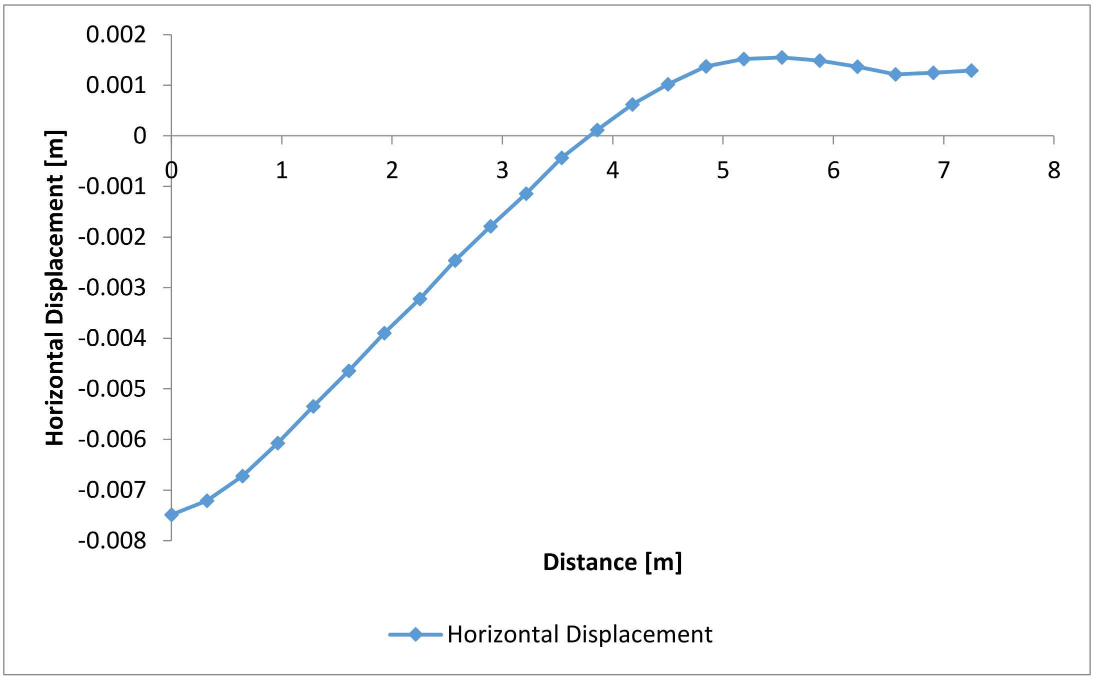

M 200.4: Horizontal displacement of soil along retaining wall

Retaining wall maximum horizontal displacement: -0.0835m

Distance from point of maximum displacement in retaining wall to the top of backfill soil: 0.0m

Test Model (TM) 1

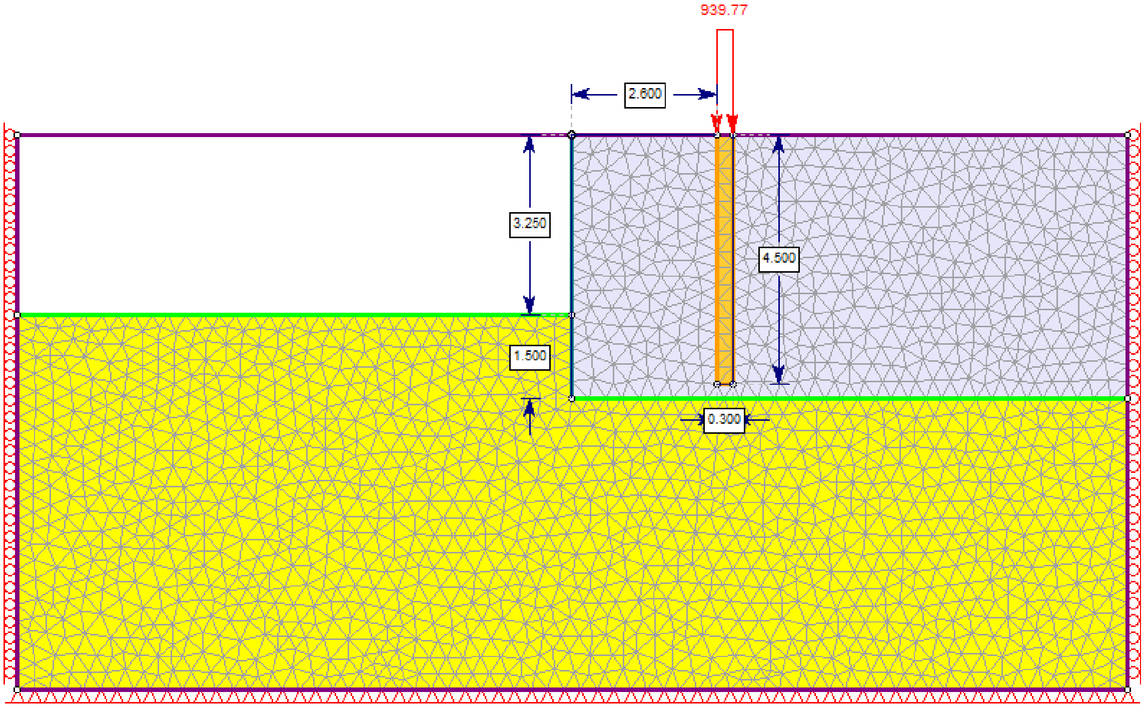

TM 1.1: Original model (stage 3)

C_1'	ϕ_1'	γ_1	E_1	C_2'	ϕ_2'	γ_2	E_2	H_1	H_2	H_3	E_3	D_1	D_2	L	Qult
0	29	20	287	48	16	19	6.2	3.25	1.5	0.75	1045397	2.6	0.3	4.5	939.77

TM 1.2: Parameter values

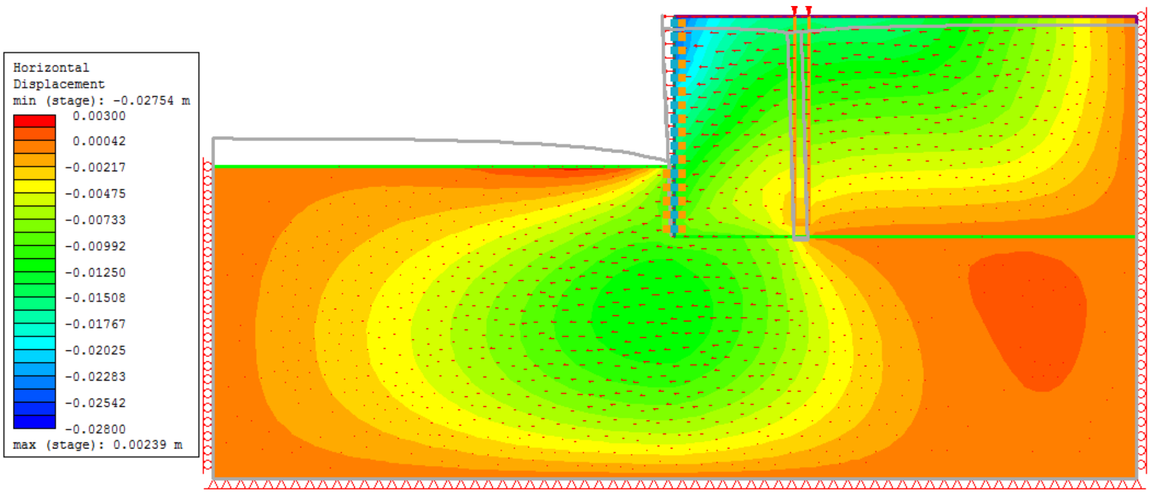

TM 1.3: Deformed model (stage 3)

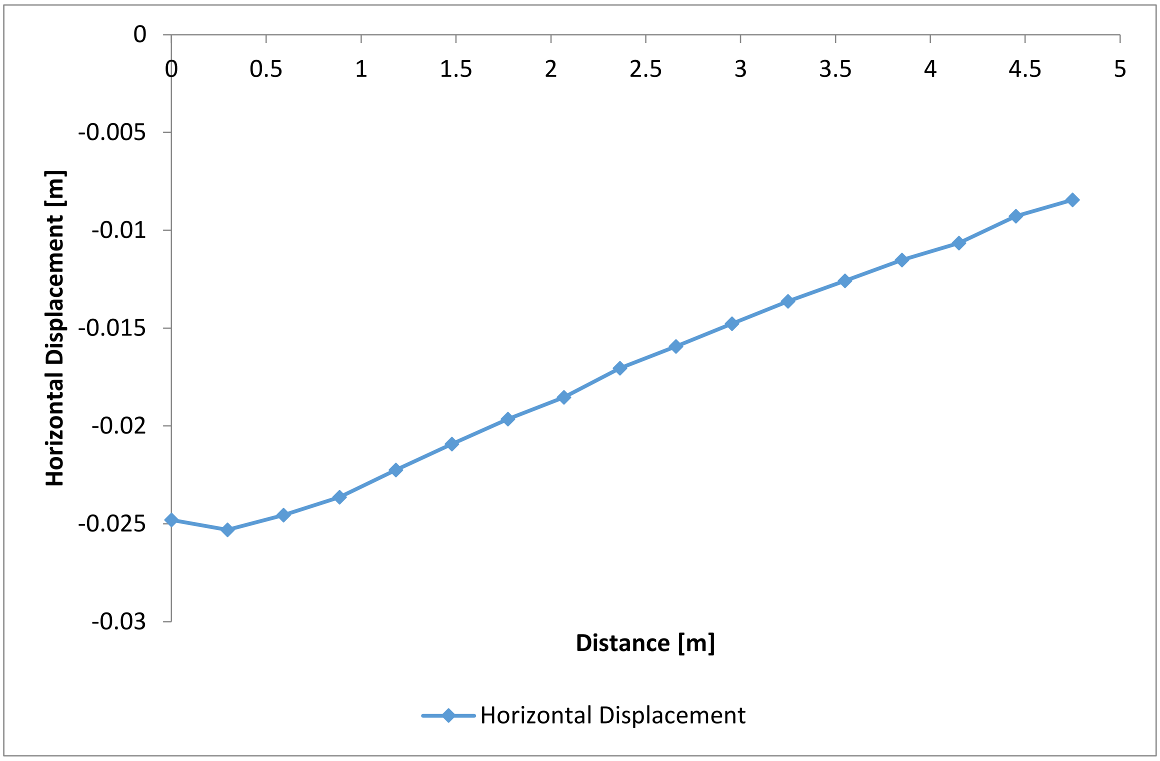

TM 1.4: Horizontal displacement of soil along retaining wall

Retaining wall maximum horizontal displacement: -0.02754m

Distance from point of maximum displacement in retaining wall to the top of backfill soil: 0.0m

Test Model 2

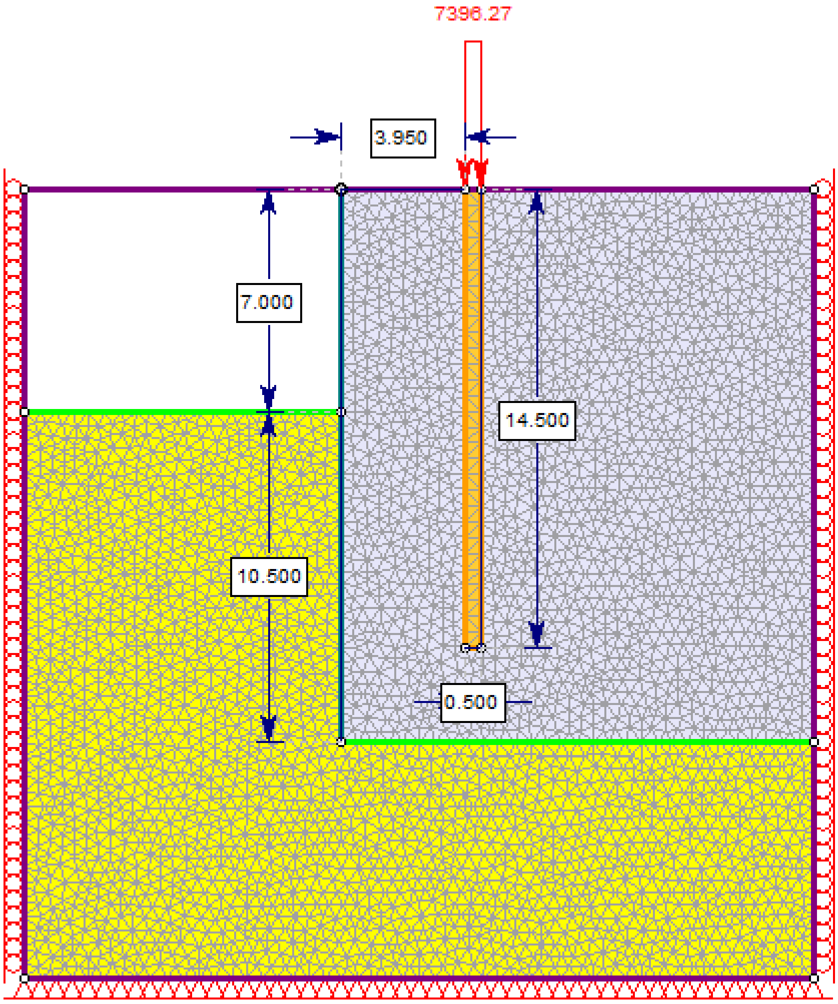

TM 2.1: Original model (stage 3)

C_1'	ϕ_1'	γ_1	E_1	C_2'	ϕ_2'	γ_2	E_2	H_1	H_2	H_3	E_3	D_1	D_2	L	Qult
0	37	18	65	39	31	23	36.9	7	10.5	1.25	775995	3.95	0.5.	14.5	7396.27

TM 2.2: Parameter values

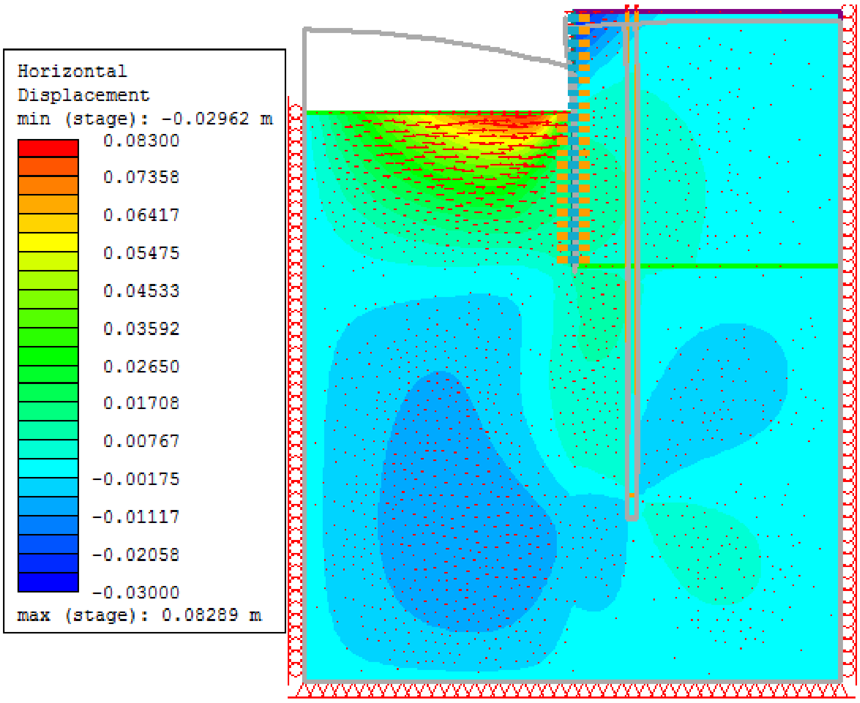

TM 2.3: Deformed model (stage 3)

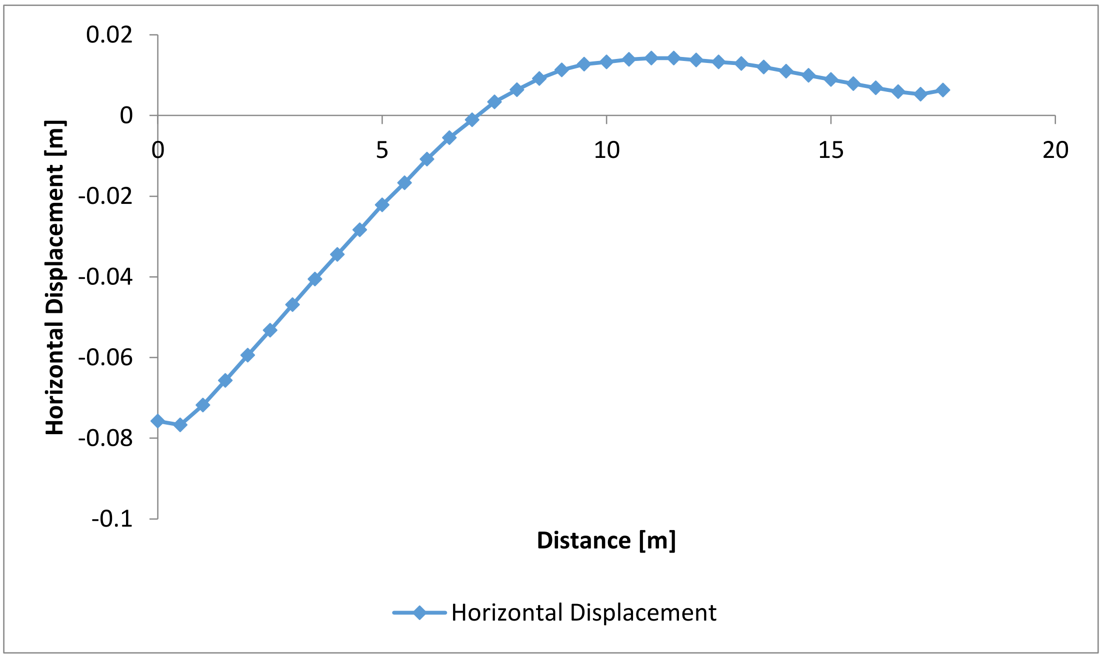

TM 2.4: Horizontal displacement of soil along retaining wall

Retaining wall maximum horizontal displacement: -0.02962m

Distance from point of maximum displacement in retaining wall to the top of backfill soil: 0.0m

Test Model 3

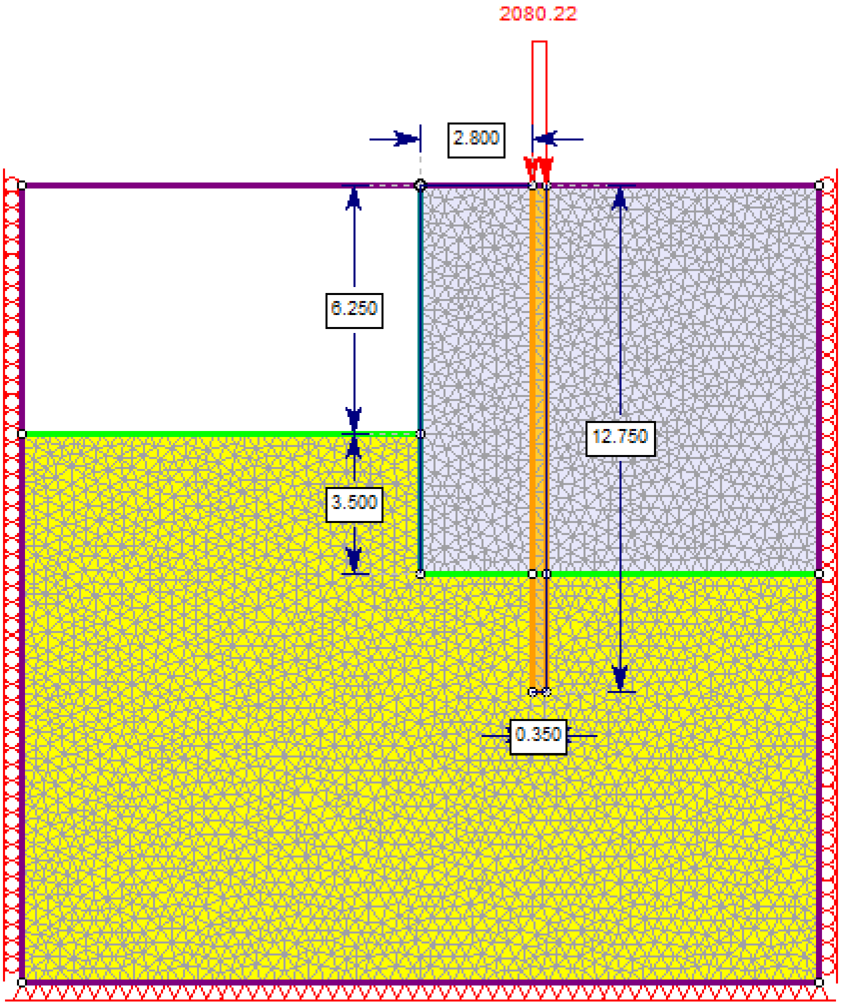

TM 3.1: Original model (stage 3)

C_1'	ϕ_1'	γ_1	E_1	C_2'	ϕ_2'	γ_2	E_2	H_1	H_2	H_3	E_3	D_1	D_2	L	Qult
0	42	20	142	51	13	24	46.5	6.25	3.25	1.25	775995	3.95	0.5	14.5	2080.22

TM 3.2: Parameter values

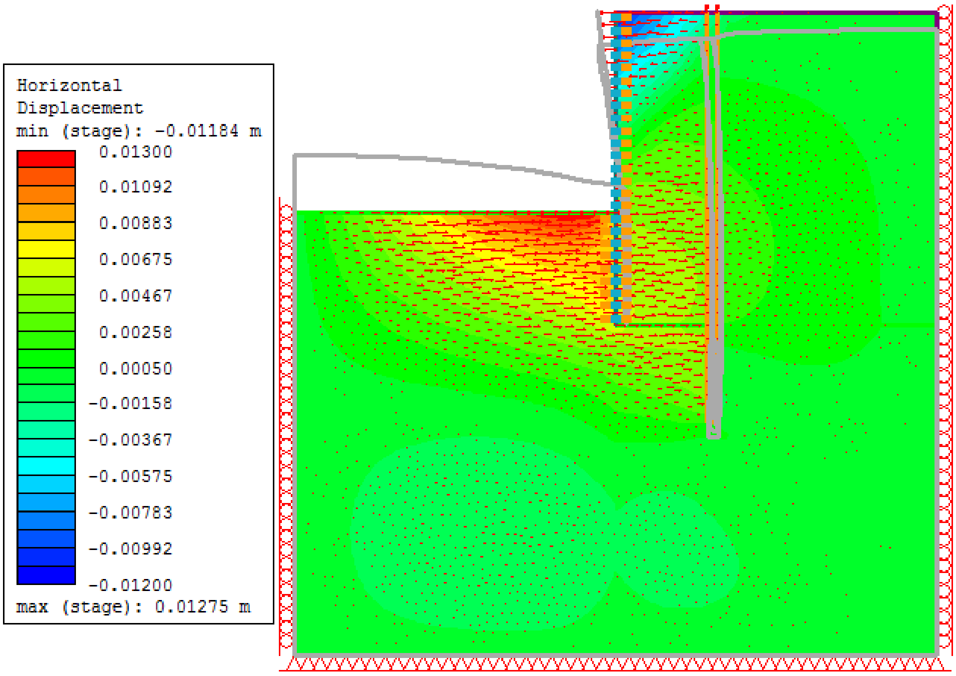

TM 3.3: Deformed model (stage 3)

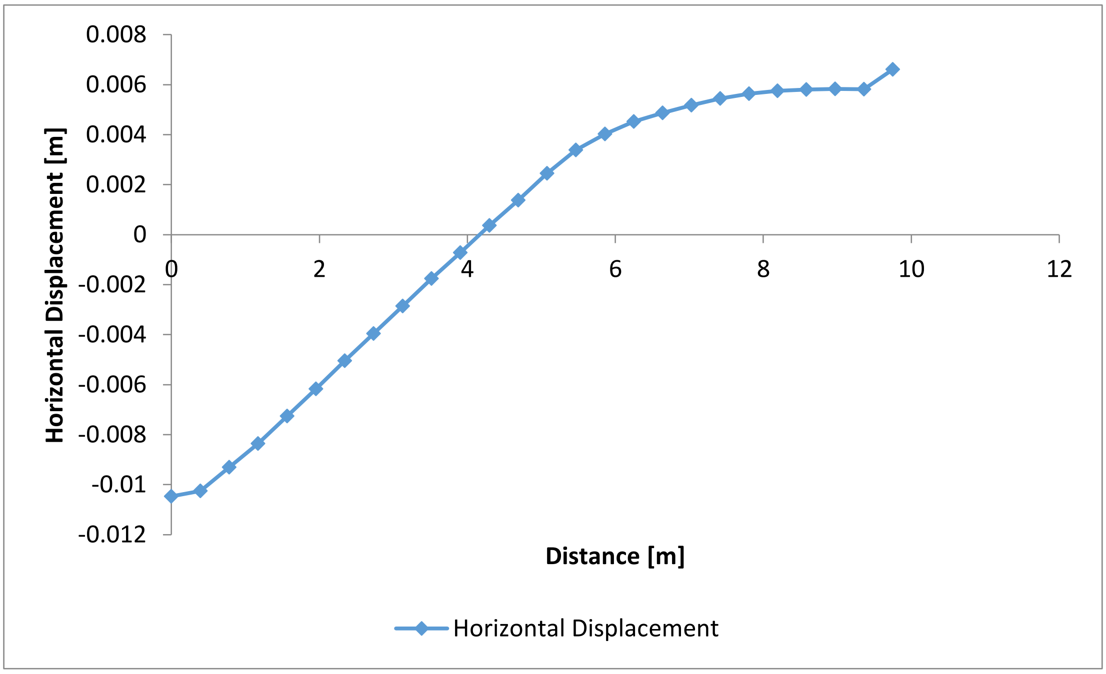

TM 3.4: Horizontal displacement of soil along retaining wall

Retaining wall maximum horizontal displacement: -0.01184m

Distance from point of maximum displacement in retaining wall to the top of backfill soil: 0.0m

Teat Model 4

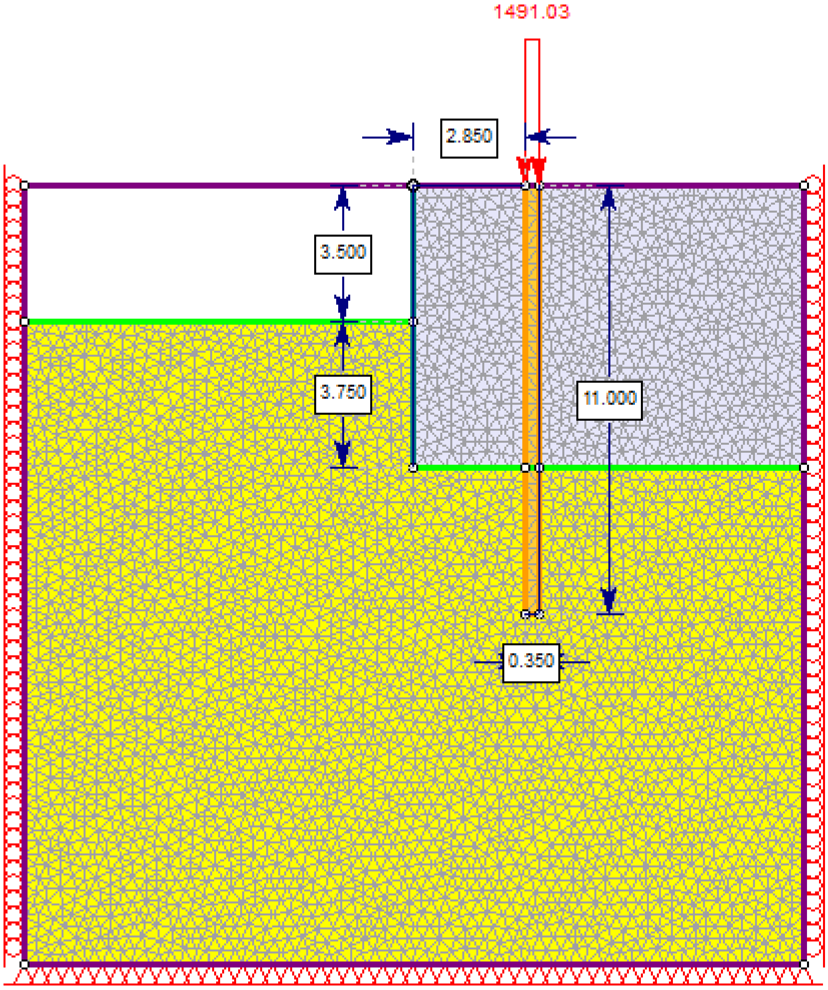

TM 4.1: Original model (stage 3)

C_1'	ϕ_1'	γ_1	E_1	C_2'	ϕ_2'	γ_2	E_2	H_1	H_2	H_3	E_3	D_1	D_2	L	Qult
0	35	19	89	23	15	18	47.2	3.5	3.75	1.25	978106	2.85	0.35	11	1491.03

TM 4.2: Parameter values

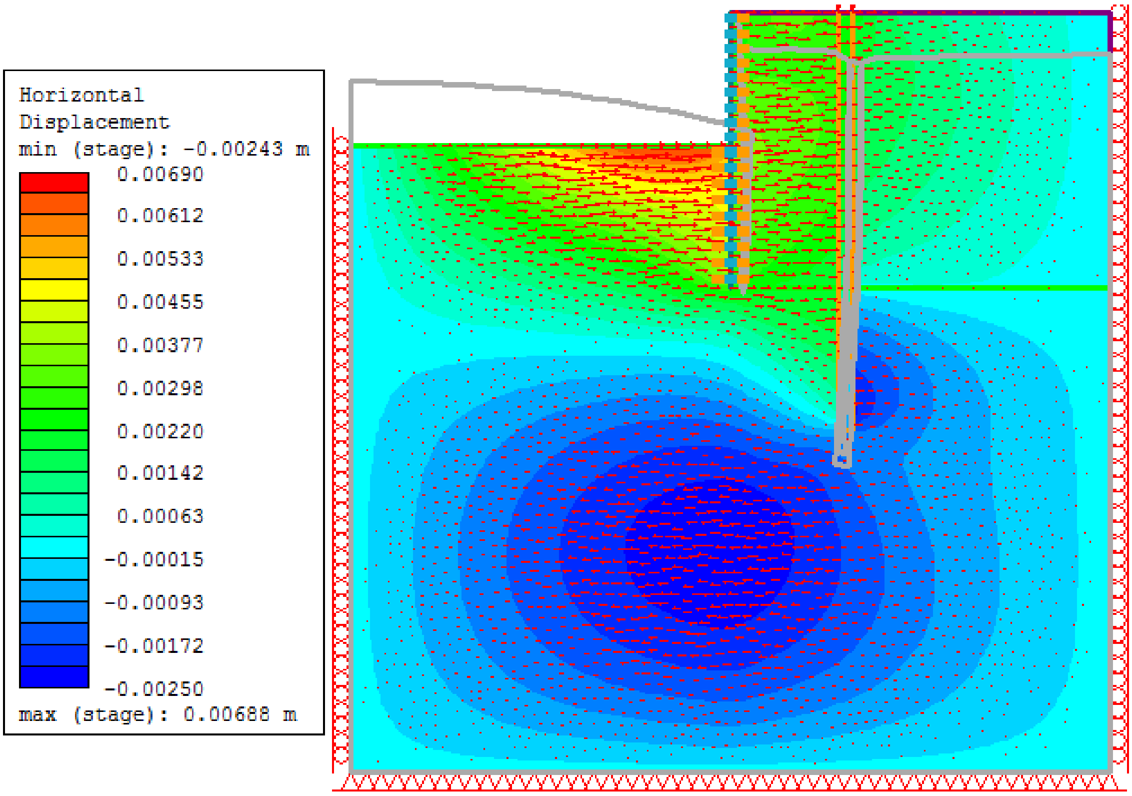

TM 4.3: Deformed model (stage 3)

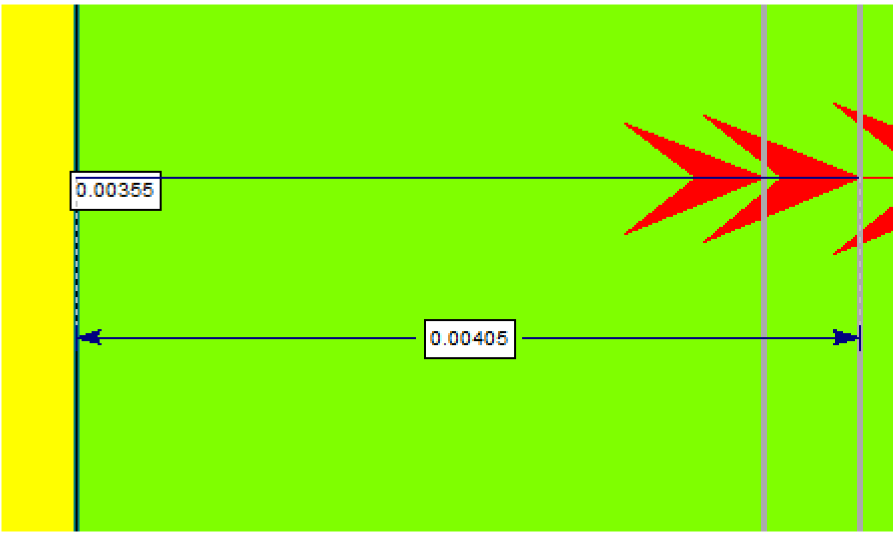

TM 4.4: Detailed view of cross-section of retaining wall and soil (stage 3)

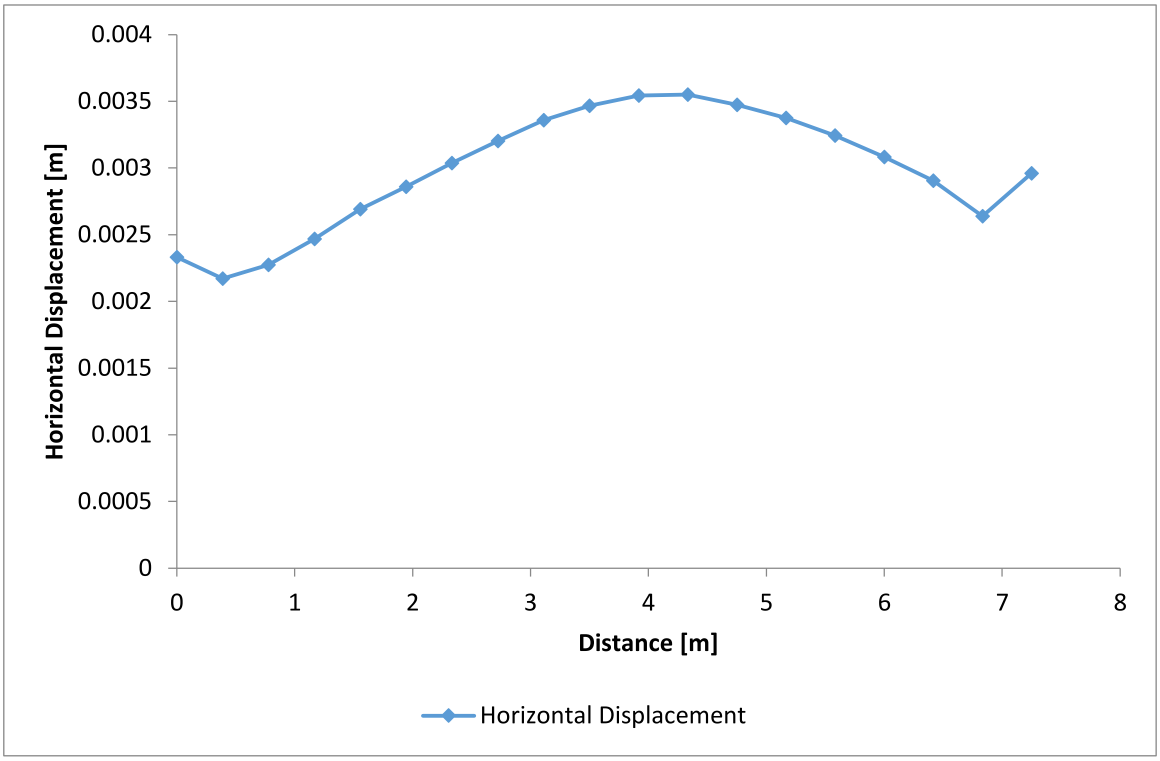

TM 4.5: Horizontal displacement of soil along retaining wall

Retaining wall maximum horizontal displacement: 0.00405m

Distance from point of maximum displacement in retaining wall to the top of backfill soil: 4.33m

Test Model 5

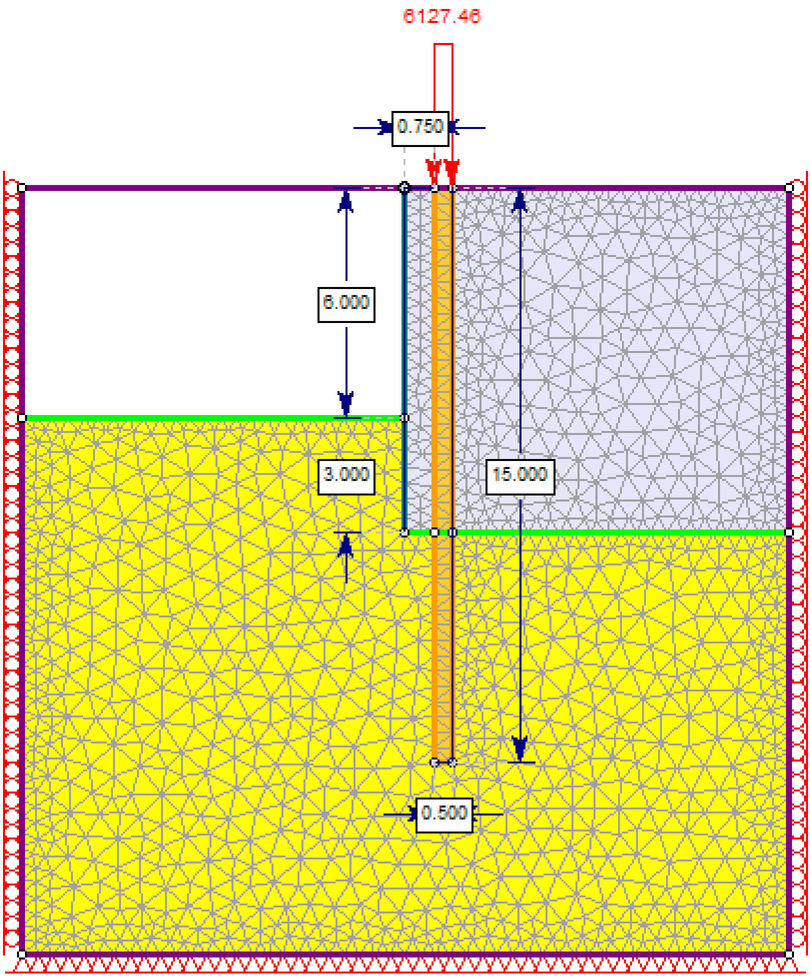

TM 5.1: Original model (stage 3)

C_1'	ϕ_1'	γ_1	E_1	C_2'	ϕ_2'	γ_2	E_2	H_1	H_2	H_3	E_3	D_1	D_2	L	Qult
0	41	20	40	53	26	25	33.9	6	3	1.25	1010299	0.75	0.5	15	6127.46

TM 5.2: Parameter values

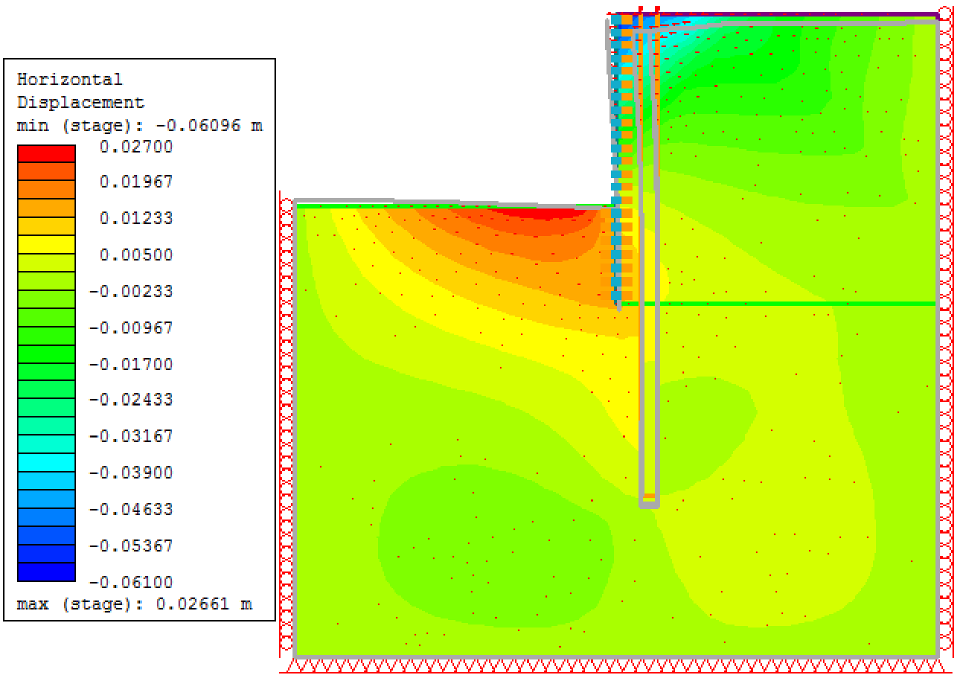

TM 5.3: Deformed model (stage 3)

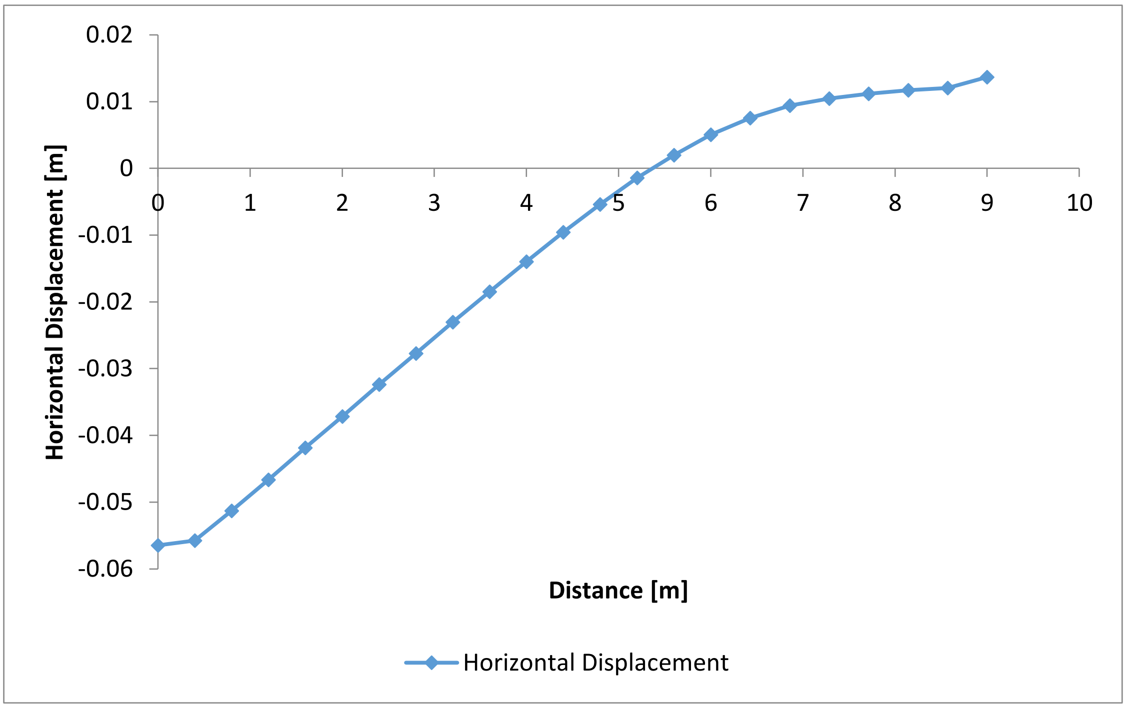

TM 5.4: Horizontal displacement of soil along retaining wall

Retaining wall maximum horizontal displacement: -0.06096m

Distance from point of maximum displacement in retaining wall to the top of backfill soil: 0.0m

Test Model 6

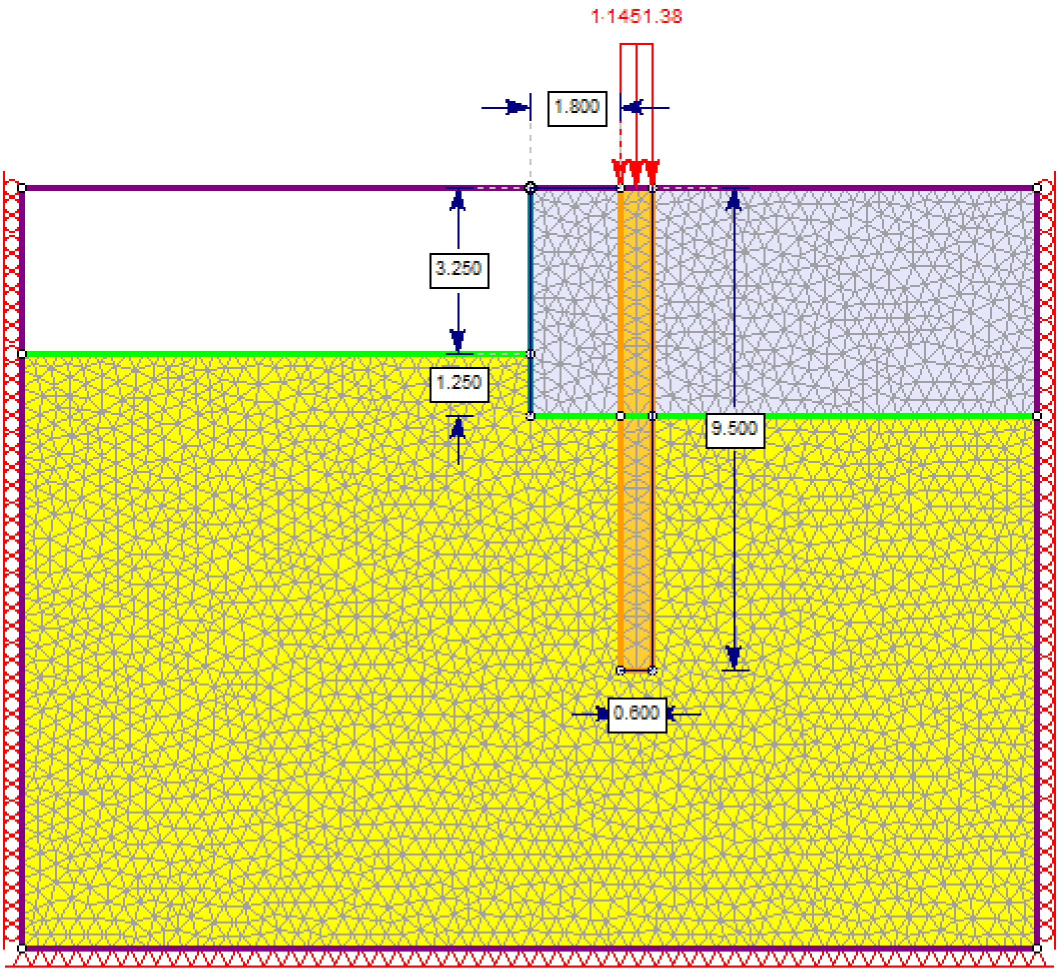

TM 6.1: Original model (stage 3)

C_1'	ϕ_1'	γ_1	E_1	C_2'	ϕ_2'	γ_2	E_2	H_1	H_2	H_3	E_3	D_1	D_2	L	Qult
0	33	21	136	49	18	22	29.5	3.25	1.25	0.75	805595	1.8	0.6	9.5	1451.38

TM 6.2: Parameter values

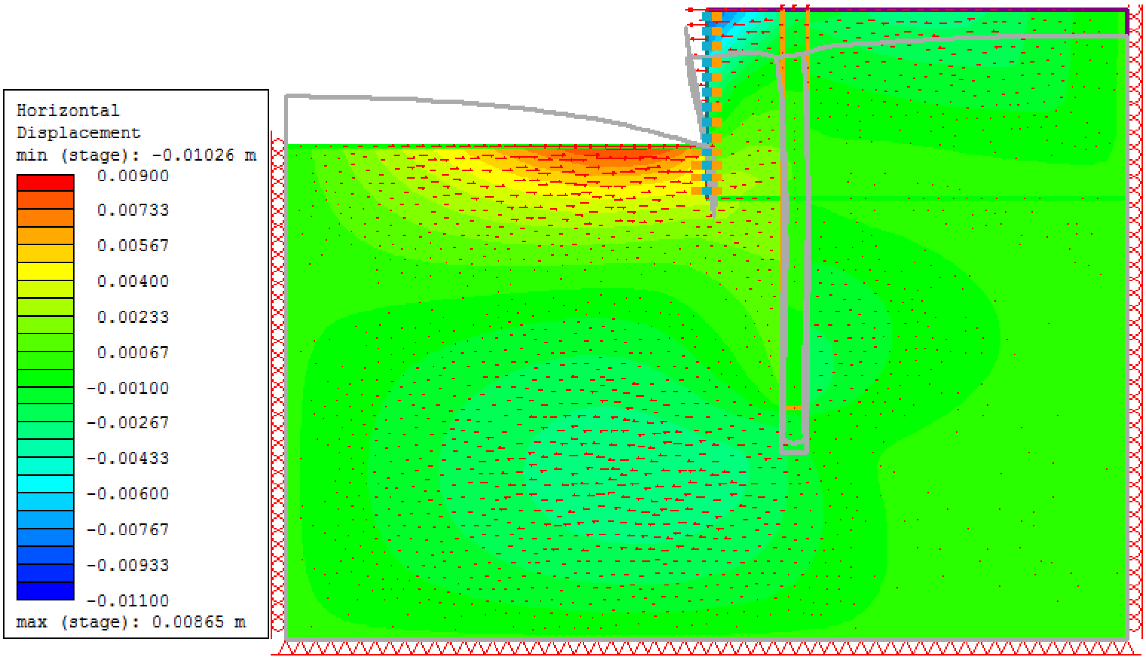

TM 6.3: Deformed model (stage 3)

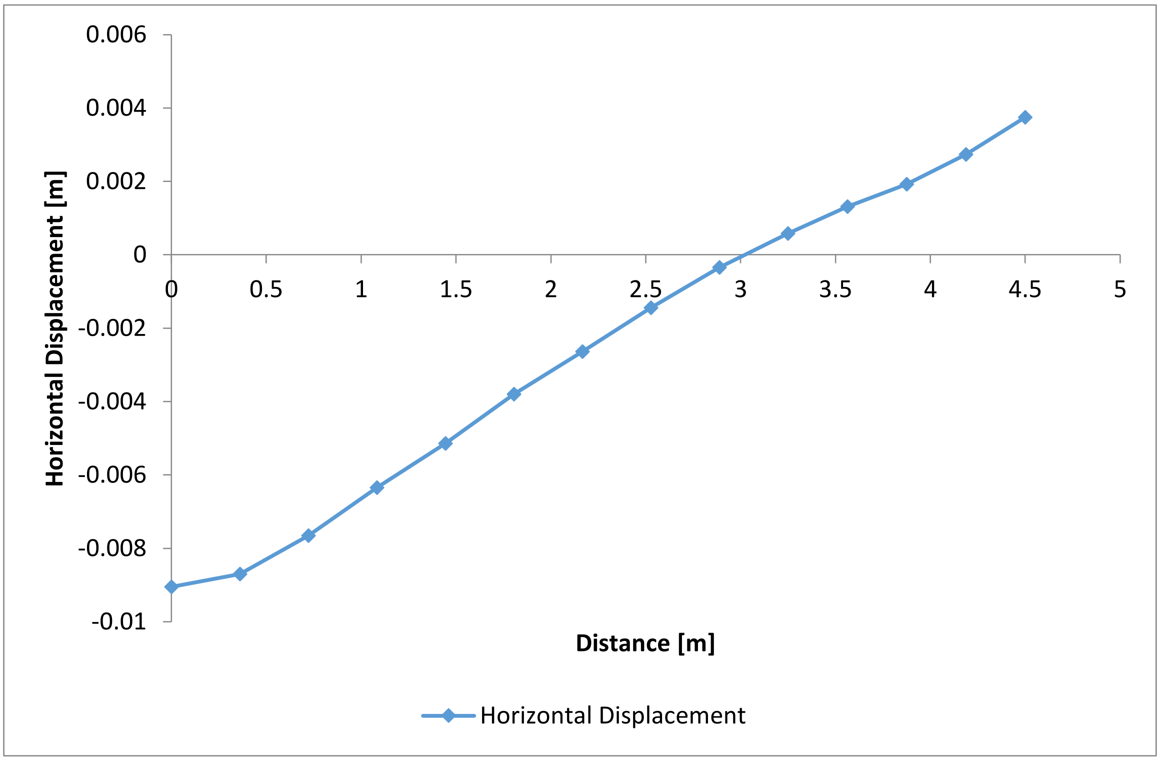

TM 6.4: Horizontal displacement of soil along retaining wall

Retaining wall maximum horizontal displacement: -0.01026m

Distance from point of maximum displacement in retaining wall to the top of backfill soil: 0.0m

Test Model 7

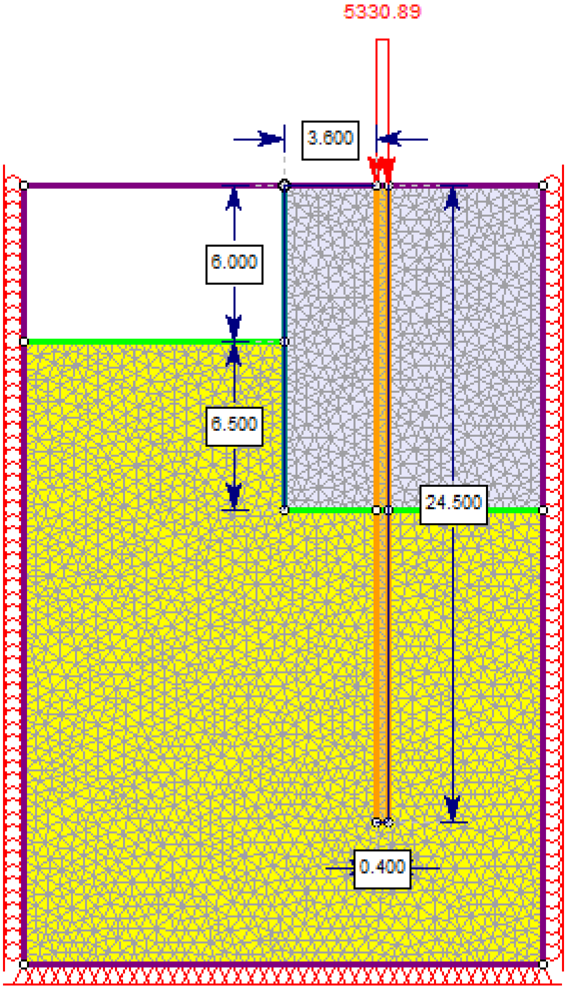

TM 7.1: Original model (stage 3)

C_1'	ϕ_1'	γ_1	E_1	C_2'	ϕ_2'	γ_2	E_2	H_1	H_2	H_3	E_3	D_1	D_2	L	Qult
0	29	18	253	40	20	23	26.7	6	6.5	1.25	692511	3.6	0.4	24.5	5330.89

TM 7.2: Parameter values

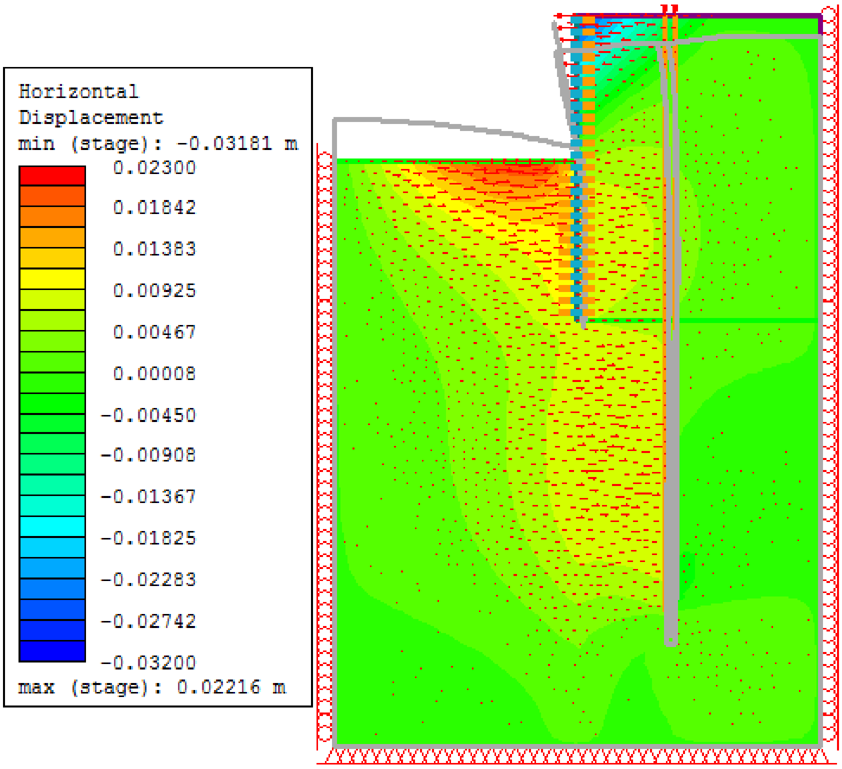

TM 7.3: Deformed model (stage 3)

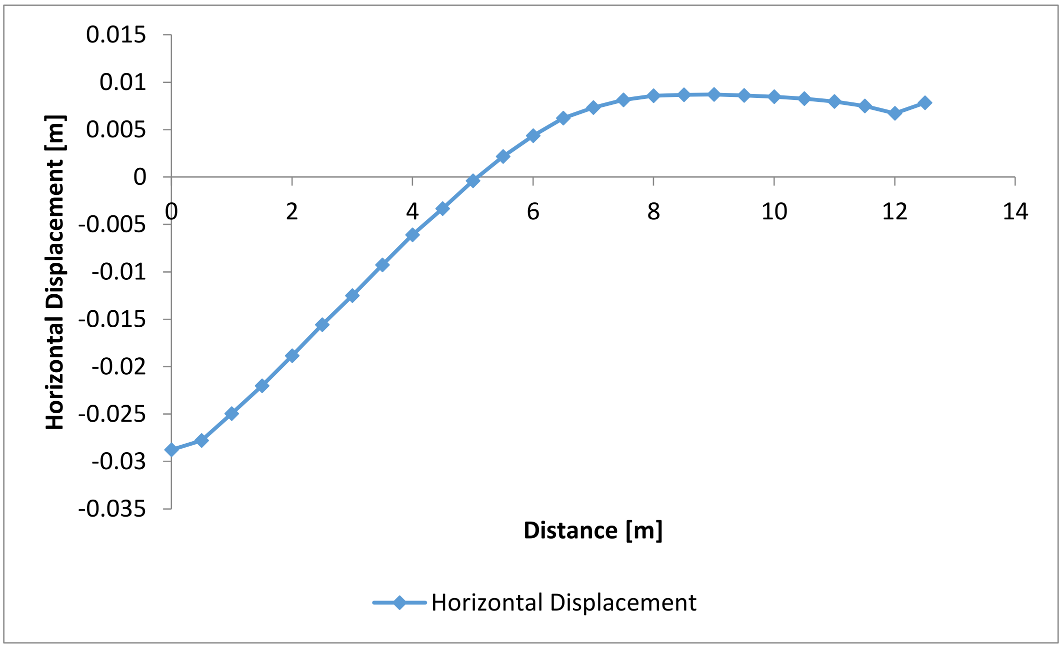

TM 7.4: Horizontal displacement of soil along retaining wall

Retaining wall maximum horizontal displacement: -0.03181m

Distance from point of maximum displacement in retaining wall to the top of backfill soil: 0.0m

Test Model 8

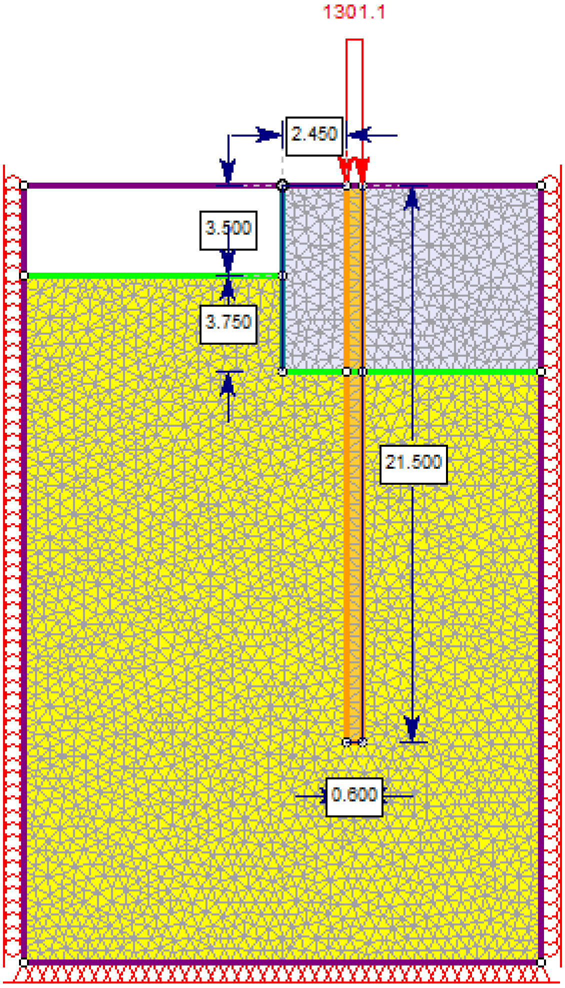

TM 8.1: Original model (stage 3)

C'_1	ϕ'_1	γ_1	E_1	C'_2	ϕ'_2	γ_2	E_2	H_1	H_2	H_3	E_3	D_1	D_2	L	Qult
0	42	21	96	24	7	18	45.0	3.5	3.75	0.5	1047976	2.45	0.6	21.5	1301.1

TM 8.2: Parameter values

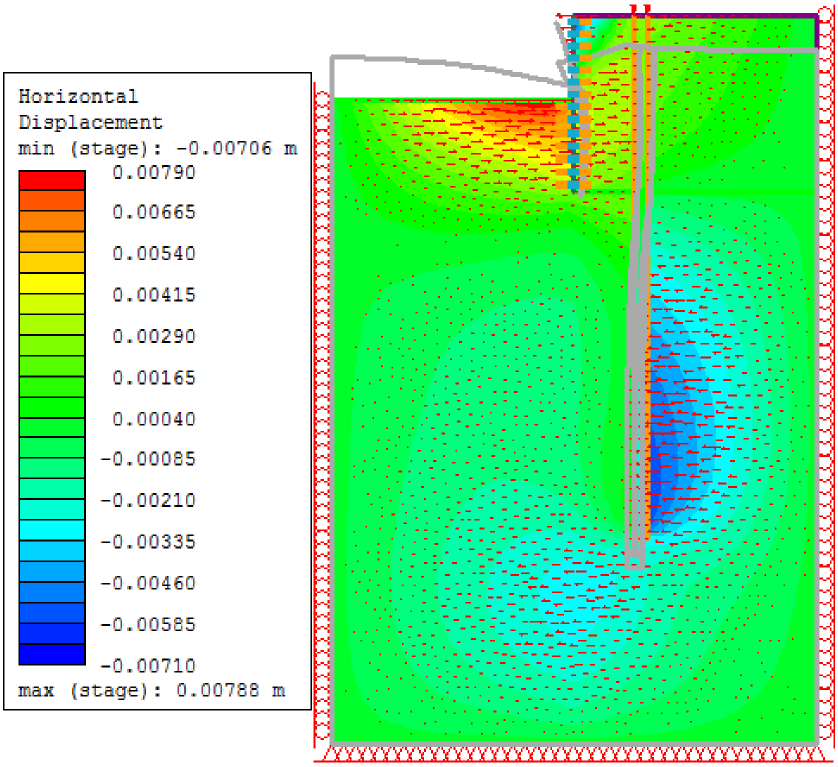

TM 8.3: Deformed model (stage 3)

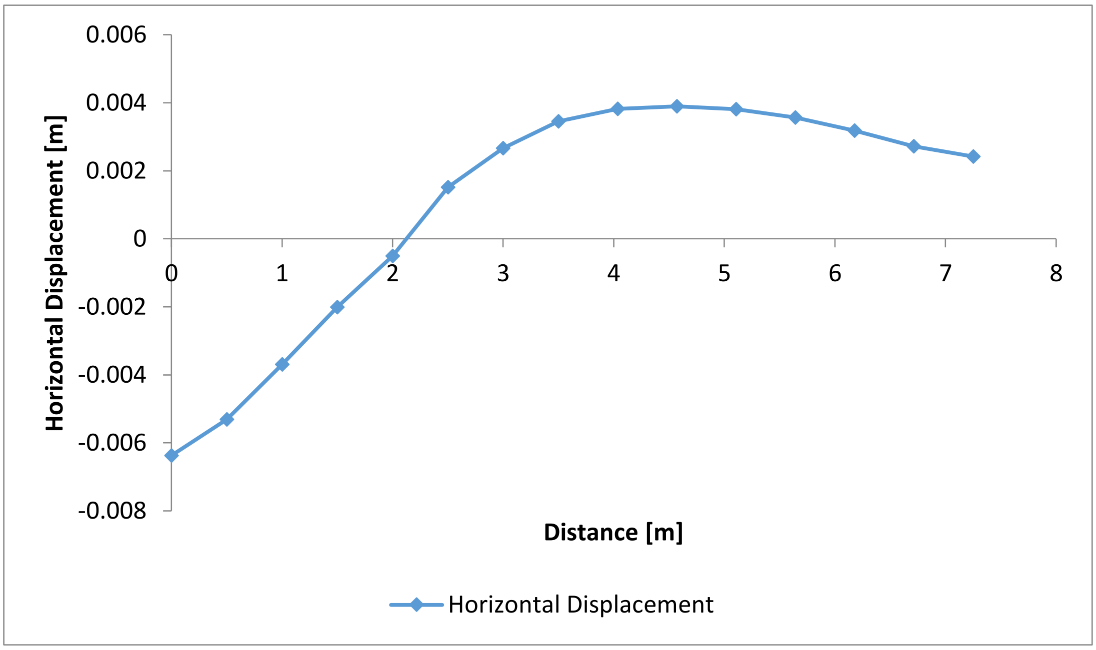

TM 8.4: Horizontal displacement of soil along retaining wall

Retaining wall maximum horizontal displacement: -0.00706m

Distance from point of maximum displacement in retaining wall to the top of backfill soil: 0.0m

Test Model 9

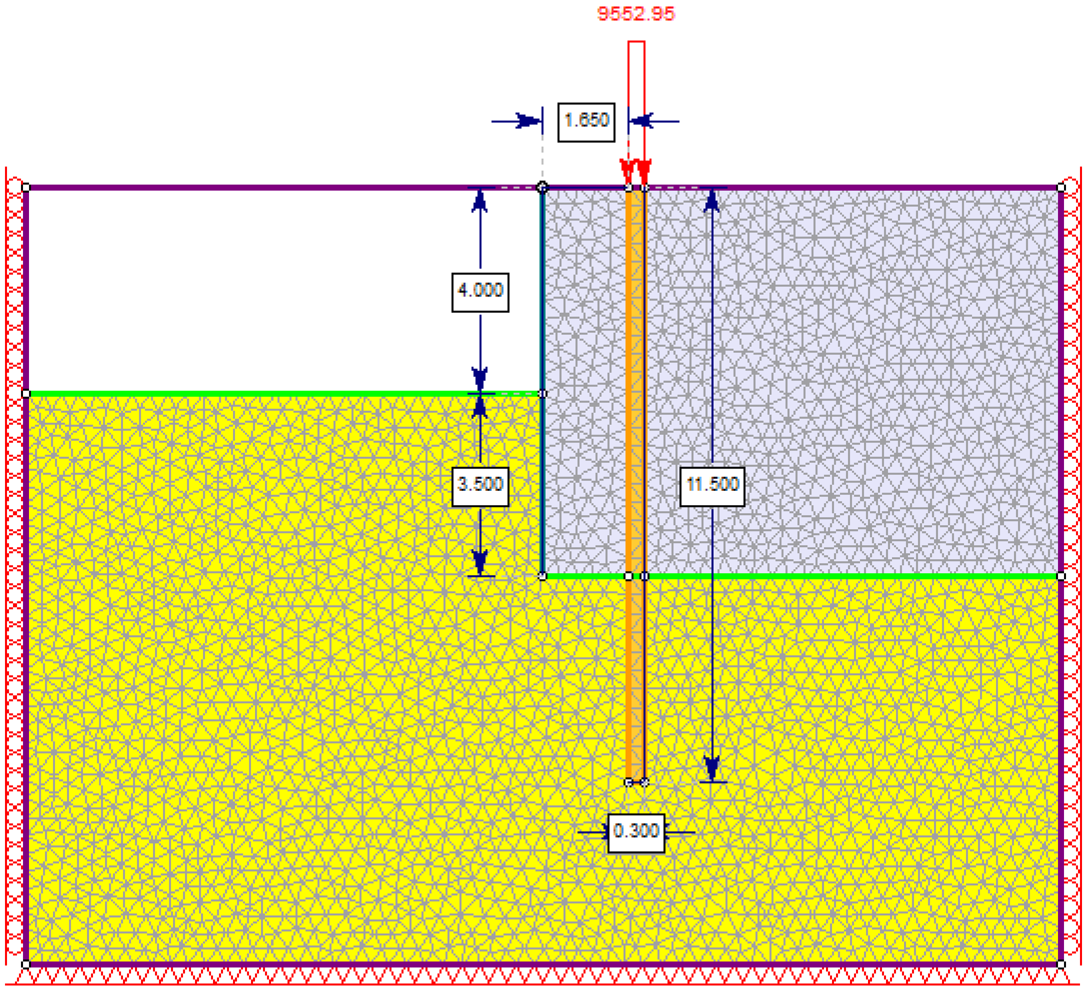

TM 9.1: Original model (stage 3)

C_1'	ϕ_1'	γ_1	E_1	C_2'	ϕ_2'	γ_2	E_2	H_1	H_2	H_3	E_3	D_1	D_2	L	Qult
0	37	22	53	31	32	23	42.6	3.5	4	3.5	737967	1.65	0.3	11.5	9552.95

TM 9.2: Parameter values

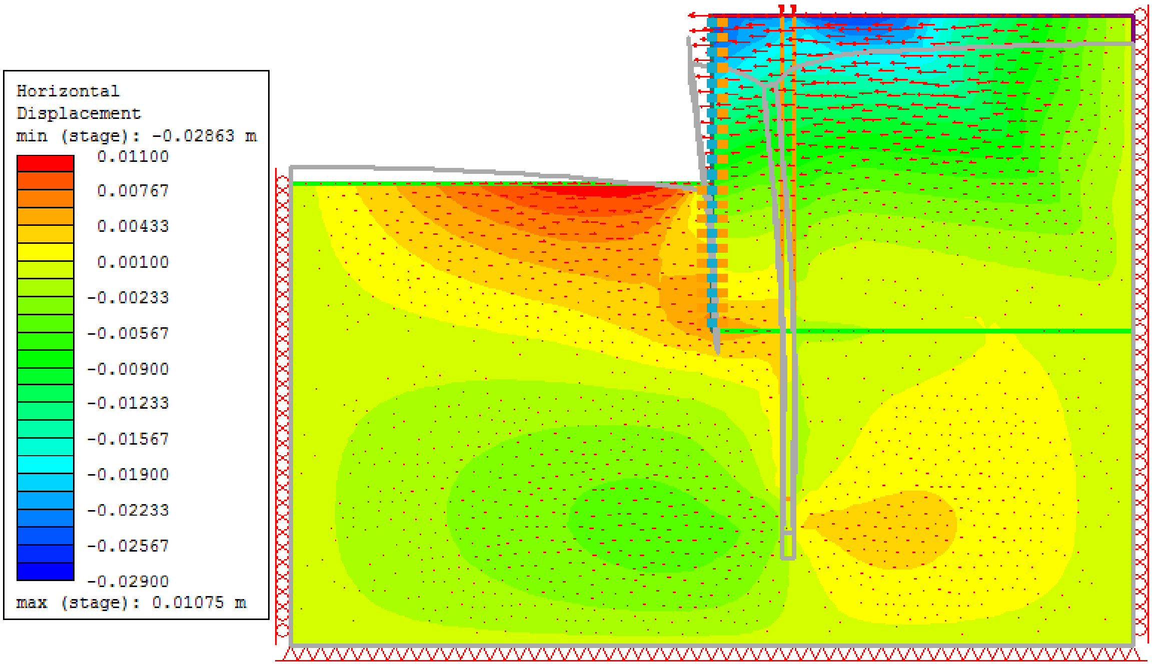

TM 9.3: Deformed model (stage 3)

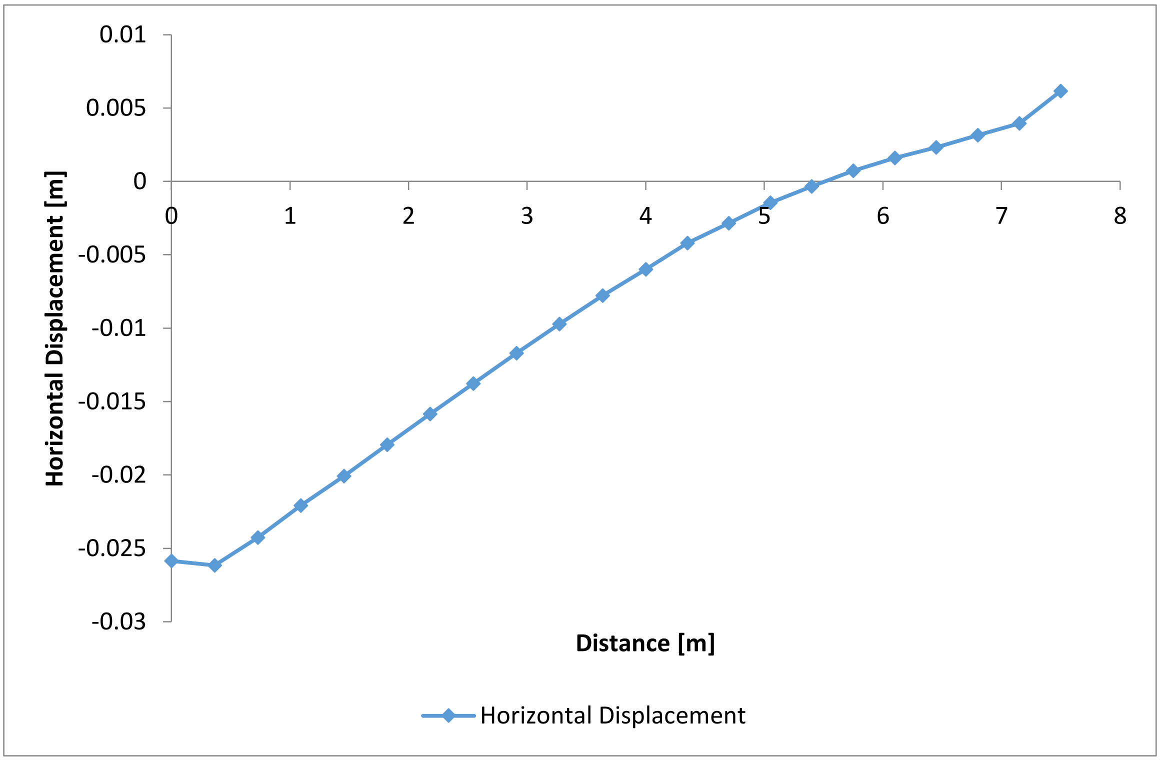

TM 9.4: Horizontal displacement of soil along retaining wall

Retaining wall maximum horizontal displacement: -0.02863m

Distance from point of maximum displacement in retaining wall to the top of backfill soil: 0.0m

Test Model 10

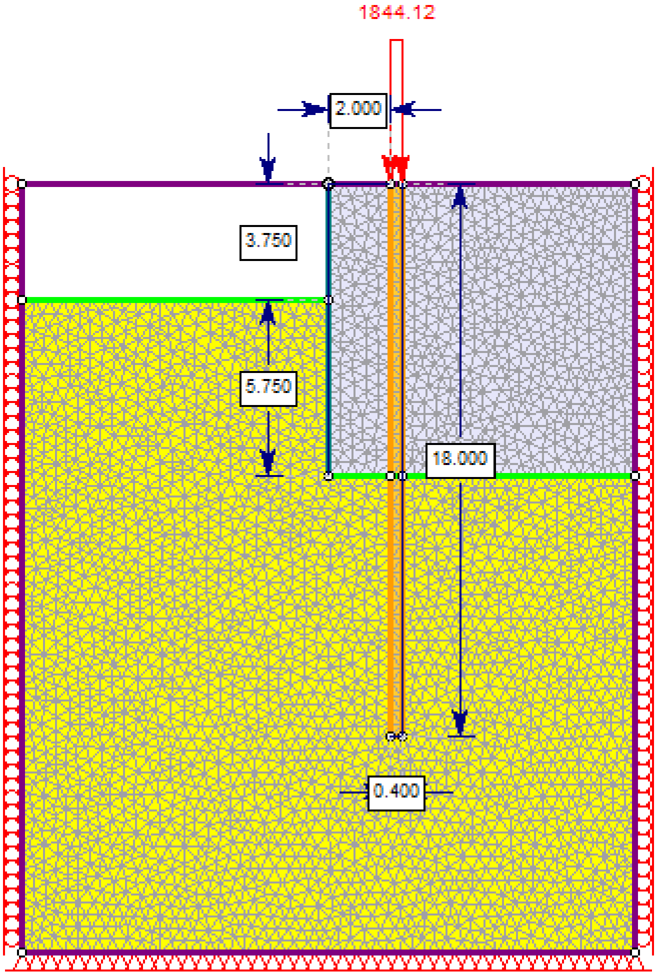

TM 10.1: Original model (stage 3)

C_1'	ϕ_1'	γ_1	E_1	C_2'	ϕ_2'	γ_2	E_2	H_1	H_2	H_3	E_3	D_1	D_2	L	Qult
0	31	19	132	22	9	21	3.2	3.75	5.75	2	1024512	2	0.4	18	1844.12

TM 10.2: Parameter values

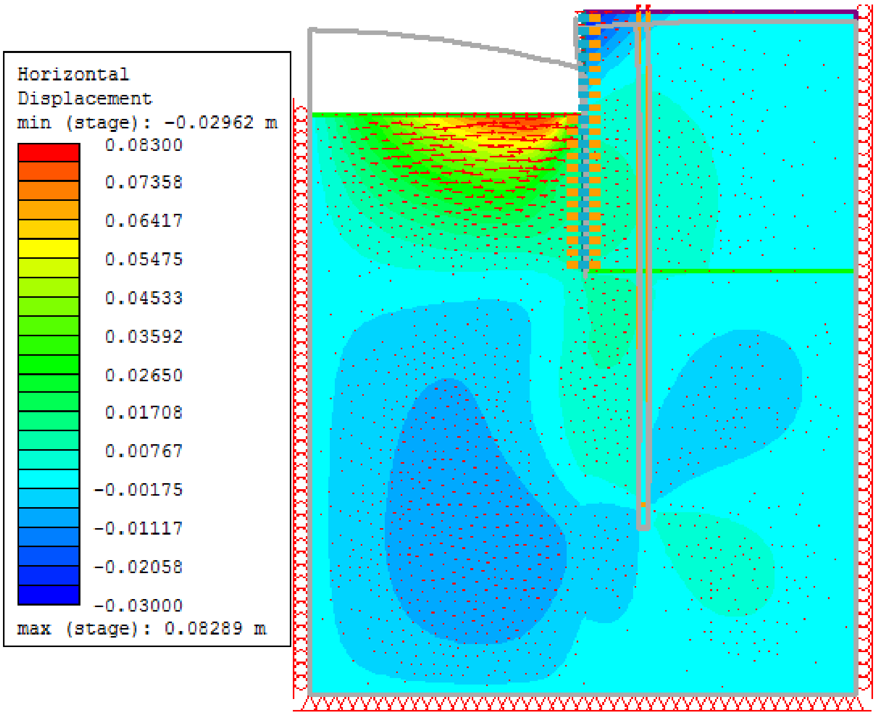

TM 10.3: Deformed model (stage 3)

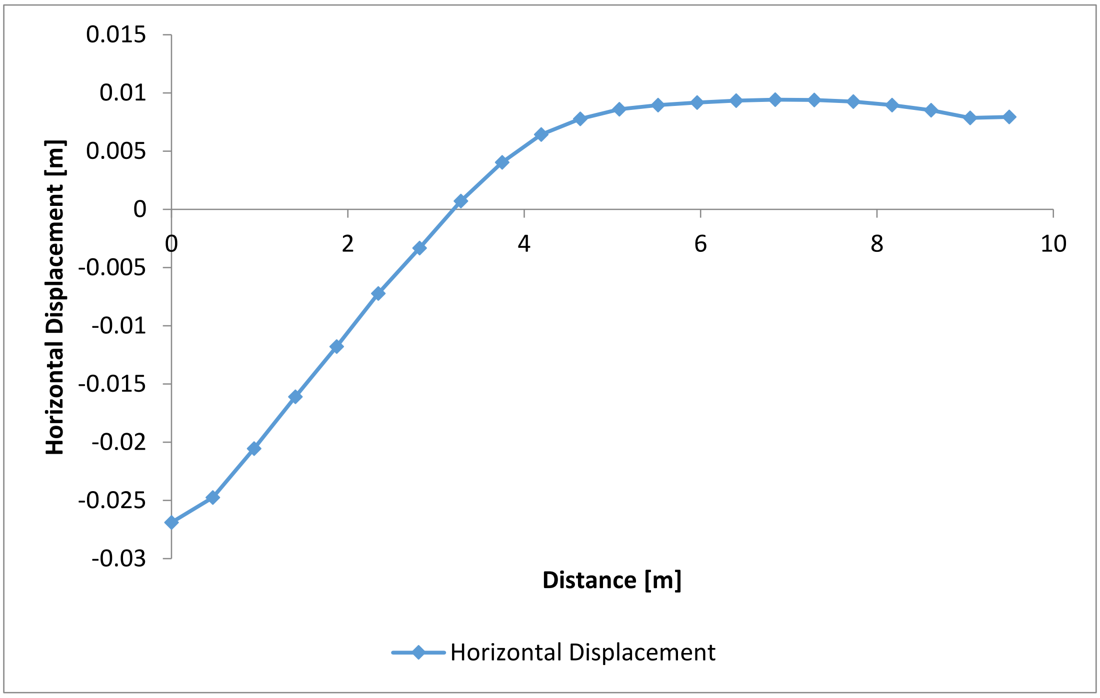

TM 10.4: Horizontal displacement of soil along retaining wall

Retaining wall maximum horizontal displacement: -0.02962m

Distance from point of maximum displacement in retaining wall to the top of backfill soil: 0.0m

Test Model 11

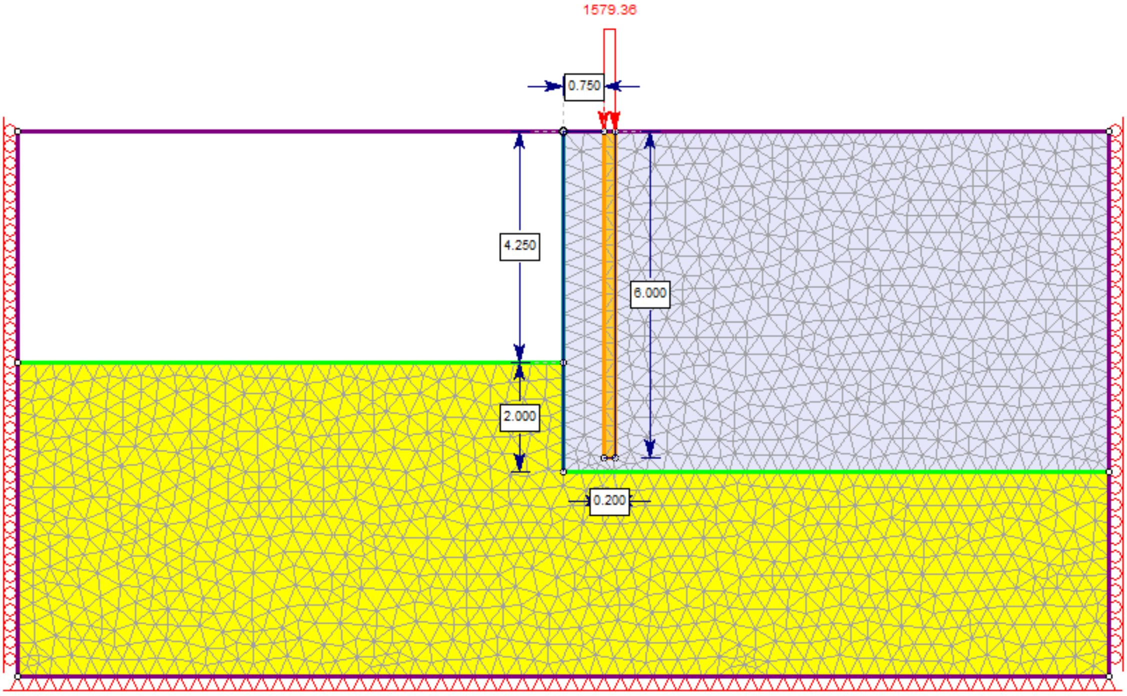

TM 11.1: Original model (stage 3)

C_1'	ϕ_1'	γ_1	E_1	C_2'	ϕ_2'	γ_2	E_2	H_1	H_2	H_3	E_3	D_1	D_2	L	Qult
0	29	21	161	56	17	23	46.0	4.25	2	1	991211	0.75	0.2	6	1579.36

TM 11.2: Parameter values

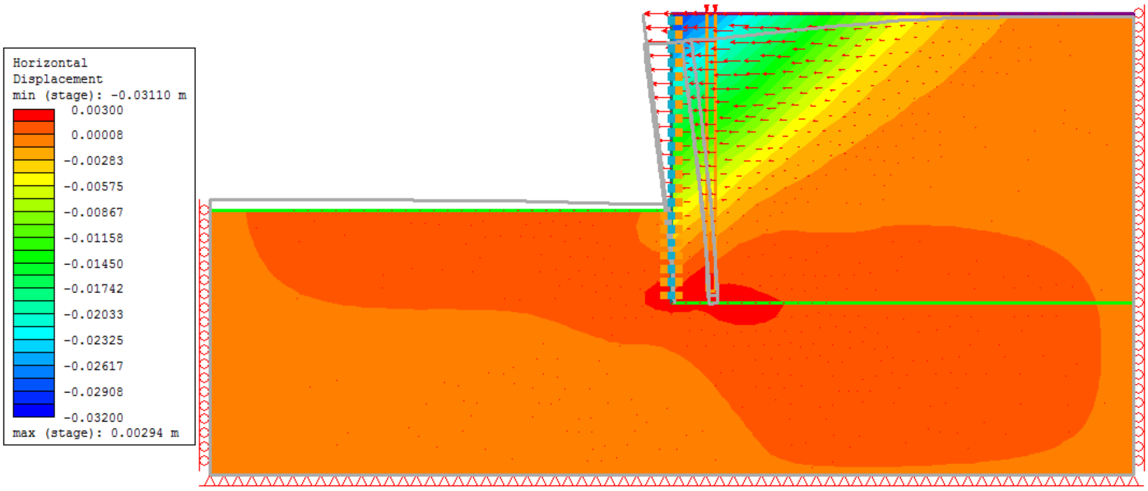

TM 11.3: Deformed model (stage 3)

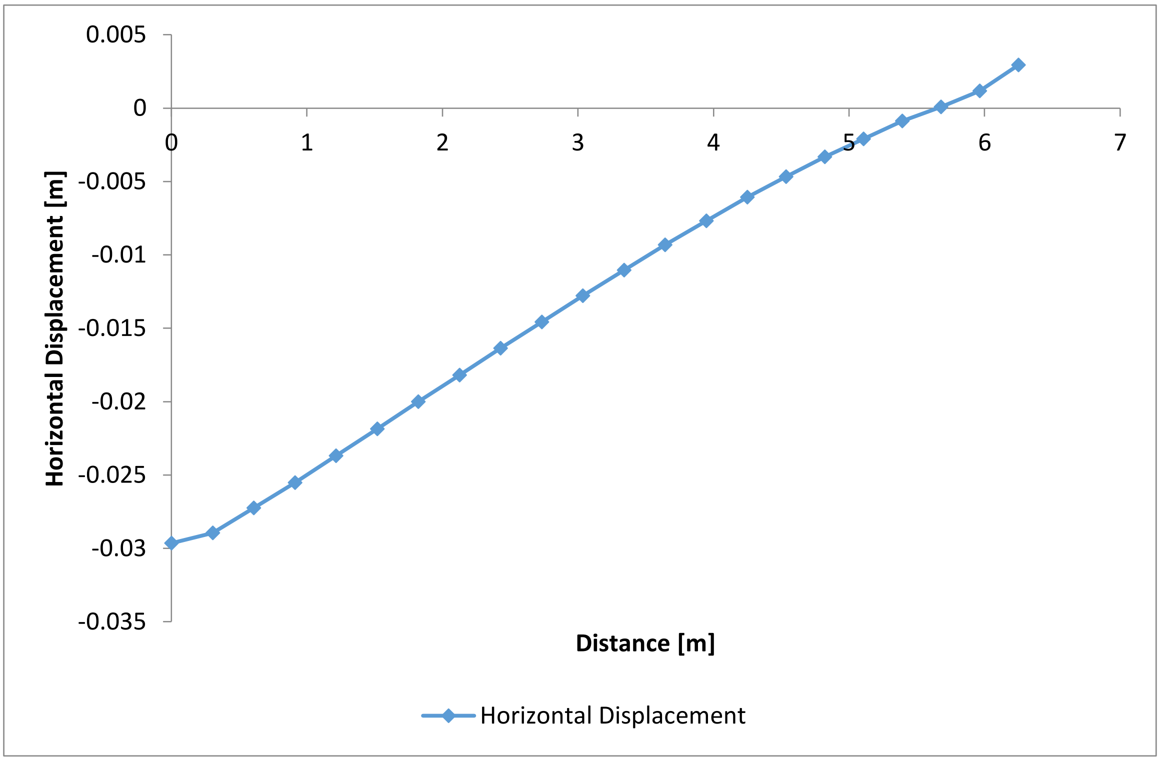

TM 11.4: Horizontal displacement of soil along retaining wall

Retaining wall maximum horizontal displacement: -0.0311m

Distance from point of maximum displacement in retaining wall to the top of backfill soil: 0.0m

Test Model 12

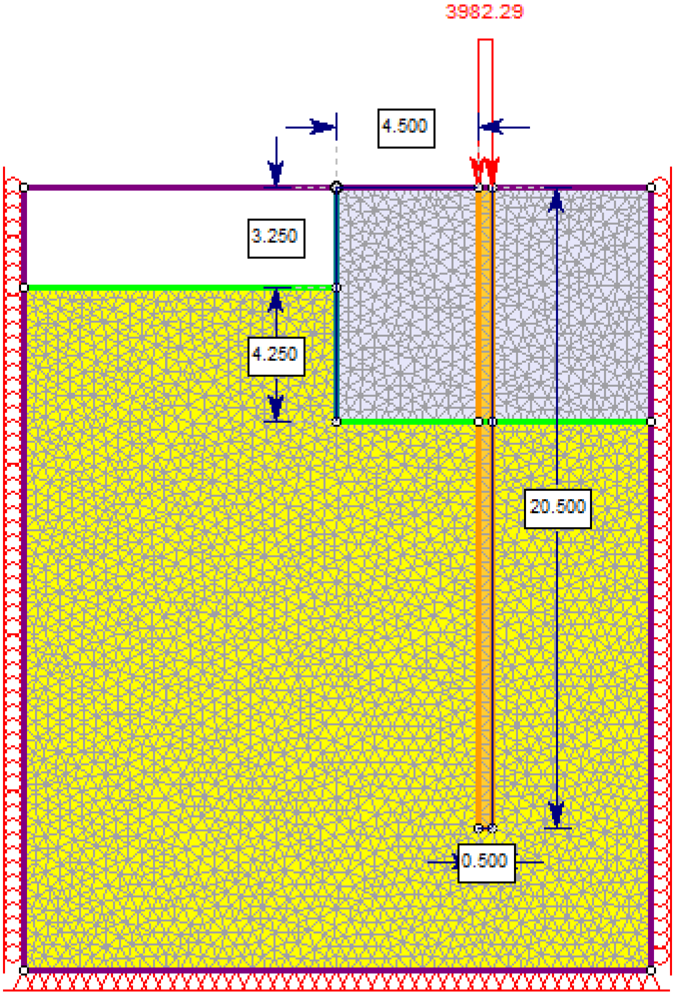

TM 12.1: Original model (stage 3)

C_1'	ϕ_1'	γ_1	E_1	C_2'	ϕ_2'	γ_2	E_2	H_1	H_2	H_3	E_3	D_1	D_2	L	Qult
0	29	20	290	22	21	22	12.4	3.25	4.25	0.75	969323	4.5	0.5	20.5	3982.29

TM 12.2: Parameter values

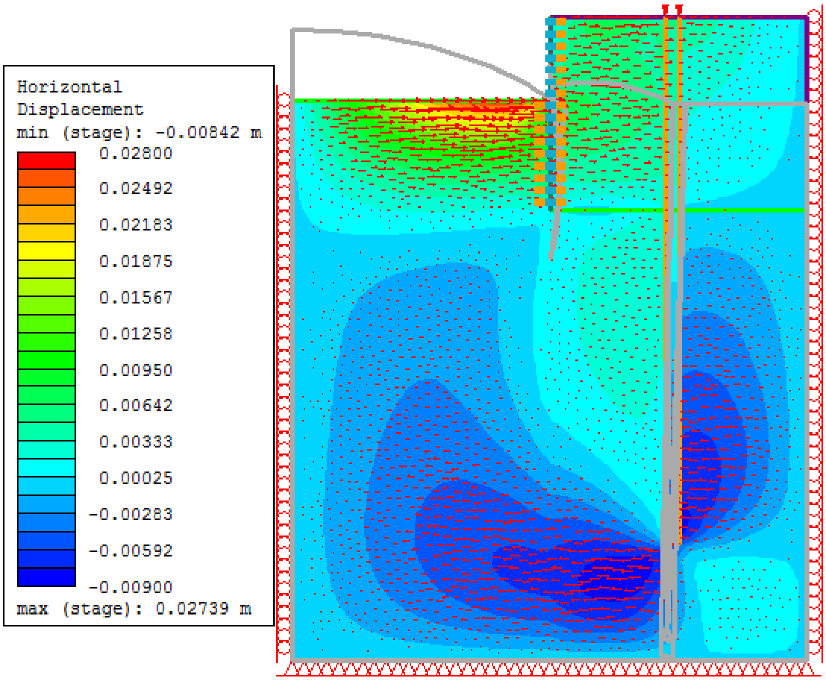

TM 12.3: Deformed model (stage 3)

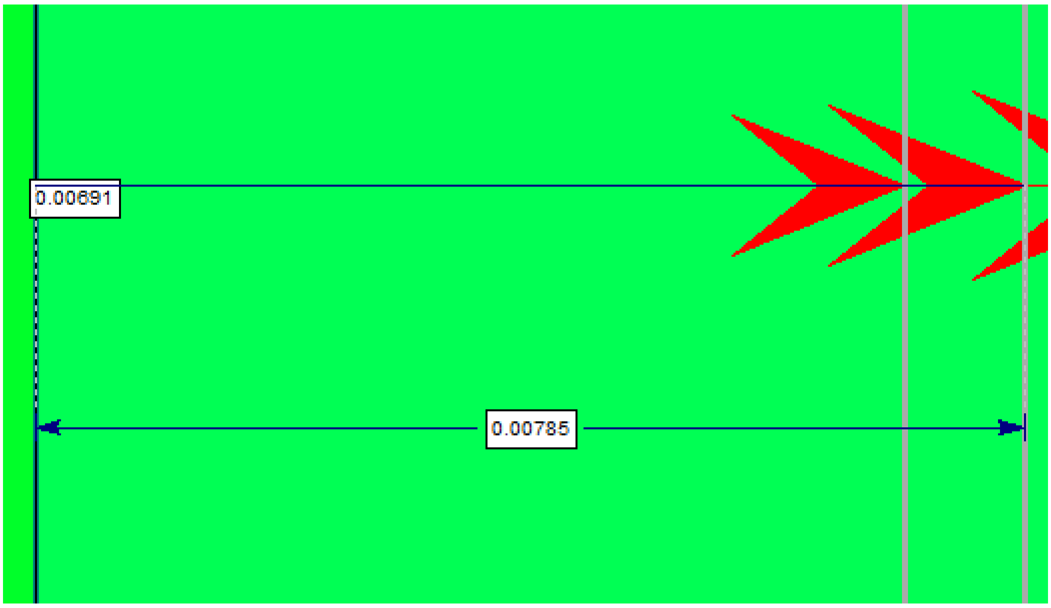

TM 12.4: Detailed view of cross-section of retaining wall and soil (stage 3)

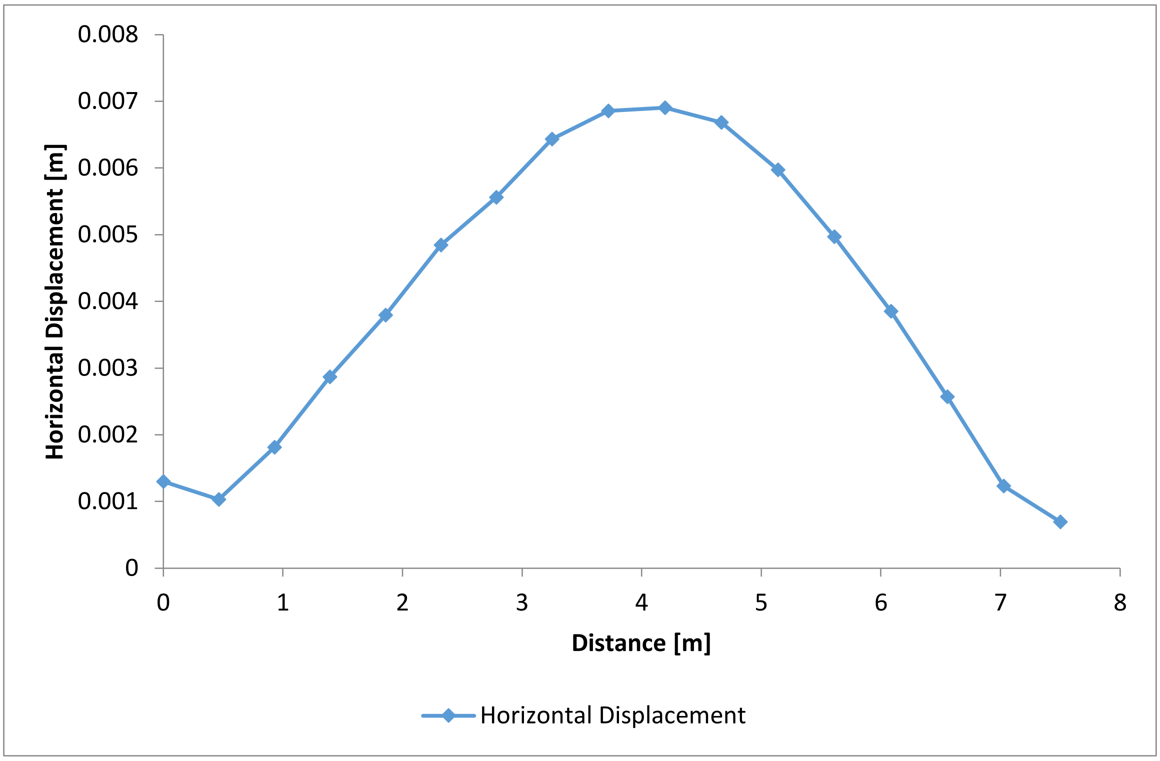

TM 12.5: Horizontal displacement of soil along retaining wall

Retaining wall maximum horizontal displacement: 0.00785m

Distance from point of maximum displacement in retaining wall to the top of backfill soil: 4.19m

Test Model 13

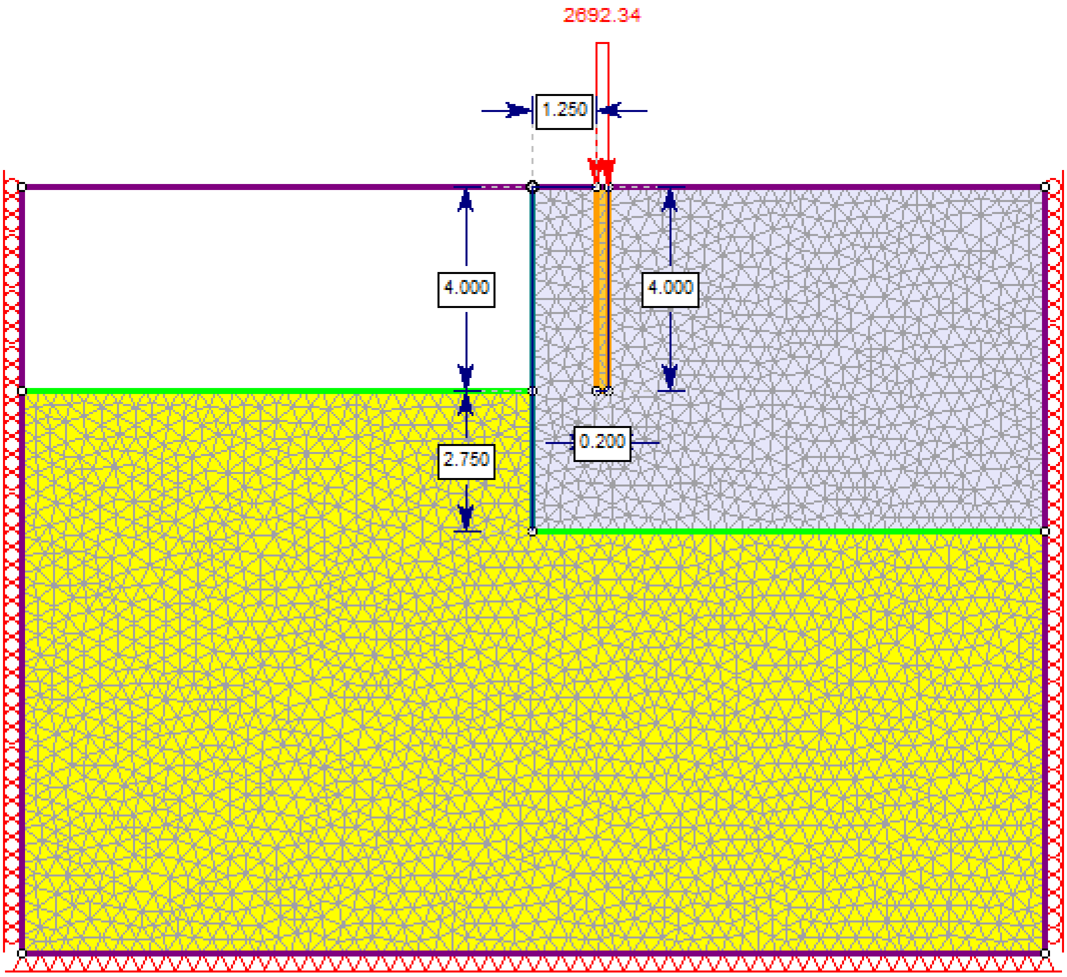

TM 13.1: Original model (stage 3)

C_1'	ϕ_1'	γ_1	E_1	C_2'	ϕ_2'	γ_2	E_2	H_1	H_2	H_3	E_3	D_1	D_2	L	Qult
0	37	21	189	33	35	17	4.1	4	2.75	1	914332	1.25	0.2	4	2692.34

TM 13.2: Parameter values

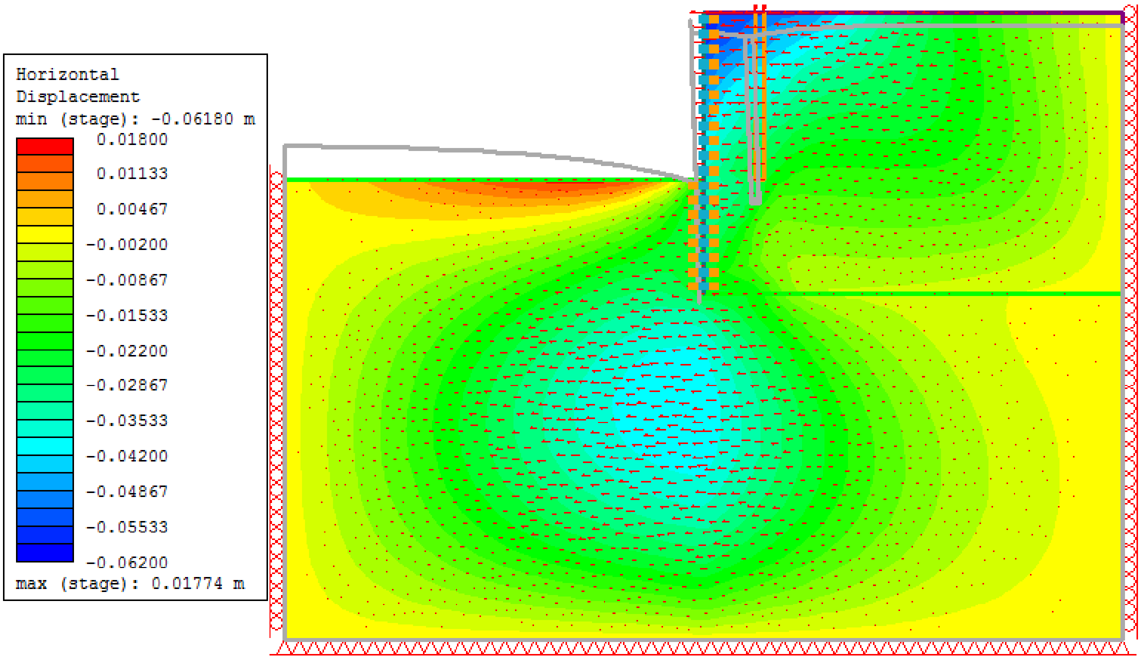

TM 13.3: Deformed model (stage 3)

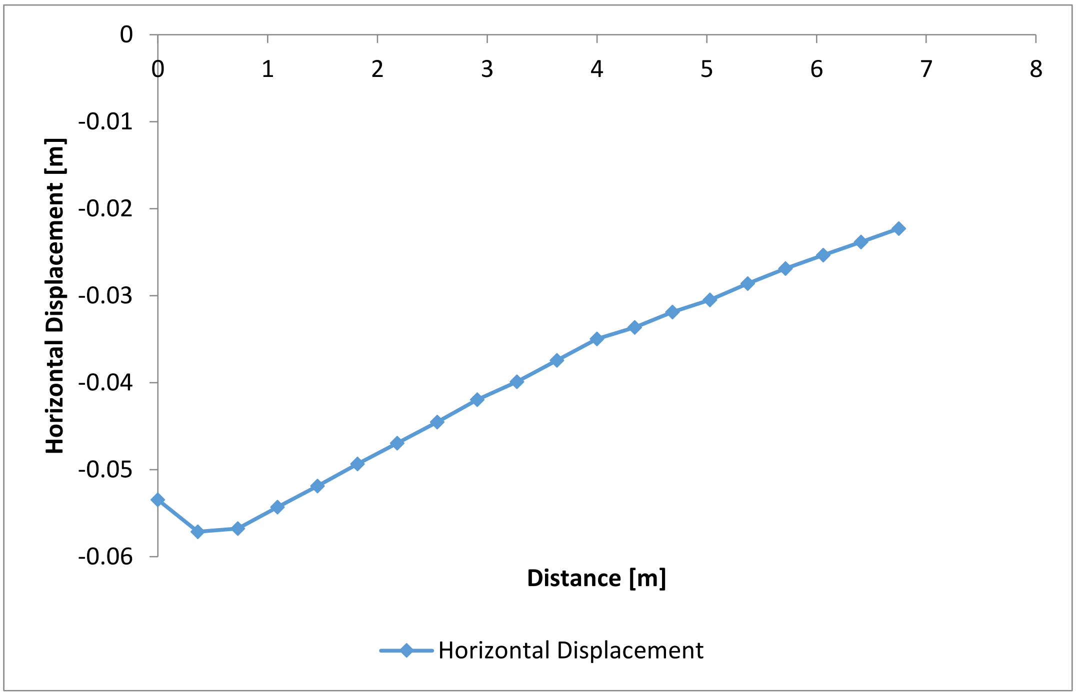

TM 13.4: Horizontal displacement of soil along retaining wall

Retaining wall maximum horizontal displacement: -0.0618m

Distance from point of maximum displacement in retaining wall to the top of backfill soil: 0.0m

Test Model 14

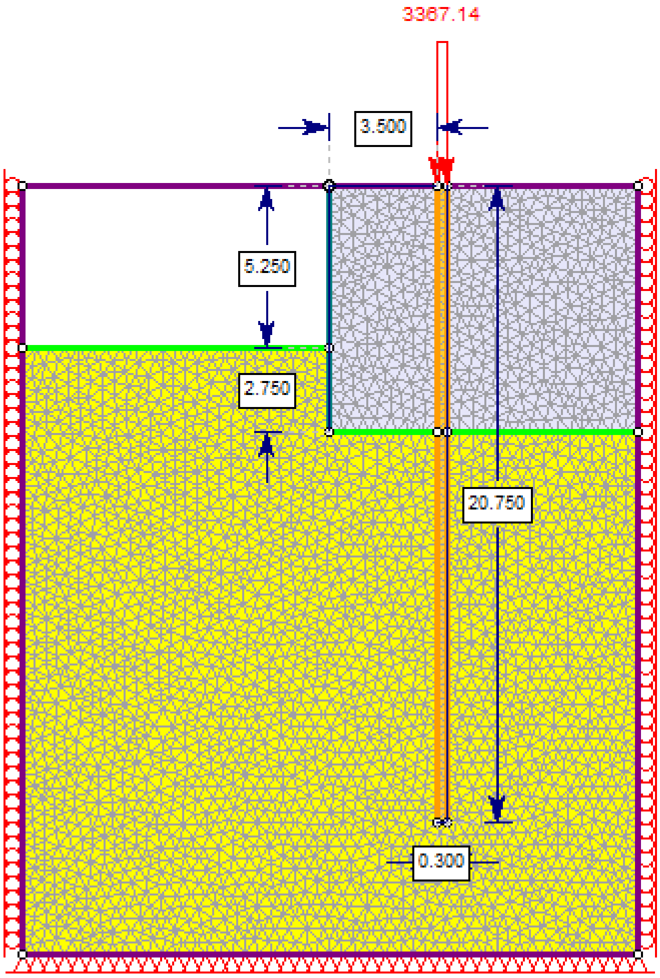

TM 14.1: Original model (stage 3)

C_1'	ϕ_1'	γ_1	E_1	C_2'	ϕ_2'	γ_2	E_2	H_1	H_2	H_3	E_3	D_1	D_2	L	Qult
0	43	22	178	47	18	17	11.6	5.25	2.75	0.75	934799	3.5	0.3	20.75	3367.14

TM 14.2: Parameter values

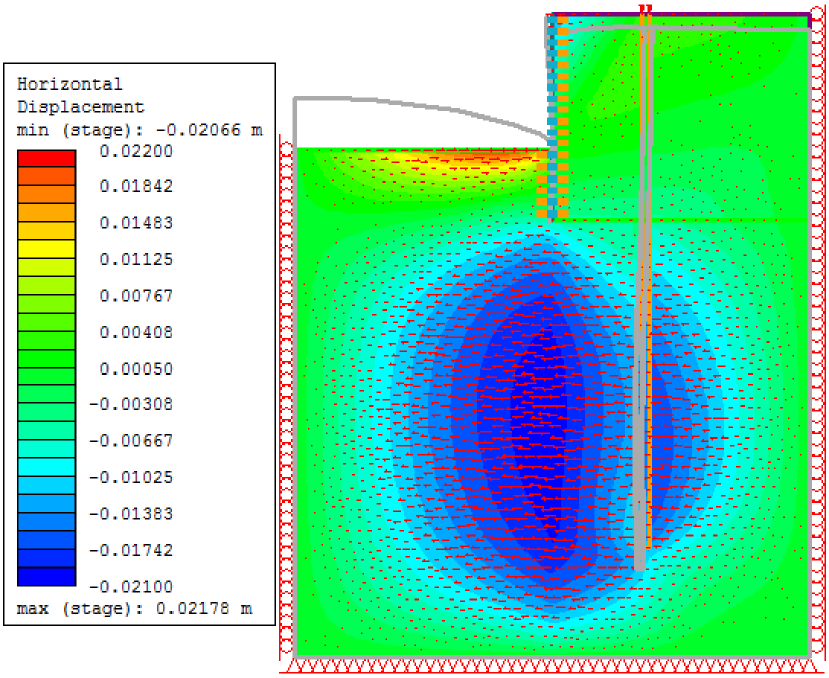

TM 14.3: Deformed model (stage 3)

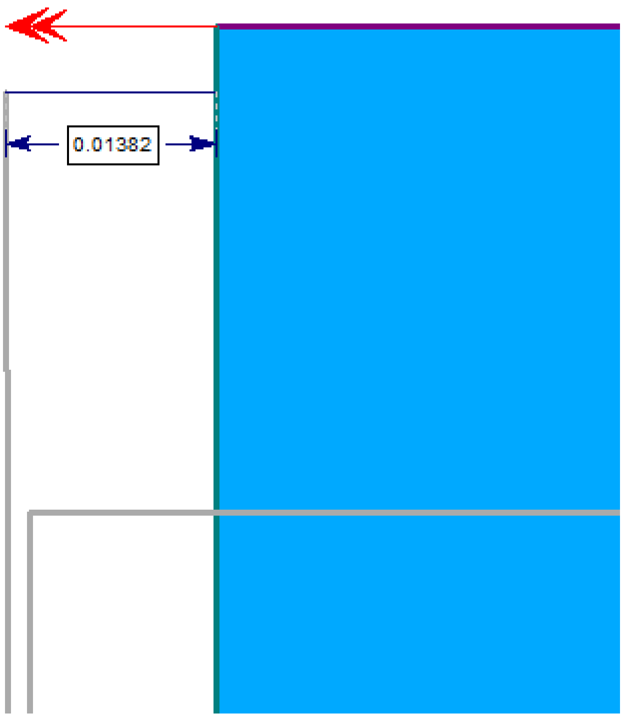

TM 14.4: Detailed view of cross-section of retaining wall and soil (stage 3)

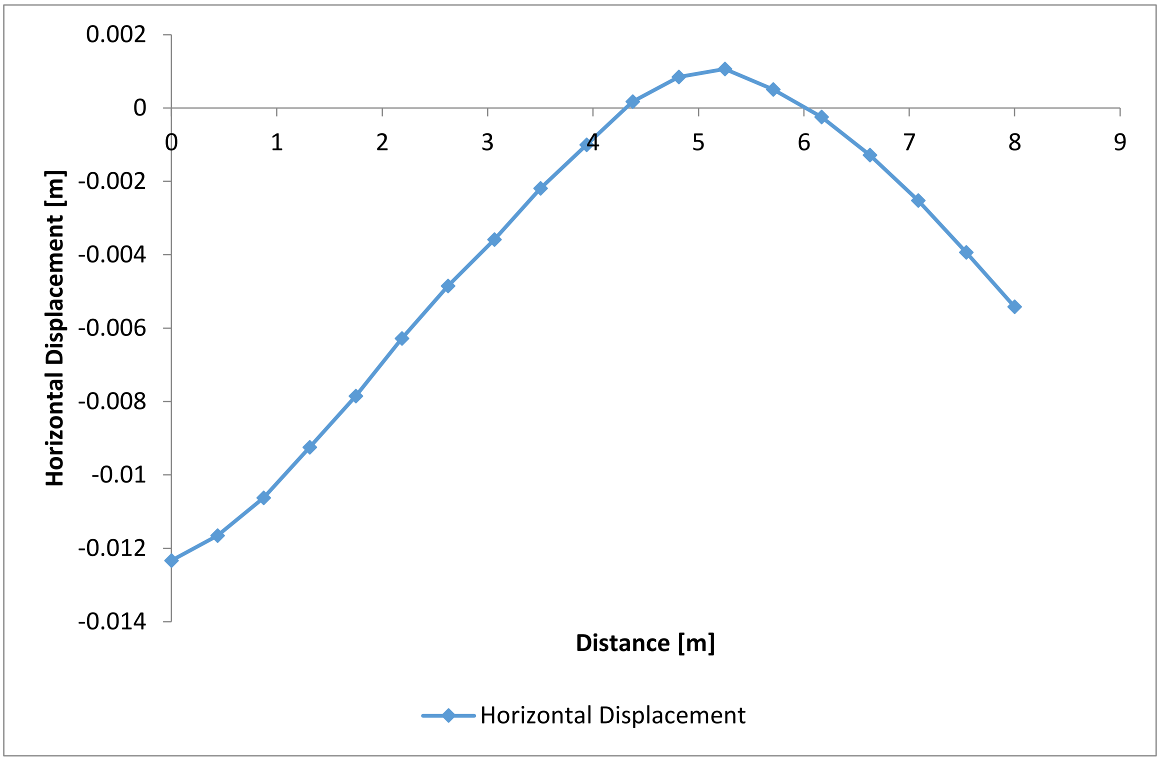

TM 14.5: Horizontal displacement of soil along retaining wall

Retaining wall maximum horizontal displacement: -0.01382m

Distance from point of maximum displacement in retaining wall to the top of backfill soil: 0.0m

Test Model 15

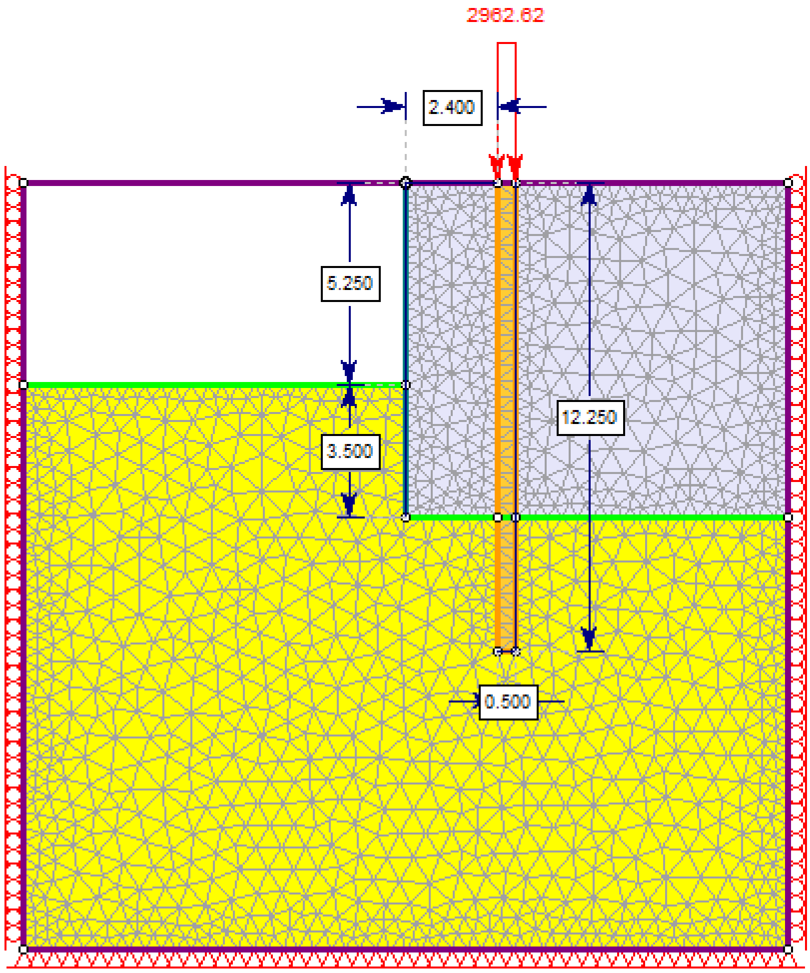

TM 15.1: Original model (stage 3)

C_1'	ϕ_1'	γ_1	E_1	C_2'	ϕ_2'	γ_2	E_2	H_1	H_2	H_3	E_3	D_1	D_2	L	Qult
0	35	18	20	41	22	24	37.0	5.25	3.5	0.5	753416	2.4	0.5	12.25	2962.62

TM 15.2: Parameter values

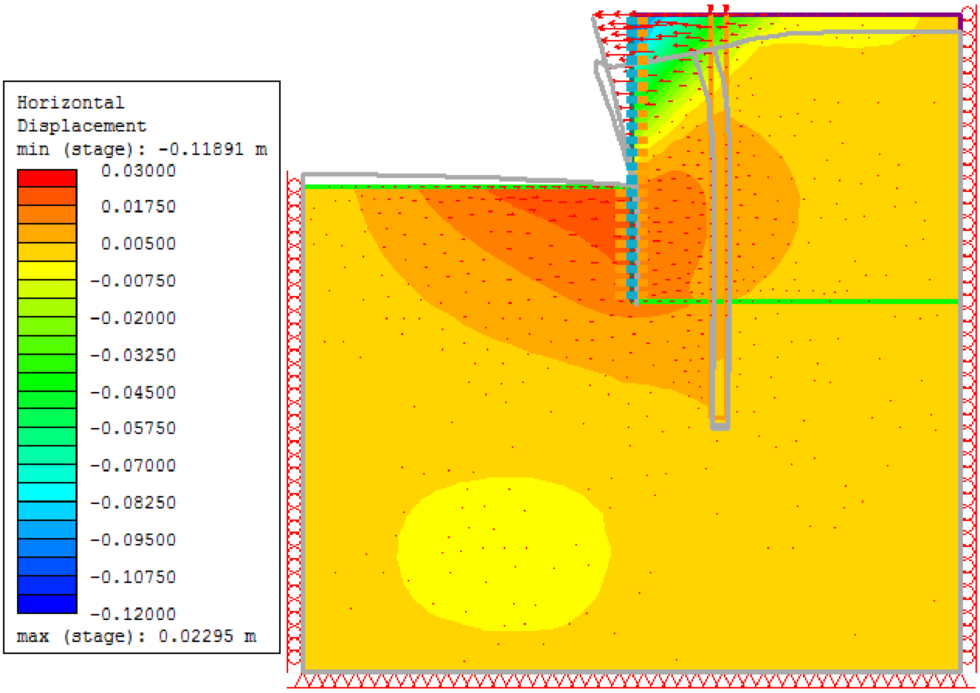

TM 15.3: Deformed model (stage 3)

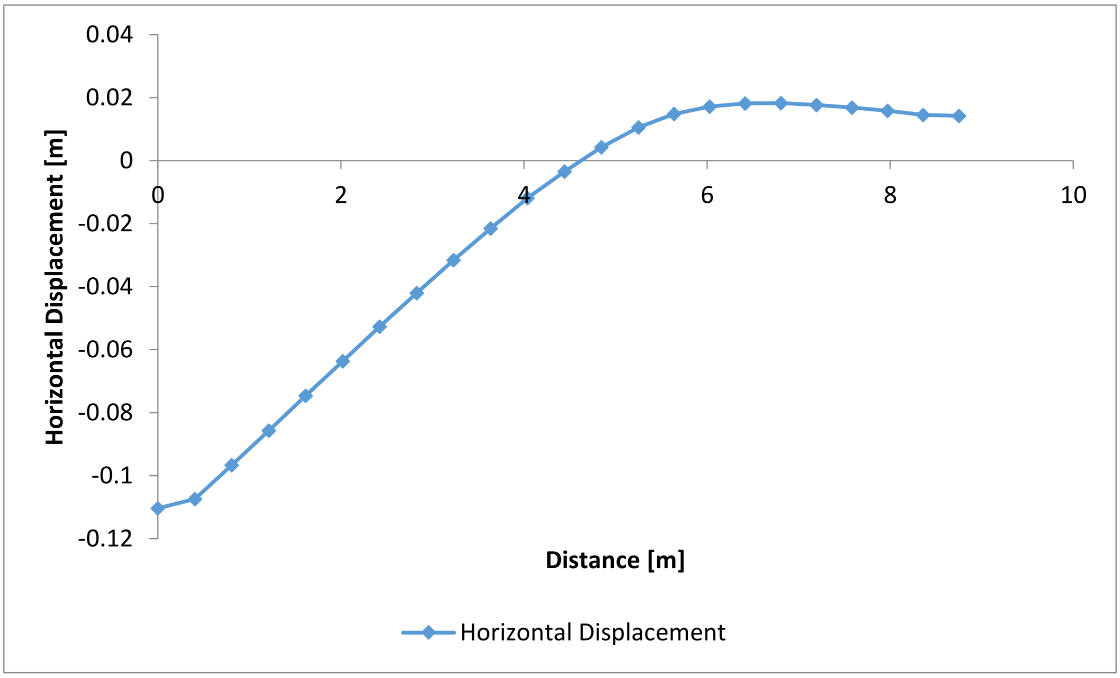

TM 15.4: Horizontal displacement of soil along retaining wall

Retaining wall maximum horizontal displacement: -0.11891m

Distance from point of maximum displacement in retaining wall to the top of backfill soil: 0.0m

Test Model 16

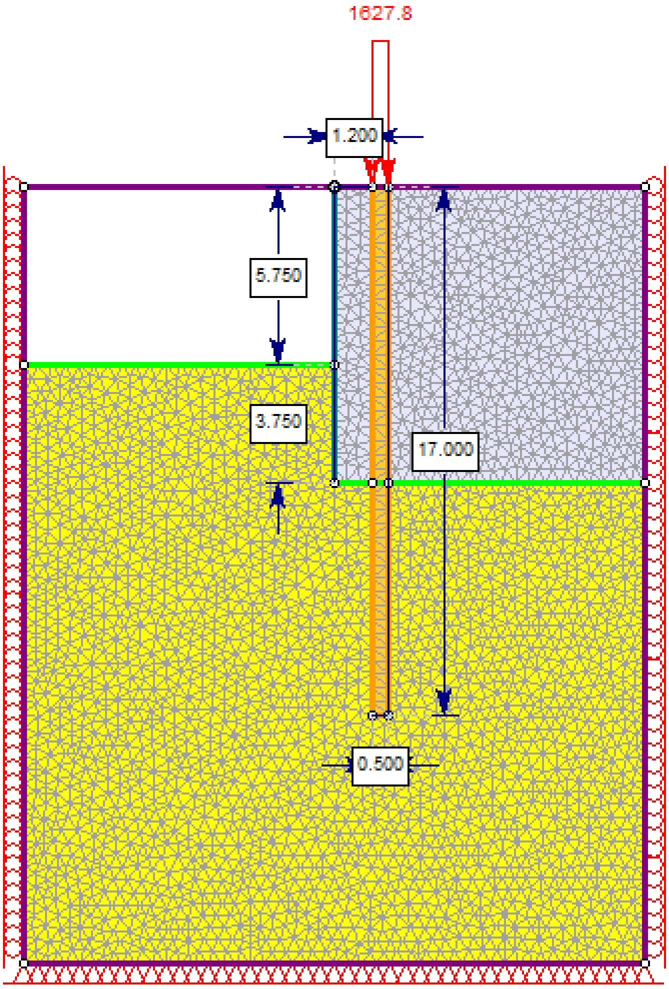

TM 16.1: Original model (stage 3)

C_1'	ϕ_1'	γ_1	E_1	C_2'	ϕ_2'	γ_2	E_2	H_1	H_2	H_3	E_3	D_1	D_2	L	Qult
0	36	21	285	51	7	19	36.0	5.75	3.75	1.25	844429	1.2	0.5	17	1627.8

TM 16.2: Parameter values

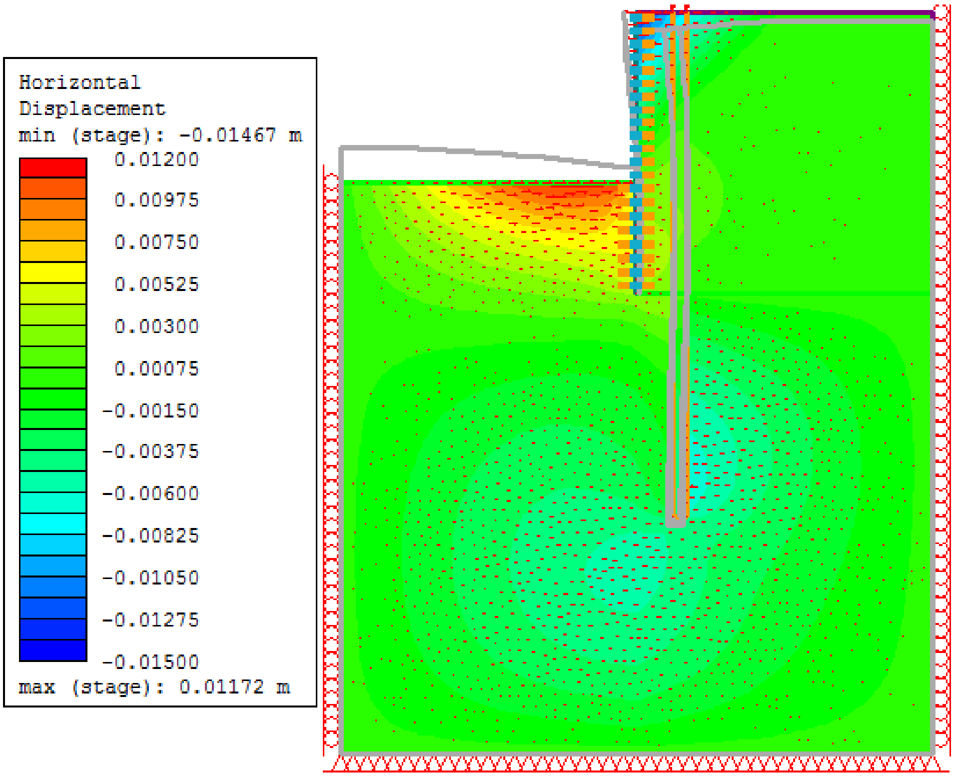

TM 16.3: Deformed model (stage 3)

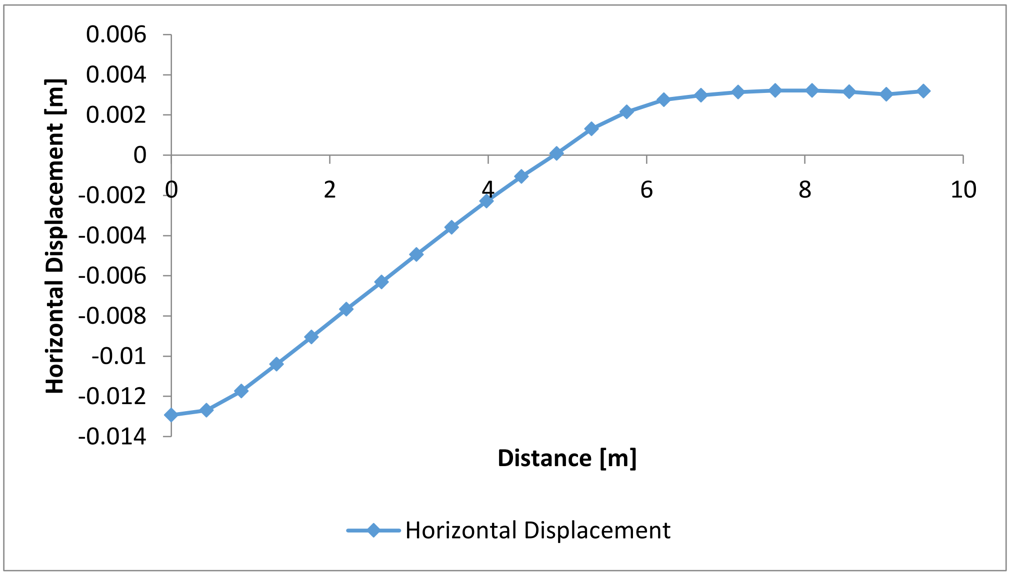

TM 16.4: Horizontal displacement of soil along retaining wall

Retaining wall maximum horizontal displacement: -0.01467m

Distance from point of maximum displacement in retaining wall to the top of backfill soil: 0.0m

Test Model 17

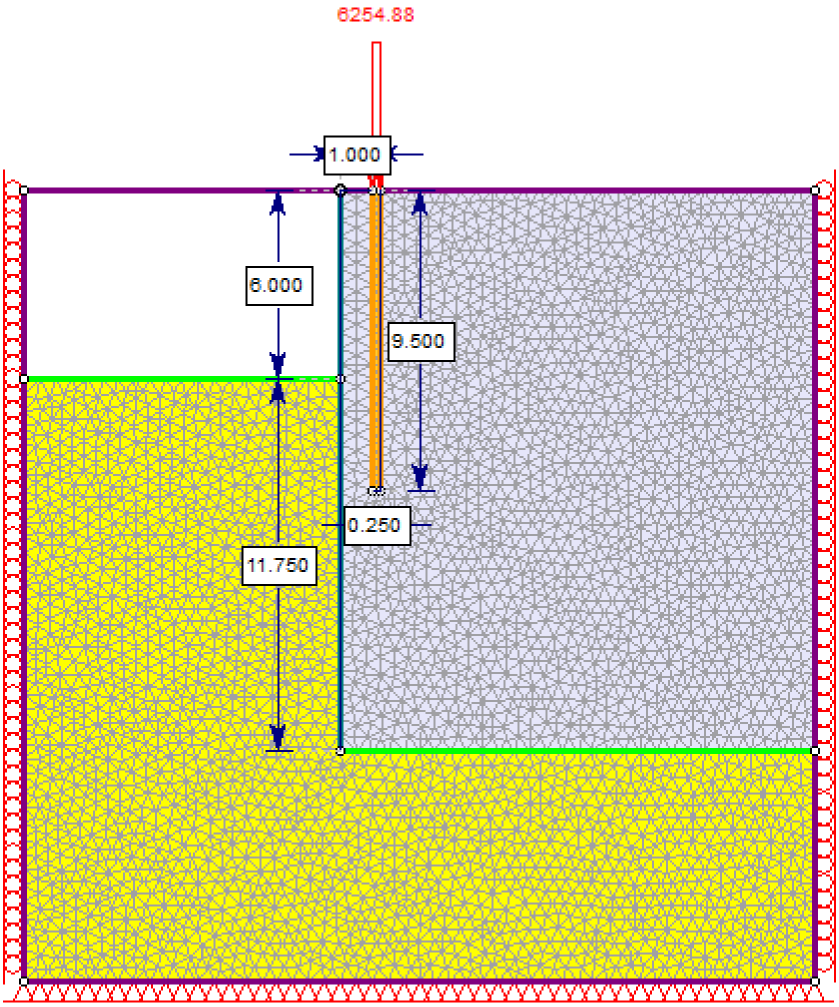

TM 17.1: Original model (stage 3)

C'_1	ϕ'_1	γ_1	E_1	C'_2	ϕ'_2	γ_2	E_2	H_1	H_2	H_3	E_3	D_1	D_2	L	Qult
0	40	21	268	36	2	16	23.3	6	11.75	0.5	797878	1	0.25	9.5	6254.88

TM 17.2: Parameter values

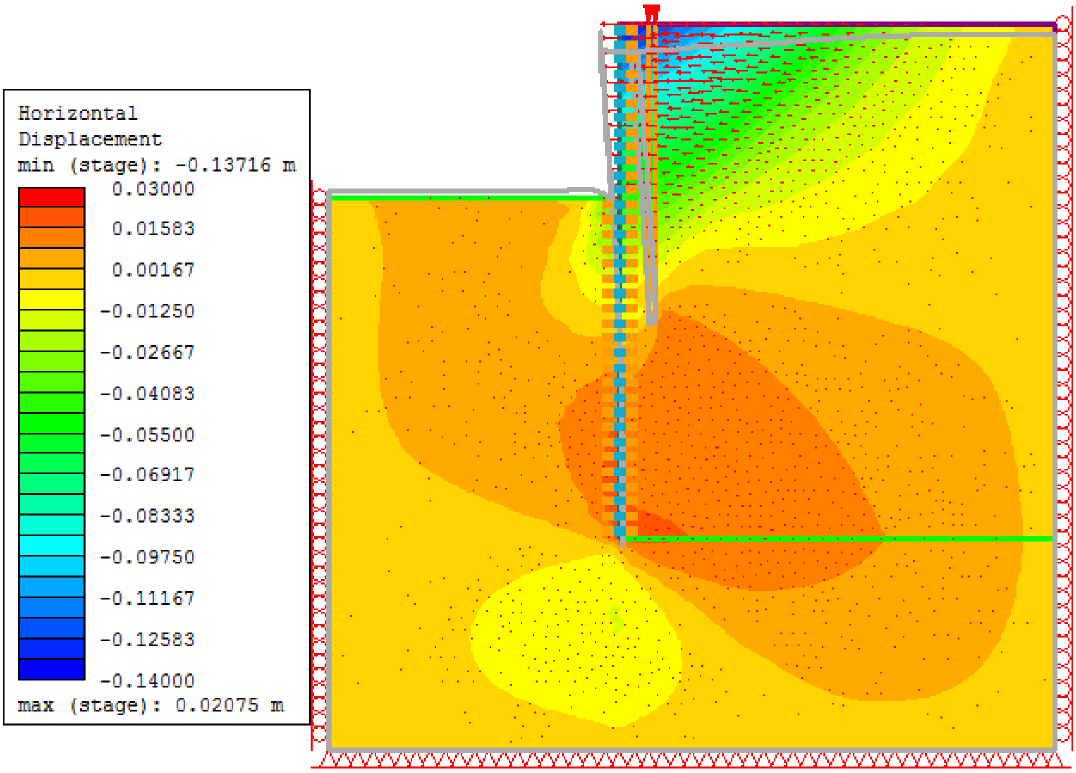

TM 17.3: Deformed model (stage 3)

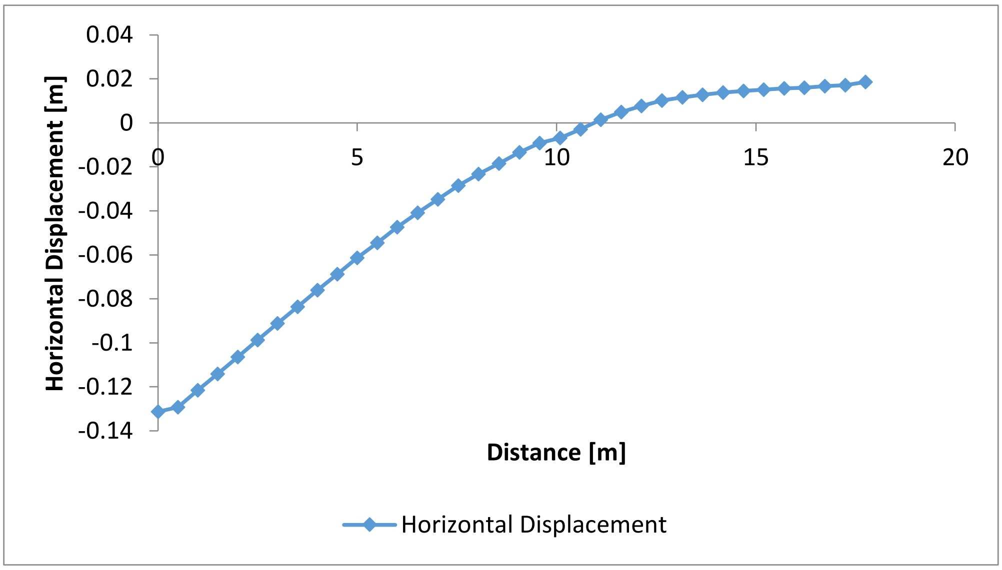

TM 17.4: Horizontal displacement of soil along retaining wall

Retaining wall maximum horizontal displacement: -0.13716m

Distance from point of maximum displacement in retaining wall to the top of backfill soil: 0.0m

Test Model 18

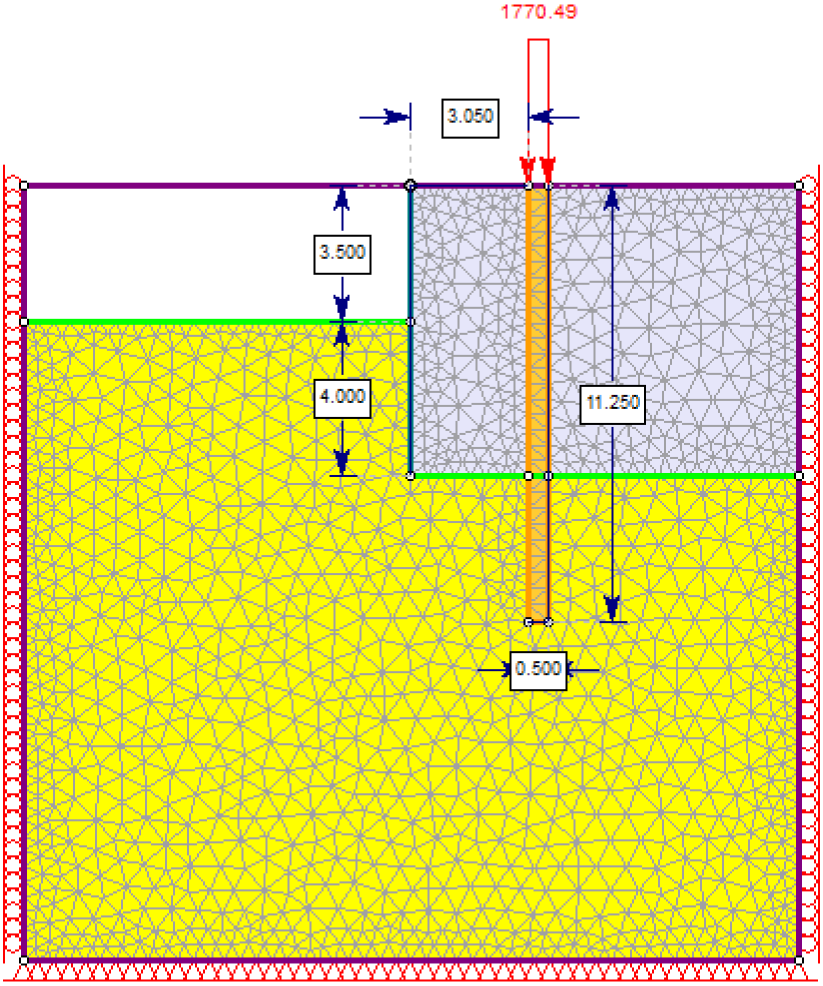

TM 18.1: Original model (stage 3)

C_1'	ϕ_1'	γ_1	E_1	C_2'	ϕ_2'	γ_2	E_2	H_1	H_2	H_3	E_3	D_1	D_2	L	Qult
0	39	22	80	25	19	18	45.9	3.5	4	0.5	713630	3.05	0.5	11.25	1770.49

TM 18.2: Parameter values

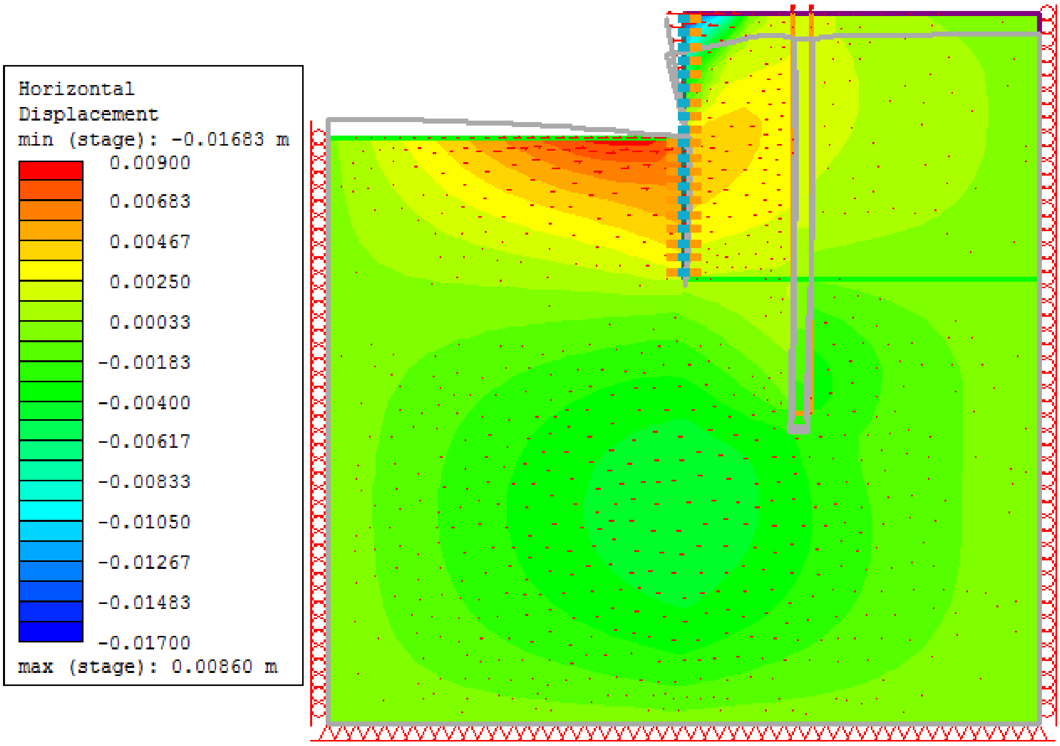

TM 18.3: Deformed model (stage 3)

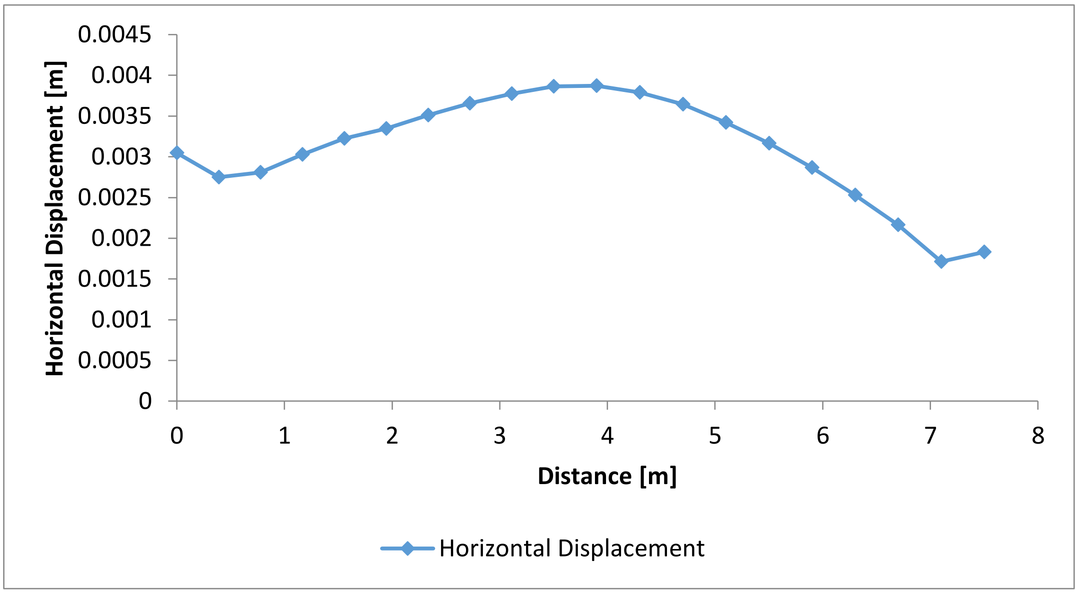

TM 18.4: Horizontal displacement of soil along retaining wall

Retaining wall maximum horizontal displacement: -0.01683m

Distance from point of maximum displacement in retaining wall to the top of backfill soil: 0.0m

Test Model 19

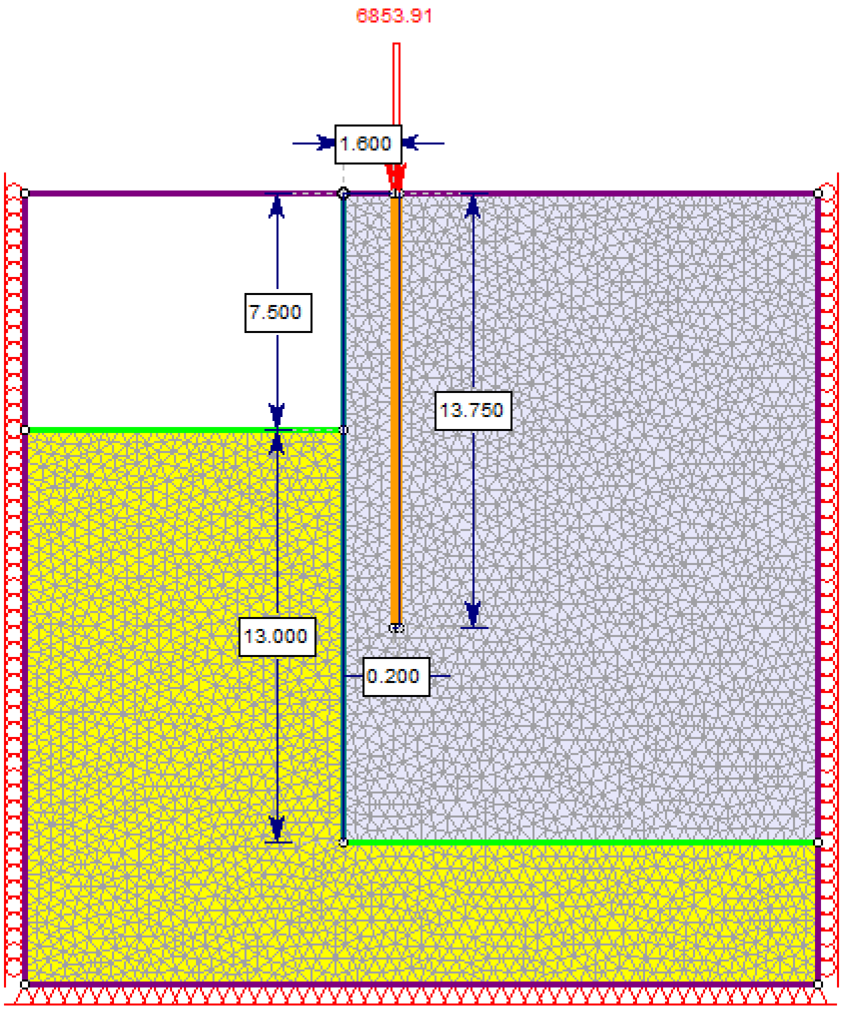

TM 19.1: Original model (stage 3)

C_1'	ϕ_1'	γ_1	E_1	C_2'	ϕ_2'	γ_2	E_2	H_1	H_2	H_3	E_3	D_1	D_2	L	Qult
0	40	19	228	41	3	16	2.3	7.5	13	1.5	729321	1.6	0.2	13.75	6853.91

TM 19.2: Parameter values

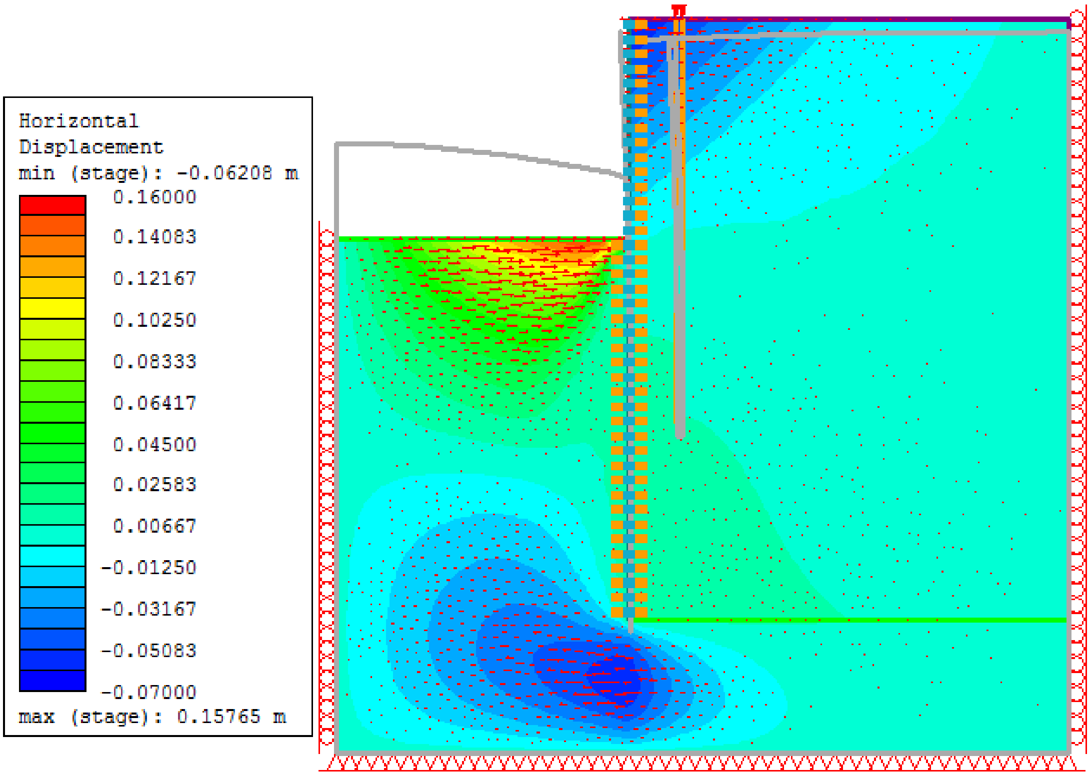

TM 19.3: Deformed model (stage 3)

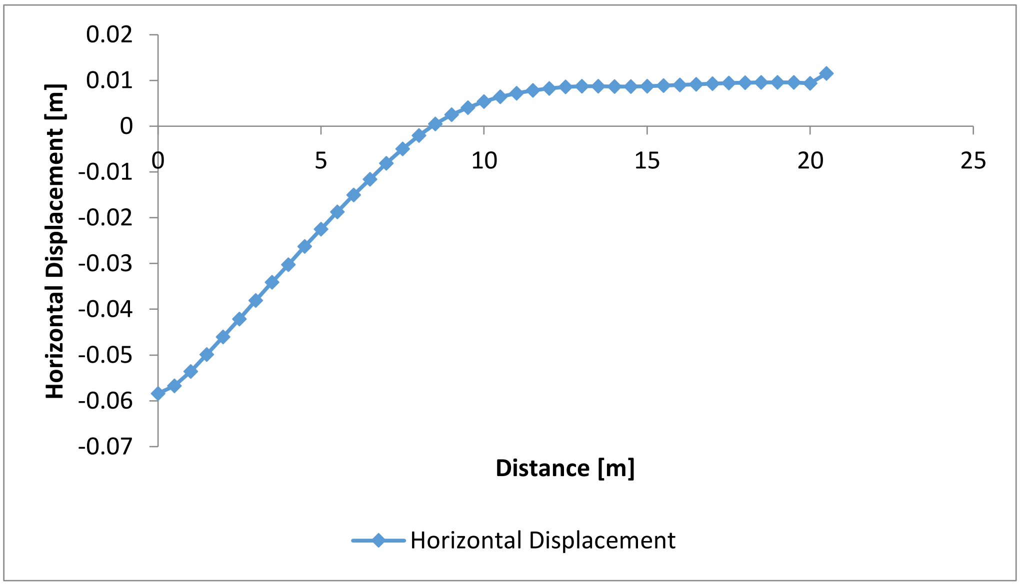

TM 19.4: Horizontal displacement of soil along retaining wall

Retaining wall maximum horizontal displacement: -0.06208m

Distance from point of maximum displacement in retaining wall to the top of backfill soil: 0.0m

Test Model 20

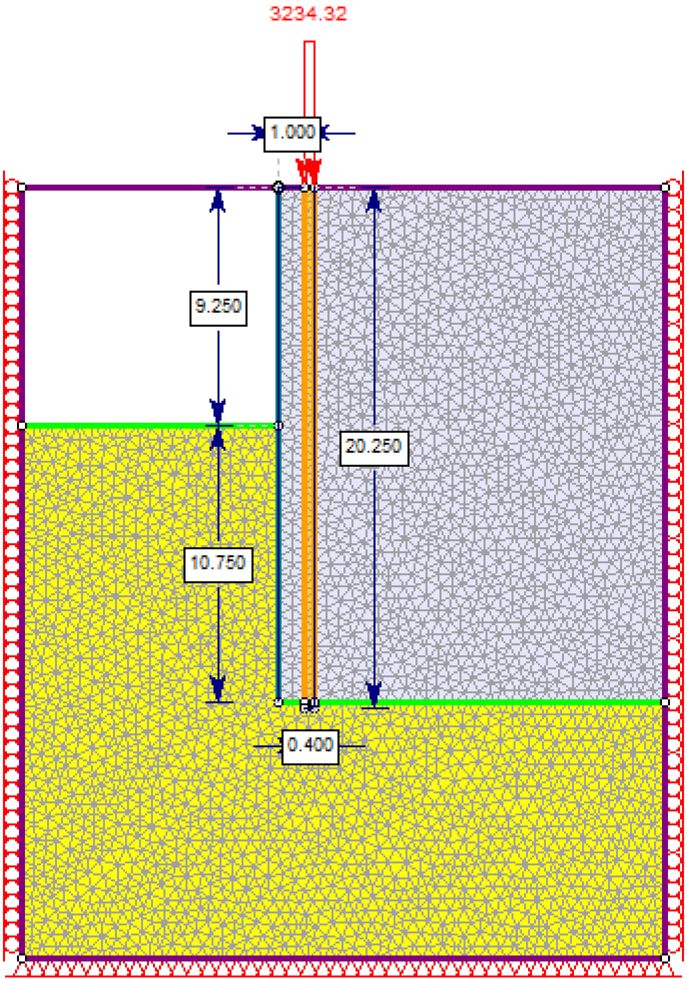

TM 20.1: Original model (stage 3)

C_1'	ϕ_1'	γ_1	E_1	C_2'	ϕ_2'	γ_2	E_2	H_1	H_2	H_3	E_3	D_1	D_2	L	Qult
0	37	18	103	54	8	20	38.7	9.25	10.75	1.25	1043888	1	0.4	20.25	3234.32

TM 20.2: Parameter values

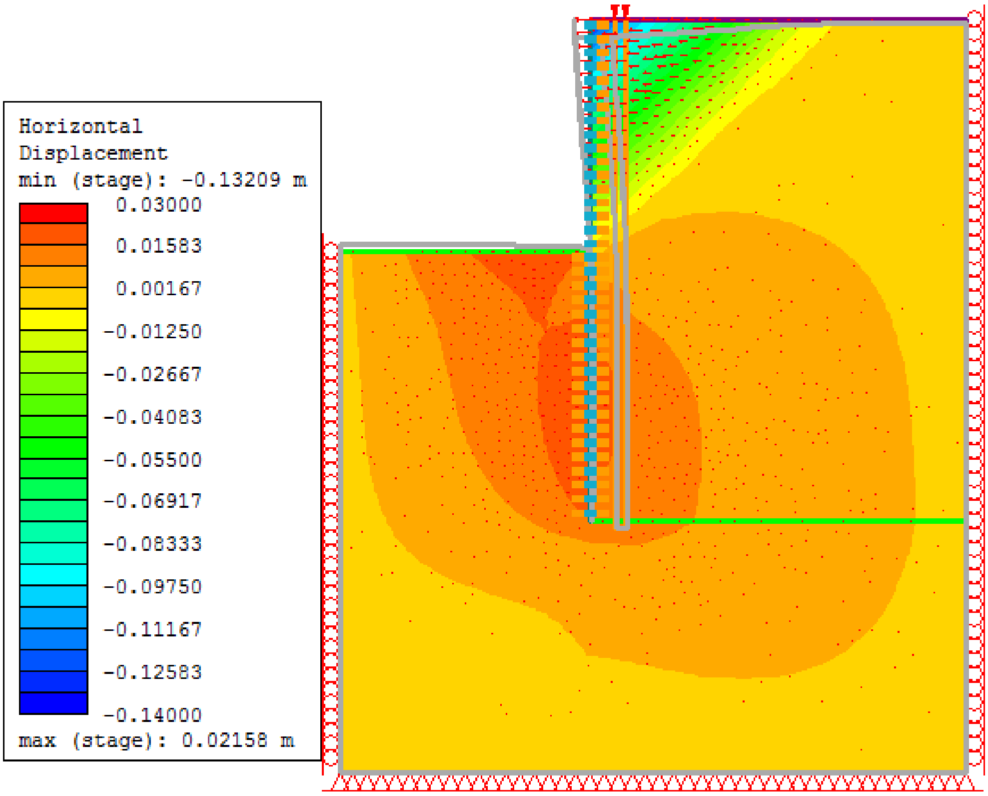

TM 20.3: Deformed model (stage 3)

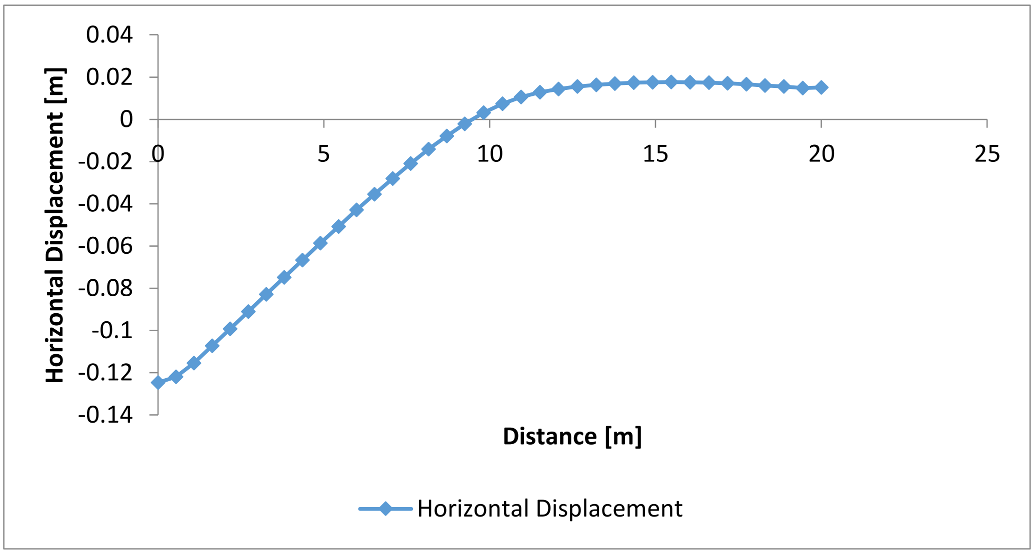

TM 20.4: Horizontal displacement of soil along retaining wall

Retaining wall maximum horizontal displacement: -0.13209m

Distance from point of maximum displacement in retaining wall to the top of backfill soil: 0.0m